ABSTRACTS

Sixth International Symposium on Antarctic Earth Sciences

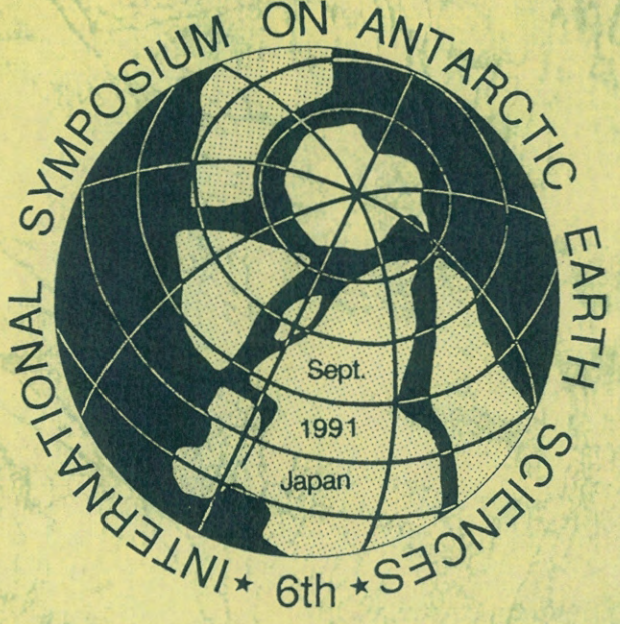

National Institute of Polar Research

9-13 September
1991

SIXTH INTERNATIONAL SYMPOSIUM ON ANTARCTIC EARTH SCIENCES

National Women's Education Center
Ranzan-machi, Saitama, Japan
9-13 September 1991

Preface

Abstracts of papers to be delivered at the Sixth International Symposium on Antarctic Earth Sciences are set out in alphabetical order of first authors in the volume.

Sponsors

Scientific Committee on Antarctic Research
International Union of Geological Sciences
Science Council of Japan
National Institute of Polar Research

METAMORPHIC HISTORY OF LATE PRECAMBRIAN-EARLY CAMBRIAN METASEDIMENTARY BASEMENT AT THE ANTARCTIC SHIELD MARGIN IN NORTH VICTORIA LAND AND MARIE BYRD LAND, ANTARCTICA

C.J. Adams, Nuclear Sciences Group, DSIR Physical Sciences,
Lower Hutt, New Zealand

Recent geochronological investigations, mainly from K-Ar and Rb-Sr studies of low-grade metasedimentary sequences in North Victoria Land and Marie Byrd Land are reviewed. The low-grade metamorphic rocks, originating from high structural levels provide the simplest method of dating the early regional metamorphism of very widespread monotonous greywacke sequences seen in three major areas :

1. Berg Group and Preistley Formation; occurring at the westernmost margin of the Wilson Terrane of North Victoria Land, consistently yield K-Ar and Rb-Sr age evidence from slates and phyllites for metamorphism only at 530-540 Ma (probably early Cambrian). Higher grade equivalents of these (Rennick Schists) occur within Wilson Group gneisses of the Wilson Terrane.

2. Roberston Bay Group; forming a distinctive terrane in the northern and eastern parts of Northern Victoria Land. Possible late Cambrian-early Ordovician sediments may show a transitional relationship to Bowers Supergroup sediments and volcanics and yield K-Ar and Rb-Sr ages on slates and phyllites, 480-500 Ma (early Ordovician).

3. Swanson Formation; a distinctive unit of unfossiliferous metagreywacke and argillite recognised in the Ford Ranges of Marie Byrd Land, but possibly correlative with similar rocks in South Island, New Zealand (Greenland Group) and Campbell Island, Campbell Plateau (Complex Point Formation), yielding K-Ar and Rb-Sr metamorphic ages, 440-450 Ma (mid-Ordovician).

These age patterns demonstrate a zonation of early Palaeozoic of metamorphism becoming younger away from the Antarctic craton proper and there is as yet no conclusive evidence for early Proterozoic-Archaean metamorphic basement in the North Victoria Land/Marie Byrd Land sector of Antarctic.

ATTENUATION OF SEISMIC WAVES IN THE LÜTZOW-HOLM BAY REGION, EAST ANTARCTICA

Junpei AKAMATSU, Disaster Prevention Research Institute, Kyoto University, Gokasho, Uji, Kyoto 611, Japan

Seismic observations with a local radio-telemetry network were carried out by the Japanese Antarctic Research Expedition teams from June 1987 to October 1989 at Syowa Station, a Japanese Antarctic facility (69°S, 39° E), to study wave characteristics and local seismicity in the Lützow-Holm Bay region (Akamatsu et al., 1989, 1990; Akamatsu, 1991). Although the seismicity in the study region is very low, nine micro earthquakes were located and discussed in relation to possible faults and geological structures inferred from surface geology and submarine topography (Akamatsu et al., 1989, 1990). In this paper, attenuation of coda waves from local events are studied to discuss heterogeneity of lithosphere.

Coda waves from local earthquakes are considered as ensembles of back-scattered S waves from randomly distributed scatterers in the lithosphere (e.g. Aki and Chouet, 1975). Heterogeneities of velocities and/or density as well as cracks and faults are supposed to be the main scatterers. Attenuation of coda amplitude with lapse time is considered to reflect scattering loss of energy and intrinsic absorption. In particular, regional variation of coda Q, Q_c, attracts considerable interest in relation to tectonics and seismicity.

Q_c^{-1} varies with frequency and can be expressed as Q_0^{-1} f^{-q} for frequency higher than about 1 Hz. Value of Q_c^{-1} around 1 Hz and dependence of Q_c^{-1} on frequency vary to a considerable extent from place to place according to tectonic activity (Singh and Herrmann, 1983; Jin and Aki, 1988). Both Q_c^{-1} around 1 Hz and q in the active regions appear larger than those in the stable regions. It is, therefore, very interesting to know the frequency characteristics of Q_c^{-1} in the Lützow-Holm Bay region, East Antarctica, one of the most stable and aseismic continental shield in the world.

Another important reason for analyzing Antarctic events is that there are no sedimentary layers in the Lützow-Holm Bay region. The P-wave

velocity of surface layer is estimated to be 6.0 km/s by explosion experiments (Ito and Ikami, 1984). This value corresponds well with velocities found in the granitic layers of seismically active regions, for example, the velocity of granitic layer deeper than 5 km in Kyoto, Japan (Okano and Kuroiso, 1986). The distribution of scatterers seems to be thick in the shallower portion of crust (Kanao and Ito, 1990). Therefore, it is possible to examine the coda characteristics free from the effects of surface sedimentary layers.

On the basis of single isotropic scattering model, Sato (1977) derived a space-time distribution of the mean energy density for the scattered wave field. Using his functional form, $K(t/t_s)$, for geometrical spreading factor, coda amplitude A(f,t) can be expressed as,

$$A(f,t) \propto S(f)\ (\ K(t/t_s))^{0.5}\ e^{-bt} \qquad \text{for } t > t_s, \qquad (1)$$

where S(f) is source spectrum, t is lapse time measured from source origin time, t_s is S travel time, b is attenuation coefficient and $K(t/t_s) = (t_s/t)\ \ln(\ t+t_s\ /\ t-t_s\ )$. Attenuation coefficients, b, were estimated for logarithmic amplitude, ln A(f,t), of band-pass filtered seismograms. Q_c^{-1} is given by $b/\pi f$.

The network consisted of a large aperture array of 3 sites with 3-component 1-s seismometers along Soya Coast, and a small tripartite array with vertical ones in East Ongul Island. The vertical components of 6 sites were analyzed for the 6 local events, the locations of which are shown in figure 1. An example of band-pass filtered traces is shown in figure 2. The center frequencies of pass-bands are 1, 2, 4, 8, 16 and 24 Hz, respectively. Figure 3 shows the logarithmic decay, in which ln A(f,t) is the mean amplitude of envelope for 1 sec interval. Analyzing intervals are from about 1.5 t_s to the time having a S/N ratio over 3. As a result, two analyzing intervals are used; 10 - 50 sec for the group of short distance, and 150 - 210 sec for that of long distance. In figure 3, decay curves fitted with least square method are drawn on the analyzing intervals. The mean values of Q_c^{-1} thus obtained are plotted in figure 4 together with the data at Kyoto, Japan for an example of an active region (Akamatsu, 1980). In figure 5 the compiled Q_c^{-1} data in the regions of various activity (Jin et al., 1985) are shown for comparison.

Main features of Q_c^{-1} for the Lützow-Holm Bay region are: (1) strong dependence on frequency with considerably large Q_c^{-1} at low frequency and extremely small values in higher frequency range, and (2) decrease of Q_c^{-1} with lapse time. The strong frequency dependence appears apparently to be different from the general relations between Q_c^{-1} and tectonic activity shown in figure 5. The small value at high frequency seems to be typical for the stable continental shield. This should also be attributed to the regional condition of no sedimentary layers. If it can be assumed that Q due to intrinsic absorption does not depend on frequency, then large Q_c^{-1} toward the low frequency range should be caused by the scattering loss of energy. Taking account of the low seismicity (Adams et al., 1985; Kaminuma, 1976), it seems likely that there are hardly any faults and cracks, which would be responsible for scattering of waves. Therefore, the large Q_c^{-1} in the low frequency range is supposed to be mainly caused by scattering loss by heterogeneities such as perturbation of velocity and/or density. The feature (2) suggests that the existing heterogeneities decrease with increase of depth in the lithosphere.

References

Adams, R. D., Hughes, A. A. and Zhang, B. M. 1985. A confirmed earthquake in continental Antarctica. Geophys. J. R. astr. Soc., 81:489-492.

Akamatsu, J., 1980. Attenuation property of coda parts of seismic waves from local earthquakes. Bull. Disas. Prev. Res. Inst., Kyoto Univ., 30:1-16.

Akamatsu, J., 1991. Coda attenuation in the Lützow-Holm Bay region, East Antarctica. PEPI, 67:65-75.

Akamatsu, J., Ichikawa, N. and Kaminuma, K., 1989. Seismic observation with local telemetry network around Syowa Station, East Antarctica. Proc. NIPR Symp. Antarct. Geosci., 3: 1-12.

Akamatsu, J., Ichikawa, N. and Kaminuma, K., 1990. Seismic observation with local telemetry network around Syowa Station, East Antarctica (2). Proc. NIPR Symp. Antarct. Geosci., 4: 90-99.

Aki, K. and Chouet, B., 1975. Origin of coda wave; source, attenuation, and scattering effects. J. Geophys. Res., 80: 3322-3342.

Ito, K. and Ikami, A., 1984. Upper crustal structure of the Prince Olav Coast, East Antarctica. Mem. Natl Inst Inst. Polar Res., Ser.C (Earth Sci.), 15: 13-18.

Jin, A and AKI, K., 1988. Spatial and temporal correlation between coda Q and seismicity in China. Bull. Seis. Soc. Am., 78: 741-769.

Jin, A., Cao, T. and AKI, K., 1985. Regional change of coda Q in the oceanic lithosphere. J. Geophys. Res., 90, B10: 8651-8659.

Kaminuma, K., 1976. Seismicity in Antarctica. J. Phys. Earth.,24: 381-395.

Kanao, M and Ito, K., 1990. Attenuation property of coda waves in the middle and northern parts of Kinki District. Zisin (J. Seism. Soc. Japan), 2, 43:311-320 (in Japanese with Engl. abstract).

Okano, K. and Kuroiso, A., 1986. Crustal structure in the northern part of Kinki District, southwest Japan. Zisin (J. Seism. Soc. Japan), 2, 39: 443-455 (in Japanese with Engl. abstract).

Sato, H., 1977. Energy propagation including scattering effects, Single isotropic scattering approximation. J. Phys. Earth, 25: 27-41.

Singh, S and Herrmann, R. B., 1983. Regionalization of crustal coda Q in the continental United States. J. Geophs. Res., 88, B1: 527-538.

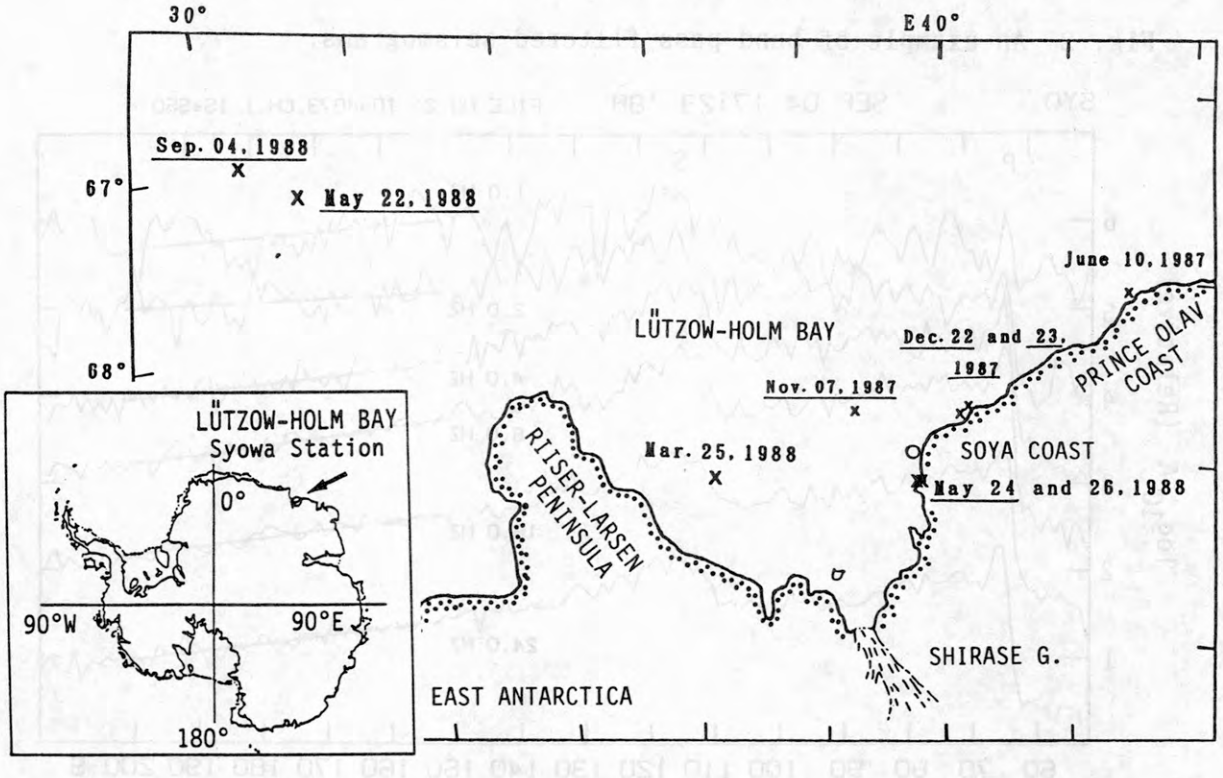

Fig. 1 Locations of local earthquakes (x). Events underlined were used for coda analysis. o: Syowa Station.

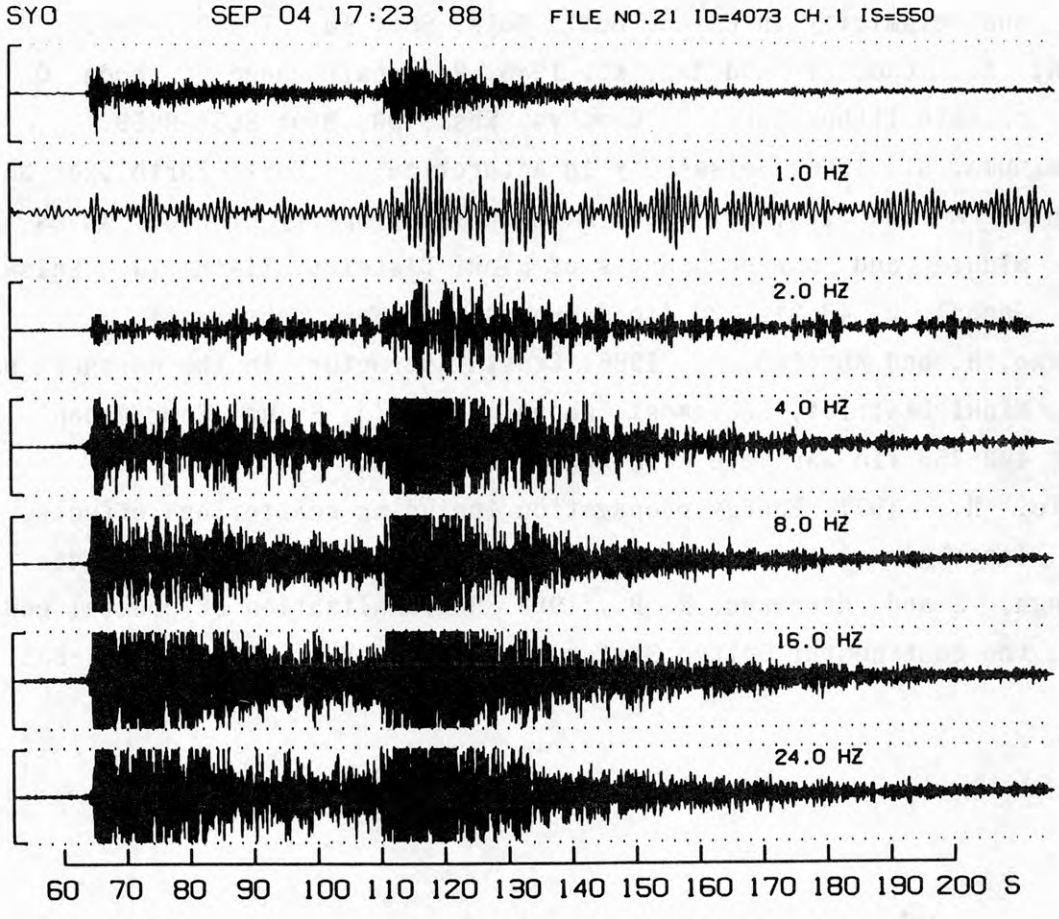

Fig. 2 An example of band pass filtered seismograms.

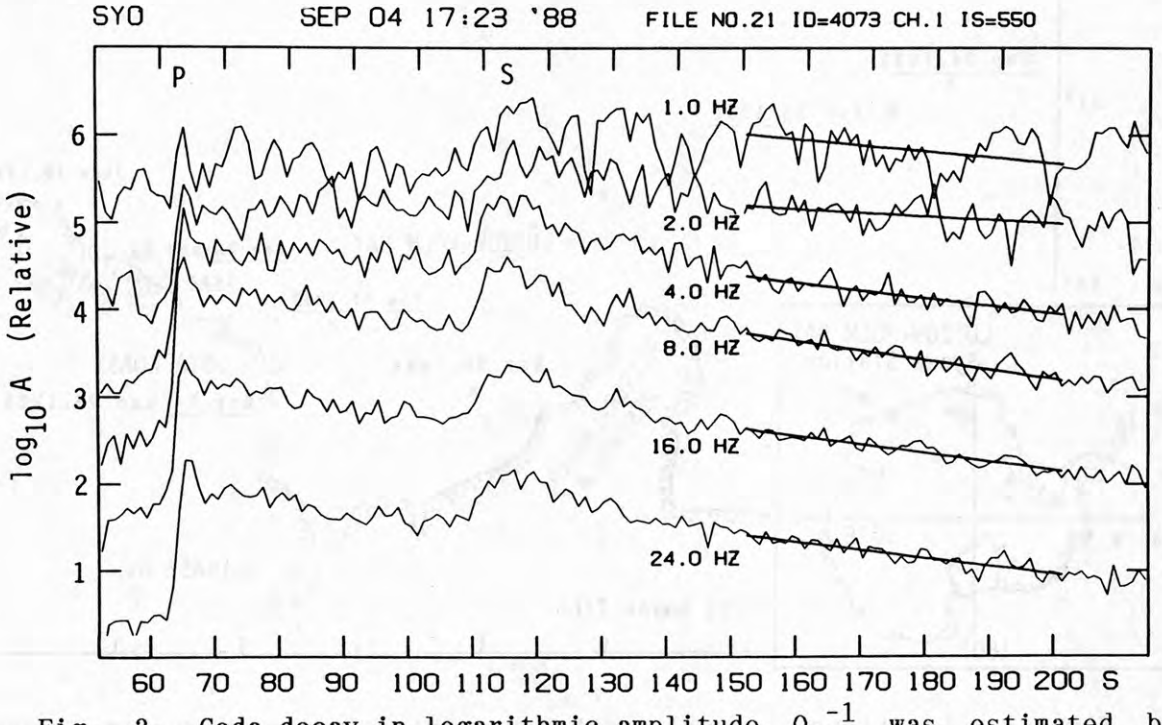

Fig. 3 Coda decay in logarithmic amplitude. Q_c^{-1} was estimated by least square method as shown on the analyzing interval, 150-200 s.

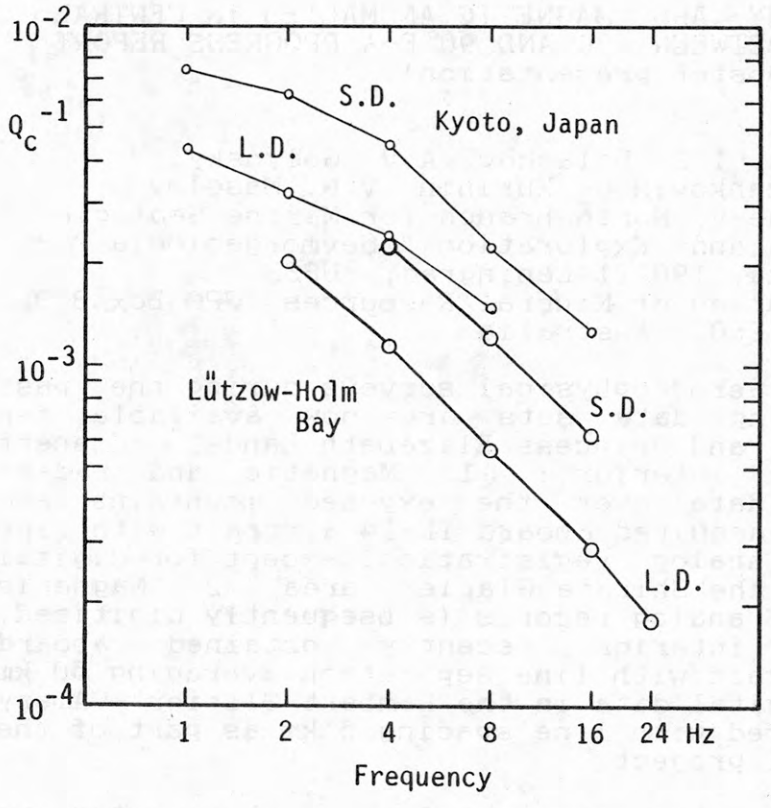

Fig.4
Q_c^{-1} in the Lützow-Holm Bay region together with Q_c^{-1} at Kyoto, Japan.
S.D.:long lapse time
L.D.:short lapse time.

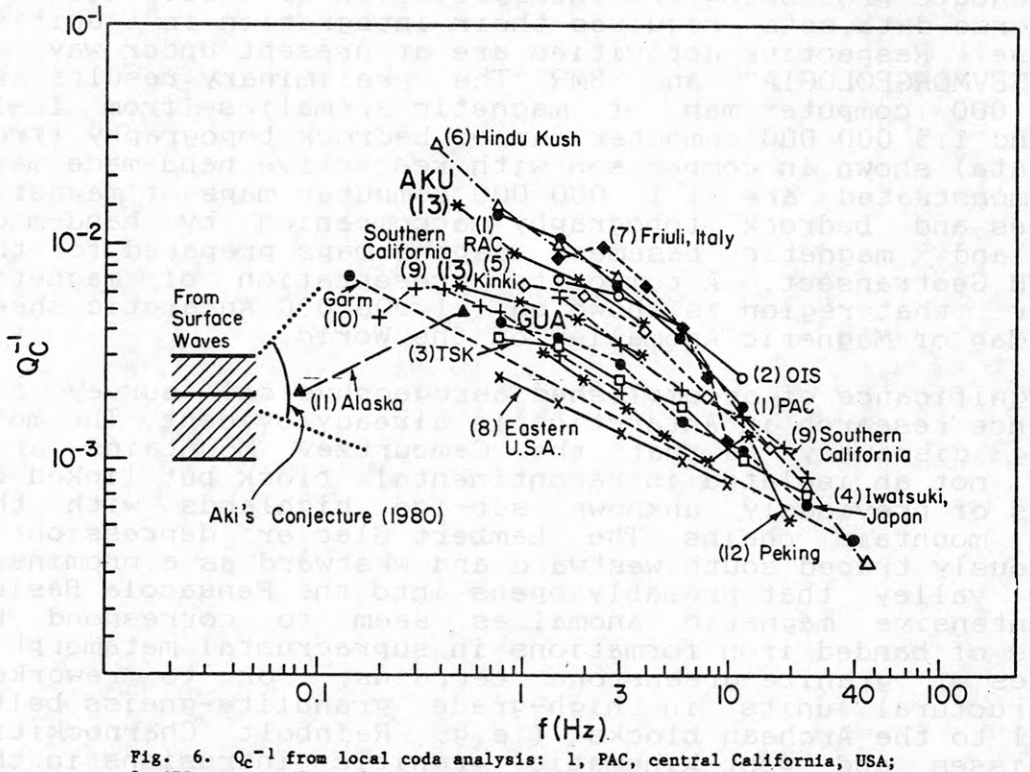

Fig. 6. Q_c^{-1} from local coda analysis: 1, PAC, central California, USA; 2, OIS, western Japan [Aki and Chouet, 1975]; 3, TSK, Kanto, Japan [Aki and Chouet, 1975]; 4, Iwatsuki, Japan [Tsujiura, 1978]; 5, Kinki, Japan [Akamatsu, 1980]; 6, Hindu Kush, Afghanistan [Roecker et al., 1982]; 7, Friuli, Italy [Rovelli, 1982]; 8, eastern United States, (New England area) [Pulli, 1983]; 9, southern California, [Phillips, 1984]; 10, Garm, central Asia, USSR [Rautian and Khalturin, 1978]; 11, Alaska, [Aki, 1982]; 12, Peking, China [R. B. Shi et al., personal communication, 1980]; 13, this study.

Fig. 5 Q_c^{-1} in various regions (after Jin et al., 1985).

BEDROCK TOPOGRAPHY AND MAGNETIC ANOMALIES IN CENTRAL EAST ANTARCTICA BETWEEN 30° AND 90° E-A PROGRESS REPORT (poster presentation)

N.D. Aleshkova, I.Z. Balashov, A.V. Golynsky, A.Yu. Kazankov, R.G. Kurinin, V.N. Masolov, V.S. Pozdeev, North Branch for Marine Geologic Research and Exploration " Sevmorgeologia ", 120 Moyka, 190121 Leningrad, USSR
P. Wellman, Bureau of Mineral Resources, GPO Box 378, Canberra 2601, Australia

As the result of aerogeophysical surveys during the past 20 years, the following data sets are now available for Enderby, MacRobertson and Princess Elizabeth Lands, adjacent shelf and Antarctic interior : 1. Magnetic and radio-echosounding (RES) data over the exposed mountains and surrounding ice cover acquired aboard IL-14 aircraft with line spacing 15-20 km and analog registration, except for digital magnetic records in the Shirase Glacier area. 2. Magnetic digital data and RES analog records (subsequently digitized) in the ice covered interior recently obtained aboard long-range IL-18 aircraft with line separation averaging 50 km. 3. Similar sets of digital data in the Lambert Glacier - Amery Ice Shelf area gathered with line spacing 5 km as part of the ANTALITH international project.

Adequate processing and interpretation of these extensive but diverse data sets requires their integration in a unified data base. Respective activities are at present under way at both "SEVMORGEOLOGIA" and BMR. The preliminary results are 1:2 500 000 computer map of magnetic anomalies (from IL-14 data) and 1:5 000 000 computer map of bedrock topography (from IL-18 data) shown in comparison with respective hand-made maps. Also demonstrated are 1:1 000 000 computer maps of magnetic anomalies and bedrock topography accompanied by hand-made gravity and magnetic basement depths maps prepared for the ANTALITH Geotransect. A composite presentation of magnetic data for that region is shown on 1:1 000 000 Antarctic sheet of the Map of Magnetic Anomalies of the World.

Significance of accomplished aerogeophysical survey for geoscience research in Antarctica is already evident. The most striking discovery is that the Gamburtzev Mountains are, in fact, not an isolated intracontinental block but linked by a series of previously unknown sub-ice highlands with the exposed mountain chains. The Lambert Glacier depression is continuously traced south-westward and westward as a prominent sub-ice valley that probably opens into the Pensacola Basin. Some intensive magnetic anomalies seem to correspond to outcrops of banded iron formations in supracrustal metamorphic complexes of granite-greenstone terrains, or to reworked infrastructural units in high-grade granulite-gneiss belts marginal to the Archean blocks (e.g. Reinbolt Charnockitic Ortogneisses and post-kinematic granitic intrusions in the Rayner mobile belt). However, reliable criteria for identifying these and other likely magnetic sources (such as post-cratonization tectonic zones or mafic igneous suites) from magnetic field fabric must be developed before the accumulated aerogeophysical evidence can be effectively used for structural extrapolations over Precambrian Shield terrains.

MAGNETIC ANOMALIES IN RELATION TO CRUSTAL STRUCTURE IN THE WEDDELL PROVINCE AND THE SOUTHERN SCOTIA ARC - A PROGRESS REPORT

N.D. Aleshkova, A.V. Golynsky, V.N. Masolov, North Branch for Marine Geologic Research and Exploration " SEVMORGEOLOGIA ", 120 Moyka, 190121 Leningrad, USSR
P.F. Barker, A.C. Johnson, M.P. Maslanyj, A.M. Smith, British Antarctic Survey, High Cross, Madingley Road, Cambridge CB3 OET, UK
J.L. LaBrecque, Lamont-Doherty Geological Observatory, Palisades, N.Y.10964, USA
M.E. Ghidella, Instituto Antartico Argentino, Cerrito 1248, 1010 Buenos Aires, Argentina

The past decade witnessed a remarkable increase in degree of international cooperation in Antarctic geoscience research. One of the most spectacular multinational efforts is an extensive aerogeophysical survey accomplished in the Weddell Sea and the southern Scotia Arc by the Soviet, British and joint US-Argentinian-Chilean expeditions [Masolov,1980; Renner at al.,1985; LaBrecque,1987; Golynsky,in press]. As the result,a vast and largely inaccessible region has been covered by aeromagnetic survey (Fig.1) partly accompanied by airborne gravity and radio-echosounding observations.This unique set of data is unparalleled elsewhere in Antarctica in both the completeness of aerogeophysical exploration and the areal extent of the survey encompassing a key structural junction between the ancient East Antarctic fragment of Gondwanaland, its Pacific rim and the South Atlantic Ocean.

In view of an extremely complex tectonic nature of the region, the whole available evidence must be incorporated into a unified data base before it can effectively be used for modelling crustal structure and evolution. At present it appears very difficult to compare individual data sets even in terms of their acquisition procedures that differ in time of the survey, type of the aircraft, measuring equipment, navigation systems, recording techniques, flying altitude, variation and reference field reduction, etc..Additional constraints may arise from the manner of presentation of results influenced by geologic outlook of the surveyors - essentially "cratonic" for the Soviet, "accretional" for the British and "oceanic" for the Lamont scientists.

Until integration and subsequent reprocessing of the data is attempted, only few observations can be made in regard of the major features of magnetic field and probable nature (fig. 2). Two prominent magnetic lineations stand out in the Antarctic Peninsula area; the WCMA associated with the Andean mafic plutons and the BSMF that broadly outlines the western limit of the Weddell Sea Sedimentary Basin [Renner et al., 1985; Garrett, 1990]. The EGML marks the boundary between the Antarctic Peninsula magmatic arc and the Haag Nunatak Precambrian block. The DMMA correspond to well known layered mafic intrusion of the Middle(?) Jurassic age exposed in the

Pensacola Mountains; synchronous early breakup structural assemblages may be responsible for the BIMA, the EWMA and the EML farther to the north-east. This array of magnetic lineations delimits the ancient East Antarctic Shield and marks a system of failed-rift basins in the eastern Weddell Sea [Hinz and Kristoffersen, 1987].

Structural interpretation of other magnetic features shown in Fig.2 is more problematic. The AEMA and the OMA are believed to follow the continent/ocean boundary formed during Gondwana breakup [Kristoffersen and Haugland, 1986; LaBrecque and Ghidella, in press]. However, great thickness of sediments northward of the presumed COB position (as far as deep water seabed beyond anomaly 34) is not entirely consistent with postulated spreading nature of underlying relatively young oceanic basement. Moreover, the Soviet magnetic data indicate that some of the fracture zones defined from the USAC data as transform faults displacing M-anomalies seem to intersect the COB-OMA zone and continue southward across the Weddell Sea shelf.

Initial results of the data base construction are now being compiled on a contour map of magnetic anomalies jointly by "SEVMORGEOLOGIA" and BAS. Further cooperative efforts aimed at incorporating this map with the USAC data will facilitate comprehensive presentation of magnetic fabric and better understanding of its relation to crustal history in the whole surveyed area.

REFERENCES:

Golynsky A.V., 1991. Magnetic anomalies in Antarctica. In: Solovjeva N.N.,ed. Map of magnetic anomalies of the World, 1:10 000 000. Sheet 26 (in press).

Hinz K., Kristoffersen Y. 1987. Antarctica recent advances in the understanding of the continental shelf. Geol. Jb., E, H. 37, 54 pp.

Kristoffersen Y., Haugland K., 1986. Geophysical evidence for the East Antarctic plate boundary in the Weddell Sea. Nature, v. 322, no. 6079, p. 538-541.

LaBrecque J.L., 1987. The USAC aerosurvey: accelerating exploration of the Antarctic. In: Lamont- Doherty Geol. Observ. Yearbook 1987, p.52-59.

LaBreque J.L., Ghidella M.E., 1991. Bathymetry, depth to magnetic basement and sediment thickness estimates from aerogeophysical data over the Westerrn Weddell (in press).

Masolov V.N., 1980. Structure of magnetic basement in sotheastern Weddell Sea Basin. In: Gaponenko G.I., ed. Geophysical Investigations in Antarctica. Leningrad, NIIGA, p. 16-28.

Renner R. G. B., Sturgeon L. J. S., Garrett S. W. , 1985. Reconnaissance gravity and aeromagnetic survey of the Antarctic Peninsula. Brit. Antarct. Surv. Sci. Rep., no. 110, 50 pp.

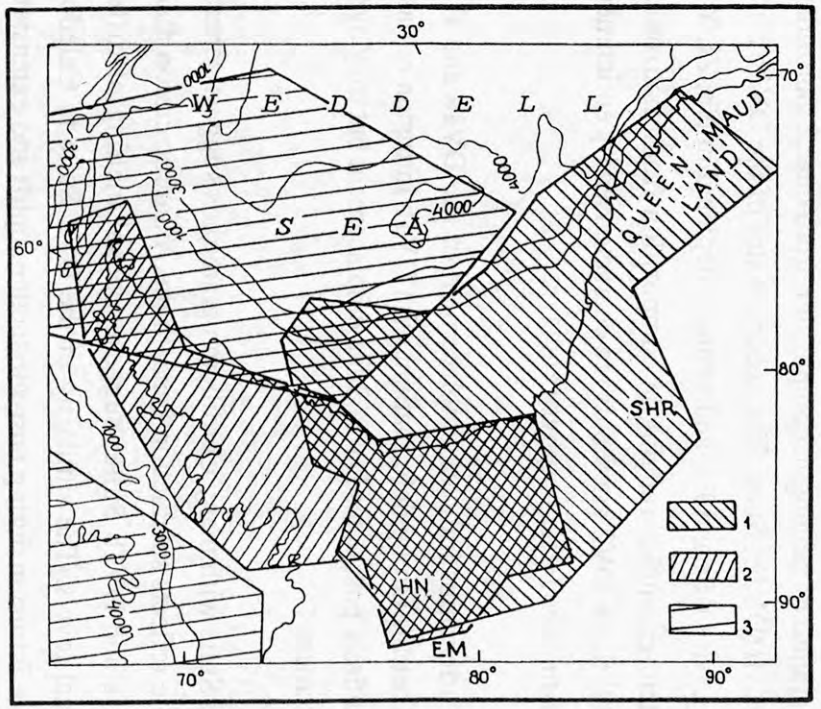

Fig. 1. LOCATION MAP OF AEROGEOPHYSICAL SURVEYS BY "SEVMORGEOLOGIA" (1), BAS (2) AND USAC PROGRAM (3).

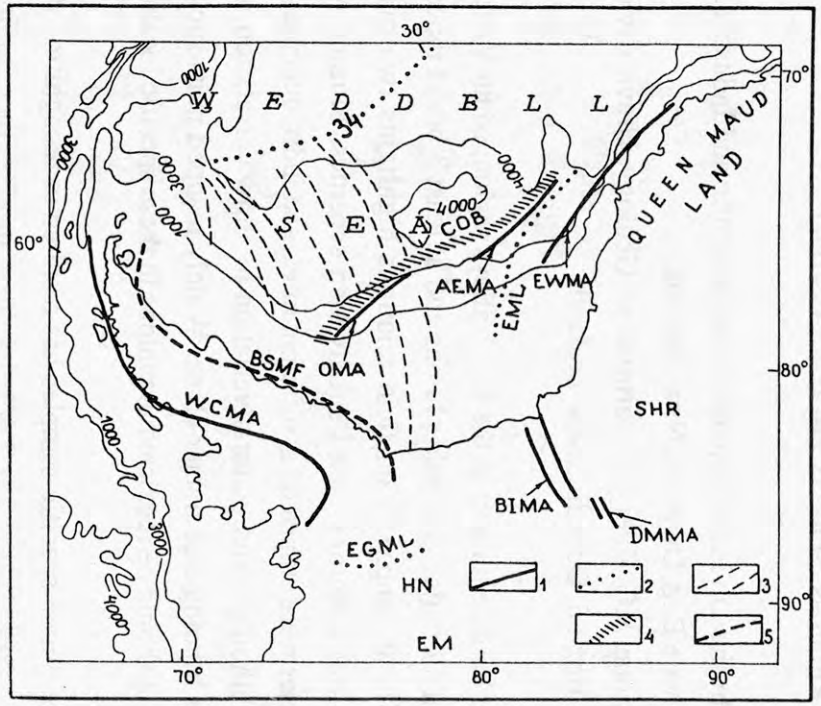

Fig. 2. MAJOR MAGNETIC FEATURES IN THE WEDDELL PROVINCE AND THE SOUTHERN SCOTIA ARC. 1 - magnetic anomalies, 2 - magnetic lows, 3 - fracture zones, 4 - continent/ocean boundary (COB), 5 - boundary of smooth magnetic field (BSMF).

WCMA - West Coast Magnetic Anomaly, OMA - Orion Magnetic Anomaly, AEMA - Andenes Escarpment Anomaly, EWMA - Explora Wedge Magnetic Anomaly, BIMA - Berkner Island Magnetic Anomalies, DMMA - Dufek Massif Magnetic Anomalies, EGML - Evans Glacier Magnetic Low; SHR - Shackleton Range, HN - Haag Nunatak, EM - Ellsworth Mountains.

SUITE - SUBDIVISION AND PETROGENESIS OF GRANITOID PLUTONS FROM THE DRY VALLEYS REGION, SOUTH VICTORIA LAND

A.H. Allibone, Geology and Geophysics Division, Department of Scientific and Industrial Research, Private Bag, Dunedin, New Zealand.
R.W. Smillie, S.C. Cox, R.D. Johnstone, S.G. Ellery, Department of Geology, University of Otago, P.O.Box 56, Dunedin, New Zealand.

Recent 1: 50.000 mapping of basement rocks in the Dry Valleys region, south Victoria Land has resulted in identification of 11 major granitoid plutons and at least 3 broad types of dike lithology. Pluton mapping with an emphasis on field relations highlights two major shortcomings associated with previous lithology-based subdivision schemes. Plutons with essentially identical lithologic character were emplaced at different times and individual plutons commonly have sufficient internal lithologic and textural variation to allow correlation with several units defined on the basis of lithologic character alone. Widely mapped units such as Larsen Granodiorite and Irizar Granite should be restricted to plutons in these specific localities.

Whole-rock geochemistry of pluton specific samples has resulted in recognition of at least 3 distinct suites of plutons. The Dry Valleys 1a, (DV1a) Suite comprises metaluminous I-type granitoids ranging from monzodiorite to granite in composition. Variably porphyritic mafic enclaves occur within all plutons of the DV1a Suite. Relatively leucocratic, metaluminous-peraluminous I-type granitoids ranging in composition from quartz monzodiorite to granite comprise the Dry Valleys 1b (DV1b) Suite. The geochemistry of the DV1b Suite is distinctive, being enriched in Al_2O_3, Na_2O, Sr and Ba, and strongly depleted in Nb, Zr, Y and LREE. Relatively young alkali-calcic granitoids ranging in composition from monzonite to granite form the Dry Valleys 2 (DV2) Suite. DV2 granitoids are characterised by enrichment in K_2O, Rb, Pb, Zr, and LREE, and distinctive felsic porphyry enclaves.

Intrusive and structural relationships indicate emplacement of the DV1a and DV1b Suites began prior to cessation of Koettlitz Group deformation, with DV1b intrusion outlasting DV1a. Intrusion of the DV2 Suite entirely post-dates DV1a Suite emplacement but may overlap with the end of DV1b Suite emplacement.

The similarity of the DV1a Suite with many Cordilleran granitoids suggest generation and emplacement of the DV1a Suite reflects subduction beneath the Antarctic craton margin. Overlapping intrusion of the DV1a and DV1b Suites suggests coeval melting of different sources, possibly at different crustal levels. The similarity of the DV2 Suite to Caledonian I-type granitoids suggests DV2 Suite intrusion during post-subduction, uplift and extension.

Seismic Stratigraphy of the Northwestern Weddell Sea Continental Shelf

John B. Anderson and Stephanie Staples Shipp
Rice University, Houston, Texas 77251

During USAP91, approximately 2,000 km of high resolution seismic reflection data were collected on the northwestern Weddell Sea continental shelf west of James Ross Island. Data collection employed 100 in^3 and 15 in^3 water guns fired independently. Heavy to moderate sea ice forced the use of a short streamer, but the data are of very good quality and well suited for high resolution sequence stratigraphic analysis. The trackline grid consists of five north-south and five east-west profiles with a line spacing of 18 to 20 km and tighter coverage in areas of interest (Fig. 1).

An extensive basin, the Palmer Basin, occupies the shelf and contains up to 3.5 km of sediment fill resting on highly tectonized basement, assumed to be Trinity Peninsula Group strata. Based on extrapolation to outcrops on adjacent Seymour Island, most of the basin fill is of Tertiary age. Sediments were sourced from the west and the north. The glacial sequence exhibits broad troughs and till tongues (Fig. 2) on the inner shelf and grades offshore into a more laminated sequence which thickens to over 500 m on the outer shelf. A major northeast-southwest oriented strike-slip fault zone extends through the center of the basin; this is the only major Tertiary tectonic feature of the basin. It does not offset the younger glacial sequence. It may be possible to estimate the timing of the initial advance of the ice sheet onto the shelf if the timing of strike-slip deformation can be constrained.

Glacial erosion of the seaward dipping sequences has resulted in exposure of virtually the entire stratigraphic section on various portions of the shelf, thus making this a key area for future shallow drilling that focuses on the study of the climatic evolution of the continent.

Figure 1. Location of seismic tracklines acquired during the USAP91 cruise in Weddell Sea.

Figure 2. Representative seismic line from the study area showing offshore dipping strata that have been eroded by glacial ice. Glacial deposits overlie the dipping strata and thicken in a seaward direction. Location of line PD91-28A is shown on Figure 1.

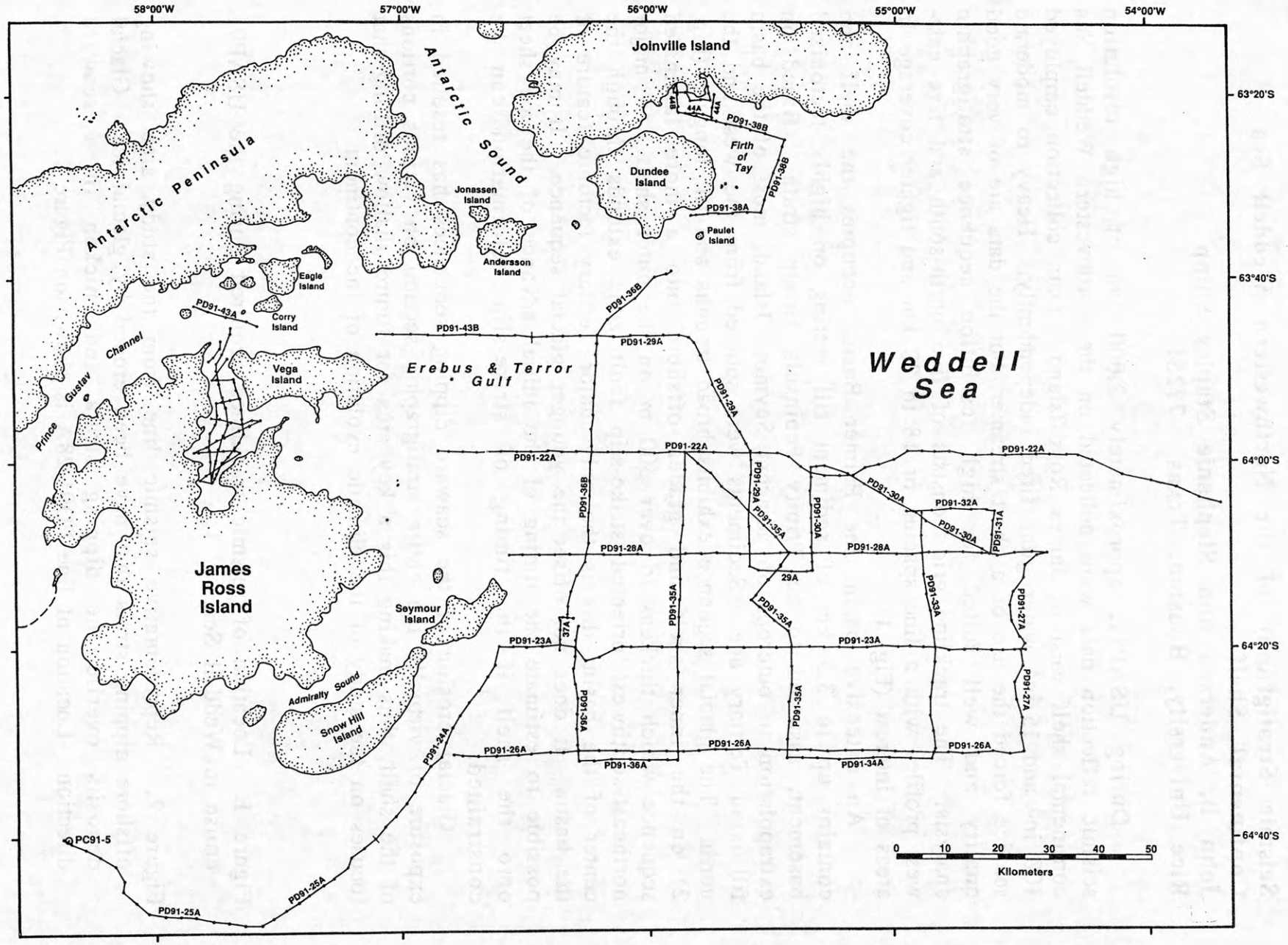
58°00'W
57°00'W
56°00'W
55°00'W
54°00'W
63°20'S
63°40'S
64°00'S
64°20'S
64°40'S
Joinville Island
Antarctic Peninsula
Antarctic Sound
Jonassen Island
Dundee Island
Firth of Tay
Paulet Island
Andersson Island
Eagle Island
Corry Island
Prince Gustav Channel
Vega Island
Erebus & Terror Gulf
Weddell Sea
James Ross Island
Seymour Island
Admiralty Sound
Snow Hill Island
PD91-43A
PD91-43B
PD91-36B
PD91-29A
PD91-22A
PD91-30A
PD91-32A
PD91-31A
PD91-28A
PD91-35A
PD91-33A
PD91-27A
PD91-23A
PD91-36A
PD91-26A
PD91-34A
PD91-24A
PD91-25A
PD91-38A
PD91-38B
PC91-5
0 10 20 30 40 50
Kilometers

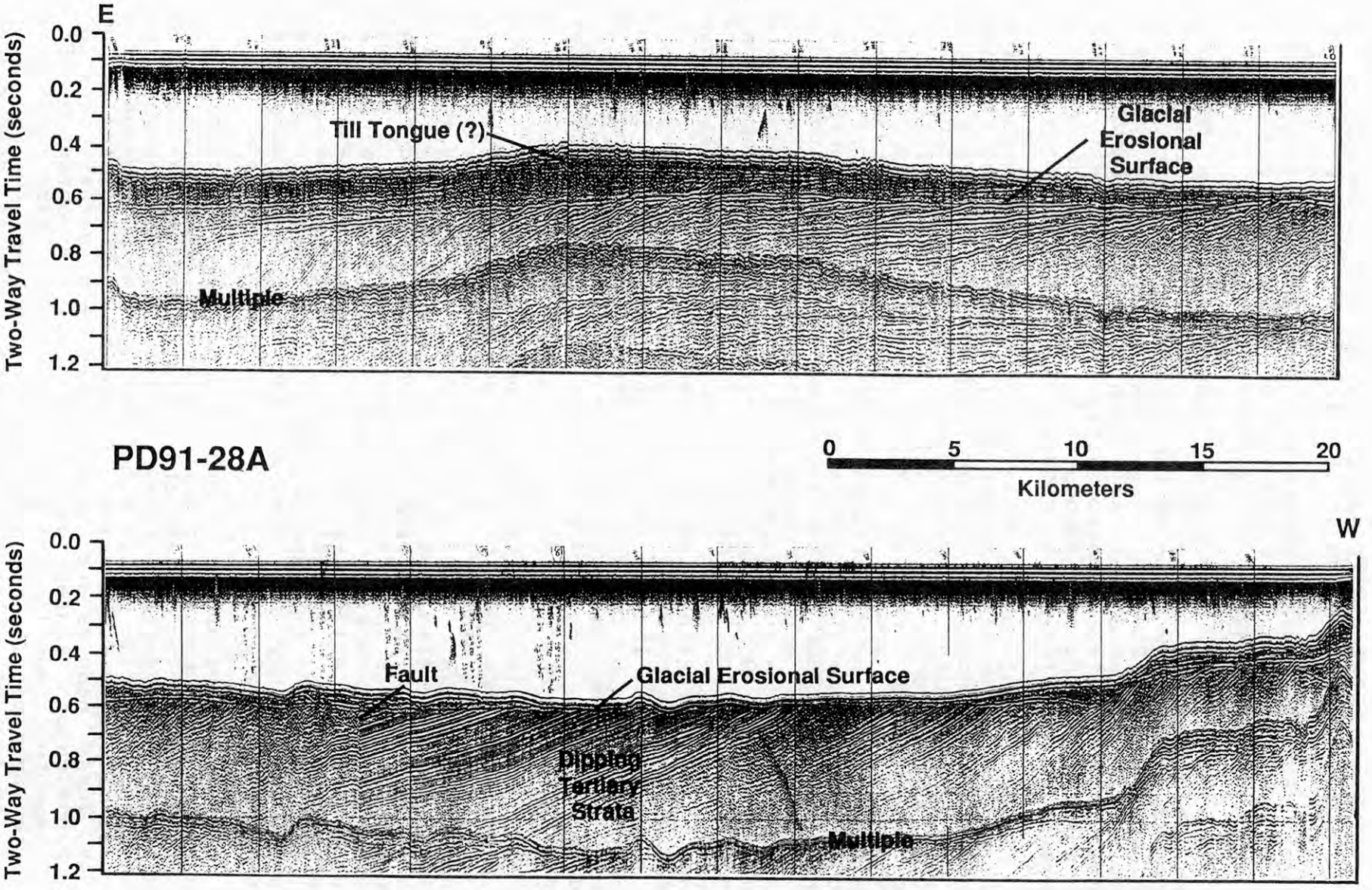
E
W
Two-Way Travel Time (seconds)
0.0
0.2
0.4
0.6
0.8
1.0
1.2
Till Tongue (?)
Glacial Erosional Surface
Multiple
PD91-28A
0
5
10
15
20
Kilometers
Fault
Glacial Erosional Surface
Dipping Tertiary Strata
Multiple

FIRST UPPER MANTLE PROBING IN THE PRINCE CHARLES MOUNTAINS, EAST ANTARCTICA.

A.V. Andronikov, North Branch of Marine Geologic Research and Exploration "Sevmorgeologia", 120, Moyka, 190121 Leningrad USSR

Examination of deep-seated nodules from the Mesozoic alkaline-ultramafic intrusions in the Beaver Lake area provided first information on the composition and structure of the upper mantle. Five main varieties of deep-seated rocks are distinguished: garnet-bearing and spinel lherzolites, garnet-free dunites, harzburgites and wehrlites. Spinel lherzolites are the most abundant. All the inclusions are to a variable degree affected by exogenetic serpentinization.

The P-T equilibrium conditions of mantle rocks were deduced from chemical composition of co-existing rock-forming minerals in the nodules. The geothermometers used were based on : thermodynamical analysis of the reactions: $Mg_2Si_2O_6$ (Opx)= $M_2Si_2O_6$ (Cpx)(Ehrenberg, 1982; Wells, 1977); the examination of constant of the reaction $Mg_2Si_2O_6$ (Opx) + $MgAl_2O_4$ (Sp) = $MgAl_2SiO_8$ (Opx) + Mg_2SiO_4 (Ol) (Sachtleben, Seck, 1981); and the ratio of Ca and Mg contents in clynopyroxene, co-existing with orthopyroxene (Boyd, Schairer, 1964). For garnet-bearing varieties of peridotites the geobarometers used were based on: Al O content in orthopyroxene (Ringwood, 1975) and the distribution of Ca and Mg between the garnet and clynopyroxene (Ukhanov et al.,1988). For garnet -free varieties of rocks we used the geobarometer based on Al / Al ratio in pyroxene (Mysen, Boettcher, 1975). The following conclusions have been made: 1. Garnet-bearing lherzolites formed at 875°-1150° C under 20-27 kbar pressure that correspond to the depths of 60-80 km. 2. Spinel lherzolites equilibrated at 825 - 1050 C and 12-19 kbar, i.e. at the 40 - 60 km depths. 3. Other inclusions (dunites, harzburgites, wehrlites) equilibrated at 905°-970° C and 16-17 kbar, i.e. under the same P-T conditions as spinel lherzolites.

If compositional variations of peridotites are believed to represent the result of their partial melting (Uhanov et al., 1988), the examined nodules may be subdivided into "undepleted" rocks ($CaO + Al_2O_3 > 5.0$ wt %; Fe /(Fe + Mg) > 0.10 %) and "depleted" peridotites ($CaO + Al_2O_3 < 3.0$ wt%, Fe/ (Fe + Mg) < 0.10) formed by incomplete eutectic melting. "Undepleted" rocks include garnet-bearing and some of spinel lherzolites, while "depleted" rocks are represented predominantly by spinel lerzolites. Wehrlites and rare spinel lherzolites are probably the residue of low partial melting. Low $CaO + Al_2O_3$ and high Fe/ (Fe + Mg) in dunites suggest that they are high-melting restites from partial peridotite melt.

The following groups of mantle material are recognized on the basis of REE content in the nodules: 1. The rocks with low fractionation of lantanoides ahd insignificant deviation from a standard chondrite. These nodules can be asigned to derivates of fertile mantle substance. 2. Rocks residual from partial melting accompanied by removal of REE of the cerium group. These nodules are characterized by a garnet type of distribution of lantanoides with overall low content of REE. 3. Fragments of mantle enriched in light REE. These rocks were affected by mantle metasomatism responsible for supply of light lantanoides. They constitute the bulk of deep-seated

inclusions in alkaline ultrabasites. 4. Dunites with low fractionation of lantanoides due to supply of light elements during cryptic metasomatism.

In two harzburgite nodules a pronounced Eu low was observed which may indicate an intrusion of basic/ultrabasic composition beneath the base of the crust.

The following conclusions can be made on the basis of complex geochemical, petrographic and mineralogical studies : 1."Depleted" garnet-free peridotites occur in the higher parts of the mantle section while at greater depths the rocks are less "depleted". 2. Strong depletion of spinel lherzolites suggests that different types of magmas could originate at respective mantle level, including sub-alkaline basic melts parental to numerous Paleozoic dykes. 3. The rocks at the uppermost mantle level are most affected by metasomatic processes. However, this metasomatism was of cryptic type and did not lead to formation of new minerals. 4. In some of spinel lherzolites a replacement of garnet by chrome pleonaste and clinopyroxene is observed. It indicates that such inclusions experienced removal from lower to higher levels. This conclusion is confirmed by the presence of thick kelyphytic rims on garnet crystals in the lherzolite nodules suggesting that the pyrope-graphitic mantle facies had been transported to higher lithospheric horizons by an ascending convection current.

A composite section of lithosphere in the Beaver Lake area is schematically presented (Figure 1).

Lack of mantle eclogite nodules is a specific feature of the studied area and may reflect the absence of eclogitic layer. This observation is consistent with an anomalous, low-density upper-mantle model derived from gravity data (Kurinin et al., 1988).

REFERENCES:

Boyd F.R., Schairer J.F., 1964. The system MgSiO3 - CaMgSi2O6. Journal of Petrologie, vol.5, N 1, p.275-309.

Ehrenberg S.N., 1982. Petrogenesis of garnet lherzolite and megacristalline nodules from Thumb, Navajo volcanic field. Journal of Petrologie, vol.23, p.507-547.

Kurinin R.G., Grinson A.S., Dun Tczun In, 1988. Riftovaya zona lednika Lamberta kak vozmozhnaya stchelochno-ultraosnovnaya provinciya v Vostochnoy Antarctide, in Russian (The rift zone of Lambert Glacier as possible alkaline-ultrabasic province in East Antarctica). Reports of Academy of Sciences of USSR, vol.299, N 4, p.944-947.

Mysen B.O., Boettcher A.L., 1975. Melting of hydrous mantle. Journal of Petrologie, vol.11, p.520-593.

Ringwood A.E., 1975. Composition and Petrology of the Earth's Mantle. McGrew-Hill, New York, 618 p.

Sachtleben Th., Seck H.A., 1981. Chemical control of Al-solubility in orthopyroxene and its implications on pyroxene geothermometry. Contrib. Miner. and Petrol., vol. 78, p.157-165.

Ukhanov A.V., Rjabchikov I.D., Harkiv A.D., 1988. Lithospheric mantiya Jakutskoy kimberlitovoy provincii, in Russian (Lithospheric mantle of Jakutskaja kimberlite province). Moscow, "Nauka", 286 p.

Wells P.R.A., 1977. Pyroxene thermometry in simple and complex systems. Contrib. Miner. and Petrol., vol.62, p.129-139.

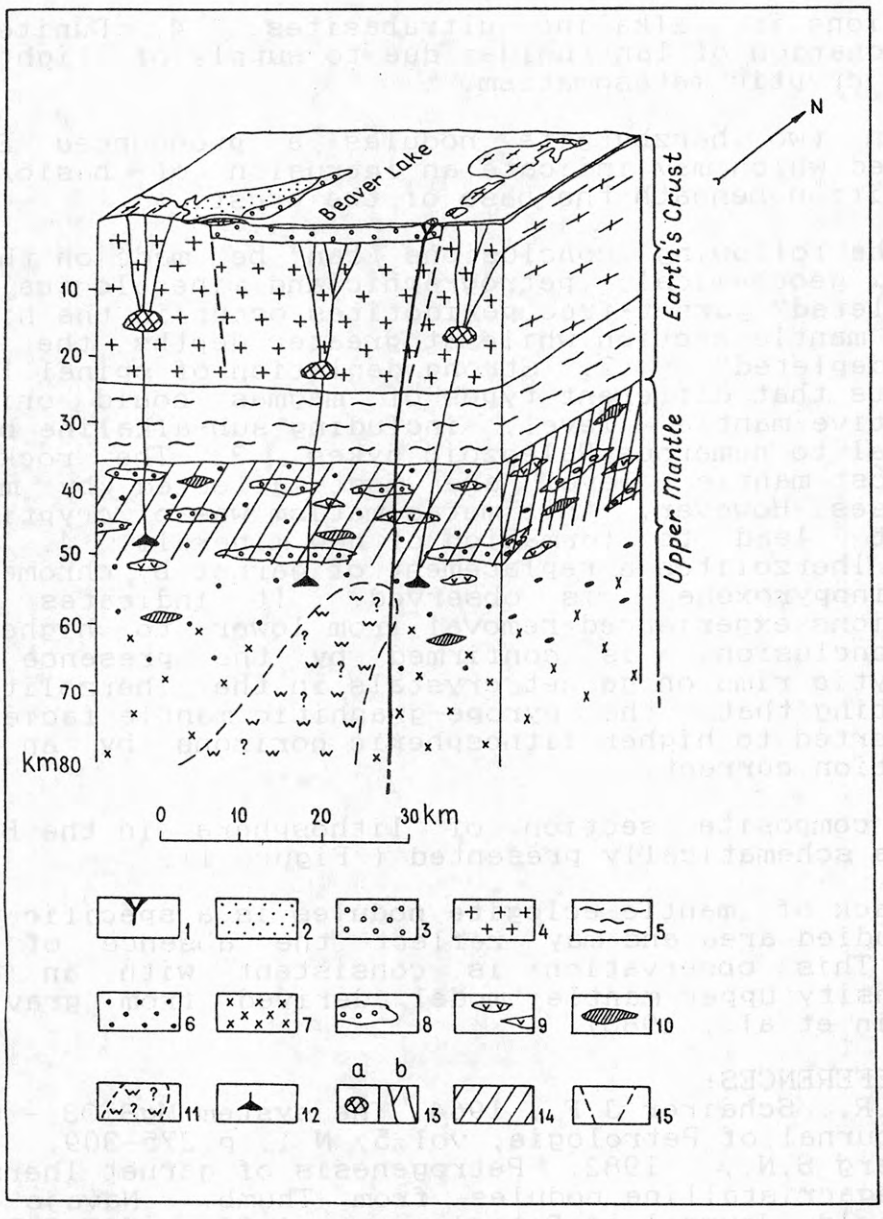

Figure 1. A composite section of lithosphere in the Beaver Lake area.

1 - feeders to alkaline-ultrabasic bodies; 2-5 - Earth's Crust rocks: 2 - moraine, 3 - Permian deposits, 4 - "granitic" layer, 5 - "basaltic" layer; 6-11 - Mantle rocks: 6 - spinel lherzolites, 7 - garnetbearing lherzolites, 8 - dunites, 9 - harzburgites, 10 - wehrlites, 11 - hypothetical intramantle intrusion; 12 - mafic magma sourses; 13 - a: intermediate magma chambers, b: mafic dykes; 14 - zone of cryptic mantle metasomatism; 15 - faults bounding the Beaver Graben.

UPLIFT MOVEMENTS IN KING GEORGE ISLAND ASSOCIATED WITH BRANSFIELD RIFT ACTIVITY

M. Araneda and O. González-Ferrán

University of Chile, Department of Geology and Geophysics

Recent geophysical and geological investigations in the South Shetland Islands confirm that the Bransfield Strait is an active rift. The gravimetric measurements made in October 1983 and October 1987 at Marsh Station and Punta Arenas, yielded a negative difference of 107 μgal (this value was obtained by means of 2 Lacoste Romberg, model G, gravimeters. The adjustment yielded a standard error of 30 μgal, a value that does not have a bearing on the observed trend. It is important to note that transportation was by air) that has been interpreted as an uplift of King George Island as part of the South Shetland Islands block, due to the rift process combined with eustatic movements. Changes in coast level were evident from observations of uplifted marine terraces. If the mentioned figure only means a variation in the free air anomany caused by altitude change there would be an average rise of about 35 cm. Considering that the opening of the Bransfield Strait and magmatism associated with rifting occurred during the last 2 Ma, and the last historical eruptions were recorded in 1967, 1969 and 1970 at Deception Caldera and 1842(?) at Penguin Volcano, as well as the permanent seismic activity, one of those earthquakes reaching Ms 7.0 (February 8, 1971), it can be estimated that tectono-volcanic activity along the Bransfield is still in process of development. In consequence, new eruptions both subaerial and submarine could be recorded in the future at any point along the rift, characterizing the region as a potential zone of high Natural Hazard.

SEDIMENTOLOGY OF THE MIERS BLUFF FORMATION, LIVINGSTON ISLAND, SOUTH SHETLAND

A. Arche, Instituto de Geología Económica, CSIC, Facultad de Geología, 28040 Madrid, Spain.
J. López-Martínez, Departamento de Geología, Facultad de Ciencias, Universidad Autónoma, 28049 Madrid, Spain.
E. Martínez de Pisón, Departamento de Geografía, Facultad de Letras, Universidad Autónoma, 28049 Madrid, Spain.

Introduction

The Miers Bluff Formation crops out in the Hurd Peninsula, Livingston Island (Fig. 1), at 62°40'S and 60°23'W, in a series of wide exposures along the SE coast of South Bay, from Bulgaria Point to the N to Miers Bluff to the S and in a series of small nunataks along the NW coast of False Bay.

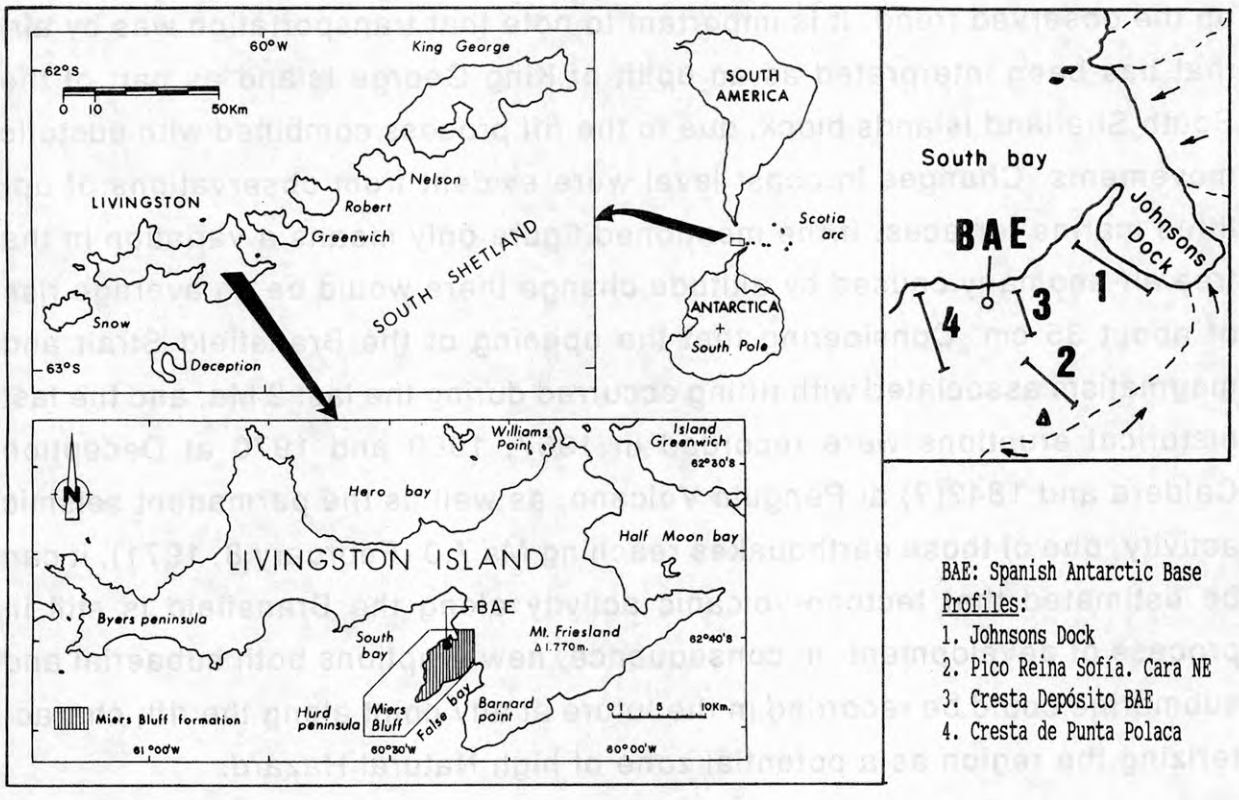

Fig. 1: Situation of Livingston Island and Hurd Peninsula and location of the studied profiles.

The type section is located at Miers Bluff, a cape at the Southern end of the Hurd Peninsula and was interpreted as a turbiditic deposit in the early surveys of the area (Adie, 1964, Hobbs, 1968, Dalziel, 1969). It was thought to be about 3,000 m thick, a figure difficult to ascertain, but certainly not excessive.

The sediments are tightly folded and affected by low-grade metamorphism. The structure of the Hurd Peninsula is unknown in detail due to lack of precise mapping and a large glaciated area, therefore its true thickness is unknown, but the interpretations

of Dalziel (1972) and Smellie et al. (1984) are correct according to our observations: most of the outcrops have inverted beds, trending NE-SW and dipping to the NW, forming the inverted flank of a kilometric syncline with subhorizontal axis and axial plan dipping 10°-30° to the W. The first-order structure is deformed by many smaller folds, intruded by tonalites, cut by at least two generations of quartz and dolerite dykes and cut by very recent tensional faults.

Its age is poorly constrained and ages from Late Carboniferous to Jurassic have been proposed by correlations with the Trinity Group of the Antarctic Peninsula (Hobbs, 1968), structural considerations (Dalziel, 1972), classification of some plant remains (Schopf, 1973) and radiometric methods (Dalziel, 1982, Pankhurst, 1983).

Sedimentology

More than 400 m of the lower part of the Formation have been surveyed in outcrops near the Spanish Antarctic Base "Juan Carlos I" and many local observations were made in the rest of the outcrops of the Hurd Peninsula (Fig. 2).

These sediments can be divided into three coarsening-thickening cycles, the last one not wholly exposed. They can be defined as medium to coarse greywackes with lithic fragments (slates, volcanic rocks, sandstones) and quartz grains, with a clay-silt-sericite matrix. There are also silty slated, laminated or massive and clay chips. Poligenic conglomerates with well-rounded quartzite, sandstone, slate and volcanic rock pebbles crop out in some nunataks to the N of False Bay. They are younger than the South Bay exposures, but the exact relationship is still unknown.

The major cycles can be subdivided into smaller ones, also of coarsening-thickening of fining-thinning character; there are frequent complete or incomplete Bouma sequences, many sole marks as flute casts, chevron marks, rills and tool marks are found, but contain no marine fossils nor wave structures, so we follow the general interpretation of these sediments as turbidites sensu Walker and Mutti (1973) and Walker (1976).

There are two main types of facies: channelized and non-channelized.

Channelized facies have a flat erosional base (banks are only excepcionally observed), lenticular geometry, up to 35 m thick and a general thinning-upwards organization. Sequences inside the channel consist of amalgamated thick to thin massive greywackes (Facies B_2, Walker and Mutti, 1973) with some mudstone horizons and rare beds with trough cross-stratification and current ripples or matrix-supported conglomerates (Facies A_3).

Within the channel facies or laterally there are fine-grained greywackes with stacked current ripples and mudstones, forming centimetric couplets repeated several times (Facies E).

These facies are interpreted as channel fill (Facies B_2 and A_3) and associated overbank deposits (Facies E) as they compare

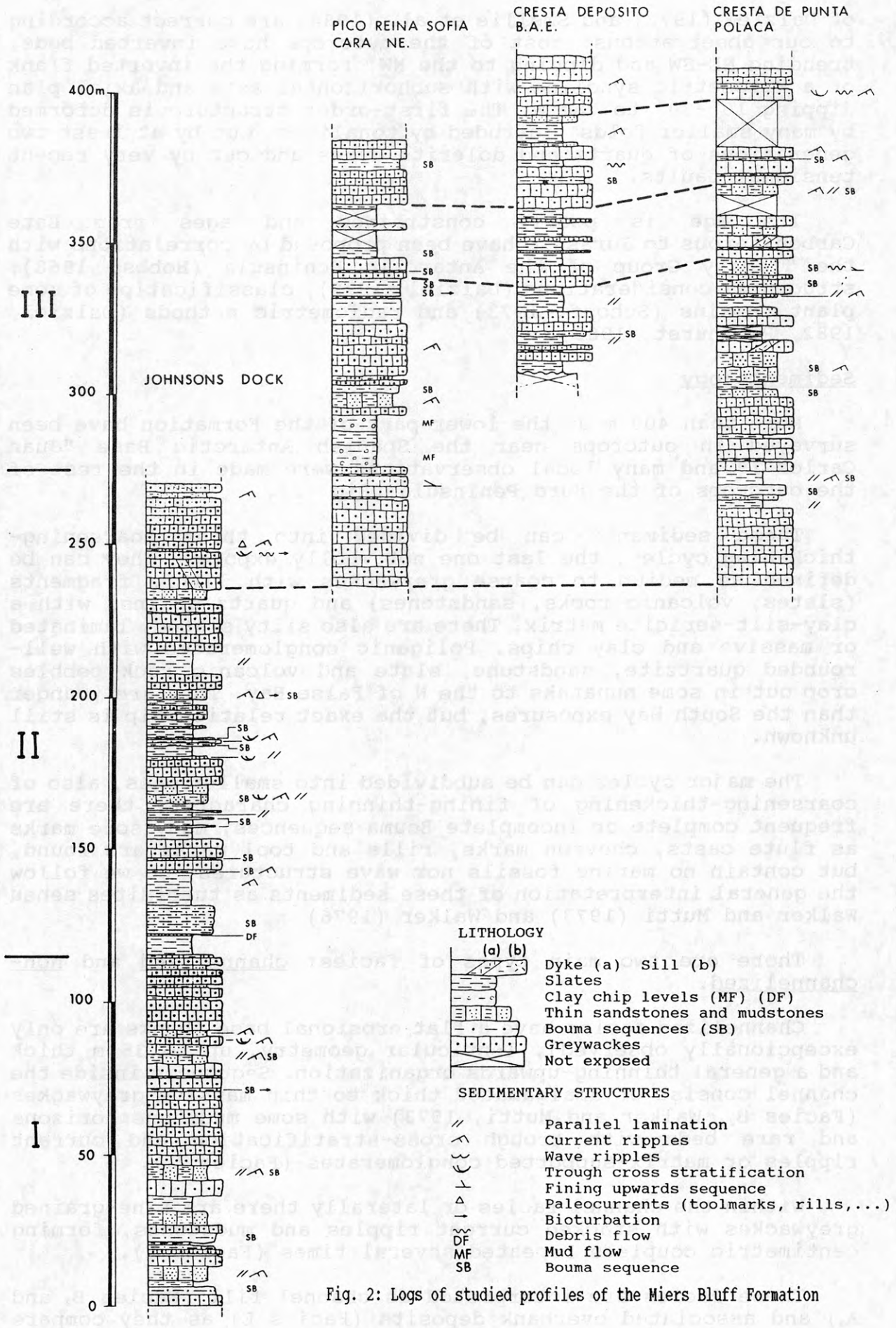

Fig. 2: Logs of studied profiles of the Miers Bluff Formation

well with classical examples described by Mutti and Ghibaudo (1972), Mutti (1977), Walker (1975), Hiscott (1981) and Pickering (1981). The general fining-thinning trend reflects the progressive infill and abandonment of the channel.

Non-channelized facies are dominated by thin- to medium greywacke beds, either massive or with complete or incomplete Bouma sequences and thin mudstone horizons (Facies C and D); there are some rare clay chips breccias and matrix-supported conglomerates. Thickening-upwards trends have been observed in some bed successions, similar to the "compensation cycles" of Mutti and Sonino (1981).

Non-channelized facies are interpreted as suprafan lobes as they compare well with some classical examples in size, geometry and internal structures and sequences (i.e., Normark, 1970, Mutti and Ghibaudo, 1972, Walker, 1978). Monomictic breccias result of the impact of turbidity currents on semi-indurated fine sediments on the floor of the lobes and the conglomerates are debris flows that escape exceptionally from the feeding channel.

A few meters of mudstones have been observed at the contact of non-channelized and channelized facies. They could correspond to the hydraulic jump zone described between channel and lobe by Mutti (1977) and observed in flume experiments by García and Parker (1989).

As the volcanic fragments in greywackes and conglomerates are fresh and of similar size and roundness than the slate or sandstone fragments, it is possible that the source area was formed by active volcanoes and low-metamorphic terranes. Paleocurrents show a N to S transport path along the margin of Gondwana.

Acknowledgements

This work was financed by the Special Action ANT-89-0821-E of the CICYT as part of the Spanish Antarctic Program.

References

ADIE, R.J. (1964) Sea level changes in the Scotia Arc and Graham land. In R.J. Adie (ed.) Antarct. Geol. SCAR Proceedings. II Geomorphology, 27-32.

DALZIEL, I.W.D. (1969) Structural studies in the Scotia Arc: Livingston Island. Antarct. Journ. of the Un. States, 4(4), 137.

DALZIEL, I.W.D. (1972) Largescale folding in the Scotia Arc. In R.J. Adie (ed.) Antarct. Geoscience, Symp. on Antartc. Geology and Geophysics. Oslo, Universitetforlaget, Series B, Number 1, 47-55.

DALZIEL, I.W.D. (1982) The Early (Pre-Middle Jurassic) History of the Scotia Arc Region: A Review and Progress Report. Antarct. Geoscience, Symp. on Antarct. Geology and Geophysics, Series B, Number 4, 137.

GARCIA, A.; PARKER, G. (1989) Flume experiments on the hydraulic jump zone. Science, 245, 393-396.

HISCOTT, R.N. (1980) Depositional framework of sandy mid-fan complexes of the Tourelle Formation, Ordovician, Quebec. A.A.P.G. Bull., 64, 1052-1077.

HOBBS, G.J. (1968) The Geology of the South Shetland Islands. IV. The Geology of Livingston Island. Scientific Reports, Br. Antarct. Surv., 47, 34.

MUTTI, E. (1977) Distinctive thin-bedded turbidite facies and depositional environments in the Eocene Hecho Group, South Central Pyrenees, Spain. Sedimentology, 24, 107-131.

MUTTI, E.; GHIBAUDO, G. (1972) Un essempio di conoide sottomarina esterna. Mem. Acad. Sci. Torino, 4, 40 p.

MUTTI, E.; SONNINO, M. (1981) Compensation cycles, a diagnostic feature of turbidite sandstone lobes. IAS 2nd European Meeting Abstracts, 120-123.

NORMARK, W.R. (1970) Growth patterns of deep-sea fans. A.A.P.G. Bull., 54, 2170-2195.

PANKHURST, R.J. (1983) Rb-Sr constraints on the ages of basement rocks of the Antarctic Peninsula. In: R.L. Oliver, P.R. James, J.B. Jago (eds.) Antarctic Earth Science (Fourth International Symposium), Cambridge Univ. Press, 367-371.

PICKERING, K.T. (1981) Two types of outer fan lobe sequence, Late Precambrian Kongsfjord Formation, Finnmark, N. Norway. J. Sed. Petrol., 51, 1277-1286.

SMELLIE, J.L.; PANKHURST, R.; THOMSON, M.; DAVIES, R. (1984) The Geology of the South Shetland Islands: VI. Stratigraphy, Geochemistry and Evolution. Scientific Reports, Br. Antarct. Surv., 87, 85.

SCHOPF, J.M. (1973) Plant material form the Miers Bluff Formation of the South Shetland Islands. Scientific Reports, Br. Antarct. Surv. Bull., 45, 45 p.

WALKER, R.G. (1975) Nested submarine fan channels in the Capistrano Formation, San Clemente, California. Geol. Soc. Am. Bull., 86, 915-924.

WALKER, R.G. (1976) Turbidite facies. Geos. Canada, 3, 25-36.

WALKER, R.G. (1978) Deep water sandstone facies and ancient submarine fans. A.A.P.G. Bull., 62, 932-966.

WALKER, R.G.; MUTTI, E. (1973) Turbidite facies and facies associations. S.E.P.M. Pacific Sect. Short Course, 4, 119-158.

METAMORPHIC EVOLUTION OF THE SØR RONDANE MOUNTAINS, EAST ANTARCTICA

M. Asami, Department of Geological Sciences, College of Liberal Arts, Okayama University, Tsushima Naka, Okayama 700, Japan
Y. Osanai, Department of Earth Sciences and Astronomy, Fukuoka University of Education, Akama, Munakata, Fukuoka 811-41, Japan
K. Shiraishi, National Institute of Polar Research, Kaga, Itabashi-ku, Tokyo 173, Japan
H. Makimoto, Geological Survey of Japan, Higashi, Tsukuba, 305, Japan

The Sør Rondane Mountains are underlain by a high-grade gneissic complex, consisting mainly of intermediate to basic rocks with subordinate pelitic to psammitic, calcareous and acid rocks, intruded by granitic and syenitic plutonic rocks. Regional metamorphism in the granulite-facies is indicated by the common occurrence of mineral assemblages such as Opx-Cpx-Grt-Hbl-Pl-Ilm±Mag, Opx-Bt-Kfs-Pl-Ilm±Grt and Sil-Grt-Bt-Kfs-Pl-Ilm in quartz-bearing rocks and Crn-Grt-Sil-Spl-Bt-Pl-Ilm-Mag in quartz-free rocks. The granulite-facies temperatures and pressures based on pyroxene, garnet and plagioclase compositions are 750-800°C and 7-8.5 Kb. Among the granulite-facies rocks, kyanite and staurolite relics in garnet have been found in some pelitic gneisses, and secondary mineral associations of amphibolite facies, including kyanite-biotite-muscovite-quartz aggregates embaying garnet, are developed in many rocks of various compositions; for the latter conditions 530-630°C and about 5.5 Kb are estimated. Moreover, high-temperature mafic minerals are altered to calcite, chlorite, epidote, muscovite and margarite,suggesting a late greenschist-facies event. Their occurrences imply a medium pressure-type, prograde and retrograde P-T-t trajectory with the peak conditions of the granulite facies.

The regional metamorphism was followed by a contact metamorphic event as suggested by the local development of granoblastic andalusite and cordierite in some pelitic rocks adjacent to the acid plutonic intrusives. Compositions of garnet, biotite and plagioclase in these metapelites give T-P values around 550°C and 3 Kb for this low-pressure metamorphism.

From a Sm-Nd whole rock age of 1000 Ma obtained on granulites by Shiraishi and Kagami (1989, Proc. NIPR Symp. Antarct. Geosci., 3, 152) and well-known 400-550 Ma ages on metamorphic and plutonic rocks throughout the Sør Rondane Mountains, it is inferred that the former regional, at least granulite-facies, metamorphism took place during a late Proterozoic crustal event and the later low-P metamorphic event during Ordovician plutono-metamorphic activity after uplift.

THE SERIS EXPERIMENT : CRUSTAL SEISMIC INVESTIGATION ACROSS THE BOUNDARY BETWEEN EAST AND WEST ANTARCTICA

Stephen Bannister[1], Uri ten Brink[2], Tim Stern[1], Bruce Beaudoin[2]

[1]*DSIR Geology and Geophysics, Wellington, New Zealand*
[2]*Department of Geophysics, Stanford University, Stanford CA 94305*

INTRODUCTION

The Transantarctic Mountains, with a total length of 3000-3500 km and elevations of up to 4500 m, are one of the major Cenozoic mountain ranges in the world. They are characterised by a lack of folding or thrust faulting, are bounded on their eastern margin by steep normal faulting, and are generally described as a gently tilted block-faulted mountain range. They are one of the most striking global examples of rift-shoulder mountains. Running parallel and just offshore along the Ross Sea sector of the Transantarctic Mountains is the Cenozoic-age Terror Rift (Cooper et al.,1987). The Ross Embayment as a whole is a vast submerged region of extended continental crust which has been dissected by several Mesozoic (?) and Cenozoic age rifts (e.g. Cooper and Davey, 1985). Thus it is generally thought (e.g. Elliott, 1975) that the Transantarctic Mountains form the boundary between the two major continental plates of East and West Antarctica.

SERIS EXPERIMENT

Over the 1990-1991 austral summer Seismic Experiment Ross Ice Shelf (SERIS) was carried out across the Transantarctic Mountain front, latitudes 82° - 83°S. This experiment involved a 134 km long seismic reflection profile together with a 96 km long coincident wide-angle reflection/refraction profile. Gravity and relative elevation (using barometric pressure) were also measured along the profile. The primary purpose was to examine the boundary between the rift system and the uplifted rift margin (represented by the Transantarctic Mountains) using modern multichannel crustal reflection/refraction techniques. The results should provide insight into the nature of the faulting across the transition, the variation in crustal thickness across the plate boundary and the presence or otherwise of the southward continuation of the Terror rift.

SERIS represents one of the first large-scale, modern multichannel seismic experiments in the remote interior of Antarctica. As such the project was designed to test different seismic acquisition techniques which will be involved in future seismic exploration of the continent.

The experiment objectives required that the seismic profile crossed the Transantarctic mountain front (using glaciers). Only one glacier along the 1500 km long Central Transantarctic Mountains, the Skelton, had been previously traversed by heavy vehicles but the orientation and location of this glacier was not suitable. After extensive inquiry and 2 reconnaissance flights two interconnected glaciers 80 km north of the Beardmore Glacier, the Robb and Lowery glaciers, were selected for the seismic profile (FIG 1). These glaciers offered moderate topographic slope and were relatively free of crevasses. This location is also nearly windless because the Markham plateau to the west blocks the flow of katabatic (gravity-driven) winds from the Polar Plateau. The total passable profile length perpendicular to the mountain front was 40-50 km using these glaciers.

The profile line passes across the north end of the 3000 m high Holland Range (Fig 1) which rises steeply at the boundary between the Ross Embayment and East Antarctica. The topography down the Robb glacier (intersecting the range) however is slight, varying by only 350 m. The western end of the profile terminated against the 4350 m high Markham plateau where geological markers indicate a 4-6 km of uplift. To the east the remaining 2/3 of the profile stretched across the 200-500 m thick floating Ross Ice Shelf (FIG 1). The experiment thus sampled two acquisition environments: a grounded glacial ice overlying crystalline basement and a floating ice layer overlying both water and sediments.

REFLECTION DATA ACQUISITION

The seismic sources for the reflection experiment were ammonium-nitrate explosive charges specially designed for low temperature. These were placed at 200 m intervals at the bottom of 17-18 m holes in the ice. A limited amount of less-expensive and safer watergel explosive was also used at times, but this has problems detonating in temperatures lower than -25°C and therefore cannot be left in 17m deep holes for long periods.

85% of the reflection profile was shot with 7.5 kg charges and the remainder with 5 kg. Single shots of 10 kg were also tested while the data also be compared to that from the wide-angle reflection shots involving 57.5 and 100 kg. Shot depths of 3, 6, 9, and 13 m were tested. Shot holes were drilled in the ice by a hose ejecting hot (80°C) water at high pressure. An improved nozzle design saved physical labour, but the drilling rate was slow, 3-5 holes an hour.

Two receiving systems were compared during the experiment. The first involved a conventional seismic cable with 48 groups of 14-Hz geophone strings, 6 geophones per string, at 50 m interval. This system was used over the first 51 km, traversing down the glaciers. The remainder of the profile (83 km, over the ice shelf) was recorded using a 1.5 km-long 60-channel experimental snow streamer which belongs to Norsk-Hydro (Norway). Two shots, 1.6 km apart, were shot into each streamer location, resulting in an effective receiving array of 120 groups of 14-Hz geophone strings, 6 geophones per string, with a 25 m group interval. The streamer was towed by a Hagglund which also housed the DFS-V recording unit (recording to 15 seconds with 2 ms sampling rate).

Preliminary analysis of the data indicates that records from the two systems have similar noise levels despite the fact that the geophones connected to the conventional cable were buried while the geophones dragged by the streamer lay on the surface. However selected streamer-geophone groups became considerably noisier above wind speeds of 5-6 knots (2.5-3 m/s). In all other respects the streamer proved superior to a conventional cable - a pair of shots was fired every 6-7 minutes, more than double the acquisition speed of a conventional cable. An example of a record from the snow streamer is shown in Fig 2 where coherent energy can be seen to at least 5 seconds.

WIDE-ANGLE REFLECTION/REFRACTION ACQUISITION

The wide-angle reflection/refraction experiment consisted of 4 deployments of a 23-25 km long receiving array, with a group interval of 100-300 m. 3-5 shots were detonated in each deployment. Two of the deployments were situated mostly over the glaciers of the Transantarctic Mountains while the other two were on the Ross Ice Shelf. Reftek recording instruments, cables and phones (8 Hz vertical geophones, 6 phones per string), all belonging to IRIS, comprised most of the length of the receiving array in each deployment. All or almost all of the available cables and geophones and the corresponding number of recording instruments were utilized in each of the deployments. The length of the receiver array in each deployment was further extended by the use of the reflection cable (7.2 km at 150 m interval) or the snow-streamer (1.5 km at 25 m interval) connected to the DFS-V recorder.

The refraction shots involved shots at each end of the receiving array (for each deployment) and additional offset shots into the arrays, with a maximum offset of 90 km on the ice shelf and 51 km on the glacier. Shot sizes ranged (with offset) between 100-400 kg and the charges were placed at the bottom of 20 m holes. Data was recorded on the 2.5 MByte internal RAM of each Reftek and was dumped to a portable SCSI disk in the field immediately following shooting. Continuous reception of both GPS and Omega time signals allowed accurate absolute time determination and the calibration of internal clocks.

Analysis of the multichannel reflection and refraction data is currently underway at both the DSIR, New Zealand and Stanford University.

REFERENCES

Cooper, A.K. & Davey, F.J. (1985). Episodic rifting of phanerozoic rocks in the Victoria Land basin, western Ross Sea, Antarctica. Science, 229: 1085-1087.

Cooper, A.K., Davey, F.J. & Behrendt, J.C. (1987). Seismic stratigraphy and structure of the Victoria Land basin, western Ross Sea, Antarctica. In: The Antarctic continental margin: geology and geophysics of the western Ross Sea, Cooper,A.K. & Davey,F.J. (eds.). Circum-Pacific Council for Energy and Mineral Resources, Earth Science Ser. Vol. 5B: 7-76.

Elliott,D.H. (1975). Tectonics of Antarctica : A review, American Journal of Science, 275-A: 45-106.

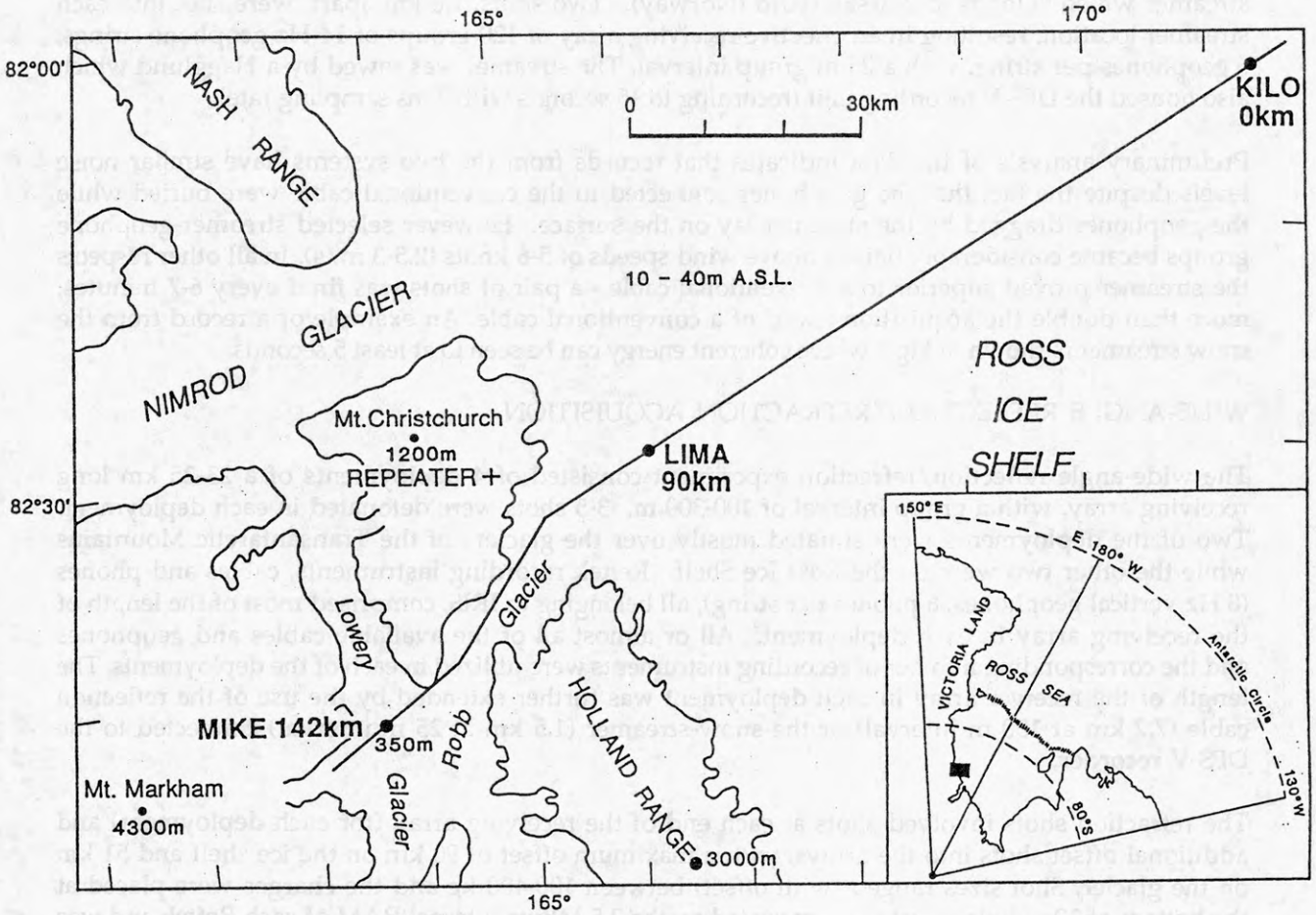

Figure 1. Location of the SERIS profile, across the eastern edge of the Transantarctic mountains and on the Ross Ice Shelf. Three logistical camps, KILO, LIMA and MIKE are marked.

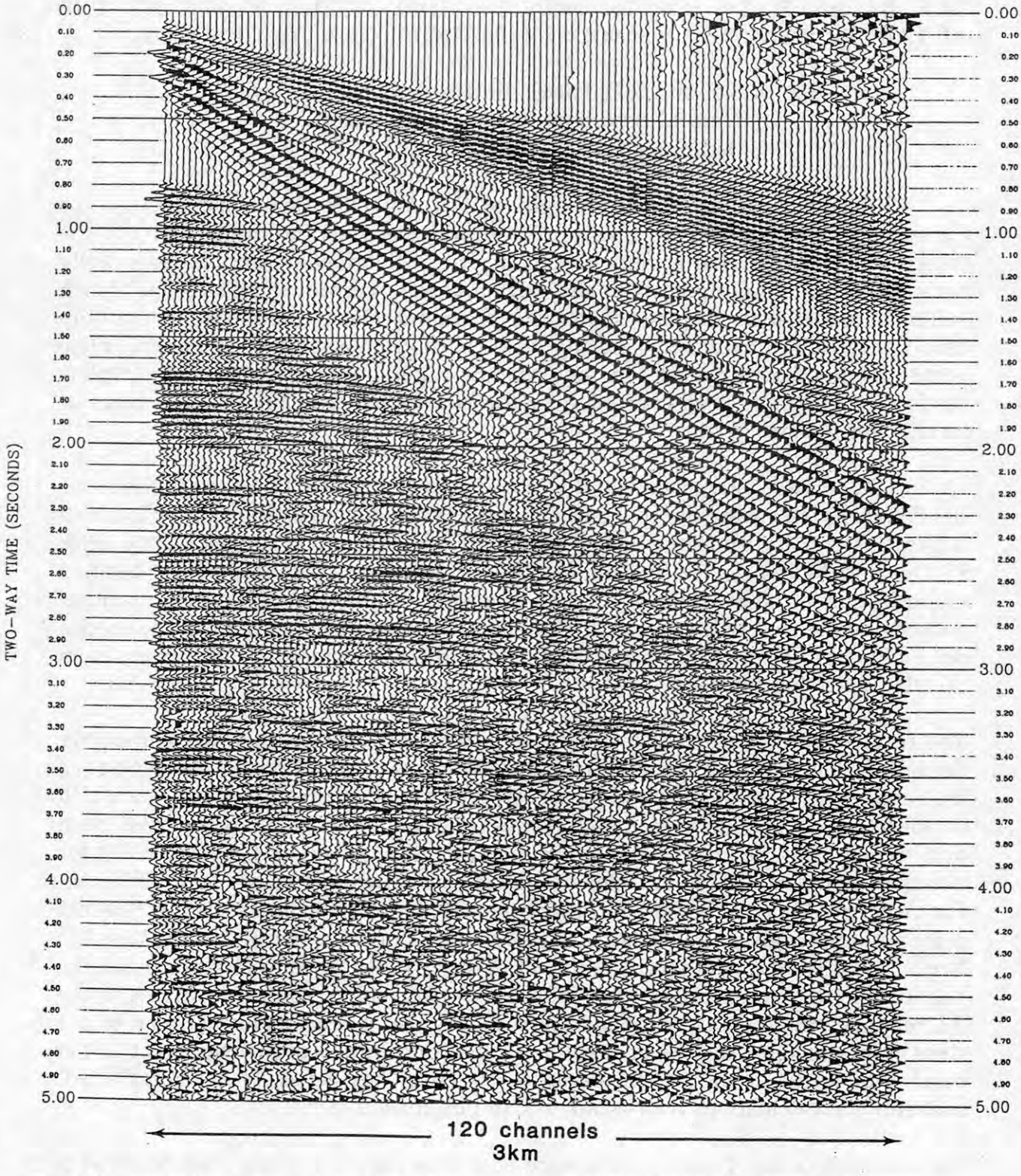

Fig. 2 Example of a data recorded on Norsk-Hydro streamer linked to a DFS-V recording system. This is an effective 120 channel shot gather , 25 m geophone group interval and with a 3km maximum offset. Shot size was 7.5 kg shot at the bottom of a 18 m deep hole in the Ross Ice Shelf. Only 5 seconds of data are shown here although 15 seconds were recorded. Data are 10-40 Hz band-passed filtered.

THE BALANCE OF FORCES ON THE SUBDUCTING PLATE AT THE ANTARCTIC PENINSULA MARGIN THROUGH THE LATE CENOZOIC

P.F. Barker and R.D. Larter, British Antarctic Survey,
(Natural Environment Research Council),
Madingley Road, Cambridge CB3 0ET, U.K.

Subduction at the Pacific margin of the Antarctic Peninsula through the Cenozoic was terminated by a series of collisions between the ridge crest and the trench (Barker, 1982; Larter and Barker, in press). Subduction stopped essentially because both the trailing flank of the ridge and the over-riding plate at the trench belonged to the Antarctic plate, so that the remaining relative motion was identically zero. For most of the Cenozoic, during these collisions, the subducting Phoenix plate was surrounded on three sides by the Antarctic plate, so that Antarctic-Phoenix plate motion has probably been controlled by the local rather than the global balance of forces over the last 35 Ma.

Under these circumstances, it is possible to examine the balance of forces on the Phoenix plate, using the conventional models of ridge push and slab pull, which depend essentially upon the age of ocean floor at the trench (eg McKenzie 1969; Richter and McKenzie, 1978). This has been determined by means of the detailed identification of ocean floor age on an extensive set of marine magnetic profiles collected to the west of the Antarctic Peninsula. The same data set permits the precise determination of spreading rates, which may then be compared with changes in calculated driving forces.

The results are of great interest. Driving forces were smaller than are commonly thought necessary to sustain subduction, a consequence of the young average age of the subducting plate. In addition, however, this implies that resistive forces are also smaller than is generally assumed (since resistive forces have in the past been determined from the need to balance driving forces). England and Wortel (1980), for example, calculate total forces (per unit length of trench) of the order of 10^{13} Nm^{-1}. For Antarctic-Phoenix interaction, the total effective driving force on the Phoenix plate per unit length of trench is calculated to have ranged between 2.6 and 3.6 x 10^{12} Nm^{-1}. This is in line with recent estimates of shear stress beneath the trench, for the subduction of young plates, by Van den Beukel (1990), but the driving force discrepancy remains to be explained. We believe that extensional disruption of old slabs at intermediate depths severely limits the contribution of the entire slab to the balance of forces at the trench. Because this effect has generally been neglected, conventional calculations over-estimate slab pull for old slabs.

The variation of this Phoenix plate force with time shows a strong correlation with observed spreading rates, which would suggest that resistive forces were largely velocity-dependent. This dependence runs counter to conventional wisdom, since the only resistive force generally taken to be velocity-dependent is viscous drag, which previous calculations (eg Forsyth and Uyeda, 1975) have shown to be small.

An explanation for this apparent dilemma may lie in the uniquely self-contained circumstances of Antarctic-Phoenix plate interaction, in which spreading and subduction are so closely coupled. A change in spreading rate, for whatever reason, causes immediate changes in conditions within the subduction zone. The upward migration of fluids, affecting both crustal buoyancy and the depth of the brittle-ductile transition, may create the enhanced velocity-dependence of resistive forces in the region of the Benioff Zone in this particular case. It may also reduce their magnitude (in the general case) below that derived from calculations that neglect convective heat transfer by these means.

REFERENCES

BARKER, P.F., 1982. The Cenozoic subduction history of the Pacific margin of the Antarctic Peninsula: ridge crest-trench interactions. J. geol. Soc. 139, 787-802.

ENGLAND, P. & WORTEL, R., 1980. Some consequences of the subduction of young slabs. Earth Planet. Sci. Lett. 47, 403-415.

FORSYTH, D. & UYEDA, S., 1975. On the relative importance of the driving forces of plate motion. Geophys. J. R. astr. Soc. 43, 163-200.

LARTER, R.D. & BARKER, P.F., in press. Neogene interaction of tectonic and glacial processes at the Pacific margin of the Antarctic Peninsula. In: MacDONALD, D.I.M. (ed.). Sedimentation, Tectonics and Eustasy. Special Publication No. 12 of the International Association of Sedimentologists. Blackwell, Oxford.

McKENZIE, D.P., 1969. Speculations on the consequences and causes of plate motions. Geophys. J. R. astr. Soc. 18, 1-32.

RICHTER, F. & McKENZIE, D., 1978. Simple plate models of mantle convection. J. Geophys. 44, 441-471.

VAN DEN BEUKEL, J., 1990. Breakup of young oceanic lithosphere in the upper part of a subduction zone: implications for the emplacement of ophiolites. Tectonics 9, 825-844.

HOLOCENE RAISED BEACHES AND ENVIRONMENTAL CHANGES AT TERRA NOVA BAY (VICTORIA LAND, ANTARCTICA)

C. Baroni, Museum of Natural Sciences,
via Ozanam 4, 25128 Brescia, Italy.
G. Orombelli Department of Earth Sciences, University of Milan,
via Mangiagalli 34, 20133 Milano, Italy.

During the Last Glacial Maximum (Late Wisconsin) a marine-based piedmont glacier extended along the coast of Terra Nova Bay. It was originated by the thickening of ice shelves and ice tongues and it merged into the ice sheet developed after the grounding and the northern expansion of the Ross Ice Shelf. In the coastal area, the glacial deposits related to the L.G.M. (Terra Nova drift) occur up to the maximum altitude of about 400 m above the present sea level. A.M.S. and conventional ^{14}C dates bracket the age of these deposits between about 26,000 and 7500 yr B.P. when deglaciation was entirely accomplished.

The deglaciation occurred in two main phases. During the first one the marine-based ice sheet was replaced by a great ice shelf. In the second phase this ice shelf retreated toward south while smaller ice shelves developed in the main inlets of the Victoria Land.

Abandoned penguin nesting sites as old as 6500-7000 years BP testify that environmental conditions similar to the present ones, in terms of favorable nesting areas and open sea conditions, characterized Terra Nova Bay at that time. During the last 6000 yr BP the continuous presence of penguin rookeries is testified by several ^{14}C dates from abandoned nests.

The deglaciation was followed by an isostatic uplift of at least 30 m in the coastal belt. In fact, Holocene raised beaches are present in several localities of the area, where the marine limit, at about 30 m a.s.l., is marked by a sharp boundary between the marine deposits and the Terra Nova drift. Several ^{14}C dates ranging from the present to 7500 yr BP have been obtained from shells collected in raised marine sediments. Organic horizons of ornithogenic soils from abandoned penguin nesting sites resting on the raised beaches supplied many other ^{14}C dates ranging from the present to about 7000 yr BP. The age of the highest and oldest beaches of the area has been estimated to be comprised between 7000 and 8000 yr BP.

The study and dating of the Holocene raised beaches allowed the first reconstruction of a relative sea-level curve for the central part of the Victoria Land. The rate of emergence ranged from about 10 mm/yr following deglaciation and 2 mm/yr in the last three millennia.

Holocene fluctuations of glaciers and ice shelves have been recognized. Groups of Holocene ice-cored moraines, differentiated on the basis of weathering degree, colour of staining, lichen cover, development of deflation pavement and patterned ground, document small fluctuations of the extent of outlet glaciers. The Nansen and Hells Gate ice shelves retreated farther inland of their present positions and then readvanced after 5000 yr BP sealing the highest Holocene raised beaches of Inexpressible Island. The Nansen ice shelf expanded toward the south more than 5 km along the western side of Inexpressible

Island. The same is testified by the Hells Gate ice shelf which advanced more than 2 km.

At the termini of small local glaciers minor neoglacial advances have been recognized. The Strandline Glacier (Tethys Bay) advanced onto raised beaches 13 m high after about 6000 yr BP.

At the foot of the Mt Melbourne volcano, the local glacier of Edmonson Point advanced more than 130 m later than about 600 yr BP, during the Little Ice Age. A complex of ice-cored moreines testifies oldest Holocene variations of the same glacier.

In this Century the small local glaciers seem to be in slight retreat. The same is true for the small Hells Gate ice shelf that retreated several hundred metres since 1912, when it was first surveyed by the Scott Northern Party. On the contrary, the Nansen ice shelf increased about 56 km^2 between 1972 and 1988.

EARLY PERMIAN GLACIATION IN ANTARCTICA - EVIDENCE FROM ALLAN HILLS (EXTENDED ABSTRACT)

P.J. Barrett, Antarctic Research Centre, Victoria University of Wellington, P.O. Box 600, Wellington, New Zealand.
N.D. Smith, Department of Geological Sciences, University of Illinois, Chicago, IL 60680, United States of America.
K.J. Woolfe, Antarctic Research Centre, Victoria University of Wellington, P.O. Box 600, Wellington, New Zealand.

The Gondwana sequence in Antarctica begins with late Carboniferous glacial beds (Metschel Tillite and equivalents), followed by early Permian alluvial strata (Weller Coal Measures and equivalents). In the past the coal measures have been considered the product of cool climate but ice-free terrestrial deposition (Barrett 1981). However, early Permian Gondwana sequences on several other continents include diamictites and dropstones, considered to have been deposited directly or indirectly from glacial ice (Veevers 1987). Paleomagnetic data show the pole to have crossed Antarctica from early Carboniferous to early Permian times (Fig. 1), consistent with the broader Gondwana climate history.

New field evidence from strata in Allan Hills, Antarctica, indicates quite plainly that there was glacial ice in the region in early Permian times, as well as massive flood events typical of glacio-fluvial activity. The evidence comes from Member C of the Weller Coal Measures, a 70-m-thick interval of sandstone, shale and coal about 200 m stratigraphically above the top of the Metschel Tillite. Member C is considered late early Permian in age (~265 Ma) based on palynomorphs assigned to the *Protohaploxypinus* zone and correlated with Stage 4 of the Permian of Eastern Australia (Kyle and Schopf 1982).

The most striking piece of evidence is a boulder marked by fine striae and embedded in shale about 5 m above the base of Member C (Fig. 2). We think the striae formed as the boulder was carried in the basal debris layer of a wet-based glacier prior to its transport by a floating ice block to its muddy depositional site in the early Permian. The striae could not have formed from over-riding ice during the present erosional cycle because striations can be seen to emerge from the buried part of the boulder. Furthermore, striae on the exposed surface are oriented in many directions, suggesting that they formed as the boulder turned with respect to the flow of the surrounding ice. Glacial striae are easily destroyed by abrasion in rivers, and their fine preservation here indicates protection and transport by floating ice.

Smaller boulders (less than 30 cm across), cobbles and pebbles are quite common individually and as lenses in the basal sheet sandstone of Member C, and could well represent fluvially reworked glacial debris. The overlying mudstone also has pebbles and cobbles both singly and in clusters, and are probably ice-rafted.

Member C has been described in terms of fluvial fining-upwards cycles (Ballance 1964), though the style of deposition might be better characterized as one of slow coal accumulation interrupted by brief periods in which fluvial sand was deposited quickly in sheets a few metres thick and of the order of a kilometre across (Woolfe et al. this volume). Most of the sand sheets were deposited from shallow low sinuosity streams flowing to the west, though three of the sheets are thought to represent a condensed record of a meandering system that

flowed in a more northerly direction. The sand sheets contain a variety of sedimentary features indicating high flow intensities and rapid sedimentation, such as shale fragments up to 1 m long, and climbing ripple lamination. Although these are not evidence of glaciofluvial sedimentation, they are consistent with it.

Lithologic features that suggest that sedimentation in Member C was controlled by glacial melting can be found in an alternating mud and fine sand facies that commonly followed the sand sheet deposition. The facies commonly has depositional dips of as much as 15 degrees and appears to have been deposited by lateral accretion in low sinuosity channels several metres deep and several tens of metres across. The facies comprises regular alternations of siltstone and fine sand with ripple lamination consistently indicating flow along the strike of the lateral accretion surfaces. Two features in particular support the view that sedimentation was controlled by glacial melting;

- the regular alternations of sand and mud on a decimetre scale (Fig. 3). This is unusual in fine-grained alluvial sediments, but could be a response to the regular variation in stream flow from glacial melting.

- the dominance of silt in the fine-grained sediment.

These data represent the first clear evidence of glaciers in Antarctica in early Permian times, and though they offer little help in defining their extent, it does provide, in association with evidence from other parts of Gondwana, a more consistent view of Permian Gondwana glaciation.

REFERENCES

BALLANCE, P.F. 1977. The Beacon Supergroup in the Allan Hills, central Victoria Land, Antarctica. New Zealand Journal of Geology & Geophysics 20: 1003-16.

BARRETT, P.J. 1991. The Devonian to Triassic Beacon Supergroup of the Transantarctic Mountains and correlatives in other parts of Antarctica. In Tingey R.J. (ed.), Geology of Antarctica, Oxford University Press, Oxford.

KYLE, R.A., SCHOPF, J.M. 1982. Permian and Triassic stratigraphy of the Victoria Group, Transantarctic Mountains. In Craddock, C. (ed.), Antarctic Geoscience, University of Wisconsin Press, Madison: 649-659.

TRUSWELL, E.M. 1991. Antarctica: A history of terrestrial vegetation. In TINGEY R.J. (editor), Geology of Antarctica, Oxford University Press, Oxford.

VEEVERS, J.J. and POWELL, C.McA. 1987. Late Paleozoic glacial episodes in Gondwanaland reflected in transgressive-regressive depositional sequences in Euramerica. Geological Society of America Bulletin 98: 475-87.

WOOLFE, K.J., ARNOT, M.J.,BARRETT, P.J. & FRANCIS, J.E. (this volume). Contrasting fluvial styles in the Weller Coal Measures at Allan Hills.

FIGURES

Figure 1. Antarctica and adjacent continents reconstructed for the early Permian using ATLAS Version 2.0 (Cambridge Paleomap Services Ltd.), showing the location of Allan Hills. The path of the magnetic pole (A.G. Smith, personal communication, 1990) and the 60° line of latitude at 265 Ma are also shown.

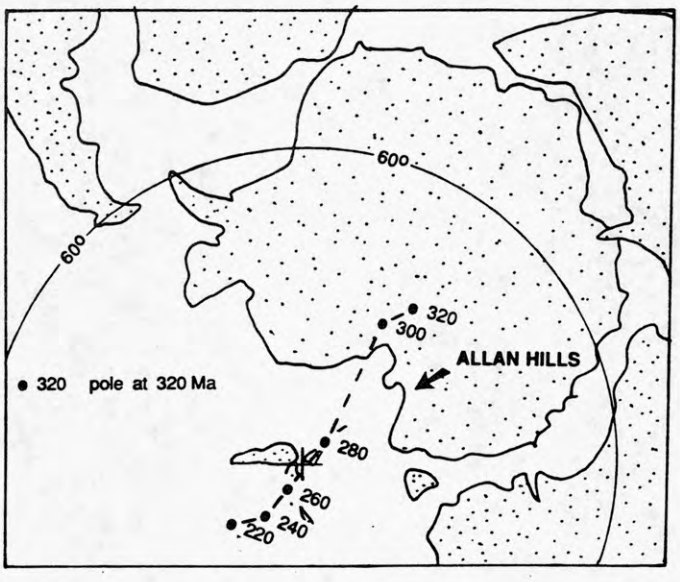

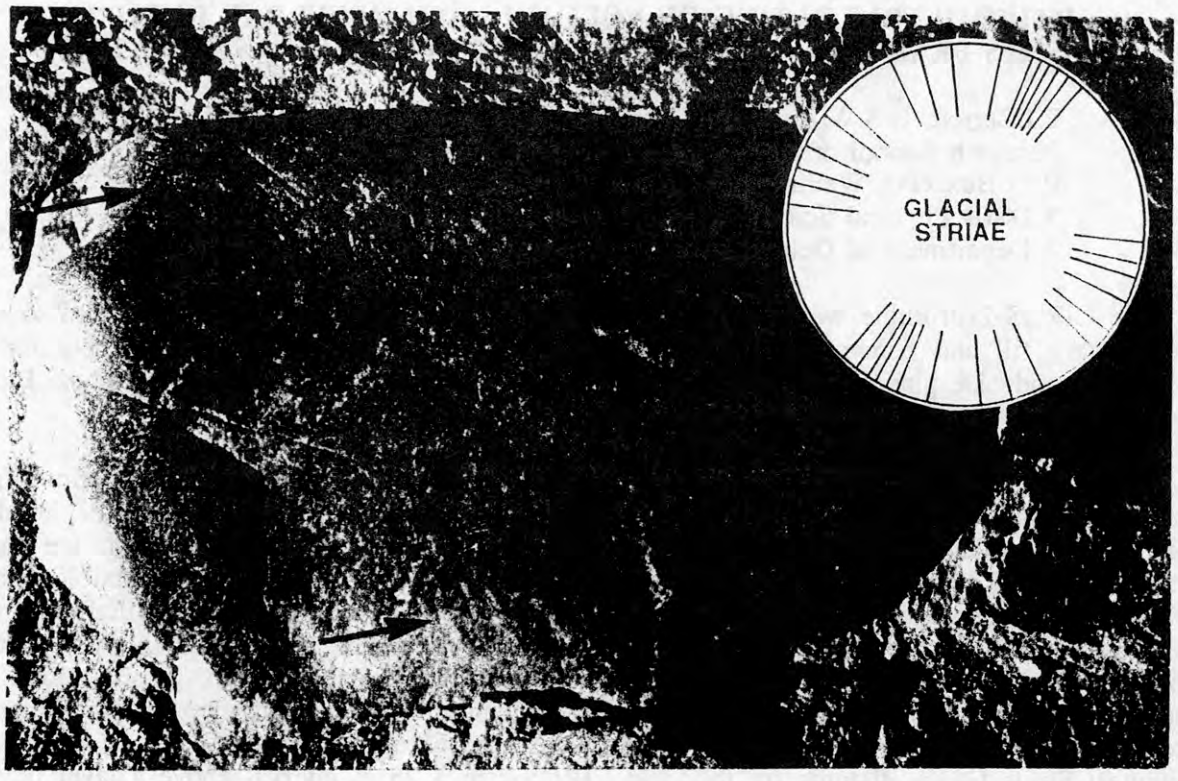

Figure 2. Striated boulder 45 cm long in late Permian mudstone in the floor of Camp Valley, Allan Hills. Arrows indicate striae. Circular diagram records striae directions.

Figure 3. Alternating mudstone and ripple laminated sandstone formed by lateral accretion during episodic flows near the base of Member C, Allan Hills.

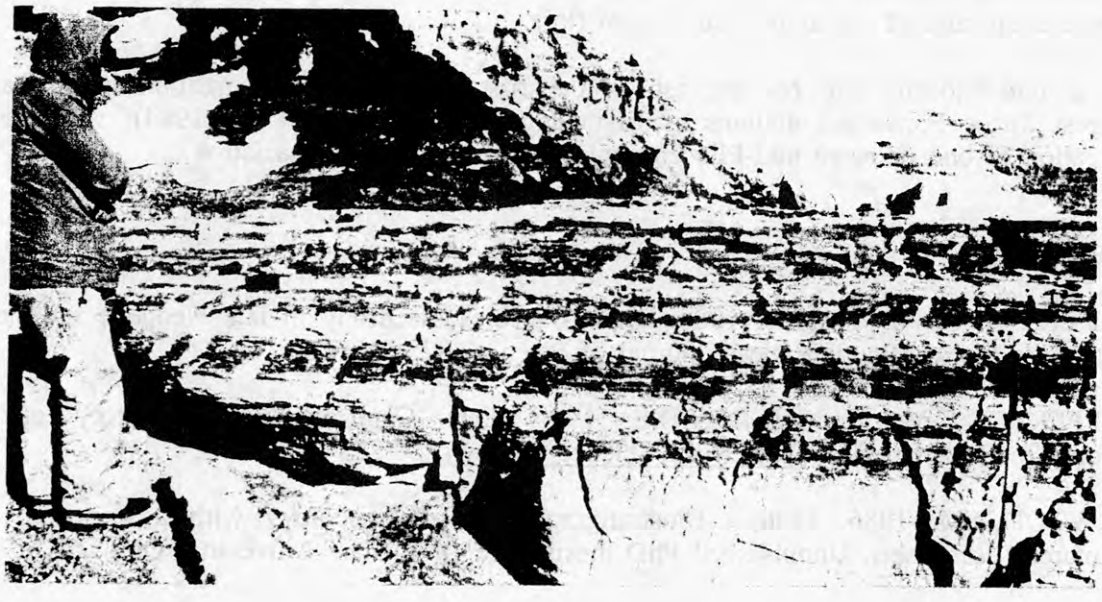

RADIOMETRIC DATING OF VOLCANIC ASH IN FERRAR FJORD AND ITS BEARING ON PLIOCENE DEGLACIATION OF ANTARCTICA

P.J.Barrett, G.S.Wilson, C.J.Adams*, G.J.Gossan, D.M.Harwood+ & A.R.Pyne,
Research School of Earth Sciences, Victoria University of Wellington,
P O Box 600, Wellington, New Zealand.
* DSIR Physical Sciences, P O Box 31312, Lower Hutt, New Zealand.
+ Department of Geology, University of Nebraska, Lincoln NE 68588, USA.

The CIROS-2 drillhole was sited in 210 m of water in the middle of Ferrar Fjord to core the sedimentary fill and hence provide a record of sedimentation, glaciation and climate for coastal Victoria Land. Despite logistic problems, the hole was successfully cored through 166 m of sedimentary strata to plutonic basement rock in November 1984.

The CIROS-2 core was found to record a series of glacial advances down the fiord from the East Antarctic ice sheet followed by a series up the fjord from a grounded ice sheet in the Ross Sea. Dating by diatom biostratigraphy (Harwood, 1986) indicated that East Antarctic ice dominated from 4.5 to 2.0 Ma ago and Ross Sea ice from 2.0 Ma to the present. This chronology assumed that diatom zones are essentially synchronous between the Antarctic and lower latitude regions, but this assumption has been disputed (Burkle and Abrams, 1986) and questioned recently (Clapperton and Sugden 1990) because similar diatoms discovered in the Sirius Group, glacial debris high in the Transantarctic Mountains, imply that at least a considerable part of the Antarctic interior was ice free on one or more occasions as recently as the middle Pliocene (Webb et al. 1984). The youngest Sirius Group diatoms are found in CIROS-2 in a 25 m interval above a layer of volcanic ash, thus providing an opportunity for a means of dating the diatoms independently.

The ash layer, which is 30 cm thick, consists largely of silt-size shards of phonolitic glass with only slight signs of devitrification. However, the layer also includes some detrital feldspar, probably from the local 450-500 Ma granite basement. The first K-Ar ages on whole subsamples gave ages of 12 and 17 Ma because of this contamination, but subsequent separates of relatively pure glass gave 7.8 and 8.3 Ma. There was still, however, a possibility that both samples were "contaminated" to a similar degree, and a new attempt was made to date the ash. This time both the volcanic glass concentrate and the "non-volcanic" or basement residue were used, with the percentage of young volcanic and old basement debris in each determined by optical microscopy. Once the age and composition of each fraction were known (243 Ma, 0.54 basement and 0.46 volcanic; 14.6 Ma, 0.03 basement and 0.97 volcanic), it was possible to solve two simultaneous equations and obtain ages for the "pure" basement and volcanic material. These were 445 ± 117 Ma (corresponding to the Ordovician age of the granitic rocks of the region), and 3.01 ± 0.60 Ma, the age of the volcanic event and of the associated diatom flora.

This mid-Pliocene age for the ash is the first radiometric confirmation of the age of the youngest Sirius Formation diatoms as first suggested by Webb et al. (1984), with the attendant implication of one or more mid-Pliocene episodes of Antarctic deglaciation.

REFERENCES

BURKLE,L.H. & ABRAMS,N. 1986. Diatom species diachrony in late Neogene sediments of the Southern Ocean. South African Journal of Science, 82: 505-506.

CLAPPERTON,C.M. & SUGDEN,D.E. 1990. Late Cenozoic glacial history of the Ross Embayment, Antarctica. Quaternary Science Reviews, 9: 253-272.

HARWOOD,D.M. 1986. Diatom Biostratigraphy and Paleoecology with a Cenozoic history of Antarctic ice sheets. Unpublished PhD thesis, The Ohio State University, Ohio: 592p.

WEBB,P.N., HARWOOD,D.M., McKELVEY,B.C., MERCER,J.H. & STOTT,L.D. 1984. Cenozoic marine sedimentation and ice volume variation on the East Antarctic craton. Geology, 12: 287-291.

Seismic Stratigraphic Evidence of Multiple, Neogene Glacial Advances on the Ross Sea Continental Margin

Louis R. Bartek, Dynamac Corporation, Rockville, Maryland, U.S.A. 20852

John B. Anderson, Department of Geology and Geophysics, Rice University, Houston, Texas, U.S.A. 77251

High resolution seismic data were acquired during Leg 2 of the 1990 R/V Polar Duke expedition in the Ross Sea with the objective of acquiring a data base on the continental shelf that, when correlated with existing drill core from the shelf (DSDP Leg 28 sites 270, 271, 272, and 273) and McMurdo Sound (MSSTS and CIROS), will provide a basis for developing a high resolution seismic stratigraphy for the late Paleogene and Neogene strata of the Ross Sea margin. Recent seismic studies on the Canadian shelf, the North Sea, and at Ice Stream B in Antarctica provide important information about the nature of seismic facies associated with both subglacial and glacial marine sequences and they therefore provide models that can be utilized in interpretations of the Ross Sea data.

Only preliminary analysis of the Polar Duke seismic data has been performed to date, but the results indicate that grounded ice sheets existed on the Ross Sea continental shelf at least as early as late Oligocene time. This is based on the first occurrence of glacial erosional surfaces and till tongues that are similar to those described on the Canadian shelf and in the North Sea. These surfaces have been tied to DSDP site 270 and the width of the scours associated with the till tongues is also comparable with the width of modern ice streams. The massive (acoustically transparent, lens-shaped), tongue-like units are at least 70 to 80 kilometers wide; modern ice streams have widths on the order of 100 to 150 kilometers. The widths of the trough-like scours on the Ross Sea continental shelf also exceed the widths of incisions carved by fluvial entrenched valley systems which are typically 10 to 20 kilometers wide.

Extensive shelf aggradation and progradation followed the late Oligocene grounding event. Waxing and waning of ice sheets on the continental shelf appears to be intimately related with the aggradation and progradation of the shelf. In dip sections the stratigraphy is very similar to temperate continental margins except that the aggradation and progradation of the shelf is characterized primarily by toplap rather than basinward and landward shifts in coastal onlap. Toplap has been generated by erosion of preceding units during glacial advances onto the continental shelf. Strike sections are characterized by an alternation of a cut and fill stratigraphy comprised of cross-cutting subparallel reflectors, acoustically massive units, and units of relatively continuous, subparallel reflectors. The cut and fill stratigraphy described above appears to be unique to glaciated margins.

In the data that are currently available, the massive, lens shaped units that characterize the subglacial cut and fill stratigraphy of the late Paleogene strike sections from the Eastern Basin of the Ross Sea are followed by an interval of early-middle Miocene shelf margin aggradation (dip sections). Strike sections of the early-middle Miocene aggradational interval are composed of continuous subparallel reflectors and may indicate an interval of less extensive glacial conditions. This interval is followed by late-middle and late Miocene progradational episodes. Strike sections of the late-middle Miocene progradational interval comprise very well defined massive lenses and trough shaped units. The extensive shelf margin progradation that has been documented in other seismic data bases along with the massive troughs of the Polar Duke '90' data suggest that middle to late-middle Miocene time was an interval of extensive ice sheet grounding on the Ross Sea continental shelf. The Late Miocene was also an interval of shelf margin progradation, but strike sections comprised of cross-cutting subparallel reflectors, but not massive lens and trough shaped units, suggest that the nature of ice sheet grounding in this interval may have been less extensive than that of the middle Miocene. The succession culminates in Plio-Pleistocene high frequency progradations and retreats (dip sections). Large troughs that are visible in the relatively

continuous, subparallel reflectors of the Plio-Pleistocene strike sections indicate that glacial scouring of continental shelf also accompanied the Plio-Pleistocene progradations and retreats.

The ice grounding stratigraphy appears to have been produced by two mechanisms. The till tongue-like stratigraphy, which appears to be the most prevalent, may have been produced by the buoyancy line migration mechanism discussed by King and Fader (1986). In this model tongues of till are deposited on the shelf as wet-based ice sheets wax and wane. Data from the eastern side of the Eastern Basin of the Ross Sea suggest that the subglacial delta model discussed by Alley et al. (1989) may also be responsible for generating the ice grounding stratigraphy of the Neogene strata on the Ross Sea continental margin.

References

Alley, R.B., Blankenship, D.D., Rooney, S.T., and Bentley, C.R., 1989, Sedimentation beneath ice shelves--The view from Ice Stream B: Marine Geology, v. 85, p. 101-120.

King, L. H., and Fader, G., 1986, Wisconsinan glaciation of the continental shelf, southeast Atlantic Canada: Geological Survey of Canada Bulletin 363, 72 pp.

THE WEST ANTARCTIC RIFT SYSTEM --A "CAPTURED" PROPAGATING RIFT?

J. C. Behrendt, United States Geological Survey,
Federal Center, Denver, CO, 80225, U.S.A.
A. K. Cooper, United States Geological Survey,
Menlo Park, CA, 94025, U.S.A.
F. Tessensohn, Federal Institute for Geosciences
and Natural Resources, Hannover, Germany
W. LeMasurier, University of Colorado,
Denver, CO, 80202, U.S.A.
D. Damaske,Federal Institute for Geosciences
and Natural Resources, Hannover, Germany
A. Trehu, Oregon State University, Corvallis,
OR, 97331, U.S.A.

The West Antarctic rift system (Figure 1) extends over a 3000 x 750 km, largely ice covered area from the Ross Sea to the base of the Antarctic Peninsula, comparable in area to the Basin and Range and the East African rift systems. A spectacular rift-shoulder scarp along which peaks reach 4-5 km maximum elevation extends from northern Victoria Land-Queen Maud Mountains to the Ellsworth-Whitmore-Horlick Mountains. The rift shoulder has maximum present physiographic relief of 5 km in the Ross Embayment and 7 km in the Ellsworth Mountains-Byrd Subglacial basin area. The rift system is characterized by bimodal alkaline volcanic rocks ranging from at least Oligocene to the present. These are exposed asymmetrically along the rift flanks and at the south end of the Antarctic Peninsula. The trend of the Jurassic tholeiites (Ferrar dolerites, Kirkpatrick basalts) marking the Jurassic Transantarctic Rift is coincident with exposures of the Cenozoic volcanic rocks along the section of the Transantarctic Mountains from northern Victoria Land to the Horlick Mountains. The Cenozoic rift shoulder diverges here from the Jurassic tholeiite trend and the tholeiites are exposed continuously (including the Dufek intrusion) along the lower-elevation (1-2 km) section of Transantarctic Mountains to the Weddell Sea (Behrendt and Cooper, 1991)

Widely spaced aeromagnetic profiles in West Antarctica indicate the absence of Cenozoic volcanic rocks in the ice covered part of the Whitmore-Ellsworth-Mountain block and suggest their widespread occurrence beneath the western part of the ice sheet overlying the Byrd Subglacial Basin. A BGR-USGS aeromagnetic survey over the Ross Sea continental shelf indicates rift fabric and suggests numerous submarine volcanoes along discrete NNW-trending zones. An approximately 200 (+50 to -150) mGal Bouguer anomaly, having 4-7 mGal/km gradients where measured in places, marks the rift shoulder from northern Victoria Land possibly to the Ellsworth Mountains (where data are too sparse to determine

maximum amplitude and gradient). The steepest gravity gradients (4-7 mGal/km) across the rift shoulder require high density (mafic or ultramafic?) rock within the crust as well as at least 12 km thinner crust beneath the West Antarctic rift system in contrast to East Antarctica. Sparse land seismic data reported along the rift shoulder where velocities are greater than 7 km/s and marine data indicating velocities above 7 km/s beneath the Ross Sea continental shelf support this interpretation. The maximum Bouguer gravity range in the Pensacola Mountains area of the Transantarctic Mountains, is only about 130 mGal with a maximum 2 mGal/km gradient, which can be explained solely by 8 km of crustal thickening. Large offset seismic profiles over the Ross Sea shelf collected by the German Antarctic North Victoria Land Expedition V (GANOVEX V) combined with earlier USGS and other results indicate 17-21 km thickness for the crust in the Ross Sea which we interpret as evidence of extended rifted continental crust. A regional positive gravity anomaly (0-50 mGal), the width of the rift, extends from the Ross Sea continental shelf throughout the Ross Embayment and Byrd Subglacial Basin area of the West Antarctic rift system and indicates that the Moho beneath the extended crust is approximately 20 km deep (probably coincident with the top of the asthenosphere) rather than the 30 km reported in earlier interpretations. The interpretation of horst and graben structures in the Ross Sea made from marine seismic reflection data probably extends beneath the Ross Ice shelf and the Byrd subglacial basin.

The near absence of earthquakes in the West Antarctic rift system probably results from a combination of primarily sparse seismograph coverage, and secondarily suppression of earthquakes by the ice sheet (e.g., Johnston, 1987) and very high seismicity shortly after deglaciation in the Ross Embayment followed by abnormally low seismicity at present (e.g., Muir Wood, 1989).

The evidence of high temperatures at shallow depth beneath the Ross Sea continental shelf and adjacent Transantarctic Mountains is supportive of thermal uplift of the mountains associated with lateral heat conduction from the rift, and can possibly also explain the volcanism, rifting and high elevation of the entire rift shoulder to the Ellsworth-Horlick-Whitmore Mountains.

The age of the oldest Cenozoic volcanism is at least Oligocene in the Ross Embayment and progressively decreases towards the end of the rift near the Antarctic Peninsula, while remaining active at the Ross Sea end. Probably no part of the rift is inactive. We infer that the Gondwana breakup and the West Antarctic rift are part of a continuously propagating rift that started in the Jurassic when Africa separated from East Antarctica (including the failed Jurassic Transantarctic rift). Rifting proceeded clockwise around East Antarctica to the separation of New Zealand and the Campbell Plateau about 85-95 Ma and has continued with a spreading center jump) to its present location in the Ross Embayment and West Antarctica. The Cenozoic activity of the West Antarctic rift system appears to be continuous in time with rifting in the same area that began only in the late Mesozoic,when New Zealand separated from Antarctica. Although the mechanism for rifting is not completely explained, we suggest a combination of the flexural

rigidity model (Stern and ten Brink, 1989) proposed for the Ross Embayment and the thermal plume or hot spot concepts. The propagating rift may have been "captured" by the thermal plume in West Antarctica.

REFERENCES

Behrendt, J.C. and Cooper A., Evidence of rapid Cenozoic uplift of the shoulder escarpment of the West Antarctic rift system and a speculation on possible climate forcing, Geology, v. 19, p. 315-319.

Craddock, C., et al., 1969, Geologic maps of Antarctica: American Geographical Society, Folio 12, scale 1:10,000,000.

Drewry, D.J., 1983, Antarctica--Glaciological and geophysical folio: University of Cambridge, Scott Polar Research Institute, 9 sheets.

Gonzales-Ferran, O., 1982, The antarctic Cenozoic volcanic provinces and their implications in plate tectonic processes, in Craddock, C., ed., Antarctic Geoscience: Madison, Wisconsin University of Wisconsin Press, p. 687-694.
Johnston, A.C., 1987, Suppression of earthquakes by large continental ice sheets: Nature, v. 330 p. 467-469.

LeMasurier, W.E., and Thomson, J.W., eds. Volcanoes of the Antarctic plate and southern oceans: Antarctic Research Series Volume 18, American Geophysical Union, 487p.

Muir Wood, R., 1989, Extraordinary deglaciation reverse faulting in northern Fennoscandia, in Gregersen S., and Basham, P.W., eds., Earthquakes at North Atlantic passive margins, neotectonics and postglacial rebound: Dordrecht, Kluwer Academic Publishers, p. 141-173.

Stern T.A., and ten Brink, 1989, Flexural uplift of the Transantarctic Mountains: Journal of Geophysical Research, v. 94, p. 10315-10330.

Figure 1. Generalized isostatically adjusted bedrock elevation map after ice removal. Contour interval 500m (modified from Drewry, 1983). Location of Late Cenozoic volcanic centers from Gonzales-Ferran (1982) and LeMasurier and Thomson (1990). Locations of Jurassic tholeiites (basalt, dolerite, and gabbroic Dufek intrusion) from Craddock, (1969). The area beneath the rift zone (elevations below sea level) is probably underlain by extended crust about 20 km thick based on interpretation of Bouguer anomaly, the Bentley (1960) interpretations adjusted to seismic determinations of Moho depth beneath the Ross Sea Shelf. Grid north is at the top.

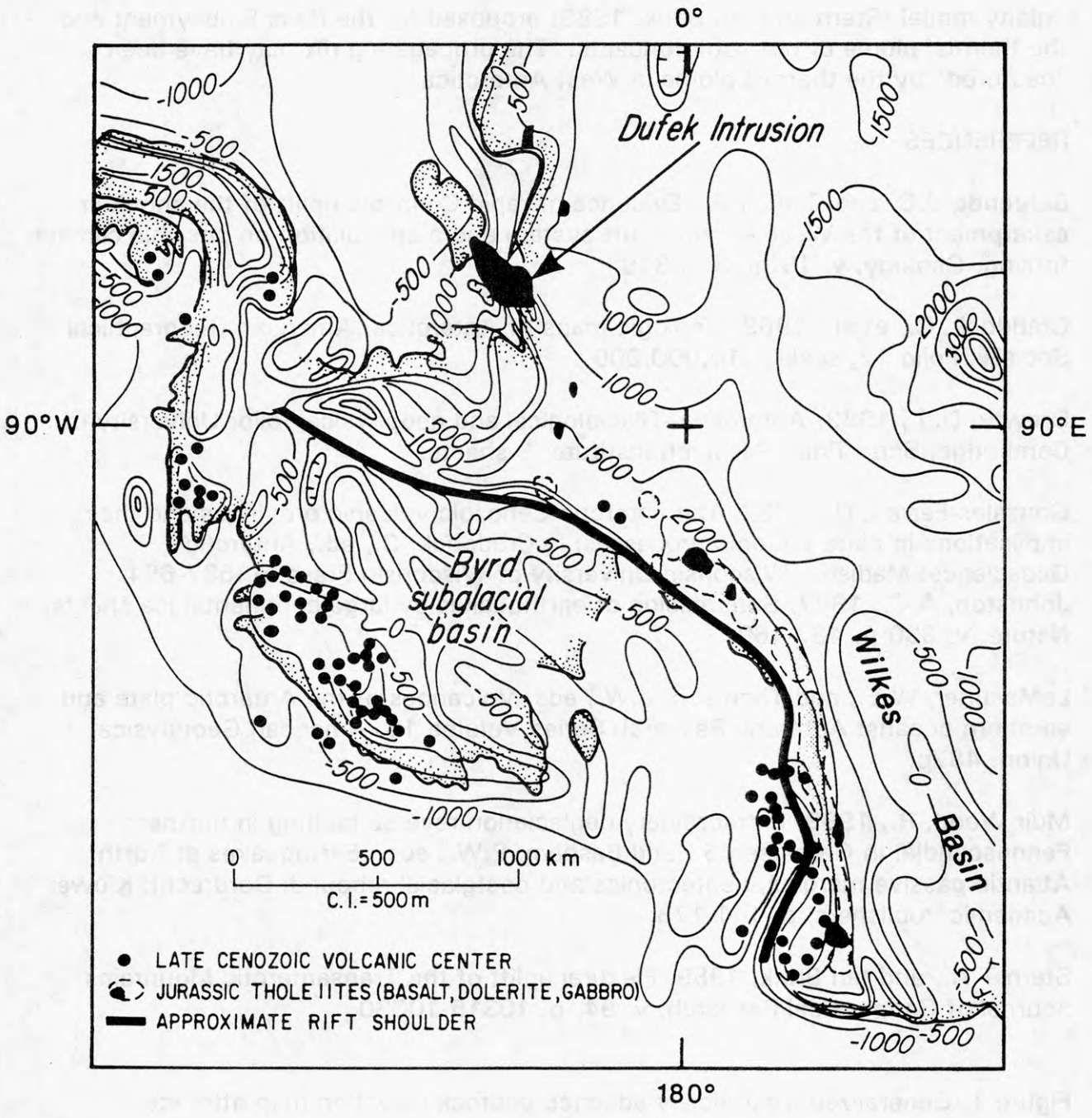
0°
90°W
90°E
180°
Dufek Intrusion
Byrd subglacial basin
Wilkes Basin
0 500 1000 km
C.I.=500m
LATE CENOZOIC VOLCANIC CENTER
JURASSIC THOLEIITES (BASALT, DOLERITE, GABBRO)
APPROXIMATE RIFT SHOULDER

AIRBORNE GRAVITY FROM A LIGHT AIRCRAFT: CASERTZ, 1990-1991

R.E. Bell and B.J. Coakley, Lamont-Doherty Geological Observatory, Palisades, New York, U.S.A.

D.D. Blankenship, Byrd Polar Research Center, The Ohio State University, Columbus, Ohio, U.S.A.

S.M. Hodge, U.S. Geological Survey, Tacoma, Washington, U.S.A.

J. Brozena and J. Jarvis, Naval Research Laboratory, Washington, D.C., U.S.A.

During the 1990-91 field season an underway marine gravity meter was integrated with accurate horizontal and vertical positioning systems and installed on a de Havilland Twin Otter for aerogeophysical surveying in the Ross Transect Zone, West Antarctica. Earlier work at Lamont-Doherty Geological Observatory suggests that such airborne gravity systems can result in measurements accurate to better than 2.7 mGal and recover anomalies with wavelengths as short as 5 kilometers. The system configured for the Antarctic field program included a Bell Aerospace BGM-3 sea gravity system, a Paroscientific pressure altimeter and both P-code and CA-code GPS receivers.

The BGM-3 gravity meter is a standard marine gravity system capable of sub-mGal accuracies when mounted on a ship. The sensor consists of an accelerometer which is maintained at a constant temperature by a series of ovens and is mounted on a two axis gyro-stabilized table capable. High quality navigation is critical to recovering free air gravity anomalies as the gravity meter is sensitive to accelerations introduced by the aircraft motion.

The horizontal position of the Twin Otter was recovered by psuedo-range GPS, kinematic GPS and a radio navigation system. The TI-4100 P-code receiver recovers the position of the aircraft horizontally to 10 meters and velocities to better than 0.1 cm/sec. The two Trimble 4000 receivers mounted on board recorded both L1 and L2 frequencies and were used in conjunction with a fixed receiver at the base camp. The differential solution from the GPS receivers results in vertical and horizontal positions good to several centimeters. The radio navigation system provided positions good to several meters.

In addition to the differential GPS navigation, the Paroscientific altimeter, a digital quartz pressure transducer, provided accurate vertical positions. A static pitot port was mounted above the cockpit on a 50 cm wand to avoid contamination of the signal by the aircraft bow shock. A second pressure altimeter was maintained as a base station at the camp.

The airborne gravity system was flown extensively over a 9,000 square kilometer region in conjunction with the magnetometer and the TUD ice penetrating radar. Tracklines were 130 kilometers long with track spacing of 5 kilometers. Cross tracks traverse the survey area every 20 kilometers. Several long reconnaissance lines were flown including one over the Horlick Mountain Traverse between Byrd Station and the Wisconsin Range.

ARCHAEAN GEOCHRONOLOGY IN ANTARCTICA - ISOTOPIC SYSTEMATICS, GEOLOGIC SETTINGS AND SOME PALEOTECTONIC IMPLICATIONS

B. V. Belyatsky, North Branch for Marine Geologic Research and Exploration "Sevmorgeologia", 120 Moyka, 190121 Leningrad, USSR.

Recent advances in isotopic studies and zircon geochronology have significantly advanced the knowledge of early stages of crustal evolution in Antarctica. A number of Archaean cratonic nuclei surrounded by Proterozoic metamorphic complexes has been recognized in the East Antarctic Shield. Poor exposure of Archaean terrains and multiple tectono-thermal overprints constrain a detailed analysis of their early history, although several major events can now be correlated throughout the key structural areas.

The Napier Complex of Enderby Land includes the best studied Archaean assemblages composed predominantly of felsic orthogneisses and subordinate mafic granulites, pyroxenites and sequences of metasedimentary rocks. It contains the oldest rocks currently recognized in Antarctica that were formed at least about 3900 Ma ago (Black et al.,1986a)and subsequently underwent extensive tectonothermal reworking. The oldest deformation and metamorphism in high-grade granulite facies environment is recorded at 3500 Ma (Belyatsky et al.,1990; Black & McCulloch,1987). A significant crustal growth indicated by Nd-isotopic framework is commonly recognized in association with tectono-metamorphic granulite facies event at 3100 Ma (see also Black et al.,1986b;Sheraton & Black,1983). During the final cratonization at 2500 Ma (Sheraton et al.,1987; Black et al.,1986b;Grew & Manton,1979) more mantle material was added with variable granites emplaced in the lower crust under conditions transitional from granulite to amphibolite facies.

Another Archaean terrain known in the Vestfold Hills is composed of tectonically interlayered orthogneisses and subordinate metasediments cut by numerous Proterozoic mafic dyke swarms. Earlier Sr and Nd isotopic data (Collerson et al.,1983) indicate recycling of granulite facies orthogneisses at 3000-2800 Ma and 2500-2400 Ma, broadly in agreement with the Napier Complex events. Later SHRIMP data (Kinny et al.,1990) seem to disagree with this conclusion and to suggest that both metamorphic episodes occurred within only 50 Ma interval (between 2530 and 2480 Ma) immediately subsequent to formation of felsic crust. However, the same workers demonstrate the presence of zircon crystallization ages ca.3270 and ca.2800 Ma in tonalitic orthogneisses on the Rauer Islands only 25 km south of the Vestfold Hills.

Recent studies in the southern Prince Charles Mountains demonstrate existence here of a major Archaean granite-greenstone terrain (Kamenev and Krasnikov,this volume). The first Late Archaean Rb-Sr ages obtained by the Australian workers (Tingey,1982) are now supplemented by an extensive set of isotopic data indicating the presence of Lower Archaean (ca.3300

Ma) protolith (Kovach and Belyatsky,this volume).

Other localities where the presence of Archaean crust may be suspected on the basis of available data are known in the Bunger Hills (2600,3000 Ma, Sheraton et al.,1990), the Windmill Islands (3500 Ma, Lovering et al.,1981), Queen Maud Land (3000 Ma, Halpern,1970; Nakajima et al.,1988), Shackleton Range (ca.2600 Ma, Pankhurst et al.,1983; our unpublished data). It appears that the earliest Precambrian protoliths had always preceded subsequent formation of mobile metamorhic belts. Our data (U-Pb on zircon, Sm-Nd WR) show that the Proterozoic metamorphic belt conventionally recognized in Enderby, MacRobertson and Princess Elizabeth Lands by the presence of ca.1000 Ma Rayner Complex is, in fact, a composite crustal assemblage that consists not only of the Late Proterozoic granulite facies rocks but also incorporates essential amount of Archaean remnants dated at 2600, 3100 and 3500 Ma (see also Black et al.,1987; Sheraton et al.,1987; Grew et al.,1988).

References:

Belyatsky B.V.,Krylov D.P.,Levsky L.K. & Grikurov G.E.,1990: Zircon geochronology of the granulite complexes of Enderby Land, East Antarctica. - *Zbl.Geol.Paläont.*,v.1,1/2,pp.1-18.

Black L.P.,Williams I.S. & Compston W.,1986a: Four zircon ages from one rock: the history of a 3930 Ma-old granulite from Mount Sones,Antarctica. - *Contrib.Mineral.Petrol.*,v.94,pp.427-437.

Black L.P.,Sheraton J.W. & James P.R.,1986b: Late Archaean granites of the Napier Complex, Enderby Land,Antarctica: a comparison of Rb-Sr,Sm-Nd, and U-Pb isotopic systematics in a complex terrain. - *Precambrian Research*,v.32,pp.343-368.

Black L.P. & McCulloch M.T.,1987: Evidence for isotopic equilibration of Sm-Nd whole-rock systems in early Archaean crust of Enderby Land, Antarctica. - *Earth Planet.Sci.Lett.*, v.82,pp.15-24.

Black L.P., Harley S.L., Sun S.S. & McCulloch M.T.,1987: The Rayner Complex of East Antarctica: complex isotopic systematics within a Proterozoic mobile belt. - *Journal Metam.Geology*, v.5,pp.1-26.

Collerson K.D., Reid E., Millar D. & McCulloch M.T.,1983: Lithological and Sr-Nd isotopic relationships in the Vestfold Block: implications for Archaean and Proterozoic crustal evolution in the East Antarctic Shield. *In* Oliver R.L.,James P.R. & Jago J.B.(Eds), *Antarctic Earth Science*, Australian Academy of Science, Canberra,pp.77-84.

Grew E.S. & Manton W.I.,1979: Archaean rocks in Antarctica: 2.5 billion-year uranium-lead ages on pegmatites from Enderby Land. - *Science*,v.206,pp.443-445.

Grew E.S.,Manton W.I. & James P.R.,1988: U-Pb data on granulite facies rocks from Fold Island, Kemp Coast, East Antarctica. - *Precambrian Research*,v.42,pp.63-75.

Halpern M.,1970: Rubidium-strontium date of possibly 3 billion years for a granitic rock from Antarctica. - *Science*, v.169,pp.977-978.

Kamenev E.N. & Krasnikov N.N.,1991: The granite-greenstone terrains in the sothern Prince Charles Mountains. *In Sixth International Symposium on Antarctic Earth Sciences, Abstracts*, this volume.
Kinny P.D., Black L.P., Sheraton J.W & Delor C.P.,1990: New isotopic and field evidence for the ages and distribution of Archaean rocks in East Antarctica. *In Extended Abstracts Volume, Third International Archaean Symposium, Perth,1990*, pp.27-28.
Kovach V.P. & Belyatsky B.V.,1991: Geochemistry and age of granitic rocks of the Ruker granite-greenstone terrain, Southern Prince Charles Mountains, East Antarctica. *In Sixth International Symposium on Antarctic Earth Sciences, Abstracts*, this volume.
Lovering J.F., Travis G.A., Comaford D.J. & Kelly P.R.,1981: Evolution of the Gondwana Archaean Shield: zircon dating by ion microprobe and relationships between Australia and Wilkes Land. *In* Glover J.E. & Groves D.I.(Eds), *Archaean Geology*, Geological Society of Australia Special Publication,v.7,pp.193-203.
Nakajima T.,1988.(Abstact), *Proceedings NIPR Symposium on Antarctic Geoscience*,2,p.172.
Pankhurst R.J., Mursh P.D. & Clarkson P.D., 1983: A geochronological investigations of the Shackleton Range. *In* Oliver R.L.,James P.R. & Jago J.B.(Eds), *Antarctic Earth Science*, Australian Academy of Science, Canberra,pp.176-182.
Sheraton J.W. & Black L.P.,1983: Geochemistry of Precambrian gneisses: relevance for the evolution of the East Antarctic Shield. - *Lithos*,v.16,pp.273-296.
Sheraton J.W.,Tingey R.J.,Black L.P.,Offe L.A. & Ellis D.J.,1987: Geology of an unusual Precambrian high-grade metamorphic terrane - Enderby Land and western Kemp Land, Antarctica. - *Aust. Bur. Mineral. Res., Geol.Geophys., Bull.*,v.223, 51p.
Sheraton J.W.,Black L.P.,McCulloch M.T. & Oliver R.L.,1990: Age and origin of a compositionally varied mafic dyke swarm in the Bunger Hills, East Antarctica.- *Chemical Geology*,v.85,pp.215-246.
Tingey R.J.,1982: The geologic evolution of the Prince Charles Mountains - an Antarctic Archaean cratonic block. *In* Craddock C.(Ed), *Antarctic Geoscience*, University of Wisconsin Press,pp.455-464.

CRUSTAL XENOLITHS FROM CAPE McCORMICK CRATER, NORTHERN VICTORIA LAND

J.H. Berg, Department of Geology, Northern Illinois University, DeKalb, Illinois 60115, USA.

The prominent crater at Cape McCormick, toward the southern end of the Adare Peninsula along the northwestern side of the Ross Sea, consists of Cenozoic alkali basalt containing abundant xenoliths of crustal granulites and gneisses. The xenoliths range from basic two-pyroxene granulites to nearly mafic-free granite gneisses. The absence of metasedimentary inclusions suggests that all of the inclusions come from the lower or middle crust and none from the upper crust. Assuming that the basal lower crust has been sampled by the eruptions, the absence of garnet in the basic granulites suggests that crustal thickness in this region is less than 25-30 km.

There is a distinct gap in major-element composition between the basic granulites and the granitic gneisses. In terms of SiO_2 content, the gap is between 50 and 63 wt%. The granulites cluster between 47-50 wt% SiO_2, and the gneisses range from 63-75 wt%. This is in striking contrast to xenoliths from Foster Crater in southern Victoria Land where the bulk of those xenoliths fall in the range 50-60 wt% SiO_2. The basic granulites from Cape McCormick Crater have very low P_2O_5 contents and almost certainly formed originally as cumulates from mafic magmas. By analogy with the Foster Crater xenoliths, which exhibit evidence for extensive assimilation of felsic crust in their evolution, the magmas which formed the protoliths to the Cape McCormick Crater granulites probably did not interact extensively with the prexisting lower crust. In that respect, they resemble the granulite inclusions from Ross Island and other islands in the vicinity of McMurdo Sound. However, the Cape McCormick Crater granulites differ from those granulites in that they have generally lower *mg* numbers.

Not surprisingly, the granitic xenoliths differ compositionally from granite xenoliths at Foster Crater. More significantly, and perhaps more surpisingly, they also are quite different from granites exposed at the surface in northern Victoria Land (i.e., Admiralty Intrusives). The Cape McCormick Crater granites are essentially plagiogranites or tonalites and have very low potash contents, 0.2-2.5 wt%. Although the low potash could be interpreted as potash having been lost during metamorphism, the data show no trend away from K_2O on a ternary plot of CaO-Na_2O-K_2O, as might be expected with variable loss of K_2O. In fact, the data form a trend that is more consistent with igneous derivation. Like the Admiralty Intrusives, they could be considered I-type granites, but they might better be described as M-type. In that case they could represent juvenile addition to the crust during the Paleozoic or they might represent original crustal growth in the Precambrian.

LOWER CRUSTAL PROCESSES AND COMPOSITIONS ASSOCIATED WITH THE ROSS OROGENY IN THE McMURDO SOUND REGION

J.H. Berg, R.I. Kalamarides, J.E. Matheney, D.N. Dickey, Jr.,
Department of Geology, Northern Illinois
University, DeKalb, Illinois 60115, USA.
V.C. Bennett, M.T. McCulloch, Research School of Earth Sciences,
The Australian National University, GPO Box 4,
Canberra, ACT 2601, Australia

Crustal xenoliths from Foster Crater and other sites in the foothills of the Royal Society Range consist of two-pyroxene granulites, scapolite- or clinopyroxene-rich granulites, charnockites, and granites, whereas xenoliths from Ross Island and sites in the Ross Sea consist of two-pyroxene granulites and very rare granites. The two-pyroxene granulites from under the Ross Sea have basic-cumulate compositions and very restricted isotopic compositions of $^{87}Sr/^{86}Sr$=0.7026-0.7031 and ϵ_{Nd} ranging from +6 to +8, corrected to 450 Ma. Interestingly, these compositions are close to what one might expect for early-Paleozoic oceanic crust derived from depleted mantle, but whatever their origin, they have "seen" little or no continental crust in their history.

The two-pyroxene granulites dominate in the Royal Society Range and have an average composition of andesite. Corrected to 450 Ma, $^{87}Sr/^{86}Sr$ varies from 0.7038 to 0.7122 and ϵ_{Nd} ranges from +4.2 to -6.9. Their relatively coherent covariation can be reasonably modeled by combined assimilation/fractional crystallization (AFC). The primitive endmember is consistent with a mantle-derived basalt generated in a Cambro-Ordovician mantle wedge above a subduction zone, and the likely assimilant is represented by a mid-crustal charnockite xenolith ($^{87}Sr/^{86}Sr$=0.71267 and ϵ_{Nd}=-26.0). Most of the two-pyroxene granulites can be derived from the primitive endmember by AFC where F_L=0.5-0.65, whereas the most evolved granulites require F_L=0.9. A striking feature of the AFC modeling is that granulites representing the first 50% of the AFC process are almost completely lacking. This, combined with the rarity of clinopyroxenites and the complete absence of eclogites and garnet clinopyroxenites, supports a model whereby part of the lower crust (perhaps as much as 20 km) was delaminated into the mantle at the end of or after the Ross Orogeny. Such a model has been hypothesized by others as one explanation for the andesitic composition of the post-Archean bulk crust despite the evidence for basalts being the primary magma at subduction zones. These xenoliths may represent direct evidence for such a process. Depleted-mantle Nd model ages (T_{DM}) of the granulites and charnockite imply that the pre-existing lower crust (prior to the Ross Orogeny) had an age of at least 2 Ga. Preliminary Pb isotope data on the charnockite suggest that that crust may, in fact, have been Archean.

The scapolite granulites and clinopyroxenites have an alkaline geochemical signature (high Nb, high LREE, etc.) and may represent carbonatitic melts or CO_2-rich silicate melts that assimilated crust. For most of them, $^{87}Sr/^{86}Sr$ is 0.708 to 0.710 and ϵ_{Nd} is -4.5 to -7.0. However, the most primitive one isotopically is 0.70654 and +6.2. Although highly speculative at this stage, the relatively high $^{87}Sr/^{86}Sr$ ratio in conjunction with the primitive ϵ_{Nd} might suggest an ultimate derivation of these CO_2-rich melts, perhaps indirectly, from sea-water altered or carbonate-bearing oceanic crust.

DIGITAL PROCESSING OF MULTISPECTRAL IMAGES OF ANTARCTICA

R. Bianchi, R. Casacchia, A. Picchiotti, M. Poscolieri, R.Salvatori, Consiglio Nazionale delle Ricerche, Via E. Fermi 70, C.P.27 00044 Frascati (Roma) - Italy

The work presented in this paper is focused on the processing and the analysis of satellite multispectral data of Victoria Land, Antarctica, to test the contribution of different digital techniques to the enhancement of geologic and morphologic information. This work is currently performed in the framework of the Italian National Research Programme of Antarctica (PNRA).

Two sets of multispectral satellite data have been used in this study: SPOT images, the high resolution of which (20 m/pixel) is particularly suitable to investigate the shape and the geometry of the surface features, and Landsat 4 Thematic Mapper (TM) data, having a lower spatial resolution (about 30 m/pixel) than SPOT, but characterized by a larger number of spectral bands, thus allowing to estimate the spectral response of surface materials. References concerning the topography and the geology of the region were provided respectively by the USGS 1:250.000 maps and by the map compiled by Carmignani et al. (1988).

The progress actually achieved is mostly concerned with the detection of morphologic features from enhanced SPOT images.

The problem of enhancing surface features in remotely sensed data by means of digital image processing techniques has been addressed in several papers (Odegaard and Helle, 1982; Lucchitta et al., 1985; Orheim and Lucchitta, 1988; Bianchi et al., 1990); the methods that are generally discussed include image contrast stretching, convolution filtering, and FFT applications. Major problems in selecting the best procedure to apply to a given area are concerned with its geomorphic and brightness characteristics and also with the efficiency of a particular method in terms of required computer time and reliability of the results. Three test areas have been selected, respectively the Northern Foothill region (where the Italian base is located; Figure 1a), a portion of Priestly Glacier and of the Deep Freeze Range and an area south of Priestly almost centered on the O'Kane Glacier (Figure 2a). The selected images show a variety of landforms such as high density features (on the slopes of some snow-free reliefs), almost flat surfaces characterized by subdued features and high brightness contrast areas; a portion of the Northern Foothill region has been mapped in detail by Baroni (1989) and represents the only large-scale field map in the study area, thus providing a good check for the results obtained by processing SPOT images.

Among the image enhancement techniques that we adopted best results have been obtained by using 3x3 Laplacian operators (high-pass filters) and 5x5 directional filters. In the application of directional filters the main issues have been the choice of the weights to construct the filtering kernel and its dimensions. Weights ranging from -4

to 4, built in a 5x5 kernel, provided the most interesting results in particular when displaying a combination of the original image and of the filtered image (Figure 1b). In this way the resulting image contains both the radiometric information of the original data plus the structural information of the filtered image. These "mixed images" allow a fairly detailed description of some glacier features such as very subdued glacial flow lines. The outline of a number of differently shaped features is much better detectable in the "mixed images", especially in those areas having originally poor surface detail.

Laplacian operators have been used to enhance features in any direction; this technique revealed to be very efficient in detecting edges in areas showing high-density spatial features (Figure 2b). Ice-covered and snow-covered areas can also be discriminated by this technique and, if the snow cover is relatively thin, Laplacian operators can contribute to enhance the morphology of the bedrock. Both Laplacian operators and directional filters permit to improve the geomorphological information of the shaded and cloud-covered areas if the DN values are not zero.

Landsat TM data have been acquired only recently and, for this reason, their processing is still preliminary. However, the results obtained so far allow a fairly good discrimination between sea and continental ice, encouraging to further improve the edge enhancement techniques to apply to snow-covered areas. Furthermore, the thermal band of the TM may permit a better estimation of the physical properties of the ice-sheet such as the detection of eventual thermal surface gradient, through the calculation of the surface brightness temperature (Orheim and Lucchitta, 1988).

The results of our work is going to be compared and integrated with the results achieved by other geoscience experiments and investigations performed within the PNRA.

REFERENCES

Baroni C., 1989. Geomorphological map of the Northern Foothill near the Italian station. Mem.Soc.Geol.It., 33 (1987), 114-117.

Bianchi R., et al., 1990. Image processing techniques applied to Landsat MSS images of Victoria Land, Antarctica. Mem.Soc.Geol.It., 43 (1988), 155-163.

Carmignani L., et al., 1989. Geology of the Wilson Terrane in the area between David and Mariner glaciers, Victoria Land, Antarctica. Mem.Soc.Geol.It., 33 (1987), 79-99.

Lucchitta B.K., et al., 1985. Multispectral digital mapping of Antarctica with Lansat images. Antarctic J. U.S., 19, 249.

Odegaard H. and Helle S.G. 1982. Polar mapping using Landsat data-Svalbard and Dronning Maud Land. IBM and Norsk Polarinstitut, Final Report, 66p.

Orheim O. and Lucchitta B.K., 1988. Numerical analysis of Landsat TM images of Antarctica: Surface temperatures and physical properties. Annals of Glaciology, 11, 109-120.

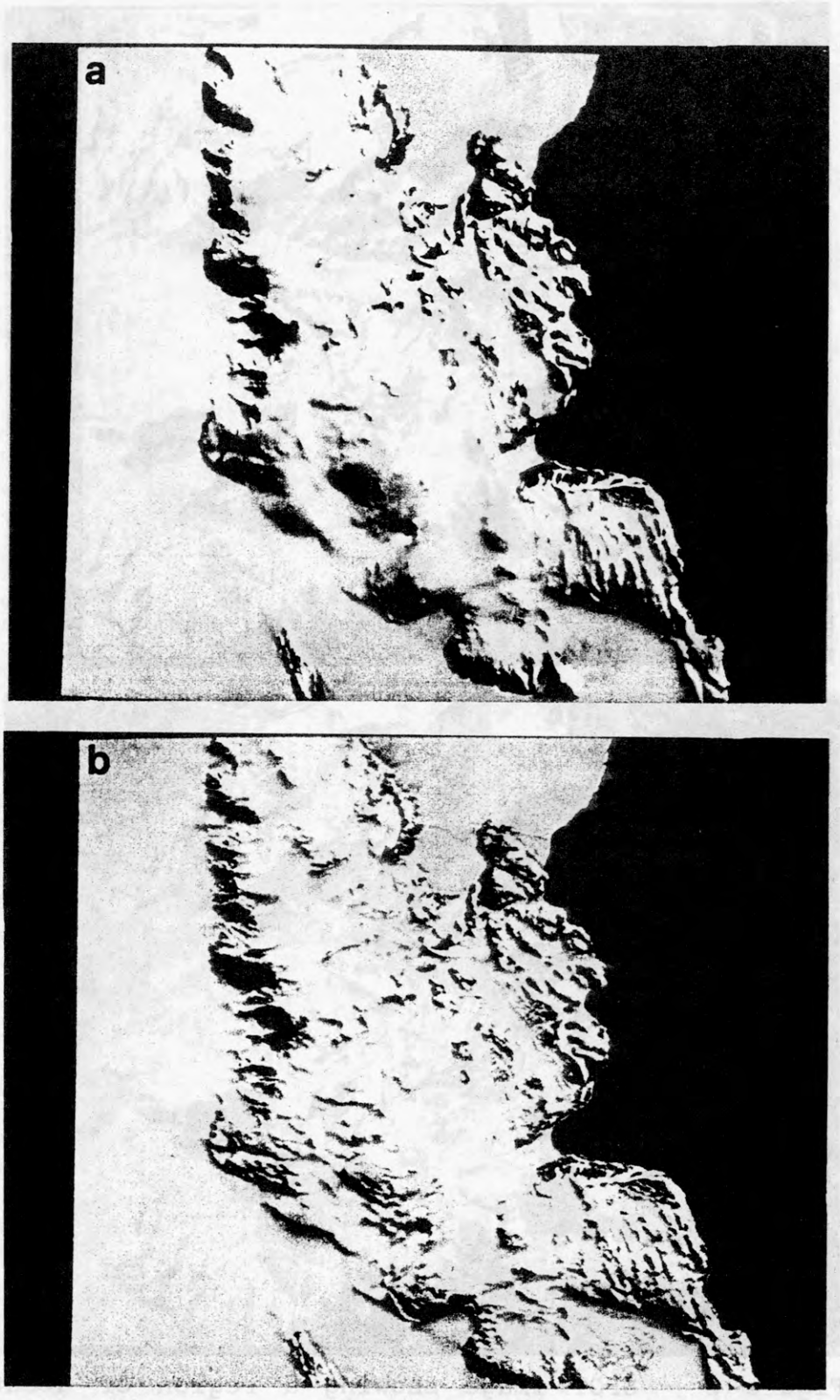

Figure 1 - SPOT image showing the Northern Foothill region and covering an area of about 20x20 km. North is at the top. a) original data; b) combination of the original image and of the image filtered in order to emphasize E-W trends.

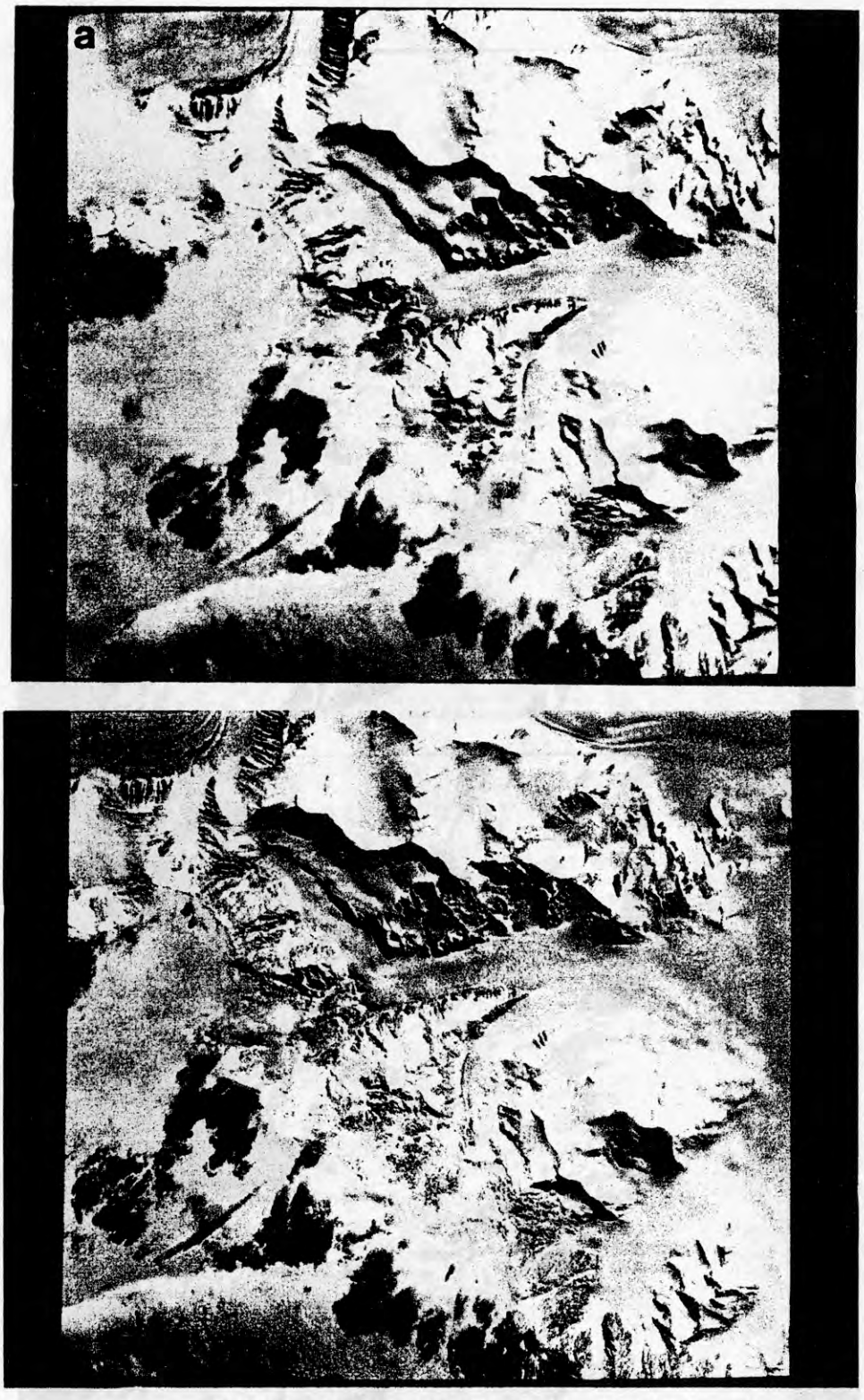

Figure 2 - SPOT image showing a region of about 20x20 km almost centered on the O'Kane Glacier. North is at the top. a) original data; b) image filtered by a Laplacian operator, used to emphasize high-density spatial features in any direction.

COMBINED USE OF AERIAL PHOTOGRAPHS AND SATELLITE DATA FOR THE GEOMORPHOLOGIC INVESTIGATION OF VICTORIA LAND, ANTARCTICA.

A. Biasini, Dipartimento Scienze della Terra
Universita' La Sapienza, Roma, Italy
R. Casacchia, CNR-ARF Via E. Fermi, 70 C.P.27
00044 Frascati (Roma), Italy
O. Fanucci, CNR Commissione Polare,
Via Tiburtina 770, Roma, Italy
M.C. Salvatore, PNRA, Roma, Italy

The work presented in this paper represents the preliminary result of a joint effort of two working groups performing their research activity on the use of aerial photographs and of satellite data respectively, to produce geomorphologic maps of the Antarctic surface. This research is currently carried on in the framework of the Italian National Research Programme in Antarctica (PNRA).

The region under study is the Terra Nova Bay area, in Victoria Land; the data sets used in this work are Trimetrogon panchromatic aerial photos taken by the US Navy and multispectral data from the SPOT satellite. Topographic data were provided by the USGS 1:250.000 maps.

We have focused our attention on the definition of a method to systematically classify the landforms detectable from the aerial photos, and on the digital processing of satellite multispectral data for the enhancement of surface features. The idea is to perform an integrated study of the glacial features of Antarctica by taking into account the results obtainable from different experiments. To achieve this it has been necessary to check the results of satellite data processing with the geomorphologic maps produced on the basis of the aerial photos and with the geologic and geomorphologic maps produced after field surveys.

Features detectable in the aerial photos have been classified and mapped by using parameters able to describe in detail the surface geometry; these parameters are defined by the combination of alphanumeric codes and of graphic symbols. In this method particularly important was the morphometric description of each feature in order to allow an efficient and rapid geomorphologic analysis, especially if these data are organized into a digital cartographic data-base. Based on the aerial photos, two sets of geomorphologic maps have been produced at scales respectively of 1:250.000 and of about 1:50.000.

In processing Spot data the most interesting results have been obtained by the application of high-pass and directional filtering procedures. High-pass filtering revealed to be a good method to improve surface details in areas characterized by high-density spatial features and in contributing to get information about the morphology of the bedrock in snow and ice-covered areas. The application of directional filters involved the use of 5x5 kernels that provided the best results when a combination of the original image and of the filtered image was performed. These data allow a fairly detailed description of some glacial features such as very subdued glacial flow lines, especially in those areas having originally poor surface detail.

FIRST GEOMORPHOLOGICAL DATA ALONG A TRANSEPT FROM PRIESTLEY GL. TO CAMPBELL GL. MAPPED BY AERIAL PHOTOGRAPHS (VICTORIA LAND - ANTARCTICA).

A. Biasini, Dipartimento di Scienze della Terra - Università degli Studi " La Sapienza " 00185 Roma, Italy.

O. Fanucci, Consiglio Nazionale delle Ricerche - Commissione Scientifica Polare Via Tiburtina n° 770 - 00159 Roma, Italy.

M.C. Salvatore, Programma Nazionale di Ricerche in Antartide, Roma, Italy.

The present study concerns the preliminary results of the scientific unit working at the Earth Sciences Dep. of the University " La Sapienza" of Roma, and supported by the Italian National Research Programme in Antarctica.

This group is performing an extensive geomorphological investigation of a part of Victoria Land, (about 30'000 sq.km) by the interpretation of large scale aerial photographs.

The data sets investigated are Trimetrogon panchromatic aerial photos taken by the US Navy during about ten years (1954-1964).

In this work, in particular, a geomorphological map is proposed, derived from a photointerpretative analysis made along a transept from Priestley Glacier to Campbell Glacier, across the Deep Freeze Range.

The ends of this area (about 650 sq.km) are located between Ogden Heights (73°58' S, 161°30' E) and Mills Pk (74°13' S, 163°58' E) and are covered by stereoscopic vertical photos at a scale about 1:48'000.

The main characteristics of outcrops have been drawn from the geological map carried out by direct surveys made by Italian expeditions started in 1985 (Carmignani et Al., 1988).

The results of photointerpretation are correlated with the Landsat-TM images which also form the cartographic base at the scale 1:50'000; this allows a detailed representation of features recognized in a region, like all Antarctica, lacking in topographic maps at a suitable scale.

The original symbolism used allows to identify the features shown not only by restricted outcrops but also by large areas covered with ice and snow; this offers more helpful elements for a first geomorphological interpretation of this particular region.

The legend used for the outcrops is the same of the geomorphological map of Northern Foothills district near the Italian station in Terra Nova Bay (Baroni, 1989); for areas covered with ice and snow there has been used a symbolic representation of several morphometric elements; these elements may be useful for the fixed aim and may better explain situations neither pointed out by the maps at a scale 1:250'000, nor by the Landsat images.

Thus the dependence of features on lithology, local structure, regional tectonic features, and present and past morphogenic processes has been evidenced.

The investigation carried out along this and other transepts - covered by vertical aerial photograps - will be used for improving the utilization of oblique photographs, the only source of detailed data on neighbouring areas.

Essential Bibliography

Carmignani L. et alii (1988) " Geological map of the area between David and Mariner Glaciers, Victoria Land - Antarctica", PNRA, CNR, ENEA.

Baroni C. (1989) " Geomorfological map of the Northern Foothills near the Italian station (Terra Nova Bay, Antarctica)". Mem. Soc. Geol. It., 33 (1987), 195-211 .

Baroni C., Orombelli G. (1989) " Glacial geology and geomorphology of Terra Nova Bay (Victoria Land, Antarctica)". Mem. Soc. Geol. It., 33 (1987), 171-193 .

EVOLUTION OF THE BRANSFIELD RIFT, WEST ANTARCTICA

K. Birkenmajer, Institute of Geological Sciences,
Polish Academy of Sciences, Senacka 3, 31-002 Krakow, Poland

The Bransfield Rift is a Cenozoic structure barely 15-20 km wide which separates the Mesozoic magmatic arc of Antarctic Peninsula from Late Mesozoic-Cenozoic magmatic island-arc of the South Shetlands. The rift is part of the Bransfield Basin (backarc) some 100 km wide, which includes also a wide submarine platform adjacent to Antarctic Peninsula, and a narrow submarine platform adjacent to the South Shetland Islands.

The oldest evidence for marine incursion in the Bransfield Basin area comes from King George Island (South Shetland Islands). It is represented by fossiliferous glacio-marine strata passing upward into basaltic marine hyaloclastites (with calcareous nannoplankton in the matrix), and overlain by basaltic lavas dated at Early Eocene. The sea covered at least a part of the area during the succeeding Arctowski Interglacial (Middle Eocene - base Oligocene) as evidenced by pelitic volcaniclastic rock fragments with calcareous nannoplankton found in volcanic breccias at Deception Island.

During the Early Oligocene continental glaciation (Polonez Glaciation), the area was at first covered by ice-sheet, then flooded by shallow sea rich in invertebrate fauna. The area was dry again during the Wesele Interglacial (mid-Oligocene), and the succeeding Legru Glaciation (Late Oligocene), probably as a result of regional uplift.

Rifting started at the end of Oligocene and continued through Early Miocene, as evidenced by a system of antithetic faults cutting through Upper Oligocene and older rocks along outer margin of the Bransfield Basin on King George Island, followed by basaltic to andesitic dyke and plug intrusion K-Ar-dated at 20 to 14 Ma. The Upper Miocene through Pliocene stages of rift formation have not been geologically documented so far.

The Pleistocene to Holocene stages of rift evolution are evidenced by mildly alkaline to calc-alkaline subaerial and submarine volcanoes (Deception - Bridgemen Line), following the rift axis. The Deception caldera is still active. A subparallel volcanic line links Penguin Island (dormant volcano) with Melville Peak (extinct Pleistocene volcano); this volcanic line cuts through the outer, southern margin of the South Shetland crustal block.

TERTIARY GLACIAL HISTORY OF THE SOUTH SHETLAND ISLANDS, WEST ANTARCTICA

K. Birkenmajer, Institute of Geological Sciences,
Polish Academy of Sciences, Sanacka 3, 31-002 Krakow, Poland

(Poster)

The Tertiary glacial history in the South Shetland Islands is recorded in terrestrial glacial and fossiliferous glacio-marine deposits. Evidence for interglacial and pre-glacial history of the islands comes mainly from terrestrial plant-bearing deposits.

The Late Cretaceous and Paleocene terrestrial volcaniclastic deposits yielded forest-plant assemblages indicative of subhumid mesothermal climate (pre-glacial). The first glaciation (Early Eocene: Krakow Glaciation) is recorded by glacio-marine fossiliferous strata. The centre of glaciation was located probably in Antarctic Peninsula area.

Rich forest-plant communities reappeared during the Arctowski Interglacial (Middle-Late Eocene and base of Oligocene).

During the second glaciation (Polonez Glaciation: Early Oligocene) a large continental ice-sheet crossed Bransfield Strait area to reach the South Shetlands. Terrestrial plant communities were completely wiped-off from the islands, while shallow-sea environments hosted a new cold-water invertebrate fauna.

During the succeeding Legru Glaciation (Late Oligocene), the South Shetland Islands were covered by a local ice-cap disconnected from that of Antarctic Peninsula.

Recolonization of the islands by *Nothofagus* forests took place during the Wawel Interglacial (Oligocene/Miocene boundary). During Early Miocene times, the islands were submerged (at least in part) by epicontinental-type sea in which glacially-controlled fossiliferous deposits had formed (Melville Glaciation: Early Miocene).

No Middle Miocene through Pleistocene deposits have so far been distinguished in the South Shetland Islands, save for unfossiliferous volcaniclastic rocks (Melville Peak volcano: Late Pleistocene).

ARCHAEAN TERRANES OF ANTARCTICA

L.P. Black, J.W. Sheraton, Bureau of Mineral Resources, G.P.O. Box 378, Canberra, A.C.T. 2601, Australia.

P.D. Kinny, Research School of Earth Sciences, Australian National University, G.P.O. Box 4, Canberra, A.C.T. 2601, Australia.

INTRODUCTION

It has long been recognised that the East Antarctic Shield is dominantly composed of Precambrian rocks, most of which are of Proterozoic age. Isolated Archaean cratonic blocks (which are most probably volumetrically subservient in their natural or concealed outcrop) were often initially identified on the basis of enclosed mafic dyke swarms. They are bounded by Middle to Late Proterozoic high-grade metamorphic belts such as those in the northern Prince Charles Mountains (MacRobertson Land), the Rauer Islands region (Princess Elizabeth Land) and the Rayner Complex of Enderby and Kemp Lands.

Some of the rocks ascribed an Archaean age are less rigorously dated than others. Erroneously old ages have arisen through the adoption of imperfectly understood methodology (e.g., as occurred in the Windmill Islands - Lovering et al., 1981), or the grouping together of unrelated samples (e.g., some of the Vestfold Hills samples studied by Collerson et al., 1983). However, most early Antarctic geochronology involved techniques which yield ages now known to be too young, having been reset by high- (and sometimes even low-) grade tectonothermal processes. The purpose of this article is to outline the geochronology of regions of indisputable Archaean age, as determined by U-Th-Pb chronology, either by the A.N.U. ion-microprobe SHRIMP or, where simple systematics were encountered, by conventional analysis. New, as well as previously published data are reported and the geochronological similarities and differences of the Archaean blocks are summarised.

Although no relevant U-Pb zircon data are yet available, it seems inescapable that at least part of the southern Prince Charles Mountains (Tingey, 1982) represent an Archaean terrane, probably at least 2800 Ma in age. Similarly, Barton et al. (1987) have shown (from Rb-Sr and Pb-Pb total rock isochrons) that the Annandagstoppane granite of Western Dronning Maud Land is about 3000 Ma old. In contrast, Williams et al. (1983) demonstrated that precursors of orthogneiss in the Windmill Islands (Wilkes Land) formed at about 1500 Ma, and not at 3500 Ma, as had originally been claimed. The two grains of approximately 3000 Ma zircon discovered by those authors in a Windmill Island paragneiss are not necessarily indicative of nearby Archaean rocks, because this region was once proximal to the Yilgarn Block (Western Australia), from which they might have been derived.

THE VESTFOLD HILLS

Although Collerson et al. (1983) concluded, mainly on the basis of Rb-Sr and Sm-Nd isotopic data, that the 400 km^2 essentially ice-free area of the Vestfold Hills experienced a prolonged Late Archaean history in which the major tectonothermal events (D_1 and D_2) were separated by several hundred million years, this has been shown to be incorrect. An extensive collection of SHRIMP analyses (Black et al., in press) shows that the igneous precursors of exposed felsic orthogneiss units (the paragneisses of the Chelnok supracrustals and the mafic and ultramafic orthogneisses have yet to be analysed) were emplaced, metamorphosed and deformed, and the region cratonised, within a 50 Ma interval. D_1 (not older than 2501±4 Ma) and D_2 (2487±6 Ma) were separated by no more than 20 Ma. The igneous precursors of the Mossel gneiss range in age from 2526±6 Ma to 2501±4 Ma, with the older age representing the "type" area in the south of the block. The igneous precursors of the Crooked Lake gneiss are also not isochronous, having an age range from south to north of 2501±4 Ma to 2486±6 Ma. A newly defined, variably deformed, syn-tectonic unit, the Grace Lake granodiorite was emplaced at 2487±6 Ma. An undeformed, post-granulite facies quartz diorite dyke was emplaced at 2477±5 Ma.

Evidence of older rocks underlying the northern part of the Vestfold Hills exists in 2800 Ma xenocrysts and zircon cores from a sample of the Grace Lake granodiorite, and grains with a minimum age of 2700 Ma within a sample of the Mossel gneiss.

THE RAUER ISLANDS

The 200 km^2 outcrops of this region adjoin the the southwestern margin of the Vestfold Block, but the contact between the two terranes is obscured by the Sorsdal Glacier. Using Sm-Nd model ages, Sheraton et al. (1984) were the first to demonstrate the presence of an Archaean component within this Middle to Late Proterozoic mobile belt. Harley (1987) estimated its abundance at 10%. However, on the basis of SHRIMP data Kinny and Black (1990) have now concluded that about half of the rocks exposed in the Rauer Islands are Archaean in age. Their occurrence in the eastern sector might suggest that these rocks are Vestfold Block equivalents which were caught up in the Late Proterozoic tectonism, but this is not the case. The Archaean of the Rauer Islands is older than that exposed in the Vestfold Hills, though it might be the same age as part of the unexposed Vestfold basement (see above).

Two distinct Archaean ages (unpublished analyses summarised in Kinny and Black, 1990) were obtained from chemically and petrologically similar, and spatially associated, tonalitic orthogneisses. Two samples of the younger of these yield indistinguishable ages (2797±9 Ma and 2810±14 Ma) for the crystallisation of their igneous precursors. That of the older gneiss

crystallised at 3269±6 Ma. A nearby paragneiss contains populations of detrital zircon grains of both ages, indicating that its sedimentary precursor was deposited later than 2800 Ma.

BUNGER HILLS REGION

Geochronologically this region appears to be quite complicated, possibly comprising elements of two, or perhaps even three discrete geological terranes. No Archaean rocks have been identified in the Bunger Hills or immediately adjoining archipelago, which consist of Early to Middle and Late Proterozoic protoliths which underwent granulite-facies metamorphism and deformation about 1190 Ma ago. However, the Obruchev Hills to their southwest contain a tonalitic orthogneiss whose precursor is dated by conventional U-Pb zircon chronology (Sheraton et al., in prep) at 2641^{+16}_{-14} Ma. A still older tonalitic orthogneiss occurs at Cape Charcot, to the west of the Denman Glacier. SHRIMP analyses show that it was derived by the deformation and granulite-facies metamorphism at 2889±9 Ma of 3003±8 Ma igneous rocks (Black et al., in prep.). The Archaean ages from the Bunger Hills region are broadly similar to values reported from the Yilgarn Block of Western Australia, which is placed nearby in Gondwana reconstructions.

NAPIER COMPLEX

The 50,000 km^2 Napier Complex of Enderby Land, which lies to the north of the dominantly Middle to Late Proterozoic Rayner Complex, contains the oldest rocks yet recognised in Antarctica, and the second oldest known terrestrial rocks. Its history extends back to at least 3870 Ma (modified after Black et al., 1986a), the age of tonalitic precursors to high-grade granulites at Mount Sones. Unpublished SHRIMP analyses show that nearby paragneiss contains the same zircon populations as the orthogneiss, which should indicate that the paragneiss was derived from locally eroded rocks, and that deposition of the original sediments post-dated emplacement of the tonalite. Intense tectonism has destroyed all unequivocal field evidence of their relative ages. Morphological and isotopic complexity of zircon in these and other Napier Complex rocks supports structural and metamorphic evidence that the region experienced a long, involved history. Three major tectonothermal events are deduced (see Black et al., 1986b) to have occurred at about 3000 Ma (D_1), about 2900 Ma (D_2) and 2456^{+8}_{-5} Ma (D_3). The first two of these events occurred under high granulite-facies conditions and the last at transitional granulite grade. A recent (unpublished) study has focussed on the delineation of the age of the felsic orthogneiss precursors. It shows that the precursor of orthogneiss at Gage Ridge is of similar age to that of the orthogneiss at Mount Sones, and that orthogneisses at Proclamation Island and Dallwitz Nunatak were derived from ca. 3000 Ma igneous precursors, the intrusion of which heralded the onset of the first major deformation in the area, nearly 900 Ma after the initial formation of felsic crust. The igneous protoliths of the Napier Complex orthogneisses were derived from two distinct source materials (Sheraton and Black, 1988),

although there is no apparent correlation with their primary ages. One suite, comprising both ca. 3870 Ma and 3000 Ma precursors, was derived from the mantle by a two-stage process involving the partial melting of mafic rocks under hydrous conditions. The other suite, for which the ca. 3000 Ma Proclamation Island charnockite is currently the only reasonably dated example, formed by intracrustal melting at low P_{H2O}.

MAJOR ARCHAEAN EVENTS IN ANTARCTICA

U-Pb dating has temporally quantified at least some of the more important geological events to have fashioned the East Antarctic Shield. Some ages are currently unique to a particular block, whereas others occur in more than one. The significance of the common ages, and in particular their relevance to previous configurations of the Archaean blocks of Antarctica, must await considerably more investigation. Each of the studied regions has a unique total chronological signature, and it will be interesting to see if this trend continues when terranes such as the southern Prince Charles Mountains are investigated in detail.

Components of the Napier Complex yield by far the oldest Antarctic age (3870 Ma). The next most ancient age (3270 Ma) is also currently unique, representing part of a composite Archaean terrane within the Rauer block. The 2800 Ma age for this terrane is also currently unique for Antarctica, with the possible exception of as yet imprecisely dated rocks from the southern Prince Charles Mountains. Approximately 3000 Ma ages are very common within the Napier Complex, where they record metamorphism-tectonism (D_1) and igneous emplacement. Relatively imprecisely defined 2900 Ma U-Pb discordia are believed to date D_2 within the Napier Complex. Both of the latter ages are also recorded in the Bunger Hills region to the west of the Denman Glacier, where igneous emplacement occurred at 3000 Ma and high-grade deformation-metamorphism at 2900 Ma. The 2640 Ma age for igneous emplacement in the Obruchev Hills is not yet duplicated elsewhere in Antarctica. In contrast, ages of about 2500 Ma, marking the end of the Archaean, are ubiqitous in both the Napier Complex (where there was igneous emplacement and the major D_3 tectonothermal event) and in the Vestfold Hills, which is the unique region of this study in terms of its very compressed (i.e., probably no more than 50 Ma) history of felsic intrusion and ductile deformation.

In terms of the evolution of the entire Antarctic continent, it is relevant to note the occurrence of 2825±100 Ma (which could correlate with either the 2800 Ma or 2900 Ma events reported above) and about 2500 Ma detrital zircon components in S-type granite of the Wilson Plutonic Complex, in northern Victoria Land, adjacent to the eastern margin of the East Antarctic Shield (Black and Sheraton, 1990). These zircons are of suitable age to have been derived from Archaean blocks within the East Antarctic Shield itself, though they might alternatively have originated from once adjoining, but now separated parts of Gondwana.

REFERENCES

BARTON, J.M. Jr, KLEMD, R., ALLSOPP, H.L., AURET, S.H. and COPPERTHWAITE, Y.E. 1987. *Contributions to Mineralogy and Petrology,* **97**, 488-496.

BLACK, L.P., WILLIAMS, I.S. and COMPSTON, W., 1986a. *Contributions to Mineralogy and Petrology,* 94, 427-437.

BLACK, L.P., SHERATON, J.W. and JAMES, P.R., 1986b. *Precambrian Research,* 32, 343-368.

BLACK, L.P., KINNY, P.D., SHERATON, J.W. and DELOR, C.P., in press. *Precambrian Research.*

BLACK, L.P., SHERATON, J.W., TINGEY, R.J. and McCULLOCH, M.T., in prep.

COLLERSON, K.D., REID, E., MILLAR, D. and McCULLOCH, M.T., 1983. *Antarctic Earth Science,* Australian Academy of Science, Canberra: 77-84.

HARLEY, S.L., 1987. *Australian Journal of Earth Sciences,* 34, 175-207.

KINNY, P.D. and BLACK, L.P., 1990. *Gondwana: Terranes and Resources*, Tenth Australian Geological Convention, Hobart. Geological Society of Australia, Abstracts, 25, 251-252.

LOVERING, J.F., TRAVIS, G.A., COMAFORD, D.I. and KELLY, P.R., 1981. In Glover,J.E. and Groves, D.I. (Eds). *Archaean Geology,* Geological Society of Australia Special Publication, 7, 193-203.

SHERATON, J.W., BLACK, L.P. and McCULLOCH, M.T, 1984. *Precambrian Research,* 26, 169-198.

SHERATON, J.W. and BLACK, L.P., 1988. *Lithos,* 21, 37-52.

SHERATON, J.W., BLACK, L.P. and TINDLE, A.G., in prep.

TINGEY, R.J. 1982. *Antarctic Geoscience,* University of Wisconsin Press, Madison: 455-464.

WILLIAMS, I.S, COMPSTON, W., COLLERSON, K.D., ARRIENS, P.A. and LOVERING, J.F. 1983. *Antarctic Earth Science,* Australian Academy of Science, Canberra: 73-76.

CORRIDOR AEROGEOPHYSICS OF THE SOUTHEASTERN ROSS TRANSECT ZONE OF WEST ANTARCTICA (CASERTZ), 1990-1991

D.D. Blankenship, Byrd Polar Research Center, The Ohio State University, Columbus, Ohio, U.S.A.

S.M. Hodge, U.S. Geological Survey, Tacoma, Washington, U.S.A.

R.E. Bell, Lamont-Doherty Geological Observatory, Palisades, New York, U.S.A.

K.A. Najmulski, Byrd Polar Research Center, The Ohio State University, Columbus, Ohio, U.S.A.

D.L. Wright and J.C. Behrendt, U.S. Geological Survey, Denver, Colorado, U.S.A

During the 1990-91 Antarctic field season a program of airborne geophysics was begun under the auspices of the U.S. Antarctic Program in the Ross Transect Zone of West Antarctica. This project fielded an ice-penetrating radar as well as airborne gravity and aeromagnetic systems in a de Havilland Twin Otter. This aircraft was positioned using GPS satellite navigation and a radio transponder network as well as by high-resolution pressure altimetry. The integration of these instruments in a Twin Otter was made possible by the recent reduction in size, power consumption, and complexity of systems for digital data acquisition, transmission and recording.

The ice-penetrating radar is a pulsed 60 Mhz system with 10 kw of peak power that will penetrate up to 3,500 meters of the relatively "warm" ice of West Antarctica. The radar unit was originally built by the Technical University of Denmark (TUD) for a specially modified LC-130 transport aircraft. The antenna system for this radar consists of a flat-plate folded dipole suspended 1.25 meters beneath each wing of the Twin Otter. These antennas, which were also constructed by TUD as part of the original LC-130 radar system, are capable of transmitting or receiving simultaneously. The radar signals were digitized at a 50 Mhz sample rate and stacked over 2,000 sweeps which corresponds to a track-line distance of about 20 meters. The digitizer/stacker unit (DSU) was built by the U.S. Geological Survey. During the course of the season both the TUD radar and the DSU proved completely reliable and the data quality were excellent.

The aeromagnetic system consisted of a proton precession magnetometer (a Geometrics 813 supplied by the U.S. Geological Survey) with its sensor mounted in a bird towed 30 meters below the aircraft. The aeromagnetic tow system proved to be quite stable aerodynamically, and the magnetometer provided high quality data.

Airborne gravity was obtained with a Bell Aerospace marine gravity meter (BGM-3) on loan from the Unisys corporation coupled to a data buffer constructed by Lamont-Doherty Geological Observatory. Results of gravity experiments are described in a companion abstract by Bell and others.

The primary horizontal positioning of the aircraft is provided by a UHF radio-navigation network consisting of five remote transponders operating at 427.5 MHz that are polled by an aircraft-mounted master transponder. The system reliably yielded horizontal positions to better than five meters; these positions were updated at one-half second intervals. Ranges of over 100 kilometers were obtained routinely using six-meter antenna towers at the remote sites although unexpected topographic relief of several tens of meters caused some shadowing. No interference was experienced between the master radio transponder and any of the geophysical or navigation instruments mounted in the aircraft.

Satellite positioning was provided by both P-code (a Texas Instruments 4100) and CA-code (two Trimble 4000's) GPS receivers that were on loan from The Ohio State University and Massachusetts Institute of Technology, respectively. Both satellite positioning and pressure altimetry are explained in the companion abstract of Bell and others.

The gravity and magnetic measurements as well as the radio navigation, P-code GPS, and pressure altimetry information were transmitted by fiber-optic link to a single control computer where they were combined with the digitized radar signals and recorded on 8 millimeter video tape. All data streams were examined continuously during flight on a pair of color monitors.

The field work was performed in a 9,000 square kilometer survey block on the eastern edge of interior Ross Embayment as well as along 1200 kilometers of reconnaissance profiles over the sinuous ridge that lies along the axis of the Byrd subglacial basin as well as the Horlick Mountains traverse route of 1958-59 that extends from Byrd Station to the Wisconsin Range in the Transantarctic Mountains. Systems tests were flown repeatedly along a 130 kilometer profile over the extremely rugged topography on the western flank of the Ellsworth-Whitmore crustal block. In addition to about 2,000 kilometers of profiles flown for systems testing and integration, about 3,000 kilometers of simultaneous radar and gravity and 1,000 kilometers of simultaneous gravity and magnetics were accomplished. A prototype of the radar suppression circuitry that will allow simultaneous radar, gravity and magnetic experiments has been ground tested and will be fielded in the 1991-92 season.

SOME FEATURES OF THE LATE PLEISTOCENE AND HOLOCENE HISTORY OF THE BUNGER HILLS (EAST ANTARCTICA)

D.Bolshiyanov, Arctic and Antarctic Research Institute (AARI), 38 Bering Street, 199226 Leningrad, USSR.
S.Verkulich, AARI.
Z.Pushina, VNIIOceangeologiya, 1 Maclin Street, 190121 Leningrad, USSR.
E.Kirienko, Geographical Institute of the Leningrad University, 41 Sredniy Street, 199004 Leningrad, USSR.

Soviet investigations of the Bunger Hills, the biggest coastal oasis of East Antarctica, were resumed between 1987 and 1990. The present research concentrates on paleogeography. Our investigations include geomorphology, fresh water lake and marine sediments, chemical hydrology, as well as organic and mineral deposits on land. Bottom sediments are the major witness of the most important events, which occurred in the process of interaction between glaciers and the sea in the region of Bunger Hills. These hills constitute an archipelago of islands which are surrounded by ice shelf on the North and West and by the grounded ice sheet to the South and East.

The geomorphology of the oasis is particularly rugged. The oasis as a whole was formed before the glacial stage of its history. Block structure is a main feature of its tectonic composition. There are many valleys which were formed along fault lines. Glaciers were not the main cause of the relief observed in the oasis.

Bottom sediments occur in the lakes, which occupy the deepest parts of the valleys. The biggest lakes are Figurnoe, Dolinnoe, Dalekoye and Ptichye. They are elongate and very deep. Maximum depth discovered is 145 m (Figurnoe lake). In the course of sampling more than 40 cores from 0,02 to 1,9 m

long, we were able to establish the stratigraphy of the bottom sediments. The main components are thin layered mineral and organic (algae, moss) deposits. Sediments, which consist of only minerals, were recovered from 75 m in Lake Dalekoye. Varvometric analysis of a 0,5 m core showed that the thickness of paired layers deposited during one year ranges from 0,02 to 7,8 mm. There are 3000 pairs of layers in this core. Statistical analysis of the sampled data shows a periodicity of intensive sedimentation in the lake at 5, 13, 21 year rhythmical intervals.

Below 1393 pairs of annual layers (varves) of the fresh water Lake Dalekoye at 0,2 m there is a 5,25 mm thick interbed. It contains marine diatoms among which the dominant one is Hyalodiscus obsoletus Sheshuk.

In most cases bottom sediments of fresh water lakes are characterised by complex interstratification of mineral and organic silts. At present blue-green algae and mosses live in depths as great as 140 m. In some lakes mosses and algae form compact organic silts with known thikness of 1,9 m.

Radiocarbon dating of organic silts in the lower parts of cores demonstrated their Early Holocene age (Fig.1). Usually aleurites and clays lay under the organic silts. Marine diatoms have been discovered in such sediments of Burevestnik Lake. By their stratigraphic position and diatom composition they relate to the preholocene stage of sea basin development.

Diatom analysis of fresh water lake sediments also showed changing conditions in different lakes. On the whole the dominant diatom species in fresh water sediments is Amphora sp. Usually in the middle parts of cores there are no diatoms. That fact proves that conditions for their existence were unfavorable during long periods of the lake development.

Bottom marine sediments are evidenced by coarser, sandy, aleuriteceous deposits with megaclastic material resulting from a considerable influence of ice which limited the interaction between the basins and the sea.

Transkriptsii Bay is the basin which is separated from sea by an ice shelf. This basin has never been free of ice

during at least the last 30 years. Rybiy Khvost Bay is connected with the sea more closely. Sometimes its ice breaks up in the summer. Irregular diurnal tides are one of the proofs of the connection between the bays and the sea.

Diatom analysis of a 0,75 m core from Transkriptsii Bay showed that ecological conditions were very unfavorable during the basin's existence. Lower layers were deposited in conditions of access by oceanic water masses, when the oceanic subantarctic species Thalassiosira Lentiginosa (Janisch) Hasle dominated among the diatoms.

After that, sea level was falling during the transitional period, in which Hyalodiscus obsoletus Sheshuk, dominated. At the same time the quantity of oceanic diatom valves decreased while the sublitoral diatom species increased.

The third phase is characterised by the further drop of sea level. During that phase the sublitoral diatoms Pinnularia quadratarea A.S. and Cocconeis Sp. dominated. In depth of 0,18 to 0,22 m there occur in the core diatoms dominated by the oceanic Thalassiosira gracilis. This fact proves a new penetration of oceanic masses into the ice dammed marine basin. The upper layers of the core (0,0 - 0,18 m) contain cold water diatoms dominated by marine sublitoral Cocconeis sp., sea ice Eucampia balaustium Castr. Sedimentation conditions during this interval were very much the same as the modern ones.

Microfaunal analysis of deposits has shown that the conditions for foraminifers were more favourable in Rybiy Khvost Bay; however the quantity of foraminifer species and shells is low. In the bay sediments, the agglutinated Trochammina squamata and Trochammina sp. dominated. There are no such foraminifer associations in deposits of Mawson Sea and under the Apfel Glacier, that prove a long isolation of sea bays formed during ice shelf damming.

Organic sediments at nesting sites of petrels (Pagodroma nivea) are the life activity product of birds and they have a clear lamination. Petrel occupation time of the oasis and its parts was determind by radiocarbon dating of organic sediments. Oldest dating relate to the Early Holocene.

The thickness of organic material shows the duration of nest inhabitance (Fig. 1).

The distribution of lichens on the oasis is an indirect criterion for the mapping out of the "ancient" and "modern" territory sectors. One of the most widespread lichen species (Buellia frigida Darb.) was subjected to analysis. The maximum diameter of the specimen found in each station has been plotted on the map (Fig. 1).

Terrace marine deposits were subjected to radiocarbon and microfaunal analyses. Only one section of marine deposits has been discovered in 5 - 7 m terraces of Thomas Island. Valves of Laternula elliptica occured in it, and have been dated at 5480 ± 40 years B.P. (LU - 2292). Foraminifer shells and sponge spicule have been found in sediments of terraces at 20, 25 -27, 22 - 35, 40m.

Chemical hydrological analysis of fresh water and marine basins showed marine cation-anion relations both in basins connected with sea, and in most cases, in fresh water lakes. Such relations show that almost all the basins of this oasis were recently connected with the ocean. Some of them have a considerable mineralisation, which is much higher than in the modern sea water masses.

Results. Marine diatom associations in the base of Transkriptsii Bay core, foraminifers, ostracods and sponge spicule in marine terrace sediments and marine water chemistry of fresh water lakes prove that large scale transgression occurred in Bunger Hills when the whole of the oasis was submerged under marine waters. Probably, this event took place in the Late Pleistocene. Glaciers spread here after the reggression of marine conditions. However, that spread was not caused by spreading of the Antarctic ice sheet, because deglaciation began from the central parts of the oasis. The proof for this deglaciation is found in unfundamental transformation of water bonds in inland basins and in distribution of petrel nests.

The deglaciation of hills, the occupation of fresh water basins by algae and mosses and the nesting in the hills by birds had started in the Early Holocene.

The hills were glaciated several times during the Holocene. Valleys were dammed by firn and small glaciers. That is why large masses of water accumulated in the valleys and periodically drained out of them after ice dams broke. The erosion was of a catastrphic character and deposited an anomalous thickness of the lake sediments. Lichen distribution on hills shows that glaciers and firn were local.

In the middle of the Holocene sea level rose again relatively to about 10 metres above its modern position.

1400 years ago marine waters penetrated into the modern fresh water Lake Dalekoye.

Even small oscillations in sea level resulted in obvious changes in the position of ice shelve and of the Antarctic ice sheet margin.

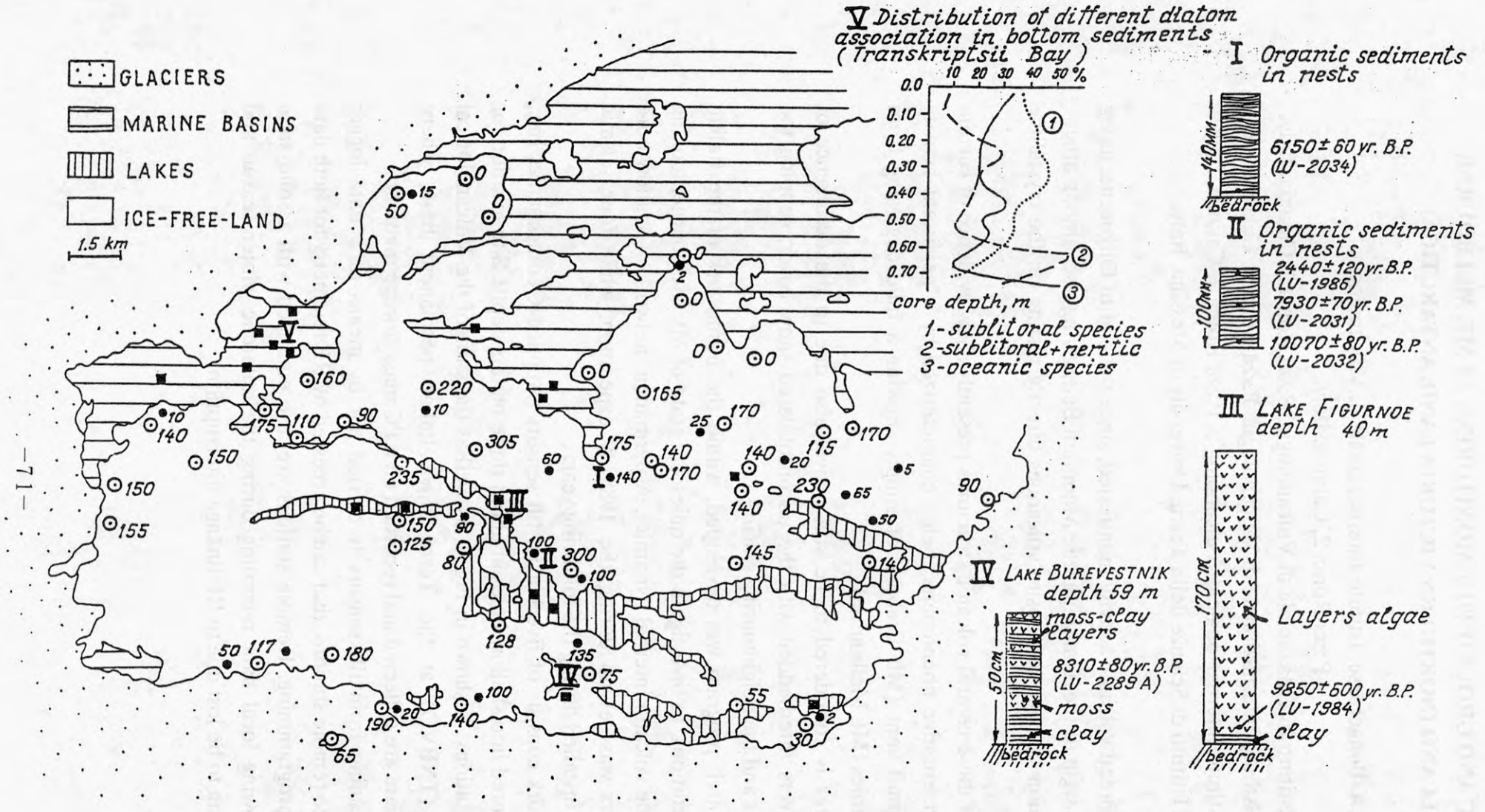
GLACIERS
MARINE BASINS
LAKES
ICE-FREE-LAND
1.5 km
V Distribution of different diatom association in bottom sediments (Transkriptsii Bay)
10 20 30 40 50 %
0.0
0.10
0.20
0.30
0.40
0.50
0.60
0.70
core depth, m
1-sublitoral species
2-sublitoral+neritic
3-oceanic species
I Organic sediments in nests
140mm
6150±60 yr. B.P. (LU-2034)
bedrock
II Organic sediments in nests
100mm
2440±120 yr. B.P. (LU-1986)
7930±70 yr. B.P. (LU-2031)
10070±80 yr. B.P. (LU-2032)
III Lake Figurnoe depth 40 m
170 cm
Layers algae
9850±600 yr. B.P. (LU-1984)
clay
bedrock
IV Lake Burevestnik depth 59 m
50 cm
moss-clay layers
8310±80 yr. B.P. (LU-2289 A)
moss
clay
bedrock
•10 – thickness of organic sediments in nests (mm)
⊙305 – maximum diameter of Buellia frigida (cm)

Fig. 1

SEISMIC AND GROUND TILT MONITORING AT MT. MELBOURNE VOLCANO (NORTHERN VICTORIA LAND, ANTARCTICA)

A. Bonaccorso, Istituto Internazionale di Vulcanologia, P.zza Roma 2, Catania, Italy.
G. Falzone, Istituto Internazionale di Vulcanologia, P.zza Roma 2, Catania, Italy.
E. Privitera, Istituto Internazionale di Vulcanologia, P.zza Roma 2, Catania, Italy.
L. Villari, Istituto Internazionale di Vulcanologia, P.zza Roma 2, Catania, Italy, and Istituto di Scienze della Terra, University of Messina, Italy.

A widespread volcanic activity manifested, since the end of Oligocene, along the eastern margin of the Transantarctic Mountain Belt, giving rise, among others, to the formation of huge composite volcanoes directly resting on the crystalline basement.

A few of those central volcanic structures presently show evidence of current and/or recent eruptive phenomena, being characterized by a persistent activity from the summit vent (Mt. Erebus), or simply showing a mild degassing from summit fumaroles (Mt. Melbourne).

The latter is considered to be still active, also due to the occurrence of pyroclastic layers interbedded with the unconsolidated snow cover, capping the volcano slopes and the neighbouring glaciers.

A research program was developed, within the framework of the Italian antarctic expeditions, to investigate the quiescent state of Mt. Melbourne, looking deeper into the volcano internal dynamics. A permanent network of shallow bore hole tiltmeters was set up during the 1988/89 expedition, while four seismic stations were installed during the following year.

The tilt network consists of five biaxial tilt sensors (Applied Geomechanics Inc., 700 series), bored into shallow holes at about three meters depth. Site location for the remote stations is shown in Fig. 1, as well as the sitingof the Volcanological Observatory (TNBVO) at the Terra Nova Italian permanent base, where telemetered data are collected and recorded on a PC mass storage memory.

Data reading from tilt sensors is carried out by means of a data logger installed at the remote stations, that can be accessed by RF telemetry for both data retrival and programming. Remote stations are also equipped with a solid state memory, allowing local data recording during the antarctic winter season and preventing data to be lost due to RF linkage interruption.

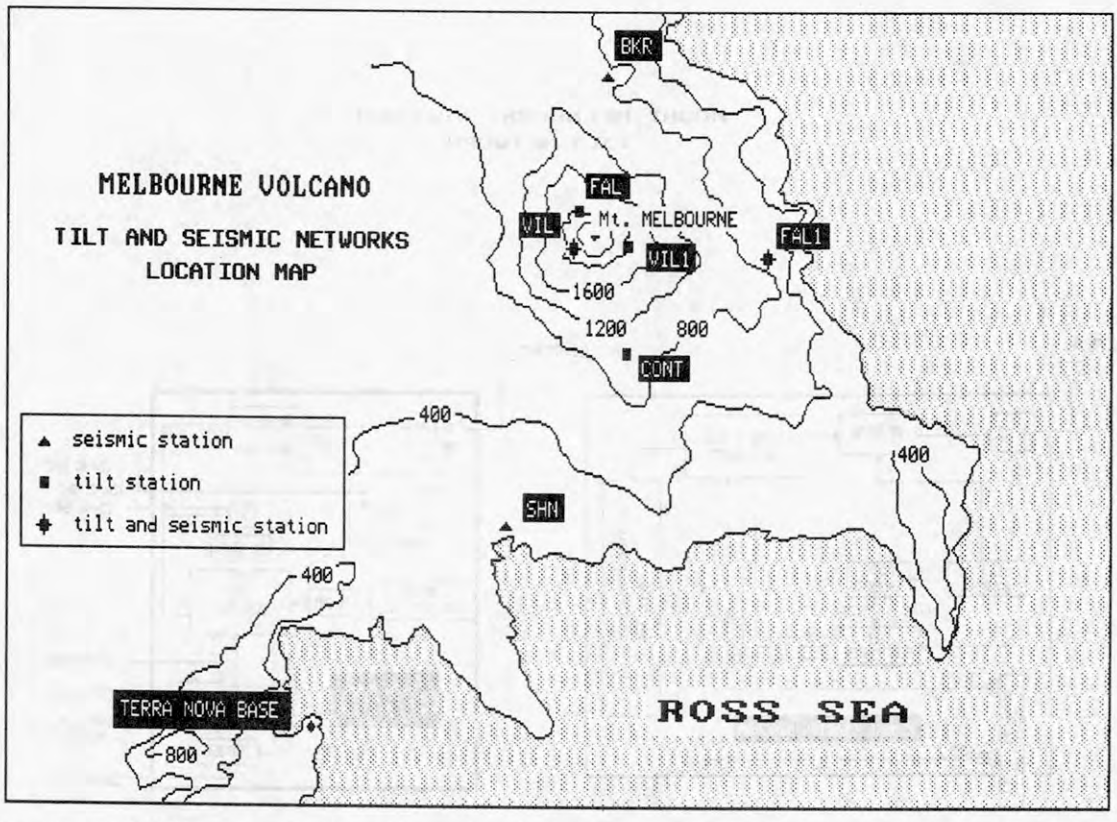

Fig. 1 - Location map of the tilt and seismic permament networks of Mt. Melbourne Volcano (Northern Victoria Land, Antarctica)

Temperature at the tilt stations is measured by three thermocouples, two of which are located at different depth inside the bore hole, allowing an extimate of the vertical temperature gradient affecting the permafrost, while the third monitors the external (atmosferic) temperature. A block diagram showing the tilt network architecture is presented in Fig. 2.

A permanent seismic network, consisting of four digital stations, have been set up, during the 1989/90 Italian antarctic expedition, in the Mt. Melbourne area.

Seismic stations are equipped with short period Geotech S-13 geophones and signal conditioning is carried out by an expressly designed data acquisition systems, based on Geotech Pdas-100. A 50 Hz signal sampling at the remote station is constrained by a local trigger and the detected events are recorded on a non volatile memory.

Two of the four seismic stations (3 components), located in a line of sigth to the Terra Nova Italian base, are programmed to send daily, by RF digital telemetry, the collected data to the Volcanological Observatory, where they are recorded on a PC hard disk. At the other two stations (only vertical component) of the network, on the opposite side of the volcanic structure, data are locally stored on a solid state memory and periodically retrived by a "lap-top" computer.

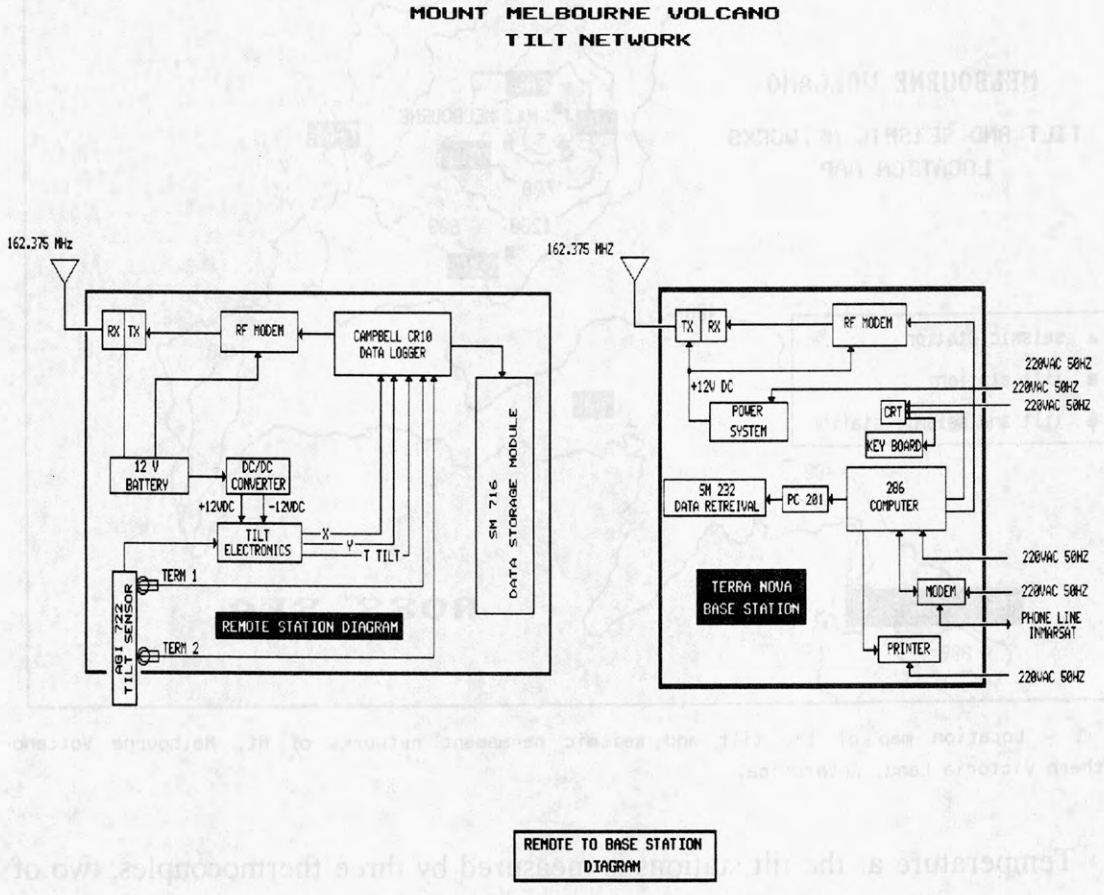

REMOTE TO BASE STATION
DIAGRAM

Fig. 2 - Block diagram of Mt. Melbourne Volcano tilt network (Northern Victoria Land, Antarctica)

Time tic for syncronization is produced by a GPS receiever, sited at TNBVO (Trimble Navigation, Mod. 5000A), and transmitted to the remote stations: a radio repeater is located on the Mt. Melbourne summit to ensure propagation towards seismic stations in the shadow area.

The seismic network architecture is illustrated in the block diagram of Fig. 3.

A project is currently in progress to convey both seismic and tilt data, progressively stored on the PC terminals, to the VAX main frame operating at the Italian Base, for a subsequent transmission to Italy by satellite telemetry (INMARSAT).

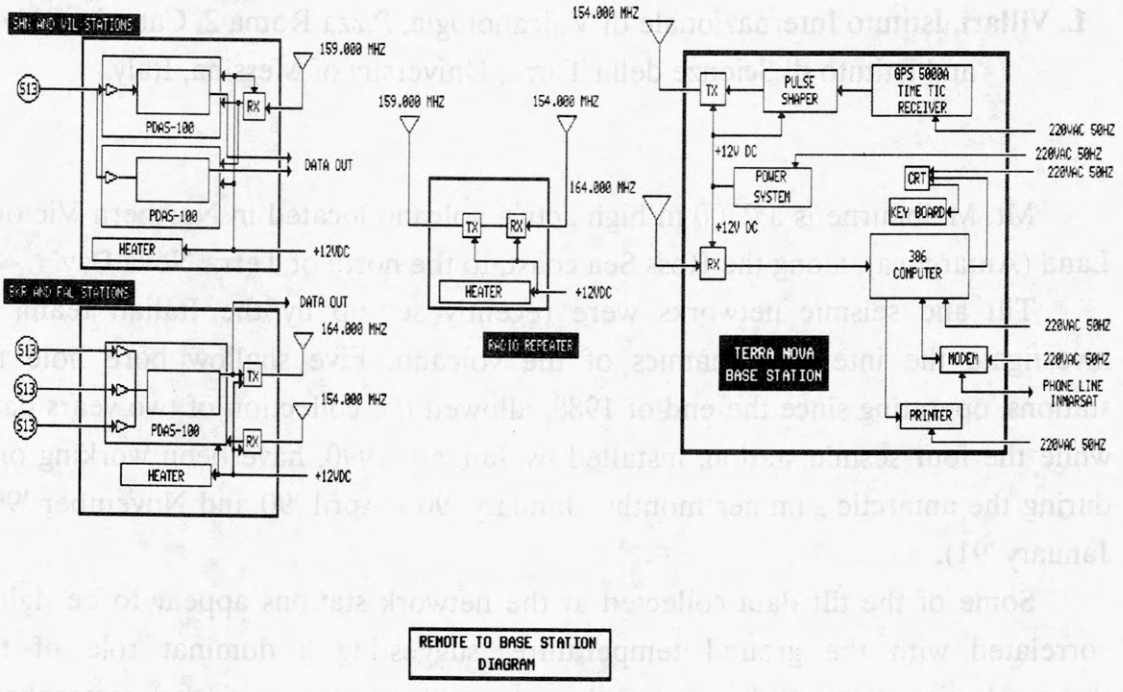

Fig. 3 - Block diagram of Mt. Melbourne Volcano seismic network (Northern Victoria Land, Antarctica)

SEISMICITY AND GROUND DEFORMATION AT MT. MELBOURNE VOLCANO (NORTHERN VICTORIA LAND, ANTARCTICA)

A. Bonaccorso, Istituto Internazionale di Vulcanologia,
P.zza Roma 2, Catania, Italy.
E. Privitera, Istituto Internazionale di Vulcanologia, P.zza Roma 2, Catania, Italy.
L. Villari, Istituto Internazionale di Vulcanologia, P.zza Roma 2, Catania, Italy,
and Istituto di Scienze della Terra, University of Messina, Italy.

Mt. Melbourne is a 2700 m high active volcano located in Northern Victoria Land (Antarctica), along the Ross Sea coast, to the north of Terra Nova Bay.

Tilt and seismic networks were recently set up by the Italian team, to investigate the internal dynamics of the volcano. Five shallow bore hole tilt stations, operating since the end of 1988, allowed the collection of two years data, while the four sesmic station, installed by January 1990, have been working only during the antarctic summer months (January '90 - April '90 and November '90 - January '91).

Some of the tilt data collected at the network stations appear to be tightly correlated with the ground temperature, suggesting a dominat role of the thermoelastic effect, induced by the seasonal variation of the atmospheric temperature. The application of different filtering procedure to remove the thermoelastic noise, allowed to point out the presence of a deformation phase exceeding the confidence limit, which affected two (VIL and FAL) of the five stations, respectively located on the western and northern high slopes of the volcano.

In spite of the short operating time lapse, several hundreds of seismic events were recorded at the permanent seismic network, whose efficiency was temporarly implemented by portable stations during summer 1990/91. Most of the recorded events appear to be icequakes, related to the dynamics of the neighbouring glaciers. Regional earthquakes were also recorded, showing typical signature of crustal faulting. Data analysis carried out on wave forms and associated spectra, allowed a preliminar characterization of the identified event classes.

LATE PROTEROZOIC–PALEOZOIC EVOLUTION OF THE TRANSANTARCTIC MOUNTAINS: EVIDENCE FROM ISOTOPIC STUDIES OF GRANITIC AND METAMORPHIC ROCKS

Scott G. Borg and Donald J. DePaolo

Berkeley Center for Isotope Geochemistry
University of California
Berkeley, California, 94720, USA

The crystalline basement rocks of the Transantarctic Mountains record the late Proterozoic–Paleozoic development of a large portion of the Panthalassa margin of Gondwana. This region is unaffected by later compressive tectonism. Traditional geologic field studies aimed at understanding the tectonic evolution of this region have been severely limited by problems associated with difficult access. Consequently, we have approached this problem via regional studies aimed at 1) identifying, delineating, and characterizing major crustal provinces through studies of Paleozoic granites and xenoliths from Late Tertiary volcanic rocks, which are geochemical probes of the continental crust, and 2) understanding relations between crustal provinces through isotopic constraints on tectonodepositional models of metasedimentary rocks. Toward this end, we have developed a model for interpretation of crustal structure and tectonic environment from granite isotopic data and we are assembling an isotopic-geochemical database of granitic and metamorphic rocks that allow us to model the tectonic evolution of a 2000 km stretch of the Transantarctic Mountains from Victoria Land to the Horlick Mountains. We are in the process of extending this data base to southeastern Australia.

Early Paleozoic granitic rocks are found throughout the Transantarctic Mountains except in the NE part of northern Victoria Land. In the central Transantarctic Mountains the granites define three crustal age provinces (from west to east): a 2.0 Ga province along the margin of the Archean East Antarctic Craton, a ≈1.7 Ga province outboard of the 2.0 Ga province, and a province with no Precambrian crystalline basement furthest outboard. To the north, we have identified the outboard two provinces in southern Victoria Land but in northern Victoria Land we have so far only identified the central (≈1.7 Ga) province. Provenance of metasediments in the ≈1.7 Ga province and an occurrence of oceanic basalt between the 2.0 and ≈1.7 Ga provinces in the central Transantarctic Mountains indicate an allochthonous origin of the ≈1.7 Ga province.

Middle Paleozoic granites in northern Victoria Land define another Proterozoic (2.0 Ga) province allochthonous to pre–Permian Gondwana. With correlation of provinces to southeastern Australia, the tectonic history deduced for northern Victoria Land suggests that much of southeastern Australia (including Tasmania, western Victoria and New South Wales) was also allochthonous to pre–Permian Gondwana.

In addition to inferences about crustal structure at the time of pluton emplacement, the isotopic province boundaries provide a baseline for evaluating younger plate movement. Apparent offsets of the isotopic province boundaries suggest several right–lateral strike–slip faults approximately parallel to the Transantarctic Mountains. These are most likely associated with opening of the Ross Sea.

THE ABSOLUTE GRAVITY STATION AND THE MT. MELBOURNE GRAVITY NETWORK IN TERRA NOVA BAY (VICTORIA LAND, EAST ANTARCTICA).

E. Bozzo, G. Caneva, Dipartimento Scienze della Terra, Sez. Geofisica, Università di Genova, Viale Benedetto XV, 5, 16132 Genova, Italy.

G. Cerutti, Istituto di Metrologia Colonetti, CNR, Strada delle Caccie,73, 10123 Torino, Italy.

R. Lanza, Dipartimento Scienze della Terra, Università di Torino, Via Accademia delle Scienze,5, 10123 Torino, Italy.

I. Marson, Istituto di Miniere e Geofisica Applicata, Università di Trieste, Via Valerio 10, 34127 Trieste, Italy.

Within the framework of the Earth Sciences Project in Antarctica sponsored by the Italian government (CNR and ENEA), a gravity program was initiated during the 1989/90 expedition. Its main purpose was to establish the gravity datum, through an absolute measurement of the gravity acceleration, and a gravity network to monitor ground deformation and mass or density variations in the volcanic area of Mount Melbourne. 14 gravity sites were established during the Antarctic summer 1989/90. In the 1990/91 expedition, the Italian team of the Istituto di Metrologia "G. Colonetti", Torino, established the first absolute gravity site on the Antarctic continent. The measurement of the gravity acceleration g, based on the symmetrical rise and fall method, was performed at the Terranova Bay Italian Station, at a site (IAGS) of coordinates Lat (S) 74^{o} 41' 36.13" Long (E) 164^{o} 05' 59.26" Height 54.3 m calculated in WGS84 system, from December 20 to December 27, 1990. A total of 166 independent measurements were carried out, with a resulting standard error of 1.2 μgal (1 μgal = 10^{-8} m sec^{-2}). Estimating an error budget up to 3-4 μgal due to systematic sources, the final g value, measured at 0.91 m above the floor level, has been computed to be 982 854 919 + 4 μgal. The most relevant conclusions of this experiment regard the establishment of the gravity datum in Antarctica with the highest accuracy allowed by modern technology, which, in turn, may serve as reference site for further detailed gravity surveys and for long term time-dependent gravity variations associated for instance to volcanic activity. This work also contributes to the definition of the geodetic reference level.

GROUND MAGNETICS IN CENTRAL VICTORIA LAND (EAST ANTARCTICA).

E. BOZZO, A. COLLA, Dipartimento di Scienze della Terra, Sez. Geofisica, Università di Genova. Viale Benedetto XV,5 - 16132 Genova, Italy.

A. MELONI, Istituto Nazionale di Geofisica, Via di Villa Ricotti,42 - 00161 Roma,Italy.

Ground magnetic surveys across Central Victoria Land (CVL), East Antarctica, were carried out during the Antarctic summers 1985-1990 within the "Progetto Nazionale di Ricerche in Antartide". These surveys were helicopter-supported and cover an area of about 15,000 km^2 located between latitudes 73^o 55' and 75^o 15' (i.e. between the Aviator Glacial and the Drygalski Ice Tongue) and longitudes 161^o 30'E and 165^o 30'E (i.e. along the coast of the Ross Sea).

The variometric data collected at Scott Base (N.Z.) during the first expedition and at the Italian Geomagnetic Observatory in the Terra Nova Bay Station area during the other expeditions, were used to correct for the daily and the secular variations of the geomagnetic survey data.

The corrected values of the field data were interpolated to produce the contour maps. The first of these shows the residual field map of the area. Further elaboration of our measurements has produced three other geomagnetic maps : (1) a high pass filter (cut-off wavelength of 20 km) map; (2) a low pass filter (cut-off wavelength of 80 km) map; and (3) an upward continuation of the geomagnetic field up to 12,000 ft map.

Magnetic susceptibility measurements (k) accompanied the entire ground survey; they were taken either on outcrops or near the stations themselves, or on samples collected during geological surveys (3,000 rock samples). A KT5 Geofyzica susceptometer was used for the measurements. Frequency distribution histograms, along with mean values, standard deviation and relative dispersion of susceptibility k values for the main bedrock types are presented. The data were used to obtain a " Magnetic Susceptibility Domains Map" . It shows that four magnetic susceptibility patterns control the induced magnetization features in the main geological units of the area: 1) Low k Domain : representing the metamorphic basement; 2) Medium-High k Domain: comprising Gabbro and Dolerite of Ordovician age; 3) High k Domain: comprising Triassic Basalts and Dolerites and Quaternary Volcanics; 4) Granite Harbour k Domain : presenting a very variable distribution in the magnetic properties of the rocks.

The maps indicate that: intense positive anomalies occur along two corridors, one near Mt. Nansen and the other near Mt. Melbourne, all the more intense of them are of surficial nature, all rock types characterized by high susceptibility produce geomagnetic anomalies, even if their outcrop is not extensive . These rocks belong to the Mt. Melbourne volcanics, Jurassic dolerites and Granite Harbour plutons. None of the formations of the metamorphic complex are responsible of intense magnetic signals.

THE SOUTHERN RIM OF THE PACIFIC: NEW WORK ON THE PRE-CENOZOIC ROCKS OF MARIE BYRD LAND.

J D Bradshaw, University of Canterbury, Christchurch, New Zealand.
I W D Dalziel, Institute for Geophysics, University of Texas, Austin, Texas, USA.
V. Di Venere, Lamont Doherty Geological Observatory, Palisades, New York, USA.
S B Mukasa, University of Michigan, Ann Arbor, Michigan, USA.
R B Pankhurst, British Antarctic Survey, Cambridge, U.K.
B C Storey, British Antarctic Survey, Cambridge, U.K.
S D Weaver, University of Canterbury, Christchurch, New Zealand.

(South Pacific Rim International Tectonics Expedition, SPRITE)

Marie Byrd Land is one of the least studied parts of Antarctica and represents a lacuna in our knowledge of the southern rim of the Pacific between New Zealand and the Andes. In the austral summer of 1990/91 a joint New Zealand-United Kingdom-United States geological programme was launched to make detailed field studies supported by extensive geochemical, geochronological and paleomagnetic analysis.

The first seasons field work in the Hobbs and Ruppert Coast areas and preliminary analysis suggest a need to revise earlier reconnaissance data. (For example, Sporli and Craddock, 1981, Wade and Wilbanks, 1972)

The Demas Range is a magmatic complex rather than a gneissic terrane. Metamorphic rocks are restricted to paragneiss and early granitoid orthogneiss enclaves. The bulk of material comprises host granitoids cut by stocks, dikes and sills of gabbro and diorite. These magmatic phases are broadly contemporaneous with abundant evidence of mutual intrusion and magma mingling.

In the central part of the area, grey hornblende-biotite granodiorites appear to be older and may be equivalent to the Devonian Ford Granodiorite of the Ranges to the west (Adams, 1987). They are variably foliated, epidotized and cut by mafic and feldsparphyric dikes. Closer to the coast in the Perry Range, the older granitoids are cut by more abundant dikes subparallel and normal to the continental margin that have previously been termed the "breakup dikes". Field relationships suggest a more complex kinematic and petrological history with early basic to intermediate east-west dikes cut by diorite sills and north-south diorite and microgranite dikes prior to a second suite of east-west mafic dikes.

The monzogranite at Kinsey Ridge is also cut by abundant dikes in a complex conjugate pattern. Sinistral and dextral offsets of the dike margins can be demonstrated and the dike rocks (and locally the granite margins) are sheared to form well developed mylonites that suggest penecontemporaneous dike intrusion and development of ductile shear zones. Nearby at Nichols Rock outcrops previously reported as Swanson Formation slates are also mylonites derived from a volcanoclastic protolith. A sinistral transtensional regime is indicated.

Pre-Cenozoic volcanogenic sequences form the country rock of many of the plutons. They comprise mainly unsorted volcanic breccia, conglomerate and sandstone of intermediate to felsic composition, with subsidiary volcanogenic mudstone, massive feldspar porphyry flows, basalts or basaltic andesites. The proposed subdivision (Grindley and Mildenhall, 1981) of the volcanic rocks into discrete Devonian and Cretaceous formations seems difficult to sustain in the field and the relationship to erratics with Devonian plant fossils to the volcanic rocks requires further scrutiny.

An alkali gabbro-syenite-alkali feldspar granite complex is widely developed in the Ruppert Coast-Hobbs Coast and appears to be the youngest plutonic suite. It intrudes the foliated granodiorite with abundant dikes and is in turn cut by occasional mafic dikes. Near Cape Burks the gabbro is cut by the syenite-alkali feldspar granite. In the Ickes Mountains suspected Cretaceous lavas said to rest unconformably on granite are roof pendants cut by the syenite-granite suite. The suite may in part be equivalent to the Byrd Coast Granite of the Ford Ranges and Edward VII Peninsula.

Satellite gravity data strongly support previously suggested relationships between Marie Byrd Land and the Chatham Rise-Campbell Plateau region of the New Zealand continent. There are however strong contrasts in pre- and post-breakup history of the two margins. Marie Byrd Land was uplifted and remained emergent, while the New Zealand margin has subsided and become the site of major sedimentary basins. Breakup magmatism also appears to be strongly asymmetric. The widespread development of alkali gabbro, syenite and "A" type granitoids in Marie Byrd Land is consistent with major continental rifting and the splitting away of the New Zealand continent. Similar rocks are not widely developed in New Zealand.

References.

Adams, C. J. 1987, Geochronology of granite terranes in the Ford Ranges, Marie Byrd Land, West Antarctica. New Zealand J. Geology and Geophysics, 30, 51-71.

Grindley, G. W. and Mildenhall, D. C. 1981, Geological background to a Devonian plant fossil discovery, Ruppert Coast, Marie Byrd Land, West Antarctica. In, Cresswell, M. M. and Vella, P. eds., Gondwana Five, Balkema, Rotterdam, pp. 23-30.

Sporli, K. B. and Craddock, C., 1981, Geology of the Ruppert Coast, Marie Byrd Land Antarctica. In, Cresswell, M. M. and Vella, P. eds., Gondwana Five, Balkema, Rotterdam, pp. 243-250.

Wade, F. A. and Wilbanks, J. R. 1972, Geology of Marie Byrd and Ellsworth Lands. In Adie, R. J. ed., Antarctic Geology and Geophysics, Universitetsforlaget, Oslo, pp. 207-14.

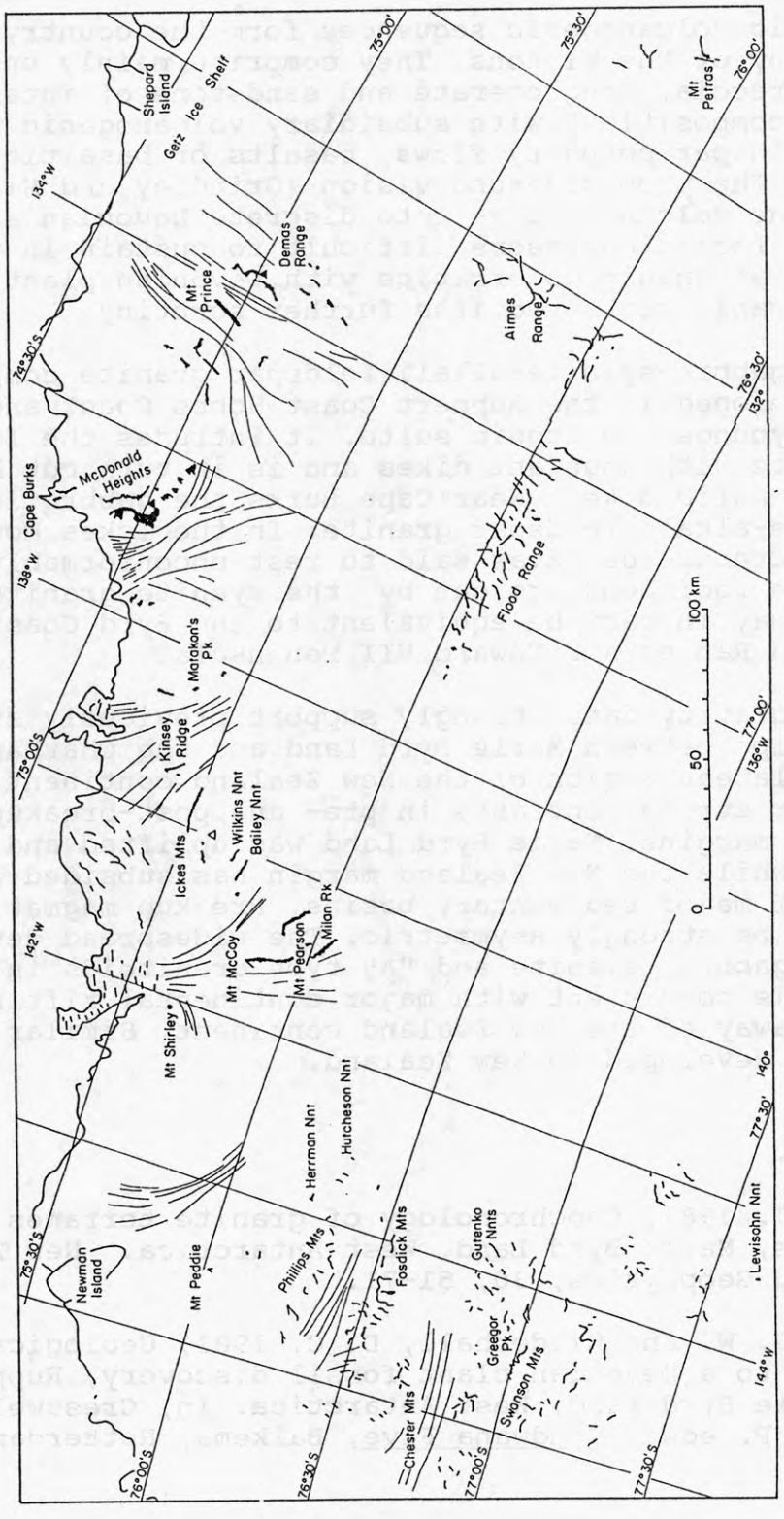

Figure 1. Main outcrop areas in the Ruppert Coast-Hobbs Coast areas.

THE STRUCTURE OF THE SHACKLETON RANGE, ANTARCTICA

Hans-Martin Braun, Geologisch-Paläontologisches Institut der Universität,
Senckenberganlage 32-34, 6000 Frankfurt / Main, Germany

The German Expedition to the Shackleton Range (GEISHA) in 1987/88 allowed detailed structural investigations in the southern and western parts of the Shackleton Range (Weddell Sea sector, Antarctica). These examinations base on earlier studies giving first insight into the distribution of the main rock units and their metamorphism and tectonics (see e.g. CLARKSON 1982; MARSH 1983a, 1983b; HOFMANN & PAECH 1983). The aim of the present study is to further elucidate the tectonometamorphic evolution of the Shackleton Range in space and time, and to establish the plate tectonic processes in this part of the Antarctic continent.

1. Tectonic structures in the Read Mountains, southern Shackleton Range

The crystalline basement of the Read Mountains, stratigraphically defined as the Read Group (see figure), comprises layered, amphibolite facies metamorphics of intermediate to mafic composition, intruded by granites, granodiorites and diorites. The metamorphic foliation generally runs parallel to the layering. Irrotational boudinage of competent layers and a local stretching lineation manifest layer-parallel extension, while ductile shear zones due to southbound thrusting followed under retrograde conditions. Structures of both extensional and compressional tectonics indicate an overall N-S sense of deformation. While the metamorphic foliation usually continues within stocks of fine-grained granites, ductile fabrics in granites containing large feldspar porphyroblasts are restricted to few mylonitic shear zones. Prominent normal faults dip steeply N or S. Another, orthogonal system of faults and minor cleavage planes strikes NW-SE or NE-SW, respectively.

The Read Group is surrounded by sedimentary rocks of very low to low grade metamorphism - however, the stratigraphic sequence shows specific regional differences.

In the southern and central Read Mountains, Read Group metamorphics and granites are cut by an erosional surface, which has been covered by sediments of the Watts Needle Formation (for localities see arrows in figure). Low illite crystallinity of paleosoil relics at the unit boundary rules out, that the sediments underwent remarkable regional metamorphism (BUGGISCH ET AL. 1990).

In the southern Read Mountains, Turnpike Bluff Group metaclastics rest upon the Watts Needle Formation (though recent dating seems to necessitate further differentiation - see BUGGISCH ET AL. 1990 - the stratigraphic term Turnpike Bluff Group is maintained for convenience here). A distinct biotite foliation dips mostly north, but curves into the basal plane of the unit inclined towards the south. Along the geological boundary, spindle shaped bodies of crystalline rocks up to about one metre in length have been encountered, showing a NW-SE lineation on their outer surfaces. Within the sediments, two generations of tight to isoclinal folds occur.

At Watts Needle, central Read Mountains, the Watts Needle Formation is topped by brecciated quartzofeldspathic basement rocks, which today form the mountain peak. These cataclasites most probably derive from porphyroblastic granites, which have been severely deformed in a regime of the brittle-ductile transition. Below this crystalline block, carbonate shales of the Watts Needle Formation are multiply folded with SE vergency, and competent limestone layers have been sheared to form mylonites with intense calcite recrystallization. According to strain determinations within basal sandstones, however, the lower parts of the formation never suffered considerable internal deformation.

In the northern Read Mountains, the basement seems to have direct contact with Turnpike Bluff Group metaclastics (the exact boundary remains hidden under ice). Within a couple of metres distance, porphyroblastic granites show mineral alignment parallel to the boundary, and heavy fragmentation of feldspar blasts.

Throughout the Read Mountains, the profiles of metamorphic grade and deformational style support a tectonic nature of the basal plane of the Turnpike Bluff Group. Internal deformation of the Turnpike Bluff Group, as well as structures from the units below consistently indicate SE directed thrusting. These observations lead to the interpretation of the whole Turnpike Bluff Group as a nappe. In the S, the basal thrust plane contains allochthonous, tectonically emplaced slices of crystalline basement. Though much larger in size, the crystalline block at Watts Needle is interpreted as a similar slice, which originally has been incorporated in the basal parts of the nappe and today represents a 'tectonic clippe'.

2. Tectonic structures in the southwestern Range (Stephenson Bastion, Otter Highlands)

In the northern outcrops of Stephenson Bastion (see figure), clastic metasediments are overturned and dip steeply to the N. Younger shear zones accomodating N-S

movements dip north at medium angles. In order to explain the situation at Stephenson Bastion, BRAUN ET AL. (1988) suggested southbound thrusting of the basement further north upon the sedimentary rocks. Similarities with the Read Mountains are corroborated by samples from a small, isolated basement outcrop some kilometres to the W, which are comparable to the cataclastic rocks at the top of Watts Needle. MARSH (1983b) similarily quoted thrusting of basement rocks upon Turnpike Bluff Group sediments for the southern Otter Highlands, which is confirmed by slices of Turnpike Bluff Group clastics tectonically intercalated with crystalline rocks (BRAUN ET AL. 1988). A large variety of microstructures indicates southerly transport of the hanging wall. As already established in the Read Mountains, deformation took place in a transitional brittle-ductile regime.

3. Tectonic structures of the northern Haskard Mountains, northwestern Shackleton Range

The northern Haskard Highlands comprise a series of layered metasediments (Nostoc Lake Formation and Mount Gass Formation, MARSH 1983a), stratigraphically assigned to the Pioneers Group. They rest upon the gneisses at Mount Weston, which are regarded to represent basement rocks belonging to the Haskard Group. Again, mineral foliation and layering are roughly parallel, but different to the south porphyroblastic granites are foliated and contain strongly elongated xenoliths. Fine grained, leucocratic granites intruded after the main deformational event and show agmatitic contacts with the country rocks. The Pioneers Group also contains punctuate outcrops of mafic to ultramafic rocks, as well as a large pyroxenite body.

All over the northern part of the Shackleton Range, granoblastic high grade minerals suffered pronounced retrograde overprint and mylonitization caused by thrust movements. Related microstructures have been found to indicate northwesterly transport in the Mount Weston area. The axes of early, isoclinal folds, as well as a pronounced stretching lineation plunge at medium angles to the WSW-WNW. Within the metasediments of the Pioneers Group, major tight to open folds constantly plunge to the NW with westerly dipping axial planes. At Mount Gass, widespread shearing with normal fault character has been encountered. Though the trace of movement - as derived from the orientation of boudins and domino structures - roughly parallels the axes of folding and stretching, the shear zone developed under brittle-ductile conditions, therefore clearly postdating the early deformations. All observations point to NW-directed downglide of the hanging metasediments from updoming basement gneisses of the Haskard Group. Late, gentle folding with wavelengths of several kilometres has subhorizontal axes oriented in N-S direction.

4. Structural interpretation, tectonic evolution, and timing of events

Radiometric ages reach back as far as 2700 Ma (PANKHURST ET AL. 1983), but further information about the early history of the Shackleton Range is lacking. In the Read Mountains, the first major tectonic event visible today is N-S directed extension, contemporaneous to amphibolite facies metamorphism. Syntectonic granites yield Rb/Sr whole rock ages of 1820 ± 160 Ma and have remarkable low $^{87}Sr/^{86}Sr$ initial ratios, precluding a long crustal prehistory (PANKHURST ET AL. 1983). Porphyroblastic granites intruded postkinematically with respect to the foliation, but several narrow ductile shear zones crosscut these granites as well as the layered metamorphics. A K/Ar whole rock determination of 1401 ± 70 Ma for one of these granites (HOFMANN ET AL. 1980) falls into the same range as the 1454 ± 60 Ma K/Ar age from a granodiorite dyke (REX 1972).

Subsequent to ductile deformation and metamorphism, the basement has been elevated from roughly 15 - 25 km (according to thermobarometry) to at least sea level. This first stage of uplift has been compensated by erosion and terminated at the latest when sedimentation of the Watts Needle Formation initiated in a fluviatile, and later continued in a shallow marine environment (BUGGISCH ET AL. 1990). Acritarchs preserved in the weathering horizon below the sediments have been dated as Riphean (at latest Vendian, WEBER 1989), which is in accordance with reports on Riphean stromatolites in Watts Needle Formation limestones by GOLOVANOV ET AL. (1979). For the Watts Needle Formation, PANKHURST ET AL. (1983) yielded a Rb/Sr model age of 720 Ma.

The Turnpike Bluff Group has been deposited in an unknown area to the NW. With the exception of the Stephenson Bastion Formation, *Oldhamia* trace fossils indicate early Cambrian age and a flysch-like sedimentational environment (BUGGISCH ET AL. 1990). PANKHURST ET AL. (1983) have been able to assess a maximum age of 700 Ma for the source rocks, while 526 ± 6 Ma may be the time of metamorphism - which is compatible with cooling ages between 540 and 490 Ma, determined by K/Ar measurements on micas (BUGGISCH ET AL. 1990). Since the growth of biotite is related to the NW-SE transport of the Read Nappe, these data also give an estimate for the time of thin skinned tectonics in the southern Shackleton Range. Following nappe emplacement, the units of the Read Mountains have been elevated during a second stage of uplift. When looking at the actual geometrical relationships, earlier images of a simple, W-E stretching anticline as suggested by the geological map and the gross orientation of structures (e.g. HOFMANN & PAECH 1983) have to be modified, however. N-S crossections reveal an appreciable amount of horizontal extension, which resulted in tilting of the northern and southern outcrops.

Samples from basement gneisses in the Haskard Highlands yield Rb/Sr ages of about 1550 Ma (PANKHURST ET AL. 1983), thus falling into the same time span as peak metamorphism in the Read Mountains. Secondary, retrograde mineral fabrics developed during widespread thrust movements, preferably localized at the unit boundaries. The probable time of compressional tectonics is given by a large number of radiometric ages ranging from about 530 Ma to 460 Ma, i.e. roughly contemporaneous to the time of nappe transport in the Read Mountains. Non-metamorphic conglomerates and sandstones of the Blaiklock Glacier Group, which are assigned to the Ordovician (PANKHURST ET AL. 1983, BUGGISCH ET AL. 1990), autochthonously rest on the metamorphic rocks, and therefore give an upper time constraint for tectonometamorphism in the Haskard Highlands.

As outlined above, the history of the Shackleton Range is clearly divided into two major tectonothermal events. According to the observations in the southern Shackleton Range, metamorphism during the Late Proterozoic has been coupled with firstly extensional, then compressional tectonics, followed by uplift and erosion of the basement rocks. Close relationships between the northern and southern Shackleton Range can be proved at latest since the upper Cambrian. However, while structures in the north show NW vergency and are bound to intense mylonitization, tectonic movements in the south have been localized in brittle-ductile shear zones and were SE directed. Taking into account the position of the Shackleton Range close to the Pacific margin of Antarctica during Paleozoic times, it seems reasonable to interprete the mountains as part of the Ross Orogen, for which subduction of the Pazific ocean under the Antarctic continent is discussed. Within this model, the Haskard Highlands may represent remnants of the accretionary wedge, whereas the Read Mountains - positioned further inland - are a zone of backward thrusting. As alternative setting, collision of the continent with an island arc has been discussed by BUGGISCH ET AL. (1990).

5. References

BRAUN, H.-M., KLEINSCHMIDT, G. & SPAETH, G. (1988): Geologische Expedition in die Shackleton Range. – *In:* FÜTTERER, D. K. (Ed.), Die Expedition ANTARKTIS-VI mit FS "Polarstern" 1987/1988. Ber. z. Polarforsch., **58**: 208-218.

BUGGISCH, W., KLEINSCHMIDT, G., KREUZER, H. & KRUMM, S. (1990): Stratigraphy, metamorphism and nappe-tectonics in the Shackleton Range (Antarctica). – Geodät. u. geophys. Veröff., Reihe I, **15**: 64-86.

CLARKSON, P. D. (1982): Tectonic significance of the Shackleton Range. – *In:* CRADDOCK, C. (Ed.), Antarctic Geoscience: 835-839; Madison (Univ. Wisconsin Press).

GOLOVANOV, N. P., MIKHAILOV, V. M. & SULJATIN, O. G. (1980): Pervye diagnostiruemye stromatolite Antarktidy i ikh biostrategrafecheskoe znachenie [First diagnostic stromatolites from Antarctica and their biostratigrafic significance] . - Antarktika, **19**: 152-159.

HOFMANN, J. & PAECH, H.-J. (1983): Tectonics and relationships between structural stages in the Precambrian of the Shackleton Range, western margin of the East Antarctic Craton. - *In:* OLIVER, R. L., JAMES, P. R. & JAGO, J. B. (Eds.), Antarctic Earth Science: 183-189; Canberra (Austral. Acad. Sci.).

HOFMANN, J., KAISER, G., KLEMM, W. & PAECH, H.-J. (1980): K/Ar-Alter von Doleriten und Metamorphiten der Shackleton Range und der Whichaway Nunataks, Ost- und Südumrandung des Filchner-Eisschelfs (Antarktis). - Z. geol. Wiss., **8**: 1227-1232.

MARSH, P. D. (1983a): The stratigraphy and structure of the metamorphic rocks of the Haskard Highlands and Otter Highlands of the Shackleton Range. - Brit. Antarct. Surv. Bull., **60**: 23-43.

——— (1983b): The Late Precambrian and Early Paleozoic history of the Shackleton Range, Coats Land. - *In:* OLIVER, R. L., JAMES, P. R. & JAGO, J. B. (Eds.), Antarctic Earth Science: 190-193; Canberra (Austral. Acad. Sci.).

PANKHURST, R. J., MARSH, P. D. & CLARKSON, P. D. (1983): A geochronological investigation of the Shackleton Range. - *In:* OLIVER, R. L., JAMES, P. R. & JAGO, J. B. (Eds.), Antarctic Earth Science: 176-182; Canberra (Austral. Acad. Sci.).

REX, D. C. (1972): K-Ar age determinations on volcanic and associated rocks from the Antarctic Peninsula and Dronning Maud Land. - *In:* ADIE, R. J. (Ed.), Antarctic geology and geophysics: 133-136; Oslo (Univ.forlaget).

WEBER, B. (1989): Late Proterozoic microbiota from the Turnpike Bluff Group, Shackleton Range. - Symposium on Antarctic Research Abstracts: 52; Potsdam (Akad. Wiss. GDR).

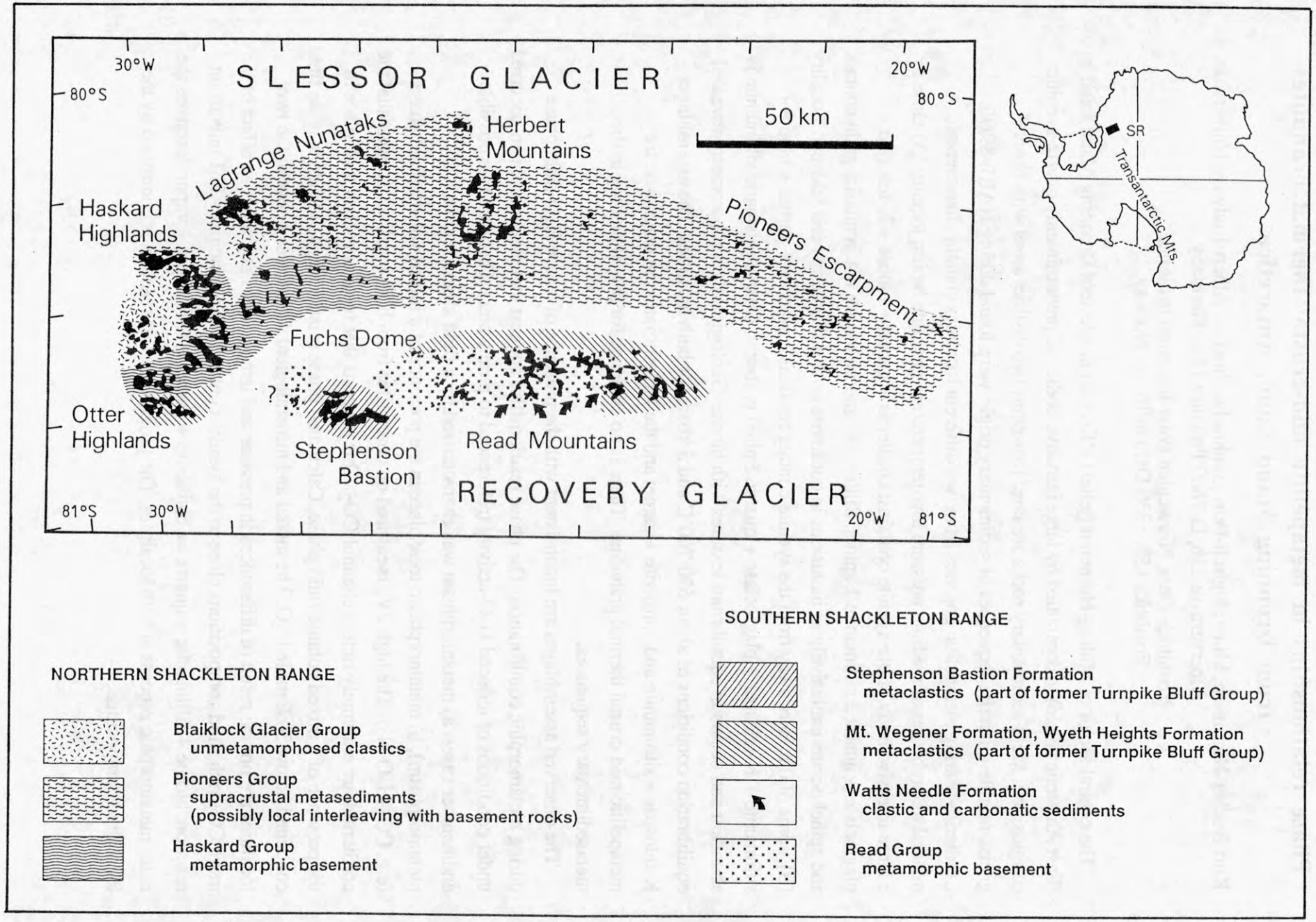

Figure: Topography and stratigraphic units in the Shackleton Range, Antarctica.

Phase relationships in metapelitic mid-crustal thermal granulites from Dronning Maud Land, Antarctica.

Kurt Bucher-Nurminen, Mineralogisch-Petrographisches Institut, Albert-Ludwigs Universität, Albertstrasse 23b, D-7800 Freiburg i.Br., Germany

Yoshihide Ohta, Norwegian Polar Research Institute, Postboks 158, 1330 Oslo lufthavn, Norway

The central sector of Mühlig-Hofmann fjellet (3°E/71°S) in Western Dronning Maud Land (East Antarctic shield) is dominated by large intrusive bodies of predominantly quartz-syenitic composition. Meta-sedimentary rocks are rare. However, two distinct areas with banded gneiss-marble-quartzite sequences of sedimentary origin were found during NARE 89/90. Cordierite-bearing metapelitic gneisses from two different localities contain characteristic mineral assemblages of medium pressure low-temperature granulite facies: locality (A) close to a large intrusive body of qtz-syenite contains: cordierite + garnet + biotite + K-feldspar + plagioclase + quartz ± sillimanite ± spinel. Sillimanite and biotite are not in mutual grain contact and spinel occurs exclusively as inclusions in cordierite or/and sillimanite and feldspar. Locality (B), some 500 meters away from the syenite contact contains cordierite + garnet + biotite + sillimanite + K-feldspar + plagioclase + quartz. Spinel is absent. Coarse prismatic sillimanite is abundant and occurs in equilibrium textures with biotite. Geological thermobarometry revealed equilibration conditions of about 650-700°C and 5 kbars for both localities. The assemblages K-feldspar + sillimanite and cordierite + garnet and the PT-estimates are diagnostic for metapelitic mid-crustal thermal granulites. There is no evidence for partial melting in the metasedimentary sequences.

The observed assemblages are inconsistent with the presence of a pure H_2O-fluid phase during metamorphic equilibration. The phase relationships suggest that metamorphism occurred under conditions of reduced H_2O-activity (referenced to pure water). There are two possible endmember cases: a) metamorphism was characterized by a fluid absent regime ("dry" metamorphism), b) metamorphism took place in the presence of a mixed volatile fluid phase (e.g. CO_2-H_2O-N_2). The high $2V_x$ measured on cordierites from both localities suggest that the cordierites are extremely rich in channel-CO_2. This suggests that metamorphism took place in the presence of a mixed volatile fluid phase. Calculated phase relationships indicate that the fluid contained below 30% mole H_2O. The modal and mineralogical differences between the two localities are not the result of differences in pressure and temperatures but rather an effect of more CO_2-rich fluid compositions close to the syenite contacts. The principal AFM-univariant reaction: biotite + sillimanite + quartz ⇔ cordierite + garnet + K-feldspar + vapor describes the main metamorphic process at both localities. The progress of this reaction is controlled by the local fluid composition.

STRATIGRAPHY AND FACIES OF THE (META-)SEDIMENTS IN THE SHACKLETON RANGE, ANTARCTICA

W. Buggisch, Institut für Geologie und Mineralogie,
Universität Erlangen, Schloßgarten 5, D 8520 Erlangen, Germany.

G. Kleinschmidt, Geologisch-Paläontologisches Institut,
Universität Frankfurt, Senckenberganlage 32-34, 6000 Frankfurt 1, Germany.

The stratigraphy of the Shackleton Range which was established by STEPHENSON (1966) and CLARKSON (1972) was revised during the German Expedition GEISHA 1987/88. The correlation of the "Turnpike Bluff Group" is still unclear. Probably, the four recognized formations belong to different units: the Stephenson Bastian and Wyeth Hights Formations probably are of Late Precambrian age, Lower Cambrian fossils were found in the Mount Wegener Formation and the Late Precambrian Watts Needle Formation was recognized as an independent formation which lies unconformably upon the Read Group. It is separated from the allochthonous Mount Wegener Nappe by a thrust. Fossils like *Oldhamia* sp., *Epiphyton* sp., *Botomaella* (?) sp. and echinoderms prove an Early Cambrian age for the Mount Wegener Formation of the former "Turnpike Bluff Group" in the Read Mountains. The Middle Cambrian trilobite shales at Mount Provender which form the Haskard Highlands Formation are probably in fault contact with the basement complex (Pioneer and Haskard Groups). They are overlain by the Blaiklock Glacier Group. An Ordovician age for this group is suggested by trilobite tracks and trails, low inclination of the paleomagnetic field and the similarity to the basal units of the Table Mountain Quartzite in South Africa. The Watts Needle Formation represents epicontinental shelf sedimentation, the Mount Wegener Formation was deposited in a (continental) back arc environment and the Blaiklock Glacier Group is a typical molasse sediment of the Ross Orogen.

References:

CLARKSON, P.D. (1972): Geology of the Shackleton Range: A preliminary report.- Bull. Br. Antarct. Surv. **31**: 1-15; Cambridge.

STEPHENSON, P. J. (1966): Geology. 1. Theron Mountains, Shackleton Range and Whichaway Nunataks (with a section on palaeomagnetism of the dolerite intrusion by D. J. BUNDELL).- Scient. Rep. Transantarct. Exped. **8**: 1-79; London.

Table 1: Stratigraphy of the Shackleton Range.

	South		North	New evidence by
JURASSIC	tuffaceous pelites and arenites			K-Ar
ORDOVICIAN		~ ~ ~ ~ ~ ~ ~	Blaiklock Glacier Group ~ ~ ~ ~ ~ ~ ~	Paleomagnetism Trace fossils ← K-Ar
CAMBRIAN UPPER				
CAMBRIAN MIDDLE			Haskard Highlands Fm.	
CAMBRIAN LOWER		Mt. Wegener Formation	~ ~ ~ ? ~ ~ ~	*Oldhamia* sp. *Epiphyton* sp.
LATE PRECAMBRIAN	Watts Needle Formation	Stephenson Bastion + Wyeth Hights Formation	Haskard and Pioneer Groups	K-Ar and Rb-Sr
PRECAMBRIAN	Read Group			

HIGH TEMPERATURE DIFFUSIONAL METASOMATISM: CALCSILICATE BOUDINS FROM THE RAUER GROUP, EAST ANTARCTICA.

I.S. Buick, Department of Geology, University of Melbourne, Parkville, Vic. 3052, Australia.
S.L. Harley, Grant Institute of Geology, University of Edinburgh, West Mains Rd., Edinburgh, EH9 3JW, United Kingdom.

High variance metasomatic rinds are a characterisitc feature of calcsilicate bodies intercalated with Proterozoic-age granulite facies Fe-rich metapelitic and felsic gneisses in the polymetamorphic Rauer Group of Prydz Bay, East Antarctica. This sequence was metamorphosed during the last major metamorphism (M3, (7-9 kbar,840±40 ^{o}C)) to affect the Rauer Group. Calcsilicates occur as rare 5-25 cm thick eliptical bodies, produced through early D3 boudinage of folded layers. Metasomatic rinds cut internal layering within the boudins, but contain an Ls lineation correlated with M3 lineations (L3) in the surrounding gneisses. Concentric metasomatic rinds around the calcsilicates are thus interpreted to be of M3 age, and are overprinted by post-M3 symplectites (Harley & Buick, this symposium).

Boudin cores are characterised by granoblastic mosaics, and contain combinations of grandite garnet (Gro Grt), clinopyroxene (Cpx), scapolite (Scp),wollastonite (Woll), calcite (Cal), quartz (Qtz), anorthitic plagioclase (An) and sphene (Spn). The most common assemblages lack primary plagioclase (e.g. [An,Cal] or [An,Qtz]) and contain wollastonite, scapolite, grandite garnet and clinopyroxene. In silica-saturated calcsilicates the following mineral assemblage zones occur between boudin cores and the surrounding metapelites:
1) Grandite Garnet Zone : Gro Grt-Scp-Cpx-Sphene±Cal±Plg,
2) Clinopyroxene Zone: a) Cpx-Scp-Spn, b) Cpx-Scp-Pl-Spn, c) Cpx-Pl-Spn, d) Cpx-Pl-Ilm,
3) Orthopyroxene Zone: Opx-Pl-Ilm ±Cpx±Hbd±Bt.,
4) Almandine Garnet Zone: a) Alm Grt-Opx-Pl-Ilm±Bt, b) Alm Grt-Pl-Ilm±Bt, c) Alm Grt-Pl-Rt-Bt ±Ilm.
Textures are well equilibrated in the grandite garnet, clinopyroxene, and almandine garnet zones, whereas the orthopyroxene zone is characterised by arrested reaction textures indicative of orthopyroxene growth at the expense of clinopyroxene, hornblende and biotite with increasing distance rimwards. The original pelite-calcsilicate boundary must occur at least as far inwards as the orthopyroxene zone. Across these zones plagioclase, scapolite, clinopyroxene, garnet and orthopyroxene exhibit systematic compositional variation. Inflection in compositional trends for different phases occur at differnt zone boundaries.

Metasomatic reaction bands developed between lithologies of greatly different bulk composition are often present in high-level contact aureoles (e.g Joesten, 1974), and in regional amphibolite facies terranes (Hewitt, 1973). In the upper and middle crust some combination of infiltration- and diffusion-driven mass transfer is usually invoked to explain these reaction zones. Variation in the activity of volatile species (low a_{CO2} in boudins, low a_{H2O} in pelites) could account for the development of metasomatic rinds in the calcsilicates if a pervasive fluid phase attended the M3 event. However, the common domainal distribution of wollastonite, calcite and quartz in Rauer Group calcsilicate boudins indicates internal buffering of the core assemblages, most probably under vapour-absent conditions. The small length scale of alteration and the variation in boudin bulk chemistry from core to rim is more consistent with the development of metasomatic rinds by diffusion as a response to chemical potential gradients in oxide components (principally μCaO) between boudin cores and the surrounding metapelites.

References

Hewitt, D.A. 1973. The metamorphism of micaceous limestones from South-central Connecticut. *American Journal of Science*, **273-A**, 444-469.

Joesten, R. 1974. Local equilibrium and metasomatic growth of zoned calcsilicate nodules from a contact aureole, Christmas Mountains, Big Bend Region, Texas. *American Journal of Science*, **274**, 876-901.

LOWER CRUSTAL FLUIDS: STABLE ISOTOPIC CONSTRAINTS FROM THE RAUER GROUP, EAST ANTARCTICA.

I.S. Buick, Department of Geology, University of Melbourne, Parkville, Vic. 3052, Australia.
S.L. Harley, Grant Institute of Geology, University of Edinburgh, West Mains Rd., Edinburgh, EH9 3JW, United Kingdom.
D.Mattey, Department of Geology, Royal Holloway and Bedford New College, University of London, Egham, Surrey, United Kingdom.

The role of volatile species in the stabilisation of the lower (granulitic) crust is contentious. Models for granulite genesis which invoke pervasive infiltration of deep-seated CO_2-rich fluids to account for the stabilisation of anhydrous granulite facies assemblages have recently received much attention. Integrated petrological and stable isotopic studies of lithologies which are sensitive monitors of fluid flow (e.g. metacarbonates and calcsailicates) have the potential to place constraints on lower crustal fluid budgets. In this study data are presented from two types of metacarbonate from the polymetamorphic Rauer Group of Prydz Bay, East Antarctica: **a)** Metre-scale calcite-forsterite-spinel-clinopyroxene± phlogopite ±pargasite marbles which occur as boudins in Archaen granulitic orthogneisses preserved within the largely late Proterozoic terrain. **b)** Decimetre-scale wollastonite-grandite garnet-scapolite-clinopyroxene± quartz± calcite±plagioclase calcite-poor calcsilicate boudins hosted in Fe-rich metapelites in the late Proterozoic portion of the terrain.

Forsterite Marbles: do not contain suitable buffering assemblages to allow calculation of a_{CO2}, but preserve heterogeneous calcite stable isotopic compositions ($\delta^{13}C$ = -9.0 to -3.0 ‰ PDB , $\delta^{18}O$ = + 4 to +12.2 ‰ SMOW) on a centimetre to metre scale. From boudin cores to rims oxygen ($\Delta\delta^{18}O$ = 5-6‰), and to a lesser extent carbon ($\Delta\delta^{13}C$ = 1-2 ‰) exhibit isotopic compositional gradients, becoming progressively lighter over 2-3 m distances. The magnitude of oxygen isotope gradients are too large to be explained soley by decarbonation, and the lengthscale of alteration requires that a free fluid phase existed at some time at the orthogneiss-marble contacts. The small shift in $\delta^{13}C$ relative to $\delta^{18}O$ suggests that this fluid was water-rich. The relative contribution of diffusion and advection to maintenance of the isotopic gradients is at present unclear, although limited evidence from the calcite (C,O) profiles suggests that some infiltration perpendicular to the orthogneiss/marble contact has occurred. More narrow zones of much lighter carbon and oxygen are superimposed on these $\delta^{18}O$ and $\delta^{13}C$ profiles. These zones correlate with decimetre-scale metasomatic reaction bands (massive clinopyroxene or amphibole skarns), which are the locus of locally intense decarbonation. These reaction bands may have acted as channelways for the channelised infiltration of fluids during granulite facies metamorphism. Although the calcite ($\delta^{13}C$,$\delta^{18}O$) data require the presence of fluids during high grade metamorphism the isotopic heterogeneity within individual marble boudins precludes communication with a large fluid reservoir of uniform isotopic composition, and the timing of fluid flow both at the orthogneiss/marble contacts and in the clinpyroxene skarns is poorly constrained..

Wollastonite-grandite Calcsilicates: solid buffering assemblages such as wollastonite-calcite-quartz, or calcite-scapolite-quartz-grossular limit a_{CO2} to be ≤ 0.35-0.5, in comparison to a_{H2O} ≤ 0.2-0.4 in the surrounding metapelites. Given the widespread distribution of these calcsilicates, this result is incompatible with pervasive flooding of the terrain by CO_2-rich fluids. The low modal % calcite in these boudins makes them very sensitive monitors of fluid/rock interaction. Calcite from boudin cores shows an appreciable range in composition ($\delta^{13}C$ = -20.4 to -5.5 ‰ PDB, $\delta^{18}O$ = + 7.3 to +13.5 ‰ SMOW). This isotopic heterogeneity is also inconsistent with the cores of the calcsilicate boudins having equilibrated with an external fluid reservoir of uniform isotopic composition, such as is required for CO_2-flushing models.

LATE CRETACEOUS AND EOCENE PALYNOFLORAS FROM FILDES PENINSULA, KING GEORGE ISLAND (SOUTH SHETLAND ISLANDS), ANTARCTICA

Cao Liu, Nanjing Institute of Geology and
Palaeontology, Academia Sinica,
Nanjing 210008, China

Rock samples from the volcanic sedimentary series in the Fildes Peninsula of King George Island, Antarctica, contain two palynofloras indicating different geological ages.

The Half Three Point Formation contains a late Late Cretaceous palynoflora, including about 40 species of fungal spores, and 60 species of pteridophyrte spores, gymnosperm and angiosperm pollen grains. The main elements are *Cyathidites*, *Gleicheniidites*, *Clavifera*, *Asterisporites*, *Klukisporites*, *Aequitriradites*, *Dacrydium*, *Araucariacites*, *Podocarpidites*, *Nothofagidites*, *Gothanipollis*, *Cranwellia* and *Tricolporites*, etc. The palynoflora is composed of Late Mesozoic terrestrial plants, which indicate a rain forest vegetation growing on the shores of marsh lakes in the mountainous or hilly areas. Because no marine fossils are present, the Half Three Point Formation is probably a terrestrial deposit.

The lower part of the Fossil Hill Formation contains fossil leaves and abundant palynomorphs, mainly spores of Cyatheaceae and Lygodiaceae, pollen grains of *Araucariacites*, *Nothofagidites* and *Proteaceae*. These are probably of Early and Middle Eocene in age.

The upper part of the Fossil Hill Formation also contains abundant palynomorphs. Of them, pteridophyte spores occupy 38% with *Laevigatosporites*, *Polypodiaceaesporites*, *Lycopodiumsporites*, *Cyathidites*, *Tschyosporites*, *Concavisporites* and *Leiotriletes*, etc. as the main forms. Gymnosperm pollen grains account for 30%, with *Trisaccites*, *Podocarpidites*, *Dacrycarpites*, *Microcachrydites* and *Araucariacites*, etc. as the main elements. Angiosperm pollen grains amount to 32% with *Nothofagidites*, *Proteacidites*, *Myrtaceidites*, *Momipites* and *Triorites* as the dominant elements. Therefore, its geological age is the same as, or younger than, the lower part of the formation.

PETROLOGY OF THE TUCKER AND BURRILL PLUTONS, VICTORY MOUNTAINS (NORTH VICTORIA LAND ANTARTICA).

Cavazzini GC., C.N.R., C.S. Orogeno Alpi Orientali c/o Department of Mineralogy and Petrology, University of Padova, corso Garibaldi 37, I-35100 PADOVA, ITALY.
Lombardo B., C.N.R., Orogeno Alpi Occ., c/o Department of Earth Sciences, University of Torino, via Valperga Caluso 37, I-10125 TORINO, ITALY.
Visonà D., Department of Mineralogy and Petrology, University of Padova, corso Garibaldi 37, I-35100 PADOVA, ITALY.
Zantedeschi C., C.N.R., C.S. Orogeno Alpi Orientali c/o Department of Mineralogy and Petrology, University of Padova, corso Garibaldi 37, I-35100 PADOVA, ITALY

This paper presents geochemical and mineralogical data on two members of the Devonian-Carboniferous Admiralty Intrusives of north Victoria Land. The Tucker pluton is an elliptical epiplutonic body with an area of about 130 Km^2 and a local topographical relief of 2.5 Km, which cuts across the structural trend of the host Robertson Bay turbidite greywacke-shale sequence. The Mt. Burrill pluton is larger, with a surface outcrop of at least 150 Km^2, and is apparently parallel to the dominant NW-SE trend of folds in the Robertson Bay Terrane but far less well exposed than the Tucker pluton and not yet fully sampled.

Both plutons were emplaced in the Robertson Bay Terrane close to the boundary with the Cambrian volcano-sedimentary Bowers Terrane: Mt. Burrill pluton sitting right off the boundary and the Tucker pluton 50 Km farther NE. Emplacement depth of the Tucker pluton is 7-9 km as estimated from Hbl-Pl barometry.

Coarse- to medium-grained, equigranular to porphyritic horneblende tonalite and granodiorite, with minor granite, compose the Tucker pluton. Biotite granite is apparently the dominant lithology in the Burrill pluton. Mafic (dioritic) xenoliths of mm to dm size are common in the Tucker pluton, suggesting interaction of an acidic magma with a mafic one of the same age. Data from the Tucker pluton define in the QAP diagram a compositionally expanded, low- to-intermediate K, calc-alkaline association, in agreement with low values of normative corundum and diopside.Inter-element correlation suggests that fractional crystallization of an intermediate magma may account for the lithological spectrum observed in the Tucker and Burrill plutons.

An emplacement age of 400 Ma (Early Devonian) is indicated for the Tucker pluton by a seven-point whole rock Rb-Sr isochron, with isotopic closure of the biotite-whole rock system between 363 and 375 Ma. The Sr isotope ratio at 400 Ma is 0.7073 for the Tucker pluton and 0.7039 for the Burrill pluton, suggesting an I-type calc-alkaline affinity and a significant crustal contribution.

PALEOECOLOGY OF LATE CRETACEOUS SEYMOUR ISLAND, ANTARCTICA: NEW EVIDENCE FROM VERTEBRATE REMAINS

Sankar Chatterjee, The Museum, Texas Tech University, Lubbock, Texas 79409-3191, USA.

During the Late Cretaceous period, Antarctica was the site of profound geological, biological, and climatic events associated with regression of the sea, mass extinctions, and the final breakup of Gondwana. The marine deposits of Seymour Island and associated vertebrate fauna provide important clues to recognize the paleoecology of the Southern Hemisphere during this critical period of the earth's history.

Vertebrate remains from the Late Cretaceous Lopez de Bertodano Formation include a variety of fish, plesiosaurs, mosasaurs, and a foot-propelled diving bird. Both beryciform teleosts and hexanchiform sharks are common in the Cretaceous deposits, but they do not live in the Antarctic region today. The marine reptiles such as plesiosaurs and mosasaurs were abundant in the Maastrichtian Antarctic sea, and filled the role of large mobile predators similar to that of seals and whales in the present-day Southern Ocean. However, these reptiles may not have been pursuing prey in the same way. Three predator guilds are recognized on the basis of body shape, mode of swimming, tooth morphology, and prey preferences. The mosasaurs were active swimmers like crocodiles and used axial undulatory mode for propulsion. They composed the 'Cut guild', and were the top carnivores in the Antarctic biota. The two lineages of plesiosaurs, the elasmosaurids and cryptoclidids, shared a similar mode of locomotion, that of subaqueous flying, using their two pairs of wing-like appendages as hydrofoils.The elasmosaurids constituted the 'Pierce guild, while the cryptoclidids formed the 'Trap guild'. These reptiles exploited various pelagic resources such as sharks, bony fish, cephalopods, and crustaceans that abound in the same deposits. The remains of plesiosaurs and mosasaurs in Seymour Island indicate that the ocean temperatures in the Antarctic Circle were equable and warm temperate to support the various ectothermic reptiles. During this period, Antarctica was still in contact with South America, and there was no circumantarctic gyre to cool the deep sea. Both plesiosaurs and mosasaurs, however, were the victims during the K/T mass extinction, as a consequence of the collapse of the marine food chain.

A beautiful avian skeleton recovered from the Late Cretaceous of Seymour Island represents not only the oldest Antarctic bird, but also the world's oldest loon. The specimen is very similar to the modern red-throated loon and is entirely toothless and neognathous unlike other Mesozoic sea birds. The discovery of the loon from Antarctica sheds new light on the pattern and process of evolution of diving birds. Morphologically loons are the closest relatives to penguins and shared a most recent common ancestry. Yet, their fossil distributions previously had not supported this close phyletic relationship. The extant loons, as well as their past fossil record, are confined to Northern Hemisphere, whereas living and fossil penguins are restricted to Southern Hemisphere. The new Antarctic bird may resolve this long-standing evolutionary puzzle about the common origin of loons and penguins. This remarkable fossil may be as much as 25 million years older than previously described loon from the Eocene of England. Its discovery in Seymour Island corroborates the concept of high latitude heterochroneity observed in mollusks and other marine organisms whereby taxa originated at high latitudes in the Southern Hemispehere and dispersed northward in the Early Tertiary.

AN INTRODUCTION TO THE GEOLOGICAL AND METALLOGENETIC MAP OF ANTARCTICA

Chen Tingyu[1], Zhao Yue[1], Li Guangcen[2], Ren Liudong[1], Shen Yanbin[3], Xie Liangzhen[1], Wang Zhenyang[1], Wang Yanbin[1]and Liu Ping[1]

1. Institute of Geology, Chinese Academy of Geological Sciences, Baiwanzhuang Road, 100037, Beijing, China.
2. Chinese Academy of Geological Sciences, Baiwanzhuang Road, 100037, Beijing, China.
3. Nanjing Institute of Geology and Paleontology, Academia Sinica, China

Early in 1972, C.Craddock compiled the first geological map of Antarctica on the scale of 1:5,000,000. Thereafter, UNESCO published the Geological World Atlas including a sheet of the geological map of Antarctica. In 1977, French geologists published a geological map and in 1978, Soviet geologists compiled another. Since then, more than ten years have passed. The study of geological sciences has much advanced, through papers which were presented in the fourth and fifth symposia as well as many other publications. It thus is necessary and possible to compile a new geological map. Moreover, as progress of study of geology, more and more attention is paid to the potential of mineral resources of Antarctica, to which many political, economic and environmental problems are related. So,in 1988, supported by State Antarctic Committee of China, National Natural Science Foundation of China, and Geological Science Foundation of China, We began to compile a geological and metallogenetic map of Antarctica on the scale of 1:5,000,000.

The geographic map is compiled on the basis of the Map of Antarctica published by State Antarctic Committee of China. Some geographic names are added to or left out of the map for geological purposes.

The geological map of Antarctica is compiled on the basis of progress in geological study during the past years.

Geotectonically, Antarctica can be divided into four units: East Antarctic shield, Transantarctic Mountains orogen , West Antarctic basins and Antarctic Peninsula orogen.

The East Antarctic shield consists of green schist facies and granulite facies rocks, mainly of Archean and Proterozoic age. On the map, we line out Archean(Ar), Lower Archean(Ar_1), Upper Archean–Lower Proterozoic (Ar_2–Pt_1), Lower Proterozoic(Pt_1), Middle Proterozoic(Pt_2) and Proterozoic undivided(Pt). Permian rocks also crop out in the area.

In the Transantarctic Mountains and Marie Byrd Land, Upper Proterozoic–Lower Paleozoic (Pt_3–Pz_1), Cambrian–Ordovician(including Silurian)(C–O), Devonian(D), Carboniferous––Permian(C–P), Permian––Triassic(P–T) are shown on the map. The most important progress in the area may be the discovery of youngest Cambrian or oldest Ordovician fossils in the Robertson Bay Group which was previously referred to as late Precambrian, and now is mapped as Cambrian––Ordovician.

In the Ellsworth Mountains, middle and late Cambrian trilobites were discovered during the 1979–1980 geological investigation, indicating that the Minaret Group be referred to late Cambrian. This group was previously considered as Precambrian.

The Antarctic Peninsula and East Ellsworth Land consists of Cenozoic and Mesozoic magmatic arcs. Nonetheless, Upper Paleozoic––Mesozoic (Pz_2–Mz), Permian––Triassic(P–T), Middle and Lower Jurassic(J_{1-2}), Upper Jurassic(J_3), Lower(K_1) and Upper Cretaceous(K_2), Tertiary(R) and Pliocene––Pleistocene(N_2–Q_1) are observed.

As to intrusive rocks, acid varieties were developed from late Archean––early Proterozoic through late Proterozoic, early Paleozoic, late Paleozozic, Mesozoic up to Tertiary; intermediate varieties from late Proterozoic––early Paleozoic, late Paleozoic, Mesozoic to Tertiary; Basic varieties from late Archean––early Proterozoic, Proterozoic, Mesozoic to Tertiary. Besides, alkaline rocks were developed in Paleozoic and ultrabasic rocks in late Mesozoic.

About 130 locations of mineral resources are shown on the map. 37 of them are located in East Antarctica, 27 in the Transantarctic Mountains and 64 in West Antarctica and the Antarctic Peninsula. As is known to all, the most important mineral resources are Precambrian iron–formation in East Antarctica, coal in the Transantarctic Mountains and copper and gold in the Antarctic Peninsula. Besides, we plot 17 locations of Fe, 40 of Cu,9 of Mo,2 of Mn,5 of U and Th,5 of Sn,5 of Pb and Zn,12 of Au and Ag,3 of Cr, Ni and Co,1 of Bi,3 of gem,3 of crystal, 2 of topaz and fluorite,1 of muscovite,1 of phlogopite,2 of beryl, 1 of zircon, 2 of graphite, 2 of coal,3 of phosphor,4 of sulphur,1 of salt and 1 of oil and gas, etc.

Modeling of Cenozoic Stratigraphy in the Ross Sea Using Sonobuoy Seismic-refraction Data

Guy R. Cochrane and Alan K. Cooper

U.S. Geological Survey
Mailstop 999
345 Middlefield Road
Menlo Park, CA 94025 USA

During the 1988/89 and 1989/90 austral field seasons, seismic sonobuoy data were acquired at 67 locations throughout the Ross Sea to gain detailed information on the velocity of Cenozoic glacial strata and older pre-glacial rocks that fill the major sedimentary basins (fig. 1). The sonobuoy data were recorded during geophysical surveys conducted cooperatively with the German Geological Survey (BGR) and the Observatorio Geofisico Sperimentale (OGS). Most sonobuoys were recorded along OGS multichannel seismic reflection (MCS) tracklines that crossed major sedimentary basins and structural highs beneath the Ross Sea. Wide-angle reflection and refraction arrivals were recorded out to distances of up to 35 km giving information on rock velocities and structural discontinuities at depths of up to approximately 10 km below the seafloor.

Wide-angle sonobuoy seismic data from the Ross Sea commonly have the following characteristics: (1) Linear refraction arrivals originating from the upper sedimentary layers and from basement rock; (2) Curved refraction arrivals originating from lower sedimentary layers and, in places, "acoustic" basement; and (3) Wide-angle reflections originating from sedimentary and intra-basement layers. We have used two-dimensional ray-trace modeling (Cervany et al., 1977) to construct velocity depth models from reflection and refraction arrivals recorded in the sonobuoy data. Such models improve the reasonable of estimates of the subsurface geologic structure and rock velocities beneath the sonobuoys in areas where there are changes in travel time caused by two-dimensionally varying structure, stratigraphy, and rock physical properties. In the ray-trace method an initial geologic (velocity-depth) model is designed using geometries from the MCS data and velocities from one-dimensional analysis of the sonobuoy data. The geologic model is modified until the computed seismic wave arrival times match the observed times in the sonobuoy data. Linear velocity gradients within model layers are used to match the curvature of the observed seismic arrivals and velocity discontinuities between layers are used to match exact times of first seismic arrivals.

Initial analysis of the data shows that velocity discontinuities commonly exist within the upper 1 km of sedimentary section. These discontinuities probably occur at unconformities between near surface units. These near surface units have nearly uniform velocities that result in linear refraction arrivals. In contrast, underlying units have large velocity gradients that result in curved arrivals as also noted by Houtz and Davey, (1973), and Davey, et al., (1983). We suspect that this change in velocity gradient occurs regionally at unconformity U5 of Hinz and Block (1983). We show one

example from the western side of the Eastern basin (Sonobuoy 72, fig. 2), to illustrate the change from the two short, distinct linear refractions to a later curved refraction. All of these refractions originate in glacial marine strata lying above unconformity U6, but only the curved arrival passes below U5 (fig. 2). The ray-trace model shows that a highly variable and discontinuous vertical sequence of velocities is required above U5 to explain why the deep curved refraction first arrives at a closer range and greater travel time than the two overlying linear refractions. A large velocity reversal is required at a depth of about 500 meters below the sea floor. Below U5, however, velocities must increase smoothly with depth to produce the continuous curved refraction we observe. The smoothly increasing velocities below U5 suggest that sediments may be progressively consolidated without major discontinuities (Gregory, 1977; Davey et al., 1982).

Sonobuoy 72 was deployed about 100 km from DSDP sites 270 and 272 where diatomaceous sand-silt-clay glacial units were recovered from above U5 and more highly indurated glacial marine clastics were sampled below U5 (Hayes, Frakes, et al., 1975). Visual inspection of DSDP core photos suggests that units above U5 have greater variability in degree of induration (and inferred velocity) than those below U5.

Prydz Bay is another area of Antarctic continental shelf thought to have been effected by glacial advance and retreat (Barron, Larsen, et al., 1989). In Prydz Bay downhole logging and sonobuoy refraction models at ODP Site 739 show similarities to the Ross Sea. At Site 739, highly variable velocities, including large velocity reversals, occur in the shallow part of the sedimentary section (upper 315 meters, Cochrane and Cooper, 1991). Low velocities are associated with interbedded diatomaceous and inferred sandy units, and high velocities are found in massive diamictites. Below 315 meters, velocities increase uniformly in friable diamictites.

We suspect that in the Ross Sea the more highly variable layer velocities above U5 may occur at regionally mapped unconformities (e.g. U1 through U4, Hinz and Block, 1984) and at other unconformities, presently not mapped. Such variability of velocities in the glacial sedimentary section at near-seafloor depths, observed at sonobuoy 72 and elsewhere in the Ross Sea, suggest that large changes in glacial depositional processes are likely since U5 (early Miocene) time. These changes may be related to the motion of grounded ice sheets across the Ross Sea (our preferred interpretation) or solely to changes in sea level. Between U5 and U6 the sonobuoy data suggest that a regionally more stable glacial depositional environment existed, in which sediment compaction was the principle agent controlling sediment velocities.

At depths within the sedimentary section below U6 refraction arrivals are recorded in sonobuoy 72 from the sedimentary fill and bounding basement structure of the large early-rift graben (Cooper et al., in press) beneath the Eastern basin. The ray-trace model further supports the existence of this deep graben structure, which is difficult to define in MCS data. The velocity of rock in the graben is 3.6 km/sec. These deep sedimentary units are likely pre-glacial rocks that also lie beneath all of the major sedimentary basins of the Ross Sea.

REFERENCES

Barron, J., Larsen, B., and et al., 1989, Proc. ODP, Init. Repts.: 119, College Station, TX, Ocean Drilling Program.

Cervany, V., Molotkov, I. A., and Psencik, I., 1977, Ray method in seismology: Praha, Univerzita Karlova, 214 p.

Cochrane, G. R. and Cooper, A. K., in press, Sonobuoy seismic studies at ODP drill sites in Prydz Bay, Antarctica, *in* Proc. ODP, Sci. Results: v. 119, Ocean Drilling Program, College Station, TX, .

Cooper, A. K., Barrett, P. J., Hinz, K., Traube, V., Leitchenkov, G., and Stagg, H. M. J., in press, Cenozoic prograding sequences of the Antarctic continental margin: a record of glacio-eustatic and tectonic events: Marine Geology.

Davey, F. J., Bennett, D. J., and Houtz, R. E., 1982, Sedimentary basins of the Ross Sea, Antarctica: N.Z. Jour. of Geol. and Geophys., v. 25, p. 245-255.

Davey, F. J., Hinz, K., and Schroeder, H., 1983, Sedimentary basins of the Ross Sea, Antarctica, *in* Antarctic Earth Science: Australian Academy of Science, Canberra, p. 533-538.

Gregory, A. R., 1977, Aspects of rock physics from laboratory and log data that are important to seismic interpretation, *in* Seismic stratigraphy-applications to hydrocarbon exploration: Amer. Assoc. Petroleum Geologists, Tulsa, Oklahoma, p. 15-46.

Hayes, D. E. and Frakes, L. A., 1975, *in* Initial Reports of the Deep Sea Drilling Project: v. 28, U.S. Government Printing Office, Washington, p. 211-334.

Hinz, K. and Block, M., 1983, Results of geophysical investigations in the Weddell Sea and in the Ross Sea, Antarctica, *in* Proceedings of 11th World Petroleum Congress: v. PD 2, London, p. 1-13.

Houtz, R. and Davey, F. J., 1973, Seismic profiler and sonobuoy measurements in Ross Sea, Antarctica: Jour. Geophysical Research, v. 78, p. 3448-3468.

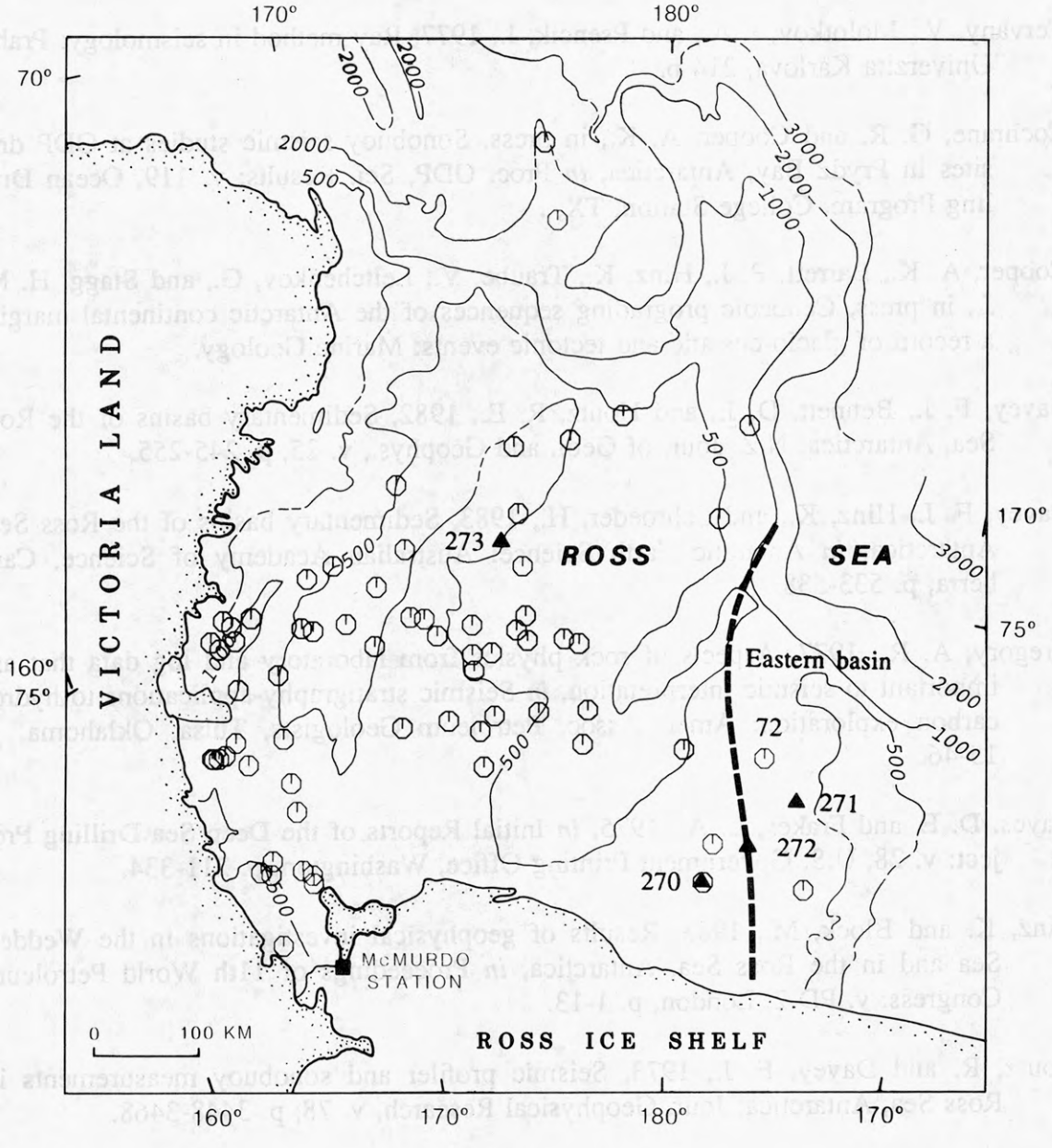

Figure 1. Map showing locations of 1989-1990 sonobuoys (circles) and DSDP sites in (filled triangles) the Ross Sea. Dashed line represents western boundary of the Eastern Basin. DSDP sites and sonobuoy 72 are labeled on the map.

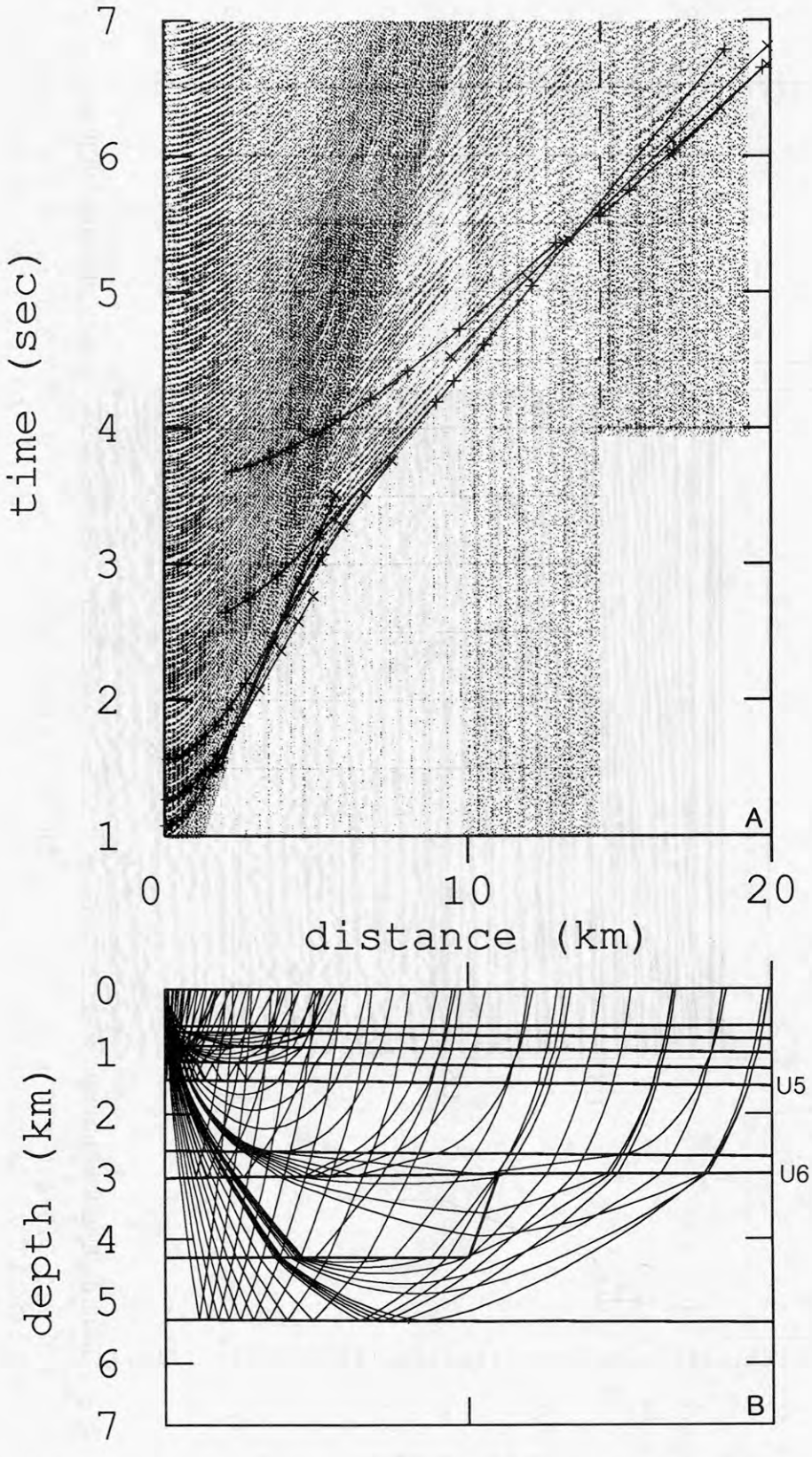

Figure 2. Ray-trace modeling of sonobuoy 72 data. A. Sonobuoy data and ray-tracing arrival times. X's indicate refracted arrivals and +'s indicate reflected arrivals. B. Velocity-depth model for ray-tracing with superimposed raypaths. Sonobuoy location is at 0 km distance. See figure 3 for velocity-depth profiles at west and east edges of the model.

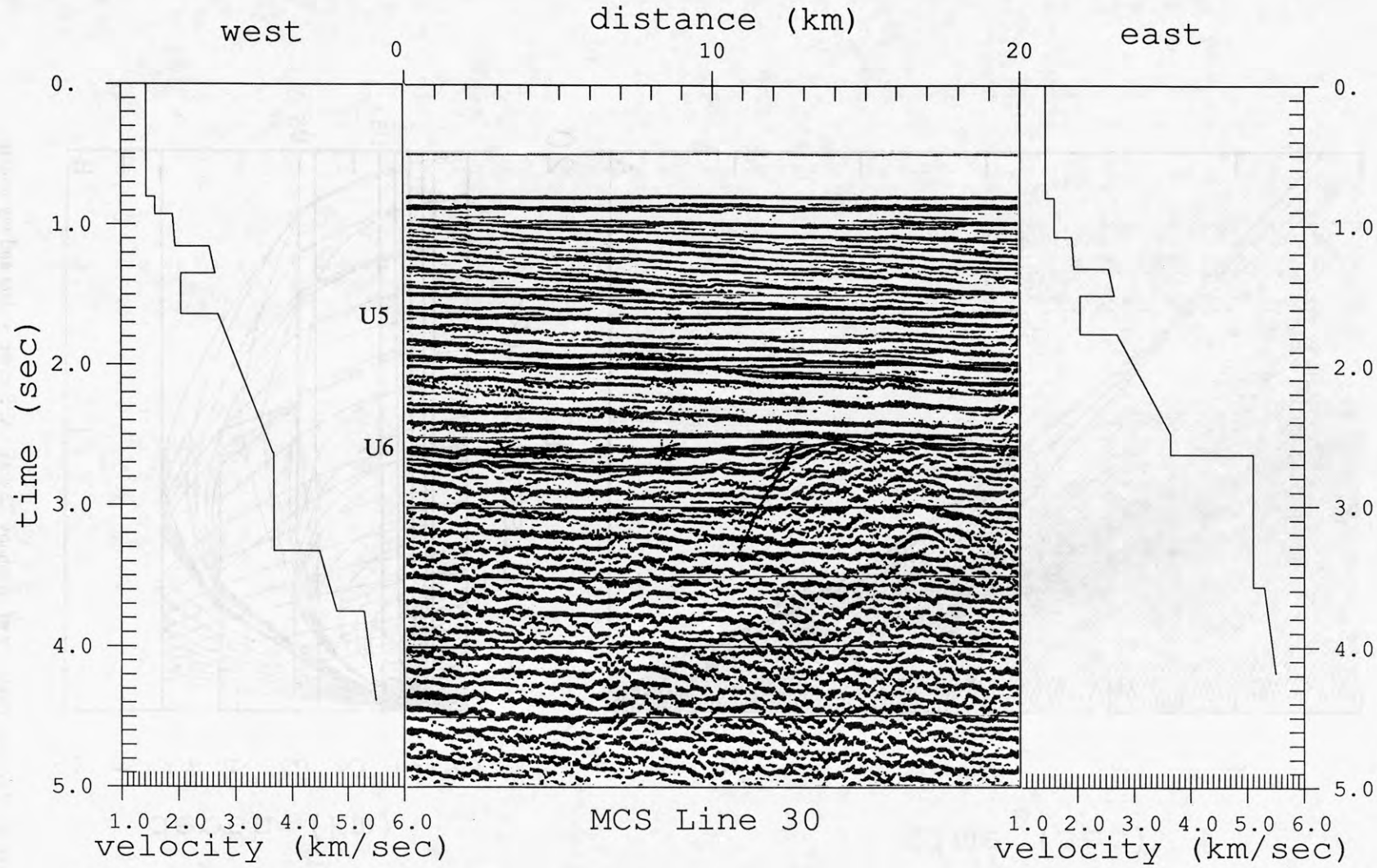

Figure 3. MCS data recorded simultaneously with sonobuoy 72 data. Location of sonobuoy 72 is at 0 km distance. Times are two-way traveltimes. Location of unconformities in the section are indicated on the western edge of the data by U5 and U6. Eastern edge of graben below U6 is shown as a line drawn on the data. Velocity depth profiles derived from sonobuoy data using ray-tracing method (Fig. 2)

LATE QUATERNARY HISTORY OF THE BUNGER HILLS, EAST ANTARCTICA

Eric A. Colhoun, Department of Geography,
University of Newcastle, Shortland,
New South Wales 2308, Australia.
Donald A. Adamson, School of Biological Sciences,
Macquarie University, North Ryde,
New South Wales 2113, Australia.

The Bunger Hills protrude from the inner continental shelf of East Antarctica (66°S and 101°E). The Antarctic ice sheet expanded northwestwards and submerged the ice-free oasis during the last glaciation. The limited degree of glacial erosion and presence of thick glacial deposits in the northwestern part of the oasis suggests that the ice sheet may not have extended far onto the continental shelf or been much thicker than the highest hills (163 m). Glacial retreat was caused by the rise of sea level which flooded the major inlets within the hills during the early to middle Holocene (before 7.7 ka BP to 5.6-5 ka BP). Sea level rise caused collapse of the thin margin of the ice sheet into the inlets without systematic southward retreat of the ice sheet edge. Several ice-dammed lakes, with eroded shore terraces, existed during the period of glaciation.

Raised beaches occur extensively in the main inlets up to 7.5 ± 1 m above the modern wave and sea ice limit. Middle and late Holocene (post 5.6 ka BP) uplift occurred at 1.4 m/ka. Morphological forms suggest that openwater wave action was more important in the inlets during the middle Holocene and that sea ice has increased in the late Holocene. The low altitude of the beaches suggests a thin ice cover of >140 m and <330 m. Similar evidence from Vestfold Hills and Windmill Islands also points to the margin of the East Antarctic ice having been much thinner than postulated by Hollin (1962) and Hughes *et al.*, (1981).

Within the Bunger Oasis two sets of moraines occur marginal to the Edisto Ice Tongue and Apfels Glacier; the Older and Younger Edisto Moraines which are dated to after 6.2 ka BP and the last few centuries respectively. A major end moraine located at the junction of the Antarctic ice sheet with the rising hills and perennial snow-wedge in the south represents the ice margin position since at least 5.6 ka BP.

SEISMIC EVIDENCE FOR MAJOR LATE CENOZOIC ICE-VOLUME VARIATIONS ON THE ROSS SEA AND WILKES LAND CONTINENTAL MARGINS, ANTARCTICA

A.K. Cooper, U.S. Geological Survey, 345 Middlefield Road, Menlo Park, CA 94025, USA
S.L. Eittreim, U.S. Geological Survey, 345 Middlefield Road, Menlo Park, CA 94025, USA
J. Wannesson, Institut Francais du Petrol, 1&4 Ave deBoise-Preau, BP 311, 92506 Rueil Malmaison Cedex, France
K. Hinz, Bundesanstalt fur Geowissenschaften und Rohstoffe, PO Box 51053, D-3000 Hannover 51, Germany

BACKGROUND

Multichannel seismic-reflection surveys of the Ross Sea and Wilkes Land continental shelf and rise reveal that sedimentary sequences reaching several kilometers thickness have prograded across the paleo shelf up to 85 km since about middle Cenozoic time. The Cenozoic prograding sequences have some stratal geometries and velocity characteristics that suggest grounded ice sheets episodically advanced across the continental shelf to the paleo shelf edge. These advances, which correspond to inferred major build-ups of ice on the Antarctic continent, deposited large quantities of sediment in the prograding sequences.

Cores obtained from scientific drilling of the Antarctic margin indicate that a large East Antarctic ice sheet has existed since about 40 Ma, and that this ice sheet extended to the continental shelf edge in Prydz Bay by 36 Ma (early Oligocene time). In the Ross Sea region, ice sheets have existed near the Transantarctic Mountains since early Oligocene time. Yet, the acoustic geometry of the Ross Sea prograding sequences suggest an episodic history of ice-volume growth during which ice was first grounded at the continental paleo-shelf edge in early Miocene time. In the Ross Sea, and elsewhere around Antarctica (e.g. Larter and Barker, 1989; Cooper et al., 1991; Kuvaas and Kristoffersen, in press), the ice-volume fluctuations seem to have been more intense during latest Cenozoic time, based on seismic data. However, few drilling data exist to provide age control for the seismic sequences.

ACOUSTIC GEOMETRIES

Acoustic geometries within the inferred Cenozoic sedimentary sections beneath the Ross Sea and Wilkes Land outer continental shelf generally become more complex and disrupted upsection from the regional unconformity at the base of these sections. Near the base of the sections, reflections are generally well layered, continuous, nearly-flat, and downlap seaward (type IIA sequences of Cooper et al., in press). Upsection, strata first make a transition to steeper dips (on the paleo shelf) and then

to steep and sometimes discontinuous sigmoidal geometries (type IA sequences) that aggrade and prograde the paleo shelf. Numerous unconformities exist and separate individual sigmoidal sequences, especially in type IA sequences. The upsection transition from type IIA to IA sequences is believed to mark the initial overdeepening of the entire continental shelf, the first movement of grounded ice sheets seaward to the continental shelf edge, and an apparent shift in the location of the paleo shelf edge. Before this transition, ice sheets were likely to have existed onshore, but did not extend far onto the continental shelf.

Prograding strata (i.e. type IA sequences) were deposited on the paleo continental slope, and on the flanks of old erosional troughs on the continental shelf, from apparent linear sediment-sources. The linear sources and high observed sea-floor velocities from overcompacted sediments (e.g. Solheim et al., 1991) indicate likely deposition of the sequences from the basal-front of grounded ice sheets. Seismic unconformities underlying the continental shelf can, in places, be traced seaward beneath overlying dipping and downlapping sequences into the abyssal basin. The unconformities, mark erosional (and depositional) events believed to be associated with the seaward movement of grounded ice-sheets to the paleo continental shelf edges, and consequent delivery of glacial debris directly to the upper continental slope. These unconformities may be continuous (and coeval) along much of the continental margin from the Ross Sea to Prydz Bay; however, seismic data are presently inadequate to confirm this.

ROSS SEA

Prograding sedimentary sequences are found over large areas of the eastern Ross Sea and in places near the continental shelf edge of the western Ross Sea. DSDP drilling has shown that these sequences are exclusively of glacial marine origin. The seismic data in the eastern Ross Sea, like that from Wilkes Land, indicates that the earliest prograding (and aggrading) sequences may have been deposited on and across an overdeepened paleo continental shelf, which is now deeply buried. The present continental shelf edge, which is a depositional feature, lies close to the former pre-glacial, structural edge of the continental shelf (i.e. the shelf edge before the prograding sequences were deposited). Near the buried paleo shelf edges, the acoustic geometry includes terminated flat reflectors, mounded reflections, angular discordances and other features that may be explained by episodic movement of grounded ice sheets to the continental shelf edge (e.g. Cooper et al., in press; Hambrey et al., in press). Although these characteristics are observed in strata of early Miocene and younger age, they do not occur in older strata (i.e. below unconformity U5 of Hinz and Block, 1984).

WILKES LAND

Seismic data show that in places up to 80 km of progradation of Cenozoic deposits has occurred on the Wilkes Land continental shelf (Eittreim and Smith, 1987; Wannesson, 1990). Near the present continental shelf edge, several buried troughs 25 to 70 km wide are floored by a prominent unconformity that can be traced nearly 300 km along the margin. These troughs, which are the likely seaward pathway for former late Cenozoic grounded ice sheets, have been infilled from along both flanks (and from the landward mouth) with up to 1 km of prograding strata. The infilled troughs are eroded and partly covered by flat-lying strata that have since been cut into banks and swales that form the present sea floor.

The unconformity that floors the troughs is a strong reflector that can be traced down the continental slope at or below the base of most of the sedimentary units that have been incised to make the large submarine canyons. On one seismic line, 23 km of shelf prograding has occurred above this unconformity. We suggest an age of late Miocene to early Pliocene for this unconformity, based on comparison of seismic and drilling data from the Ross Sea (and Prydz Bay).

MODEL

The acoustic geometry of Cenozoic deposits of the outer continental shelves in the Ross Sea and Wilkes Land areas is characterized by a deep regional unconformity (U6 in the Ross Sea; Hinz and Block, 1984) overlain by gently dipping strata that change to strongly prograding and aggrading strata with many discontinuities, which are especially prominent in the young sediments. Our interpretation is that the gently dipping strata (type IIA sequences) were deposited on a normal depth continental shelf during early glacial times when ice-sheets may have existed at or near the coast. The transition to strongly prograding strata (type IA sequences) marks the first advance of grounded ice sheets to the paleo shelf edge, and the initial over-deepening of the shelf due to the ice load. Numerous individual prograding sequences and unconformities mark later episodes during which grounded ice sheets again advanced to the continental shelf edge. Such advances are probably closely tied to the variations in the size of the adjacent East Antarctic ice sheet. These variations have seemingly increased in their intensity during latest Cenozoic times (i.e. late Miocene and younger times), based on the offshore sedimentary record.

REFERENCES

Cooper, A. K., Stagg, H., and Geist, E., 1991. Seismic stratigraphy and structure of Prydz Bay, Antarctica: Implications from ODP Leg 119 drilling. In: J. Barron, B. Larsen (Editors), Proc. ODP, Sci. Results, 119. Ocean Drilling Program, College Station, TX., in press

Cooper, A.K., Barrett, P.J., Hinz, K., Traube, V., Leitchenkov, G., Stagg, H.M.J., in press. Cenozoic prograding sequences of the Antarctic continental margin: a record of glacio-eustatic and tectonic events. Marine Geology.

Eittreim, S. L., and Smith, G. L., 1987. Seismic sequences and their distribution on the Wilkes Land margin. In: S. L. Eittreim, M. A. Hampton (Editors), The Antarctic Continental Margin: Geology and Geophysics of offshore Wilkes Land. Circum-Pacific Council for Energy and Mineral Resources Earth Science Series, Houston, 5A: pp.15-43.

Hambrey, M. J., Barrett, P. J., Ehrmann, W. U., and Larsen, B., in press. Cenozoic sedimentary processes on the Antarctic continental margin and the record from deep drilling. In: M. G. Marcus, H. M. French, G. Staglein (Editors), Proceedings of the ICG Symposium No. 5: Glacial and Polar Geomorphology. Zeitschrift fur Geomorphologie Spec. Issue, Bremen.

Hinz, K., and Block , M., 1984. Results of geophysical investigations in the Weddell Sea and inthe Ross Sea, Antarctica. Proceedings of 11th World Petroleum Congress, London (1983), PD 2: 279-291.

Kuvaas, B., and Kristoffersen, Y., in press. The Crary Fan: A trough-mouth fan on the Weddell Sea continental margin, Antarctica. Marine Geology.

Larter, R. D., and Barker, P. F., 1989. Seismic stratigraphy of the Antarctic Peninsula Pacific margin: A record of Pliocene-Pleistocene ice volume and paleoclimate. Geology, 17: 731-734.

Solheim, A., Forsberg, C. F., and Pittenger, A., 1991. A stepwise consolidation record for the glacigenic sediments of Prydz Bay and its relationship to the glacial history of East Antarctica. In: J. Barron, B. Larsen (Editors), Proc. ODP, Sci. Results, 119. Ocean Drilling Program, College Station, TX, in press.

Wannesson, J., 1990. Geology and petroleum potential of the Adelie Coast margin, East Antarctica. In: B. St. John (Editor), Antarctica as an Exploration Frontier--Hydrocarbon Potential, Geology, and Hazards. American Association of Petroleum Geologists Studies in Geology #31, Tulsa, pp.77-88.

THE ANTOSTRAT PROJECT - INTERNATIONAL OFFSHORE STUDIES ON ANTARCTIC CENOZOIC HISTORY, GLACIATION, AND SEA-LEVEL CHANGE

A.K. Cooper, U.S. Geological Survey, 345 Middlefield Road
Menlo Park, CA 94025, USA
P.N. Webb, Department of Geology, Ohio State University,
125 South Oval Mall, Columbus, OH 43210, USA

In April 1989, the Scientific Committee on Antarctic Research (SCAR) Group of Specialists on the Evolution of Cenozoic Paleoenvironments of the Southern High Latitudes proposed a multi-year International project to study the Cenozoic sedimentary deposits around Antarctica, focusing in particular on the extensive sedimentary sections beneath the continental margin. The project, as adopted in July 1990, seeks to integrate a variety of offshore geophysical, geological and glaciological data bases, and to incorporate them with ongoing studies to better understand the relationships between Cenozoic terrestrial and marine glacial-interglacial histories and between Cenozoic ice-volume and global sea-level variations.

The new project is ANTOSTRAT (Antarctic Offshore Acoustic Stratigraphy) in recognition that much of what is currently known about the Antarctic continental margin is derived from the vast quantity of acoustic data (e.g. high- and low-resolution seismic-reflection, bathymetry and side-scan data) that has been collected since the 1960s. Although extensive data exist, ANTOSTRAT is the first major international effort to compile and integrate all existing offshore acoustic data sets to study circum-continental Cenozoic events in Antarctica and to help plan future offshore geophysical and geological studies.

Several investigators have noted that the continental shelf is underlain in many places by Cenozoic sedimentary sequences that are many kilometers thick and have prograded the continental shelf up to 85 km (e.g. Hinz and Block, 1984; Haughland et al., 1985; Larter and Barker, 1989; Cooper et al., in press). The Cenozoic sequences have been drilled on the continental shelves in the Ross Sea and Prydz Bay and are composed of glacial-marine rocks of at least early-Oligocene and younger age. These sequences have acoustic signatures suggesting that grounded ice sheets have episodically moved out to the continental shelf edge, and back, many times during the Cenozoic. The erosion and deposition of strata by these grounded ice sheets have left geologic records of the growth and decay of the Antarctic Ice Sheet, and these records can be used to infer ice-volume changes. Deciphering the proximal record of Antarctic ice-volume changes and its link to global sea-level variations is a significant goal of the ANTOSTRAT project.

The record of Cenozoic sea level changes is controlled by many factors, all of which must be considered to unravel this record in absolute rather than relative terms. The glacial strata of

the Antarctic continental shelf and slope must first be understood in terms of its depositional environment. Factors controlling relative depths of the Antarctic continental margin include Cenozoic (and Mesozoic) tectonism, ice-sheet loading, rates and times of erosion and sediment supply, and degrees of sediment compaction. For example, as a result of these factors, the Antarctic continental shelf presently lies mostly in water depths greater than 400 m, which is too deep to expose the shelf to subaerial erosion (but not to ice erosion) during common sea-level fluctuations of 100-300 m. Studies by the ANTOSTRAT project will also address the direct and indirect effects that these factors have had throughout Cenozoic time to correctly resolve the history of ice sheet movements as it is recorded in glacial rocks beneath the Antarctic continental margin.

The scientific goals and procedures for the ANTOSTRAT project are established and implemented by a nine-member international steering committee that is guided by advice from the geoscience community. As such, ANTOSTRAT presently functions in advisory and coordinating roles to national programs within the Antarctic geoscience community. Scientific interchange is through workshops and regional working group meetings dedicated to topics on Antarctic Cenozoic history of global scientific interest. At the first ANTOSTRAT workshop in June 1990 (Cooper and Webb, 1990), existing data holdings were displayed, and topics relating to factors controlling the deposition of offshore Cenozoic glacial strata were discussed. Additionally, working groups with regional coordinators were established for five areas of the Antarctic continental margin (Antarctic Peninsula, Ross Sea, Wilkes Land, Prydz Bay, and Weddell Sea) to facilitate multinational data compilations and interpretations and to investigate regional problems.

Future thematic workshops are planned, and geoscience researchers who are interested in contributing data (existing or planned) and ideas to ANTOSTRAT's scientific objectives are encouraged to participate. Further major advances in the resolution of Cenozoic glacial history are likely to come, in the near future, from offshore areas where the Cenozoic record is preserved. Multidisciplinary geoscience studies of these areas are needed, especially scientific drilling programs that can sample below the ubiquitous surficial diamictons. The greatest benefits to Antarctic Cenozoic geoscience will come through coordinated international studies, which ANTOSTRAT strongly advocates and encourages.

REFERENCES

Cooper, A.K. and Webb, P.N. (Editors), 1990. International Workshop on Antarctic Offshore Acoustic Stratigraphy (ANTOSTRAT): Overview and Extended Abstracts. U.S. Geological Survey Open-File Report 90-309, Menlo Park, 290 p.

Cooper, A.K., Barrett, P.J., Hinz, K., Traube, V., Leitchenkov, G., Stagg, H.M.J., in press. Cenozoic prograding sequences of the Antarctic continental margin: a record of glacio-eustatic and tectonic events. Marine Geology.

Haugland, K., Kristoffersen, Y., and and Velde, A., 1985. Seismic investigations in the Weddell Sea embayment. Tectonophysics, 114: 293-313.

Hinz, K., and Block , M., 1984. Results of geophysical investigations in the Weddell Sea and inthe Ross Sea, Antarctica. Proceedings of 11th World Petroleum Congress, London (1983), PD 2: 279-291.

Larter, R. D., and Barker, P. F., 1989. Seismic stratigraphy of the Antarctic Peninsula Pacific margin: A record of Pliocene-Pleistocene ice volume and paleoclimate. Geology, 17: 731-734.

MAJOR MAGNETIC ANOMALIES IN WESTERN DRONNING MAUD LAND; THEIR POSSIBLE ORIGIN AND CORRELATES IN SOUTHERN AFRICA

B Corner, University of the Witwatersrand, Johannesburg,
J C Maccelari 2050, South Africa.
S Niccol. Geodass (Pty) Ltd, Johannesburg, South Africa.

In this study, magnetic data from South Africa, Dronning Maud Land (DML) in Antarctica, and the Falklands plateau, are compared and interpreted within a Gondwana reconstruction.

The Beattie magnetic anomaly occurring in the poly-metamorphic Namaqua-Natal belt of South Africa, beneath Phanerozoic cover, has a strike length of some 900 km. The anomaly has no gravity expression, is semi-linear, and can be modelled by a slab with a depth-to-top of roughly 6 km and bounded by low-angle faults dipping to the south (suggestive of thrusting northwards towards the Kaapvaal craton). The origin of the anomaly is speculative, with some workers favouring serpentinised mafic material. However, anomalies with a similar signature and strike direction occur to the north of the Beattie anomaly and correlate with outcropping basement granite-gneisses in Natal. The authors interpret high susceptibilities measured in these outcrops to arise from pervasive recrystallisation of iron to magnetite, and favour a similar setting for the Beattie anomaly. The timing is uncertain, possibly relating to the Cape orogeny at circa 500 Ma.

Fütterer et al (1989) synthesized and interpreted aeromagnetic data, derived primarily from surveys by the USSR and Germany, in a geotraverse crossing western DML. We extend this study in the light of additional South African airborne data and of marine magnetic data available for the Falklands plateau. A number of major semi-linear magnetic anomalies are observed in DML with signatures remarkably similar, in terms of amplitude (100-900nT), strike-length (›600km) and wavelength, to the Beattie anomaly. The southernmost of these anomalies coincides in the east with the granite-gneisses of the Kirwanveggen and Sverdrupfjella. Field observations and magnetic modelling indicate low-angle thrusting from the south east (toward the Kaapvaal craton in a Gondwana context). The signatures of the Beattie and DML anomalies also make them useful as continental-scale marker units. Their positions, as well as our postulated extension of the Beattie anomaly into the Falklands plateau within Gondwana, clearly mimic the boundaries of the Kaapvaal craton. The inference from our observations is that both the Beattie and DML anomalies have a common origin in the evolution of the poly-metamorphic terrains which surround the Kaapvaal craton.

Reference. Fütterer, D, (1989). Convener on behalf of: the Alfred Wegener Institute for Polar and Marine Research (FRG); the Federal Institute of Geosciences and Mineral Resources (FRG); the Northern Research Corporation for Marine Geology, SEVMORGEOLOGYA, (USSR); the Universities of Aachen (FRG), Gottingen (FRG), Munster (FRG), Natal PMB (RSA) and Witwatersrand (RSA). **Crustal transects from the Weddell sea to Dronning Maud Land, east Antarctica.** Poster presented at the IGC, Washington DC.

LATE CRETACEOUS PALAEOENVIRONMENTS OF ANTARCTICA

J.A. Crame, British Antarctic Survey, Natural Environment Research Council, High Cross, Madingley Road, Cambridge CB3 0ET, U.K.

The concept of the Late Cretaceous as a period of globally warm, equable climates is coming under increasingly closer scrutiny. In particular new data from the polar regions is pointing to significant phases of cooling in both the Campanian and Maastrichtian stages. Within Antarctica and contiguous regions, cooling trends have been identified in the late Campanian-early Maastrichtian and the late Maastrichtian. They are coincident with major basin-wide shallowing events and thus may be eustatically driven. However, the possibility of local tectonic influences cannot be excluded.

The nature and scale of Late Cretaceous biotic extinctions in the high southern latitudes is being re-assessed. Whereas certain molluscan groups, such as belemnites and inoceramid bivalves, became extinct well before the Cretaceous-Tertiary boundary, others, such as the ammonites, are present right up to it. An unusual combination of environmental parameters (lower temperatures, high seasonality, etc.) may well have governed processes such as taxonomic origination and extinction in polar regions. Nevertheless, the presence of certain terrestrial taxa, such as dinosaurs, indicates that the "polar winter" scenario may not have been as potentially lethal as was once imagined.

PERMIAN THROUGH TRIASSIC PALAEOCLIMATIC EVOLUTION IN ANTARCTICA BASED ON PALAEOVEGETATIONAL DATA

R.Cuneo, Byrd Polar Research Center-OSU, Columbus, Ohio, USA.
E.L.Taylor and T.N.Taylor,Dept.of Plant Biology and Byrd Polar Research Center-OSU, Columbus, Ohio, USA.

The plant record in Antarctica indicates a continuous change from the Permian to the Triassic as a consequence of paleoclimatic and palaeogeographic dynamics. As a result, the physiognomy, composition and distribution of plant communities, as well as some anatomical, climatically-sensitive features (e.g. growth rings), were constantly adapting to new macroclimate parameters. The poorest climatic conditions for plant growing (very cold and dry) occurred by the earliest Permian, a time when the peak of the Gondwanian glaciation took place with the South Pole located on Antarctica. The record of vegetation is limited to a few palynomorphs recovered from glacial sediments. Immediately above the glacial sediments are lacustrian deposits that contain the first record of Permian megafossils. This vegetation is believed to have occupied those habitats that originated during glacial retreat. The flora at this time consisted of small trees and shrubs that produced *Gangamopteris* foliage.The climate was periglacial but showed some increase in humidity.

The next vegetational step in Antarctica was much more successful and is recognized throughout the Transantarctic basin. It was probably the result of a general warming due to the northward drifting of the Gondwana plate. This stage is characterized by a forest vegetation occupying different habitats associated with fluvial systems. The forest had a deciduous character as suggested by large numbers of *Glossopteris, Gangamopteris* and *Cordaites* leaves found in the taphocenosis. Growth rings in petrified logs are very narrow, suggesting a short growing season. Thus, a highly seasonal, cold or cool and moist temperate climate is suggested; high humidity is assumed from the presence of thick coal measures. A similar vegetational/climate framework is thought to have occured during the Late Permian, especially in the central Transantarctic Mountains where very dense "in situ" palaeoforests occur; *Glossopteris* was the main leaf type produced by this vegetation.

The first Triassic phytosuccessional step is not well defined in Antarctica. Formational units of this age (lower Fremouw Formation and most of the Feather Conglomerate) contain monotonous taphocenosis of *Neocalamites*-like stems in restricted communities. Palynological records were not found in this part of the sequence. Thus, this low diversity flora may suggest some kind of climatic control due to drier conditions. This is also in accordance with a small amount of original phytomass available prior to coal formation, which is contrasted with the late Permian and mid Triassic stages. The changes in climate may be associated with a geographic barrier related to the volcanic arc located along the Antarctic and Australian gondwanian

margin; this would have played a key role as a barrier for humid winds.

The following successional step took place during the upper Early and Middle Triassic and is recognized through mega and microplant assemblages of southern Victoria Land and the central Transantarctic Mountains (Lashly and mid-upper Fremouw Formations). Its main feature, in comparison with the Lower Triassic, is that of a much more diversified vegetation as a direct result of improving in both temperature and humidity. Gymnosperm forests were well developed, and consisted of communities dominated by *Rhexoxylon?/Dicroidium* stands in levee and floodplain environments of braided fluvial systems. Understory vegetation in the same forests was represented by shrubby ferns of the *Osmunda* type; pure communities of *Neocalamites*, although restricted, still occupied hygrophyllous biotopes of river banks and small lakes. Growth rings in petrified logs may be up to 1 cm wide, suggesting an important growth period in a seasonal climate.

The Late Triassic vegetation (lower Falla Formation) shows a slightly greater diversification as a result of the final consolidation in the *Dicroidium* flora, also recognized in other Gondwanian regions. Climatically, the same features as in the previous step could be suggested for this time.

Finally, a continuous increase in temperatures is suggested in Antarctica beginning in the Late Permian and is reflected through the palaeovegetation. It has been also suggested that this increase was related to a higher level of CO_2 in the atmosphere which contributed to a "greenhouse effect", especially during the Mesozoic. The increased volcanic activity in Antarctica from Late Permian times would have been an important source for CO_2 in high latitudes of the Southern Hemisphere.

Neighbors?: Implications for Antarctic geology of the East Antarctic and Laurentian Pacific margins as a conjugate rift pair

I.W.D. Dalziel, Institute for Geophysics, University of Texas at Austin,
8701 Mopac Boulevard, Austin, Texas 78759-8345, USA.

Evidence supports the hypothesis (E. Moores, *Geology*, 1991, in press) that the Laurentian and East Antarctic-Australian cratons were continuous in the late Precambrian and that their Pacific margins were initiated as a conjugate rift pair (I. Dalziel, *Geology*, 1991, in press). Both margins extend for approximately 40° of latitude. They have a similar rift history throughout their length, i.e. Late Proterozoic rifting and Early Cambrian carbonate platform development. A geometrically acceptable computer-generated reconstruction for the latest Precambrian can be achieved. This reconstruction juxtaposes and aligns the Grenville front that is truncated at the Pacific margin of Laurentia and a closely comparable tectonic boundary in East Antarctica that is truncated along the Weddell Sea margin. These may prove to be critical, perhaps even unique, "piercing points" for relating the northern and southern continents.

Geologic and paleomagnetic evidence also suggest that the Atlantic margin of Laurentia rifted from the proto-Andean margin of South America in the earliest Cambrian. Early Phanerozoic sea-floor spreading that isolated Laurentia from South America and East Antarctica-Australia in an Eocambrian supercontinent appears to balance convergence along the Mozambique suture that resulted in final amalgamation of the smaller Gondwana supercontinent at ~500 Ma.

This new view of the origin of the southern Pacific Ocean basin has many implications for Antarctic geology. These include: the relation of the Antarctic and Laurentian cratons; the tectonic significance of Late Proterozoic rifting along the Transantarctic margin; the nature and tectonic significance of the Ross orogeny; and constraints on terrane displacements in West Antarctica. The oral presentation will focus on these issues.

GLACIERIZATION OF THE CENTRAL PART OF THE SOR RONDANE, ANTARCTICA : GLACIOLOGICAL EVIDENCE

H. DECLEIR, F. PATTYN and Ph. HUYBRECHTS

Geografisch Instituut, Vrije Universiteit Brussel,
Pleinlaan 2, B-1050 Brussel, Belgium

The Sor Rondane (Dronning Maud Land, Antarctica) is a marginal mountain area, situated some 200 km from the coast -250 km long and parallel to the coast line- and damming the main flow from the ice sheet. The damming effect can clearly be seen by (i) the stepwise topography of the glaciers at the southern margin where they cut through the range (ii) the divergent and convergent ice flow pattern resp. south and north of the range (iii) the considerable reduced ice mass transport through the central part of the range. In the Sor Rondane extensive ice free areas are found, which were once overridden by ice and whose geological and geomorphological aspects are at present being extensively studied by Japanese earth scientists. On the basis of field work carried out during JARE 28 (1987-88), 31 and 32 (1990-1991) we were able to study the glacial characteristics of the central part of the range in relation to its glacierization and deglaciation.

Ice thickness measurements, carried out by radio echo sounder and gravimeter, reveal a subglacial topography of the outlet glaciers and its tributaries characterized by U-shaped valley profiles and overdeepened bedrock. Seen the absence of any blockfaulting this patterns is apparently caused by deepening of a pre-existing fluvial network caused by a considerable, mainly south-north flowing, ice cover.

The mass-flux measurements highlight the reduced flow of at least one outlet glacier (Jenningsbreen). This glacier is in the process of being cut off from the main ice supply and may serve as an example for the deglaciation process. An interesting feature of this deglaciation is that, once decoupled from the main ice supply, this glacier is probably characterized by an increasingly lowering of the ice surface gradient due to the ablation which is characteristic for the upper part of the present outlet glacier. In the end this will result in a reversed flow (north to south) of which examples can be found elsewhere in the range. Also, inverted moraine arcs testify at many places of the compensating advance of ice lobes into the -now ice free- valleys.

On basis of the field evidence, a numerical one-dimensional model is presented to simulate the glacier behaviour in the central part. The glacial expansion experiment shows the expected increase in ice thickness under reasonal assumptions for mass balance, temperature and sea level. These result are then compared with the paleo ice sheet reconstruction as inferred from glacio-geological evidence by Hirakawa et al. (1988 and 1990). Finally, the paleoenvironments pertaining to maximum and minimum ice extents are discussed.

HEAT FLOW AND ACTIVE TECTONICS OF THE WESTERN ROSS SEA

B. Della Vedova, G. Pellis, Istituto di Miniere e Geofisica Applicata, Università di Trieste, Via Valerio, 10 34127 Trieste, Italy.
L.A. Lawver, Institute for Geophysics, University of Texas at Austin, 8701 Mopac Blvd., Austin, Texas 78759-8345, USA.

As part of the 1990-91 sixth Italian Antarctic Program, single channel high resolution and multi-channel reflection seismics, gravity, magnetics, bathymetry, coring and heat flow (HF) have been collected in the western Ross Sea. The main targets of the R/V OGS-Explora program during January 1991 were: the recent tectonic evolution of the Victoria Land Basin (VLB) as connected to the broad and active tectonism affecting the Transantarctic mountains, a HF survey of the Drygalski Basin, Terror Rift and Franklin Basin, and sediment transport and deposition processes in the western Ross Sea. Particular effort was made to select appropriate sites where reliable HF measurements could be obtained. One goal was to map the present tectonic activity in the VLB and to relate that activity to the uplift of the Transantarctic mountain belt.

Extensional and listric faults have been recognized on the single channel seismic lines both in the Drygalski Basin and Terror Rift, which suggests a tectonic origin for the entire VLB. Its evolution seems to be controlled by extensional tectonic processes, including rifting, faulting, subsidence and locally associated magmatic and volcanic activity.

Despite the coarse and stiff sediment, which limited the penetration of the HF probe to about 3-4 meters, two reliable HF measurements in the Drygalski Basin and nine in the Terror Rift were obtained. Thermal gradients in the bottom sediment of these two deep basins (>700-800 m) were fairly linear. Exceptionally high in situ thermal conductivity values, some of which exceeded 2 W m^{-1} K^{-1}, were measured below the uppermost 0.5-1.5 m of soft sediment. These thermal conductivity values are in good agreement with the 350 needle probe thermal conductivity measurements taken on seven cores collected in the area. Preliminary mean observed HF values of 118 ± 10 mW m^{-2} (n=2) in the Drygalski Basin and of 103 ± 15 mW m^{-2} (n=9) in the Terror Rift were calculated. The sedimentation correction factor is positive and will be estimated from the interpreted seismic sections.

Geological and geophysical data collected in the central part of the VLB support a tectonic origin for the Terror Rift and for the Drygalski Basin. In particular, the latter basin is proposed as a possible example of a propagating rift. Why the VLB rift system is active within an apparently stable and aseismic plate, poses another question which may be answered by knowledge of the deep thermal conditions within the basin.

THE VELOCITY STRUCTURE OF EREBUS VOLCANO, ANTARCTICA, AND ITS ACTIVE LAVA LAKE

R.R. Dibble and B. O'Brien,
Victoria University, Wellington, New Zealand.
C.A. Rowe, Geophysical Institute,
University of Alaska, Fairbanks, AK 9975-0800

Erebus of 3.7km altitude is a phonolitic volcano on Ross Island with an active lava lake in its summit crater. A combination of 3 seismic refraction lines up to 1.4km long, 6 large seismic shots up to 300kg, and many strombolian explosions recorded by video surveillance in the crater and on the 10 station seismic net reveals the following velocity structures:

The surface permafrost layer of ejecta on the summit cone has a velocity of about 3km/s, and prevents refraction arrivals from lower velocity layers. Shooting in warm ground shows a 1.3km/s layer up to 100m thick under the summit plateau of the volcano, with lateral changes in the underlying refractor from 1.6 to 3.7km/s along the line of fumaroles from the Side Crater to the somma rim. Over 1.4km, the maximum delay relative to a 4.0km/s arrival is 0.21s. A ray tracing model will be presented.

The seismic net records of the large shots define a model (Rowe 1988) with a linear vertical gradient from 3.55km/s at the summit to 4.6km/s at 7km depth, overlying a 6.1km/s half space. With this model and epicenter program HYPOELLIPSE, the shots can be relocated from the sometimes poor recordings with errors averaging 0.8±1.1s in time, 1.3±1.6km in position, and 1.5±0.54km in depth. Most well recorded explosion earthquakes accompanying cannon-like strombolian explosions are found to occur at shallow depth under the summit crater.

Several families of explosion earthquakes with cross-correlation coefficients between waveforms exceeding 0.7 have been recorded for which the time and location of the explosion are known by video surveillance. The stacked seismic onsets and explosion instants are reliable and show that the explosions occur 1.47 ± 0.1s before the intercept time of the seismic time/distance curve, which has an apparent velocity of 3.8±0.3km/s between 0.7 and 10.1km distance. The refraction lines show that a seismic delay of such magnitude is not occurring under the summit plateau, but it could occur in the lava lake where it is easily explained by reduction in velocity caused by the vesiculation of the liquid lava observed in ejected bombs. The velocity structure in the lava lake has been modelled using Sparks' 1976 analysis of vesiculation in rising magma columns and Woods' 1946 equation (confirmed by Miksis and Ting, 1989, for vanishing Reynolds number) for the velocity in bubbly liquids. Assuming 50% vesiculation at the surface, the theoretical velocity there is only 18m/s, increasing with depth at gradients of up to 25/s, to the nominal bubble free velocity of 2.3km/s at 250m depth. Ray paths from sources in such a lava lake are strongly curved, and inhibited from escaping from the lake at shallow depth by large critical angles and high reflection coefficients. Those recorded should originate steeply downwards, and the observed apparent velocity of 3.8±0.3km/s is close to that expected at the depth of the path in Rowe's model.

PALEOMAGNETISM OF MARIE BYRD LAND, WEST ANTARCTICA

V.J. DiVenere, Lamont-Doherty Geological Observatory, Palisades, New York
South Pacific Rim International Tectonics Expedition, *SPRITE

Marie Byrd Land is one of four major crustal blocks which make up west Antarctica. Recent paleomagnetic studies in the Antarctic Peninsula, Thurston Island, and Ellsworth-Whitmore Mountains crustal blocks, combined with geochemical and structural analyses have placed constraints on the position and relative motions of these with respect to the east Antarctic craton and Gondwana. Only two paleomagnetic studies have been published on rocks from Marie Byrd Land. Scharnberger and Scharon (1972) got results (pole long/lat=116.3 E/36.0 S, α_{95}=27.7) with a high degree of scatter from Cretaceous igneous rocks which indicated a low paleolatitude discordant with the rest of Gondwana. Grindley and Oliver (1983) studied rhyolitic and mafic dike swarms radiometrically dated at 90-110 Ma. These rocks yielded stable results (pole long/lat=242 E/65 S, α_{95}=4.5) with a high paleolatitude similar to the rest of Gondwana.

Six hundred-thirty five oriented cores and 60 oriented hand samples were collected during the 1990-1991 austral summer from formations ranging in age from late pre-Cambrian through Cretaceous, as well as from dikes of probable Cenozoic age. Upon coring of hand samples there will be 900 to 1000 oriented cores for paleomagnetic analysis. This was part of the tripartite United States-New Zealand-United Kingdom expedition to Marie Byrd Land, SPRITE (South Pacific Rim International Tectonics Expedition). Paleomagnetic sampling was conducted in conjunction with structural analysis and sampling for geochemical analysis.

Samples were collected from turbidites and intercalated volcanics of the late pre-Cambrian Swanson Formation from Lewisohn Nunatak, Greegor Peak, and the Swanson Mts. The formation was folded in late Ordovician-early Silurian times (Adams, 1987). Three separate bedding orientations, including two limbs of a syncline, will allow the performance of a paleomagnetic fold test. Samples were collected from three locations in the Devonian Ford Granodiorite (Gutenko Nunataks, Herman Nunatak, and Chester Mts), as well as several other formations which have been suggested to be Devonian in age. Samples were collected from 22 locations across central Marie Byrd Land in igneous rocks expected to be Cretaceous in age. Sampling was conducted in bedded volcanics to allow the performance of a fold test for these rocks. Dikes were collected at several locations in order to perform contact tests.

All samples are subjected to progressive alternating field or thermal demagnetization and the magnetic remanence is measured in a cryogenic magnetometer. Preliminary results from Cretaceous syenites in the McDonald Heights area yield a stable component of magnetization indicating a high paleolatitude similar to the results of Grindley and Oliver (1983).

*SPRITE
J.D. Bradshaw and S.D. Weaver (University of Canterbury, Christchurch, New Zealand)
I.W.D. Dalziel (Institute for Geophysics, University of Texas, Austin, Texas)
V.J. DiVenere (Lamont-Doherty Geological Observatory, Palisades, New York)
S.B. Mukasa (University of Michigan, Ann Arbor, Michigan)
R.B. Pankhurst and B.C. Storey (British Antarctic Survey, Cambridge, U.K)

GPS DEFORMATION CONTROL IN THE MOUNT MELBOURNE AREA (TERRA NOVA BAY - ANTARCTICA)

D. Dominici, A. Gubellini, M. Marsella, D. Postpischl, F. Radicioni, L.Vittuari

Istituto di Topografia, Geodesia e Geofisica Mineraria
Università di Bologna - Italy

The Mount Melbourne volcanic complex is located in the area of the Italian Base and is part of the Trans-Antarctic chain that is accompanied by the Ross Depression for more than 2000 kilometres. This area is characterized by typically expansive tectonic events, which appear as a principal rifting system with deep vertical faults, lifting and rotation of the blocks, and alkaline volcanic activity. The orientation of this rifting system in Victoria Land, where the Italian Base lies (Terra Nova Bay), is approximately NW-SE.

The tectonic scheme is completed by the presence of structures, once again with an expansive character, but with an orientation (NE-SW) perpendicular to the preceding one. These structures are evidenced by a series of glaciers (Browning Pass, Corner Glacier, Turmalin Plateau, Nansen Fall, etc.) parallel to the chain and by sedimentary basins that border Victoria Land toward NE to Cape Hallet.

The same features can be found in the Mount Melbourne area; the volcanic complex is, in fact, oriented toward NNW-SSE, but it is also characterized by a NE-SW direction, which is clearly identifiable in the morphological discontinuities that tie the Browning Pass to Edmonson Point.

The same deformation pattern also results from micro-tectonic analysis, with normal micro-faults found in the deposits derived from the area's most recent activity.

This aspect leads to the hypothesis that both directions of discontinuity are still active and that in the recent past both experienced magmatic upwellings.

The multi-disciplinary interest in a geodetic network in the Italian Base area required the development of a network project divided in two parts: a fundamental network covering the area close to the base and a detail network on the Mount Melbourne volcanic cone.

The results of the analysis of the data collected during the three GPS campaign 1988-1989, 1989-1990 and 1990-1991, which were processed using the same techniques, are discussed. A preliminary comparison of individual solutions is performed and few considerations on the performance of different receivers used are presented.

Owing to the very high latitude of the region under investigation, the disturbance effects caused by the ionospheric layer turns out to be a dominant factor influencing the quality of the solutions.

ACCRETED OCEAN-FLOOR AND OCEAN-ISLAND MATERIAL IN THE MESOZOIC SUBDUCTION COMPLEX OF ALEXANDER ISLAND, ANTARCTICA

P.A. Doubleday, British Antarctic Survey, High Cross, Madingley Road, Cambridge. CB3 0ET. United Kingdom.
T.H. Tranter, Shell Internationale Petroleum Maatschappij B.V., Postbus 162, 2501 AN, Den Haag, Netherlands.

The LeMay Group (LMG) of Alexander Island is one of the best exposed Mesozoic accretionary prisms along the south-east Pacific rim. It was formed by the eastward subduction of proto-Pacific ocean crust beneath the Antarctic Peninsula margin of Gondwanaland. It consists of autochthonous trench-slope and trench-fill sedimentary rocks, mélange belts, and accreted ocean-floor lavas, pelagic sediments and ocean-islands. Bouguer gravity anomaly data show a marked positive anomaly down the centre of Alexander Island (Figure 1), representing a belt of accreted oceanic rocks more than 150 km long. This contribution describes three areas where this belt is exposed in central and southern Alexander Island (Figure 1). Similar lithologies have been described previously from northern Alexander Island by Nell (1990).

Ocean-island material

Ocean-island material is exposed in the Lully Foothills, central Alexander Island, over an area of at least 55 km² (Figure 2). It consists of pillowed and massive basaltic lava flows, tuffs, jaspers and fine-grained sedimentary rocks, with a total thickness of at least 4 km (Garrett and Storey 1987). Lavas have geochemical affinities to tholeiitic within-plate basalts and to transitional mid-ocean ridge basalts. Vesicles within the basalts indicate eruption at relatively shallow water depths, and volcanic bombs suggest subaerial volcanism. Ammonite, bivalve, echinoid, gastropod and plant remains recovered from tuffs indicate an Early Jurassic age for this sequence (Thomson and Tranter 1986). The evidence for shallow-water or subaerial volcanism, coupled with the lack of clastic sediment, leads us to conclude that these rocks were formed on an ocean island away from a continental margin.

The rocks of the Lully Foothills have not been severely deformed, with tectonic fabrics only poorly developed. Anastomosing pressure-solution seams are present in tuffs but are irregularly distributed. Minor veins filled with quartz, calcite and chlorite occur in most lithologies, indicating limited fluid flow through the rock, and replacement by quartz and calcite is widespread. Pillow lavas retain their characteristic ovoid morphology, and ammonites shows strain ratios of only 1.15-1.20.

The mechanism for emplacement of the ocean-island into the accretionary prism is indicated by several factors. First, accretion-related veins are not filled by

mineral assemblages characteristic of deep burial depths, suggesting deformation occurred at shallow crustal levels. Second, the general scarcity of shear-deformation fabrics indicate a relatively low stress regime, with material failure occurring only in the weakest horizons. Third, the absence of any material other than ocean-island or ocean-floor assemblages suggests that these rocks were emplaced *en masse* after becoming detached from the underlying ocean-floor. Therefore, we conclude that the ocean-island was accreted near to the toe of the prism.

Ocean-floor material

Ocean-floor lithologies are exposed in two areas - in the NW LeMay Range and at Herschel Heights (Figure 1).

i) NW LeMay Range

In the NW LeMay Range highly deformed interbedded sequences of pillow lavas, bedded cherts and siliceous mudstones are tectonically interleaved with arc-derived clastic sedimentary rocks (Figure 2). Lavas are vesicular, and have geochemical affinities to modern mid-ocean ridge basalts. Radiolaria contained within cherts and mudstones have been extensively recrystallised and cannot be dated. Depositional styles and facies within arc-derived clastic sediments are similar to those described from modern trenches. Therefore we interpret them as representing trench-fill sediments accreted with the ocean-floor sequences.

Accretionary deformation within the ocean-floor and trench-fill facies is intense and widespread. The earliest phase is represented by stratal disruption within trench-fill sediments, with boudinage and pinch-and-swell structures, and mobilisation of material along thrust planes indicating high fluid contents. In thin section, it is evident that independent particulate flow was the primary deformation mechanism at this time, but was superseded by grain cataclasis and the formation of discrete shear zones. Voids were filled by phyllosilicate growth. In igneous rocks, ocean-floor metamorphic fabrics are cut by accretion-related anastomosing fractures, initially lined with red opaque minerals and quartz. Later vein-fills of these and cross-cutting fractures include chlorite and green-amphibole, marking the onset of greenschist facies metamorphism. In places, blue amphiboles are present, indicating that conditions for blueschist facies metamorphism were reached for a short time. Cherts and siliceous mudstones are widely recrystallised and veined with quartz, calcite and chlorite. Pressure solution follows cataclastic deformation in all lithologies, but is best developed in the clastic sedimentary rocks. In the most highly metamorphosed areas pressure solution was superseded by crystal plasticity, which can be indicative of higher temperatures (Moore 1989).

The variation in deformation mechanisms within ocean-floor and trench-fill rocks provides evidence for the emplacement mechanism. Soft-sediment deformation features within the trench-fill rocks indicate that fluids were a major factor in determining deformation style. It is well known that fluids can be instrumental in decreasing the effective confining stress by increasing the pore-fluid pressure, which can encourage cataclasis (eg Lucas and Moore 1986). Microstructural analysis of ocean-floor basalts indicates this occurred in varying degrees throughout emplacement (Figure 3), and hence that fluids remained in the system for some considerable time. The growth of greenschist and blueschist mineral assemblages synchronous with cataclasis therefore suggests rapid burial in a closed environment to depths at which the above metamorphic conditions could be achieved. They then became detached from the subducting slab and incorporated into the accretionary complex. Such a mechanism has been termed underplating and has been described within rocks of similar lithology, depositional and tectonic environment, deformation style and metamorphic grade by many authors (eg Fisher and Byrne 1987, Moore 1989, Brandon and Calderwood 1990).

ii) Herschel Heights

Herschel Heights is situated 120 km south of the NW LeMay Range (Figure 1). It consists of pillow lavas, tuffs, volcaniclastic sandstones, cherts and slates tectonically interleaved with arc-derived sandstones. Lavas are highly deformed, vesicular, and have geochemical similarities to modern mid-ocean ridge basalts. Using the same criteria as for the NW LeMay Range, we interpret the arc-derived sandstones as trench-fill sediments and the other lithologies as representing the upper layers of oceanic crust. No datable fossils have been recovered from this area.

Accretionary deformation shows a similar style to that described above. A history of stratal disruption of fluid-rich sediments accompanied by independent particulate flow, followed by fracture and the formation of discrete cataclastic shear zones is an indication of the effective stress levels inherent early in the burial history. Pressure solution seams postdate these fabrics. The filling of fractures with chlorite, quartz and calcite is an indication of the P-T conditions reached at that time. All these indicate a similar accretion history to the rocks of the NW LeMay Range, with near-identical deformation paths and metamorphic grade. Hence we conclude a similar emplacement mechanism for the Herschel Heights rocks, by the same criteria outlined above.

The Quinault Pass Mélange Belt

Ocean-island material of the Lully Foothills and ocean-floor material of the NW LeMay Range are separated only by the Quinault Pass mélange belt (Figure 2). At 15 km long and at least 150 m wide, this belt marks a major

structural boundary within the accretionary prism. It consists of inclusions derived from both areas in a sheared mudstone matrix, cut by an anastomosing network of faults and exhibiting a variety of deformation styles. Tranter (in press) interpreted this belt as a major accretionary thrust that may have been reactivated by later accretionary events, placing rocks of the NW LeMay Range upon those of the Lully Foothills. Zircon fission track ages of 161.9+/-14.1 Ma from the NW LeMay Range and 167.8+/-11.6 Ma from autochthonous trench-slope sequences in the eastern LeMay Range (analyses by University of London Fission Track Research Group) may represent this uplift.

Conclusions

The Mesozoic accretionary complex in central and southern Alexander Island contains a belt of accreted oceanic material. An ocean-island of Early Jurassic age is exposed in the Lully Foothills, and was accreted near the toe of the prism. It is bound on its east side by a mélange belt formed along an accretionary thrust, upon which sequences of mid-ocean ridge basalts and pelagic sedimentary rocks of the NW LeMay Range have been uplifted. These ocean-floor sequences are tectonically interleaved with trench-fill deposits and are interpreted as having been underplated before or during the Middle Jurassic. To the south of these two areas lies Herschel Heights, also consisting of ocean-floor lavas and pelagic sedimentary rocks, and tectonically interleaved with trench-fill sediments. On the basis of deformation styles and metamorphic grade, it is also interpreted as having been underplated.

References

BRANDON, M.T. and CALDERWOOD, A.R. (1990). High-pressure metamorphism and uplift of the Olympic subduction complex. Geology, 18, p.1252-1255.

FISHER, D. and BYRNE, T. (1987). Structural evolution of underthrusted sediments, Kodiak Island, Alaska. Tectonics, 6, p.775-793.

GARRETT, S.W. and STOREY, B.C. (1987). Lithospheric extension on the Antarctic Peninsula during Cenozoic subduction. In: COWARD, M.P., DEWEY, J.F. and HANCOCK, P.L. (eds.) Continental Extensional Tectonics. Geological Society Special Publication 28. Blackwell, Oxford. p.419-431.

LUCAS, S.E. and MOORE, J.C. (1986). Cataclastic deformation in accretionary wedges: Deep Sea Drilling Project Leg 66, southern Mexico, and on-land examples from Barbados and Kodiak Islands. In: MOORE, J.C. (ed.) Structural Fabrics in Deep Sea Drilling Project Cores from Forearcs. Geological Society of America Memoir 166. Boulder, Colorado. p.89-103.

MOORE, J.C. (1989). Tectonics and hydrogeology of accretionary prisms: role of the décollement zone. J. Struct. Geol., 11, p.95-106.

NELL, P.A.R. (1990). Deformation in an accretionary mélange, Alexander Island, Antarctica. In: KNIPE, R.J. and RUTTER, E.H. (eds.) Deformation Mechanisms, Rheology and Tectonics. Geological Society Special Publication 54. The Geological Society, London. p.405-416.

THOMSON, M.R.A. and TRANTER, T.H. (1986). Early Jurassic fossils from central Alexander Island and their geological setting. Br. Antarct. Surv. Bull., 70, p.23-39.

TRANTER, T.H. (in press). Accretion and subduction processes along the Pacific margin of Gondwana, central Alexander Island. In: THOMSON, M.R.A., CRAME, J.A. and THOMSON, J.W. (eds.) Geological evolution of Antarctica. Cambridge University Press, Cambridge.

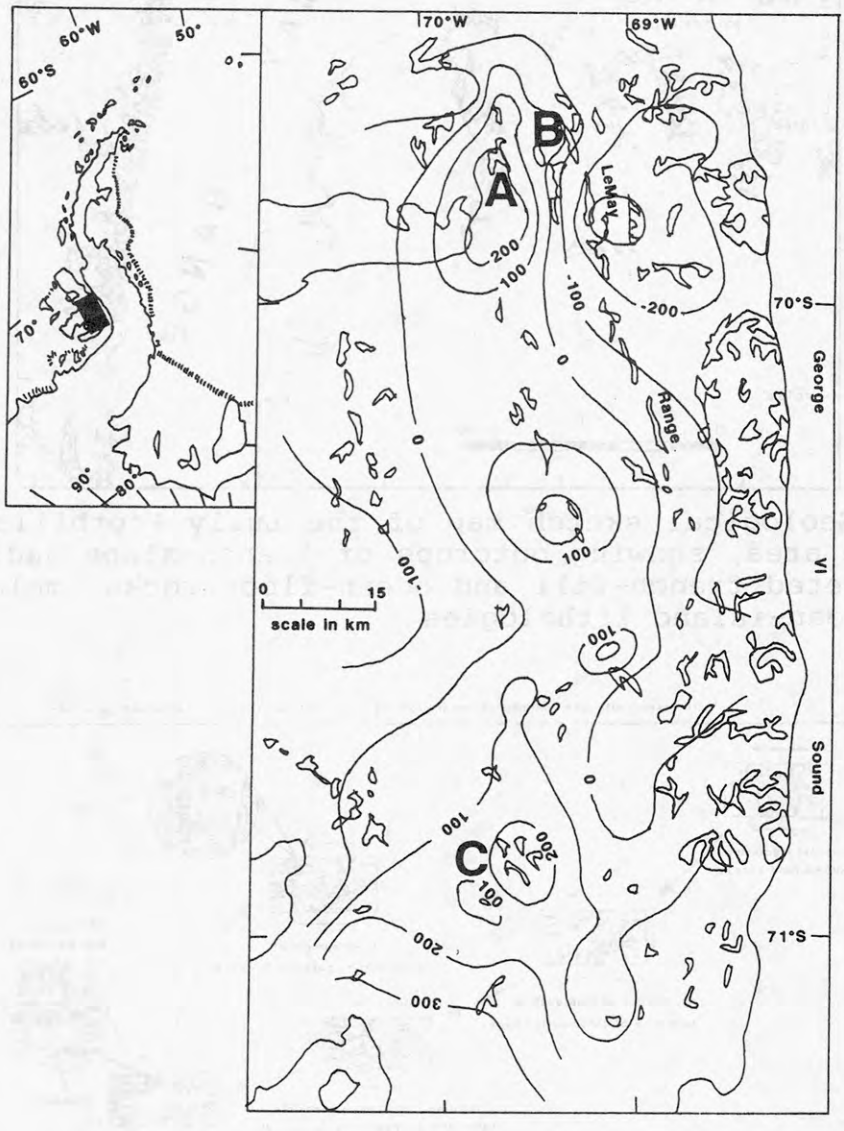

Figure 1. Location map of study area, with Bouguer gravity anomalies contoured at 100 gu intervals. A = Lully Foothills, B = NW LeMay Range, C = Herschel Heights.

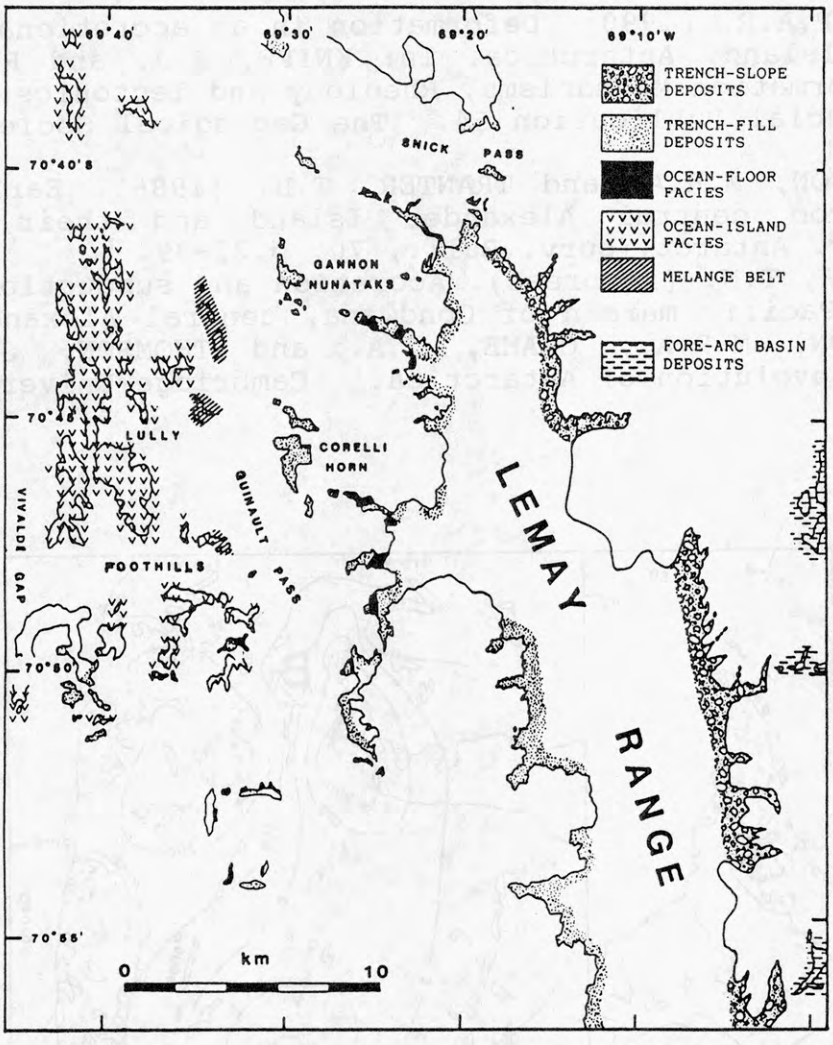

Figure 2. Geological sketch map of the Lully Foothills and NW LeMay Range area, showing outcrops of trench-slope sedimentary rocks, accreted trench-fill and ocean-floor rocks, melange and accreted ocean-island lithologies.

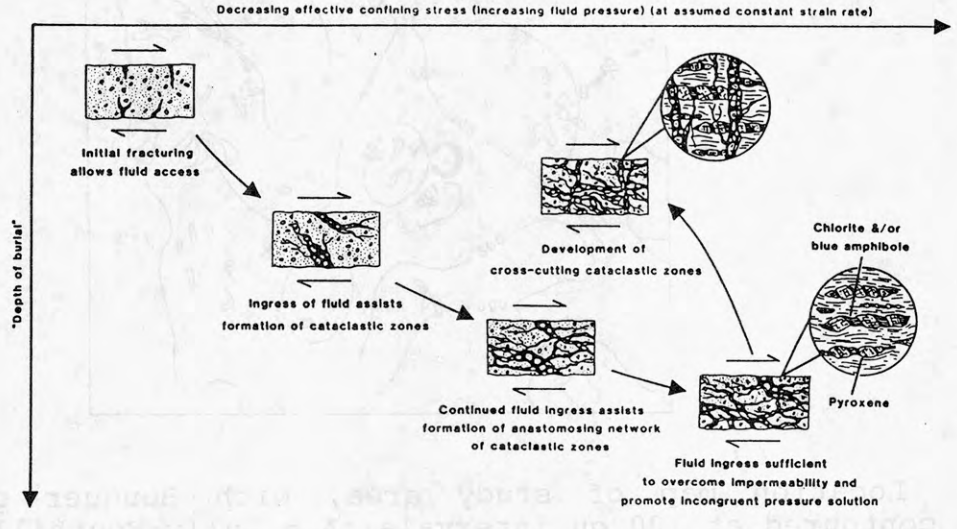

Figure 3. Model to explain the evolution of microstructures in underplated ocean-floor basalts of the NW LeMay Range.

LOW PRESSURE CRYSTALLIZATION OF ANORTHOCLASE CRYSTALS FROM PHONOLITIC MELT, MOUNT EREBUS, ANTARCTICA: EVIDENCE FROM VOLATILE CONTENTS OF MELT INCLUSIONS.

N.W. Dunbar, Geoscience Dep't. NMIMT, Socorro, NM, USA,
P.R. Kyle, same address

Mount Erebus, Antarctica, is a large, active, phonolitic volcano which contains presently contains two convecting, and continuously degassing lava lakes. Bombs erupted from the lava lakes contain abundant large (up to 10 cm in length) anorthoclase crystals, as well as pyroxene crystals up to 1 cm in length. The glass and phenocryst compositions from all recent Mount Erebus eruptive material is very similar, and composition of bombs erupted over the last 20 years is identical, suggesting that the magmatic system is in equilibrium, and that the crystal:melt ratio has been relatively constant through time.

Melt inclusions (MI) are abundant in anorthoclase and pyroxene phenocrysts from Mt. Erebus, and occur in 2 morphologies: 1) irregularly-shaped up to 600 microns in diameter; 2) smaller, negative crystal-shaped MI. Both types of inclusions contain one to many shrinkage bubbles, which are generally more abundant in the irreguarly-shaped inclusions. Electron and ion microprobe analyses indicate that the major and trace element composition of the MI are homogeneous, and are mostly very similar to degassed matrix glass, suggesting that MI are representative of magmatic composition. Only elements Ba and Sr are depleted in the MI relative to matrix glass, possibly because a small amount of anorthoclase was deposited on the inclusion walls. The volatile contents of inclusion and matrix glass are also very similar, and are, respectively: 1960 and 1910 ppm Cl; 650 and 530 ppm S; 3500 and 3100 ppm F; and 0.20 and 0.16 wt.% H_2O. The MI and matrix glass both contain around 1900 ppm P, 40 ppm Li, and 30 ppm B.

The similarity between volatile contents of MI and degassed matrix glass from Mt. Erebus is unusual. Phenocrysts in other magmatic systems contain volatile-rich MI which apparently grew in a volatile-rich magma. There are three possible explanations. The inclusions could have trapped non-representative melt, could have degassed after entrapment, or, most likely, the anorthoclase may have grown under near-surface conditions, thereby trapping degassed melt. Depth estimates made for crystal growth are between ~200 meters and the surface. However, due to the lack of H_2O solubility data for phonolitic melts, this estimate is tentative. Experimental determinations will help clarify this depth. Degassing of the magma during ascent may trigger rapid, low-pressure crystallization. The high abundance of MI in the Erebus anorthoclase crystals is consistent with rapid crystal growth. The lack of significant major and trace element zonation in crystals and MI suggest that major and trace element diffusion rates in this phonolitic melt are equal to, or faster than, crystal growth rates.

MOHO MORPHOLOGY ACROSS THE WILKES-ADELIE MARGIN OF EAST ANTARCTICA

Stephen L. Eittreim, United States Geological Survey, Menlo Park, CA 94303.

The Wilkes-Adelie margin of East Antarctica, a passive margin rifted in the Cretaceous, has a seismically reflective Moho that can be traced across the continent-ocean transition. Velocity models and depth sections were constructed for the combined multichannel seismic data sets of the United States Geological Survey and the Institute Francais du Petrole, allowing the following observations, some of which are illustrated in the figure below:

1 The continent-ocean boundary (COB; the boundary between oldest oceanic crust and the transitional crust to the south) is marked by the thinnest crust, and on some seismic lines, an upwarp of Moho.
2 The Moho is morphologically continuous across the COB, and, at varying distances landward from the COB, gradually increases in depth beneath the continent, with typical gradients of about 50 m/km.
3 The Moho consists of a single or doublet reflector, except on one line where it appears as a series of laminated reflectors below an isolated shallow spot in the base of the crust. This latter line implies that underplating has occurred here, at a location landward of the edge of oceanic crust in the transition zone of thickening-landward, stretched, and intruded, continental crust.
4 The bulge of thickened oceanic crust that has often been observed at the oldest edge of oceanic crust is underlain here by a generally flat Moho showing no compensating "root" for the topography.
5 Sub-oceanic Moho has generally rougher morphology than sub-transitional crust Moho, and wavelengths of the roughness are similar to oceanic basement surface roughness.

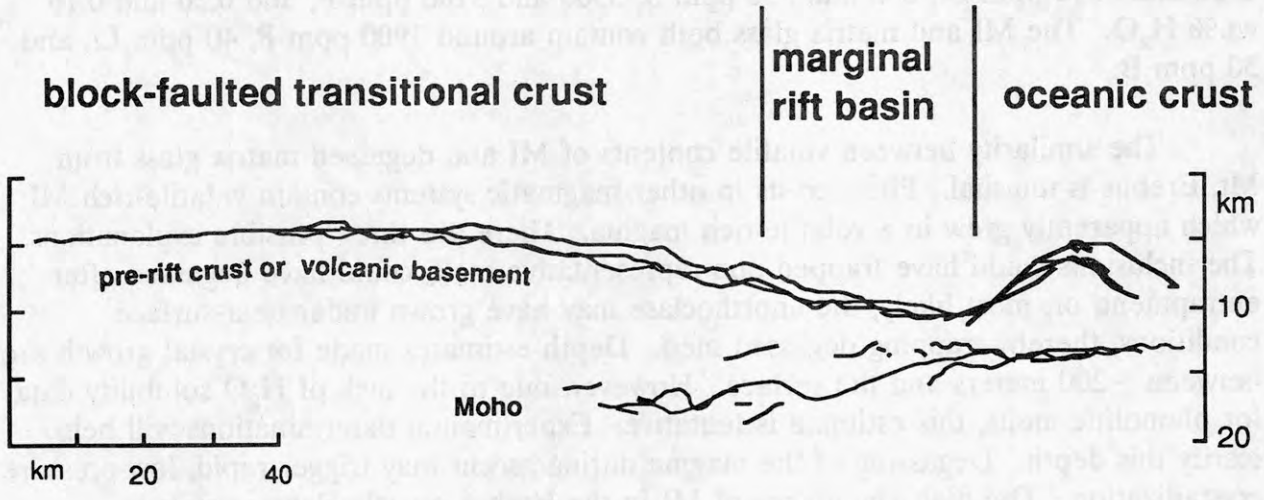

Figure: Composite view of crustal surface (post-rift sediment removed) and Moho along three western-most seismic lines.

PROVENANCE OF PALEOCENE STRATA, SEYMOUR ISLAND, ANTARCTIC PENINSULA

D. H. Elliot, S. M. Hoffman, and D. E. Rieske
Byrd Polar Research Center and Department of Geological Sciences
The Ohio State University, Columbus, Ohio 43210, U.S.A.

Paleocene strata are exposed on Seymour Island at Cape Wiman, and in and to the south of Cross Valley. The strata include the uppermost unit (Unit 10) of the Lopez de Bertodano Formation, the Sobral Formation, the Cross Valley Formation and beds of uncertain affinities near Cape Wiman (informally referred to as the "Wiman" Formation). Unit 10 of the Lopez (up to 95 m thick) consists of silty sands with glauconite beds near the base and sparsely distributed clay-rich (tuffaceous) beds. The Sobral (265 m thick) comprises five mappable units that form an upward coarsening sequence of marine clastic sediments; the lower three and the uppermost also contain clay-rich (tuffaceous) beds. The Cross Valley (117+ m thick) consists of a lower coarse grained and volcaniclastic unit overlain by 20 m of medium to fine sands. The "Wiman" (66 m thick) also consists of two units of clastic sediment that is upward fining.

The provenance of these strata has been examined through study of the sandstone petrology, heavy minerals, and chemical compositions of selected heavy minerals and glass shards. The Sobral sandstones are quartz rich arenites (quartz mean ~50% of sand-sized grains); the Cross Valley and the lower unit in the "Wiman" are volcanic litharenites (lithic grain mean ~59%), and the upper unit of the "Wiman" shows a return to quartzose compositions (quartz mean ~48%). Heavy mineral suites are dominated by garnet and pyroxene in the Sobral samples examined and by amphibole in the "Wiman". Garnet compositions, in general, correspond with those recorded for metamorphic rocks of the Antarctic Peninsula. Tuffaceous sediments carrying glass shards are sparsely distributed throughout the Paleocene section, being conspicuous in Unit 10 of the Lopez and in parts of the Sobral and Cross Valley Formations.

The provenance for the Paleocene beds was a magmatic arc terrain consisting of a basement of igneous and metamorphic rocks overlain by active or recently active volcanoes. The glass shards indicate contemporaneous andesitic volcanism in Unit 10 of the Lopez, but the subsequent intermittent activity was dominantly silicic. Sandstone petrology, however, indicates erosion of volcanic rocks of intermediate to silicic composition, principally during the time of deposition of the lower parts of both the Cross Valley and the "Wiman." Paleocene magmatism is unknown in the northern Antarctic Peninsula and only sparsely represented by andesitic to basaltic volcanic rocks in the offshore islands to the northwest and in the South Shetland Islands. The tuffs in the Paleocene strata of Seymour Island expand the history of volcanism in the northern Antarctic Peninsula region.

EROSION AND DEPOSITION IN THE TERRA NOVA BAY (ROSS SEA - ANTARCTICA): FIRST RESULTS OF THE STUDIES OF 3.5 KHz PROFILES

P. Fabretti, T. Pescatore, M.R. Senatore, Dipartimento di Scienze della Terra -Università di Napoli - Largo S. Marcellino,10 - 80138 Napoli, Italy
A. Stefanon, Istituto Universitario Navale - Via Acton, 38 - 80133 Napoli, Italy

INTRODUCTION

The first Italian oceanographic survey in Antarctica was carried out in the western Ross Sea with the M/N Polar Queen. In the Terra Nova Bay between Cape Washington and Cape Russel 1,174 nautical miles of high resolution seismic profiles (3.5 kHz) trending NW-SE were collected. This paper concerns the analysis of these profiles to obtain preliminary information about the morphology and sedimentary processes in this sector.

The chart of the Terra Nova bathymetry used in the work was made by Istituto Idrografico della Marina (Italy).

GEOMORPHOLOGICAL FRAMEWORK

The Ross Sea physiography has been studied by several authors (HAYES & DAVEY, 1975; VANNEY et al., 1981; ANDERSON et al., 1984; BARRETT et al., 1987) who have identified on the shelf depressions and reliefs with NE-SW direction.

The bathymetry of the shelf is particularly rugged near the coast of Northern Victoria Land; in general the shelf is deepest near the continent (to about 1,100 m) and becomes shallower in the off-shore direction to ca. 500 m near the shelf-break. Banks shoal to less than 250 m in this area.

The most western depression is the Victoria Land Basin which comprises three smaller basins: the Drygalski Basin, the Nordenskjold Basin and the Erebus Basin underlying McMurdo Sound.

Surficial holocenic sediments on the continental shelf consist of compound glacial-marine sediments near the coast and of siliceous ooze and siliceous mud in deeps (ANDERSON, 1989). Residual glacial-marine sediments are present on the banks (ANDERSON et al., 1980, 1984).

The thickness of the holocenic sediments ranges from a few centimeters to some meters (EDWARDS et al., 1987).

In the Western Ross Sea the compound glacial-marine sediments are restricted to a coastal belt (ANDERSON et al., 1984) and contain ice-rafted gravel, sand and silt, dispersed in a muddy matrix with marine fossils.

In the sub-surface, several authors (ANDERSON et al., 1980, 1984; BARRETT et al., 1985; EDWARDS et al., 1987) have also identified overconsolidated diamictons and basal tills deposited at the base of the grounded Ross Sea ice sheet. Marine fossils are absent in these deposits.

MORPHOLOGY AND ECHO TYPES

The studied area has a very rough topogrophy. Near the coast there are depressions and reliefs trending almost N-S; the depths range from 200 to 800 m. Towards S-E the morphology becomes smooth, with a slope trending SW-NE lowering into the Drygalski Basin to a depth of 1,100 m.

Preliminary analysis of 3.5 kHz profiles has led to the identification of five echo types according to the model of DAMUTH (1975), DAMUTH & HAYES (1977), DAMUTH (1980) and SENATORE et al., (1982) and of the following morphological units (Fig. 1).

-Hills: small and isolated hills with 50-100 m elevations above the sea floor (Fig. 2 - d); the bottom echo is distinct, with no sub-bottom reflectors (type IA of DAMUTH, 1975).

- Sharp banks: N-S trending reliefs with sharp top and steep sides (Fig. 1); the elevation above the sea floor is greater than 200 m (Fig. 2 - c). The bottom echo is distinct with no sub-bottom reflectors (type IA of DAMUTH 1975).

-Flat banks: NE-SW trending reliefs with flat top mainly present in the southern and eastern sectors of the studied area. Their top is frequently rugged (Fig. 2 - f). The bottom echo is generally indistinct, with irregular, overlapping hyperbolae having varying vertex elevations above the sea floor; no sub-bottom reflectors are present (type IIIC of DAMUTH, 1975). Amplitudes range from 10 to 100 m whereas wavelengths are usually less than one kilometer, although longer wavelengths are occasionally observed.

- Rough areas: zones near the coast with very rugged morphology (Fig. 2 - a). The bottom echo is indistinct with large hyperbolae (from 10 to 200 m), overlapping or single, having widely varying vertex elevations above the sea floor (type IIIA of DAMUTH & HAYES, 1977). The wavelengths can reach one kilometer.

- Valleys: elongate U-shaped sub-flat areas surrounded by slope areas (Fig. 2 - e). The topography of these areas varies from smooth to rough, with isolated hills. The bottom echo is generally indistinct with regular, overlapping hyperbolae having vertices approximately tangent to the sea floor (type IIID of DAMUTH & HAYES, 1977). The amplitudes of the hyperbolae are usually less than 50 m while the wavelengths are limited between 100 and 500 m.

- Slope areas: these zones comprise the sides of the reliefs and the Drygalski Slope. When the slope is greater than 5%, small slumps are often observed. The bottom echo is generally distinct, with no sub-bottom reflectors (type IA of DAMUTH, 1975).

-Troughs (Terra Nova Trough): depressed area with U-shaped cross profile separating the flat banks (Fig. 1). Width and depth of the trough increase from NE to SW. The bottom echo has the same characteristics as the morphological unit previously described (type IIIC of DAMUTH, 1975).

- Basins (Drygalski Basin): sub-flat area almost entirely covered with a veneer of acoustically transparent sediment. The bottom echo is distinct with a single indistinct reflector in the sub-bottom. This type of echo is

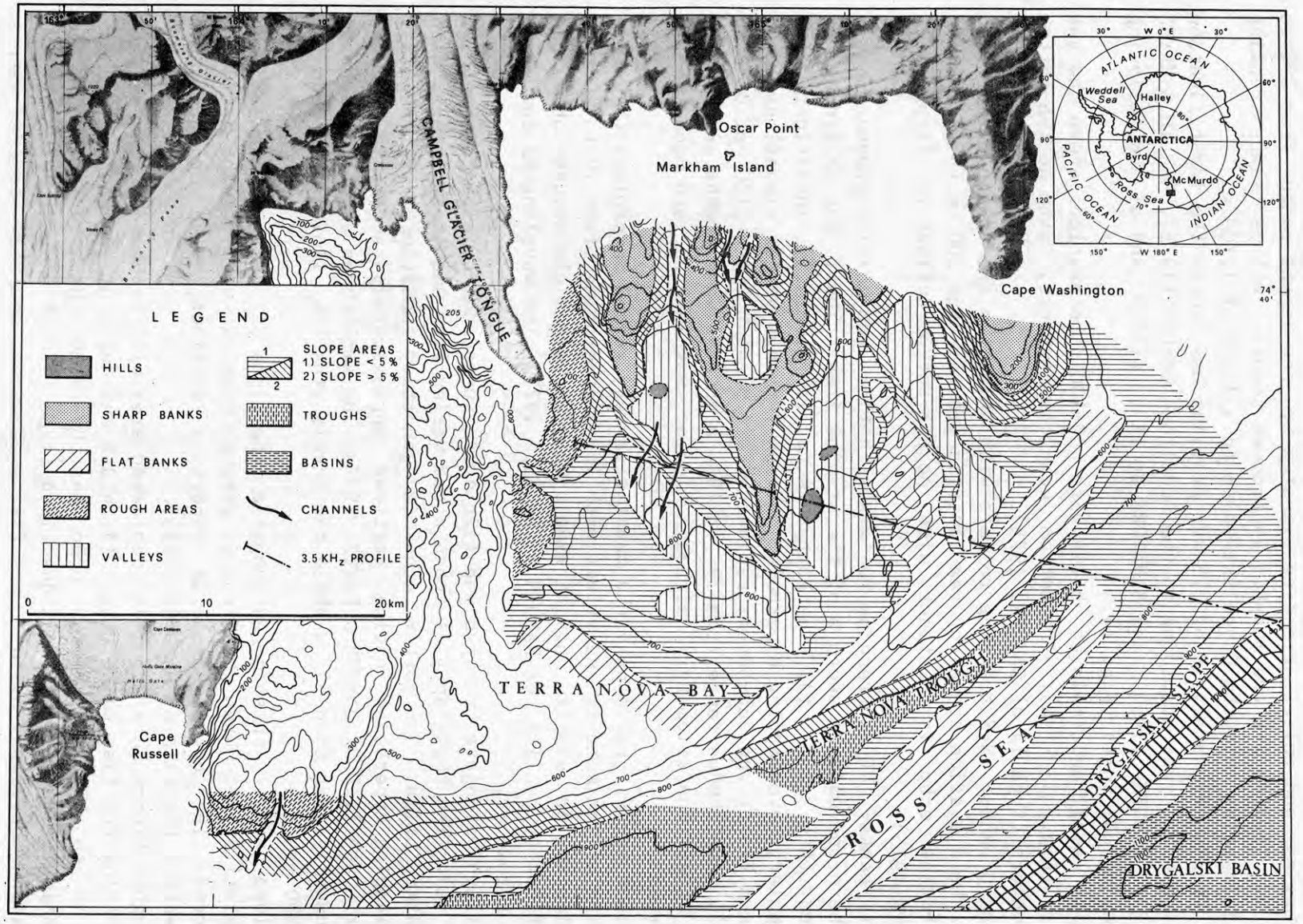

Fig. 1 - Morphological map of the Terra Nova Bay

not found in the classification of DAMUTH & HAYES (1977) and DAMUTH (1980). A similar echo has been identified by SENATORE et al. (1982) and classified as IID.

- Channels: small V-shaped channels (Fig. 2 - b) found in the northernmost part of the studied area (Fig. 1) and terminating in the valleys. The echo in some places is type IIID and in others type IA (DAMUTH, 1975; DAMUTH & HAYES, 1977).

DISCUSSION

The recognized morphological units lead to the subdivision of the studied sector into a northern and southern area.

The morphology in the northern area is very rough and dominated by the presence of sharp banks with N-S trending. On the coast morpho-structures with the same orientation are built up by lava flows from Mount Melbourne (Cape Washington, Oscar Point). The sharp banks are therefore interpreted as the prolongation of on land structures.

The erosional phenomena are prevalent in this area. Elongate U-shaped valleys separate the sharp banks and have different depth with respect to one another. These seem to be related to a N-S flow of the recent movements of ice sheet.

The southern area is characterized by the presence of NE-SW trending flat banks separated by the Terra Nova Trough. Their interpretation is quite problematic. In this same zone WONG & CHRISTOFFEL (1981) have located, on seismic profiles, stratified depositional features interpreted as delta moraine deposited when an expanded Ross Ice Shelf invaded the bay from south. Our data are insufficient to arrive at a clear interpretation of these morpho-structures but we may assume, as WONG & CHRISTOFFEL (1981) and several other authors (ANDERSON, 1989; KARL, 1989; EDWARDS et al., 1987) that their origin is glacial, formed during a phase of advance and retreat of the grounded Ross Sea ice sheet.

The types of echoes recognized in Terra Nova Bay, mainly hyperbolic, indicate the presence of consolidated sediments or unconsolidated coarse sediments on the sea floor. The presence in this zone of coarse sand with a scarce clay fraction is reported by BRAMBATI et al. (1989).

REFERENCES

ANDERSON J.B. (1989) - Antarctica's glacial setting. In: ANDERSON J.B. & MOLNIA (eds), Glacial-marine sedimentation. Short Course in Geology, American Geophysical Union, 9, 11-59.

ANDERSON J.B., KURTZ D.D. DOMACK E.W., BALSHAW K.M. (1980) - Glacial and glacial marine sediments of the Antarctic continental shelf. Journal of Geology, 88, 399-414.

ANDERSON J.B., BRAKE C.F., MYERS N.C. (1984) - Sedimentation on the Ross Sea continental shelf, Antarctica. Marine Geology, 57, 295-333.

BARRETT P.J., PYNE A.R., GOSSON G. (1985) - Late Cenozoic glacial sequence cored at Ciros-2, Ferrar Fjord, Western McMurdo Sound. In: Abstracts - Workshop on Cenozoic Geology of the Southern High Latitudes,

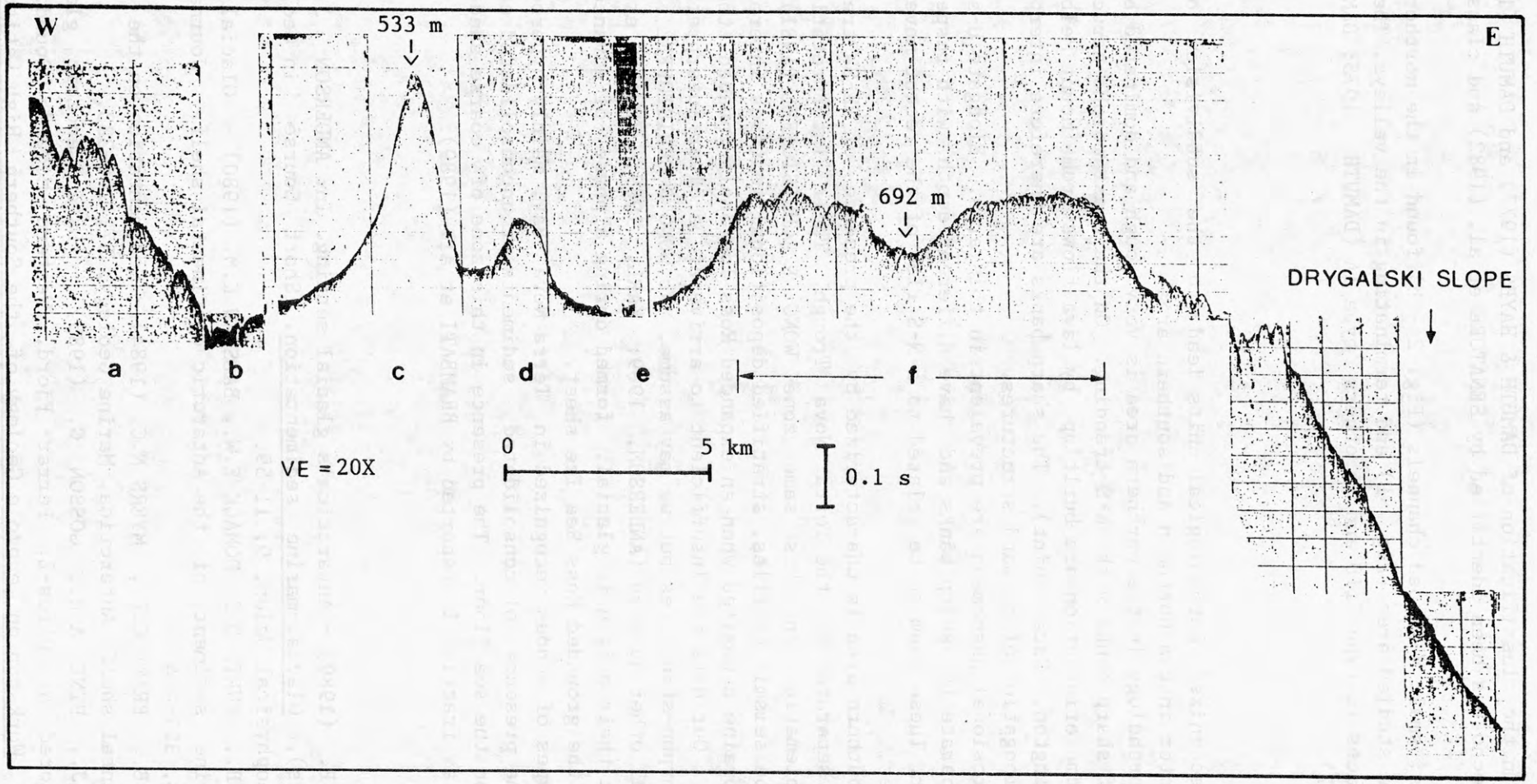

Fig. 2 - 3.5 kHz profile (see location in Fig. 1).
a) Rough area; b) channels; c) sharp bank; d) hill; e) valley; f) flat banks separated by an U-shaped valley.

Sixth Gondwana Symposium, Ohio State University, p.37.
BARRETT P.J., ELSTON D.P., HARWOOD D.M., McKELVEY B.C., WEBB P.N. (1987) - Mid-Cenozoic record of glaciation and sea level change on the margin of the Victoria Land Basin, Antarctica. Geology,15, 634-637.
BRAMBATI A., FANZUTTI G.P., FINOCCHIARO F., SIMEONI U. (1989) - Sediments and sedimentological process in the Ross Sea continental shelf (Antarctica): results and preliminary conclusions. Boll. Oceanol. Teor. e Appl., 7, (1-2), 159-188.
DAMUTH J.E. (1975) - Echo character of the western Equatorial Atlantic floor and its relationship to the dispersal and distribution of terrigenous sediments. Mar. Geol. 18, 17-45.
DAMUTH J.E. (1980) - Use of high-frequency (3.5 kHz) echograms in the study of near-bottom sedimentation process in the deep-sea: a review. Marine Geology, 38, 51-75.
DAMUTH J.E. & HAYES D.E. (1977) - Echo character of the East Brazilian continental margin and its relationship to sedimentary process. Marine Geology, 24, 73-95.
EDWARDS B.D., LEE H.J., KARL H.A., REIMNITZ E., TIMOTHY L.A. (1987) - Geology and physical properties of Ross Sea, Antarctica, continental shelf sediment. In: COOPER A.K. & DAVEY F.J. (eds), The Antarctic continental margin: Geology and geophysics of the western Ross Sea. Circum-Pacific Council for Energy and Mineral Resources, Houston, 5B, 191-216.
HAYES D.F. & DAVEY F.J. (1975) - Geophysical study of the Ross Sea, Antarctica. In: HAYES D.E. et al. (eds), Initial reports of the Deep-Sea Drilling Project. Washington D.C., 28, 887-908.
ISTITUTO IDROGRAFICO DELLA MARINA - Mare di Ross, Baia Terra Nova (Antartide)- Carta Batimetrica n.883 alla scala 1:100.000, 1989.
KARL H.A. (1989) - High-resolution interpretations of some sediment deposits, Antarctic Continental Margin: focus on the Western Ross Sea. In: POWELL R.D. & ELVERHOI (eds), Modern glaciomarine environments: Glacial and marine controls of modern lithofacies and biofacies. Marine Geology, 85,205-223.
SENATORE M.R., DIPLOMATICO G., MIRABILE L., PESCATORE T., TRAMUTOLI M. (1982) Franamenti sulla scarpata continentale pugliese del Golfo di Taranto (Alto Ionio - Italia). Geol. Romana, 21, 497-510.
VANNEY J.R., FALCONER R.K.H., JOHNSON G.L. (1981) - Geomorpholgy of the Ross Sea and adjacent oceanic provinces. Marine Geology, 41, 73-102.
WONG H.K. & CHRISTOFFEL D.A. (1981) - A reconnaissance seismic survey of McMurdo Sound and Terra Nova Bay, Ross Sea. In: McGINNIS L.D. (ed), Dry Valley Drilling Project: Antactic Research Series. Amer. Geophys. Union, 33, 37-62.

THE MANTLE ORIGINS OF PRIMARY THOLEIITIC MAGMAS ASSOCIATED WITH THE BREAKUP OF SOUTHERN GONDWANALAND

T.J.Falloon, R.J.Sweeney, D.H.Green and N.Ortez, Geology Department, The University of Tasmania, GPO Box 252C, Hobart, Tasmania 7001, Australia.

During mid-Mesozoic times mafic tholeiitic magmas were voluminously emplaced into the upper crust as thick dolerite intrusions or extruded onto the surface as extensive basaltic flows as part of an extensive eruptive event associated with the breakup of southern Gondwanaland. This magmatism is now represented by the Tasmanian dolerites, the Ferrar tholeiites of Antarctica and the Karoo Igneous Province of Southern Africa.

Within the Karoo Igneous Province a substantial accumulation of picritic volcanics occur in the Northern Lebombo-Tuli-Nuanetsi region of SE Africa. These picrites, which are considered to be close to or actual primary compositions, are divided into a volumetrically dominant high Ti-Zr (HTZ) group and a less abundant low Ti-Zr (LTZ) group. The major element compositions of the Karoo picrites are compared with experimentally determined partial melts of mantle peridotite systems to constrain the depth of magma segregation and the nature of source and residual mantle materials from which such segregation may have occurred. The LTZ group show uniformly shallow pressures (ca. 13-15kb) of magma segregation and the HTZ group a range of pressures (10kb to >30kb) of segregation which are correlated with incompatible element abundance. Both picrite groups have segregated from sources more refractory, with respect to basaltic constituents, than MORB or OIB sources.

The Tasmanian dolerites and the Ferrar tholeiites of Antarctica together comprise a geochemically uniform magmatic province of the continental tholeiitic association. Regional sampling of fine-grained (chill margin) occurrences, representing initially liquid (magmatic) compositions both in Tasmania and Antarctica indicate:

1) That crystal fractionation and post magmatic alteration can fully account for the geochemical variation within the magmatic suite. These variations are evident in the sequence olivine- to orthopyroxene- to clinopyroxene-phyric tholeiites with decreasing MgO content.

2) Recognition of the role of crystal fractionation processes in generating the observed liquid compostions permits estimation of more primitive magmatic liquids which may be both parental and primary magmas.

An experimental study of the liquidus phase relationships of a calculated parental composition (containing 15.5 wt% MgO) for the Tasmanian/Ferrar suite demonstrates that this composition is in equilibrium with olivine and orthopyroxene at 15kb and 1400°C, suggesting that such a parental liquid can be derived by partial melting of an upper mantle peridotite composition leaving a harzburgitic residue. This residue is very magnesian suggesting that the source peridotite itself was refractory in major element composition.

The depth of magma segregation is similar to that inferred for the LTZ picrite group of the Karoo Igneous Province. This suggests a uniformity in the depth of magma segregation for primary magmas during the most voluminous eruptive phase associated with the breakup of southern Gondwanaland.

Evolution of the Lutzow-Holm Complex, East Antarctica: Geological, petrological and geochronological constraints

M. Fanning, Research School of Earth Sciences, Australian National University, GPO Box 4, Canberra, ACT 2601, Australia
Y. Hiroi, Department of Earth Sciences, Faculty of Science, Chiba University, Yayoicho, Chiba 260, Japan
Y. Motoyoshi and K. Shiraishi, National Institute of Polar Research, Kaga, Itabashi-ku, Tokyo 173, Japan
Y. Nakai, Department of Earth Sciences, Aichi University of Education, Kariya 448, Japan
D. J. Ellis, Department of Geology, Australian National University, GPO Box 4, Canberra, ACT 2601, Australia
L. Black, Division of Petrology and Geochemistry, Bureau of Mineral Resources, GPO Box 378, Canberra, ACT 2601, Australia

The Lutzow-Holm Complex in East Antarctica between 30 and 45 °E has been well characterized geologically and petrologically. However, previous geochronological data was insufficient and the techniques applied were not suitable for unraveling the complex metamorphic history. An ion-microprobe (SHRIMP) U-Pb zircon dating study of the metasedimentary rocks was therefore undertaken.

Rocks of the Lutzow-Holm Complex show diversity including calcareous, pelitic, quartzo-feldspathic, intermediate, basic and ultrabasic rocks. Tectonically significant is the ubiquitous occurrence of ultrabasic rocks, though small in amount, as isolated blocks and sheets enclosed within meta-sedimentary rocks. They are inferred to have been derived from various parts of layered gabbro including allivalite and pyroxenites.

Progressive and prograde metamorphic features are well documented in the Lutzow-Holm Complex. Metamorphic grade continuously increases southwestwards from the upper amphibolite facies to the granulite facies up to the thermal peak located near the outlet of the Shirase Glacier and then decreases further westwards. Six isograds have been mapped to date. Prograde meta-morphic evolution of the rocks from the kyanite to the sillimanite stability fields is constrained by the well-preserved reaction textures of mineralsin various rock types.

Both complex and simple zircon populations have been separated from a regional scale sampling of the metasedimentary rocks. Two discrete high-grade metamorphic ages are recorded at *c.* 1000 Ma and 500-550 Ma. The former is considered to date the first and main high-grade metamorphism that resulted in the presently observed regional metamorphic thermal structure of the Lutzow-Holm Complex. This has been overprinted during the Early Paleozoic (500-550 Ma) at which time there was a widespread granitic activity and related high-grade metamorphism. It is noteworthy that the Early Paleozoic ages tend to become younger as the grade of previous regional metamorphism increases, suggesting that the overall thermal structure of *c.* 1000 Ma metamorphism was preserved up to the Early Paleozoic and controlled the closure timing of the U-Pb system (metamorphic zircons). In addition, the ion-microprobe analyses have identified a range of inherited zircon components, from *c.* 1680 Ma to *c.* 2900 Ma. The heterogeneous inherited zircon populations in some of the metasediments reflect a range of provenance, and due to the fine structure of these grains it has only been possible to unravel their complex history using the ion-microprobe.

Maximum and Minimum Configuration for Antarctic Ice Sheet

James L. Fastook
Computer Science
University of Maine
**
Michael Prentice
Quaternary Institute
University of Maine
**
Sathya Rajavelu
Computer Science
University of Maine

Extreme climatic conditions have existed in the past which resulted in extreme configurations for the Antarctic Ice Sheet.

One extreme leads to overriding of the Transantarctic Mountains with ice surface elevations at least 1000 m thicker along the Tranantarctic Mountains. In this configuration the ice sheet is likely grounded out to the continental shelf boundary. Present regions of sliding do not exist and the ice sheet dynamics are dominated by flowing ice.

The existence of a warmer climate is indicated by the presence of trees and marine microfossils along the Transantarctic Mountains. The degree of warming consistent with the marine microfossils produces an ice sheet more restricted in areal extent, yet approximating the present in volume. This rules out the possibility of a significant deglaciation in East Antarctica. This configuration does not allow for marine microfossils to originate from behind the Tranantarctic Mountains.

A distinct and different climate scenario of even greater warmth consistent with the existence of trees produces a smaller ice sheet restricted to southern-most East Antarctica. This ice sheet continues to bridge the gap between the southern Transantarctic Mountains and the Gamburtsev Mountains of central East Antarc-

tica.

A model of these three configurations as they may have existed in the past has been developed using the finite-element method to solve the equation for mass conservation. Primary input to the model consists of a parameterization of the mass balance relationship which is based on sea level temperature, surface elevation, and surface slope. By linking the mass balance relationship to the sea level temperature, reasonable bounds on the climatic extremes which produced these extreme configurations can be applied.

Average isotopic content and volumes of the two configurations have been related to measured deep-ocean core isotopic records. These three climate scenarios have been put into the framework of the geologic record by comparing modeled isotope content of the ice sheets with the deep-sea record, and agreement for particular instances in time has been achieved.

Paradoxically, the warmer climate scenarios required to generate the minimum configurations produces much higher accumulation rates in the interior of the ice sheet, resulting in relatively high dome elevations, and consequently higher volumes than might have been anticipated.

New Geological Data and Maps of Greenwich Island, South Shetland Islands, Antarctica.

H. C. Fensterseifer*, M. A. F. Hansen*, G. C. Azevedo**, F. L. Troian*.

* Geology Department, University of Vale do Rio dos Sinos-UNISINOS, Av. Unisinos, 950, 93.020, Sao Leopoldo, RS, Brazil.

** National Department of Mineral Production- DNPM, Ministry for Infraestructure, Rua 24 de Outubro, 1557, 90.470, Port Alegre, RS, Brazil.

This geological research shows maps (scale 1:10.000) from areas of Greenwich Island, South Shetland Islands. The correspondent field works at this island were developed during the austral summers of 1988-91, under the auspices of the Brazilian Antarctic Programme.

The maps from Duff, Atrio and Muleta points in the west of the island and Lenqua, Sartorius and Hardy points in the east, contain also geological profiles and columnar sections of these localities together with their respective petrographic descriptions.

Two main volcanic-sedimentary units of different ages are identified. These are separated by angular unconformity and each shows different depositional and volcanogenic facies, some of wich contain plant fossils. Basaltic lava flows of the oldest sequence gave ages of 77.6 + or - 2.3 M.y. and 70.3 + or - 1.9 M.y. (Late Cretaceous) by K-Ar whole-rock samples.

Also, two large intrusive units are defined and described:

1. Greenwich Intrusive Suite - a granodiorite-granite rock association located in the east of the island;

2. Atrio Intrusive Suite - a gabbro, dolorite and basalt rock association, located in the western part of the island. A basalt intrusion of this suite gave an age of 55.3 + or - 5.0 M.y. (Early Paleocene to Early Eocene) by K-Ar whole-rock sample.

SATELLITE DETERMINATION OF ICE FRONT CHANGES IN ANTARCTICA

J.G. Ferrigno, U.S. Geological Survey, Reston, VA 22092, USA
B.F. Molnia, U.S. Geological Survey, Reston, VA 22092, USA
B.K. Lucchitta, U.S. Geological Survey, Flagstaff, AZ 86001, USA
R.S. Williams, Jr., U.S. Geological Survey, Reston, VA 22092, USA

Between 1987 and 1991, the Scientific Committee on Antarctic Research (SCAR) consortium acquired Landsat data of the coastal regions and outlet glaciers of Antarctica to document current ice extent and compare this with older and future data sets so the location and magnitude of changes can be ascertained. Approximately 400 Landsat thematic mapper (TM) scenes were acquired that give cloud-free coverage of about 90 percent of the Antarctic coastline.

Inspection of these recently acquired images and older Landsat multispectral scanner (MSS), return beam vidicon (RBV), and TM data, NOAA AVHRR data, and SPOT data has shown that substantial changes have taken place in the area and volume of ice in several coastal areas. In 1986, AVHRR data revealed that more than 11,225 km^2 of the Larsen Ice Shelf and 11,500 km^2 of the Filchner Ice Shelf (15-20 percent of the total areas) calved into the Weddell Sea. Landsat TM and AVHRR imagery acquired during the same year showed that about 1,600 km^2 of the Thwaites Iceberg Tongue and the Thwaites Glacier Tongue broke away. Landsat TM imagery acquired in 1990 showed further loss in the Thwaites Glacier area. In 1987, a large tabular iceberg (B-9) with an area of more than 4,000 km^2 calved from the eastern side of the Ross Ice Shelf. Landsat TM data from the western side of the Ross Ice Shelf acquired in 1990 and AVHRR data acquired in 1991 show two large crevasses that will soon generate two tabular icebergs of more than 2,800 km^2 in total area.

Because of the high resolution (30-m pixel) of the TM data, it is possible to observe changes in several smaller ice shelves also. Landsat TM imagery acquired in 1989 and 1991 shows almost total disintegration of the Wordie and Cook Ice Shelves. Similarly, the ice shelf covering Larsen Inlet has totally disappeared. Lesser reductions in the size of Muller Ice Shelf and several other areas around the continent have been noted. Less dramatic and noticeable, but not any less significant are the advances of the ice front of as much as several hundred meters in some areas in Marie Byrd Land and Queen Maud Land.

A computer technique developed by the U.S. Geological Survey in Flagstaff, AZ, makes it possible to map and measure ice front changes accurately if multiple image coverage is available. Considerable cyclic fluctuation is expected in the coastal regions of Antarctica, but it is important to monitor these recent changes to determine if they are indeed cyclic, or if they are random or signals of global climate change.

UPLIFT HISTORY OF THE TRANSANTARCTIC MOUNTAINS FROM VICTORIA LAND (~70°S) TO SCOTT GLACIER (~86°S): EVIDENCE FROM FISSION TRACK ANALYSIS.

Paul G. Fitzgerald and Edmund Stump, Department of Geology, Arizona State University, Tempe, Arizona 85287-1404, U.S.A.

The Transantarctic Mountains (TAM) define the boundary between cratonic East Antarctica and the microplate mosaic of West Antarctica. The mountains extend for some 4000 km, are on average ~150 km wide and commonly reach elevations of 4000 m. Prior to the application of fission track dating techniques to the uplift history of the TAM, their uplift was only constrained only as post-Jurassic and pre-late-Cenozoic. Apatite fission track analysis has now been applied to the TAM in four widely spaced regions along their length. These are northern Victoria Land (NVL), southern Victoria Land (SVL), the Beardmore Glacier (BG) and the Scott Glacier (SG) areas. In all of these areas a major period of synchronous uplift and denudation of the TAM has been recognized in apatite fission track profiles taken over significant vertical relief. This event began in the early Cenozoic and is believed responsible for typically 5-6 km of uplift and denudation along the front of the range (adjacent to the Ross Embayment), although in NVL, some 10 km of uplift is evident in the southeastern area near Mt Murchison and the lower Tucker Glacier. Data from the Mt Griffith - Fission Wall profile in the SG indicate that the uplift and formation of the TAM in that region actually began in the late Cretaceous. Approximately 1 km of late Cretaceous uplift and denudation is seen in this profile, followed by a period of quiescent and then the main period of uplift starting in the early Cenozoic. This late Cretaceous event is also tentatively identified in data from NVL. However, only the main period of uplift, that initiated in the early Cenozoic, is seen in data from SVL and BG. This indicates that the uplift history of the TAM is more complicated than originally thought and that more work on new areas is required to delineate the variation of uplift along the TAM.

The style and timing of faulting along the Transantarctic Mountain Front (TMF) can be delineated from mapping and the offset of apatite age profiles. In the Dry Valleys area of SVL, the TMF is characterized by a zone of steeply dipping normal faults, dominantly downfaulted towards the coast with offsets of 40-1,000 m. The amount of uplift and denudation is greatest just inland of the TMF, at the axis of maximum uplift, but then generally decreases away from the front of the mountains, that is, away from the Ross Embayment and towards the East Antarctic Ice Sheet. In the simplest case, e.g in the Dry Valleys area of SVL, where the TAM can be likened to one large fault block tiled gently to the west, the amount of uplift decreases inland at the same rate as the dip of the fault block. In this area the amount of erosion also decreases inland, hence the elevation of the mountains increase. Some 4-5 km of erosion is estimated along the axis of maximum uplift, but only 1-2 km of erosion along the range adjacent to the East Antarctic Ice Sheet. The north-south striking range-front faults within the TMF in the Dry Valleys area of SVL lie at an acute angle to the axis of maximum uplift indicating a dextral component to the dominantly east-west extension direction.

The timing of the uplift of the TAM can now be directly related to the timing of plate tectonic events in the southwestern Pacific region, specially the separation of Australia and Antarctica. The initial separation of these two continents began in the late Cretaceous (~100 Ma) but the rate of spreading remained slow until the early Cenozoic (~55 Ma) (Cande and Mutter, 1982). The TAM, an area of thick continental crust (40-45 km) lie adjacent to the Ross Embayment, an area of extended and thinned continental crust. Formation of the TAM has been linked, both temporally and spatially to the formation of the Ross Embayment. Cretaceous sediments are suspected to be present in the lower parts of sedimentary basins of the Ross Embayment, but have yet to be found. The discovery of late Cretaceous uplift in the TAM indicates that sediments of this age are almost certainly present in the Ross Embayment and further links the evolution of these two contrasting physiographic regions. Models for the formation of the TAM and adjacent tectonic features will now have to take account of this late Cretaceous tectonic event.

UPLIFT HISTORY OF THE VINSON MASSIF, ELLSWORTH MOUNTAINS: CONSTRAINTS FROM APATITE FISSION TRACK ANALYSIS AND IMPLICATIONS TO THE TECTONIC HISTORY OF WEST ANTARCTICA.

Paul G. Fitzgerald and Edmund Stump, Department of Geology, Arizona State University, Tempe, Arizona 85287-1404, U.S.A.

The Ellsworth Mountains (EM) lie on the eastern side of the Ellsworth-Whitmore Mountains crustal block (EWM), one of five blocks that make up the tectonic collage of West Antarctica. The timing of the uplift of the EM offers important constraints on the evolution of the EWM and hence on the movement of this block relative to East Antarctica and the other crustal blocks of West Antarctica.

The geology of the EM is dominated by a thick folded succession of Cambrain-Permian sedimentary rocks which have been correlated to the Paleozoic cover sequence of the Transantarctic Mountains (TAM) , although they lack the conspicous mid-Paleozoic unconformity seen in the TAM from the Ohio Range to northern Victoria Land. Strata in the EM show an increased metamorphic grade with depth of section, from laumontite grade in the uppermost unit, the Permian Polarstar Formation, to pumpellyite-actinolite and lower greenschist facies in the lower units of the Cambrian Heritage Group. Both the Sentinel and Heritage Ranges are topographically higher on their western flanks than to the east, and in both ranges stratigraphically lower rocks are exposed in their western portions. These observations suggest that the present day EM can be simply envisaged as a block tilted to the east. With the expectation that sampling a profile over the maximum vertical relief would yield the most information on the timing of the uplift and denudation of the EM, the western side of the Sentinel Range was targeted for collection.

Antarctica's highest mountain, the Vinson Massif (4,897 m) forms part of the high spine of the Sentinel Range, and has vertical relief of ~4 km on its western flank. A vertical sampling profile was collected from the summit of the Vinson Massif down its western flank to its base on Nimitz Glacier (1,397 m). The profile was extended down to an elevation of 690 m at Bowers Corner, making the total vertical range ~4.2 km. All samples were taken from the Crashsite Quartzite and almost all samples yielded abundant apatite for dating purposes. In all, 31 samples were taken from this profile. The results of the first batch of 12, which cover the entire vertical range, are presented here. Apatite fission track ages ranged from 139 ± 8 Ma from the top of the Vinson Massif to 117 ± 5 Ma for the lowermost sample at Bowers Corner. Ages increase systematically with increasing elevation and define a slope of approximately 250 m/Myr. Length distributions ranged from 14.1 μm to 13.4 μm, with an average of 13.8 μm. All standard deviations were relatively small (less than 1.6 μm, average of 1.4 μm). The data indicate substantial uplift and denudation in the Early Cretaceous, at least 4 km over a ~20 Myr period. A further period of uplift and denudation since the time covered by the data here is required in order to raise the samples to their present elevation. This later activity is in the order of 3 km. A rather poorly defined erosion surface is present at an elevation of ~4,000 m in the vicinity of the Vinson Massif. It is possible that this erosion surface is a post-Early Cretaceous remnant of the Early Cretaceous uplift and denudation.

From one sample collected in the Heritage Range by G. Webers in 1979, we obtained an apatite age of 169 ± 17 Ma, with a mean length of 13.3 μm and a standard deviation of 1.7 Ma. The results from this sample indicate that information prior to the Early Cretaceous thermal and denudation history are preserved in the less uplifted portions of the EM, and it is likely that future data from the EM will therefore enable us to place constraints on the exact timing and magnitude of this "Early Cretaceous" tectonic event.

Tectonic models of the evolution of Antarctica during the breakup of Gondwana rely on data from paleomagnetics, sea-floor magnetic anomalies, aeromagnetics, bedrock geology and topography. Uncertainties exist in interpretations of some of the basic data and hence disagreements exist between the models. In broad terms, a chronology since the mid-Mesozoic is generally agreed on. Initial rifting at ~180-175 Ma indicating the initial breakup of Gondwana as evidenced by bimodal volcanism of the Ferrar Group and Prebble Formation in the TAM and peraluminous granites in the EWM. Initial separation of East and West Gondwana and formation of oceanic crust beginning, with accompanying differential movements between East and West Antarctica. Opening of the Weddell Sea and South Atlantic beginning at ~135-130 Ma (there is less of a concensus on the timing of this event), with more differential movement of West Antarctica relative to East Antarctica. Subsequent block faulting within West Antarctica at an unspecified later time to produce some of the present day topography.

Our data indicates that uplift and denudation of the EM was occurring during the period following initial separation of East and West Antarctica, and continued into the period of opening of the Weddell Sea. The data indicates that there is no dramatic change in the thermal history of the EM during the initial opening of the Weddell Sea. Further study of samples from the eastern side of the Sentinel Range and within the Heritage Range may permit a determination of the time of initiation of uplift in the EM. The uplift to form the present day EM and elevation of the erosion surface to high elevations in the Sentinel Range is probably due to later block faulting events.

STRUCTURAL AND METAMORPHIC EVIDENCE FOR EXTENSIONAL COLLAPSE OF THICKENED CRUST: THE BRATTSTRAND BLUFFS PARAGNEISS, PRYDZ BAY

I.C.W. Fitzsimons & S.L. Harley, The Grant Institute, Department of Geology & Geophysics, University of Edinburgh, West Mains Road, Edinburgh EH9 3JW, Scotland.

The Brattstrand Bluffs coastline of Prydz Bay (Figure 1) comprises some 15 km^2 of island and coastal outcrop scattered along the 70 km of coastline between the Rauer Group and the Larsemann Hills. It consists of Proterozoic granulite with a polyphase metamorphic and deformational history, and subordinate discordant intrusions (Fitzsimons & Harley, 1991). Two gneissic associations have been identified, a basement orthogneiss association correlated with the orthogneiss-dominated Rauer Group (Harley, 1987), and a cover paragneiss association correlated with the paragneiss-dominated Larsemann Hills (Stüwe *et al.*, 1989). The relationships between structure and mineral assemblage development in the paragneiss units, which are not complicated by relics of early deformational and metamorphic events, can be used to constrain the Proterozoic tectonic evolution of the area.

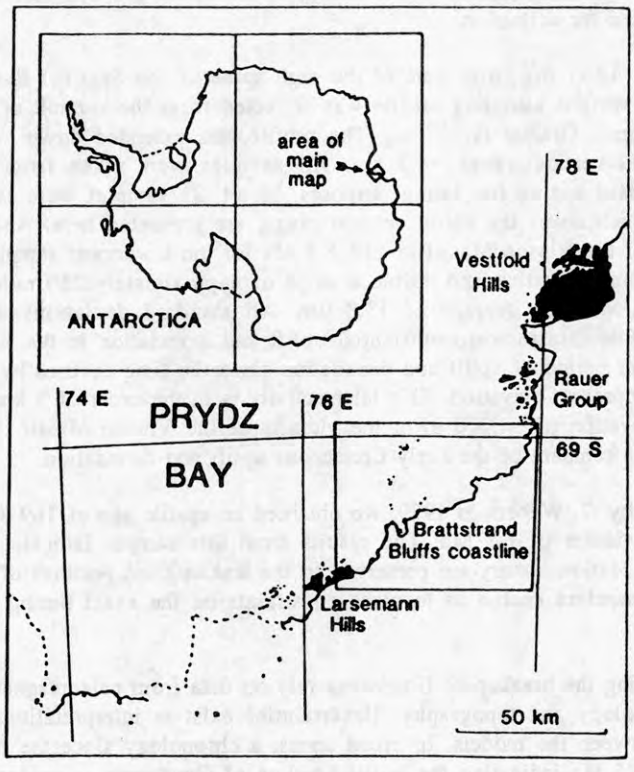

Figure 1. Map of south-east Prydz Bay. The box on the main map represents the area of study.

1. Structural evolution of the Brattstrand Bluffs paragneiss

The dominant fabric elements in the Brattstrand Bluffs paragneiss are a lithological banding of pelite, semi-pelite and intermediate gneiss units, and a layer parallel foliation defined by modal variation and preferred orientation of mineral grains and grain clusters. This fabric (termed S_3 by Fitzsimons & Harley, 1991), is truncated by widespread leucogneiss sheets and lenses. Earlier structures are generally transposed by S_3, although rare F_3 helicitic inclusion trails preserved within garnet porphyroblasts are interpreted as relics of prograde deformation. Structures attributed to D_1 and D_2 are only preserved in the basement orthogneiss, and are correlated with Archaean events identified in the Rauer Group which pre-date deposition of the paragneiss precursors (Harley *et al.*, this symposium).

Metre-scale asymmetric F_4 structures are sub-parallel to S_3, and fold both S_3 and leucogneiss units. They are commonly non-cylindrical, and developed during non-coaxial

simple bulk shear. Orientation and vergence data imply that F_4 had a single sense of asymmetry over most of the Brattstrand Bluffs coastline, and that both F_4 and S_3 were flat-lying, before the area was deformed into an upright regional F_5 antiform (Figure 2).

F_4 folds are locally transposed in discrete zones of high strain, characterized by ductile shear and a penetrative planar fabric (S_4). These high-strain zones developed initially along the long limbs of F_4 folds and then in zones of S_4 non-coaxial ductile shear up to 20 m wide or more, in which no S_3 or F_4 structures are preserved. The relationship between S_3 and S_4 structures is similar to the S-C structures described by Berthé *et al.* (1979). However, the relationship of S_3 (S surfaces) and S_4 (C surfaces) with leucogneiss units indicates a two-stage formation rather than the simultaneous development described by Berthé *et al.* (1979). A mineral lineation of variable intensity (L_4) is most intense in areas exhibiting the greatest attenuation of S_3 and F_4 fabrics, in particular the high-strain S_4 zones. F_4 fold axes parallel this lineation, which is attributed to rotation of fold-axes towards the direction of extension during progressive high bulk strain (Escher & Watterson, 1974).

An increase in intensity of S_4 fabrics with D_4 structural depth along the Brattstrand Bluffs coastline (Figure 3) is consistent with a major D_4 detachment zone somewhere below present outcrop levels, perhaps beneath the Ranvik Glacier. This detachment zone is interpreted as a transposed basement-cover boundary, representing the principal discontinuity between the Rauer Group orthogneiss and Larsemann Hills paragneiss.

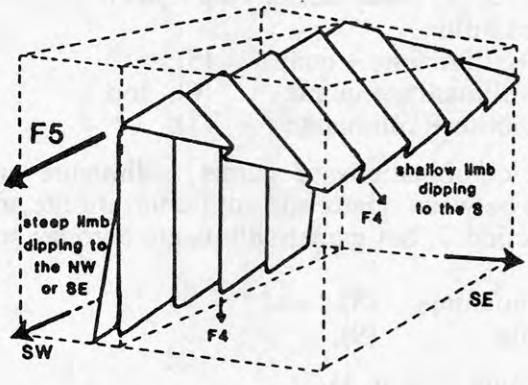

Figure 2. Block diagram showing a single S3 layer, folded by asymmetric F4 folds of uniform vergence, all deformed by a regional F5 antiform. Not to scale.

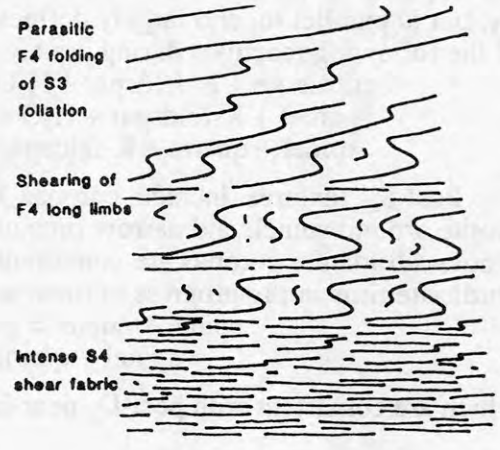

Figure 3. Cartoon depicting the variation in intensity of D4 structures with increasing D4 structural depth. No scale is implied.

2. Metamorphic evolution of the Brattstrand Bluffs paragneiss

Mineral assemblages in the paragneiss are consistent with low to medium pressure granulite-facies conditions. Peak metamorphic conditions have been estimated from garnet-orthopyroxene-plagioclase-quartz semi-pelite. Thermometry based on iron-magnesium exchange between garnet and orthopyroxene, and barometry based on the reaction:

$$\text{garnet} + \text{quartz} = \text{plagioclase} + \text{orthopyroxene} \quad (1),$$

and the solubility of alumina in orthopyroxene coexisting with garnet, were used to yield peak pressure-temperature estimates of *c.* 6 kbar and 850°C. Migmatitic textures and leucogneiss sheets reflect syn to post-S_3 partial melting of pelitic and semi-pelitic lithologies at the metamorphic peak (Harley *et al.*, this symposium).

The metapelite records a complex metamorphic evolution during D_3 and D_4. Assemblage evolution at the metamorphic peak indicates that partial melting proceeded via incongruent biotite-melting reactions (Harley *et al.*, this symposium) to produce a peak metamorphic assemblage of garnet-cordierite-sillimanite-quartz-K-feldspar, which commonly preserves an S_3 sillimanite fabric. The S_3 fabric is locally overgrown by xenoblastic green spinel, which forms in two different textural settings depending on the local assemblage. In quartz-absent domains, spinel forms symplectitic intergrowths with cordierite, whereas in cordierite-absent domains it forms lobate intergrowths with quartz. Both types of texture enclose resorbed garnet and sillimanite, and are attributed to progress of the reactions

garnet + sillimanite = cordierite + spinel, (2), and
garnet + sillimanite = spinel + quartz (3),

which are both indicative of decompression (Figure 4). Barometry involving the phases garnet, sillimanite, cordierite, spinel and quartz yields conditions of *c.* 5 kbar at 800°C, assuming low water contents in cordierite (which is consistent with cordierite channel volatile analysis; Harley *et al.*, this symposium). Limited plagioclase growth adjacent to resorbed garnet is attributed to progress of the reaction

garnet + sillimanite + quartz = plagioclase (4),

which is also consistent with decompression. Barometry based on this equilibrium yields pressures of 3 to 4 kbar, although these values are associated with relatively large uncertainties due to the low grossularite content of garnet. Further metapelite assemblage development is characterized by the reappearance of biotite as a matrix phase. It overprints S_3, but is parallel to, and largely defines, the localized S_4 shear fabric. This reflects progress of the following reactions during pre to syn-S_4 water influx

cordierite + K-feldspar + H_2O = biotite + sillimanite + quartz (5),
garnet + K-feldspar + H_2O = biotite + sillimanite + quartz (6), and
spinel + quartz + K-feldspar + H_2O = biotite + sillimanite (7).

Post-S_4 textures include coronas of various combinations of garnet, sillimanite and biotite around spinel, and narrow rims of cordierite between quartz and cordierite. Biotite and biotite-sillimanite coronas are consistent with Reaction 7, but garnet-sillimanite coronas and cordierite rims imply progress of the reactions

spinel + quartz = garnet + sillimanite (8), and
spinel + quartz = cordierite (9),

which are consistent with post-D_4 near-isobaric cooling (Figure 4).

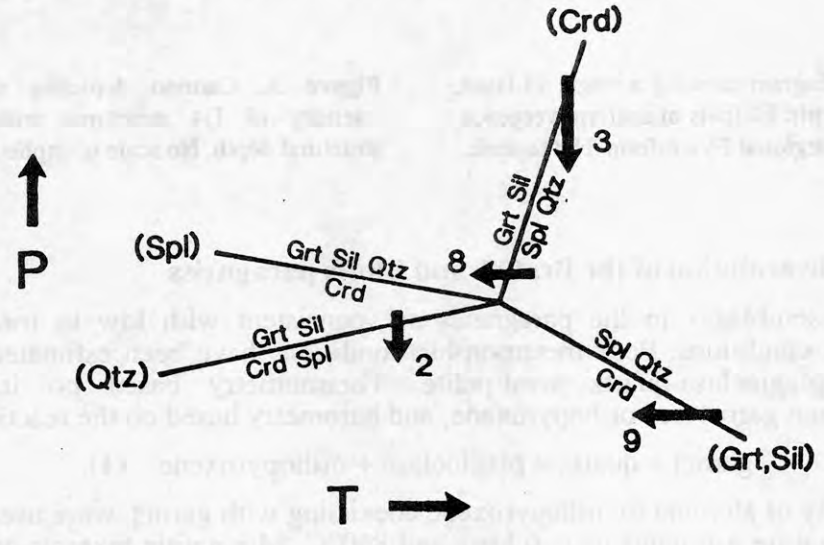

Figure 4. Schematic P-T plot of univariant reactions between the phases garnet (Grt), sillimanite (Sil), spinel (Spl), cordierite (Crd) and quartz (Qtz), for pure iron or magnesium end-member compositions. The reactions become divariant bands for iron-magnesium solid solutions. The arrows refer to the pressure-temperature evolution inferred for numbered reactions in the text.

3. Pressure-temperature-deformation path and tectonic implications

The clockwise pressure-temperature path defined above, with 2 to 3 kbar of decompression after peak metamorphism followed by post-D_4 near-isobaric cooling (Figure 5), is consistent with metamorphic studies of other localities in Prydz Bay (Harley, 1988; Stüwe & Powell, 1989), and indicates that the tectonic event responsible for the Proterozoic metamorphism involved crustal thickening. Evidence for the tectonic evolution of the overthickened crust after peak metamorphism is provided by the structural history. The combination of decompression and sub-horizontal, non-coaxial ductile shear during the D_3 to D_4 interval is attributed to progressive extension, and the post-peak decompressional history is correlated with extensional collapse of overthickened crust (Sandiford, 1989).

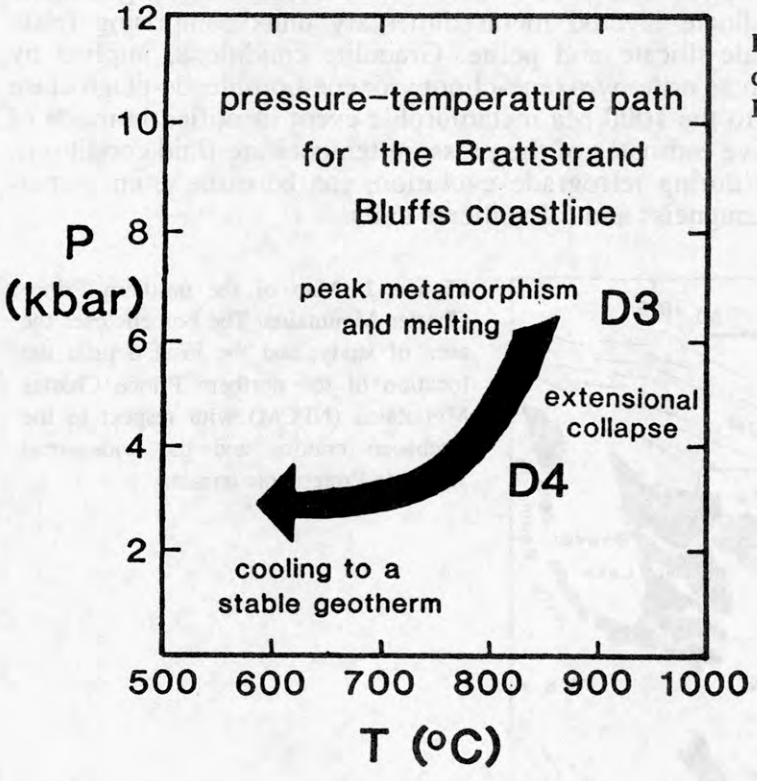

Figure 5. The pressure-temperature-deformation evolution of the Brattstrand Bluffs Coastline.

Flat-lying post-peak extensional structures have not been reported from the Rauer Group, and although asymmetric folds post-dating peak metamorphism have been identified in the Larsemann Hills (Stüwe *et al.*, 1989), no penetrative zones of ductile shear equivalent to S_4 are developed. This implies that extension is concentrated along the Brattstrand Bluffs coastline, and is consistent with this area being close to an inferred basement-cover boundary, which would act as a focus for much of the sub-horizontal deformation.

References

Berthé, D, Choukroune, P. & Jegouzo, P., 1979. *Journal of Structural Geology* **1**, 31-42.
Escher, A. & Watterson, J., 1974. *Tectonophysics* **22**, 223-231.
Fitzsimons, I.C.W. & Harley, S.L., 1991. *Australian Journal of Earth Sciences* (in press).
Harley, S.L., 1987. *Australian Journal of Earth Sciences* **34**, 175-207.
Harley, S.L., 1988. *Journal of Petrology* **29**, 1059-1095.
Sandiford, M., 1989. *Geology* **17**, 449-452.
Stüwe, K., Braun, H-M. & Peer, H., 1989. *Australian Journal of Earth Sciences* **36**, 219-241.
Stüwe, K. & Powell, R., 1989. *Journal of Metamorphic Geology* **7**, 465-483.

PRESSURE-TEMPERATURE-FLUID HISTORY OF GRANULITES FROM THE NORTHERN PRINCE CHARLES MOUNTAINS: CONSTRAINTS FROM GARNET-ORTHOPYROXENE PARAGNEISS AND WOLLASTONITE-SCAPOLITE CALC-SILICATE

I.C.W. Fitzsimons & S.L. Harley, The Grant Institute, Department of Geology & Geophysics, University of Edinburgh, West Mains Road, Edinburgh EH9 3JW, Scotland.

High-grade gneiss of the northern Prince Charles Mountains (Figure 1) has a complex intrusive and deformational history (McKelvey & Stephenson, 1990; Fitzsimons & Thost, 1991). Outcrop is dominated by homogeneous felsic orthogneiss enclosing boudinaged mafic and ultramafic dykes, with subordinate layered metasedimentary units comprising felsic paragneiss, semi-pelite and rare calc-silicate and pelite. Granulite conditions, implied by diagnostic mineral assemblages such as orthopyroxene-clinopyroxene-hornblende-plagioclase ± quartz mafic units, are attributed to the 1000 Ma metamorphic event identified in much of the East Antarctic shield. Quantitative estimates of the pressure-temperature-fluid conditions, both at the metamorphic peak and during retrograde evolution, can be made from garnet-orthopyroxene-plagioclase-quartz paragneiss and calc-silicate units.

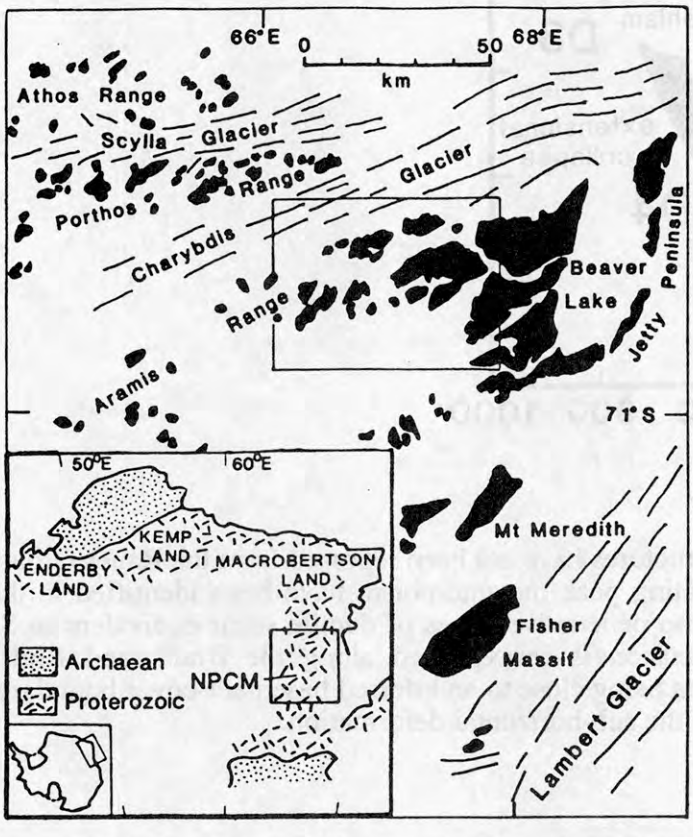

Figure 1. Map of the northern Prince Charles Mountains. The box encloses the area of study, and the inset depicts the location of the northern Prince Charles Mountains (NPCM) with respect to the Archaean cratons and the widespread 1000 Ma Proterozoic terrain.

1. Garnet-orthopyroxene-plagioclase-quartz thermobarometry

The most-suitable lithology for thermobarometric study is garnet-orthopyroxene-plagioclase-quartz ± biotite ± K-feldspar paragneiss, for which a number of well-calibrated thermometers and barometers are available. Peak pressure-temperature (*P-T*) estimates (Figure 2) were derived by substituting mineral-core compositional data into the thermometer of Harley (1984*a*), which is based on the iron-magnesium exchange reaction between garnet and orthopyroxene:

$$\text{pyrope} + \text{ferrosilite} = \text{almandine} + \text{enstatite} \qquad (1),$$

and into barometers based both on the reaction:

plagioclase + orthopyroxene = garnet + quartz (2)

(Newton & Perkins, 1982; Bohlen *et al.*, 1983), and on the solubility of alumina in orthopyroxene co-existing with garnet (Harley & Green, 1982; Harley, 1984*b*).

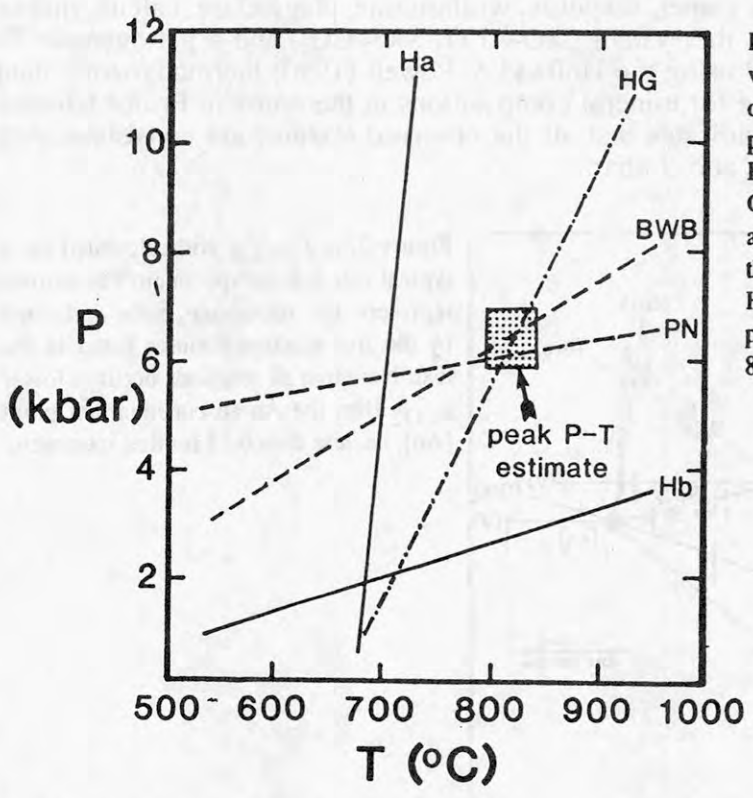

Figure 2. A pressure-temperature plot of various thermobarometric calibrations discussed in the text for a typical paragneiss specimen. Ha = Harley 1984*a*, Hb = Harley 1984*b*, HG = Harley & Green 1982, BWB = Bohlen *et al.* 1983 and NP = Newton & Perkins 1982. Note the low temperature and pressure of the Harley calibrations. This specimen gives peak *P-T* estimates of *c.* 6.5 kbar and 800°C.

The exchange thermometer yields temperatures between 550 and 750°C. This cannot reflect a real variation in peak conditions given the proximity of many specimen locations, but rather reflects a variable extent of retrograde iron-magnesium exchange. The garnet-orthopyroxene-plagioclase-quartz barometers (Reaction 2) yield consistent pressures of 6 to 7 kbar at their intersection, which are interpreted as peak metamorphic pressures. These barometers are based on mass-transfer of calcium, aluminium and silicon which is not as easily reset during retrograde *P-T* evolution as iron and magnesium. Peak temperatures of 700 to 800°C are estimated from the intersection of garnet-orthopyroxene-plagioclase-quartz barometers with the Harley & Green (1982) calibration, which has a relatively steep d*P*/d*T* slope (Figure 2) and a position which is not greatly affected by retrograde iron-magnesium exchange. This is in contrast to the Harley (1984*b*) calibration of the same equilibrium, which is highly sensitive to iron-magnesium distribution, and yields variable pressures which are up to 4 kbar below those derived from garnet-orthopyroxene-plagioclase-quartz barometers.

Chemical zonation profiles in garnet, orthopyroxene and plagioclase imply progress of Reactions 1 and 2 from left to right. The profiles in garnet and orthopyroxene confirm that retrograde iron-magnesium exchange via Reaction 1 has been important in these specimens, and profiles resulting from both reactions 1 and 2 are consistent with a retrograde evolution dominated by cooling. However, the various diffusing species involved in Reactions 1 and 2 have different closure temperatures, which can produce a zonation profile that does not reflect the actual pressure-temperature path of the rock (Frost & Chacko, 1989).

2. Calc-silicate reaction textures and petrogenetic grid *P-T* estimates

Less-equivocal evidence of pressure-temperature evolution is derived from mineral reaction textures. Wollastonite-scapolite calc-silicate layers and boudins, enclosed within garnet-orthopyroxene paragneiss, exhibit spectacular reaction textures including:

(1) garnet coronas between calcite and scapolite,

(2) garnet-quartz coronas between scapolite and wollastonite,

(3) garnet-quartz coronas between plagioclase and wollastonite,
(4) calcite-quartz intergrowths in wollastonite, and
(5) calcite-plagioclase symplectites in scapolite.

Reactions involving the phases garnet, scapolite, wollastonite, plagioclase, calcite, quartz and vapour have been modelled in the system CaO-Al_2O_3-SiO_2-CO_2, and a petrogenetic T-a_{CO2} grid (Figure 3) was calculated using the Holland & Powell (1990) thermodynamic data set with phase activities appropriate for mineral compositions in the northern Prince Charles Mountains calc-silicate. The grid indicates that all the observed textures are consistent with near-isobaric cooling from *c.* 830°C at *c.* 7 kbar.

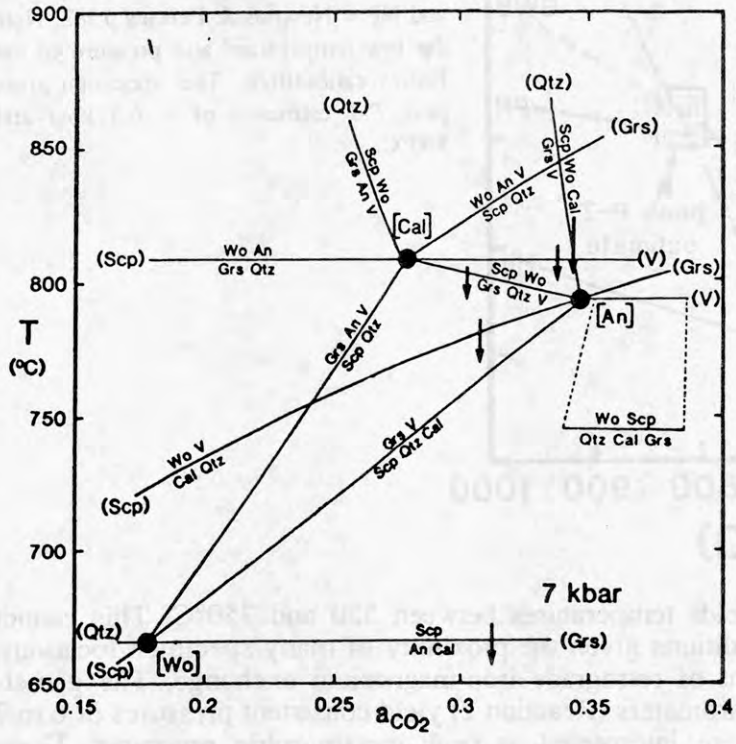

Figure 3. A T-a_{CO2} grid calculated for a typical calc-silicate specimen. The arrows represent the retrograde paths indicated by the five reaction textures listed in the text. Note that all reactions occur at lower a_{CO2} than the An-absent invariant point [An], i.e. less than 0.35 for this specimen.

This *P-T* path is consistent with geothermobarometric and mineral zonation studies of the garnet-orthopyroxene paragneiss, but suggests that some of the lower thermobarometric estimates for peak metamorphic conditions actually reflect retrograde conditions.

3. Constraints on fluid conditions during peak and retrograde metamorphism

The petrogenetic grid (Figure 3) does not constrain *peak* CO_2 activities in the calc-silicate, but does constrain retrograde CO_2 activities to be low (less than 0.5, and in some specimens less than 0.35). It is unlikely that CO_2 activities were significantly higher at the metamorphic peak, since there is no evidence of substantial CO_2 loss, or H_2O influx before textural development. The enclosing garnet-orthopyroxene-plagioclase-quartz-K-feldspar-biotite paragneiss buffers water activities to values less than 0.35 (Hansen *et al.*, 1984) during the metamorphic peak and retrograde evolution via the reaction:

$$\text{biotite} + \text{quartz} = \text{orthopyroxene} + \text{K-feldspar} + H_2O \quad (3).$$

Given that the calc-silicate and paragneiss host are interlayered on a scale of 0.5 m, and that the sum of volatile activities for a free fluid phase should equal unity (assuming ideal mixing), these units cannot have equilibrated with the same volatile fluid phase unless a volatile species other than H_2O or CO_2 was present in significant amounts. Lower crustal volatile fluids are generally considered to be H_2O-CO_2 binary mixtures, implying that either:
(1) fluid composition was buffered on a local (less than 0.5 m) scale, or

(2) CO_2 and H_2O activities were controlled only by the solid assemblage and were able to vary independently (i.e. conditions were fluid absent).

4. Conclusions: pressure-temperature-fluid history

Phase composition and textural relationships in garnet-orthopyroxene paragneiss and wollastonite-scapolite calc-silicate from the northern Prince Charles Mountains, are consistent with peak granulite metamorphism at 6 to 7 kbar and *c.* 800°C. Reaction textures indicate that the retrograde evolution from these conditions was dominated by cooling.

Similar garnet-corona textures have been described in scapolite-wollastonite calc-silicate from the Arunta Block of central Australia (Warren *et al.*, 1987). These textures were interpreted using the calc-silicate grid of Ellis (1978), which predicts growth of garnet coronas between wollastonite and scapolite during decompression or water influx (Figure 4). This contrasts with other Arunta lithologies which record an evolution dominated by cooling. This paradox can be resolved using the T-a_{CO2} grid presented here (Figure 3), which predicts that garnet coronas in scapolite-wollastonite calc-silicate are indicative of a cooling history. This difference between the two interpretations derives from the dT/da_{CO2} slope of the garnet-forming, wollastonite-scapolite decarbonation reactions:

$$\text{scapolite} + \text{wollastonite} + \text{calcite} = \text{garnet} + CO_2 \quad (4), \text{ and}$$
$$\text{scapolite} + \text{wollastonite} = \text{garnet} + \text{quartz} + CO_2 \quad (5),$$

which have a positive dT/da_{CO2} in the Ellis (1978) grid (i.e. decarbonation proceeds with increasing temperature) and a negative dT/da_{CO2} in the grid presented here (i.e. decarbonation proceeds with decreasing temperature). Although the Ellis (1978) grid is consistent with common sense, the orientation of decarbonation reactions in Figure 3 can be explained by the high degree of aluminium-silicon disorder in scapolite (Moecher & Essene, 1990; Harley & Buick, this symposium).

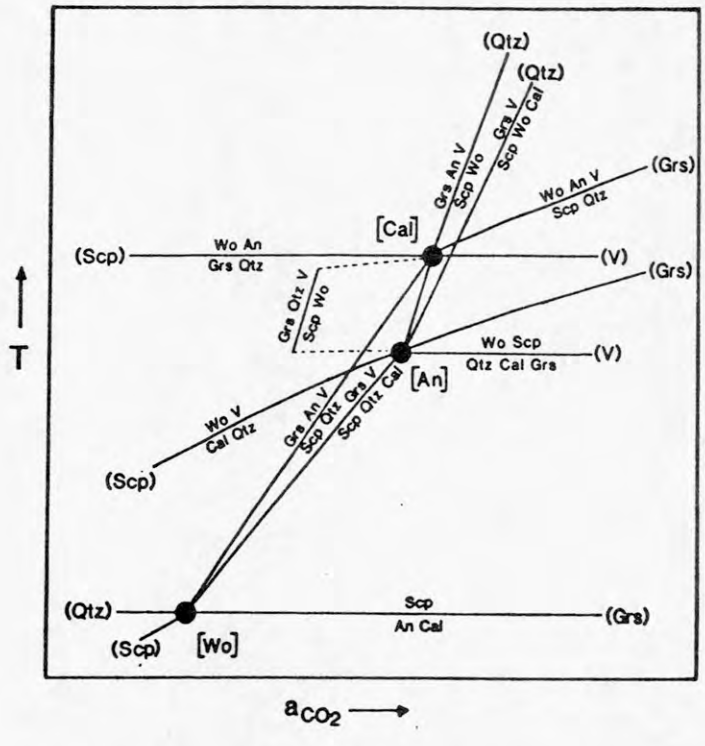

Figure 4. The T-a_{CO2} grid of Ellis (1978). Note the different positions of the [An] and [Cal] invariant points, and the different slopes of the three wollastonite-scapolite decarbonation reactions, compared with Figure 3.

The stabilization of anhydrous granulite assemblages requires dehydration of precursor lithologies, and the role of volatile fluids during dehydration is particularly controversial. The two principal models of granulite formation are:

(1) partition of H_2O into hygroscopic silicate melts produced by a combination of anatexis and magmatism (Fyfe, 1973), and

(2) dilution of H_2O-rich fluids with pervasive CO_2-rich fluids (Newton *et al.*, 1980).

Both alternatives given in Section 3 for metamorphic fluid conditions in the northern Prince Charles Mountains preclude pervasive CO_2-rich fluid infiltration as a viable means of granulite stabilization in this region.

References

Bohlen, S.R., Wall, V.J. & Boettcher, A.L. 1983. *Contributions to Mineralogy & Petrology* **83**, 52-61.

Ellis, D.E., 1978. *Geochimica & Cosmochimica Acta* **42**, 1271,1281.

Fitzsimons, I.C.W. & Thost, D.E., 1991. *Australian Journal of Earth Sciences* (in press).

Frost, B.R. & Chacko, T., 1989. *Journal of Geology* **97**, 435-450.

Fyfe, W.S., 1973. *Philosophical Transactions of the Royal Society of London* **A273**, 457-461.

Hansen, E.C., Newton, R.C. & Janardhan, A.S., 1984. *Journal of Metamorphic Geology* **2**, 249-264.

Harley, S.L., 1984*a*. *Contributions to Mineralogy & Petrology* **86**, 359-373.

Harley, S.L., 1984*b*. *Journal of Petrology* **25**, 665-696.

Harley, S.L. & Green, D.H., 1982. *Nature* **300**, 697-700.

Holland, T.J.B. & Powell, R., 1990. *Journal of Metamorphic Geology* **8**, 89-124.

McKelvey, B.C. & Stephenson, N.C.N., 1990. *Antarctic Science* **2**, 53-66.

Moecher, D.P. & Essene, E.J., 1990. *Journal of Petrology* **31**, 997-1024.

Newton, R.C. & Perkins, D., 1982. *American Mineralogist* **67**, 203-222.

Newton, R.C., Smith, J.V. & Windley, B.F., 1980. *Nature* **288**, 45-50.

Warren, R.G., Hensen, B.J. & Ryburn, R.J., 1987. *Journal of Metamorphic Geology* **5**, 213-223.

DEPOSITIONAL ENVIRONMENT OF THE KIRKPATRICK BASALT IN THE CENTRAL TRANSANTARCTIC MOUNTAINS

T. H. Fleming and D. H. Elliot, Department of Geological Sciences and Byrd Polar Research Center, Ohio State University, Columbus, Ohio, USA 43210

In the central Transantarctic Mountains the Jurassic Kirkpatrick Basalt is represented by a 500 meter thick sequence of tholeiitic lava flows. Individual lava flows that are apparently ponded range up to 220 meters thick and flows over 40 meters thick are very common. These thick flows occur throughout the lava sequence suggesting the continuous presence of topographic barriers during the accumulation of the basalts. Several thick flows show a lateral transition to sequences of thinner flows and suggest that other sequences of thinner flows may represent rapid accumulation of numerous flow lobes.

Water has also played an important role in the eruptive environment. The Prebble Formation, which underlies the basalts and consists largely of lahars, is thought to represent the interaction of magma and water during the initial stages of basaltic magmatism. The continued importance of water in the eruptive environment of the basalts is shown by hyaloclastite deposits and commonly associated pillow lavas, and finely laminated lacustrine interbeds which contain freshwater fossils. These features have been found throughout the basalt sequence. Fracture pattern analysis of several thick glassy lava flows indicates that crystallization progressed downward from the upper surface of the flows to within a few meters of the flow base. This rapid downward cooling from the flow tops forming thick entablatures may reflect post-depositional flooding of the lavas by water, as has been suggested for some Columbia River Basalt Flows.

The thick flows and abundant evidence of water/magma interaction at all stratigraphic levels in the lava sequence suggest that the basalts were deposited in a topographic low in which subsidence probably persisted during eruptive activity. Structural data suggest monoclinal warping and basement block faulting during or before accumulation of Prebble beds. Basaltic volcanism probably occurred in a rift settting in which the flood basalts were confined by rift shoulders and intra-rift horsts, however, bounding faults for this inferred rift system have not yet been identified in the underlying Beacon sequence or basement rocks.

Kinematics of major structures of northern Victoria and Oates Lands, Antarctica

Thomas Flöttmann, Georg Kleinschmidt, Geologisch Paläontologisches Institut,
Johann Wolfgang Goethe Universität
Senckenberganlage 32, D-6000 Frankfurt/Main Germany

Major thrust structures developed during the Cambro-Ordovician Ross orogeny separate northern Victoria Land's main geological units which comprise from west to east: the Antarctic craton, the highly metamorphic Wilson terrane magmatic arc, the Bowers terrane, consisting of a basal Cambrian volcanic arc, and the Cambro-Ordovician turbidites of the Robertson Bay terrane. This paper discusses the thrust kinematics and their implications for the early Paleozoic structural evolution of northern Victoria Land.

The magmatic arc of the central Wilson terrane is thrust towards the Antarctic craton in the west along the Exiles thrust which occurs along the westernmost Wilson terrane, and oppositely towards the east along the Wilson thrust which crops out at the the eastern edge of the Wilson terrane. Both thrusts show a dominant component of orogen normal displacement kinematics. The Lanterman fault marks the suture between the Wilson terrane mobile belt and the easterly adjacent Bowers terrane, which again is thrust bound along the Leap Year Fault with the easternmost Robertson Bay terrane. In the north the terrane boundary faults dip steeply towards the west and display west over east directed kinematics, whereas in the south top to the northeast directed transpression along moderately west dipping reverse faults occurs.

The thrust kinematics suggest dominant overall orogen normal convergence and are consistant with west directed subduction during the Ross orogeny resulting in the formation and exhumation of the Wilson terrane mobile arc and the accretion of the Bowers/Robertson Bay terranes at the active Paleo Pacific margin of the Antarctic craton.

ANALYSIS OF TERRA NOVA AND WOOD BAY ICE TONGUES AND ICE SHELVES INFERRED FROM SATELLITE IMAGES AND AIR PHOTOS (NORTH VICTORIA LAND, ANTARCTICA)

Dr. FREZZOTTI Massimo
ENEA- CRE Casaccia- C.P. 2400- 00100 Roma A.D. Italy

The analysis and comparison of U.S. Navy Trimetrogon system air photos (taken from 1956 to 1985) and of satellite images LANDSAT 1 MSS (recorded from 1972 to 1973), LANDSAT 4 TM (recorded from 1988 to 1990) and SPOT XS (recorded from 1988 and 1990) allow a first evaluation of ice surface velocity and ice cliff variation. This study concerns the Drygalski, Larsen, Campbell, Random Hills, Tinker and Aviator ice tongues and Nansen Ice Shelf.

Drygalski is the name of the David Glacier Tongue that floats in the southern part of Terra Nova Bay. This is the major outlet glacier of North Victoria Land; it drains an area of East Antarctic Plateau of 224,000 km^2. The flow rate is between 615±30 m a^{-1}, closed to the grounding line, and 730±5 m a^{-1} at the end of the Ice Tongue. The section of the Ice Tongue at the grounding line is about 14 km and the thickness of ice is from 1,190 m and 2,530 m. Taking into account this value the annual ice discharge is between 10 and 22 km^3. The Ice Tongue area increased by 27.5 km^2 a^{-1} from 1960 to 1972, 15 km^2 a^{-1} from 1972 to 1990.

The Larsen Glacier Tongue is a small outlet glacier floating in Terra Nova Bay between the Drygalski Ice Tongue and the Nansen Ice Shelf. Its medium ice flow rate is 151 m a^{-1}, with a speed of 170±5 to 115±5 m a^{-1}. The Ice Tongue area increased by about 0.6 km^2 a^{-1} between 1957 and 1988.

The Nansen Ice Shelf cover an area of about 1,800 km^2 and it is fed by the Reeves and Priestley outlet glacier. The mean flow rate is about 181 m a^{-1}, with a speed of 120±5 to 360±5 m a^{-1}. The ice surface discharge is about 3.5 km^2 a^{-1} at Inexpressible Tarn Flat section. The Ice Shelf area decreased from 1957 to 1972 by a 124 km^2 because a portion of 170 km^2 of the Ice Shelf broke away as icebergs between 1963 and 1972. From 1972 to 1988 the Ice Shelf area increased by 3.5 km^2 a^{-1}. This value represents the annual ice surface discharge, so that during this period very little ice was lost by iceberg calving. The satellite images show that the ablation zones, evidenced by blue ice area, are continuous features of the Ice Shelf and cover an area of about 720 km^2. Considering a mean ablation rate of about 20 cm a^{-1} the ice lost by the Nansen Ice Shelf surface is about 14 km^3 a^{-1}.

The Campbell Glacier Tongue is fed by névés of Southern Cross Mountains and the Deep Freeze Range, the catchment area is about 4,000 km^2. The Ice Tongue floats in Terra Nova Bay. The mean flow rate is 187 m a^{-1} with a speed of 140±20 to 240±20 m a^{-1}. The Ice Tongue area is about 78 km^2 and did not vary between 1963 and 1990. The mean Ice Tongue height is 43 m with a maximum of 74 m near the grounding line and 33 m at 13 km from Shield Nunatak. Considering the value of the area and the mean height of the cliff, the volume of the Ice Tongue is about 25 km^3.

The Random Hills Glacier Tongue is fed by a local catchment of about 76 km^2 at the northern foot of Mt. Melbourne. The mean flow rate is 40 m a^{-1} with a speed of 31±5 to 54±5 m a^{-1}. The Ice Tongue area was about 4.6 km^2 in 1963, and increased at 6.1 km^2 in 1972 and decreased by 1989 to 5.7 km^2.

The Tinker Glacier Tongue floating in Wood Bay is fed by névés of Southern Cross Mountains; the catchment area is about 1,400 km^2. The mean flow rate is 76 m a^{-1} with a speed of 91±5 to 50±5 m a^{-1}. The Ice Tongue area estimated as 76 km^2 in 1960, 76 km^2 in 1972

and 77 km^2 in 1989. The mean height of the ice cliff is 20 m varying from 32 m to 12 m. Using the mean height of the ice cliff, the volume of the Ice Tongue in 1990 was of about 1.5 km^3.

The Aviator Glacier Tongue floating in Wood Bay is fed by névés of Southern Cross Mountains, Evans, Hercules and Mountaineer Range, the catchment area is about 7,300 km^2. The mean flow rate is 166 m a^{-1} with a speed of 119±5 to 185±5 m a^{-1}. The Ice Tongue area has been estimated as 400 km^2 in 1960; 379 km^2 in 1972 and 410 km^2 in 1989. The mean height of ice cliff is 24 m varying from 14 to 54 m. Using the mean height cliff the volume of the Ice Tongue in 1990 is of about 74 km^3.

THE RELEVANCE OF BIOTURBATION IN REWORKING PROCESSES OF ROSS SEA RECENT SURFICIAL SEDIMENTS

M. Frignani, L .Langone, M. Ravaioli, M. Taviani, Istituto Geologia Marina, CNR, via Zamboni 65, 40127 Bologna, Italy
C. Gambi, Laboratorio Ecologia Benthos, 80077 Ischia, Italy

Bioturbation plays an important role in syn- and post-depositional modifications of sediments. Most studies have focussed on examples from middle-low latitude seas while only a few took into consideration the importance of such a phenomenon in the polar seas. On the contrary, it should be stressed that modality of animal-induced reworking in these extreme environments is indeed an important factor to be assessed for sedimentary facies analysis. In fact, Antarctic continental shelf marine sediments are widely dominated by apparently structureless diamictons whose discrimination would be difficult also in absence of animal disturbance. We have approached the problem of evaluating the relevance of bioturbation in the polar marine record by means of visual inspection and core sampling Ross Sea surficial sediments. Selected experimental sites included very shallow (<30 m) stations in Terra Nova Bay and deeper ones (>300 m) offshore the same bay. Study of bioturbation included the identification of major reworkers, i.e. those organisms responsible for significant (>1 cm) sediment remodeling, combined with radionuclide profiles on suitable fine sediments. Major reworkers of the shallow, sandy-gravelly dominated areas are mostly polychaetes, molluscs and irregular echinids. Polychaetes are the major reworkers of the offshore fine-grained sediments. Complete homogeneization of the uppermost 6-9 cm of the deeper stations is well documented by the ^{210}Pb activity-depth profiles showing a depth interval with quite constant unsupported ^{210}Pb activities.

PERMAFROST OCCURRENCE IN JAMES ROSS ISLAND AND SEYMOUR ISLAND, ANTARCTIC PENINSULA REGION

M. Fukuda, Institute of Low Temperature Science, Hokkaido University, Sapporo 060, Japan.
J. Strelin, Instituto Antartico Argentino, Corrito 1248, Buenos Aires, Argentina.
K.Shimokawa, Sapporo University, Sapporo 062, Japan.
N.Takahashi, Hokkai-gakuen University, Sapporo 062, Japan.
T.Sone, Institute of Low Temperature Science, Hokkaido University, Sapporo 060, Japan.
D.Trombott, Centro Nacional Patagonico, Puerto Madryn-CH, Argentina.

The authors conducted the field survey related to the genesis and occurrence of permafrost in James Ross Island and Seymour Island, Antarctic Peninsula region, in 1989-1990 summer season. Mean annual air temperature in both islands is estimated about -10°C.

Ice-free ground spreads to the north-western part of James Ross Island. Coastal terraces of different three levels develop around Santa Marta Point along Croft Bay; upper terrace (21-24m, 32-35m a.s.l.), middle terrace (10-17m a.s.l.) and lower terrace (3-5m a.s.l.). Detailed topographical mapping and geological survey were conducted in this area. The upper terrace is composed of glacial till deposit. Shell samples were collected from deltaic deposit which composes the middle terrace, and from marine sand and gravels which cover the surface of the lower terrace. Then ^{14}C dating was done with the results of about 25,000 y.B.P. and 3,000 y.B.P., respectively. According to geo-electric resistivity measurements, the depths of permafrost base on the upper and lower terraces are estimated at 40 m deep and 3-5 m deep, respectively. It is considered that permafrost on the upper terrace occurred prior to the last glacial maximum age. The comparison between Antarctic and Arctic permafrost suggests that the permafrost in Antarctic regions is shallower than in Arctic regions under similar annual mean temperature in present time.

The transitional distribution from sorted circles to stone pits was mapped in detail on the slope near Mt.Santa Marta in this island. The internal structures of the patterned ground were examined by means of geo-electric resistivity measurement.

Seymour Island is located near James Ross Island. Marine terraces of different three levels are distributed in the island; upper terrace at Meseta (about 200 m a.s.l.), middle terrace at Sub-Meseta (about 60 m a.s.l.) and lower terrace at Larsen (about 5 m a.s.l.). In order to check the thickness of permafrost, geo-electric resistivities were surveyed at several sites. In the lower terrace at Larsen, two-year monitoring of ground temperature profiles was carried out. Annual mean ground temperature and the temperature gradient indicate that the depth of permafrost base is 32 m deep. This value coincides with the one obtained by geo-electric resistivity measurements.

DETERMINATION OF THE GRAVITY FIELD AROUND ANTARCTICA USING SATELLITE ALTIMETER DATA AND SURFACE GRAVITY DATA

Yoichi FUKUDA, Ocean Research Institute, University of Tokyo,
15-1, Minamidai 1-chome, Nakano-ku, Tokyo 164, Japan.

Jiro SEGAWA, Ocean Research Institute, University of Tokyo,
15-1, Minamidai 1-chome, Nakano-ku, Tokyo 164, Japan.

Katsutada KAMINUMA, National Institute of Polar Research,
9-10, Kaga 1-chome, Itabashi-ku, Tokyo 173, Japan.

During the past few years, we have investigated the determination of the gravity field around Antarctica. A significant point in these studies was the use of the GEOSAT altimeter data which have revealed the sea surface heights around Antarctica in the austral summer season for the first time. Thus we could determine a large scale geoid and gravity anomalies around Antarctica using the GEOSAT data. The results were compared with those of former studies and improvement of the accuracy was confirmed.

Although the altimeter data are very effective for covering large areas uniformly, their accuracy and resolution are worse than those of surface ship gravity data. In the continental margin, in particular, we can hardly use the altimeter data. Thus, combined use of both altimeter data and gravity data is important. As an attempt of the combined use of heterogeneous data, we estimated a geoid and gravity anomalies around the Japanese Antarctic stations where surface gravity data obtained by Japanese Antarctic Research Expedition as well as the GEOSAT data were available.

The method employed for the estimation is the Least Squares Collocation with an empirical covariance function. The method, by which both data can be dealt with simultaneously, enables us to evaluate formal error estimates and to budget for future measurement campaigns. The formal error estimates of the results show the values of 10 mgal for gravity anomaly and 20 cm for geoidal undulation.

Among the scant geophysical data in the Antarctic region, the gravity anomalies and the geoid obtained in this study provide significant new information on the area. The gravity anomalies in the area show a periodical undulation which seems to be correlated with the topographical structures. We also discuss other remarkable points of the results from the geophysical and the topographical perspectives.

PALEOMAGNETIC AND Ar^{40}/Ar^{39} DATING STUDIES OF THE MAWSON CHARNOCKITE AND SOME ROCKS FROM CHRISTENSEN COAST

Minoru FUNAKI[1], Kazuo SAITO[2]

1: National Institute of Polar Research, 9-10 Kaga 1-chome, Itabashi-ku, Tokyo 173, Japan.

2: Yamagata University, Faculty of Sciences, Yamagata 990, Japan

Rock samples of gneiss, charnockite, granite, pegmatite and dolerite dike were collected from Mawson Station, Scullin Monolith, Larsemann Hills and Vestfold Hills in the Christensen Coast. Characteristics of natural remanent magnetization (NRM) and magnetic properties of the samples were measured. The mean NRM directions of the stable NRM components are listed in Table 1. An age of the representative Mawson charnockite was determined by Ar^{40}/Ar^{39} and K/Ar methods.

The samples of Mawson charnockite from Mawson Station and Mt. Burnett have stable NRM component against AF demagnetization. The best precision of NRM distribution was obtained by thermal demagnetization at 480°C and the mean direction is decided as in Table 1. Magnetite and pyrrhotite are estimated for magnetic carrier of the charnockite. However, the gneiss rocks from the Rumdoodle Peak and Painted Hill have only unstable NRMs. A radiometric age of the Mawson charnockite was determined by Ar^{40}/Ar^{39} to be 445±27Ma (isochron age) which is younger than K/Ar age (475±15Ma).

The NRM of granitic gneiss from Scullin Monolith was relatively stable against AF demagnetization up to 20 mT. The best clustering was observed by thermal demagnetization at 380°C (α_{95}=20.8), although number of samples is only 5. Significant NRM directions were not obtained from the biotite gneiss rocks.

The NRM directions of biotite and pyroxene gneisses from the Larsemann Hills scattered widely, but almost all the directions clustered after thermal demagnetization at 330° or 380°C, as shown in Table 1, but those of several samples dispersed from the clusters. However, We have not obtained any significant NRMs from the rocks of Vestfold Hills in present.

Thermal demagnetization proved more effective than AF demagnetization during analyses of NRM's which are considered associated with pyrrhotite. The VGP positions obtained from the stable NRM components in these area may be located along the APWP of Antarctica from late Proterozoic to Silurian Periods.

Table 1. Paleomagnetic results obtained from this study.

SITE	MAWSON ST.	SCULLINM.	LARSEMANN HILLS	
Rock type	Charnockite	Granitic gn.	Biotite gn.	Pyroxene gn.
Demag	450°C	380°C	380°C	330°C
N	88	5	23	13
I	44.3	49.5	62.9	46.8
D	315.0	273.4	295.5	199.0
K	44	15	16	8
α_{95}	2.3	20.8	7.8	15.2
LAT	9.3S	26.5S	32.8S	45.6S
LON	22.9E	7.4W	27.8E	76.8W

LITHOSPHERIC ARCHITECTURE OF EAST AND WEST ANTARCTICA CONSTRAINED BY XENOLITHS FROM BASALTS.

J.A. Gamble, Dept. of Geology and Antarctic Research Centre, Victoria University of Wellington, Wellington, New Zealand.
R.J. Wysoczanski, Dept. of Geology and Antarctic Research Centre, Victoria University of Wellington, Wellington, New Zealand.

The Ross Sea Embayment which roughly parallels the mountain front of the Transantarctic Mountains (TAM) is an extensional region characterised by Miocene to Recent intraplate volcanism. The siting of large strato volcanoes composed largely of evolved lavas such as trachyte and phonolite was controlled by basement lineaments or fracture systems whereas small monogenetic scoria cones of basanite and alkali basalt randomly pepper the basement. Many of the latter have carried xenoliths to the surface from which we can piece together incomplete stratigraphic sections of the lithosphere. Presently available geophysical data constrains the continental crust to thin from ~ 40 km beneath the TAM to 20 km or less beneath Ross Island in the Ross Sea Embayment.

In a transect normal to the TAM fifteen xenolith bearing scoria cones have been sampled in detail. Granulite xenoliths confirm this geophysical model; garnet bearing samples coming only from localities in the foothills of the TAM whereas olivine (+ spinel) bearing samples typify those from Ross Island. The granulites vary compositionally from felsic (plagioclase dominated) to mafic (cpx + opx ± olivine dominated) types. Interlayering between these types is relatively common. Ultramafic xenoliths include black clinopyroxenite (with olivine + Cr-spinel ± kaersutite ± apatite), spinel bearing lherzolite, websterite and dunite. Rare phlogopite ± pargasite bearing xenoliths have been recorded from Ross Island and an unusual suite of phlogopite and pargasite bearing high-Ca pyroxenite (HCPS-suite) samples from Foster Crater in the foothills of TAM.

The late Cenozoic volcanic province of West Antarctica covers an area in excess of 150,000 km^2 with volcanic activity recorded over a period from early Miocene to Recent. Major volcanic features include linear ranges of volcanoes such as the Executive Committee Range (ECR), USAS Escarpment, Flood Range, Crary Mountains and Toney Mountain together with variably eroded edifices at Mount Murphy, Mount Takahe, the Kohler Ranges and the Fosdick Mountains. As part of the joint US-NZ-UK West Antarctica Volcano Exploration (WAVE) project in the field seasons of 1989/90/91 comprehensive suites of xenoliths were collected from ECR, the USAS Escarpment and Mount Murphy and these are now being compared to the suites from the Ross Sea Embayment. In many of these locations pre-volcanism basement to the volcanoes is not exposed and only the summit calderas of large strato volcanoes penetrate the surrounding ice-cap. Like the large strato volcanoes of the Ross Embayment, these are composed of evolved trachyte, phonolite or peralkaline rhyolite and, similarly, we also conjecture a strong structural control in their siting. Satellitic scoria cones of basanite and alkali basalt contain rich xenolith assemblages which range from supra crustal to lower crustal and upper mantle. Because of the lack of surface exposure, these scoria cones become vital probes from which to glean important, but imperfect, sections through the lithosphere.

The xenolith assemblages from West Antarctica are similar petrographically to those from the Ross Sea Embayment, although no HCPS types are recorded. Granulites are spinel bearing, mostly mafic and dominated by clinopyroxene - no orthopyroxene or garnet bearing granulites were recorded from the southern ECR (Mts Sidley and Waesche). A number of samples display a distinctive layering between felsic (plagioclase) and mafic (cpx + olivine) varieties. Ultramafic xenoliths also vary from black clinopyroxenites (with Cr-spinel ± olivine ± kaersutite) to spinel lherzolite with conspicuous bright green Cr-diopsides. Xenoliths showing interlayering of these types have also been recorded. Textures range from coarse grained protogranular to porphyroclastic - mylonitic.

The xenolith assemblages from the Ross Sea Embayment and West Antarctica are a record of lithospheric attenuation and modification associated with major asthenospheric upwelling. Current and planned work will address the geochemical consequences of lithospheric growth and modification during episodes of rifting.

STROMATOLITES FROM THE PALEOGENE POLONEZ COVE FORMATION OF KING GEORGE ISLAND, ANTARCTICA: STRATIGRAPHIC AND PALEOCLIMATIC IMPLICATIONS

A. Gaździcki
Institute of Paleobiology
Polish Academy of Sciences
Al. Żwirki i Wigury 93
02-089 Warszawa, Poland

The Low Head Member (= *Chlamys*-bearing conglomerate) of the Polonez Cove Formation on King George Island (South Shetland Islands) which contains discussed stromatolites consists of glacially-controled sediments formed during the Polonez Glaciation *i. e.* the largest Cenozoic glaciation in the Antarctic Peninsula sector.

These isolated, abiophoric stromatolites are turbinate and unbranched with smooth surface. The height of individual specimens ranges from 12 mm to 40 mm and their width from 25 mm to 80 mm. It is the first record of such stromatolites from the continent of Antarctica.

The results of studies of the $^{87}Sr/^{86}Sr$ isotope ratios on stromatolites from King George Island (Barrera, *pers. comm.*) show that the Low Head Member as well as the Polonez Glaciation are of Late Eocene - Early Oligocene age. The high Sr concentrations and the preservation of stromatolite structures suggest that Sr isotope ratios are original and have not been modified by diagenesis.

The stratigraphic and paleoclimatic implications of those data are discussed.

ISOTOPICAL EVIDENCE FOR GLACIATION IN THE PALEOGENE LA MESETA FORMATION, SEYMOUR ISLAND, ANTARCTICA

A. Gaździcki, M. Gruszczyński, A. Hoffman,
K. Małkowski, Institute of Paleobiology,
Polish Academy of Sciences, Al. Żwirki i Wigury 93,
02-089 Warszawa, Poland
S. Hałas, Institute of Physics, UMCS University,
Pl. Skłodowskiej-Curie 1, 20-031 Lublin, Poland
A. Tatur, Institute of Ecology, Polish Academy
of Sciences, Dziekanów Leśny, 05-092 Łomianki, Poland

Stable carbon and oxygen isotopic relations have been analyzed in brachiopod, gastropod, and bivalve fossils from the La Meseta Fm. (Eocene to possibly early Oligocene), Seymour Island, West Antarctica. The results indicate a bipartite vertical division of the stable carbon isotopic curve through time. The lower segment represents delta-13-carbon values largely the same as observed in the Lopez de Bertodano Fm. (Campanian to Paleocene). In the middle part of the Unit II informally distinguished by Elliot and Trautman (1982) within the La Meseta Fm., the carbon isotopic curve begins to radically shift toward negative values and this trend continues up to the top of the La Meseta Fm. The shift is by roughly 6 permil; it is so large that it demands an explanation in terms of the oceanographic model proposed by Małkowski *et al.* (1989) which presumes a change from largely stratified to vigorously mixed ocean. The carbon isotopic shift implies the onset of mixing, which must also have severe consequences both for the oxygen isotopic relations and for climatic cooling. As reflected in delta-18-O values, these consequences counteract each other and this is why the oxygen isotopic curve does not decline parallel to the carbon curve. Therefore, divergence of the carbon and oxygen isotopic curves in the upper part of the Unit II and Unit III of the La Meseta Fm. implies a considerable climatic cooling. This effect is so profound that it should be interpreted as evidence for glaciation, which may then be correlated with the Polonez Glaciation of King George Island, that is, the largest Cenozoic glaciation in the Antarctic Peninsula sector.

INTRUSIVE ROCKS IN THE AREA BETWEEN DAVID AND TUCKER GLACIERS, NORTH VICTORIA LAND, ANTARCTICA

C.Ghezzo, Dipartimento di Scienze della Terra, Università di Siena, Italy.
B.Lombardo, Centro Studi Orogeno Alpi Occidentali-CNR, Dipartimento di Scienze della Terra, Università di Torino, Italy.
A.Montrasio, Centro Studi Stratigrafia e Petrografia Alpi Centrali-CNR, Dipartimento di Scienze della Terra, Università di Milano, Italy.
P.Pertusati, Dipartimento di Scienze della Terra, Università di Pisa, Italy.

The area between David and Tucker Glaciers comprises three terranes accreted to the Precambrian East Antarctic Craton during Early Paleozoic times: the Wilson, Bowers and Robertson Bay Terranes.

Plutonic rocks invaded all three terranes during two Paleozoic magmatic cycles (Cambro-Ordovician Granite Harbour Intrusives: GHI and Devono-Carboniferous Admiralty Intrusives: AI) and one Tertiary cycle (Meander Intrusives: MI).

As a result of previous studies and of a research programm by an Italian team, a preliminary map of the granitoid types characterizing this region is here presented. The distinction within each cycle is based on field, petrographic and chemical data.

- Granite Harbour Intrusives. For these intrusives, believed to be an orogenic magmatic sequence, a subdivision according to relative emplacement age, petrographic type and chemical affinity is outlined. Several suites are distinguished: a metaluminous calcalkaline suite, a shoshonitic suite and a peraluminous suite. Within the first two suites the mafic, intermediate and felsic types are distinguished; the third suite is composed only by felsic rocks. A further distinction is made between older foliated, syntectonic intrusives and late-to post-tectonic intrusives.

These distinctions outline a regional zonation of the Cambro-Ordovician magmatism in the study area.

- For the Devono-Carboniferous Admiralty Intrusives only a post tectonic calcalkaline suite has been detected (a metaluminous dioritic to monzogranitic association). These plutonic complexes occur in all three terranes in the Eastern part of the region.

- The Tertiary Meander Intrusives comprise several small intrusive bodies whose composition varies from gabbro to alkaligranite. Like the AI, they occur in all three terranes and belong to the anorogenic alkaline volcano-plutonic province associated to the Ross Sea rift system.

THE ZEOLITISATION MODEL OF KERGUELEN ISLANDS, SOUTH INDIAN OCEAN

A. Giret, Laboratoire de Pétrologie, C.N.R.S. - U.R.A. 10,
Université Jean Monnet, 23 rue du Docteur Paul Michelon,
42023 Saint-Etienne Cédex 02, France.

O. Verdier, Laboratoire de Pétrologie, Université Pierre et Marie Curie,
4 place Jussieu, 75252 PARIS Cédex 05, France.

P. Nativel, Laboratoire de Pétrologie-Volcanologie, Université Paris-Sud,
Bâtiment 504, 91405 Orsay Cédex, France.

Kerguelen Islands present many subjects of geological interest: a sequencial magmatism beginning with tholeiitic product and evolving to very alkaline ones (Giret and Lameyre, 1985), a bimodality of the alkaline suites with a silica-oversaturated and a silica-undersaturated trends (Giret, 1990), magmatic sources which characteristics determine an isotopic pole of reference (Gautier et al., 1990), the existence of several plutonic complexes which is anusual in oceanic provinces (Giret, 1983), a geological history related to the Kerguelen-Gaussberg ridge (Schlich, 1975) which is one of the largest in the world, a more than 40 Ma longevity (Giret and Lameyre, 1983). Recent investigations (Verdier, 1989) point at the zeolitisation as an instructive model which may be added to the attractive geological characteristics of those fascinating islands.

Descriptions of zeolites in Kerguelen date back to the last century (Roth, 1875, Lacroix, 1915, Aubert de la Rüe, 1929) and a review has been published by Nativel and Nougier (1983) who recognized 8 species of zeolites and a twenty different associations of them: analcite, chabazite, epistilbite, heulandite, mesolite, phillipsite, stilbite and thomsonite. A new program of research focusing on Kerguelen paleo-hydrothermalism and supplemented by several

TABLE 1

ZEOLITES OF KERGUELEN

STRUCT. (SBU)	SPECIES	IDEAL FORMULAE	RANGE OF COMPOSITION IN KERGUELEN ISLANDS
4-1	Natrolite	$Na_{16}(Al_{16}\ Si_{24}\ O_{80})\ 16\ H_2O$	$Na_{15}\ Ca_{0.5}\ (Al_{16}\ Si_{24}\ O_{80})\ 25\ H_2O$
	Mésolite	$Na_{5.3}\ Ca_{5.3}\ (Al_{16}\ Si_{24}\ O_{80})21.3\ H_2O$	$Na_{2.5}\ Ca_{8.75}\ (Al_{16}\ Si_{24}\ O_{80})26\ H_2O$ ↔ $Na_6\ Ca_5\ (Al_{16}\ Si_{24}\ O_{80})24\ H_2O$
	Scolécite	$Ca_8\ (Al_{16}\ Si_{24}\ O_{80})\ 24\ H_2O$	$Ca_8\ (Al_{16}\ Si_{24}\ O_{80})\ 27\ H_2O$ ↔ $Na_2\ Ca_7\ (Al_{16}\ Si_{24}\ O_{80})\ 26\ H_2O$
	Thomsonite	$Na_4\ Ca_8\ (Al_{20}\ Si_{20}\ O_{80})\ 24\ H_2O$	$Na_4\ Ca_{7.5}\ (Al_{19}\ Si_{21}\ O_{80})\ 26\ H_2O$ ↔ $Na_{5.8}\ Ca_6\ (Al_{17.8}\ Si_{22.2}\ O_{80})\ 26\ H_2O$
	Gonnardite	$Na_5\ Ca_2\ (Al_9\ Si_{11}\ O_{40})\ 12\ H_2O$	$Na_{6.2}\ Ca_{1.15}\ (Al_{8.5}\ Si_{11.5}\ O_{40})11H_2O$
S4R	Analcime	$Na_{16}\ (Al_{16}\ Si_{32}\ O_{96})\ 16\ H_2O$	$Na_{15}\ (Al_{15}\ Si_{33}\ O_{96})\ 17.5\ H_2O$
	Laumontite	$Ca_4\ (Al_8\ Si_{16}\ O_{48})\ 16\ H_2O$	$(Na,K)_{0.24}Ca_{3.68}(Al_{7.6}Si_{16.4}O_{48})16.5H_2O$
D4R	Glamondine	$Ca_4\ (Al_8\ Si_8\ O_{32})\ 16\ H_2O$	$Na_{1.5}\ Ca_3\ (Al_{7.5}\ Si_{8.5}\ O_{32})\ 17\ H_2O$
	Phillipsite	$K_2\ (Ca_{0.5},Na)_4(Al_6\ Si_{10}\ O_{32})12\ H_2O$	$K_{1.5}\ Ca_{1.85}\ Na_{0.5}(Al_{5.7}\ Si_{10.3}\ O_{32})11H_2O$
6R	Chabazite	$Ca_2\ (Al_4\ Si_8\ O_{24})\ 12\ H_2O$	$(Na,K)_{0.7}\ Ca_{1.7}\ (Al_{4.1}\ Si_{7.9}\ O_{24})10.5\ H_2O$
	Levyne	$Na\ Ca_{2.5}\ (Al_6\ Si_{12}\ O_{36})\ 18\ H_2O$	$K_{0.2}\ Na_{1.4}\ Ca_{2.5}\ (Al_{6.6}\ Si_{11.4}\ O_{36})\ 15\ H_2O$
	Erionite	$Na\ K_2\ Mg\ Ca_{1.5}(Al_8\ Si_{28}\ O_{72})28\ H_2O$	$Na_{0.5}K_{1.7}Mg\ Ca_{2.5}(Al_{9.2}\ Si_{26.8}\ O_{72})26H_2O$
	Offrétite	$K\ Ca\ Mg\ (Al_5\ Si_{13}\ O_{36})\ 15\ H_2O$	$K\ Na_{0.2}Ca_{1.7}Mg_{0.35}(Al_{5.3}Si_{12.7}O_{36})15H_2O$
5-1	Mordénite	$Na_3\ K\ Ca_2\ (Al_8\ Si_{40}\ O_{96})\ 28\ H_2O$	$Na_3\ K_{0.5}\ Ca_{2.15}\ (Al_{7.8}\ Si_{40.2}\ O_{96})\ 28\ H_2O$
	Dachiardite	$(Na,K,Ca_{0.5})_4\ (Al_4\ Si_{20}\ O_{48})\ 18\ H_2O$	$Na_{2.7}\ K_{0.5}\ Ca_{0.4}\ (Al_4\ Si_{20}\ O_{48})14.5\ H_2O$
	Epistilbite	$Ca_3\ (Al_6\ Si_{18}\ O_{48})\ 16\ H_2O$	$Na_{0.4}\ Ca_{2.8}\ (Al_6\ Si_{18}\ O_{48})\ 16.5\ H_2O$
4-4-1	Heulandite	$(Na,K)\ Ca_4\ (Al_9\ Si_{27}\ O_{72})\ 24\ H_2O$ ↔ $(Na,K)_6\ (Al_6\ Si_{30}\ O_{72})\ 20\ H_2O$	$(Na,K)\ Ca_4\ (Al_9\ Si_{27}\ O_{72})\ 24\ H_2O$ ↔ $(Na,K)_{2.5}\ Ca_2\ (Al_{6.5}\ Si_{29.5}\ O_{72})\ 22\ H_2O$
	Stellérite	$Ca_4\ (Al_8\ Si_{28}\ O_{72})\ 28\ H_2O$ ↔ $Na\ Ca_4\ (Al_9\ Si_{27}\ O_{72})\ 30\ H_2O$	$Ca_4\ (Al_8\ Si_{28}\ O_{72})\ 27.5\ H_2O$ ↔ $Na_{1.5}\ Ca_4\ (Al_{9.5}\ Si_{26.5}\ O_{72})\ 28\ H_2O$
	Stilbite		

methods of analyse - X.R. diffr., I.R. spectr., X-fluo spectr.,electron microprobe, scanning microscope and D.T.A.- led to the description of 11 other species of zeolites (Yerdier, 1989): scolecite, natrolite, gonnardite, laumontite, gismondite, levyne, erionite, offretite, mordenite, dachiardite and stellerite (see table 1).

Some of these zeolites remain only occasionnal and are of restricted interest for the following interpretations. On the other hand, few hydrothermal minerals as quartz, calcite, aragonite, celadonite and saponite are genetically associated with zeolites. Thus, it is a number of 16 minerals which have been used as geothermal references. Hydrothermal mineralisations are observed mainly in the basalts, in which they fill geodes of 1 to 10 cm in diameter, and they are more abundant at the roof and floor of scoriaceous lava flows. They also appear as a ground mass cementing the porous interlayers. These deposits present a fifty associations of 2, 3 and sometimes 4 cogenetic minerals. 28 of them have been considered as geothermal indexes (see table 2). It has been established that the associations of more then 4 minerals represent in fact successive crystallisations delayed over long time intervals, the reason why they cannot be accepted as paragenesis sensu-stricto.

ZONES	TYPICAL MINERALS	*MAIN PARAGENESIS*	TEMP.(°C)
I	PHILLIPSITE CHABAZITE	*CHABAZITE+PHILIPSITE* *THOMSONITE+CHABAZITE+PHILLIPSITE* *ARAGONITE+CHABAZITE*	40 - 80
II	SAPONITE ANALCITE THOMSONITE	*THOMSONITE+CHABAZITE+SAPONITE* *THOMSONITE+ANALCITE+CHABAZITE* *THOMSONITE+ANALCITE+SAPONITE* *THOMSONITE+SAPONITE* *THOMSONITE+ANALCITE* *MESOLITE+THOMSONITE+SAPONITE* *MESOLITE+THOMSONITE+ANALCITE*	70 - 110
III	MESOLITE STILBITE	*STILBITE+MESOLITE+THOMSONITE* *STILBITE+MESOLITE* *SCOLECITE+STILBITE+MESOLITE*	100 - 140
IVa	SCOLECITE STELLERITE HEULANDITE	*STELLERITE+STILBITE+SCOLECITE* *STELLERITE+SCOLECITE+MESOLITE* *HEULANDITE+SCOLECITE+MESOLITE* *HEULANDITE+STELLERITE+STILBITE* *HEULANDITE+STELLERITE+SCOLECITE*	130 - 180
IVb	CELADONITE MORDENITE HEULANDITE	*CELADONITE+HEULANDITE+SCOLECITE* *HEULANDITE+QUARTZ+MORDENITE* *CELADONITE+HEULANDITE+MORDENITE* *CELADONITE+QUARTZ+CALCITE* *CELADONITE+HEULANDITE+STELLERITE*	
V	LAUMONTITE CHLORITE	*LAUMONTITE+HEULANDITE+STELLERITE* *LAUMONTITE+HEULANDITE* *LAUMONTITE+QUARTZ+HEULANDITE* *CHLORITE+LAUMONTITE+HEULANDITE* *CHLORITE+LAUMONTITE*	170 - 240

TABLE 2

INDEX ZEOLITES AND ZONES OF ZEOLITES

Field occurences and reciprocity relationships amongst the main paragenesis allow the definition of 5 zones which may be recognized then by a few index minerals coexisting together or not depending on environmental chemical constraints. The field location of these zones as well as the physical and chemical conditions of crystallisation of the index minerals confer to them the quality of P-T indicator, that is to say hydrothermal facies which intensity growths from zone I to zone V (see table 2 and figure 1). The isograd planes which separate the different zones of facies are parallel, dipping from 2 to 4° to the East. This hydrothermal structure cut the general structure of

the basalts according to their regional dip of 5° to the E.S.E. Geological evidences as well as the extent of the zeolitisation all over the Kerguelen archipelago involves a 2000 m thickness of the mineralized pile of basalts. The zonality which is pointed out here recalls the zeolite model of Iceland as it has been published by Walker, 1960. Nevertheless the Kerguelen zeolite model is of better accuracy since the third and fourth icelandic zones have been respectively divided in zones III and IVa and in zones IVb and V in Kerguelen.

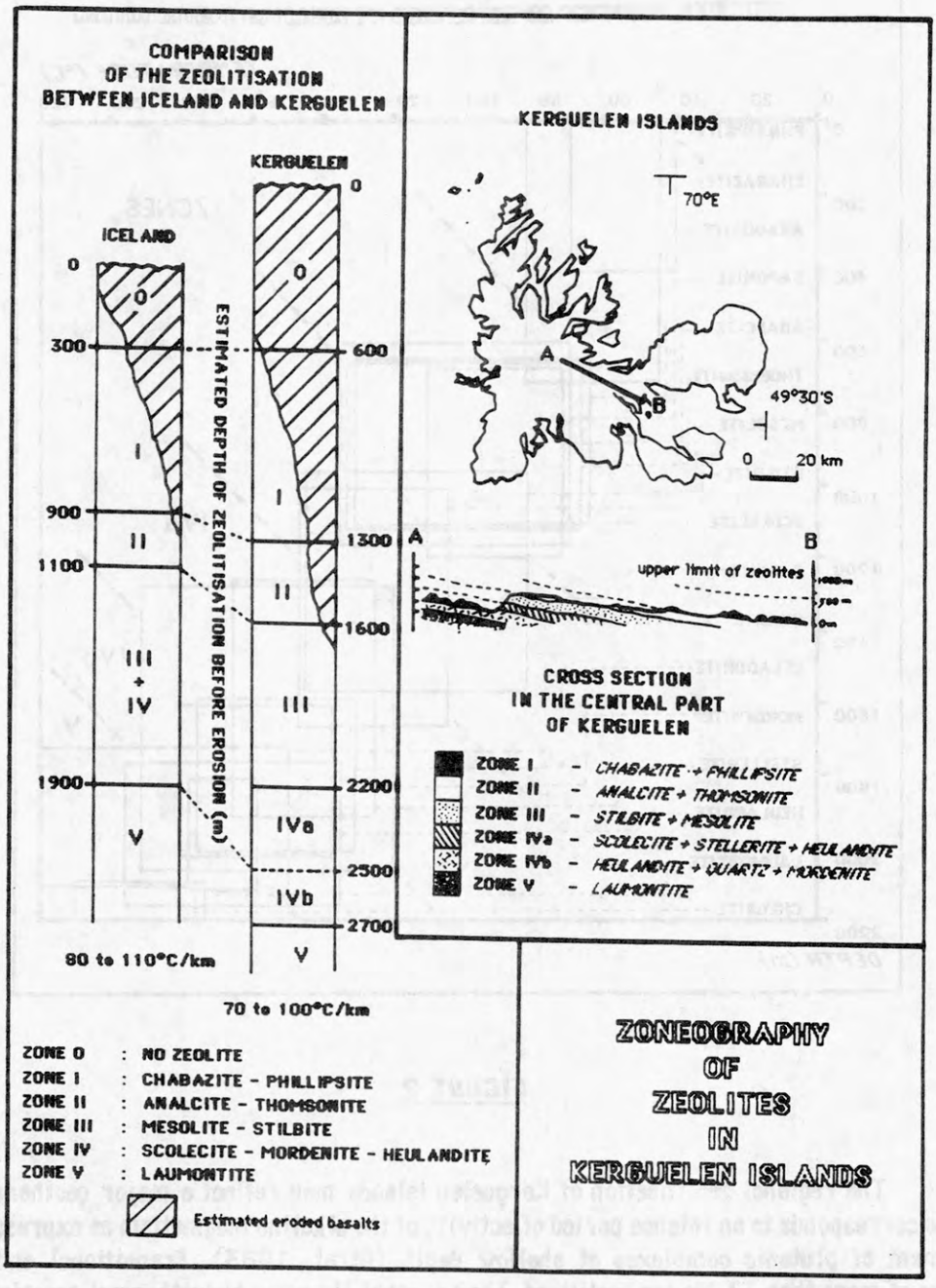

FIGURE 1

Experimental data (Thompson, 1970, Liou, 1971a, 1971b, 1971c, Zeng and Liou, 1982, Cho et al., 1987, Miyashiro and Shido, 1970) and field observations reveal close relationships between the crystallisation temperature range of zeolites and their depth of occurence in Kerguelen. This lead (figure 2) to a T-D diagram in which the existence areas of the different zeolites are controlled by a geothermal gradient ranging from 70 to 100°C.km-1 .

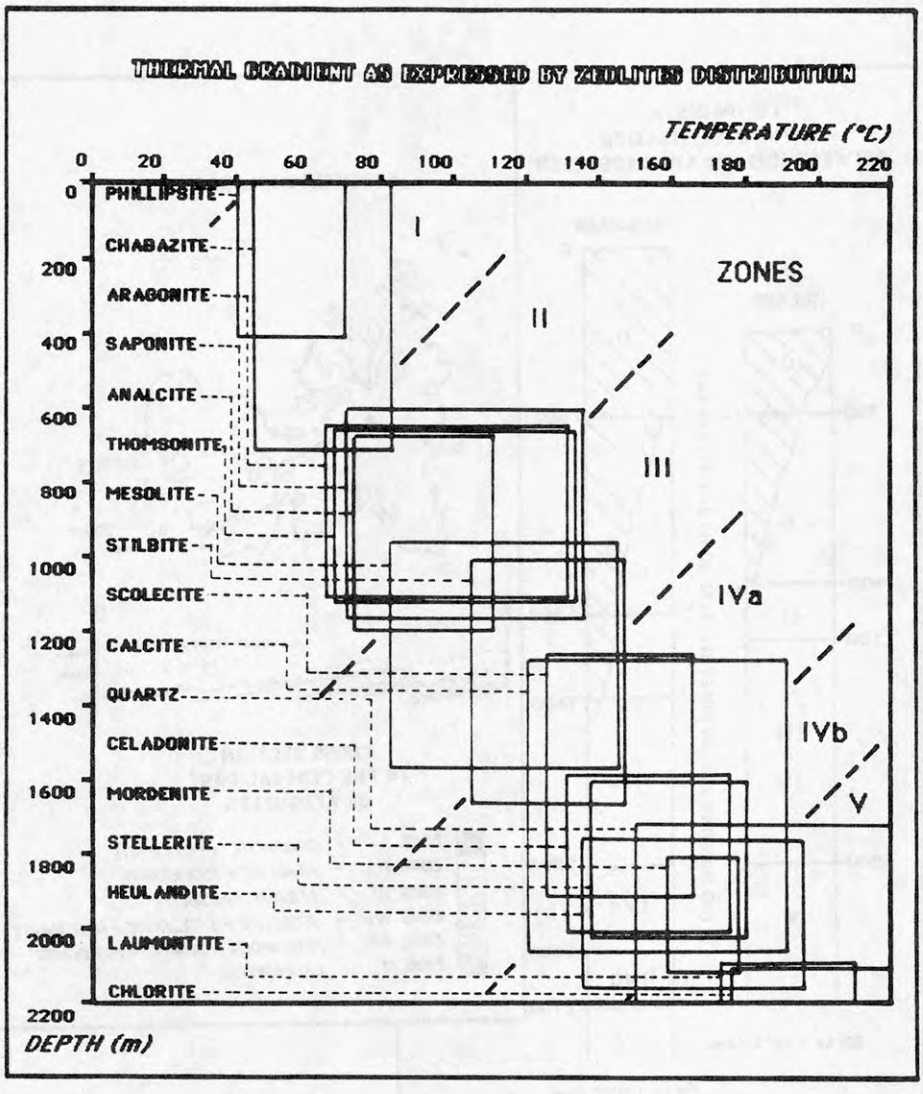

FIGURE 2

The regional zeolitisation of Kerguelen Islands may reflect a major geothermal event which age corresponds to an intense period of activity of the alkaline magmatism as expressed by the emplacement of plutonic complexes at shallow depth (Giret, 1983). Transitional and alkaline complexes of more than 13 Ma are zeolitised. They present the same hydrothermal associations that those of the surrounding basalts, except the fact of zeolite compositions slightly more sodic in differentiated rocks such as nepheline-syenites, quartz-syenites and granites. Moreover, the zeolite associations are surimposed to the contact metamorphism paragenesis in the periphery of the intrusions. On the contrary, zeolites are absent from younger plutonic complexes (Rallier du Baty,

12 to 4 Ma, Mt. Ross, 4 to 2 Ma) . In this case, the surrounding basalts, in which the regional zeolitisation is well observed elsewhere, zeolites are replaced by typical minerals of contact metamorphism around the intrusions. In the plutonic intrusions of intermediate ages (Mts. Ballons, 14 to 12 Ma, Société de Géographie peninsula, 15 to 12 Ma), the zeolites associations are of lower facies than in their surrounding basalts. Thus, the relationships between plutonic complexes and zeolites occurences clearly date the major zeolitisation in the range of 15 Ma, with an intensity decreasing until 12 Ma. Taking into account an erosion speed ranging from 1,2 to 1,5 cm. per century, such dating is consistent with a 1 500 m thickness of the eroded pile of basalts since the end of the zeolitisation.

References:

Aubert de la Rüe, E., 1929 - Sur quelques minéraux des îles Kerguelen. *Bull. Soc. Fr. Mineral.*, 52, 144-146.

Cho, M., Liou, J.G., Maruyama, S., 1986 - Transition from the zeolite to prehnite pumpellyite facies in the Kartmuntsen metabasite, Yancouver Island, British Columbia. *Journ. Petrol.*, 27, 467-494.

Gautier, I., Giret, A., Loubet, M., Vidal, P., Weis, D., 1990 - Petrology and geochemistry of the Kerguelen archipelago basalts (South Indian Ocean): evolution of the mantle source from ridge to intraplate position. *Earth Planet. Sci. Letters*, 100, 59-76.

Giret, A., 1983 - Le plutonisme océanique intraplaque, exemple des îles Kerguelen. Thèse doct. ès Sci., Université Pierre et Marie Curie, Paris, Published in *Bull. C.N.F.R.A.*, Paris, 54, 289 p.

Giret, A., 1990 - Typology, evolution, and origin of the Kerguelen plutonic series, Indian Ocean, a review. Geol. Journ., 25, 239-247.

Giret, A., Lameyre, J., 1983 - A study of Kerguelen plutonism: petrology and geochronology, geological implications. In: Oliver R.L., James P.R., and Jago, J.B. (Eds), *Antarctic Earth Sciences n°4*. Australian Academy of Sciences, Australia, 645-661.

-1985 - Inverted alkaline tholeiitic sequences related to lithospheric thickness in the evolution of continental rifts and oceanic islands. *Journ. Afr. Earth Sci.*, 3, 1, 261-268.

Lacroix, A., 1915 - Les zéolites et les produits siliceux des basaltes de l'archipel Kerguelen. *Bull. Soc. Fr. Mineral.*, 58, 134-137.

Liou, J.G., 1971 a - Stilbite-Laumontite equilibrium. *Contrib. Mineral. Petrol.*, 31, 171-177.

-1971 b - P-T stabilities of laumontite, wairakite, lawsonite and related minerals in the system $CaAl_2Si_2O_8 - SiO_2 - H_2O$. *Journ. Petrol.*, 12, 379-411.

-1971 c - Analcime equilibrium. *Lithos*, 4, 389-402.

Miyashiro, A., Shido, F., 1970 - Progressive metamorphism in zeolite assemblages. *Lithos*, 3, 251-260.

Nativel, P., Nougier, J., 1983 - Les faciès zéolitiques des basaltes des plateaux des îles Kerguelen. (T.A.A.F.); implications volcanologiques. *Bull. Soc. Géol. Fr.*, 25, 957-961.

Roth, J., 1875 - Uber die gesteine von Kerguelen's Land. *Monatsberitchte der König., Pruss. Akad. der Wissensch., Berlin*, 60, 723-735.

Thompson, A.B., 1970 - Laumontite equilibria and the zeiolite facies. *Amer. J. Sci.*, 269, 267-275.

Verdier, O., 1989 - Champs géothermiques et zéolitisation des îles Kerguelen: implications géologiques. Thèse Univ. Pierre et Marie Curie, Paris, n°89-29, 271p.

Walker, G.P.L., 1960 - Zeolite zones and dyke distribution in relation to the structure of the basalts of Eastern Iceland. *Journ. Geol.*, 68, 515-528.

Zeng, Y., Liou, J.G., 1982 - Experimental investigations of yugawarakite-wairakite equilibrium. *Amer. Mineral.*, 67, 937-943.

PETROTECTONIC HISTORY OF HIGH-GRADE METAMORPHIC ROCKS IN THE CENTRAL TRANSANTARCTIC MOUNTAINS, ANTARCTICA, AND IMPLICATIONS FOR PROTEROZOIC CRUSTAL EVOLUTION

John W. Goodge, Department of Geological Sciences, Southern Methodist University, Dallas, Texas 75275, USA.
Vicki L. Hansen, Department of Geological Sciences, Southern Methodist University, Dallas, Texas 75275, USA.
Simon M. Peacock, Department of Geology, Arizona State University, Tempe, Arizona 85287, USA.

Precambrian metamorphic rocks of the Nimrod Group, exposed in the central Transantarctic Mountains, represent a small part of the East Antarctic cratonal mass that formed a portion of the Gondwana supercontinent. The importance of these rocks lies in their inferred position near a proto-Antarctic plate boundary, offering a unique opportunity to study the relation between the Archean-Proterozoic craton and younger crustal elements formed along the active plate margin. On the basis of emerging age data, high-grade metamorphic rocks from this terrain appear to record multiple Precambrian tectonothermal events prior to ~1.45 Ga. Two of these Middle Proterozoic or older events, represented by (1) high-P tectonic blocks within (2) a wide zone of mylonitic tectonites, reflect involvement of deep crust in a mobile continental lithosphere. These events pre-date the Late Proterozoic Beardmore orogeny, which formed shallow-level structures in outboard assemblages that differ from those in the Nimrod Group in terms of style, geometry and kinematic history.

Cryptic evidence for the first of these events is derived from numerous mafic and ultramafic tectonic blocks hosted by layered, ductilely-deformed schist and gneiss. Mafic blocks contain cores of partially preserved eclogitic mineral assemblages, surrounded by rinds of garnet amphibolite. Block metamorphism in the eclogite facies is indicated by pyrope-rich relict garnets, Mg-rich staurolite (Mg/Mg+Fe = 0.58) inclusions in one garnet from a block rim, and plagioclase reaction rims around garnets. Complex intergrowths of low-Na Cpx + Opx + Hbl + Pl + Qtz may have formed from the breakdown of omphacitic pyroxene. These mineral data indicate the mafic blocks were metamorphosed under conditions of P = 12-25 kbar and T ≈ 600°C. The ultramafic rocks indicate the involvement of deep crustal or upper mantle material within the deforming zone, either as relict subduction zone entrainments, or as tectonic slivers introduced during ductile flow.

A younger event affecting Nimrod Group rocks formed a regionally SW-dipping zone of pervasive mylonitic L-S tectonites that contain a gently-plunging, NW-trending elongation lineation. Macro- and microscopic kinematic indicators record regionally consistent along-strike displacement (present-day coordinates) throughout an exposed structural thickness of ~20 km. Deformation within this zone also occurred under high P-T conditions (≥8 kbar; ~700°C), as shown by syn-kinematic Ky (± Sil) + Grt + Ms + Bt + Qtz in pelites, Hbl + Pl ± Grt ± Cpx ± Czo in mafic rocks, and by thermobarometry. High temperatures of deformation are also indicated by the presence of migmatite zones, and syn-kinematic granitic sills and pegmatitic veins, which may have enhanced ductility. The preservation of high-T tectonite fabrics over such a wide structural zone, in which mineral recrystallization did not keep pace with deformation, indicates that strain rates were high. The inferred high strain rates required to allow for the formation and preservation of this ≥20 km-thick zone of L-S tectonites may suggest that extremely rapid Precambrian displacement rates operated along this ancient crustal boundary. High displacements may have allowed for tectonic incorporation of the earlier-formed deep-crustal or mantle materials into the crustal-penetrating zone, and for movement of sedimentary protoliths to deep crustal levels.

The width of the shear belt, homogeneity of structures, high temperatures of deformation, and syn-kinematic magmatism suggest that Proterozoic crust in this region was extremely dynamic but kinematically simple. Nimrod tectonites may thus provide valuable insight into the growth of Gondwana, the Proterozoic thermal structure of the lithosphere, and the physical nature of lithospheric boundaries.

CRETACEOUS-TERTIARY SEAFLOOR OFF DRONNING MAUD LAND, ANTARCTICA

D. Gopala Rao, A.K. Chaubey and T. Ramprasad
National Institute of Oceanography, Dona Paula, Goa-403004, India

A study of the bathymetric and linear magnetic anomalies between Dronning Maud Land, Antarctica and the South West Indian Ridge (SWIR) revealed a Mesozoic sequence of linear magnetic anomalies, MO to M12 (108 to 126 Ma), fracture zone offsets (≈130 km), and the Cretaceous magnetic quiet zone between isochrons MO and 34 (108 to 80 Ma). The study sheds light on : 1) the evolution of an anomalous "stretched" pattern of seafloor anomalies during magnetic isochrons MO and 34 and associated offset (>10°) in some segments of the northeast part of the SWIR and, 2) continuation of a proposed, buried fracture zone to the south where it abuts the Astrid Ridge off Dronning Maud Land. The history of spreading is related to declining dynamic pressures at the plate margin due to the Kergeulen-Heard mantle plume during Cretaceous times (≈110 Ma).

TECTONIC DEVELOPMENT OF GRABEN OVER THE ASTRID RIDGE OFF DRONNING MAUD LAND, ANTARCTICA

D. Gopala Rao, M.V. Ramana and K.V.L.N.S. Sarma
National Institute of Oceanography, Dona Paula, Goa-403004, India

High resulution seismic reflection and bathymetric surveys have been carried out on the 280 km wide and 450 km long Astrid Ridge off Dronning Maud land Antarctica (Fig. 1). These studies helped in identifying the various structural elements and sedimentary sequences. They are (i) thick sedimentary strata of about 1.3 sec (TWT) comprised of four seismic sequences identified based on the acoustic impedence over the study area. (ii) ridge crest which is deformed and down faulted along N to NNW-S to SSE trending normal and upthrust faults, and (iii) large scale incision of sediments (Fig. 2). These sequences possess wavy pattern and are parallel to the upwarped acoustic basement (unit IV). Distinct and higher order reliefs within the basement and overlying sediments are seen on the crestal part of the ridge. Abrupt truncation of reflectors in south of the study area (Seismic units I to III), diverging reflection patterns on the eastern flank of the ridge, sheet drape structure over the ridge flanks, contorted reflection patterns in the deformed/down faulted parts of the acoustic basement, onlap fill structures, folds normal faults bounding the graben and upthrust crustal blocks are some of the structural elements observed within the sediments and basements (Fig. 2). The incision marked by truncated reflectors extends to a maximum depth of 0.58 sec. with its axis aligned towards west which may be due to the currents at the near bottom depths. Further, the seismic records show a broad graben like structure trending north south and the sediment sequences within the graben attain upward convexity.

The upwarped acoustic basement of the ridge crest between 2000 m isobath in the study area is maximum deformed and down faulted. The zone of deformation trends NNW-SSE and the graben structure is more conspicuous towards north. A tentative chronostratigraphy has been established based on the identified conformities in the adjacent Weddle sea and age of the acoustic basement is attributed to late-middle Jurassic (~ 120 Ma).

The zone of deformation (110 km wide is associated with a seaward prograded graben (~20 km wide) which is seen in three different stages of development i. e. deformed, intermittent and well developed with 240-320 m of down throw (Fig. 3) at sea bed level. In the basence of the identifiable zone of subduction in the vicinity of Astrid Ridge, the stages of development are explained as result of compressional forces (from spreading and stretching ridge push) and stretching lead to subsidence and upthrust crustal blocks controlled by faults, thus causing the graben like feature on the crest of Astrid Ridge.

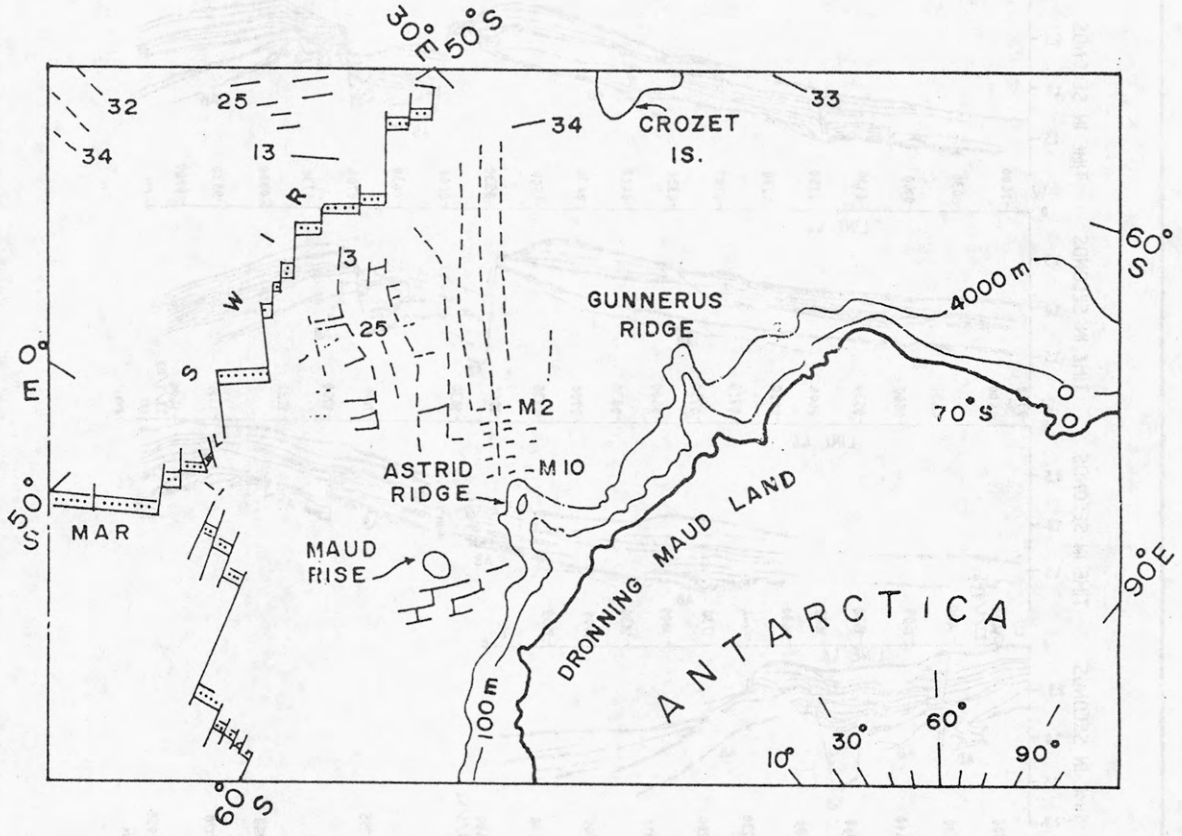

Fig 1. Map showing the study area on the Antarctica continental margin.

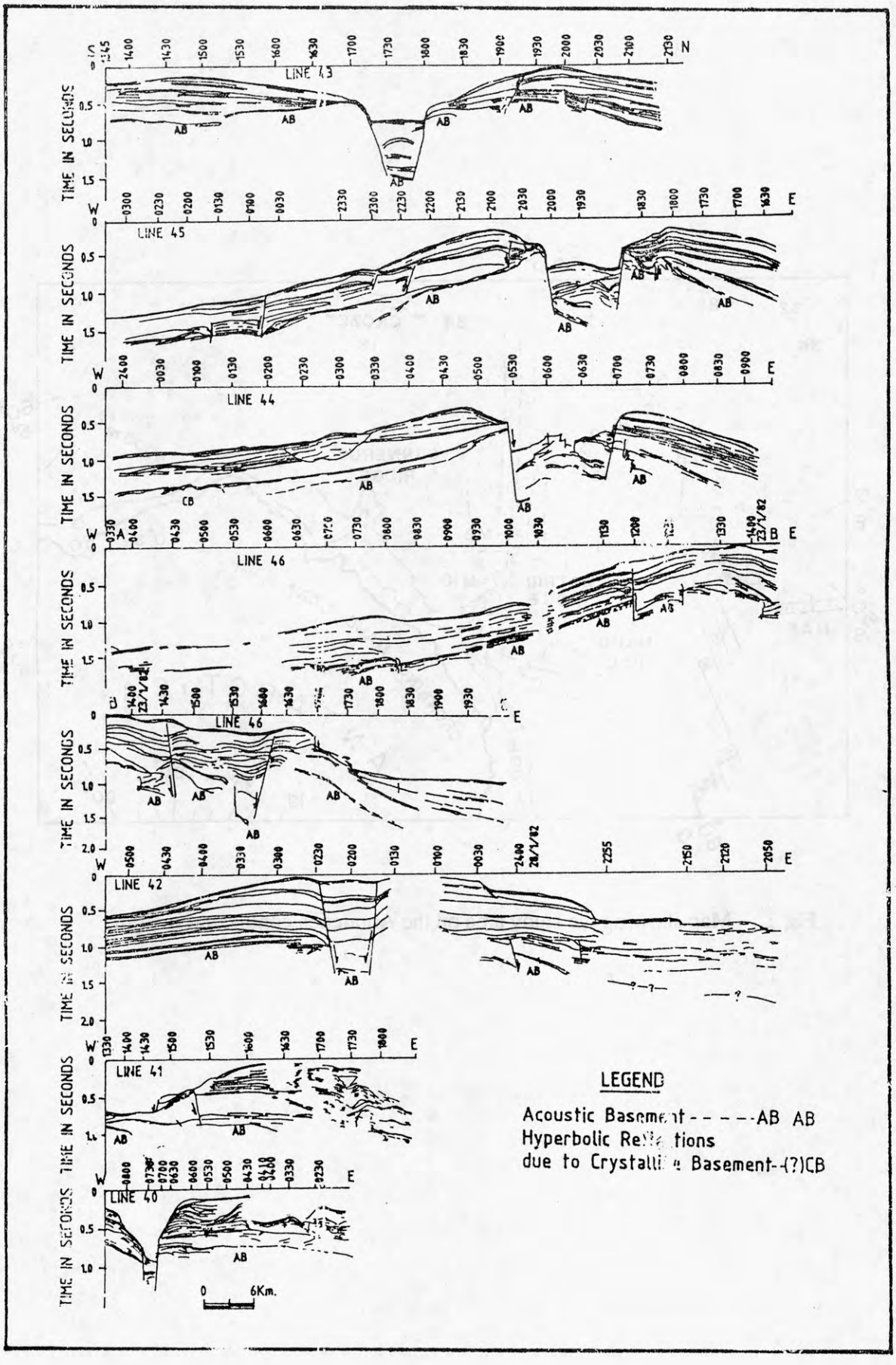

Fig 2. Interpreted seismic sections (24 kj sparker record) showing various geomorphic units within the sedimentary strata and acoustic basement.

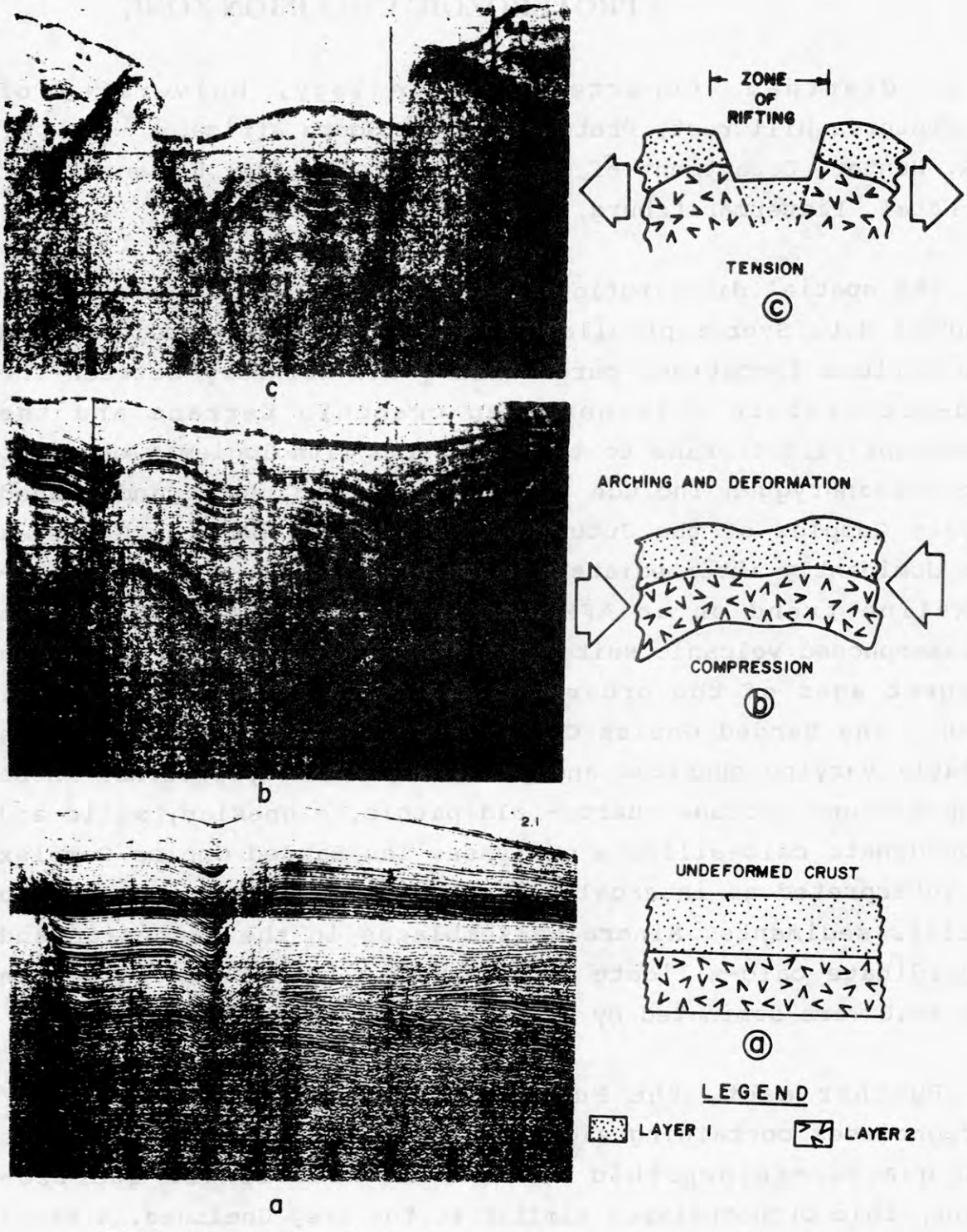

Fig 3. Shows selected seismic reflection records (two way travel time in seconds) of the Astrid Ridge in the study area and two layered conceptual models to explain mechanism of compression / extension. Seismic reflection records of line 42(6a), 46(6b) and and 45(6c) depict the deformed, intermittent to down faulted and down faulted (graban development) stages respectively.

THE GEOLOGY OF THE WESTERN AND CENTRAL H.U. SVERDRUPFJELLA,ANTARCTICA: A PROTEROZOIC COLLISION ZONE

G. H. Grantham, Department of Geology, University of Pretoria,Hillcrest, Pretoria, 0002, South Africa.
D.R. Hunter, Department of Geology, P.O. Box 375, University of Natal, Pietermaritzburg, 3200, South Africa .

The spatial distribution of lithologies in the western and central H.U. Sverdrupfjella show a lithological zonation with the various formations parallelling the boundary between the mid-Proterozoic Ahlmannryggen cratonic terrane and the Sverdrupfjella terrane to the east. The lithologies closest to the Ahlmannryggen include the Grey Gneiss Complex and Banded Gneiss Complex of the Jutulrora Formation. The Grey Gneisses are dominantly intermediate orthogneisses which define a calc-alkaline trend on an AFM plot and are interpreted as a metamorphosed volcanic suite. Preliminary Rb/Sr whole rock data suggest ages of the order of $\pm$ 1000 Ma (Moyes and Barton, 1990). The Banded Gneiss Complex is more heterogeneous with greatly varying chemical and mineralogical compositions. These compositions include quartz-feldspathic, magnesian, mafic and subordinate calc-silicate gneisses. The Banded Gneiss Complex is interpreted as intercalated meta-volcanics and arenitic to pelitic sediments. Mineral assemblages in the magnesian and subordinate calc-silicate rocks suggest that fluid phases in the west were dominated by H_2O.

Further east, the Fuglefjellet Formation comprises paragneisses containing significant proportions of carbonates and quartzo-feldspathic rocks with subordinate quartzo-feldspathic orthogneisses similar to the Grey Gneisses. Mineral assemblages are consistent with upper amphibolite facies metamorphism with a fluid phase containing significant CO_2. These lithologies are interpreted to represent a miogeosynclinal shelf-facies.

Further east, paragneisses dominated by quartz, feldspars and biotite and commonly containing sillimanite, form the

Sveabreen Formation. These paragneisses are interpreted to represent a eugeosynclinal facies consisting of metapelites and impure arenites. At Salknappen a porphyroclastic orthopyroxene-bearing granitoid is intercalated with the Sveabreen Formation paragneisses. The contact relationships are no longer preserved, having been sheared during D_2. Metamorphosed mafic boudins (gt + cpx + plag + hbl + qz bearing) in the Sveabreen Formation may represent intrusions or intercalated volcanics which have been dismembered during deformation.

The area exhibits a polyphase deformation history. D_1 appears to have involved tight isoclinal folding of a recumbent nature with axial planes dipping shallowly toward the south and south-east. D_2 involves folding of a similar nature to D_1 but in the east also involved large scale thrust faulting with rocks being overthrust toward the west from the south and southeast. An indication of the timing of D_2 is provided by a post-D_1 pre-D_2 mafic sheet (now amphibolite) which has yielded a poorly constrained isochron of 796$\pm$ 102 Ma, the large error resulting from the similarity of Rb/Sr ratios in the analyzed samples (Moyes and Barton, 1990). D_3 involves steep dipping thrust faults and associated folding. The thrust faults and axial planes of the folds dip steeply toward the northwest with fold axes plunging toward the northeast and southwest. The D_3 folds commonly have an axial planar foliation defined by biotite. The syn-D_3 emplacement of the Dalmatian Granite occurred at ~470Ma (Grantham et al, in press).

The paragneisses of the Sveabreen Formation are characterized by biotite + garnet + sillimanite with kyanite developed and partially replaced by sillimanite in the southerly areas. These relationships may supports the interpretation of a decompression regime or isothermal uplift for these lithologies. The assemblage (M_1?) garnet - clinopyroxene - plagioclase - hornblende - quartz preserved in mafic boudins in the paragneisses of the Sveabreen Formation display corona textures. In the textures amphibole + plagioclase symplectites separate garnet from a matrix mass assemblage of clinopyroxene + hornblende + quartz. The bulk

composition of the mafic rocks are comparable with compositions used by Green and Ringwood (1967) and the co-existence of garnet and clinopyroxene suggests M_1 pressures in excess of 10kb at 700°C. These pressures are confirmed by barometry on the assemblage clinopyroxene + plagioclase + quartz utilizing Ca-Tschermaks solubility in the pyroxene (Ellis, 1980) and the assemblage garnet + plagioclase + hornblende + quartz (Kohn and Spear, 1989) yields pressure estimates of 8-12kb (Fig. 1). The higher pressure estimates from the Kohn and Spear (1989) calibration are derived from core compositions whereas the lower estimates utilized rim compositions. Thermometry based on garnet + clinopyroxene and garnet + hornblende yields temperatures of approximately 750°C (Fig.1). The corona textures therefore suggest decompression.

Post M_2 assemblages in discordant, post D_2, garnet amphibolites from Dyna include garnet + hornblende + plagioclase + quartz. Garnet + hornblende thermometry yields temperatures of 600°C and garnet + hornblende + plagioclase + quartz barometry yields pressures of approximately 3-6kb (Fig. 1). These physical conditions are considered to represent post-D_2 conditions in the east. The preservation of orthopyroxene in the granitoid intrusions in the Sveabreen Formation rocks indicates that they are charnockitic in nature. At the temperatures indicated above, the co-existence of orthopyroxene + K feldspar suggests that the activity of H_2O in the fluid phase was $<<1$. The development of biotite axial planar to D_3 folds indicates that M_3 involved partial rehydration and associated mobility of K. The subsequent partial alteration of the sillimanite to muscovite provides further evidence of fluid and K mobility.

Structures displayed in the paragneisses of the Fuglefjellet Formation and Sveabreen Formations in the east indicate that the eugeosynclinal facies has been thrust-faulted over the miogeosynclinal facies to the west during D_2 and has been responsible for emplacing rocks, containing M_1 high-pressure assemblages, to higher crustal levels. In the east the P-T-t path for M_1-M_3 describes a typical isothermal decompression path in support of that recognized by Groenewald

and Hunter (1991) (Fig. 1).

In the west, high pressure assemblages are absent with M_1 temperatures of approximately 550°C based on thermometry on garnet + hornblende assemblages and biotite inclusions in garnet. Barometry using clinopyroxene + plagioclase + quartz suggests pressures of the order of 4-6kb with garnet + hornblende + plagioclase + quartz barometry yielding similar estimates (Fig.2). Garnet + hornblende thermometry on post M_1 (M_{2-3}?) amphibolite dykes yield slightly higher temperatures of the order of 600°C (Fig. 2). These slightly higher temperatures are supported by lenses of granitic leucosome in the Grey Gneisses of the Jutulrora Formation. These lenses are commonly oriented axial planar to D_2 folds and are commonly characterized by the presence of epidote. Significantly M_3 biotite + garnet thermometry suggests slightly higher temperatures as well (Fig. 2).

The genesis and emplacement of the water-saturated, two-mica Dalmatian Granite during D_3 at approximately 470Ma (Grantham et al, in press) suggests temperatures approaching 700°C and pressures of approximately 6kb. A P-T-t path for the western portion of the Sverdrupfjella therefore appears to define a clockwise prograde orientation and may possibly be the result of depression of the western areas to greater depths as a consequence of Pan-African or Ross Orogeny over-thrusting from the west (Fig. 2).

Rapid uplift in Dronning Maud Land followed as indicated by the deposition of the Urfjell Group in the Kirwanveggen in Lower Paleozoic times (Wolmarans and Kent, 1982) followed by the pre-Jurassic age basalts and associated dolerite dykes in the Kirwanveggen and H.U. Sverdrupfjella. The dolerite dykes intrude the 180Ma Straumsvola Alkaline Complex. Significantly, the dolerite dykes contain amygdales suggesting that they crystallized not far from surface. A rate of uplift from the end of D_3/M_3 to the deposition of the Urfell Group at approximately 300Ma is of the order of 105m per m.y.

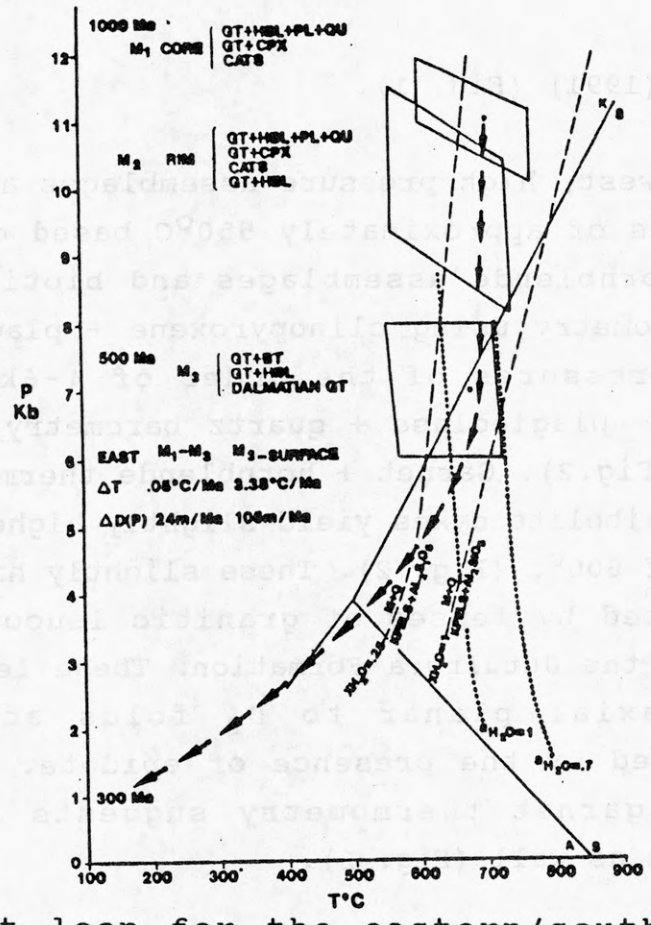

Figure 1. P-T-t loop for the eastern/southeastern Sverdrupfjella.

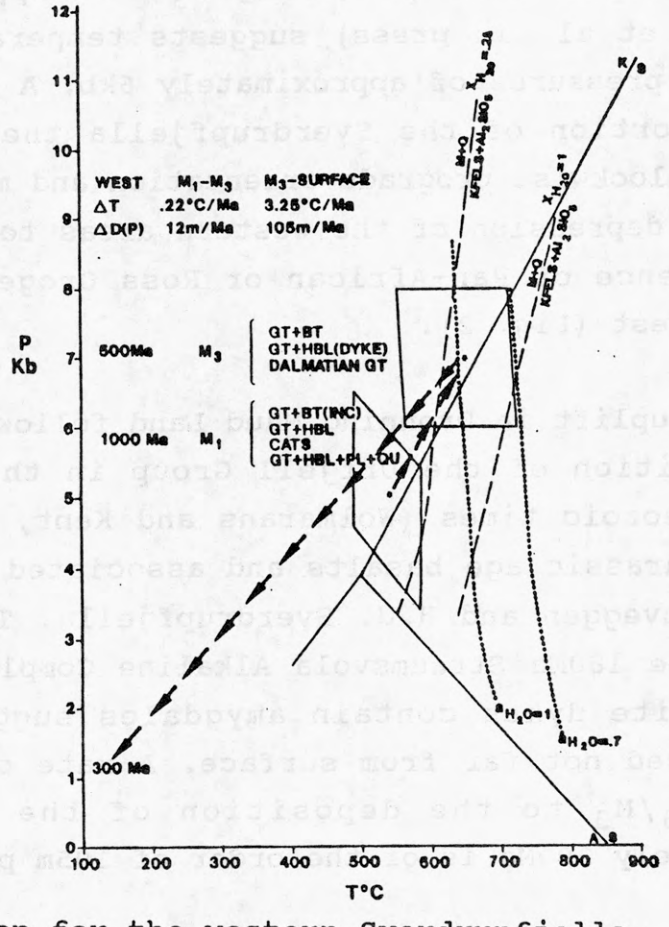

Figure 2. P-T-t loop for the western Sverdrupfjella.

REFERENCES

Ellis D.J. (1980) Osumilite-Sapphirine-Quartz Granulites from Enderby Land, Antarctica: P-T conditions of Metamorphism, implications for garnet-cordierite equilibria and the evolution of the deep crust. *Contrib. Mineral. Petrol.*, 74, 201-210.

Grantham, G.H., Moyes, A.B. and Hunter, D.R. (In press) The age, petrogenesis and emplacement of the Dalmatian Granite, H.U. Sverdrupfjella, Dronning Maud Land, Antarctica. *Antarctic Science*.

Green, D.H. and Ringwood, A.E. (1967) An experimental investigation of the gabbro to eclogite transformation and its petrological applications. *Geochim. Cosmochim. Acta*, 31, 767-833.

Groenewald, P.B. and Hunter D.R (1991). Granulites of northern Sverdrupfjella, western Dronning Maud Land : metamorphic history from garnet-pyroxene assemblages, coronas and rehydration reactions. In *Geological Evolution of Antarctica*. eds Thompson, M.R.A., Crame, J.A. and Thomson, J.W.,.pp 61-66. Cambridge: Cambridge University Press.

Kohn, M. J. and Spear, F.S. (1989) Empirical calibration of geobarometers for the assemblage garnet + hornblende + plagioclase + quartz. *Amer. Mineral.*, 74, 77-84.

Moyes, A.B. and Barton, J.M. (1990) A review of isotopic data from western Dronning Maud Land, Antarctica. *Zbl. Geol. Paläont.* Teil I. 19-31.

Wolmarans, L.G. and Kent, L.E. (1982). Geological investigations in western Dronning Maud Land, Antarctica - a synthesis. *S. Afr. J. Ant. Res.*, supplement 2. 93pps.

GEOCHRONOLOGIC DATA ON PROTEROZOIC POLYMETAMORPHIC ROCKS OF THE EASTERN SØR RONDANE MOUNTAINS, EAST ANTARCTICA

E.S. Grew, Department of Geological Sciences,
University of Maine, Orono, ME 04469, USA
W.I. Manton, Program in Geosciences, University of Texas
at Dallas, Richardson, TX 75083-0688, USA
M. Asami, Department of Geological Sciences,
College of Liberal Arts, Okayama University,
Tsushima-naka, Okayama 700, Japan
H. Makimoto, Geological Survey of Japan,
Higashi, Tsukuba 305, Japan

Migmatitic gneisses of the eastern Sør Rondane Mountains were first metamorphosed under upper amphibolite- to granulite-facies conditions, then, after a certain time interval, under amphibolite-facies conditions, and lastly, under greenschist-facies conditions. Four biotitic (Bt) granitic gneisses from the dominantly amphibolite-facies northern and central parts of the area and an orthopyroxene-bearing (Opx) dioritic gneiss from the dominantly granulite-facies southern part were analysed for U-Pb (zircon), Sm-Nd (whole rock), and Rb-Sr (whole rock, biotite, feldspar) isotopes. U-Pb data on two Bt gneisses lie on chords with intercepts 1095±51--340±230 Ma (MSWD=0.164) and 1180±120--533±120 Ma (0.524). The upper intercepts are interpreted to date the earliest metamorphic event, which soon followed original formation of the rocks dated by 990-1220 T_{DM} ages on two Bt gneisses and the Opx gneiss. However, a 2220 T_{DM} age on another Bt gneiss suggests considerable crustal evolution prior to metamorphism at some localities. Mineral Rb-Sr isochron ages on three Bt gneisses are 448-479 Ma and Bt ages on all four are 390-489 Ma. In contrast, the Bt age of the Opx gneiss is 622 Ma, suggesting that this rock was less affected by early Paleozoic resetting of the Rb-Sr system, which, most likely, corresponds to the second metamorphic event. This event is roughly coeval with plutonic activity in the northern Sør Rondane dated at 520 Ma with U-Pb isotopes in zircon (Pasteels and Michot,1968, Ann. Soc. Geol. Belg. 91(3), 283-303). The earliest event is probably the same as the granulite-facies event at Brattnipene (100 km to the west) dated at 1000 Ma with a Sm-Nd isochron on whole rock samples (Shiraishi and Kagami,1989, Proc, NIPR Symp. Antarctic Geosci., 3, 152). This event appears to be coeval with Late Proterozoic metamorphism in the Rayner complex of Enderby Land, Antarctica, and with the Kibaran orogeny in the Mozambique Province of southern Africa.

STRUCTURE AND EVOLUTION OF SEDIMENTARY BASINS IN THE WEDDELL PROVINCE

G.E. Grikurov, V.L. Ivanov, V.V. Traube, G.L. Leitchenkov, N.D. Aleshkova, A.V. Golynsky, R.G. Kurinin, North Branch for Marine Geologic Research and Exploration " SEVMORGEOLOGIA", 120 Moyka, 190121 LENINGRAD, USSR

The Weddell Province (WP) is defined as a complex structural junction between the South Atlantic oceanic opening(s) and the Transantarctic intraplate discordance. Its greater part is occupied by sedimentary basins linked together within a vast crustal depression which is unparalleled elsewhere in Antarctic plate in both the areal dimensions and the volume of sedimentary fill. The following basins are recognised: Jane Basin (JB), Powell Basin (PB), Larsen Basin (LB), Ronne-Filchner Basin (RFB), Explora Basin (EB) and Abyssal Plain Basin (APB). Positions of the basins in WP and locations of the seismic surveys are shown in Fig.1.

JB is underlain by the South Orkney microcontinent acoustic basement downfaulted to approximately 2 km subbottom depth between the shelf break and the shear-related Endurance Ridge (Fig.2a).

PB is a steep-sided bathymetric depression which represents an oceanic-type "window" in the South Scotia Ridge and is characterized by more than 2 km of sediments on a relatively flat acoustic basement resembling the second layer of oceanic crust (Fig.2b).

Back-arc LB underlies much of the Weddell Sea western shelf and slope. The first seismic data obtained by "SEVMORGEOLOGIA" in 1990 for the northern LB support the earlier USAC conclusions [LaBreque and Ghidella,in press], and the data indicate that as much as 9 km of sediments lie below the outer shelf. There is more than 5 km of sediments at almost 4000 m water depth (Fig.2c).

The evolution of shelf RFB where sedimentary cover may locally exceed 15 km in thickness is best explained in terms of extensional regime which dominated the southern WP lithosphere since at least late Paleozoic time (Fig.3). The pre-breakup phase is represented by paleorifts underlying the central RFB. Subsequent syn- and post-breakup events caused further stretching and lateral growth of continental margin which supported vigorous sag sedimentation. These processes presumably involved a detachment-fault mechanism providing for a very low-angle displacements in the upper lithosphere.

The slope/rise EB is underlain by a series of buried failed-rift grabens formed by extension and modification of ancient continental crust in connection with a major breakup event (Fig.4).

Scarce geophysical data available for APB indicate the presence within the 4000 m isobath of a substantial thickness (3-4 km) of sediments probably continuous with a similar sequence immediately seaward of Explora- Andenes Escarpment [Okuda et.al., 1983; Kudryavtzev et al., this volume] and/or post - breakup cover strata elsewhere in WP. We do not know whether APB is comparable to EB (and other basins discussed above) or whether APB it represents, in terms of basement evolution, an entirely different structural terrane related exclusively to post-breakup spreading processes.

REFERENCES:

Hinz K., Kristoffersen Y., 1987. Antarctica recent advances in the understanding of the continental shelf. Geol. Jb., E, H.37, 54 pp.

Kudryavtzev G.A., Butzenko V.V., Kadmina I.N. (this volume). Crustal section across the western Queen Maud Land continental margin from geophysical data.

LaBreque J.L., Ghidella M.E., 1991. Bathymetry, depth to magnetic basement and sediment thickness estimates from aerogeophysical data over the Western Weddell (in press).

Okuda Y., Yamazaki T., Sato S., Saki T., Oikawa N., 1983. Framework of the Weddell Basin inferred from the new geophysical and geological data.In: Nagata T., ed. Proc. Third Symp. Antarct. Geosci. Tokyo, NIPR, p. 93-114.

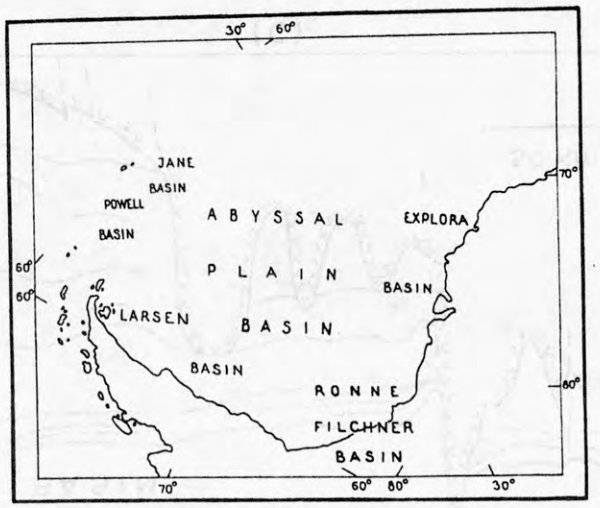

(a)

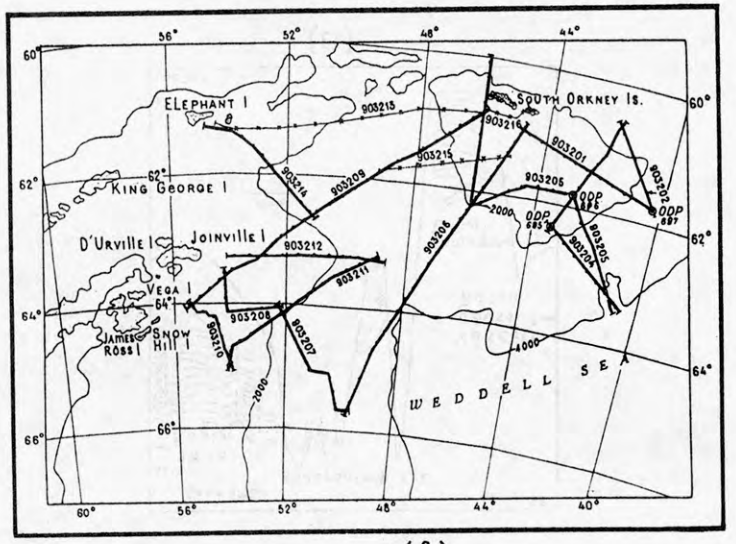

(b)

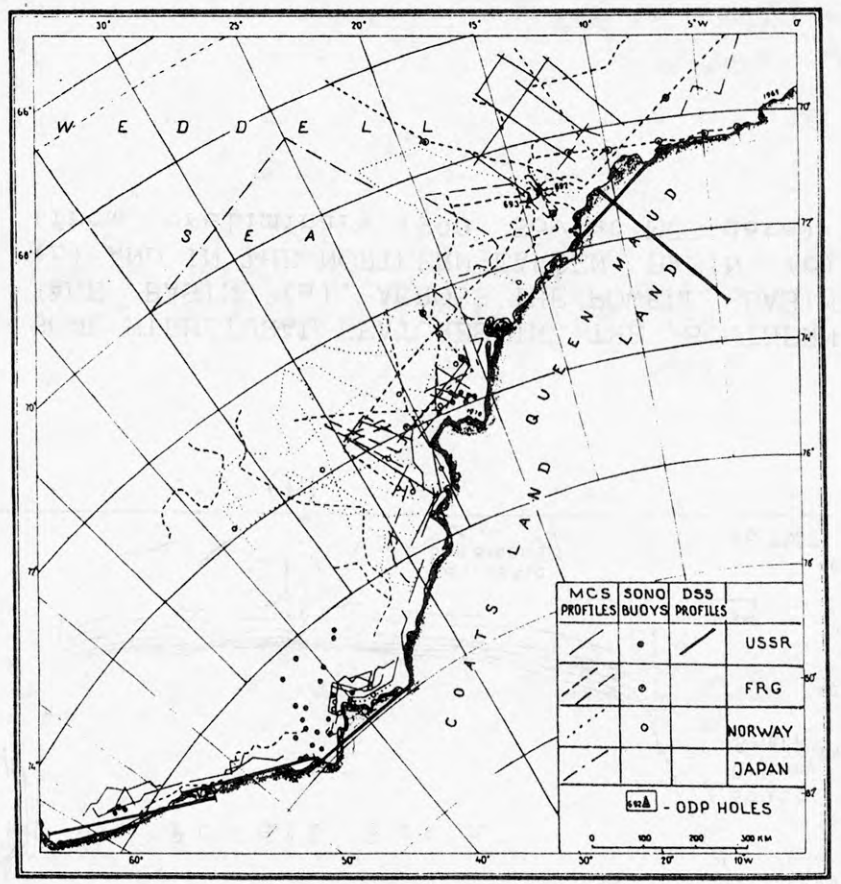

C)

Fig.1. POSITION OF SEDIMENTARY BASINS IN THE WEDDELL PROVINCE (a) AND LOCATION OF 1990 SOVIET MCS LINES IN THE NORTH-WESTERN WEDDELL SEA (b) AND MULTINATIONAL SEISMIC SURVEYS IN THE SOUTHERN AND NORTH-EASTERN WEDDELL SEA (c).

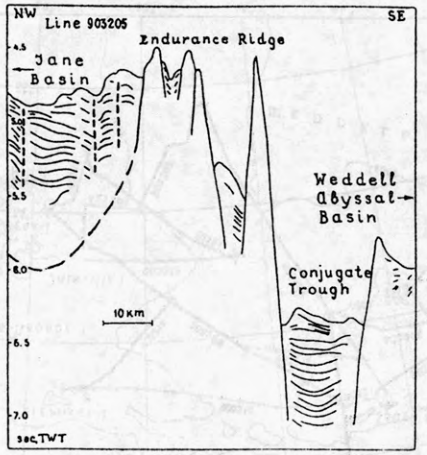

(a)

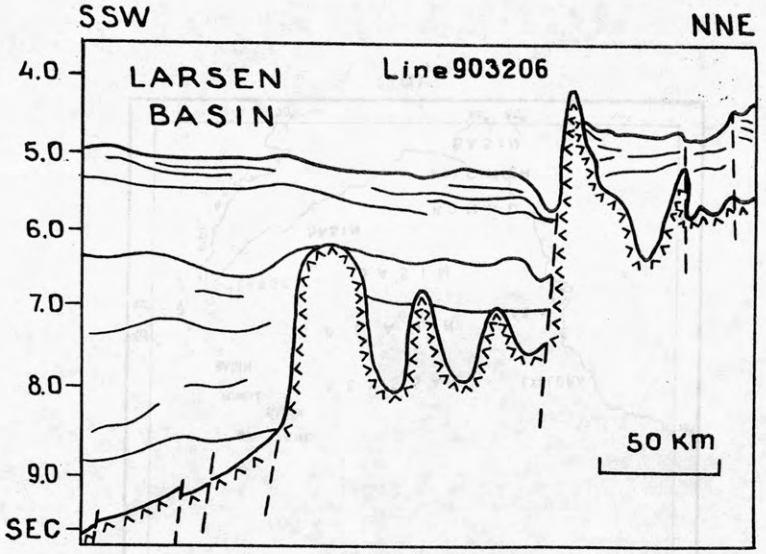

(C)

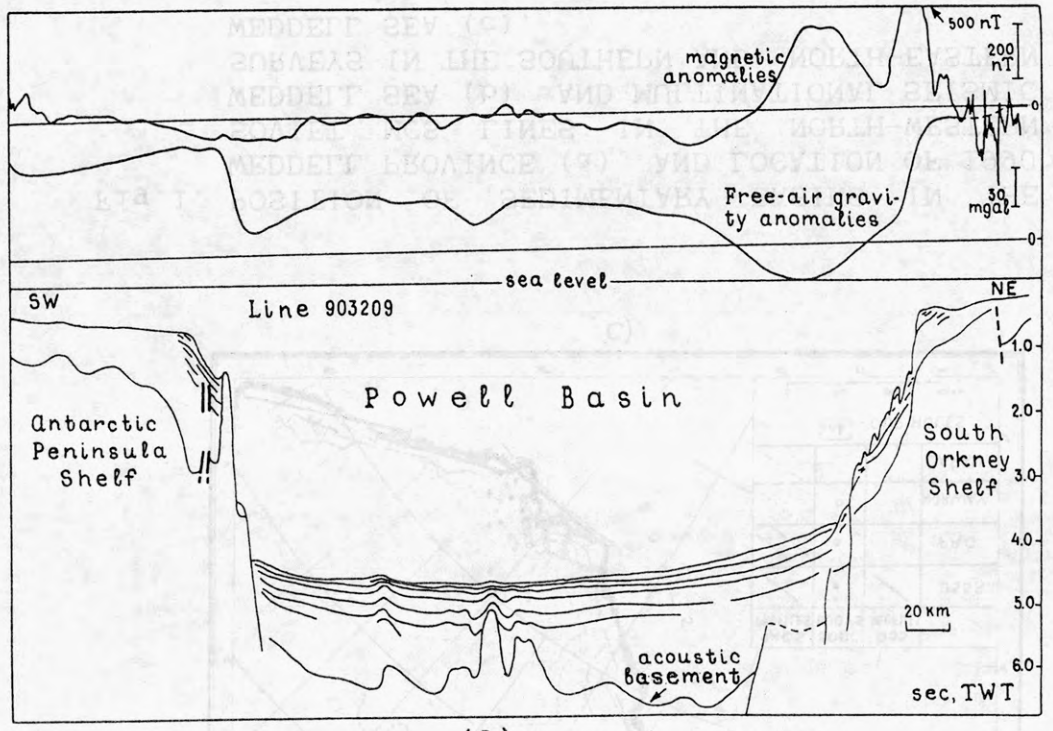

(b)

Fig.2. SOME STRUCTURAL FEATURES IN THE SOUTHERN JANE BASIN (a), ACROSS THE POWELL BASIN (b) AND IN THE NORTHERN LARSEN BASIN (c) (from preliminary 1990 Soviet MCS data).

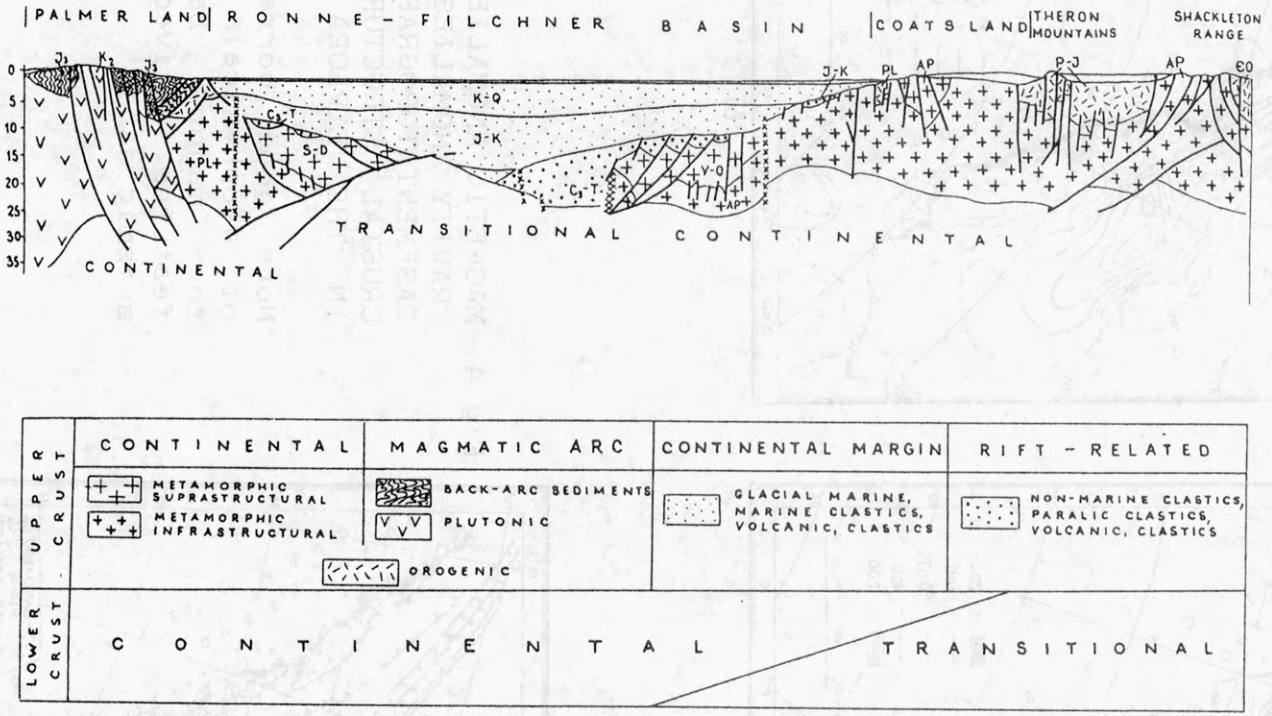

Fig.3 INTERPRETATIVE CRUSTAL SECTION
ACROSS THE RONNE-FILCHNER BASIN

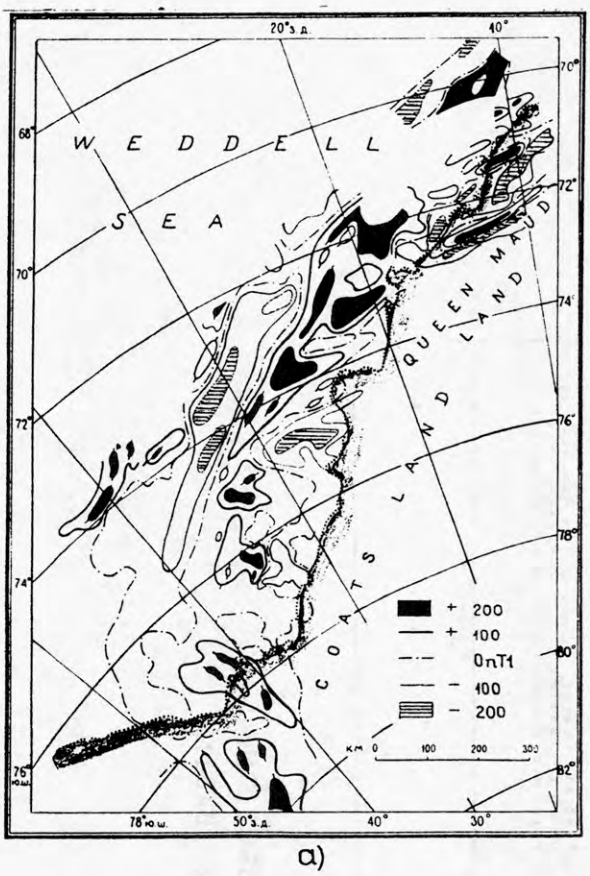

a)

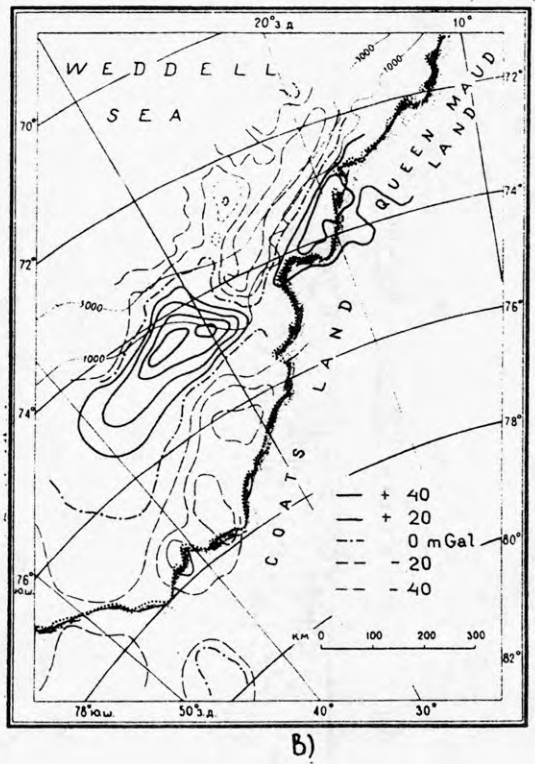

b)

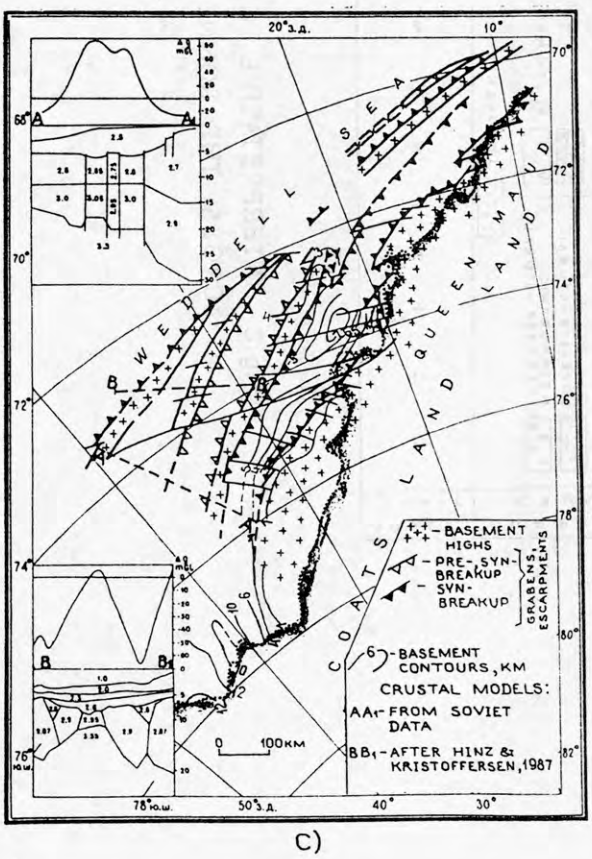

c)

Fig.4. MAGNETIC ANOMALIES (a), GRAVITY ANOMALIES (b), BASEMENT TOPOGRAPHY AND CRUSTAL STRUCTURE (c) IN THE EXPLORA BASIN.

Note good correlation of geophysical fields to major basement features derived from seismic data.

CRUSTAL PROVINCES IN THE SOUTHERN HIGH LATITUDES IN RELATION TO GONDWANA BREAKUP

G.E. Grikurov, R.G. Kurinin and A.V. Golynsky,
North Branch for Marine Geologic Research and Exploration "Sevmorgeologia",120 Moyka, 190121 Leningrad, USSR

On the basis of recent geodynamic models (Lister et al.,1986), global gravity and magnetic data (Segawa et al.,1984, Karasik et al., 1982), the paleotectonic history of Antarctic plate is presented in terms of increasing extension and transformation of primeval sialic lithosphere. It is believed that since the earliest stages of evolution this lithosphere has been affected by destructive tectonic processes which virtually led to disruption of Gondwanaland and isolation of the Antarctic continent in the middle of Southern high latitudes oceanic terranes (figure).

A subconcentrical distribution of major crustal types in Antarctic plate is clearly manifested in a continuous transition (away from the South Pole) from older continental to younger oceanic provinces. A prominent intraplate suture named the Transantarctic Discordance is evident between the Scotia Sea and Tasman Sea. This structural divide delineates a long-lived system of failed rifts which connects the West Pacific mobile belt and the Mid-Atlantic Ridge.

The present-day crustal mosaic in the Southern high latitudes is viewed as a complex juxtaposition of different lithospheric types forming a continuous evolutionary series. A primary sialic domain is represented by widely separated relics of ancient Gondwana supercontinent with predominantly pre-breakup crustal features only slightly affected by breakup -related events. Around these almost unaltered fragments there are vast extensional margins evolved by pre-, syn- and post-breakup stretching and thinning of primary continental crust. Such "metacontinental" crust normally still shows ensialic affinities but in places is modified beyond reliable recognition from a simatic ("orthooceanic") type evolved by spreading between separated extensional margins (table).

REFERENCES:

Karasik A.M., Desimon A.U., Pozdnyakova R.A., Sotchevanova N.A., Shreider A.A., 1982. Paleomagnetic anomalies in the World Ocean. In: Pushkov A.N., ed. Anomalies of geomagnetic field and crustal structure. Kiev, "Nauka" Publ. House, p. 99-101.

Lister G.S., Etheridge M.A., Symonds P.A., 1986. Detachment faulting and the evolution of passive continental margins. Geology, v. 14, no. 3, p. 246-250.

Segawa J., Matsumoto T., Kaminuma K. 1984. Free air gravity anomaly of Antarctic Region. NIPR Spec. Map. Ser. no. 3, Tokyo, Midorikawa Print. Co.

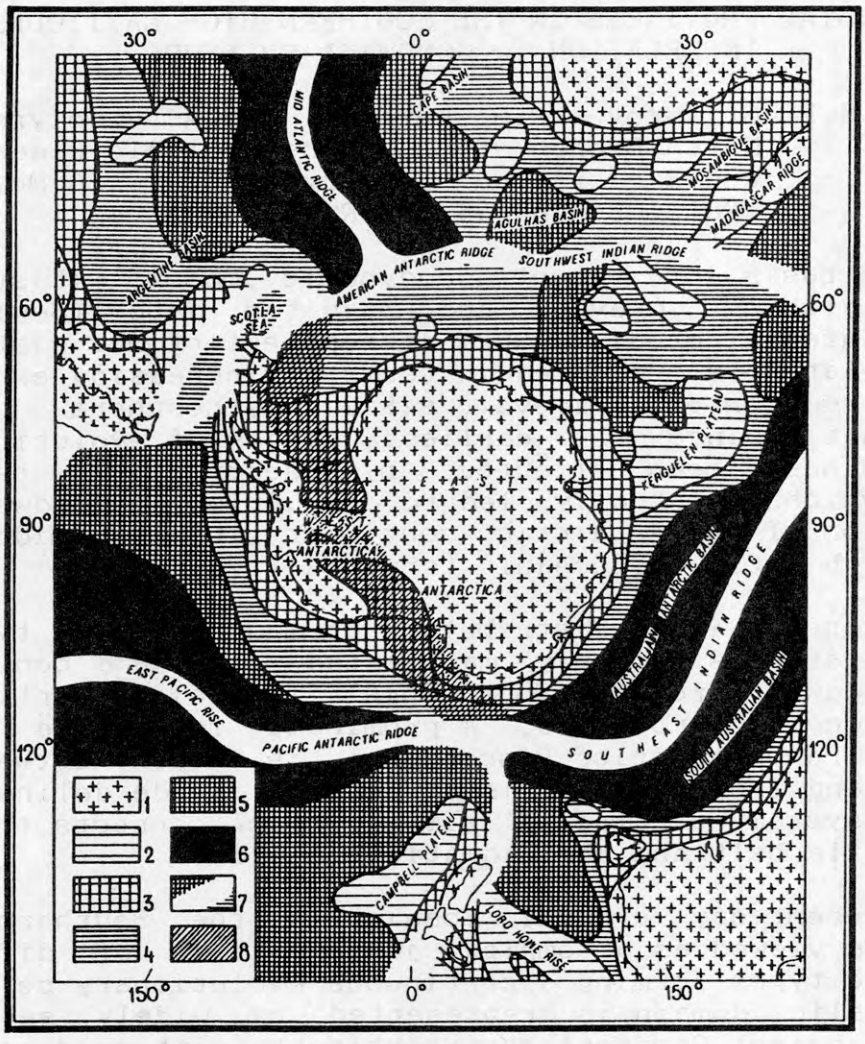

CRUSTAL PROVINCES IN THE SOUTHERN HIGH LATITUDES. 1 - continental (sialic) crust; 2-5 - metacontinental (reworked ensialic) crust: 2 - subcontinental "positive", 3 - subcontinental "negative", 4 - suboceanic, 5 - paraoceanic, 6 - intercontinental (simatic) orthooceanic crust; 7 - zones of high seismicity associated with oceanic ridges, island arcs and Andean-type active margins; 8 - Transantarctic Discordance.

CRUSTAL TYPES IN THE ANTARCTIC

TYPE	SUBTYPE	INTERNAL STRUCTURE	HYPSOMETRIC LEVEL	GRAVITY ANOMALIES	MAGNETIC ANOMALIES	MAGSAT ANOMALIES	CONVENTIONAL TECTONIC TERMS, DEFINITIONS, DESCRIPTION	PROPOSED MODEL OF EVOLUTION
CONTINENTAL		Mean thickness in excess of 30 km; "granitic" and "basaltic" layers well defined	Above and/or close to sea level	Linear to mosaic short wavelength large-amplitude highs and lows	Linear to mosaic short wavelength highs and lows	Highs and lows of considerable amplitude	Continental platforms, shields and basement inliers; fold belts related to metaplatform provinces and active margins	PRIMARY ENSIALIC DOMAIN: widely separated remains of Gondwanaland with predominantly ancient pre-breakup crustal features; breakup-related phenomena are restricted to active margins (orogenic shortening and associated crustal accretion) and intracontinental rifts (limited crustal extension and attenuation)
MARGINAL CONTINENTAL	SUBCONTINENTAL "POSITIVE" (+)	Thickness approximately 20km; "granitic" layer partly reduced	Isometric intra oceanic elevations of limited extent rising to 2 000-3 000m depths within abissal plains	Large-amplitude highs	Same as above, subdued	Same as above	Microcontinents, oceanic rises, oceanic plateaux, "oceanic lands", etc.	REWORKED ENSIALIC DOMAIN: vast extensional margins evolved around present-day Gondwana remnants by prolonged pre-, syn- and post-breakup stretching and thinning of primary continental crust which in places is modified beyond recognition from oceanic types
	SUBCONTINENTAL "NEGATIVE" (-)	Thickness less than 30 km; "granitic" layer substantially reduced; very thick sedimentary layer	Shelf, continental slope and upper continental rise	Mosaic to linear short wavelength highs and lows	Long-period highs and lows with subdued linear to mosaic fabric	Mainly large-amplitude lows	Passive margin basins : sediment-filled (on continental shelves), sediment-starved (on continental rise)	
	SUBOCEANIC	"Basaltic" layer c.10 km thick with fragments of "granitic" and sedimentary layers	Lower continental rise, abyssal plains and outer slopes of mid-oceanic ridges at 4 000-5 000 m depths	Mosaic short wavelength highs and lows	Indistinct long-period mosaic fabric and / or fragmentary, often randomly spaced linear features lacking definite correlation ("X" anomalies)	Low-amplitude anomalies	Distal parts of spreading zones, or zones of "diffuse", "disseminated", "rhomboidal", "scattered", "patchy", "irregular", etc. spreading; zones of "oceanization", "basification", etc.	
	? ? PA- ? RA- ? OCEA- ? NIC	Essentially "basaltic" layer less than 10 km thick	Abyssal plains and basins at c.5 000 m depth	Long-period low-amplitude anomalies	Semi-regular lineations of limited extent with inconsistent correlation (mainly anomalies 20-34)	Low-amplitude anomalies	? ? ?

METAMORPHIC EVOLUTION OF H.U. SVERDRUPFJELLA IN THE CONTEXT OF MAUDHEIM OROGENIC PROVINCE, WESTERN DRONNING MAUD LAND, ANTARCTICA.

P. Bruce Groenewald, Department of Geology, University of Natal, Pietermaritzburg, South Africa.

The H.U. Sverdrupfjella, Kirwanveggen and Heimefrontfjella areas in Western Dronning Maud Land constitute an orogenic belt termed the Maudheim Province. This is separated from the adjacent cratonic Grunehogna Province by the Jutulstraumen-Pencksokket rift zone, a distinct structural boundary representing major thrust- or transcurrent-faulting which was probably reactivated after the main orogeny. The three areas are correlated on the grounds of lithology and chronology, but metamorphic and orogenic histories require elucidation. Synthesis of available metamorphic data, principally those from H.U. Sverdrupfjella, provides some constraints on crustal evolution in the region. The early metamorphism (c. 1100 Ma, on the basis of dating of syn-orogenic granite) attained granulite facies conditions under which dehydration, anatectic melting and intense deformation took place. Locally, unfoliated mafic boudins have preserved high-pressure granulite facies assemblages (8 kb, 800°C), and kelyphitic reaction evidence for decompression. Most lithologies re-equilibrated at 6kb, 650°C, but later rehydration also occurred. The cooling path cannot be attributed entirely to the early orogeny, because major thrust faulting, although close in orientation to the early foliations, is locally transgressive to these and therefore postdates the main folding event. An estimate of 520 Ma for the age of thrusting is provided by a syn-kinematic alkaline granitic intrusion. The long interval requires separation of the events on the P-T-t path, if it is to aid inference of the tectonic setting.

The succession in the H.U. Sverdrupfjella has lithological characteristics of a marginal basin - volcanic arc sequence, and the early condition of high pressure metamorphism followed by decompression is characteristic of collision tectonics. Thus, the first orogeny is interpreted as having accreted a marginal basin and volcanic arc to the cratonic Grunehogna Province.

The second orogeny was initially extensional, as inferred from the alkaline/peralkaline magmatism. The pervasive rehydration and renewal of anatexis is attributed to thrusting of the granulites over lower grade metamorphites during compressional tectonism. The thrusting resulted in the interleaving of major units containing kyanite with those containing sillimanite. Generation of sillimanite in the kyanite-bearing rocks and the nature of the associated mylonites indicate that the thrusting occurred under high-temperature conditions. Lithostatic pressure was in the range 3-4 kb, and temperature > 500°C, implying a geothermal gradient of about 50°C/kilometer. The high temperatures during this time, and rapid cooling (shown by the passage through biotite isotopic blocking temperature at 475 Ma) are different in character from the early event. Crustal underplating, providing high heat flow, and uplift associated with extensive thrusting may be significant aspects of this orogeny.

High grade conditions have been reported from Kirwanveggen, but no P-T-t path is available. An early high grade event, followed by retrograde tectonothermal overprinting, has been reported in the Heimefrontfjella. These two stages were dated at c. 1100 and c. 500 Ma respectively, suggesting similar metamorphic histories throughout the Maudheim Province.

GEOLOGY OF H.U. SVERDRUPFJELLA, DRONNING MAUD LAND, ANTARCTICA

P. Bruce Groenewald, Department of Geology, University of Natal, Pietermaritzburg, South Africa.
G.H. Grantham, Department of Geology, University of Pretoria, Pretoria, South Africa.

H.U.Sverdrupfjella provides outcrop close to the western limit of East Antarctica, where this abuts on the cratonic Grunehogna Province. Recently completed mapping has identified a substantial lithological succession which underwent a complex magmatic, metamorphic and deformational history spanning the period from 1200 to 160 Ma. At the eastern limit of the N-S trending area, the lithologies are predominantly quartzofeldspathic, quartzose and pelitic paragneisses that host major bodies of porphyroclastic megacrystic granite. Along the western limit of the main range the most common lithologies are carbonates and intermediate gneisses. The outlying nunataks still further west consist predominantly of intermediate biotite-hornblende-plagioclase orthogneisses interlayered with banded paragneisses. The orthogneisses have the chemical characteristics of calc alkaline volcanics.

Granitic intrusions of several ages and diverse character are recognised in the area. Pre- or syn-tectonic granites are of typical orogenic compositions, with many characteristics of S- and I-type granites, and provide Rb-Sr ages of 1000-1200 Ma. The late syn-tectonic Brattskarvet intrusion, a large stratified alkalic granite body, yields a Rb-Sr age of 520 Ma. This was postdated by further S-type granitic magmatism, the emplacement of diorite on the western boundary of the area, and then by the intrusion of syenitic bodies and widespread mafic dyking.

The deformation of this succession began with intense isoclinal folding and foliation. This was followed by further folding and large scale thrust faulting directed northwestwards towards the cratonic province. The thrusting emplaced granulite facies lithologies at high structural levels, above an amphibolite facies sequence. The inverted metamorphic gradients are complex in that kyanite and sillimanite gneisses are extensively interleaved. Ages obtained from the granites allow discrimination between two major orogenies in the area. The earlier, 1000-1200 Ma, high-grade event was followed by another in the period 520-475 Ma, which was of lower pressure, but similar temperature. The first orogeny may have been accretionary, adding a marginal basin - volcanic arc succession to the craton through collision. The second was probably related to underplating by mantle-derived magmas. Cataclastic deformation, represented by normal faults with predominant ENE to E strikes, was tha last orogenic activity.

The Kirwanveggen and Heimefrontfjella lie to the west of H.U. Sverdrupfjella. The similarities in geological features suggest that they are correlates. It is proposed that the three ranges be combined to form the Maudheim Province. Current re-assemblies of Gondwana bring Dronning Maud Land into juxtaposition with southeastern Africa, which allows correlation of the orogenic Maudheim, Mozambique and Namaqua-Natal Provinces.

TECTONIC AND MORPHO-CLIMATIC ASPECTS AS CONDITIONING FACTORS IN THE GLACIO-MARINE SEDIMENTATION PROCESSES - ADMIRALTY BAY, KING GEORGE ISLAND, ANTARCTICA.

N.L.S. GRUBER & N.O. HORN FILHO
Centro de Estudos de Geologia Costeira e Oceânica
CECO/IG/UFRGS, P.O. BOX 15.009, Porto Alegre,RS ,
BRAZIL,91.500.

Results from the 3rd through 6th Brazilian Antarctic Expeditions (1985-1988) to Admiralty Bay, King George Island are presented. They include analysies from 88 sea floor samples and 23 water column samples, glacial characteristics and physiographic field observations and detailed studies of bottom morphology.

King George Island comprises several faulted blocks resulting from two main fault trends (ESE-WNW and NNE-SSW) that have produced a complex horst and graben topography. This has been emphasized by glacial excavation.

International literature mention the main trend faults related to generation process of island arc evolution history. Our studies regarding "bottom morphology" and "sedimentation patterns" suggest strong tectonic control over the subaerial and submarine physiography that affects the intensity degree of glacio-marine processes.

Under subpolar climatic conditions, this region is dominated by tidewater glacier processes. Specifically on Admiralty Bay we observated and identified in subaqueous and beach sectors, two main types of tidewater glaciers: outlet and piemont terminus.

From our studies we suggest four distinct glacier-fjord sedimentation systems: Martel Inlet, Mackellar Inlet, Ezcurra Inlet and Bay Channel.

Based on environmental characteristics observed, we suggest a glacio-estuarine model to explain its glacio-marine deposits patterns and circulation behavior of water masses into the fjord system. This model is constitued by a estuarine fjord glaciers dominated type.

Granulometric analysies of sea floor sediments were used to identify textural facies and infer depositional mechanisms:

Textural Facies	Depositional Mechanisms
Mud with sand and gravel	Grounded glacial ice
Sandy mud	Ice rafting and melt water flows
Muddy sand	Wave/current winnowed
Mud with gravel	Gravity flows; mass flows
Mud	Pelitic deposition; turbidity flows

These results provide a texturaly-based model for sedimentation in glacier-fed sub-polar fjords.

TECTONIC AND MORPHO-CLIMATIC ASPECTS AS CONDITIONING FACTORS IN THE GLACIO--MARINE SEDIMENTATION PROCESSES - ADMIRALTY BAY, KING GEORGE ISLAND, ANTARCTICA.

N.L.S. GRUBER & N.O. HORN FILHO
Centro de Estudos de Geologia Costeira e Oceânica
CECO/IG/UFRGS, P.O. BOX 15.009, Porto Alegre,RS ,
BRAZIL,91.500.

Results from the 3rd through 6th Brazilian Antarctic Expeditions (1985-1988) to Admiralty Bay, King George Island are presented. They include analysies from 88 sea floor samples and 23 water column samples, glacial characteristics and physiographic field observations and detailed studies of bottom morphology.

King George Island comprises several faulted blocks resulting from two main fault trends (ESE-WNW and NNE-SSW) that have produced a complex horst and graben topography. This has been emphasized by glacial excavation.

International literature mention the main trend faults related to generation process of island arc evolution history. Our studies regarding "bottom morphology" and "sedimentation patterns" suggest strong tectonic control over the subaerial and submarine physiography that affects the intensity degree of glacio-marine processes.

Under subpolar climatic conditions, this region is dominated by tidewater glacier processes. Specifically on Admiralty Bay we observated and identified in subaqueous and beach sectors, two main types of tidewater glaciers: outlet and piemont terminus.

From our studies we suggest four distinct glacier-fjord sedimentation systems: Martel Inlet, Mackellar Inlet, Ezcurra Inlet and Bay Channel.

Based on environmental characteristics observed, we suggest a glacio--estuarine model to explain its glacio-marine deposits patterns and circulation behavior of water masses into the fjord system. This model is constitued by a estuarine fjord glaciers dominated type.

Granulometric analysies of sea floor sediments were used to identify textural facies and infer depositional mechanisms:

Textural Facies	Depositional Mechanisms
Mud with sand and gravel	Grounded glacial ice
Sandy mud	Ice rafting and melt water flows
Muddy sand	Wave/current winnowed
Mud with gravel	Gravity flows; mass flows
Mud	Pelitic deposition; turbidity flows

These results provide a texturaly-based model for sedimentation in glacier-fed sub-polar fjords.

TECTONIC AND MORPHO-CLIMATIC ASPECTS AS CONDITIONING FACTORS IN THE GLACIO-MARINE SEDIMENTATION PROCESSES - ADMIRALTY BAY, KING GEORGE ISLAND, ANTARCTICA.

N.L.S. GRUBER & N.O. HORN FILHO
Centro de Estudos de Geologia Costeira e Oceânica
CECO/IG/UFRGS, P.O. BOX 15.009, Porto Alegre,RS ,
BRAZIL,91.500.

Results from the 3rd through 6th Brazilian Antarctic Expeditions (1985-1988) to Admiralty Bay, King George Island are presented. They include analysies from 88 sea floor samples and 23 water column samples, glacial characteristics and physiographic field observations and detailed studies of bottom morphology.

King George Island comprises several faulted blocks resulting from two main fault trends (ESE-WNW and NNE-SSW) that have produced a complex horst and graben topography. This has been emphasized by glacial excavation.

International literature mention the main trend faults related to generation process of island arc evolution history. Our studies regarding "bottom morphology" and "sedimentation patterns" suggest strong tectonic control over the subaerial and submarine physiography that affects the intensity degree of glacio-marine processes.

Under subpolar climatic conditions, this region is dominated by tidewater glacier processes. Specifically on Admiralty Bay we observated and identified in subaqueous and beach sectors, two main types of tidewater glaciers: outlet and piemont terminus.

From our studies we suggest four distinct glacier-fjord sedimentation systems: Martel Inlet, Mackellar Inlet, Ezcurra Inlet and Bay Channel.

Based on environmental characteristics observed, we suggest a glacio-estuarine model to explain its glacio-marine deposits patterns and circulation behavior of water masses into the fjord system. This model is constitued by a estuarine fjord glaciers dominated type.

Granulometric analysies of sea floor sediments were used to identify textural facies and infer depositional mechanisms:

Textural Facies	Depositional Mechanisms
Mud with sand and gravel	Grounded glacial ice
Sandy mud	Ice rafting and melt water flows
Muddy sand	Wave/current winnowed
Mud with gravel	Gravity flows; mass flows
Mud	Pelitic deposition; turbidity flows

These results provide a texturaly-based model for sedimentation in glacier-fed sub-polar fjords.

TECTONIC AND MORPHO-CLIMATIC ASPECTS AS CONDITIONING FACTORS IN THE GLACIO-MARINE SEDIMENTATION PROCESSES - ADMIRALTY BAY, KING GEORGE ISLAND, ANTARCTICA.

N.L.S. GRUBER & N.O. HORN FILHO
Centro de Estudos de Geologia Costeira e Oceânica
CECO/IG/UFRGS, P.O. BOX 15.009, Porto Alegre,RS ,
BRAZIL,91.500.

Results from the 3rd through 6th Brazilian Antarctic Expeditions (1985-1988) to Admiralty Bay, King George Island are presented. They include analysies from 88 sea floor samples and 23 water column samples, glacial characteristics and physiographic field observations and detailed studies of bottom morphology.

King George Island comprises several faulted blocks resulting from two main fault trends (ESE-WNW and NNE-SSW) that have produced a complex horst and graben topography. This has been emphasized by glacial excavation.

International literature mention the main trend faults related to generation process of island arc evolution history. Our studies regarding "bottom morphology" and "sedimentation patterns" suggest strong tectonic control over the subaerial and submarine physiography that affects the intensity degree of glacio-marine processes.

Under subpolar climatic conditions, this region is dominated by tidewater glacier processes. Specifically on Admiralty Bay we observated and identified in subaqueous and beach sectors, two main types of tidewater glaciers: outlet and piemont terminus.

From our studies we suggest four distinct glacier-fjord sedimentation systems: Martel Inlet, Mackellar Inlet, Ezcurra Inlet and Bay Channel.

Based on environmental characteristics observed, we suggest a glacio-estuarine model to explain its glacio-marine deposits patterns and circulation behavior of water masses into the fjord system. This model is constitued by a estuarine fjord glaciers dominated type.

Granulometric analysies of sea floor sediments were used to identify textural facies and infer depositional mechanisms:

Textural Facies	Depositional Mechanisms
Mud with sand and gravel	Grounded glacial ice
Sandy mud	Ice rafting and melt water flows
Muddy sand	Wave/current winnowed
Mud with gravel	Gravity flows; mass flows
Mud	Pelitic deposition; turbidity flows

These results provide a texturaly-based model for sedimentation in glacier-fed sub-polar fjords.

MESOZOIC TECTONIC EVOLUTION OF WEST ANTARCTICA: A SYNTHESIS OF NEW AND EXISTING PALEOMAGNETIC DATA

A.M. Grunow, Byrd Polar Research Center, 125 South Oval Mall, Ohio State University, Columbus, Ohio, 43210
I.W.D. Dalziel, Institute for Geophysics, Univ. of Texas at Austin, Austin, Texas 78759
D.V. Kent, Lamont-Doherty Geological Observatory, Palisades, New York, 10964

The position of West Antarctica with respect to cratonic East Antarctica prior to and after the Mesozoic break-up of Gondwanaland is critical to the opening history of the Weddell Sea and the paleoclimatic history of the region. Paleomagnetic and geologic data from Thurston Island (TI) and the Ellsworth-Whitmore Mountains (EWM) blocks in West Antarctica suggest that major rotation of the EWM and possibly the TI blocks occurred prior to the first formation of ocean floor associated with the disassembly of the supercontinent. We suggest that major rotation of the EWM block and the Falkland/Malvinas Islands in the Late Triassic to Middle Jurassic resulted from post-Gondwanide Orogeny reaccomodation of the continental crust along transcurrent shear zones.

The relative motion of three of the West Antarctic crustal blocks (the Antarctic Peninsula (AP); TI and EWM)) appears to be linked during the mid- to- Late Mesozoic to three major events in the evolution of the southern ocean basins:

Event 1 (~160 to 130 Ma)

Opening in the Mozambique-Somali -Weddell Sea ocean basins at < 160 Ma may have caused counterclockwise rotation of the TI block with respect to East Antarctica between the Jurassic and Early Cretaceous based on a new TI Late Jurassic pole (145°E, 64.5°S, A95=7°). The TI rotation, as well as the Palmer Land deformational event in the southern AP block, may have been caused by collision and shearing of the EWM block against the other two as the EWM block moved southward with East Antarctica.

Event 2 (~130 to ~110 Ma)

An Early Cretaceous paleomagnetic pole (232°E, 49°S, A95=7.9°) from the TI block requires that between the Early and mid- Cretaceous there was clockwise rotation with respect to East Antarctica, of the AP-TI-EWM block (an entity we call Weddellia). A change in the opening history of the Weddell Sea basin caused by initiation of speading in the South Atlantic ocean basin at ~130 Ma probably started Weddellia's clockwise rotation.

Event 3 (~110 Ma to ~90 Ma)

Two new ~110 and ~90 Ma poles from the TI block (210°E, 73°S, A95=7.6° and 161°E, 81°S, A95=4.9°, respectively) are similar to equivalent age poles from the AP block (Watts et al., 1984; Kellogg and Rowley, 1989) and East Antarctica and indicate that Weddellia was at or near its present day position with respect to East Antarctica by ~110 Ma. This corresponds to the time of a major plate reorganization in the South Atlantic and southeast Indian Oceans.

Based on previously reported paleomagnetic data from Marie Byrd Land (MBL) (Grindley and Oliver, 1983), dextral shearing would be expected to have occurred between MBL and Weddellia since the mid-Cretaceous. Pine Island Bay, the area between the TI and MBL blocks, marks a fundamental and complex tectonic boundary in West Antarctica that we propose has largely been a zone of trancurrent shearing.

Paleomagnetic samples from the EWM and TI blocks were collected as part of the joint US-UK West Antarctic Tectonics Project. We plan to incorporate new paleomagnetic data from the AP block obtained as part of Grunow's US Antarctic Peninsula Paleomagnetics Project.

AN OBS-LAND REFRACTION SEISMOLOGICAL EXPERIMENT IN THE BRANSFIELD TROUGH, WEST ANTARCTICA, 1990/1991

A. Guterch, Institute of Geophysics, Polish Academy of Sciences, Warsaw 01-452, POLAND,
H. Shimamura, Laboratory for Ocean Bottom Seismology, Hokkaido University, Sapporo 060, JAPAN
Polish-Japan-Argentina Research Group (Institute of Geophysics, Polish Academy of Sciences, Warsaw, POLAND; Laboratory for Ocean Bottom Seismology, Hokkaido University, Sapporo, JAPAN; Instituto Antartico Argentino, Buenos Aires, ARGENTINE)

The first detailed deep refraction seismological study in the Bransfield Strait, by the use of sensitive OBSs (Ocean Bottom Seismographs) and digital land seismographs was carried out successfully during the Polish Geodynamic Expedition to West Antarctica in Antarctic summer 1990/91. The experiment was a cooperation by Institute of Geophysics, Polish Academy of Sciences and Laboratory for Ocean Bottom Seismology, Hokkaido University, Japan, in collaboration with the Instituto Antartico Argentino, Argentine

The experiment was focused on the deep crustal and upper mantle structure beneath the Bransfield strait between the South Shetland Islands and the Antarctic Peninsula. Three refraction profiles, ranging with lengths from 180 to 250 km, were taken in the Bransfield Strait. Main profile was located exactly in the Bransfield Trough, which is suspected as a young rift system, where nobody has seen Moho. On the profiles 10 OBSs and 5 land digital refraction stations were deployed. Both OBS and land seismographs have threecomponents, with a wide dynamic range. All the deployed OBSs were recovered. The seismographs and shots were located by by GPS (Global Positioning System).

The distances between the OBSs , 40-50 km, and those of shots fired in the sea, 5 km in average, were short enough to obtain detailed structure. The records obtained by OBS and land seismographs were very clear, up to the distance of 250 km, or sometimes up to 350 km. The figure shows a record section of profile 20, obtained by an OBS on the bottom of Bransfield Trough, which shows clear onsets up to 240 km.

From Polish previous refraction works, made between 1979 and 1988, it

was known that the pattern of the seismic wave field and crustal structure of the Bransfield Trough are very complex and highly anomalous. Two seismic discontinuities had been found in the crust, about 7.0 km/s at 10-15 km depth, and about 7.5 km/s at 20-25 km depth, however no deeper structure, including Moho, had been found. With the present experiment, we have first seen Moho velocity, 8 km/s on the profile which is situated exactly in the Bransfield Trough.

From the refraction data from the present experiment, together with previous Polish refraction studies, we have succeeded to obtain structure of the Bransfield Trough as well as to construct 3-dimensional crustal model for transition zone from the South Shetland Islands to the Antarctic Peninsula across Bransfield Trough.

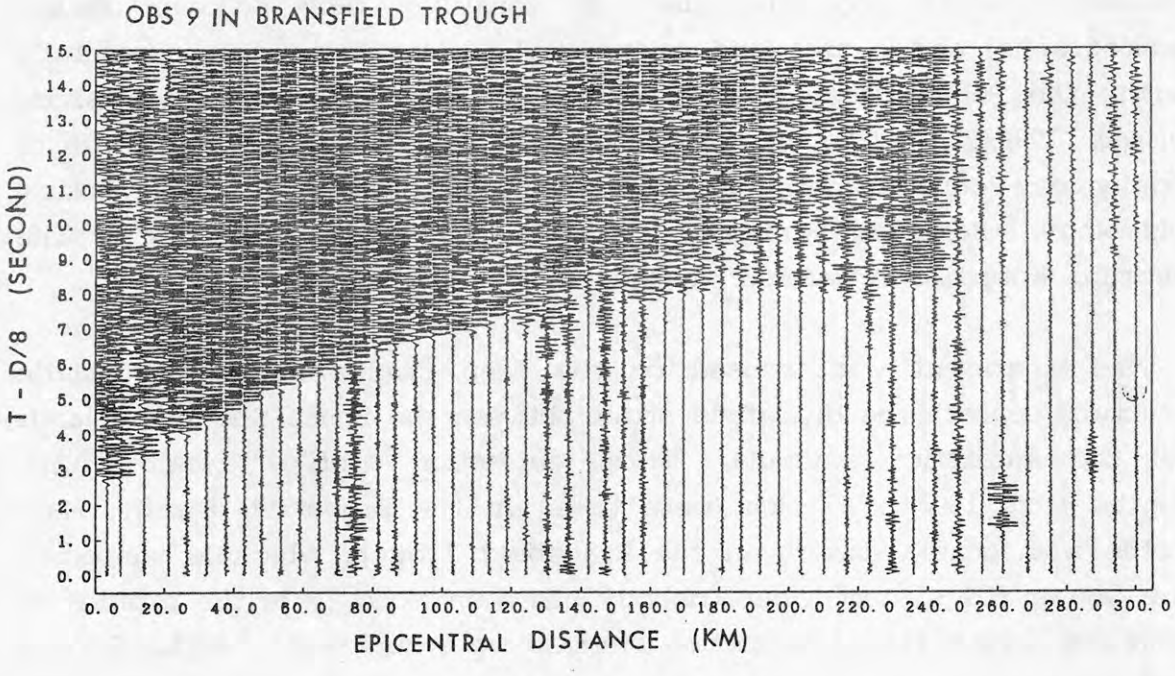

Figure explanation : An example of record section obtained in the present experiment. The record was obtained by the OBS9, which is on the southwestern end of the profile 20 which runs on the Bransfield Strait. Note that records up to 240 km were quite clear. The depth of the OBS9 was 530 m. The time axis is reduced by the wave velocity of 8 km/s. Seismograms of vertical component, with high gain amplification channel of the OBS, are shown. The seismograms were processed with a band-pass filter of 5-15 Hz. No correction for the seabottom topography was made in the picture. The amplitude of each seismogram was corrected by the square root of the epicentral distance.

MECHANICAL WEATHERING ON LIVINGSTON ISLAND, SOUTH SHETLAND ISLANDS, ANTARCTICA.

Kevin Hall,
Geography Department,
University of Natal,
Pietermaritzburg 3200,
South Africa.

Although mechanical weathering has been cited as operative in the Antarctic since the very first explorations of that continent and many researchers allocate one process or another to explain shattered bedrock, very little quantitative data with respect to weathering controls, processes or rates are actually available. In addition, most major texts usually only consider the Antarctic continent in any detail and the climatically different maritime Antarctic is all but ignored.

In order to obtain a broader view of weathering in the Antarctic, the British Antarctic Survey initiated a series of studies in the early 1980's on Signy Island (South Orkney Islands) as a representative maritime Antarctic location. As an extension of this project, work was undertaken during the 1990/91 austral summer close to the Antarctic Peninsula on Livingston Island. Although the climate of Livingston Island is still maritime Antarctic it has a different and more varied geology.

Unlike on most of the continent, the environment is one within which rocks may be subject to frequent wetting and drying cycles as well as summer freezing together with severe winter freezing, probable to a point below the eutectic temperature of NaCl with the consequent possible formation of a rock damaging cryohydrate. Thus the potential exists for wetting and drying, freeze-thaw and salt weathering to take place. In addition, strong radiation inputs on cloudless days also gives rise to the possibility of thermal stress fatigue.

Field data were collected on rock moisture content, rock temperatures and rock strength in order to evaluate and quantify the role of the various mechanical weathering processes. A summary of this background data will be presented together with a preliminary assessment of the weathering regime and its role in landscape development on Livingston Island.

CLAST SHAPE AND LITHOLOGY IN GLACIOMARINE SEDIMENTS OF THE WEDDELL AND LAZAREV SEAS AS AN INDICATOR OF GLACIAL TRANSPORT PATHS

M. J. Hambrey, Scott Polar Research Institute, University of Cambridge, Lensfield Road, Cambridge CB2 1ER, England.

G. Kuhn, M. Melles & W. U. Ehrmann, Alfred-Wegener-Institut für Polar- und Meeresforschung, Postfach 12 01 61, D-2850 Bremerhaven, Federal Republic of Germany

The gravel component in the marine sediments of the continental shelf, continental slope and ocaen basins around Antarctica is almost totally the result of transport by glacier ice: by grounded ice, ice shelves and ice tongues, and by icebergs. However, few systematic observations have previously been made linking the gravel component in Antarctic glaciomarine sediments to these specific glaciological settings.

The main aim of Leg ANT IX/3 of RV *Polarstern* during January to March 1991 inclusive was to visit the SW Weddell Sea, but severe ice conditions led to a change of programme. Instead, sedimentological studies were undertaken in both shallow and deep seas around more than 1500 km of the Antarctic margin bordering the eastern Weddell Sea and the Lazarev Sea as far as 12°E. In addition, onshore observations were made in ice-marginal areas at Schirmacher Oasis. Gravel clasts were examined at approximately 40 sites, and nearly 3000 clasts were measured for roundness, Zingg shape and Krumbein sphericity. Surface characteristics, such as facetting, striations and other specific glacigenic shapes were recorded, as well as lithology.

Although we sampled each glaciological setting several times, no systematic differences in clast shape can be detected; the variation in shape for a particular setting is greater than that between different settings. In particular, we find no sign of increased angularity of clasts as one moves offshore, as has previously been argued on the basis of a much smaller data-set.

Comparisons with previous work indicates that most clasts in marine sediments fall within the basal transport zone defined by G. S. Boulton in 1978 for temperate glaciers. However, compacted diamictons beneath the surficial sediments, which are believed to be Pleistocene lodgement tills, fall within the same field, but not within Boulton's lodgement till field. We believe, therefore, that the thermal regime of the Antarctic glaciers is such that abrasion of clasts at the ice-bed interface is less important than in temperate regions. This hypothesis is confirmed by the similarity of shape with debris from basal ice and sandy basal tills at Schirmacher Oasis. Exceptions to the general shape pattern occur in gravel off grounded ice margins in Coats Land. In these more southerly latitudes (76°30'S), debris supplied to the continental shelf is more angular, and falls within the rock-fall field. However, there are no nunataks inland to supply such debris. We provisionally propose that the angular debris is derived as a result of rock fracturing at a relatively dry, frozen bed.

Studies of surface features on clasts indicate that more than half, and sometimes nearly all, the clasts are facetted. Examination of clasts of different lithology, indicate that facetting, roundness and sphericity are independent of lithology. In contrast, striae on clasts are very much lithology-dependent: few gneissic clasts have striae, but nearly half the clasts of fine grained basic igneous or metavolcanic rocks are striated.

Lithological studies on clasts indicate that each area has a distinct population of rock types of limited variety, suggesting that deposition is predominantly from the nearest land ice source, and that mixing of sediment with that from far-travelled icebergs is unimportant. This confirms the belief of some glaciologists that most sediment is released by icebergs close to their source, and that debris is confined predominantly to the basal ice zone.

NEW FOSSIL VERTEBRATES FROM THE FREMOUW AND FALLA FORMATIONS BEARDMORE GLACIER REGION, ANTARCTICA

William R. Hammer
Department of Geology
Augustana College
Rock Island, Illinois 61201 USA

During the 1990-91 austral summer vertebrate fossils representing several new taxa were collected in the Beardmore Glacier region of the Transantarctic Mountains. Included are new genera of therapsid reptiles and temnospondyl amphibians from the late Early to early Middle Triassic upper Fremouw Formation of the Gordon Valley and portions of at least two dinosaurs from the Upper Falla Formation on Mt. Kirkpatrick. While the Fremouw specimens represent additions to a fauna first discovered in 1985-86, the Kirkpatrick specimens represent both the first record of dinosaurs from the Antarctic mainland and the first vertebrates of any kind from the Falla Formation.

The upper Fremouw Formation produced approximately 100 specimens from two sites in the Gordon Valley. The previously known taxa from the upper Fremouw include a large kannemeyeriid dicynodont, the cynodonts Cynognathus (also occurs in South Africa and South America) and Acrognathus (endemic to Antarctica), the gomphodont Crymodon (endemic to Antarctica) and two or three large capitosaurid temnospondyls. While additional specimens of these fairly large animals were found, it is interesting to note that some of the new material represents smaller animals, including smaller dicynodonts and temnospondyls. All of the Gordon Valley material occurs in a coarse channel-form sandstone with large intraclasts. The fossils are largely fragmentary, but a variety of elements occur including many cranial pieces, limbs, and large temnospondyl clavicles.

The specimens collected from the Falla Formation are more complete and occur in a low energy, fine-grained deposit. Most of the bones come from one localized area of exposure. This concentration of bones appears to contain much of the skeleton of one medium-sized herbivore (possibly a prosauropod). Included are the skull, lower jaw, several limb bones, vertebrae, ribs and a scapula. In addition, the lone tooth of a carnivorous theropod was found associated with the disarticulated skeleton. This tooth was probably broken off as the carnivore attacked or scavenged the other animal. Three additional isolated bones were collected from the same general area, two of them could possibly belong to the above individual, but one represents a much smaller animal.

This level of the Falla Formation provisionally is considered to be Late Triassic to Early Jurassic in age, depending upon exactly what type of dinosaur the skeleton represents. Whatever the age, these are both the first dinosaurs of any type and the youngest vertebrates known from the Transantarctic Mountains and the Antarctic mainland.

New Geological and Geochemical Data from Nelson Island, South Shetland Islands, Antarctica

M. A. F. Hansen, H. C. Fensterseifer, F. L. Troian and J. Beckel,
Geology Department, University of Vale do Rio dos Sinos-UNISINOS, Av. Unisinos, 950, 93.020, Sao Leopoldo, RS, Brazil.

This poster session reports the results of a field work carried out at the South Shetland Islands (Nelson Island - Stansbury Peninsula, O'Cain, Miró, Duthoit, Ross, The Toe and Harmony points) during 1985 and 1986/87 summer.

The field work was supported by the Brazilian Antarctic Programme.

The studied area is composed by interlayered volcanic, volcaniclastic and intrusive rocks.

The volcanic rocks and associated intrusives are low-K (0.13-2.4 %), calc-alkaline to tholeiitic, subalkaline basaltic andesites, basalts, dacites and dolerites of intermediate to basic composition.

The Zr, Ti, Sr contents of the calc-alkaline volcanics indicate an island arc tectonic setting for these rocks.

MAGNESIAN METAPELITES FROM THE RAUER GROUP, PRYDZ BAY: 1000°C METAMORPHISM AND HIGH-TEMPERATURE DECOMPRESSION IN A REWORKED GRANULITE TERRAIN.

S.L. Harley, Geology & Geophysics, Kings Buildings, University of Edinburgh, Scotland, EH9 3JW.

Unusual magnesian metapelites preserving assemblages and mineral compositions indicative of anomalously high pressure-temperature (P-T) metamorphic conditions occur as rafts and discontinuous layers within felsic orthogneisses at Long Point in the Rauer Group. The host gneisses, which are dissected by deformed metabasic dykes, are correlated with tonalitic orthogneisses yielding Archaean (3300 and 2830 Ma) zircon U-Pb ages (Kinny & Black, 1990) and form part of an extensive block of reworked Archaean granulites which outcrops in the NE Rauer Group.

Quartz-bearing migmatitic metapelites contain highly magnesian garnet (X_{Mg} (Mg/Mg+Fe) = 0.57-0.59) coexisting with sillimanite and feldspar and indicate minimum equilibration pressures of 10 kbar at 1000°C. A quartz-deficient, migmatitic metapelite contains orthopyroxene (X_{Mg} = 0.80; Al_2O_3 = 8 wt %) -mesoperthite-antiperthite veins produced by in-situ anatexis. The gneissose paleosome in this sample preserves initial garnet-orthopyroxene-sillimanite assemblages featuring the most pyropic garnets yet reported (X_{Mg} = 0.69-0.72) coexisting with orthopyroxene (X_{Mg} = 0.80; Al_2O_3 = 9.5 wt %) in granulites. Calculated metamorphic P-T conditions are 10-13 kbar and 1000-1050°C.

Symplectite and corona textures involving the formation of cordierite (Crd), sapphirine (Spr) and spinel (Spl) from garnet (Grt) with or without orthopyroxene (Opx) and sillimanite (Sil), indicate a P-T history involving post-peak near-isothermal decompression at high-T. The Mg/Mg+Fe (X_{Mg}) ratio of reactant garnet exerts a major control on the phase assemblage produced on garnet breakdown through decompression, as many of the relevant equilibria have shallow dP/dT slopes.

The most magnesian garnets (X_{Mg} = 0.70) in quartz-absent samples break down on decompression through c. 11 kbar (at c. 950 °C) to form graphic intergrowths of orthopyroxene +sillimanite+sapphirine, via the FMAS divariant reaction:

$$Grt = Opx + Sil + Spr \quad (1).$$

The related garnet-absent reaction:

$$Opx + Sil = Spr + Crd \quad (2),$$

is responsible for the generation of sapphirine-cordierite symplectites and overgrowths within orthopyroxene-sillimanite layers in the same samples. Garnets with lower X_{Mg} (0.65-0.58) are stable to lower pressures on the same decompressional path, and breakdown to yield bladed, graphic, and leaf-like symplectites of orthopyroxene+sapphirine and coarser areas of cordierite, explained by the divariant reaction:

$$Grt = Opx + Spr + Crd \quad (3),$$

which occurs at progressively lower P for garnets with lower X_{Mg}.

Decompressional reaction textures developed between garnet and sillimanite also display systematic differences dependent on the garnet X_{Mg}. Magnesian garnet (X_{Mg} = 0.55-0.60) reacts with sillimanite to yield sapphirine+cordierite intergrowths via the reaction:

$$Grt + Sil = Spr + Crd \quad (4)$$

at higher pressures than the breakdown of Fe-richer garnets (X_{Mg} = 0.48-0.38), which occurs through the alternative reaction:

$$Grt + Sil = Spl + Crd \quad (5)$$

at pressures of only 8-6 kbar.

All these textures and reactions can be generated on a single decompressional P-T path, but at different points or segments along it (figure 1). This P-T path traverses from c. 12-13 kbar to 8 kbar at temperatures in the range 900-1000°C (figure 2). The initial high-T metamorphism and decompressional P-T path recorded as relics in these metapelites are

considered to be responses to magmatic accretion and crustal overthickening in Archaean tectonic events, and are unrelated to the c. 1000 Ma Proterozoic granulite metamorphism documented in the Rauer Group (Harley, 1988). Reworking of these older granulites in this younger metamorphism is manifested in the development of overprinting biotite fabrics and subsequent formation of Crd+Opx symplectites on further decompression from 7-8 kbar to 4-5 kbar at 700-800°C (figure 2).

References:
Harley, S.L., 1988. *J. Petrol.* **29**, 1059-95.
Kinny, P.D. & Black, L.P., 1990. *Abs. Geol. Soc. Aust.* **25**, 251-52.

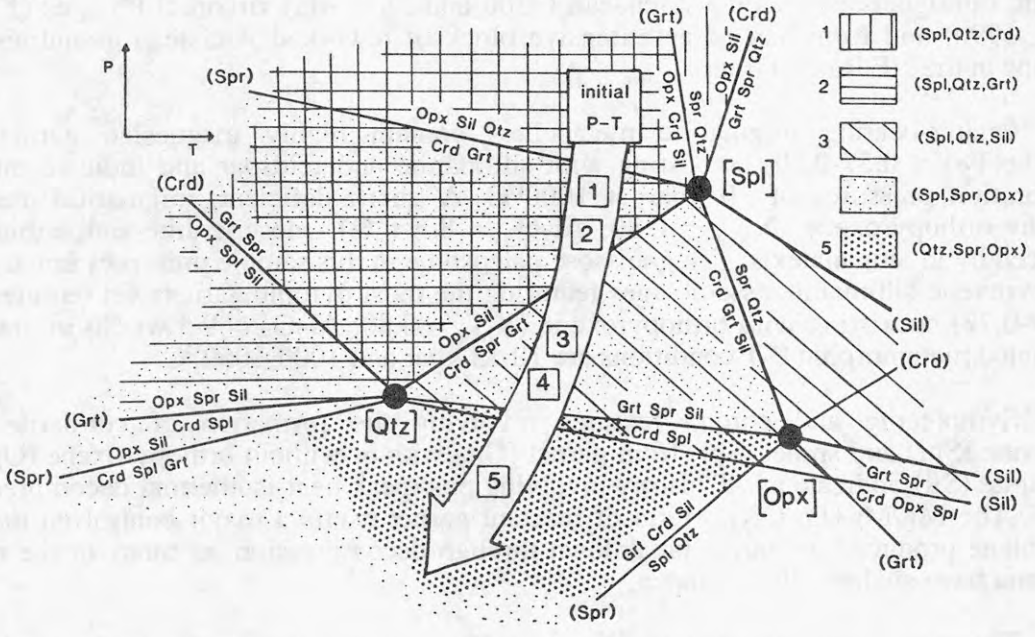

Figure 1: Schreinemakers grid showing high-T reactions between the FMAS phases Grt, Opx, Spr, Crd, Qtz, Sil and Spl and the sense of P-T change indicated by the observed reactions (large arrowed path). Numbers in squares correspond to the FMAS divariant reactions noted in the text, also indicated as fields labelled using absent-phase notation in the key.

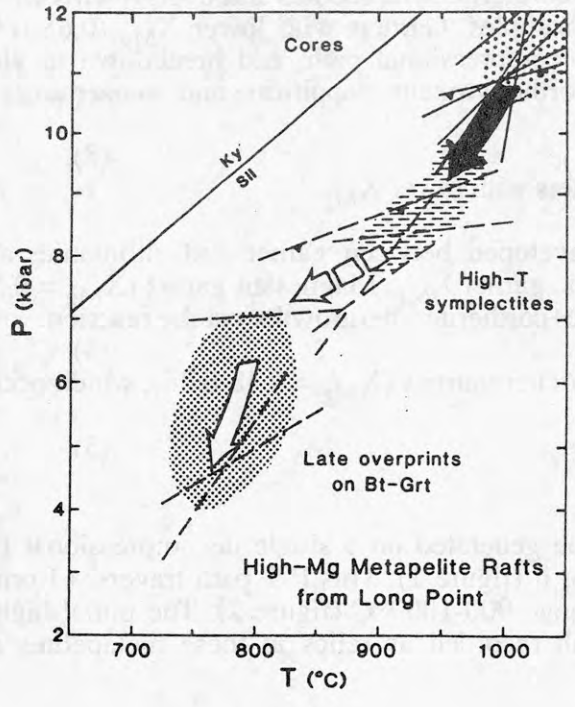

Figure 2: P-T estimates for the high-T decompressional path (filled arrows) and later overprint (open arrow) on the Long Point metapelites. Estimates (dashed and barred lines) are based on a range of geothermobarometers, and define the shaded P-T areas related to peak conditions (large dots), initial high-T decompression (dashes) and later, 1000 Ma, overprints (small dots).

WOLLASTONITE-SCAPOLITE CALC-SILICATE GRANULITES FROM THE RAUER GROUP: IMPLICATIONS FOR P-T-FLUID HISTORIES.

S.L. Harley, Geology & Geophysics, Kings Buildings, University of Edinburgh, Scotland, EH9 3JW.
I.S. Buick, Department of Geology, University of Melbourne, Parkville, Victoria, Australia 3052.

Granulite facies calc-silicates from the Rauer Group, East Antarctica, contain grossular+wollastonite+scapolite+ clinopyroxene assemblages, with either quartz or calcite (figure 1), which preserve spectacular symplectite and corona textures often involving the growth of secondary wollastonite:

(1) wollastonite-scapolite-clinopyroxene symplectites replacing grossular;

(2) wollastonite-plagioclase symplectites replacing grossular or the earlier symplectites involving wollastonite and scapolite, (1);

(3) wollastonite-plagioclase rims and intergrowths between quartz and scapolite; and,

(4) wollastonite rims between quartz and calcite.

Only in domains lacking wollastonite and quartz is the breakdown of scapolite to symplectitic plagioclase-calcite seen.

Calculated mineral reactions between the phases garnet (Grs), scapolite (Scp), wollastonite (Wo), calcite (Cc), quartz (Qtz), plagioclase (An) and vapour (V) in the $CASHCO_2$ system show that *these textures are indicative of near-isothermal decompression (ITD)* at 800-850 ^{o}C, and in this case imply a decrease in P from 8 to 6 kbar, consistent with P-T paths determined from textural and thermobarometric studies of other rock types in the Rauer Group.

The reaction topologies have been calculated and adjusted for activity-composition relations for Ca-end members in calc-silicate garnets (Grs) and scapolites using the dataset of Holland & Powell (1990). The resulting P-T (vapour-absent), T-a_{CO2} and P-a_{CO2} (figure 2) grids show that important reactions limiting the stability of scapolite+wollastonite paradoxically involve *carbonation* with increasing T, rather than decarbonation. For example, texture (1) is considered to be the result of the high-T carbonation reaction (labelled using absent-phase notation):

$$3Grs + 2Qtz + CO_2 = Scp + 5Wo \qquad (An,Cc)$$

progressing with increasing T, or on decompression, at 8-7 kbar, 820-850 ^{o}C, and a_{CO2} of 0.40-0.48. Texture (3) is consistent with progress of the the decarbonation reaction:

$$Scp + Qtz = Wo + 3An + CO_2 \qquad (Cc,Grs)$$

from left to right with increasing T, or decompression, at similar T-a_{CO2} conditions but slightly lower pressures (6.5 kbar).

Localisation of the reaction textures, systematic variations in modal proportions of product phases (e.g. wollastonite : clinopyroxene) in relation to initial grossular composition, and a clear relation between reaction progress and mineral composition, preclude open system behaviour or the involvement of an external fluid phase in the generation of these reaction textures. The vapour-absent reactions

$$3Grs + Cc + 3Qtz = 6Wo + Scp \qquad (An,V)$$

and

$$Grs + Qtz = 2Wo + An \qquad (Scp,Cc,V),$$

are inferred to have produced textures (1) and (2) respectively, at ca. 7.5 kbar 850^{o}C and under low a_{CO2} conditions (0.4-0.5). The occurrence of orthopyroxene+ Kfeldspar+plagioclase assemblages adjacent to these calcsilicates is consistent with this vapour-absent P-T evolution.

The broader implications of the occurrence of carbonation with increasing temperature, and liberation of CO_2 on cooling, in such calc-silicate granulites are discussed. For example, post-metamorphic CO_2-rich fluid inclusions reported from some granulite

terrains may be produced by fluids released during cooling of volumetrically important scapolite calc-silicates.

Reference:
Holland, T.J.B. & Powell, R., 1990. *J. Metamorphic Geol.* 8, 89-124.

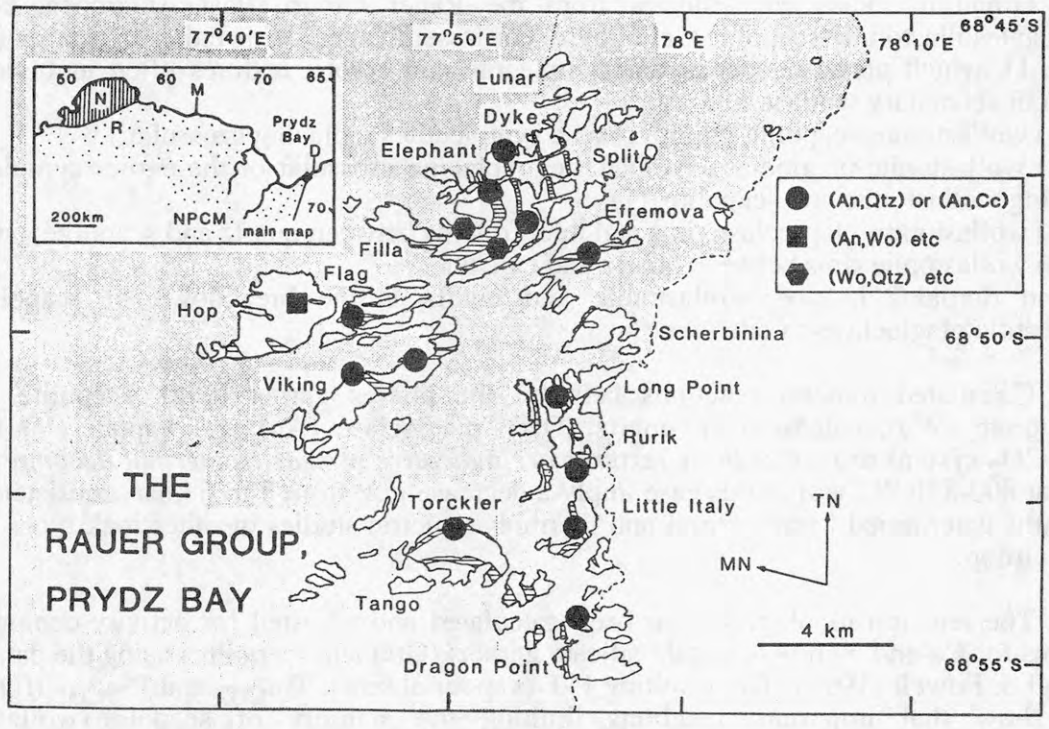

Figure 1: Distribution of calc-silicate assemblages in the Rauer Group. Assemblages labelled using absent-phase notation. Inset map: location of the Rauer Group in relation to Davis (D), Mawson (M), Napier Complex (N), Northern Prince Charles Mountains (NPCM) and the Rayner Complex (R). Horizontal ruled areas: outcrops of Fe-rich metapelite suites.

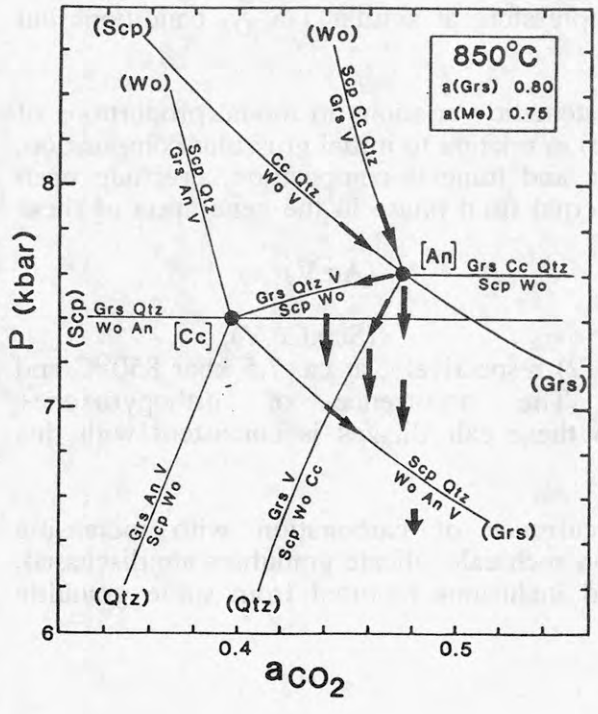

Figure 2: P-aCO_2 diagram (at 850°C) showing positions of calc-silicate reactions adjusted for appropriate activities of grossular in garnet, a(Grs), and meionite in scapolite, a(Me), using the Holland & Powell (1990) dataset. Arrowed paths are consistent with the textural evolutions in the scapolite-wollastonite rocks.

TITANIAN 2:2:1 SAPPHIRINE IN Mg-Al RICH GNEISS XENOLITHS FROM THE NORTHERN VESTFOLD HILLS: A FIRST RECORD AND IMPLICATIONS FOR EMPLACEMENT PRESSURES OF THE LONG PENINSULA NORITE COMPLEX

S.L. Harley, Geology & Geophysics, Kings Buildings, University of Edinburgh, Scotland, EH9 3JW.
A.G. Christy, Department of Earth Sciences, Downing St., Cambridge, England, CB2 3EQ.

A new compositional variety of Mg-sapphirine containing up to 1.5 wt% TiO_2 (titanian sapphirine), and close to the synthetic $2MgO:2Al_2O_3:SiO_2$ (2:2:1) end-member previously not found in nature, has been formed through partial melting of a Mg-Al rich granulite xenolith entrained in the Long Peninsula Norite Intrusive Complex, Vestfold Hills.

Basement gneisses in the Taynaya Bay area include a suite of rare silica-undersaturated sapphirine (Spr) + enstatite (En) ± spinel (Spl) ± phlogopite (Phl) (X_{Mg} = Mg/Mg+Fe values 0.95-0.98; 0.94-0.96; 0.89-0.94; 0.96-0.98 respectively) Mg-Al granulites (Harley, 1987) occurring as boudins within ca. 2526-2490 Ma felsic orthogneisses (Black et. al., 1990). These boudins record a granulite event at > 8 kbar and 900°C which precedes the major 2500 Ma granulite metamorphism (7-8 kbar and 750-850°C) responsible for most of the orthogneiss assemblages. A suite of post-metamorphic norite intrusives correlated with the high-Mg tholeiite dyke suite of Collerson & Sheraton (1986), emplaced into the basement granulites at ca. 2420 Ma, contain spectacular xenoliths (3 cm to 20 cm diameter) similar to the outcropping Mg-Al granulites. These xenoliths preserve unusual assemblages and textures formed as a consequence of their entrainment. Pink-rose to yellow-orange coloured titanian sapphirine occurs in 2-4 mm pink patches within a pale 10 cm diameter Mg-Al granulite xenolith. A darker spinel-rich rim (5-10 mm) occurs next to enclosing norite. These unique features reflect partial melting and melt crystallisation within the xenolith, and xenolith/norite host reaction, respectively.

The titanian sapphirine is magnesian (X_{Mg} = 0.985), contains 0.5-1.5 wt% TiO_2, and is highly silicic. The principal substitution causing minor departures from a 2:2:1 composition is $Ti^{VI}Al^{IV}Al^{IV}$ = $Mg^{VI}Si^{IV}Si^{IV}$. The tschermaks' substitution, $Al^{VI}Al^{IV}$ = $Mg^{VI}Si^{IV}$, and calculated Fe^{3+} contents are negligible. This sapphirine has the formula $Mg_{1.98}Fe_{0.02}Al_{4-4.06}Ti_{0.02-0.05}Si_{0.94-0.97}O_{10}$, a unique composition which contrasts with the earlier aluminous sapphirines in this and other Mg-Al granulites (figure 1).

Another extreme variety of sapphirine is also present, but only as rare inclusions within coarse resorbed rutile. This sapphirine also contains Ti (up to 1 wt%), but is markedly peraluminous ($Mg_{1.1}Ti_{0.04}Al_{4.83}Si_{0.55}O_{10}$). Hence, sapphirines in this one rock cover an Al-Si compositional spectrum greater than that shown by the collection of all previously reported sapphirines!

Initial granoblastic and radiating textures within the xenolith correlate with those in the basement Mg-Al granulites, and involve colourless enstatite (X_{Mg} = 0.984, Al_2O_3 = 5-6 wt%), sapphirine, and minor rutile and phlogopite (X_{Mg} = 0.99). These granulite facies textures are modified and overprinted in "pools" showing igneous features:

(a) spinel (X_{Mg} = 0.966, negligible Cr, Fe^{3+}) euhedra and clusters set in interstitial feldspar (Ab30-60Or30-60An5-10) and feldspar+cordierite (Crd) pools;

(b) euhedral Ti-phlogopite (X_{Mg} = 0.99) poikilitically enclosing spinel (a) and other euhedral phases (Ti-sapphirine, perovskite).

Titanian sapphirine occurs as euhedral prisms associated with the feldspathic "pools". It forms euhedral overgrowths on earlier resorbed Spr+En, and encloses strongly resorbed spinel adjacent to the "pools". Both titanian sapphirine and enstatite (Al_2O_3 = 6-9 wt%, TiO_2 up to 1.3 wt%) overgrowths exhibit Ti-rich growth zones parallel to euhedral faces. In contrast, rutile (Rut) is strongly resorbed, ragged, and rimmed by phlogopite.

Partial melting occurred through the reaction:

Phl + Spr + En + Rut = Spl + KMASHTi Liquid

Subsequent crystallisation of this melt and reaction with spinel resulted initially in the formation of titanian sapphirine and enstatite:

Spl + Liquid = Ti-Spr + En + Ti-phase (perovskite)

followed at successively lower T by phlogopite, interstitial feldspars and minor cordierite. The unexpected composition of the unique 2:2:1 sapphirine (Seifert, 1974), therefore, reflects equilibrium with a crystallising Ti-saturated aluminous melt.

Temperatures of this partial melting were in the range 1150-1200°C:

(a) magmatic temperatures near 1200°C are estimated for the host norite using pyroxene thermometry (Kuehner, 1987);

(b) melting of Spr+En only occurs at 1450-1545°C in the pressure range 4-15 kbar (Taylor, 1973). However, Phl+En melts at 1100-1140°C under vapour-absent conditions, and Phl+En+Spr will melt at similar or higher temperatures (Modreskii & Boettcher, 1973), given the presence of Ti in the phlogopite and alumina in enstatite.

(c) although Spl+Fo Fe-Mg exchange thermometry yields low temperatures for the xenolith margins (700-800°C), the high Al-contents in orthopyroxene (X_{Mg} = 0.91; Mgts = 0.16 mol%) coexisting with Spl (X_{Mg} = 0.81) and Fo (X_{Mg} = 0.9) in these domains yield calculated temperatures of 1180 $\pm$ 50°C.

The emplacement depth of the Long Peninsula Norite Intrusive Complex is constrained by the xenolith melting relations. Coexistence of En+Spr in the melting interval implies *minimum* pressures of 3.5-4 kbar (Seifert, 1974). Furthermore, interstitial cordierite in the former melt pool areas may reflect pressures near the reaction:

Spl + Crd = Spr + En,

which defines these minimum pressures. Emplacement pressures of 4.5 kbar are calculated assuming that the xenolith margins formed under the same conditions as melting reactions in the core. The relatively shallow emplacement pressures inferred here for the norite and related high-Mg tholeiites contrast with previous estimates (Kuehner, 1987; 7-8 kbar). Substantial *decompression* and exhumation of the Vestfold Hills block (ca. 12 km) occurred in this area in the 2480-2420 Ma interval, prior to norite intrusion. A post-metamorphic near-isobaric cooling history and prolonged deep crustal residency, inferred from previous studies, is not supported by this new data.

References:
Black, L.P., Kinny, P.D. & Sheraton, J.W., 1990. *Abs. Geol. Soc. Aust.* **25**, 253.
Collerson, K.D. & Sheraton, J.W., 1986. *J. Petrology* **27**, 853-886.
Harley, S.L., 1987. *Abs. 5th ISAES*, Cambridge.
Kuehner, S.M., 1987. Unpubl. PhD Thesis, Univ. Tasmania.
Modreskii, S. & Boettcher, A., 1973. *Am. J. Sci.* **273**, 385-414.
Seifert, F., 1974. *J. Geol.* **82**, 173-204.
Taylor, H.C.J., 1973. *Bull. Geol. Soc. Am.* **84**, 1335-1348.

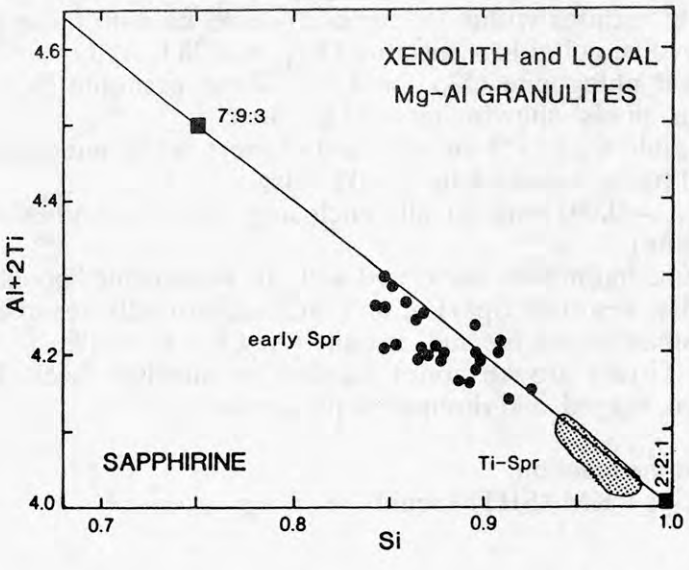

Figure 1: compositions of Mg-sapphirines expressed as cations Al+2Ti versus Si per formula unit. This plot includes both the tschermaks and Ti-tschermaks substitutions noted in the text. Note the distinctive fields occupied by the initial low-Ti (solid circles) and later high-Ti (shaded area) sapphirines. The peraluminous sapphirines included in rutile plot well above the 7:9:3 composition along the diagonal line, and lie off the scale of this diagram.

GRANULITE METAMORPHISM IN PRYDZ BAY, EAST ANTARCTICA: THE SIGNIFICANCE OF REWORKING, FLUIDS AND PARTIAL MELTING

S.L. Harley, I.C.W. Fitzsimons & G.R. Watt, Geology & Geophysics, Kings Buildings, University of Edinburgh, Scotland, EH9 3JW.

The high-grade basement gneisses of the Rauer Group-Brattstrand Bluffs coastal region, Prydz Bay, exhibit a complexity of structural, metamorphic, and overprinting features. This reflects the presence of monocyclic granulites, which only record the effects of the regionally extensive c. 1000 Ma event correlated with the Rayner metamorphism in Enderby and Kemp Lands (Black *et. al.*, 1987), and interleaved polycyclic or reworked granulites which preserve deformational and migmatitic structures, and initial metamorphic assemblages, related to substantially earlier high-grade events.

1. Polycyclic granulites and reworking in the Rauer Group

In the Rauer Group, domains of reworked Archaean basement containing polymetamorphic granulites are defined on the basis of distinctive lithological associations and geological relationships (figure 1) coupled with zircon U-Pb SHRIMP geochronology (Kinny & Black, 1990) which indicate Archaean ages of 3270 Ma and 2800 Ma for felsic orthogneisses. The minimum extent of this reworked domain is indicated in figure 1.

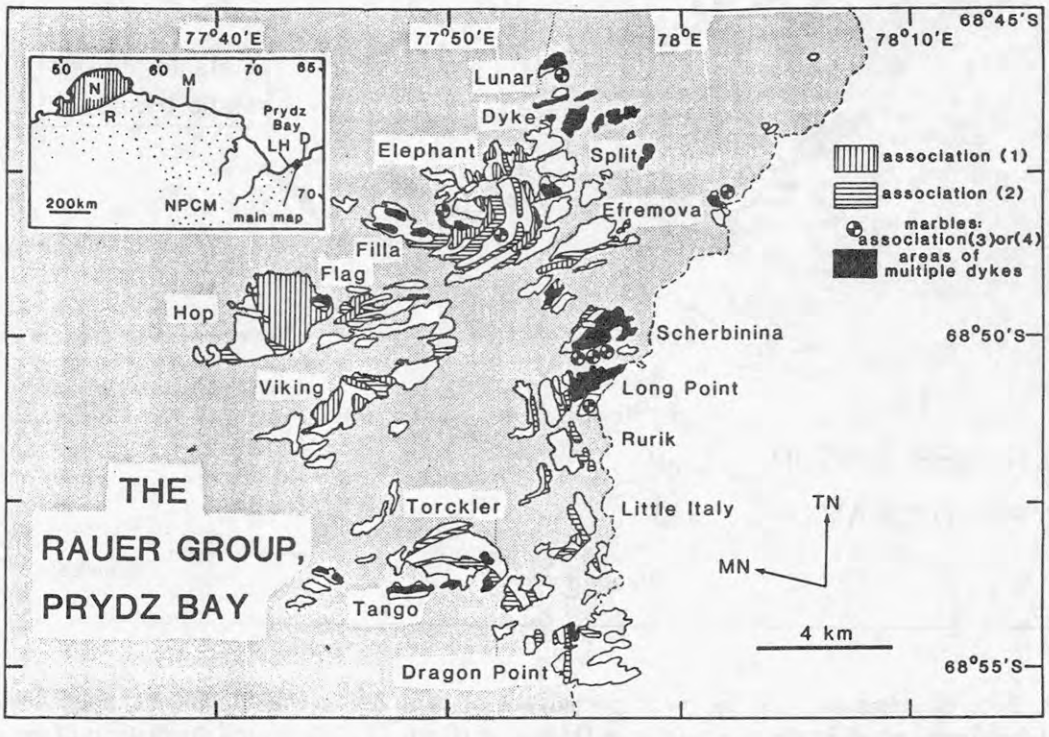

Figure 1: Map of the Rauer Group showing the distribution of lithological associations described in the text and locations of forsterite marbles. The black shaded areas containing multiple dyke generations and early structures define the minimum extent of reworked old (Archaean) granulites. Gross layering orientations are a result of D4 and later deformations

Diagnostic geological features of these reworked domains are:

(a) An extensive array of deformed metabasite dykes, often of several orientations and generations (figure 2) dissect basement lithologies dominated by felsic orthogneisses and composite felsic-mafic layered gneisses (c and d below).

(b) Deformation events (D1, D2, D3) and overprinting relations between orthogneisses and enclosed lithologies pre-date the emplacement of these metabasite dykes. Events grouped

as D4 (Harley, 1988) deform the dykes and have given rise to open to tight south-plunging upright folds in the southern Rauers and NS and EW trending upright ductile shear zones in the north and NW Rauers.

(c) Relatively homogeneous to weakly banded felsic (granitic) to intermediate (tonalitic) orthogneisses showing strong fabrics host forsterite marble boudins (Fo-Di-Cal±Spl) (Buick & Harley, *this symp.*) and rarer magnesian metapelite rafts (association (3), Harley & Fitzsimons, 1991). These rafts preserve internal folds and fabrics cut by those in the orthogneisses. Such structurally early magnesian metapelite rafts from one area record extreme peak P-T conditions of 10-12 kbar and 1000-1050°C and an initial decompression to 8 kbar at temperatures of greater than 950°C (Harley, this symp.).

(d) Composite felsic-mafic gneisses comprised by mafic granulite rafts and layers enclosed in or interleaved with gneissic (tonalitic) and later granular felsic veins also host rare forsterite marble and magnesian metapelite lenses (association (4), Harley & Fitzsimons, 1991).

(e) A marked correlation is seen between the outcrop area of forsterite marble bodies and the region of intense dyking.

(f) Layered mafic-ultramafic complexes preserving relict igneous features (e.g. graded and rhythmic layering, internal dykes, xenolith zones) and early folds are intruded by, or form tectonic blocks enclosed in, orthogneisses of association (3).

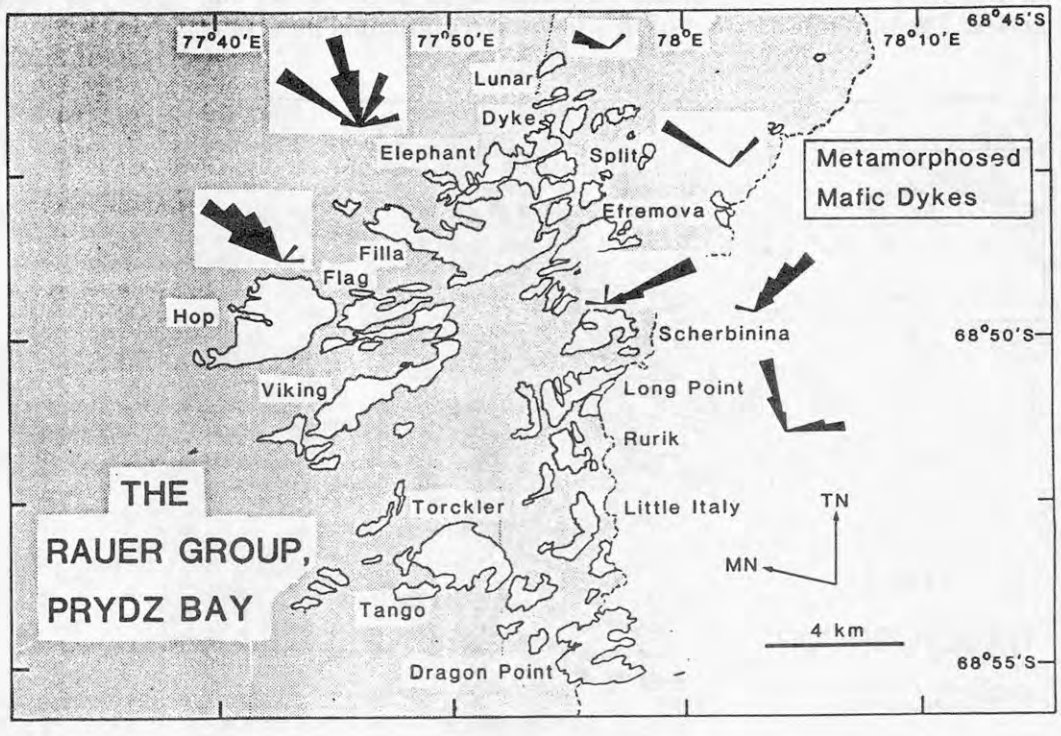

Figure 2: Rose diagrams showing the mean orientations of generally steeply-dipping deformed metabasite (mafic) dykes, uncorrected for the effects of gross D4 folding (figure 1). Note several orientations of dykes from the N and NW islands.

Homogeneous felsic orthogneisses (I-types) of association (3) include at least two suites with geochemical signatures very similar to those of the Napier Complex depleted and undepleted orthogneisses (Sheraton *et. al.*, 1985). Depleted tonalitic to granitic orthogneisses show very low REE abundances, highly fractionated REE patterns (Ce_N/Yb_N = 36) with severe HREE depletions and positive Eu anomalies (figure 3a), and are characterised by high Ti/Y, low Nb, and high Sr: features generally considered to reflect an origin through high-pressure hydrous melting of a garnet ± amphibole bearing mafic source. Undepleted granitic orthogneisses (mainly charnockites) have much higher REE abundances. They show either relatively unfractionated REE patterns with no Eu anomaly (Ce_N/Yb_N = 5; figure 3b), or

fractionated REE and negative Eu anomalies (Ce_N/Yb_N = 35; figure 3a); Nb is variable, but Sr and Ti/Y are both low. The undepleted types may have formed through dry melting of mafic to intermediate granulite crustal precursors.

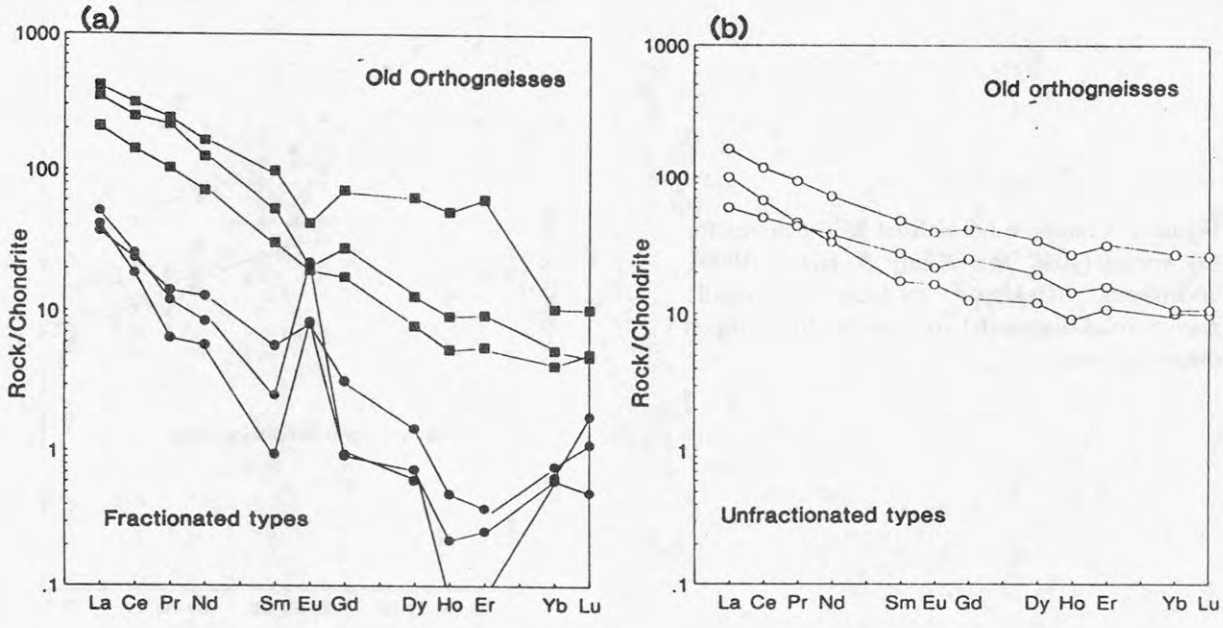

Figure 3: Chondrite-normalised REE plots for (a) fractionated and (b) relatively unfractionated (open circles) orthogneisses defined as "old" on the basis of structural and overprinting relations. The highly depleted (filled circles) and undepleted suites (filled squares) in (a) both include granitic to tonalitic types (charnockites and enderbites).

Partial melting of mafic granulite has played a significant role in the production of tonalitic material within composite gneisses, prior to dissection by dykes and the late deformation phases. Patch, agmatic, and schollen migmatitic structures featuring euhedral orthopyroxene (Opx) (+ garnet, Grt), preserved in mafic granulites within low strain zones, are consistent with dehydration-melting of amphibole (Hbl) at > 950°C and > 8 kbar via the generalised reaction:

$$Hbl + Plag = Cpx + Opx + Grt + L$$

The observation that these migmatite structures are little affected by metamorphism and partial melting associated with the 1000 Ma overprinting indicates that these low-strain zones were generally impervious to any fluids generated in or related to that younger event.

2. The 1000 Ma events: P-T-fluid conditions in the Rauer Group

Two gneiss associations in the Rauer Group post-date most of the metabasic dyke suites and preserve relatively simple deformational histories:

(1) Felsic to intermediate (granitic to dioritic) I-type orthogneisses which commonly preserve relict igneous features, including Kfeldspar megacrysts and rhythmic layering, overprinted by a simple foliation (association (1), Harley & Fitzsimons, 1991). These comagmatic rock-types are related by crystal fractionation at mid-crustal levels, are undepleted in terms of total REE and trace element contents, and show moderately to highly fractionated REE patterns (Ce_N/Yb_N = 4-30, figure 4) and high Ti/Y . A SHRIMP zircon U-Pb age of 1030 Ma has been obtained on one of these "young" orthogneisses (Kinny & Black, 1990).

(2) Layered paragneiss successions consisting of Fe-rich pelites and semipelites, quartzites, leucogneisses, impure calcsilicates, and rare mafic granulite (association (2)). The migmatitic metapelites and associated leucogneisses indicate that the metapelites underwent partial melting mainly early in D3, although locally podiform leucogneisses related to post-

D3 but pre-D4 melting are also present. A SHRIMP zircon U-Pb age of 1000 Ma for one leucogneiss from Filla Island (Kinny & Black, 1990) provides a good estimate for the age of the main metamorphism affecting affecting these younger lithological associations.

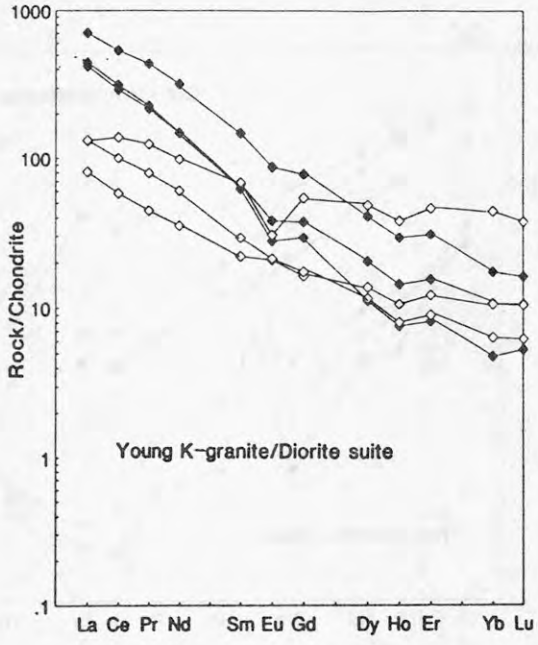

Figure 4: Chondrite-normalised REE patterns for the young (1030 Ma: Kinny & Black, 1990), undepleted, Kfeldspar megacrystic granitic gneiss (solid diamonds) and dioritic gneiss (open diamonds) suite.

The Fe-rich metapelites are garnet (Grt)-sillimanite (Sil) gneisses with additional ilmenite (Ilm) and/or rutile (Rut), quartz (Qtz), feldspars (Plag, Kfs) and minor biotite (Bt). These record syn- to post-deformational decompression through 2 to 4 kbar from maximum pressure (P)-temperature (T) conditions of 7-9 kbar and 800-850^{o}C. This P-T path is consistent with that deduced from earlier studies of felsic granulites from association (1) (Harley, 1988), and is further refined through P-T calculations on interlayered and boudinaged impure calcsilicates. The latter rock-types feature grossluar-wollastonite-scapolite assemblages which define initial P-T conditions near 8 kbar and 850^{o}C and initial decompression at temperatures of >800^{o}C (Harley & Buick, *this symp.*). Water activities (a_{H2O}) associated with metamorphism of the metapelites, calculated using the equilibrium:

$$Bt + Sil + Qtz = Grt + Kfs + H_2O$$

are in the range 0.3-0.4, and a_{CO2} deduced from the calcsilicates are 0.4-0.48 (Harley & Buick, *this symp.*). These results, stable isotope measurements on calcsilicate calcites (Buick *et. al., this symp.*), and undepleted K/Rb signatures in the diorites of association (1), are evidence against the existence of a *pervasive* fluid related to the 1000 Ma granulite metamorphism.

3. The 1000 Ma events: P-T conditions and partial melting in the Brattstrand Bluffs region, Ingrid Christensen Coast.

Two gneissic associations, one comprising interlayered felsic and mafic orthogneiss and the other dominated by metapelitic paragneisses, occur the Brattstrand Bluffs region, 30-60 km south-west of the Rauer Group (figure 5). A tectonically disrupted and transposed basement/cover relationship is inferred between these associations as the orthogneiss association (basement) preserves structural and migmatitic features not recorded in the paragneisses, which underwent widespread partial melting in a later event correlated with the 1000 Ma metamorphism dated in the Rauer Group.

Well-layered to migmatitic pelitic and semi-pelitic lithologies record maximum granulite conditions of *c.* 6 kbar, 850^{o}C. There is abundant field evidence for the generation and extraction of leucocratic melts in equilibrium with garnet and cordierite (Crd) from the metapelitic gneisses during and immediately after peak metamorphism:

(a) Migmatitic textures are frequently developed. Pelitic schlieren and pods in a leucocratic garnet- and cordierite-bearing matrix are interpreted as restite and recrystallized partial melt respectively.

(b) Leucogneiss sheets and lenses, often containing minor garnet and cordierite, cut across layered and migmatitic units and are interpreted as recrystallized bodies of extracted melt.

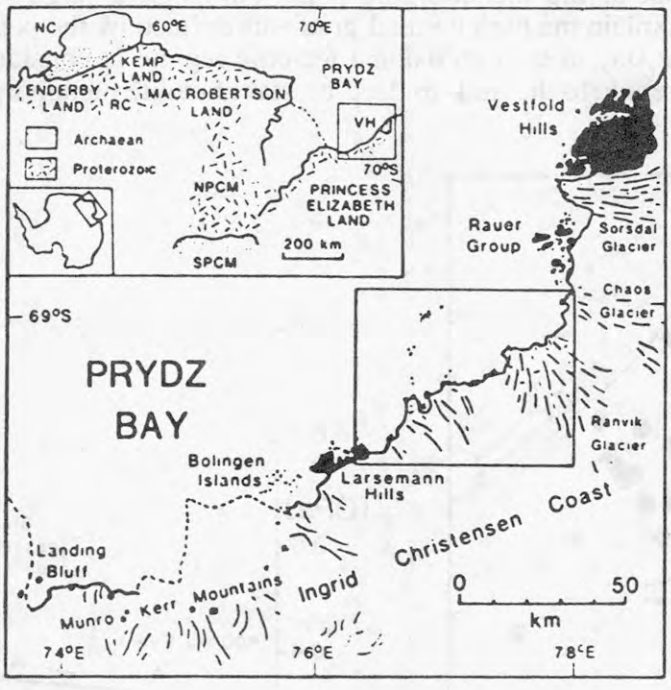

Figure 5: Location map of the East Prydz Bay area, showing the extent of outcrop and geographic position of the Brattstrand Bluffs area (region enclosed in the outlined box) with respect to the Rauer Group and Larsemann Hills.

The equilibria involved in this melting event are best preserved in the layered pelites, where apparent melt production was low, and products and reactants are retained in close proximity. In such granulites, an early Grt(1)-Sil-Bt(1)-Qtz assemblage is preserved in garnet cores, but is replaced in the matrix by an assemblage characterized by absence of biotite and presence of cordierite and second generation garnet (Grt(2)-Crd(1)-Sil-Qtz-Kfs). Garnet(2) and cordierite(1) are correlated with garnet and cordierite present in leucogneisses, and interpreted as the solid products of incongruent vapour-absent melting of biotite by *fluid-absent* reactions such as:

$$Bt(1) + Sil + Qtz = Grt(2) + Kfs + L, \text{ and}$$
$$Bt(1) + Sil + Qtz = Grt(2) + Crd(1) + Kfs + L$$

The proposed development of cordierite as a peritectic phase in equilibrium with a H_2O-undersaturated silicate melt has been tested through analysis of several cordierites for channel volatile (CO_2 and H_2O) contents using newly-developed secondary ion mass spectrometry techniques. Total volatile contents are considerably less than both the equilibrium values for fluid-saturated cordierites under the deduced P-T conditions and those contents reported for most other natural cordierites (figure 6). The proportion of CO_2 is also low (X_{CO2} = 0.1 to 0.4), in contrast to many granulite-facies cordierites. These initial results are consistent with cordierite equilibration with a melt rather than a free fluid phase, but require further testing in order to exclude other possible explanations such as post-granulite volatile leakage from the channels. On the basis of the present data, it is suggested that the peak metamorphism in this region occurred in the presence of melt but did not involve the pervasive influx of a fluid from reserviors external to the metamorphic pile itself.

The post-peak P-T evolution of the Brattstrand Bluffs granulites involved decompression through 1-2 kbar prior to cooling (Fitzsimons & Harley, *this symp.*), a P-T history rather similar to other parts of the Prydz Bay area (Harley, 1988; Stüwe & Powell, 1989) but occurring at crustal levels between those exposed in the deeper Rauer Group and shallower Larsemann Hills (figure 7). In addition, in contrast to pelites from the Larsemann Hills (Stüwe & Powell, 1989), spinel-bearing assemblages only formed during decompression and not at the metamorphic peak. Although a large-scale magmatic heat source is required to explain the high thermal gradients defined by the peak metamorphic P-T data in the East Prydz Bay area, a collisional tectonic regime is considered to have been a prerequisite for and prelude to the mid- to deep-crustal granulite metamorphism.

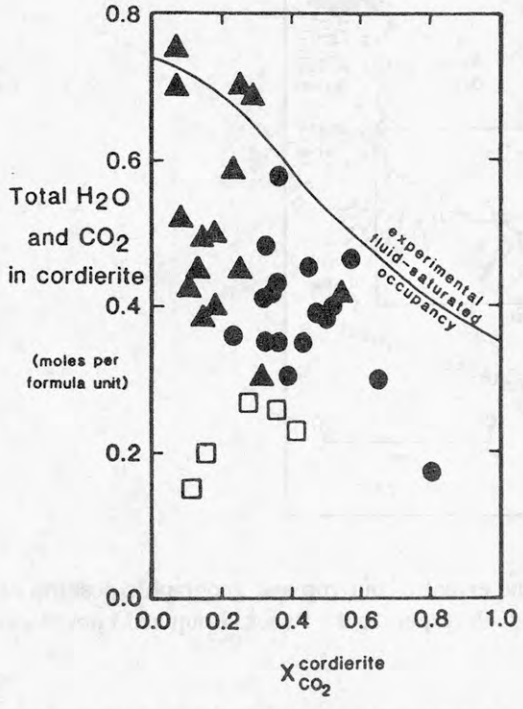

Figure 6: Total volatile contents of Brattstrand cordierites (open squares) compared with data for cordierites from other granulites (filled circles) and miscellaneous rocks (triangles).

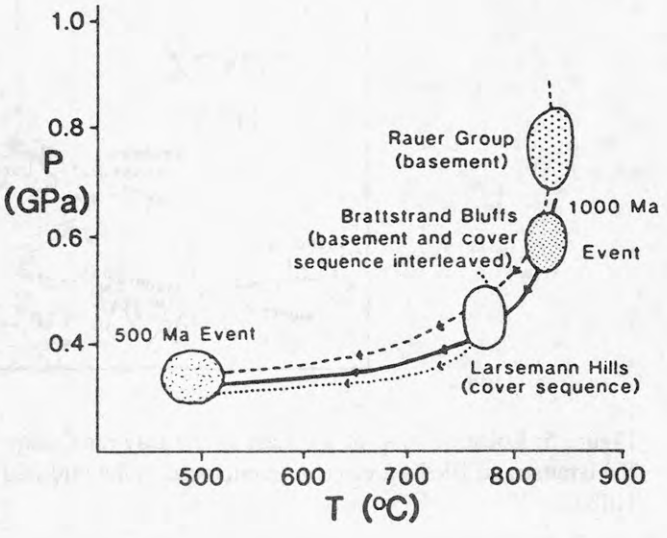

Figure 7: P-T evolutions defined for areas in the Prydz Bay region.

References:

Black, L.P., Harley, S.L., Sun, S.S. & McCulloch, M.T., 1987. *J. Metamorphic Geol.* **5**, 1-26.

Harley, S.L., 1988. *J. Petrol.* **29**, 1059-1095.

Harley, S.L. & Fitzsimons, I.C.W., 1991. *J. Metamorphic Geol.* **9**, in press.

Kinny, P.D. & Black, L.P., 1990. *Abs. Geol. Soc. Aust.* **25**, 251-52.

Sheraton, J.W., Ellis, D.J. & Kuehner, S.M., 1985. *BMR J. Aust. Geol Geophys.* **9**, 207-218.

Stüwe, K. & Powell, R., 1989. *J. Metamorphic Geol.* **7**, 465-483.

Tertiary Marine Molluscs from the Pagodroma Tillite, Prince Charles Mountains, East Antarctica

C.P. Hart, Department of Geological Sciences and Byrd Polar Research Center, Ohio State University, Columbus, Ohio 43210 United States of America.

B.C. McKelvey, Department of Geology and Geophysics, University of New England, Armidale, NSW 2351 Australia.

The widespread Pliocene Pagodroma Tillite (McKelvey and Stephenson 1990, Bardin 1982) of the Prince Charles Mountains contains Tertiary marine megafossils unknown from elsewhere in East Antarctica. Recent field work has revealed *in situ* articulated bivalve molluscs in the Pagodroma Tillite at Pagodroma Gorge in the Amery Oasis. This fossil assemblage indicates Pliocene marine sedimentation some 270 km south from the present coastline. The frequent occurrence of articulated bivalves, and the preservation of their fine shell growth sculpture offers compelling evidence for the autochthonous nature of these fossils. In some localities the specimens are crushed indicating sequence deformation beneath readvancing East Antarctic ice.

The Pagodroma Gorge fauna consists of five species of small (<25 mm long) infaunal bivalves, representing four families, preserved in a sandy, clay-rich diamicton. Three species, one from the Nuculidae and two Nuculanidae, dominate this assemblage. These three species are also known from early Oligocene marginal marine strata of the CIROS-1 and DSDP Site 270 Antarctic drill sites. Two additional species have apparently not been previously described from the Antarctic.

The low diversity of this Pagodroma Tillite fauna contrasts with that of the Pliocene shelly fauna found some 450 km to the northeast in the Vestfold Hills at Marine Plain (Pickard *et al.* 1986). This latter fauna contains nine species of molluscs, but only one species in common with the Pagodroma fauna. The infaunal mode of life for the Pagodroma Gorge fauna suggests an environment featuring high rates of terrigenous input, an environment compatible with the tidewater glacier depositional model. The members of the Pagodroma Gorge fauna are known from shallow subtidal to abyssal depths. This eurybathic distribution, together with small individual size, are two characteristics found in modern Antarctic molluscan faunas. The Pagodroma Tillite features another older bioclastic facies, containing comminuted coarse shell hash unrelated to the autochthonous facies.

Micropaleontological studies of the Pagodroma Tillite reveal recycled late Cretaceous and early Paleogene foraminifera (P.N. Webb, this volume). The preservation of internal molds, and of silica-replaced foraminifera contrasts with the unaltered shell material found in the Pagodroma Tillite. Recycled mid-Pliocene diatoms in the Pagodroma Tillite (D.M. Harwood, this volume) establish its maximum age.

Bardin, V.I. 1982. Lithology of East Antarctic Moraines and some problems of Cenozoic history. In Craddock, C., ed. *Antarctic geoscience.* Madison: University of Wisconsin Press, 1069-1076.

McKelvey, B.C. and Stephenson, N.C.N. 1990. A Geological Reconnaissance of the Radok Lake area, Amery Oasis, Prince Charles Mountains. *Antarctic Science* 2(1), 53-66.

Pickard, J., Adamson, D.A., Harwood, D.M., Miller, G.H., Quilty, P.G. and Dell, R.K. 1986. Early Pliocene marine sediments in the Vestfold Hills, East Antarctica: implications for coastline, ice sheet and climate. *South African Jounral of Science* v.82:520-521.

THE CHANGING STYLE OF CENOZOIC ANTARCTIC GLACIATIONS

D.M. Harwood, Dept. of Geology, Univ. of Nebraska, Lincoln, NE 68588-0340 USA
P.N. Webb, Dept. of Geological Sci., The Ohio State Univ., Columbus, OH 43210 USA
P.J. Barrett, Antarctic Research Centre, Victoria University of Wellington, New Zealand
B.C. McKelvey, Dept. of Geology, Univ. of New England, Armidale NSW 2351, Australia

Cenozoic Antarctic glacial history is more complex than suggested by existing interpretations of deep-sea data. Physical evidence from Antarctic drillcores and terrestrial outcrops documents the repeated growth and decay of numerous ice sheets over the last 40 million years. Recycled marine microfossils in the glacigene upper Pliocene Sirius Group and Pagodroma Tillite record repeated periods of Cenozoic deglaciation, when marine seas covered vast areas of East Antarctica. This history is consistent with periods of global warmth, high-stands of sea-level, and with oxygen isotope interpretations that accommodate a progressive cooling of the deep-sea through the Cenozoic. Major ice volume changes occurred every 1 to 3 m.y., with peak deglaciations during the early Pliocene, early Miocene and late Oligocene and peak glaciations during the late Pliocene-Pleistocene, late Miocene, middle Miocene, mid-Oligocene, and latest Oligocene.

The presence of in situ *Nothofagus* (southern beech) leaves and twigs in the Pliocene Sirius Group indicates that climate during Oligocene and Miocene glaciations was never as cold as today, otherwise this vegetation would have been dispelled from Antarctica by the increasing cold. The survival of Antarctica's terrestrial vegetation until the late Pliocene indicates temperatures estimates at least 15°to 20°C warmer than today, for all pre-Pliocene glaciations, with higher values during deglacial periods. This climatic regime lends strong support to the dynamic ice sheet history presented above by suggesting a 'temperate' glacial setting where multiple deglaciations would be more easily accommodated. The major change in character of Antarctic glaciations from 'temperate' and cyclic to 'polar' and permanent is thought to have occurred in the late Pliocene, coincident with other records of global cooling.

The modern Antarctic environment is thus a poor analog for the warmer and wetter pre-late Pliocene glacial, conditions and for the interpretation of past marine shelf and oceanic sediment records. Glacial and eustatic variations seen in long drillcores on the Antarctic shelf, such as CIROS-1 in McMurdo Sound, provide a good record of major changes in ice volume and exemplify the dynamic character of Cenozoic 'temperate' ice sheet history in Antarctica. Interpretations of Cenozoic ice sheet history from deep-sea proxy records (isotopes, IRD, bottom-water, etc.) are guided by our understanding of modern processes. However, given the complex history of Antarctic glaciation/deglaciation we present here, and the change from 'temperate' to 'polar' glacial conditions at ~2.5 Ma, it is clear that many interpretations from these deep-sea data need to be reconsidered, with guidance from nearshore and onshore stratigraphic evidence emerging from the Antarctic continent. Because there can ultimately be only one history of past Antarctic glaciations, we search for consistency among all of the available data. Do deep-sea sediments selectively record and amplify the climate signal of a particular phase of a glaciation or deglaciation? Are different climate signals produced in separate regions of this large continent during the same glacial/deglacial phase? A complex climatic history produced by dynamic ice sheets of varying size and character through time should replace the simplistic deep-sea view of stable Cenozoic Antarctic ice sheets.

TILL GENESIS OF SUPRAGLACIAL MORAINE IN THE CENTRAL SØR-RONDANE MOUNTAINS, EAST ANTARCTICA

H. Hasegawa, Graduate Student, Department of Geography,
Meiji University, Kanda Surugadai, Chiyoda-ku,
Tokyo 101, Japan.
S. Iwata, Department of Geography, Mie University,
Kamihamacho, Tsu, Mie 514, Japan.
N. Matsuoka, Institute of Geoscience, the University of
Tsukuba, Tenno Dai, Tsukuba, Ibaragi 305, Japan.

From the observation of supraglacial till and englacial debris, till genesis was clarified at two moraine fields, central Sør-Rondane Mountains, East Antarctica. In these areas the till was classified into two types according to their sizes : one is clayey till composed of fines (clay and silt) with semiangular-semiround gravels and the other is sandy till of angular gravels with coarse (sand) matrix.

In Bergersen area the youngest moraine ridge, located at the southern fringe of the ice lobe, consists of clayey till. The cross section of this moraine ridge was observed in trench excavated by the authors. Thickness of the clayey till is about 10-20 cm and underlying glacial ice consists of regelation ice with thin debris-rich layers which inclined obliquely to the surface. Their structures dipping to the glacier show that the regelation ice with debris-rich layers is basal ice, and the clayey till was transported from the glacier bed. The existence of clayey till suggests that basal sliding occurred at the glacier bed, as a result of pressure melting.

On the snout zone of the ice lobe, the sandy till is deposited on dirty ice layers in foliations, and it stretches to medial moraine of the glacier. This indicates that entrainment and transport processes of the sandy till are different from those of the clayey till.

Since the clayey till is distributed on the moraine field of older stages in the Mefjell area, it is suggested that the conditions for basal sliding of the glacier has occurred continuously or intermittently for a long time.

A HIGH PRESSURE- HIGH TEMPERATURE METAMORPHIC EVENT PRECEEDING PROTEROZOIC GRANULITE METAMORPHISM IN THE PRYDZ BAY AREA, ANTARCTICA

B.J. Hensen, D.E. Thost[1] and Y. Motoyoshi[2]
1) University of New South Wales, Kensington 2033, Australia
2) National Institute of Polar Research, Itabashi-ku, Tokyo 173, Japan

Granulite facies metasediments and associated metaigneous/metavolcanic felsic gneisses occurring along the Prydz Bay coastline (74-78°E, 69°S) have generally been regarded as a supracrustal sequence, deformed and metamorphosed during a single low to medium pressure tectonothermal event at c. 1000Ma. This scenario is brought into question by the recognition of an earlier higher pressure(P)-temperature(T) event in mafic granulite from Søstrene Island, 10km south-west of the Bolingen Islands.

Garnet-bearing mafic granulites from Søstrene Island occur as remnants in deformed concordant layers of amphibolite and pyroxenite within a felsic host. Maximum P-T estimates based on garnet core-matrix orthopyroxene-clinopyroxene-hornblende pairs are *c.* 0.95GPa at 950±50°C. These P-T conditions are comparable to those recorded by similar mafic rocks of Archaean age from the Rauer Islands (Harley 1988), and are much higher than for metasediment occurring along the coastline between the Bolingen and Rauer Islands.

The larger garnets from Søstrene Island exhibit two-stage symplectic coronas which formed after peak metamorphic conditions. A medium-grained corona of orthopyroxene+plagioclase+(hornblende) surrounds a fine-grained inner corona of orthopyroxene+plagioclase+spinel which mantles the garnet and occurs along a fracture cleavage within it. This "inner symplectite" gives P-T estimates of *c.* 0.7 GPa at 850°C. The host felsic gneiss yields P estimates of 0.5-0.7 GPa, which compare closely with conditions of *c.* 0.6 GPa and 775°C for metasediments in the neighbouring Bolingen Islands. This suggests that the garnet breakdown correlates with the widespread 1000Ma metamorphic event recognized in outcrops along the Prydz Bay coast. These observations can be interpreted in a number of ways:

1.The rocks on Søstrene Island belong to a separate probably Archean terrane wich was tectonically juxtaposed, prior to Proterozoic metamorphism,to the main Prydz Bay terrane.

2. The Prydz Bay metasediments were derived from predominantly felsic basement rocks (Archaean to mid-Proterozoic) wich locally preserve evidence for a previous high-grade metamorphic history. Subsequently, basement and cover were deformed, interleaved and metamorphosed at *c.* 1000Ma.

3. The metasediments and felsic gneisses have undergone the same polymetamorphic history, with evidence of early high P-T conditions having been largely obliterated by the 1000Ma event.

In the Bolingen Islands area, contacts between metapelite and felsic orthogneiss associations coincide with high strain zones and layer parallel mylonites which obscure the original rock unit relationships. Structural evidence suggests that both rock associations have been subjected to the same tectonic history, favouring scenarios 1or 3 above.

The high-P, high-T estimates derived from the garnet relics provide evidence for an earlier, possibly Archaean, higher-grade metamorphic event which has been largely overprinted in the surrounding rocks by the lower-grade 1000Ma metamorphism. In the surrounding rocks, evidence for a two stage metamorphic history is very rare to absent. The generally concordant relationships of different lithologies on Søstrene Island also suggests the rocks have undergone a common metamorphic history, and the high pressure rocks are not allocthonous tectonic inclusions. The possibility that the entire terrane may once have experienced higher P-T conditions than are indicated by the present mineral assemblages deserves further investigation.

GEOLOGY OF CAPE DUBOUZET, NORTHERN ANTARCTIC PENINSULA

Francisco Herve, Ignacio Ugalde, Jorge Lobato

Departamento de Geologia y Geofisica, Universidad de Chile,
Casilla 13518 Correo 21, Santiago; Chile

During the XXVIIth Scientific Antarctic Expedition of Instituto Antartico Chileno in January-February 1991, the authors mapped the Cape Dubouzet area, a sharp rocky "arête" surrounded by glaciers located near the northern tip of the Antarctic Peninsula (Fig. 1).

Previous work in this area included sampling of moraine blocks of tonalite with metamorphic xenoliths (Loske et al., 1980 a,b). Detailed mapping of Cape Dubouzet, allowed us to determine the provenance of the metamorphic rock xenolith bearing tonalite whose geological setting is given below.

GEOLOGY

The most extensive lithologic unit at Cape Dubouzet (Fig. 1) is a sequence of volcanic breccias of rhyolitic composition. Thick flow units of ca. 10 m thickness prevail, with flattened pumice clasts which suggest possible ignimbritic eruptions. Most of the clasts are angular and of banded rhyolite composition. The sequence is monoclinal with smooth dips to the SE, with a minimum estimated thickness of more than 200 m.

The rhyolitic breccias are intruded by two tonalite stocks, by a banded rhyolitic dome and by dikes of andesitic composition. A third tonalitic stock crops out in the coastal areas, but its contact with the breccias is not exposed. However, it is intruded by the banded rhyolitic dome.

Only one of the tonalitic-dioritic stocks contains xenoliths of metamorphic rocks (see Fig. 1). It constitutes a semi annular body of about 600 m of external diameter. It shows about 15% in volume of inclusions of metamorphic rocks, most of them less than 5 cm long but some up to 50 cm. The tonalitic host rock is porphyritic, with clinopyroxene and plagioclase phenocrysts. The matrix is composed of chlorite, epidote, biotite, plagioclase and granophyric quartz-K feldspar intergrowths. Corroded quartz and garnet xenocrysts are present. Zircon, apatite, sphene-leucoxene and opaque minerals are accessories.

The rhyolitic dome is finely flow banded, with scarce quartz phenocrysts embedded in a devitrified quartz-feldspar-opaque mineral groundmass. This body is probably subcontemporaneous with the breccia flows and it intrudes the coastal tonalitic stock which is thus possibly older than the breccias.

Coarse block moraines are well developped in the area. The lithology of the blocks indicate a local provenance. The samples dated by Loske et al. (1990 a, b) were taken from the moraines.

THE XENOLITHS

As indicated by Loske et al. (1990 a), three petrographically distinct groups of xenoliths occur in the hemiannular tonalite body: A) plagioclase-biotite gneisses. B) amphibolites and C) metatonalites.

In the present study, in rocks of group A, cordierite and sillimanite bearing gneisses were observed which were not previously identified; sillimanite occurs in well oriented needle-like crystals, which probably preclude an origin by the heating in the process of inclusion in the tonalite. Some bands have patchy micropegmatitic quartz-K feldspar inergrowths which might indicate partial melting in them.

Gneisses and amphibolites thus represent rocks which attained the higher part of the amphibolite facies, probably in a low pressure metamorphic environment, previous to their ascent to the present levels of occurrence in the magma.

AGE

Loske et al. (1990 a, b) have dated zircons in the inclusions which indicate a Late Carboniferous (ca. 300 Ma) event which is considered as a minimum age of the metamorphism of the inclusions. The tonalite host rock gave imprecise Triassic-Jurassic U-Pb ages in zircons. Dating of some of the other units of the area is in progress.

DISCUSSION

The sequence of volcanic breccias which is intruded by the tonalite was probably deposited unconformably over the TPG. Their subhorizontal structural attitude is similar to the mount Flora Formation (MFF, Elliot & Gracanin, 1983) which outcrops at Hope Bay, 20 km SE from Cape Dubouzet, where it overlies the folded TPG strata. Mount Flora Formation is mainly conglomeratic, but has tuffaceous intercalations which underlie Middle to Upper Jurassic plant bearing horizons.

A broad time correlation is here suggested between the breccia sequence of Cape Dubouzet and the Mount Flora formation on the basis of structural similarity, lithologic similarity of the breccias and the tuffaceous intercalations in MFF, and the Triassic-Jurassic age of the tonalite intruding the breccias.

However, in the Jurassic the Cape Dubouzet area was an active volcanic area, maybe including caldera related activity, as indicated by the presence of ignimbritic flows, an annular ring intrusive body and a subvolcanic rhyolitic dome.

This Triassic-Jurassic acid volcanic activity would be part o the acid magmatic event which developed extensively in South America (Choiyoi province of central and northern Chile, Chon-Aike province in Patagonia, Mpodozis and Kay, 1990) and has been also recognized mainly as granitic intrusions in the eastern coast of the peninsula (Pankhurst et al., 1988) and in the Ellsworth-Withmore Mountains (Storey et al., 1988). This magmatic event preceeded the disagregation of the Gondwana supercontinent.

Acknowledgments

Instituto Antartico Chileno (INACH) project 061 financed this work. Eduardo Garcia solved the mountaineering problems during the field work.

REFERENCES

Elliot, D.H. & Gracanin, T.M. (1983) Conglomeratic strata of Mesozoic age at Hope Bay, Northern Antarctic Peninsula. In Antarctic Earth Science, (Oliver, R.L., James, P.R. and J.B. Jago Editors), 303-307, Canberra.

Loske, W; Miller, H; Milne, A. & Herve, F. (1990). U-Pb zircon ages of xenoliths from Cape Dubouzet, northern Antarctic Peninsula. Zbl. Geol. Palaont., T. 1, H1/2, 87-95, Stuttgart.

Loske; W; Miller, H; Milne, & Herve, F. (1990). Lithology and age of the basement at Capa Dubouzet, Antarctic Peninsula. ICOG 7, Abstracts, 61, Canberra.

Millar; I.L; Milne, A. & Pankhurst, R.J. (1990). Early proterozoic detrital garnet in Mesozoic accretionary complex rocks, West Antarctica. ICOG 7, Abstracts, 66, Canberra.

Mpodozis, C. & Kay, S.M. (1990). Provincias magmaticas acidas y evolucion tectonica de Gondwana: Andes chilenos (28°-31°S). Revista Geologica de Chile, 17, 2, 153-180.

Pankhurst; R.J., Hole; M.J. & Brook, M. (1988). Isotope evidence for the origin of Andean granites. Transactions of the Royal Society of Edinburgh. Earth Sciences, vol. 79, p. 123-133.

Storey, B.C; Hole. M.J; Pankhurst, R.J., Millar, I.L; & Vennum, W. (1988). Middle Jurassic within plate granites in West Antarctica and their bearing on the breakup of Gondwana-land. Journal of the Geological Society of London, vol. 145, p. 999-1007.

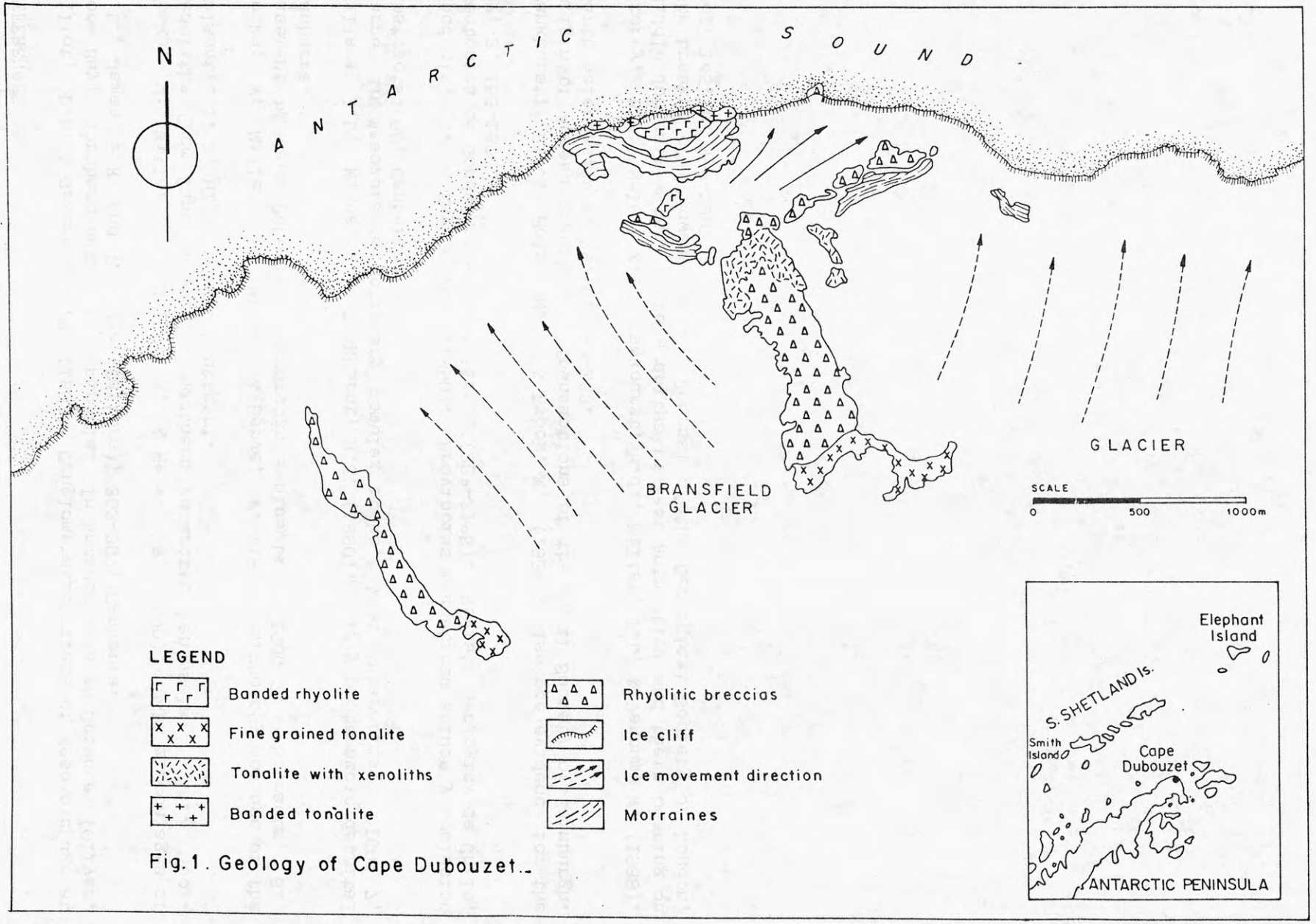

Fig. 1. Geology of Cape Dubouzet.

Interaction between salt weathering, wind action and frost action in the Sor Rondane Mountains, East Antarctica

K. HIRAKAWA, Department of Geography, Tokyo Metropolitan University, Hachiouji-shi, Tokyo 192, Japan

The landforms of the inland Mountains, the Sor Rondane, East Antarctica are produced through the interaction of salt weathering, wind action and frost action, except for the majour sculpturing effect of glaciers. Of these processes, wind action plays a dominant role in various indirect ways.

The measurement of temperature of rock surface and slope debris shows the occurrence of a number of diurnal freeze-thaw cycles and an active layer of 10 to 30 cm depth during the summer season, although the air temperature does not rise above 0 ° c. However, frost heave and related frost creep occur only on the restricted windward slope where exceptionally adequate snow redistribution by wind and subsequent melting of the snow produce high moisture conditions in the active layer. Thus, frost weathering and periglacial mass movement are thought to be limited due to the low water content of subsurface materials. Even on the slopes with high moisture conditions, the very strong katabatic wind prevent the ground from thawing, reaching only 3-5 cm in depth, and therefore from the occurrence of active periglacial slope processes.

Salt weathering is a dominant geomorphic process, particularly in relation to the wind action. The snow redistribution as well as the effective evaporation due to the katabatic wind result in the mechanical disintegration through the growth of salt crystals. Salt segregation is easily recognized almost everywhere, not only on the mountain bed rock slopes but also on the individual morainic blocks. Salt weathering is the majour process of taffoni development or carvaeous weathering. Where the cover of lag gravels prevents the ground surface from down-wearing by wind erosion, the subsurface materials beneath the lag gravels have been frequently totally weathered to show a perfectly disintegrated powder-like horizon, which indicates the very stable condition of ground surface for a long period. On the contrary, where the lag gravels are not formed, wind erosion operates more effectively to produce a mashroom-like form or honeycomb-structure, because the wind has removed the fine materials produced by salt weathering.

It must be stressed that the thickness of the powder-like horizon caused by salt weathering coincides with the thickness of active layer. Such subsurface structure is observed even on the smoothed mountain slopes, which topographically looks like a representative slope due to the periglacial mass movements.

The case hardning layer resistant to weathering should be developed in relation to the evaporation due to the katabatic wind, which is found on the mashroom-like form or on the surface of lag gravels.

Ultramafic granulites from the Lützow-Holm Complex, East Antarctica

Y. Hiroi and Y. Shimizu-Kozaki, Department of Earth Sciences, Faculty of Science, Chiba University, Yayoicho, Chiba 260, Japan
K. Shiraishi and Y. Motoyoshi, National Institute of Polar Research, Kaga, Itabashi-ku, Tokyo 173, Japan

Ultramafic granulites occur as isolated blocks and sheets enclosed in metasedimentary rocks of the Late Proterozoic Lützow-Holm Complex. Their bulk rock compositions and internal structures indicate that they are derived from various parts of layered gabbro including allivalite and pyroxenites. They show various mineral assemblages and textures, offering some insights into their metamorphic evolution.

The ultramafic granulites have neither olivine + plagioclase nor olivine + garnet associations but commonly contain the olivine + spinel + orthopyroxene + pargasite assemblage, indicating that they belong to the spinel-amphibole-lherzolite facies.

The following reactions are written among coexisting olivine, orthopyroxene and spinel in normative olivine-rich rocks, and are used as thermometers.

$1/2Mg_2SiO_4 + FeAl_2O_4 = 1/2Fe_2SiO_4 + MgAl_2O_4$.

$Mg_2Si_2O_6 + MgAl_2O_4 = MgAl_2SiO_6 + Mg_2SiO_4$.

Both the Mg-Fe partitioning between olivine and spinel and the mats-content of orthopyroxene coexisting with olivine and spinel suggest a gradual increase in temperature southwestwards up to the thermal peak located near the outlet of the Shirase Glacier and decrease further westwards, which is in good harmony with other petrological data obtained from pelitic, calc-silicate and basic-intermediate rocks. In general, however, temperatures obtained by the olivine-spinel Mg-Fe exchange thermometers are much lower than those obtained by the "mats" thermometers, indicating recrystallization upon relatively slow cooling.

In some pyroxenites and related rocks, the following continuous prograde reaction is written.

$Ca_2(Mg, Fe)_5Si_8O_{22}(OH)_2 = 2Ca(Mg, Fe)Si_2O_6 + 3(Mg, Fe)SiO_3 + SiO_2 + H_2O$.

The gradual change in chemical composition of amphibole intergrown with two pyroxenes and quartz clearly documents that the reaction was in operation during prograde and progressive metamorphism.

The garnet + orthopyroxene + anorthite + spinel + pargasite ± sapphirine assemblage of normative plagioclase-rich rocks offers other insights. In particular, decompression upon heating is indicated by the partial replacement of Mg-rich garnet (e.g., $prp_{55}alm_{33}sps_3grs_9$) by the orthopyroxene + spinel + anorthite symplectite.

THE LAST MAJOR DEGLACIATION IN THE ANTARCTIC PENINSULA REGION

Christian Hjort, Svante Björck & Olafur Ingolfsson
Department of Quaternary Geology, Lund University, Sölvegatan 13, S-223 62 Lund, Sweden

When northern hemisphere ice-sheets melted at the end of the Wisconsinan/Weichselian glaciation this led to an eustatic rise in global sea level which pushed the grounding line around Antarctica southwards, leading to large scale destruction of fringing ice shelves. The sea inundated isostatically depressed land and this initial deglaciation period, probably ending before 10 000 BP, may be correlated to some undated intermediate altitude shorelines ($\leq$60 m) in the South Shetland Islands. However, most of the presently ice-free areas in the South Shetlands, on the Antarctic Peninsula itself and on the islands in the northwestern Weddell Sea seems to have become ice-free much later. On northern James Ross Island, east of the peninsula, the initial deglaciation occurred between 10 000 and 8000 BP, but it was soon followed by renewed glacier advances, of 20 km or more. In the case of one marine-based glacier this advance was short-lasting, starting after c. 7300 BP and terminating before 6700 BP, whereas the advanced position of one large terrestrial glacier may have lasted until around 5000 BP. Studies of lake sediments and a critical review of ^{14}C-dates throughout the region indicates that in most cases the post-glacial lacustrine sedimentation did not start until between 6000 and 5000 BP, in some cases even later. A corresponding timing is shown by moss banks in the South Shetland- and South Orkney Islands, which did not start growing until around 5000 BP. The only reasonable explanation for this late start seems to be ice cover. This early/mid Holocene glacial readvance, or in some areas perhaps only strongly retarded deglaciation, closely predated or directly corresponded to the formation of the youngest, very distinct marine limit, at 15-20 m. We favour an interpretation of this oscillation, affecting both terrestrial and marine-based glaciers, as due to regionally increasing precipitation - perhaps a combined effect of the encroaching sea and increasing Milankovich-type solar insolation ?

CARBONATE BRECCIAS AND PSEUDOTACHYLITES, STRUCTURALLY RELATED TO ALKALINE LAMPROPHYRE DYKES IN THE VESTFOLD HILLS: A POSSIBLE PHANEROZOIC EVENT IN THE EAST ANTARCTIC SHIELD.

J.D. Hoek & C.W. Passchier Department of Structural Geology, Institute of Earth Sciences, P.O.Box 80.021, TA 3508 Utrecht, Netherlands

Carbonate breccias are relatively widespread in the Vestfold Hills. They generally occur on the border of alkaline lamprophyre dykes, less often along tholeiitic dykes of similar orientation. Pseudotachylite is often associated with carbonate breccias parallel to alkaline dykes.

A case study is made of the association of carbonate-rich breccia, pseudotachylite, and alkaline lamprophyre. Pseudotachylite is present in the dyke as veins of up to 1 cm wide, as the remains of a vein on the border of the dyke, and as inclusions in the breccia. The breccia forms a vein of up to 5 cm wide between dyke and host-rock. Apart from the presence of ± 15 wt% CO2 in the breccia, its chemical composition is roughly equivalent to that of the orthogneiss host-rock. The pseudotachylite is chemically equivalent to the dyke material and contains abundant bubbles, indicating that the pseudotachylite formed as a friction melt. The boiling of this melt is due to the composition of the lamprophyric dykes, containing up to 5 wt% CO2. Pseudotachylite inclusions in the breccia have amoeboid shapes, indicating that both pseudotachylite and breccia-matrix both behaved as viscous fluids during brecciation. Pseudotachylite and breccia must have been formed simultaneously during a single, short-lived, deformation event involving seismic slip on the contact between dyke and host-rock. The fluid state of the breccia was due to fluidization by a CO2-rich volatile phase. This phase boiled off from the friction melt and pervaded a zone of fractured gneiss immediately next to the slip plane.

The alkaline dykes are cut by tholeiite dykes, dated at 1250 Ma. These dykes pre-date a 1000 Ma, amphibolite grade, metamorphic event. Pseudotachylite shows no evidence of porphyroblast growth and in one instance contains non-devitrified glass. Therefore, the formation of carbonate breccias cannot be related to the intrusion of the alkaline dykes, and must be younger that 1000 Ma.

Typical displacements along breccia zones are in the order of 1-10 meters. Larger displacements occur along non-exposed valleys which form the most conspicuous lineaments in the Vestfold Hills. Breccia material can generally be found along these zones. The ubiquity of carbonate breccias in the Vestfold Hills and in the Rauer Islands, where they also form the last event, implies that they represent a significant brittle deformation phase of possible Phanerozoic age.

THE PROTEROZOIC STRUCTURAL EVOLUTION OF THE VESTFOLD HILLS, AN ARCHAEAN CRATON IN A PROTEROZOIC METAMORPHIC BELT, EAST ANTARCTIC SHIELD.

J.D. Hoek & C.W. Passchier Department of Structural Geology, Institute of Earth Sciences, P.O.Box 80.021, TA 3508 Utrecht, Netherlands

The Vestfold Hills are part of an Archaean nucleus in the East Antarctic Shield, surrounded by an extensive Proterozoic Belt exposed along the Prydz Bay coast.

The Proterozoic Belt underwent extensive deformation and metamorphism at granulite facies conditions around 1000 Ma ago. Petrological data indicate near-isothermal decompression accompanied by ductile deformation. This has been interpreted as a crustal thickening event, possibly accompanied by anomalously high heat flow conditions (Harley, 1988; Stüwe & Powell, 1990). In the Vestfold Hills, ± 25 Km NE of the Rauer Islands in the southernmost part of the Belt, the effects of the 1000 Ma event are much less pronounced. Dolerite dykes which intruded around 1250 Ma ago were metamorphosed around 1025 Ma ago (Black *et al.*, 1990). In the SW Vestfold Hills this led to growth of garnet + hornblende in the dykes. A maximum estimate for the depth of intrusion of the dykes is equivalent to 4-5 Kb, while metamorphic assemblages in the dykes indicate 5-6 Kb (Kuehner 1986, unpubl. Ph.D., Hobart). A ductile deformation event, at greenschist to amphibolite facies conditions, post-dates dyke intrusion and largely pre-dates metamorphism. This event involves thrusting towards the NE on mylonite zones up to 1 m wide (PASSCHIER *et al.*, 1991). In the SW, pegmatites which cut across the dykes are mylonitized. These pegmatites are possibly related to the orthogneisses that formed in the Rauer Islands during the 1000 Ma event.

The 1250 Ma dykes cut across pseudotachylite veins, indicating that brittle conditions prevailed in the Vestfold Block prior to the 1000 Ma event. The overprinting of a brittle by a ductile deformation phase and independent barometry indicate that the Vestfold Hills underwent burial during the 1000 Ma event (PASSCHIER *et al.*, 1990). The presence of pegmatites and metamorphic assemblages in the SW Vestfold Hills indicate a metamorphic gradient towards the Rauer Block, but a strain gradient is absent in the Vestfold Hills. The Vestfold Block, with only limited internal deformation along isolated ductile shear zones, was relatively rigid compared to the Rauer Block. Burial of the Vestfold Block contemporaneous with syn-kinematic decompression of the Rauer Block into the presently observed juxtaposition, indicates that the Rauer Islands formed part of a regional hanging wall, overthrusting the Vestfold Hills.

references

Black,L.P., Sheraton,J.W., Kinny,P.D. & Maxwell,S. (1990) in *Geol.Soc. Australia* **28**, abstracts.
Harley,S.L. (1988) *J.Petr.***29**, 1059-1095.
Passchier,C.W., Hoek,J.D.,Bekendam,R.F. & De Boorder,H. (1990) *Prec.Res.* **47**, 3-16
Passchier,C.W., Bekendam,R.F. Hoek,J.D., Dirks,P.H.G.M. & De Boorder,H. (1991) *Geol.Mag.* **128**
Stüwe,K. & Powell,R. (1990). *J.Metam. Geol.* **7**, 465-484

COMPOSITIONAL CHANGE OF CONTINENTS THROUGH GEOLOGIC TIME, AND THE RIFTING OF A SUPERCONTINENT

R. Hori and S. Maruyama, Department of Earth Science and Astronomy, University of Tokyo at Komaba, Tokyo 153, Japan.

A new method of estimating the secular variation of average continental compositions through geologic time, is proposed. The method uses the compositions of deep-sea clays intercalated with bedded cherts with or without BIF (banded iron formation). The range of compositional variations of present-day red clays is examined in the Atlantic, Pacific and Indian Oceans, and it is concluded that the red clays were derived from the loesses mainly of arid areas on the continents. Compositions of red clays roughly correspond to the average chemical compositions of continents estimated by several different methods such as average shale composition in a global scale etc.

Using the compositions of ancient deep-sea sediments in orogenic belts back to 3.5Ga, the secular variations of average continental compositions are estimated. The result does not seem to support the well-known secular variations proposed by many authors (e.g., Condie, 1982). For example, the K_2O/Na_2O ratio lies in the range 0.5-4.08 through the last 3.5Ga, and does not show any significant difference between Archean and Proterozoic times. Instead, anomalous pulses, with ratios up to 20, occur twice at 0.21Ga and 1.9Ga(Fig. 1). Ratios for shales behave similarly to those for deep-sea sediments, and the 0.5-0.6 Ga shale compositions suggest the presence of a third anomalous peak. These pulse periods correspond well to the frequency peaks of carbonatites through the Earth history (Wooly, 1989), and to the geologically estimated times supercontinent break up. The first supercontinent is estimated to have been formed at 1.9Ga(Hoffman, 1989), the second at 0.6Ga is Gondwanaland, and the third is Pangaea at 0.2-0.3 Ga.

The correlation between MgO and K_2O of deep-sea sediments indicates that the anomalously high K_2O/Na_2O ratios are due to the input of volcanic ashes with high MgO and K_2O contents. The explosive magmas called Group II kimberlite are characterized by high MgO(30wt.%) and high K_2O(15wt.%), and are formed only at the onset of break-up of a supercontinent. Other volcanic rocks with different tectonic settings, do not show such high K_2O/Na_2O rations usually less than 1.0. For example, the ratio does not increase even if the subduction magma becomes abnormally active. Thus, we speculate that the K_2O/Na_2O ratio monitors well the timing of break-up supercontinent through geologic time. Secondly, the abrupt change in average composition of continents between the Archean and Proterozoic is doubted.

Chert/BIF around 1.1Ga and 0.6Ga is critical to discuss the formation of supercontinents during the late Proterozoic time. It occurs in Pan-African orogenic belts, but has not well described. The information from Antarctica would contribute to our understanding on the compostional evolution of continents and the presence or absence of supercontinent(s) in those periods.

References cited

Condie,K.C.(1982): "Plate tectonics and Crustal Evolution". 2nd edition, Pergamon Press. 310p.
Hoffman,P.E.(1989): Speculation on Laurentia's first gigayear (2.0 to 1.0Ga). Geology,17, 135-138.
Wooly,A.R.(1989): The spatial and temporal distribution of carbonatites. *In* "Carbonatites". Unwin Hyman, London, 15-69.

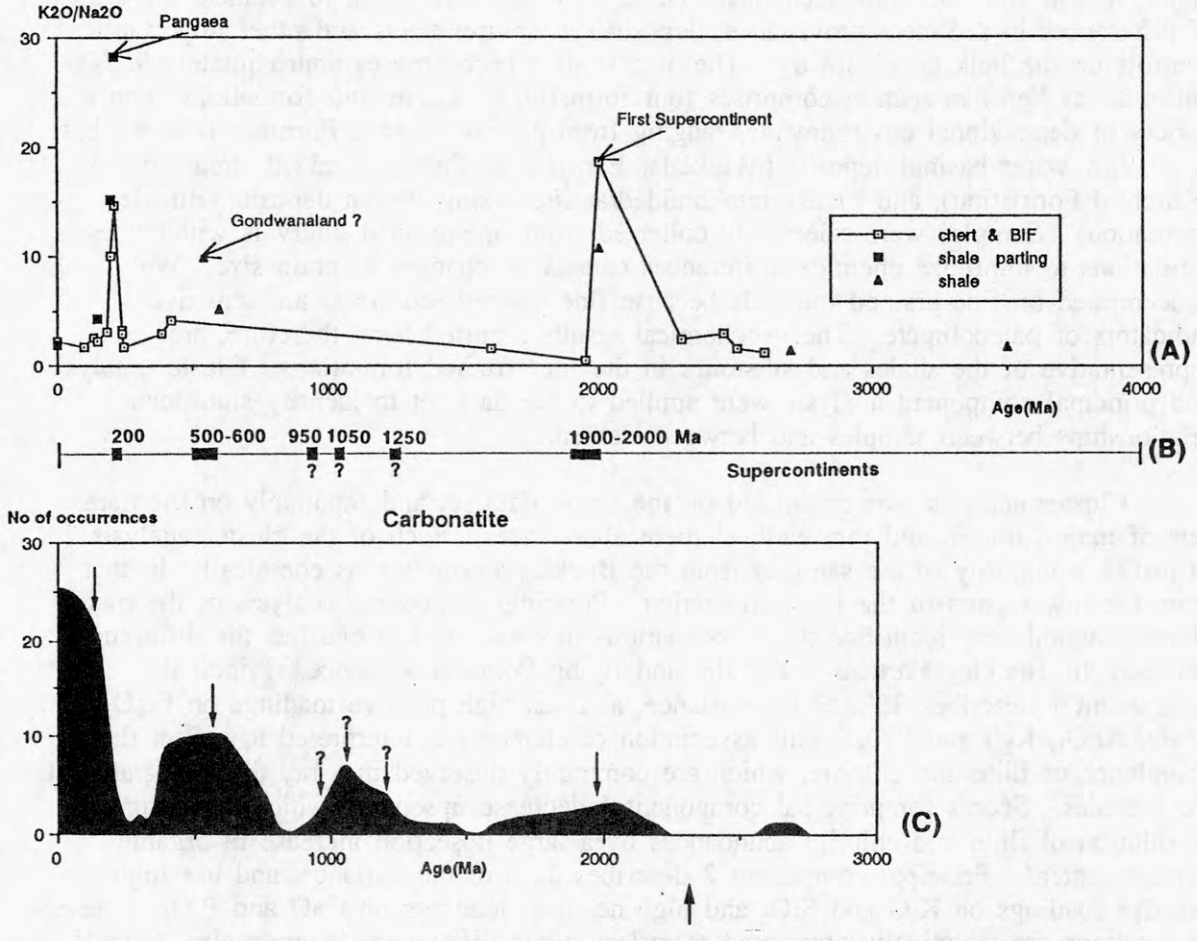

Figure 1. (A): Seqular variation of K_2O/Na_2O ratios of chert & BIF, shale parting of bedded chert, and shale. (B): Appearance of supercontinents in the earth history. (C): Frequency of carbonatites through geologic time, modified from Wooly (1989).

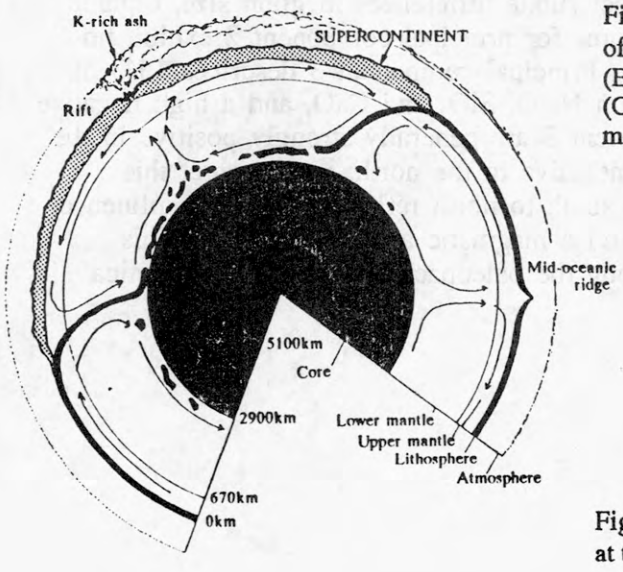

Figure 2. A speculative model to explain K_2O-pulse at the onset of break-up supercontinents.

STATISTICAL ANALYSIS OF GEOCHEMICAL PATTERNS IN FINE-GRAINED PERMIAN SEDIMENTS FROM THE BEARDMORE GLACIER REGION, ANTARCTICA

T. C. Horner and L. A. Krissek, Dept. of Geological Sciences and
Byrd Polar Research Center, The Ohio State University,
Columbus, Ohio 43210

Ninety-one samples of fine-grained Permian sediments from the Beardmore Glacier area of the Central Transantarctic Mountains, Antarctica, have been analyzed for 47 major, minor, and rare earth elements. These data have been used to evaluate the effects of differences in sediment provenance, depositional environments and other important controls on the bulk geochemistry. The area studied encompasses approximately 90,000 km^2, and its Permian section comprises four formations. These four formations span a variety of depositional environments, ranging from glacial (Pagoda Formation) at the base, to shallow water basinal deposits (Mackellar Formation), through braided stream deposits (Fairchild Formation), and finally into braided/anastomosing stream deposits (Buckley Formation). Samples were selectively collected from fine-grained intervals within these formations to minimize chemical differences caused by changes in grain size. We concentrated on fine-grained intervals because fine-grained sediments are sensitive indicators of paleoclimate. The geochemical results reported here, therefore, are representative of the shales and siltstones in the four studied formations. Cluster analysis and principal component analysis were applied to the data set to identify significant relationships between samples and between elements.

Cluster analysis was conducted on the entire data set and separately on the data sets of major, minor, and rare earth element abundances. Each of the cluster analysis identifies a majority of the samples from the Buckley Formation as chemically distinct from the lower parts of the Permian section. Principal component analysis of the major element abundances identifies three associations of elements and clarifies the differences between the Buckley Formation and the underlying Permian sequence. Principal component 1 describes 36% of the variance, and has high positive loadings on Fe_2O_3, MgO, Al_2O_3, K_2O and P_2O_5. This association of elements is interpreted to reflect the abundance of illite and chlorite, which are commonly observed in x-ray diffractograms of the samples. Scores for principal component 1 decrease upsection, which is interpreted as dilution of illite and chlorite abundances by a large upsection increase in organic carbon content. Principal component 2 describes 22% of the variance, and has high positive loadings on K_2O and SiO_2 and high negative loadings on CaO and P_2O_5. These associations are tentatively interpreted to reflect subtle differences in grain size, organic carbon content or diagenetic effects, since scores for principal component 2 exhibit no consistent geographic or stratigraphic pattern. Principal component 3 describes 15% of the variance, and has high positive loadings on Na_2O, SiO_2 and CaO, and a high negative loading on K_2O. Scores for principal component 3 are generally strongly positive in the southern part of the study area and strongly negative to the north; we interpret this pattern in terms of provenance changes from south to north reflecting stronger influence of a continental/granitic source to the north and a magmatic arc to the south. This pattern is consistent with overall relations along the paleopacific margin of Antarctica during Permian time.

A P-WAVE VELOCITY STRUCTURE OF MT. EREBUS AS DERIVED FROM A SEISMIC EXPLOSION EXPERIMENT

A. Ikami, Earthquake Research Institute, University of Tokyo, Yayoi, Bunkyo-ku, Tokyo 113, Japan
K. Kaminuma, National Institute of Polar Research, Kaga, Itabashi-ku, Tokyo 173, Japan
M. Shimizu, T. Taniguchi, and H. Nishinaka, Department of Earth Science, Aichi University of Education, Kariya 448, Japan

Seismic observations have been made at Mt. Erebus (3794 m) in Ross Island, Antarctica, to study the seismicity and volcanic activity. A seismic explosion experiment was conducted on Mt. Erebus from Nov. to Dec., 1984 during the IMESS (International Mt. Erebus Seismological Studies) program. In addition to the seismic network installed by IMESS, three temporary stations on the summit and four on the side of the mountain were set to observe the seismic explosion experiment. At these temporary stations, a magnetic tape recorder of a direct recording system was operated. Seven shots were detonated at four sites, nearby one of the seismic stations.

The experiment was not designed as in the normal explosion experiment style. Shot points and observation station were not on a special profile line, so ordinary refraction analysis technique could not be applied. In addition to the station configuration, station altitudes varid from sea level to over 3000 m. The observation data are not good enough to elucidate a precise structure. Therefore, we determined a simplified structure, assuming a linear increase of velocity with depth, namely

$$V = Vo + a\,z$$

where Vo is the velocity at the horizontal datum plane, V the velocity at a depth z below the datum plane and a is a constant. In this case, there are only two unknown parameters, Vo and a. The ray path calculated from a linear velocity increase model is a circle. Therefore, we can calculate a ray path and the travel time along the path between a shot and a station, even if their altitude difference is large.

In this study, we calculated travel times for models with Vo (3.0 km/s to 4.9 km/s with an interval of 0.1 km/s) and a (0.20/s to 0.39/s with an interval of 0.01/s), and then compared between the calculated travel times and the observed ones. The minimum deviation picked up as the best solution was:

$$Vo = 3.9 \text{ km/s}$$
$$a = 0.26 \text{ /s}$$

The model shows slightly slower velocity structure than that derived by Murakami et al. (1988), who assumed a layered structure.

The derived crustal structure is applied to hypocenter determination in the area, and we discuss the seismicity recalculated form the model.

MAJOR COVER SEQUENCES IN THE ANTARCTIC SEDIMENTARY BASINS AND APPROACH TO THEIR CORRELATION

V.L.Ivanov, North Branch for Marine Geologic Research and Exploration "Sevmorgeologia", 120 Moyka, 190121 Leningrad, USSR

1. During two last decades considerable progress was achieved in studying the offshore Antarctic sedimentary basins (ASB) and, to a lesser extent, those beneath the continental ice sheet [Ivanov and Kamenev, 1990; Ivanov et al.,1990; Hinz and Kristoffersen, 1987; Ivanov, 1989; Kimura, 1982; Eittreim and Hampton, 1987; Cooper and Davey, 1987]. About 20 ASB are recognized that underlie up to 40% of the Antarctic continent and adjacent shelf (Fig.1).

2. Formation of ASB was influenced by different geodynamic environments which overlapped both spatially and in time. Three principal evolutionary trends are distinguished:

- interaction between a stable platform (the Precambrian Shield of East Antarctica) and a mobile belt (the Pacific active margin of West Antarctica);this trend is rather typical of continental crust evolution elsewhere in the world and is characterized by mutual influence of controversial geodynamic processes at the junction of "antagonistic" continental geoblocks;

- destruction of continental crust that simultaneously leads to opening of the Southern Ocean and formation of new sedimentary crustal layer on the Antarctic passive margin;

- development in Cenozoic time of a specific circum-Polar morphostructural grain defined by the central position of the Antarctic continent among surrounding oceanic abyssal plains with anomalously high sedimentation rates.

3. The cyclic nature of evolution of ASB is reflected in stratigraphic range and composition of major structural units recognized in several studied cover sections (Fig.2).

3.1. In late Proterozoic and early Paleozoic time accumulation of platform sediments and subordinate volcanic activity were related to moderate extension and thinning of sialic crust along the margins of rising continental landmass. Such platform sequences were subsequently incorporated in the basement and/or basal cover complexes of Gondwana basins (South Weddell Sea Basin), or remained uncovered by younger basin deposits and were later locally exposed in bedrock outcrops (Western Queen Maud Land).

3.2. Renewal of basin accumulation during Carboniferous - Triassic time resulted in extensive Beacon sedimentation, although the paleotectonic scenario was at this stage quite different. Predominance of essentially epicontinental trough facies indicates deposition in linear, graben-like depressions

that dissected the ancient platform or followed its junction with the active paleomargin. The system of Beacon grabens is now largely involved in the Transantarctic Mountains uplift, although their off-branches are believed to continue beneath the adjacent Victoria Land Basin and correspond to embryonic phases of basin evolution that occurred here predominantly in Cenozoic time.The existence in East Antarctica of other intracontinental failed rift basins with the earliest cover units in the same stratigraphic range (Lambert Glacier Basin, Jutulstreumen Basin, etc.) suggests that the Beacon grabens represented an Antarctic component of initial breakup network which must have emerged at that time throughout the Gondwana supercontinent.

3.3. After a relative decline in Late Triassic - early Jurassic time, the intensity of cover accumulation reached its peak due to combined effect of basin-forming geodynamic processes and especially destruction of continental crust by rifting. Breakup-related epicratonic basins of East Antarctica that were generated at that stage include the Brunt Basin, the Princess Martha Basin, inferred basins of the Lasarev, the Riiser-Larsen and the Cosmonaut Seas, the Cooperation Sea Basin, the Dumont D'Urville Sea Basin; beginning of their formation ranges, respectively, from 180 - 150 Ma (Jurassic) to 55-50 Ma (Eocene). The Ross Sea Megabasin was formed by the Cenozoic extensional rifting superposed on the Late Mesozoic active margin. The Weddell Sea Megabasin encloses the most complicated structural mosaic controlled by overlapping influence of two principal paleoenvironments - (1) interaction between the East Antarctic Precambrian shield and the West Antarctic Meso-Cenozoic active margin, and (2) transformation of continental crustal assemblages into oceanic lithosphere along the East/West Antarctica junction. Both factors led to predominant subsidence of vast crustal terrains, despite significant lateral heterogeneities that might have existed in these terrains prior to Gondwana breakup and formation of the Southern Ocean. The term "borderline areal downwarps" is suggested to designate transregional geostructural features of that kind.

Finally, formation of the circum-Polar morphostructural grain was completed by the Bellingshausen Sea and the Amundsen Sea Basins, as well as by other, as yet very poorly studied, abyssal basins in the outer part of the Antarctic plate.

4. The common features recognized in cover sequences of ASB reflect a similarity of major tectonic processes that controlled the basin formation, while specific characteristics of individual basins apparently result from different combinations of these processes. The following major tectono-stratigraphic units are typically present in the ASB covers:

(1) "paraplatform" or "intermediate" unit related to early post-cratonization stages (late Precambrian to early Paleozoic) of evolution of an ancient platform:

(ii) "pre-breakup" unit that includes variable sequences accumulated in similar depositional environments (relatively open, mostly linear depressions - rift grabens, aulacogens, foredeeps, marine embayments of limited extent, etc.) prior to Gondwana breakup or during the initial phases of the supercontinent's destruction (predominantly in late Paleozoic and early Mesozoic time);

(iii) "breakup" unit represented by a uniform sedimentary cover of late Mesozoic to Cenozoic age formed in connection with oceanic openings around the Antarctic continent.

ASB are believed to belong to a single evolutionary succession initiated in pericratonic paleobasins adjacent to the East Antarctic ancient platform and terminating in abyssal structural provinces of the present-day Southern Ocean. Transitional members of that succession are represented by vast passive margin basins characterized by the thickest and most composite sedimentary cover: the latter incorporates, as a rule, all three or at least two of the major tectono-stratigraphic units (Fig.3).

Most common in the studied sections is the "pre-breakup" unit. It makes up the bulk of cover volume in both the basins superposed on relatively well preserved sialic basement and those where the original structure of continental crust has been strongly affected by extension and deep incision of syn-rift deposits. The "breakup" unit and especially its uppermost syn-glacial sequences occur predominantly in the off-shore parts of ASB as a rather continuous, although often diachronous cover.

REFERENCES:

Cooper A.K., Davey F.J., 1987, eds.The Antarctic continental margin: geology and geophysics of the Western Ross Sea. Circ.-Pacif.Counc. Energy Miner. Resourc..Earth Sci.Ser., v.5B, Houston, 253 pp.

Eittreim S.L., Hampton M.A., 1987, eds. The Antarctic continental margin: geology and geophysics of offshore Wilkes Land. Circ.-Pacif.Counc. Energy Miner. Resourc., Earth Sci.Ser., v.5A, Houston, 221 pp.

Hinz K., Kristoffersen Y.,1987. Antarctica recent advances in the understanding of the continental shelf. Geol.Jb., E, H.37, 54 pp.

Ivanov V.L., Kamenev E.N.,1990, eds. The geology and mineral resources of Antarctica. Moscow, "Nedra", 232 pp.(in Russian).

Ivanov V.L., Grikurov G.E., Kurinin R.G., 1990. The Antarctic continental margin: structure, evolution and study approach. The Soviet Geology, 12, p.47 - 58 (in Russian).

Ivanov V.L., 1989. Evolution of Antarctic prospective sedimentary basins. Antarctic Science, 1 (1), p.51 - 56.

Kimura K.,1982. Geological and geophysical survey in the Bellingshausen Basin off Antarctica. Antarct. Rec.,75, p.12-24.

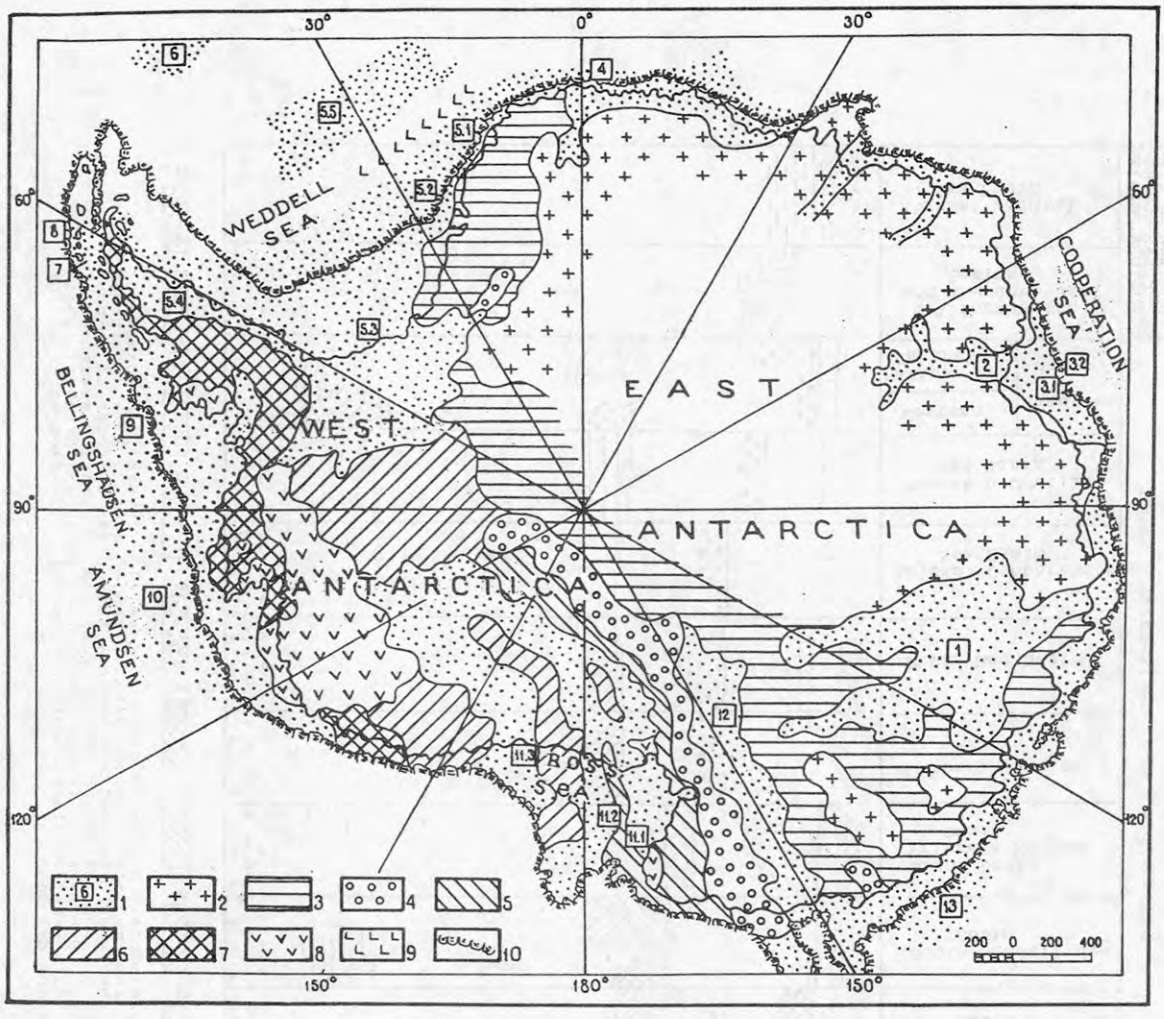

Fig.1. Location of sedimentary basins with respect to structural provinces of the Antarctic continent. 1 - sedimentary basins. Structural provinces and/or tectonotypical complexes: 2-4 - ancient platform of East Antarctica (2 - Precambrian crystalline basement, 3 - Upper Proterozoic to Lower Paleozoic platform cover, 4 - Middle Paleozoic to Lower Mesozoic Beacon sequences); 5-7 - fold belts (5 - Precambrian to Lower Paleozoic folded complexes of the Ross Orogen, 6 - Precambrian to Upper Paleozoic(?) folded complexes in the West Antarctic interior, 7 - Mesozoic to Cenozoic folded and undeformed rocks of the Andean Orogen); 8 - Cenozoic plateau basalts; 9 - oceanic floor. 10 - shelf break.

Sedimentary basins (numbers in boxes): 1 - Wilkes Land Basin, 2- Lambert Glacier Basin, 3-Cooperation Sea Megabasin (3.1-Prydz Bay Basin, 3.2- Abyssal Cooperation Sea Basin), 4- Jutulstreumen Basin, 5 - Weddell Sea Megabasin (5.1 - Princess Martha Basin, 5.2 - Brunt Basin, 5.3 - South Weddell Sea Basin, 5.4 - West Weddell Sea Basin, 5.5 - Abyssal Weddell Sea Basin), 6 - South Orkney Basin, 7 - Bransfield Strait Basin, 8 - South Shetland Basin, 9 - Bellingshausen Sea Basin, 10 - Amundsen Sea Basin, 11- Ross Sea Megabasin (11.1- West Ross Sea Basin, 11.2- Central Ross Sea Basin, 11.3 - East Ross Sea Basin), 12 - Victoria Land Basin, 13 - Dumont D'Urville Sea Basin.

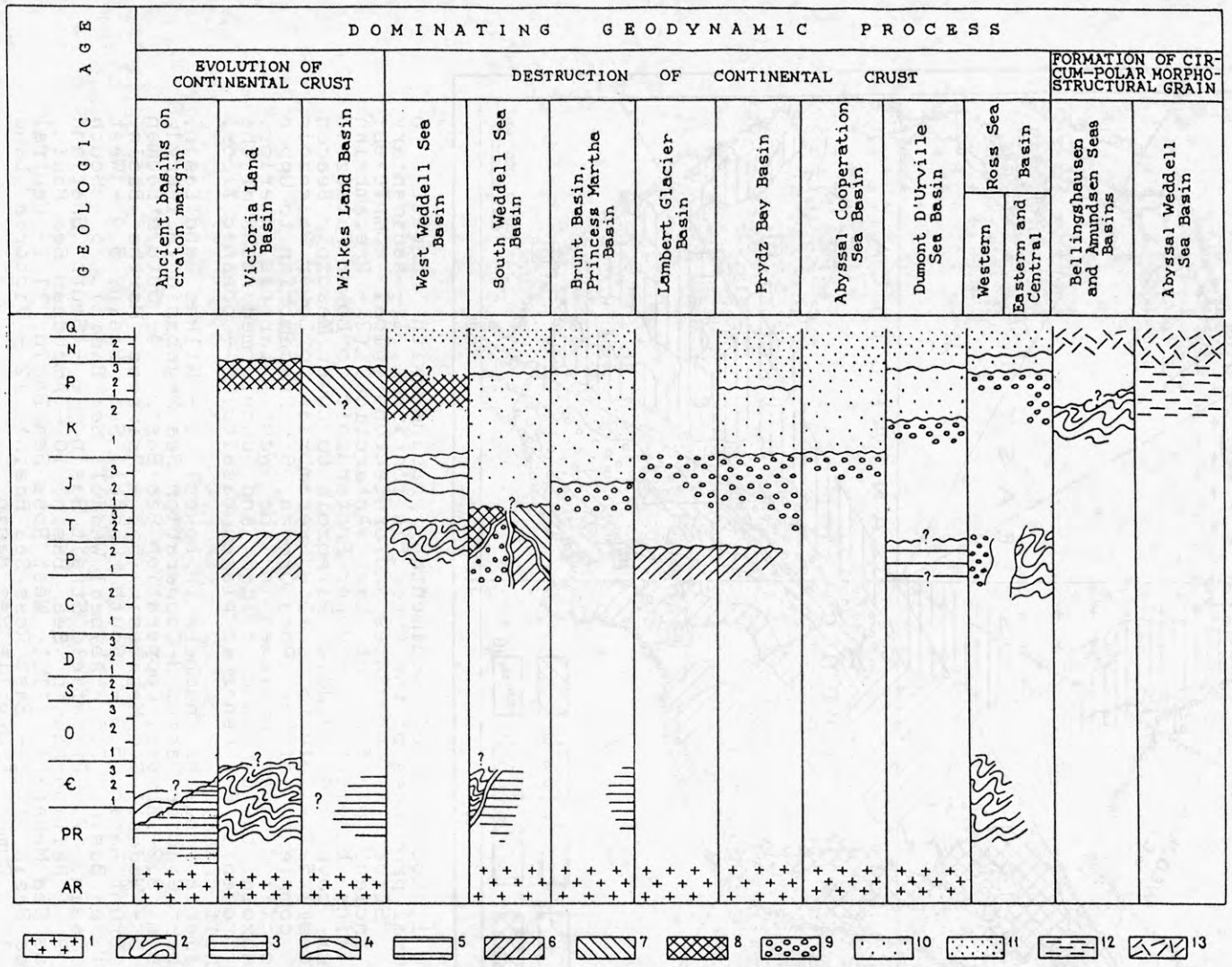

Fig.2. Evolution of Antarctic sedimentary basins in geologic time. 1 - crystalline basement; 2 - folded basement; 3-5 - "intermediate" tectono-stratigraphic unit; 3 - undeformed metasedimentary sequences, 4 - gently deformed metasedimentary sequences, 5 -rocks of unknown origin; 6-9 - "pre-breakup" unit: 6 - non-marine and paralic clastics, 7 - marine sequences of restricted extent, 8 - molasses, 9 - synrift trough deposits; 10-13 - "breakup" unit: 10 -shallow marine sediments, 11 -shallow glacial-marine clastics, 12 -deep-water marine facies, 13 -deepwater glacial marine deposits

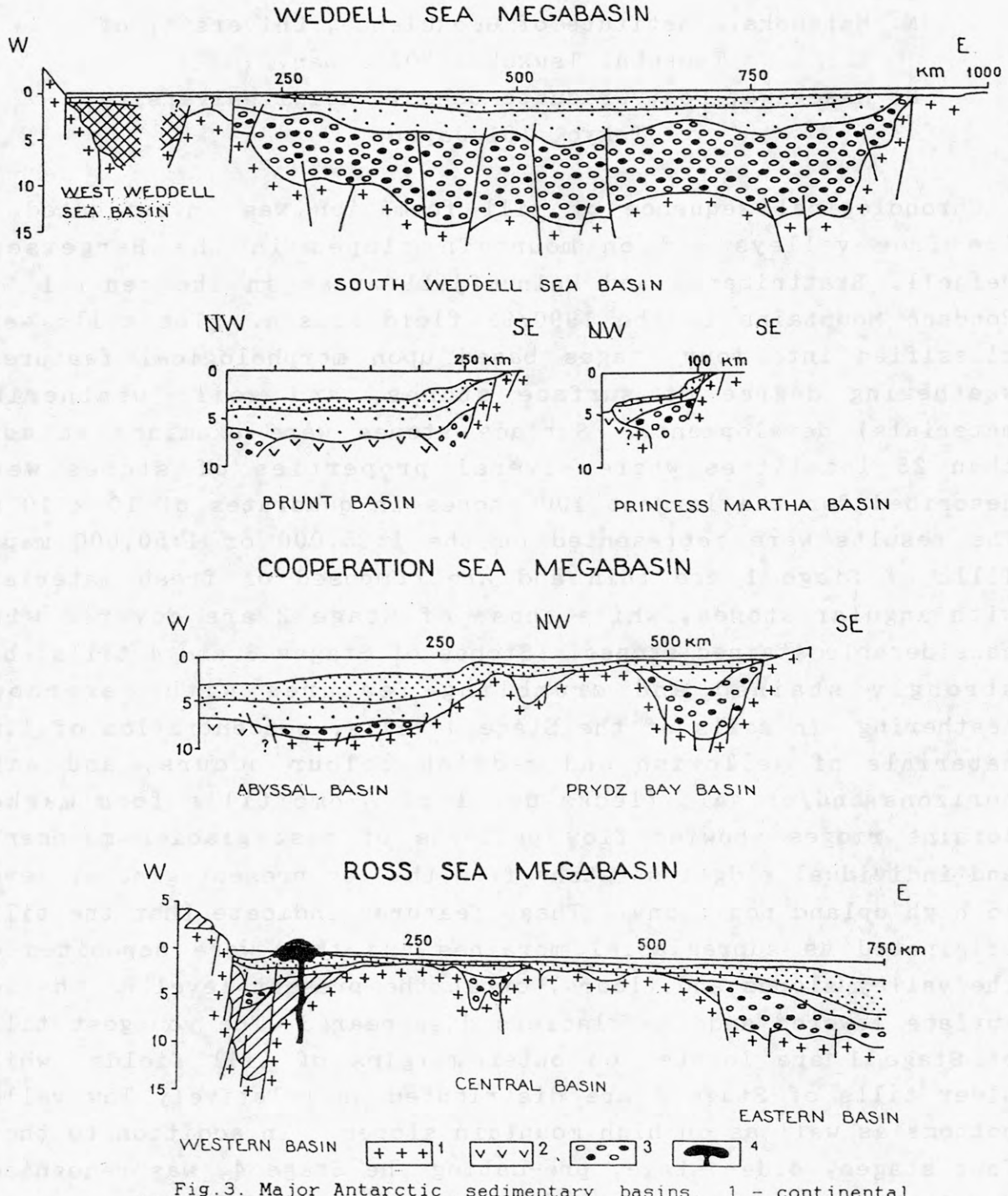

Fig.3. Major Antarctic sedimentary basins. 1 - continental basement, 2 - oceanic basement, 3 - heterogeneous tectono-stratigraphic cover unit, 4 - Cenozoic volcanoes; for other symbols see explanation to Fig.2. For better comparison all sections are shown at one scale.

MAPPING OF TILL DISTRIBUTION IN THE SØR RONDANE MOUNTAINS, EAST ANTARCTICA

S. Iwata, Department of Geography, Mie University, Tsu, 514 Japan.
N. Matsuoka, Institute of Geoscience, University of Tsukuba, Tsukuba, 305 Japan.
H. Hasegawa, Post Graduate School, Meiji University, Tokyo, 101 Japan.

Chronological sequence of till formation was investigated in ice free valleys and on mountain slopes in the Bergersen, Mefjell, Brattnipene, and Walnumfjell areas in the central Sør Rondane Mountains in the 1990/91 field season. The tills were classified into four stages based upon morphological features, weathering degree of surface stones, and soil (weathering materials) development. Surface stones were examined at more than 25 localities where several properties of stones were described for the largest 100 stones in quadrates of 10 x 10 m. The results were represented on the 1:25,000 or 1:50,000 maps. Tills of Stage 1 are thin and are composed of fresh materials with angular stones, while those of Stage 2 are covered with considerable stained stones. Stones of Stages 3 and 4 tills show strongly stained and crumbling features with cavernous weathering. In soils of the Stage 4 tills, concentration of fine materials of yellowish and reddish colour occurs, and salt horizons and/or salt flecks develop. Some tills form marked moraine ridges showing flow patterns of past glacier movement, and individual ridges stretche from the low present glacier level to high upland positions. These features indicate that the tills originated as supraglacial moraines and then were deposited on the valley slopes and floors, or at the present level as the ice surface lowered and the glaciers disappeared. The youngest tills of Stage 1 are located on outer margins of till fields, while older tills of Stage 4 are distributed on relatively low valley bottoms as well as on high mountain slopes. In addition to these four stages, older stage, pre-dating the Stage 4, was recognized on the high plateau in Mefjell. These till sequences seem to correspond with those in the Transantarctic Mountains (Campbell and Claridge, 1987). Although no absolute dating was obtained, exposure ages of bedrock dated by analyzing cosmic ray bombardment products (Nishiizumi, 1989; Moriwaki et al., 1991) suggest that the oldest till formed more than 3 Ma ago and even the younger four stages are of considerable antiquity.

UPLIFT HISTORY OF THE HEIMEFRONTFJELLA METAMORPHIC COMPLEX (DRONNING MAUD LAND), ASSESSED BY FISSION TRACK ANALYSIS

J. Jacobs & K. Weber, Institut für Geologie und Dynamik der Lithosphäre, Goldschmidtstr. 3, 3400 Göttingen
E. Hejl & G.A. Wagner, Max-Planck-Institut für Kernphysik, Saupfercheckweg 1, 6900 Heidelberg (F.R.G.)

The "Heimefrontfjella Metamorphic Complex" (HMC) in Dronning Maud Land is an 1100 Ma old mountain belt which can be correlated with the Kibaran event in southern Africa (Arndt et al., 1991; Weber et al., this volume). K/Ar mineral-data from white mica and biotite indicate a second thermal event during Pan-African times (Jacobs, in prep.). A non-metamorphic sequence of 100 m Permo-Carboniferous sandstone overlies the HMC horizontally. The Palaeozoic erosion surface is exposed in the northern part of the studied area at three localities at a constant elevation of ≈2100 m (Fig. 1). Basement outcrops above this level, up to 2700 m, appear only in the central part of this mountain range. The youngest features are mafic Jurassic dykes, sills and flows indicating the initiation of the Gondwana breakup.

Apatite fission track (AFT)-ages and confined/projected track length distributions have been determined for 20 samples from basement rocks of the HMC. AFT-ages have an effective closing temperature of ≈100°C and thus offer important information about the very low temperature and uplift history. Samples were collected from three vertical profiles between 1000 and 2700 m. Sample locations are indicated on Fig. 1.

The exposed Palaeozoic erosion surface indicates that the basement must have been cooled down to temperatures below 100°C during Palaeozoic times. However, all AFT-ages display Mesozoic ages between 90 and 220 Ma. The ages fall into two groups, one having Upper Cretaceous ages of around 100 Ma, the other having older ages of 130 to 220 Ma. We assume that this age-reduction is due to a thermal event at the beginning of Gondwana breakup and the loading/burial caused by a thick pile of Jurassic lava flows.

Most samples with Upper Cretaceous AFT-ages were collected from profile A of approximately 2000 m elevation and at Mannefallknausane. They show a positive correlation with elevation (Fig. 2). The confined track length distribution of ≈14,5 µm indicate that these ages are cooling ages (Fig. 1 + 2). Uplift must have been quite rapid (≈100 m/Ma from the elevation/age profile). The calculation of the 60°C cooling ages using the cs/ci-method of WAGNER (1988) gave ages of about 50 Ma.

Profile C consists of only two samples. Sample A718 (1200 m) also yields a cooling age of ≈100 Ma. The second sample is a granite dropstone from the lower beds of the Permo-Carboniferous sediments (2120 m). This dropstone must have cooled down long before the incorporation into the sediments, however, it revealed an age of only 150 Ma. The confined track length distribution revealed a mean track length of only ≈13 µm and the shape of the length distribution (Fig. 1) clearly indicates a mixed age. Thus, it can be concluded that this sample has been reheated up to temperatures of the apatite "partial annealing zone" (PAZ = 60 - 125°C) but not above it and that the base of the fossil PAZ must have lain somewhere between the samples.

Profile B consists of seven samples collected from elevations between 1750 and 2500 m.

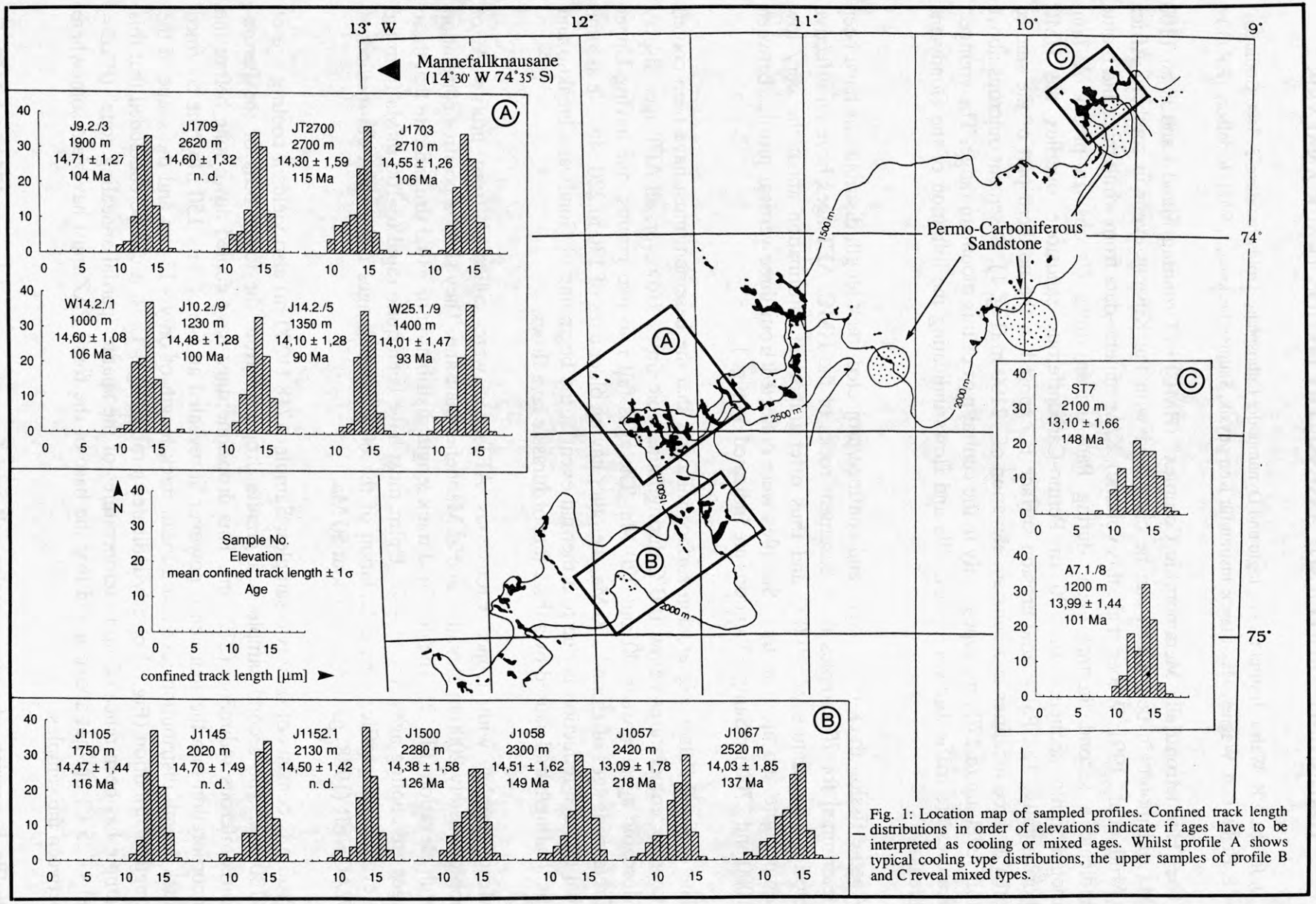

Fig. 1: Location map of sampled profiles. Confined track length distributions in order of elevations indicate if ages have to be interpreted as cooling or mixed ages. Whilst profile A shows typical cooling type distributions, the upper samples of profile B and C reveal mixed types.

Only five of them proved to be suitable for dating, but the confined track length distribution has been determined for all of them. The five ages scatter from 110 to 220 Ma, but only the highest age can clearly be interpreted as a mixed age. The lower three samples (Fig. 1) show cooling type length distributions, whereas the upper four ages show slightly reduced mean confined track length and the shape of the confined track length distributions get closer to typical mixed age types with elevated standard deviations. We conclude that the ages and confined track length distributions of the four highest samples (2300 m to 2500 m) indicate that they are located at the base of a fossil PAZ, probably equal to the PAZ identified in profile C.

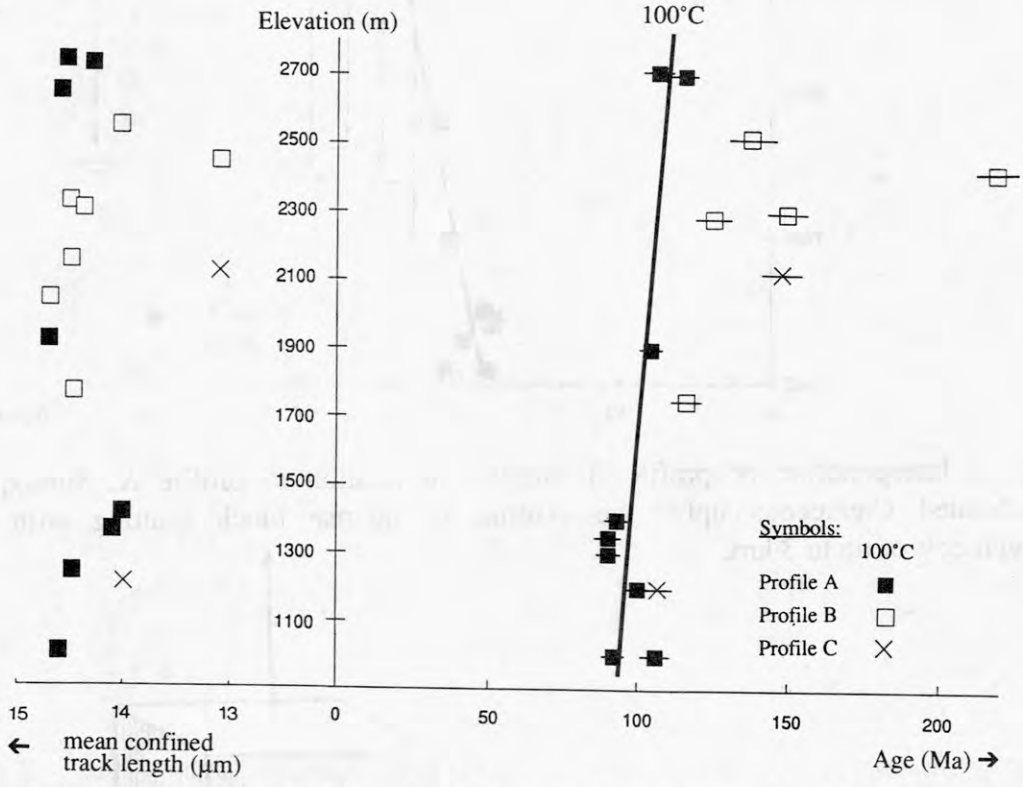

Fig. 2: The age-elevation diagram of apatite fission track ages show that the cooling ages of profile A samples fit into a linear regression. Note that profile A samples reveal relatively high mean confined track length typical of cooling ages, whilst the largest ages of profile B and C yield lengths of typical mixed ages. Error bars represent 1σ.

In two of the three elevation-AFTA profiles a fossil PAZ has been identified at different levels. At profile B the base of the fossil PAZ has been estimated at 2400 m, whilst at profile C the base should be situated somewhere between 1200 and 2100 m. No fossil PAZ has been identified at profile A, but should be expected above the recent outcrop level (> 2700 m). From the vertical slip of this fossil PAZ we conclude that the rapid uplift in the Upper Cretaceous was accompanied by an intense block faulting.

The relative downthrow of profiles B and C in respect to profile A can be estimated if the linear regression of profile A shown in Fig. 2 is prolonged to an elevation up to about 5000 m. The restoration of the block faulting to the pre-Cretaceous situation has been done by moving the profile B samples some 2500 m upwards until the cooling age samples fitted best with the linear regression of profile A. The assessment for profile C then amounts to about 3 km vertical differential offset (Fig. 4).

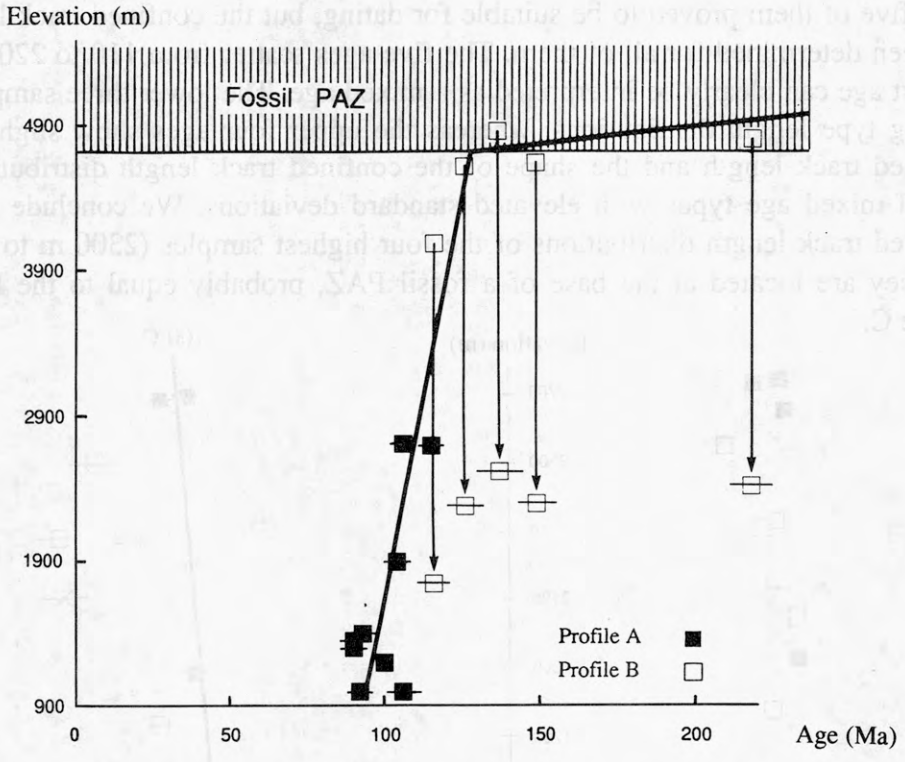

Fig. 3: Interpretation of profile B samples in relation to profile A. Subsequent to the accelerated Cretaceous uplift we assume an intense block faulting with differential movements of up to 3 km.

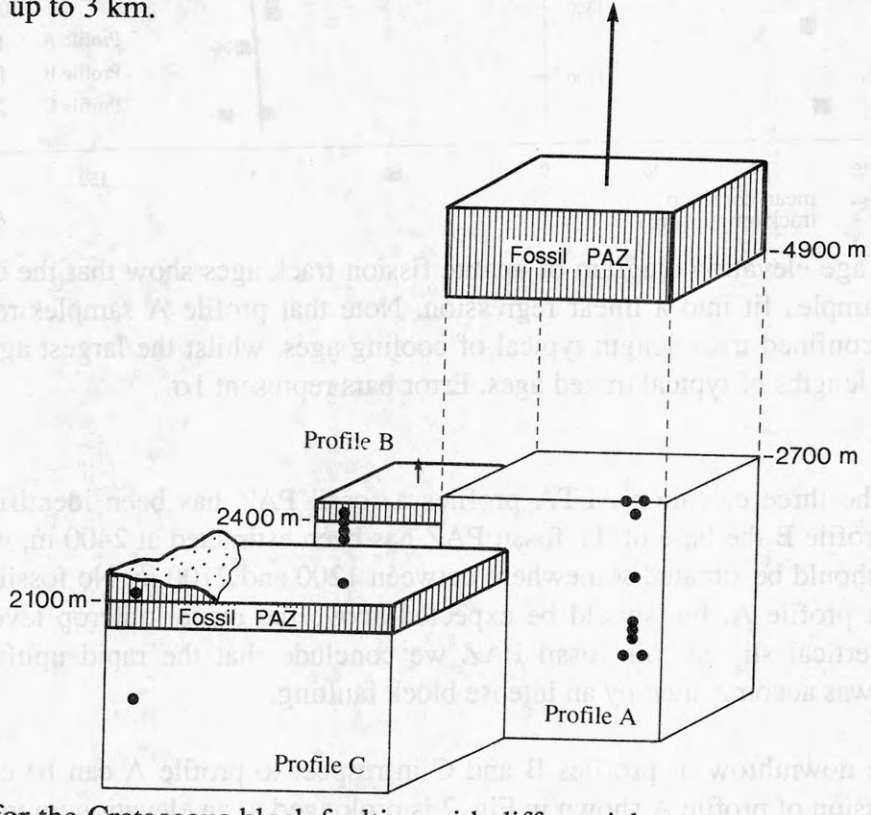

Fig. 4: Model for the Cretaceous block faulting with differential movements which are shown by the arrows in relation to profile C. Dots schematicaly indicate the sample positions. The offset of the apatite fission-track partial annealing zone proves that the block faulting must syn- or postdate the fast uplift during the Upper Cretaceous.

It should be noted that the topographically highest regions successively underwent the highest degrees of uplift.

Conclusions:

❑ Cretaceous apatite fission track cooling ages and older mixed ages indicate that the exposed basement level was reheated during Mesozoic times (> 100 Ma) to temperatures of the apatite fission track annealing zone (60 - 125°C) and above it.

❑ Reheating was probably due to an elevated geothermal gradient at the inital stage of Gondwana breakup and due to the loading of Jurassic lava flows.

❑ The Upper Cretaceous is a time of fast uplift (≈100 m/Ma) with subsequent block faulting.

❑ The fast uplift in the Cretaceous must have been accompanied by high erosion rates implying a high sedimentation rate elsewhere.

❑ The final separation of Africa from Antarctica with the formation of ocean floor might be responsible for the episode of fast uplift in the Upper Cretaceous.

References:

ARNDT, N.T., TODT, W., CHAUVELT, C., TAPFER, M., WEBER, K. (1991). U-Pb zircon age and Nd isotopic composition of granitoids, charnockites and supracrustal rocks from Heimefrontfjella, Antarctica. Precambr. Res. (in press).

JACOBS, J. (1991): Strukturelle Entwicklung und Abkühlungsgeschichte der Heimefrontfjella (Westliches Dronning Maud Land / AnTraktika). Unpubl. PhD-thesis.

WAGNER, G.A. (1988). Apatite fission-track geochrono-thermometer to 60°C: projected length studies. Chem. Geol. (Isot. Geosic. Sect.), 72, 145-153.

WEBER, K.; ARNDT, N.T., JACOBS, J.; PETERS, M. (1990). The Proterozoic evolution of New Schwabenland and its correlation with the southern part of Africa. Geodät. and geophys. Veröffentlichungen, Reihe I, Berlin (1990) 15, 62-63.

SEISMIC ANISOTROPY IN ANTARCTIC FIRN

E.P.Jarvis
British Antarctic Survey
Madingley Road
Cambridge
CB3 0ET, UK.

Refraction seismic experiments were undertaken in March 1991 on the Wormald Ice Piedmont, Adelaide Island, Antarctic Peninsula (fig 1) in order to determine the seismic velocity structure of the surface firn layer and the firn-ice transition region. The experiment was conducted at Latitude 67°29.84' South, Longitude 68°10.18' West on grounded ice of 300 to 400m thickness. Variation in surface elevation over the experiment area was a maximum of 6m. Four composite 36 channel 300m long refraction profiles were recorded at azimuths of 000, 090, 120 and 240 degrees using a 24 channel seismograph. Four different hammer and explosive source configurations were employed on each profile at offsets of 2 to 5m from the first geophone. Three-component geophone sets spaced at maximum intervals of 10m were used to record both P and S-wave refraction arrivals.

The use of a variety of source techniques has yielded high quality field records with high energy refracted arrivals (fig 2a). S-wave records (fig 2b) have been obtained by stacking traces recorded on horizontal geophones from shot records with horizontal impulse energy sources. Pairs of traces with similar S-wave and opposite P-wave polarities are stacked together to eliminate P-wave energy and stack S-wave energy.

P and S-wave arrivals recorded along the different profiles determine the behaviour of any azimuthally dependant seismic P and S-wave velocity anisotropy present. Travel time curves for the refracted arrivals along the different azimuths have been reduced to velocity distance and then velocity depth relationships for both P and S-waves. P and S-wave velocity variation with depth in the near surface firn and firn-ice transition region will be presented for the different azimuths. Density depth relationships for the surface firn layer and firn ice transition region are calculated empirically from the P-wave velocity depth relationship.

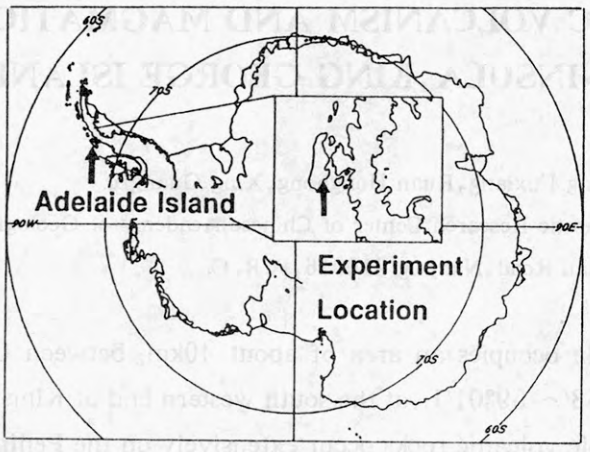

Figure 1. Location of seismic refraction experiments, Adelaide Island, Antarctic Peninsula.

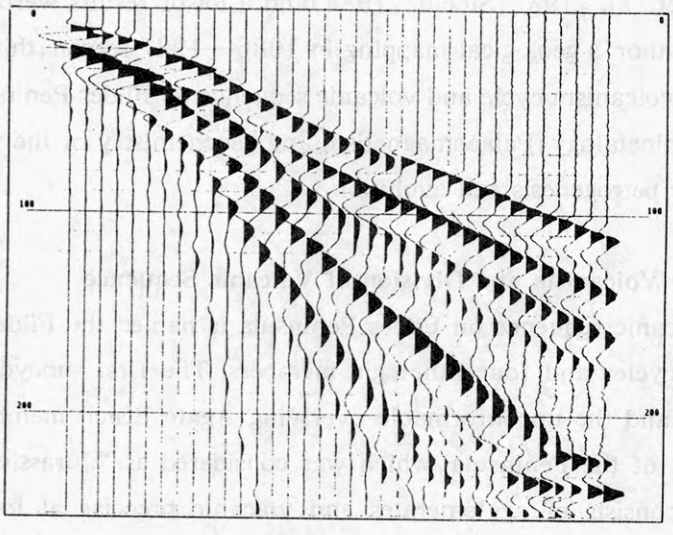

Figure 2a. P-wave refracted energy recorded from an explosive source.

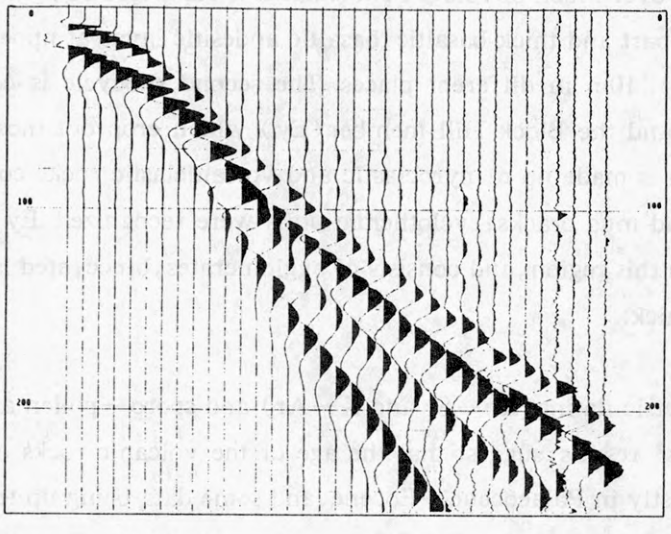

Figure 2b. S-wave refracted energy recorded on horizontal geophones after removal of P-wave energy by stacking.

ISLAND ARC VOLCANISM AND MAGMATIC EVOLUTION IN FILDES PENINSULA, KING GEORGE ISLAND, ANTARCTICA

Jin Qingmin, Kuang Fuxiang, Ruan Honghong, Xing Guangfu
Antarctic Research Center of Chinese Academy of Geological Sciences
534 East Zhongshan Road, Nanjing 210016, P. R. C.

Fildes Peninsula occupies an area of about 40km$_2$ between Latitudes 62°10′～62°13′S and Longitudes 58°53′～59°01′E, at the south western end of King George Island, South Shetland Islands. Cenozoic volcanic rocks occur extensively on the Peninsula and lots of work have been made by researchers from different countries in the area (Hawkes, 1961; Barton, 1965; Schauer et. al., 1961, 1963, 1964; Grikurov et al, 1968, 1973; Covacevich et. al., 1972; Birkenmajer et. al., 1982; Smellie, 1984) and a lot of results were accumulated. On the basis of the first author's geological mapping in 1986—1987 season, this study is expected to make a division of volcanism cycle and volcanic sequence on Fildes Peninsula, to carry out studies of chronology, minetalogy, Palaeomagnetism and geochemistry of the volcanic rocks, so as to understand their petrogenesis and evolution.

Cycle of Volcanism and Division of Volcanic Sequence

The volcanic sequence on Fildes Peninsula is named the Fildes Cycle. It may be divided into two subcycles and four lithologic members. The first subcycle includes the Jasper Hill member (Eb) and the unconformable overlying Agate Beach member (Em). Eb occurs in the southern part of the Peninsula, which was considered as "Jurassic volcanic rocks" by Barton (1965). It consists of agglomerates and volcanic breccias at lower part and basaltic and basaltic andesitic lavas intercalated by thin tuff breccia beds at upper part, in which develop red jaspers. The bed show NEE gentle dips with thickness of 60m to 120m from east to west. Em crops out over much of Fildes Peninsula. It is composed of agglomerates and volcanic breccias at lower part and thick basaltic, basaltic andesitic lavas at upper part. The thickness varies from 50m to 240m in different places. The second subcycle is composed of the Fossil Hill member (Eh) and the Block Hill member (Ey) which crop out mostly over the eastern Fildes Peninsula. Eh is made up of pyroclastic and volcaniclastic rocks containing fossil plants, cross—bedding, and mud cracks; cyclothemic units were recognized. Ey is the youngest of the volcanic rocks in this region, and consists of agglomerates, brecc; ated lavas and volcanic breccias, 10—100m thick.

Radiometric dating (Rb—Sr and K—Ar) and sporo—pollen analysis, combining with pre—researchers' results, suggest that the age of the volcanic rocks on Fildes Peninsula is early Tertiary (mostly in Palaeocene—Eocene, and some data being up to Oligocene). But the lower limit may be as early as late Cretaceous.

Volcanic Structuye

There are two main kinds of volcanic edifices in the area. One is the positive edifice characterized by stumps of volcanic neck facies and radiating dikes, such as Horatio Stump, Gemel Peaks and Shanhaiguan Peaks. The other is the negative edifice with agglomerates (lava), agglomerate breccias(lava) of volcanic vent facies, showing negative topography, such as windstorm Cove and Norma Cove.

Cenozoic volcanic activity in the area was controlled by regional tectonics, and there are some trends in time—space distribution. From the south to the north, four eruptive zones, spaced about 2km apart, were recognized, including Flat Top—Shanhaiguan Peaks volcanic eruption zone, Gemel Peak—Ardley Island zone, Winstorm Cove—Suffield Point zone, and Great wall Rock zone, corresponding to four major NE—trending structural zones. The structures controlling the eruptive zones are extentional faults, related to subduction of the Pacific plate beneath the Antarctic Peninsula. Early eruption occurred almost all over Fildes Peninsula, and had a progressive north easterly maigration, consistent with that of whole South Shetland Islands; late etuption had a north easterly migration, showing local characteristics.

Palaeomagnetism

Palaeomagnetic determination of 18 samples from Agate Beach member, Fossil Hill member, Block Hill member and Long Hill hypabissal body in the centre of Fildes Peninsula show that the maximum value of natural remanent magnetization of these samples is 2. 6A/m, the minimum value is 1.1×10^{-2}A/m. The average values of volume magnetic susptibility are $5.140\times10^{-3}$to $3.987\times^{-3}$SI and the anisotrop of magnetic susptibility(A. M. S.)is not evident.

The samples from Agate Beach member and Fossil Hill member have similar magnetization. Their mean magnetic inclination and declination are —76. 9°and 59. 7°, respectively, corresponding to the normal subzone of middle—lower Cenozoic mixed polarity zone. Block Hill member has dispersive palaeomagnetic directions, suggesting that some remelting may have occurred. The magnetic inclination and declination which are different from those of Agate and Fossil Hill member are 77. 6° and 211. 6°, respectively , corresponding to the reversal subzone of the above—mentioned mixed polarity zone.

Petrochemistry and Geochemistry

Chemical determination shows that the volcanic rocks are predominantly basaltic and basaltic andesitic, subordinately andesitic and rarely dacitic. Nearly all of them are typically high in Al_2O_3 and have tholeiitie K—low and Ti—depleted features. Average Al_2O_3 content of the basaltic rocks is 20. 90%(N = 50, recalculated to 100% on an hydrous basis) with the highest 24. 13%, and those of K_2O and TiO_2 are 0. 40% and 0. 66%, respectively. On the diagram of (K_2O+Na_2O) versus SiO_2, most of the rocks are plotted in the tholeiitic field. On graphs of K_2O against SiO_2, TFe/MgO against SiO_2, and AFM, the majority of the rocks are

fallen in the intersect area of both calc —alkaline and tholeiitic fields, while the basaltic rocks are mostly in tholeiitic field. These chemical features suggest that the volcanic rocks have both calc—alkaline and tholeiitic characteristics , with the basic members more similar to tholeiite, and more and more evolutive towards calc—alkaline with increasing SiO_2 contents.

The volcanic rocks on Fildes Peninsula have low transitional element abundances, particularly Ni, Cr, Co. The average Ni, Cr and Co abundances of the basalts are 20. 4ppm, 53. 8ppm and 32. 3ppm, respectively. The sharp low Ni, Cr abundances indicate that the basalt in the studied area could not be the products of direct crystallization of a primary basaltic magma, and may undergo the fractional crystallization of olivine and clinopyroxene. with increasing siO_2 content in the rocks, the abundances of Cr, Co, V decrease gradually and that of Ni remains constant, suggesting the fractional crystallization of pyroxene in the magmatic evolution, while olivine was not a main fractionation phase.

It is showed that studied volcanic rocks are usually high in incompatible elements, indicating the calc—alkaline affinity. The contents of Sr are even higher than those of typical calc—alkaline rocks. The enrichment of Sr, Rb, Ba, Th etc. , can be directly observed on the MORB —normalized pattern, which are similar to those of typical calc—alkaline rocks. In addition, with the magmatic evolution from basaltic to dacitic, nearly all the incompatible elements increase, but that of Sr decrease, which indicates fractional crystallization of sr—bearing phase, plagioclasc.

For all kinds of volcanic rocks of discussed area show similar REE patterns which are slightly enriched in LREE ($(La/Yb)_N = 3.24-5.66$), suggesting that these rocks are products of comagmatic evolution under close condition. The total REE concertrations and distribution patterns of the basaltic rocks are similar to those of circum—Pacific calc—alkaline high—Al basalts (such as those in Japan, western America, New Zealand, southern Chile) (L. Lopez—Escobar et. al. , 1977), but are different from those of typical arc tholeiites (Hawkesworth et. al. , 1977). With increasing SiO_2 contents, REE concertrations of the volcanic rocks increase and Eu anomaly changes from low positive to low negative, but ratios of $(La/Yb)_N$ usually remain constant, reflecting the effect of fractional crystallization during the magmatic evolution. The change of Eu anomaly is consistent with fractional crystallization of plagioclase.

The $\delta^{18}O$ values of the studied rocks range from 5. 5 to 7. 5‰. Most of them lie in the range of OIB and MORB. Higher $\delta^{18}O$ values of some samples may be due to the low temperature alteration. The $^{87}Sr/^{86}Sr$ ratios of the volcanic rocks on Fildes Peninsula are in the range 0. 703230—0. 703791. Such low ratios and narrow variation range suggest the rocks have mantle—derived and comagmatic feature. The $^{143}Nd/^{144}Nd$ ratios of the volcanic rocks in question is 0. 512885—0. 513011, and $\in_{Nd}$ are 4. 82—7. 28 (CHUR = 0. 512638) similar to those of Patagonia, Mexico, Ecuador and Northeast Japan (S. Nohda, 1984). On the graph of

$^{143}Nd/^{144}Nd$ against $^{86}Sr/^{87}Sr$, the samples essentially plot on or near the main correlation line of mantle—derived magmatic rocks, suggesting little continental crust contamination to the magma. The Pb isotope compositions of the volcanic rocks are: $^{206}Pb/^{204}Pb$ 18.5032—18.6413, $^{207}Pb/^{204}Pb$ 15.5877—15.6250, showing more radiogenic than MORB, especially ^{207}Pb. On the graph of $^{207}Pb/^{204}Pb$ against $^{206}Pb/^{204}Pb$, the samples plot in the field between MORB and recent oceanic sediments, and forming steeper slopes than MORB, suggesting the effect of sudbucted oceanic crust or oceanic sediments or less on the volcanic rocks through their forming process.

Petrogenesis and Evolution

Using various geothmometers and geobarometers, crystallization temperatures and pressures of the major rock—forming minerals from Fildes Peninsula were estimaed: Pl, t=1276—1231℃; ol, t=1120—1291℃; cpx, t=1053—1150℃, p=0.31—1.05GPa. It was estimated that the pressure of the magatic chamber was 0.31—1.05 GPa, equivalent to 16.5—26.4km depth.

High—Al basalts are developed in several places of circum—Pacific orogenic belt. They may belong to tholeiitic series as well as calc—alkaline series (L. Lopez—Escobar et. al., 1977). It has been a long time for the study on petrogenesis of high—Al basalts. For example, Green and Ringwood (1967)proposed that a primary high—Al olivine tholeiite might be resulted from magma segregation from a pyrolite source at pressures of $15-35\times10^8$Pa, and that the Al_2O_3 content could be successively enriched by low level olivine and pyroxene fractionation. Similarly, Lewis(1971) suggested that circum—oceanic high—Al basalts are fractionation products of olivine tholeiite . Based on the experimental studies of Hawiian tholeiite, Holloway and Barnham (1972) concurred that high—Al basalts may be produced from low—Al tholeiites by subtraction of olivine and clinopyroxene. In recent years, based on the studies of Volcanic suite in Aleutian Arc and calc—alkaline magma of Jorullo Volcano, Mexico (Conrad et. al., 1983; Kay, 1982; Gust et. al., 1987)(Luhr et. al., 1985), it is considered that the high—Al basalts are derived from high—Mg basaltic magma by frational crystallization of olivine and clinopyroxene.

As mentioned above, the strong depletion of Ni and Cr indicates that the basalts in this area do not represent a primary magma, but one that may have undergone fractional crystallization of mafic phases. The basalts on Fildes Peninsula are believed to have a two—stage genesis. In the first stage, a diapiric uprising of the upper mantle wedge formed primary olivine tholeiitic magma by way of partial melting along the boundary between the crust and mantle. During the process, there might be a fluid, produced by dehydration of subducted oceanic crust, which migrated upwards and entered into the mantle wedge. This enhanced the partial melting of upper mantle and was accompanied with fluid metasomatism and enrichment of LILE elements. In the second stage, widespresd fractional crystallization of ol, cpx in the

primary basaltic magma formed high—Al basaltic magma and also reduced abundances of Cr, Co, Ni and content of MgO in residual magma.

Supposed that a primary magma from which the studied high—Al basalts were derived was formed by 20—25% partial melting of pyrolite whose mineral composition is $Ol_{50}Opx_{30}Cpx_{15}Sp_5$, using 2000 and 3000 ppm as the Ni and Cr abundances of pyrolite, respectively, and introducing Frey and Prinz's(1978) and Frey's(1978) distribution coefficients, we can calculated from the eqution, $(C_l/C_l = 1/F + D(1-F))$, the values of Ni and Cr in derived primary magma being 246—260 ppm and 1270—1320 ppm, respectively. The Ni and Cr abundances of subsequent magma which is derived from the supposed primary magma by fractional crystallization of 40%(ol+cpx) are, calculated from Reyleigh eqution, $C_l = C_o F^{(D_i-1)}$, 20—21 ppm and 56—60 ppm, respectively, which are consistent with that of studied high—Al basalts. On the contrary, by adding 12wt% olivine and 28wt% clinopyroxene (ol/cpx is 30%/70%)to the studied high—Al basalts, the compostition of the resulted rocks would be similar to that of olivine tholiite.

Geochemistry involving the aspects of isotope, trace element, and REE shows cognate relationship among the basalts, andesites and dacites on Fildes Peninsula. The variation of some trace elements in magmatic evolution is consistent with the fractional crystallization of plagioclase and pyroxene. In the light of above consideration, a model calculation of major oxides for evolution of the volcanic rocks has been made. The results of major oxides least—squares approximation of fractional crystallization demonstrated that none of the squared residuals are greater than unity, which indicates the success of the model calculation, and that fractional crystallization of plagioclase and pyroxene is dominant in magmatic evolution.

In order to make further verification on the major oxides model calculation, we have calculated, using Reyleigh equation and proper distributions coefficients, the variation of REE in fractionation process. The results show that from the basalt to the basaltic andesits, REE model calculation coincided with the major oxides in evolution, and from the basaltic andesite to the andesite REE model calculation yields systimatical deviation, except Eu, in the evolution process, Therefore, the model calculation can be considered to be successful.

The good results of major oxides model calculation and further verification in REE show that fractional crystallization of plagioclase and pyroxene in the magmatic evolution process controls the evolution; high—Al basalts to basaltic andesites to andesites and to dacites on Fildes Peninsula. Certainly, because of the comlexity of volcanism, in additon to the fractironal crystallization to be considered as a predominant factor, subordinate influences of other factors involved in magmatic evolution cannot be entirely excluded

References

C. M. Barton, 1965, The geology of South Shetland Islands III, The stratigraphy of King George Island, Sci. Repts. Ant. Surv. , 44: 1—33, London

K. Birkenmajer, 1982, Report on geology investigation of King George Island and Nelson Island (South Shetland Islands), Studia Pol. IXXIV, part III, 175—197, Warszawa.

W. K. Conrad, S. M. Kay and R. W. Kay, 1983, Magma mixing in the Aleutian Arc: Evidence from cognate inclusions and composition of xenoliths, J. Volcanol. Geothermal. Res. , 18, 279—295.

V. Covacevish & C. Lamperein, 1972, Ichnites from Fildes Peninsula, King George Island, South Shetland Islands, In R. A. Adie, ed. Antarctic Geology and Geophysics, 71—74.

F. A. Frey & M. Prinz, 1978, Ultramafic inclusion from San Carlos, Arizona: Petrogentic and geochemical data bearing on their petrogenesis, Earth and Planet. Sci. Lett. , 38, 129—176.

F. A. Frdy, D. H. Green & S. D. Roy, 1978, Intergrated model of basalts petrogenesis: A study of quartz tholeiite olivine melilitites from southeastern Australia, utilizing geochemical and experimental petrological data, J. Petrol. , 19, 463—513.

D. H. Green & A. E. Ringwood, 1967, The genesis of basaltic magma. Contrib. Mineral. Petrol. , 15, 103—190.

D. A. Gust & M. R. Perfit, 1987, Phase relation of high—Mg basalts from the Aleutian Island Arc: Implications for primary island arc basalts and high—Al basalts, Contrib. Mineral. Petrol. , 97, 7—18.

D. D. Hawkes, 1961, The geology of South Shtland Islands, I. The petrology of King George Island, Sci. Rept. Falkd. Dep. Surv. , 26, 1—28, London.

C. J. Hawkesworth et. al. , 1977, A geochemical study to island arc and back—arc tholeiite from the Scotia Sea, Earth Planet. Sci. Lett. , 36, 253—262.

J. R. Holloway & C. W. Burnham, 1972, Melting relations of basalt with equilibrium water pressure less than total pressure, J. Petrol. , 13, 1—29

S. M. Kay, R. W. Kay & G. P. Citron, 1982, Tectonic controls on tholeiitic and calc—alkaline magmatism in the Aleutian Arc, J. Geophys. Res. , 87, 4051—4072.

J. F. Lewis, 1971, Composition origin, and differentiation of basalt magma in the Lesser Antilles In: Caribbean, Geophysical, tectonic, and petrologic studies (T. W. Donnelly et. al.), 159—179, Geol. Sco. Am. Mem. , 130.

L. Lopez—Escobar, F. A. Frey & M. Vergarn, 1977, Andesites and high—alumina basalts from the Central—South Chile High Andes: Geochemical evidence bearing on their petrogenesis, Contrib. Mineral. Petrol. , 63, 199—228.

J. F. Juhr & I. S. E. Carmichael, 1985, Jorullo Volcano, Micheacan, Mexico (1759—1774): The earlist stage of frationation in calc—alkaline magmas. Contrib. Mineral. Petrol. , 90, 142—161.

J. L. Smellie et. al. 1984, The geology of South Shetland Islands: VI. Stratigraphy, Geochemistry and evolution, Bull. Brit. Antarct. Surv. , 53, 39—84

THE GEOLOGICAL CHARACTERISTICS OF VINSON MASSIF IN ELLSWORTH MOUNTAINS, ANTARCTICA

Jin Qingmin, Qiu Jingrong, Kuang Fuxiang

Antarctic Research Center (Nanjing), Chinese Academy of Geological Sciences, 534 East Zhongshan Road, Nanjing, 210016 China

Vinson Massif, as the summit of the Antarctic continent, lies in the northern Ellsworth Mountains, West Antarctica. Its main peak is 5140m above sea level. Because of steep relief, vile climate, very low temperature and always being covered by ice and snow, it was a neglected area of geological research.

Prof. Jin Qingmin, the first author, took part in a Sino—American Joint Scaling and Sciences Expedition to Vinson Massif in 1988. She Completed routing geological investigation in an area about 80km^2; collected rock (ore) samples of 40 Kg; studied the stratigraphy, lithological characteristics, ore—bearing property and tectonics of a late Palaeozoic low—grade metamophic sequence that occurred in the region, and found a large scale iron—bearing rock sequence and iron—ore belt.

The low—grade metamophic rocks exposed in Vinson Massif region is composed of sedimentary rocks of neritic and shore facies in Devonian. They consist of dark brown—pale green garnet quartz sandstone, iron—bearing garnet quartz sandstone with hematite interlayers, light grey quartz sandstone, variegated quartz sandstone and calcareous quartz sandstone, more than 650m thick. It can be divided into five lithologic members, described from lower to upper: (1) the first member: grey—violet striped iron—bearing quartz sandstone, ferruginous garnet quartz sandstone with hematite interlayers, more than 150m thick, showing cross—bedding; (2) the second member: grey white, pale green calcareous sandstone, 0—30m thick; (3) the third member: interbedded green quartz sandstone and grey violet iron—bearing garnet quartz sandstone with thickness of 200—250m; (4) the fourth member: thick—bedded pale green quartz sandstone, intercalated with violet striped garnet quartz sandstone and conglomerate, 150—200m thick; (5) the firth member: grey white quartz sandstone, more than 50m thick. The rocks we describe may be similar to or lie within the Crashsite formation of Hjelle et al (1982) and Webbers et al (1983) and the Crashsite Quartz group of Craddock

(1986).

The sandstone shows fine sorting and high compositional maturity and has giant wave—formed cross—bedding, parallel bedding, graded bedding and rhythmic bedding etc. . Major mineral assocition of this clastic rock series consists of quartz and almandine (abundant, sometimes more than 50%) and minor illite. The trace element, REE, sedimentary structure and typomophic peculiarities of clay minerals of the studied almandine—bearing quartz sandstone and intercalated iron ore beds suggested that they were deposited in submarine and shoreside environment, and formed a marine transpression sequence.

In the area investigated, located in the east limb of the Ellsworth Mountains anticlinorium, stratigraphy was complicated by folding. There are two closed anticlines and a wide syncline and a post ore—forming fault zone.

Iron—ore layers occurred in garnet quartz sandstone of the first lithologic member. Total thickness of the ore belt, composed of 5—10 hematite layers, each 0. 5—10m thick, is about 30—40m. Fe—bearing rock is 100—150m thick, and extends over 15Km. Ore layers and country rocks suffered regional metamorphism and were folded. There are three sorts of ore, including striped, massive and colloidal ore. Mean tenor is 35%, rising to 54. 28—64. 39% in pay ore. XRD and Mossbauer spectrum study shows that major mineral is hematite; Fe_2O_3: 98. 66—99. 35%; TiO_2: 0. 00—0. 40%; MnO: 0. 06—0. 08%; MgO: 0. 00—0. 27%.

Ferrous ions are suggested to come from volcanic rocks, metamorphic rocks and other source rocks. Iron ore is conformable with the country rocks, therefore consided to be syngenetic type. The age of the ore is the same as that of the country rocks in Devonian.

TECTONIC AND PETROGENETIC EVALUATION OF THE PETERMANN RANGES, EAST ANTARCTICA

A.Joshi, N.C.Pant, B.R.Bejarniya and M.L.Parimoo

Antarctica Division, Geological Survey of India, NH-5P, N.I.T., Faridabad-121001, Haryana, India.

The Petermann Ranges in Wohlthat Region, East Antarctica expose low pressure granulite facies gneisses intruded by anorthositic dykes and stocks, a ferrogabbro- ferro monzogabbro-monzonite (FG-FMG-MZ) suite and alkali feldspar granites.

The gneisses are dominated by garnet-sillimanite-K feldspar-quartz-biotite bearing lithology with interbands of hornblende-biotite, garnet- K feldspar-quartz gneisses, marbles and calc silicates. Indicating derivation from pelitic-psammatic sediments with minor carbonates, the bulk rock geochemistry of the gneisses appears to control the development of varied mineral assemblages. Garnet-biotite geothermometry and garnet-sillimanite-plagioclase-quartz geobarometry of the Petermann gneisses reveal garnet core temperature of 625°C at 5.3 Kb and garnet rim temperature of 540°C at 4.2 Kb. Peak metamorphic conditions in the same sequence have been recorded from the adjacent Humboldt Mountain and are of the order of 800°C and 6 Kb. These gneisses have undergone three phases of deformation and the granulite facies metamorphism has been inferred synchronous or prior to the second deformation.

Close spatial association of the Petermann anorthosites (An_{40}) with the Gruber anorthosite massif may indicate a genetic linkage. Mineral chemistry of the FG-FMG-MZ suite shows continuous trend in the plagioclase composition with anorthite content decreasing from An_{47} (FG) to An_{35} (FMG) and An_{30} (MZ). From FG to FMG, the clinopyroxene compositon shows variation in Fe/Fe+Mg from 0.24 to 0.75 while fayalite (Fe/Fe+Mg: 0.95) forms the main mafic silicate in MZ, defining an iron enrichment trend. Such mineral chemical traits supported by gradational field relationships, interpret the rocks of FG-FMG-MZ suite to be the fractional crystallization products of a single magma while their being comagmatic to the anorthosites is not supported by the present data. Associated alkali feldspar granites of the Petermann Ranges exhibit characters of A-type.

The Petermann granulites are similar to the 1100 Ma granulites of the Larsemann Hills in dominantly metasedimentary character and peak metamorphic conditions. In contrast to several other mid-Proterozoic granulites of East Antarctica, the post granulite decompression (2-4 Kb) appears to be absent in the Petermann Ranges besides the presence of diverse, mantle activated plutonism.

Geochronology and geochemistry of the igneous rocks from the Barton and Fildes Peninsula, King George Island

Yong-Joo Jwa*, Byong-Kwon Park* and Yeadong Kim*

* Korea Ocean Research and Development Institute,
Ansan, P.O.Box 29, Seoul 425-600, Korea

Abstract

From the K-Ar age determinations, it is known that volcano-plutonic rocks in the Barton Peninsula have ages of 36-49Ma (Eocene - Oligocene) and that volcanic rocks in the Fildes Peninsula yield 53-61Ma (Paleocene - Eocene) ages. The apparent age difference between these areas can be explained by eastward migration of magmatism in western King George Island.

Trace and major element geochemistry of the igneous rocks from these areas indicates that the fractionation trend of the rocks is calc-alkaline type. The volcano-plutonic magmas of Tertiary western King George Island were possibly originated from subducted oceanic crust - mantle wedge system during island-arc formation. The chemical nature of the rocks in the Barton Peninsula is slightly different from that in the Fildes Peninsula. The eastward migration of magmatism would be responsible for the difference between both areas. The geochemical difference would be due to the different degree of partial melting or fractional crystallization of the magmas.

SUBMARINE CANYONS IN THE BELLINGSHAUSEN SEA, OFFSHORE DRONNING MAUD LAND AND WILKES LAND, ANTARCTICA

Hideo Kagami, Faculty of Science, Josai University, Sakado 350-02 Japan
Hiromi Kuramochi and Yoko Shima, Department of Geology, Kochi University, Kochi 780 Japan

The Antarctic continental margin is presently characterized by three different submarine canyons. These include young continental margins where canyons show the existence of a leveed channel on the deep-sea fan, and old continental margins whose continental rise is incised by canyons with terraced walls and a flat channel floor which subsequently join in a deep-sea channel. The former is observed in the Bellingshausen Sea and the latter is in the offshore of the Dronning Maud Land. The third type of continental margins is seen offshore Wilkes Land where canyons show a large-scale erosive valley on the sediment starved margin.

We suspect that the canyons were formed by rigorous activities of turbidity currents and debris flows, as DSDP drilling results indicated that the canyons in the Bellingshausen Sea and offshore Dronning Maud Land were formed during the last advancement of the Antarctic ice sheet, and that those offshore Wilkes Land were formed during the "interglacial" period at around 3-4 Ma BP. The canyons in the Bellingshausen Sea are so incorporated to build up deep-sea fans, that they develop dominantly at the upper continental rise and disappear apparently at the base of the lower continental rise. The canyons in the Dronning Maud Land have a large-scale entrenchment throughout their course and construct a canyon-deep sea channel complex. This is caused by thermal cooling effect of lithosphere to deepen the oldest ocean basin in Antarctica. On the contrary, the canyons in the offshore of the Wilkes Land have been maintaining their channels in the same place by downward erosion indicating that the bottoms of the canyon incised sea-bed formation of Miocene.

We found also that the buried canyons observed in the Bellingshausen Sea and offshore Dronning Maud Land were mostly formed during the maximum advancement of the Antarctic ice sheet at around 5-7 Ma BP. We can not observe any buried canyons in the continental slope offshore Wilkes land, because they have been keeping the same course.

STRUCTURE AND EVOLUTION OF PRECAMBRIAN CRATONS AND METAMORPHIC BELTS IN EAST ANTARCTICA
(Review)

E.N.Kamenev, North Branch for Marine Geologic Exploration "Sevmorgeologia" 120, Moyka, Leningrad 190121 USSR.

East Antarctica between 30 W and 100 E is a giant Precambrian shield where cover strata have been eroded or never accumulated. Mountain chains, isolated nunataks and ice-free hills facing the Indo-Atlantic coast are predominantly built up of intensively deformed Precambrian rocks with prevailing granulite and amphibolite facies assemblages. Recent aeromagnetic and bedrock topography data indicate that these partly exposed coastal highlands may be continuous with sub-ice Gamburtzev Mountains in the Antarctic interior.

Because of extremely lengthy Precambrian geologic record many geological features and events typical of Precambrian history, such as the order and peculiarities of deformational episodes, metamorphic and magmatic processes, lithology of individual units, metallogenic considerations, etc. are often used to define and correlate paleotectonic environment of widely variable age. A similar approach has been applied in Antarctic Precambrian studies carried by the Australian, Belgian, British, German, Norwegian, Soviet, South African and other expeditions since the early days of Antarctic research. As the result of these multinational cooperative efforts, it appeared possible to recognize four major types of paleotectonic environments (Fig.1).

A - belts of highly metamorphosed rocks (gneiss-granulite terrains) characterised by intense and repeated tectonic deformations, granulite and high-grade amphibolite facies metamorphism, post- kinematic subalcaline plutonic activity and the presence of some supracrustal rocks and mafic suites, including stratified and anorthosite complexes;

B - granite-greenstone belts (granite-greenstone terrains) built up of granitic block-intrusions, domes, slabs and nappes in complex combination with nappes, slabs, piles of slabs and lenses of supracrustal sedimentary-volcanic rocks; the latter are usually characterized by a relatively weak, often zonal metamorphism ranging from the low-grade greenschist facies to the initial migmatic grade of amphibolite facies, and by intensive Alpine-type deformations;

C - linear zones or troughs with a thick sedimentary and volcanic fill underformed or slightly deformed and metamorphosed under prehnite-pumpellyite to low-grade greenschist facies and/or hydrothermally altered; mafic and subalcaline intrusions of subcrustal derivation are common;

D - areas of tectono-thermal activization superimposed on all other terrains; they control distribution of the so-called post-cratonic basic, ultrabasic, alkaline magmatism mainly related to the Phanerozoic rifting.

Belts of highly metamorphosed rocks are further subdivided into three subtypes:

AI - relics of the most ancient belts or cores of shields (of charnockite-enderbite or granite-tonalite composition) with linear fragments ("xenoliths") of the oldest supracrustal folded sequences; the latter are typically composed of metavolcanic rocks and do not contain carbonate rocks;

AII - charnockite-granulite belts where charnockites are associated with abundant supracrustal rocks with carbonate and other metasedimentary and metavolcanic lithologies, as well as stratified anorthsites;

AIII - granite-gneiss-schist belts of predominantly supracrustal rocks metamorphosed in the high grade amphibolite facies; abundant migmatites and post-deformational veins of granite and pegmatite are common; in places the granite-gneiss -schist belts represent transitional zones between the granite -greenstone and charnockite-granulite belts.

The distribution of the proposed tectonic environments throughout the shield and advances of Antarctic geochronology support the existence of the following major structural types in the Precambrian Antarctic shield: 1. Early Archean protocratonic blocks (fragments of protocratonic basement); 2.Late Archean-Proterozoic Wegener-Mawson mobile belt (a part of the huge ancient protogeosynclinal belt) and 3. Proterozoic sedimentary-volcanogenic protoaulacogens or protorifts. Each type reflects successive stages of evolution of the Antarctic shield in the Precambrian.

Protocratonic blocks (Napier, Westfold, Bunger, West Ritscher, inferred South Lambert and Read) were formed between 3900 and 2400 Ma ago. They are dominated by ultrametamorphic plutonic domes built up of enderbitic and charnockitic gneisses and granite gneisses, garnetiferous granite gneisses, tonalitic and trondhjemitic gneisses and granite gneisses. Relics of the oldest greenstone belts, ultramafic bodies and mafic plutons occur between theese domes and as xenoliths. Metamorphism of protocratonic blocks, except for the West Ritscher and Read blocks, primarily corresponds to the highest grade granulite facies; relics of the oldest greenstone belts show evidence of the low gradient metamorphism.

The Wegener-Mawson mobile belt (WMMB) strikes throughout the whole shield from east to west. It was formed between 3000 and 500 Ma ago and is characterized by a polycyclic evolution. The WMMB consists of charnockite-granulite belts (reworked marginal zones of protocratons), granite-gneiss-schist belts (reworked zones of protocratons and high-grade zones of granite-greenstone belts), and granite-greenstone metamorphic belts. Regional combinations of exposed metamorphic belts form distinct tectonic and mineragenic provinces separated by regional transcurrent or thrust faults. Metamorphic prograde and retrograde zoning in the WMMB is best explained by its

nappe-block structure, caused by collision and accretion of protocratons. Six cycles of tectonic activity in the WMMB culminating approximately (+ 200 Ma) 2900, 2400, 1700, 1100 and 600 Ma are recognized. Initial stages of the first and fourth cycles are the most prominent (greenstone troughs, ultrabasites, low-gradient metamorphism). Final stages of the cycles (high gradient metamorphism, granites) are most evident in the second, fourth and fifth cycles. The cycles of tectonic activity are separated by epochs of partial or complete cratonization, marked by mafic dyke swarms, subalkaline and alkaline plutons, or plutons of stratified basic rocks. Cratonizations subsequent to 2400, 1100 and 600 Ma events were most extensive.

Proterozoic proto-aulacogens (Ritscher, Sandow-Amundsen, possibly Turnpike) were formed 1800 to 600 Ma ago. Various volcanic and volcanoclastic rocks of the contrasted series and differentiated intrusive traps dominate in the fill of the proto-aulacogens. Formations of proto-aulacogens marked transition to the rift stage of development of the Antarctic shield. Tectono-thermal activity in the Phanerozoic also related to a rifting stage.

THE GRANITE - GREENSTONE TERRAINS IN THE SOUTHERN PRINCE CHARLES MOUNTAINS
(poster presentation)

E. N. Kamenev, N. N. Krasnikov. North Branch for Marine Geologic Exploration "Sevmorgeologia" 120 Moyka, Leningrad 19121 USSR

Two granite-greenstone terranes are recognized in the southern Prince Charles Mountains (PCM). The larger Ruker Terrain comprising several individual greenstone belts intermingled with different kinds of granites extends for about 400 km east and west of the southern Mauson Escarpment and varies in width from 50 to 150 km. The smaller Fisher Terrain is named after the Fisher Massif from where it extends SW and NE; it is about 200 km long and 50 km wide.

The Rukeer terrain is entirely thrust bounded against the Proterozoic granite-gneiss-schist belt on the north and a hypothetical Archean high-grade protocratonic block in the south. Variable rock assemblages that compose that terrane are collectively named the Ruker Complex and subdivided into the Menzies Supracrustals, the Sodruzhestvo Supracrustals and the Mauson Granitoids.

The Menzies Supracrustals consist of epidote-amphibolite, cummingtonite-amphibolite and garnet-amphibolite facies assemblages. The base of the section is represented by tectonic melange of mica-quartz-amphibole-plagioclase schists (locally with garnet and epidote), anphibolites (mafic metavolcanics and dykes), talc-actinolite rocks with olivine relics (meta-ultramafics), mica-quartz rocks , plagioclasites, epidothites. Many of mafic and ultramafic rocks have chemical composition of komatiitic volcanics. The melange sequences are easily recognized in the outcrop by their variegated appearance: white, grey, black, dark-green, bluish-green rocks deformed in chaotic mesoscopic folds with elongated infolded bands of crushed mafic and ultramafic inclusions and rolled massive blocks, deformed mafic slabs and boudins in banded schists. The size of melange exposures often exceeds 4 km in width, 7 km in length and 0.8 km in height. The melange forms synclinal nappe-folds, wedges and lenses in zones of thrusting.

The middle part of the Menzies Supracrustals is represented by fuchsite-, iron-,mica-, garnet-bearing quartzites interbedded and interfingered with metapelites (with kyanite, staurolite,garnet, mica sillimanite), mafic schists and acid gneisses.

In the upper part of the Menzies Supracrustals there are grey and black schists consisting of biotite, actinolite, hornblende, epidote, carbonates,acid plagioclase and guartz (calcareous metasediments), minor metapelites, quartzites, amphibolites, conglomerates, tremolite marbles and carbonate gyprocks.

The Sodruzhestvo Supracrustals are characterized by greenschist facies assemblages. In the lower parts of this sequence metabasalts and metadiabases include chains of blocks and lenses of banded iron formation and are overlapped by meta-andesites, acid metavolcanics, metacherts (quartzites) and metatuffs. Higher up the section there are metamorphosed acid tuffs, pyroclastics and epivolcanic sediments with minor conglomerates. Intensive carbonatization is common in all rocks.

The Mawson Granitoids include biotite-amphibole, biotite, micaceous quartz-feldspar gneisses or granite-gneisses, locally with migmatitic textures. In the greenschist facies zone these granitoides are highly sheared and transformed to cataclasites and mylonites, chloritized and seritized, locally altered to quartzites. In the amphibolite facies zones they show clear lineation, schistosity, irregular banding, mottling and folding. Granitoids appear to form tectonic domes, slabs or piles of slabs. The size of outcrops composed of granitoids is 5 - 10 km in length and 0.6 - 1.0 km in height. Minor slabs are tens or hundreds meters in width. The supracrustals are sendwiched between the granitoid slabs. Bands of metabasites, dykes and sills (or their fragments), as well as xenoliths of supracrustals are included in the presence of deformed and folded veins or lenses of pegmatite. Some of the granitoids may represent the blocks of sialic basement of greenstone belts, but more often they are derived from pretectonic and syntectonic acid intrusives, extrusives or even volcanics.

The structure of the Ruker Terrain is dominated by tightfolding, thrusting and shearing. The majority of large geological bodies are tectonic slabs, nappes, fold-nappes and domes with intensive internal folding, shearing and cleavage. Tectonic breccias, melange and tectonic conglomerates are very common. Tectonic features strike mostly in W-E direction, and metamorphic zonation is subparallel to that trend. Increase in metamorphic grade is associated with intensity of tectonic deformation.

Underformed dykes and sills of amphibolites (metabasetes) intersect both supracrustals and granitoids and constitute an important feature related to the period of cratonization of the Ruker Terrain.

Syntectonic movement is represented mainly by thrusts, overthrusts and underthrusts. Some of strike-slip transportation also occurred. The latest normal faults cut undeformed amphibolite dykes. Fig.1 illustrates the structure of the Ruker Terrain in the amphibolite facies zone at the Southern Mawson Escarpment.

In the central part of the Ruker Terrain the metamorphic grade corresponds to greenschist facies (chlorite and biotite zones of intermediate pressure), in adjacent zone - to epidote-amphibolite facies (staurolite-biotite-kyanite-

muscovite subfacies), and in the marginal part - to almandine-amphibolite and cummingtonite-amphibolite facies (garnet-kyanite-biotite-muscovite,cordierite-staurolite-gerdite and garnet-sillimanite-biotite-orthoclase subfacies). In a high-grade amphibolite facies zone there is a clear evidence of retrograde alteration to epidote-amphibolite facies zone is retrogressively metamorphosed to the greenschist facies.

Pb-Pb and U-Pb isotopic data on zircons, Rb-Sr model and isochron ages and Sm-Nd model ages indicate that evolution of the Ruker greenstone belts (volcanism, sedimentation, granite intrusion, deformation and metamorphism) occurred between 3100 and 2700 Ma. Initial volcanic-sedimentary troughs developed upon, and laterally to, a much older granulite-gneissic terrain that existed here since about 3300 Ma. Underformed metabasic dykes were intruded about 2400Ma ago. Subsequent tectono-thermal activation manifested by intrusion of granite and pegmatite veins and plugs occurred at 2100, 1500, 1300 and 950 Ma ago.

The Fischer Terrain is entirely fault bounded from NW to SE against Proterozoic granulite-gneiss belts. The rocks of mafic, intermediate and felsic composition metamorphosed into epidote-amphibolite facies assemblages and consisting of epidote, bluish-green hornblende, biotite, quartz, muscovite, oligoclase, albite, microcline and relics of andesine-labradorite, pyroxenes, rare olivine, garnet (staurolite-biotite-kyanite-muscovite and staurolite-chlorite-muscovite subfacies). Regressive minerals are chlorite, muscovite and actinolite. Features of igneous origin, such as feldspar phenocrysts,ophitic, gabbroic textures are locally well preserved.

At Fisher Massif the metavolcanics are interleaved with minor intrusive bodies of porphyritic rocks, lenses of banded iron formation, calcareous tuffs, felsic tuffaceous pyroclastic rocks and metacherts. The metavolcanics of mafic and intermediate composition dominate in the northern and central parts of Fisher Massif, while metavolcanics of felsic composition prevail in the southern part (Fig.2). Thickness of bands, horizons and lenses of uniform material varies from 5 to 200 m. The metavolcanics form tectonic slabs intercalated with the slabs of coarse-grained plutonic rocks. Thickness of slabs appears to be more than 2 km. Configuration of plutonic bodies is variable; lensoid , sill-shaped forms are most abundant.

Willing Massif , Mount Collins and Nelson Rocks consist almost entirely of plutonic rocks. Their bodies extend colaterally with thrust faults and fold axes in the enclosing metavolcanic sequences. The largest plutonic rock outcrop extends for more than 10 km and is almost 5 km wide. Petrographic composition of plutonic rocks varies from gabbro to granite and syenite and reflects the succession of their intrusion. Gabbro and diorite plutons are most abundant.

Usually they have a layered structure and occasionally include metapyroxenite layers (Willing Massif). The plutonic rocks are deformed and metamorphosed similar to the volcanics.

Metamorphosed and slightly deformed dykes inside the plutons are represented by biotite-amphibole, biotite-amphibole-plagioclase, biotite-amphibole-clinopyroxene-plagioclase rocks, metadolerites, metaporphirites of intermediate composition, blastocataclasites of granitic and granodioritic composition and pegmatites.

The structure of the Fisher Terrain is not clear. There are piles of tectonic slabs, thrust fault zones, internal isoclinal folding, schistosity in metavolcanics, and shear zones inside the plutons. Locally there is evidence of two folding episodes.

No age determination are available for metavolcanic sequences of the Fisher Terrain. However, some of the intrusive bodies have been dated. Pb-Pb isotopic investigation on zircons from gabbro of the Willing Massif show a probable age of the intrusion close to 1300 Ma. Rb-Sr · isochron determinations on a granodiorite pluton in the northern Fisher Massif indicated 870 ± 0.001).Therefore it is likely that metavolcanic sequences in the Fisher Terrain are also of Late Proterozoic age.

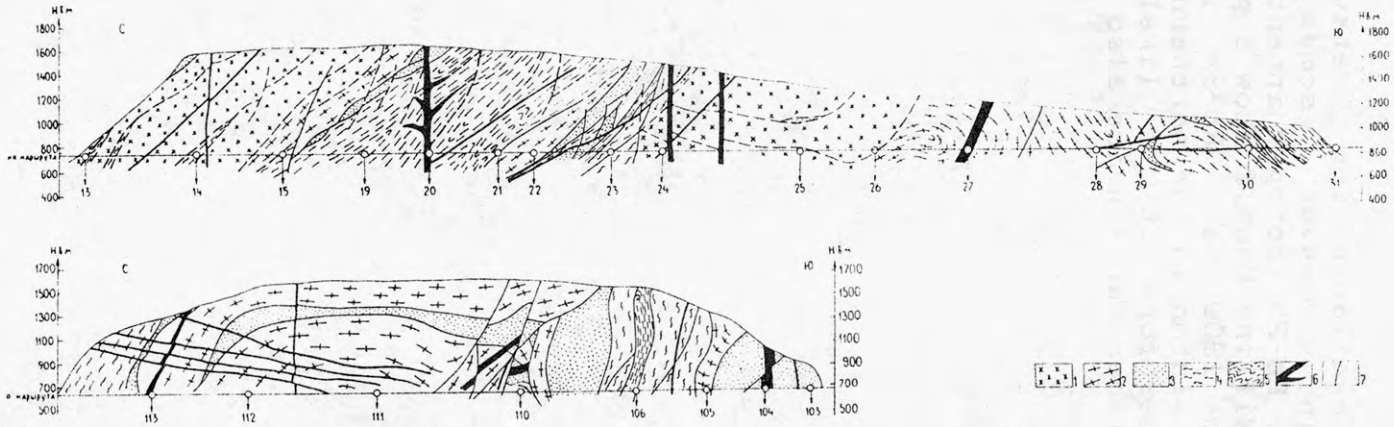

Fig.1. GEOLOGICAL SECTIONS THROUGH THE SOUTHERN MAWSON ESCARPMENT (THE MENZIES SUPRACRUSTALS AND THE MAWSON GRANITOIDS OF THE RUKER GRANITE-GREENSTONE TERRAIN). 1 - linear quartz-feldspatic gneisses with amphibolite bands and deformed dykes ; 2 - granite-gneisses with deformed amphibolite dykes ; 3 - rock unit with metaultramafic lenses and blocks; 4- biotite-amphibole-quartz-feldspar schists; 5- quartzites and metapelites; 6 - undeformed amphibolite dykes ; 7 - faults.

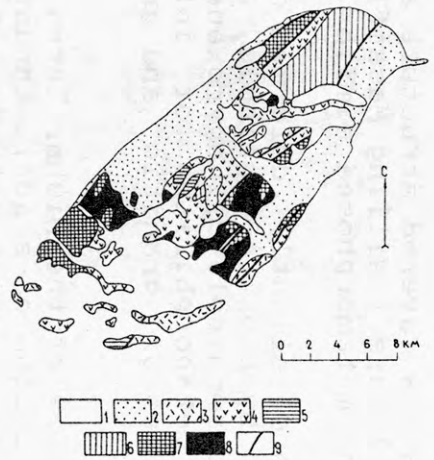

Fig 2. SIMPLIFIED GEOLOGICAL MAP OF ~~THE~~ FISHER MASSIF. 1 - ice and snow; 2 - moraine deposits; 3 - felsic metavolcanics and tuffaceous pyroclastic rocks; 4 - mafic and intermediate metavolcanics; 5 -granites; 6 -granodiorites; 7 - metadiorites; 8 - metagabbro; 9 - faults.

THE MAGMATIC COMPLEXES ROUEN AND ELGAR FROM ALEXANDER ISLAND, ANTARCTIC PENINSULA - PETROLOGICAL, GEOCHEMICAL AND GEOCHRONOLOGICAL CONSTRAINTS

B.K. Kamenov and C.T. Pimpirev
Sofia University "Kliment Ochridsky", Faculty of Geology, 15 Russky Bd., 1000 - Sofia, Bulgaria

The outcrops of Rouen pluton and Elgar volcanics recorded on Alexander Island represent an calc-alkaline assemblage which is an important accent of the subduction-related Mesozoic-Cenozoic magmatism within Antarctic Peninsula. New radioisotope dating (K-Ar and Rb-Sr) indicates that the both magmatic complexes are coeval (Early Plaeocene). Isotopic ratios show mantle-derived source for the melts with a weak degree of magma-crust interaction. The lavas and hypabyssal intrusions overlie or intrude the metasedimentary LeMay Group.

New finds of miospores in sections across turbidite sequences of the country rocks points upon Tertiary age of these deposits.

Undescribed up to now plutonic and volcanic rock varieties were found thus the compositional range of the igneous rocks is extended. Many of the observed chemical and mineralogical variations are compatible with the differentiation of a single parental magma. New whole rock and mineral chemistry data, combined with trace element and REE geochemistry confirm the analogy with the other magmatic complexes of the Andean Intrusive Suite and Antarctic Peninsula Volcanic Group. The typical features of subduction-related island arc on the margin of the continental Antarctic plate left their specific geochemical signitures. The extent of fractionation, crystal accumulation, contamination and mixing of rising magma is figured out of the geochemical plots and general mixing model calculations. Temperature, pressure and oxygen fugacity conditions of crystallization have been calculated using different geothermomenters and geobarometers.

The study supports the idea of gradual rejuvenation of the magmatism in the southern part of Antarctic Peninsula westwards which may be explained by assuming the change of the geometry of the subducted proto-Pacific oceanic slab.

PRESENT STATUS OF SEISMIC NETWORK IN ANTARCTICA

K. Kaminuma, National Institute of Polar Research, Kaga, Itabashi-ku, Tokyo 173, Japan

At its meeting in Sãn Paulo, Brazil in July 1990 the Working Group on Solid Earth Geophysics (WG/SEG) of SCAR decided to review the present status of earthquake seismology in Antarctica, and the author was nominated to undertake the review. Accordingly, a Questionnaire was sent out to the group members of WG/SEG. The Questionnaire included following items: Country, Contact person, Station name, Location and elevation, Seismographs, Report of Phase readings, Data Report, Detection Capability etc.

Completed Questionnaires were returned from group members or contact persons of eleven countries. Ten countries out of the eleven operated 13 seismic stations in Antarctica in 1990/91 as shown in Fig. 1. Figure 1 shows station locations with symbols for long- and short-period seismographs and digital seismographs. Long period seismographs in the figure are those with a period of pendulum longer than 10 s. Short period seismographs have a pendulum period of about 0.5 ~ 2 s. The establishment and development of world wide networks of broadband digital seismographs have been emphasized by seismologists during the last decade. The broadband digital seismograph networks that are developing in the lower latitude regions are named GEOSCOPE (by European countries), IDA/IRIS (by the United States), POSEIDON (by Japan), etc. However, digital seismographs in Antarctica are operated at only two stations, Dumont D'Urville and Syowa Stations. Dumont D'Urville is one of the GEOSCOPE stations and Syowa is part of POSEIDON. USGS has a plan to install digital seismographs at South Pole in 1991/92. A set of broadband digital seismographs has been installed at VNDA by Albuquerque Seismological Laboratory of US and the seismic signal is transmitted to Scott Base by radio-telemetry. However, digital tape recording is not yet operational. Germany also has a plan to install an ultra long period three-component seismograph somewhere on the grounded ice near Georg-von-Neumayer Station.

It should be mentioned that a seismic array with four stations is operated by Germany in the vicinity of Georg-von-Neumayer Station. The array, with four 1 s period seismographs, is established on the floating ice shelf. Another two stations with three-component short period seismographs are operated on grounded ice sheet.

During IGY in 1957/58, seismic stations had been operated by Argentina and Chile on the Antarctic Peninsula, but no information from the two countries were available for this review. Only two seismic stations, Faraday and Great Wall Stations have been operated in the Antarctic Peninsula region. According to the author's personal knowledge, three-component

seismographs are also installed at King Sejon Station of Korea in King George Island, but he has no detailed information at present. The seismicity in the Antarctic Peninsula region is an important aspect of Antarctic Earth Science.

Phase readings of seismic events are currently reported to NOAA/NEIC and ISC from CSY, DRV, SNA, SPA, SBA, SYO and MAW by telex/telegram etc. It is easy to find the data from these stations in the Bulletin of ISC, but the data of only four stations; DRV, SBA, SPA and MAW are used frequently on the Earthquake Data Report by USGS. Recently, the author could not find phase reading reports of SYO on the Earthquake Data Report, even though they are continue to send the data at least once a week. This might be a result of the difficulty of telecommunications in Antarctica.

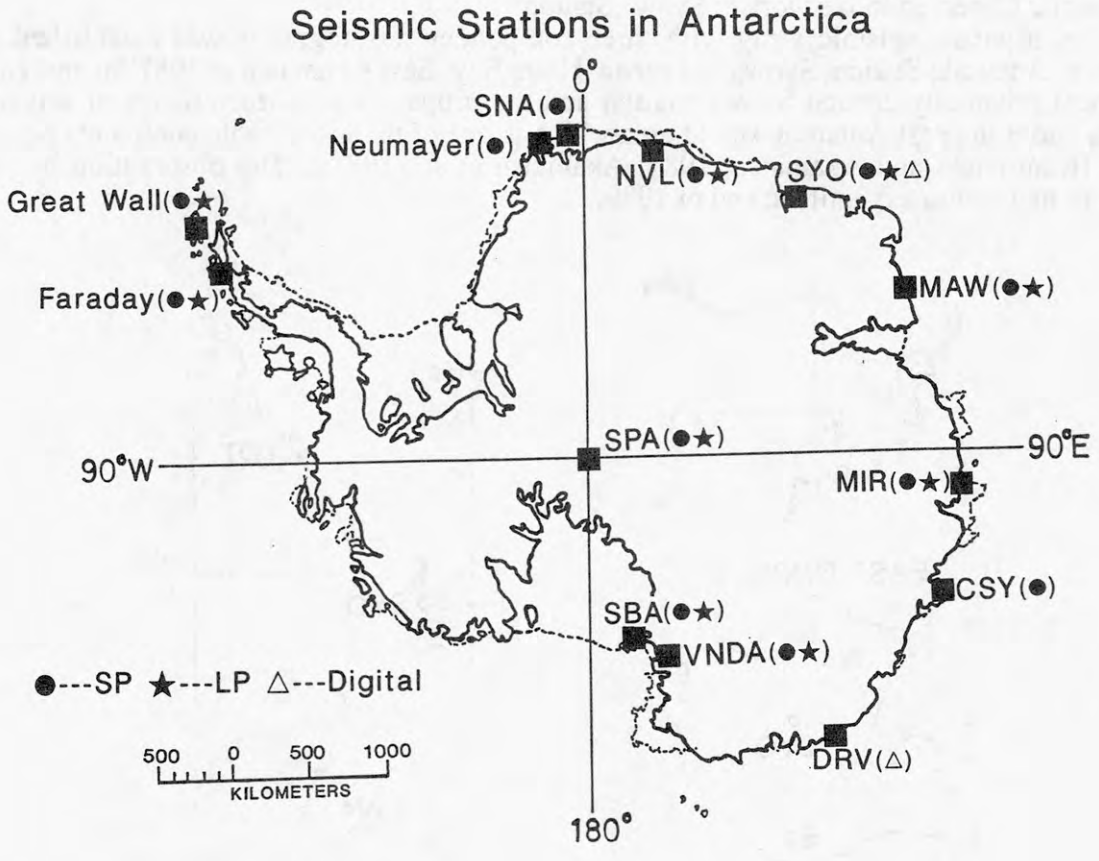

Fig. 1 Seismic Stations in Antarctica operated in 1990/91. Solid circles and solid stars show short-period and long- period seismographs respectively. Open triangles show broadband digital seismographs. The code of stations are as follows; NVL (Novolazarevskaya, USSR), SYO (Syowa, Japan), MAW (Mawson, Australia), MIR (Mirny, USSR), CSY (Casey, Australia), DRV (Dumount D'Urville, France), VNDA (Vanda in Dry Valley, USA), SBA (Scott Base, New Zealand) and SPA (South Pole, USA): The full name of the other stations is Georg-von-Neumayer (Germany), Great Wall (China) and Faraday (UK).

INTERMITTENT MICRO-SEISMIC ACTIVITIES IN THE VICINITY OF SYOWA STATION, EAST ANTARCTICA

K. KAMINUMA, National Institute of Polar Research, Kaga, Itabashi-ku, Tokyo 173, Japan
J. AKAMATSU, Disaster Prevention Research Institute, Kyoto University, Gokasho, Uji, 611, Japan

A tripartite seismic array was established in Syowa Station (69°S, 39°E) in 1987 for studying the local seismicity. Ten micro-earthquakes were recorded by the tripartite array during 20 months from June 1987 to January 1989. These earthquakes are located in the geological and geophysical structural boundaries of the coastal area in the Antarctic continent and offshore. There are many well-developed elevated beaches and marine terraces in the coastal ice-free area of the Antarctic continent. These have been formed by the relative lowering of sea level, caused by the crustal uplift after the deglaciation. It seems that the local micro-earthquakes are caused by the tectonic stress which is accumulated by the slow-moving crustal uplift.

1. Seismic Observation Network at Syowa Station

A tripartite seismic array with three-component seismographs was established at Japanese Antarctic Station, Syowa in Lützow-Holm Bay, East Antarctica in 1987 for studying the local seismicity around Syowa Station and the propagation characteristics of seismic waves under the east Antarctic shield area which is one of the most stable continents on the earth (Kaminuma and Akamatsu, 1987; Akamatsu et al., 1988). The observation by the network had continued until the end of 1989.

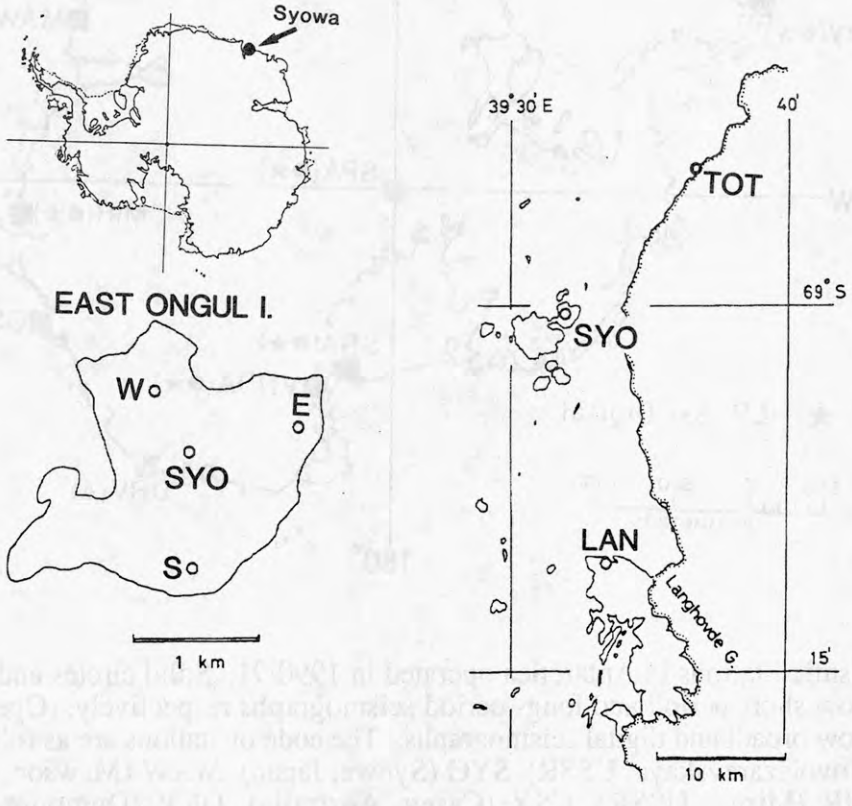

Fig. 1. The tripartite seismic array with three-component seismographs around Syowa Station operated from June 1987 to October 1989. The small tripartite array (W, S and E) in East Ongul Island was occupied from February 1988 to December 1989.

The seismic observation network consisted of three sites with a three-component 1-s seismograph as shown in Fig. 1; Syowa Station (SYO), Tottuki Point (TOT) and Langhovde (LAN). TOT and LAN were located on the outcrops at the edge of the east Antarctic shield. These two stations were linked by radio-telemetry to Earth Science Laboratory of Syowa Station. The distances between the sites ranged from 15 to 30 km (Akamatsu et al., 1988).

A smaller tripartite array with three 1-s vertical seismographs had been operated in East Ongul Island from February 1988 to December 1989 (E, S and W in Fig. 1). The seismic signals were transmitted by cable wire to the recording system at the Earth Science Laboratory (Akamatsu et al., 1989).

2. Seismic Activity

More than 17,000 events were recorded during 29 months from June 1987 to October 1989. About 25 percent of the total events were sea-ice shocks, 66 percent were icequakes, 8 percent were teleseisms and 1 percent were the events caused by glacier movements. Only ten local events were located by the system during the 20 months from June 1987 to January 1989 as shown in Fig. 2. The magnitude ranges from -0.8 to 3.0, most of them being micro-earthquakes in the range of 1.0-3.0.

Five events out of ten are located along the Prince Olav Coast, three are in Lützow-Holm Bay and the others are in the northwestern offing of the Riiser-Larsen Peninsula.

Magnitudes of the two events on May 24 and 26, 1988 located near the Langhovde glacier are 0.2 and -0.8. The event of May 26 is inferred to be the aftershock of the event of May 24 on the basis their magnitudes (Akamatsu et al., 1989). Three aftershocks of the Nov. 7, 1987 event were recognized on the seismograms of the routine seismic observation. These two events are mainshock-aftershock type among the micro-seismic activities around Syowa Station (Akamatsu et al., 1989).

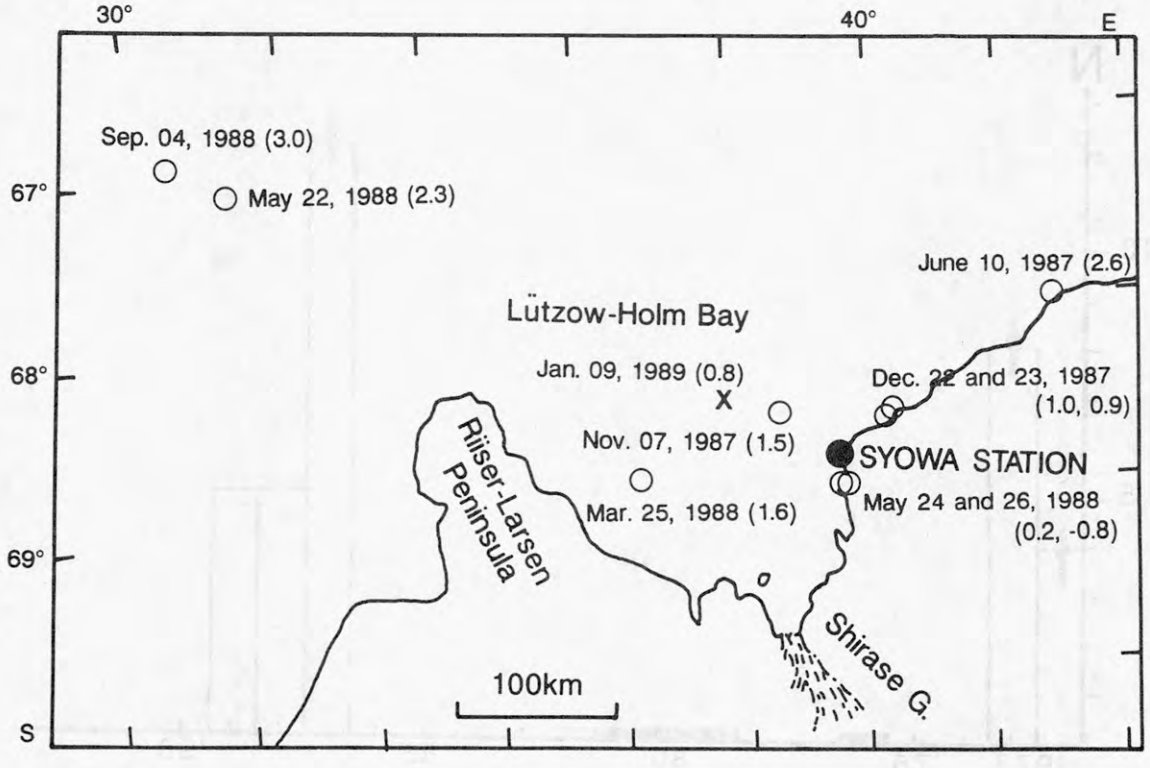

Fig. 2. The locations of local earthquakes with magnitude in the vicinity of Syowa Station recorded from June 1987 to January 1990.

The earthquake of June 10, 1987 has about 20s S-P time at Syowa Station and a magnitude of 2.6. It must be pointed out that nine events with similar wave forms were recorded during the preliminary observation period from March to May 1987, but no such event was recorded after the June 10 event. Akamatsu et al. (1988) mentioned that these earthquakes are located in the boundary between the two geological complexes, Lützow-Holm Complex and Layner Complex. The earthquakes are considered to be tectonic earthquakes occurring along the geological fault, and a kind of earthquake swarm.

Two events of Dec. 22 and 23, 1987 located near TOT has a similar magnitude, being 1.0 and 0.9 and their wave forms are alike. The two events are probably a multiple shock.

The events located in the northwestern offing of the Riiser-Larsen Peninsula have relatively large magnitudes among the earthquakes detected by the network. As the earthquakes, which occurred in the area, were far from the network, only the ones with magnitude larger than about 3 (small-earthquake) may have been detected.

Although seismic activity in the vicinity of the Syowa Station is very low, but still one could see a variety of earthquakes: swarms, main-shock-aftershock, multiple shocks etc. This pattern of seismic activities is similar to the activities in Japan where is the most high seismicity on the earth.

Figure 3 shows annual number of micro-earthquakes counted on the seismograms of the routine observation and the tripartite seismic array at Syowa Station from 1972 to 1989. As the magnification of seismographs are not the same through the period, the figure does not show the seismicity but minimum number of local earthquakes detected on the seismograms. The arrows in Fig. 3 indicate that the number of earthquakes occurred is more than that shown in the figure. The solid lines in 1976 and 1979-1982 show the periods that no local-earthquakes were detected in spite of seismologists were wintering during that time and scaled seismogram carefully. The earthquakes occurred only in 1972-73 and 1987-89. It must be pointed out from the figure that the local-earthquakes occur intermittently in the vicinity of Syowa Station.

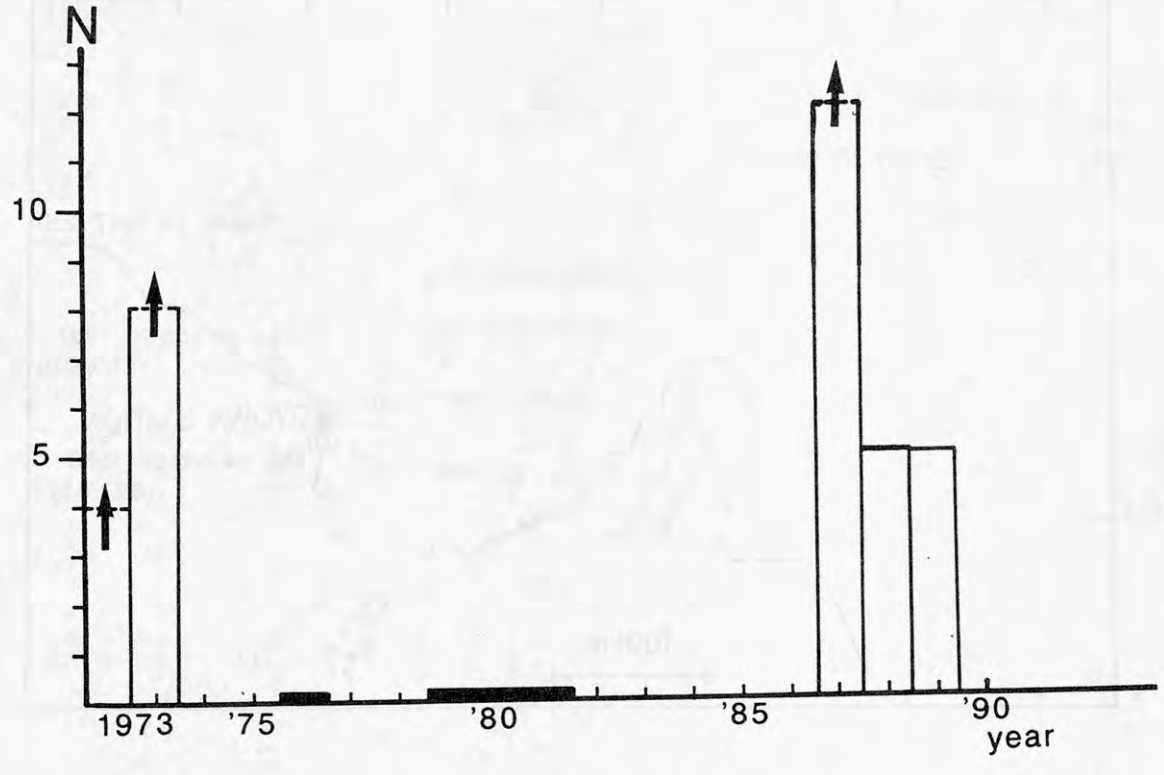

Fig. 3. Annual number of earthquakes in the vicinity of Syowa Station counted on the seismograms of the routine observation and the tripartite array from 1972 to 1989.3.

3. Discussion

There are many well-developed elevated beaches and marine terraces in the broad coastal ice-free areas of the Antarctic continent. The well-developed elevated beaches and the marine terraces are found around Syowa Station and along the eastern coast of Lützow-Holm Bay. These elevated beaches and marine terraces have been formed by the relative lowering of sea level (Omoto, 1977; Yoshida and Moriwaki, 1979), caused by the crustal uplift after the deglaciation. The maximum heights of elevated beaches around Syowa Station are 22 m in East Ongul Island, 19 m in Teöya (Island), 3 km south from East Ongul Island, and 35 m in Ongulkalven (Island), 5 km west from East Ongul Island as shown in Fig. 4. No elevated beaches are found in West Ongul Island. The origin of the horizontal axis in Fig. 4 is taken as the edge of the continent, the front of the Antarctic ice sheet.

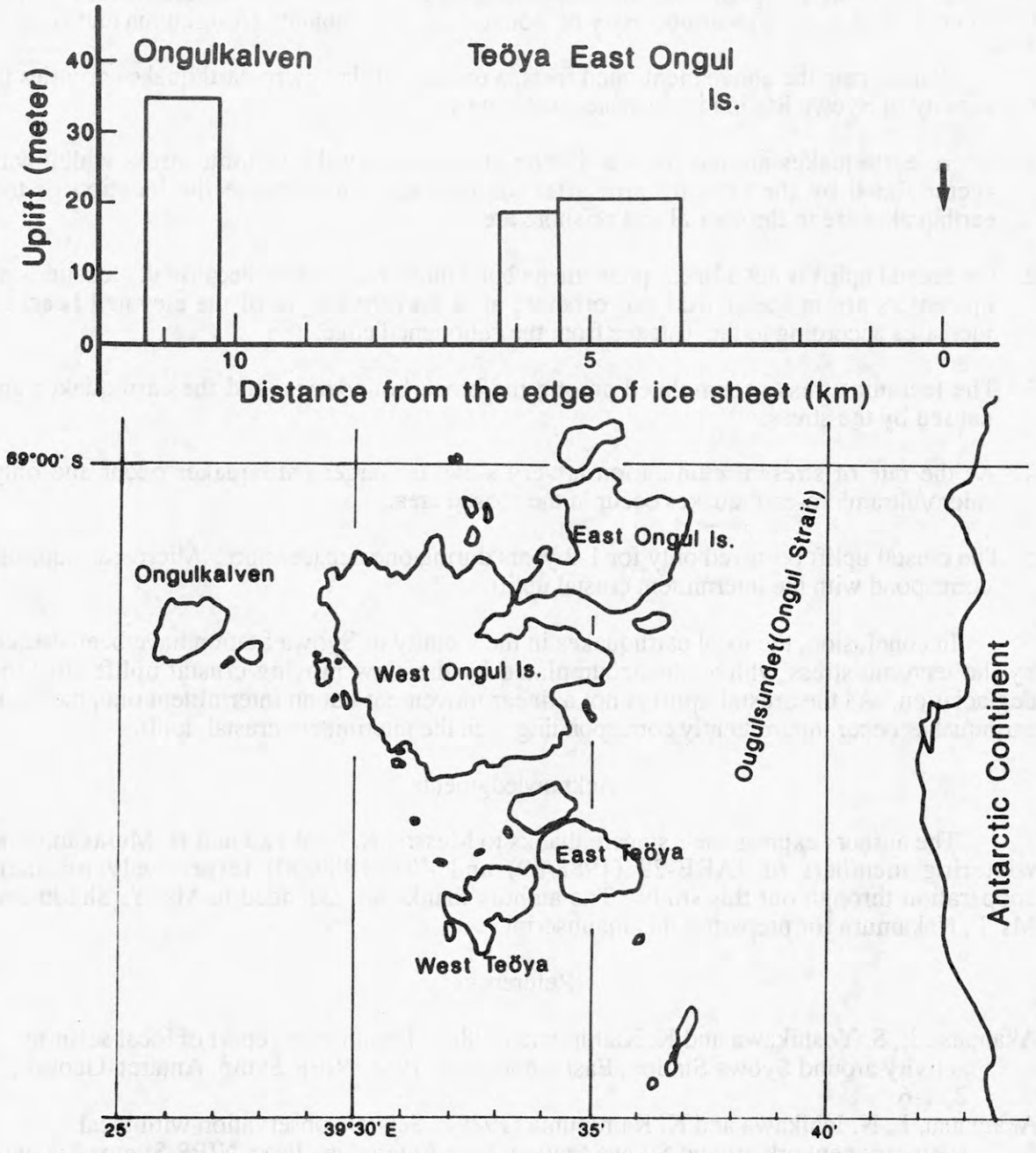

Fig. 4. The maximum heights of elevated beaches around Syowa Station.

The uplift movement seems a block movement, because the height of the elevated beaches increases according to the distance from the edge of the continent and each beach is horizontal. The uplift movement of the Ongulkalven block in Fig. 4 is more than that of the East Ongul-Teöya block. As there is the Ongul strait, 4 km wide and 700 m deep between the East Ongul-Teöya block and the continent, the movement of East Ongul-Teöya block is independent from that of the continent.

As the dates of submarine fossils found in East Ongul Island are about 6,000 years BP, the rate of the uplift of the submerged area relative to the sea level seems to be 2.5 mm/y on the average, possible maximum being 5-6 mm/y (Yoshida and Moriwaki, 1979). The crustal uplift seems to have continued during the last 6,000 years. Kaminuma (1990) estimated that the micro-earthquakes around Syowa Station have been caused by the tectonic stress which was accumulated by the slow-moving crustal uplift after the deglaciation.

As shown in Fig. 1, the local earthquakes are located in the mouths of glaciers in the coastal area. There is a geological boundary located in the center part of Lützow-Holm Bay (Hiroi et al., 1991) and a clear boundary of Bouguer gravity anomaly (Kaminuma and Nagao, 1984).

Considering the above mentioned facts, a process of the micro-earthquake activities in the vicinity of Syowa Station is suggested as follows:

1. Micro-earthquakes around Syowa Station are caused by the tectonic stress which was accumulated by the crustal uplift after the deglaciation, because the location of the earthquakes are in the coastal and offshore area.

2. The crustal uplift is not a linear phenomena but a block movement, because the locations of epicenters are in the coastal and offshore area, and the height of the elevated beaches increases according to the distance from the continental edge.

3. The tectonic stress accumulated among the block boundaries, and the earthquakes are caused by the stress.

4. As the rate of stress accumulation is very slow, no larger earthquakes occur and only micro/ultramicro-earthquakes occur in the coastal area.

5. The crustal uplift occurred only for 1-2 years during one decade/more. Micro-earthquakes correspond with the intermittent crustal uplift.

In conclusion, the local earthquakes in the vicinity of Syowa Station have been caused by the tectonic stress which was accumulated by the slow moving crustal uplift after the deglaciation. As the crustal uplift is not a linear movement but an intermittent one, the local earthquakes occur intermittently corresponding with the intermittent crustal uplift.

Acknowledgments

The authors express their sincere thanks to Messrs. N. Ichikawa and H. Murakami, the wintering members of JARE-29 (1988/89) and -30 (1989/90) respectively for their cooperation through out this study. The authors thanks are extended to Ms. Y. Shudo and Ms. F. Nakamura for preparing this manuscript.

References

Akamatsu J., S. Yoshikawa and K. Kaminuma (1988): Preliminary report of local seismic activity around Syowa Station, East Antarctica. Proc. NIPR Symp. Antarct. Geosci., 2, 1-6.

Akamatsu, J., N. Ichikawa and K. Kaminuma (1989): Seismic observation with local telemetry network around Syowa Station, East Antarctica. Proc. NIPR Symp. Antarct. Geosci., 3, 1-12.

Hiroi, Y., K. Shiraishi and Y. Motoyoshi (1991): Late Proterozoic paired metamorphic complexes in East Antarctica. Proc. of the 5th International Symp. on Antar. Ear. Sci. (in press).
Kaminuma, K. (1990): Local earthquake activities around Syowa Station, East Antarctica. Tohoku Geophys, J. 35, 127-136.
Kaminuma, K. and J. Akamatsu (1987): Nankyoku Syowa Kiti Fukin no Zishin (Local earthquakes around Syowa Station, Antarctica). Nankyoku Shiryo (Antarctic Rec.), 31, 177-185.
Kaminuma, K. and T. Nagao (1984): Gravity survey in Lützow-Holm Bay and the Mizuho Plateau, East Antarctica, 1981. JARE Data Rep. No. 89, 59-87.
Omoto, K. (1977): Geomorphic development of the Soya Coast, East Antarctica-Chronological interpretation of raised beaches based on levelling and radiocarbon datings, Sci. Rep. Tohoku Univ., Ser. 7 (Geogr.), 27, 95-148.Yoshida, Y. and K. Moriwaki (1979): Some consideration on elevated coastal features and their dates around Syow Station, Antarctica. Mem. Natl Inst. Polar Res., Spec. Issue, 13, 220-226.
Yoshida, Y. and K. Moriwaki (1979): Some consideration on elevated coastal features and their dates around Syowa Station, Antarctica. Mem. Natl Inst. Polar Res., spec. Issue, 13, 220-226.

GRAVITY SURVEY IN ROSS ISLAND, ANTARCTICA

K. KAMINUMA, National Institute of Polar Research, 9-10, Kaga 1-chome, Itabashi-ku, Tokyo 173
S. MIURA and S. UEKI, Faculty of Science, Tohoku University, Aramaki Aoba, Sendai 980
E. KOYAMA, Earthquake Research Institute, University of Tokyo, 1-1, Yayoi 1-chome, Bunkyo-ku, Tokyo 113

Gravity surveys have been carried out in Ross Island during four summer seasons from 1982/83 to 1985/86 in order to investigate the subsurface structure of the active volcano Mount Erebus, Antarctica. The Bouguer anomaly has been calculated at each station. The pattern of anomaly distribution on this island can be summarized that the anomaly is high in the whole island except the western and southwestern coast, where anomalies are about zero or negative, and that a higher anomaly exists in the summit area of Mount Erebus. The structure of Mount Erebus might be classfied as a type similar to the Kilauea Volcano of Hawaii Island and the Osima Volcano of Japan.

1. Measurments

Gravity surveys at Mount Erebus (77.5°S, 167.0°E, 3794m), Ross Island started in the austral summer of 1982/83, have been carried out using a LaCoste & Romberg gravity meter, G-type. The locations of the gravity stations are shown in Fig. 1. The absolute gravity base station 59676C, the bench mark at Earth Sciences Laboratory of McMurdo Station, was chosen as the references point for the relative measurements of gravity. All the measurments started from the reference point and ended there to correct instrumental drift of the gravimeter. The location of 59676C is 77°51.0'S, 166°40.4'E and 43.18m in elevation above mean sea level, and its gravity value in the IGSN71 (International Gravity Standardization Net 1971) is 982969.771 mgal. The results in the 1982/83 season were reported by KAMINUMA et al. (1984). MIURA et al. (1987) presented results from the surveys conducted in the 1983/84 and 1984/85 summer seasons as well as recalculated results of the 1982/83 surveys.

The accuracy of the locations of the measurment points is directly related to the accuracy of the gravity survey. The climate and the general conditions for land surveys in Antarctica are so severe that there are not many points whose altitude is precisely determined. KAMINUMA et al.(1984) discussed the estimated error in altitude at the measurment points.

In the case of measurment points in the summit area (see small frame in Fig.1), the accuracy of altitude at each point was better than 1 m because it was determined on the 1: 5000 topographic map of "Mt. Erebus, Antarctica" which was published by Depatment of Lands and Survey, New Zealand, with a contour interval of 5 m. This uncertainty of elevation corresponds to an error in gravity value of about 0.2 mgal in the Bouguer anomaly value.

For other measurment points in Ross Island, the altitude of each station was determined by means of a barometric altimeter; the accuracy was estimated to be within about 10 m after applying corrections for the altimeter. Therefore, the estimated error in gravity values is up to 2 mgal for these points. The same procedure was taken for all measurments.

2. Terrain Correction

The values of terrain corrections are very important for gravity surveys particularly conducted in mountain areas because Bouguer corrections are made by assuming an infinite plate whose thickness is equal to the elevation of the observation point, so the mass at the convex place higher than the observation point is not considered and the mass at the concave place is overestimated. Unfortunately, the terrain of Ross Island is not yet well determined.

The most detailed topographic map has been published by the U.S. Geological Survey. It has a scale of 1 to 250000 and a contour interval of 200 m. Figure 2 shows the contour lines read from this map (NAGAO, personal communication) and the corresponding three-dimensional topographic map. Here, as a preliminary study (KAMINUMA et al., 1984), we adopted Talwani's three-dimensional method (TALWANI and EWING, 1960) to calculate the terrain corrections. Figure 3 shows the spacial distribution of the terrain correction values calculated at 1.5' (latitudinal direction) × 6' (longitudinal direction) grid points by Talwani's method. The correction values are normalized by a unit density. Therefore, the actual correction values are derived from multiplying these values by the assumed density. As expected, the large corrections are necessary to the observation points at high elevation.

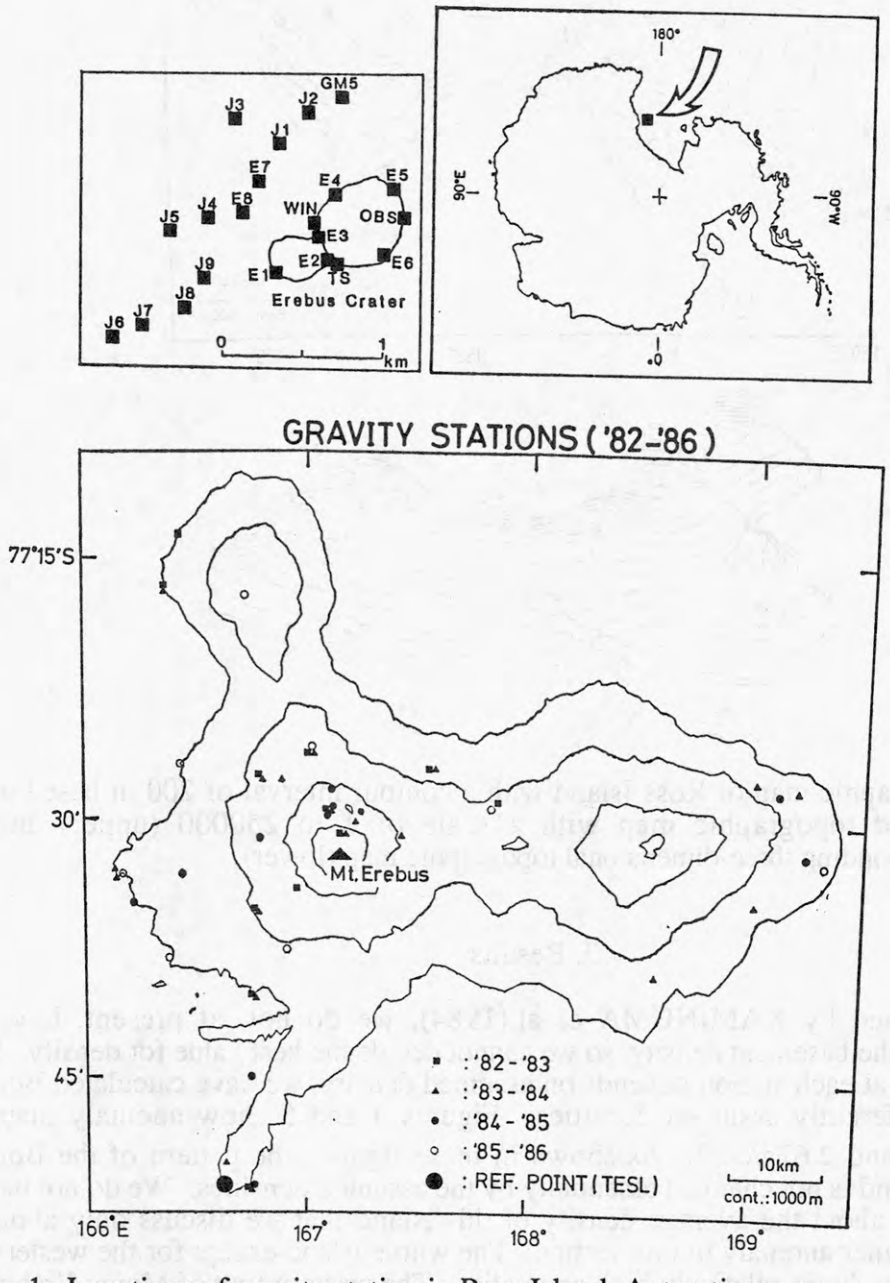

Fig. 1. Locations of gravity station in Ross Island, Antarctica.

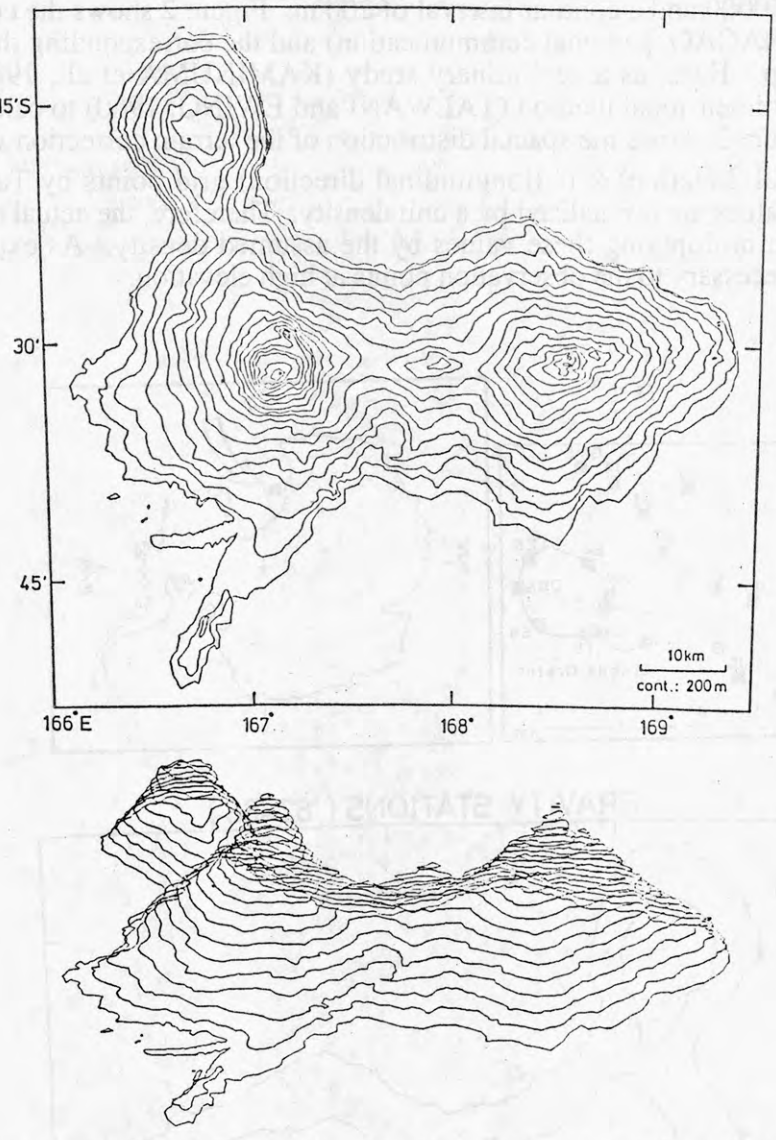

Fig. 2 Topographic map of Ross Island with a contour interval of 200 m based on the detailed topographic map with a scale of 1 to 250000 (upper) and the corresponding three-dimensional topographic map (lower).

3. Results

As mentioned by KAMINUMA et al.(1984), we do not, at present, have any information about the basement density, so we cannot decide the best value for density. Since the anomaly value at each station depends on assumed density, we have calculated Bouguer anomalies for differently assumed densities. Figures 4 and 5 show anomaly maps for densities of 2.20 and 2.67g/cm^3. As shown in these figures, the pattern of the Bouguer anomaly in the island is not changed essentially by the assumed densities. We do not have so much information about the average density of this island that we discuss only about the pattern of the Bouguer anomaly in this section. The whole island except for the western and southwestern coasts shows relatively high anomalies. The western foot of Mount Erebus can be noted as a negative anomaly and the southwestern part as nearly zero.

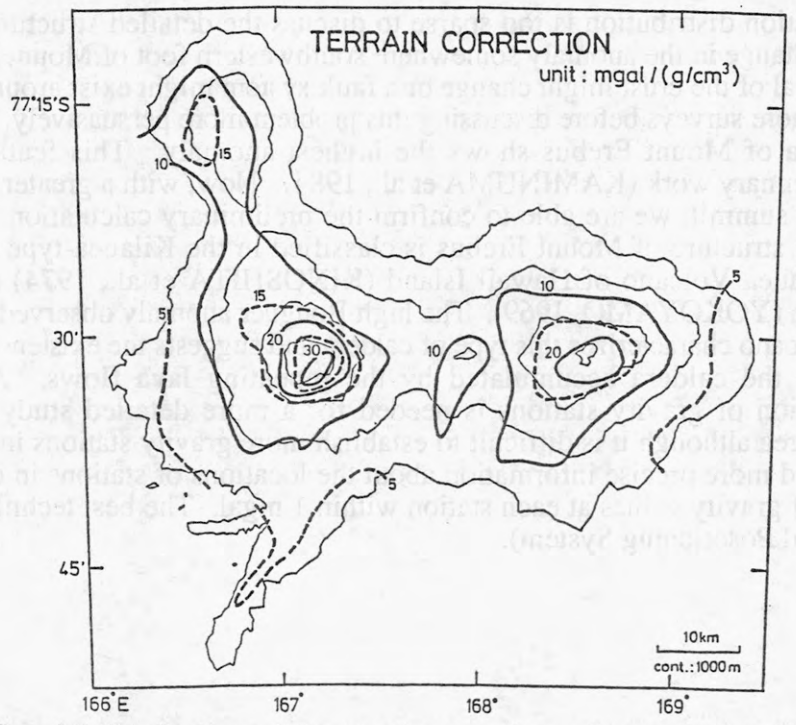

Fig. 3. Spacial distribution of the terrain corrction values calculated by Talwani's three-dimensional method. Contour lines were drawn by using 1.5'(latitudinal direction) x 6'(longitudinal direction) grid point value. Values are normalized by a unit density, unit being mgal/(g/cm^3).

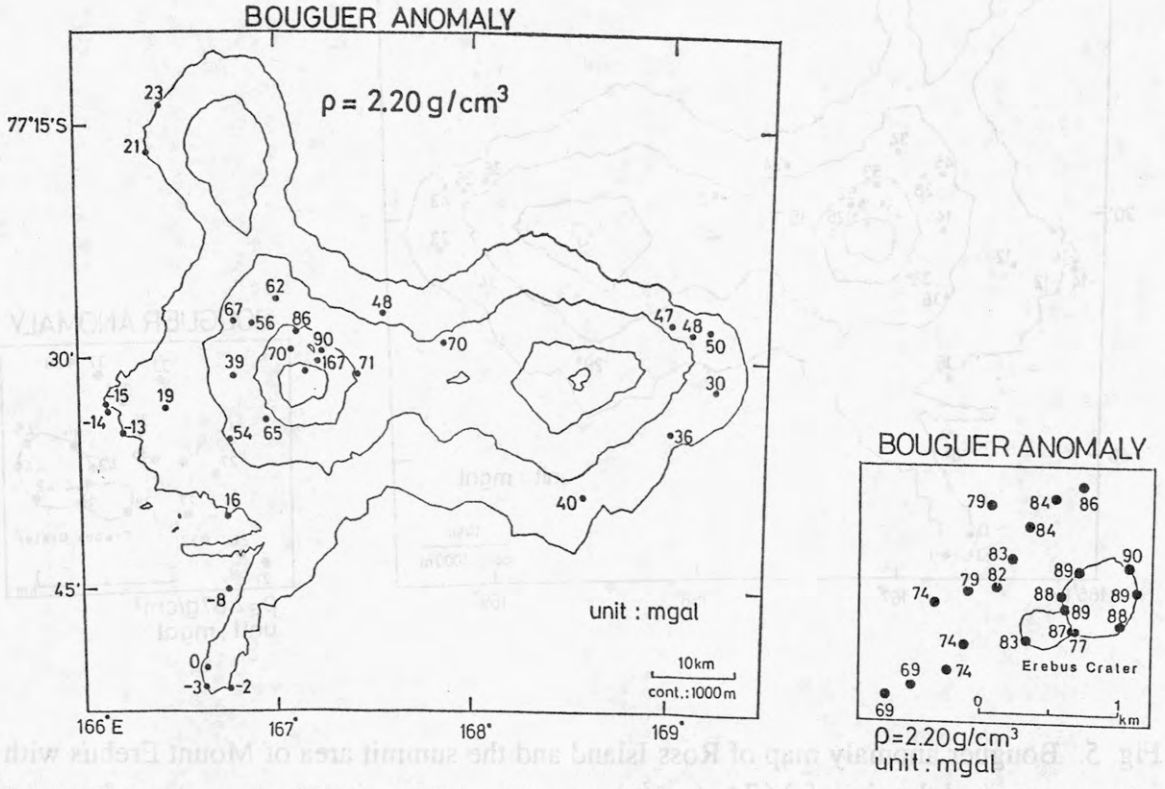

Fig. 4. Bougure anomaly map of Ross Island and the summit area of Mount Erebus with assumed density of 2.20g/cm^3

Although the station distribution is too sparse to discuss the detailed structure, there seems to be an abrupt change in the anomaly somewhere southwestern foot of Mount Erebus. If this is true, the material of the crust might change or a fault system might exist around here. We will have to make more surveys before discussing this problem more persuasively.

The summit area of Mount Erebus shows the highest anomaly. This feature was pointed out in the preliminary work (KAMINUMA et al., 1984). Now, with a greater density of observation near the summit, we are able to confirm the preliminary calculation. These results indicate that the structure of Mount Erebus is classified in the Kilauea-type caldera represented by the Kilauea Volcano of Hawaii Island (KINOSHITA et al., 1974) and the Osima Volcano of Japan (YOKOYAMO, 1969). The high Bouguer anomaly observed around the summit area of a volcano characterizes this type of caldera and suggests the existence of the denser material inside the caldera accumulated by the repeating lava flows. A more homogeneous distribution of gravity stations is needed for a more detailed study on the structure of the island area although it is difficult to establish more gravity stations in the icy mountain area. We need more precise information about the locations of stations in order to improve the accuracy of gravity values at each station within 1 mgal. The best technique for this may be GPS (Global Posotioning System).

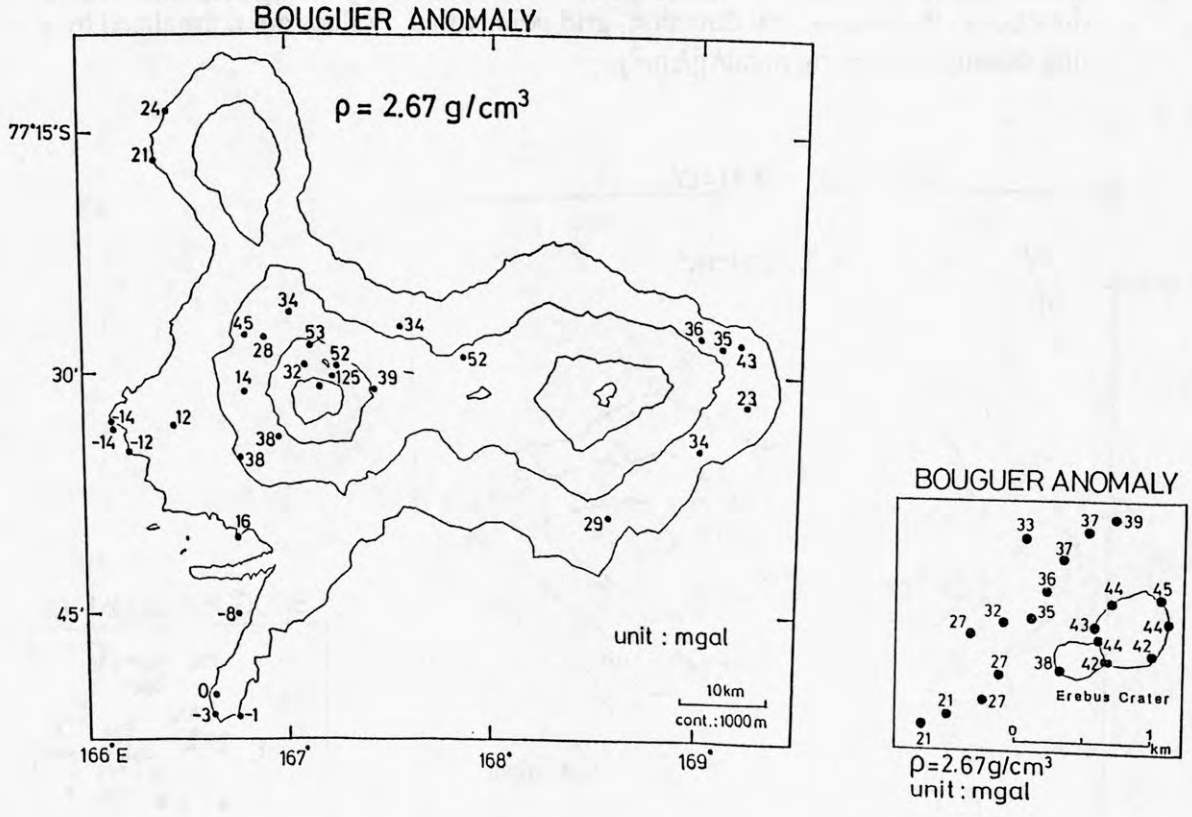

Fig. 5. Bouguer anomaly map of Ross Island and the summit area of Mount Erebus with assumed density of 2.67 g/cm³.

Acknowledgments

The authors express their sincere thanks to Dr. T. NAGAO, Faculty of Science, Kanazawa University , for his assistance in calculating the gravity anomaly and kindly providing us with topographic data. The authors also acknowledge Ms Y. Shudo and Ms F. Nakamura for preparing this manuscript.

References

KAMINUMA, K., KOYAMA, E. and UEKI, S. (1984): A preliminary report of gravity survey in Ross Island, Antarctica. Mem. Natl Inst. Polar Res., Spec. Issue, 33, 41-46.

KINOSHITA, W.T., SWANSON, D.A. and JACKSON, D. B. (1974): The measurement of crustal deformation related to volcanic activity at Kilauea Volcano, Haweaii. Physical Volcanology, ed. by L. Civetta et al. Amsterdam, Elsevier, 87-115.

MIURA, S., KAMINUMA, K. and KOYAMA, E. (1987): Gravity survey in Ross Island Antarctica, Proc. NIPR Symp. Antarct. Geosci., 1, 6-14.

TALWANI, M. and EWING, M. (1960): Rapid computation of gravitational attraction of three-dimention bodies of arbitary shape. Geophysiscs, 25, 203-225.

YOKOYAMA, I. (1969): The subsurface structure of Oosima Volcano, Izu. J. Phys. Earth, 17, 55-68.

SEISMIC ACTIVITY OF MOUNT EREBUS IN 1981-1989

K. KAMINUMA and K. SHIBUYA, National Institute of Polar Research, 9-10, Kaga 1-chome, Itabashi-ku, Tokyo 173
R. R. DIBBLE,Victoria University of Wellington, Private Bag, Wellington, New Zealand
T. TAKANAMI, Research Center for Earthquake Prediction, Faculty of Science, Hokkaido University, Kita-ku Sapporo 060
S. UEKI and S. MIURA, Faculty of Science, Tohoku University, Aramaki Aoba, Sendai 980
H. SHIMIZU, Shimabara Earthquake and Volcano Observatory, Kyushu University, Maeyama Shimabara, Nagasaki 855
S. ASAKAWA, Faculty of Science, Ibaraki University, Bunkyo, Mito, Ibaraki 310

A program to monitor the seismic activity of Erebus Volcano in Antarctica started in December 1980 as an international cooperative program among Japan, New Zealand and the United States. A new volcanic episode began on 13 September 1984 and continued until December. A remarkable change was recognized in the seismic activity of Mount Erebus before and after the 1984 activity.

1. Seismic Network

The seismic network of Mount Erebus (77°37'S, 167°09'E, 3794m) in Ross Island, Antarctica was established in December 1980 by IMESS (International Mount Erebus Seismic Study) of Japan, New Zealand and the United States, and the observations by the network were continued until December 1986 (KIENLE et al., 1981; TAKANAMI et al., 1983a,b; Dibble et al., 1984; KAMINUMA, 1987). The network has been used by IMEEMS (International Mount Erebus Eruption Mechanism Study) of New Zealand and Japan. Since January 1987, the number of stations has been reduced from ten to five since January 1987 (KAMINUMA et al., 1987). The goal of IMEEMS is to study the eruption mechanism and the seismic activity of Mount Erebus.

The seismic network of Mount Erebus is shown in Fig. 1, and was operated in 1989 using five stations ; E1 and TRC in the summit area and HOO, ABB and BOM on the flanks. The seismic signals were transmitted to Scott Base of New Zealand by radio-telemetry, and recorded on a 14-channel FM data recorder and a one-channel chart recorder for monitoring.

A TV camera has been installed at the rim of the main crater of Mount Erebus for observing eruptions from the lava lake since December 1986. The camera and TV transmitter were operated with solar power between spring (September) and autumn (April) each year, but in 1987 and 1988 corrosion of the camera window by volcanic gas obscured the pictures between September and December.

A distinctive feature of Mount Erebus volcano is that a lava lake has presented in the inner crater at the summit for more than ten years in 1972-1984. A new volcanic eruptive episode started on 13 September 1984 with a number of large explosions and lasted until the end of the year. The lava lake disappeared after this September 1984 activity. By December 1985, a new lava lake reappeared in the inner crater .

2. Daily counts and Hypocenter location

The daily number of earthquakes counted at Hooper Shoulder Station (HOO) has been an index of the seismic activity of Mount Erebus since 1981 when the IMESS seismic network was established. Only the events with S-P times not greater than 10s were picked from the monitor seismogram. Figure 2 shows the daily counts in 1984, 1985 and 1986. Earthquake swarms are shown as 84-A, 85-A, 86-B etc. in Fig. 2. An earthquake swarm described here

is defined as one group with more than 250 events occurring within 24 hours, and the events occurring within one or two days on either side of the 250-event day. The magnitude of the events in Fig. 2 could not be exactly determined, but all events were estimated to be less than 2. A remarkable change is recognized in the daily counts before and after the 1984 activity. The number of earthquakes decreased after the activity. The average daily number of earthquakes in 1985 was 23 events per day which is less than 20% of those in the previous three years. Several earthquake swarms occurred every year in 1982-1984, before the 1984 activity, but one or two swarms were recorded in 1985 and 1986, and no swarms recorded in 1987-1989.

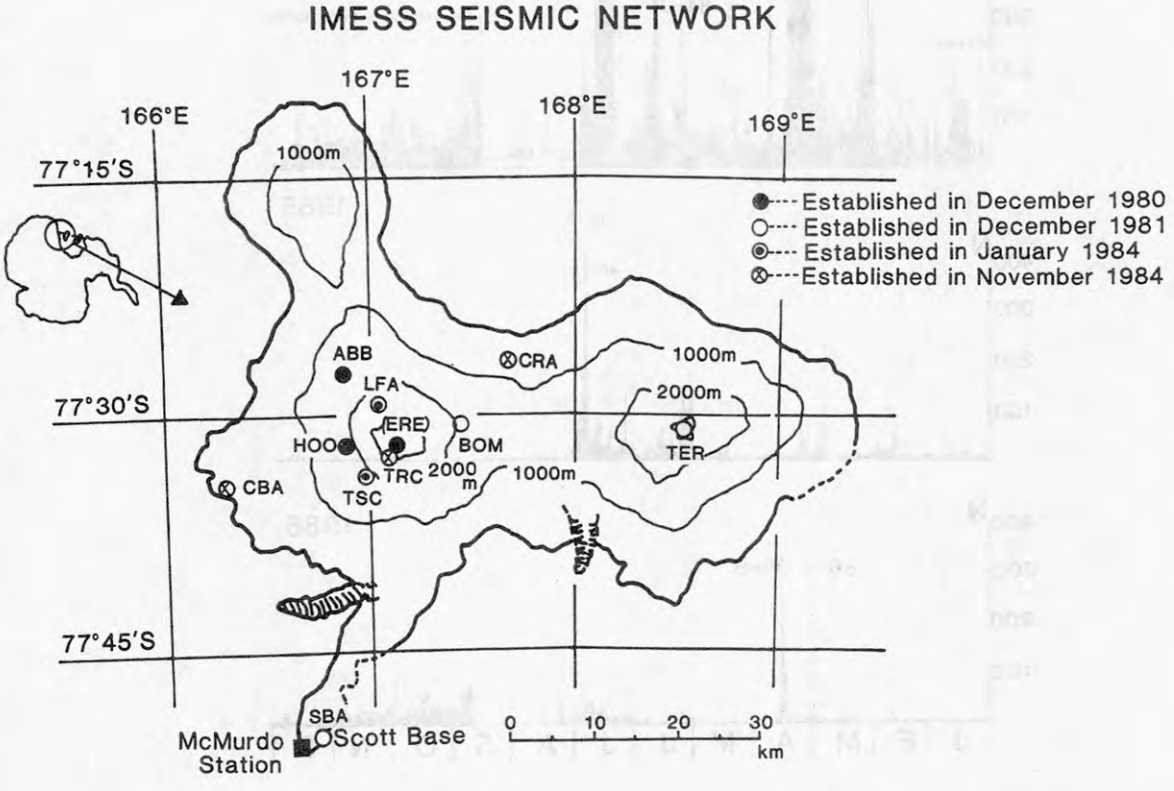

Fig. 1. The configuration of the radio-telemetered IMESS seismic network on Ross Island. The abbreviations of the stations are as follows: Abbott Peak (ABB), The Erebus Summit (ERE: operated until 13 September 1984, but was moved to the E1 survey station on Mt. Erebus), Hoopers Shoulder (HOO), Bomb (BOM), Mount Terrer (TER), Lower Fang (LFA), Three Sisters Cone (TSC), Truncated Cone (TRC), Cape Barne (CBA), Crash Site (CRA) and Scott Base(SBA).

The duration, total number of earthquakes and average number of earthquakes for each earthquake swarm were shown in Fig. 3. Sixteen earthquake swarms were recorded during three years of 1982-1984. However, only three swarms were recorded during following five years after the 1984 activity. Not only the number of earthquake swarms but also swarm activity itself decreased after the 1984 volcanic episode.

The hypocenter distributions of earthquakes before and after the 1984 activity are shown in Fig. 4. There is a clear difference in the hypocenter distributions before and after the activity. The earthquakes were located throughout Ross Island before the activity. The earthquake locations however became more localized around the summit area after the activity.

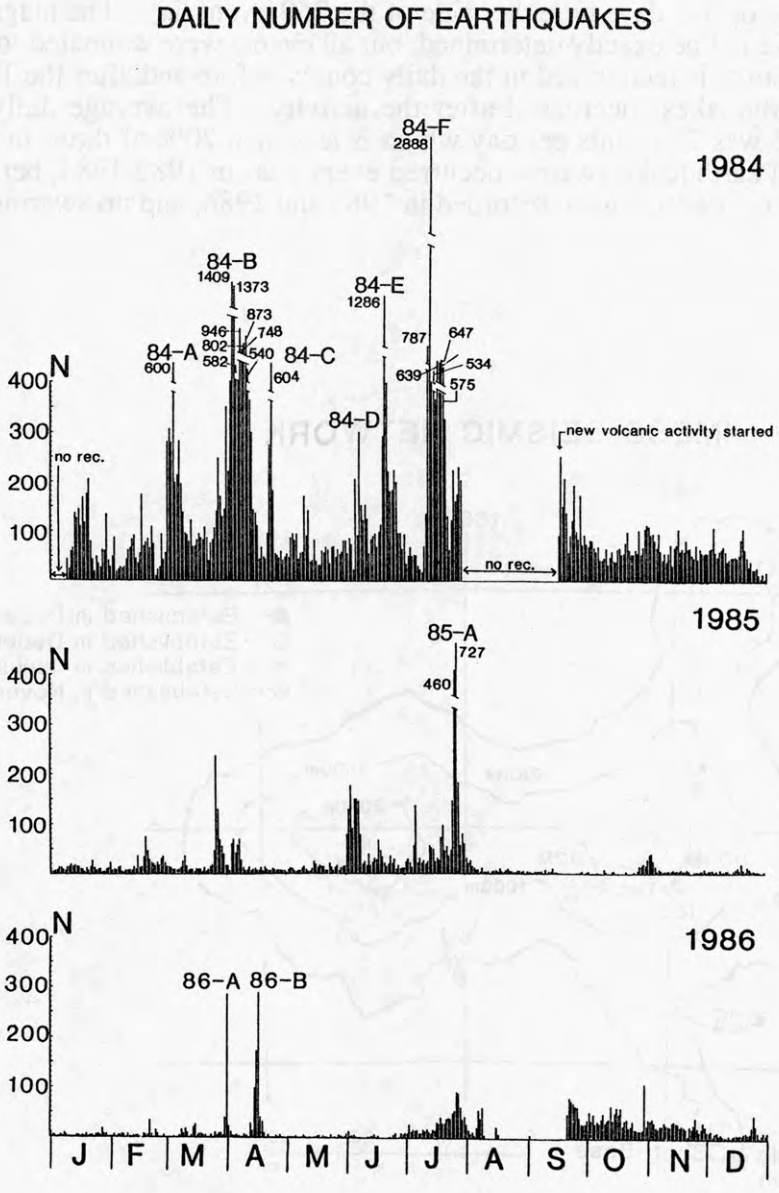

Fig. 2. Daily number of earthquakes counted at Hoopers Shoulder Station (HOO in Fig. 1) in 1984, 1985 and 1986. 84 -A, -B etc., show earthquake swarms.

3. Seismic Activity in 1981-1989

Figure 5 shows the mean number of earthquakes per day in each month from 1981 to 1989. In 1987-1989, the numbers were counted at TRC. The daily numbers at TRC are about four times larger than those at HOO. A reduced number is given for HOO with dotted line in Fig. 5. It is clear in the figure that the number of earthquakes was increasing until the 1984 activity occurred. The mean numbers were 64 per day in 1982, 134 in 1983, and 146 in January-July 1984. The number of earthquake swarms in 1982 was three, but increased to seven in 1983 and six during seven months in 1984 (KAMINUMA et al., 1986).

In 1985 and 1986, soon after the activity occurred, the mean numbers were around 20 earthquakes per day. The reduced daily counts at HOO in 1987 was 16. It decreased to several earthquakes per day in 1988. The number of earthquake swarms in 1985 and 1986 was one and two, respectively, but no earthquake swarms were recorded in 1987 (KAMINUMA and MURAKAMI, 1989), or 1988 and 1989.

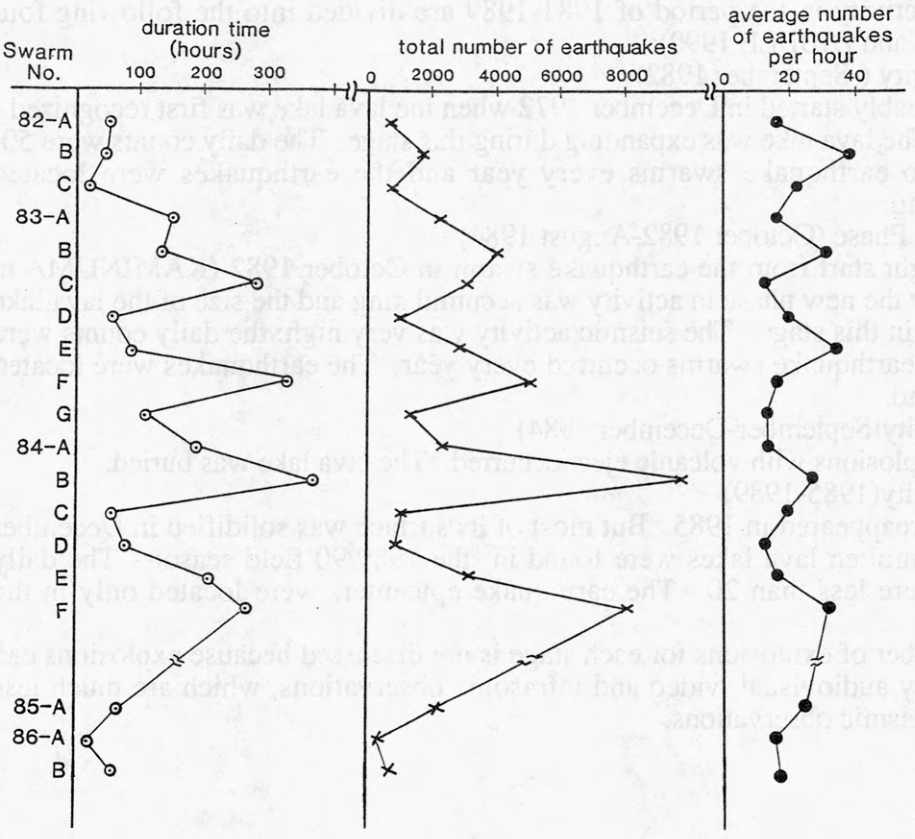

Fig. 3. The duration, total number of earthquakes and average hourly number of earthquakes for each earthquake swarm.

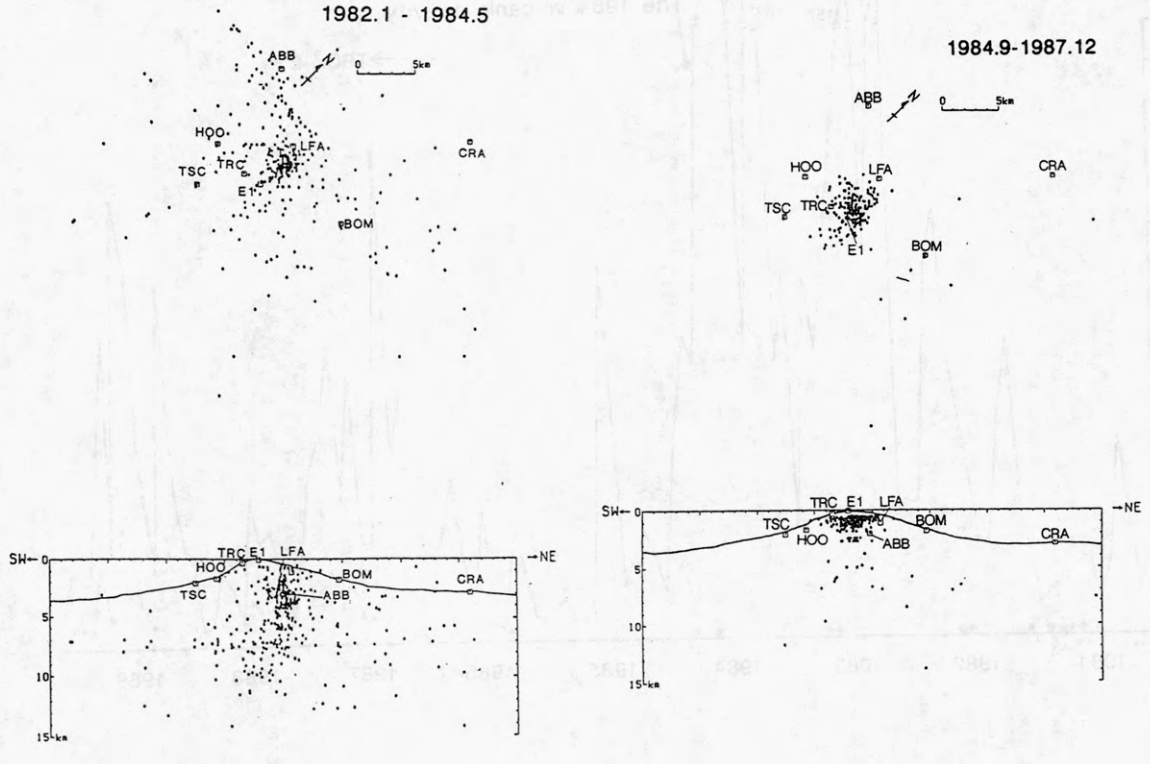

Fig. 4. Earthquake location before and after the 1984 activity.

The seismic activity in the period of 1981-1989 are divided into the following four stages (KAMINUMA and DIBBLE 1990):

1) Normal High Activity (-September 1982)

This stage probably started in December 1972 when the lava lake was first recognized (KYLE et al. 1982). The lava lake was expanding during this stage. The daily counts were 50-100 with one or two earthquake swarms every year and the earthquakes were located throughout Ross Island.

2) Preceding the New Phase (October 1982-August 1984)

This stage might start from the earthquake swarm in October 1982 (KAMINUMA et al., 1985). Energy for the new phase in activity was accumulating and the size of the lava lake was in the maximum in this stage. The seismic activity was very high: the daily counts were over 100 and several earthquake swarms occurred every year. The earthquakes were located throughout Ross Island.

3)New Phase in Activity(September-December 1984)

A lot of big explosions with volcanic eject occurred. The lava lake was buried.

4) Low Seismic Activity(1985-1989)

The lava lake reappeared in 1985. But most of its surface was solidified in December 1988 and two small molten lava lakes were found in the 1989/90 field season. The daily earthquake counts were less than 20. The earthquake epicenters were located only in the summit area.

The daily number of explosions for each stage is not discussed because explosions can be recognized only by audiovisual, video and infrasonic observations, which are much less continuous than the seismic observations.

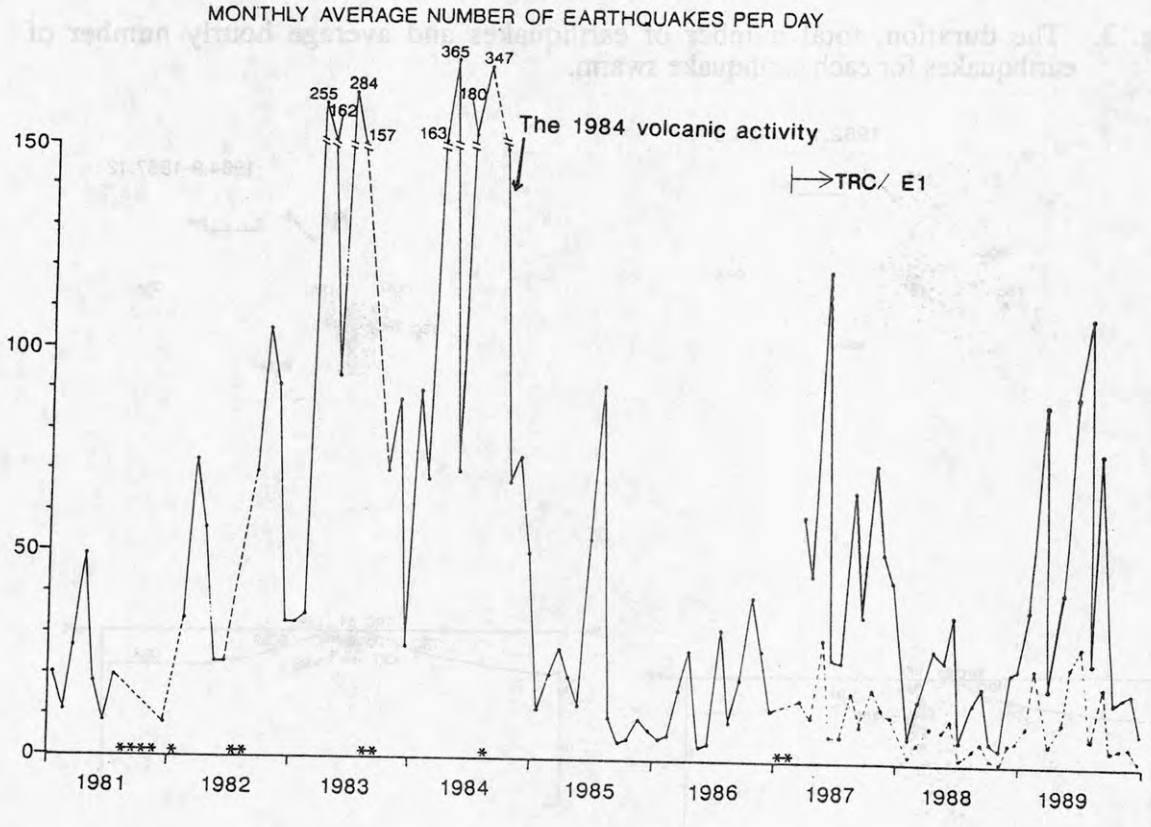

Fig. 5 Monthly mean daily counts at HOO in 1981-1986 and at TRC (or E1 at the summit) in 1987-1989. The dotted line shows the reduced daily counts to HOO.

Acknowledgments

The authors express their sincere thanks to the laboratory technicians of Scott Base wintering party for their kind cooperation. The authors' thanks are extended to Ms Y. SHUDO her help throughout this study, and to Ms F. NAKAMURA for preparing this manuscript.

References

DIBBLE, R, R,., KIENLE, J., KYLE, P. R. and SHIBUYA, K. (1984): Geophysical studies of Erebus Volcano, Antarctica, from 1974 December to 1982 January. N. Z. J. Geol. Geophys., 27, 425-455.

DIBBLE, R.R., BARRETT, S. I. D., KAMINUMA, K., MIURA, S., KIENLE, J., ROWE, C.A., KYLE, P. R. and MCINTOSH, W.C. (1988): Time comparisons between video and seismic signals from explosions in the Lava Lake of Erebus Volcano, Antarctica. Bull. Disas. Prev. Res. Inst., Kyoto Univ., 38, Part 3, 49-63.

KAMINUMA, K. (1987): Seismic activity of Erebus Volcano, Antarctica. Pure Appl. Geophys., 125, 993-1008.

KAMINUMA, K. and DIBBLE, R. R. (1990): Seismic activity of Mount Erebus in 1981-1988. Proc. NIPR Symp. Antarct. Geosci., 4, 142-148.

KAMINUMA, K.and MURAKAMI, K (1989): Seismic activity of Mount Erebus in 1987. Proc. NIPR Symp. Antarct. Geosci., 3, 13-19.

KAMINUMA, K., UEKI, S. and KIENLE, J. (1985): Volcanic earthquake swarms at Mt. Erebus, Antarctica. Tectonophysics, 114, 357-369.

KIENLE, J., KYLE, P. R., ESTES, S., TAKANAMI, T. and DIBBLE, R. R. (1981): Seismic activity of Mount Erebus 1980-1981. Antarct. J. U. S., 16 (5), 35-36.

KYLE, P. R., DIBBLE, R. R. , GIGGENBACH, W. F. AND KEYS, J. (HARRY) (1982): Volcanic activity associated with the Anorthoclase phonolite lava lake, Mount Erebus, Antarctica. Antarctic Geoscience, ed. by C. Craddoc K, The Univ. of Wisconsin Press, Wisconsin, 735-745.

TAKANAMI, T., KAMINUMA, K., TERAI, K. and OSADA, N.(1983a): Seismological observation on Mount Erebus, Ross Island, Antarctica, 1980-1981. Mem. Natl Inst. Polar Res., Spec. Issue, 28, 46-53.

TAKANAMI, T., KIENLE, J., DIBBLE, R.R., KAMINUMA, K. and SHIBUYA, K. (1983b): Seismological observations on Mount Erebus, 1980-1981. Antarctic Earth Science, ed. by R. L. OLIVER et al. Canberra, Aust. Acad. Sci., 671-674.

CONSTRUCTION OF THE GRAVITY OBSERVATORY AND THE ESTABLISHMENT OF AN ABSOLUTE GRAVITY STATION AT SYOWA STATION, ANTARCTICA

K. Kaminuma and K. Shibuya: National Institute of Polar Research, Kaga, Itabashi, Tokyo 173
I. Nakagawa: Faculty of Science, Kyoto University, Sakyo-ku, Kyoto 606
Y. Fukuda: Ocean Research Institute, Tokyo University, Minamidai, Nakano ,Tokyo 165
M. Ishihara, M. Kaidzu and Y. Kuroishi: Geographical Survey Institute, Kitago Tsukuba, Ibaraki 305
T. Tsubokawa, H. Hanada and T. Sato: National Astronomical Observatory, Mizusawa, Iwate 023

The gravity station at Syowa Station (39°E, 69°S), Antarctica was established in 1962 using a pendulum -type gravimeter. This station has been the reference point for relative gravity measurements in the ice plateau and in the vicinity of Syowa Station since its establishment. Tidal gravity observations had been made at Syowa Station using LaCoste and Romberg gravity meters model G in 1987 and 1990.

IAG has selected Syowa Station as one of 36 absolute gravity stations that were proposed to establish a new world-wide network of absolute gravity ; This network is named the International Absolute Gravity Basestation Network (IAGBN). A new gravity observation hut (8.0m x 6.0 m) was constructed at Syowa Station in January 1991. The hut was built on a solid foundation of granitic gneiss and has three basement blocks for installing gravimeters. The first measurements of absolute gravity are going to be carried out in January 1992 using a Sakuma-type transportable absolute gravimeter. Geographical Survey Institute has responsibility to carry out the measurements. The second measurements will be made in January 1993 using two transportable absolute gravimeters . One of the two gravimeters is an absolute gravimeter with a rotating vacuum pipe which has been developed recently. The measurements will be conducted by the staff of Mizusawa Astrogeodynamics Observatory of the National Astronomical Observatory .

Continuous observations by a superconducting gravimeter are planned from February 1992 in the gravity observation hut. The observations will be continued for five years. Seismic, geomagnetic and oceanic tidal observations have been continued at Syowa Station since 1966. A set of broadband digital seismograph has been also installed at Syowa Station as one of the stations of the global digital seismograph networks. GPS measurements have been made for geodetic control in the vicinity of Syowa Station. Current measurements of VLBI are planned to be started in 1993. Because of these programs, Syowa Station is now one of the most important reference points for geodetic and geophysical studies on earth.

ANTARCTIC GEOSCIENCE TRANSECTS QML-1A AND -1B

K. KAMINUMA, K. SHIBUYA, K. SHIRAISHI, M. FUNAKI, K. MORIWAKI and Y. YOSHIDA: National Institute of Polar Research, Kaga-1, Itabashi, Tokyo 173
J. SEGAWA and Y. FUKUDA: Ocean Research Institute, the Universityof Tokyo, Minamidai, Nakano, Tokyo 165
T. NAGAO: Faculty of Sciences, Kanazawa University, Marunouchi, Kanazawa 920
K. ITO: Disaster Prevention Research Institute, Kyoto University, Gokasho, Uji, Kyoto 611
A. IKAMI: Earthquake Research Institute, the University of Tokyo, Yayoi-1, Bunkyo, Tokyo 113
Y. HIROI: Faculty of Science, Chiba University, Yayoi-cho, Chiba 260

We propose two transects, QML-1A and -1B, in the East Queen Maud Land where Japanese Antarctic stations Syowa and Mizuho are located. Many geophysical surveys have been conducted between Syowa and Mizuho stations, the central part of QML-1A. Most of the continental area is covered by a huge ice sheet, the thickness of which is more than 2000 m. The existence of the ice sheet is the distinctive character of the Antractic continent transects.

A chain of outcrops is located along the coastal area in QML-1B. There are, however, very few geophysical data available. This transect is proposed for deriving mainly geological information. The area in QML-1B is underlain by Lützow-Holm and Yamato-Belgica complexes. The Lützow-Holm complex is mainly composed of Late Proterozoic medium pressure-type metamorphic rocks, and the Yamato-Belgica complex is Late Proterozoic igneous and low pressure-type metamorphic rocks.

All data of transect QML1 were obtained by Japanese Antractic Research Expedition (JARE).

Deep seismic sounding experiments have been carried out along the measurement line between Syowa and Mizuho stations in 1980-1982, and a crustal thickness of 40 km was revealed. Gravity surveys through oversnow traverses were repeated along the measurement line of the deep seismic soundings. Aeromagnetic surveys along the line were also made several times. We think that the profile between Syowa and Mizuho stations provides sufficient data to represent transects in Antarctica and a model cross-section for studying the crustal structure in East Antarctica.

The geophysical data in the oceanic area of transect QML-1A is mainly gravity through both sea gravity surveys and the values to be obtained from satellite altimetric sea surface topography. A map of bathmetry in Lüzow-Holm Bay is published by National Institute of Polar Research.

Only one paleomagnetic measurement is available at Syowa Station. The heat flow measurements in the Antarctic are very few, and no data have been obtained in the area. Several earthquakes with magnitudes of 4.3-4.9 were located in the Antarctic continent. However, no earthquakes of which magnitude is larger than 3 were located in the transect area.

According to the Global Geoscience Transect (GGT) printing and publishing policy, all display of the transects is requested to be compiled under the same guideline. However, there are many different situations in the Antarctic Geoscience Transects to compare the transects with other continents such as very few geological data, no earthquake location, a huge ice sheet covered on the continent, etc.

This display was compiled by the GGT guideline basically. However, because of the scarcity of data we decreased the scale of map size.

A COMPARISON OF ANTARCTIC ICE CORES WITH CHINESE LOESS RECORDS AND ITS REFLECTION OF ENVIRONMRNTAL CHANGE OVER LAST 150,000 YEARS

Kang Jiancheng, Wen Jiahong,
Polar Research Institute of China, 451 Shangchuan Road, Pudong Shanghai, 200129, P.R.China

Many studies indicate that polar ice cores and loess deposits in middle latitudes contain good information of terrestrial environmental changes. In recent years, research on both ice cores and loess deposits covering over the last 150,000 years has rapidly developed, so far several works have been done (Burbank and Li, 1985; Liu *et al.*, 1985; Lorius *et al.*, 1985; Jouzel *et al.*, 1987; Kukla, 1987, 1988, 1989; Li *et al.*, 1990; Petit et al., 1990). By studing the Linxia loess section in China, and comparing with the reords from Antarctic ice cores, the authors have tried to expound the general rules of global environmental change and regional differentiation.

1. The ice core records of environmental change over the last 150,000 years

The environmental change revealed by Antarctic ice cores over the last 150,000 years was divided into 8 stages of A-H (Lorius *et al.*, 1985; Jouzel *et al.*, 1987; Fig. 5). Among these, stage H was about the same as the 6th stage of deep sea core $\delta^{18}O$, or the Penultimate Glacial period. Stages E, F and G matched the 5th stage of $\delta^{18}O$. Stage D corresponded to the 4th $\delta^{18}O$, or early period of the last Glaciation; stage C, the 3rd $\delta^{18}O$; stage B, the 2nd $\delta^{18}O$, or the main Wurm Glaciation. Stage A was about the same as the 1st stage of $\delta^{18}O$, or Holocene. The temperature variations revealed by ice core records were: at cold phases, stage B, D and H were about the same level. Stage F was about 2 °C higher than stages B, D and H, the cold phase of middle stage E was warmer than stage F, even about the same as the warm phase of middle stage C. At warm phases, temperature in the Holocene was about 8 °C higher than that in the last Glaciation. The temperature of the warm term in the last Full Interglacial age (stage G) (equal to substage 5e of deep sea $\delta^{18}O$, but lasted for a longer time), was 3 °C higher than that in the Holocene. The highest temperature at stage E (about the same as 5a, 5c) was about 3 °C lower than that in the Holocene, and it was 5 - 6 °C lower at interstadial of the last Glaciation (stage C) than in the Holocene.

2. Environmental records of Chinese loess over the last 150,000 years

Because of its continuity, large thickness and long-covered period, more complete records of palaeoenvironmental change, Chinese loess is one of the best records of the environmental change (Heller and Liu, 1982, 1984; Sasajima and Wang, 1984; Burbank and Li, 1985; Liu *et al.*, 1985; Kukla, 1987, 1988, 1989). According to the previous research, the Linxia loess section can be a standard of the stratigraphic section containing the good records of the environmental changes since 150,000 Y.B.P. Depositional rate in this area was 4 - 5 times as fast as that in the other areas, paleosol layers were also more than that in other places, which

allowed this section to reveal the environmental changes with sensitibility and highly distinguishability.

Linxia section is located at the second terrace of Daxia River (a first branch of Yellow River), north side of Linxia city. Its geographic coordinates are: 35 °35'N, 103 °11'E and 1,900m a.s.l. (Figs. 1 and 2). Fig. 3 shows the relationship between the thickness and the age of the individual loess layers.

The alternated sequence of loess and paleosol deposits is the good indicator for the environmental change. According to the stratigraphy of loess and paleosols, stages of the deposits at the Linxia loess section can be divided into: S_0 < 8,500 Y.B.P.; L_{1-1}, 25,000 - 8,500 Y.B.P.; S_m 53,000 - 25,000 Y.B.P.; L_{1-2}, 80,000 - 53,000 Y.B.P.; S_1, 140,000 - 80,000 Y.B.P. and L_0 > 140,000 Y.B.P. Among these, stage S_m was composed of three weak pedogenic paleosol layers interbedded with two layers of loess, stage S_1 included three paleosol layers of drab soil type and two loess layers, and L_{1-2} contained two slightly weathered layers.

The variation of the magnetic susceptibility among loess and paleosols, as a substitute showing environmental changes, can be compared with that of $\delta^{18}O$ profile of deep sea cores (Wang, 1987; Kukla *et al.*, 1988; An Zhisheng *et al.*, 1990; Beget *et al.*, 1990). The results of the magnetic susceptibility measured at 5cm intervals at Linxia loess section by the Bartington SM2 magnetic susceptibility system are consistent with the eye-distinction of the loess and paleosols. The magnetic susceptibility of loess stages was about 20 C.G.S.; that of paleosol at stage S_m, 30 C.G.S.; and at S_0 S_1, about 60 - 90 C.G.S., this means that the magnetic susceptibility of paleosol at stage S_m was 1.5 times as high as that of loess stage, and at stages S_0 and S_1, was 3 - 4 times higher than that of loess stages.

Pollen records from loess and paleosols can reveal paleovegetation features. Fig. 4 shows the results of the pollen analysis at the Linxia section. The concentration of pollen was higher in paleosols than in loess. There was considerable amount of lignosa in paleosols, but herbs were dominant in loess. The period from paleosol to loess, just as the early cold phase, was the developing time of dark coniferous forests mainly with pine, dragon spurce and fir. In the middle of the cold phase (about 60,000 Y.B.P. and 18,000 Y.B.P.), the major plants were sage, chenodiaceae, lompositae, just liked vegetation of an arid desert steppe.

According to pollen assemblages, we can conclude that the precipitation in the last Interglacial age was more than 200 mm, and that the temperature was 3 °C higher than that at present. In the last Full Glacial age, the temperature was 7.8 °C lower, and the precipitation (0.3 time as much as today) was 350 mm less than that at present.

3. A comparison between Chinese loess and Antarctic ice cores

The Linxia loess in China and Vostok ice core in Antarctica show remarkably similar environmental changes (Fig. 5): the similar points are phase L_0 of Linxia loess section corresponded to phase H of Vostok ice core; S_1 corresponded of E, F and G ; and L_{1-2}, S_m, L_{1-1}, S_0 corresponded respectively to D, C, B, A. There were two weak pedogenic layers at lower part of L_{1-2} of Linxia section, along with peak values of magnetic susceptibility the short developing periods of dark coniferous forests, and the periods of precipitation increase. Correspondingly, at early phase D of Vostok, there were two terms with slightly higher temperature. Four peak values of magnetic susceptibility were at Linxia section during 53,000 - 25,000 Y.B.P. and also, Vostok and Byrd ice cores indicate four relatively high temperature

periods at interstadial of the last Glaciation during 58,000 - 30,000 Y.B.P. (Jouzel *et al.*, 1987, 1989). Linxia section shows that there were two short developing periods for herb at about 12,000 Y.B.P. and 15,000 Y.B.P., and Byrd ice core shows two periods of temperatural fluctuation at the same time. These, therefore, indicate the concordance and comparability of the global environmental change. It means that the environmental changes have been synchronous in the southern and northern hemispheres. This conclusion agrees with the results obtained from deep sea records by Hays *et al.* (1976).

There are, however, several differences among records of loess sediments, ice cores and deep sea cores. First, environmental charateristics estimated by Linxia section at early and late full stage of the last Glaciation (about 60,000 Y.B.P. and 18,000 Y.B.P.) were remarkably similar, which were the same as Vostok ice core. However, among deep sea records (Shackleton and Opdyke, 1973; Hays *et al.*, 1976; Martinson *et al.*, 1987), these two stages, *i. e.*, stages 2 and 4 of $\delta^{18}O$, the decline value of sea level (expressed by $\delta^{18}O$) had greater difference. Second, at stage S_1 (140,000 - 80,000 Y.B.P.) of Linxia section, two loess layers were interbedded with the three paleosol layers, the magnetic susceptibility of theses loess substages corresponded to that of loess (L_{1-1} ,L_{1-2}) deposited in the last Full Glacial age. This means that the climatic features of these two substages in S_1 were about the same as that in the last Full Glacial age, if the magnetic susceptibility can be used as a substitutive index to estimate paleoclimate (Kulka, 1987, 1988). When Lorius *et al.* (1985) used $\delta^{18}O$ as a climatic index to examine Vostok ice core, they also stated that the climate at stage F was on the same scale as that at B and D. However, there are some differences between them when 8 D is used as index (Jouzel, 1987). These different results from ice cores and loess are because of climatic differences, or the mistake from the climatic index, which should be studied furthermore. Third, at Linxia section, the maturity of the three paleosol layers S_{1-1}, S_{1-2} and S_{1-3} of stage S_1 were weakened from the older to the younger. This result is different with the records from Vostok ice core and deep sea. At stage E of Vostok ice core, the two highest values of temperature were approximately only a half of the value of stage G. Records of deep sea care RC11-120 in South Indian Ocean showed that, the substages 5a, 5c had the similar value but lower than 5e. Therefore, the record of loess at this point, is different with ice core and deep sea core. In 1972, Fairbridge modeled the ideal temperature curve for the late Quaternary, which is similar with the magnetic susceptibility curve of Linxia section (Fig. 6). From this, it can be got that the magnetic susceptibility of paleosol layer S_{1-2} at Linxia section was higher than that of S_{1-1}, lower than S_{1-3}, and the paleosol layer was thicker than S_{1-1} and S_{1-3}. The reason is that the period of S_{1-2} at Linxia section corresponded to the developing time of the B2terrace and early-subterrace in Barbadose (Fig. 6). It means that paleosol S_{1-2} developed longer, but the climate condition in the developing time was not as good as the forming time of paleosol S_{1-3}.

As to Vostok ice core records, that stage G was longer was not revealed by Linxia section or deep sea records.

Comparative research shows that fluctuation tendencies of environmental charateristics recorded by Antartic ice cores and Chineses loess over the last 15,000 years were concordant. The ranges of variation, during the last Interglacial age, have greater difference between these two records. When comparing with deep sea records, it shows that marine and terrestrial environmental records have a world of difference at early and late stage of the last Glaciation .

REFERENCES

An Zhishan *et al.* (1990): The magnetic susceptibility evidences of the monsoon variability on the loess plateau over last 130,000 years. Kexuetongbao, (China) 35 (7), 529-532.

Beget, J.E. *et al.* (1990): Palaeoclimatic forcing of magnetic susceptibility variations in Alaskan loess during the late Quaternauy. Geology, 18 (10), 40-43.

Burbank, D.W. and Li Jun (1985): Age and paleoclimatic significance of the loess of Lanzhou, China. Nature, 316 (6027), 429-431.

Fairbridge, R.W. (1972): Climatology of a glacial cycle. Quaternary Research, 2 (3), 283-302.

Hays, J.D., Imbrie, J. and Shackleton, N.J. (1976): Variation in the earth's orbit: pacemaker of the ice ages. Science, 194, 1121-1132.

Heller, F. and Liu T. (1982): Magnetostratigraphic dating of loess deposits in China . Nature, 300, 525-543.

Heller, F. and Liu T. (1984): Magnetism of Chinese loess deposits. Geophys, J.R. 77, 125-141.

Jouzel, J. *et al.* (1987): Vostok ice core: a continuous isotope temperature record over the last climate cycle (160,000 years). Nature, 329 (6138), 403-408

Jouzel, J. *et al.* (1989): A comparison of deep Antarctic ice cores and their implications for climatic between 65,000 and 15,000 years age. Quaternary Research, 31, 135-150.

Kukla, G. J. (1987): Loess stratigraphy in central China. Quaternary Science Rviews, 6, 191-219.

Kukla, G.J., *et al.* (1988); Pleistocene climates in China dated by magnetic susceptibility, Geology, 16 (9), 811-814.

Kukla,G.J. and Zhisheng An (1989): Loess stratigrtaphy in central China. Palaeogeography, Palaeoclimatology, Palaeorcology, 72, 203-225.

Li Jijun *et al.* (1990): A comparson of Lanzhou loess profile with Vostok ice core in Antarctic: for last glaciation cycle. Scientia Sinica (B), (10).

Liu Tongsheng, *et al.* (1985): Loess and Environment. Science Press, Beijing.

Lorius, C. *et al.* (1985): A 150,000 year climatic record from Antarctic ice, Nature, 316 (6029), 591-596.

Martinson, D. G. *et al.* (1987): Age dating and the orbital theory of the ice ages: Development of a high-resolution 0 to 300,000 year chronostratigraphy. Quaternary Research, 27 (1), 1-29.

Petit, J. R. *et al.* (1990): Palaeoclimatological and chronological implications of the Vostok core dust record, Nature, 343 (6253), 56-58.

Richmond (1972): Appraisal of the future climatic of the Holocene in the Rocky Mountains. Quaternary Research, 2 (3), 315-322.

Sasajima, S. and Wang, Y.Y. ed. (1984): Recent research on loess in China, Kyoto, Japan, Kyoto University.

Shackleton, N.J. and Opdyke, N.D. (1973): Oxygen isotope and Paleomagnetic stratigraphy of equatorial Pacific core V28-238: Oxygen isotope temperatures and ice volumes on a 10,000 year and 100,000 year scale. Quaternary Research, 3 (1), 39-55.

Wang Yongyan (1987): Quaterary climatic change at loess plateau of China. Scientia Sinica (B), (10), 1099-1106.

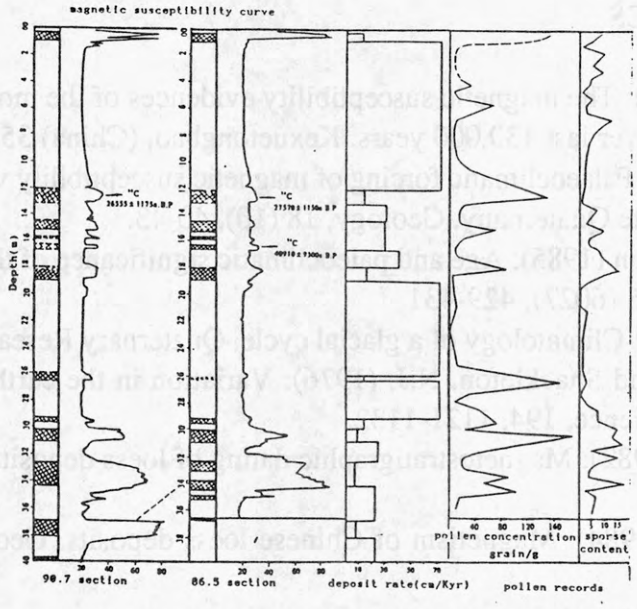

Fig.4 Magnetic susceptibility, deposit rate and pollen record of Linxia section in China

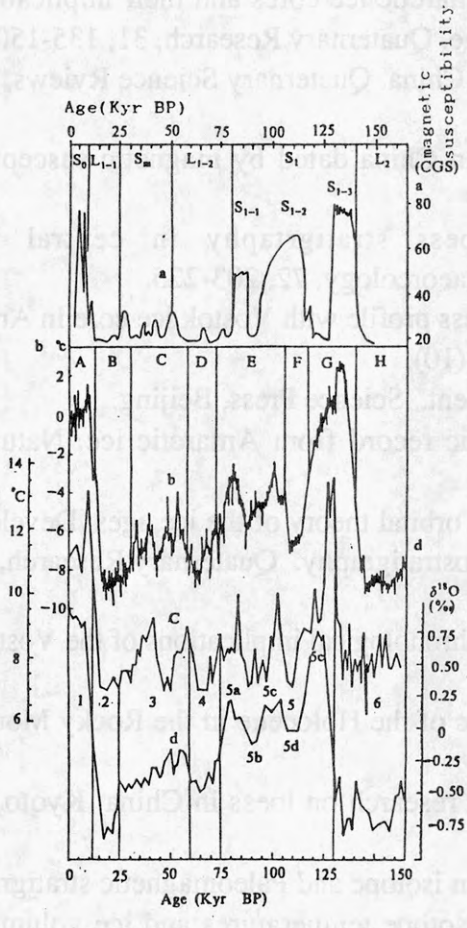

Fig.5 A comparison of loess deposit with ice-core and deep-sea core

a, The magnetic susceptibility curve of Linxia section in China. b,Variation with time of the Vostok isotope temperature record in °C as a difference from the modern surface-temperature value (T_0 = -55.5 °C) (J.Jouzel et al.,1987). c, Variation with time of estimated summer sea-surface temperature at the subpolar Indian ocean site RC11-120. d, variation with time of the RC11-120 δO^{18} record (c, d, from Martinson et al., 1987).

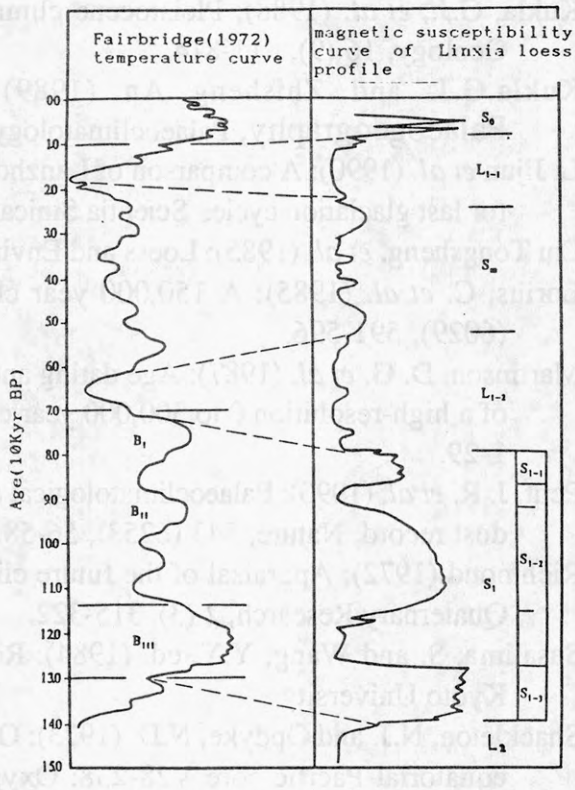

Fig.6 A comparison of magnetic susceptibility curve of Linxia loess section with ideal temperature curve modeled by Fairbridge (1972) over last 150,000 years

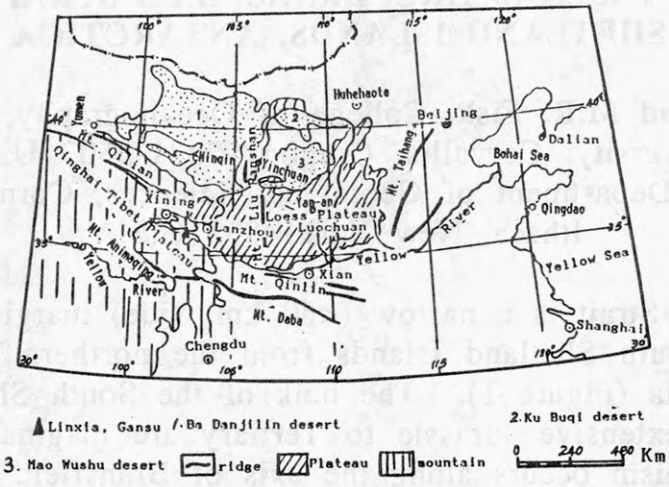

Fig.1 The position of Linxia basin, China

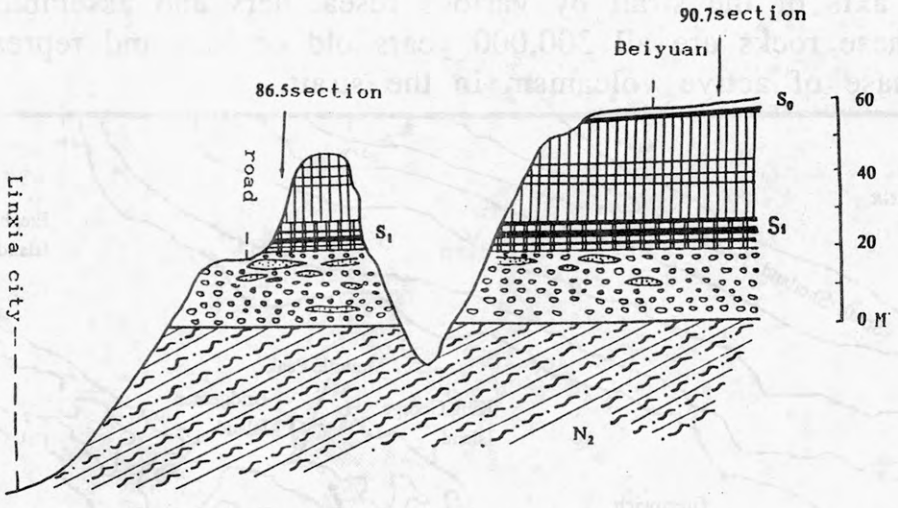

Fig.2 Schematic diagram of Linxia terrace section

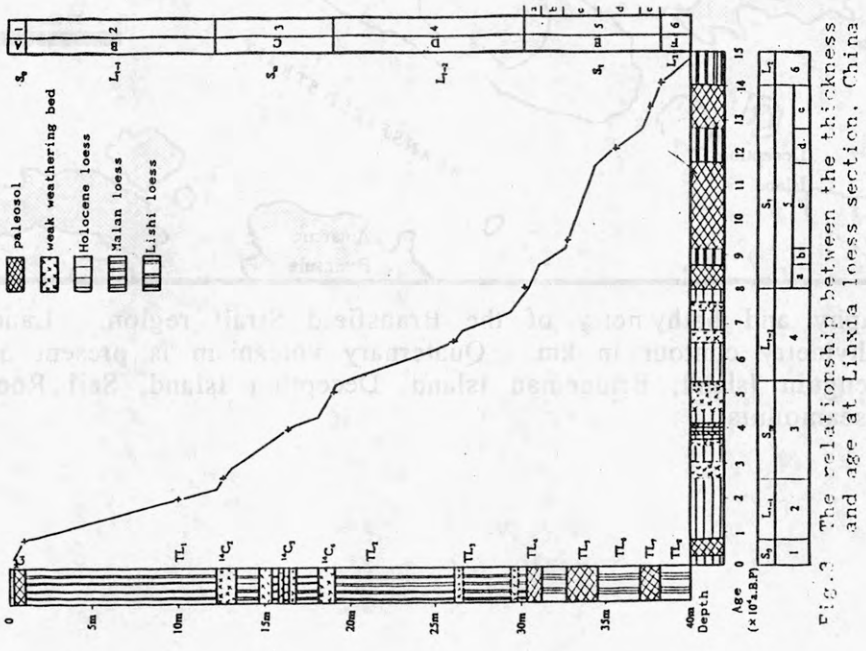

Fig.3 The relationship between the thickness and age at Linxia loess section, China

RIFTING OF AN ISLAND ARC, BRANSFIELD STRAIT AND SOUTH SHETLAND ISLANDS, ANTARCTICA

R.A. Keller and M.R. Fisk, College of Oceanography, Oregon State University, Corvallis, Oregon 97331-5503 U.S.A
W.M. White, Department of Geological Sciences, Cornell University, Ithaca, New York14853 U.S.A

The Bransfield Strait is a narrow (<60 km wide) marginal basin separating the South Shetland Islands from the northern end of the Antarctic Peninsula (Figure 1). The bulk of the South Shetland Islands was created by extensive Jurassic to Tertiary arc magmatism but Quaternary volcanism occurs along the axis of Bransfield Strait and at two off-axis locations on and adjacent to King George Island (Smellie et al., 1984; Weaver et al., 1979). Samples were collected from 8 locations along the axis of the strait by various researchers and assembled for study. These rocks are all 300,000 years old or less and represent that present phase of active volcanism in the strait.

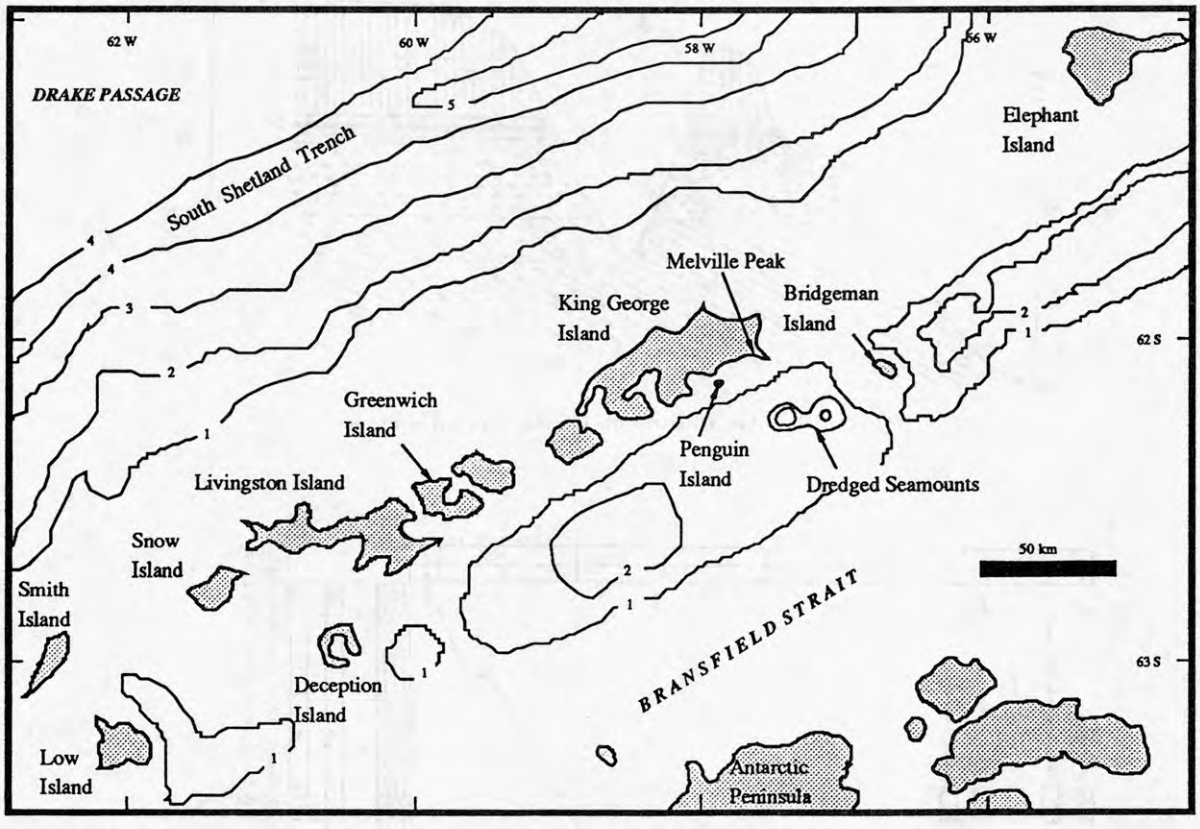

Figure 1. Geography and bathymetry of the Bransfield Strait region. Land areas are shaded. Bathymetry contour in km. Quaternary volcanism is present on Melville Peak, Penguin Island, Bridgeman Island, Deception Island, Sail Rock and the submerged seamounts.

Bridgeman Island is a 0.5 km^2 volcanic remnant in the northeastern part of the Bransfield Strait, and is aligned with Deception Island and seamounts along the rift axis of the strait (Figure 1). These seamounts (Eastern and Western Seamounts) on the floor of the Bransfield Strait were dredged from the *R/V Polarstern* in 1985 (Fisk, 1990). Deception Island is a composite stratovolcano over 30 km wide at its submerged base, and topped by a flooded caldera approximately 10 km in diameter. Sail Rock (60°57'W, 63°03'S) is a small islet of alternating lavas and breccias protruding 30 m above the sea surface 10 km WSW of Deception Island (Figure 1). The age of this material has not yet been determined but it is presumed to be contemporary with Deception Island.

Melville Peak, on the eastern tip of King George Island (Figure 1) lies on the northern margin of the Bransfield Strait, off of the present axis of rifting, but possibly associated with the normal faults bounding the northern margin of the Bransfield Strait (Ashcroft, 1972). Penguin Island is a small cinder cone on the southern shelf of King George Island that, like Melville Peak, lies off the rift axis of the Bransfield Strait (Figure 1).

Analysis and results

Concentrations of major and trace elements in the volcanic rocks were measured by X-ray fluorescence, isotope dilution mass spectrometry, and by ICP-MS. Sr, Nd, and Pb isotope ratios were measured on the VG Sector mass spectrometer.

The major and trace elements of all the samples roughly follow a trend of increased fractional crystallization starting at 49 wt. % SiO_2 and 3 wt. % total alkalis and extending to 70 % SiO_2 and 9 % total alkalis (Figure 2).

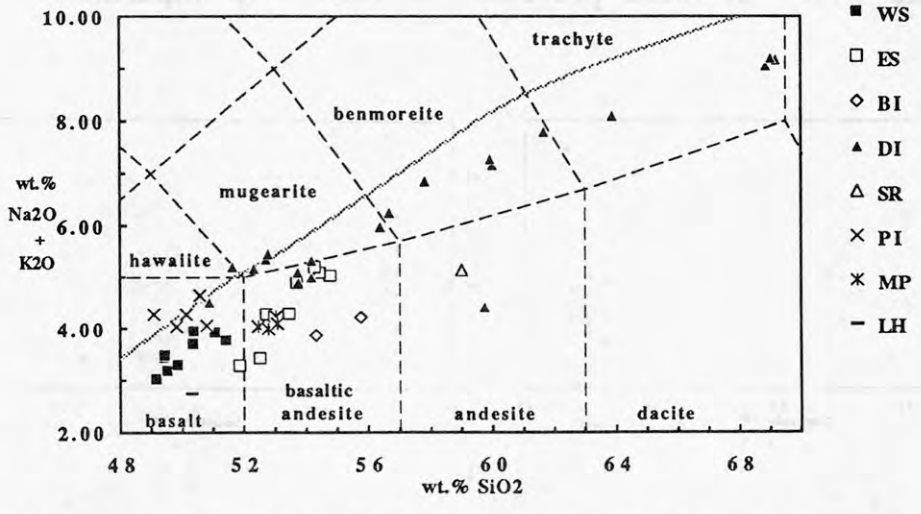

Figure 2. SiO_2 versus Na_2O+K_2O of Quaternary volcanic rocks from the Bransfield Strait. **WS**, Western Seamount; **ES**, Eastern Seamount; **BI**. Bridgeman Island; **DI**, Deception Island; **SR**, Sail Rock; **PI**, Penguin Island; **MP**, Melville Peak; and **LH**, Low Head (early Miocene basalt from King George Island).

Bridgeman Island samples are classified as basaltic andesites as are the dredged samples from Eastern Seamount, and some of the Deception Island samples and the Melville Peak samples (Figure 2). The dredged samples from Western Seamount would be classified as basalts. The Sail Rock andesite is chemically similar to, but more evolved than, samples from Bridgeman Island. The two off-axis volcanic centers, Melville Peak and Penguin Island have chemical characteristics that separate them from the on-axis volcanoes. All four of our samples classify as basaltic andesites similar to Eastern Seamount (Figure 2), but can be distinguished from Eastern Seamount and other on-axis volcanoes by low total iron and TiO_2, high Al_2O_3 and by noticeably higher K_2O, Rb, Sr, and Ba abundances than the other Bransfield Strait lavas with similar MgO contents.

A single pre-rift rock (from Low Head on King George Island) is a basalt with lower total alkalis than any of the other basalts we analyzed (Figure 2) but with the exception of TiO_2 and the alkalis it is indistinguishable from these basalts in terms of major and most trace elements.

Geographic variation

Figure 3 shows the range of Sr isotopes and Rb/Sr for rocks from the strait. The chemical diversity of basalts within this restricted geographic area implies: the mantle is heterogeneous on a small scale; there are variable extents of partial melting along the rift; and possibly there are various extents of crustal, mantle wedge, and subducted lithosphere involvement. Along-rift and cross-rift variations in chemistry may help to determine which of these processes or factors is important.

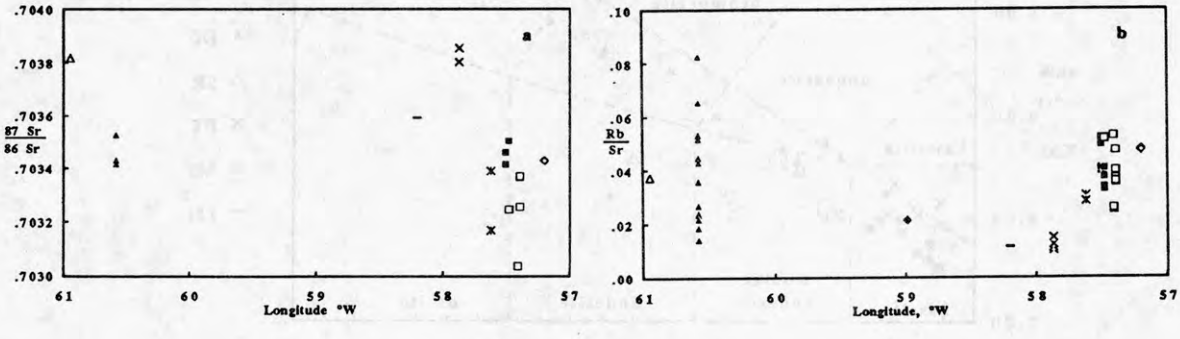

Figure 3.
Regional chemical variation plotted against latitude (°W) in Bransfield Strait. (a) $^{87}Sr/^{86}Sr$. (b) Rb/Sr.

Regional variation in mantle chemistry can be reflected in changes in isotope ratios if we ignore the possibility of assimilated crust. Figure 3 shows the Sr isotope ratios and Rb/Sr ratios plotted against longitude of the volcanic centers. Isotope ratios along the rift axis exhibit no systematic variation but Penguin Island and Sail Rock have high $^{87}Sr/^{86}Sr$.

Ratios of trace elements may indicate relatively small differences in partial melting in the mantle, or if amount of melting is large (≥20%) differences in source chemistry, or they could indicate melting of the mantle that had different residual mineralogy. The more compatible element (Sr) is in the denominator so the ratios will decrease as the amount of melting increases. Penguin Island and most samples west of Penguin Island (Figure 3b) have low Rb/Sr suggesting high degrees of melting.

Fractionation, assimilation, partial melting, mantle composition, and metasomatism

Chemical variation within single volcanoes can explained by simple fractional crystallization, but the separate volcanic centers can not be related by this simple mechanism. More complex evolutionary models (such as the assimilation and fractional crystallization - AFC- model of O'Hara, 1977; Nielsen, 1988) also show that these more complex models are not capable of generating the chemical variation seen between volcanoes. We have therefore assumed that the chemical differences are derived from the mantle.

The variable isotope ratios along the axis of the rift (Figure 3a) suggest either that the mantle is variable in composition or that there are variable amounts of contamination of the magmas between volcanic centers. It is difficult to determine whether isotope signatures are derived from mantle or crust because the chemical signatures of the two are often similar. To demonstrate the effect of the contribution of material either to the mantle source or to the magma, Figure 4 shows Sr and Nd isotope mixing lines that originate at depleted mantle (Wood et al.,1979: Sr 13.2 ppm, Nd 0.86 ppm) with $^{87}Sr/^{86}Sr$ of 0.7026, and $^{143}Nd/^{144}Nd$ of 0.51319. The other components for each of the mixing lines are continental crust (Galer et al., 1989), Atlantic sediment (White and Dupré, 1985), Pacific sediment (Elderfield et al., 1981), and Elephant Island metamorphic basement (Tanner et al., 1982). The mixing lines show that it is not possible to determine whether the contaminant is crust or sediment, and there is no way of determining from this diagram where the contamination originated in the mantle or crust.

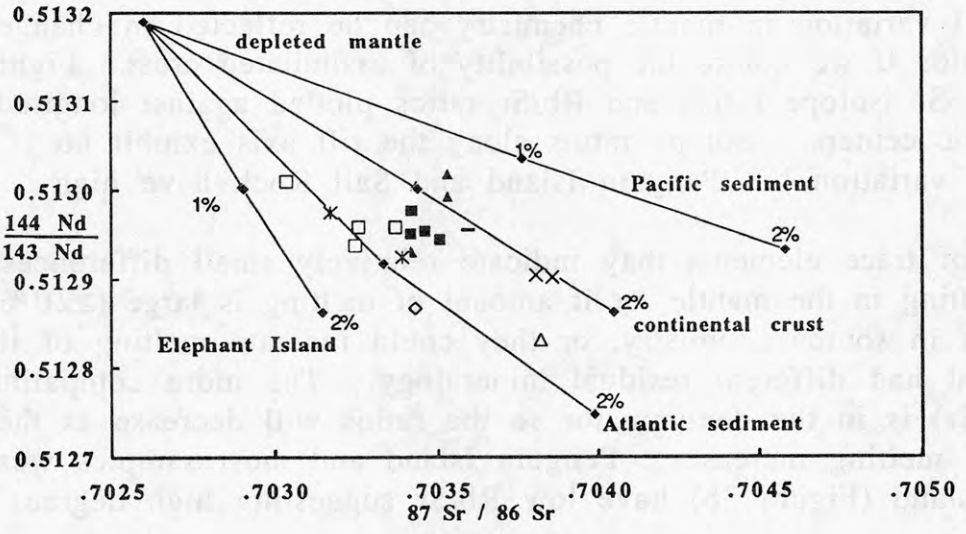

Figure 4. Nd and Sr isotope ratios of basalts and evolved rocks from Bransfield Strait. Symbols as in Figures 2. Mixing models showing the effect of adding up to 2 % of sediment or crust to a depleted mantle with a $^{87}Sr/^{86}Sr$ of 0.7026 and a $^{143}Nd/^{144}Nd$ of 0.51319.

Assuming that the source for Penguin Island, Deception Island, and Low Head basalts is the mantle wedge above the subducted slab, several chemical characteristics of this source can be identified. It must have lower Rb/Sr than the depleted mantle of Wood et al. (1979) and probably has higher Sr abundance than depleted mantle. This requires that the Rb/Sr of any mixed component (crust or sediment) of the mantle be extremely low (less than 0.001) which effectively rules out all significant crustal sources. The $^{87}Sr/^{86}Sr$ of the source mantle for Penguin Island is higher than can be produced its Rb/Sr which suggest that Rb was lost from the mantle.

Rb is known to be highly mobile during dehydration of the mantle (Tatsumi et al., 1986) so it appears possible that some portions of the mantle have been dehydrated or that they have been flushed by fluids released from the subducted slab. These fluids removed Rb from the mantle that generated Penguin Island basalts and also increase the Sr abundance and $^{87}Sr/^{86}Sr$ of the mantle.

Conclusions

Recent volcanism in Bransfield Strait has diverse chemical characteristics that indicate the mantle source for these rocks is also diverse. This can only partially be accounted for by magma chamber processes such as recharge and assimilation, although within single

volcanic centers all chemical differences between basalts can be explained by these processes. Sr and Nd isotopes suggest there is 1 to 2% of a crust or sediment component in the mantle that generated these basalts. The source for Penguin Island basalts could be either the subducted slab that partially dehydrated at low pressure (less than 15 km) followed by partial melting at high pressure (60 km). This depth of melting is below the subducted slab (Ashcroft, 1972) and we suggest that the slab separated along the axis of Bransfield Strait and the detached portion descending into the mantle. Melting of the upwelling depleted mantle which moved up to fill the gap is the source of magmas for Bransfield Strait.

References

Ashcroft, W. A., 1972, Crustal structure of the South Shetland Islands and Bransfield Strait. *British Antarct. Surv. Sci. Reports,* No. 66, 43 pp.

Elderfield, H., C.J. Hawkesworth, M.J. Greaves, and S.E. Calvert, 1981, Rare earth element geochemistry of oceanic ferromanganese nodules and associated sediments. *Earth Planet. Sci. Lett.* v. 45, p.513-528.

Fisk, M. R., 1990, Volcanism in the Bransfield Strait, Antarctica. *J. South Am. Earth Sci.*, v. 3, p. 91-101.

Galer, S.G.J., S.L. Goldstein, and R.K. O'Nions, 1989, Limits on chemical and convective isolation in the Earth's interior. *Chemical Geology*, v. 75, p. 257-290.

Nielsen, R. L., 1988, A model for the simulation of combined major and trace element liquid lines of descent. *Geochim. Cosmochim. Acta,* v. 52, p. 27-38.

O'Hara, M.J., 1977, Geochemical evolution during fractional crystallization of a periodically refilled magma chamber. *Nature*, v. 266, p. 503-507.

Smellie, J. L., R. J. Pankhurst, M. R. A. Thomson, and R. E. S. Davies, 1984, The Geology of the South Shetland Islands: VI. Stratigraphy, Geochemistry and Evolution. *British Antarct. Surv. Sci. Reports,* No. 87, 85 pp.

Tanner, P.W.G., R.J. Pankhurst, and G. Hyden, 1982, Radiometric evidence for the age of the subduction complex in South Orkney and South Shetland Islands, West Antarctica. *J. Geol. Soc. London,* v. 139, p. 683-690.

Tatsumi, Y., D.L. Hamilton, and R.W. Nesbitt, 1986, Chemical characteristics of fluid phase released from a subducted lithosphere and origin of arc magmas: evidence from high-pressure experiments and natural rocks. *J. Volcanol. Geotherm. Res.* v. 29, p. 293-309.

Weaver, S. D., A. D. Saunders, R. J. Pankhurst, and J. Tarney, 1979, A geochemical study of magmatism associated with the initial stages of back-arc spreading. The Quaternary volcanics of Bransfield Strait, from South Shetland Islands. *Contrib. Mineral. Petrol.*, v. 68, p. 151-169.

White, W.M., and B. Dupré, 1985, Isotope and trace element geochemistry of sediments from the Barbados Ridge-Demerara Region, Atlantic Ocean, *Geochim. Cosmochim. Acta,* v. 49, p. 1875-1886.

Wood, D.A., J.-L. Joron, M. Treuil, M. Norry, J. Tarney, 1979, Elemental and Sr isotope variations in basic lavas from Iceland and the surrounding ocean floor. *Contrib. Mineral. Petrol.* v. 70, p. 319-339.

Gravity Study of the Rennick Graben and the Mt. Melbourne Quadrangle in North Victoria Land, Antarctica and the Relation of the Rennick Structure to Rifting Processes in the Ross Sea

Juergen Kienle and Thomas F. Redfield
Geophysical Institute
University of Alaska Fairbanks
Fairbanks, AK 99775-0800, USA

In the austral summer of 1988/89, the University of Alaska participated in an international campaign to study the tectonics and origin of the Transantarctic Mountains in North Victoria Land. North Victoria Land offers the widest cross section of this major mountain range separating East and West Antarctica. Recently acquired marine seismic, magnetic, and gravity data show that the Ross Sea, an ocean basin south of North Victoria Land, has been created by crustal rifting (Cooper et al., 1987a,b). A major rift in North Victoria Land, the Rennick Graben, may be the landward extension of the Terror Rift, a central rift zone of the Victoria Land Basin in the Ross Sea. The University of Alaska's gravity study of the Transantarctic Mountains in the Mt. Melbourne Quadrangle and in the Rennick Graben area was only one of several geological and geophysical projects that were carried out during the fifth German Antarctic North Victoria Land Expedition (Ganovex V).

A set of high quality gravity data was acquired in the Mt. Melbourne Quadrangle during the first leg of the Ganovex V expedition to Terra Nova Bay, North Victoria Land, 12 December 1988 through 10 January 1989. Elevation control for 33 of 60 gravity stations was obtained with the Global Positioning satellite navigation System (GPS). Most GPS elevations were accurate to within 1 meter or less. All stations were located on bedrock and have been fully terrain-corrected. In addition, corrections for the gravitational effects of ice were estimated from two- and three-dimensional gravity models of plausible ice-rock interfaces. A complete Bouguer anomaly gravity map of the Mt. Melbourne quadrangle reveals a strong negative gravity gradient of about 2 mgal/km from Terra Nova Bay towards the Transantarctic Mountains. The gravity field changes from about +20 mgal near the coast to approximately -150 mgal at the crest of the Transantarctic Mountains. The Ganovex V data link well with those of Duerbaum and others (1989) on the Polar Plateau to the west. Their lowest Bouguer gravity value is about -300 mgal, 200 km inland from the coast.

Fifty nine gravity stations were established during the second leg of the Ganovex V expedition to the Rennick Glacier area and the north coast of North Victoria Land, 13 January 1989 to 2 March 1989. Fifty four stations were located on bedrock. All but 5 stations were controlled by GPS measurements. Again, all stations were terrain-corrected. The region has extensive ice cover. Corrections for the gravitational effect of glacier ice were again estimated from two- and three-dimensional gravity models of plausible ice-rock interfaces at each station. A complete Bouguer anomaly map of the North Victoria Land coast between the Rennick and Matusevitch Glaciers shows long wavelength regional features, including pronounced gravity lows over the northern end of the USARP Mountains and beneath the Morozumi Range in the Rennick Graben. The two lows are not believed to be artifacts due to insufficient correction for ice. We interpret them to represent a deep crustal root underlying the northern end of the Transantarctic Mountains.

Preliminary crustal modeling of the gravity data in both field areas suggests flexural uplift of the Transantarctic Mountains (Stern and tenBrink, 1989) along the rifted boundary between East and West Antarctica, marked by high heat flow, normal faulting, rapid uplift and active volcanism. Gravity data suggest a thickened lithosphere and crust in East Antarctica contrasting with a thinned and stretched crust in West Antarctica. According to Stern and tenBrink, active uplift of the older East Antarctic lithosphere along a suture expressed by the Transantarctic Mountain Range appears to be largely thermal and associated with an active rifting process.

References

Cooper, A.K., Davey, F. J., Behrendt, J. C., 1987a. Seismic stratigraphy and structure of the Victoria Land Basin, Western Ross Sea, Antarctica, in The Antarctic Continental Margin: Geology and Geophysics of the Western Ross Sea, edited by A. K. Cooper and F. J. Davey, pp. 27-76, Vol. 5B, Circum-Pacific Council for Energy and Mineral Resources, Earth Sciences Series, Houston, Texas.

Cooper, A. K., Davey, F. J., Cochran, G. R., 1987b. Structure of extensionally rifted crust beneath the Western Ross Sea and Iselin Bank, Antarctica, from sonobouy seismic data, in The Antarctic Continental Margin: Geology and Geophysics of the Western Ross Sea, edited by A. K. Cooper and F. J. Davey, pp. 93-118, Vol. 5B, Circum-Pacific Council for Energy and Mineral Resources, Earth Sciences Series, Houston, Texas.

Duerbaum, H. J., Druivenga, G., Geipel, H., and Merkel, G., 1989. Gravity measurements along a traverse from Mt. Melbourne to the Polar Plateau in North Victoria Land, Antarctica, Geol. Jb., E-38, 14 pp.

Stern, T., tenBrink, U., 1989. Flexural uplift of the Transantarctic Mountains, J. Geophys. Res., 94(B8), 10,315-10,330.

THE CHARNOCKITE MAGMA SUITE: A NEW WIDESPREAD MAGMA TYPE DISTINCTIVE FROM METAMORPHIC CHARNOCKITES. ITS PETROGENESIS AND ROLE IN GONDWANA.

J.A. Kilpatrick, and
D.J. Ellis
Department of Geology, Australian National University, GPO Box 4, Canberra, ACT 2601, Australia.

The Ardery Charnockitic Intrusions of the Windmill Islands, Antarctica, have unambiguous intrusive characteristics (Kilpatrick et al., 1990), evidence of high magmatic temperatures (pigeonite, inverted pigeonite, complex pyroxene exsolution, and antiperthites), and show a wide range in cogenetic compositions with SiO_2 values of 45 to 78%. The bulk of the magma chamber has an approximate SiO_2 value of 58 to 64% and has been modelled to produce the observed cogenetic cumulates and differentiates through simple fractionation of observed mineral assemblages and whole rock compositions. The Ardery Charnockitic Intrusions contain extreme TiO_2 and P_2O_5 and low CaO for given SiO_2 values.

Magmatic charnockites can be defined as a distinct, previously unrecognised magma type, the "Charnockite Magma Suite" (CMS). Documented charnockites from three continents (Antarctica, Australia, and Africa) have been compiled and it has been found that they all have the same range in chemical compositions. These characteristics, in terms of high P, Ti, and depletion in Ca for a given SiO_2 content distinguish them from other felsic intrusive rocks (i.e. I and S types).

Charnockite has been used to describe almost all orthopyroxene+K-feldspar +biotite+quartz bearing rocks. Recent research has proven that both magmatic and metamorphic charnockites occur. Metamorphic charnockites, principally occur in India and Sri Lanka, and have been the focus of much recent debate (Newton et al., 1980; Janardhan et al., 1982; Burton and O'Nions, 1990), over the viability of regional CO_2 flushing which causes widespread dehydration of deep crustal rocks resulting in pre-existing granitoids recrystallising to the characteristic orthopyroxene+biotite bearing charnockite mineral assemblage. Whilst some charnockites show field evidence for an igneous origin (Kilpatrick et al., 1990) it is not always discernible. Igneous and metamorphic charnockites are essentially identical in handspecimen, however they can be discriminated petrographically by a subtle difference in the modal abundance of apatite and ilmenite. Charnockites studied from Mawson and Casey Stations (Antarctica), Musgrave Ranges (Central Australia), and compiled analyses of charnockites from elsewhere in the world show that the majority of reported charnockites from occurrences other than India and Sri Lanka are in fact igneous in origin and members of the CMS.

Charnockites of igneous origin are geochemically distinct from metamorphic charnockites (Figures 1 and 2). Magmatic charnockites contain relatively lower CaO for given SiO_2 values than the metamorphic charnockites. The combined K_2O and TiO_2 enrichment of the magmatic charnockites is also distinctive. Very little overlap occurs between the two fields on figures 1 and 2. The use of these figures and others not presented here very clearly discriminate magmatic charnockites from most other magma types. It is significant that the CMS can be distinguished almost solely by the use of major element plots which contain restricted fields which confine the CMS. Whilst the CMS is restricted to defined major element fields, the CMS covers an extensive SiO_2 range from 45 wt.% to 78 wt.%. Most recent data from Antarctica

(unpublished data), Central Australia (unpublished data), and South Africa suggests that the range of primary magma SiO_2 is large, and these primary magmas all share the same geochemical characteristics indicating consanguinity.

The CMS with its high K_2O and SiO_2,and low MgO, Cr, Ni, and U has been considered to most likely represent an unusual crustal melt. This was supported by the rare earth element data from the Mawson Charnockites (unpublished data) which has been interpreted as indicating either the presence of residual garnet in the source rocks of some of the Mawson Charnockites, or crystallisation of garnet from melts generated in thickened crust (D. Young pers. comm.; Young and Ellis, 1990 & 1991). The Mawson Charnockites also represent some of the few charnockites that have been analysed for Nd and Sr isotopes, and which show a highly evolved signature (generally interpreted to be of crustal origin). However this may relate to the enrichment of the upper mantle or basal lower crust similar to and possibly related to the enrichment proposed to account for some tholeiites.

It has been found that a number of Continental Flood Basalts share many of the major element characteristics of the CMS (Figure 3). These tholeiites are part of the high P_2O_5 and TiO_2 type (HPT) that occurs in the Karoo, Parana, and East Antarctic Shield areas and which is itself geochemically distinct from the other basalt types. Brooks and Hart (1978) recognised two zones of different average Sr isotopic compositions for Mesozoic tholeiites of Gondwana, one comprising the Parana, Karoo, Deccan, and Queen Maud Land tholeiites, and the other the Ferrar and Tasmanian tholeiites, and proposed the existence of an enriched lithospheric component within a heterogeneous mantle source. Hergt (1987) speculated that the apparent chemical and isotopic zones (Figure 4) may be related to the subduction proposed by Cox (1978), with subducted components enriching mantle source regions, and the zones of figure 4 reflecting the changing composition of fluids released from the subducting slab and sediments. To account for the enrichment of mantle 1000's of kilometres from the zone of subduction Hergt (1987) speculated that Gondwana had over-ridden contaminated mantle sources.

The isotopic variation found within the Continental Flood Basalts of Gondwana is considerable and has been variably interpreted as originating through mantle enrichment processes, which may or may not be related to subduction, or by crustal contamination. Where the HPT and LPT (low P and Ti types) occur in close proximity and can be readily compared, the relative role of crustal contamination is debated (eg. Parana, and Karoo). It is mostly agreed that much of the isotopic variation in the LPT-type basalts results from crustal contamination of a relatively geochemically homogeneous parental magma (Dupuy and Dostal, 1984; Fodor, 1987; Petrini et al., 1987), the origin of the much more varied isotopic signature of the HPT-type basalts (where they are identified) is debated, either invoking contamination (Fodor et al., 1985; Bellieni et al., 1986; Hughes et al., 1986), or no crustal contamination (Brooks and Hart, 1978; Collerson and Sheraton, 1986; Bellieni et al., 1990).

It can be seen from figure 4 that in the reconstruction of Gondwana there are distinct geochemical types of tholeiites, with the magmatic charnockites from Mawson and Casey (Antarctica), Musgrave Ranges (Central Australia), Limpopo (South Africa), and the Prince Charles Mountains (Antarctica) occuring in the broad HPT band that sweeps across Gondwana. It is of interest that evidence for a supposed enriched mantle source is based on Jurassic and younger tholeiitic basalts. The late Proterozoic high Ti and P magmatic charnockites apparently also occur within the HPT zone and suggest a long term enrichment in the sub-Gondwana mantle. The coincidence of a high TiO_2

and P_2O_5 signature is problematical in its origin. It is possible that discreet areas of enriched heterogeneous lithospheric mantle could be the source for the CMS, and that the HPT zones reflect ancient enrichment processes, since the charnockites are generally > 500 million years old (eg Mawson charnockite 985 Ma. (Young and Ellis, 1990)). However it is not certain as to whether the enrichment processes relate to ancient subduction and the construction of the early proto-continents. The shared signatures may also indicate that the enrichment process that occurred in the subcontinental mantle extended up into basal crustal level. The work of Collerson and Sheraton (1986) showed the occurrence of HPT-type tholeiites occurring in the Archaean Vestfold Block, Antarctica, which is in relative proximity to the Prince Charles Mountains and in light of the CMS signature of the known charnockite analyses from the Prince Charles Mountains (Ravich et al., 1985) strongly points to a link between subcontinental mantle enrichment processes and the potential fertility of source regions (be they mantle or lower crustal) to produce CMS-type magmas.

This possible link between the CMS and subcontinental mantle enrichment processes could verify the suggestion of Collerson and Sheraton (1986) that ancient subcontinental lithosphere has been and possibly is still attached to the component continents of Gondwana, in particular the East Antarctic Shield. The existence of mantle keels to Gondwana segments is significant in our understanding of the development of the continents.

REFERENCES

Bellieni, G., Comon-Chiaramonti, P., Marques, L. S., Melfi, A. J. G., Nardy, A. J. R., Papatrechas, C., Piccirillo, E. M., Roisenberg, A., & Stolfa, D. (1986) Petrogenetic aspects of acid and basaltic lavas from the Parana plateau (Brazil): geological, mineralogical and petrochemical relationships. J. Petrol. 27; 915-944.

Bellieni, G., Piccirillo, E. M., Cavazzini, G., Petrini, R., Comon-Chiaramonti, P., Nardy, A. J. R., Civetta, L., Melfi, A. J., & Zantedeschi, P. (1990) Low- and high-TiO_2 Mesozoic tholeiitic magmatism of the Maranhao basin (NE-Brazil): K/Ar age, geochemistry, petrology, isotope characteristics and relationships with Mesozoic low- and high-TiO_2 flood basalts of the Parana basin (SE-Brazil). Neues Jahr. Miner. Abh. 162; 1-33.

Brooks, C. & Hart, S. R. (1978) Rb-Sr mantle isochrons and variations in the chemistry of Gondwanaland's lithosphere. Nature 271; 220-223.

Burton, K. W., & O'Nions, R. K. (1990) The timescale and mechanism of granulite formation at Kurunegala, Sri Lanka. Contrib. Mineral. Petrol. 106; 66-89.

Collerson, K. D. & Sheraton, J. W. (1986) Age and geochemical characteristics of a mafic dyke swarm in the Archaean Vestfold Block, Antarctica: Inferences about Proterozoic dyke emplacement in Gondwana. J. Petrol. 27; 853-886.

Cox, K. G. (1978) Flood basalts, subduction and the breakup of Gondwanaland. Nature 274; 47-49.

Dupuy, C. & Dostal, J. (1984) Trace element geochemistry of some continental tholeiites. Earth. Planet. Sci. Lett. 67; 61-69.

Fodor, R. V., Corwin, C., & Roisenberg, A. (1985) Petrology of the Serra Geral (Parana) continental flood basalts, southern Brazil: crustal contamination, source material, and South Atlantic magmatism. Contrib. Mineral. Petrol. 91; 54-65.

Fodor, R. V. (1987) Low- and high-TiO_2 flood basalts of southern Brazil: origin from picritic parentage and a common mantle source. Earth. Planet. Sci. Lett. 84; 423-430.

Hergt, J. M. (1987) The Origin and Evolution of the Tasmanian Dolerites. Unpul. Ph.D. thesis A.N.U.

Hughes, S. S., Schmitt, R. A., Wang, Y. L. & Wasserburg, G. J. (1986) Trace element and Sr-Nd isotopic constraints on the compositions of lithospheric primary sources of Serra Geral continental flood basalts, southern Brazil. Geochem. J. 20; 173-189.

Janardhan, A. S., Newton, R. C. & Hansen, E. C. (1982) The transformation of amphibolite facies gneiss to charnockite in southern Karnataka and northern Tamil Nadu. Contrib. mineral. Petrol. 79; 130-149.

Kilpatrick, J. A., Ellis, D. J. & Young, D. N. (1990) Field aspects of the Ardery charnockitic intrusions, Windmill Islands, Antarctica. A dynamic magma chamber. Gondwana: terranes and resources. Geol. Soc. Aust. Abst. 25: 290.

Newton, R. C., Smith, J. V. & Windley, B. F. (1980) Carbonic metamorphism, granulites and crustal growth. Nature 288; 45-50.

Petrini, R., Civetta, L., Piccirillo, E. M., Bellieni, G., Comon-chiaramonti, P., Marques, L. S., & Melfi, A. J. (1987) Mantle heterogeneous and crustal contamination in the genesis of low-Ti continental flood basalts from the Parana Plateau (Brazil): Sr-Nd isotope and geochemical evidence. J. Petrol. 28; 701-726.

Ravich, M. G., Solov'ev, D. S. & Fedorov, L. V. (1985) Geological structure of Mac. Robertson Land (East Antarctica). Russian Translations Series 24. AA Balkema/Rotterdam.

Young, D. N., & Ellis, D. J. (1990) Petrology of Proterozoic igneous charnockites from Mawson, Antarctica: high-temperature syn-orogenic granitoids produced by anatexis in a thickened crust. Gondwana: terranes and resources. Geol. Soc. Aust. Abst. 25: 261-262.

Young, D. N., & Ellis, D. J. (1991) The intrusive Mawson charnockites: evidence for a compressional plate margin setting of the Proterozoic mobile belt of East Antarctica. In Geological Evolution of Antarctica, ed. M.R.A. Thomson, J.A. Crame and J.W. Thomson, pp 25-31. Cambridge: Cambridge University Press.

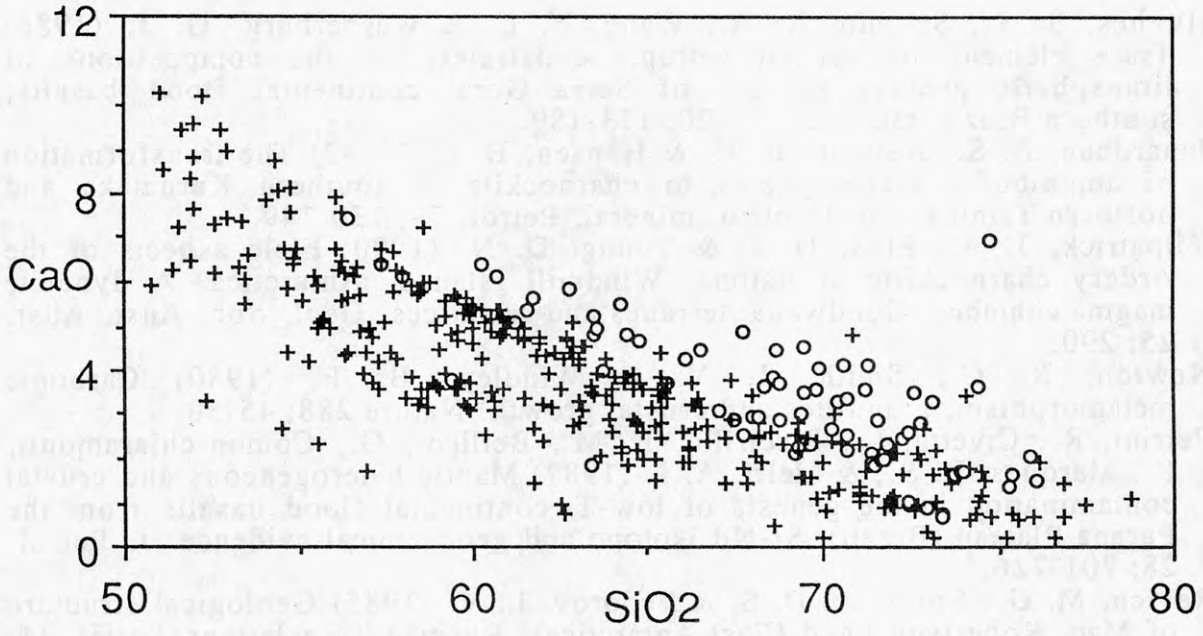

Figure 1: CaO Vs SiO_2 showing contrasting CaO contents between magmatic charnockites of the CMS (crosses) and metamorphic charnockites (circles). For Figures 1 to 3 magmatic charnockites consist of analyses from the Casey, Prince Charles Mountains, and Bunger Hills Charnockites (Antarctica), the Musgrave Charnockite (Australia), the Limpopo Belt (South Africa), and other world occurrences. Metamorphic Charnockites are principally from India and Sri Lanka.

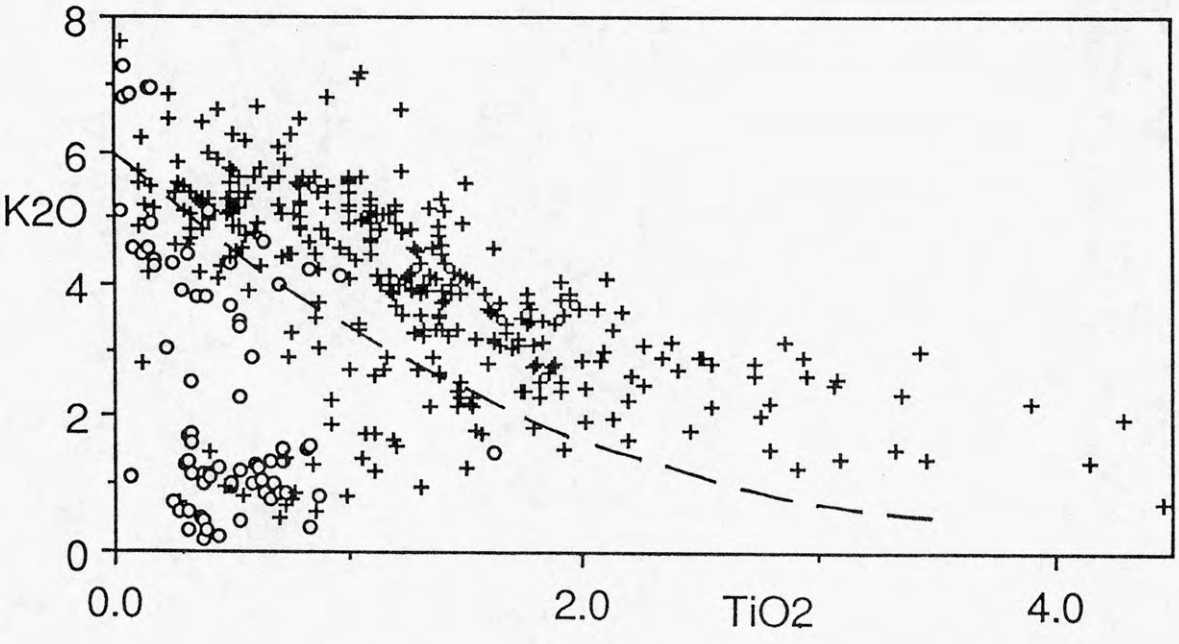

Figure 2: K_2O Vs TiO_2 showing the CMS's (crosses) characteristic enrichment in both K_2O and TiO_2 relative to metamorphic charnockites (circles). Common magmas (i.e S & I types) generally occur below the dashed line.

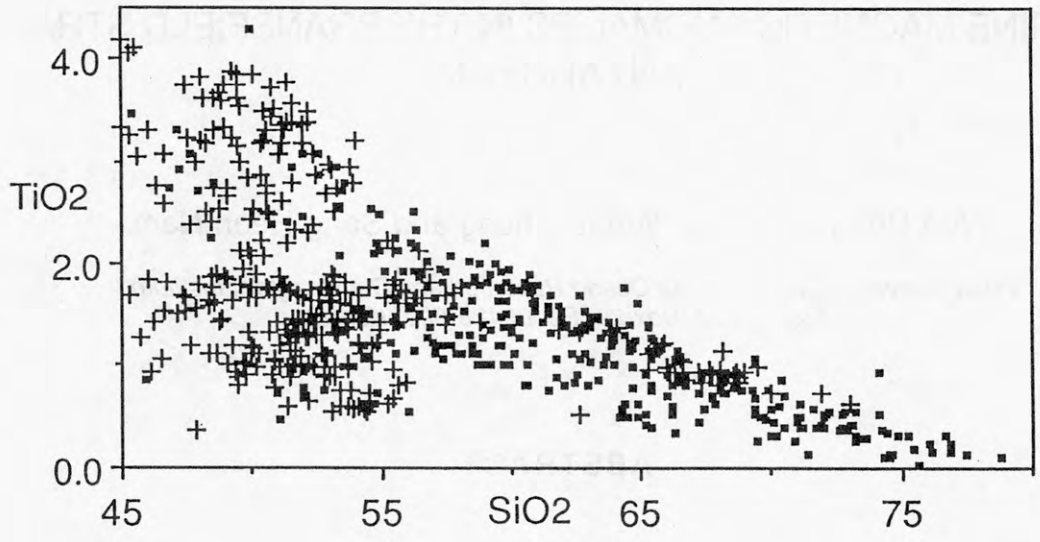

Figure 3: TiO_2 Vs SiO_2 comparing the Gondwana Continental Flood Basalts (crosses) to the CMS (small squares). Note particularly the HPT (high P_2O_5 TiO_2) and LPT (low P_2O_5 TiO_2) groupings of the basalts.

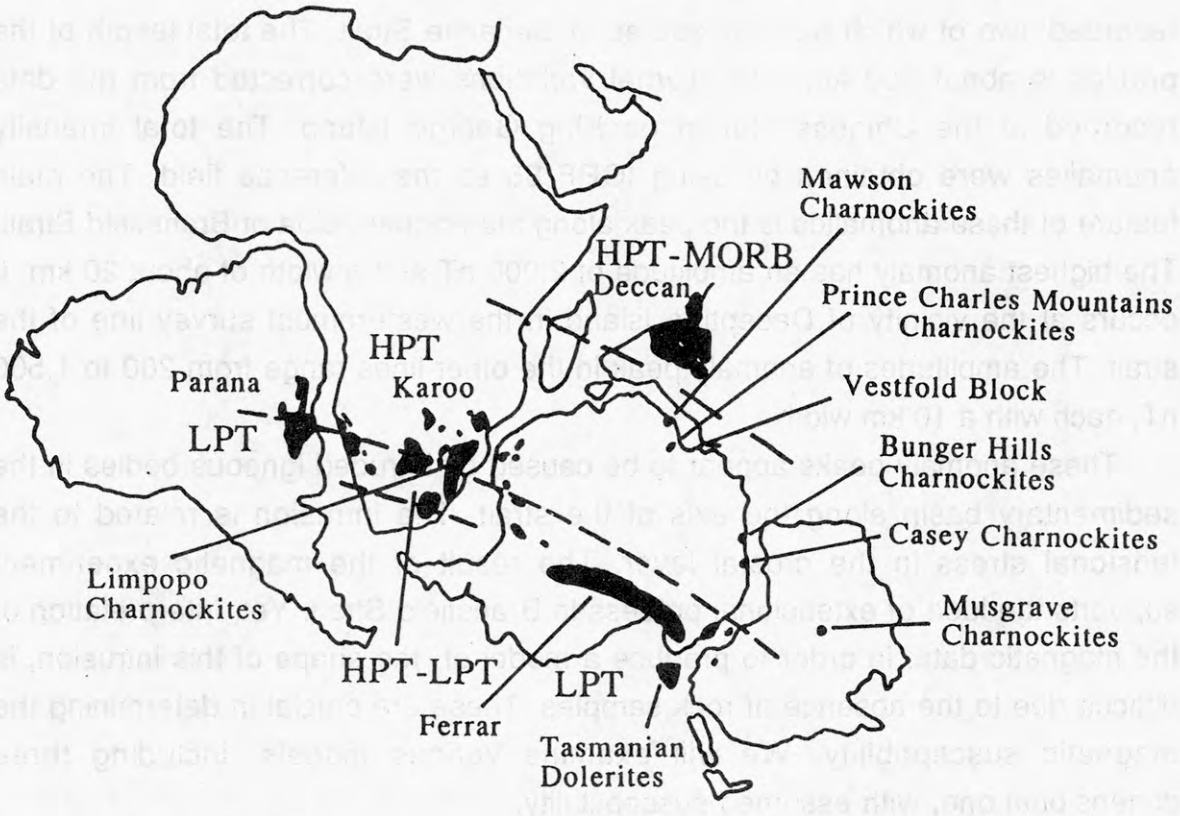

Figure 4: Representation of the zonation of Mesozoic tholeiites of Gondwana (after Hergt, 1987), and the occurrence of magmatic charnockites of the Charnockite Magma Suite.

MARINE MAGNETIC ANOMALIES IN THE BRANSFIELD STRAIT, ANTARCTICA

Yea Dong Kim, Tae Woong Chung and Sang Heon Nam

Polar Research Center, Korea Ocean Research and Development Institute, Ansan, P.O. Box 29, Seoul 425-600 (Korea)

ABSTRACT

Bransfield Strait has been believed to be extensional process which is caused by trench-arc movements. However, this process is not fully understood due to a lack of information on crustal structure. To study the structure of Bransfield Strait, a marine magnetic survey was carried out as a part of the Korea Antarctic Research Programme during the 1990/91 season.

Eleven profiles, with lengths of 40 km to 70 km, across the strait were recorded; two of which were measured in Gerlache Strait. The total length of the profiles is about 550 km. The diurnal variations were corrected from the data recorded at the Chinese station on King George Island. The total intensity anomalies were obtained by using IGRF 85 as the reference field. The main feature of these anomalies is the peak along the northern side of Bransfield Strait. The highest anomaly has an amplitude of 2,000 nT and a width of about 20 km. It occurs at the vicinity of Deception Island in the westernmost survey line of the strait. The amplitudes of anomaly peak in the other lines range from 200 to 1,500 nT, each with a 10 km width.

These anomaly peaks appear to be caused by intruded igneous bodies in the sedimentary basin along the axis of the strait. The intrusion is related to the tensional stress in the crustal layer. The result of the magnetic experiment supports the idea of extensional process in Bransfield Strait. Yet, interpretation of the magnetic data, in order to produce a model of the shape of this intrusion, is difficult due to the absence of rock samples. These are crucial in determining the magnetic susceptibility. We will examine various models, including three dimensional one, with assumed susceptibility.

GEOCHRONOLOGY OF BASEMENT ROCKS IN THE FOSDICK MOUNTAIN REGION OF WEST ANTARCTICA AND CORRELATION WITH CRETACEOUS EXTENSIONAL TERRANES OF SOUTHERN NEW ZEALAND

KIMBROUGH, David L., Baylor Brooks Institute of Isotope Geology, Department of Geological Sciences, San Diego State University, San Diego, CA 92182; RICHARD, Stephen M., Institute for Crustal Studies, University of California, Santa Barbara, CA 93106

The Ford Ranges provide the most widespread exposures of pre-Cenozoic rocks in western Marie Byrd Land continental margin. Geologic similarities have led previous workers to suggest that this area was adjacent to portions of New Zealand and the Campbell Plateau prior to Cretaceous breakup of the southern Gondwana margin (e.g. Cooper et al., 1982). The Ford Ranges are dominated by low-grade metasedimentary rocks of the Late Precambrian-Early Ordovician Swanson Formation that are intruded by mid-Paleozoic Ford Granodiorite and Cretaceous Byrd Coast Granite (Wade et al., 1977, 1978). The Fosdick Mountains, in the northern Ford Ranges, comprise an upper amphibolite facies migmatite-gneiss complex with gently dipping to subhorizontal foliations that define a broad E-W trending structural culmination. These high grade metamorphic rocks, which contrast with the bulk of the Ford Ranges, are referred to as the Fosdick Metamorphic Complex (FMC). Structural and petrologic features of the FMC are described elsewhere in this volume (Smith et al., Richard et al., and Richard). Here we report new U-Pb and ^{40}Ar-^{39}Ar geochronological data that constrain the timing and nature of magmatic, metamorphic, and tectonic events in the Ford Ranges.

The Ford Granodiorite is a metaluminous/peraluminous calc-alkaline granodiorite-monzogranite suite with initial $^{87}Sr/^{86}Sr$ ratios of 0.704-0.706, and is classified as an I-type granitoid (Weaver et al., 1991). Whole rock Rb-Sr isochrons have been determined at four widely spaced localities and range from 353 to 379 Ma (Adams, 1987). U-Pb zircon dates from a sample of the Ford Granodiorite in the Chester Mountains are discordant and define a lower intercept of 353 Ma that is interpreted as the crystallization age of the magma. This lower intercept age is consistent with the earlier Rb-Sr whole rock isochrons that indicate late Devonian to early Carboniferous emplacement of the suite. The upper intercept of ~1300 Ma reflects inherited components of Precambrian zircon derived from the source region of the magma. The upper intercept date indicates the presence of Precambrian continental crust, or material derived

therefrom, in the source region. This component may have been derived from material related to the Swanson Formation at deeper crustal levels.

The Byrd Coast Granite is a compositionally uniform suite of pink biotite leucogranite with common miarolitic cavities and local accessory fluorite. Initial $^{87}Sr/^{86}Sr$ ratios range from 0.704-0.708, and trace element contents indicate at least some of the suite are A-type granitoids (Weaver et al., 1991). These features suggest that the Byrd Coast Granite is a shallowly emplaced anorogenic suite unrelated to subduction. Zircon data from a sample of Bryd Coast Granite at Mt. Corey are slightly discordant with $^{206}Pb/^{238}U$ dates of 103 Ma and $^{207}Pb/^{206}Pb$ dates of ~130 Ma. The $^{206}Pb/^{238}U$ dates correspond to a Rb-Sr date of 103 +/- 3 Ma for Mt Corey determined by Halpern (1968). We interpret this as the crystallization age for this sample. The slightly discordant $^{207}Pb/^{206}Pb$ dates may be the result of small components of inherited radiogenic lead in the zircon.

Zircon U-Pb dates have been determined for two components of the FMC, a biotite granodiorite orthogneiss exposed at Mt Richardson, and a relatively undeformed garnet biotite leucogranite exposed at Mt Lockhart. The dates from both samples are strongly discordant and fall along similar discordia trajectories with Mesozoic lower intercept ages. The Mt Lockhart sample is interpreted as migmatitic leucosome material segregated during peak metamorphic conditions. The lower intercept date is therefore regarded as the age of migmatization and new zircon growth with the upper intercept date reflecting inherited components derived from the partially melted parent material. The Mesozoic lower intercept for the Mt Richardson sample may represent either a crystallization age or simple lead loss associated with peak metamorphism. Additional work is in progress.

Hornblende, muscovite, biotite, and potassium feldspar ^{40}Ar-^{39}Ar dates from three widely spaced localities in the FMC indicate rapid cooling (75-100°C/Ma) of the FMC between 100 and 94 Ma. Muscovite and potassium feldspar from the north-central FMC yield ~96 and 94 Ma plateau ages. In the structurally higher southeast FMC hornblende, biotite and potassium feldspar plateau ages are ~101, 97, 96 Ma. Hornblende in foliated granodiorite from Neptune Nunataks yielded disturbed spectra with a total gas date of 271 Ma while biotite yielded a plateau age of 103 Ma. The old apparent age from foliated granodiorite at Neptune Nunatak suggests a pre-Mesozoic, possibly Ford age, deformation event. We hypothesize that rapid cooling of the FMC was a result of tectonic unroofing and uplift. Northward decrease of cooling ages is consistent with southward tilting of the Fosdick/Chester block during this uplift. These

ages are consistent with seven previously reported Rb-Sr biotite ages from the FMC that range from 92 to 102 Ma (Halpern, 1972). This period of uplift was nearly coincident, or perhaps overlapped with, emplacement of Byrd Coast Granite in the area.

The cooling and uplift ages from the FMC are similar to those determined for a Cordilleran-type metamorphic core complex terrain in South Island New Zealand (Kimbrough and Tulloch, 1988; Tulloch and Kimbrough, 1989). The Cretaceous New Zealand core complex developed in response to continental extension preceding the breakup of the southern Gondwana margin. A similar mechanism of rapid tectonic uplift involving low angle normal faulting is hypothesized for the Fosdick Mountains, which resulted in omission of crustal section between the deep level FMC and relatively shallow level Ford Granodiorite and Byrd Coast Granite. The timing of extensional events in both New Zealand and the Ford Ranges of Marie Byrd Land is consistent with estimates for the initiation of continental rifting based on marine magnetic anomalies (Moore and Eittreim, 1987). The FMC is thus interpreted as the lower plate assemblage while the Byrd Coast Granite is regarded as a pre- and/or syn-extensional upper plate magmatic suite.

REFERENCES

Adams, C.J., 1987, Geochronology of granite terranes in the Ford Ranges, Marie Byrd Land, West Antarctica, New Zealand J. Geology Geophysics, 30, 51-72.

Cooper, R. A., C. A. Landis, W. E. Le Mauserier, and I. G. Speden, 1982, Geologic history and regional patterns in New Zealand and West Antarctica - Their paleotectonic and paleogeographic significance, in Craddock, C., ed., Antarctic Geoscience, Int. Union Geol. Sci. Series B - no. 4, 43-53.

Halpern, M., 1968, Ages of Antarctic and Argentine rocks bearing on continental drift. Earth Planet. Sci. Lett., 5, 159-167.

Halpern, M., 1972, Rb-Sr total-rock and mineral ages from the Marguerite Bay area Kohler Range and Fosdick Mountains. in Adie, R. J. ed., Antarctic Geology and Geophysics, Oslo, Universitetsforlaget, 197-204.

Kimbrough, D.L., and Tulloch, A.J., 1988, Metamorphic core complex in western New Zealand related to the late Cretaceous breakup of Gondwana: Geological Society of America Abstracts w/ Programs, v. 20, no. 7, p. 324.

Moore, G.W., and Eittreim, S.L., 1987, Mechanism of Extension and Rifting at the Antarctic Continental Margin, *in*: The Antarctic Continental

Margin: Geology and Geophysics of Offshore Wilkes Land, CPCEMR Earth Science Series, v. 5A: Houston, Texas, Circum-Pacific Council for Energy and Mineral Resources, p. 89-97.

Tulloch, A.J., and Kimbrough, D.L., 1989, The Paparoa metamorphic core complex, Westland-Nelson, New Zealand: Cretaceous extension associated with fragmentation of the Pacific margin of Gondwana: Tectonics, v. 8, p. 1217-1234.

Wade, F. A., C. A. Cathey, and J. B. Oldham, 1977, Reconnaissance geologic map of the Guest Peninsula quadrangle, Marie Byrd Land, Antarctica, USARP, Ant. Geol. Map, A-7.

Wade, F. A., C. A. Cathey, and J. B. Oldham, 1978, Reconnaissance geologic map of the Gutanko Nunataks quadrangle, Marie Byrd Land, Antartica, USARP, Ant. Geol., Map A-11.

Weaver, S. D., Bradshaw, J. D., and Adams, C. J., 1991, Granitoids of the Ford Ranges, Marie Byrd Land, Antarctica, *in* Thomson, M.R.A., Crame, J.A., and Thomson, J.W. (eds.), Geological Evolution of Antarctica, Cambridge University Press, p. 345-351.

SEISMIC CHARACTERISTICS OF AN AIRGUN FIRED OVER SNOW

E C King, E P Jarvis and E A Mowse
British Antarctic Survey
Madingley Road
Cambridge UK

A small airgun was tested as an over-snow seismic source during the 1990/91 Antarctic field season. The tests were carried out at Rothera Base, Antarctic Peninsula (figure 1). It has been known for some time that explosive charges fired above the ground can produce good seismic records. This method is still used in areas where the drilling of shot holes is difficult or undesirable. The tests described here were intended to determine whether or not airguns could be used in the same fashion.

The device used was a 0.65l (40cu.in) sleeve-gun, which was fired in the air above the snow surface at heights of 2 m; 1 m and 0.5 m, it was also fired when resting on the snow surface and buried at a depth of 0.5 m. It is possible to fire such a device in air without damage to the mechanism but there is a need for increased maintenance because the bearing surfaces have to be renewed more frequently than when firing in water.

Comparison shots were obtained using buried and surface-laid explosives and using a sledge hammer. Shots were recorded by a spread of 24 geophones with 40 Hz natural frequency, spaced 10 m apart. The sample interval was 0.5 ms and filters were open between 4 and 500 Hz for the recording. Figure 2 shows shot records for a single shot with the sleeve-gun (fired at 1m above the surface), 200 g of high explosive fired on the surface and 5 hammer blows stacked together.

The reflection which can be seen on the sleeve-gun and hammer shots is from the ice/bedrock interface (near-vertical incidence time of 125 ms). The ice thickness at the test site is approximately 200 m.

On the unprocessed, true amplitude records (figure 2) the exposive and hammer shots show much stronger ground-roll than on the sleeve-gun shot. This means that the reflection signal to ground-roll noise ratio on the far-offset traces is very much better for the sleeve-gun shot. At near offsets the airwave and debris-fall noise affects the sleeve-gun and explosive records but not the hammer.

Explosive shots buried at various depths from 6 to 26 m were also fired during the

season. Such shots display greatly reduced ground-roll compared to the surface shot, as would be expected, and the bedrock reflection is clear. The amplitude of the reflection when using 200 g of high explosive at 16 m depth is 26 dB greater than when using the airgun.

The ground-roll can be well attenuated on all the surface shot records if a 90Hz highpass filter is applied (figure 3). The reflection is just discernible on the explosive and hammer records but the signal to noise ratio is poor. In contrast the airgun record displays a very good reflection at all offsets between 60 and 240m. It should be noted that the airgun record is from a single shot but the source is a repeatable one, so an even better signal to noise ratio is achievable.

Discussion and Conclusions

For speed of operations a surface seismic source is preferable. On safety, environmental and cost grounds it is desirable to use explosives as little as possible in Antarctic seismic work. On the basis of data obtained in the 1990/91 field season it is clear that the airgun has the potential to be further developed as a viable non-explosive surface seismic source, useful for some types of investigation. Use of the airgun in conjunction with a short drag cable should provide a rapid means of profiling ice-shelf thickness and seabed depth.

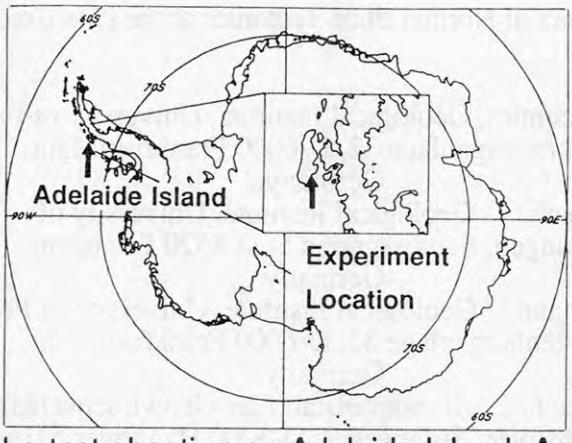

Figure 1. Location of the test shooting on Adelaide Island, Antarctic Peninsula.

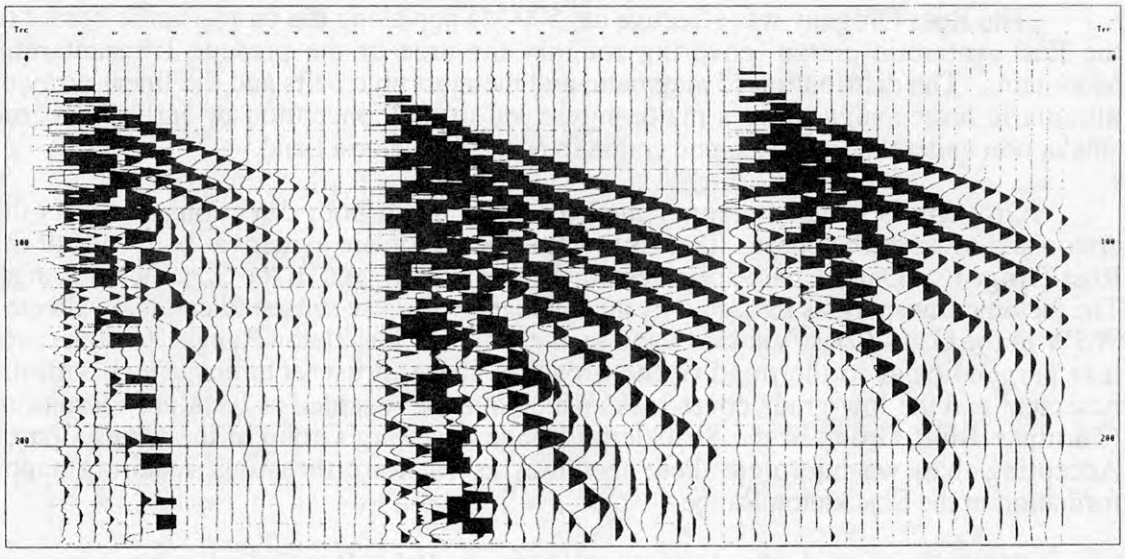

Figure 2. Unprocessed shot records with amplitudes preserved. From left to right: airgun fired at a height of 1m above the snow; 200g high explosive fired on the surface; vertical stack of 5 blows with a 7.5kg hammer. Trace spacing is 10m. Timing lines are at 10ms intervals.

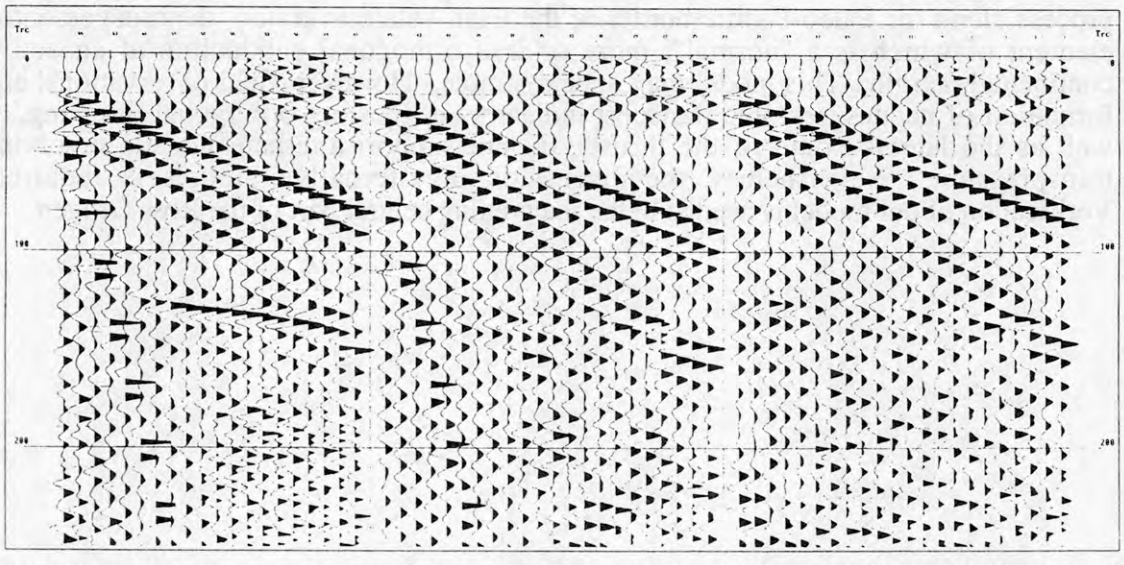

Figure 3. The same records as figure 2 with a 90hz highpass filter applied and displayed with an 80ms AGC.

The Ross Orogen - Product of Normal Plate Tectonics at the Paleozoic Antarctic Margin?

G. Kleinschmidt, Geological Institute, University of Frankfurt, Seckenberganlage 32, D-6000 Frankfurt/Main, Germany.
W. Buggisch, Geological Institute, University of Erlangen, Schlossgarten 5, D-8520 Erlangen, Germany.
T. Floettmann, Geological Institute, University of Frankfurt, Seckenberganlage 32, D-6000 Frankfurt/Main, Germany.
T. Tessensohn, Bundesanstalt fuer Geowissenschaften und Rohstoffe, Stilleweg 2, D-3000 Hannover 51, Germany.

The Ross Orogeny was effective ca. 500 Ma ago along the proto-Pacific border of the East Antarctic craton, covering roughly the area of the present Transantarctic Mountains. The distribution of magmatic and metamorphic belts and the linear array of ultramafic lenses suggesting a major suture led to the conception of early Paleozoic subduction under the East Antarctic craton in northern Victoria Land.

Orogeny is usually accompanied by thrusting in both directions, towards the craton and towards the ocean. Thrusts towards the craton are evident at both ends of the Ross Orogen: at Oates Coast/northwestern Victoria Land, and in the Shackleton Range. The tectonic transport, as indicated by an abundance of shear-sense indicators, is directed WSW in the Oates Coast/Victoria Land sector, S in the Shackleton Range. In both cases it is perpendicular to the trend of the orogen. These thrust tectonics affect both the basement and the low-grade cover rocks which may be regarded as back-arc formations (Turnpike Bluff Group in the Shackleton Range and Berg Group at the Oates Coast). Accepting that, we interprete these tectonics as back-arc thrusting, reaching nappe formation in the Shackleton Range.

Thrusting towards the ocean, in this case the Paleo-Pacific, is known up to now only in northern Victoria Land. Three major thrust systems are traceable for several 100 km. Here, too, the thrust directions are clearly orthogonal and the formation of nappes is probable.

All these features indicate that the Ross Orogen is the product of an accretionary process along the Paleo-Pacific border of the East Antarctic craton, the most essential element of which is a "normal", more or less orthogonal subduction at an active continental margin. This model may appear simple. However, field observations, e.g. formation of nappes, tectonic transport indicators suggesting orthogonal thrusting, as well as the lateral extent of the thrusts, do not support alternate models involving transpression. Nevertheless, the discussion of alternative models is required. Verification of our model is needed in the intervening central part of the Ross Orogen.

GEOCHEMISTRY AND AGE OF GRANITIC ROCKS IN THE RUKER GRANITE-GREENSTONE TERRAIN, SOUTHERN PRINCE CHARLES MOUNTAINS, EAST ANTARCTICA

(poster presentation)

V.P.Kovach, B.V.Belyatsky, North Branch for Marine Geologic Research and Exploration "Sevmorgeologia", 20 Moyka, 190121, Leningrad, USSR.

Preliminary results of analysis of U-Pb zircon systems, as well as Sm-Nd whole-rock, REE and other trace elements studies of granitic rocks from the Ruker granite-greenstone terrain (Kamenev & Krasnikov, this volume) are reported. The analyzed specimens were collected from the Southern Mawson Escarpment (SME) and at Mount Ruker (MR) during 1987/88 and 1989/90 field seasons (Fig. 1).

Four distinct groups of granitic rocks are recognized in the SME on the basic of their geological setting, geochemistry and isotopic age.

Ancient sialic basement is represented by granulite facies assemblages found at one locality as lensoid relics included in amphibolite facies granitic gneisses. These assemblages are represented by high-alumina hy-am and am-bt tonalite-trondhjemitic gneisses (boxes 1 and 2 in Fig. 2) typical of grey gneiss terrains (Barker et al.,1979; Condie, 1981; Hunter et al.,1979). They are characterized by fractionated REE patterns with steep L- and HREE sloping and with no or positive Eu anomaly (Nos. 111 and 111-4 in Fig. 3A), high Sr and low Rb, Ba, Zr, Nb and Hf concentrations. Geochemical and isotopic data indicate that tonalite-trondhjemitic basement protolith was derived by partial melting about 3.2 Ga ago (T Nd(CHUR), 147Sm/144Nd=0.1046-0.1062) from mafic source depleted in LREE (E Nd(T)=+1.3) with ga+/-hb in residue.

Bt- and hb-bt-qu-fsp gneisses with prominent lineation are the most abundant granitic rocks in the SME. They are interleaved with mafic-ultramafic metavolcanics and metasedimentary rocks metamorphosed in upper amphibolite facies and are often changed to

migmatites along the contacts. Abundant tectonic clasts of mafic and ultramafic metavolcanic rocks, layered amphibolite bodies, metabasic dykes, pegmatite veins and lenses occur in the slabs of gneisses. These gneisses were previously described as granite-gneisses (Kamenev, 1990); however, their major- and trace-elements characteristics are more similar to low-alumina rhyodacites and rhyolites (boxes 3 in Fig. 2). They have weakly fractionated REE patterns with gently sloping L- and HREE, small positive and prominent negative Eu anomaly (Nos. 014-1, 025-1, 027-6 in Fig. 3A; 014-3 and 014-6 in Fig. 3B); Sr and Rb contents are relatively low, whereas Ba, Zr, Nb and Hf concentrations are high. The geochemical affinities of low-alumina gneisses are similar to undepleted felsic volcanics of greenstone belts (Condie, 1981), siliceous gneisses of the Mkhondo metamorphite suite of the Ancient Gneiss Complex (AGC) of Kaapvaal Shield and one sample (No. 025-1;) may be compared with low-alumina siliceous gneisses of the bimodal suite of AGC (Hunter et al.,1978) or with Webb Canyon gneisses (metarhyodacites) in Wyoming (Barker et al., 1979). Magmatic protoliths of low-alumina linear gneisses may be derived 3.0-3.1 Ga ago (U-Pb zircon age) by partial melting of short-lived mixed tonalite-greenstone or enriched in LREE tholeiitic basalts source (E Nd(3.0-3.1)=-0.2 to +0.9) with pl+px+/-hb in residue and subsequent crystal fractionation.

Locally low-alumina gneisses incorporate leucocratic and melanocratic segregations with obscure boundaries that differ significantly from the host rocks in geochemical properties. A leucogneiss sample (No. 027-3 in Fig. 3B) shows fractionated REE pattern with steep LREE and gently sloping HREE, positive Eu anomaly and low Sr, Ba, Zr, Nb and Hf contents. A melanocratic sample (No. 027-5 in Fig. 3B) is characterized by steep LREE and gently sloping HREE pattern with negative Eu anomaly. Genetic relationships between segregations and host low-alumina gneisses are not clear, but their T Nd(CHUR) model age is the same (ca. 3.1 Ga). Some of low-alumina am-bt gneisses lack obvious lineation and show low Ba contents and FeO /MgO ratio (box 4 in Fig. 2). They may be classified as low-alumina trondhjemites derived 2.5 Ga ago (Pb-Pb zircon method).

The fourth group is represented by granite pegmatite (box 7 in Fig. 2). They are 2.3 Ga old (Pb-Pb zircon) and differ from all other granitic rocks in the SME (No. 025-4 in Fig. 3A), although they might have formed by partial melting of the high-alumina tonalite-trondhjemitic gneisses.

Granitoids at MR (Fig.1) occur in tectonic relationship with volcanic-sedimentary rocks deformed and metamorphosed in greenschist facies environment. Coarse-grained porphiritic slightly banded subalkaline bt-fsp granites, granodiorites and leucogranites (box 8 in Fig. 2) are dominant. They include vein bodies of medium-grained Bt-granites concordant with banding and chemically similar to enclosing rocks (box 9 in Fig. 2). All granitic rocks at MR have strongly fractionated REE patterns with steep L- and HREE sloping and prominent negative Eu anomaly (Fig. 3C), relatively high Rb and Ba and low Sr and Zr contents. These features of the MR granites resemble syn- and post tectonic granites of the Eastern Kaapvaal Shield (Glikson & Jahn, 1985). Granites from the MR have a U-Pb zircon age about 3.0 Ga (Fig. 10) with E Nd(3.0)=-1.75+/-0.4. They were probably derived by partial melting with pl+px+/-hb in residue of preexisting sialic rocks similar to high-alumina tonalite-trondhjemites at the SME.

Thus, distinct groups of granitic rocks in the Ruker granite-greenstone terrain are: at least 3.2 Ga old tonalite-trondhjemitic basement; granite-gneisses presumably derived from 3.0-3.1 Ga old felsic volcanics or formed at that time at the expense of older volcanic rocks; 3.0 Ga old subalkaline granites formed by remobilization of preexisting sialic crust; 2.5 Ga old low-alumina trondhjemites and 2.3 Ga old granite pegmatites. The relation of 2.5 Ga old low-alumina trondhjemites with respect to above groups is not clear. Age and geochemical affinities of the Ruker GGT granitic rocks are similar to Archaean granitoids elsewhere in Gondwanaland - Kaapvaal Shield, South Africa (Glikson & Jahn, 1985).

References.

1. Barker F.,1979. Trondhjemite: definition environment and

hypotheses of origin.In: F.Barker (ed.),Trondhjemites, Dacites and Related Rocks. Elsevier, Amsterdam, pp. 1-12.
2. Barker F., Millard H.T.,Jr., Lipman P.W., 1979. Four low-K siliceous rocks of the western U.S.A.In: F.Barker (ed.),Trondhjemites, Dacites and Related Rocks. Elsevier, Amsterdam, pp. 415-433.
3. Condie K.C., 1981. Archaean Greenstone Belts. Elsevier, Amsterdam, 434pp.
4. Glikson A.Y., Jahn B.M., 1985. REE and LIL elements, eastern Kaapvaal shield, South Africa: evidence of crustal evolution by 3-stage melting. - Geol. Assoc. Canada, Spec. Pap., 28: 303-324.
5. Hunter D.R., Barker F., Millard H.T.,Jr., 1978. The geochemical nature of the Archean Ancient Gneiss Complex and Granodiorite Suite, Swaziland: a preliminary study. - Precambrian Res. 7: 105-127.
6. Kamenev E.N.,1990. Prince Charles Mountains. In: V.L.Ivanov, E.N.Kamenev (eds.), Geology and Mineral Resources of Antarctica. Moscow, Nedra, pp .67-113 (in Russian).
7. Kamenev E.N., Krasnikov N.N., 1991. The granite-greenstone terrains in the Southern Prince Charles Mountains. Sixth International Symposium on Antarctic Earth Sciences. Extended abstracts, this volume.

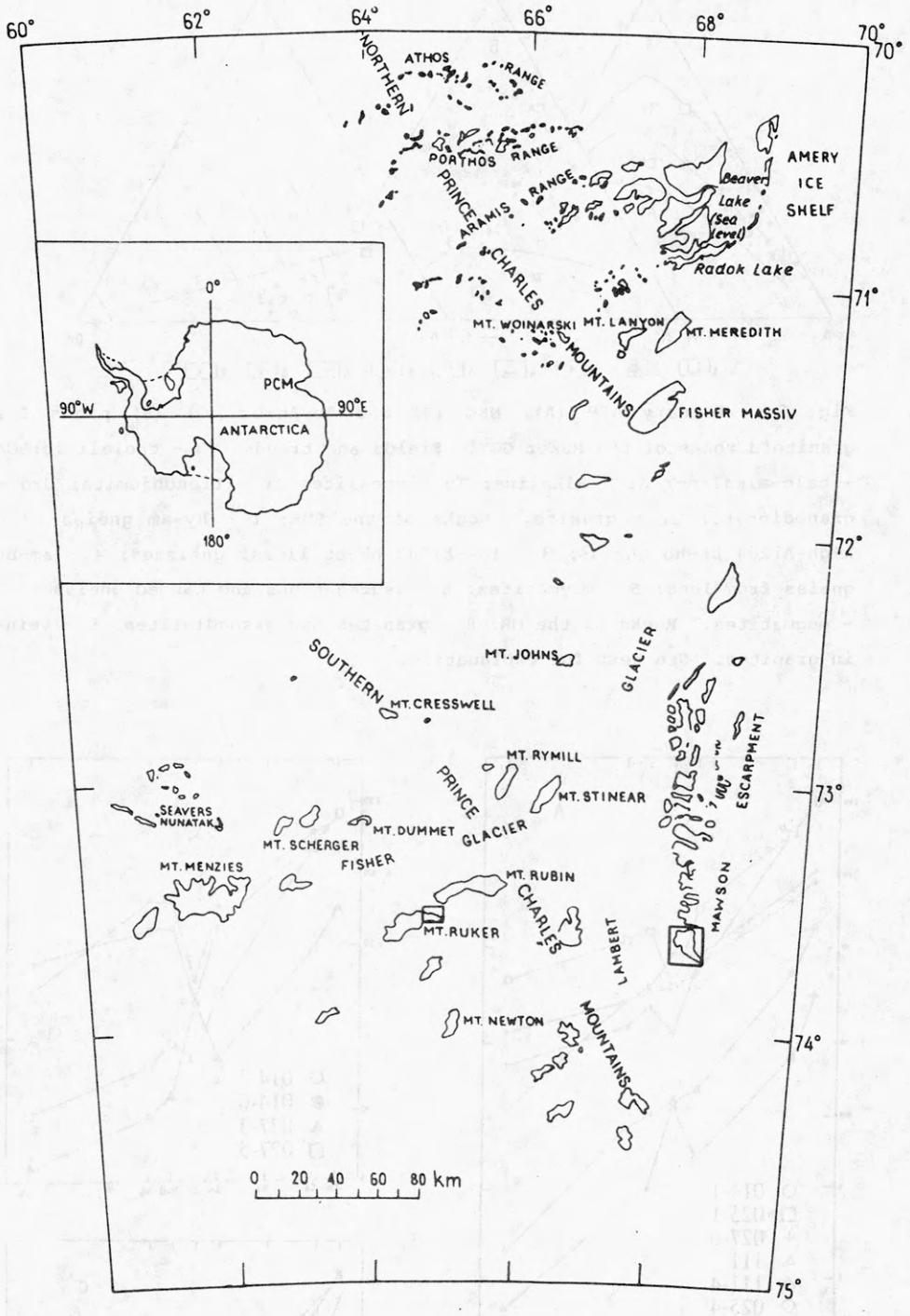

Fig. 1. Location of study areas (boxes) in the Prince-Charles Mountains.

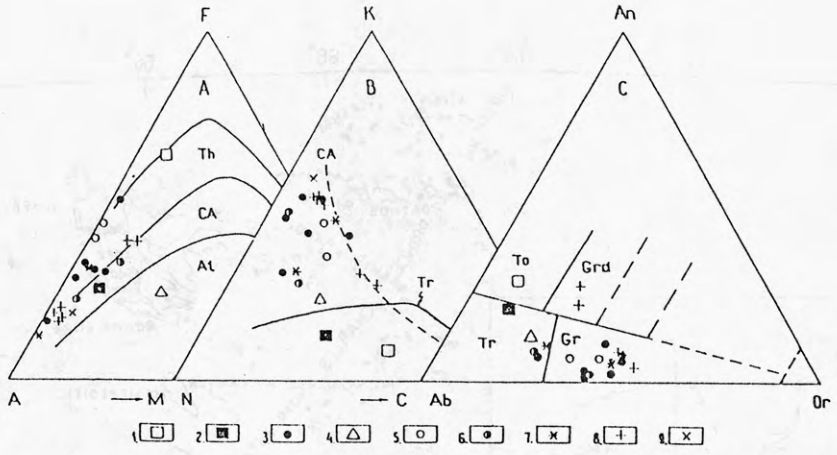

Fig. 2. Ternary AFM (A), NKC (B) and Ab-An-Or (C) (8) plots for granitoid rocks of the Ruker GGT. Fields and trends: Th - tholeiitic; CA - calc-alkaline; Al - alkaline; To - tonalite; Tr - trondhjemite; Grd - granodiorite; Gr - granite. Rocks of the SME: 1 - hy-am gneiss; 2 - high-Al2O4 bt-hb gneiss; 3 - low-Al2O3 hb-bt linear gneisses; 4 - am-bt gneiss from lens; 5 - migmatites; 6 - segregations and banded gneisses; 7 - pegmatites. Rocks of the MR: 8 - granites and granodiorites; 9 - veins in granites. See text for explanation.

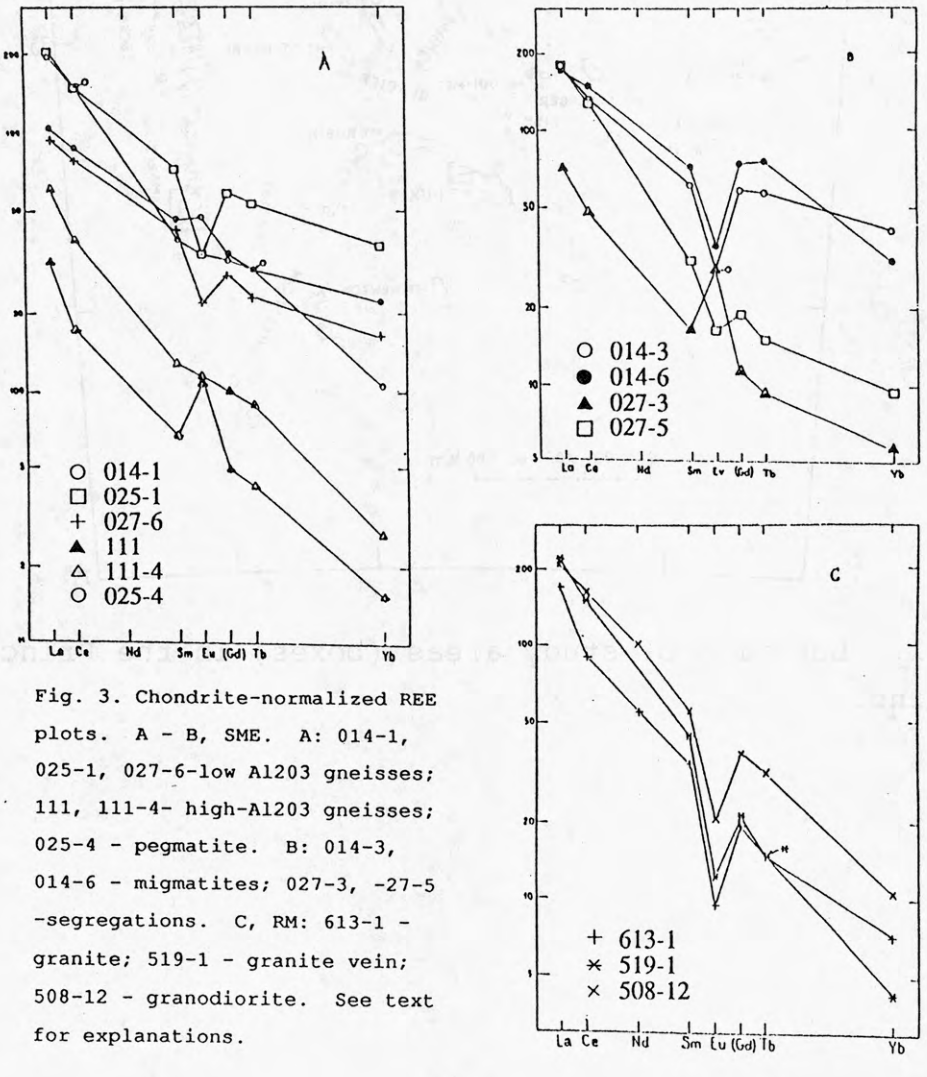

Fig. 3. Chondrite-normalized REE plots. A - B, SME. A: 014-1, 025-1, 027-6-low Al2O3 gneisses; 111, 111-4- high-Al2O3 gneisses; 025-4 - pegmatite. B: 014-3, 014-6 - migmatites; 027-3, -27-5 -segregations. C, RM: 613-1 - granite; 519-1 - granite vein; 508-12 - granodiorite. See text for explanations.

GEOCHEMICAL RECORDS OF PROVENANCE AND PALEOCLIMATE IN FINE-GRAINED PERMIAN CLASTIC ROCKS OF THE CENTRAL TRANSANTARCTIC MOUNTAINS

L.A. Krissek and T.C. Horner, Byrd Polar Research Center and Department of Geological Sciences, Ohio State University, Columbus, Ohio 43210, U.S.A.

The Beacon Supergroup in the central Transantarctic Mountains records the transition from a glacial regime (Pagoda Formation), through subaqueous fan/delta environments (Mackellar Formation), to fluvial environments (Fairchild Formation) with coals (Buckley Formation) during the Permian. Geographic and stratigraphic records of source lithologies and source area weathering regimes have been investigated using major element compositions of 100 samples from fine-grained facies within this sequence. Source lithologies are characterized by the Al_2O_3/TiO_2 ratio, which increases as the source becomes more silicic. Weathering intensity is characterized by the chemical index of alteration (CIA) of Nesbitt and Young (1982), which increases with increased chemical weathering.

Average Al_2O_3/TiO_2 ratios range from 17 to 27, indicating intermediate source area compositions (equivalent to diorite to granodiorite). Ratios in the Pagoda and Mackellar formations are generally lowest in the southern and southeastern portions of the study area, suggesting a greater influence of basic source rocks in those regions. Ratios consistently decrease upsection throughout the study area, recording an increase in volcaniclastic input that is readily observable in Buckley Formation sandstones.

CIA values generally increase upsection, reflecting the transition from glacial conditions dominated by physical weathering to more equitable conditions dominated by chemical weathering. This transition is also recorded by upsection changes in clay mineralogy. The style and exact stratigraphic position of this transition vary across the study area, however, suggesting local variability in weathering regimes.

Indicators of source lithologies, paleoclimate, and paleocurrents in the southernmost portion of the study area are consistently anomalous, perhaps reflecting the location of a connection between the Beardmore Glacier region and the elongate basin that existed along the paleo-Pacific margin of Gondwanaland during the Permian.

Reference: Nesbitt, H.W., and Young, G.M., 1982. Early Proterozoic climates and plate motions inferred from major element chemistry of lutites. Nature, 299: 715-717.

STRATIGRAPHY AND SEDIMENTOLOGY OF VERTEBRATE BONE-BEARING BEDS IN THE TRIASSIC (AND JURASSIC?) FREMOUW AND FALLA FORMATIONS, BEARDMORE GLACIER REGION, ANTARCTICA

L.A. Krissek, T.C. Horner, D.H. Elliot, and J.W. Collinson, Byrd Polar Research Center and Department of Geological Sciences, The Ohio State University, Columbus, Ohio 43210, U.S.A.

Vertebrate-bearing horizons are present in the Fremouw Formation, a lower to middle Triassic fluvial sequence in the central Transantarctic Mountains. During the 1990/91 field season, a bone-bearing horizon in the upper Fremouw Formation was examined at Gordon Valley, and an additional vertebrate locality was discovered and described at Mount Kirkpatrick in the upper Falla Formation, an upper Triassic (to lower Jurassic?) sequence of fluvial sediments and tuffs. The sedimentology of each locality was examined to determine environments of deposition and to evaluate the effects of transport/deposition on the vertebrate faunas.

The local stratigraphic section at the vertebrate site in the upper Fremouw Formation at Gordon Valley begins with a basal greenish-gray siltstone to sandy siltstone, which contains moderate amounts of root traces. The siltstone is overlain discontinuously by thin trough cross-stratified medium sands that fill laterally restricted, low-relief channels. A thin matrix-supported, siltstone-cobble conglomerate blankets both the discontinuous channel-form sands and the intervening siltstones; the basal contact of the conglomerate is sharp, slightly irregular, and shows no evidence of large-scale scouring. Clasts in the conglomerate are predominantly greenish-gray rounded siltstone, lithologically identical to the underlying siltstone. The conglomerate is overlain gradationally by a thick sequence of white, medium-grained, trough cross-stratified sandstone.

Vertebrate bones and wood are dispersed throughout the lower sandstones and the conglomerate, but are significantly more abundant in the latter lithology. Cross-bedding in the sands consistently indicates paleoflow to the northwest, in agreement with data from the rest of the Fremouw Formation. Elongate bones and wood within the conglomerate, however, exhibit a wide range of orientations. This sequence records minor channelling of an existing floodplain, followed by rapid deposition from a large flow of relatively high viscosity and moderate to low velocity (i.e., a relatively fluid debris flow). This large flow spread laterally from an unidentified major channel, blanketing the floodplain and its low-relief channels. "Normal" fluvial processes were re-established following this flood event. This interpretation suggests that fluvial discharge was variable during deposition of the upper Fremouw Formation, perhaps indicating a relatively arid climate. The abraded surfaces of the bones and their concentration within the conglomerate suggest that these bones were eroded from floodplain deposits further upstream and dispersed during transport.

The local stratigraphic section at the vertebrate site in the upper Falla Formation on Mount Kirkpatrick begins with a basal greenish gray coarse siltstone to fine-grained sandstone that contains root traces. This fine-grained interval is overlain by a clast-supported cobble conglomerate, which exhibits a lenticular form over the restricted scale of the outcrop. Clasts within the conglomerate are predominantly greenish gray mudstone; the remainder are angular pieces of parallel-laminated, fine-grained sandstone. The conglomerate is overlain gradationally by another root-bearing, light greenish gray mudstone to sandy siltstone. Sedimentary rocks throughout this section may contain an abundant volcanogenic component.

Vertebrate bones at the Mount Kirkpatrick site appear to be the relatively complete remains of at least one individual. Lateral relationships are not entirely clear, but the bones appear to be concentrated in a small area of the fine-grained facies that is just outside the conglomeratic lens and approximately 1.5 m thick. This sequence records deposition by a localized mass flow on a floodplain, followed by a return to "normal" floodplain deposition. The vertical distribution of bones suggests the effect of transport/mixing, but the spatial concentration of bones indicates that such processes were very limited. Several alternative depositional interpretations are under consideration: 1) whole carcasses were carried off the flank of the mass flow by a small, late-stage, clast-poor flow; 2) animals were trapped in liquified floodplain fines adjacent to the conglomerate soon after the mass flow occurred; and 3) bones were mixed vertically by taphonomic processes, perhaps including predation, after animals died on the floodplain.

FLUID INCLUSION STUDIES OF THE BORGMASSIVET SUITE, WESTERN DRONNING MAUD LAND, ANTARCTICA

J.R. Krynauw, Department of Geology, University of Natal, P.O. Box 375, Pietermaritzburg, 3200 South Africa.
H.-J. Behr, Institut für Geologie und Dynamik der Lithosphäre, Universität Göttingen, Goldschmidtstr 3, D3400 Göttingen, Germany.

The Borgmassivet Suite (BMS) of western Dronning Maud Land consists of ultramafic to intermediate dykes and sills, which intruded the Mid-Proterozoic Ritscherflya Supergroup, and basalts, andesitic basalts and pyroclastic deposits which form the uppermost Straumsnutane Formation of the Supergroup. The low-grade tectonic setting is probably an early- or pre-Gondwana extension of the Kaapvaal Province of southern Africa, referred to here as the Grunehogna Province (GSP - However, see Barton and Moyes, 1990). The Borgmassivet igneous event probably occurred during the mid- to late-Proterozoic, but Rb-Sr, Pb-Pb and Sm-Nd isotope data show a complex scatter of radiogenic ages between 850 to 1800 Ma, which has not been resolved (Moyes and Barton, 1990).

Krynauw *et al.* (1988, 1991) showed that some of the BMS sills intruded a wet, unconsolidated sedimentary environment, and that they have been subjected to various degrees of retrograde alteration. Possible origins of the alteration and problematic isotope data include:

a) contamination by crustal material;
b) extensive deuteric alteration owing to incorporation of juvenile water during intrusion;
c) hydrothermal alteration resulting from a circulating groundwater system initiated during intrusion; and
d) hydrothermal alteration during a later event, possibly related to GSP-directed thrusting within the high-grade H.U. Sverdrupfjella sub-Province.

This paper presents preliminary results of fluid inclusion and cathodoluminescence studies on quartz grains in selected BMS sills and Ritscherflya sedimentary rocks. Possible resolution of some of the problems mentioned above and the significance of these results towards a better understanding of the tectonic history of western Dronning Maud land are discussed.

REFERENCES

Barton, J.M., Jr., and Moyes, A.B. 1990. Cooling patterns in western Dronning Maud Land, Antarctica, and southeastern Africa and their implications to Gondwana. *Zbl. Geol. Paläont. Teil I*, H.1/2, 33-43.

Krynauw, J.R., Hunter, D.R., and Wilson, A.H. 1988. Emplacement of sills into wet sediments at Grunehogna, western Dronning Maud Land, Antarctica. *J. geol. Soc. Lond.*, 145, 1019-1032.

Krynauw, J.R., Watters, B.R., Hunter, D.R., and Wilson, A.H. 1991. A review of the field relations , petrology and geochemistry of the Borgmassivet intrusions in the Grunehogna Province, western Dronning Maud Land, Antarctica. In: Geological Evolution of Antarctica. Eds. M.R.A. Thomson, J.A. Crame, and J.W. Thomson. Cambridge University Press, Cambridge.

Moyes, A.B., and Barton., J.M., Jr. 1990. A review of isotopic data from western Dronning Maud Land, Antarctica. *Zbl. Geol. Paläont. Teil I*, H.1/2, 19-31.

CRUSTAL SECTION ACROSS THE WESTERN QUEEN MAUD LAND CONTINENTAL MARGIN FROM GEOPHYSICAL DATA
(poster presentation)

Kudryavtzev G.A., Butzenko V.V., Kadmina I.N.,
North Branch for Marine Geologic Research and Exploration "Sevmorgeologia", 120 Moyka, 190121 Leningrad, USSR

In accordance with Antarctic geotransect international program developed by SCAR GOSL, WGG and WGSEG, "Sevmorgeologia" accomplished in 1988-1990 a composite geophysical survey in the W-2,3 geotransect corridor across the NE Weddell Province (Fig.1). The survey included deep seismic sounding (DSS) sublongitudinal profile more than 300 km long accompanied by land gravity observations, reflection soundings and aeromagnetic measurements in western Queen Maud Land; the profile was supplemented by offshore gravity, magnetic and MCS recording. The preliminary results were incorporated in poster presentations at the 28 th IGC in Washington [Ivanov, 1989; Futterer, 1989].

Most observations were conducted using standart methods described elsewhere [Ivanov and Grikurov, 1987] However, for the DSS profile some new technologies had to be developed to ensure efficient energy sources in the continental ice sheet environment (Fig.2).

A direct continuation of DSS profile by marine observations was impossible because of ice conditions. The MCS data were obtained between middle slope and abyssal deep along approximately 200 km line (Fig.3). The remaining gap of about 60 km between the middle slope and outer shelf was filled in by projecting on the line of results of MCS earlier observations [Hinz and Krausze, 1982) and aerogeophysical data.

A composite interpretative crustal section is shown in Fig.4. Three crustal blocks are recognized across the western Queen Maud Land continental margin that correspond to (1) continental land and inner shelf, (2) outer shelf and upper slope, and (3) lower slope transitional to abyssal plain.

1. The continental crustal block has a uniform thickness in the range between 40 and 35 km; it is defined by a very gentle rise of the Moho discontinuity from inland towards ice shelf. An important feature of the upper crust is the presence of two distinct layers bounded by F,K1 and K2 refractors. We correlate F with the surface of Precambrian crystalline basement, K1 - with the base of the uppermost brrittle crustal layer, and K2 - with the Conrad boundary at the base of intermediate crust characterized by appreciable increase in density and, presumably, in ductility.

2. The next block is defined as subcontinental. The Moho rises sharply from 35 to 15 km b.s.l., while the sea bottom deepens in the same direction to 3000-4000 m b.s.l. Another

critical variation is observed in the upper crust where graduate decrease in thickness is accompanied by dramatic structural change represented by substitution of infracrustal basement by a lower density supracrustal sequence of great thickness presumably related to Gondwana breakup. 3. The third block shows suboceanic appearance defined by thin (5 -7 km) basement overlain by undisturbed sedimentary cover of moderate thickness (up to 2 km). Available evidence suggests the presence in the basement of abundant faults and related horsts and grabens probably associated with rifting and reworking of stretched continental crust.

REFERENCES:

Futterer, D., 1989. Crustal Transects from Weddell Sea to Dronning Maud Land, East Antarctica. 28 th IGC, Abstracts, v.1, Washington, p.519.

Hinz, K., Krause, W., 1982. The continental margin of Queen Maud Land, Antarctica: seismic sequences, structural elements and geological development. Geol. Jb.E., Bd.23, p.17-41.

Ivanov, V.L., 1989. Weddell Sea crustal transect, West Antarctica. Abstracts, v.2, 28 th IGC, Washington, p.103-104.

Ivanov, V.L., Grikurov, G.E. (eds.), 1987. The geological and geophysical research in Antarctica. Leningrad, "Sevmorgeologia", 153 p.p. (in Russian).

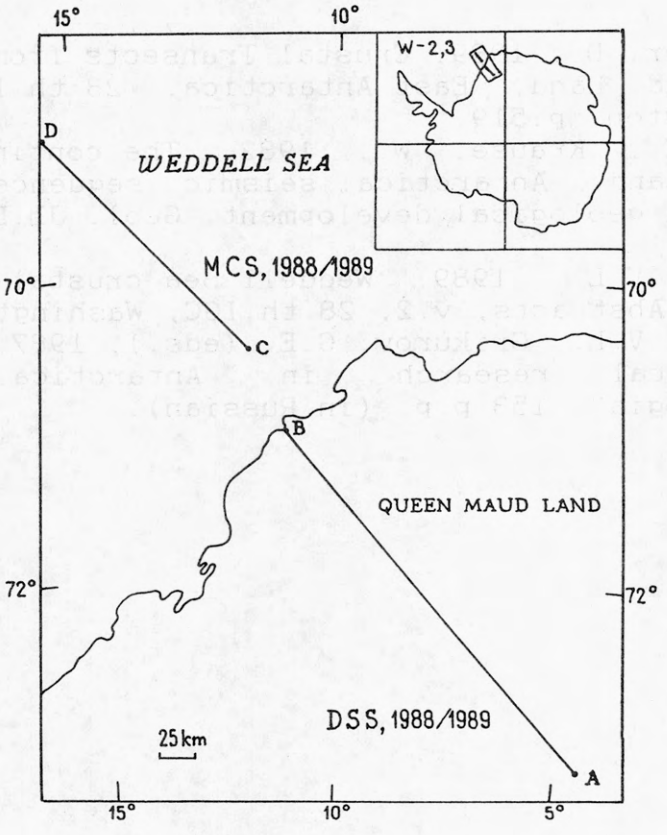

Fig.1. Location of deep seismic sounding profile (A–B) and multichannel seismic line (C–D) used to construct composite crustal section shown in Fig.4. Inset indicates approximate position of W – 2,3 geotransect corridor.

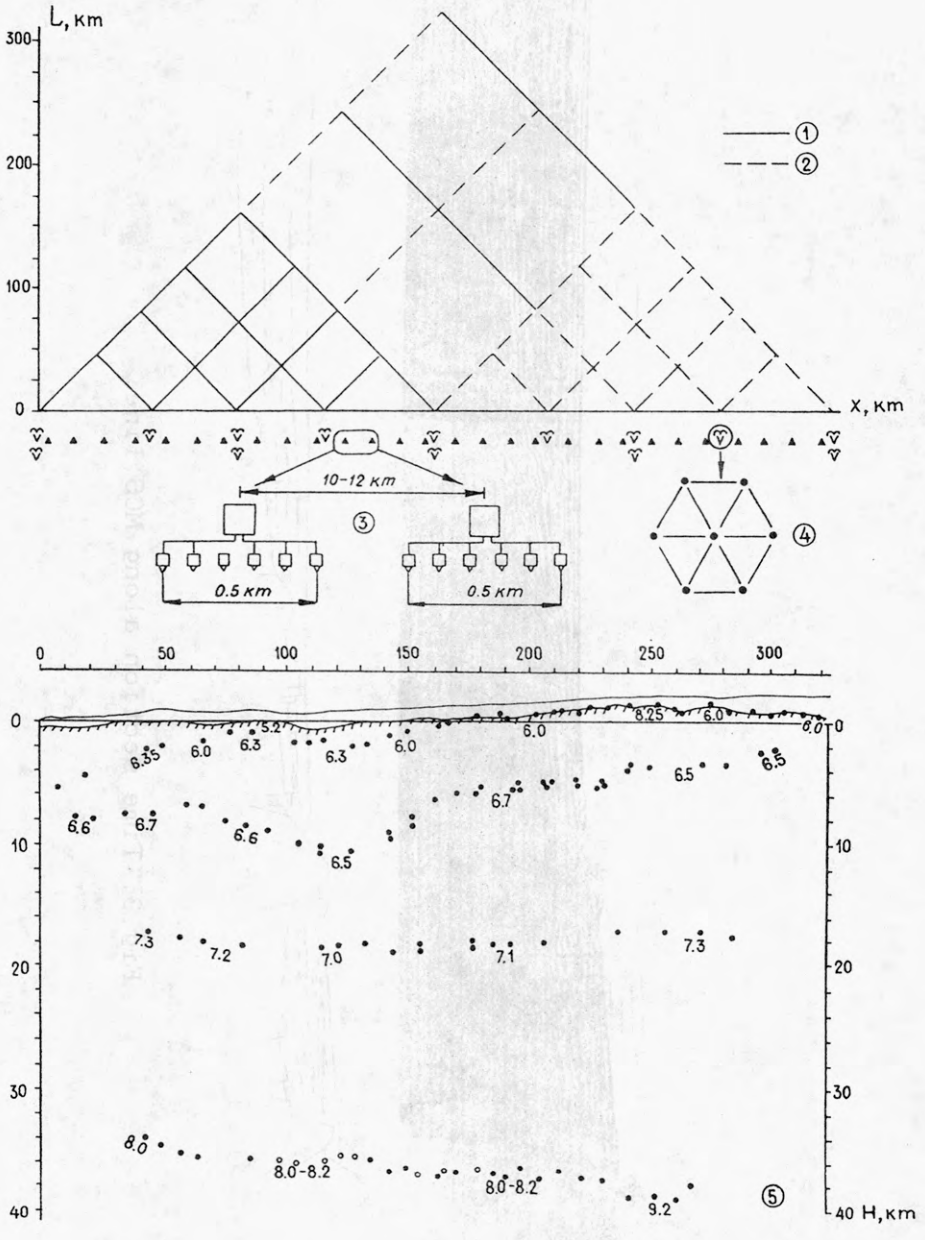

Fig.2. DSS arrays and processed section. Numbers in circles: 1 - first array; 2 - second array; 3 - arrangement of seismographs (telecontrolled from the aircraft) and geophones; 4 - arrangement of charges at shot sites: from 460 to 3570 kg of explosive at each site in seven holes drilled in snow cover; depth of holes from 6 to 15 m, respectively; 5 - seismic section: solid circles - depths from refraction data, open circles - depths from reflection data, figures - boundary velocities, km/s.

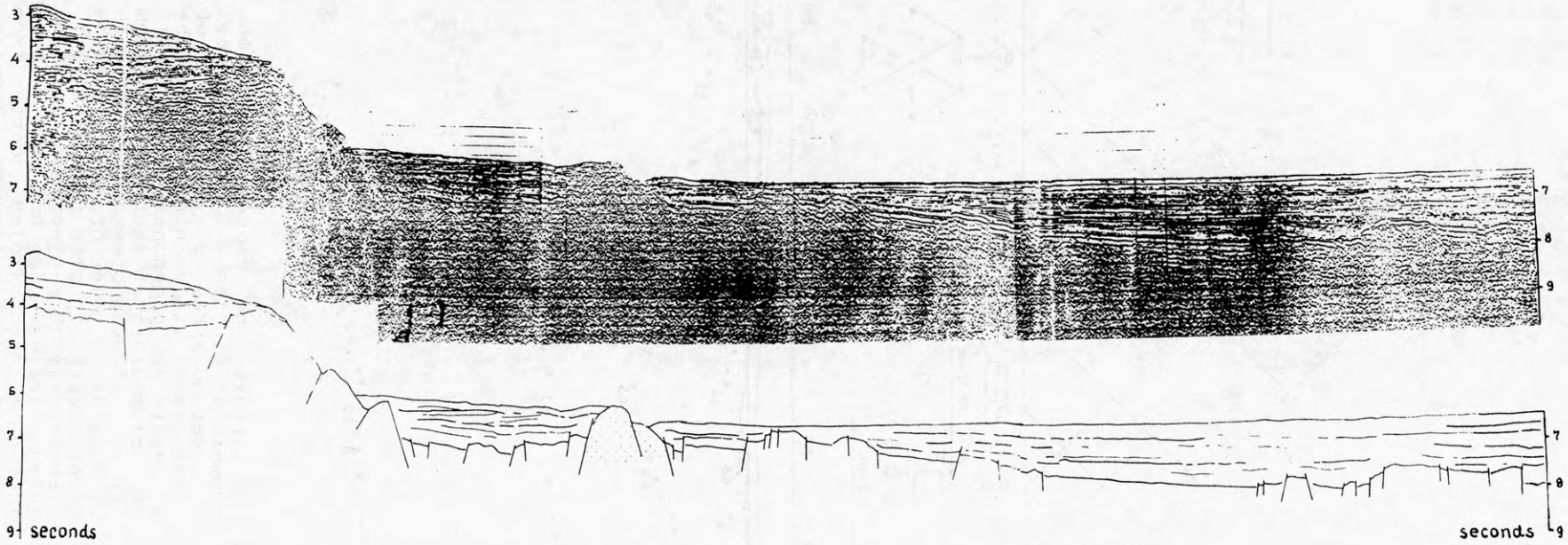

Fig.3. Time section along MCS line.

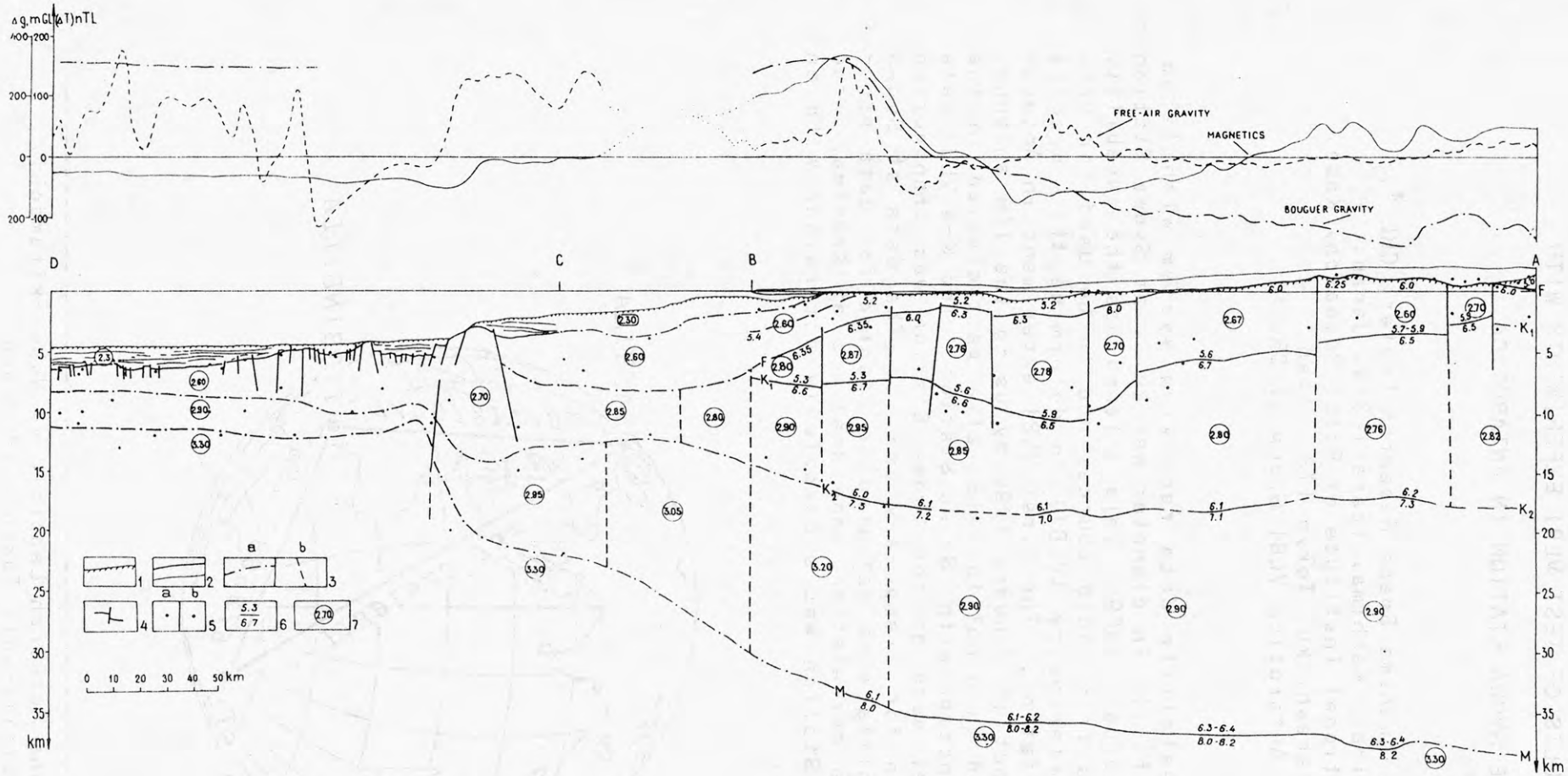

Fig.4. Composite crustal section in the Western Queen Maud Land continental margin. 1 – sea bottom and bedrock surface; 2 – seismic boundaries (thin lines – in sedimentary cover); 3 – boundaries calculated from density modelling (a – of crustal layers, b –of crustal blocks); 4 – faults displacing seismic boundaries; 5 – calculated position of magnetic bodies (a – top, b – base), 6 – seismic velocities, km/s: effective/boundary; 7 – density values, g/cm3 calculated from gravity data.

THE RESULTS OF TEST VLBI EXPERIMENTS WITH THE SYOWA STATION IN ANTARCTICA

N. Kurihara, Kashima Space Research Center, CRL *,
893-1 Hirai, Kashima, Ibaraki 314, Japan.
M. Ejiri, National Institute of Polar Research, Kaga,
Itabashi-ku, Tokyo 173, Japan.
and Antarctica VLBI Group of CRL.

A multipurpose satellite data receiving system with large parabolic antenna of 11m in diameter was built at Syowa Station in Antarctica in February 1989. This antenna has the capability to receive signals from radio sources and to be used for very long baseline interferometry (VLBI) to determine the precise position of Syowa Station. The first VLBI experiment in Antarctica was carried out in January 1990 by using the 11m antenna. Kashima, Japan and Tidbinbilla, Australia participated in the experiment in conjunction with Syowa Station. The K-4 VLBI data acquisition terminal used at the Syowa Station was transported from Kashima, Japan for temporary use. The data at Syowa Station and Tidbinbilla were gathered to Kashima for data processings. After data correlation and analysis at Kashima, the position of Syowa Station was successfully determined with an error of decimeters.

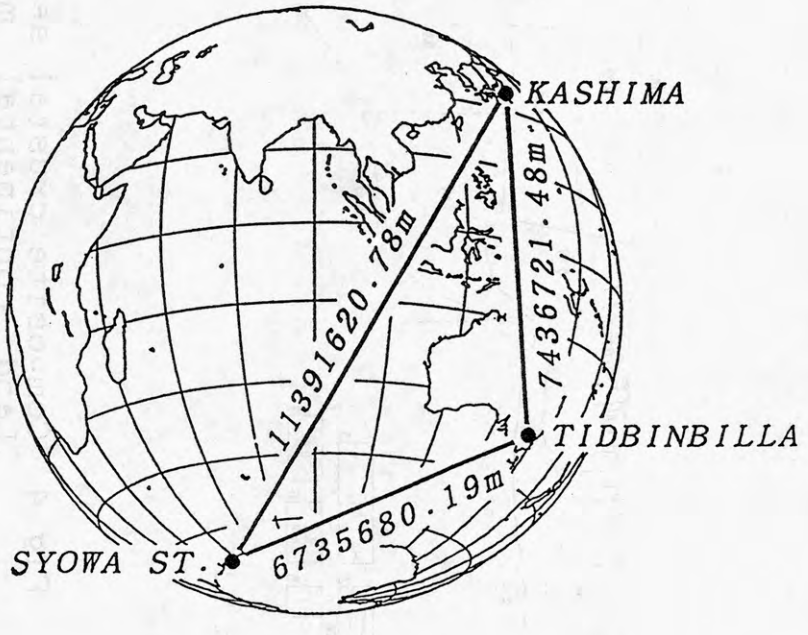

* Communications Research Laboratory, Nukui-kitamachi,
Koganei-shi, Tokyo, 184 Japan

IS VOLCANISM IN MARIE BYRD LAND RELATED TO A MANTLE PLUME?

Philip R. Kyle[1], William C. McIntosh[1], Kurt Panter[1], John Smellie[2]
[1]Dept. of Geoscience, New Mexico Institute of Mining
and Technology, Socorro, N.M. 87801 USA
[2] British Antarctic Survey, Cambridge CB3 OET, UK

LeMasurier and Rex (1989) first recognized that volcanism in Marie Byrd Land shows distinct radial patterns in the timing of felsic volcanism and elevation of prevolcanic basement surfaces. Published conventional K/Ar age determinations show that Mt. Petras (22-25 Ma) and USAS Escarpment (19-28 Ma) in central Marie Byrd Land are the oldest exposed eruptive centers. Ages of felsic volcanoes young progressively outward towards the four youngest volcanoes, Mt. Takahe (<0.5 Ma), Mt Waesche (<0.5 Ma), Mt Siple (<2 Ma) and Mt. Berlin (<0.1 Ma), which are located approximately 90 degrees apart along the outer edge of the volcanic province. Particularly well-defined younging trends have been recognized along the Executive Committee Range, Flood Range and Ames Range. New high-precision $^{40}Ar/^{39}Ar$ age determinations in progress (Panter et al., this meeting) are helping to refine the geochronology of migration of Marie Byrd Land volcanism. Where exposed, elevation of the prevolcanic erosion surface likewise shows a radial pattern. This erosion surface is highest beneath the oldest centers of volcanism, although interpretation of the data is somewhat complicated by recent observations of significant prevolcanic topographic relief at some localities (McIntosh et al., this volume).

LeMasurier and Rex (1989) suggested that radial patterns in Marie Byrd Land volcanism and basement topography may be related to a 550-600 km hotspot on the shoulder of a continental rift, but they do not expand on the concept. They interpret within-range age trends as consequences of propagating fractures related to tectonic doming.

We believe that Marie Byrd Land's radial volcanic and tectonic features are best explained by a model involving a single large stationary mantle plume beneath the also stationary Antarctic plate. The plume initially upwelled > 30 m.y. ago beneath the present site of Mount Petras and the USAS Escarpment, doming the Mesozoic and older basement rocks to elevations as high as 2700 m. Outward flow of the plume beneath the lithosphere may have been channelled by progressive underplating of the crust above the plume axis, resulting in the radial younging trend seen in Marie Byrd Land felsic volcanism.

The mantle plume model offers a unifying theory for Marie Byrd Land volcanism and tectonism and furthermore is attractive because it can be tested. The proposed geophysical investigations of the Antalith project could document sub-ice basement surface topography and search for subcrustal evidence of upwelling hot mantle beneath the region. Field observations and mapping of the basement could further constrain the extent of crustal doming. Finally, helium isotopes can provide distinct signatures for mantle plumes and would be an ideal method to verify the existence of upwelling deep mantle beneath Marie Byrd Land.

VOLCANIC EMISSION RATES FROM MOUNT EREBUS, ANTARCTICA

Philip R. Kyle[1], L. Sybeldon[1], G. Zreda-Gostynska[1], D. Finnegan[2], W. C. McIntosh[1]
[1]Department of Geoscience, New Mexico Institute of Mining and Technology, Socorro, N.M. 87801, USA
[2]Los Alamos National Laboratory, Los Alamos, N.M. 87545, USA

Mount Erebus on Ross Island is one of two active volcanoes in the southern Ross Sea. A persistent convecting lava lake of anorthoclase phonolite magma has been present in the crater since 1972.

SO_2 emission rates have been measured annually, usually in December and/or January, since 1983 by correlation spectrometer (COSPEC V). From 1984 to 1987 (inclusive) observations were made using a stationary hand-held scanning technique. Since 1988 measurements have been made using an automated scanner and computer data acquisition and analysis. The rise rate or wind speed of the plume is a necessary requirement to determine the SO_2 emission rate. We have used video observations to obtain high precision estimates of these parameters. The automated system has resulted in a significant increase in the number and quality of the observations allowing us to examine short term fluctuations in SO_2 emission rates and relate these to magma convection rates. The yearly average SO_2 emission rates were:

Month/Year	SO_2 Emission Rate Mg/day	Number of Scans	Lava Lake Area (m^2)
12/1983	230±90	27	2800
12/1984	25±10	41	200
12/1985	15±7	67	180
12/1986	20±11	244	300
12/1987	44±27	327	380
12/1988	27±9	777	240
12/1989	59±27	1405	630
1/1991	75±20	400	650

The SO_2 emission rate is proportional to the surface area of exposed magma in the crater.

Filter packs consisting of a 1-2 micron Teflon particulate filter followed by 2 to 4 filters treated with ^{7}LiOH or tetrabutyl ammonium hydroxide have been used to examine the nature and composition of particulate and acid gas aerosols. Using element/sulfur ratios measured on the filters and the COSPEC SO_2 emission rates, estimates have been made of emission rates for over 25 elements. Filters collected in 1986 (Kyle et al., 1990) had Cl/S = 10 and F/S = 5; however filters collected in 1988, 1989 and 1991 show Cl/S = 1-2 and F/S = 1. The reason for the differences are not known at this time but may be analytical. The implied emission rates of F and Cl are therefore lower than those given by Kyle et al., (1990) and are in the range of 30-40 and 60-80 Mg/day, respectively.

Mount Erebus is a major and significant source of aerosols to the troposphere in the southern Ross Sea area. The residence time and dispersal of these aerosols are poorly known at this time, but it is possible that Erebus may be a source of inorganic HCl found in snow and ice cores from East Antarctica.

MAGNETIC ANOMALY MAP FOR THE CIRCUM-ANTARCTIC BASINS

John L. LaBrecque, Lamont-Doherty Geological Observatory,
Palisades, New York 10964
John Brozena, U.S. Naval Research Laboratory, Washington, D.C.
Juan Carlos Parra, Servicio Nacional de Geologia y Mineria
Santiago de Chile
Marcelo Keller, Instituto Antartico Argentino,
Buenos Aires, Argentina
Carol Raymond, Jet Propulsion Lab, California Inst. of Tech.
Pasadena, CA 91109
Gonzalo Yanez, Lamont-Doherty Geological Observatory,
Palisades, New York 10964

We present a magnetic anomaly map for the basins surrounding the Antarctic Peninsula which incorporates all available magnetic anomaly data sets including marine data, the USAC aerosurvey, and the Chilean aerosurvey. The data base clearly displays anomalies associated with fracture zone and continental margin structure as well as the seafloor spreading anomalies of the Weddell, Bellingshausen and Scotia Basins. The continental margin anomalies have been used to examine the reconstruction of Antarctica with respect to New Zealand and South America.

BATHYMETRY, DEPTH TO MAGNETIC BASEMENT, AND SEDIMENT THICKNESS ESTIMATES FROM AEROGEOPHYSICAL DATA OVER THE WESTERN WEDDELL

John L. LaBrecque, Lamont-Doherty Geological Observatory
Palisades, N.Y. 10964

and

Marta E. Ghidella, Instituto Antartico Argentino
Buenos Aires, Argentina

The USAC aerogeophysical survey (U.S., Argentina, Chile), has devoted 53 flights to collect magnetic and gravity data over the basins surrounding the Antarctic Peninsula. Thirty-six of these flights were used to calculate bathymetry and depth to magnetic basement estimates for the western Weddell. Both wavenumber and space domain techniques along individual profiles were applied in an automated fashion to obtain depth to magnetic basement estimates. The bathymetric estimates were obtained by gravity admittance inversions. The results were then gridded for the region 60°W, 44°W, 73°S, and 62°S. Bathymetric estimates and depth to magnetic basement layer estimates were differenced at each grid point to obtain a regional estimate of the sediment layer thickness. Contour maps show the following features: the magnetic basement gets gradually deeper from the Antarctic Peninsula margin to the East with increasing slope, until a north-south band is reached where the estimated sediment layer is very thick (10 km) around meridian 54°W. Further eastward, the basement steps upwards, with the corresponding thinning of the sediment layer. Along the east coast of the Peninsula, results agree well with seismic studies on James Ross Island, magnetotelluric studies on Marambio Island and the Larsen nunatak, as well as the British Antarctic Survey estimates from aeromagnetic data.

THE DEPOSITIONAL PATTERN AND DISTRIBUTION OF GLACIAL-INTERGLACIAL SEQUENCES ON THE ANTARCTIC PENINSULA PACIFIC MARGIN

R.D. Larter and A.P. Cunningham
British Antarctic Survey, Natural Environment Research Council,
High Cross, Madingley Road, Cambridge CB3 0ET, U.K.

Previous investigation of the Antarctic Peninsula Pacific margin using multichannel seismic reflection data revealed a series of oblique progradational sequences of Pliocene-Pleistocene age. On individual multichannel seismic profiles across the margin these sequences exhibit a variety of unusual characteristics interpreted to indicate that they were produced mainly by the action of ice sheets grounded out to the shelf edge at times of glacial maximum. The grounded ice sheet model implies supply of sediment to the continental margin from a line source, in contrast to the point sources which characterise lowstand deposits on low-latitude margins. Thus, one of the most important distinguishing characteristics of depositional sequences produced by grounded ice sheets is predicted to be their three-dimensional external form.

The available multichannel seismic reflection data on one part of the Antarctic Peninsula Pacific margin allow a crude description of the three-dimensional form of depositional sequences. Age constraints obtained by following sequence boundaries into sediments overlying young oceanic basement near the margin indicate that rapid progradation of the shelf in this area began no earlier than latest Miocene. Isopachyte maps show that the prograded sequences have very elongate depocentres on the upper palaeoslope. Two-way time and crude depth maps of selected sequence boundaries illustrate the broad oceanward advance and steepening of the continental slope. This depositional pattern is consistent with the hypothesis that sediment was supplied from a line source. However, each depositional sequence recognised on the multichannel seismic profiles may represent several ice sheet advances, so the possibility that the observed depositional pattern has been produced by depocentre switching or migration cannot be discounted at this stage. A planned high resolution seismic survey may reveal a more detailed stratigraphy.

Seismic profiles on the continental rise show an abrupt change in seismic facies which is interpreted to correlate with the start of glacial progradation on the shelf. Earlier rise sediments appear to constitute a broad slope-front fill whereas later sedimentation has been dominated by large channel-levee systems. A similar change in seismic facies has been reported in continental rise sediments off East Antarctica, and has been interpreted to correlate with the Oligocene onset of glacial progradation of the East Antarctic shelf. The difference in age of this facies change off East Antarctica and off the Antarctic Peninsula is consistent with other evidence which suggests development of the ice sheet on the Antarctic Peninsula lagged behind that of the East Antarctic Ice Sheet.

PETROGRAPHIC COMPARISON OF PALEOZOIC ROCKS FROM THE ENGLISH COAST, EASTERN ELLSWORTH LAND AND THE ELLSWORTH MOUNTAINS

T.S. Laudon, The University of Wisconsin Oshkosh
Oshkosh, Wisconsin 54901, U.S.A.
Campbell Craddock, The University of Wisconsin Madison
Madison, Wisconsin 53706, U.S.A.

The English Coast of eastern Ellsworth Land is the location of the southwesternmost exposures of the Antarctic Peninsula Tectonic Province (**APTP**). FitzGerald quartzite beds of unknown pre-Cretaceous age, and Glossopteris bearing Erehwon beds of Upper(?) Permian age, are previously unknown units that were discovered during exploration of the English Coast in 1985. Stratigraphic linkages of FitzGerald quartzite beds with the lower Paleozoic Crashsite Quartzite Group of the Ellsworth Mountains (**EM**), and of Erehwon beds with the Middle-and-Upper Permian Polarstar Formation of the **EM** have been suggested.

FitzGerald quartzite beds consist of cross bedded, cross laminated, gray-green, vitreous, quartz-mica hornfels. Photomicrographs of thin sections of FitzGerald quartzite beds and of similar quartzite from the Crashsite Group reveal that they are petrologically nearly identical, with granoblastic polygonal frameworks consisting of <90% quartz. Protoliths were quartz-wackes with frameworks composed of well sorted, well rounded, medium sand sized quartz grains, accessory lithic clasts, and no sand-sized feldspar. Both units are of continental interior provenance.

Erehwon beds are composed of dark colored mudstone, siltstone, and fine grained sandstone. Photomicrographs of thin sections of sandstone from Erehwon beds and from the Polarstar Formation are strikingly similar. Sandstones from both units are characterized by textural and compositional immaturity. Textural characteristics include poor sorting, and extreme angularity of sand sized clasts. Both units contain abundant detrital feldspar and volcanic rock fragments. Their average modal compositions are almost identical. Sandstones from both units are lithic arenites and wackes of magmatic arc provenance.

FitzGerald quartzite beds were deposited in a passive margin environment that predated the onset of subduction of the paleo-Pacific margin of Antarctica (**PPM**). They are known from only a single locality, but reported occurences of quartzite pebbles in Mesozoic conglomerates indicate that similar rocks are widespread in pre-Mesozoic basement of the southern **APTP**. Erehwon beds are of magmatic arc provenance and indicate that subduction related vulcanism of the **PPM** began in the southern **APTP** by Permian.

Stratigraphic linkages of FitzGerald quartzite beds with the Crashsite Quartzite Group, and of Erehwon beds with the Polarstar Formation, although highly speculative because of sparse evidence, are consistent with models of the **PPM** characterized by lower Paleozoic passive margin sedimentation followed by subduction beginning in late Paleozoic.

CONSTRAINTS ON MESOZOIC TRANSTENSION IN ANTARCTICA

L.A. Lawver and L.M. Gahagan, Institute for Geophysics, University of Texas at Austin, 8701 Mopac Boulevard, Austin, Texas 78759-8345, USA.

Reconstructions of the Mesozoic positions of the major plates of Gondwana provide constraints on the later stretching between East and West Gondwana. The early stretching phase of breakup extended along the Transantarctic margin of East Antarctica and provided the mechanism for the intrusives of the Ferrar and Beacon Supergroups. The Mesozoic breakup of Gondwana may have started with extension between Madagascar and Africa during Late Permian to Early Triassic time as evidenced by a marine incursion in that area. Actual seafloor spreading between East and West Gondwana did not begin until Late Middle Jurassic or later. From the pre-Mesozoic tight fit reconstruction, Gondwana must have undergone stretching during Early Jurassic so that Madagascar could move away from Africa. This is required so that the second phase of breakup which included seafloor spreading in the Somali Basin would not produce an overlap between Madagascar and Africa/East Antarctica. First phase stretching is also required on the Early Mesozoic Mozambique Plateau and the West Coast of the Dronning Maude Land region of East Antarctica in order to explain the truncated seaward dipping reflectors found there. An additional problem of the tight fit reconstruction of Gondwana has always been the overlap of the North New Zealand block with the stretched continental margin of the Campbell Plateau. In previous reconstructions, the overlap has resulted from the assumption that the North New Zealand block was rigidly attached to the "continental" Lord Howe Rise that was in turn part of the Australian block. If instead, it is assumed that there was Jurassic stretching between North New Zealand and the Lord Howe Rise then the overlap disappears. The same pole of rotation that solves the overlap problem of Madagascar with respect to Africa, as well as the Explora Wedge/Mozambique Ridge formation, also solves the North New Zealand/Lord Howe Rise/Campbell Plateau overlap problem. Therefore we propose that the first phase of Mesozoic Gondwana breakup involved stretching between West Gondwana which consisted of Africa, South America, the pieces of West Antarctica, Marie Byrd Land, the Campbell Plateau and North New Zealand, and East Gondwana which included at least Madagascar, India, Sri Lanka, East Antarctica, Australia and the Lord Howe Rise. Figure 1 shows the transantarctic margin of the East Antarctic craton as a zone of translation between East and West Gondwana. Our reconstructions suggest that during the Middle Jurassic, there may have been as much as 400 km of translation and pull-apart basin formation between East and West Gondwana along the Transantarctic margin (Figure 1) and less than 300 km of extension (Figure 2). The nearly linear occurence of the Ferrar dolerites and their extrusive and felsic equivalents along the Transantarctic Mountain range may not be due merely to exposure along a Cenozoic uplift but rather, may reflect a relatively narrow zone of Mesozoic transtension.

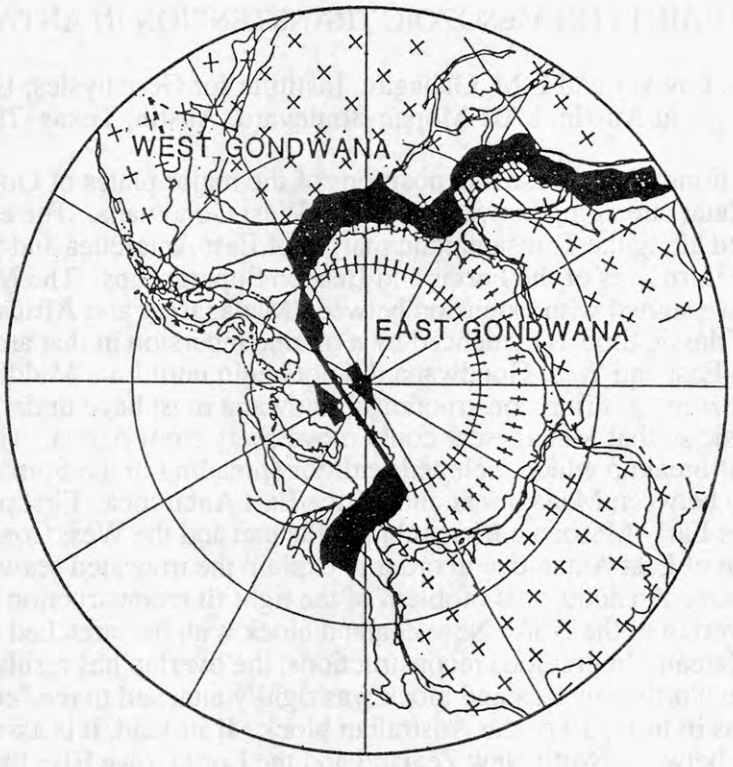

Figure 1. Maximum stretching phase (240 - 160 Ma) translation along the Transantarctic margin was less than 400 km. The right lateral translation moved Madagascar away from its tight-fit position with Africa and may have produced extension in the western Ross Sea and off the present-day west coast of New Zealand.

Figure 2. Maximum stretching phase extension along the Transantarctic margin was less than 300 km. The stretching phase extension translated Madagascar with respect to India and may have produced extension at the Lord Howe Rise along the eastern margin of Australia.

HEAT FLOW MEASUREMENTS IN THE KING GEORGE BASIN, BRANSFIELD STRAIT

L.A. Lawver and S. Nagihara, Institute for Geophysics,University of Texas at Austin, 8701 Mopac Boulevard, Austin, Texas 78759-8345, USA.

We collected 54 heat flow measurements in the King George Basin of Bransfield Straits which indicate that the area is tectonically active. Our new heat flow instrument, with three outrigger-bows, each 1.5 meters in length and 6.4 mm in diameter, spirally mounted on a 5-meter-long strength member, was used for the first time on this cruise. Each outrigger-bow sensor string contained four equally spaced thermistors and a heater wire which used the pulse-heating method to measure *in situ* thermal conductivity at 22 of the sites. Thermal conductivity measurements on six piston cores were made on board using the needle-probe technique. The objective of *R/V Polar Duke* cruise PD IV-89 was to investigate the tectonic history of the basin and the presumed occurrence of hydrothermal activity. In conjunction with the heat-flow survey, seismic surveys were made with a 3.5 kHz echo sounder and a single-channel seismic reflection system which used a 100-cubic-inch water gun. The seafloor of the King George Basin is flat (1,960-1,990 m) and well sedimented. The flat part of the basin is roughly 10 to 18 km by 45 km which we partially covered with a 1 to 2 km station spacing. The measured heat flow values range from ~50 to >600 mW m^{-2}, are generally high, and show significant variation. A quarter of the values are greater than 220 mW m^{-2}. The highest values are in the central part of the basin and along the southeast and northeast edges of the basin. In contrast, the values in the west and northwest parts of the basin are generally less than 100 mW m^{-2}. The highest value was measured in the central southeast part of the basin. In our attempt to duplicate the highest value, we took five measurements within a few hundred meters of the original high value. These measurements show a large variation from 150 to 250 mW m^{-2} in a small area, typical of regions with active hydrothermal circulation. A second high value (370 mW m^{-2}) was measured on the northeast edge of the basin in an area where the 3.5 kHz data indicate that there are mounds of a few meters height and up to a kilometer in width.

In February, 1991, *R/V Ewing* ran two lines across the flat part of the King George Basin and collected MCS, magnetics, and Hydrosweep data. The 3.5 kHz, GPS-navigated *R/V Polar Duke* data agree remarkably well with the Hydrosweep data and the datasets have been combined in a new bathymetric chart of Bransfield Strait. The bathymetric data reveal a very narrow, very linear line of submarine volcanic features that are roughly parallel to the South Shetland Islands and are only a few km at most from the base of the South Shetland Islands scarp. The volcanic features range from small mounds a few meters high, found on the 3.5 kHz data to two large subsea volcanoes about 10 km in diameter, one to the southwest and the other to the northeast of the flat part of the King George Basin. On the two Hydrosweep lines, one shows a 25 m high circular mound that is 500 m or less in diameter. The other line has a 280 m high ridge that is at least 2 km long and defines the volcanic trend.

The highest heat flow value measured is 8.5 km to the southeast of the linear volcanic trend. The second highest value was on the trend in the northeast part of the basin. The near channel monitor record of the MCS data does indicate an anomalous sub-seafloor feature on line with the highest heat flow value. Unfortunately, ice conditions prevented heat flow measurements in the southwest region of the basin where the majority of the mounds were found. The lower west and northwest heat flow values noted above, support the idea that active hydrothermal circulation depletes the normal convective heat transfer near the linear volcanic line. All evidence indicates that the active volcanic line is extremely asymmetric and off-axis even with the flat part of the King George Basin which is much closer to the South Shetland Islands than it is to the Antarctic Peninsula. The heat flow data with the MCS data suggest a central to northern Gulf of California type of extension rather than a back-arc basin type of extension.

STRUCTURE, SEISMIC STRATIGRAPHY AND EVOLUTION OF THE PRYDZ BAY

G.L. Leitchenkov, North Branch for Marine Geologic Research and Exploration "Sevmorgeologia", 120 Moyka, 190121 Leningrad, USSR

Geophysical surveys by Australian and Japanese expeditions in the Prydz Bay (PB) and adjacent slope of the Cooperation Sea [Stagg et al., 1982; Mizukoshi et al., 1986] were supplemented in 1985-1988 by the Soviet marine geophysical research (Fig.1). It included 7700 km of MCS profiling accompanied by gravity (Fig.2) and magnetic (Fig.3) observations and sonobuoy measurements at 19 sites. In addition to the hydromagnetic survey, the coastal part and eastern PB shelf have been covered by aeromagnetic observations with line spacing ranging between 5 and 20 km; the results of this airborne survey are also incorporated in Fig.3.

Seismic techniques and preliminary interpretation of the collected data have been previously published [Leitchenkov et al., 1990]. In this paper we present more advanced geological results based on ODP data and implementation of better processing procedures.

Stagg et al. (1982) recognized 5 pre-Quaternary seismic units of the cover (PS.1-5) and acoustic basement (PS.6). Cooper et al. (in press) used HRS data to correlate these units along the ODP line and additionally subdivided unit PS.2. We extrapolate these results over the whole PB sedimentary basin (Fig.4-6).

ACOUSTIC BASEMENT. The major structural feature on the PB shelf is a broad NE-trending graben which represents a seaward continuation of the Lambert-Amery continental rift zone. On its south-eastern flank the basement is exposed at the sea floor along the Princess Elizabeth Land (PEL) coast from where it deepens to about 1.5 s below the sea floor (b.s.f.) and then sharply drops towards the graben axis (Fig.4, lines 32009, 32002) where its depth reaches, according to refraction and magnetic data, 9 - 10 km (Fig.5). Towards the shelf edge and slope, the PB graben is defined mainly by a gravity low (Fig.2) and series of elongated magnetic anomalies (Fig.3) terminating over a bathymetric channel in the lower slope.

In the NW, the graben is bounded by a prominent basement high underlying the central PB. Its surface descends to the NE from 0 - 0.2 s in the inner shelf to 1.5 s towards the outer shelf where it is downfaulted by a series of latitudinal listric steps to 2.5 s and more (Fig.4, line 32006, Fig.5). The basement surface is characterized by distinct reflections and gently undulating topography (fig.4, lines 31001, 32006), except in the southern part where it is broken by numerous faults (Fig.4, line 32007).

In the NW, the central high is downfaulted from 1.5-2.0 s b.s.f. depths to 3.5-4.0 s (7-8 km). This marginal half-graben presumably cuts across the PB graben on continental slope (Fig.6). Its position is also well defined by gravity and magnetic data (Figs. 2, 3).

We believe that the SE flank of the PB graben is built of the ancient complexes continuous with the East Antarctic

shield terrain. Sublatitudinal magnetic fabric of this terrain is traced beneath the PB graben to the southern part of central basement high that may also consist of the Precambrian crystalline rocks. Such interpretation is consistent with measured boundary velocity 6.0-6.2 km/s (Fig.5) and does not exclude the presence of younger igneous rocks suggested by Cooper et al. (in press) on the basis of local magnetic anomalies. Some indications of igneous activities in the cover are also found in seismic records (Fig.4, line 31001, left). Judging by configuration of magnetic anomalies accompanied by relative gravity highs, in graben structures, magmatic activity was an important component in rifting process.

SEDIMENTARY COVER. We recognized four regional cover units: PS.5, PS.4, PS.2B and PS.2A (Fig.4). the boundaries of these units correspond to major unconformities defined by Cooper et al. (in press), although we do not agree with their interpretation of unit PS.5 as Precambrian metamorphic basement.

In our view, unit PS.5 constitutes a very considerable part of the PB graben fill where its thickness reaches 2.0-2.5 s (5-6 km), despite sea-floor exposures of that unit on steep basement slopes bounding the graben from where its top deepens inward at 3° - 5° (from NW side) and 7° - 9° (from SE); along the PB graben, the surface of unit PS.5 descends to the NNE at about 1° (Fig.5). The top of unit PS.5 is generally smooth and defined by distinct high amplitude reflections. Internal bedding of PS.5 is obscure, and the seismic velocities are in the range 3.5 - 4.5 km/s.

The age of unit PS.5 is defined by the following considerations. In the PB sedimentary basin seismic section it underlies the oldest of drilled sequences - unit PS.4 assigned by Cooper et al.(in press) to late Paleozoic-early Mesozoic interval. A great thickness of unit PS.5 and its seismic characteristics are comparable to acoustic and density values measured on reliably dated specimens of thick Permian sediments of the Amery Group in the Beaver Lake area (4.5-5.0 km/s and 2.45-2.47 g/cm^3, respectively). Therefore we conclude that unit PS.5 is probably of a Permian age. Beginning in late Paleozoic time, rift-related processes are confirmed by the presence in the area of deep-seated magmatic rocks of that age (Mikhalsky and Andronikov, this volume).

Unit PS.4 is reliably recorded in seismic sections not only in the PB graben, but also in listric-bounded basement tilts on the central high (Fig.4, line 32006). Its top is represented by a distinct reflector that is conformable to internal bedding of the unit on the PEL side of the PB graben (Fig.4, lines 32009, 32002) but on the opposite side of the PB graben the top forms a flat-lying angular unconformity. The seismic indications of the presence of unit PS.4 in marginal half-graben are obscure (Fig.4, line 31001, left).

The thickness of unit PS.4 in the PB graben (1.5-2.0 s or 3-4 km) suggests that its formation was related to a renewed trough sedimentation. The upper age limit of the unit is constrained by its stratigraphic position below the paleontologically dated lower Cretaceous unit PS.2B in ODP hole 741. Therefore we conclude that the most likely age of unit PS.4 is Jurassic, and that its accumulation was associated with early rifting in the Southern Indian Ocean

directly preceding Gondwana breakup. If this assumption is correct, then unit PS.4 must constitute a major component in the sedimentary fill of marginal half-graben. Seismic stratigraphy of unit PS.4 suggests that the central high must have been an important source area for Jurassic trough sedimentation.

Unit PS.2B occurs extensively throughout the entire PB sedimentary basin and wedges out against underlying units only in the southermost central high and near the PEL coast. Northward it is overlapped by glacial-marine cover of unit PS. 2A (fig.5,6). The thickness of unit PS.2B increases towards the outer shelf to 1.2-1.5 s (2.5 km) and is almost not controlled by the shape of the PB basement graben (Fig.4, line 31001, right), although unit PS.2B seems to thicken more rapidly in the marginal half-graben (Fig.4, line 31001, left). The character of thickness changes of unit PS.2B is clearly reflected in its internal seismic structure.

The lower Cretaceous (Albian) age and fluvial origin of unit PS.2B are directly determined by drilling (Cooper et al., in press). Apparently, formation of that unit reflected slow subsidence on an evolving continental margin with predominantly terrestrial paleoenvironment in place of the present inner shelf and shallow marine sedimentation in more distant offshore areas. More vigerous delta conditions were probably responsible for PS.2B accumulation in the marginal half-graben.

The unconformity at the top of unit PS.2B corresponds to sedimentation hiatus during late Cretaceous and early Paleogene time. The uppermost unit PS.2A constitutes a thin uniform cover (0.25-0.4 s) in the central PB shelf from where it thickens dramatically (to more than 2 s, or 2.5 km) into prominent prograding sequences extending seaward for more than 40 km (on east) - 60 km (on west) in the vicinity of PB shelf break (Fig.5). Structural and paleoenvironmental features of unit PS.2A are described elsewhere (Cooper et al., in press).

REFERENCES:

Cooper A.K., Stagg H.M.J., Geist E., in press. Seismic stratigraphy and structure of Prydz Bay, Antarctica : Implications from ODP Leg 119 drilling: In Barron, I., Larsen B., eds., Scientific results of ODP Leg 119 drilling, volume B: College Station, TX, Ocean Drilling Program, 57 p.

Leitchenkov G.L., Shelestov F.A., Gandjuhin V.P., Butsenko V.V., 1990. Outline of structure and evolution of the Cooperation Sea Sedimentary Basin: In Cooper A.K. and Webb P.N., conveners, International Workshop on Antarctic Offshore Seismic stratigraphy (ANTOSTRAT):Overview and Extended Abstracts: U.S. Geological Survey Open-File Report 90-309, p.202 -211.

Mikhalsky E.V., Andronikov A.V. and Beliatsky B.V. (this volume). Mafic and ultramafic igneous suites in the Lambert-Amery Rift Zone.

Mizukoshi I., Sunouchi H., Saki T., Sato S., Tanahashi M., 1986. Preliminary report of geological and geophysical surveys off Amery Ice Shelf, East Antarctica. Mem. Nation Inst. Polar Res., Spec. Issue 43, p.48-61.

Stagg H.M.J., Ramsay D.C., Whitworth R., 1983. Preliminary report of marine geophysical survey between Davis and Mawson Stations. In Oliver R.L., James P.R., Jago J.B., eds. Antarctic Earth Science. Canberra, Austral. Acad. Sci., p.527-532.

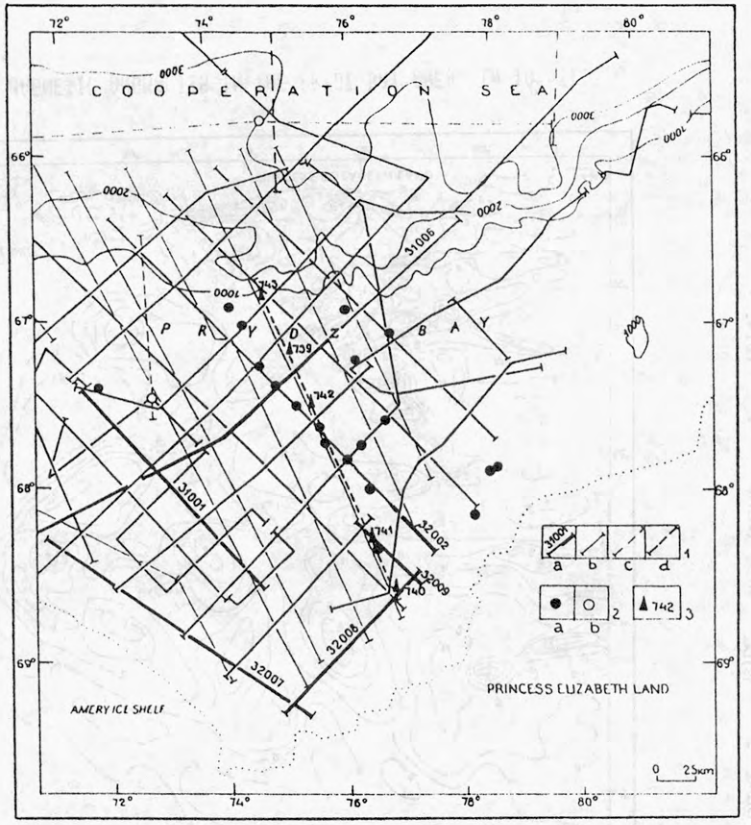

Fig.1. LOCATION MAP OF SEISMIC INVESTIGATIONS IN THE PRYDZ BAY. 1 - seismic lines: MCS - USSR (a), Australia (b) and Japan (c); HRS -USA (d); 2-sonobuoys: USSR (a), Japan (b); 3 - ODP holes. Heavier lines indicate profile shown in Fig.4.

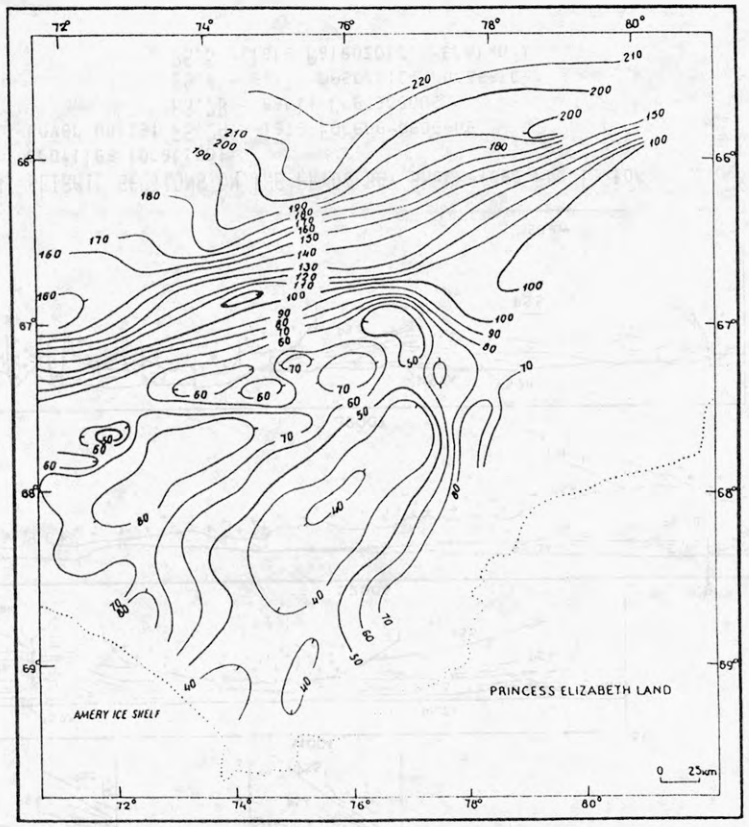

Fig.2. BOUGUER GRAVITY ANOMALIES IN THE PRYDZ BAY, in mGal.

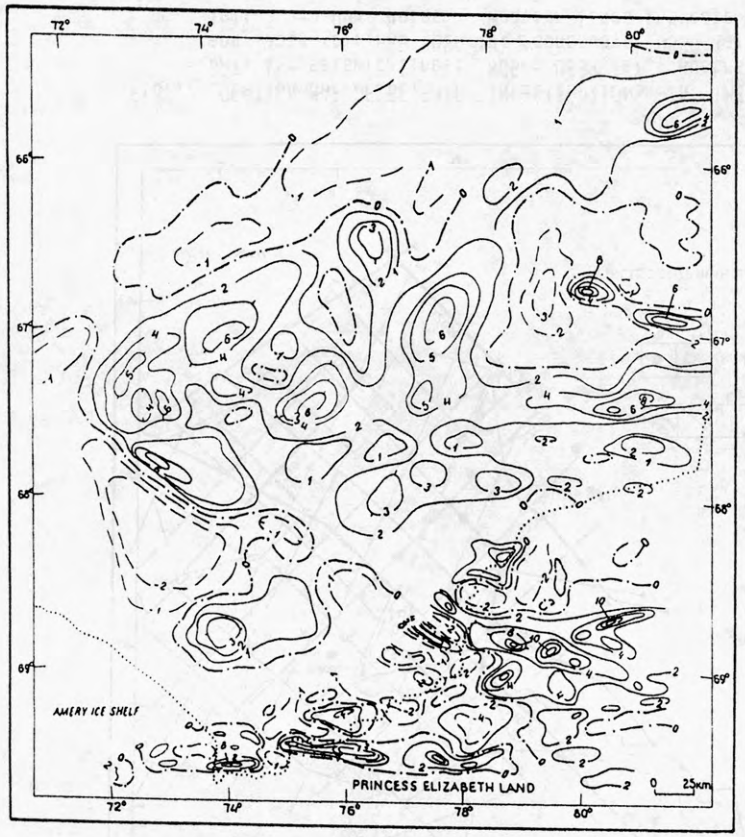

Fig.3. MAGNETIC ANOMALIES IN THE PRYDZ BAY AREA, in 10^2nTl.

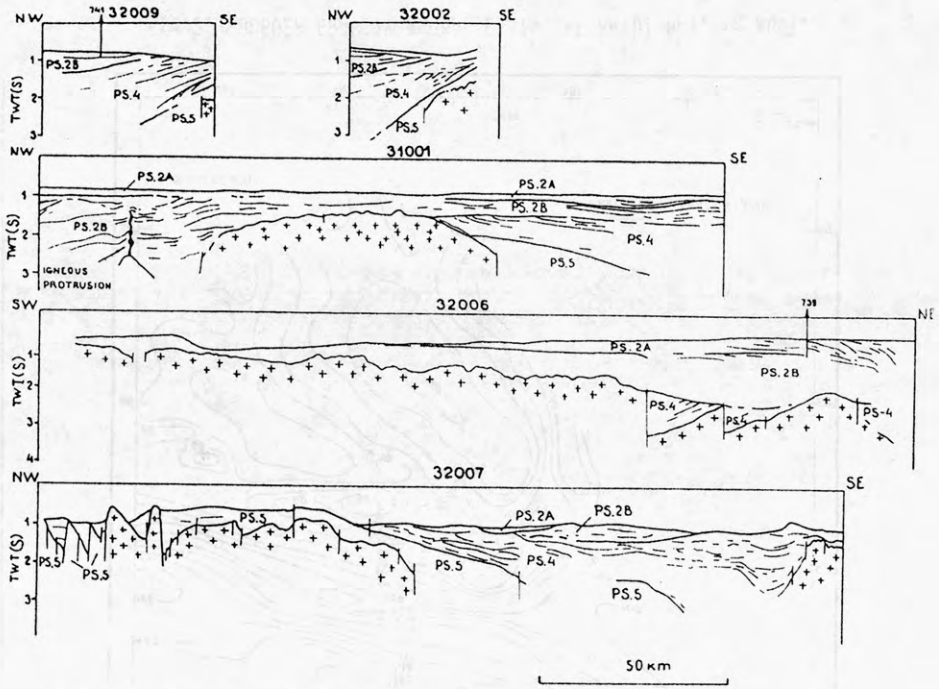

Fig.4. SEISMIC SECTIONS ON THE PRYDZ BAY SHELF (see Fig.1 for profiles location).
Cover units: PS.2A - late Eocene-Neogene
PS.2B - early Cretaceous
PS.4 - early Mesozoic (Jurassic?)
PS.5 - late Paleozoic (Permian?)

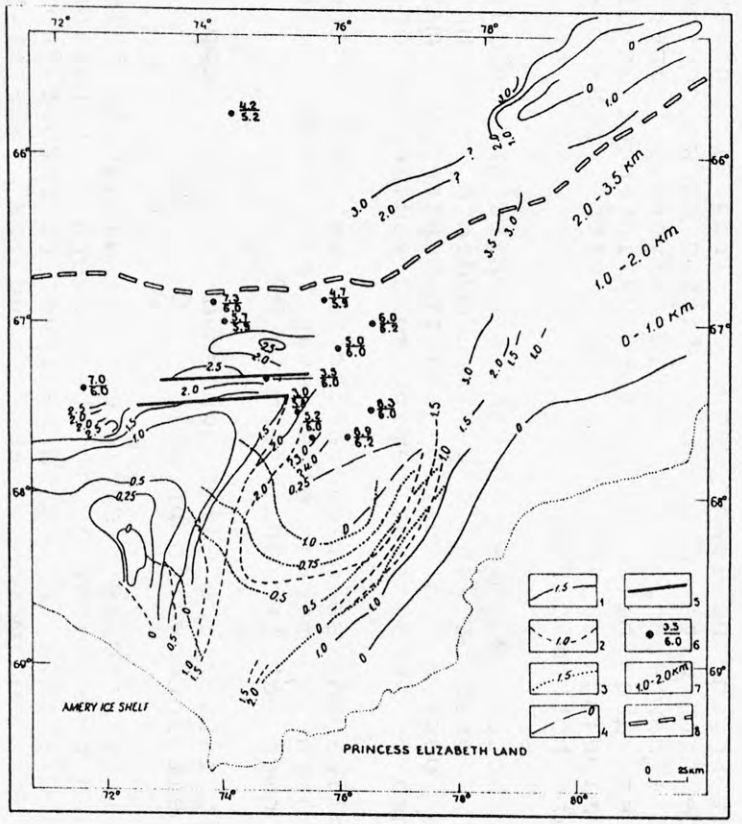

Fig.5. STRUCTURAL MAP FOR THE PRYDZ BAY. 1-4: reflection time interval between Sea floor and tops of basement (1), PS.5 (2), PS.4 (3) and PS.2B (4); 5 - listric faults; 6 - sonobuoy data: depth to basement (km) / boundary velocity (km/s); 7 - depths to basement from magnetic data in the eastern Prydz Bay; 8 - prograding shelf edge.

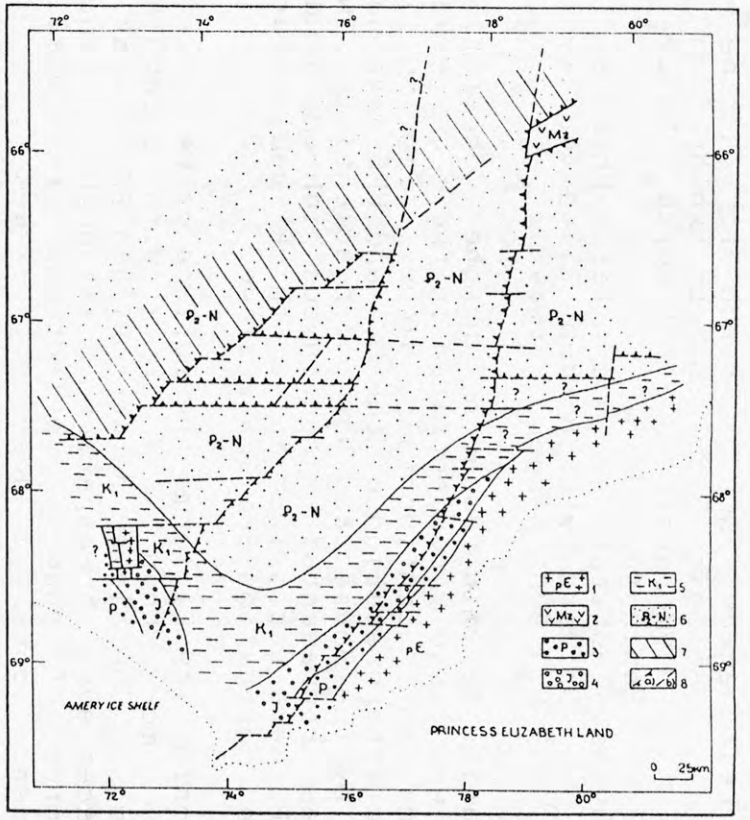

Fig.6. MAJOR FEATURES OF SEA-FLOOR GEOLOGY AND BASEMENT STRUCTURE IN THE PRYDZ BAY. 1 - Precambrian basement; 2 - sub-bottom protrusion of Mesozoic (?) igneous rocks; 3 - Permian (?) strata; 4 - Jurassic (?) non-marine sediments; 5 -early Cretaceous fluvial deposits; 6 - Eocene/Oligocene - Neogene glacial marine cover; 7 - deep downwarp of ensialic basement in marginal half-graben ; 8 - major fault escarpments (a) and faults (b) in the basement mostly buried by sediments.

SEISMIC FACIES ON THE COOPERATION SEA LOWER SLOPE
(poster presentation)

G.L.Leitchenkov, North Branch for Marine Geologic Research and Exploration "Sevmorgeologia", 120 Moyka, 190121 Leningrad, USSR
B.Kuvaas, Institute of Solid Earth Physics, University of Bergen, Allegaten 41, N - 5007 Bergen, Norway

1.The Soviet marine seismic research in the Cooperation Sea in 1986 - 1988 was largely concentrated in the outer Prydz bay shelf and adjacent continental slope (Fig. 1). Seismostratigraphic interpretation of the MCS and HRS data was jointly undertaken by the Soviet and Norwegian scientists. Two major unconformities represented by continuous high-amplitude reflectors P1 and P2 were recognized in a thick sedimentary pile underlying the Cooperation Sea lower slope.

The lower unconformity P1 forms the surface of relatively homogenous sequence more than 2 s thick with irregular internal boundaries. The layer between P1 and P2 is weakly stratified, in places even transparent, although distinct interfaces and zones of chaotic reflections are locally observed. The sequence above P2 does not exceed 2 s in thickness and consists of well stratified combination of different seismic facies.

Reflection pattern in the lower sequence (Fig.2) gives reasons to compare it with deep-water facies known on the continental margins elsewhere in the world [Myers, Piper, 1986]. Such facies are believed to form by interaction of turbidite and hemipelagic sedimentation with possible influence of moderate bottom currents.

Typical slope facies, such as channel deposits and debris flows, are locally present in the intermediate sequence (Fig.2), while its general acoustic semitransparency may indicate predominance of persistent hemipelagic sedimentation.

The most complicated seismic reflection pattern in the upper sequence apparently marks a substantial change in depositional environment at the unconformity P2.

2. Five seismic facies are distinguished in the upper sequence [Kuvaas, Leitchenkov, in prep.]:

(i) wavy-stratified facies restricted exclusively to this sequence and recorded predominantly in the western Cooperation Sea slope (Fig.2A,B,C); this facies is believed to result from eastward migration of sediment waves caused by westerly currents;

(ii) mounded-stratified facies that is also present only above P2 unconformity and interpreted as the result of bottom-

current controlled moulding of sediments (Fig.2A,B,C);

(iii) well stratified cut-and-fill facies (locally observed in the intermediate sequence as well) thought to represent deep-sea fan channel and levee deposits; the latter are usually found on western flanks of the channels (Fig.2 A,B);

(iv) local well stratified facies with parallel continuous boundaries reflecting episodes of relatively stable depositional environments similar to those inferred for the lower sequence;

(v) chaotic facies (olistostromes) that in places penetrate the unconformity P2 from respective lithologies in the underlying sequence.

Predominance of the first three facies suggests channelized mass overflow by downslope turbidity currents in combination with strong contour bottom currents of mainly western direction.

3. Observed paleodepositional features are consistent with common paleotectonic and paleoclimatic reconstructions [Leitchenkov, this volume; Cooper et al., in press; Norton, 1982]. Deep-water sedimentation on the East Antarctic continental margin presumably began in early Cretaceous time during initial stages of formation of the Southern Indian Ocean. Next major event was the separation of Antarctica from Australia in early Tertiary time and establishing of quasicircumpolar paleocurrent; as the result, considerable erosion of the lower sequence and formation of P1 unconformity occurred. This early Cenozoic event was probably accompanied or immediately succeeded by activization in the Lambert Glacier area and on adjacent continental margin of rift-related sublongitudinal faults that controlled distribution of downslope mass flows and overlapping canyon generation (Wild Canyon).

Dramatic change in hydrodynamic regime must have occurred in connection with final separation in Mid-Tertiary time of Antarctica from Gondwana by opening of the Drake Passage, closing of Antarctic circulation and associated increase in bottom currents activity [Barker, 1977]. These events were marked by P2 unconformity and appearance in the overlying seismic facies of distinct indications of westerly component in bottom currents. This component was probably related to a clock-wise circulation in the Cooperation Sea area caused by blocking effect of the Kerguelen Plateau (probably, in combination with the Coriolis force).

Breakup-related paleotectonic events and associated paleoenvironmental changes that led to formation of regional unconformities P1 and P2 were also responsible for two major phases of rapid growth of the Antarctic ice sheet commonly attributed to the Lower Tertiary glaciation of East Antarctica

and the Middle Tertiary expansion of ice sheet over the whole continent [Cooper et al., in press; Webb, 1990]. Consequently, all seismic facies above unconformity P1 were deposited offshore the already ice-covered landmass, and the bulk of clastic material for these sequences must have been derived from a glaciated source area, whether the latter only included the Antarctic land (at times of glacial retreats) or extended over the adjacent shelf (at times of glacial maxima and offshore advances of ice sheet).

5. Resolution of seismic images of the lower slope deposits is not sufficient to detect an unambiguous glacial component directly supplied by grounded and/or floating ice; nevertheless, it is logical to assume that a seaward movement of ice sheet would be of vital importance for sediment transportation. On the other hand, the process of sediment supply and distribution could depend on repeated glacial retreats to a much greater extent than is commonly realized, especially if they were deep and lengthy enough to allow limited development of humid conditions and fluvial systems.

6. Thus, the dimensions and internal structure of a thick sedimentary pile on the lower slope of the Cooperation Sea are comparable to large fan bodies formed in deep-water, high-energy hydrodynamic environments on other continental margins. Available data suggest that accumulation of the greater part of the lower slope sequences took place parallel and subsequent to onset of the full-scale Antarctic glaciation. However, the role of that factor in sediment supply and depositional processes remain to a large degree uncertain.

REFERENCES:

Barker P.F. and Burrell J., 1977. The opening of the Drake Passage. Marine Geology, v.25, No 1/3, p.15-34.

Cooper A.K., Stagg H. and Geist E., in press. Seismic stratigraphy and structure of Prydz Bay, Antarctica: Implications from ODP Leg 119 drilling. In: Barron J. and Larsen B.,eds. Scientific Results of ODP Leg 119 drilling, Volume B. College Station, TX, Ocean Drilling Program.

Kuvaas B. and Leitchenkov G.L., in prep. Glacigenic turbidite and current controlled deposits in Prydz Bay, Antarctica.

Leitchenkov G.L. (this volume). Structure, seismic stratigraphy and evolution of the Prydz Bay.

Myers R.A. and Piper D.J.W., 1988. Seismic stratigraphy of late Cenozoic sediments in the northern Labrador Sea: a history of bottom circulation and glaciation. Can.J.Earth Sci., 25, p.2059-2074.

Norton I.D., 1982. Paleomotion between Africa, South America and Antarctica, and implications for the Antarctic Peninsula. In: Craddock C., ed. Antarctic Geoscience. Madison, Univ.Wisconsin Press, p.99-106.

Webb P.-N., 1990. The Cenozoic history of Antarctica and its global impact. Antarctic Science, v.2(1), p.3 - 21.

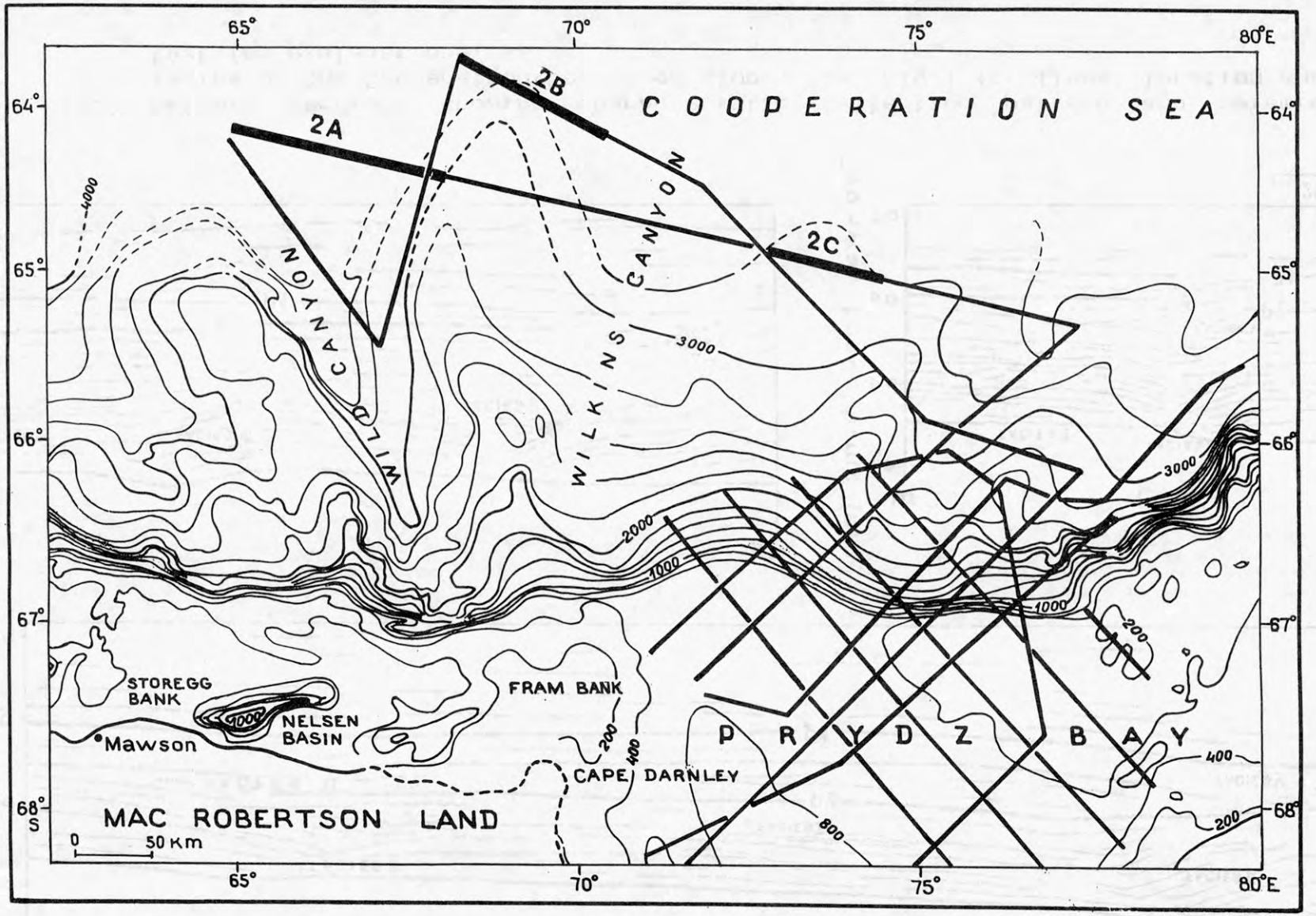

Fig.1. Location of MCS lines used in the present study in relation to bathymetry and the Soviet marine seismic network. Heavy lines indicate profiles shown in Fig.2.

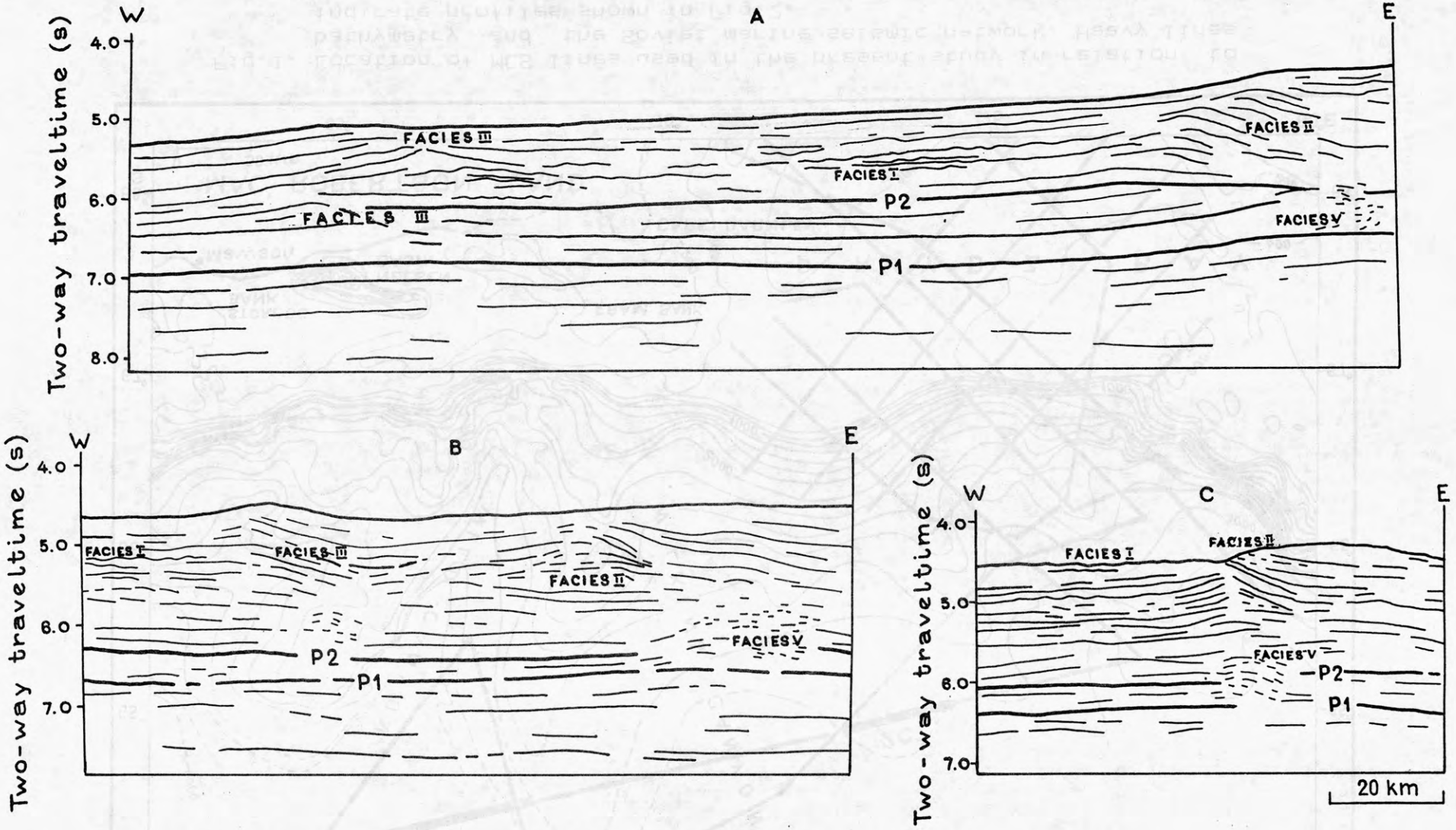

Fig.2. Seismic sections showing characteristic reflection pattern and seismic facies on the Cooperation Sea lower slope. See Fig.1 for lines location and text for explanations.

EARLY TERTIARY FOSSIL HILL FLORA FROM FILDES PENINSULA OF KING GEORGE ISLAND, ANTARCTICA

H.M. Li, Nanjing Institute of Geology and Palaeontology Academia Sinica, Nanjing, 210008,China

The Fossil Hill flora consists of more than 40 forms of ferns, gymnosperms and angiosperms, which are a mixture of subantarctic and neotropical elements, mostly resembling the Early Tertiary South American palaeoflora.

According to "the nearest living relative method" and "leaf physiognomical analysis", the plants of the Fossil Hill flora probably grew under the following environmental conditions : 1. The mean annual temperature was approximately 14-16^{o}C. 2. The mean temperature of the coldest month was about 10^{o}C. 3. The mean temperature of the warmest month was about 20^{o}C. 4. The mean annual range of temperature was probably 7-10C^{o}. 5. There was a lack of solar radiation during winter as a result of being the high latitude. 6. There was high precipitation (more than 1000mm per year). 7. The area where the plants of the Fossil Hill flora were growing was at rather low altitudes.

The author tried to determine what caused the warm and humid climate during the time when the plants were growing, and proposes the following hypothesis. During Cretaceous and Early - Middle Palaeogene, Antarctica, Australia and South America as parts of the Gondwana formed a nearly continuous landmass along the southern margin of the Pacific Ocean. The Southern Pacific was effectively separated from other oceans and continents at that time and it is reasonable to assume that in the Southern Pacific the oceanic circulation of a warm current southward from the equator transported huge quantity of heat to Gondwana. The Circum-Polar Current developed about 38 Ma ago; since then the antarctic climate began deteriorating. The development of a Circum- Polar Current as it exists today requires deep sea conditions around the whole of Antarctica; this did not appear until the end of the Oligocene (23.5 Ma ago).

The palaeontologically determined age of the Fossil Hill flora is most likely Early to Middle Eocene. This is in good agreement with the isochron age of the Fossil Hill Member and the Block Hill Member (52 $\pm$ 1 Ma - 43 $\pm$ 2 Ma B.P.) (Li Zhaonai et al., 1989).

A DISCUSSION ON THE CHARACTERISTICS AND EVOLUTION OF THE CRUST IN THE TRANSANTARCTIC MOUNTAITNS BASED ON GEOGHEMICAL AND PALEOMAGNETIC RESULTS

Li Huamei Wang Shenyuan Xie Guanghong
Liu Yimao Chen Xianpei Zhu Bingquan
Institute of Geochemistry, Chinese Academy of Seiences
P. O. Box 1131, Wushan, Guangzhou 510640, P. R. China

Extended Abstract

This paper reports a study of an area of the Transantarctic Mountains and Ross Island (161°-167°E, 77. 2°-78. 2°S). The basement rocks consist of metamorphic rocks, migmatite and granitoid with injection of basic dikes. The protolith of the metamorphic rocks was a complex of andesite to basalt. The granitoid rocks include intermediate-acid granites and acid granites, the former largely occurring as batholiths or giant masses and the later predominantly occurring as small rock bodies or dykes. K-Ar and $^{40}Ar-^{39}Ar$ isotopic dating indicates that the ages of basement rocks in this area within the range of 400—550 Ma, mostly between 490 and 440 Ma. A few samples of fine-grained diorite, monzonitic granite and granite yielded isotopic ages ranging from 400to 200 Ma . Two groups of rock bodies and dykes gave Rb-Sr isochron ages of 488 Ma and 438 Ma, respectively. The major granites in this area have initial $^{87}Sr/^{86}Sr$ ratios ranging from 0. 705 to 0. 709, with Al index of 0. 94—1. 06, low differentiation index of 24—58 and high solidified index of 18—41. An content of plagioclase is between 34—46. Mica belongs to Mg—Fe biotite. LREE is enriched, LREE/HREE 3. 7—16. 4 Eu negative anomaly is not striking. Li, Be,Rb, Ta, W, Sn are poor and V, Ti, Cr, Ni, Co, Sr are slightly enriched in granitoids. The above features indicate that the intermediate-acid granitoid rocks are of crust-mantle type. Their formation is interpreted as a deep-source andesitic magma interacting with the Cambrian-Ordovician or even older strata when moving upwards along deep faults, resulting in the formation of some semi-autochthonous quartzdiorite and granodiorite under high temperature and high pressure condition. In other words, they were formed in a compressional environment marginal to the plate, and are syntectonic granites with the characteristics of collisionzone granites.

The Taylor group of Beacon supergroup is composed mainly of orthoquartzite

with quartz sands accounting for 95—99%, of which single quartz grains account for 85—95%, composite quartz grains, 5—15%, and rock fragments, 1% or even lower. Medium-sized sand grains are well sorted (the sorting coefficient: 1. 08—1. 49) and exhibit roundness, perfect aphericity and frosted surfaces. The stable heavy minerals zircon and rutile are dominant, accounting for at most 95—100%. Tourmaline and magnetite come next, the ZTR index is over than 0. 9. The sandstones show high component and textural maturity. Aeolian sandgrains of unusual shapes are observed in thin section. These grains are cubic, tetrahedral and concave in form, and V-shaped hollows are generally developed in the aeolian concave surfaces of quartz grains or on their margins. Overlapping of these two kinds of surface textures indicates that the transport mediums of these sands was predominantly moving water and to a lesser extent. The sandstone cements are thuringite, goethite and illite, most of which has reacted to pyrophyllite and some interlayered pyrophyllite-smectite-thringite. Quartz grains of the sandstiones display overgrowths. The interstral clays have been all transformed into mica minerals which are interstitially distributed in the form of lamelliform crystals or penetrate into the sand grains. There features suggest a stable geotectonic environment with a terrestrial source region characterized by strong chemical weathering. The sandstones were deposited in middle to low latitudes. The cements in the sandstones were all strongly recrystallized during late diagensis. During the middle Jurassic, deep fault activity in the Transantarctic Mountains became intense, leading to extensive intrusion of basic magmas. According to P. R. Kyle, the Ferrar dolerite has initial $^{87}Sr/^{86}Sr$ ratios ranging from 0. 7089 to 0. 7153. Higher $^{87}Sr/^{86}Sr$ ratios may be due to crustal contamination when deep-seated magmas find their way upwards through the basement and covering strata of great thickness.

A preliminary AWP for the rocks includes the paleopole positions of 36. 4°S, 222. 2°E with $A_{95}=1.2°$ (200—400 Ma), 47. 1°S, 228. 1°E with $A_{95}=2.6°$ (160—170 Ma), 69. 8°s, 221. 2°E with $A_{95}=4.9°$ (0. 9 Ma), and 76. 2°S, 122. 5°E with $A_{95}=9.2°$ (0. 3—0. 6 Ma). The paleolatitudes of sampling locations are 41. 7°S, 50. 6°S, 73. 5°S and 80. 2°S, respectively. In the light of the reconstruction of Gondwanaland by Smith and Hallam (1970), rotation of the Antarctic continent together with its Jurassic paleopole (47. 1°S, 228. 1°E) through an angle of 58. 4° relative to Africa around the Eura pole (1. 3°N, 324°E) (McElhinny, M. W., 1976), places Antarctica next to the southeast edge of Africa. The Jurassic pole of rotated Antarctica, located at 74°S, 67. 6°E, is close to the southern end of

the APW of reconstructed Gandwanaland by Thompson and Clark (1982). The above results show that Antarctica was a part of Gandwanaland before middle Jurassic, and at that time Antarctica lay at middle latitudes around 40—50°S. The antarctica has separated from Gondwanaland and moved southwards since about 165 Ma. From the time when basaltic magmas were widely injected until 40 Ma when the Antarctic glacial sheet was formed, Antarctica moved southwards about 2800 km.

The Cenozoic volcanic rocks in this area can be divided into two types: trachyphonolites, and tephrite and basanite. K—Ar age determinations show that the ages of the two trachyphonolites at Cape Royds are 0.27±0.06 Ma and 0.62±0.04 Ma, respectively, the age of tephrite and basanite from Crater Hill is 0.9±0.18 Ma, and those of the three flows at Cape Bird are 4.47±0.17 Ma (the second flow), 4.93±0.04 Ma (the fourth flow) and 4.95±0.17 Ma (the fifth flow), respectively. The chondrite-normalized Ti, V, Cr, Mn, Fe, Co, Ni, Cu distribution patterns in volcanic rocks exhibit remarkable positive Ti anomalies and negative Cr and Ni anomalies. The patterns are of strong differentiation "W" type. The contents of REE and LREE tend to increase in the order of basanite-tephrite and tephrite-trachyphonolite. In the $(La/Sm)_N$—La diagram the data points for the volcanic rocks from five location basically fall near an oblique line. It is found that Rb, Ba, Cs, Pb, U, Th, Ta, Zr, Hf, Y, Se and REE are negatively correlated with MgO, but positively with K_2O. Mantle-derived F tends to increase in parallel with K_2O. It can be seen from the above that volcanic rocks from the five location in this area were formed through co-magmatic crystal differentiation and evolution. Twelve samples were measured for their Sr isotopes, most have initial $^{87}Sr/^{86}Sr$ ratios ranging from 0.7300—0.70316 three have slightly high isotopic ratios (0.7033—0.7045). No obvious Eu anomaly has been observed. The composition of melt inclusions is basically consistent with that of the host rocks. The homogenization temperatures were estimated at 1190— 1350 ℃ and pressure at 7200—7500 bars for basalt glassy inclusions. The magma was derived from the mantle. Relatively low Th/U ratios suggest that the magma was derived from depleted mantle materials and belong to the oceanic-island type at volcanism. The source region is closely related with that of oceanic basslts in the south hemisphere. In the ternary system, they are mainly controlled by the Kerguelen and St. Helena members.

Quaternary Diatoms from Xihu Lake on Fildes Peninsula of King George Island. Antarctica and the Paleoenvironmental Analysis by Fuzzy Mathematics

Li Jiaying, Zhang Yucai Institute of Geology, Chinese Academy of Geological Sciences, Beijing, 100037, China

The Xihu Lake is located in an ice-free area of the King George Island, which is the biggest one on South Shetland Islands. It is the only source of drinking water in the Great Wall Station area. The Xihu Lake is 160 m long from north to south and 100 m wide from east to west, with a maximum water depth of 10 m. Xie Youyu made a drilling through the 3.5 - 4 m deep water in the Xihu Lake by using a gravity rig. The drill hole was 2.6 m deep and 102 samples were collected there.

There are very abundant diatoms, completely preserved, in the 43 samples from the core and the diatom flora contains 21 genera, 131 taxa. Using the method of the fuzzy mathematics, this comprehensive study of the diatom assemblages graphically shows the development and variations of the diatom.

The diatoms and Cysts(Chrysophyta) from the sediments in the Xihu Lake are represented by 9 diatom assemblages distinguished in W5-3 of the core from bottom to top as follows:

1, *Fragilaria construens* var. *subsalina-Frag. construens* var. *venter-Melosira italica* subsp. *subarctica*(respective percentages: 18%, 14.5%, 11.6%).

2, *Fragilaria construens* var. *binodis-Frag. vaecheriae-Synedra rumpens*(12.5%, 9.6%, 11.6%).

3, *Opephora martyi-Achnanthes delicatula-Fragilaria vaecheriae*-Cysts(19.5%, 11.0%, 10.0%, Cysts abundant).

4, *Opephora martyi-Navicula pseudoscutiformis-Melosira roeseana* (13.5%, 11.5%, 10.0%).

5, *Achnanthes lanceolata* var. *rostrata-Navicula hungarica-Painnularia subcapitata*-Cysts(7.5%, 9.0%, 4.5%, Cysts abundant).

6, *Melosira roeseana* var. *epidendron-Gomphonema longiceps* var. *subclarata-Achnanthes delicatula-Ach. lanceolata* var. *rostrata*(12.5%, 12.1%, 11.5%, 9.5%).

7, *Fragilaria vaecheriae-Achnanthes delicatula-Ach. lanceolata* var. *rostrata*(14.1%, 11.5%, 8.1%).

8, *Synedra rumpens-Fragilaria vaecheriae-Achnanthes inflata-Ach. linearis* var. *pusilla*(25.1%, 17.5%, 13.3%, 13.2%).

9, *Pinnularia gibba* f. *subundulata-Pinn. microstauron-Melosira roeseana* var. *epidendron*(13.5%, 11.1%, 10.1%).

The variation of the assemblages reflect the Paleoclimatic and Paleoenvironment change over the last 3600 years.

1, It is proved from the characteristics of the present diatom assemblages that the Palaeoecological environment was nonmarine during the diatom deposition.

2, The change of the number and diversity of the cold water species in that period veflects warm-cold-warm climatic variation: assemblages of 1, 9 reflect warmth, 2, 4, 6, 8 represent show cool and 3, 5, 7 cold.

EVOLUTION OF MORAINES AND BEACHES AND RECENT UPLIFT RATES IN HURD PENINSULA, LIVINGSTON ISLAND, SOUTH SHETLAND

J. López-Martínez, Departamento de Geología, Facultad de Ciencias, Universidad Autónoma, 28049 Madrid, Spain.
E. Martínez de Pisón, Departamento de Geografía, Facultad de Letras, Universidad Autónoma, 28049 Madrid, Spain.
A. Arche, Instituto de Geología Económica, CSIC, Facultad de Geología, 28040 Madrid, Spain.

Introduction

The Hurd Peninsula is situated between South Bay and False Bay, southern part of Livingston Island, the second largest of the South Shetland Island (Fig. 1). It is about 20 km^2, culminates at 420 m near its south end. The shape of the peninsula is controlled by active faults and most of the details of the landscape are also tectonically controlled.

Outcrops in the Hurd Peninsula are the largest in Livingston Island except the Byers Peninsula; they consist of turbidites of the Miers Bluff Formation (Hobbs, 1968, Dalziel, 1972, 1982, 1984, Smellie et al. 1984) and small areas of granites and dyke swarms.

A series of interrelated raised beaches and moraine arcs has been found in several coves along the coast; here we present some of these data (Fig. 1) and a fist approach to their common evolution, their relative ages and the uplift history of the peninsula. A detailed geomorphological map of the area is already finished and will be related to other areas of Livingston Island in a near future.

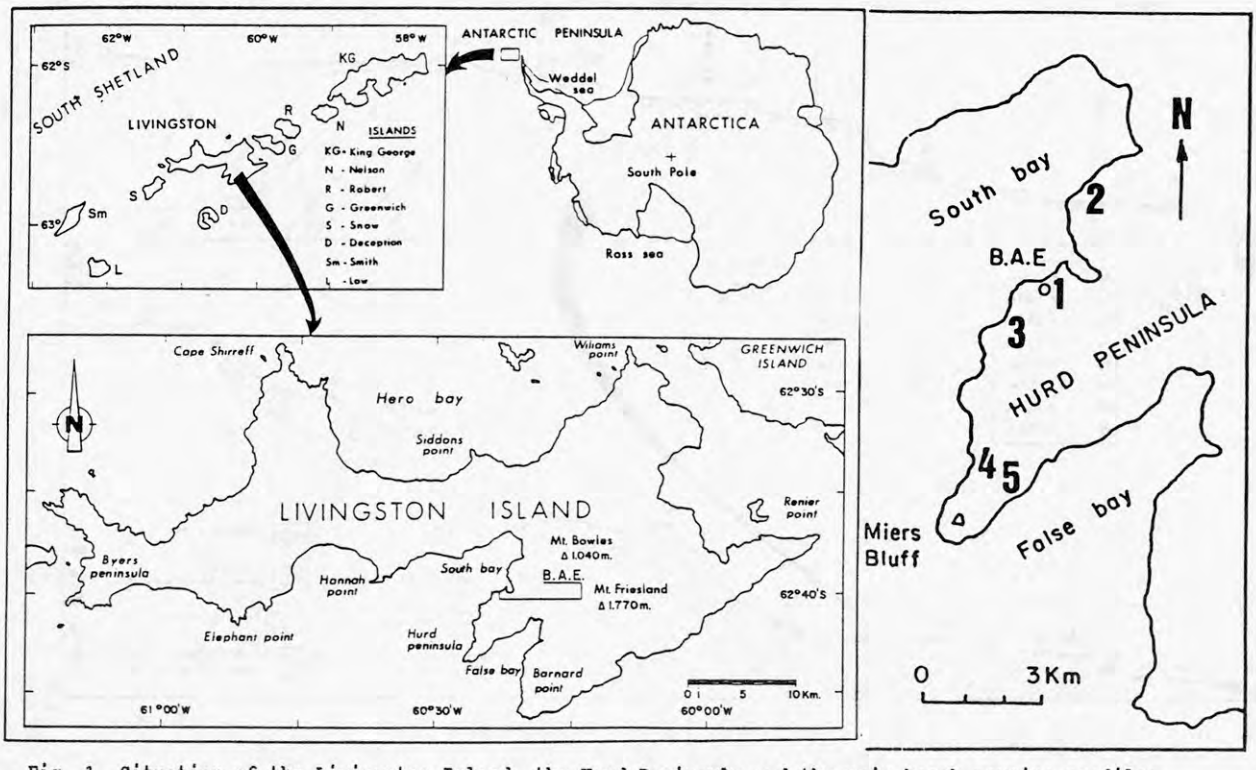

Fig. 1. Situation of the Livingston Island, the Hurd Peninsula and the main beach-moraine profiles.
1: Spanish Base Cove, 2: Bulgaria Point, 3: Argentinian Cove, 4: Sally Rocks Area, 5: Rocky Glacier Cove.
B.A.E.: Spanish Antarctic Base Juan Carlos I.

Previous work

The Holocene glacial retreat and the presence of raised beaches are known in several Antarctica localities, specially in the South Shetland (Corte, 1959, Adie, 1964, Nichols, 1966, John and Sugden, 1971,...). Hobbs (1968) pointed out the succession of moraine arcs in the Johnsons Dock area and the raised beaches, paleocliffs and raised marine platforms of the island. There are good descriptions of the Byers Peninsula raised beaches (Adie, 1964, John and Sugden, 1971,...), where some radiocarbon dating was obtained (Sugden and John, 1973, Hanson, 1979).

Two main glacial episodes, probably of the Pleistocene, have been described (John and Sugden, 1971) in the South Shetland. Everett (1971) suggested two main episodes in Livingston Island, a minor readvance and the present day retreat, without precise ages, and tied up the raised beaches with interglacial stages.

Geometry of moraine and beaches

The locations of the best profiles for the study of the raised beaches and moraine arcs of the Hurd Peninsula are shown in Fig. 1.

1. Spanish Base Cove: There are eight raised beaches and six moraine arcs in succession (Fig. 2).

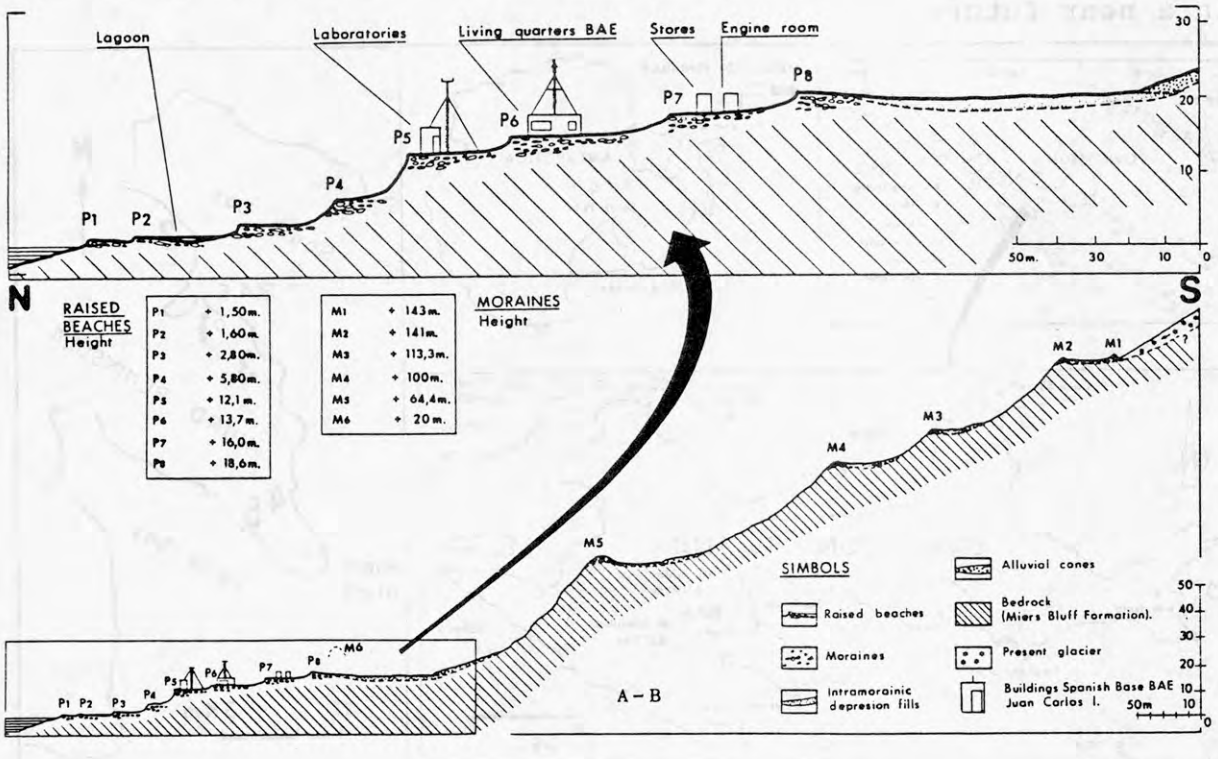

Fig. 2. Profile of the Spanish Base Cove

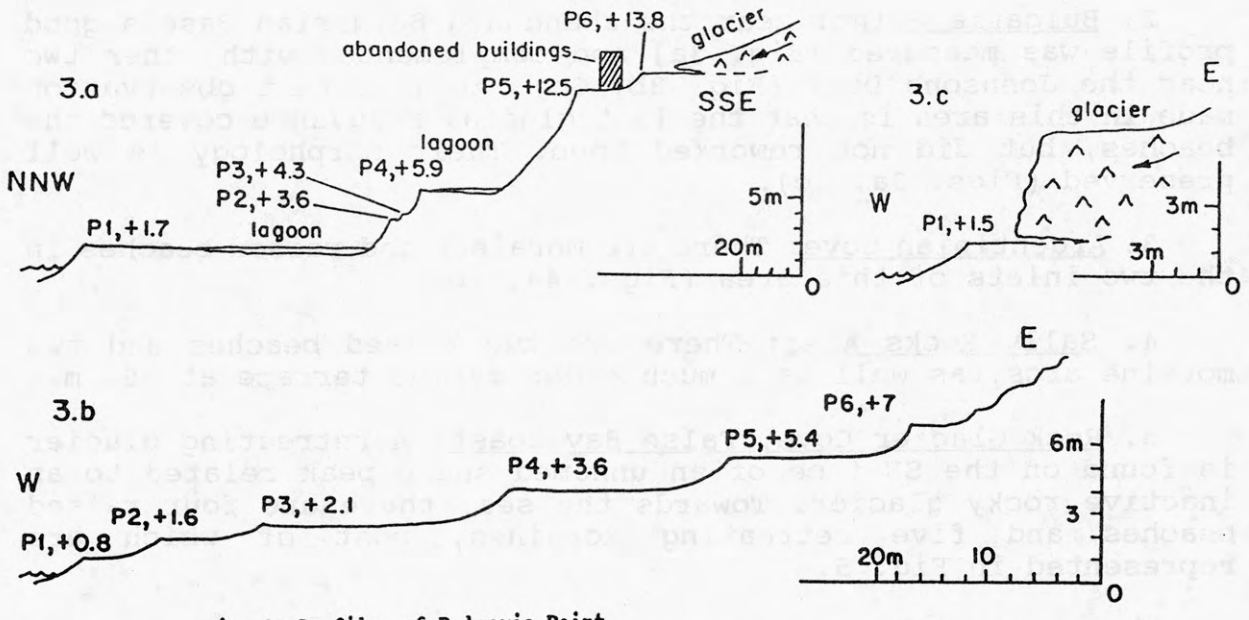

Fig. 3: Profiles of Bulgaria Point.

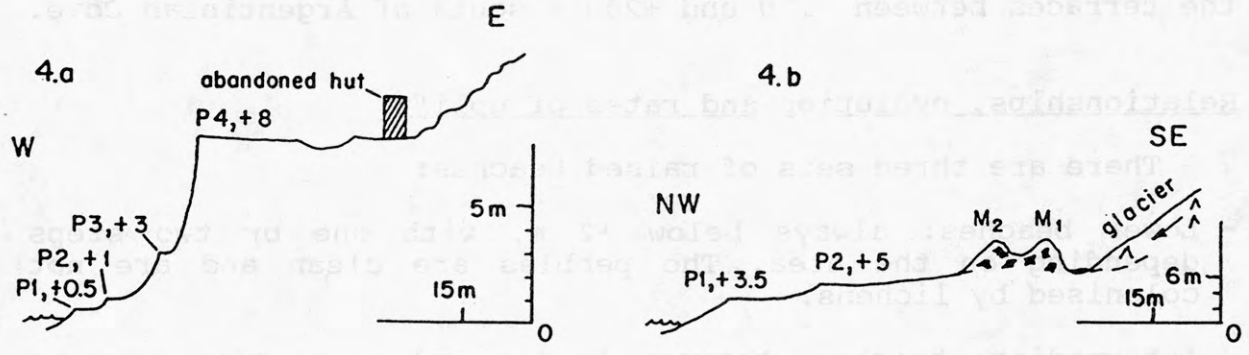

Fig. 4: Profiles of the Argentinian Cove.

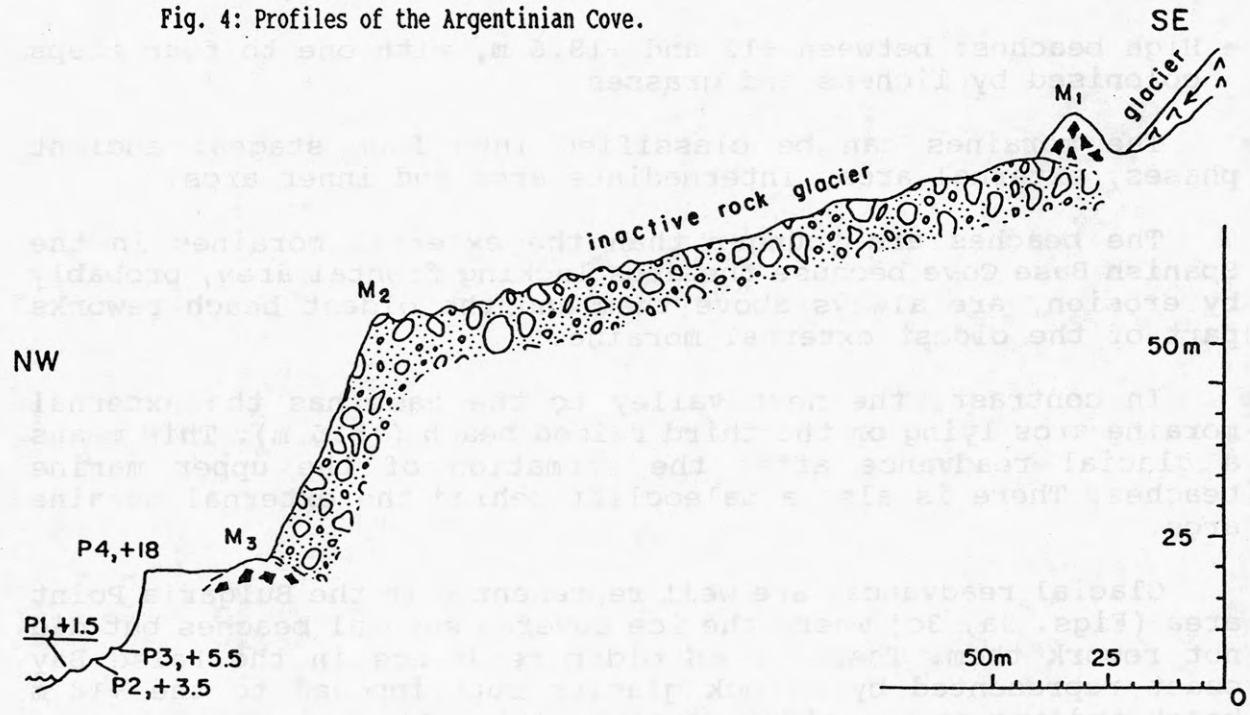

Fig. 5: Profile of the Rock Glacier Cove, False Bay.

2. Bulgaria Point: near the abandoned Bulgarian Base a good profile was measured (Fig. 3a) and complemented with other two near the Johnsons Dock (Fig. 3b, 3c). An important observation made in this area is that the last glacial readvance covered the beaches, but did not reworked them. Their morphology is well preserved (Figs. 3a, 3c).

3. Argentinian Cove: There are moraines and raised beaches in the two inlets of this area (Figs. 4a, 4b).

4. Sally Rocks Area: There are two raised beaches and two moraine arcs, as well as a much older marine terrace at +60 m.

5. Rock Glacier Cove, False Bay coast: A retreating glacier is found on the SE face of an unnamed sharp peak related to an inactive rocky glacier. Towards the sea, there are four raised beaches and five retreating moraines, most of which are represented in Fig. 5.

There are also erosional features of possible marine origin in the Hurd Peninsula, such as the +60 m terrace near Sally Rocks, the +70 m and +120 m terraces of the Johnson Dock area and the terraces between +150 and +200 m south of Argentinian Cove.

Relationships, evolution and rates of uplift

There are three sets of raised beaches:

- Lower beaches: always below +2 m, with one or two steps depending on the area. The pebbles are clean and are not colonised by lichens.

- Intermediate beaches: between +2.8 m and +8 m, with four to eight steps partially colonised by lichens and grasses.

- High beaches: between +12 and +18.6 m, with one to four steps colonised by lichens and grasses.

The moraines can be classified into four stages: ancient phases, external arcs, intermediate arcs and inner arcs.

The beaches are younger than the external moraines in the Spanish Base Cove because the arcs lacking frontal area, probably by erosion, are always above them and the oldest beach reworks part of the oldest external moraine.

In contrast, the next valley to the east has the external moraine arcs lying on the third raised beach (+5.5 m). This means a glacial readvance after the formation of the upper marine beaches. There is also a paleocliff behind the external moraine arcs.

Glacial readvances are well represented in the Bulgaria Point area (Figs. 3a, 3c) where the ice covered several beaches but did not rework them. There is an older readvance in the False Bay coast represented by a rock glacier superimposed to the +18 m beach and one of the older moraines (Fig. 5).

These facts show a history of several glacial pulses in recent times, with different number and position in each valley, taking place during the general retreat of the ice. The raised beaches indicate that a recent rise of Livingston Island, difficult to be explained by glacioeustatic or isostatic causes, needs more time or more ice, but is related to recent tectonic activity along the normal faults. Although we have found no beaches or moraines cut by these faults, a structural morphology controlled by them is clearly exposed in the reliefs and coasts of the Hurd Peninsula.

It is difficult to give a precise chronology of the beaches and moraines, in spite of some radiocarbon datings. Mausbacher, Muller and Schmidt (1989) give an age of 8,000 years for the deglaciation of the Fildes Peninsula (King George island), and of 6,000 years for the maximum sea level rise (+20 m) in the Holocene.

As the highest beaches that we have found in Hurd Peninsula are at 18.6 m, and as they can be about 6,000 years old, the mean uplift rate of the area can be estimated at about 3 m/1000 yrs.

Acknowledgements

This work was financed by the Special Action ANT-89-0821-E of the CICYT as part of the Spanish Antarctic Program.

References

ADIE, R.J. (1964) Sea level changes in the Scotia Arc and Graham land. In R.J. Adie (ed.) Antarct. Geol. SCAR Proceedings. II Geomorphology, 27-32.

B.A.S. (1985) Tectonic map of the Scotia arc, E. 1:3.000.000. BAS (Misc) 3. British Antarctic Survey.

CORTE, A.; SOMOZA, A.L. (1959) Observaciones criopedológicas y glaciológicas en las islas Decepción, Media Luna y Melchior. In R. Cordini (ed.) Publ. nº 6. Inst. Antárt. Argentino, 65-131.

DALZIEL, I.W.D. (1972) Largescale folding in the Scotia Arc. In R.J. Adie (ed.) Antarct. Geoscience, Symp. on Antartc. Geology and Geophysics. Oslo, Universitetforlaget, Series B, Number 1, 47-55.

DALZIEL, I.W.D. (1982) The Early (Pre-Middle Jurassic) History of the Scotia Arc Region, A Review and Progress Report. Antarct. Geoscience, Symp. on Antarct. Geology and Geophysics, Series B, Number 4, 137.

DALZIEL, I.W.D. (1984) Tectonic evolution of a forearc terrane, southern Scotia Ridge, Antarctica. Geol. Soc. Am. Spec. Paper, 200, 32 pp.

EVERETT, K.R. (1971) Observations on the glacial history of Livingston Island. Artic, 24(1), 41-50.

HANSON, J.D. (1979) Radiocarbon dating of a raised beach at 10 m in the South Shetland Islands. Br. Antarct. Surv. Bull., 49, 287-288.

HOBBS, G.J. (1968) The Geology of the South Shetland Islands. IV. The Geology of Livingston Island. Scientific Reports, Br. Antarct. Surv., 47, 34.

JOHN, B.S.; SUGDEN, D.E. (1971) Raised marine features and phases of glaciation in the South Shetland Islands. Br. Antarct. Surv. Bull., 24, 45-111.

MAUSBACHER, R.; MULLER, J.; SCHMIDT, R. (1989) Evolution of postglacial sedimentation in Antarctic lakes (King George Island). Zeitch. fur Geomorphologie, 33(2), 219-234.

NICHOLS, R.L. (1966) Geomorphology of Antarctic. In J.C.F. Tedrow (ed.) Antarct. soils and soil forming processes, Amer. Geoph. Union Publ., 1418, 1-46.

SMELLIE, J.L.; PANKHURST, R.; THOMSON, M.; DAVIES, R. (1984) The Geology of the South Shetland Islands, VI. Stratigraphy, Geochemistry and Evolution. Scientific Reports, Br. Antarct. Surv., 87, 85.

SUGDEN, D.E.; JOHN, B.S. (1973) The ages of glacier fluctuations in the South Shetland Islands, Antarctica. In: E.M. van Zinderen Bakker (ed.) Palaeoecology of Africa, the Surrounding Islands and Antarctica, 8, 141-159. Balkema.

U-PB AND RB-SR GEOCHRONOLOGY ON CONGLOMERATE BOULDERS FROM VIEW POINT, GRAHAM LAND, ANTARCTIC PENINSULA

W. Loske and H. Miller,
Institut für Allgemeine und Angewandte Geologie,
Ludwig-Maximilians-Universität München, Luisenstr. 37
8000 München 2, Federal Republic of Germany

Introduction

The geology of the View Point Peninsula, near Duse Bay in north-east Graham Land (Fig. 1), is dominated by sandstone/shale alternations which include important beds of conglomerate (Aitkenhead 1965). This is not the only, but the best developed exposure of conglomerates within the (?Carboniferous to) Triassic Trinity Peninsula Group (TPG) of Antarctic Peninsula. Aitkenhead (1965) describes the groundmass of the conglomerate as low grade ("chlorite zone") metamorphic. In a polished specimen he counted 55.6 % sedimentary, 4.3 % low-grade metamorphic, 35,7 % acid volcanic and 4.4 % plutonic and orthogneiss phenoclasts.

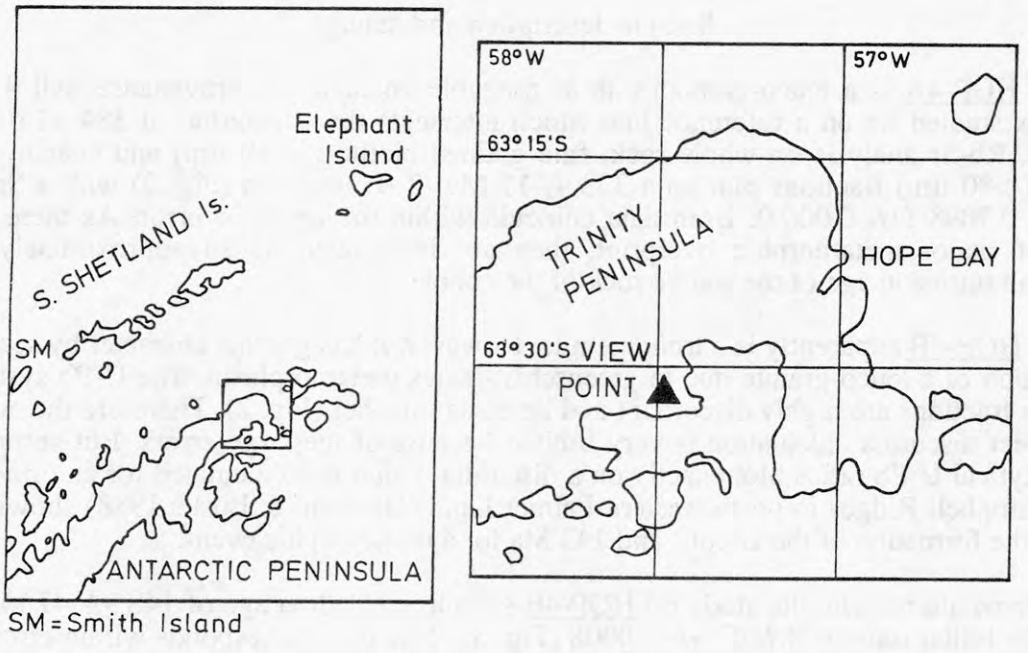

Fig. 1
Geographic sketch map of the northern Antarctic Peninsula

Smellie (1981, Fig. 4) includes the View Point area in the "fore-arc basin" of a arc-trench system of Gondwana sequences. He classifies the rocks (Smellie 1987) as belonging to a petrofacies characterized by high quartz contents and not well identified provenance (maybe magmatic arc mixed with mature sedimentary rocks). Loske et al. (1988a,b) and Miller et al. (1987) concluded from U-Pb geochronology on detritic zircons for a mostly Carboniferous and magmatic provenance area for the TPG sediments at Livingston Island and Cape Legoupil.

On a suite of granophyric cobbles recollected from the base of the sequence at View Point, Pankhurst (1983) calculated a Rb-Sr errorchron of 386+/-39 Ma and interpreted this date as a maximum age for the View Point Formation.

Geology

In order to bring forward the discussion on the maximum age of TPG and to improve the knowledge of the type and age of the conglomerate's source area, we sampled once more the type locality at View Point.

The visited area is composed of massive quartzite beds with intercalated phyllites and conglomerates. Many quartzites show cross bedding. Some conglomerate beds are up to 20 m thick. At the visited area the components are mostly quartzites (80 %), approx. 10 % granitoids and 10 % phyllites and others. Bedding of the quartzite/phyllite series strikes ENE dipping steeply (65 to 70) to NNW.

2 cobbles of a 20 m thick granitoid dominated boulder conglomerate, which did not show visible bedding, were selected for geochronology and individually dated using the U-Pb (zircons) and Rb-Sr (wr/biotite) systems. Analytical results are given in Table 1.

Sample description and dating

Sample HOP-4A is a leuco-granodiorite of probable volcanic-arc provenance. All 3 zircon fractions studied lie on a reference line which intersects the concordia at 384 +15/-19 Ma (Fig. 2). Rb-Sr analysis on whole rock, fine grained biotite (< 80 µm) and coarse grained biotite (>80 µm) fractions plot on a 398 +/-17 Ma (2 σ) isochron (Fig. 3) with a Sr initial ratio of 0.7098 (+/- 0.0007). Both data coincide within the limits of error. As there are no signs of major metamorphic overprint, they are interpreted as an approximately Early Devonian intrusion age of the source rock of the cobble.

Sample HOP-4B apparently is a trondhjemite. However, it has got this character by secondary albitization of a leuco-granite due to greenschist-facies metamorphism. The U-Pb systems of 5 zircon fractions are highly discordant and lie close together (Fig. 2). Therefore the evidence of a direct discordia calculation is very limited because of the large errors. But surprisingly the analytical U-Pb ratios plot exactly on a discordia which was calculated for an orthogneiss from Campbell Ridges in north-western Palmer Land (Harrison & Loske 1988) showing 506 Ma for the formation of the zircons and 143 Ma for a metamorphic event.

A Rb-Sr whole rock/biotite study on HOP-4B sample yielded an age of 148 +/- 47 Ma (2 σ) with a Sr initial ratio of 0.7109 +/- 0.0008 (Fig. 3). This date corresponds within error limits to the U-Pb lower intercept age of the Campbell Ridge, and even the Rb-Sr wr-biotite age at Campbell Ridge (130 Ma, RI 0.712) indicates certain similarities in their geological history.

The apparent one event history of HOP-4A resembles much the Silurian orthogneisses of Target Hill (Milne & Millar 1989), although the Carboniferous metamorphism affecting those rocks cannot be recognized in the cobble of View Point. The most remarkable characteristics of the HOP-4B sample is the Middle to Upper Jurassic overprinting which is documented by both the U-Pb and Rb-Sr isotopy. Within the limits of error this sample shows the same geochronological history as the Late Cambrian/Early Ordovician Campbell Ridge Orthogneiss in north-western Palmer Land.

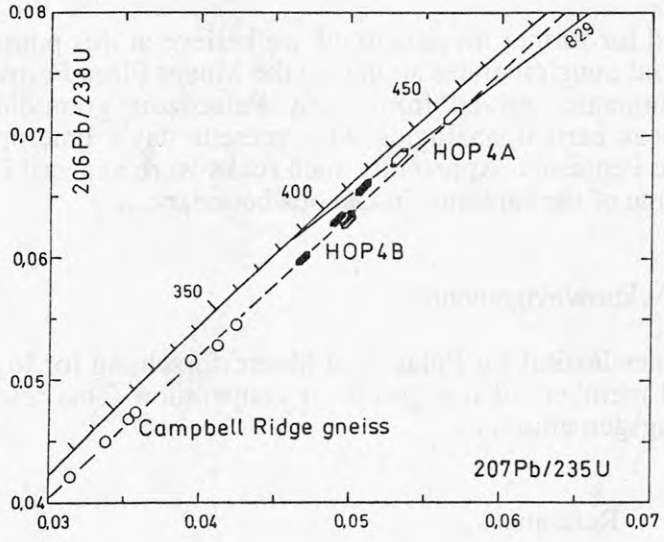

Fig. 2
U-Pb Concordia diagram of View Point Granite cobbles; for reference the isotope ratios of Campbell Ridge Gneiss are included

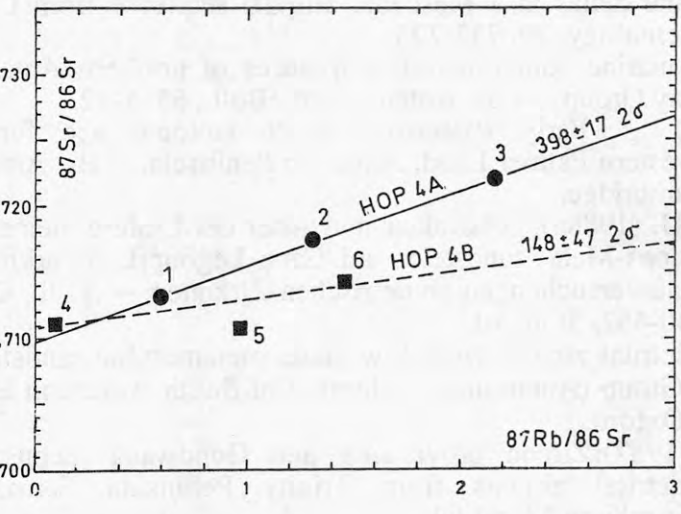

Fig. 3
Rb-Sr Isochron plot of View Point Granite Cobbles

Discussion

The two samples show obvious differences in petrographic composition and in Rb-Sr and U-Pb isotopy, indicating that they are not cogenetic and may derive from different places.

To explain the Mesozoic overprinting of HOP-4B one might suppose a metamorphic event which affected View Point Peninsula after deposition of the conglomerate. This assumption is contradictory to the fact that the other sample (HOP-4A) was not affected by this metamorphism. We suppose that there are two different conglomerates present at View Point. One intercalated with the TPG quartzites and phyllites, weakly metamorphosed together with these during the Peninsula Orogeny at the end of Triassic, and anotherone which postdates TPG. The latter is composed of granitoids, acid volcanics and material derived from TPG (quartzites and phyllites). This particular coarse conglomerate can be compared with the conglomerates of Mount Flora Formation at Hope Bay (Elliot & Gracanin 1983) and with the basal conglomerates of Camp Hill beds at Botany Bay (Farquharson 1982, 1984). Unfortunately, time did not allow for detailed mapping of the area of sampling.

The U-Pb isotopic ratios of the zircons of both samples differ basically from the U-Pb system of the detritic zircons of TPG sandstones (e.g. Miller et al. 1987). Their mostly Carboniferous, subordinately Precambrian to Cambrian zircons do not appear in the cobbles of the conglomerate.

Results

Placing ahead that there is urgent need for further investigations we believe at this point that on the top of View Point Peninsula basal conglomerates similar to the Mount Flora Formation are exposed. Cobbles of this conglomerate derived from Early Palaeozoic granitoids of different age and lithology. They bear certain analogies with present day's outcrops of crystalline rocks in Northern Antarctic Peninsula. Apparently such rocks were exposed in the former Peninsula area already at the time of the Jurassic/Cretaceous boundary.

Acknowledgements

We gratefully thank the Alfred-Wegener-Institut für Polar- und Meeresforschung for logistic support during the field work and all members of our group for cooperation. This research was granted by the Deutsche Forschungsgemeinschaft.

References

Aitkinhead, N. (1965): The geology of the Duse Bay - Larson Inlet area, northeast Graham Land (with particular reference to the Trinity Peninsula Series). -- Scient. Rep. Br. antarct. Surv., 51: 62 pp; London.

Elliot, D.H. & Gracanin, T.M. (1983): Conglomeratic strata of Mesozoic age at Hope Bay, northern Antarctic Peninsula. -- In: Oliver, R.L., James, P.R. & Jago, J.B. (eds.): Antarctic Earth Science: 303-307.

Farquharson, G.W. (1982): Lacustrine deltas in a Mesozoic alluvial sequence from Camp Hill, Antarctica. -- Sedimentology, 29: 717-725.

"" (1984): Late Mesozoic, non-marine conglomeratic sequences of northern Antarctic Peninsula (The Botany Bay Group). -- Br. Antarct. Surv. Bull., 65: 1-32.

Harrison, S.M. & Loske, W.P. (1988): Early Palaeozoic U-Pb isotopic age for an orthogneiss from north-western Palmer Land, Antarctic Peninsula. -- Br. Antarct. Surv. Bull., 81: 11-18; Cambridge.

Loske, W.P., Miller, H. & Kramm, U. (1988a): Charakter und Alter der Liefergesteine des Trinity-Peninsula-Formations-Meta- sandsteins auf Cape Legoupil, Antarktische Halbinsel: U-Pb--Isotopenuntersuchungen an detrischen Zirkonen. -- N. Jb. Geol. Paläont. Mh., 1988(7): 440-452; Stuttgart.

"" (1988b): U-Pb systematics of detrital zircons from low-grade metamorphic sandstones of the Trinity Peninsula Group (Antarctica). -- Journal of South American Earth Sciences, 1(3): 301-307; Oxford.

Miller, H., Loske, W. & Kramm, U. (1987): Zircon provenance and Gondwana reconstruction: U-Pb data of detrital zircons from Trinity Peninsula Formation metasandstones. -- Polarforschung 57: 59-69.

Milne, A.J. & Millar, I.L. (1989): The significance of mid-Palaeo-zoic basement in eastern Graham Land, Antarctica. -- J. Geol. Soc. Lond., 146: 207-210; London.

Pankhurst, R.J. (1983): Rb-Sr constraints on the ages of basement rocks of the Antarctic Peninsula. -- In: Oliver, R.L., James, P.R. & Jago, J.B. (eds.): Antarctic Earth Science: 367-371.

Smellie, J.L. (1981): A complete arc-trench system recognized in Gondwana sequences of the Antarctic Peninsula region. -- Geol. Mag. 118(2): 139-159.

"" (1987): Sandstone detrital modes and basinal setting of the Trinity Peninsula Group, northern Graham Land, Antarctic Peninsula: A preliminary survey. -- In: G.D. McKenzie (ed) Gondwana Six: Structure, tectonics and geophysics. Geophysical Monograph 40: 199-207.

No.	Sieve fraction (μm)	Remarks	Sample weight (mg)	Concentrations			Observed atomic ratios			Atomic ratios corrected for common Pb and blank			Apparent ages (Ma)		
				U_{tot} (ppm)	Pb_{tot} (ppm)	$^{206}Pb_{rad}$ (μmol/mg)	$^{206}Pb/^{204}Pb$	$^{207}Pb/^{206}Pb$	$^{208}Pb/^{206}Pb$	$^{206}Pb/^{238}U$	$^{207}Pb/^{235}U$	$^{207}Pb/^{206}Pb$	$^{206}Pb/^{238}U$	$^{207}Pb/^{235}U$	$^{207}Pb/^{206}Pb$
HOP-4A															
1	100-80	i	1,6	347	25	0,16006	461	0,08826	0,21803	0,06817	0,53215	0,05661	425	433	477
2	80-63	i	1,6	453	36	0,20776	459	0,08825	0,21857	0,06832	0,53249	0,05653	426	434	473
3	63-53	t	1,0	387	33	0,11778	406	0,09334	0,23311	0,07152	0,56703	0,05750	445	456	511
HOP-4B															
4	125-100	i	0,4	267	23	0,02633	235	0,11818	0,28269	0,06578	0,50839	0,05606	411	417	455
5	100-80	i	0,7	411	30	0,07586	431	0,09081	0,21594	0,06330	0,49742	0,05699	396	410	491
6	80-63	i	0,9	437	30	0,10243	1045	0,07044	0,16517	0,06312	0,49173	0,05650	395	406	472
7	63-53	i	0,2	641	44	0,03037	927	0,07303	0,17209	0,06309	0,49860	0,05732	394	411	504
8	<53	t	4,2	776	52	0,80505	755	0,07601	0,18354	0,05994	0,46868	0,05671	375	390	480

Table 1

Rb-Sr isotopic data of View Point cobbles

No.		Remarks	Concentrations		Observed atomic ratios	
			Rb (ppm)	Sr (ppm)	$^{87}Rb/^{86}Sr$	$^{87}Sr/^{86}Sr$
HOP-4A						
1	1	wr	53	256	0,5977	0,7130
2	2	<80m	16	36	1,305	0,7174
3	3	>80m	11	14	2,159	0,7219
HOP-4B						
1	4	wr	3,4	93	0,1046	0,7112
2 ***	5	<80m	6,9	21	0,9692	0,7108
3	6	>80m	7,1	14	1,460	0,7142

errors for Rb / Sr concentrations 1.5 / 0.3 %
$^{87}Sr/^{86}Sr$-ratio 0.1 %
*** error on $^{87}Sr/^{86}Sr$-ratio exceeds 0.8 %
wr: whole rock m: mica (chlorite/biotite)

Table 2

U-Pb isotopic data of View Point zircons

RB-SR AND U-PB GEOCHRONOLOGY OF BASEMENT XENOLITHS AT CAPE DUBOUZET, ANTARCTIC PENINSULA

W. Loske and H. Miller,
Institut für Allgemeine und Angewandte Geologie,
Ludwig-Maximilians-Universität München, Luisenstr. 37,
8000 München 2, Federal Republic of Germany

We like to dedicate this paper to Prof. Dr. Borwin Grauert. This year he will be able to look back at sixty years of fruitful life and a brilliant scientific career.

Introduction

The exposed pre-Middle Jurassic geology of northern Antarctic Peninsula is dominated by low-grade metasedimentary rocks of the (?) Carboniferous-Triassic Trinity Peninsula Group (TPG). Due to the lack of outcrops, the nature and age of any higher grade basement rocks of the northern Antarctic Peninsula have for a long time been the subject of discussion.

Milne & Millar (1989) and Harrison & Loske (1988) showed for the first time that in central Graham Land and in Palmer Land, Palaeozoic ages (300-500 Ma) are present. The metamorphic rocks of the South Shetland Islands and Elephant Island Group display only a doubtful Late Palaeozoic age of deposition and metamorphism (Hervé et al. 1987; 1990).

The question of whether the northern Antarctic Peninsula rests on old continental crust or not, is of significant importance for the position of West Antarctica within Gondwana. Overlapping models of the Antarctic Peninsula with the Falkland Plateau (e.g. Smith & Hallam 1970) would be possible if the northern part of the Peninsula formed after the Palaeozoic, but would be impossible if the sediments of the TPG were deposited on a Palaeozoic or even older continental crust.

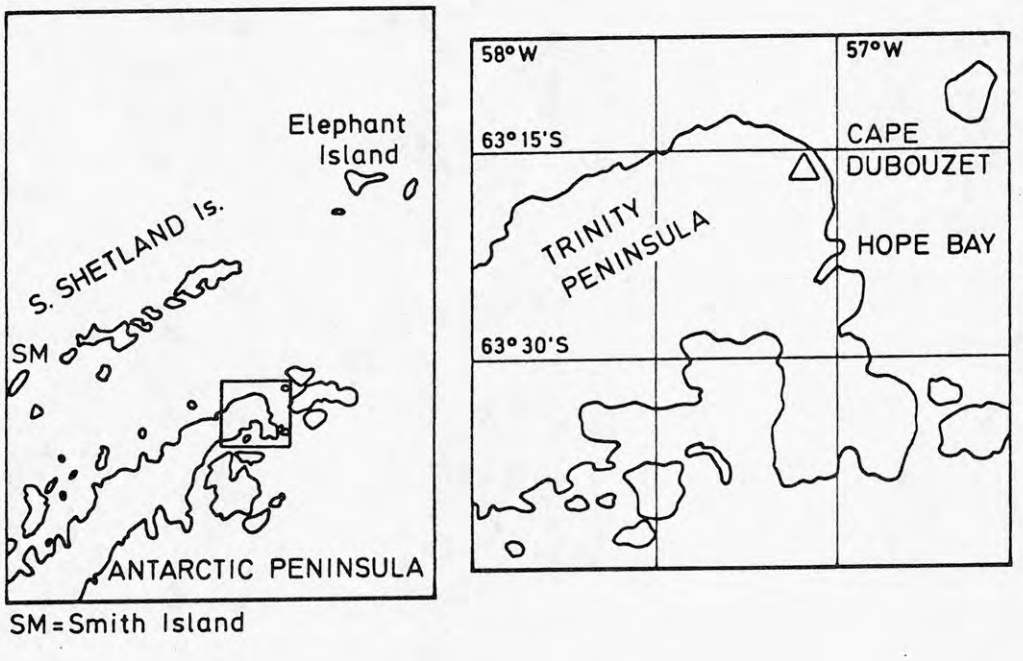

Fig. 1
Geographic sketch map of the northern Antarctic Peninsula

Petrography

On occasion of a helicopter reconnaissance flight large boulders (up to 0.6 m) of medium grade metamorphic xenoliths in a granitoid matrix were found by A. Milne and F. Hervé (Loske et al. 1990) in a local moraine of a glacier coming from the Mount Bransfield region (Fig. 1). About 100 m north of the moraine, rocks of the Antarctic Peninsula Volcanic Group and conglomerates composed of pebbles of TPG quartzites are exposed.

The host rock of the xenoliths is a quartz-diorite/tonalite composed mainly of plagioclase and quartz besides the mafic minerals chlorite, biotite and epidote. Muscovite is scarce. Accessory minerals are zircon, sphene/leucoxene, carbonate, apatite, clinozoisite, allanite and opaques. Small xenocrysts (3-4 mm) of quartz, plagioclase and garnet are present. Sometimes the garnets show rims of fine-grained phyllosilicates and inclusions of biotite. The garnets suggest an anatectic origin of the granitoid.

Three petrographically distinct groups of xenoliths were collected:
(I) Plagioclase-biotite-hornblende gneisses with variable amounts of chlorite, garnet, epidote, muscovite, actinolite and/or other minerals of the amphibole group.
(II) Amphibolites composed of plagioclase and two generations of amphibole. The first generation is poikiloblastic, forming xenomorphic and corroded blasts, the second generation is represented by small euhedral, needle-shaped crystals. Quartz, biotite, epidote and chlorite are common; clinopyroxene occurs only exceptionally.
(III) Metatonalites of similar composition as the matrix. Schistosity is documented by quartz or garnet-rich layers and by parallel alignment of biotite.

Dating of the matrix

The micas of the reddish and bleached white matrix were analysed using the Rb-Sr method. Together with the whole rock data the biotites (intergrown with chlorite) suggest an age of approx. 80 Ma for the final event (chloritisation ?) that affected the micas (Fig. 2).

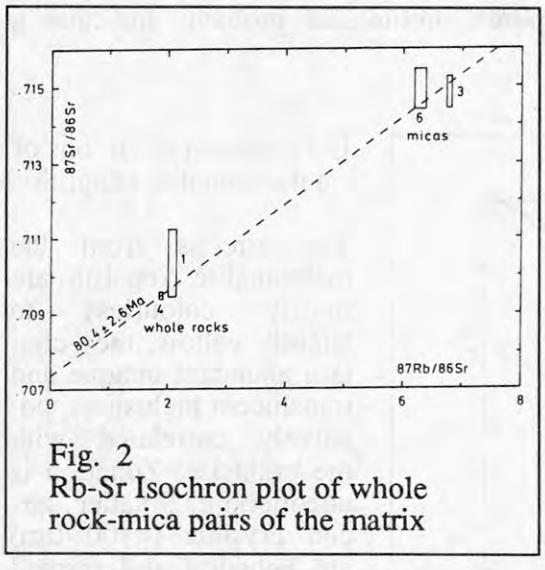

Fig. 2
Rb-Sr Isochron plot of whole rock-mica pairs of the matrix

The majority of the zircons of the granitoid matrix are euhedral, prismatic and colourless. On the temperature-alkalinity diagram of Pupin (1980) they plot in the overlapping fields of tonalites and calcalkaline rhyolites. The dominance of the prism (100) over (110) indicates a relatively high temperature of about 750-850°C during the formation of these crystals.

The U-Pb systematics of the zircons show a conspicious scatter. A calculated regression line (Fig. 3) intersects with the concordia at 224 +21/-31 Ma (1 sigma scatter error). Assuming that the matrix tonalite in contact with the large xenoliths is not of the same age as the reddish and bleached matrix, this date might represent an early stage of anatectic processes.

The metamorphic event at approx. 140 Ma (Rb-Sr, see below) is not clearly documented in the zircons. This may be due to the fact that (i) they were not affected by this event or that (ii) their crystal lattice did not allow for a loss of large amounts of radiogenic lead. But we have still to consider that the scatter and non-linearity of U contents, grainsize and degree of discordance may be due to composite growth structures.

Rb-Sr isotopics of thin slabs of a banded amphibolite xenolith

Four fine grained, feldspar-banded slabs plot in an isochron diagram on a line which allows to calculate a 141 +/-5 Ma regression line (Fig. 4). Two biotite rich layers display considerably higher $^{87}Sr/^{86}Sr$ ratios, but lie also on a line whose slope represents 147 Ma. The majority of the nebulitic slabs plot into a cloud in between the Rb-Sr systems of the banded amphibolite slabs and the mica bands.

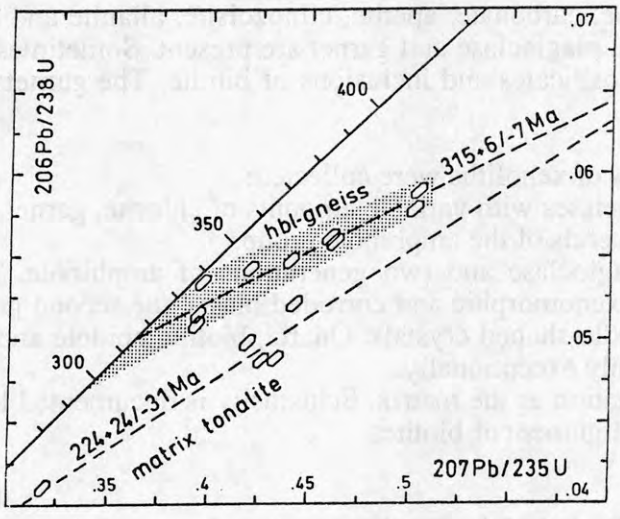

Fig. 3
U-Pb Concordia diagram of the granitoid matrix zircons and the hornblende gneiss xenolith zircons (see below)

We believe that this approx. 140 Ma date could represent a metamorphism affecting the amphibolite during the late Jurassic.

A reference line drawn through the cluster of the nebulitic parts of the slices and the purest biotite layer points to a date of approx. 222 Ma (Fig. 4). This date clearly correlates to the U-Pb 224 Ma date for the assumed primary matrix formation. Adding the information of the U-Pb systems of zircons from a hornblende gneiss and a metatonalite, a further reference line, calculated from the banded amphibolites and the purest biotite slab probably indicates a speculative 299 Ma date.

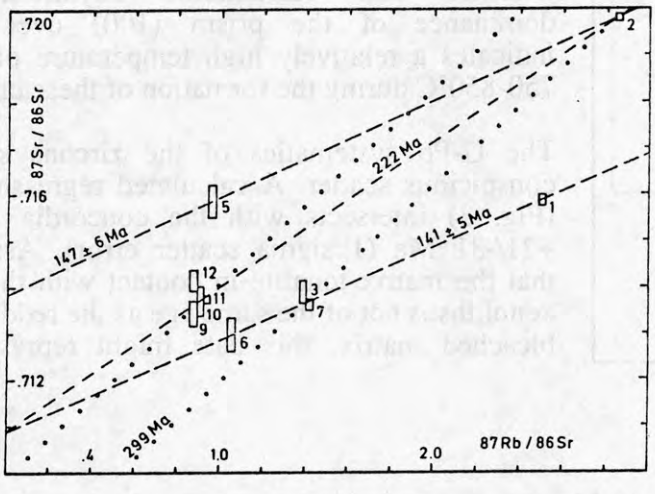

Fig. 4
Rb-Sr isochron plot of thin slabs of a banded amphibolite xenolith

U-Pb system of zircons of a metatonalite xenolith

The zircons from the metatonalite xenolith are mostly colourless to slightly yellow; they contain abundant opaque and translucent inclusions, positively correlated with the grainsize. Zonation is uncommon. Smaller zircon crystals (<100 µm) are euhedral and formed of one or two prisms and pyramids, similar to the zircons from the unmetamorphosed granitoid matrix. Within the larger grainsize fractions (>100 µm), the dominant crystal habit is rounded; sometimes elongate.

The U contents of the zircons from the metatonalite xenolith ranges between 266 and 938 ppm. They are discordant and their apparent $^{206}Pb/^{238}U$ ages range from 438 to 638 Ma, excluding the grain-size fraction 125-100 µm. Simple correlation between grain-size, uranium contents and degree of discordance indicates that this zircon population might be cogenetic (Table 2).

Seven of the eight analysed grain-size fractions (ranging from <40 µm to >125 µm) define a reasonable reference line (MSWD 1.5) which intersects the concordia at 291 +24/-26 Ma and 1698 +88/-82 Ma (1-sigma scatter error; Fig. 5).

U-Pb system of zircons of a hornblende gneiss xenolith

The isotopic ratios of the mostly euhedral zircons of the hornblende gneiss are closer to a lower intercept compared with the metatonalite zircons. The scatter of uranium contents, grain-size and degree of discordance displays a typical pattern of inherited, probably detrital zircons (Fig. 3).

A calculated regression line (MSWD 0.9) indicates at least a two stage history of the zircons. The initial growth during the Precambrian (approx. 1635 Ma) and a major overprinting event with a minimum age of 315 +6/-7 Ma (1 sigma scatter error). Within the limit of errors this age is identical with the Sm-Nd isochron age of garnet-whole-rock pairs from gneisses of Target Hill, central Graham Land (Milne & Millar 1989).

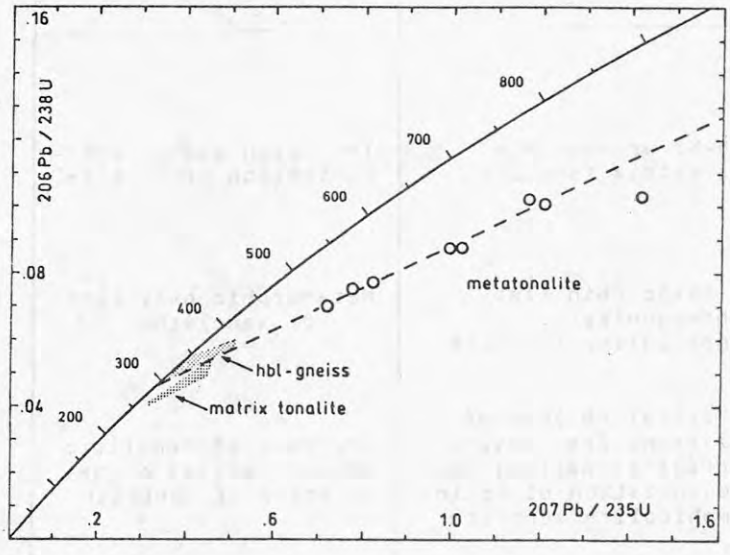

Fig. 5
U-Pb Concordia diagram of zircons of the metatonalite xenolith

Discussion

The geologic history of the xenoliths' zircons is characterized at least by three events. (I) Parts of the zircons must have a history extending back into the Precambrian; (II) a metamorphic overprinting that occurred during the Carboniferous and (III) the incorporation of these metamorphic rocks into the granitoid during the Mesozoic. Obviously, the U-Pb system of the zircons from both samples was not, or at least not visibly affected by a late Jurassic event, as indicated by the Rb-Sr system from the banded amphibolite.

Our interpretation of the geological history of the xenoliths derived from isotopic data shows a polygenetic evolution with five major steps, as shown in Table 1.

The until now only known Late Palaeozoic age from the South Shetland Islands is thought to represent a metamorphic event at Gibbs Island (Hervé et al. 1987; 287 +/-48 Ma). This date is consistent with the 291 Ma U-Pb date obtained from Cape Dubouzet. Both dates suggest the existence of Palaeozoic crust in the northern Antarctic Peninsula. Consequently reconstruction models of Gondwana which overlap the Falkland Plateau with the Antarctic Peninsula have to be critically rethought.

Acknowledgements

We gratefully thank the Alfred-Wegener-Institut für Polar- und Meeresforschung for logistic support during the field work and all members of our group for cooperation. This research was granted by the Deutsche Forschungsgemeinschaft.

References

Harland, W.B., Cox, A.V., Llewellyn, P.G., Pickton, C.G.A., Smith, A.G. & Walters, R. (1982): A geologic time scale. 131 p; Cambridge University Press.

Harrison, S.M. & Loske, W.P. (1988): Early Palaeozoic U-Pb isotopic age for an orthogneiss from north-western Palmer Land, Antarctic Peninsula. Br. Antarct. Surv. Bull., 81: 11-18.

Hervé, F., Loske, W.P., Miller, H. & Pankhurst, R.J. (1987): Chronology of provenance, deposition and metamorphism in the southern limb of the Scotia Arc. 5th Intern. Symp. on Antarctic Earth Science, Abstracts: 65; Cambridge.

Hervé, F., Miller, H., Loske, W.P., Milne, A. & Pankhurst, R.J. (1990): New Rb-Sr age data on the Scotia Metamorphic Complex at Clarence Island. Zbl. Geol. Paläont. Teil 1, 1990 H.1/2: 119-126.

Loske, W., Miller, H., Milne, A. & Hervé (1990): U-Pb zircon ages of xenoliths from Cape Dubouzet, northern Antarctic Peninsula. Zbl. Geol. Paläont. Teil 1, 1990 H.1/2: 87-95.

Milne, A.J. & Millar, I.L. (1989): The significance of mid-Palaeo-zoic basement in eastern Graham Land, Antarctica. J. Geol. Soc. Lond., 146: 207-210.

Pupin, J.P. (1980): Zircon and granite petrology. Contrib. Mineral. Petrol., 73: 207-220; Heidelberg.

Smith, A.G. & Hallam, A. (1970): The fit of the southern continents. Nature, 225: 139-144.

Table 1. Geological processes at Cape Dubouzet deduced from isotopic events. Time scale after Harland et al. 1982.

Time	Ma	Isotopic event	Geological process
Cenozoic			
	80	Rb-Sr wr mica age of matrix tonalite	Intrusion age or chloritization of biotite
Cretaceous			
	140	Rb-Sr thin slab homogenization of amphibolite xenolith	Metamorphic overprint of xenoliths
Jurassic			
		Partial Pb-loss of zircons from matrix tonalite; partial homogenization of Sr in amphibolite xenolith	Anatexis of tonalitic magma; partial migmatization of xenolith
Triassic	220		
Permian			
	300	Pb loss and new growth of zircons in xenoliths; partial Sr homogenization	Major metamorphic event in basement rocks
Carbonifer.			
Proteroz.	1600	Crystallization of zircons	Major event in basement educt

No.	Sieve fraction (μm)	Remarks	Sample weight (mg)	Concentrations			Observed atomic ratios			Atomic ratios corrected for common Pb and blank			Apparent ages (Ma)		
				U_{tot} (ppm)	Pb_{tot} (ppm)	$^{206}Pb_{rad}$ (μmol/mg)	$^{206}Pb/^{204}Pb$	$^{207}Pb/^{206}Pb$	$^{208}Pb/^{206}Pb$	$^{206}Pb/^{238}U$	$^{207}Pb/^{235}U$	$^{207}Pb/^{206}Pb$	$^{206}Pb/^{238}U$	$^{207}Pb/^{235}U$	$^{207}Pb/^{206}Pb$
DUB-4	Metatonalite xenolith														
1	>125	r	0,5	266	29	0,06000	2364	0,08980	0,14306	0,10400	1,20408	0,08397	638	803	1292
2	125-75	r	1,5	390	41	0,24518	1002	0,09663	0,10995	0,10251	1,16940	0,08273	629	786	1263
3	125-100	r,e	0,7	328	35	0,10176	4967	0,10262	0,10279	0,10322	1,42108	0,09985	633	899	1621
4	100-75	r,e	2,7	458	41	0,47926	7881	0,08370	0,11352	0,08772	0,99075	0,08191	542	699	1243
5	75-61	r,e	1,2	432	39	0,19652	4962	0,08668	0,11066	0,08789	1,01737	0,08395	543	713	1291
6	61-53	e	1,5	450	36	0,21900	4887	0,07951	0,11061	0,07726	0,81607	0,07661	480	606	1111
7	53-42	e	1,1	542	41	0,17863	4836	0,07719	0,10614	0,07525	0,77040	0,07425	468	580	1048
8	<42	e	0,3	938	67	0,08523	3558	0,07763	0,11054	0,07025	0,71322	0,07363	438	547	1031
DUB-3	Hornblende gneiss														
1	>150		2,3	282	15	0,13607	5835	0,05816	0,13439	0,05135	0,39403	0,05565	323	337	439
2	150-125	w	1,0	265	14	0,05726	3351	0,06048	0,14934	0,05086	0,39357	0,05612	320	337	457
3	150-125	b	0,5	352	19	0,04062	3016	0,06113	0,12280	0,05419	0,42052	0,05629	340	356	464
4	125-100	w	1,3	283	16	0,08067	3470	0,06263	0,13325	0,05891	0,50445	0,06211	369	415	678
5	125-100		0,5	360	22	0,04244	2934	0,06705	0,11923	0,05466	0,44043	0,05844	343	371	546
6	100-80	b	0,7	428	24	0,06608	6089	0,06182	0,11174	0,05615	0,46013	0,05944	352	384	583
7	100-80	w	1,0	277	15	0,06368	2107	0,06083	0,13602	0,05343	0,39691	0,05388	336	339	366
8	80-63		0,8	347	20	0,06720	5424	0,06267	0,12535	0,05588	0,46220	0,05999	351	386	603
9	63-40		0,8	509	30	0,09564	6902	0,06505	0,11844	0,05782	0,50189	0,06296	362	413	707
DUB-10	Granitoid matrix / quartz-diorite														
1	>150	e	1,5	206	9	0,05333	2235	0,06272	0,12402	0,04109	0,31849	0,05622	260	281	461
2	150-125	e	1,9	232	12	0,09141	2906	0,06833	0,13207	0,04868	0,42586	0,06345	306	360	723
3	125-75	e	2,4	321	16	0,15652	3580	0,06837	0,12926	0,04876	0,43318	0,06443	307	365	756
4	75-61	e	2,0	480	25	0,20818	4339	0,06503	0,12256	0,05203	0,44262	0,06170	327	372	664
5	61-42	e	1,7	470	24	0,16550	7296	0,06311	0,11389	0,04971	0,41899	0,06113	313	355	644

e = euhedral zircons, r = rounded zircons
b = brown zircons, w = white zircons

No.	Remarks	Concentrations		Observed atomic ratios	
		Rb (ppm)	Sr (ppm)	$^{87}Rb/^{86}Sr$	$^{87}Sr/^{86}Sr$
DUB-11	Amphibolite thin slabs				
1	1 wr	221	257	2,492	0,71584
2	2 wr	315	321	2,844	0,71981
3	3 wr	172	361	1,384	0,71390
4	5 wr	92	279	0,9537	0,71585
5	6 wr	104	286	1,049	0,71297
6	7 wr	119	245	1,406	0,71362
7	9 wr	85	279	0,8803	0,71343
8	10 wr	90	288	0,9042	0,71370
9	11 wr	75	237	0,9225	0,71375
10	12 wr	88	289	0,8827	0,71414
DUB-5	Matrix tonalite				
1	1 wr	176	246	2,066	0,71036
2	3 mica	77	33	6,754	0,71484
DUB-18	Matrix tonalite				
1	4 wr	172	265	1,879	0,70949
2	6 mica	56	26	6,262	0,71493

Rb and Sr concentrations analysed by isotope dilution technique, isotope ratios measured using a Finnigan MAT quadrupole mass spectrometer system. Analytical errors are shown in the figures.

Tables 2 and 3

U-Pb isotopic data of Cape Dubouzet xenoliths and matrix zircons

Rb-Sr isotopic data of Cape Dubouzet xenoliths and matrix

LATE QUATERNARY ICE-SURFACE FLUCTUATIONS OF THE LOWER LAMBERT GLACIER, NORTHERN PRINCE CHARLES MOUNTAINS.

M.C.G. Mabin, Department of Geography
James Cook University of North Queensland
TOWNSVILLE Q 4811, AUSTRALIA

The Lambert and associated outlet glaciers that drain through the Prince Charles Mountains into the Amery Ice Shelf constitute a drainage system covering 13.5% of the East Antarctic Ice Sheet, with flowlines extending far inland to Dome Argus, the central dome of the ice sheet. It is thus an area of central importance for our understanding of the late Quaternary glaciation of Antarctica. In the area of the Northern Prince Charles Mountains four ice systems are recognised; land-terminating alpine glaciers in the mountain massifs, large slow-moving outlet glaciers draining from peripheral parts of the ice sheet, the fast-flowing Lambert Glacier ice stream draining from the interior of the ice sheet, and the inner part of the Amery Ice shelf fed by the Lambert and large outlet glaciers. Moraines and drift sheets on numerous massifs provide a record of fluctuations of these glacial systems.

The ice-free parts of Fisher Massif are extensively mantled by various drift sheets and moraine complexes that have been formed by the Lambert, large outlet, and alpine glaciers. Ice-cored moraines with well preserved constructional morphologies occur close to the margins of the alpine glaciers, and up to about 100m above the Lambert Glacier. Moraines with subdued surface form and more extensive frost polygon development occur at higher levels, up to 700m above the present glacier surface. while the Lambert Glacier has declined from its most recent moraine, the alpine glaciers are close to their maximum extent, having advanced across the Lambert lateral moraines. Similar patterns occur in the higher morains and drift sheets. It is interpreted from this that the small alpine glaciers advance out of phase with advances of the large ice sheet-fed glaciers.

Denton *et al* (1986, *Quat. Resc.* 26; 3-26) present a reconstruction of the Antarctic ice sheet during the Last Glaciation based largely on data from the Ross Embayment region. Their model predicts ice-level increases of more than 1000m for the lower reaches of the Lambert and outlet glaciers, and complete grounding of the Amery Ice Shelf. However those predictions cannot be reconciled with the field data from Fisher Massif. The moraines that are most likely to be of Last Glaciation age occur less than 100m above the present ice surface, and none of the older lateral moraines occur at the high elevations predicted in the Denton *et al* model. It is suggested that during the Last Glaciation the Lambert and outlet glaciers did not expand greatly and the Amery Ice Shelf may not have become grounded. This has important implications for Antarctic Ice Sheet volume and its contribution to sea level fall during the Last Glaciation.

EARLY PALAEOZOIC SEDIMENTATION AND TECTONICS IN THE PENSACOLA MOUNTAINS, ANTARCTICA

David I.M. Macdonald & Bryan C. Storey, British Antarctic Survey, Natural Environment Research Council, High Cross, Madingley Road, Cambridge CB3 0ET, UK.
Ian W.D. Dalziel, Institute for Geophysics, The University of Texas at Austin, 8701 North Mopac Boulevard, Austin, Texas 78759, USA.
Anne M. Grunow & John L. Isbell, Byrd Polar Research Center, Ohio State University, 125 South Oval Mall, Columbus, Ohio 43210, USA

The Pensacola Mountains are towards the Atlantic end of the Transantarctic Mountains (TAM). The TAM lie on a major tectonic boundary, separating the Precambrian craton of East Antarctica from the mainly Phanerozoic crustal blocks of West Antarctica. The Pensacola Mountains are important as the area was re-activated during three major co-axial orogenic episodes: late Precambrian Beardmore folding, the Cambro-Ordovician Ross Orogeny, and the Permo-Triassic Weddell (Gondwanide) Orogeny.

Recent structural and sedimentological studies as part of a joint UK/US tectonics project has revealed that the Ross orogeny is progressive. Three tectono-sedimentary sequences have been recognized, defined by unconformities and correlative conformities. The three sequences are:

S1. A Middle Cambrian shelf limestone (Nelson Formation) conformably overlain by 1.5 km of silicic volcanic rocks (Gambacorta Formation).

S2. A mixed carbonate-clastic sequence of terrestrial and shallow marine origin (Wiens Formation).

S3. A thick sequence of alluvial fan and fluvial deposits (Neptune Group).

These sequences are folded about the same large-scale upright folds, and contain a single, common cleavage. However, the basal conglomerates of each sequence contain randomly oriented cleaved clasts of the underlying strata. This indicates progressive development of both folds and cleavage. Furthermore, the Wiens Formation thins across an anticlinal structure within Gambacorta formation, and both facies and palaeocurrents are controlled by the geometry of the developing folds. At one locality, basal strata of the Neptune Group are involved in the Ross deformation, with sedimentation being controlled by growth folds. Unlike other areas of the TAM, there is no clear unconformity between rocks deformed in the Ross Orogeny and post-Ross strata.

The TAM are generally accepted as having been a subducting margin during Late Cambrian - Ordovician times, but the tectonic setting of the Pensacola Mountains is equivocal. We suggest that the shelf limestones of S1 represents a former passive

continental margin, pre-dating subduction. The S2 and S3 sequences may represent a foredeep setting, related to outboard crustal loading along a convergent margin. If this is the case, the outboard sequences, including a magmatic chain have subsequently been removed from this margin. The S-type silicic volcanic rocks of the Gambacorta Formation may be part of the inboard, craton-ward fringe of this magmatic belt.

GRANITIC ROCKS OF THE JETTY PENINSULA, AMERY ICE SHELF AREA, EAST ANTARCTICA

W.I. Manton, Program in Geosciences, University of Texas at Dallas, Richardson, TX, 75083-0688 USA
E.S. Grew, Department of Geological Sciences, University of Maine, Orono, ME 04469 USA
J. Hofmann, Sektion Geowissenschaften, Bergakademie Freiberg, 9200 Freiberg, Germany
J.W. Sheraton, Bureau of Mineral Resources, Canberra, 2601 A.C.T., Australia

Granulite facies rocks dated at 952 +4/-3 Ma (U-Pb zircon on a granulite containing Opx ± Cpx + Br +Pl) are intruded by two suites of granitic rocks: (1) a gneissic leucogranite that crops out in a band 1 x 0.2km and contains dominant microcline, subordinate plagioclase, minor biotite and sporadic garnet; (2) biotite granites that comprise a dike of a porphyritic variety at least 0.5km long and 2 - 5m thick, and masses up to 20m across of nonporphyritic rock. Quartz, K-felspar, plagioclase and biotite are major constituents; garnet is local; monazite and zircon are ubiquitous. The gneissic leucogranite is dated at ~850Ma by U-Pb zircon, and at 717 ± 32Ma (Ri = 0.761) by an Rb-Sr mineral isochron. The porphyritic biotite granite is dated at 507 +18/-9Ma by zircon and 487 ± 3Ma (Ri = 0.724) by Rb-Sr on minerals; and the non porphyritic at 542 ± 2Ma and 483 ± 13 (Ri = 0.714) by the same methods. Whole rock geochemistry suggests that both suites were probably derived by anatexis of sedimentary source materials. The gneissic granite has geochemical features in common with many other synorogenic, sedimentary-derived (S-type) granitic rocks of the East Antarctic shield and elsewhere. Like many other early Paleozoic postorogenic (anorogenic or A-type) intrusives in the Prince Charles Mountains-Amery Ice Shelf area, the biotite granites are strongly enriched in Zr and light rare earth elements. However, they are also markedly peraluminous, depleted in Y, and have unusually high Th/U ratios. All these compositional features can be attributed to high-temperature melting of relatively anhydrous granulite-facies metasediments containing garnet and depleted in U.

SEA BOTTOM MORPHOLOGIES OF THE ROSS SEA AREA, ANTARCTICA.

A. Marchetti(1), C. Baroni(2), C. Gantar(1), E. Lodolo(1), G. Orombelli(3), A. Stefanon(4)

(1) Osservatorio Geofisico Sperimentale di Trieste
Po. Box 2011 34016 Trieste, Italy
(2) Museo di Scienze Naturali
Via Oznam 4 25128 Brescia, Italy
(3) Universita' di Milano, Dipartimento di Scienze della Terra
Via Mangiagalli 34 20133 Milano, Italy
(4) Istituto Universitario Navale
Via Acton 38 80133 Napoli, Italy

During the Antarctic 1987-88, 1988-89, 1989-90 and 1990-91 summers and in the frame of the italian PROGRAMMA NAZIONALE DI RICERCHE IN ANTARTIDE (PNRA) conducted by ENEA, multichannel seismic reflection, gravity and magnetic surveys have been performed by the Osservatorio Geofisico Sperimentale (OGS) of Trieste in the the Ross Sea using the research vessel "OGS-EXPLORA".

Gravity and magnetic data have been collected along all the tracks with only few small interruptions due to bad sea conditions.

The seismic data were collected along 60 profiles, totalling more than 9640 Km. Moreover, 21 sonobuoys were dropped by USGS to record refraction seismic data.

Processing of data has been made at the OGS Processing Center in Trieste.

An AIRGUN array was used as source, consisting of two 31 meters long strings, each with 14 guns having a total volume of 45.16 liters of compressed air at about 140 bar.

The strings were kept at a mutual distance of 20 meters and, using suspension buoys, at an operating depth of 6 meters.

During the first survey, an analogic cable of PRAKLA-SEISMOS, stronger than a digital cable, with 96 channels, 25 metres intertrace and 32 hydrophones per trace, was used at an operating depth of 12-18 metres. A coverage of 2400% was obtained by shooting at 50 metre intervals.

For the subsequent surveys a streamer with 120 channels was employed: keeping constant all the other parameters, a coverage of 3000% was obtained.

In this paper, after an analysis of the interrelated problems of the area, three of the most evident morphological features of the sea bottom in the Ross Sea and their spatial distribution are identified and investigated. A comparison is made with data collected by other investigators using sparkers, side-scan sonars and sub-bottom profilers.

The classification of this features is based on an assemblage of morphogenetically related elements and their geometric relationships.

Erosional patterns are quite common in the sub-bottom morphology: the discrepancy between structural highs and bathy-

metry in the Ross Sea can be explained by the prevailing erosional phenomena.

The analisys of the seismic data carried out by OGS contributes to a more complete and detailed knowledge of the morphology in the Ross Sea, expecially for the erosional "terraces" of which the deeper implications are shown. They appear as a series of gently sloping terraces that truncate the sedimentary sequence.

Another interesting feature shown in the seismic lines is the presence in some area of "rough" sea bottom surfaces. Moreover, in the same areas, many shallow diffraction phenomena are present, expecially in the proximity of volcanic events. Detailed interpretation of these areas needs direct sampling: some hypotheses are considered.

Two seismic sections representing the Ross Sea continental slope are presented.

The first one is characterized by a prograding reflection pattern which shows two distinct clinoform depositional cycles in which the uppermost prograding sequence presents a typical slanted pattern interpreted as a depositional unit originated in a low standing of the sea level (regression).

The second section, which crosses the continental margin of Antarctica, does not show evidence of prograding, and the slope is generally unstable with gravitative deposits, slumping and sliding at its base. The slope profile is probably controlled by a local feature (canyon ?) which denotes erosion.

Moreover, integrating the data known in literature with those recorded during the OGS surveys, a bathimetric sketch of the Ross Sea is given.

TRIPLE JUNCTION POINT AREA.
RESULTS OF THE FIRST THREE O.G.S. GEOPHISYCAL SURVEYS

A. Marchetti(1), C. Gantar(1), L. A. Lawver(2), E. Lodolo(1), D. Postpischl (3)

(1) Osservatorio Geofisico Sperimentale di Trieste
Po. Box 2011 34016 Trieste,Italy.
(2) University of Texas in Austin, Institute for Geophysics
8701 Mopac Boulevard Austin, Texas 78759-8345, USA.
(3) Istituto di Topografia, Geodesia e Geofisica Mineraria
Viale Risorgimento 2 40136 Bologna, Italy.

During the 1988-89, 1989-90 and 1990-91 Antarctic summers, in the frame of the italian PROGRAMMA NAZIONALE DI RICERCHE IN ANTARTIDE (PNRA) conducted by ENEA, three multichannel seismic reflection, gravity and magnetic surveys were carried out by the Osservatorio Geofisico Sperimentale of Trieste (OGS) in the Southern part of the Pacific Ocean with the research vessel "OGS - EXPLORA".

Specific purpose of these geophysical surveys was the investigation of the existing structural interactions among the Antarctic, Indian and Pacific plates in the area between parallels 60° and 70° South and meridians 150°and 180° West. Final aim of the study is a contribution to the knowledge of the evolution of Gondwanaland.

About 6265 Km. of seismic data were collected along 24 profiles; gravity and magnetic data were recorded during all the tracks except few small interruptions due to bad sea conditions.

The instruments employed are:

- for navigation, the integrated positioning sistem NAVDATA 3000 devised by Prakla-Seismos;
- for gravimetry, the marine surface gravimeter BODENSEEWERK KSS31.
- for magnetometry, the magnetometer GEOMETRIC G801-803 and, in the last cruise, the gradiometer GEOMETRICS G811G;
- for seismic data, an airgun source, a recorder SERCEL 358 and an analogic streamer PRAKLA-SEISMOS.

The geometry of the system streamer - airgun array was selected from the available information on signature diagrams and radiation spectra and in the light of the previous survey; it was kept constant troughtout all the campaigns.

An AIRGUN system was used as source. It consisted of one ar-ray of two 31 meters long strings, each with 14 guns, having a total volume of 45.16 liters of compressed air at about 140 bars.

These strings were kept at a mutual distance of 20 meters and, using suspensions buoys, at an operating depth of 6 meters.

A seismic transformless analogic cable PRAKLA-SEISMOS, stronger than a digital one, with 120 channels, 25 metre intertrace and 32 hydrophones per trace was used at an operating depth of 12-18 meters.

The resulting streamer consisted of an active section of 3000 meters, behind three elastic passive sections each of 50 metres between the active section and the tow rope, terminated with a final elastic section with the tailbuoy, for a total length of 3400 meters.

All the lines were recorded by shooting every 50 metres, thus obtaining a coverage of 3000%, with record lenght 16 seconds and sample rate 4 milliseconds.

All the data have been processed by the OGS Processing Center in Trieste.

A standard processing sequence was applied: only data on which the velocity analysis and the tests were performed have been filtered in the F/K domain to attenuate the main multiples.

Particular programs (F/K filtering, dip move out, before stack migration) could be applied to data of particular areas according to interpretation problems.

The following main processing steps have been applied:
REFORMAT The field tapes were recorded in Seg-D format. Thus the first step was the reading of the tapes and transcription into Seg-Y format.
BINATION Antialias filter and resample to 8 msec.
TRACE SUM Adiacent trace summing;the traces per record were reduced from 120 to 60.
GAIN In order to compensate for amplitude decay due to sferical divergence and absorption, a gain curve of the form

$$db = 2.00*t+1.00 * \log t$$

were db is the gain in decibels and t the time in seconds, was applied.
SORT The data were reordered from shot to common middle point order.
VELOCITY ANALYSIS One analysis every 5 Km using VELSTACK.
STACK Normal move out corrected gathers were muted and stacked. The coverage is 3000%.
MIXING A three traces mixing, weighted 100/100/100, was applied to attenuate the steeper dipping events, mainly multiples or noise.

This triple junction area represents a key area for the study of the Antarctic plate evolution. This investigation represents our first approach to uderstand the geological and geophysical characteristics of the area.

The triple junction between Indian plate, Pacific plate and Antarctic plate is a complex area that is currently interpreted in different ways. A key role for its evolution is played by the transcurrent faults that extends so far northward (Macquarie Ridge) and southward (Balleny Islands) and by the transform faults which dissects the Indian-South Pacific Ridge (e.g. Balleny fracture zone).

Our data indicate that the general tectonics of the region include lineations produced by transpression between the Australian and Pacific plates. This transpressive regime is superimposed on the oceanic crust of the region and indicates that there is an incipient subdution of the Australian plate beneath the Pacific plate.

The anomalies produced by the major offset transform

faults having trend roughly NNW-SSE South of 60° S dominate the Geosat altimeter data. The offset of these faults along the eastern end of the Indian-Antarctic ridge produces significant contrasts in the crustal thickness and stucture across these fracture zones.

The offset is sufficiently great in at least one case where the Geosat data produce a classic example of reversal in signature across the transform fault going from older to younger crust.

The multychannel seismic lines across these segments show seismic reflections within the oceanic crust that reveal both tectonic and magmatic processes. A series of extensional faults observed in the oceanic crust may be the simple result of sea-floor spreading or may be a result of complex magmatic layering that reflects variations in physical properties of basaltic rocks.

An anomalus region immediatly west of the so-called Hjort trench could be a continental fragment according to the observed seimic facies. The seismic profile patterns include folded and thrusted layers not normally present in the oceanic crust. Also the Geosat data as well as an anomalous bathymetry support the idea that this is a continental fragment. If it is continental it may have been left behind by the Tasman rise as it was rifted northward. This fragment may have also resulted in the probable reversal of subduction direction at the Hjort trench which originally showed eastward subduction but, the 1988 Macquarie Island earthquake clearly indicates westward subduction.

AEROMAGNETIC ANOMALY MAP OF WEST ANTARCTICA (WEDDELL SEA SECTOR)

M.P. Maslanyj, S.W. Garrett, A.C. Johnson,
R.G.B. Renner and A.M. Smith
British Antarctic Survey, Natural Environment Research Council,
High Cross, Madingley Road, Cambridge, CB3 OET. UK.

Over 114,000 line-kilometres of aeromagnetic data collected between 1973 and 1987 are presented on a 1:2,500,000 scale map. The most important anomalies on the map are:

(a) A 2,000 km-long linear anomaly belt along the Pacific coast of the Antarctic Peninsula and Ellsworth Land, caused by a subduction-related batholith complex.

(b) An extensive area of high amplitude, high frequency anomalies between the Antarctic Peninsula and the Ellsworth Mountains. These are caused by Precambrian metamorphic basement which is exposed in a single outcrop at Haag Nunataks.

(c) A long-wavelength anomaly over Berkner Island, interpreted as shallowing magnetic basement.

Areas of low magnetic gradients, as well as local, isolated high amplitude anomalies cover the rest of the map. The map improves our understanding of the structure and extent of the major igneous and metamorphic complexes and the nature of the basins and boundaries which separate the crustal blocks of West Antarctica.

DETERMINATION OF WATER CONTENT IN QUARTZ FROM THE NAPIER COMPLEX, EAST ANTARCTICA

Hiromi Matayoshi, Takako Yuko, Toshiaki Masuda:
Institute of Geosciences, Shizuoka University, Shizuoka 422, Japan.
Yoichi Motoyoshi: *Polar Research Institute, Tokyo 173, Japan.*
Satoru Nakashima: *Department of Mining Geology, Akita University, Akita 010, Japan.*

Water content in quartz grains of a quartzite from the Napier Complex, East Antarctica, was measured by Fourier Transform Infrared Spectroscopy (FT-IR). The quartzite in the Complex consists mostly of quartz, and subordinately sapphirine and zircon. Quartz grains are usually large, and their diameters sometimes exceed 8 mm. The Napier Complex suffered from a high P-T metamorphism at around 10kbar and 1000°C (e.g.,Ellis, 1980; Motoyoshi and Matsueda, 1984). The quartzite is regarded as a dry rock because of the absence of hydrous minerals. The aim of this study is to determine water content of the quartz grain in such dry rocks.

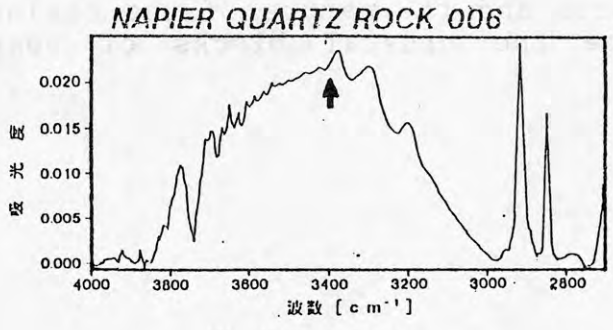

約 40 ppm

Existence of water was detected by Infrared absorption spectra, as shown left. The absorption peak of 3400cm^{-1} corresponds amount of water. Using the molecular coefficient of water proposed by Thompson(1965), the water content in this quartz is estimated as approximately 40 ppm.

This result indicates that even quartz grains in the rocks without hydrous minerals do contain a small amount of water. We measured water contents in some Japanese metamorphic rocks of lower grade, which comprise muscovite, biotite and amphibole in order to compare the amount of water in a wide range of metamorphic grades. The water content of quartz in these rocks ranges from about 200 to 1000 ppm.

Thus, the water content of quartz in the Napier Complex with no hydrous minerals is affirmed to be low when compared with metamorphic rocks with hydrous minerals in Japan.

CHEMICAL FOSSILS OF VASCULAR PLANT ACTIVITY IN THE McMURDO DRY VALLEYS DURING THE PRE- AND INTER-GLACIAL PERIODS, ANTARCTICA

Genki I. MATSUMOTO[1], Yoshio YOSHIDA[2], Kunihiko WATANUKI[1] and Tetsuya TORII[3]

[1]Department of Chemistry, College of Arts and Sciences, University of Tokyo, 8-1, Komaba 3-chome, Meguro-ku, Tokyo 153, Japan
[2]National Institute of Polar Research, 9-10, Kaga 1-chome, Itabashi-ku, Tokyo 172, Japan
[3]Japan Polar Research Association, 8-7, Kojimachi 1-chome, Chiyoda-ku, Tokyo 100, Japan

INTRODUCTION

Antarctica is extremely harsh for biological activity and presently no vascular plants are distributed in the continent, except in the northern part of the Antarctic Peninsula. Antarctica was a part of Gondwanaland from late Precambrian to Jurassic ages, and would have provided a favorable habitat for vascular plants throughout the continent, except in the period of Paleozoic continental glaciation. After the breakup of Gondwanaland, relatively warm climatic conditions in the pre- and inter-glacial periods of Antarctica are believed to be suitable for biological activity, including vascular plants.

Although Antarctica is covered with an ice sheet with an average thickness of 2450 m, at present ice-free areas are sparsely distributed in coastal regions and inland mountains. The McMurdo Dry Valleys of Southern Victoria Land are the largest ice-free areas in Antarctica, extending approximately 2500 km^2. Moraines containing various glacially eroded materials are distributed in the valley depressions, and are considered to be a key material to elucidate the paleoenvironment of Antarctica. Here we discuss organic components in soil samples obtained from moraines in the McMurdo Dry Valleys in relation to distribution of vascular plants during the pre- and inter-glacial periods in Antarctica.

STUDIED SITES

The McMurdo Dry Valleys mainly consist of Taylor, Wright and Victoria Valleys (Fig. 1). Floors and some parts of walls of these valleys are covered with morainic and fluvioglacial deposits of Pliocene to Holocene ages. Soil-like materials can be found in the deposits in many places. In December 1981 and 1983, surface soil samples (0-10 cm) were collected from the east side of Don Juan Pond (Don Juan samples) in the Wright Valley, and the surroundings of Lake Bonney (Bonney samples) in the Taylor Valley.

CHARACTERISTICS OF ORGANIC COMPONENTS

Analytical results of organic components in soil samples are reported elsewhere (MATSUMOTO *et al.*, 1981, 1990a, b, c; Table 1). A series of *n*-alkanes (C_{13}-C_{35}) and *n*-alkenes (C_{15}-C_{35}) were detected with a predominance of odd-carbon numbers, as evidenced by high carbon preference indices. Normal-

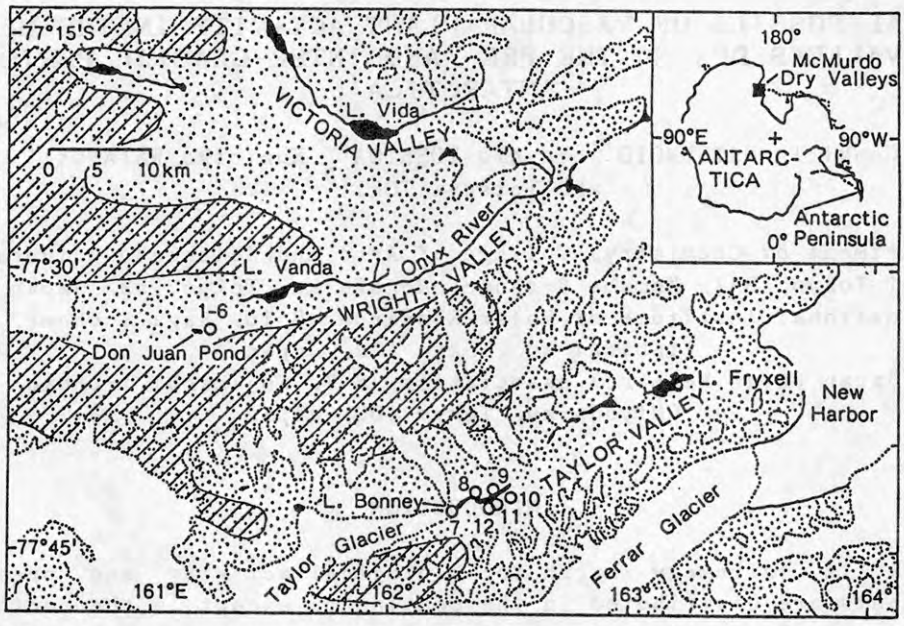

Fig. 1. Sampling locations in the McMurdo Dry Valleys of Southern Victoria Land, Antarctica. ⊡: Ice-free areas. ▨: Beacon Supergroup (modified from BARRETT and KYLE, 1975). Sampling site: 1-6, Don Juan-1 to Don Juan-6; 7, Bonney-W1; 8, Bonney-C1; 9, Bonney-E2; 10, Bonney-E8; 11, Bonney-E9; 12, Bonney-E12.

alkanoic acids (C_8-C_{40}) with a predominance of even-carbon numbers were found, together with small amounts of iso- and anteiso-alkanoic, and n-alkenoic acids. 3-Hydroxy (C_8-C_{30}) and (ω-1)-hydroxy (C_{22}-C_{30}) acids were detected with a predominance of even-carbon numbers, but 2-hydroxy (C_8-C_{30}) and ω-hydroxy (C_8-C_{30}) acids showed no even-carbon predominance. Small amounts of iso- and anteiso-2-hydroxy and 3-hydroxy acids were present in the soil samples. α,ω-Dicarboxylic acids (C_8-C_{31}) were detected with near unity values of carbon preference indices; mainly the C_{13} dicarboxylic acid predominated.

The major pentacyclic compounds in the Don Juan samples were triterpenes, such as hop-17(21)-ene, neohop-13(18)-ene and hop-22(29)-ene as well as triterpanes i.e., 17β(H)-22,29,30-trisnorhopane, 17β(H),21β(H)-hopane and/or 17β(H),21β(H)-homohopane, while those in the Bonney samples were mainly 17β(H)-22,29,30-trisnorhopane, 17α(H),21β(H)-30-norhopane and 17α(H),21β(H)-hopane. The major steranes and diasteranes in the Don Juan samples were (20S)-5α(H),14α(H),17α(H)-cholestane, (20R)-5α(H),14α(H),17α(H)-cholestane, (20R)-24-methyl-5α(H),14β(H),17β(H)-cholestane/(20R)-24-methyl-5β(H),14α(H),-17α(H)-cholestane, (20R)-24-ethyl-5α(H),14β(H),17β(H)-cholestane/(20R)-24-ethyl-5β(H),14α(H),17α(H)-cholestane, and/or (20R)-24-ethyl-5α(H),14α(H),-17α(H)-cholestane. Generally, the pentacyclic compounds and sterane compositions of the Bonney samples are more complex than those of the Don Juan samples, and comprise many isomerized forms (MATSUMOTO et al., 1990b).

(20S/20R)-24-Ethyl-5α(H),14α(H),17α(H)-cholestane ratios (0.03-0.66) and (22S/22R)-17α(H),21β(H)-homohopane ratios (0.01-1.1) revealed that organic components in the soil samples have been received various thermal stresses (e.g. SEIFERT and MOLDOWAN, 1981; PHILP, 1986; Table 1).

Table 1. Geochemical markers for sources and thermal maturation of organic components found in soil samples from the McMurdo Dry Valleys of Southern Victoria Land, Antarctica

Sample	n-Alkane		n-Alkene		n-Alkanoic acid		2-Hydroxy acid		3-Hydroxy acid		ω-Hydroxy acid		α,ω-Dicarboxylic acid		Sterane		Triterpane
	Long/short*	CPI#	Long/short*	CPI#	Long/short*	CPI#	Long/short*	CPI#	Long/short*	CPI#	Long/short*	CPI#	Long/short*	CPI#	$C_{29}/C_{27}$$	(20S/20R)-C_{29}¥	(22S/22R)-C_{31}¦
Wright Valley																	
Don Juan-1	3.4	2.3	49	6.5	0.85	1.5	ND	ND	ND	ND	ND	ND	ND	ND	1.3	0.16	0.18
Don Juan-2	5.5	2.3	330	5.2	3.0	1.8	3.5	0.77	1.3	2.9	0.45	0.97	0.66	0.98	0.89	0.18	0.30
Don Juan-3	2.0	2.7	99	4.1	0.91	1.8	0.92	0.89	0.61	2.7	0.25	1.0	0.23	0.99	0.89	0.10	0.29
Don Juan-4	9.1	2.8	16	3.4	2.7	2.8	1.9	1.3	0.63	5.6	1.7	1.3	0.66	1.0	3.5	0.03	0.10
Don Juan-5	6.5	2.3	16	4.9	1.7	2.0	1.9	1.2	0.53	2.8	0.94	1.1	0.55	0.91	3.6	0.04	0.01
Don Juan-6	13	1.9	Large	3.0	2.0	2.0	3.6	1.5	0.88	3.4	0.45	1.1	0.85	0.87	1.3	0.20	0.22
Taylor Valley																	
Bonney-W1	6.1	2.0	17	17	ND	ND	0.93	3.0	0.03	22	0.13	1.4	0.46	0.80	0.46	0.49	0.55
Bonney-C1	6.9	1.5	Large	7.8	0.95	2.0	1.6	1.8	0.35	1.3	0.22	0.91	0.05	0.85	1.2	0.65	1.0
Bonney-E2	16	1.9	Large	3.5	1.0	3.0	2.3	1.6	0.27	5.6	0.20	1.0	0.42	0.80	1.0	0.56	0.71
Bonney-E8	8.9	1.4	Large	1.6	1.2	1.9	1.8	1.7	ND	ND	0.14	1.0	0.20	0.82	0.93	0.66	1.1
Bonney-E9	15	1.8	Large	3.2	1.4	2.4	1.9	1.1	0.07	6.4	0.12	0.91	0.03	0.98	1.2	0.57	1.1
Bonney-E12	11	2.0	Large	3.2	0.80	3.0	0.86	1.5	0.23	4.9	0.16	0.91	0.14	0.83	1.1	0.47	0.62

*Long (C_{20}-C_{34})/short (C_{12}-C_{19}) ratios for straight chain components.
#CPI values show odd/even-carbon ratios for n-hydrocarbons, and even/odd-carbon ratios for straight chain acid components.
$(20R)-24-Ethyl-5α(H),14α(H),17α(H)-cholestane/(20R)-5α(H),14α(H),17α(H)-cholestane ratio.
¥(20S/20R)-24-Ethyl-5α(H),14α(H),17α(H)-cholestane ratio.
¦(22S/22R)-17α(H),21β(H)-30-Homohopane ratio.
Large: No short-chain n-alkenes were found.
ND: No data.

SOURCES OF ORGANIC COMPONENTS

A large variety of organic compounds suggest that organic matter in the soil samples is derived from various organisms ranging from bacteria to vascular plants, with various ages from Devonian (Beacon Supergroup) to Holocene. Especially, abundance of long-chain n-alkanes and n-alkanoic acids in the soil samples strongly suggests that organic matter was largely derived from vascular plants. However, no vascular plants are presently distributed in the McMurdo Dry Valleys and adjacent regions. Therefore, direct contribution of vascular plants is unlikely. Also, no aeolian transport of the waxes of vascular plants from the mid and lower latitudes is important source (MATSUMOTO et al., 1981, 1990a). Detailed microscopic studies reveal that no living cyanobacteria and microalgae are occur, but small amounts of their debris are found in some soil samples (MATSUMOTO et al., 1990a). Also, no n-alkenoic acids were abundant in all the soil samples. Hence, living organisms are not important sources of these organic components. Visual kerogen implies that the main sources of organic matter are microorganisms and ancient vascular plants (MATSUMOTO et al., 1990b).

Cyanobacterial mats containing various microorganisms are commonly distributed in and around the streams, lakes and ponds of the McMurdo Dry Valleys. Katabatic wind in the valleys is strong and, thus the wind-transportation of these microbial materials may be responsible for the sources of soil organic matter. Also, some organic matter may have produced by in situ microbial activity, and accumulated for a geological time. Certain short-chain n-alkanes and n-alkanoic acids, n-alkenes, and hydroxy acids may have attributed to these cyanobacterial mats as well as microbial activity (MATSUMOTO et al., 1990a, b). However, long-chain components and organic components having low CPI values are uncommon in these cyanobacterial mats (MATSUMOTO et al., 1979; MATSUMOTO, 1989). Thus, wind-transported cyanobacterial mats are not important sources of these organic components in the soil samples, and long-chain compounds are probably attributed to the following two candidate sources: (1) Erosion of the Beacon Supergroup, and (2) vascular plant debris in the pre- and inter-glacial periods.

The Beacon Supergroup of Gondwanaland sediments is widely distributed in the high altitude areas (>1500 m asl) of the McMurdo Dry Valleys and adjacent regions (e.g., BARRETT and KYLE, 1975; Fig. 1). The Beacon Supergroup often contains fossils of vascular plants, such as Glossopteris. MATSUMOTO et al. (1986, 1987) reported hydrocarbons and fatty acids in these sedimentary rocks in the same area, although their compositions are much different from those in the soil samples. Especially, long-chain components having relatively high CPI values are not abundant in the Beacon Supergroup samples. Also, the Beacon Supergroup in this region contains triterpanes and steranes having a wide variety of maturation from near zero to equilibrium ratios (MATSUMOTO et al., 1987). It is consistent with those of the soil samples (Table 1). α,ω-Dicarboxylic acid distributions in the soil samples are very different from recent sediments where even-carbon numbered dicarboxylic acids usually predominate, but similar to those in ancient sediments, e.g. Scottish Torbanite (Carboniferous), in which no even-carbon dicarboxylic acids predominate (DOUGLAS et al., 1970; Table 1). It is probable, therefore, that these dicarboxylic acids, straight-chain compounds having low CPI values, and some cyclic compounds are derived from the Beacon Supergroup. The soil samples, however, contain considerable amounts of triterpenes and less matured triterpanes and steranes, indicating the presence of young organic matter due

to biological activity other than that in the Beacon Supergroup. Thus it is unlikely that the Beacon Supergroup is important sources of long-chain components in the soil samples.

After isolation of Antarctica from Gondwanaland, relatively warm climatic conditions may have provided a favorable habitat for various organisms, including vascular plants in the McMurdo Sound region. Palynomorphs and a Nothofagus leaf impression in the CIROS-1 drillhole (702m long, 36-34.5 Ma and 30.5-22 Ma) suggest that cool temperature forest form on the foothills of the Transantarctic Mountains and persisted through several glacial cycles (e.g., BARRETT et al., 1989; HARWOOD et al., 1989; HILL, 1989). Also, parenchymatous and woody tissues are found in the Sirius Formation (3.1-2.5 Ma) of the Beardmore Glacier region in Transantarctic Mountains (ca 85°S; ASKIN and MARKGRAF, 1986). Relatively warm climatic conditions prevailed in this region when portions of the Sirius Formation were deposited (WEBB et al., 1987). These biological materials including vascular plant debris are probably buried beneath the ice-sheet during glacial periods under a favorable condition for preservation of organic matter. These materials are glacially eroded and transported to the valley depressions as moraines. Long-chain n-alkanes and n-alkanoic acids in the soil samples are probably attributed to these vascular plant debris. Also, (20R)-5α(H),14α(H),17α(H)-C_{29}/C_{27} sterane ratios in 7 of 12 soil samples are greater than unity, supporting that organic components in the soil samples are originated from certain vascular plants, although some cyanobacteria/green algae are possible sources (MATSUMOTO et al., 1990b; Table 1).

CONCLUSIONS

Organic components in the soil samples from the McMurdo Dry Valleys of Southern Victoria Land, Antarctica were discussed focused on vascular plant activity in the past. Complex organic components in the soil samples are attributed to the mixing of various source organisms ranging from bacteria to vascular plants with different ages from Devonian to Holocene, rather than from living organisms. Especially, the predominance of long-chain compounds strongly suggests that vascular plants were distributed in the McMurdo Dry Valleys and adjacent regions during the pre- and inter-glacial periods of Eocene-Pliocene.

Acknowledgments - We are greatly indebted to the Antarctic Division, DSIR, New Zealand, US National Science Foundation, US Navy, Japan Polar Research Association and National Institute of Polar Research for their support in Antarctic research.

REFERENCES

ASKIN R. A. and MARKGRAF V. (1986): Antarct. J. U. S., 21(5), 34-35.

BARRETT P. J. and KYLE R. A. (1975): In Gondwana Geology (Edited by CAMPBELL K. S. W.), pp. 333-346, Aust. Natl Univ. Press, Canberra.

BARRETT P. J., HAMBREY M. J., HARWOOD D. M., PYNE A. R. and WEBB P. -N. (1989): In Antarctic Cenozoic History from the CIROS-1 Drillhole, McMurdo Sound (Edited by BARRETT P. J.), DSIR Bull., 245, pp. 241-251, Wellington.

DOUGLAS A. G., DOURAGHI-ZADEH K., EGLINTON G., MAXWELL J. R. and RAMSAY J. N.

(1970): In Advances in Organic Geochemistry 1966 (Edited by HOBSON G. D. and SPEERS G. C.), pp. 315-334, Pergamon Press, Oxford.
HARWOOD, D. M., BARRETT P. J., EDWARDS A. R., RIECK H. J. and WEBB P. -N. (1989): In Antarctic Cenozoic History from the CIROS-1 Drillhole, McMurdo Sound (Edited by BARRETT P. J.), DSIR Bull., 245, 231-239, Wellington.
HILL R. S. (1989): In Antarctic Cenozoic History from the CIROS-1 Drillhole, McMurdo Sound (Edited by BARRETT P. J.), DSIR Bull., 245, pp. 143-144, Wellington.
MATSUMOTO G. I. (1989): Hydrobiologia, 172, 265-289.
MATSUMOTO G., TORII T. and HANYA T. (1979): Mem. Natl Inst. Polar Res., Spec. Issue, 13, 103-120.
MATSUMOTO G., TORII T. and HANYA T. (1981): Nature, 290, 688-690.
MATSUMOTO G. I., FUNAKI M., MACHIHARA T. and WATANUKI K. (1986): Mem. Natl Inst. Polar Res., Spec. Issue, 43, 149-158.
MATSUMOTO G. I., MACHIHARA T., SUZUKI N., FUNAKI M. and WATANUKI K. (1987): Geochim. Cosmochim. Acta, 51, 2663-2671.
MATSUMOTO G. I., AKIYAMA M., WATANUKI K. and TORII T. (1990a): Org. Geochem., 15, 403-412.
MATSUMOTO G. I., HIRAI A., HIROTA K. and WATANUKI K. (1990b): Org. Geochem., 16, 781-791.
MATSUMOTO G. I., WATANUKI K. and TORII T. (1990c): Proc. NIPR Symp. Antarct. Geosci., 4, 165-171.
PHILP R. P. (Ed., 1986): In Fossil Fuel Biomarkers. Applications and Spectra. Methods in Geochemistry and Geophysics No. 23, 294 pp., Elsevier, Amsterdam.
SEIFERT W. K. and MOLDOWAN J. M. (1981): Geochim. Cosmochim. Acta, 45, 783-794.
WEBB P. -N., McKELVEY B. C., HARWOOD D. M., MABIN M. C. G. and MERCER J. H. (1987): Antrct. J. U. S., XXII(1), 8-13.

ROCK WEATHERING PROCESSES IN THE SØR RONDANE MOUNTAINS, EAST ANTARCTICA

N. Matsuoka, Institute of Geoscience, University of Tsukuba, Tennodai, Tsukuba 305, Japan

Introduction

Inland ice-free mountains in Antarctica are situated in the coldest periglacial environments in the earth as well as in extremely arid environments. The Sør Rondane Mountains, more than 100 km from the nearest coast, belong to such an extreme environment. The ground thaws to not more than 40 cm below surface, indicating that rock weathering and the transport of weathering products occur only in surface layers.

Previous studies on rock weathering in Antarctica showed that physical weathering is more important than chemical weathering because of low temperature and limited moisture availability (e.g. Kelly and Zumberge, 1961). Nevertheless, with the exception of some chemical weathering and soil studies (e.g. Campbell and Claridge, 1987), quantitative and analytical undertakings are extremely limited. This report deals with rates and products of physical weathering as well as the links between physical and chemical weathering as indicated by the measurement of rock decay and the analysis of weathering products.

Frost weathering, insolation weathering and unloading

The record of rock surface temperature indicates that north-facing

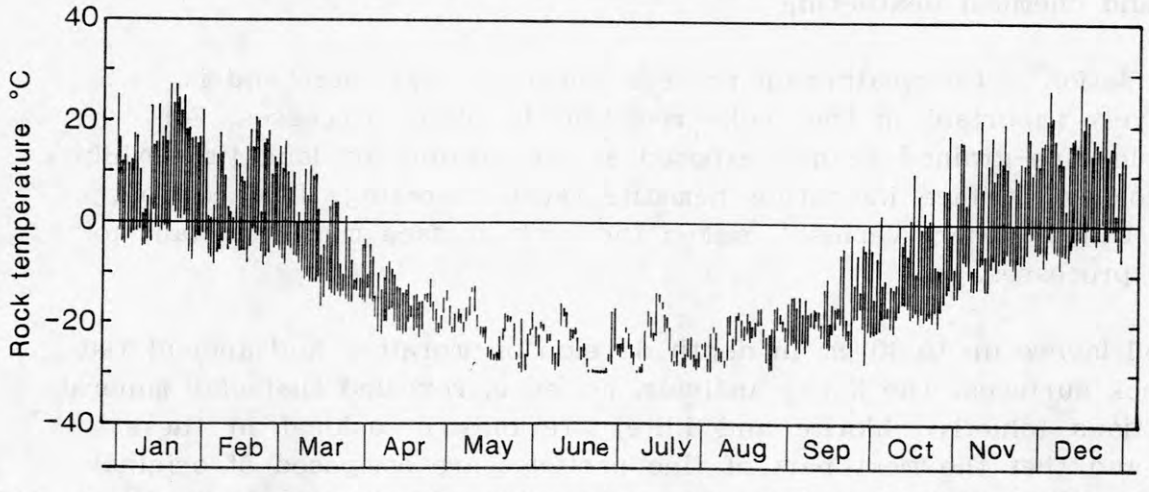

Fig. 1 Annual fluctuation in rock surface temperature (1.5 cm depth) at the northwest-facing rockwall. Daily ranges are shown with solid lines. Note that records are limited within ±30° C. (after Matsuoka et al., 1990)

rockwalls are subject to frequent diurnal freeze-thaw cycles during summer (Fig. 1). The freeze-thaw frequency is similar to that in mid-latitude alpine environments where frost weathering is predominant (e.g. Matsuoka, 1990). Rock decay from the painted rockwalls, however, was quite slow during 6 years. Only thin, small fragments less than 5 cm fell down through exfoliation or granular disintegration from the rockwalls. This is due to low moisture content in the bedrock, usually 30-40 % in the degree of saturation. Under such a limited moisture condition, ice in rock joints cannot exert enough pressure for enlarging the joint. Frost weathering is only active on the bedrock and stones with high moisture contents, sources of which are the snow spray by wind, snowpatches on rockwall and the ice core below thin moraine cover. Shattered fragments accumulating in such environments are indicative of frost weathering. The diameter of these fragments rarely exceeds several tens cm, or the maximum thaw depth.

Large temperature ranges in summer may also cause insolation weathering. Some experimental studies (e.g. Griggs, 1936) have suggested that rocks do not break ever during multiple temperature cycles. Thus it may be that insolation weathering cannot produce small fragments but large blocks.

Boulders larger than 1 m, lying on some scree slopes, are considered to be produced chiefly by unloading accompanied by glacial retreat. Sheeting joints whose intervals are similar to the diameter of the boulders developed on the surface of rockwalls above the scree slopes. This process may produce large volume of debris at a time from steep rockwalls despite operating only during the period of glacial retreat.

Salt and chemical weathering

Oxidation is the weathering process working everywhere and is relatively important in the rocks resistant to other processes. For example, fine-grained granite exposed at the ground for long time exhibits red-colored surface indicating hematite (Fe_2O_3) coating. This coating, often called 'desert varnish', makes the rock surface more resistant to other processes.

Soil layers up to 40 cm in depth develop on moraines and ancient flat bedrock surfaces. The X-ray analysis, however, revealed that clay mineral formations (chiefly chlorite and illite) are only occasional in these soils and that the most part of fine particles are composed of original minerals and salts. The salts appear either as distinct layers or scattered throughout such soils. This indicates that salt weathering is primarily responsible for the rock fragmentation and the soil development. Mineral alteration due to chemical weathering seems to be quite slow

despite solution of the bedrock being essential in the formation of salt. The most common weathering forms in the Sør Rondane Mountains are exfoliation and granular disintegration, often combined with tafoni and mushroom-like features. Frequent occurrences of salts in weathering products (soils and weathered rocks) indicate the importance of salt weathering. This finding was also supported by the field experiment on rock pieces (soft tuff) that contained thenardite, which broke down completely in only 5 years.

Table 1 Salt occurrences in soils and in weathered rocks

Salt	Formula	Number of identification
Gypsum	$CaSO_4 \cdot 2H_2O$	64
Thenardite/	Na_2SO_4	11
Mirabilite	$Na_2SO_4 \cdot 10H_2O$	
Epsomite/	$MgSO_4 \cdot 7H_2O$	10
Hexahydrite	$MgSO_4 \cdot 6H_2O$	
Jarosite	$KFe(SO_4)_2(OH)_6$	9
Calcite	$CaCO_3$	6
Bloedite	$Na_2Mg(SO_4)_2 \cdot 4H_2O$	5
Alunites	$MgAl_2(SO_4)_4 \cdot 22H_2O$	3
	$KAl(SO_4)_2 \cdot 11H_2O$	
	$FeAl_2(SO_4)_4 \cdot 22H_2O$	
	$Al_2(SO_4)_3 \cdot 18H_2O$	
Nitratite	$NaNO_3$	2

Several salt phases were identified from weathering products (Table 1). Cations in these salts probably derive from chemical solution of the bedrock, because all cations are contained in rock-forming minerals. Being negligible in the minerals, most anions may derive from precipitation. Among several phases, gypsum is most widespread. Other sulfates, for example, thenardite and epsomite mostly distribute in warm sites or in old soils. This suggests that calcium ion dissolves most readily under low temperature while the solution of sodium and magnesium ions needs much time or warmer environments.

The ice-free mountains seem to have lost their height mainly through salt weathering and subsequent transport of fine fragments by wind. Figure 2 shows the geological section of a flat bedrock surface composed of dipped layers of metamorphic and intrusive rocks. Granite and aplite (quartz dyke) occupy the high position where tafoni and mushroom-like features are common. The surface of lower parts, mainly composed of gneiss and amphibolite, exhibits desert pavement under which fine soils and salt

layers develop. Mushroom-like boulders of granite distribute only one side of the ridge and were thus left through the lowering of the dipped bedrock. This enables us to estimate the former height and denudation rate of the flat surface. The surface would have lowered 27 m in average by the subaerial processes during more than several million years: the age is estimated in terms of the weathering stage. The mean denudation rate of the surface is then calculated to be less than 2 cm/1000 yrs.

Summary of weathering processes

Interaction among weathering processes is illustrated in Fig. 3. The type of weathering is basically dependent on moisture conditions. Frost weathering works on the bedrock with high water content; however, such a condition is uncommon in the Sor Rondane Mountains. In the most parts of the mountains with limited moisture supply, chemical solution of the bedrock, combined with precipitation, leads to the salt segregation which at the same time gives physical damage to the bedrock. The salt weathering produces rock fragments and causes soil formation while the subsequent transport of the fine particles by wind lowers the ground surface despite the rate of erosion being quite small.

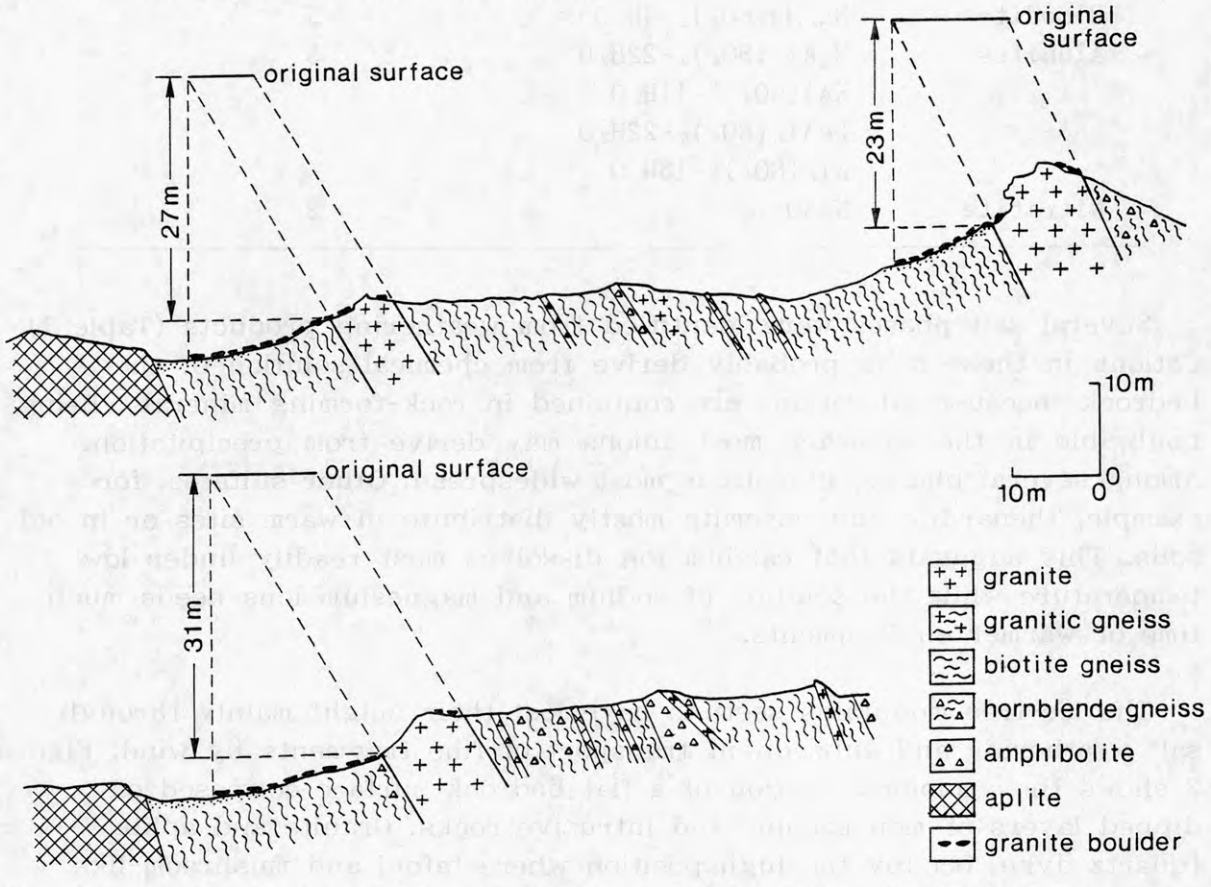

Fig. 2 Geological sections of a flat mountain ridge of Brattnipene, showing the estimated heights of the original surface.

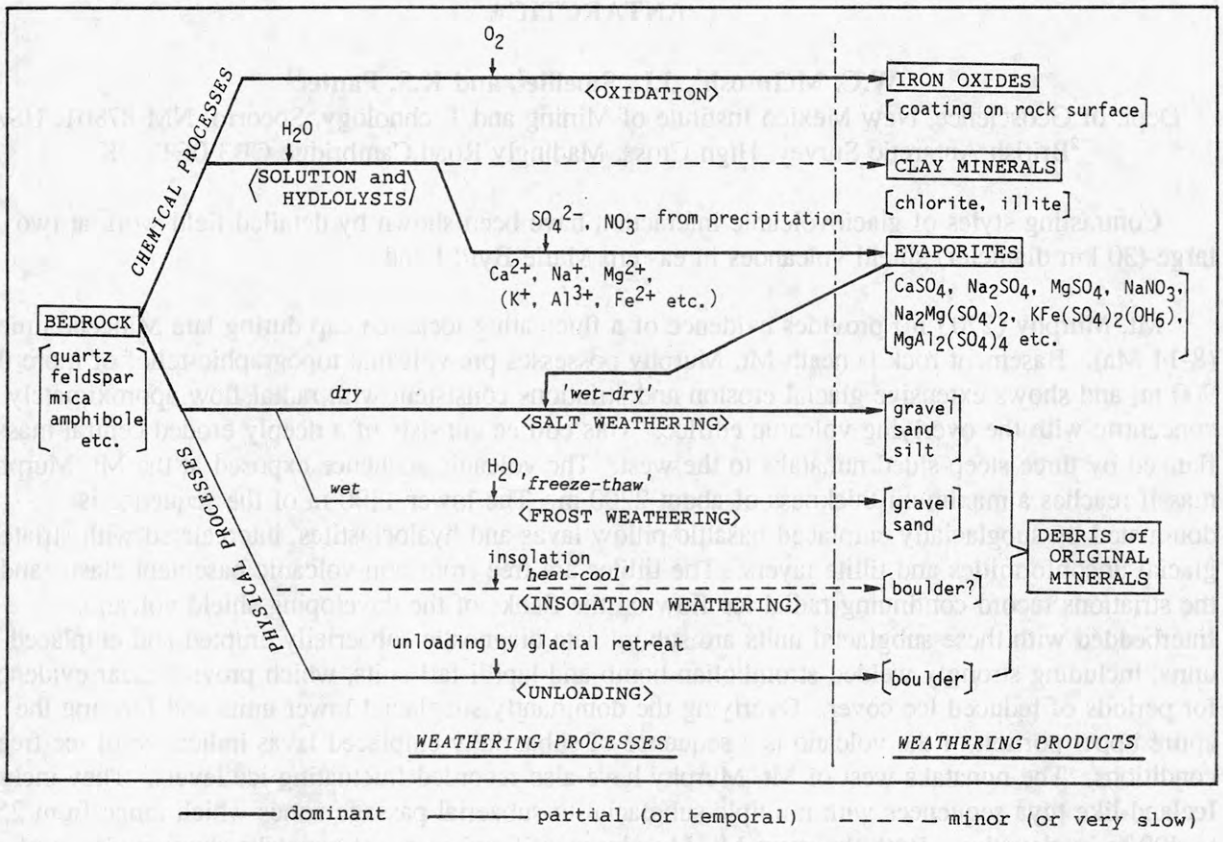

Fig. 3 Summary of rock weathering processes in the Sør Rondane Mountains.

References

Campbell, I.B. and Claridge, G.G.C. (1987): *Antarctica: Soils, Weathering Processes and Environment.* Development in Soil Sciences **16**, Amsterdam, Elsevier, 368p.

Griggs, D.T. (1936): The factor of fatigue in rock exfoliation. *Jour. Geol.*, **44**, 783-796.

Kelly, W.C. and Zumberge, J.H. (1961): Weathering of a quartz diorite at Marble Point, McMurdo Sound, Antarctica. *Jour. Geol.*, **69**, 433-446.

Matsuoka, N. (1990): The rate of rock weathering by frost action: field measurements and a predictive model. *Earth Surface Processes and Landforms*, **15**, 73-90.

Matsuoka, N., Moriwaki, K., Iwata, S. and Hirakawa, K. (1990): Ground temperature regimes and their relation to periglacial processes in the Sør Rondane Mountains, East Antarctica. *Proc. NIPR Symp. Antarc. Geosci.*, **4**, 55-66.

GLACIOVOLCANIC INTERACTIONS IN EASTERN MARIE BYRD LAND, ANTARCTICA

W.C. McIntosh[1], J.L. Smellie[2], and K.S. Panter[1]
[1]Dept. of Geoscience, New Mexico Institute of Mining and Technology, Socorro, NM 87801, USA
[2]British Antarctic Survey, High Cross, Madingly Road,Cambridge CB3 0ET, UK

Contrasting styles of glaciovolcanic interaction have been shown by detailed field work at two large (30 km diameter) shield volcanoes in eastern Marie Byrd Land.

Mt. Murphy (2703 m) provides evidence of a fluctuating local ice cap during late Miocene time (8-14 Ma). Basement rock beneath Mt. Murphy possesses pre-volcanic topographic relief of more than 900 m, and shows extensive glacial erosion and striations consistent with radial flow approximately concentric with the overlying volcanic edifice. This edifice consists of a deeply eroded central massif flanked by three steep-sided nunataks to the west. The volcanic sequence exposed at the Mt. Murphy massif reaches a maximum thickness of about 2200 m. The lower 1100 m of the sequence is dominated by subglacially emplaced basaltic pillow lavas and hyaloclastites, intercalated with striated glacial unconformities and tillite layers. The tillites are free from non-volcanic basement clasts, and the striations record continuing radial ice flow on the flanks of the developing shield volcano. Interbedded with these subglacial units are subordinate diagnostic subaerially erupted and emplaced units, including strongly welded strombolian bomb and lapilli fall units, which provide clear evidence for periods of reduced ice cover. Overlying the dominantly subglacial lower units and forming the entire upper portion of the volcano is a sequence of subaerially emplaced lavas indicative of ice-free conditions. The nunataks west of Mt. Murphy have also recorded fluctuating ice levels. They include Iceland-like tuya sequences with multiple subglacial-to-subaerial passage zones which range from 250 to 400 m in elevation. Both the main Mt. Murphy massif and adjacent nunataks show evidence of post-volcanic overriding by the continental ice sheet. Surfaces showing striations not radial to volcanic topography and strewn with non-volcanic erratics extend as high as 950 m above the present 800 m level of the surface of the continental ice sheet south of the volcano.

In contrast to Mt. Murphy, Mt. Takahe (3460 m) provides evidence for relatively small (<400 m) fluctuations in the level of the late Quaternary continental ice sheet. Located 100 km southwest of Mt. Murphy, Mt. Takahe is a little-dissected <0.5 Ma shield volcano surrounded by the continental ice sheet with a surface elevation of about 1300 m. Exposures at Mt. Takahe are dominated by subaerial lavas, some of which extend at least as low as the present continental ice level. Subglacial pillow lavas and hyaloclastites are confined to three localities, each of which includes a subglacial-to-subaerial passage zone located 350 to 400 m above the present continental ice level. No evidence was found for post-volcanic glacial overriding of Mt. Takahe's flanks.

The differences in glaciovolcanic history between Mt. Murphy and Mt. Takahe can be attributed to a number of factors. The *syn-eruptive* record at Mt. Murphy documents alternating subglacial and subaerial conditions, which are interpreted as evidence for a relatively thin and unstable *local* icecap during late Miocene time. The *post-eruptive* record at Mt. Murphy indicates fluctuations in the level of the *continental* ice sheet much larger than those shown by the *syn-eruptive* record at Mt. Takahe. This difference probably in part reflects Mt. Murphy's coastal location and ability to act as a barrier to ice flow, as compared to the isolated inland location of Mt. Takahe.

$^{40}Ar/^{39}Ar$ dating work presently in progress promises to provide much improved age constraints for the glaciovolcanic histories of these two volcanoes.

THE PAGODROMA EVENT — A LATE PLIOCENE MAJOR EXPANSION OF THE ANCESTRAL LAMBERT GLACIER SYSTEM

B.C. McKelvey, Department of Geology and Geophysics, University of New England, Armidale NSW 2351, Australia.
M.C.G. Mabin, Department of Geography, James Cook University, Townsville QLD 4811, Australia.
D.M. Harwood, Department of Geology, University of Nebraska, Lincoln NE 68588, United States of America.
P.N. Webb, Department of Geological Sciences, Ohio State University, Columbus OH 43210, United States of America.

In the northern Prince Charles Mountains the upper Pliocene glacigene Pagodroma Tillite blankets much of eastern Amery Oasis, and residuals also outcrop on the top and flanks of nearby Fisher Massif. The Pagodroma Formation includes marine lodgement tillites and other tidewater glacier facies deposited by an ancestral phase of the Lambert Glacier system. Some parts of the formation almost certainly predate others and may be terrestrial. Preservation is due to late Cenozoic uplift of the strata to above the surrounding glacier ice surfaces.

The Pagodroma Tillite occurs in sequences up to 400 m thick, although most total less than 150 m. The base of the formation ranges in altitude from sea level up to approximately 1450 m, and rests on an erosion surface cut in Proterozoic metamorphics and Permian fluvial strata. The erosion surface is a composite one. Locally pre-Pagodroma event fluvially(?) cut rugged landforms are preserved, but generally the erosion surface is glacially cut and smoothed. Striations and grooves are widespread and indicate palaeo-ice-flow directions compatible with the present Lambert Glacier drainage system. No widespread younger glacigene strata overlie the ablated rolling surface of the Pagodroma Tillite. Only relatively restricted alpine glacier moraines locally cover the tillites. However, in many places the formation has been partially or completely removed by subsequent glacial and fluvioglacial erosion.

In Amery Oasis the Pagodroma Tillite is predominantly a marine lodgement tillite containing marine and non-marine reworked microfossils ranging in age from Late Cretaceous to mid-Pliocene. Sparse reworked bivalve debris is also present. The reworked fossils are derived from higher latitude (subglacial) older strata probably located within the confines of the Lambert Graben. Abundant *in situ* Late Cenozoic bivalves occur in laminated glaciomarine facies at the mouth of Pagodroma Gorge.

The marine depositional settings of the Pagodroma Tillite contrast with that of the coeval terrestrial Sirius Group of the Transantarctic Mountains. However, the presence of reworked marine microfossils of similar ages in both these units points to the same late Pliocene expansion of the East Antarctic ice sheet following a major early to mid-Pliocene interglacial marine transgression.

THE GEOPHYSICAL OBSERVATORY AT TERRA NOVA BAY

A. Meloni, A. De Santis, A. Morelli, P. Palangio and G. Romeo, Istituto Nazionale di Geofisica, Via di Villa Ricotti 42, 00161 ROMA - ITALY.

E. Bozzo, G. Caneva, Dip. Scienze della Terra, Sez. di Geofisica, Università di Genova, Viale Benedetto XV,5, 16132 GENOVA - ITALY.

In the framework of the ItaliAntartide Project a geophysical observatory has been installed in Terra Nova Bay, Antarctica. Two disciplines were undertaken: Geomagnetism and Seismology.

The main objectives for the installation of the Geomagnetic Observatory started in 1986/87 Austral summer, were:

a) to provide a data-base for reduction of the magnetic survey measurements;

b) to measure the elements of the magnetic field in order to provide absolute values and the secular variation trend for the area;

c) to obtain data to investigate the time variation of the geomagnetic field;

d) to supply values to World Data Center for the definition of the IGRF.

All data after five Austral summer observations have been reduced and results are shown together with a discussion of time variation.

During the Austral summer 1988-89 a high quality seismic station has been installed and tested close to the Terra Nova Bay Italian Base. The sensors comply to the Very Broad Band specifications, with an instruments response flat on ground velocity in the frequency band from 8 Hz to 3 mHz, and the digitizers allow a dinamic range og 140 dB. For such a sensitive instrumentation the installation was made inside a 8-meter tunnel in granite. On the 1988-89 expedition the seismograph was kept running for a test period of about one month. Data analysis revealed a rather low background noise level, which is expected to decrease significantly after slow mechanical settling of the sensore.

Starting from the Austral summer 1990-91 the Observatory will start continuous unmanned operation. Continuous power will be provided by a new system and data acquisition will be on the micro VAX of the Base. A satellite communication link with the Base computer will allow to monitor the state of the instrumentation, as well as to view and transfer data of events of special interest.

For what concerns especially seismology the presence of this station in Antarctica, a continent otherwise devoid of such high-quality instrumentation, because of its unique location will contribute greatly to global seismology, and to the study of local seismicity.

Precambrian crustal evolution of the Adélie Land (East Antarctica) : preliminary results

R.P. Ménot, University, URA CNRS n°10, 23, rue Dr. P. Michelon,
42023 SAINT ETIENNE cédex 02, FRANCE
C. Delor, B.R.G.M. Service géologique, BP 6009, F - 45060 ORLEANS cédex 2, FRANCE
J.J. Peucat, C.A.E.S.S.- CNRS, University, Campus de Beaulieu,
35042- RENNES cédex, FRANCE
A. Giret, University, URA CNRS n°10, 23, rue Dr. P. Michelon,
42023 SAINT ETIENNE cédex 02, FRANCE

Geological data about the Adélie Land are scarce and have been drawn out from the scientific explorations of Stillwell (1923) (Mawson expeditions (1911-1914), Heurtebise (1952), Bellair (1961) and Bellair and Delbos (1962) (French Polar Expeditions). They bore evidence for a granitic and gneissic basement, mainly described in the Port Martin and Pointe Géologie areas. According to Bellair and Delbos (1962), cordierite-sillimanite and garnet bearing gneisses have been reworked by successive anatectic events and a 14OO Ma age was defined for the latest granitic intrusions.

A recent project (1990-1994) has been set up by the Scientific Commitee of the french TAAF (Terres Australes et Antarctiques Françaises), the French Polar Expeditions and the University of Saint Etienne. Its purpose involves a detailed mapping of the Adélie Land coastal area and up-to-date petrological and geochronological studies of the basement rocks.

In such scope, some results may be enhanced after the field investigations, during the 1991 antarctic summer trip, and preliminary analyses of previously sampled rocks :

(i) comparable chronological successions of magmatic and tectono-metamorphic events can be recognized in different places of the Adélie Land,

(ii) granulitic parageneses have been discovered as relics of a very early metamorphic stage,

(iii) some old granites, now outcropping as orthogneisses, have been dated. Their crystallization age is about 2.4 Ga (U-Pb, zircons).

Such data, together with the previously published results, imply a crustal evolution of Archean age that probably ended in Medium Proterozoic times. They seem to be, pro parte, at variance with the recent synthetic view of Stüwe and Oliver (1989).

The present works on the Terre Adélie geology might give a new insight into the Early Precambrian generation of the Gondwana crust.

Stillwell F.L. (1923) - The metamorphic rocks of Adélie land. Australasian Antarctic Expedition (1911-1914), Scient. reports, vol. III, part 1, sect.1.
Heurtebise G.(1952) - Sur les environs de Port Martin. C.R.Acad. Sci., Paris, 234, 1380-1382.
Heurtebise G. (1952) - Sur les formations géologiques de Terre Adélie, C.R.Acad. Sci., Paris, 234, 2209-11.
Bellair P. (1961) - Sur les formations anciennes de l'archipel de le Pointe Géologie (Terre Adélie). C.R. Acad.Sci., Paris, 252, 3087-3089.
Bellair P. (1962) - Pétrographie du socle cristallin de la Terre Adélie. C.R.Acad.Sci., Paris, 252, 3296-3298.
Bellair P. and Delbos L. (1962) - Age absolu de la dernière granitisation en Terre Adélie. C.R.Acad.Sci., Paris, 1465-1466.
Stüwe K. and Oliver R. (1989) - Geological history of Adélie Land and King George V Land, Antarctica : evidence for a polycyclic metamorphic evolution. Precamb. Res., 43, 317-334.

Sixth International Symposium on Antarctic Earth Sciences
9-13 september 1991, Kaga, Itabashi, Tokyo, Japan

MAFIC AND ULTRAMAFIC IGNEOUS SUITES IN THE LAMBERT-AMERY RIFT ZONE
(poster presentation)

E.V. Mikhalsky, A.V. Andronikov and B.V. Beliatsky,
North Branch for Marine Geologic Research and Exploration "SEVMORGEOLOGIA", 120 Moyka, 190121 Leningrad, USSR

The Lambert-Amery rift stretches across the East Antarctic Precambrian Shield from the sea cost for at least 700 km inland. Igneous rocks are widespread along the length of the rift. They vary in composition from alkaline-ultrabasic and tholeiitic to acidic and form dyke swarms, small plutons, sills, stocks and rare volcanic strata (Fig.1). Isotopic age determinations of mafic rocks have shown 2400, 1800, 1380, 420, 320, 120-145, 50 Ma (Tingey, 1976; Sheraton, England, 1980; Sheraton, 1983; Collerson, Sheraton, 1986; Hofmann,1986; Laiba et al., 1987).

Geologic setting and petrogenetic characteristics of basic and ultrabasic igneous rocks are important indications of lithospere extension and rifting. In this report the dyke swarms in Vestfold Hills, Mawson Escarpment, Mt. Collins, Beaver Lake area, plutons at Mt. Willing and Mt. Collins, stocks and sills in Jetty Peninsular are considered as manifestations of deep-seated processes preceding to and accompanying Gondwana breakup.

According to Australian geologists (Sheraton et al.,1987; Kuehner, 1987) basic dykes in the Vestfold Hills (VH) high-grade Archean metamorphic terrane belong to three intrusive episodes: (1) sublongitudinal dykes of high-Mg tholeiites dated at 2400 Ma, (2) sublatitudinal tholeiitic dykes intruded at the Low/Upper Proterozoic boundary (c.1800 Ma), and (3) N-S trending tholeiitic and alkaline basic dykes of Late Proterozoic age (1380 Ma). Our field observations show that the most ancient high-Mg tholeiites form not only sublongitudinal but also latitudinal dykes parallel to 1800 Ma system and often change their trend to NE (Fig.2a). In addition to previously described dyke groups new systems were recognized: (1) NW trending tholeiitic dykes that cut the Early Proterozoic bodies but are transected by the Riphean (c.1400 Ma) tholeiites, and (2) NNE trending (Fig.2b) alkaline lamprophyres which are cut by the dated Riphean dykes but transect all older systems. These lamprophyres are of specific significance since their alkaline character (Fig.3) and the presence of deep-seated nodules may be related to ancient rifting in the area.

Alkaline lamprophyres consist of phenocrysts of clinopyroxene (Ca_{48} Mg_{40} Fe_{12}), olivine and phlogopite (f=38, MgO=18%, TiO_2=6.5%) enclosed in relatively fresh, well

crystallized groundmass of carbonate+phlogopite and/or plagioclase. No modal alkaline minerals were recorded. Small carbonate-feldspar globules are common. Colour index varies from 55 to 95-100, and Mg number is 50-75. According to petrographical and geochemical screen of Rock (1987), these rocks are defined as (K-Na biotite-augite) camptonites although less evolved varieties resemble ultramafic lamprophyres (e.g. in SiO_2, K_2O, MgO abundances). Field evidence suggests that more salic dykes may represent a relatively older portion of a common melt responsible for generation of both melanocratic and leucocratic varieties. Zr/Nb, Zr/Y ratios are consistent with a model of heterogeneous fluid-rich source region and its advanced partial melting during progressive deepening.

In places the lamprophyre dykes thicken into lensoid bodies of similar composition with abundant small deep-seated nodules represented by dunites, plagioclase-bearing lherzolites, spinel lherzolites and harzburgites, garnet-bearing lherzolites. Some nodules may originate from the depth as much as 80 km.

In the southern part of the Mawson Escarpment numerous dykes of basic rocks intersect the upper-amphibolite to granulite facies terrane. They are of different trends (Fig.2c) and compositions. At least two chemically distinct age groups have been recognised. The earlier dykes trending WE or SW-NE are composed of high-Mg (and high-Cr) metatholeiites and amphibolites. The age of these rocks has been preliminary determined by U-Pb zircon study as 2400 Ma. Less evolved members of high-Mg suite have a higher Zr content that might be due to alkaline character of primary melt. The younger group is probably of a Late Proterozoic age as suggested by some authors (Tingey, 1982) for dyke suites in the southern Prince Charles Mountains (PCM), and is chemically comparable with the Vestfold Hills c. 1400 Ma tholeiites.

A large body of metamorphosed syenites and monzonites is exposed at Mt.Collins in the central PCM. These rocks are considered to have crystallized at 1400±80 Ma (U-Pb zircon data) and undergone subsequent thermal events at 1200, 870-900 and 500 Ma. Metasyenites are cut by numerous metamorphosed basic dykes of variable trends (Fig.2d) and composition (Fig. 3) and partly of alkaline character probably indicated by Zr- and Ba-enrichment. The presence of metasyenite intrusion and accompanying dyke suite of Late Proterozoic age confirms a Late Precambrian extensional igneous activity in the central PCM.

A layered gabbroid complex is exposed at Mt.Willing some 30 km to the south. The rocks are mainly gabbro-norites, gabbro, norites (some are Ol-bearing) with minor

hornblende gabbro and ferrogabbro-norites at the uppermost part of the exposed section. The latter is at least 3 km thick. Along shear zones the rocks are converted to amphibolites. The cumulus assemblage changes upwards from Opx+Cpx+Pl to Opx+Pl± Ol±Cpx and Pl+Cpx±Opx±Hrb±Mt. Nine samples define a Sm-Nd whole-rock isochron of 1187±145 Ma corresponding probably to a recrystallization event. Relatively high values of ε_{Nd} =1.5-3.5 are thought to indicate a low degree of crustal contamination of depleted mantle derived initial melt. The Mt.Willing layered complex might have originated during the same Late Proterozoic (c.1400 Ma) extensional event as other mafic intrusions in this region.

The Phanerozoic igneous rocks belong to alkaline series. Rare Middle Paleozoic (K-Ar age 420 Ma; Sheraton, England, 1980) high-K lamproite dykes are known from the southern PCM (Mt.Bayliss, Mt.Rubin). Late Paleozoic (K-Ar age 320 Ma) dykes of alkaline dolerites and alkaline lamprophyres are widespread in the Beaver Lake area forming a dense N-S trending swarm in Jetty Peninsula (Fig.2e). This igneous event directly predates the formation of paleorift graben filled by a Permian coal-bearing sequence.

An Early Cretaceous (120-145 Ma) complex of K-Na alkaline-ultramafic rocks in Jetty Peninsula comprises small stocks following a N-S major fault zone, sills and dykes intruded into Precambrian metamorphic terrane and Paleozoic sedimentary strata. The stocks were formed during three successive melt injections. Olivine-melilite tuffisite breccias were followed first by melilite lamprophyres and then by alkaline picrites and ultramafic foidites. Deep-seated nodules are abundant in all stocks and represented by garnet-bearing and spinel lherzolites, garnet-free dunites, harzburgites and wehrlites. Formation of this complex is believed to record an initial stage of Gondwanaland breakup. The latest igneous event in this region is dated at 50 Ma and represented by a thin flow of K-rich basalts (Ol-Lc trachybasalts) at Manning Massif.

Data presented in the paper suggest recurrent tectono-thermal events in the Lambert-Amery rift zone that were manifested in several igneous episodes. The earliest record of extensional igneous activity in brittle sialic crust is represented by Early Proterozoic (2400-1800 Ma) tholeiites. The first rift-related magmatism is believed to occur at c.1400 Ma when the oldest alkaline rocks of K-Na character were formed. Subsequent accumulation in a depleted mantle source region of K-rich mineral phases (phlogopite) was not released until Middle Paleozoic time marked by intrusion of lamproitic dykes. Ancient regional fracture zones marked by linear dyke swarms (Early Proterozoic predominantly W-E trending and Late Proterozoic N-S trending) were revived, and

a new ENE direction was developed in Phanerozoic time (Fig.2f). In late Paleozoic a renewed K-Na magmatic activity began in relation to initial pre-breakup rifting; it lasted until the major breakup event at c.145-120 Ma. This was again succeeded by a period of mantle degasation which was terminated by an extrusion of Early Cenozoic K-rich basalts coeval with final opening of the South Indian Ocean.

REFERENCES

Collerson K.D., Sheraton J.W., 1986. Age and geochemical characteristics of a mafic dyke swarm in the Archaean Vestfold Block, Antarctica: inferences about Proterozoic dyke emplacement in Gondwana. J. Petrol., 27, 4, p. 853-886.

Hofmann I., 1986. Bruchtektonik und Magmatism im kristallinen Fundament der Octantarktischen Plattform. Freiberg. Unpudlished report.

Irvine T.N., Baragar W.R.A., 1971. A guide to the chemical classification of the common volcanic rocks. Can. J. Earth Sci., 8, p. 523-548.

Kamenev E.N., Kameneva G.I., 1990. Structural and metallogenic provinces in Antarctica (in Russian). In: Ivanov V.L., Kamenev E.N., eds. The geology and mineral resources of Antarctica. Moscow, "Nedra", p. 15-40.

Kuehner S.M., 1987. Mafic dykes of the East Antarctic Shield: a note on the Vestfold Hills and Mawson Coast occurrences. In: Halls H.C., Fahrig W.F., eds. Mafic dyke swarms. Geol. Assoc. of Canada spec. paper, 34, p. 429-430.

Laiba A.A., Andronikov A.V., Egorov L.S., Fedorov L.V., 1987. Stock-like bodies and dykes of alkaline-ultramafic rocks in Jetty Peninsula (Prince Charles Mountains, East Antarctica) (in Russian). In: Ivanov V.L., Grikurov G.E. Geological and geophysical research in Antarctica. Leningrad, VNIIOkeangeologia, p. 35-47.

Sheraton J.W., 1983. Geochemistry of mafic igneous rocks of the northern Prince Charles Mountains, Antarctica. J. Geol. Soc. Austral., 30, p. 295-304.

Sheraton J.W., England R.N., 1980. Highly potassic mafic dykes from Antarctica. J. Geol. Soc. Austral., 27, p. 129-135.

Sheraton J.W., Thomson J.W., Collerson K.D., 1987. Mafic dyke swarms of Antarctica. In: Halls H.C., Fahrig W.F.,eds. Mafic dyke swarms. Geol. Assoc. Canada spec. paper, 34, p. 419-432.

Tingey R.J., 1976. Basic and alkaline intrusive rocks in the Prince Charles Mountains. Bur. Min. Res. Rep., 194, p.73.

Tingey R.J., 1982: The geologic evolution of the Prince Charles Mountains - an Antarctic Archean cratonic block. In: Craddock C., ed. Antarctic Geoscience. Univ. Wisconsin Press, Madison, p. 455-464.

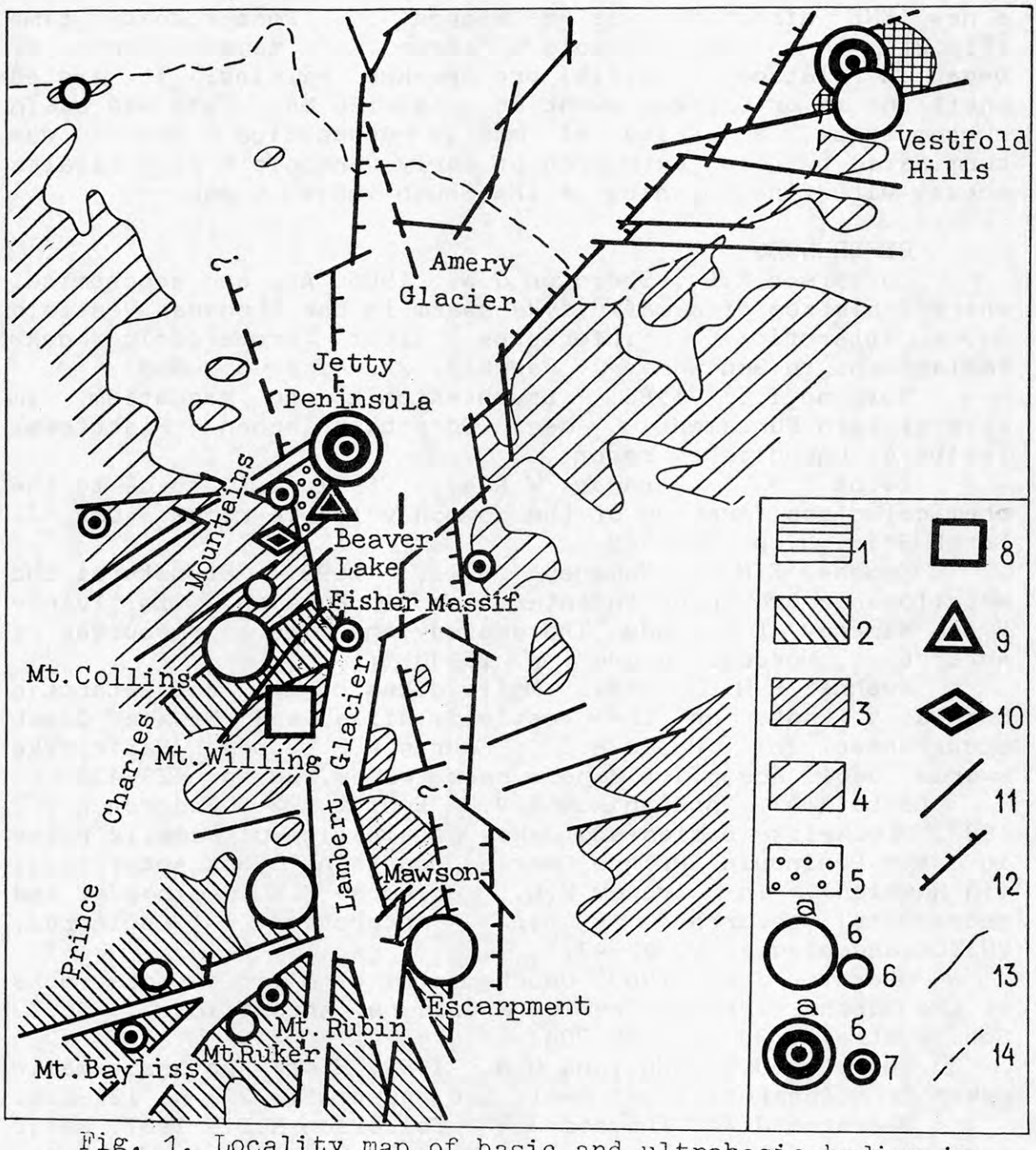

Fig. 1. Locality map of basic and ultrabasic bodies in relation to basement geology.

1-4 - basement geology (after Kamenev, Kameneva, 1990): 1-Vestfold Hills granulites (Archean), 2- Fisher and Ruker greenstone belts (respectively Late Proterozoic and Late Archean), 3-transitional granite-gneiss-schist belts, 4-granulite-gneiss mobile metamorphic belt (Proterozoic); 5-Permian coal-bearing strata; 6,7 - locations of dykes: 6-of tholeiitic and calc-alkaline composition, 7-of alkaline composition (a-dense swarms, b-rare dykes); 8 - location of gabbroid plutons; 9 - location of alkaline ultramafic stocks, sills and dykes; 10 - location of alkaline basalt flow; 11,12 - fault zones: 11-recent, 12-of Paleozoic (?) generation; 13 - contours of bedrock above sea level; 14 - coast line.

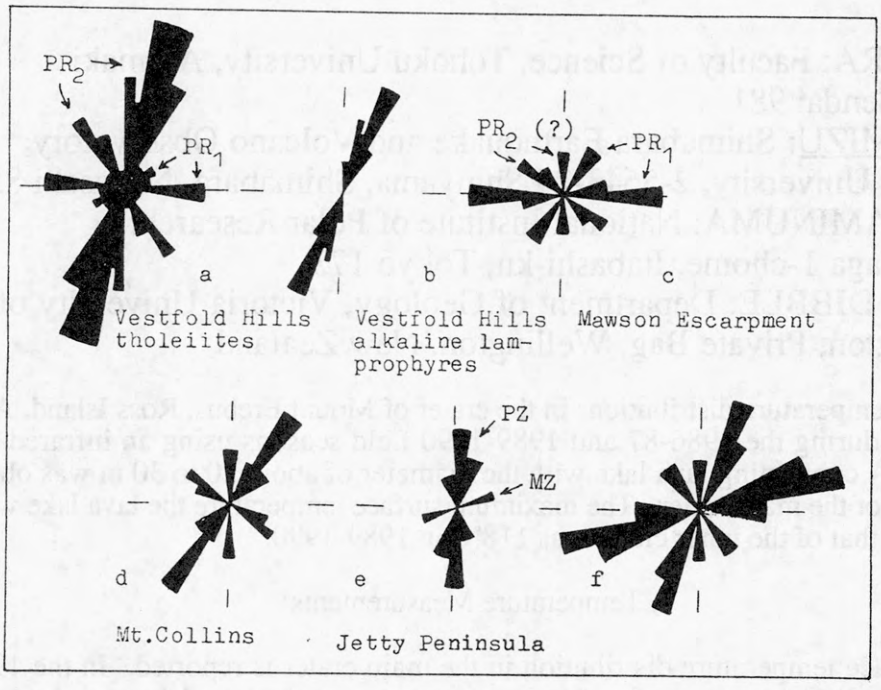

Fig. 2. Rose diagrams for main dyke swarms (a-e) and post-dyke (predominantly recent) fracture zones at Vestfold Hills (f).

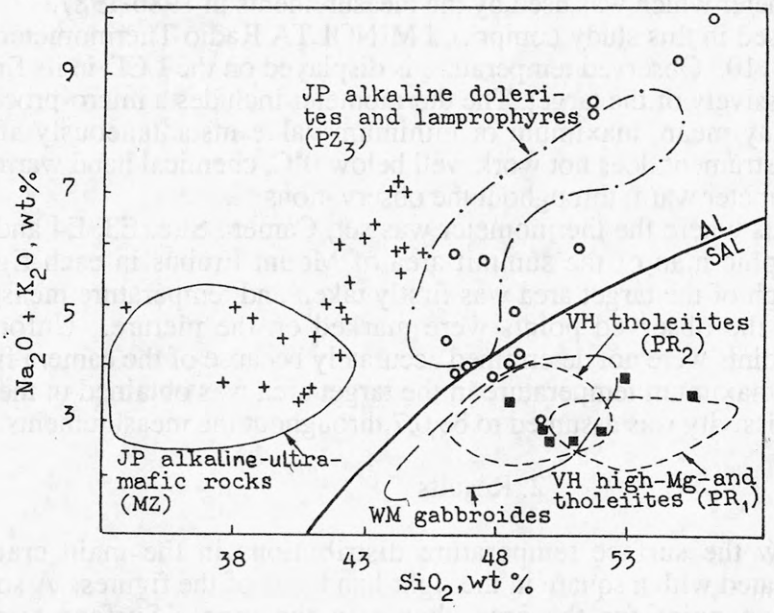

Fig 3. SiO_2 - (Na_2O+K_2O) diagram.

Crosses - Vestfold Hills alkaline lamprophyres, boxes - Mawson Escarpment metabasites, circles - Mt.Collins metabasites. Fields of different igneous rocks at individual localities are shown by contours: JP - Jetty Peninsula, WM - Mt.Willing, VH - Vestfold Hills.

Alkaline (AL) -subalkaline (SAL) dividing line after Irvine and Baragar (1971).

SURFACE TEMPERATURE MEASUREMENTS IN THE CRATER OF MOUNT EREBUS, ROSS ISLAND, ANTARCTICA

Satoshi MIURA: Faculty of Science, Tohoku University, Aramaki Aoba, Sendai 981
Hiroshi SHIMIZU: Shimabara Earthquake and Volcano Observatory, Kyushu University, 2-5643-29 Shinyama, Shimabara, Nagasaki 855
Katsutada KAMINUMA: National Institute of Polar Research, 9-10, Kaga 1-chome, Itabashi-ku, Tokyo 173
Raymond R. DIBBLE: Department of Geology, Victoria University of Wellington, Private Bag, Wellington, New Zealand

Surface temperature distributions in the crater of Mount Erebus, Ross Island, Antarctica were surveyed during the 1986-87 and 1989-1990 field seasons using an infrared radiation thermometer. A convecting lava lake with the diameter of about 20 to 30 m was observed in the inner crater of the main crater. The maximum surface temperature the lava lake was 798°C in 1986-87 and that of the inner crater was 118°C in 1989-1990.

1. Temperature Measurements

The surface temperature distribution in the main crater is reported. In the 1986-1987 field season, the measurements of surface temperatures on the lava lake and the crater wall were carried out using an infrared radiation thermometer to study the mechanism of energy transfer concerning the persisting lava lake (Miura et al. 1988). Eruptions occurred from four vents on the solidified surface of the lava lake. In December 1989, the lava lake reappeared and eruptions occurred from it. The measurements of surface temperature was carried out using the same thermometer which was used by the measurements in 1986-1987.

The equipment used in this study comprised MINOLTA Radio Thermometer IR-0510 and Data Processor DP-110. Observed temperature is displayed on the LCD in its finder after a correction for the emissively of the target. The thermometer includes a micro-processor and can calculate and display mean, maximum or minimum value instantaneously after some samplings. Since the instrument does not work well below 0°C, chemical hand warmers were used to keep the thermometer warm throughout the observations.

Observation points where the thermometer was set, Camera Site, E3, E4 and E5, are indicated on a topographic map of the summit area of Mount Erebus in each figure. An instantaneous photograph of the target area was firstly taken and temperature measurements were carried out, then the observed points were marked on the picture. Unfortunately, locations of measured points were not determined accurately because of the camera finder was broken. Then only the maximum temperature in the target area was obtained in the 1989/90 measurements. The emissivity was assumed to be 0.7 throughout the measurements.

2. Results

Figures 1-4 show the surface temperature distributions in the main crater. The measurement area indicated with a square in the right-hand side of the figures. A solid circle indicates an observation point for the area shown in the map. Surface temperature distributions in °C are shown in the left-hand side of the figures. The values at the dotted points are the temperature measured in December 1986. The maximum temperature measured in the small square in 1989 was given by larger characters. Only the maximum temperature measured in each target area as shown with a small square was given because of locations of measurement points were not determined exactly for the camera finder trouble. The values in parentheses are the maximum temperatures whose measurements were disturbed by the fumarolic activity.

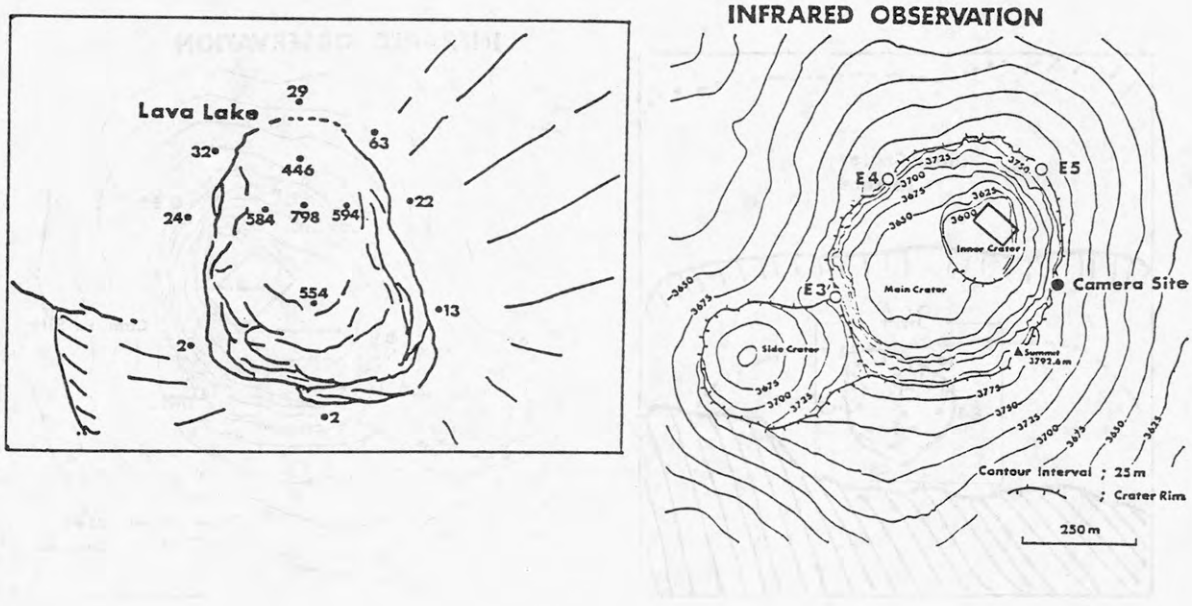

Fig.1 Surface temperature distribution in °C in the lava lake measured from Camera Site.

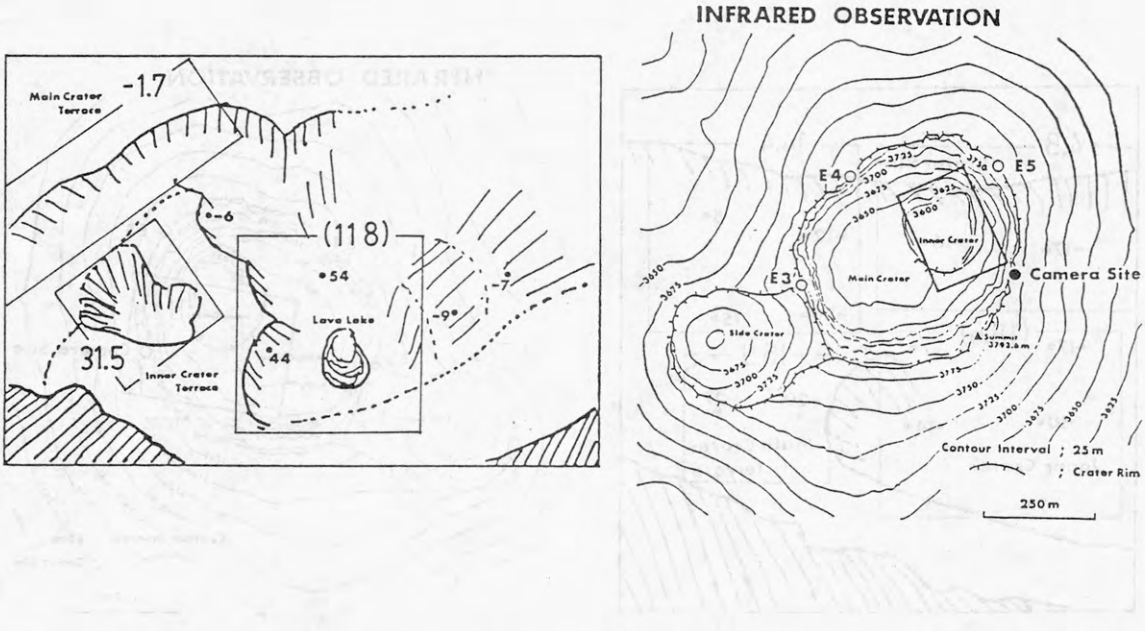

Fig.2 Surface temperature distribution in °C in the inner crater measured from Camera Site.

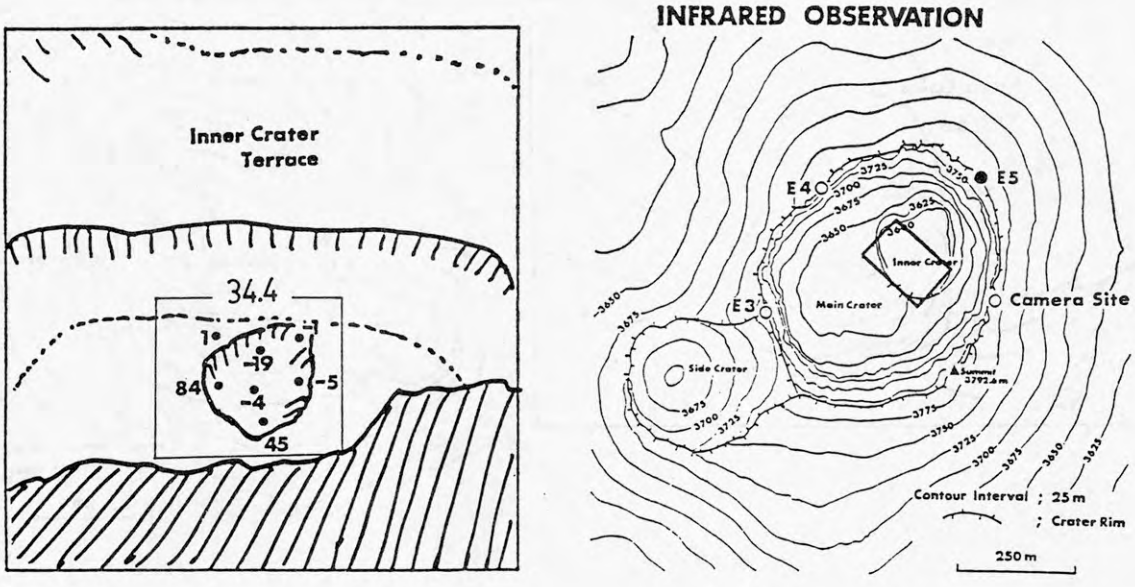

Fig 3 Surface temperature distribution in °C in the inner crater measured from E 5. A solid circle indicates the observation point.

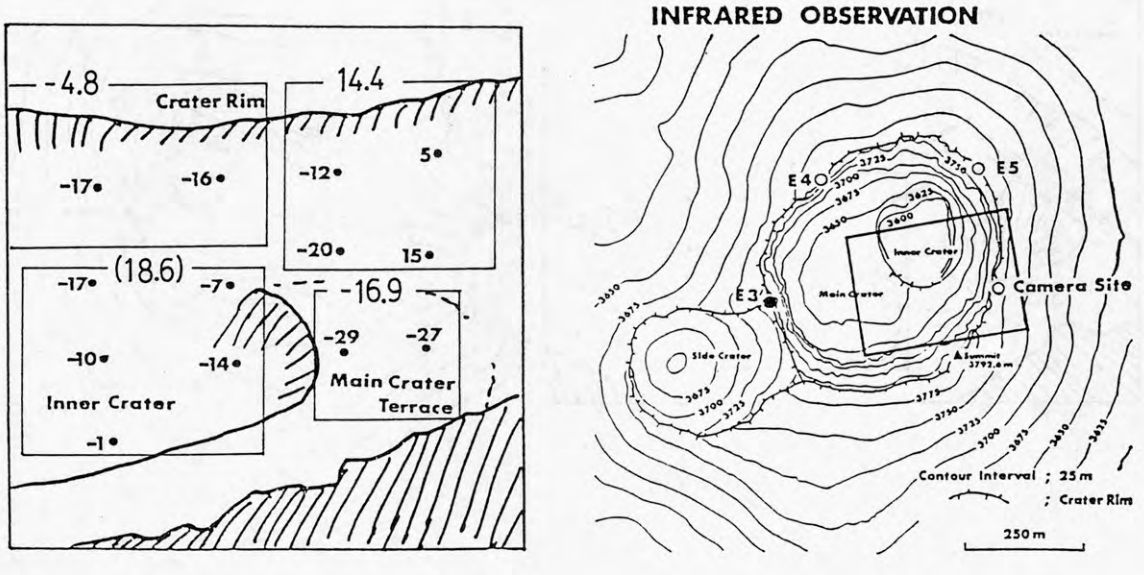

Fig. 4 Surface temperature distribution in °C in the eastern part of main crater measured from E 3.

Figure 1 is the measurments in the lava lake observed from Camera Site in December 1986. The maximum temperature observed was 798°C. In December 1989, the surface temperature of the lava lake was not measured because of novisivility of the lava lake from the rim by heavy fumarolic activity .

The temperature in the inner crater was 118°C, and those in the active vent and the northern edge of the main crater terrace were 31.5°C and -1.7°C respectively in December 1989 as shown in Fig. 2. The active vent locates in the southern part of the inner crater terrace. It was 54°C that the maximum temperature measured in the inner crater in December 1986. The observation point is also Camera Site in the measurements shown in Fig. 2.

The temperature in the inner crater measured at E5 ranged from -19°C to 84°C in December 1986 and was 34.4°C in December 1989 as shown in Fig. 3.

The observation point in Fig. 4 is E3. The temperature in the eastern part of the main crater ranged from -29° to 5°C in December 1986. The temperature in the southern part of the main crater terrace was -16.9°C and that in the southern part of the inner crater was 18.6°C in December 1989 as shown in Fig. 4. The temperatures in the eastern part of the crater wall were measured 14.4°C and -4.8°C in December 1989.

Acknowledgments

The authors express their sincere thanks to Messor Max. Wendon and Gerry Kennedy, field assistants of our party for their help in temperature measurements and stay in the summit area. The authors thanks are extended to Ms. F. Nakamura for preparing this manuscript.

References

MIURA, S., KAMINUMA, K., and DIBBLE, R. R., (1988): Temperature measurements in the crater of Mount Erebus, Ross Island , Antarctica. Proc. NIPR Symp. Antarct. Geosci., 2, 17-23.

SATELLITE IMAGERY AVAILABLE FOR THE STUDY OF GLACIAL AND GEOLOGICAL PROCESSES IN ANTARCTICA

B.F. Molnia, U.S. Geological Survey, Reston, VA 22092, USA
J.G. Ferrigno, U.S. Geological Survey, Reston, VA 22092, USA

In the last two decades, three satellite systems, Landsat, SPOT, and Sojuzkarta, have acquired about 30,000 high-resolution (between 6- and 80-m) images of Antarctica. These data have proven to be useful and cost effective for the study of glacial and geological processes in Antarctica. They have been used in a variety of research efforts, including monitoring coastal change, determining velocities of outlet glaciers and ice streams, defining blue-ice areas, tracking the movement of icebergs, and as a base for overlaying satellite radar images, radar altimetry, and geophysical data. This paper reviews the data acquired since 1972 by the three systems and illustrates where usable (minimal cloud cover) data are available.

Since 1972, the Landsat system has acquired more than 17,000 images. The Landsat 1, 2, and 3 satellites acquired approximately 10,000 multispectral scanner (MSS) (80-m pixel resolution) and return beam vidicon (RBV) (30-m pixel resolution) images of Antarctica in photographic and digital form between 1972 and 1983. The quality of the images was evaluated by the U.S. Geological Survey (USGS) to determine the feasibility of using them for glaciological, climatological, and geological research. Results plotted on a base map of Antarctica show that about 45 percent of the nominal scene centers, encompassing about 70 percent of the continent, are covered by usable imagery.

Landsat 4 started acquiring data in 1982 and Landsat 5 in 1984. Together the two satellites have acquired more than 7,000 thematic mapper (TM) (30-m pixel resolution) and MSS images of Antarctica through the 1990-91 austral summer. Computer evaluation of the Landsat 4 and 5 data indicates that about 1,700, or less than 25 percent, of the images have 10 percent cloud cover or less. However, it is difficult for automatic systems or those unfamiliar with the snow- and ice-covered areas of Antarctica to discriminate between clouds and snow. On the basis of our sampling of the data, it is more likely that 10 to 15 percent, about 700 to 1000 scenes, have 10 percent cloud cover or less. The scenes that have been examined and evaluated as part of the USGS/SCAR (Scientific Committee on Antarctic Research) cooperative acquisition project and are known to be of good quality provide cloud-free coverage of about 90 percent of the coastal and ice shelf areas. A plot combining the earlier and more recent Landsat data illustrates areas where temporal comparisons can be made.

More that 10,000 Sojuzkarta photographs, with 20 percent cloud cover or less, have been collected over Antarctica since 1976. The most useful data consist of photography from the KATE-200 system (20-m spatial resolution) and the KFA-1000 system (6-m spatial resolution). The data have been plotted by the USGS and will soon be available through the USGS open-file report series. Scenes that have been examined are excellent; however, an insufficient number of scenes have been inspected to evaluate the accuracy of the cloud-cover estimate.

The Systeme Probatoire d'Observation de la Terre (SPOT) was launched in 1986 and has acquired more that 1,500 scenes of Antarctica. SPOT data consist of multispectral (20-m pixel resolution) and panchromatic (10-m pixel resolution) images in photographic or digital format. SPOT also has the capacity to generate stereoscopic images. The coverage extends from the coastline to latitude 85°S. When the coverage of all three satellite systems is combined, more than 80 percent of Antarctica is covered by high-resolution, cloud-free, remotely-sensed data.

SEQUENCE STRATIGRAPHY OF THE CRARY FAN, SOUTHEASTERN WEDDELL SEA

*Moons, A., **Miller, H., *De Batist, M. & * °Henriet, J.P.

* Renard Centre of Marine Geology, Krijgslaan 281, B-9000 Gent, Belgium
** Alfred-Wegener-Institut für Polar- und Meeresforschung, Columbusstraße, D-2850 Bremerhaven, Germany
° present address : Département des Géosciences Marines, IFREMER, F-26280 Plouzané, France

Within the framework of the Belgian Antarctic Research Programme the Renard Centre of Marine Geology (RCMG) at the State University of Gent has participated in two cruises in the Weddell Sea organised by AWI (Bremerhaven, BRD). More than 6700 km of high-resolution reflection seismic profiles have been acquired in the eastern and southeastern Weddell Sea.

During the first cruise part of the reflection seismic profiles have been shot in association with the drilling operations of ODP Leg 113 off Cape Norvegia in the northeastern Weddell Sea. Site 693 has been used as a stratotype for an integrated seismic-stratigraphic reassessment of the Weddell Sea Basin. The depositional sequences identified on the seismic sections in the vicinity of site 693 are named W1, W2, W3, W4 and W5. The basal onlap unconformity WO1 (O : onlap) corresponds with the "Weddell Sea Continental Margin Unconformity", postulated of Late Middle Jurassic age. The top interval of sequence W3 was found to be of Aptian to Albian age. The deposits of sequence W4 have been assigned a middle Early Oligocene to Early or early Middle Miocene age. This implies that the WO4 unconformity represents a local hiatus of about 60 Myr. This seismic stratigraphic model has been extended towards the southeastern Weddell Sea. North of Halley Bay, the WO4 unconformity splits into two major sequence boundaries : a lower and strongly erosive surface WO4a and an upper WO4b.

A major feature in this southeastern part of the Weddell Sea is the Crary Fan depositional system. Its sediments, supplied through the Crary Trough, can be traced along large parts of the continental slope and rise, and in basinward direction over a distance of more than 400 km. The high resolution of the seismic data over the distal units of the Crary Fan off Halley Bay allowed a detailed analysis of sediment transport pathways and sediment accumulation mechanisms in the fan system. Eleven major submarine fan sequences, named WF0 to WF10 (Weddell Sea Fan), can be distinguished above the WO4b unconformity. They are associated with two main buried channel systems. The nine oldest sequences are associated with a N-S trending channel system situated in the western part of the study area. These sequences are outlapping against the sloping erosional surface WO4b on the eastern side of the channel. The termination of the sequences on the western side of the channel is still unknown. The two youngest sequences WF9 and WF10 are clearly associated with the second buried channel system with a NE-SW orientation, close to the foot of the upper continental slope.

The seismic facies of the channel fill sequences is very different from that of the actual fan deposits. Very large NE-SW aligned structures seem to be incorporated in the channel fill sediments, where they rest on top of the lower fill sequences. They probably can be interpreted as remnants of levee-like sedimentary units, though with a peculiar basal disharmonic stratal contact.

This detailed sequence-stratigraphic analysis of the various Crary Fan units provides a better insight in the sedimentary processes of this major fan system and in the mechanisms of sediment accumulation and distribution in the Weddell Sea basin.

Glacial history in the Sør-Rondane Mountains, East Antarctica
- Thick tills and evidence of warmer climate in the past -

K. MORIWAKI, National Institute of Polar Research, Kaga, Itabashi-ku, Tokyo 173, Japan
K. HIRAKAWA, Department of Geography, Tokyo Metropolitan University, Hachiouji-shi, Tokyo 192, Japan
S. IWATA, Department of Geography, Mie University, Kamihama-cho, Tsu 514, Japan
M. HAYASHI, Department of Geography, ShimaneUniversity, Nishikawatsu-cho, Matsue 690, Japan

A large part of the Sør-Rondane Mountains was once covered by an extended ice sheet (Van Autenboer, 1964; Iwata, 1987; Hirakawa *et al.*, 1988, 1990; Hayashi and Miura, 1989; Aniya, 1989). The mountains are in some places covered with tills which show various degrees of weathering. Relative ages of these tills have been classified into Stages 1,2,3 and 4 (from youngest to oldest) on the basis of the weathering characteristics of their surface gravels. The maximum stage of glaciation is prior to Stage 4 and has been assigned to Stage 5. The correlation with elapsed time of rocks since they were freed from ice (Nishiizumi *et al.*, 1991) gives the absolute time scale to the Stages as follows; Stage 1a: tens of thousands years ago; Stage 1b: a rather young period less than 1Ma; Stage 2: an older period less than 1Ma; Stage 3: 2-1Ma; Stage 4: 2-4Ma; Stage 5: prior to 4Ma (Moriwaki *et al.*, in press). These Stages 1-4 seem to correspond with the weathering stages 1-4 defined by Campbell and Claridge (1987). Tills of Stage 1 form thin moraine fields extending from the lower part of mountain slopes to the surrounding ice (their maximum relative height above the present ice surface (MRH): 30m), tills of Stage 2 form lateral moraines on the mountain slopes (MRH: 100m), and tills of Stages 3 and 4 are basal tills located on flat-topped mountains and on the floors of ice-free valleys (MRH: 600m).

Location and characteristics of the oldest tills: The surface of the oldest tills form reddish (2.5YR6/8 at the most) desert pavements in most places. Secondary salts are often present beneath surface gravels. Soil profiles below the desert pavement show mixed materials of silt to cobble size at every place. Salt horizons are recognized at a depth of 5 to 10cm in the soil profiles. The majority of salts are sulfates, in particular, gypsum is most common (Hayashi and Miura, 1989). Depth of the present permafrost table is between 20 and 30cm from the ground surface. Some of the tills attain several tens of meters in thickness. They outcrop at the top of steep walls of

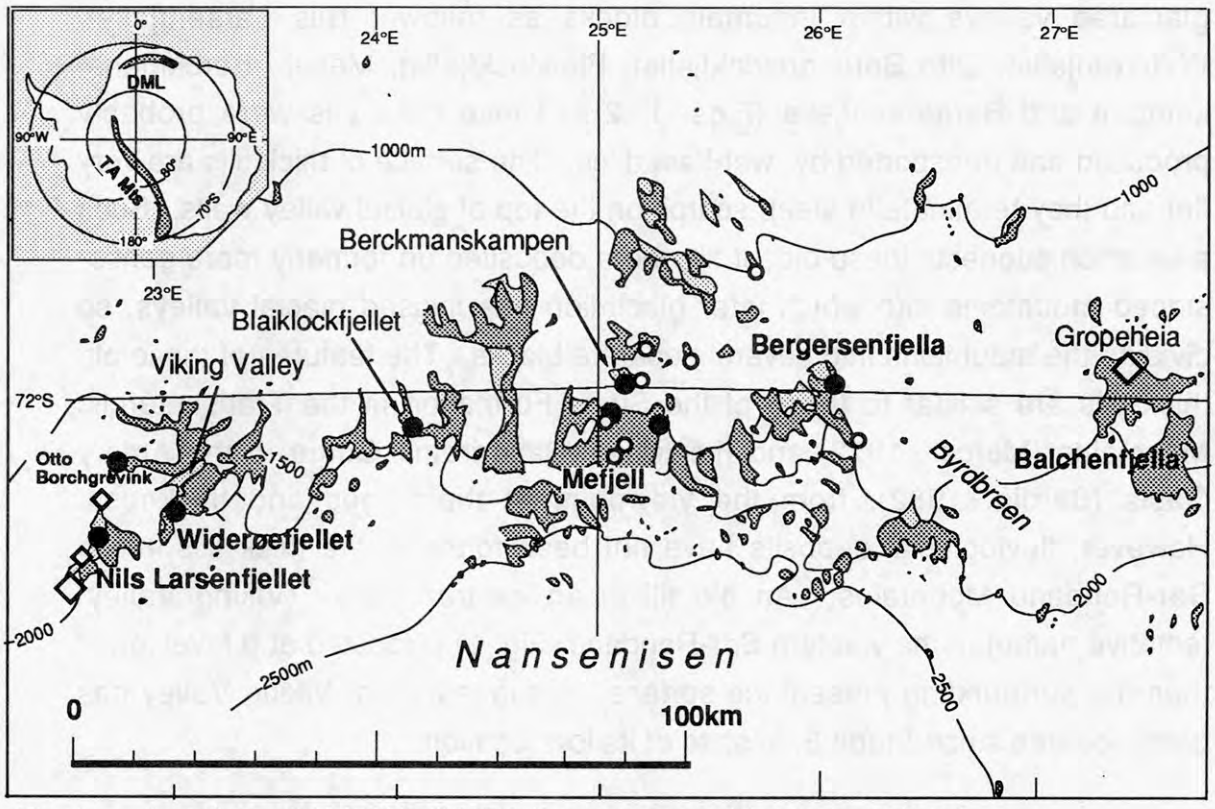

Fig. 1 Locations of thick till (solid circle), gypsum crystal (open square) and radiometrically dated rock (open circle) in the Sør-Rondane Mountains.

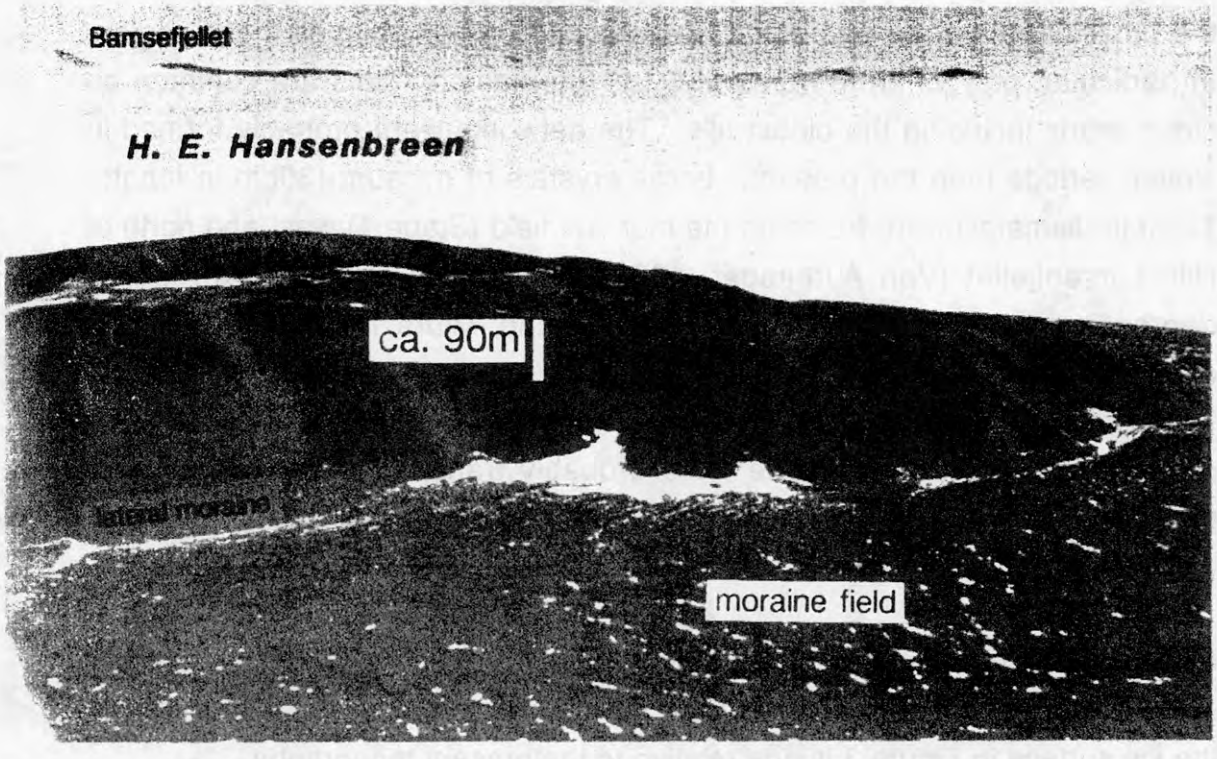

Fig. 2 Thick till in Nils Larsenfjellet, Western Sør-Rondane Mountains.

glaciated valleys within mountain blocks as follows; Nils Larsenfjellet, Widerøefjellet, Otto Borchgrevinkfjellet, Blaiklockfjellet, Mefjell, Berckmanskampen and Bergersenfjella (Figs. 1, 2). These thick tills were probably produced and transported by wet-based ice. The surface of thick tills are very flat and they terminate in steep scarps on the top of glacial valley walls. Such a situation suggests these oldest tills were deposited on formerly more gentle-sloped mountains into which later glaciation has incised glacial valleys, so dividing the mountains into several separate blocks. The features of these old thick tills are similar to those of the Sirius Formation in the Transantarctic Mountains (Mercer, 1972) and the tills of Pagodrome Gorge in the Amery Oasis (Bardin, 1982), from the viewpoint of their ages and thickness. However, fluvioglacial deposits have not been found in the thick tills in the Sør-Rondane Mountains. An old till in an ice-free valley (Viking Valley: tentative name) in the western Sør-Rondane (Fig. 1) is located at a level lower than the surrounding present ice surface. It suggests that Viking Valley has been ice-free since Stage 3, in spite of its low location.

Evidence of wetter and warmer environment in the past: This region is a periglacial environment at present. However frost action is insignificant owing to the very low water content of the ground (Matsuoka *et al.*, 1990). On the other hand, patterned ground is developed in many places in the region. In particular, polygonal networks of 5 to 10m diameter cells are common on older debris including the oldest tills. The networks were probably formed in wetter periods than the present. Large crystals of gypsum (30cm in length, 10cm in diameter) were found on the moraine field (Stage 1) west and north of Nils Larsenfjellet (Van Autenboer, 1964); and on the bottom of a ice-free depression in Gropeheia (Fig.1; Hayashi and Miura,1989). They grew obviously in water containing Ca and SO_4 ions. It suggests that lakes were formed during a former warmer climate in this region. Fragments of gypsum crystals in and on the moraine were probably transported from a place of production (*e.g.* a lake in a depression west of Nils Larsenfjellet, Fig.1) with till by subsequent glacial advance.

Glacial history (Fig. 3): We must consider tectonic and isostatic movements of the mountains, but we have not any data at present. Therefore, the level of the ice surface in Figure 3 is one relative to the present topography.

Stage 5: Former gentle-sloped Sør-Rondane Mountains with the exception of several high mountain peaks were covered by a wet-based ice sheet during

Miocene - early Pliocene. The ice sheet produced, transported and deposited a large quantity of the oldest till .

Stages 4-3: Deglaciation took place during Pliocene - early Pleistocene, and the oldest tills were exposed. Early periglacial processes possibly took place during the period. Retreated ice surface was probably lower than the present, judging from the low old till located in Viking Valley.

Stages 3-2: Subsequent glaciation eroded the valley systems that persist to the present day, dividing the mountains into several blocks.

Stage 2: A re-advancing ice sheet at around 1Ma was probably dry-based, and it formed only small lateral moraines on flanks of valley walls.

Stage 1b: Recessional or else re-advansing ice sheet formed small lateral moraines and/or thin moraine fields surrounding the mountains.

Stages 1b-1a: Deglaciation took place and lakes were formed in some ice-free depressions and on the ice surface. Gypsum crystals grew in the lakes. Periglacial processes occurred in the ice-free areas.

Stage 1a: Minor re-advancement of the ice sheet delivered gypsum crystals and formed thin moraine fields.

After Stage 1a: The ice sheet shrank a little.

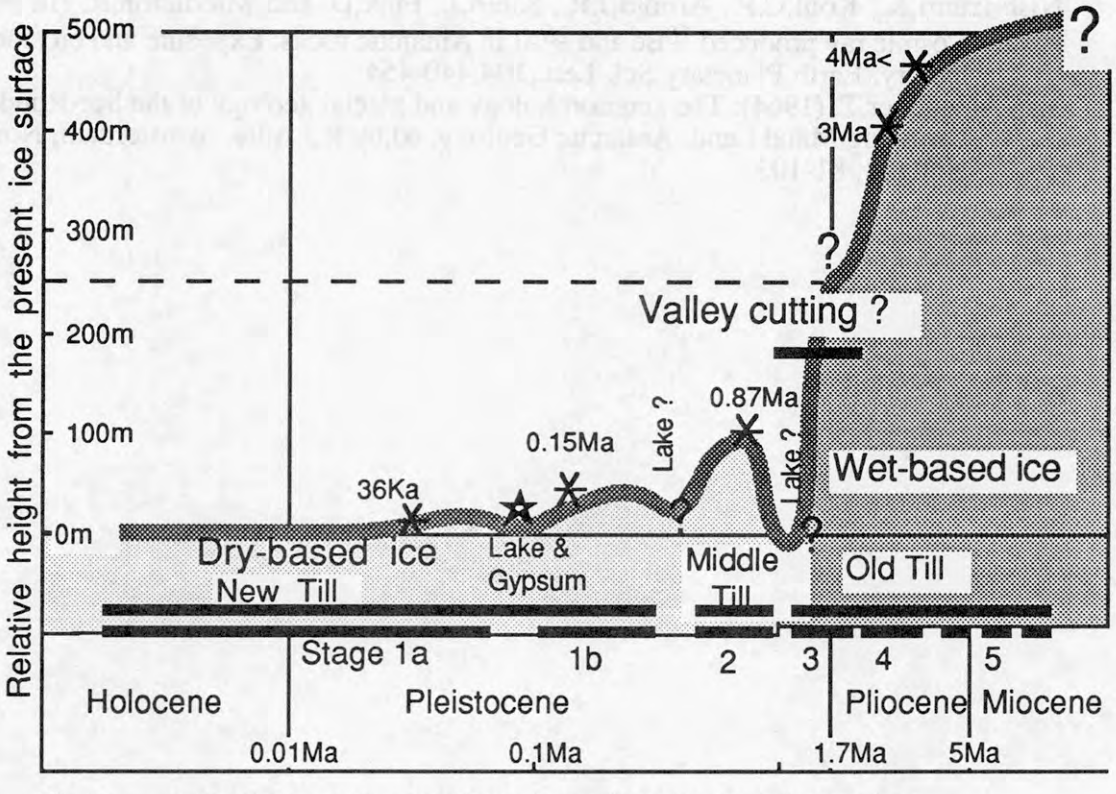

Fig. 3 Fluctuation of the ice sheet in the Sør-Rondane Mountains.

References

Aniya,M. (1989): Landforms of the Balchenfjella area, the Sør Rondane, East Antarctica. Antarct. Rec., 33, 353-375.

Bardin,V.I. (1982): Composition of East Antarctic moraines and some problems of Cenozoic history. Antarctic Geoscience, ed by C.Craddock, Univ. Wisconsin Press, 1069-1076.

Campbell,I.B. and Claridge,G.G.C. (1987): Antarctica: Soils, weathering processes and environment. Elsevier, Amsterdam, pp.368.

Hayashi,M. and Miura,K.(1989): Glacial landforms and weathering processes in the Balchenfjella region, eastern part of the Sør Rondane Mountains, East Antarctica. Proc. NIPR Symp. Antarct. Geosci., 3, 65-80.

Hirakawa,K., Matsuoka,N. and Moriwaki,K. (1988): Reconstruction of maximum glacial extent in the central Sør Rondane Mountains, East Antarctica. Proc. NIPR Symp. Antarct. Geosci., 2, 146-161.

Hirakawa,K. and Moriwaki,K. (1990): Former ice sheet based on the newly observed glacial landforms and erratics in the central Sør Rondane Mountains, East Antarctica. NIPR Symp. Antarct. Geosci., 4, 41-54.

Iwata,S. (1987): Debris-mantled rectilinear slopes in the western Sør Rondane Mountains, East Antarctica. Proc. NIPR Symp. Antarct. Geosci., 1, 178-192.

Matsuoka,N., Moriwaki,K., Iwata,S. and Hirakawa,K. (1990): Ground temperature regimes and their relation to periglacial processes in the Sør Rondane Mountains, East Antarctica. Proc. NIPR Symp. Antarct. Geosci., 4, 55-66.

Mercer,J.H. (1972): Some observations on the glacial geology of the Beardmore Glacier area. Antarctic geology and geophysics, ed. by R. J. Adie, Universitetsforget, Oslo, 427-433.

Moriwaki,K., Hirakawa,K. and Matsuoka,N. (In press): Weathering stage of till and glacial history of the central Sør Rondane Mountains, East Antarctica. Proc. NIPR Symp. Antarct. Geosci., 5.

Nishiizumi,K., Kohl,C.P., Arnold,J.R., Klein,J., Fink,D. and Middleton,R. (In press): Cosmic ray produced ^{10}Be and ^{26}Al in Antarctic rocks: Exposure and erosion history. Earth Planetary Sci. Lett.,104,440-454.

Van Autenboer,T. (1964): The geomorphology and glacial geology of the Sør-Rondane, Dronning Maud Land. Antarctic Geology, ed.by R.J.Adie. Amsterdam, North-Holland, 81-103.

CENOZOIC ANTARCTIC GLACIAL HISTORY - A PROVISIONAL SYNTHESIS

K. MORIWAKI and Y. YOSHIDA

National Institute of Polar Research,
Kaga, Itabashi-ku, Tokyo 173, Japan

Knowledge of late-Cenozoic glacial history of Antarctica is increasing rapidly, particularly in the areas of the Transantarctic Mountains - Western Ross Sea, the Antarctic Peninsula, and the Prince Charles Mountains - Prydz Bay region. The recovery of fossil floras and faunas in glacigenic and/or "interglacial" sediments were amongst the research highlights of the 1980s. More recently the analysis of isotopes in quartz grains formed by cosmic ray bombardment has been used to determine the duration of exposure of ice-free areas since ice retreat.

Using such published data, including our own, we present here in provisional form a correlation table outlining the glacial history of Antarctica. We do this in order to both invite critical comment, and to receive advice of data as yet unknown to us. Following such discussions we intend then to publish a revised and completely up-to-date version of our table.

References cited in the figure

(Bd) Bardin, V. I. (1982): Composition of East Antarctic moraines and some problems of Cenozoic history. Antarctic Geoscience, ed. by C. Craddock, Madison, Univ. Wisconsin Press, 1069-1076.

(Bi) Birkenmajer, K. (1991): Tertiary glaciation in the South Shetland Islands, West Antarctica: evaluation of data. Geological Evolution of Antarctica, ed by M.R.A. Thomson, J.A. Crame and J.W. Thomson, Cambridge Univ. Press, 629-632.

(Bk) Barker, P. F., Kennett, J. P. and Scientific Party (1988): Weddell Sea palaeoceanography: Preliminary results of ODP Leg 113. Palaeogeography, Palaeoclimatology, Palaeoecology, 67, 75-102.

(Bt) Barrett, P. J.[ed.] (1989): Antarctic Cenozoic history from the CIROS-1 drillhole, McMurdo Sound. DSIR Bulletin 245, pp.254.

(Br) Brady, H. T. (1982): Late Cenozoic history of Taylor and Wright Valleys and McMurdo Sound inferred from diatoms in Dry Valley Drilling Project cores. Antarctic Geoscience, ed. by C. Craddock, Madison, The Univ. Wisconsin Press, 1123-1131.

(Cl) Clapperton, C.M. and Sugden, D.E. (1982): Late Quaternary glacial history of George VI Sound area, West Antarctica. Quaternary Res., 18, 24-267.

(De1) Denton, G.H., Armstrong, R.L. and Stuiver, M. (1970): Late Cenozoic glaciation in Antarctica: The record in the McMurdo Sound region. Antarct. Jour. U.S., 5, 15-21.

(De2) Denton, G. H. and Wilson, S. C. (1982): Late Quaternary geology of the Rennick Glacier area, Northern Victoria Land. Antarct. Jour. U.S., 17, 49-51.

(De3) Denton, G. H., Prentice, M. L., Kellogg, D. E. and Kellogg, T. B. (1984): Late Tertiary history of the Antarctic ice sheet: Evidence from the Dry Valleys. Geology, 12, 263-267.

(De4) Denton, G.H., Stuiver, M. and Austin, K.G. (1985): Radiocarbon chronology of the last glaciation in McMurdo Sound, Antarctica. Antarct. Jour. U.S., 20(5), 59-61.
(De5) Denton, G. H., Anderson, B. G. and Conway, H. W. (1986): Late Quaternary surface fluctuations of Beardmore Glacier, Antarctica. Antarct. Jour. U.S., 21(5), 90-92.
(Dr1) Drewry, D. J. (1975): Initiation and growth of the East Antarctic ice sheet. Jour. Geol. Soc., 131, 255-273.
(Dr2) Drewry, D. J. (1979): Late Wisconsin reconstruction of the Ross Sea region, Antarctica. Jour. Glaciol., 24, 231-244.
(Dr3) Drewry, D. J. (1981): The record of Late Cenozoic glacial events in East Antarctica (60-171E). Earth's pre-Pleistocene glacial record, ed. by M. J. Hambrey and W. B. Harland, Cambridge Univ. Press, 212-216.
(El) Elston, D.P. and Bressler, S. S. (1981): Magnetic stratigraphy of DVDP drill cores and late Cenozoic history of Taylor Valley, Transantarctic Mountains, Antarctica. Dry Valley Drilling Project, Antarctic Research Series, 33, ed. by L.D.McGinnis, American Geophysical Union, 413-426.
(Gi) Gillieson, D., Burgess, J. and Spate, A. (1988): Geomorphology and limnology of the Larsemann Hills, Antarctica. Paper presented to International Geographical Union Congress, Sydney.
(Hm) Hambrey, M. J., Larsen, B. and Ehrmann, W. U. (1989): Forty million years of Antarctic glacial history yielded by Leg 119 of the Ocean Drilling Program. Polar Rec., 25, 99-106.
(Hw) Harwood, D.M.(1986): Recycled siliceous microfossils from the Sirius Formation. Antarct. Jour. U.S., 21(5), 101-103.
(Hl) Haugland, K., Kristoffersen, Y. and Velde, A. (1985): Seismic investigations in the Weddell Sea embayment. Tectonophysics, 114, 293-313.
(Hd) Hendy, C. H., Healy, T. R., Rayner, E. M., Shaw, J. and Wilson, A. T. (1979): Late Pleistocene glacial chronology of the Taylor Valley, Antarctica, and the global climate. Quaternary Res., 11, 172-184.
(Hz) Hinz, K. and Krause, W. (1982): The continental margin of Queen Maud Land / Antarctica: Seismic sequences, structural elements and geological development. Geol. Jb., 23, 17-41.
(Ke) Kennet, J. P. (1980): Paleoceanographic and biogeographic evolution of the southern ocean during the Cenozoic, and Cenozoic microfossil datums. Palaeogeography, Palaeoclimatology, Palaeoecology, 31, 123-152.
(Mb) Mabin, M. C. G. (1986): Glacial geology of Spike Cape, McMurdo Sound. Antarct. Jour. U.S., 21(5), 88-89.
(My) Mayewski, P. A. (1982): Upper Rennick Glacier ice mass fluctuation study. Antarct. Jour. U.S., 17, 51-52.
(Mk1) McKelvey, B. C. (1982): Late Cenozoic marine and terrestrial glacial sedimentation in eastern Taylor Valley, Southern Victoria Land. Antarctic Geoscience, ed. by C. Craddock, Madison, The Univ. Wisconsin Press, 1109-1116.
(Mk2) McKelvey, B. C., Mercer, J. H., Harwood, D. M. and Stott, L. D. (1984):The Sirius Formation: Further considerations. Antarct. Jour. U.S., 19, 42-43.
(Mk3) McKelvey, B.C., Webb, P.N., Harwood, D.M. and Mabin, M.C.G. (1991): The Dominion Range Sirius Group: a record of the late Pliocene - early Pleistocene Beardmore Glacier. Geological Evolution of Antarctica, ed by M.R.A. Thomson, J.A. Crame and J.W. Thomson, Cambridge Univ. Press, 675-682.
(Mg) Meguro, H., Yoshida, Y., Uchio, T., Kigoshi, K. and Sugawara, K. (1964): Quaternary marine sediments and their geological dates with reference to the geomorphology of Kronprins Olav Kyst. Antarctic Geology, ed. by R. J. Adie. Amsterdam, North-Holland, 73-80.
(Me1) Mercer, J.H. (1972): Some observations on the glacial geology of the Beardmore Glacier area. Antarctic Geology and Geophysics, ed. by R.J.Adie, Oslo, Universitetsforget, 427-433.

(Me2) Mercer, J.H. (1978): Glacial development and temperature trends in the Antarctic and in South America. Antarctic glacial history and world palaeoenvironments, ed. by Van Zinderen Bakker, E.M., Rotterdam, Balkema, 73-93.
(Mo) Moriwaki, K., Hirakawa, K. and Matsuoka, N. (In press): Weathering stage of till and glacial history of the central Sør Rondane Mountains, East Antarctica. Proc. NIPR Symp. Antarct. Geosci., 5.
(Ni) Nishiizumi, K., Klein, J., Fink, D., Middleton, R., Kohl, C.P. and Arnold, J.R. (1989): Exposure ages of rocks from the Sør Rondane Mountains, Antarctica. Papers pre. 14th Symp. Antarct. Meteorites. 6-8.
(Pc1) Pickard, J. (1986): The Vestfold Hills: A window on Antarctica. Antarctic oasis, ed. by J. Pickard, Sydney, Academic Press, 333-351.
(Pc2) Pickard, J., Adamson, D.A., Harwood, D.M., Miller, G.H., Quilty, P.G. and Dell, R.K. (1988): Early Pliocene marine sediments, coastline, and climate of East Antarctica. Geology, 16, 158-161.
(Pt1) Prentice, M. L., Wilson, S. C., Bockheim, J. G. and Denton, G. H. (1985): Geologic evidence for pre-late Quaternary East Antarctic glaciation of central and eastern Wright Valley. Antarct. Jour. U.S., 20(5), 61-62.
(Pt2) Prentice, M.L., Denton, G.H., Lowell, T.V., Conway, H.C. and Heusser, L.E. (1986): Pre-late Quaternary glaciation of the Beardmore Glacier region, Antarctica. Antarct. Jour. U.S., 21(5), 95-98.
(Pt3) Prentice, M. L., Denton, G. H., Burckle, L. H. and Hodell, D. A. (1987): Evidence from Wright Valley for the response of the Antarctic ice sheet to climate warming. Antarct. Jour. U.S., 22(5), 56-58.
(Ru) Rutford, R. H., Craddock, C., White, C. M. and Armstrong, R. L. (1972): Tertiary glaciation in the Jones Mountains. Antarctic Geology and Geophysics, ed. by R.J.Adie, Oslo, Universitetsforget, 239-243.
(Sm) Smith, A. G. and Drewry, D. J. (1984): Delayed phase change due to hot asthenosphere causes Transantarctic uplift? Nature, 309, 536-538.
(St) Stuiver, M. and Denton, G.H. (1977): Glacial history of the McMurdo Sound region. Antarct. Jour. U.S., 12, 128-130.
(Su) Sugden, D.E. and Clapperton, C.M. (1980): West Antarctic ice sheet fluctuations in the Antarctic Peninsula area. Nature, 286, 378-381.
(Th) Thomas, R.H. and Bentley, C.R. (1978): A model for Holocene retreat of the West Antarctic Ice Sheet. Quaternary Res., 10, 150-170.
(We1) Webb, P.N. (1972): Wright Fjord, Pliocene marine invasion of an Antarctic dry valley. Antarct. Jour. U.S., 7, 227-234.
(We2) Webb, P. N. and Wrenn, J. H. (1982): Upper Cenozoic micropaleontology and biostratigraphy of eastern Taylor Valley, Antarctica. Antarctic Geoscience, ed by C. Craddock, Madison, The Univ. Wisconsin Press, 1117-1122.
(We3) Webb, P.N., Harwood, D.M., McKelvey, B.C., Mercer, J.H. and Scott, L.D. (1984): Cenozoic marine sedimentation and ice-volume variation of the East Antarctic craton. Geology, 12, 287-291.
(We4) Webb, P.N. and Andreasen, J.E. (1986): Potassium/argon dating of volcanic material associated with the Pliocene Pecten Conglomerate (Cockbarn Island) and Scallop Hill Formation (McMurdo Sound). Antarct. Jour. U.S., 21(5), 59.
(We5) Webb, P.N., McKelvey, B.C., Harwood, D.M., Mabin, M.C.G. and Mercer, J.H. (1987): Sirius Formation of the Beardmore Glacier region. Antarct. Jour. U.S., 22(5), 8-13.
(We6) Webb, P. N. (1990): The Cenozoic history of Antarctica and its global impact. Antarctic Science, 2, 3-21.
(Yo1) Yoshida, Y. (1983): Physiography of the Prince Olav and Prince Harald Coasts, East Antarctica. Mem. Natl Inst. Polar Res., Ser. C (Earth Sci.), 13, 83p.
(Yo2) Yoshida, Y. and Moriwaki, K. (1979): Some consideration on elevated coastal features and their dates around Syowa Station, Antarctica. Mem. Natl Inst. Spec. Issue, 13, 220-226.

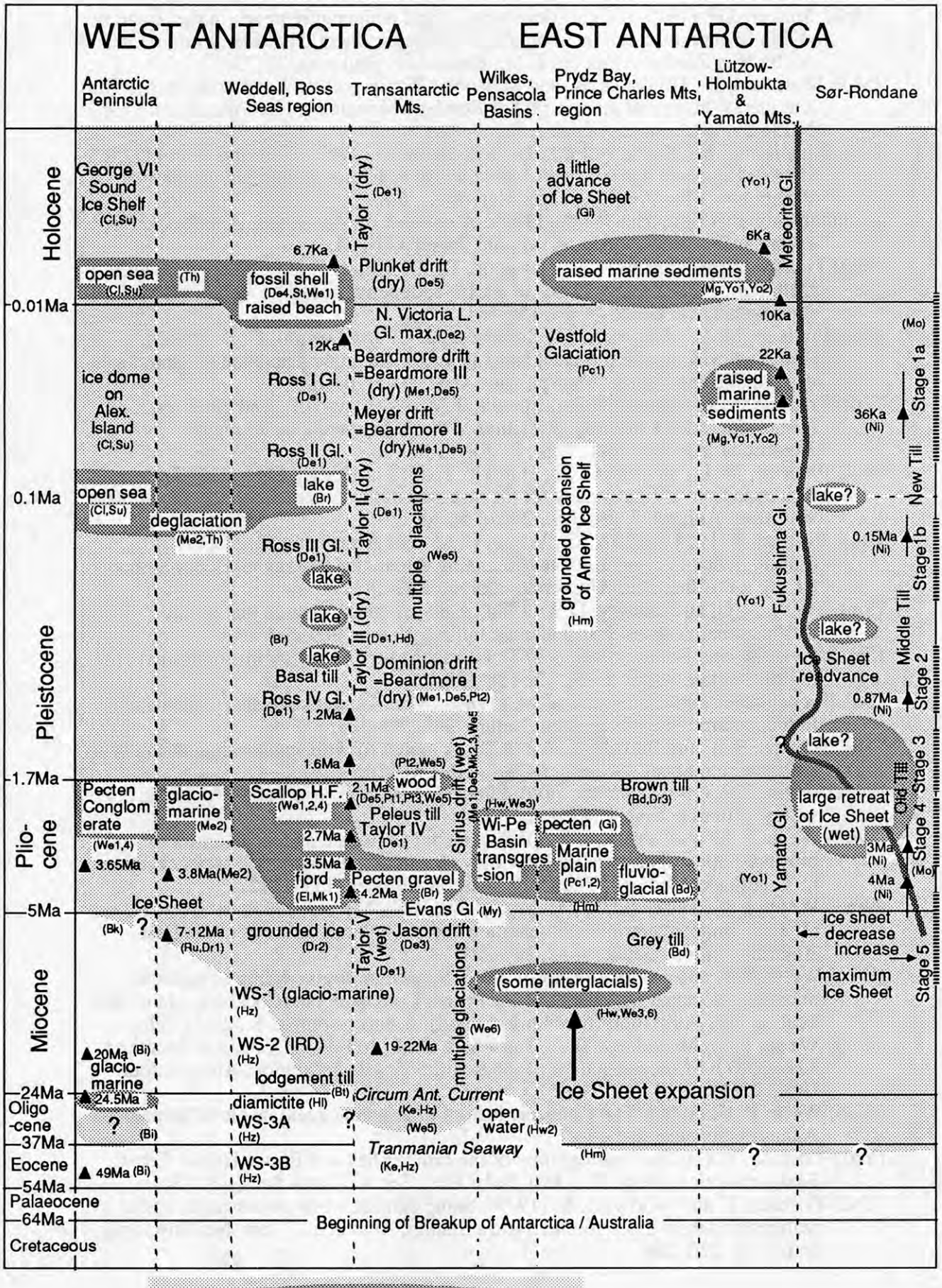
WEST ANTARCTICA
EAST ANTARCTICA
Antarctic Peninsula
Weddell, Ross Seas region
Transantarctic Mts.
Wilkes, Pensacola Basins
Prydz Bay, Prince Charles Mts, region
Lützow-Holmbukta & Yamato Mts.
Sør-Rondane
Holocene
Pleistocene
Pliocene
Miocene
Oligocene
Eocene
Palaeocene
Cretaceous
0.01Ma
0.1Ma
1.7Ma
5Ma
24Ma
37Ma
54Ma
64Ma
George VI Sound Ice Shelf (Cl,Su)
open sea (Cl,Su)
(Th)
6.7Ka
fossil shell (De4,St,We1)
raised beach
Taylor I (dry) (De1)
Plunket drift (dry) (De5)
a little advance of Ice Sheet (Gi)
raised marine sediments (Mg,Yo1,Yo2)
6Ka
(Yo1)
Meteorite Gl.
10Ka
N. Victoria L. Gl. max. (De2)
12Ka
Beardmore drift =Beardmore III (dry) (Me1,De5)
Ross I Gl. (De1)
Meyer drift =Beardmore II (dry) (Me1,De5)
Ross II Gl. (De1)
Taylor II (dry) (De1)
multiple glaciations (We5)
Vestfold Glaciation (Pc1)
grounded expansion of Amery Ice Shelf (Hm)
22Ka
raised marine sediments (Mg,Yo1,Yo2)
(Mo)
Stage 1a
36Ka (Ni)
New Till
ice dome on Alex. Island (Cl,Su)
open sea (Cl,Su)
deglaciation (Me2,Th)
lake (Br)
Ross III Gl. (De1)
lake
lake
(Br)
lake
Taylor III (dry) (De1,Hd)
Basal till
Ross IV Gl. (De1)
1.2Ma
Dominion drift =Beardmore I (dry) (Me1,De5,Pt2)
1.6Ma
(Pt2,We5)
Sirius drift (wet) (Me1,De5,Mk2,3,We5)
lake?
Fukushima Gl.
(Yo1)
0.15Ma (Ni)
Stage 1b
Middle Till
lake?
Ice Sheet readvance
0.87Ma (Ni)
Stage 2
lake?
Stage 3
Old Till
Pecten Conglomerate (We1,4)
3.65Ma
glacio-marine (Me2)
3.8Ma (Me2)
Scallop H.F. (We1,2,4)
2.1Ma (De5,Pt1,Pt3,We5)
wood
Peleus till
Taylor IV (De1)
2.7Ma
3.5Ma
fjord (El,Mk1)
Pecten gravel
4.2Ma (Br)
Wi-Pe Basin transgression
pecten (Gi)
Marine plain (Pc1,2)
fluvio-glacial (Bd)
(Hw,We3)
Brown till (Bd,Dr3)
large retreat of Ice Sheet (wet)
3Ma (Ni)
4Ma (Ni)
(Mo)
Stage 4
Yamato Gl.
(Yo1)
Ice Sheet
Evans Gl (My)
(Bk)
7-12Ma (Ru,Dr1)
grounded ice (Dr2)
Taylor V (wet) (De1)
Jason drift (De3)
Grey till (Bd)
ice sheet decrease
increase
maximum Ice Sheet
Stage 5
WS-1 (glacio-marine) (Hz)
(some interglacials) (Hw,We3,6)
multiple glaciations (We6)
WS-2 (IRD) (Hz)
20Ma (Bi)
glacio-marine
24.5Ma
19-22Ma
lodgement till (Bt)
diamictite (Hl)
Circum Ant. Current (Ke,Hz)
Ice Sheet expansion
WS-3A (Hz)
(Bi)
(We5)
open water (Hw2)
Tranmanian Seaway (Ke,Hz)
WS-3B (Hz)
49Ma (Bi)
(Hm)
Beginning of Breakup of Antarctica / Australia
period of deglaciation or warm condition
radiometric age
Ice Sheet

EXPERIMENTAL STUDY ON THE STABILITY OF OSUMILITE IN KMAS: THE NAPIER COMPLEX REVISITED

Y. Motoyoshi, *National Institute of Polar Research, 1-9-10 Kaga, Itabashi-ku, Tokyo 173, Japan*
M. Arima, *Yokohama National University, Hodogaya-ku, Yokohama 165, Japan*
B.J. Hensen, *University of New South Wales, Kensington, N.S.W. 2033, Australia*

1. Introduction

Osumilite is one of the diagnostic minerals in the Archaean Napier Complex, East Antarctica, which has been considered to be subjected to very high temperatures of metamorphism, probably higher than 1000°C at pressures of 7-11 kbar as evidenced by the regional occurrence of sapphirine-quartz, orthopyroxene-sillimanite-quartz and inverted metamorphic iron-rich pigeonite (Dallwitz, 1968; Sheraton *et al.*, 1980; Ellis 1980; Ellis *et al.*, 1980; Grew, 1980, 1982; Harley, 1985, 1987; Motoyoshi & Matsueda, 1984; Sandiford & Powell, 1986). Osumilite occurs in a number of mineral assemblages with sapphirine, orthopyroxene, garnet, sillimanite, cordierite, spinel, K-feldspar and quartz. With respect to the stability of osumilite-bearing mineral assemblages from the Napier Complex, Ellis *et al.* (1980) and Grew (1982) proposed different *P-T* grids. The main point of difference is that, in the KMAS (K_2O-MgO-Al_2O_3-SiO_2) system, an invariant point [Kfs, Os] is situated inside the osumilite stability field in Grew's grid, whereas it is outside in Ellis *et al.*'s grid.

We report the upper pressure stability limit of osumilite in the KMAS system determined experimentally, and discuss the petrogenesis of osumilite from the Napier Complex, Antarctica.

2. Natural Occurrence of Osumilite

Osumilite occurs on a regional scale in the Napier Complex. The distribution overlaps the sapphirine+quartz assemblages, but the osumilite-in isograd expands outside the sapphirine-quartz isograd (Sheraton *et al.*, 1987).

Petrographic evidence with regard to osumilite from the Napier Complex can be summarized as follows:

1. Osumilite is generally surrounded by fine-grained symplectites composed of cordierite + dendritic hypersthene + K-feldspar.
2. Osumilite + hypersthene (not dendritic) + sillimanite appears to be stable in some rocks.
3. Osumilite rarely includes spinel and sillimanite.
4. Osumilite is locally replaced by phlogopite.

3. Experimental Procedure

The experiments have been performed using 1.27 cm piston cylinder apparatus at the University of New South Wales (UNSW) and Yokohama National University (YNU).

The powdered starting materials were slightly moistened by breathing. fO_2 was unbuffered but it is believed to be between the QFM and WM buffers.

The starting materials were

1) a seeded glass composed of mixture of **20% seed crystals** of synthetic osumilite (Os), enstatite (En), sanidine (Sa), natural Antarctic sillimanite (Sil) and Brazilian quartz (Qtz), and **80% of glass** with osumilite composition ($KMg_2Al_5Si_{10}O_{30}$) prepared through fusion of mixtures of A-R grade chemicals under ~1500°C in air.
2) a completely crystalline assemblages containing mostly osumilite and seeds of enstatite, sillimanite and quartz synthesized from starting material 1) at 1050°C and 11 kbar.

We assumed a stoichiometric reaction,

$$KMg_2Al_5Si_{10}O_{30} = 2MgSiO_3 + 2Al_2SiO_5 + KAlSi_3O_8 + 3SiO_2,$$
$$\text{Os} \qquad\qquad \text{En} \qquad \text{Sil} \qquad \text{Kfs} \qquad \text{Qtz}$$

and carried out runs at 900-1200°C and at 11-14 kbar. The run products were examined and observed with the optical microscope, XRD and SEM.

4. Experimental Results

The experimental results obtained to date are shown in Fig. 1. Pressures reported are nominal "piston-in" values corrected by a -10% friction correction for UNSW apparatus and by

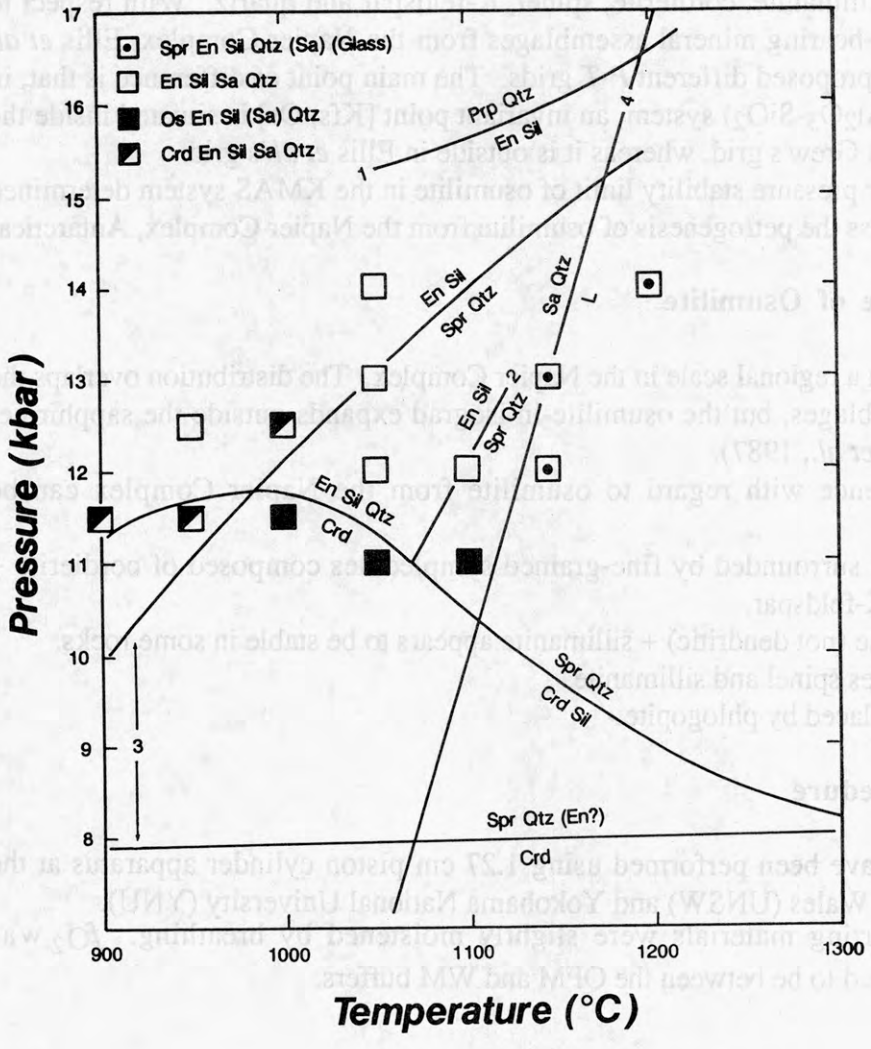

Fig. 1. *P-T* diagram for the experimental results. Data source: 1, Hensen & Essene (1971); 2, Bertrand *et al.* (1991); 3, Newton (1972); 4, Bohlen *et al.* (1983).

a -13% correction for YNU apparatus, respectively. The -10% correction has been applied to the results of Bertrand *et al.* which were carried out by the same techniques. Run times vary from 193.5 hrs at 900°C to 48-139 hrs at 1145°C.

We found abundant osumilite in the runs (1000°C, 11.5 kbar), (1050°C, 11 kbar) and (1100°C, 11 kbar). Under slightly higher pressures, osumilite disappeared in runs using starting material 2) and enstatite + sillimanite + sanidine ± cordierite assemblage is observed instead. Therefore, the upper stability of osumilite is *c.* 12 kbar for the temperature interval of 900-1100°C.

This study further confirms that the Napier Complex has undergone very high temperatures of metamorphism. The maximum pressure at the peak of metamorphism would be up to 12 kbar based on the osumilite stability.

Mineral assemblages observed in our experiments support a grid proposed by Bertrand *et al.* (1991) rather than Newton (1972) with respect to the MAS system containing sapphirine, enstatite, sillimanite, cordierite and quartz.

References

Bertrand, P., Ellis, D.J. & Green, D.H. (1991): The stability of sapphirine-quartz and hypersthene-sillimanite-quartz assemblages: an experimental investigation in the system FeO-MgO-Al_2O_3-SiO_2 under H_2O and CO_2 conditions. *Contributions to Mineralogy and Petrology*, **108**, 55-71.

Bohlen, S.R., Boettcher, A.L., Wall, V.J. & Clemens, J.D. (1983): Stability of phlogopite-quartz: a model for melting in the lower crust. *Contributions to Mineralogy and Petrology*, **83**, 270-277.

Dallwitz, W.B. (1968): Coexisting sapphirine and quartz in granulite from Enderby Land, Antarctica. *Nature*, **219**, 476-477.

Ellis, D.J. (1980): Osumilite-sapphirine-quartz granulites from Enderby Land, Antarctica: P-T conditions of metamorphism, implications for garnet-cordierite equilibria and the evolution of the deep crust. *Contributions to Mineralogy and Petrology*, **74**, 201-210.

Ellis, D.J., Sheraton, J.W., England, R.N. & Dallwitz, W.B. (1980): Osumilite-sapphirine-quartz granulites from Enderby Land, Antarctica: mineral assemblages and reactions. *Contributions to Mineralogy and Petrology*, **72**, 123-143.

Grew, E.S. (1980): Sapphirine+quartz association from Archean rocks in Enderby Land, Antarctica. *American Mineralogist*, **65**, 821-836.

Grew, E.S. (1982): Osumilite in the sapphirine-quartz terrane of Enderby Land, Antarctica: implications for osumilite petrogenesis in the granulite facies. *American Mineralogist*, **67**, 762-787.

Harley, S.L. (1985): Garnet-orthopyroxene bearing granulites from Enderby Land, Antarctica: metamorphic pressure-temperature-time evolution of the Archaean Napier Complex. *Journal of Petrology*, **26**, 819-856.

Harley, S.L. (1987): A pyroxene-bearing meta-ironstone and other pyroxene granulites from Tonagh Island, Enderby Land, Antarctica: further evidence for very high temperature (>980°C) Archaean regional metamorphism in the Napier Complex. *Journal of Metamorphic Geology*, **5**, 341-356.

Hensen, B.J. & Essene, E.J. (1971): Stability of pyrope-quartz in the system MgO-Al_2O_3-SiO_2. *Contributions to Mineralogy and Petrology*, **30**, 72-83.

Motoyoshi, Y. & Matsueda, H. (1984): Archaean granulites from Mt. Riiser-Larsen in Enderby Land, East Antarctica. *Memoirs of National Institute of Polar Research, Special Issue*, **33**, 103-125.

Newton, R.C. (1972): An experimental determination of the high-pressure stability limits of magnesian cordierite under wet and dry conditions. *Journal of Geology*, **80**, 398-420.

Sandiford, M.A. & Powell, R. (1986): Pyroxene exsolution in granulites from Fyfe Hills, Enderby Land, Antarctica: evidence for 1000°C metamorphic temperatures in Archean continental crust. *American Mineralogist*, **71**, 946-954.

Sheraton, J.W., Offe, L.A., Tingey, R.J. & Ellis, D.J. (1980): Enderby Land, Antarctica --- an anusual Precambrian high grade metamorphic terrain. *Journal of the Geological Society of Australia*, **27**, 1-18.

Sheraton, J.W., Tingey, R.J., Black, L.P., Offe, L.A. & Ellis, D.J. (1987): Geology of Enderby Land and Western Kemp Land, Antarctica. *Australian Bureau of Mineral Resources Bulletin*, **223**, 51pp.

ISOTOPIC CONSTRAINTS ON THE AGE AND ORIGIN OF THE BRATTSKARVET AND JUTULSESSEN GRANITOIDS, WESTERN DRONNING MAUD LAND

A.B. Moyes, Isotope Research Unit, BPI Geophysics, University of the Witwatersrand, Private Bag 3, Johannesburg 2050, South Africa.

The H.U. Sverdrupfjella and Mühlig-Hoffmannfjella of western Dronning Maud Land comprise a series of multiply-deformed gneisses of variable composition, intruded by a series of plutonic suites (Grantham et al., 1988; Ohta et al., 1990). Two of the largest intrusions in this metamorphic belt are the Brattskarvet and Jutulsessen granitoid suites, and previous work has correlated the two in terms of age and composition (Ravich and Solov´ev, 1966). Isotopic data (Rb-Sr, Sm-Nd, Pb-Pb and apatite fission track analysis) are presented here which indicate, however, that there are fundamental differences in both the age and source for these two intrusions.

The Brattskarvet intrusion comprises dominantly medium- to coarse-grained monzogranites, with minor monzonites and syenites, and intrudes paragneissic country rock, several large xenoliths of which are contained in the granitoid. There is also a generally developed tectonic fabric, axial planar to scarce tight folds which correlate to F3 folds in the country rocks. The Jutulsessen granitoid also intrudes paragneissic country rocks similar to those at Brattskarvet, and is dominantly granodioritic in composition; associated dykes are commonly monzogranite, and late-stage dykes syenitic in composition. Disrupted mafic dykes are monzonitic or quartz monzonitic in composition. In contrast to Brattskarvet the whole suite is extensively tectonized by at least three phases of deformation, and a gneissic texture is well developed throughout. Thus although the two intrusions appear outwardly similar in composition, their structural fabric is considerably different.

Brattskarvet granitoid suite: Rb-Sr data have been obtained from 16 whole rock samples and 7 mineral separates of the suite, in addition to 7 pyroxene granulite xenoliths and 2 hornfelses; Sm-Nd data have been obtained from 9 whole rock samples and two mineral separates of the granitoid, 6 xenoliths and 2 hornfelses; Pb-Pb data from 7 whole rock samples, and fission track data from 2 whole rock samples. The Rb-Sr whole rock data (Figure 1) scatter (MSWD=6) about a line equivalent to 482 ± 23Ma, with R_o=0.7082 ± 0.0002. However, this scatter is due to two essential linear arrays defined by both sample locality and rock type. For example, six granitic from the northern part of the complex plot along an isochron (MSWD=1.8) equivalent to an age of 556 ± 76Ma, with R_o=0.7081 ± 0.0003. Ten further samples, ranging from syenite to monzonite to granite (but from other localities) plot along an isochron (MSWD=1.7) equivalent to an age of 520 ± 17Ma, with R_o=0.7078 ± 0.0002. There is no significant difference between these results, and the preferred age is taken to be the weighted average of 522 ± 17Ma. The pyroxene-granulite xenoliths scatter widely (MSWD=24), but three of the five

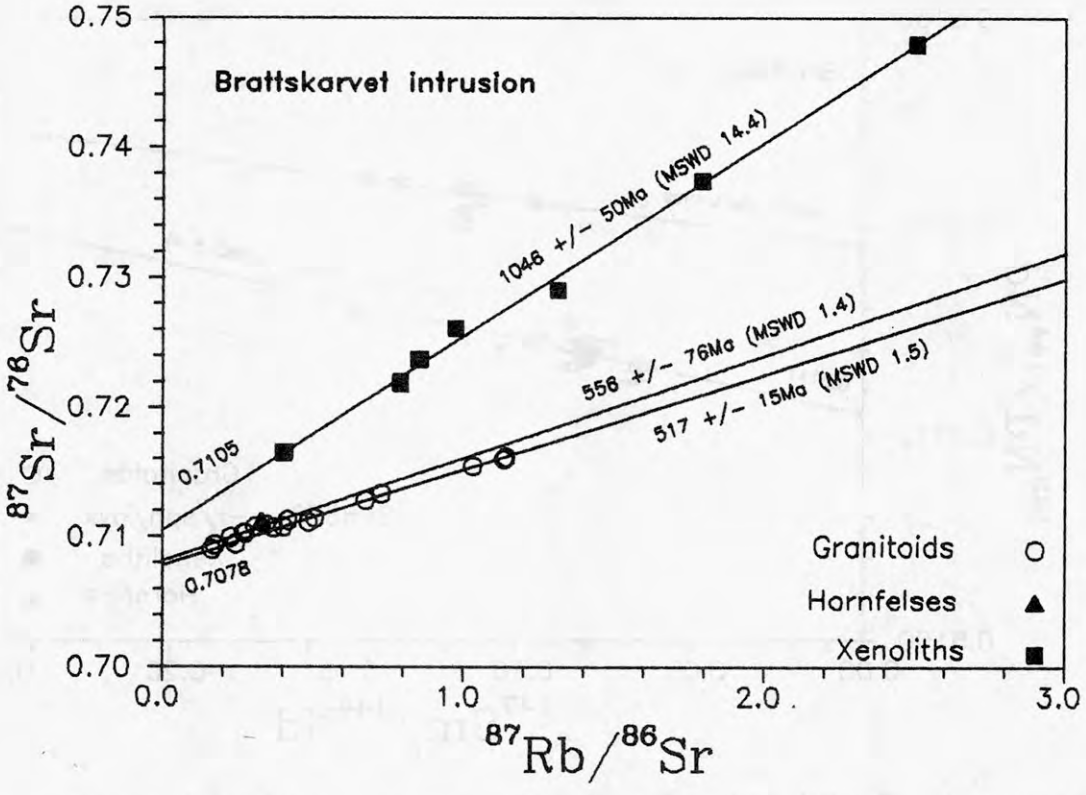

Figure 1: Rb-Sr Whole Rock Data from Brattskarvet Granitoid Suite.

samples plot along an isochron (MSWD=2.5) equivalent to an age of 1150Ma ± 48Ma, with R_o=0.7098 ± 0.0005.

Mineralogical data from two granitoid samples yield the following data: SF847 whole rock-biotite-alkali feldspar scatter (MSWD=10.5) about a line equivalent to 465 ± 14Ma, and sample SF8662 whole rock-alkali feldspar-sphene plot on an isochron (MSWD=2.06) equivalent to 482 ± 9Ma. These ages are considered to be significantly different to those obtained from the whole rock samples, indicating a period of resetting approximately 50Ma after intrusion.

The Pb-Pb whole rocks data are completely scattered, and define no linear trends. However, it is noteworthy that the Pb does not appear to be radiogenic. It is concluded that the Pb-Pb system has been severely affected some time after crystallization. The Sm-Nd whole rock data(Figure 2) are closely grouped, with the exception of one sample, and scatter (MSWD=5.4) about a line equivalent to 522 ± 120Ma with an R_o of 0.5111 ± 0.0001. Mineralogical data (sphene and pyroxene) from sample SF8663 plot close to this line (see Figure 2) but do define an isochron (MSWD=0.3) equivalent to an age of 705 ± 177Ma with R_o=0.5109 ± 0.0001. These data are within error of the whole rock age, and it is equivocal whether or not the mineralogical data represent an older event. It is interpreted here that the Sm-Nd and Rb-Sr whole rock data corroborate an intrusive age of approximately 522Ma. Nd model age data give consistent results, with an average T_{chur} of 1623Ma (range

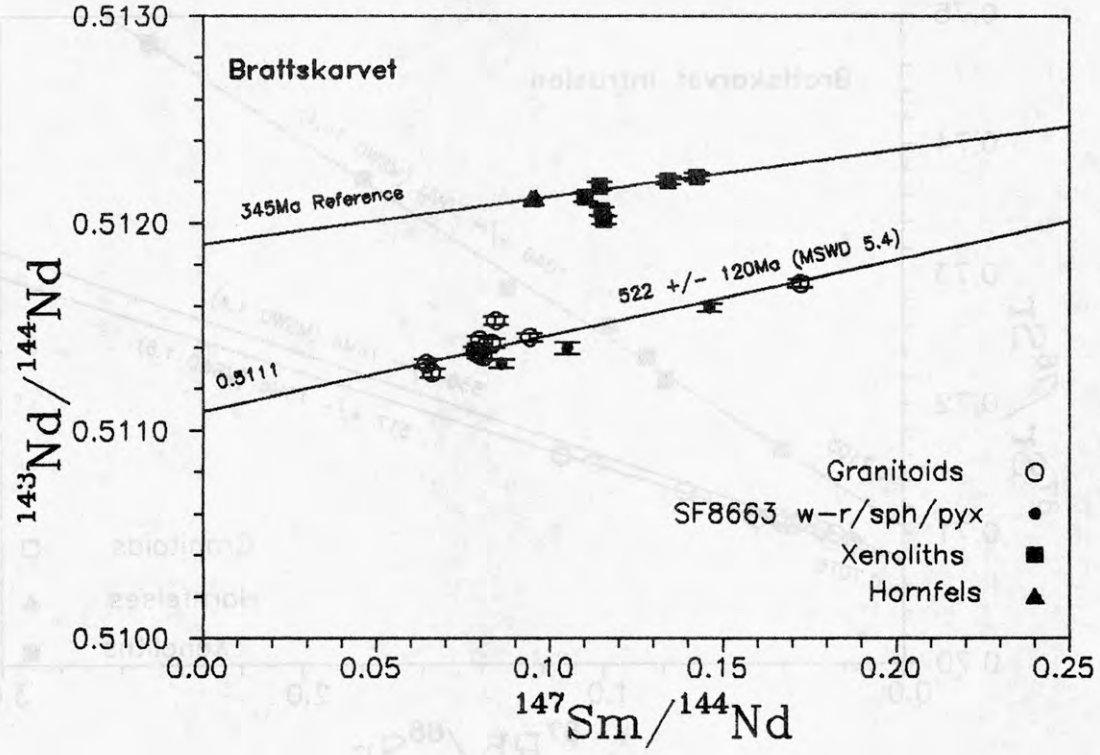

Figure 2: Sm-Nd Data for Brattskarvet granitoid suite

1812-1502Ma) and an average T_{dm} 1895Ma (range 2079-1768Ma). The average value for ϵNd at 522Ma is -16.56 (range -18.4 to -14.2).

Apatite fission track data for sample SF8662 indicate track lengths with a narrow mean distribution, typical of rocks that have cooled rapidly from temperatures >120°C to <50°C and have remained cool since that time. The mean age of this cooling is 117 ± 8Ma.

Jutulsessen granitoid suite: Rb-Sr whole rock data from 17 samples are shown in Figure 3, from which it can be seen that, with the exception of two samples, the data scatter (MSWD=19) about a line equivalent to 551 ± 29Ma, with R_o=0.7061 ± 0.0003. This scatter can also be viewed as resulting from two essentially linear trends. The first consists of 8 samples which scatter closely (MSWD=4.2) about a line equivalent to 553 ± 13Ma, with R_o=0.7057 ± 0.0002, and the second of 6 samples that plot on an isochron (MSWD=2.5) equivalent to an age of 572 ± 29Ma, with R_o=0.7064 ± 0.0002. These results are within error of each other, and yield a weighted mean average of 556 ± 12Ma.

However, Sm-Nd data for 12 whole rock samples are shown in Figure 4, from which it can be seen that, with the exception of 3 samples, the data scatter (MSWD=42) about a linear trend, equivalent to an age of 1188 ± 166Ma, with R_o=0.51116 ± 0.0001. Thus there is a fundamental contrast between the Rb-Sr data, which indicates an apparent Pan-African age, and the Sm-Nd data which suggests a Kibaran age.

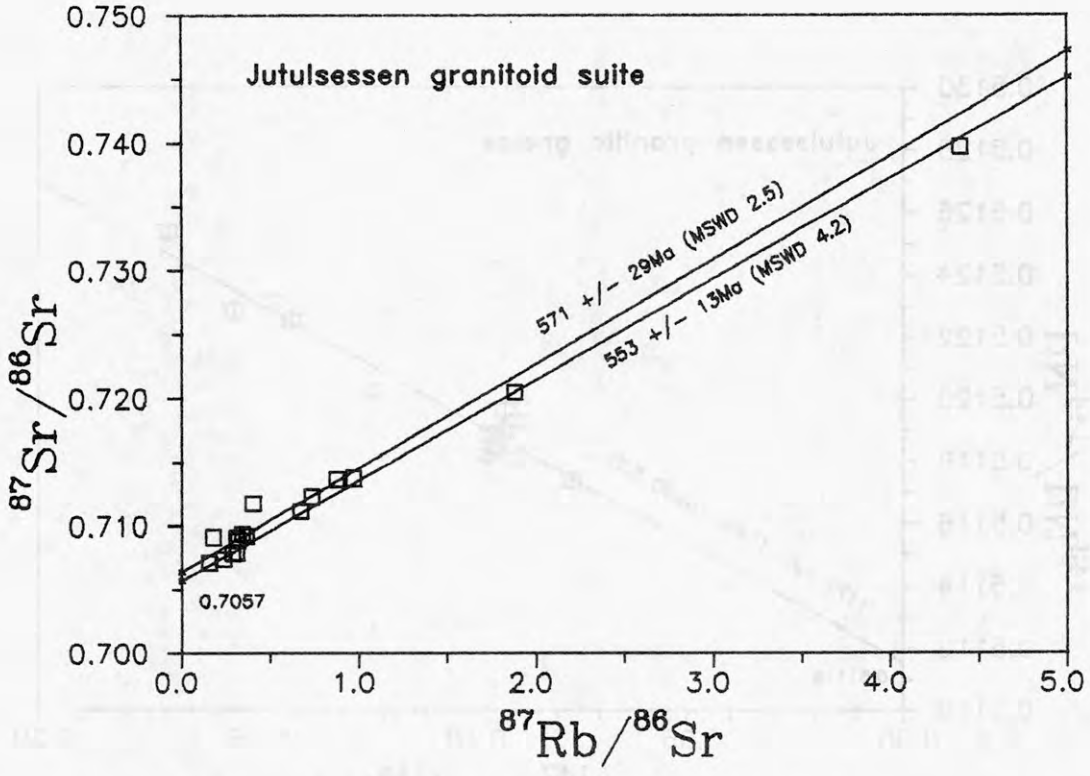

Figure 3: Rb-Sr Whole Rock Data for the Jutulsessen Granitic Gneiss

Given the structural evidence for this suite, it is inferred here that the older, Kibaran age is more likely to reflect an original intrusive age, and that near-complete resetting of the Rb-Sr system has occurred later. In addition, the Nd model ages for Jutulsessen give a T_{chur} average of 1067Ma (range 1286-895Ma) and a T_{dm} average of 1469Ma (range 1747-1246Ma); it should be noted, however, that 2 samples give much younger ages of approximately 580Ma (T_{chur}) and 1000Ma (T_{dm}) respectively.

The Rb-Sr whole rock data indicate that the Brattskarvet granitoid suite was intruded at ≈522Ma, during, or slightly prior to, the Pan-African orogeny. Mineral resetting occurred approximately 50Ma later at ≈480-460Ma, but whether this represents cooling of the intrusion or a later period of biotite growth is not known. Pyroxene granulite xenoliths included in this body retain a Kibaran overprint of ≈1150Ma, and this age is interpreted as representing peak metamorphism; this is remarkably similar to a Rb-Sr whole rock age of 1170 ± 26Ma obtained from samples of the Sveabreen paragneiss which hosts the intrusion (unpublished data). It should be noted, however, that the xenolith samples have a higher R_o than the gneisses. The apatite fission track data indicate that cooling to <50°C occurred at ≈117Ma, which corresponds to the approximate time of final Gondwana fragmentation. In contrast, the Jutulsessen granitoid was intruded during, or prior to the Kibaran orogeny, at ≈1188Ma, but the Rb-Sr system has suffered near-complete resetting during the Pan-African event at ≈556Ma. As shown in Figure 5, the ϵNd values for the two

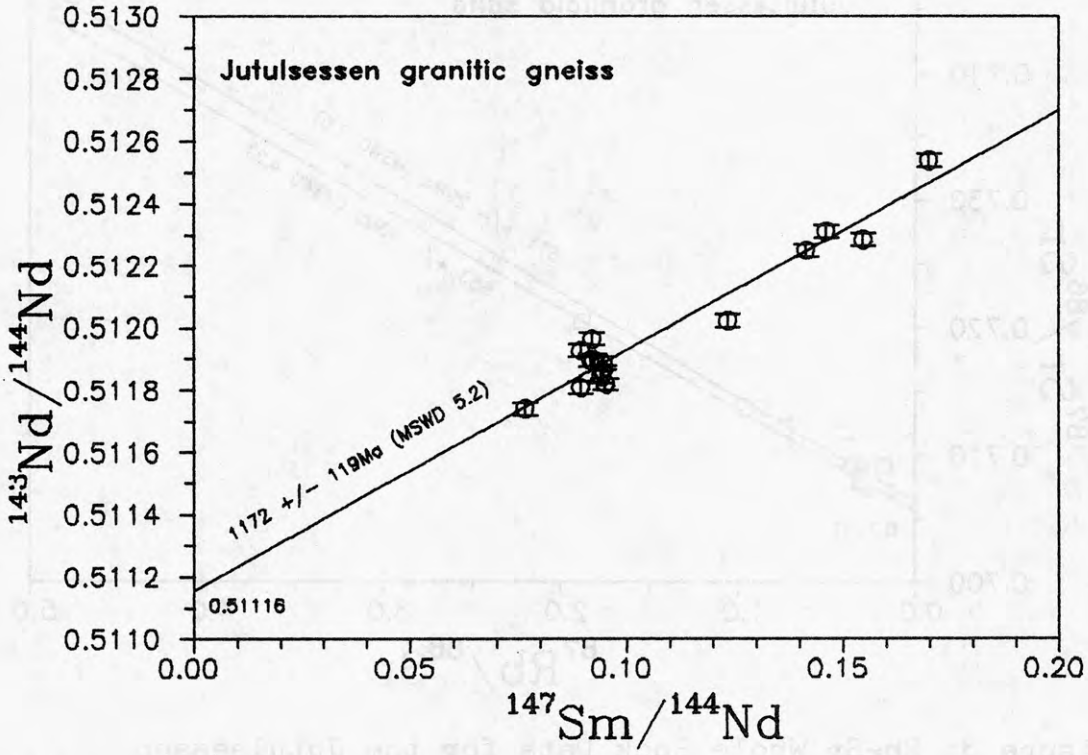

Figure 4: Sm-Nd Whole Rock Data for the Jutulsessen Granitic Gneiss

intrusions indicate very different source materials. Firstly, T_{dm} model ages are much older for the Brattskarvet samples, with an average of 1895Ma compared to 1469Ma for the Jutulsessen suite. Secondly, it should also be noted from Figure 4 that samples of the Sveabreen paragneiss country rock are similar to the Jutulsessen suite (implying a possible source) but not to Brattskarvet; samples of the metasedimentary Hogfonna Formation (which crop out on the cratonic fragment of the Ahlmannryggen-Borgmassivet) do, however, lie on the Nd evolution line for this suite. This implies that similar material underlying the H.U. Sverdrupfjella might provide a suitable source.

References

Grantham, G.H., Groenewald, P.B. and Hunter, D.R. 1988. Geology of the northern H.U. Sverdrupfjella, western Dronning Maud Land and implications for Gondwana reconstructions. South African Journal of Antarctic Research, 18 (1), 2-10.

Oht, Y., Tørudbakken, B.O. and Shiraishi, K. 1990. Geology of Gjelsvikfjella and western Mühlig-Hofmannfjella, Dronning Muad Land, east Antarctica. Polar Research, 8, 99-126.

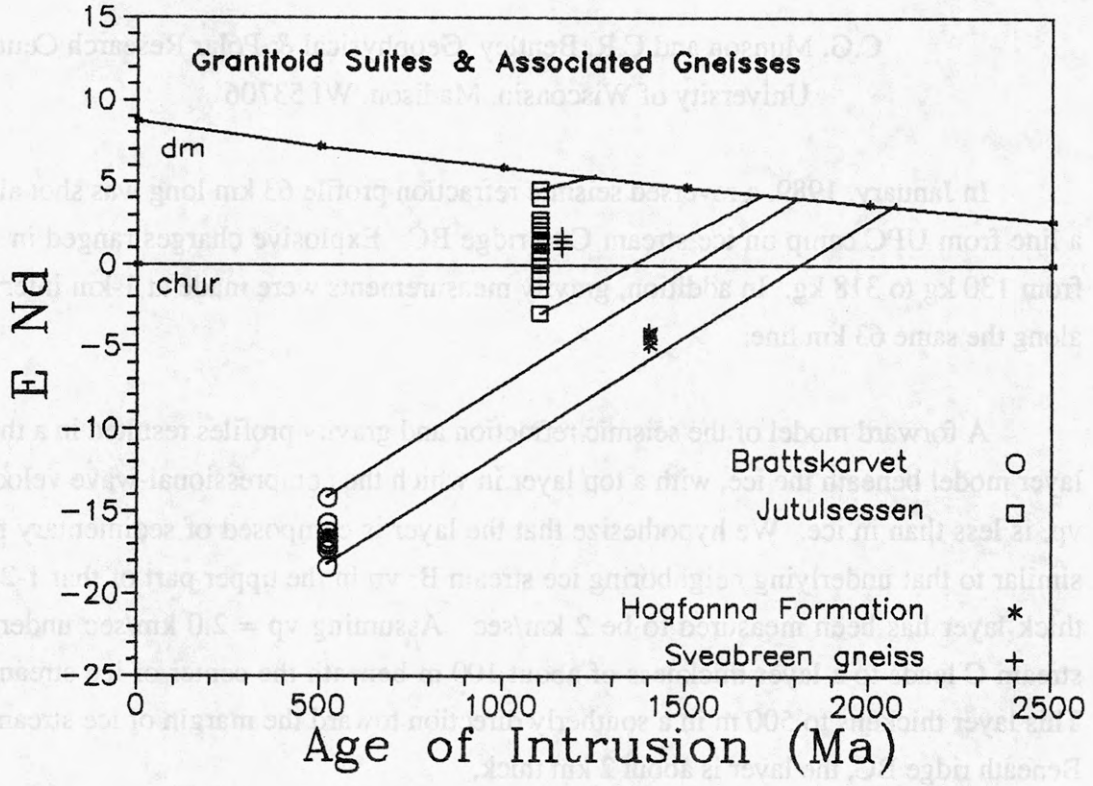

Figure 5: Nd Evolution Diagram for the Brattskarvet & Jutulsessen suites and Associated Suites

Ravich, M.G. and Solov´ev, D. 1966. (Engl. trans. 1969). Geology and petrology of the mountains of central Queen Maud Land (Eastern Antarctica). Trans Sci. Res. Institt. Geol. Arctic, Ministry Geol. USSR, Moscow 141, 348pp. Jerusalem, Israel Programme for Scientific Translations.

The Crustal Structure Beneath Ice Stream C and Ridge BC, West Antarctica from Seismic Refraction and Gravity Measurements

C.G. Munson and C.R. Bentley, Geophysical & Polar Research Center, University of Wisconsin, Madison, WI 53706

In January, 1989, a reversed seismic refraction profile 63 km long was shot along a line from UPC camp on ice stream C to ridge BC. Explosive charges ranged in size from 130 kg to 318 kg. In addition, gravity measurements were made at 1-km intervals along the same 63 km line.

A forward model of the seismic refraction and gravity profiles resulted in a three-layer model beneath the ice, with a top layer in which the compressional-wave velocity, vp, is less than in ice. We hypothesize that the layer is composed of sedimentary rock similar to that underlying neighboring ice stream B: vp in the upper part of that 1-2 km thick layer has been measured to be 2 km/sec. Assuming vp = 2.0 km/sec under ice stream C leads to a layer thickness of about 100 m beneath the center of ice stream C. This layer thickens to 500 m in a southerly direction toward the margin of ice stream C. Beneath ridge BC, the layer is about 2 km thick.

Furthermore, the forward modeling of seismic refraction travel times resulted in a vp of 5.65 km/sec at the top of layer 2 and a vp of 6.0 km/sec at the bottom of the layer. The thickness of the layer ranges from 6 km beneath ice stream C to 2 km beneath ridge BC. The third and deepest layer has a vp of 6.85 km/sec.

The forward modeling of the gravity anomalies revealed a full graben structure (~10 km wide) beneath ridge BC that may be a result of continental rifting.

THREE-DIMENTIONAL TOPOGRAPHIC AND GRAVITY ANOMALY MAPS IN AND AROUND MIZUHO PLATEAU, EAST ANTARCTICA

Toshiyasu Nagao, Faculty of Science, Kanazawa University, 1-1, Marunouchi, Kanazawa-shi, Ishikawa 920, Japan
Katsutada Kaminuma National Institute of Polar Research, 9-10, Kaga 1-chome, Itabashi-ku, Tokyo 173, Japan.

A re-compilation of gravity data around Syowa Station, East Antarctica (68-78°S, 25-55°E) was made, to present three-dimensional contour maps of free-air and Bouguer anomalies. Ice sheet and bedrock topographies contour maps were also obtained. Gravity values calculated by Potsdam System are unified to IGSN71 System, and the accuracy of the gravity values was evaluated.

In Mizuho Plateau, some free-air and Bouguer anomalies were calculated based on the ground survey by the JARE snow traverse parties, and others were by the height from WGS-72 ellipsoids (NNSS). Therefore, in the latter case, to remove this confusion, we re-calculated free-air and Bouguer anomalies using the geoid height estimated by a geoid model (GEM-10b). In this study, we regarded as that the geoid model corresponds with the mean sealevel at Syowa Station. The results are as follows: 1) the accuracy of the gravity value determination is better than 3 mgal. 2) an accuracy of free-air anomaly is about 10 mgal. The latter accuracy is depended on the accuracy of height determination.

However, an ice thickness (in other word, bedrock topography) obtained by a radio echo sounding sometimes showed large differences in values at the same observation point by different observations (The maximum difference is larger than 300 m.). This may be caused by the incorrect identification of an internal boundary of ice layer as a real boundary between ice and bedrock. Therefore, simply obtained Bouguer anomaly may have a large error in some cases. One of our final goal is to make a bedrock topography map taking into account the results of the gravity data.

SEISMOLOGICAL OBSERVATIONS BY A THREE-COMPONENT BROADBAND DIGITAL SEISMOGRAPH AT SYOWA STATION, ANTARCTICA

Ken-ichi NAGASAKA: Faculty of Science Ibaraki University, Bunkyo, Mito, Ibaraki 310
Katsutada KAMINUMA and Kazuo SHIBUYA: National Institute of Polar Research, Kaga, 1-chome, Itabashi, Tokyo 173

A three-component broadband STS (Streckeisen Seismometer) Seismograph was installed at Syowa Station to obtain digital seismic record for studying the earth's interior and earthquakes. The STS observation system at Syowa Station is introduced and some examples of digital seismogram are shown in this paper.

1. POSEIDON project

The Federation of Digital Broadband Seismograph Network (FDSN) was founded in 1986 facilitating research on earthquakes and the earth's interior, and is officially sanctioned by the International Union of Geodesy and Geophysics (IUGG). As the Japanese contribution to the FDSN research program, a project is proposed to deploy seismographs in the Western Pacific, and in Eastern and Southeastern Asia. The project has been named the POSEIDON (Pacific Orient Seismic Digital Observation Network) project.

The POSEIDON project was proposed to install a set of broadband digital seismographs in Syowa Station (69°S, 39°E), Antarctica, in addition to the three-component of short-period and long-period seismographs which have been in operation since 1966 (Kaminuma et al., 1968; Kaminuma, 1969). Although Syowa Station is far from the Western Pacific and Eastern Asia, which is the major focus of the POSEIDON project, the seismic station, when combined with few other Antarctic Stations (e.g. Dumont d'Urville, a Geoscope observatory of French), will provide important data for studying the earth's interior from a global point of view. A three-component broadband digital seismograph was installed in Syowa Station in 1989, and the observation system was developed in 1990.

2. Observation System

A three-component broadband STS (Streckeisen Seismometer) seismograph was installed at Syowa Station in 1989. The STS system has two different broadband ; BRB (Broad-Band) output (0.1~20sec/0.1~360sec) and LP(Long-Period) output (longer than 20sec), and a dynamic range of at least 10^6. The seismic signal is recorded in digital form together with analog seismogram for monitoring.

The three-component seismograph and the feed back amplifier box are installed in the seismic observation vault. The recording systems are installed in the Earth Science Laboratory, and seismic signal is transmitted by cable wire. The recording system concists of a long-term pen recorder for monitoring BRB output, a digital recording system and a cassette logger for digital recording. The STS observation system at Syowa Station is shown in Fig. 1.

A pen recorder for monitoring LP output and an adjuster for zero positioning of pendulum have been installed at the Laboratory since 1990. The position of the pendulums is continuously monitored at the Laboratory to control the drift of the pendulums (POS in Fig. 1). The installation of the adjuster makes it possible to remote control the position of the pendulums through the connector box from the Laboratory. The temperature in the observation vault and around the STS seismographs is also recorded continuously by the pen recorder in the Laboratory for monitoring and studying the relation between temperature change and pendulum drift.

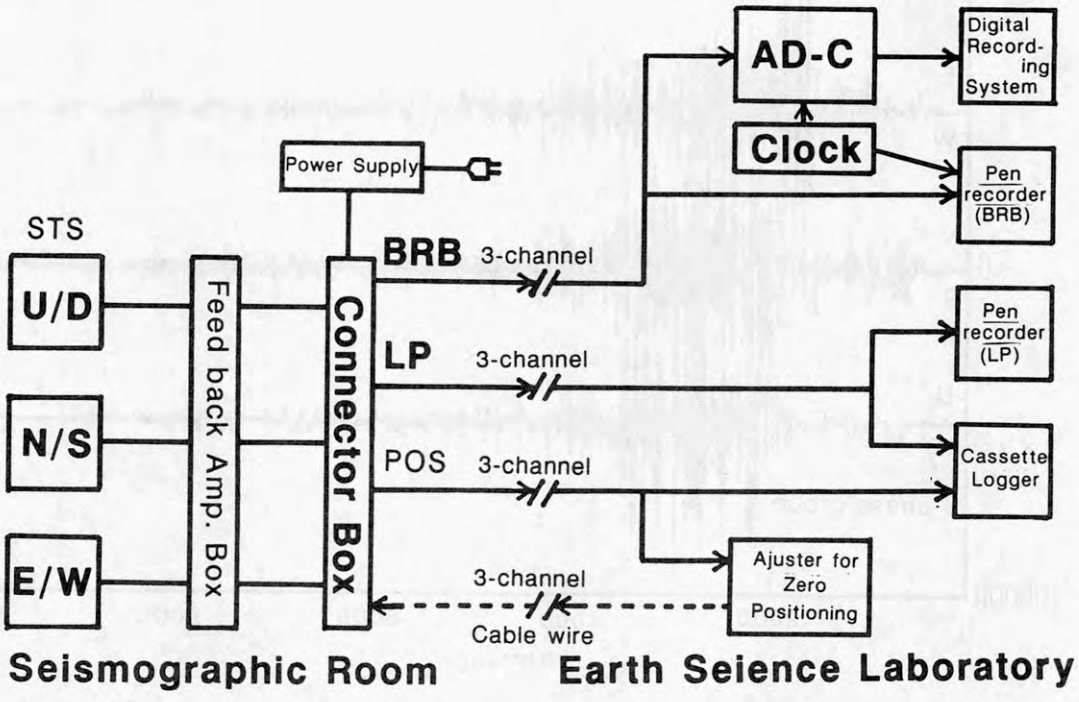

Fig. 1. A schematic diagram of STS seismic recording system at Syowa Station.

3. Observation

The BRB output is currently recorded on the long-term pen recorder and the digital rrecording system. The LP output is also recorded on the pen recorder and the cassette logger. Only the bigger events are compiled into floppy disks from the digital recording system approximately once a week. The digital record can be transmitted to National Institute of Polar Research, Japan via the satellite telecommunication system.

Figure 2 shows the output of digital recordings of a event which occurred in Western Iran (36.957°N, 49.409°E, depth 19km, mb 6.4, Ms 7.7). As Syowa Station is in the shadow zone from the epicenter of the earthquake, P phase group is not recorded. S phase group, surface waves and some other phases are well recorded. The seismogram of the initial 3000 sec in Fig. 2 was transmitted to Japan for testing the telecommunication system for sending digital seismic record and the transmitted seismogram is given in Fig. 3. Clear Love and Rayleigh waves are recognized on the seismogram.

Figure 4 shows the digital seismogram of a deep earthquake, south of Fiji Islands (23.622°S, 179.893°W, depth 531km , mb 5.9). A long period noise of about 10 min is recognized on the seismogram, and clear P and S phases are recorded. Enlarged scale seismogram of initial P and S phases are also given in Fig. 5 and 6 respectively.

The digital seismogram of a local event is shown in Fig. 7, the event has clear Pand S phases with S-P time of 263 sec, however its hypocenter is not determined by the world wide seismic network.

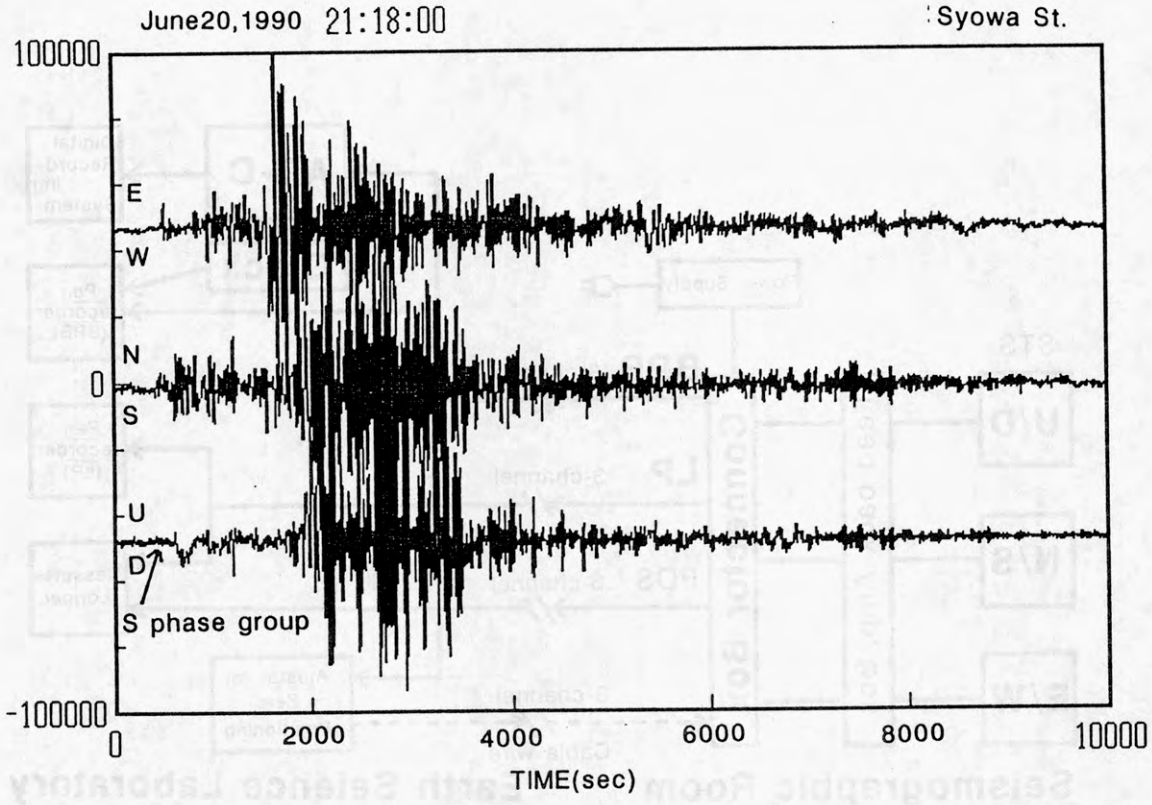

Fig. 2. Digital seismogram of the three-component STS seismograph. The earthquake hypocenter parameters are as follows: Origin time, 21h00m09.9s, June 20, 1990; Location, 36.957°N, 49.409°E; Depth, 19km; mb=6.4, Ms=7.7; Western Iran.

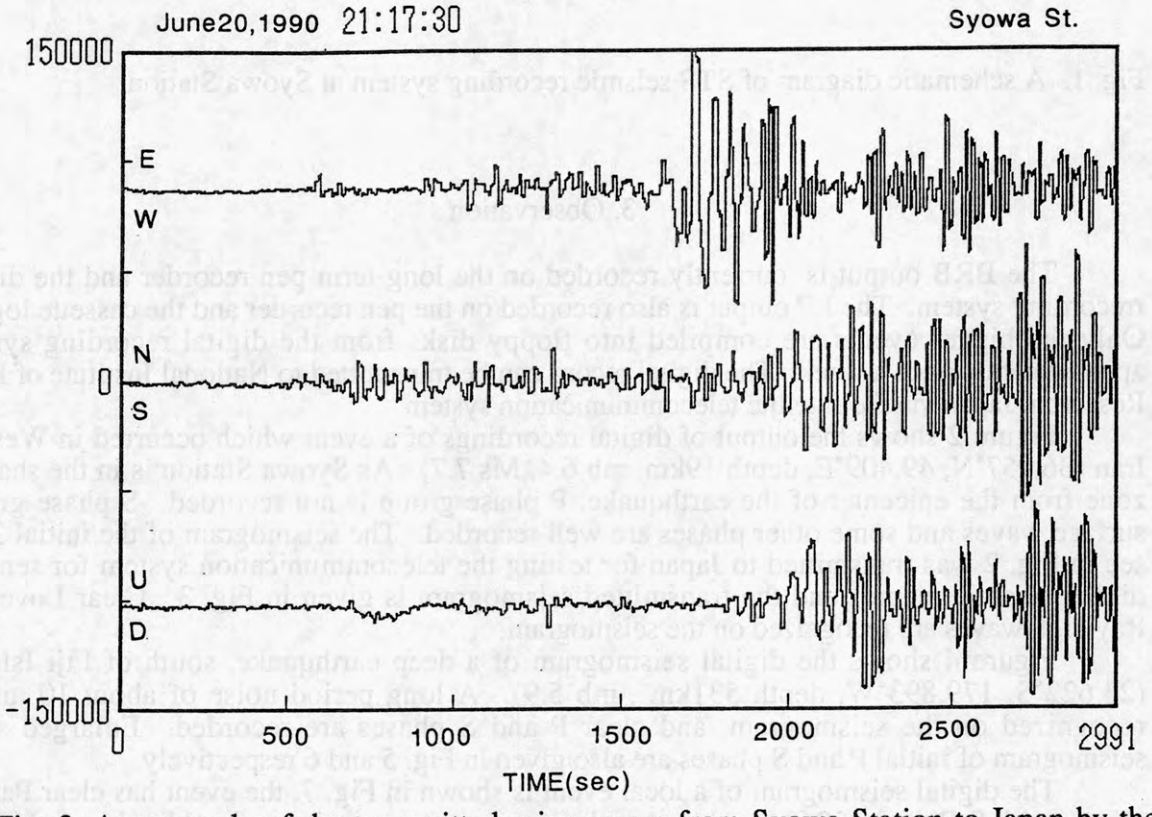

Fig. 3. An example of the transmitted seismogram from Syowa Station to Japan by the satellite telecommunication system. The initial 3000 sec phases in Fig 2 are shown.

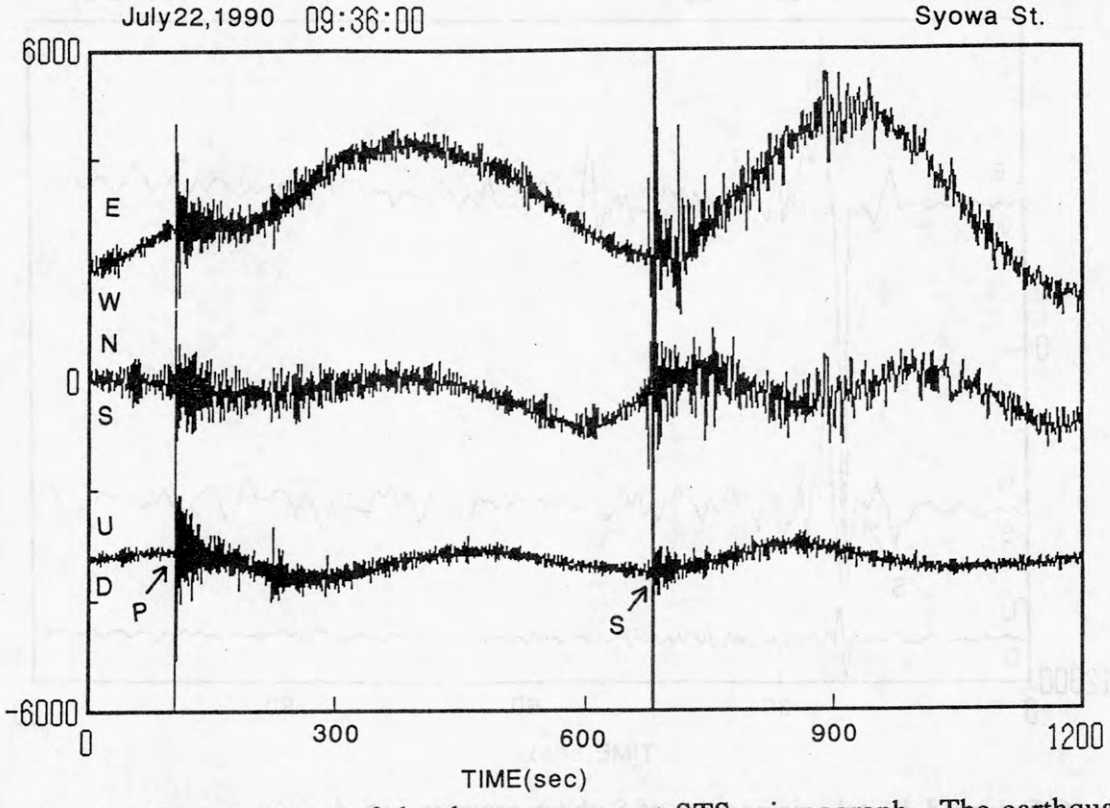

Fig. 4. Digital seismogram of the three-component STS seismograph. The earthquake hypocenter parameters are as follows : Origin time 09h26m14.6s July 22, 1990; Location, 23.622°S 179.893°W; Depth, 531km ; mb, 5.9; South of Fiji Islands.

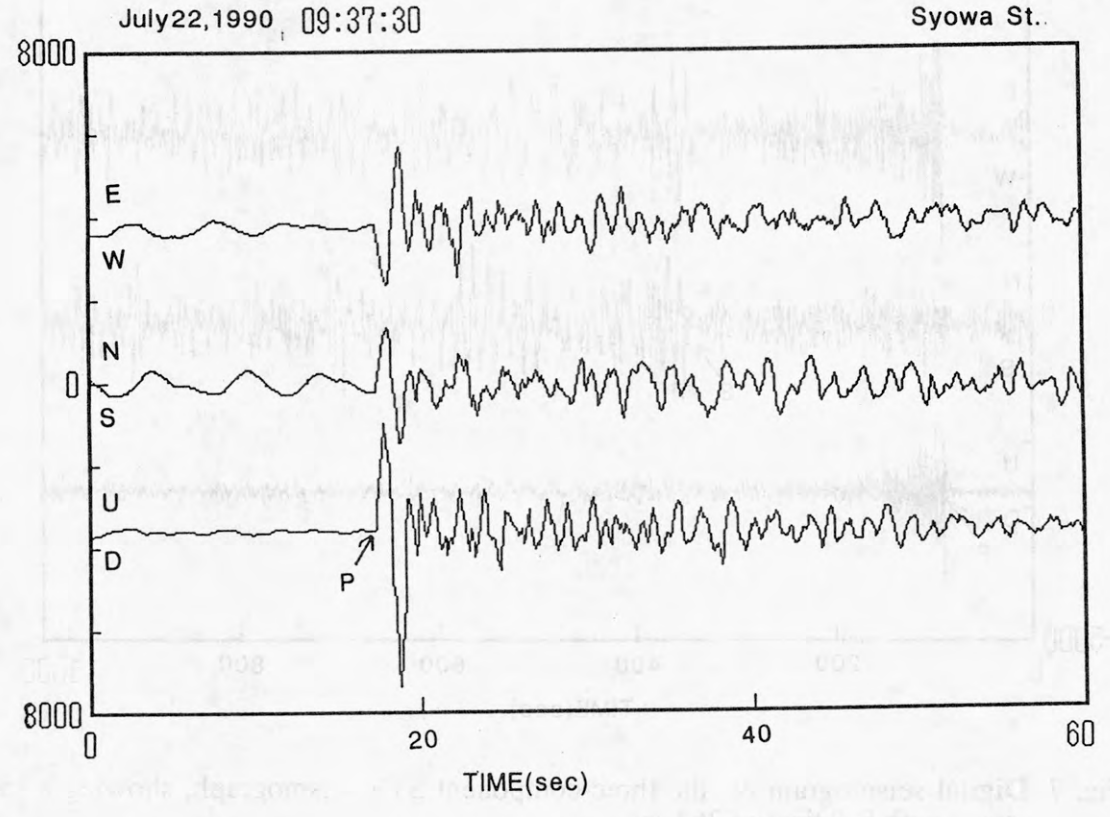

Fig. 5. Enlarged digital seismogram of P phase group in Fig. 4.

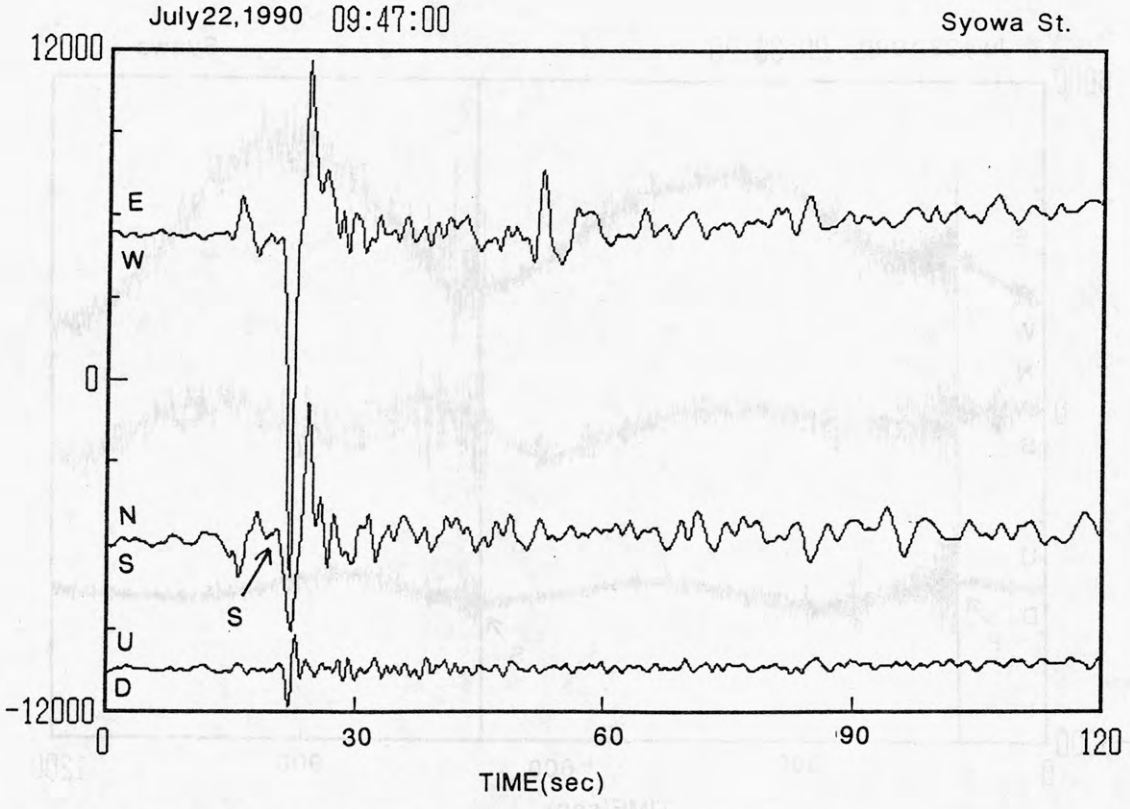

Fig. 6. Enlarged digital seismogram of S phase group in Fig. 4.

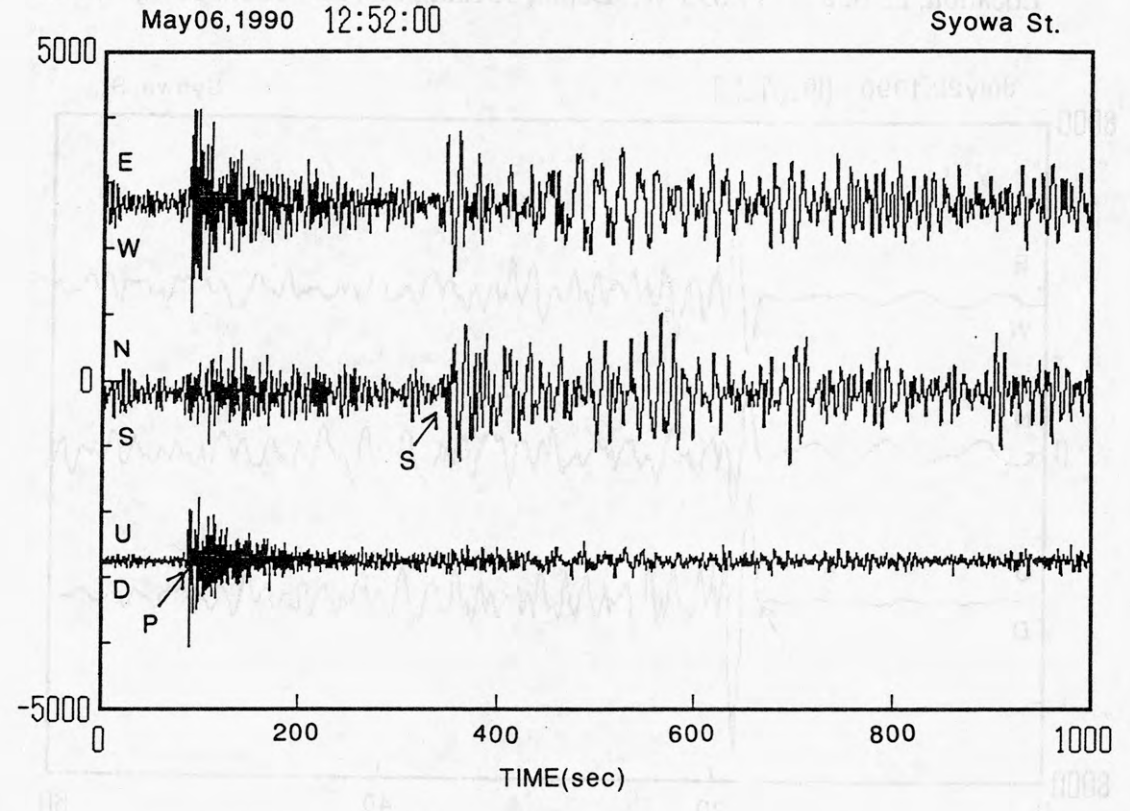

Fig. 7. Digital seismogram of the three-component STS seismograph, showing a local event with S-P time of 263 sec.

Ackowledgments

The authors express their sincere thanks to Drs. J. AKAMATSU and K. ITO for their advise in preparing the STS system. The authors' are extended to Ms. F. NAKAMURA for preparing this manuscript.

References

Kmainuma, K., Eto, T. and Yoshida, M. (1968): Seismological observation at Syowa Station, Antactica (in Japanese), Antar. Rec. 33, 65-70.

Kaminuma, K. (1969): The seismological Observation and earthquake detection capability of Syowa Station, Antarctica, Bull Earthq. Res. Inst. 47 453-466.

PRELIMINARY NOTES ON GEOLOGICAL STRUCTURE AND SEDIMENTATION OF THE SEA AREA OFF WILKES LAND, EAST ANTARCTICA

S.Nakao, Geological Survey of Japan, Higashi, Tsukuba 305 Japan.
K.Koike, Technology Research Center, Japan National Oil Corporation, Hamada, Chiba 260 Japan.

Japan National Oil Corporation conducted a marine geoscientific survey in a part of the sea area off Wilkes Land, East Antarctica in December,1990 to February,1991 as R/V Hakurei-maru cruise, TH90. Multichannel seismic reflection data over 2000km, short (several meter long) sediment cores at 9 locations and dredge samples of 4 holes were obtained.

The cruise was divided into two legs. In the 1st leg, one of the deep-sea hills situated northerly off the Dumont d'Urville Sea was studied. In addition, several submarine canyons situated northeast of Porpoise Bay were studied in the 2nd leg.

The shallowest part of the deep-sea hill, tentatively named "Ohmachi Hill" after the late Prof. H.Ohmachi at Yamagata University, is ca.3118m deep. Water depths of the foot of the hill are ca.3830m and ca.3943m, on SW- and NE-side respectively. A small elongated depression trending NW-SE, water depth of which slightly exceeds 4000m, is observed at the very NE foot of the hill. NE slope of the hill, consisting mainly of Cretaceous sequences, is a fault scarp. The depression is formed originally by erosion of Paleogene sequences at the foot of the scarp. Present topography of the depression has resulted from insufficient Neogene filling of the original depression. A similar depression was observed at the SW foot, but not at the NE foot, of another hill located ca.85km NE of the "Ohmachi Hill".

The biggest among the several submarine canyons in the area northeasterly off Porpoise Bay is tentatively named "Porpoise submarine Canyon" after the Bay. It runs over 150km long, from the edge of continental shelf to the abyssal plain. Meandering of the canyon erodes Neogene and probably a part of Paleogene sequences, attaining a depth of more than 500m. Ridges between any two canyons are extensively eroded with no flat top between them them. In general, coarse sediments thinly deposit on the bottom of the canyons. There is apparently no fault control, which may affect the initiation of erosion, in the older sequences beneath the canyons.

METASOMATIC MODIFICATION OF UPPER MANTLE MATERIALS BENEATH THE McMURDO VOLCANIC FIELD, ANTARCTICA, DEDUCED FROM MANTLE-DERIVED XENOLITHS

K. Niida, Department of Geology and Mineralogy, Faculty of Science, Hokkaido University, Sapporo 060, Japan.

Ultramafic to mafic xenoliths were collected from the Late Cenozoic basanite lava flows at Cape Bird and McMurdo Station, Ross Island, in the scoria cone deposits at Turtle Rock, 1 km off the western coast of the Hut Point Peninsula, Ross Island, and at the summit of Mt. Nubian, Black Island. The upper mantle-derived xenoliths can be classified into two groups: (1) Cr-diopside series xenoliths (spinel lherzolite, harzburgite, dunite; representing a solid mantle peridotite), and (2) Al-augite series xenoliths (dunite, wehrlite, clinopyroxenite, gabbro; representing a cumulate suite). Crustal xenoliths, dominate in basic igneous rocks, also occur in association with group (1) and (2) xenoliths. The primary assemblage of group (1) xenoliths (porphyroclasts of Mg-rich olivine, orthopyroxene, clinopyroxene, and spinel) represent solid upper mantle, formed within the stability field of spinel-lherzolite. Some xenoliths comprise vein-minerals or interstitial hydrous minerals, indicating a modal metasomatic modification of upper mantle peridotite.

The most common features observed in the vein-type xenoliths are modal addition of metasomatic minerals (Fe-olivine, fassaitic augite, kaersutitic amphibole, phlogopitic mica, Al-spinel, and apatite), which provides evidence for basanitic melt infiltration and crystallization in the upper mantle peridotites. The spinel lherzolite xenoliths (Nos. 73-2 and 73-5) from Turtle Rock contain a small amount of quenched basanitoid glass in the metasomatic veins. Compositionally zoned olivine, diopside, and Cr-spinel are dominant along the veins. From the core to rim, the composition varies from those of primary phases in the mantle-derived peridotites to those of cumulus ones in the cumulate suite. Both of the above modifications are characterized by Fe-, Mn-, Ti-, Al-, alkalis-, P-enrichment and Mg-, Cr-, Si-depletion, suggesting an extensive infiltration of basanitic melt into the source region of the group (1) xenoliths beneath the McMurdo volcanic field.

Xenoliths from Mt. Nubian contain discrete grains of interstitial pargasite and phlogopite, showing a textural and chemical equilibration. The hydrous minerals are poor in Ti, Al, Cr and K, and rich in Si and Na, in contrast to the above types. Although the metasomatic agents and the processes have not been identified, the hydration appears to have taken place prior to the basanitic melt infiltration.

THE DIRECTIONS OF THE MAGNETIC ANOMALY LINEATIONS IN ENDERBY BASIN, OFF ANTARCTICA

Y. Nogi, Meteorological Research Institute, Nagamine, Tsukuba 305, Japan.
N. Seama, Ocean Research Institute, University of Tokyo, Minamidai, Nakano-ku, Tokyo 164, Japan.
N. Isezaki, Faculty of Science, Chiba University, Yayoi, Chiba 260, Japan.
M. Funaki & K. Kaminuma, National Institute of Polar Research, Kaga, Itabashi-ku, Tokyo 173, Japan.

Vector anomalies of the geomagnetic field were obtained along the two observation lines between Africa and Antarctica across the Enderby Basin and the Southwestern Indian Ridge during the 30th Japanese Antarctic Research Expedition. The directions of two dimensional magnetic structures along the two observation lines were determined by using vector anomalies of the geomagnetic field. The direction of the geomagnetic anomaly lineations and the fracture zones were determined from the directions of two dimensional magnetic structures by using satellite gravity data and bathymetric features as well as sea surface gravity and sea bottom topography obtained during this cruise.

In Enderby basin, complicated features of the directions of the geomagnetic anomaly lineations are present as follows: (1) between 59°S-63°S and 22°E-30°E, N-S and NNE-SSW directions of the magnetic anomaly lineations; (2) between 63°S and 65°S along about 31°E and 22°E, WNW-ESE directions of the magnetic anomaly lineations.

The directions of the lineations in region (2) along about 22E° coincide with the previously suggested directions of M series lineations off the Dronning Maud Land. Although WNW-ESE directions in region (2) along about 31°E have never been reported, their directions are in good agreement with that of M series lineations. This result suggests that a mid ocean ridge which created the lineations off Dronning Maud Land extended to the west.

The directions of lineations in region (1) is quite different from previously reported direction of seafloor spreading. To explain the geomagnetic anomaly lineations obtained in this region, the existence of N-S trending ridge should be postulated. Complex features of gravity anomaly in the south of 60°S despite flat bathymetric features, indicate the ridge could be buried under thick sediments.

These directions of the magnetic anomaly lineations must suggest complex spreading history during early opening of southwestern Indian Ocean. These results imply new constraints on the evolution of the Indian Ocean.

THE DIRECTIONS OF THE TWO DIMENSIONAL MAGNETIC STRUCTURE AROUND THE KERGUELEN PLATEAU

Y. Nogi, Meteorological Research Institute, Nagamine, Tsukuba 305, Japan.
N. Seama, Ocean Research Institute, University of Tokyo, Minamidai, Nakano-ku, Tokyo 164, Japan.
N. Isezaki, Faculty of Science, Chiba University, Yayoi, Chiba 260, Japan.
T. Hayashi, Geographical Survey Institute, Kitazato, Tsukuba 305, Japan.
M. Funaki & K. Kaminuma, National Institute of Polar Research, Kaga, Itabashi-ku, Tokyo 173, Japan.

Vector anomalies of the geomagnetic field were obtained around the Kerguelen Plateau during the 30th and 31st Japanese Antarctic Research Expedition. The directions of two dimensional magnetic structures originated by the geomagnetic polarity reversals and the fracture zones around the Kerguelen Plateau were determined by using vector anomalies of the geomagnetic field.

N-S and E-W directions of magnetic structure are present above the Kerguelen Plateau (around 60°S, 71°E-88°E). Topographic and structural lineaments of the Kerguelen Plateau reflect N-S and E-W directions of magnetic anomaly lineations.

Stable NE-SW directions are present in the west of the Kerguelen Plateau (58°S-61°S, 62°E-68°E). Because topography and free-air gravity anomalies show no structural offset, stable NE-SW directions observed here indicate these NE-SW directions are due to the geomagnetic polarity reversals. These directions have never been reported. NE-SW directions obtained from vector anomalies of the geomagnetic field support presumptive directions of the geomagnetic anomaly lineations originated from an ancient abandoned ridge, that is, the mid-ocean ridge between India and Antarctica from the Late Jurassic(160Ma) to the Middle Cretaceous(96Ma).

In the farther west along 60°S, the directions of two dimensional magnetic structures turn to N-S around 62°E. Stable N-S directions in the farther west may suggest that there is an ancient plate boundary around 62°E.

These results may provide detailed kinematics of the growth of the Indian Ocean.

BREAKUP AND DISPERSAL OF GONDWANALAND: AN ANTARCTIC PERSPECTIVE

Ian Norton, Exxon Production Research Co.,
P.O. Box 2189, Houston, TX 77252-2189, U.S.A.

Antarctica has been called the 'keystone' of Gondwanaland because most Gondwana continents were once attached to it. The history of formation of the present-day rift or passive margins of Antarctica is thus also the record of breakup of Gondwanaland. Gondwana rifting started in the Permian, eventually leading to continental separation by sea floor spreading in Middle Jurassic through Early Cretaceous time.

Chronology of the various tectonic events that formed Antarctica's margins is fairly well established, with timing of initiation of sea floor spreading between India and Antarctica being the least constrained. India's separation is usually assumed to be dated by M-sequence oceanic magnetic anomalies of Early Cretaceous (Hauterivian) age in the Perth Basin off Australia. These are assumed to have formed by separation of Australia (which was still attached to Antarctica) and 'Greater India', a part of India that has subsequently been subducted beneath Tibet. Recent studies of the India/Asia collision and tectonics of Tibet, however, suggest that there is no Greater India beneath Tibet, and that the present Indus-Tsangpo Suture is close to the original edge of continental India. Even restoration of the four to five hundred kilometers of convergence within the Himalaya is not enough to increase India's size enough to fill the Perth Basin in a restored Gondwanaland.

It is also impossible to make plate reconstructions that rigorously fit all M-sequence anomalies that have been found in the Indian Ocean, if the Perth Basin anomalies are assumed to be formed between Australia and Greater India. A geometric fit of all observed magnetics can, however, be obtained if it is assumed that the Perth Basin anomalies were formed by separation of a plate that was not attached to India, and that India separated from Antarctica in the Aptian, about 10 million years later than start of Hauterivian spreading in the Perth Basin. Absence of M-sequence anomalies off the conjugate Indian and Antarctic margins could be explained by Aptian separation, as this is the start of the Cretaceous normal polarity interval.

Breakup and separation of the Gondwana continents is illustrated in this presentation with computer-generated video animations of plate motions. Plate boundaries and other tectonic features (rifts, hotspots) are traced as they evolve. Animations are run to emphasize different aspects of the plate motions:

1) Phanerozoic paleolatitudinal motion of Antarctica.
2) From start of drifting in Jurassic time to the present, showing the whole Southern Hemispere.
3) A more detailed look at Cenozoic deformation of West Antartica and New Zealand.

EXPERIMENTAL STUDY OF THE SYENITIC ROCKS FROM THE YAMATO AND THE SØR RONDANE MOUNTAINS, EAST ANTACTICA.

Takanobu Oba, Department of Geoscience, Joetsu University of Education, Yamayashiki, Joetsu 943, Japan
Kazuyuki Shiraishi, National Institute of Polar Research, 1-9-10 Kaga, Itabashi-ku, Tokyo 173, Japan

The Yamato Mountains are made up of late Proterozoic to early Paleozoic high grade regional metamorphic rocks and syenitic and granitic rocks (Shiraishi et al. 1982). A syenite(Y405) indicates about 466 Ma in isochron age by Rb-Sr isotopic data. Small syenite bodies are distributed in the Yamato Mountains. Two syenites in the present study are collected from the different places. These analytical data and CIPW norms are given in Table 1. The K_2O/Na_2O ratios of the syenites from the Yamato Mountains are higher than 1. As compared to the syenites from the Sør Rondane Mountains, they have the low K_2O/Na_2O ratios. Shiraishi et al.(1982) reported that the trend in the AFM diagram is higher in Mg/(Fe+Mg) than the calc-alkalin trend.

The Sør Rondane Mountains are underlain by various kinds of upper amphibolite to granulite facies metamorphic rocks, possibily of late Proterozoic age, followed by several stages of plutonism. In the oldest of three syenite intrusion stages, the largest body of layered syenite has a heterogeneous appearance in a mesoscopic scale. In the dark mafic layers(SR-B) and the leucocratic syenite(SR-C), constituent minerals are K-feldspar, bluish green richteritic actinolite, bluish green clinopyroxene, biotite, quartz and plagioclase. In the leucocratic layer(SR-C) of the rhythmic layered syenite, albite occurs along grain boundaries of orthoclase whereas it occurs as very thin films around orthoclase in the mafic layer(SR-B). The younger intrusive rocks(SR-A) were found as dikes. In the youngest syenite which characteristically contains green microcline (amazonite), no amphibole is observed and green clinopyroxene occurs as subhedral prisms. Bulk chemical compositions of three syenites used for the experiment in the present study are shown in Table 1. These syenites are extremely rich in K_2O and P_2O_5 and slightly rich in TiO_2, but poor in Na_2O. The chemical characters are similar to those reported by Sakiyama et al. (1988).

The syenites from the Yamato and Sør Rondane Mountains are composed of porphyritic K-feldspar, plagioclase, quartz, biotite, Ca-amphibole or Ca-Na amphibole, clinopyroxene, sphene, ilmenite and rarely magnetite. Though the syenite from both regions consists of the same mineral assemblages, the compositions of amphiboles are various as follows; Ca-amphibole in the syenites(Y904 and Y405) from the Yamato Mountains is close to edenitic. On the other hand, the bluish green hornblende in the mafic layer(SR-B) and the leucocratic layer(SR-C) from the Sør Rondane Mountains is richteritic actinolite. In the leucocratic syenite(SR-A) intruding the layered syenites(SR-B and SR-C), the

Ca-amphibole is pargasitic hornblende. Clinopyroxene from Y405 syenite is augite-salite, on the other hand clinopyroxenes from four syenites are Na-augite.

The melting relationships of two hornblende clinopyroxene syenites from the Yamato Mountains and three hornblende clinopyroxene syenites from Sør Rondane Mountains were determined in the temperature range of 665-935°C, under a water pressure of 0.5-3.0 kbar and oxygen fugacities of the FMQ buffer in standard 'cold seal' pressure vessels. The buffer technique utilized a double capsule system. Inner capsules were 2.3mm-diameter $Ag_{70}Pd_{30}$ alloy, on the other hand outer capsules were 7 mm pure Ag. H_2O was always in excess(6-10 wt. per cent). After the rock sample for the starting materials was crushed in stenless mortar, it was ground together for 5 hours with ethyl alcohol in an agate mortar. The starting material is composed for small grains averaging 30 and ranging up to 50 in maximum dimension. Generally run times were between 150-435 hours for temperatures less than 850°C and from 96-150 hours at 850-935°C.

Representative results of syenites from the Yamato Mountains at 1 kbar are: clinopyroxene quartz syenite(Y904) begins to melt at 740° C, quartz and plagioclase disappear at 780°C, edenitic hornblende disappears at 850°C(as shown in Fig.1a), clinopyroxene hornblende quartz syenite(Y405) begins to melt at 780°C, plagioclase and quartz disappear at 780°C, K-feldspar disappears at 900°C, hornblende appears at 920°C. The pargasitic hornblende(Y405) is stable under all water vapor pressure in the present experiment. The composition of edenitic hornblende from Y904 syenite shifts to actinolite-pargasite join with increasing temperature under water pressure.

The water saturated solidus temperatures of the syenites from the Sør Rondane Mountains are about 700°C at 1 kbar. With increasing temperature, quartz and plagioclase(albite) disappeared in the lower temperature range than K-feldspar, hornblende, biotite and clinopyroxene. Clinopyroxene, biotite and K-feldspar are stable at 900°C under the water pressure of 1 kbar. Richteritic actinolite in two layered syenites(SR-B and SR-C) becomes unstable at temperatures 150°C above solidus at 1 kbar. With increasing temperature, richterite content in actinolite decreases at 1 kbar. Amphibole from SR-B syenite is richteritic actinolite at 760°C and 2.9 kbar, and on the other hand it is actinolite at 775°C and 1 kbar. Pargasitic hornblende from syenite(SR-A) is stable at 875°C/1 kbar and 760°C/2.9 kbar, and it disappears at 825°C and 2 kbar. Fig.1b shows the stability field of amphibole from SR-C syenite.

In two syenites of Y904 and SR-C, solidus of syenite and the stability limit line of amphibole intersect at the lower pressure than 3 kbar. The present experimental results suggest that hornblende could have crystallized only at pressures less than 3kbar(depth 10km), probably in a shallow crustal magma chamber.

All rocks investigated are at least 40 % melted at temperatures 50°C above the solidus. The approximate K-feldspar

content of the syenite is about 30 %. The compositions of K-feldspar are $Ab_{40}Or_{60}$ and Ab_5Or_{95} at 800°C and 700° C, respectively. As compared to biotite, the behavior of K-feldspar is important to concentrate K_2O content of syenite.

References

Sakiyama,T., Takahashi,Y. and Osanai,Y. 1988, Geological and petrological characters of the plutonic rocks in the Lunckeryggen-Brattnipene region, Sør Rondane Mountains, East Antarctica. Proc.NIPR Symp.Antarct.Geosci., 2, 80-95.

Shiraishi,K., Asami,M. and Kanaya,H. 1982, Petrochemical character of the syenitic rocks from the Yamato mountains, East Antarctica. Mem.Natl.Inst.Polar Res.,Spec.Issue, 28, 183-197.

Table 1. Analyses and CIPW norms of the syenitic rocks from the Yamato and the Sør Rondane Mountains.

	SR-A	SR-B	SR-C	Y904	Y405	Y406
SiO_2	57.43	46.13	59.78	65.31	50.70	61.64
TiO_2	1.42	2.00	0.65	0.82	1.68	0.77
Al_2O_3	15.36	6.87	16.25	15.50	7.68	14.72
Fe_2O_3	-	-	-	-	-	2.66
FeO*	5.37	11.24	3.49	3.46	10.25	2.89
MnO	0.06	0.17	0.03	0.03	0.25	0.03
MgO	2.01	10.02	1.78	0.94	9.35	1.99
CaO	4.86	13.42	2.15	1.47	9.36	2.81
Na_2O	3.41	1.02	1.72	4.48	3.19	4.36
K_2O	7.84	4.57	11.84	7.51	3.50	7.04
P_2O_5	0.93	3.39	0.62	0.21	3.54	0.35
Total	98.61	98.68	98.25	99.72	99.33	99.26
			CIPW norms			
Q				5.6		3.0
Or	47.0	27.4	71.2	44.5	20.8	41.6
Ab	25.2	1.7	14.0	38.0	20.2	36.5
An	3.5	0.7	1.7	tr.		
Ne	2.2	3.8	0.5			
Ns					1.6	
Di Wo	6.2	18.5	2.1	2.5	9.8	4.9
En	2.5	10.5	1.0	0.8	5.5	3.2
Fs	3.7	7.3	1.1	1.7	3.9	1.3
Hy En				1.5		1.7
Fs				3.3		0.7
Ol Fo	1.8	10.4	2.5		4.3	
Fa	3.0	8.0	3.3		4.3	
Il	2.7	3.8	1.3	1.6	3.2	1.5
Ap	2.2	8.0	1.5	0.5	8.3	0.8
K_2O/Na_2O	2.3	4.5	6.9	1.7	1.1	1.6

* Total Fe expressed as FeO.

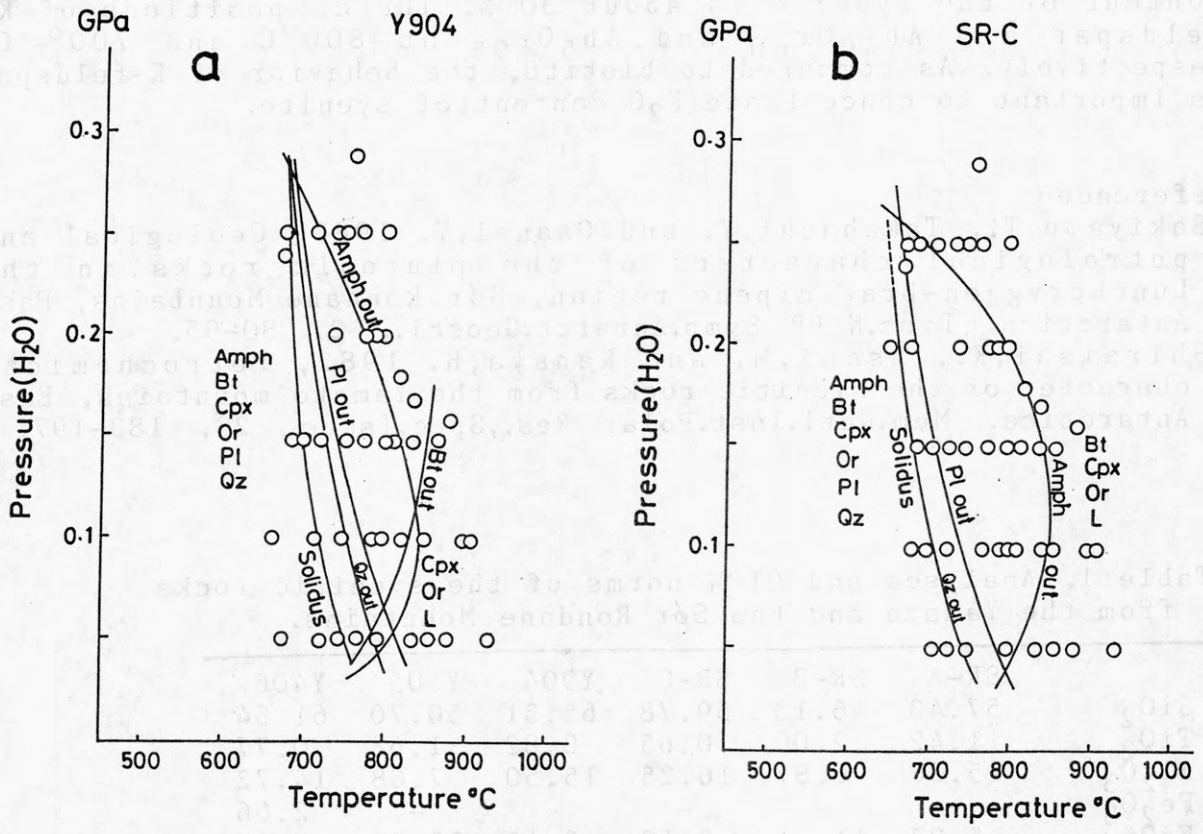

Fig.1 Pressure-Temperature diagram
a: Y904 syenite from the Yamato Mountains. b: SR-C syenite from the Sør Rondane Mountains.
Abbreviations: Amph=amphibole, Bt=biotite, Cpx=clinopyroxene, Or=orthoclase(and K-feldspar), Pl=plagioclse, Qz=quartz, L=liquid(glass)

A New Insight of Possible Correlation between the Lützow-Holm Bay Granulites (Antarctica) and the Sri Lankan Granulites

Y. Ogo[1], Y. Hiroi[1], K.B.N. Prame[2] & Y. Motoyoshi[3]

[1] *Department of Earth Sciences, Chiba University, Japan.*
[2] *Geological Survey Department, Sri Lanka.*
[3] *National Institute of Polar Research, Japan.*

1. Introduction

With respect to the *P-T* evolution of Lützow-Holm Bay granulites, relict kyanite (±quartz) and staurolite have been reported in garnet-sillimanite gneisses, which suggest a clockwise *P-T-t* trajectory for the rocks (Hiroi *et al.*, 1983a, b, 1991; Motoyoshi *et al.*, 1985, 1989). Similar petrographical characteristics have now been recognized in some Sri Lankan granulites, as represented by khondalite (garnet-sillimanite-graphite gneisses), from the Highland Series and the Southwestern Group rocks. The prograde metamorphic history of the granulites is also suggested by the rarely preserved growth zoning of some garnets in khondalites and pelitic gneisses from the central part of the Highland Series.

This paper gives new information on the *P-T* evolution of the Sri Lankan granulites, and discusses a possible correlation between the Lützow-Holm Bay granulites and the Sri Lankan granulites mainly based on petrographical evidence.

2. Petrography

We describe here some rocks which give petrographical constraints on the *P-T* evolution of the Sri Lankan granulites.

Relict kyanite+sapphirine+spinel±biotite in garnet (Sp. 88112401A): This rock contains garnet, orthopyroxene, biotite, sillimanite, kyanite, sapphirine, spinel, cordierite, magnetite, hematite, plagioclase, K-feldspar and quartz. Secondary spinel, corundum and rutile are associated with magnetite. In this rock, kyanite+sapphirine+spinel±biotite are interlocked with each other and they are totally included in garnet porphyroblasts. Because they are never present in the matrix, it is interpreted that these minerals are relict phases formed after staurolite locally in the absence of quartz. Retrograde metamorphism is suggested by the breakdown of garnet to form biotite+sillimanite+quartz and orthopyroxene+cordierite +magnetite, respectively.

Secondary andalusite (Sp. 88120403, 89090303, K89082407): Andalusite occurs in the cordierite-rich pelitic rocks cut extensively by pink granitic veins, that usually contain cordierite and are sometimes highly mylonitic. It is noteworthy that andalusite often coexists with siderite and is partially replaces cordierite together with siderite. Andalusite has been revealed to occur not only in the Southwestern Group rocks but also in the Highland Series rocks. All the modes of occurrence of andalusite indicate that it is a secondary mineral formed clearly after the widespread formation of sillimanite at the peak of regional metamorphism.

The petrographical evidence mentioned above provides constraints on the *P-T-t* trajectory of the Highland Series granulites, *i.e.* clockwise *P-T-t* path. This interpretation is at odds with Schumacher *et al.*'s (1990) idea, which suggests essentially an isobaric cooling (retrograde) *P-T* path from the very high-temperature conditions based on the textural and

mineralogical analyses on the basic to intermediate rocks. They further correlate this isobaric cooling path to that of the Archaean Napier Complex, Antarctica.

As a possible counterpart of the Highland Series and the Southwestern Group in the Gondwana reconstruction, relict kyanite+sapphirine+biotite association is also reported from the Lützow-Holm Bay region, East Antarctica (Motoyoshi, 1986). Because this association is quite unique in the East Antarctic Shield, it suggests further evidence for this juxtaposition.

3. Implications

The Highland Series and the Southwestern Group in Sri Lanka probably belong to the same metamorphic complex because of the similar mode of occurrence of relict kyanite and secondary andalusite. However, the Southwestern Group is characterized by widespread occurrence of cordierite and the local development of charnockitization.

This difference in metamorphic conditions between the Highland Series and the Southwestern Group may reflect the difference in uplift rate, *i.e.*, the Highland Series uplifted quickly which resulted in both pressure and temperature decreased markedly, whereas the Southwestern Group uplifted slowly which resulted in nearly isothermal decompression due to recovery of the geotherm.

In view of the close spatial relationship between the localities of andalusite and the sites of local charnockitization, it is inferred that local charnockitization has taken place at a relatively shallow level in the crust at a late stage of the metamorphic evolution.

References

Hiroi, Y., Shiraishi, K. Nakai, Y., Kano, T. & Yoshikura, S. (1983a). Geology and petrology of Prince Olav Coast, East Antarctica. In *Antarctic Earth Sciences*, ed. R.L. Oliver, P.R. James & J.B. Jago, 32-35. Canberra, Australian Academy of Science.

Hiroi, Y., Shiraishi, K., Yanai, K. & Kizaki, K. (1983b). Aluminum silicates in the Prince Olav and Soya Coasts, East Antarctica. *Memoirs of National Institute of Polar Research, Special Issue*, **28**, 115-131.

Hiroi, Y., Shiraishi, K. & Motoyoshi, Y. (1991): Late Proterozoic paired metamorphic complexes in East Antarctica, with special reference to the tectonic significance of ultramafic rocks. In *Geological Evolution of Antarctica*, ed by M.R.A. Thomson, J.A. Crame & J.W. Thomson, 83-87. Cambridge, Cambridge University Press.

Motoyoshi, Y. (1986). Prograde and progressive metamorphism of the granulite-facies Lützow-Holm Bay region, East Antarctica. PhD Thesis, Hokkaido University, 238p (unpublished).

Motoyoshi, Y., Matsubara, S., Matsueda, H. & Matsumoto, Y. (1985). Garnet-sillimanite gneisses from the Lützow-Holm Bay region, East Antarctica. *Memoirs of National Institute of Polar Research, Special Issue*, **37**, 82-94.

Motoyoshi, Y., Matsubara, S. & Matsueda, H. (1989). *P-T* evolution of the granulite-facies rocks of the Lützow-Holm Bay region, East Antarctica. In *Evolution of Metamorphic Belts*, ed. J.S. Daly, R.A. Cliff & B.W.D. Yardley, 325-329. London, The Geological Society.

Schumacher, R., Schenk, V., Raase, P. & Vitanage, P.W. (1990). Granulite facies metamorphism of metabasic and intermediate rocks in the Highland Series of Sri Lanka. In *High-temperature Metamorphism and Crustal Anatexis*, ed. J.R. Ashworth & M. Brown, 235-271. London, Unwin Hyman.

Shiraishi, K., Hiroi, Y., Motoyoshi, Y. & Yanai, K. (1987). Plate tectonic development of Late Proterozoic paired metamorphic complexes in eastern Queen Maud Land, East Antarctica. In *Gondwana Six: Structure, Tectonics, and Geophysics*, Geophysical Monograph 40, ed. G.D. McKenzie, 309-318. Washington D.C., American Geophysical Union.

GEOLOGY OF GJELSVIKFJELLA AND WESTERN MÜHLIG-HOFMANNFJELLA, WESTERN DRONNING MAUD LAND, AND RB/SR DATINGS

Y.Ohta, Norsk Polarinstitutt, Rolfstangen 12,
1330 Osl Lufthavn, Norway
B.O.Tørudbakken, Saga Petroleum A/S, Kjørboveien 16,
1301 Sandvika, Norway
K.Shiraishi, National Institute of Polar Research,
9-10 Kaga 1-chome, Itabashiku, 173 Japan

Gjelsvikfjella and western Mühlig-Hofmannfjella(2 E-5 35 E),Dronning Maud Land consist mainly of upper amphibolite to granulite facies rocks. The gneisses and banded migmatites, with probable meta-igneous rocks, are grouped as the Jutulsessen metasupracrustals, c.4,500m, whilst the granitic migmatites are named the Risemedet migmatites and have gradational transition. The metamorphic mineral assemblages with sillimanite, spinel and garnet in micaceous rocks, two pyroxenes in amphibolites and the Fe/Mg ratios among coexisting minerals, show the highest grade granulite facies, c.650-750°C and 7 kbar. The assemblages with cordierite and andalusite indicate retrograde process. An intermediate pressure prograde process is suggested by the inclusion of kyanite in garnet. The metamorphism is considered to be c. 1,100 Ma old, referring to the ages from the adjacent area and own preliminary isotope data from felsic gneisses of Gjelsvikfjella. Granulite--charnockites dominate in the western Mühlig-Hofmannfjella, with some banded gneisses and migmatites. The granulites here are homogeneous granitic rocks, partly showing intrusive relation to the gneisses, while the charnockites are clear intrusive rocks, having numerous angular xenoliths in the marginal parts. Fayalite-quartz-magnetite assemblages with hedenbergite are common in the charnockites, which gave the formation temperature, c. 750°C. The dark reddish charnockites often have irregular white patches of flame-like shape and sometimes in straight lines, the latter suggests that the white ones followed along joints. These two facies have similar composition and continuous texture across the boundary, whilst the dark part has two pyroxenes and the white one has hornblende-biotite. This occurrence indicates an important role of vapor phases for the transition between the granulite and amphibolite facies. A Rb/Sr age, 500+-24Ma obtained from the granulite, is the second major thermal event in this area.

METAMORPHISM OF BASEMENT ROCKS FROM THE SOUTHERN SHACKLETON RANGE

M. Olesch, FB Geowissenschaften, Univ. Bremen, PO-Box 330440, 2800 Bremen, FRG.

The Pioneers Escarpment which comprises metamorphic, proterozoic to late paleozoic rock successions, connects the mobile zones of the Transantarctic Mountains with the consolidated East Antarctic shield. Mineral analyses of garnet-kyanite-staurolite-biotite schists give an estimate of following peak metamorphic conditions: pressures range between 10 and 11 kbars at temperatures of about 600°C. This is indicated by Fe-mole ratios between 0.71 - 0.73 of garnet cores using the model of SPEAR & CHENEY (1989). Therefore, this P-T estimate resembles granulite facies conditions. The Fe-content increases towards the rim of the garnets up to Fe-mole ratios of 0.84 - 0.86), documenting a subsequent uplift. The garnet rim coexist with biotite, staurolite, and kyanite indicating amphibolite facies conditions. Thermobarometry gives pressures between 5 and 6 kbars at temperatures of 570 - 580°C. The temperatures were confirmed by the garnet-biotite geothermometer of FERRY & SPEAR (1978) and by the staurolite-garnet geothermometer of PERCHUK (1969).

The amphibolite facies conditions may either display a retrograde part of the uplift path during the Ross orogeny or may represent a distinct metamorphic event presuming an older (1100 Ma ?) granulite fazies event.

Also, biotite gneisses from the Read Mountains of the southernmost Shackleton Range indicate former granulite facies conditions. Pressures of 8 - 12 kbars at temperatures between 540 - 580°C were established using the ternary feldspar geothermobarometer.

However, P-T conditions for migmatitic cordierite-bearing gneisses from the DuToit-Nunataks, south-eastern part of the Shackleton Range range between 5 - 6 kbars at about 690°C. These peak conditions were estimated by garnet-biotite and garnet-cordierite geothermometers as well as sillimanite-plagioclase-geobarometer. These peak metamorphic conditions were continuously reduced to 2 - 3 kbars at about 515°C during a clockwise uplift path. Thus, these results clearly demand a single metamorphic evolution.

FERRY, J.M., SPEAR, F.S. (1978) Contrib Mineral Petrol 66: 113-117.
GREEN, N.L., USDANSKY, S.J. (1986) Am Mineral 71: 1100-1108.
PERCHUK, L.L. (1969) Dokl Akad Nauk SSSR 186: 1405-1407.
SPEAR, F.S., CHENEY, J.T. (1989) Contrib Mineral Petrol 101: 149-164.

METAMORPHISM AND TECTONICS OF THE DANIELS RANGE, NORTHERN VICTORIA LAND, AND POSSIBLE INTRA-AND INTERCONTINENTAL RELATIONSHIPS

R.L. Oliver
University of Adelaide, South Australia

In the Daniels Range, pelitic to semi-pelitic metasediments have been deformed by at least three folding events and intruded by an abundance of predominently felsic igneous material. The mineralogy of the metasediments is monotonously biotite-quartz-feldspar. The presence, in some localities of garnet and elsewhere of fibrolitic sillimanite and/or cordierite and/or anthophyllite together with plagioclase of intermediate composition indicates a metamorphic grade corresponding to the amphibolte facies. Some of the garnets are zoned, with peripheral compositions reflecting a cooling of crystallisation temperatures, verified by the application of garnet-biotite geothermometry. Disequilibrium compositional variation within some garnet grains is a function of proximity to adjaceant retrograde green chlorite.

Much granodioritic intrusive is closely admixed with metasediment (migmate) and is known as the Wilson Plutonic Complex (WCP). Somewhat more discreet (later?) felsic igneous bodies are classified as the Granite Harbour intrusives (GHI). Ion-microprobe U-Pb analyses of zoned zircons in a single WPC sample from the Daniels Range suggest 544±4 Ma for the WPC and infer 469±4 Ma for the GHI (black and Sheraton, 1990).

Several Gondwana reconstructions have been proposed by a number of writers. Some of these suggest correlation of the Wilson terrain in Antarctica with the Glenelg River Complex, in the southwesternmost corner of the state of Victoria, Australia, and the Kanmantoo in South Australia (e.g. Stump et al, 1986). There is some support for this, viz.

i) the lithological similarity (metagreywackes with intermittent pelitic horizons displaying greenschist to upper amphibolite facies metamorphism, the grade being a function of proximity to granitoid intrusions),

ii) ca 500 Ma age of granitoids in the Daniels Range and the Australian localities mentioned above, plus Tasmania (see Foden et al, 1990).

iii) subdivision of the granitoids intruding the Kanmantoo and within the Glenelg River Complex into post tectonic and syntectonic intrusives (Foden et al, 1990) and the subdivision of the Daniels Range granitoids into the Granite Harbour intrusives and those of the Wilson Group.

Tectonically, there are suggested similarities between the postulated allochthonous Cambrian and younger Palaeozoic terrain east of the Daniels Range in northern Victoria Land thrust westward against the Antarctic craton and postulated thrusting of the Kanamantoo against Proterozoic Adelaidean

and possibly similar histories in the Glenelg River area and in Tasmania (though see Gibson, 1989).

Reference

Black L. P. and Sheraton J. W., 1990. The influence of Precambrian source components on the U-Pb zircon age of a Palaeozoic granite from northern Victoria Land. Precambrian Research 46, 275-293.

Foden J. D., Turner S. P. and Morrison R. S., 1990. Tectonic implications of Delamarian magmatism in South Australia and western Victoria, *in* J. B. Jago and P. S. Moore (*Eds.*). Geol Soc Australia Spec. Publ. 16, 465-481.

Gibson G. M., 1989. Metamorphism and deformation of the Glenelg River Complex, western Victoria, and implications for correlations between SE Australia and northern Victoria Land. Geol Soc Australia Abstracts No. 24, 53.

Stump E., White A. J. R. and Borg S. G., 1986. Reconstruction of Australia and Antarctica: evidence from granites and recent mapping. Earth and Planetary Science Letters 79, 348-360.

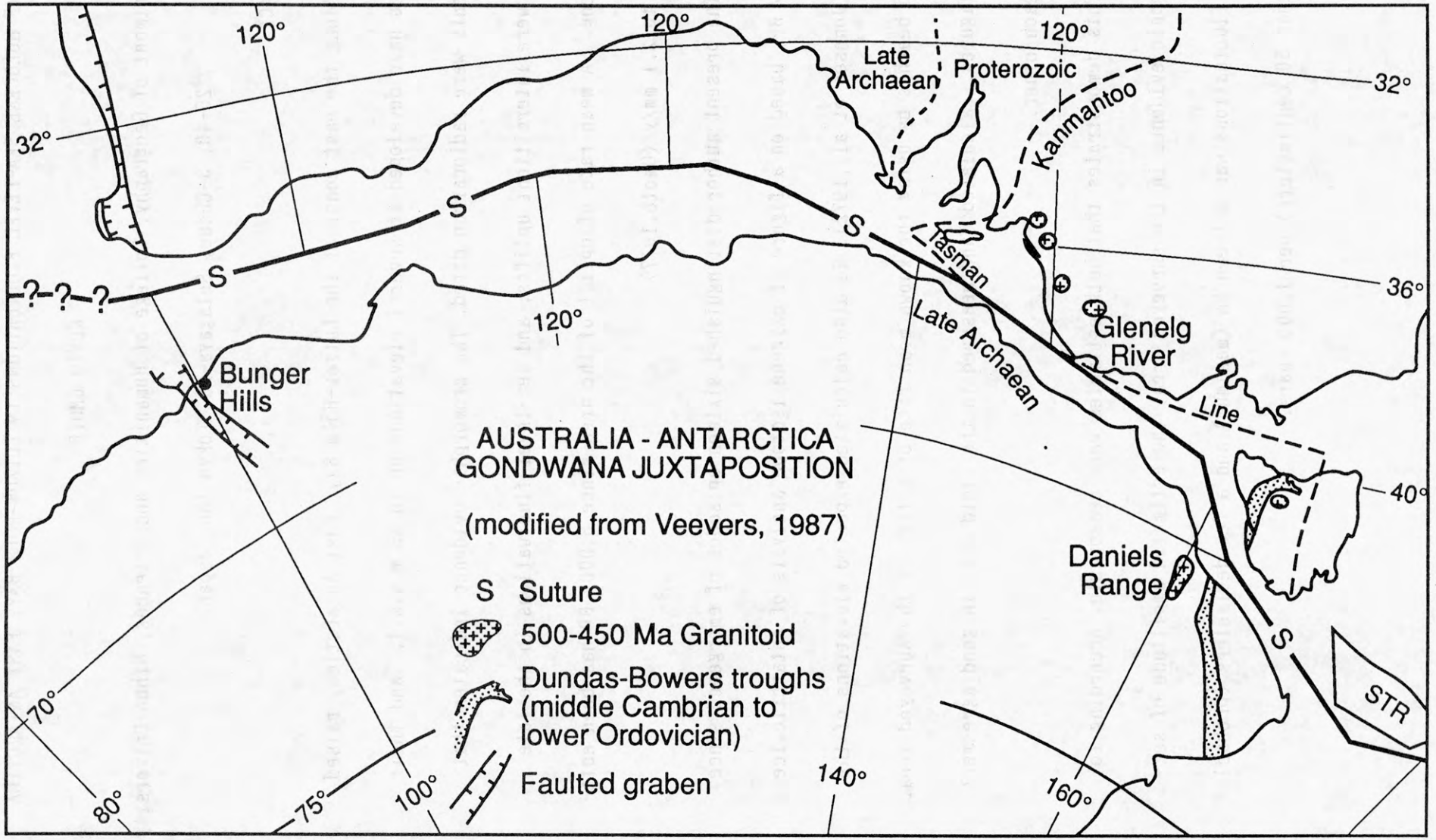
120°
120°
120°
32°
32°
Late
Archaean
Proterozoic
Kanmantoo
S
S
S
?-?-?
Tasman
Line
36°
120°
Glenelg
River
Late Archaean
Bunger
Hills
AUSTRALIA - ANTARCTICA
GONDWANA JUXTAPOSITION
(modified from Veevers, 1987)
S Suture
500-450 Ma Granitoid
Dundas-Bowers troughs
(middle Cambrian to
lower Ordovician)
Faulted graben
40°
Daniels
Range
S
STR
70°
80°
75°
100°
140°
160°

LATE HOLOCENE SEA-LEVEL FLUCTUATIONS IN LÜTZOW-HOLM BAY, EAST ANTARCTICA

KUNIO OMOTO

Department of Geography, College of Humanities and Sciences, Nihon University.

25-40, 3-Chome, Setagaya-ku, Tokyo 156, Japan.

ABSTRACT

Along the east coast of the Lützow-Holm Bay, East Antarctica, raised beaches have developed at several elevations up to 35 m.a.s.l., and their sediments were radiocarbon dated. The geomorphic evidence indicates that there were intermittent uplifts, and sea-level fluctuations in the late Holocene. A mean rate of uplift of the area since 6,000y BP has been estimated to 2.1 mm/y (Omoto,1977).

The present author distinguished sixteen episodes of emergence since 6,000y BP, based on a figure of oxygene isotope analysis of Antarctic ice core (Johnsen et al.,1972). He also calculated expected elevations of the raised beaches by using the known mean rate of uplift of the surveyed area. Both figures, calculated and measured in the field were in good agreement with each other.

This demonstrates that both estimates were reasonable. According to geomorphic evidence in the surveyed area, the estimated amplitude of sea-level fluctuations was between 2m (maximum) and a few decimeters (probably less than 50 centimeters) per 1,000 years.

GEOPHYSICAL FEATURES OF DECEPTION ISLAND

R. Ortiz, Museo N. Ciencias Naturales, CSIC, Madrid, Spain.
J. Vila, Institut d'Estudis Catalans. Barcelona, Spain.
A. Garcia, Museo N. Ciencias Naturales, CSIC, Madrid, Spain.
J.L. Díez, Museo N. Ciencias Naturales, CSIC, Madrid, Spain.
A. Aparicio, Museo N. Ciencias Naturales, CSIC, Madrid, Spain.
R. Soto, Real Observatorio Armada, S. Fernando, Cádiz, Spain.
J.G. Viramonte, Universidad N. Salta-CONICET, Rep. Argentina.
C. Risso, Universidad de Buenos Aires-IAA, Rep. Argentina.
I. Petrinovic, Universidad N. Salta-CONICET, Rep. Argentina.

Deception Island (South Shetland Island, Antarctica 62.93º S 60.57º W) is a complex strato volcano 14 km in diameter. This volcanic island has been very active during its entering evolution and it's possible to distinguish different episodes of volcanic activity. The central part of the island presents a calderic structure (BAKER and ROOBOL, 1975).

A Spanish-Argentine Cooperation Project have been developed to monitoring the present activity of volcano by application of geological and geophysical methods. Seismic, magnetic, gravimetric and thermometric surveys have been carried out during summer antarctic expeditions from 1986 to 1991. The magnetic and gravimetric land surveys cover the ice free part of the island (more than 70%) completed by a marine magnetic survey inside Port Foster Bay. The magnetic survey comprised 400 land stations and 2000 points the marine magnetic profiles. The gravimetric survey comprised 300 stations. Both surveys had a reference point located with the GPS 2001 benchmark placed near to Argentinean Station.

The Bouguer anomaly gravimetric map shows moderate values (<100 mgal). Only Fumarolic Bay presents a minimun probably reflecting the trace of the main fracture (NE-SW) in the island where the most fumarolic emissions are produced. Samples from fumaroles and thermal springs have been collected in this area. On the basis of their chemical compositions, a thermal anomaly connected to an underlying magma body and mainly distributed along the northern and eastern portions of the island can be derived.

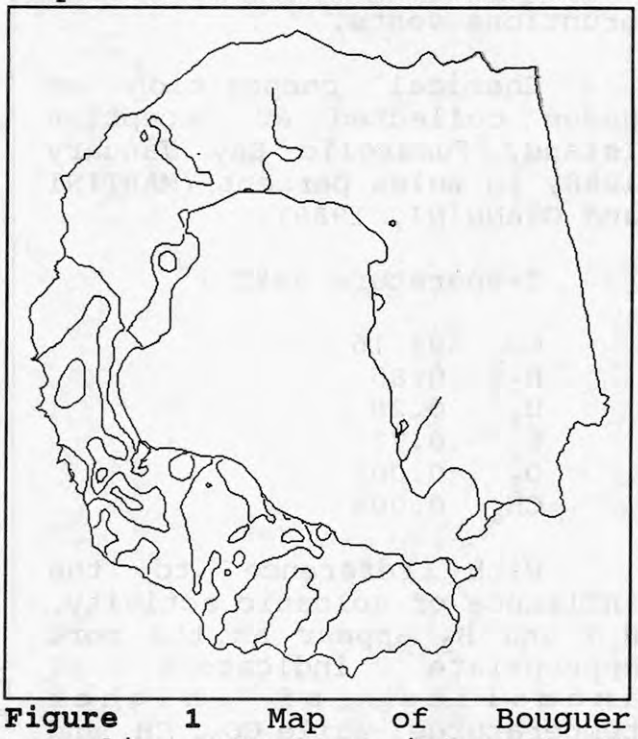

Figure 1 Map of Bouguer anomalies. Contour interval 10 mgal.

The magnetic field total intensity map (contour interval 500 γ) shows a significative low values (36800 γ) along a wide area NNW-SSE at the Port Foster NE sector. In this area was developed the last eruptions (1967, 1969, 1970). The maximun values (42700 γ) are spatially short and isolated, by that these values have been associated to dikes and massive lava flow. The long period magnetic field component (λ > 2.5 km) reveals the deep structure of the island. The results show a system of lineal structures. The large minimun magnetic anomaly (at NE sector) has been interpreted as being due to a low-magnetized body. Field changes up to several tens of γ per ºC (EMELEUS, 1977) rise in source are shown to be possible, taking into account the thermal state of the area with fumarolic emissions and the proximity of the last eruptions vents.

Chemical composition of gases collected at Deception Island, Fumarolic Bay January 1988, in moles percent (MARTINI and GIANNINI, 1989).

Temperature 99ºC

CO_2	98.16
H_2S	0.85
H_2	0.20
N_2	0.77
O_2	0.006
CH_4	0.009

With reference to the influence of volcanic activity, H_2S and H_2 appear as the more appropriate indicators of anomalies of higher temperatures, while CO_2, CH_4 and N_2 are probably the result of a lower degree of thermometamorphism.

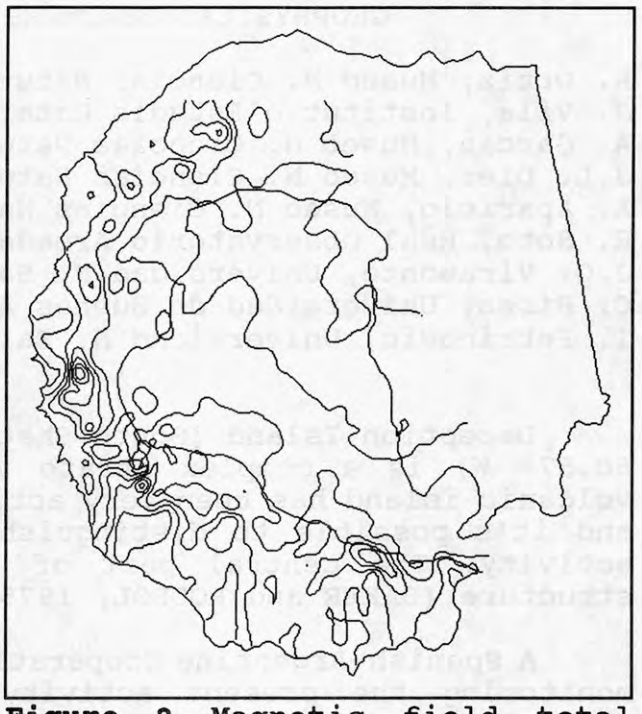

Figure 2 Magnetic field total intensity map. Contour interval 500 γ

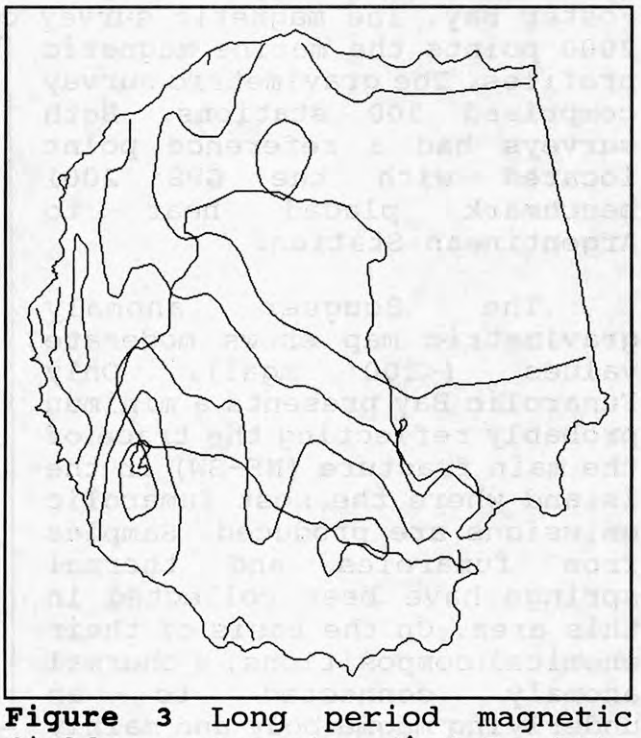

Figure 3 Long period magnetic field component (λ>2.5 km). Contour interval 500 γ

The gas geothermometry (CH_4-H_2-CO_2-H_2S), corresponding to Fumarolic Bay emissions, indicates a equilibrium temperature of 219 ºC for the superficial aquifers (VALENTIN et al., 1990). These aquifers are the shield to the deeper magmatic gas emissions. At depth temperatures higher of 600 ºC can be expected, connecting to an underlying magma body and mainly distributed along the northern and eastern portion of the island. The thermometric survey at Port Foster shows the influence of this magma body with high temperatures distributed accord to the same NE-SW structure.

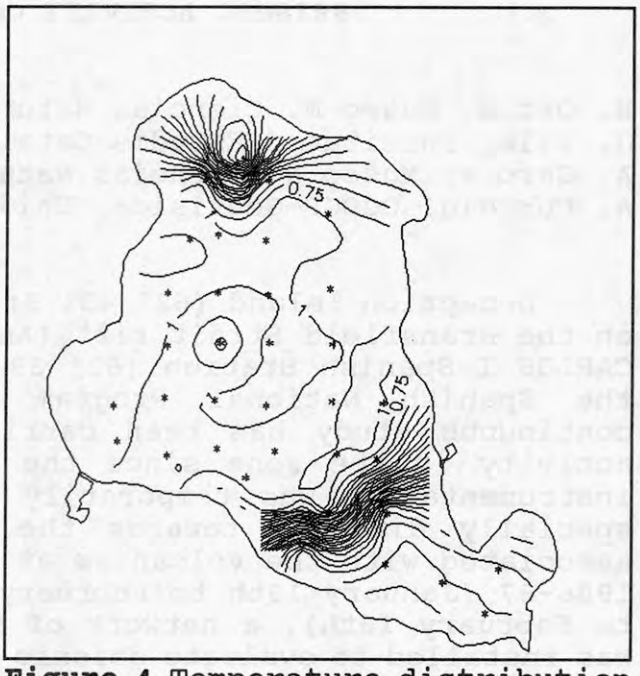

Figure 4 Temperature distribution at Port Foster Bay. Contour interval .1ºC. Dots are the points of measure.

The volcano surveillance program includes the control of ground deformation. With this aim a GPS network was installed (January, 1991). Four GPS benchmarks (Argentinean Station, Pendulum Cove, Fumarole Bay and Wallers Bay) were measured with a double frequence GPS receivers. Finally, three Dry_tilt were installed in Telephone Bay (1970 eruption area), Crater Lake (1842 eruption area) and Fumarolic Bay. Electronic distance measurements between benchmarks throughout Port Foster Bay where ground deformation is likely.

BIBLIOGRAPHY

Baker, P.F.; Roobol, M.J., 1975. The geology of the South Shetlands Islands. V. Volcanic Evolution of Deception Island. Br. Ant. Surv. Rep. 78: 3-15.

Emeleus, T.G., 1977. Thermo-magnetic measurements as a possible tool in the prediction of volcanic activity in the volcanoes of the Rabaul Caldera, Papua New Guinea. J. Volcanol. Geotherm. Res., 2: 343-359.

Martini, M.; Giannini, L., 1989. The thermal manifestations of Deception Island (South Shetlands, Antarctica). Dep. of Earth Sciences. Univ. of Florence, Italy.

Valentín, M.A.; Martini, M.; Díez-Gil J.L., 1990. Geoquímica de fluidos en la isla Decepción. Actas del III Symposium Español de Estudios Antárticos. CICYT. Madrid, 195-198.

SEISMIC ACTIVITY ON DECEPTION ISLAND

R. Ortiz, Museo N. Ciencias Naturales, CSIC, Madrid, Spain.
J. Vila, Institut d'Estudis Catalans, Barcelona, Spain.
A. Garcia, Museo N. Ciencias Naturales, CSIC, Madrid, Spain.
A. Correig, DGDGP-Geofísica, Universidad Barcelona, Spain.

Deception Island (62° 43' S; 60° 57' W), is an active volcano on the Bransfield Strait rift (Antarctica), located near the JUAN CARLOS I Spanish Station (62° 39' 46.9 S; 60° 23' 20.3 W). Under the Spanish National Program for Research in Antarctica a continuous study has been carried out of seismic and volcanic activity in the zone since the 1986-87 austral summer. Several instrumentation was temporarily installed during these surveys, specially directed towards the study of the seismic activity associated with the volcanism at Deception. During the surveys of 1986-87 (January 13th to February 11th) and 1987-88 (January 14th to February 16th), a network of 5 analog drum recording stations was installed to evaluate seismic activity at Deception. Over 2,000 events were recorded in this period. During the 1988-89 (December 29th to February 24th) and 1989-90 surveys (January 27th to February 20th) a digital seismic network was set up, with 6 FM telemetry stations on the VHF 170 MHz band, one of three components and five only vertical. The central unit included the set of receivers, demodulators and the digital recording system. The digital unit used a 14 bit analog-digital converter controlled by a laptop Pc, which operates at 64 or 128 samples per second. Data was digitally recorded on RAM-DISK, and periodically transferred to a 3.5" floppy disk. The detection algorithm employed was the STA/LTA (Short Term and Long Term Average) which was added digitals high-pass and low-pass filters. Data was only recorded when more than two stations exceeded the detection algorithm. All the geophones were of 1 Hz, Mark L4C type. A second PC was used for the real time preliminary analysis of the events registered. The electronic instruments and the software used were especially developed at the laboratories of the CSIC for operation in the Antarctica.

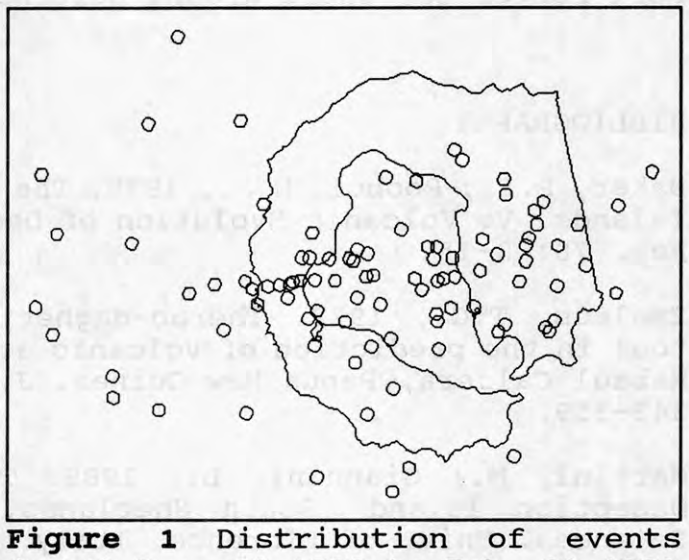

Figure 1 Distribution of events (m_l>1) Dec. 29 1988 to Feb. 23 1989

The successive surveys show that the seismic activity around Deception Island remained stationary, at approximately 500 seismic events (m_l > .8) a month. The distribution of located events be predisposed to

accumulate around fractures previously detected by field geology and photointerpretation works. The distribution of events clearly emphasized the activity in a main fracture which crosses the island from W-E, continuing outward. Otherwise, N-S alignments were observed inside and outside of Deception. These system of fractures are evidence of the impossibility of separating Deception Island from the rest of the Bransfield rift. The events are distributed throughout the island and temporarily appear grouped by zones and generally aligned in accordance with the directions of the main fractures (slightly NE-SW and interconnected). At Fumarole Bay and Telephon Bay there is a continuous seismic activity with a great number of small scale events. Regional seismicity is concentred to an important N-S active fracture approximately 10 Km to the west of Deception Island.

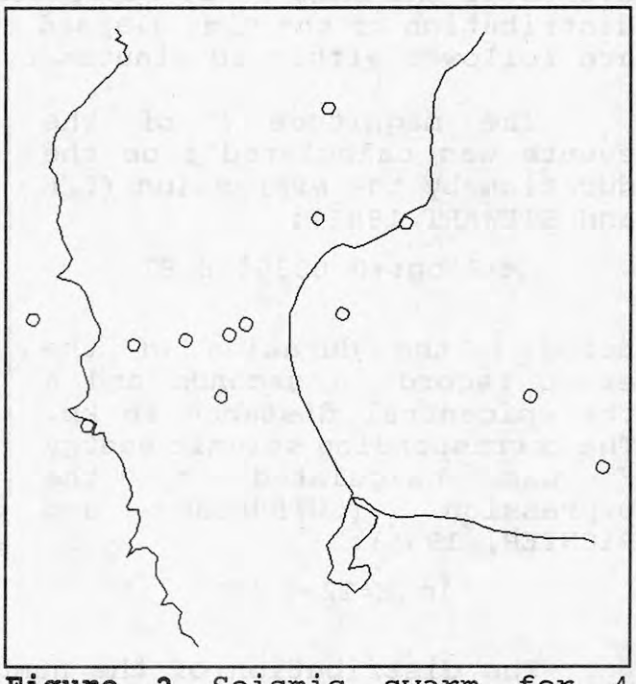

Figure 2 Seismic swarm for 4 hours occurred the January 31 1989 at Fumarolic Bay (m_l>.8)

Another regional seismic activity follows the direction line of the Bransfield rift at the southern of Deception Island. The annular morphology and the predominant pyroclastic matter on the island provides the latter with a high level of background noise, so it is not possible to operate with high gain. As a result, many events are only registered by one or two stations and so they can only be statistically analyzed.

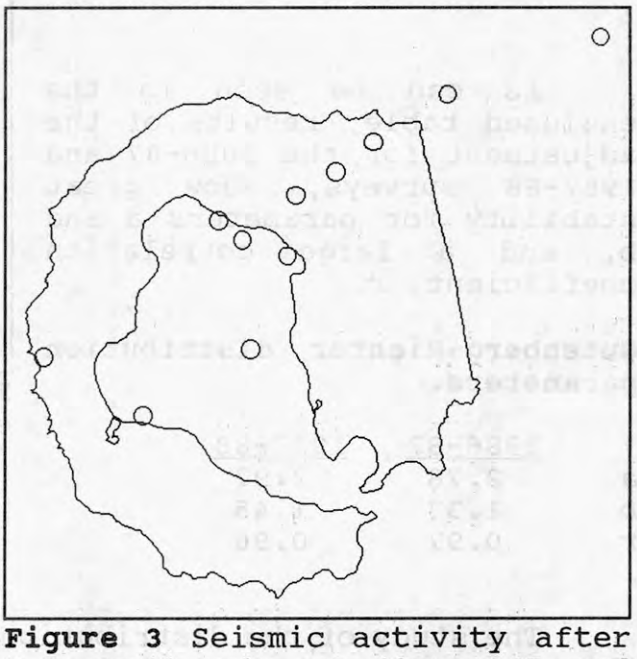

Figure 3 Seismic activity after 3.2 earthquake at the 1967 and 1970 eruptions area occurred the January 14 1991

The residues obtained in the localization of the events point towards the presence of a low velocity zone in a NW-SE direction in the eastern part of the island, which coincides with a detected magnetic anomaly. The delay is of 0.2 seconds for the seismic waves from outside the island, in E-W direction and crossing the magnetic anomaly.

In general, seismic events appear in clusters, i.e. various events at the same zone, separated by short intervals of time. The distribution of the time elapsed events shows that most earthquakes are followed within 10 minutes by another event.

The magnitude M of the events was calculated from the duration by the expression (LEE and STEWART 1981):

$$M=2\log\tau+0.0035\delta-0.87$$

being τ the duration of the event record in seconds and δ the epicentral distance in km. The corresponding seismic energy E was calculated by the expression (GUTENBERG and RICHTER, 1956):

$$\log E=12+1.5M$$

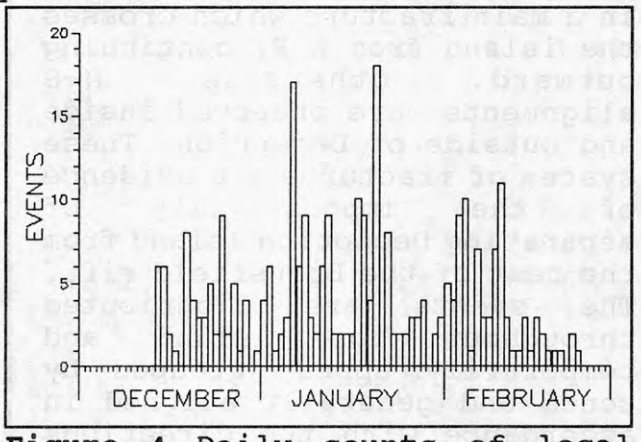

Figure 4 Daily counts of local earthquakes (m_l>0.8) in 1990-91

The distribution of the number of events, N, in relation to the magnitude, allows for the determination of the Gutenberg-Richter distribution parameters, a and b:

$$\log N=a-bM$$

As can be seen in the enclosed table, results of the adjustment for the 1986-87 and 1987-88 surveys, show great stability for parameters a and b, and a large correlation coefficient, r.

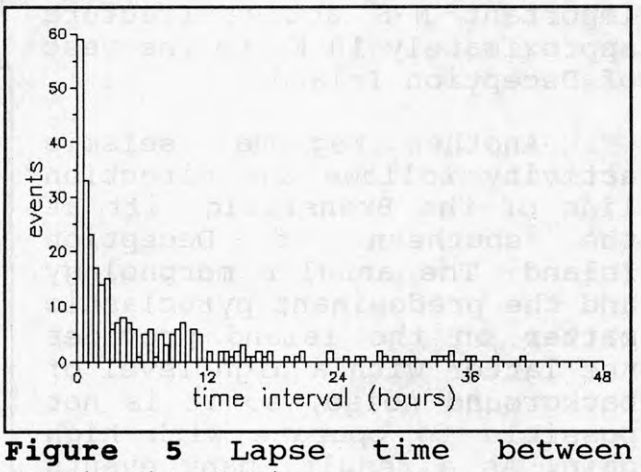

Figure 5 Lapse time between events (m_l>0.8)

Gutenberg-Richter distribution parameters.

	1986-87	1987-88
a	2.78	2.97
b	1.37	1.45
r	0.97	0.96

The study of the distribution of the seismic energy shows that this remains constant during the periods studied, with an average value of $8.8\cdot10^{14}$ ergs/day.

One common feature of active volcanic areas is the presence of tremors in the form of seismic noise. These registers are generally classified in relation to the characteristics of their signal, which in turn depend upon the zone in question; these

characteristics are: limited variation of the envelope in terms of time and large estability in the spectral content.

The volcanic tremors appear frequently at Deception Island and are especially detected at stations located them at Fumarole Bay and close to the 1969 and 1970 emission centers. Very often when a tremor is identified, this is preceded or followed by an increase in the seismic activity of the zone and in some cases by earthquakes swarms. Frequently events of different characteristics are observed superimposed with the tremor. After an important series of tremors and small earthquakes at Fumarole Bay, the whole beach appears covered in a thick layer of dead krill. This fact was probably due to a strong emission of gas in the underwater fumaroles.

Three different types of volcanic tremors were defined, associated with the high temperature fumarolic field at Fumarole Bay and in the zone of the last eruptions to have taken place on the island. Lobulated aspect tremors are to be found all over the island although they prevail in the fumaroles areas. Low frequency, long lasting tremors are to be found at Fumarolic Bay. The spectral features of these tremors are explained by the model of acoustic emission in the ducts. Tremors triggered by a local seismic event and with high frequencies appear close to the large magnetic anomaly located to the NE-SE of the island.

REFERENCES

GUTENBERG B.; RICHTER C.F.1956.- *Magnitude and Energy of Earthquakes*. Ann. Geofis., 9: 1-15.

LEE W.; STEWART S. 1981.- *Principles and Aplications of Microearthquakes Networks*. Academic Press. New York: 221 pp.

ORTIZ R.; VILA J. 1990.- *Red sísmica para su utilización en condiciones antárticas*. III Symposio de Estudios Antárticos. CICYT. Madrid: 345-349.

CHEMICAL FEATURES OF METAMORPHIC ROCKS FROM THE CENTRAL SØR RONDANE MOUNTAINS, EAST ANTARCTICA

Yasuhito Osanai, *Department of Earth Sciences and Astronomy, Fukuoka University of Education, 729 Akama, Munakata 811-41.*
Yuhei Takahashi, *Geological Survey of Japan, 1-3, Higashi-1, Tsukuba 305.*
Kazuyuki Shiraishi, *National Institute of Polar Research, Itabashi-ku, Tokyo 179.*
Tohru Sakiyama, *Hyogo Natural Science Museum, chuou-ku, Kobe 650.*
Yoshiaki Tainosho, *Department of Earth Science, Faculty of Education, Kobe University, Nada-ku, Kobe 657.*
Noriyoshi Tsuchiya, *Department of Mining and Mineral Engineering, Faculty of Engineering, Tohoku University, Aoba-ku, Sendai 980.*
Hideo Ishizuka, *Department of Earth Science, Faculty of Science, Kochi University, 2-5 Akebono-cho, Kochi 790.*

1. Introduction

The Sør Rondane Mountains consists mainly of Proterozoic high- and medium-grade metamorphic rocks and various kinds of intrusive plutonic rocks. The metamorphic rocks show evidence of c.1000 Ma granulite-facies metamorphism in the northern part and were intruded by 950 Ma and c.500 Ma plutonic rocks. During the late Proterozoic to early Cambrian orogeny, strong deformation and thrust-up movement took place with typical mylonite formation. Five distinct mylonite zones including older suture zone and younger shear zone form tectonic boundaries in the central Sør Rondane Mountains (Fig. 1). Therefore, we can divide the metamorphic rocks into six lithologic units.

To determine the geochemical characteristics of metamorphic rocks in each unit, major, trace and rare earth element analyses were carried out. The analyzed samples were collected by 25th - 28th and 31st Japanese Antarctic Research Expedition (JARE). The aim of this paper is to describe the geochemical characteristics of metamorphic rocks from the Sør Rondane Mountains, and to consider the original rock constitution in relation to the tectonic environments.

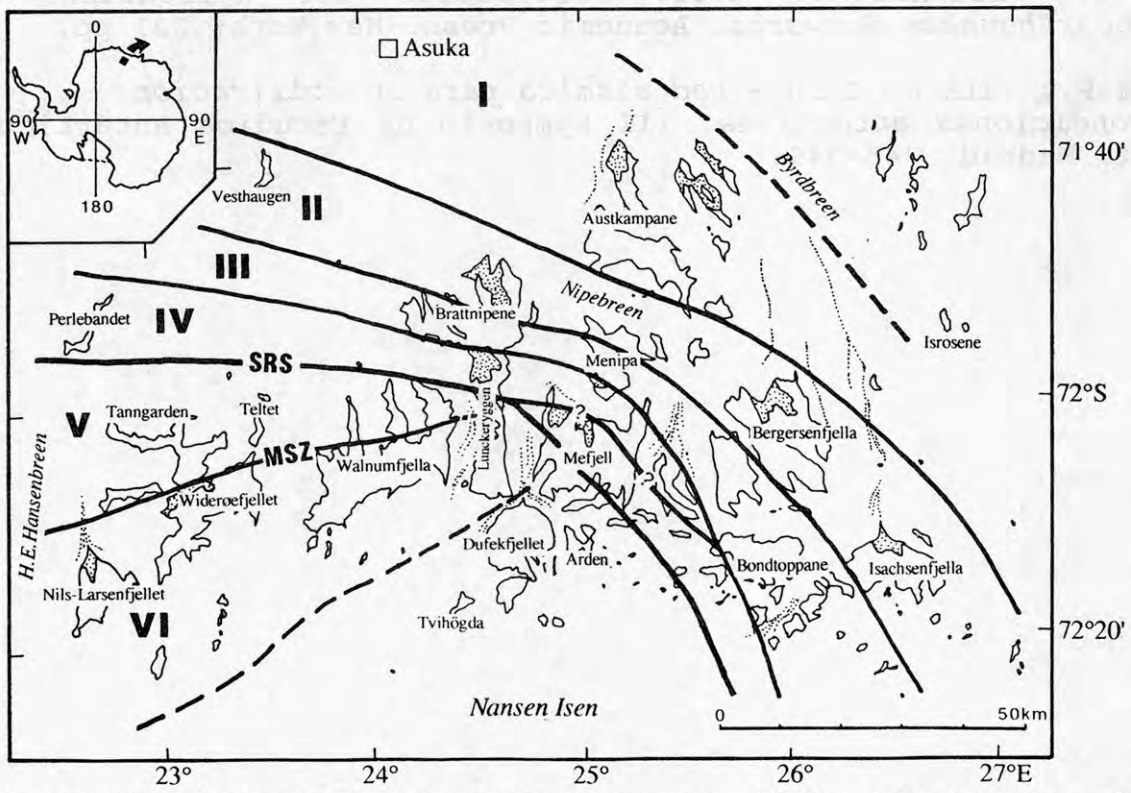

Fig. 1 Tectonic division of lithologic units in the central Sør Rondane Mountains. General geology of the region is reported by Shiraishi et al. (1990).

2. Geological Outline

2.1 Geology of the central part of the Sør Rondane Mountains

The central part of the Sør Rondane Mountains is composed of various kinds of metamorphic rocks and intrusive plutonic rocks (Kojima and Shiraishi, 1986; Ishizuka and Kojima, 1987; Sakiyama et al., 1988; Shiraishi et al., 1990). The metamorphic rocks can be divided into two groups; the northern group, which are rich in hornblende-biotite gneiss and garnet-biotite gneiss with subordinate amphibolite and calc-silicate gneiss, while the southern group consists mainly of meta-tonalite and basic schist. Van Autenboer (1969) and Van Autenboer and Loy (1972) grouped the metamorphic rocks into the Teltet-Vengen Group (TVG) in the north and the Nils-Larsen Group (NLG) in the south of the west-central part of the Sør Rondane Mountains. Therefore, it seems likely that the northern and the southern groups are equivalent to the TVG and the NLG, respectively. The boundary between the two groups is the Main Shear Zone (MSZ) (Kojima and Shiraishi, 1986).

The metamorphic rocks can be classified into following six rock types ;
(1) Bt gneiss, (2) Grt-Bt gneiss, (3) Bt-Hbl or Hbl-Bt gneiss, (4) Grt-Bt-Hbl or Grt-Hbl-Bt gneiss, (5) amphibolite and (6) calc-silicate rock. Opx is found in Hbl-Bt gneiss, Grt-Bt gneiss and amphibolite. An Mg-rich Crd-Grt-Kfs association is also found in Grt-Bt gneiss, which indicate the granulite-facies metamorphism in the TVG. However, Opx and related granulite-facies mineral assemblages are not found in the NLG and the southern TVG .

The metamorphic P-T conditions of the granulite-facies rocks have been estimated by using various geothermobarometers. P-T conditions determined on pelitic rocks are 750° to 850 °C and 7 to 8 kbar for non-mylonitized gneisses, and 530° to 630 °C and 5 to 5.5 kbar for mylonitized gneisses (Asami and Shiraishi., 1987; Osanai et al., 1988).

2.2 Division of lithologic units

The TVG is characterized by north-dipping thrust faults trending WNW-ESE which are subparallel to the metamorphic foliation. The general trend of geologic structure show E-W to ENE-WSW strike with a steeply dipping to south, while those along the thrust faults are overturned and are dipping to the north. The rocks around the thrust faults are strongly deformed into blastmylonite to ultramylonite with right-lateral strike-slip sense. The mineral lineations on these mylonite foliations dip toward the northwest. The distribution of mylonite zones is shown in Fig. 1.

On the basis of the distribution of the thrust faults with mylonite zone as the tectonic boundaries, the metamorphic rocks of the TVG and other mountain masses, which are underlain by granulite-facies rocks, can be divided into five lithologic units (unit I - V). If we use the MSZ as a tectonic boundary, the whole central part of the Sør Rondane Mountains can be divided into six units (Fig. 1). The granulite-facies metamorphic rocks lie in the units I, II, III and IV, while amphibolite-facies and lower grade metamorphic rocks lie in the units V and VI. So far the MSZ has been thought to the important tectonic boundary in the central part of the Sør Rondane Mountains (Kojima and Shiraishi, 1986; Ishizuka and Kojima, 1987; Shiraishi et al., 1990). However, there are most distinctive boundary between units IV and V, which means the boundary between the granulite and amphibolite terrains, at the northern part of the Mefjell mountain mass (Fig. 1). Therefore, it seems that this boundary, which we call the Sør Rondane Suture (SRS), is the most important tectonic boundary in the Sør Rondane Mountains.

3. Geochemistry of metamorphic rocks

In this section, we describe the chemical characteristics of the metamorphic rocks to discriminate the tectonic environments comparing to the modern plate tectonic systems. The plate tectonic systems and related lithologic associations in the Proterozoic age are very similar to those of the Phanerozoic (Condie, 1989a). The representative bulk chemical compositions are shown in Tables 1 and 2.

3.1 Basic metamorphic rocks

The basic metamorphic rocks occur in all units from I to VI in the central Sør Rondane Mountains. Most of samples have olivine and diopside normative basaltic compositions; a few have hypersthene in the norm.

Table 1 Major chemistry and CIPW norms of matamorphic rocks from the central Sør Rondane Mountains.

	Basic rocks						Intermediate rocks					Pelitic rocks					
	1	2	3	4	5	6	7	8	9	10	11	12	13	14	15	16	17
SiO_2	46.93	48.66	46.79	51.35	49.40	48.54	55.62	57.41	67.98	59.20	58.05	53.67	70.81	56.93	58.10	52.08	69.37
TiO_2	0.96	0.96	1.64	1.02	1.11	0.98	0.79	1.50	0.53	0.82	1.81	1.14	0.37	0.62	1.40	0.80	0.73
Al_2O_3	15.41	14.47	14.46	16.58	14.24	17.59	14.90	14.40	13.93	17.03	14.56	24.02	15.79	16.07	16.04	14.67	12.98
Fe_2O_3	1.06	1.43	1.33	0.84	1.43	1.06	1.29	1.14	1.05	0.62	0.68	1.21	0.28	1.39	1.08	6.47	0.65
FeO	9.58	12.90	11.95	7.51	12.86	9.58	11.63	10.23	4.49	5.59	6.12	10.86	2.56	12.54	9.71	12.65	5.82
MnO	0.23	0.17	0.20	0.13	0.34	0.17	0.48	0.18	0.08	0.11	0.09	0.11	0.03	0.47	0.16	0.39	0.07
MgO	9.55	5.94	7.37	7.71	6.79	6.62	2.95	1.42	1.38	3.04	2.35	3.24	0.75	6.38	5.05	6.63	2.44
CaO	9.48	7.98	12.26	10.21	7.76	10.10	6.65	4.29	4.33	5.43	4.85	0.34	2.56	0.86	2.52	1.08	0.80
Na_2O	1.87	4.27	2.08	3.31	3.62	3.26	3.73	3.49	4.26	5.44	4.26	0.31	4.82	2.62	2.42	0.35	2.28
K_2O	2.23	1.66	0.64	0.87	1.04	1.58	0.84	3.99	1.17	1.92	3.95	3.43	0.97	2.16	1.91	3.13	3.99
P_2O_5	0.05	0.07	0.15	0.11	0.13	0.20	0.20	0.85	0.09	0.18	1.31	0.09	0.04	0.01	0.26	0.13	0.06
LOI	1.82	1.03	1.25	0.90	0.89	0.73	0.48	0.80	0.43	0.81	1.42	0.59	1.25	0.44	1.11	1.67	0.53
Total	99.17	99.54	100.12	100.54	99.61	100.41	99.56	99.70	99.72	100.19	99.45	99.01	100.23	100.49	99.76	100.05	99.72
A/CNK	0.678	0.620	0.697	0.665	0.922	0.692	0.779	0.806	0.863	0.815	0.724	4.963	1.159	1.957	1.509	2.050	1.363
mg	0.618	0.427	0.500	0.624	0.461	0.528	0.291	0.184	0.312	0.468	0.383	0.326	0.322	0.452	0.457	0.390	0.404
								C.I.P.W. norm									
Q	---	---	---	---	---	---	5.71	6.67	26.02	2.70	5.35	25.90	30.77	12.32	16.76	18.33	31.49
C	---	---	---	---	---	---	---	---	---	---	---	19.46	2.14	7.95	5.40	9.07	3.46
or	13.36	10.0	23.90	5.01	6.12	9.46	5.01	23.37	6.68	11.13	23.37	20.03	5.57	12.80	11.13	18.36	23.37
ab	13.11	22.54	17.83	27.79	30.41	19.14	31.46	29.36	36.18	46.14	36.18	2.62	40.90	22.02	20.45	3.15	19.40
an	26.98	15.30	28.09	28.09	19.75	28.37	21.41	11.96	15.57	16.41	8.90	0.83	12.79	4.17	12.52	4.45	3.89
di	16.33	20.49	26.46	17.66	15.07	17.21	9.27	3.85	4.22	8.09	6.26	---	---	---	---	---	---
wo	8.36	10.22	13.35	9.06	7.55	8.71	4.53	1.86	2.09	4.06	3.14	---	---	---	---	---	---
en	4.85	4.26	6.56	5.38	3.35	4.43	1.29	0.37	0.75	1.88	1.41	---	---	---	---	---	---
fs	3.12	6.01	6.55	3.22	4.17	4.07	3.45	1.62	1.38	2.15	1.71	---	---	---	---	---	---
hy	---	---	0.79	5.92	1.28	---	22.56	17.41	7.81	12.13	11.02	25.38	5.73	37.63	28.25	33.88	15.20
en	---	---	0.42	3.83	0.58	---	6.20	3.30	2.80	5.80	4.42	8.10	1.90	16.00	12.55	16.60	6.10
fs	---	---	0.37	2.09	0.70	---	16.36	14.11	5.01	6.33	6.60	17.28	3.83	21.63	15.70	17.28	9.10
ol	22.61	18.53	15.73	11.23	21.53	16.73	---	---	---	---	---	---	---	---	---	---	---
fo	13.44	7.53	8.07	6.93	9.23	8.58	---	---	---	---	---	---	---	---	---	---	---
fa	9.17	11.00	7.66	4.30	12.30	8.15	---	---	---	---	---	---	---	---	---	---	---
mt	1.62	2.08	1.85	1.16	2.08	1.62	1.85	1.62	1.62	0.93	0.93	1.85	0.46	2.08	1.62	9.29	0.93
il	1.82	1.82	3.19	1.97	2.12	1.82	1.52	2.88	1.06	1.52	3.49	2.12	0.76	1.21	2.73	1.52	1.37
ap	0.12	0.16	0.35	0.26	0.31	0.47	0.47	2.02	0.21	0.43	3.10	0.21	0.10	0.02	0.62	0.31	0.14
unit	I	II	III	IV	V	VI	II	III	IV	V	V	I	II	III	IV	V	VI

1 - 6: Basic rocks, 7 - 11: Intermediate rocks, 12 - 17: Pelitic rocks

Table 2 Trace elements in parts per million.

	Basic rocks						Intermediate rocks					Pelitic rocks					
	1	2	3	4	5	6	7	8	9	10	11	12	13	14	15	16	17
V	186	272	329	219	317	191	140	70	63	97	102	146	16	72	202	360	152
Cr	248	83	236	262	130	51	8	8	9	31	10	80	10	24	300	32	60
Ni	159	14	69	10	46	11	1	1	1	12	1	13	2	6	156	14	21
Rb	159	23	11	28	11	39	3	69	43	87	70	144	22	76	73	19	304
Sr	101	137	221	364	108	607	263	370	184	446	3034	43	463	51	127	10	252
Y	22	30	27	25	30	25	41	59	39	24	27	44	16	113	29	81	53
Zr	41	45	89	61	67	167	112	745	85	168	535	191	204	167	140	36	218
Ba	136	167	81	217	90	177	360	1421	243	675	4146	535	672	646	381	760	572
Th	<1	<1	<1	---	<1	<1	<1	<1	---	8	---	18	5	<1	4	---	---
U	<1	<1	<1	---	<1	<1	<1	<1	---	4	---	3	<1	<1	2	---	---
Hf	1	1	2	---	6	---	1	4	---	5	---	9	11	5	5	---	---
La	5.0	11.0	4.0	---	11.0	2.0	3.0	10.0	---	8.0	---	59.0	42.0	20.0	20.0	---	---
Ce	13.0	32.0	7.0	---	25.0	7.0	5.0	21.0	---	28.0	---	116.0	69.0	27.0	41.0	---	---
Nd	8.0	17.0	6.0	---	21.0	5.0	5.0	11.0	---	11.0	---	59.0	27.0	6.0	18.0	---	---
Sm	3.5	6.2	2.4	---	5.6	1.7	1.2	3.6	---	4.1	---	13.2	8.3	5.6	5.2	---	---
Eu	1.6	1.1	0.7	---	1.9	0.4	0.3	0.8	---	0.8	---	1.0	1.4	1.6	1.3	---	---
Tb	0.4	1.5	0.6	---	0.5	0.3	<0.1	0.9	---	0.8	---	1.4	0.9	3.8	0.5	---	---
Yb	2.4	5.2	2.1	---	2.1	1.4	1.1	2.9	---	1.9	---	5.1	7.1	14.0	3.1	---	---
Lu	0.4	1.0	0.3	---	0.4	0.2	0.2	0.5	---	0.4	---	1.0	1.1	2.2	0.5	---	---
$(La/Yb)_N$	1.41	1.43	1.29	---	3.54	0.97	1.84	2.33	---	2.85	---	7.82	4.00	0.97	4.36	---	---
$(La/Sm)_N$	0.90	1.12	1.05	---	1.24	0.74	1.57	1.75	---	1.23	---	2.81	3.19	2.25	2.42	---	---
$(Tb/Lu)_N$	0.66	0.98	1.31	---	0.82	0.98	0.33	1.18	---	1.31	---	0.92	0.54	1.13	0.66	---	---
DF 3	---	---	---	---	---	---	0.88	2.60	2.11	4.81	4.57	-5.76	2.80	-7.21	-4.56	-10.77	-2.87
DF 4	---	---	---	---	---	---	4.85	6.04	3.29	4.03	4.27	-5.01	-0.33	1.16	-12.35	2.92	2.38
unit	I	II	III	IV	V	VI	II	III	IV	V	VI	I	II	III	IV	V	VI

1 - 6: Basic rocks, 7 - 11: Intermediate rocks, 12 - 17: Pelitic rocks

The chondrite normalized patterns are divided into two groups: (1) flat patterns ($(La/Yb)_N$=0.97-1.43) with little or no light REE (LREE) and heavy REE (HREE) fractionations ($(La/Sm)_N$= 0.74-1.12, $(Tb/Lu)_N$=0.65-1.31) and (2) slightly LREE enrichment patterns relative to HREE of $(La/Yb)_N$=2.8-3.5 with LREE and HREE fractionations are $(La/Sm)_N$=1.24-2.14 and $(Tb/Lu)_N$=0.66-0.82, respectively. Most of patterns show small negative Eu anormalies except a Pl-rich sample. However, these two groups of normalized patterns show similarities to those of E-type mid oceanic ridge basalt and/or island arc basalt.

To discriminate the tectonic environments of the protolith of basic metamorphic rocks. Condie (1989b) proposed basalt classification screens using the ratios of immobile elements (e.g. Ti/V, Ti/Y, Zr/Y, Ti/Zr) for Archaean and Proterozoic basic rocks. The rocks from unit I have high Ti/V ratios (≥30), while those from units II and VI have low (≤30). The rocks from units III, IV and V show the wide range of Ti/V ratios. Condie (1989b) suggested that the ratio of Ti/V=30 is the boundary between the arc basalt (ARCB) (or N-type mid oceanic ridge basalt (NMORB)) and the MORB (or within plate basalt (WPB)). These evidences are also clearly shown in the TiO_2-Ti/V and Ti/Y-Ti/V diagrams (not shown). Other diagrams such as Y-Cr (Pearce and Norry, 1979), Ti-Ni (Ishizuka, 1981) and Zr-TiO_2 (Pharaoh and Pearce, 1984) are also applied to the discrimination of the tectonic environments. In all these diagrams, the basic metamorphic rocks from unit I are plotted in the MORB field, while those from units II and VI are plotted in the ARCB and/or island-arc basalt (IAB) field. The rocks from units III, IV and V show the affinities to both of ARCB (IAB) and MORB (WPB). When we use the Y-Zr diagram (Condie, 1989b) to discriminate more detail of tectonic environments for the basic metamorphic rocks having ARCB (IAB) affinities from units II, III, IV, V and VI, these rocks have lower Zr/Y ratio (≤3) and are classified into IAB type.

In summary, the protoliths of the basic metamorphic rocks of unit I have derived from MORB and those of units II and VI from IAB. The units III, IV and V seem to be the mixture zone of MORB- and IAB-type basic rocks.

3.2 Intermediate metamorphic rocks

The intermediate metamorphic rocks in units II - VI have been derived from the intermediate igneous rocks. The origin and tectonic environments of the protolith of the intermediate metamorphic rocks have been classified in comparison with the modern arc andesite based on relatively immobile incompatible elements (Ti, Zr, V, Y) and REE.

Condie (1989b) defined the four categories of andesites: primitive arc andesite (PAA), island arc andesite (IAA), continental-margin andesite (CMA) and Andean arc andesite (AA). The most distinctive groups are the end-members PAA and AA with significant overlap occurring between most of the IAA and CMA geochemical affinities. Therefore, we apply two categories of CMA (AA) and IAA (PAA) to discrimination.

The rocks from unit II have low-Zr/Y ratios (1.25-7.0), while those from units III, IV, V and VI have rather high values (up to Zr/Y=20). If we apply the Condie's definitions, the protolith of the intermediate metamorphic rocks of unit II had been derived from IAA-type andesite, whereas those of units III, IV, V and VI from CMA-type andesite with subordinate IAA-type. Ti/V and La/Yb ratios also show the same characteristics such as the rocks from unit II have rather low-Ti/V ratios with low-La/Yb ratio (2.7), while those from the other units show wide range of Ti/V values and rather high-La/Yb ratios (3.5-5.2).

3.3 Pelitic metamorphic rocks

The geochemical characteristics of the pelitic metamorphic rocks from each unit are described in this section. The units I - IV underwent granulite-facies metamorphism, while units V and VI were metamorphosed under amphibolite facies and lower grade conditions, described above.

Most rocks have Cr/Ni ratios between 1 and 10. Characteristically unit I has slightly higher values than units II and VI. These rather high values (of units I and IV) are very close to the average Cr-Ni content of an oceanic crust and units II and VI have nearly the same values to the average of an island-arc andesite. These evidences reflect in the consequence of classification in the tectonic environments for basic and intermediate metamorphic rocks.

Taylor and McLennan (1985) suggested that very high abundance of Cr and Ni in shales are observed for early Archean sequences, while many late Archean sequences are either not or only slightly enriched in Cr and Ni as compared with their post-Archean counterparts. The Cr

and Ni abundances of the pelitic metamorphic rocks from the central Sør Rondane Mountains are plotted within the post-Archean field.

The K/Rb ratios in granulite-facies metamorphic rocks are known to vary widely (Tarney and Windley, 1977). However, clear differences of K/Rb ratios between unit I (K/Rb=30-200) and unit II (180-1500) are observed. Unit III have wide range from 100 to ca.1000. Heier (1973) suggested that Rb is preferentially lost as compared with K during granulite metamorphism. The K/Sr ratios of these rocks show a wide range (K/Sr=10-3000) and nearly the same values among them. Therefore, if only Rb had been removed by the fluid action (Tarney and Windley, 1977), the Rb/Sr ratios of unit I should be lower than those of unit II in ralation to the statement of K/Rb investigations, but the results show the opposite (unit I: Rb/Sr=0.2-20, unit II: 0.02-1.0).

Sheraton et al. (1985) suggested that the molar ratios of $Al_2O_3/CaO+Na_2O+K_2O$ (A/CNK) are more than 1.1 for normal sediments and less than 1.1 for sediments influenced by igneous activities. The A/CNK ratios are different among each unit as follows;

A/CNK $\geq$ 1.1: units I, III, IV and V

A/CNK $\leq$ 1.1: units II, III, IV, V and VI.

Therefore, those evidences suggest the differences among original geochemical characters of each unit with refrection of their tectonic environments such as an oceanic crust affinity in unit I, island-arc type crust affinity in units II and VI, and their mixture in units III, IV and V.

4. Discussion and conclusions

4.1 Geochemical characteristics of units

As described in the previous sections, the protoliths of the basic, intermediate and pelitic metamorphic rocks can be classified in terms of their geochemical characters in each unit.

The unit I comprises basic, pelitic and calc-silicate metamorphic rocks. The geochemical characters of the basic metamorphic rocks show the MORB-like affinities. The pelitic metamorphic rocks have high-A/CNK ratios and moderately high Cr and Ni contents, which may support the chemical effect of oceanic crustal materials. The units II, III, IV and V consist of basic, intermediate, pelitic, acidic and calc-silicate metamorphic rocks. The basic metamorphic rocks of unit II have IAB-type geochemical characters, while those of units III-V have both of MORB- and IAB-type characters. The intercalated intermediate metamorphic rocks are slightly different in chemical compositions between unit II and units III-V. The rocks of unit II are characterized by the IAA-type andesite affinities, while those of units III-V show the CMA-type with rare IAA-type chemical compositions. The unit VI mainly consists of basic and intermediate metamorphic rocks with subordinate pelitic rocks. The chemical characters of basic and intermediate metamorphic rocks of unit VI show IAB-type and CMA-type, respectively. The differences of the chemistry between the basic and the intermediate metamorphic rocks of six units can indicate the development relations of the crusts under different tectonic settings.

Most of the pelitic metamorphic rocks of all these six units have classified into graywacke, therefore we apply the discrimination diagram for sandstones in relation to the tectonic environments of Bhatia (1983) to determine the protolith of the pelitic metamorphic rocks. It may be suggested that the protoliths of the pelitic metamorphic rocks had deposited possibly in the active continental margin.

Results of these investigations indicate that the rock assemblages are classified into the following types with a zonal arrangement from north to south; oceanic type (unit I), island-arc type (unit II), mixture type of oceanic, island-arc and continental-margin island-arc types (accretional complex?: units III, IV, V) and continental-margin island-arc type (unit VI).

4.2 Tectonic implications

Shiraishi and Kagami (1988) investigated that the timing of granulite-facies metamorphism in unit II took place at around 1000 Ma by their Rb-Sr and Sm-Nd isotopic studies. As well as unit II (island-arc type), the granulite-facies metamorphism had taken place in units I (oceanic type), III and IV (accretional complex) at the same time. However, the slightly later amphibolite-facies metamorphism occurred in 950 Ma aged tonalites (Takahashi et al., 1990) of unit VI (continental-margin island-arc type). This tonalite had cut the SRS as the tectonic boundary between units IV and V. Therefore, it is regarded that the original magmatic activities and depositions of supracrustal rocks took place before 1000 Ma and subsequent collisions

with formation of the SRS occurred between 1000 Ma and 950 Ma at around the Archean continent.

Subsequently, the MSZ with only strike-slip sense was formed during 550 - 530 Ma as determined by the geochronological studies of intrusive plutonic rocks (Takahashi et al., 1991). The boundaries among units I - V are the WNW-ESE trending thrust faults with NW dipping mineral lineations. These thrust faults have also been cut by the younger intrusives of ca. 500 Ma. It is, therefore, suggested that the thrust forming deformation event and the formation of the zonal arrangement of each unit having different protolith constitutions occurred nearly the same time, but slightly later than the MSZ formation. The younger intrusions of syenite (A-type granitic rocks), which cut the MSZ, have the geochemical affinities with active plate margin igneous activity (Sakiyama and Takahashi, 1988).

It is concluded that the central Sør Rondane Mountains consists of oceanic, island-arc, accretional complex and continental-margin island arc protoliths similar to those in modern plate tectonic systems. These complicated original rock constitutions were formed during the collision event before 950 Ma and were re-arranged by the thrust faults at around 540 Ma. Subsequently, A-type igneous activity took place in the tectonic environment of active plate margins.

References

Asami, M. and Shiraishi, K. (1987): *Proc. NIPR Symp. Antarct. Geosci.*, **1**, 150-168.
Bhatia, M. R. (1983): *Jour. Geol.*, **91**, 611-627.
Black, L. P.et al. (1987): *Jour. Metamorphic Geol.*, **5**, 1-26.
Condie, K. C. (1989a): *Plate Tectonics and Crustal Evolution.* 476 pp.
Condie, K. C. (1989b): *Lithos*, **23**, 1-18.
Evensen, M. N. (1978): *Geochim. Cosmochim. Acta*, **42**, 1203.
Gill, J. B. (1981): *Orogenic Andesite and Plate Tectonics.* 390 pp.
Grew, E. S. (1978): *Geol. Soc. Amer. Bull.*, **89**, 801-813.
Harley, S. L. and Hensen, B. J. (1990): *High-temperature Metamorphism and Crustal Anatexis.* 320-370.
Heier, K. S. (1973): *Trans Roy. Soc. London*, **A273**, 429-442.
Ishizuka, H. (1981): *Jour. Geol. Soc. Japan*, **87**, 17-34.
Ishizuka, H. and Kojima, H. (1987): *Proc. NIPR Symp. Antarct. Geosci.*, **1**, 113-128.
Kojima, S. and Shiraishi, K. (1986): *Mem. Natl Inst. Polar Res., Spec. Issue*, **43**, 116-131.
Osanai, Y. et al. (1988): *Proc. NIPR Symp. Antarct. Geosci.*, **2**, 170.
Pearce, J. A. and Norry, M. J. (1979): *Contrib. Miner. Petrol.*, **69**, 33-47.
Pharaoh, T. C. and Pearce, J. A. (1984): *Precambrian Res.*, **25**, 283-308.
Sakiyama, T. et al. (1988): *Proc. NIPR Symp. Antarct. Geosci.*, **2**, 80-95.
Sakiyama, T. and Takahashi, Y. (1988): *Program • Abstr. 9th Symp. Antarct. Geosci.* 65-66.
Sheraton, J. W. et al. (1987): *Bureau Miner. Resources Bull.*, **223**, 1-51.
Shiraishi, K. et al. (1988): *Proc. NIPR Symp. Antarct. Geosci.*, **2**, 117- 132.
Shiraishi, K. and Kagami, H. (1988): *Program • Abstr. 9th Symp. Antarct. Geosci.* 67-68.
Shiraishi, K. et al. (1990): *Geological Evolution of Antarctica*, 77-82.
Takahashi, Y. et al. (1990): *Proc. NIPR Symp. Antarct. Geosci.*, **4**, 1-8.
Takahashi, Y. et al. (1991): *Proc. NIPR Symp. Antarct. Geosci.*, **5**, (in press).
Tarney, J. and Windley, B. F. (1977): *Jour. Geol. Soc. London*, **134**, 153-172.
Taylor, S. R. and McLennan, S. M. (1985): *The Continental Crust: its composition and evolution.* 312 pp.
Tingey, R. J. (1982): *Antarctic Geoscience.* 455-464.
Van Autenboer, T. (1969): *Antarct. Map Folio Ser.*, Folio 12.
Van Autenboer, T. and Loy, W. (1972): *Antarctic Geology and Geophysics*, 563-571.

LATE PROTEROZOIC TO EARLY PALEOZOIC MAGMATISM IN THE SØR RONDANE MOUNTAINS, EAST ANTARCTICA.

Masaaki Owada, *Department of Mineral Science and Geology, Yamaguchi University, Yoshida, Yamaguchi 753, Japan.*
Tsuyoshi Toyoshima, *Graduate School of Science and Technology, Niigata University, Ikarashi, Niigata 951-21, Japan.*
Kazuyuki Shiraishi, *National Institute of Polar Research, Kaga, Itabashi-ku, Tokyo 173, Japan.*
Yasuhito Osanai, *Institute of Earth Science and Astronomy, Fukuoka University of Education, Akama, Munakata, Fukuoka 811-41, Japan.*
Yoshiaki Tainosho, *Department of Geology, Faculty of Education, Kobe University, Nada-ku, Kobe 657, Japan.*
Yuhei Takahashi, *Geological Survey of Japan, Tsukuba 305, Japan.*

The Sør Rondane Mountains are largely underlain by various metamorphic and igneous rocks. Most of metamorphic rocks have undergone upper amphibolite to granulite facies metamorpohism. The Sm-Nd whole-rock isochron age for charnockitic gneiss from the Koyubi-Ridge is 999+/-164 which is inferred to be the age of granulite-facies metamorphism (Shiraishi and Kagami, 1989). Sakiyama *et al.* (1988) have divided the intrusive rocks into the Older intrusives and the Younger intrusives based on their field occurrences. The Older intrusives consist of tonalite, granodiorite, sheet of granitic rock and quartzdiorite. On the other hand, the Younger intrusives include a syenite complex, and a biotite granite (Lunckeryggen granite). Rb-Sr whole-rock isochrons indicate an age of 956+/-39 Ma for the tonalite of the Older intrusives and 525+/-32 Ma for the Lunckeryggen granite of the Younger intrusives (Takahashi *et al.*, 1990).

The Older intrusives are subdivided by this study on the basis of field occurrence in the central part of the Sør Rondane Mountains as follows: 1) charnockite, 2)gabbro-diorite, 3)tonalite, 4) pegmatite (pegmatite I), 5)hornblende-biotite granite (Older granite), 6) garnet-biotite granite (Leucocratic granite), 7) quartz diorite, and 8) granodiorite. The mutual relations of these plutonic rocks are given in Fig. 1. The charnockite is associated with granulite facies metamorphic rocks and is considered to have been emplaced during granulite-facies metamorphism.

In this presentation, we will described the petrological and petrochemical character of the intrusive rocks and will discuss the change of magmatism from the Late Proterozoic to the Early Paleozoic in the Sør Rondane Mountains.

References

Sakiyama, T., Takahashi, Y. and Osanai, Y. (1988): Geological and petrological characters of the plutonic rocks in the Lunckeryggen-Brattnipene region, Sør Rondane Mountains, East Antarctica. Proc. NIPR Symp. Antarct. Geosci., 2. 80-95.
Shiraishi, K. and Kagami, H. (1989): Preliminary

geochronological study of granulites from the Sør Rondane Mountains, East Antarctica -A comparison of Rb-Sr and Sm-Nd ages-. Proc. NIPR Symp. Antarct. Geosci., 3. 152.
Takahashi, Y., Arakawa, Y., Sakiyama, T., Osanai, Y. and Makimoto, H. (1990): Rb-Sr and K-Ar whole rock ages of the plutonic bodies from the Sør Rondane Mountains, East Antarctica. Proc. NIPR Symp. Antarct. Geosci., 4, 1-8.

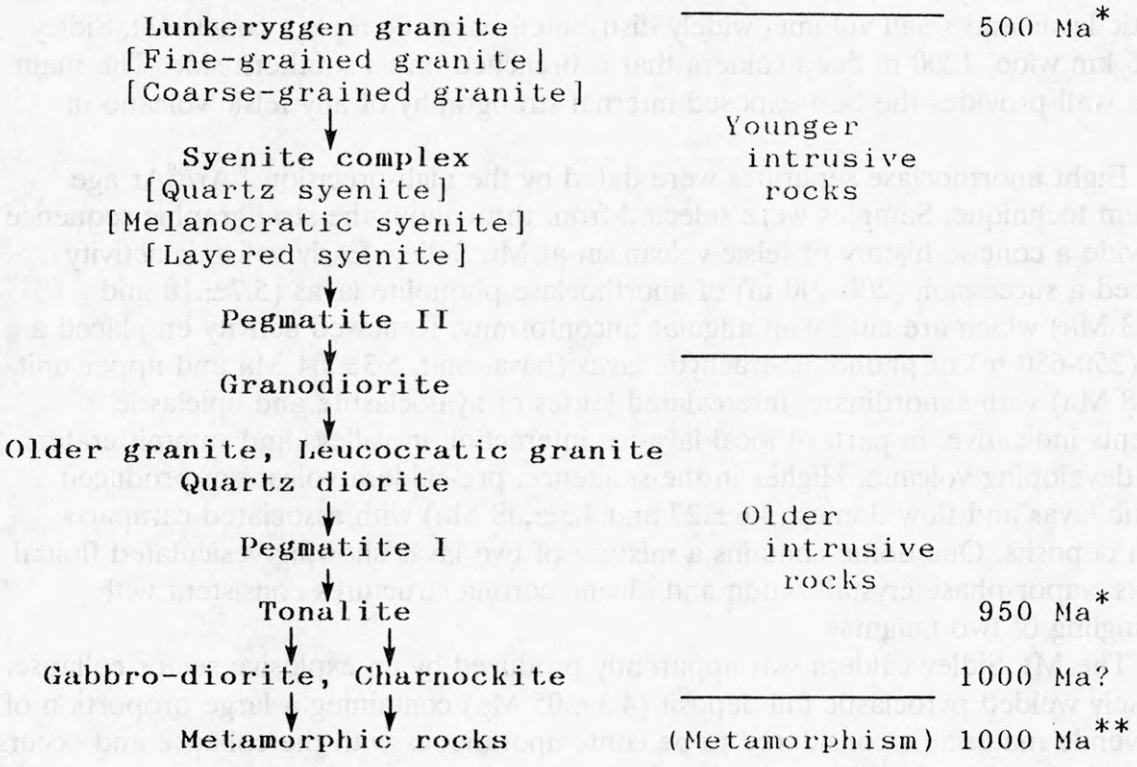

*Fig. 1 Mutual relations of the plutonic rocks for the central part of the Sør Rondane mountains. *: Takahashi et al. (1990), **: Shiraishi and Kagami (1989).*

VOLCANIC HISTORY OF MOUNT SIDLEY, MARIE BYRD LAND, ANTARCTICA

K.S. Panter[1], W.C. McIntosh[1], J.L. Smellie[2], and J.A. Gamble[3]
[1]Department of Geoscience, New Mexico Institute of Mining and Technology, Socorro, NM 87801, USA
[2]British Antarctic Survey, High Cross, Madingley Road, Cambridge CB3 0ET, UK
[3]Victoria University, Department of Geology, Box 600, Wellington, New Zealand

Mount Sidley (4181 m), is the largest and highest volcano within the Late Cenozoic Marie Byrd Land (MBL) volcanic province. It is composed of phonolitic and trachytic lavas and small volume, widely distributed basanitic tephra cones. Mt. Sidley has a 5 km wide, 1200 m deep caldera that is breached on its southern side. The main caldera wall provides the best exposed internal stratigraphy of any felsic volcano in MBL.

Eight anorthoclase separates were dated by the high-precision $^{40}Ar/^{39}Ar$ age spectrum technique. Samples were selected from throughout the stratigraphic sequence to provide a concise history of felsic volcanism at Mt. Sidley. Early volcanic activity produced a succession (200-400 m) of anorthoclase phonolite lavas (5.7±.10 and 5.6±.33 Ma) which are cut by an angular unconformity. Renewed activity emplaced a series (250-650 m) of phonolitic-trachytic lavas (basal unit, 5.3±.04 Ma and upper unit, 4.7±.18 Ma) with subordinate, intercalated lenses of hyaloclastite and epiclastic sediments indicative, in part, of local lava-ice interaction in valleys and summit craters of the developing volcano. Higher in the sequence, pre-caldera volcanism produced trachytic lavas and flow domes (4.6±.27 and 4.5±.08 Ma) with associated carapace breccia deposits. One dome contains a mixture of two lavas showing vesiculated fluidal contacts, vapor phase crystallization and olivine corona structures consistent with commingling of two magmas.

The Mt. Sidley caldera was apparently produced by an explosive sector collapse. A densely welded pyroclastic fall deposit (4.3±.05 Ma) containing a large proportion of non-juvenile material is considered to be contemporaneous with the collapse and occurs as a relatively thin unit (~5 m) capping the caldera rim. An expansive pumice-rich, unwelded ignimbrite (4.4±.09 Ma) and associated minor surge tephras flowed within and mantled the walls of the breached caldera. Stratigraphically, these two units are considered to bracket the caldera forming event and their ages are indistinguishable within analytical error. At Doumani Peak, the ignimbrite deposits are overlain by a well developed hydrovolcanic tuff cone sequence grading from base surge up into fall beds containing abundant accretionary lapilli layers. The final phase of volcanism at Mt. Sidley was eruptions of parasitic cones of basanite scoria some of which contain crustal and mantle xenoliths.

This study shows that felsic volcanic activity at Mt. Sidley occurred as several pulses over ~1.5 m.y., indicating the presence of a substantial mantle thermal anomaly beneath Mt. Sidley.

TRANSVERSE VARIATIONS IN THE GERLACHE STRAIT PLUTONIC ROCKS: EFFECTS OF THE ALUK RIDGE - TRENCH COLLISION IN THE NORTHERN ANTARCTIC PENINSULA

Miguel A. PARADA
Departamento de Geología y Geofísica, Universidad de Chile
Casilla 13518 Correo 21, Santiago-CHILE

Jean-Baptiste ORSINI
Laboratoire de Géologie-Pétrologie, Faculté de Sciences et Techniques. 23, rue du Docteur Paul Michelon, 4023 Saint-Etienne Cédex, FRANCE

Ricardo ARDILA
Departamento de Geología y Geofísica, Universidad de Chile
Casilla 13518 Correo 21, Santiago-CHILE

Raúl GUERRA
Departamento de Geología y Geofísica, Universidad de Chile
Casilla 13518 Correo 21, Santiago-CHILE

INTRODUCTION

As many Cordilleran Batholith, the Antarctic Peninsula plutonic rocks exhibit gradient in geochronological compositional and isotopic characteristics. The oldest plutonic rocks (Jurassic) are restricted to the eastern coast of the Antarctic Peninsula, whereas the younger rocks (Tertiary) developed in the western coast. Plutons of Cretaceous ages are widespread distributed throughout the Peninsula (cf. Saunders et al., 1982). Saunders and Weaver (1980), Tarney et al. (1982) and Saunders and Tarney (1982) indicate an eastward increase of LIL elements and Ce/Yb in igneous rocks of equivalent SiO_2 % wt. Similarly, there is a trend of eastward increasing initial $^{87}Sr/^{86}Sr$ ratio of the plutonic rocks of Graham Land (Pankhurst, 1982) from 0.707 to 0.704. These trends have been explained by a progressively greater depth of the source away from the trench (Saunders et al. 1988), and influence of the crustal basement (Pankhurst, 1982).

This paper is a contribution to the geochronology, whole-rock and mineral chemistry of the Gerlache Strait plutonic rocks, in relation to characterize the transverse variations and to a better understanding the influence on the Antarctic Peninsula magmatism, of the ocean-floor subduction under the peninsula. The influence of the Aluk Ridge - trench collision on the Tertiary plutonism is particulary discussed.

TRANSVERSE VARIATIONS

AGE

Previous K-Ar ages of 117 and 94 Ma and Rb-Sr isochron ages of 131 ± 4 and 114 ± 11 Ma were obtained on plutonic rocks from the Danco Coast (cf. Scott, 1965; Pankhurst, 1982; British Antarctic Survey, 1984). A new biotite K-Ar age of 113 ± 3 Ma was obtained in a hornblende-biotite granodiorite of the SE extreme of Andvord Bay.

The range of K-Ar ages from 54 to 49 Ma already obtained in the Doumer Island (cf. British Antarctic Survey, 1984) was confirmed by two new biotite K-Ar ages of 50 ± 1 and 56 ± 2.

Early Tertiary biotite K-Ar ages of 68 ± 2 and 54 ± 1 Ma were obtained in samples collected in the NE extreme of Anvers

Island.

Farther west from the Gerlache Strait, near the Palmer Station, Gledhill et al. (1982) report a whole-rock Rb-Sr isochron age of 35 Ma and three concordant biotite K-Ar ages of 20 Ma. A tonalite collected at the Palmer Station gave a new biotite K-Ar age of 20 ± 1 Ma.

With the exception of a late Cretaceous Rb-Sr age of the Cape Monaco granites (cf. Pankhurst, 1982) on the SW extreme of Anvers Island a westward migration of the plutonism with time is confirmed. The limit between the Mesozoic and Cenozoic plutonic rocks is roughly defined in figure 1. The apparent jump of the magmatic belts from the Cretaceous Danco Coast granitoids to the Tertiary Anvers Island rocks, appear to correspond to a non-magmatic interval between 68 and 94 Ma. Taking all the available radiometric dates in the Gerlache Strait, a peak of the plutonic activity in early Tertiary times (50 - 60 Ma) is recognized.

PETROGRAPHIC FEATURES

The Cretaceous Danco Coast plutonic rocks consist of a large spectrum of lithology from diorites to leucogranites (Fig. 2a). Lithological variations have been found from west to east along the Andvord Bay. Clinopyroxene, hornblende diorites dominate the western part, whereas hornblende tonalites and leucogranites occupy the intermediate and easternmost part of the Andvord Bay respectively. Farther north, on the Arctowsky Peninsula, a suite of leucogranites, biotite granites and muscovite granitoids were recognized, suggesting a N-S felsic granitoids distribution.

Along the Wiencke, Doumer and Anvers island shores, Tertiary mafic to intermediate plutonic rocks prevail, although a late Cretaceous Cape Monaco granite, on the extreme SW of Anvers Island, have been recognized (cf. Pankhurst, 1982). From the petrographic point of view, hornblende, clinopyroxene, diorites and tonalites are the most common varieties (Fig. 2a), however gabbronorite and norite exhibiting cumulate textures are present on the extreme SE of Anvers.

PHYSICAL CONDITIONS

Using the geobarometer of Hammarstrom and Zen (1986), refined by Hollister et al. (1986), a pressure range of 1.0-2.7 kbar was calculated for the pluton emplacements. Although precision is limited by sample density and accuracy of the amphibole geobarometer, it is interesting to note a westward increase of the pressure crystallization for the Tertiary intrusive rocks (Fig. 2b). This pressure gradient probably reflect sampling at different level of erosion due to uplift of westward increasing magnitude.

Water fugacity conditions for the biotite crystallization were obtained for the assemblage biotite + magnetite + alkali feldspar. Although no systematic variations of fH_2O with time and space have been found, a westward increase of $PH_2O/PTotal$ with decreasing age, but irrespective to SiO_2 content, is observed (Fig. 2c).

The geobarometer based on the Ca-Tschermaks molecule content of clinopyroxene and anorthite content of plagioclase (Ellis, 1980) was used to estimate the pressure of early clinopyroxene-bearing assemblage crystallization in Tertiary plutons. A pressure range as high as 5-6 kbar was calculated

for the westernmost analyzed sample. Assuming a crust density of 2.65 gr/cm^3, the maximum pressure corresponds to a depth range of 19-22 km. These depths most likely represent the magma source.

GEOCHEMICAL CHARACTERISTICS

Despite the limited number of analyses there is an overall increase in SiO_2 to the east that reflects the abundance of granites in the Cretaceous Danco Coast plutonic rocks. As many Cordilleran batholiths there is an inland increase in K_2O/SiO_2, but in this case, this trend opposite to the age variation pattern.

The Gerlache Strait rocks ranging from 57 to 71% SiO_2 show high Th/Nb, Sm/Ti and low Nb/La, which are characteristic of calc-alkaline rocks. However, the Tertiary rocks have higher Ce/Sr and Hf/P than the Cretaceous ones. The LIL elements contents eastwardly increase with increasing SiO_2 comparable with the LIL elements variation across Graham Land (cf. Saunders and Tarney, 1982).

CORRELATION BETWEEN THE ALUK RIDGE - TRENCH COLLISION AND PLUTONIC EVOLUTION

The plutonic activity in the Antarctic Peninsula seems to have reached its maximum at Cretaceous time particularly at 120-80 Ma (cf. Saunders et al. 1982). This maximum can be correlated with the high spreading rate prior to the Aluk Ridge formation. According to the available data,the beginning of the Cenozoic plutonism in the Gerlache Strait at 68 Ma roughly coincides with the Aluk Ridge formation, thus, the 95-68 interval of non plutonic activity may be a consequence of the reorganization of both, the spreading centers and triple junction of Antarctica, Africa and South America.

The Aluk Ridge was accreted by progressive northeastward collision along the Pacific margin of the Antarctic Peninsula, rather than subducted with the oceanic lithosphere. Such progressive northeastward collisions, which started in Eocene (≈50 Ma; cf. Meissner et al., 1988), may be responsible for important tectonic modifications that controlled the igneous activity. An important tectonic effect is the abrupt decrease of the subduction rates since 50 m.y. ago (Barker, 1982). Despite the buoyancy of the progressive younger ocean floor that was consumed, the subduction rate decline appears to cause a gradual increase in subduction angle that favored the westward shift in the loci of plutonic activity.

The observed difference in the amphibole crystallization pressures of Tertiary plutons from western to eastern Anvers Island, is thought to be a consequence of a trenchward increasing uplift during the ridge crest arrival at the trench off the Anvers Island (20-15 m.y. ago). The discrepancie between the Rb-Sr isochron age (35 Ma) and the K-Ar ages (≈20 Ma) obtained in the SW Anvers Island can be explained by the mentioned uplift event that interrupted 15 Ma of subsolidus cooling. Such a slow subsolidus cooling rate appear to be a consequence of near-trench efficient mechanism of heat transfer, compatible with the prediction of DeLong's et al. (1978) ridge-trench interaction model.

The decrease of SiO_2 content from the Cretaceous Danco granitoids to the eastern Tertiary rocks, may be correlated with

a westward decreasing involvement of continental crust as the westward migration of the plutonism proceeded. Asuming an origin in the mantle of the basic to intermediate Tertiary plutons, the estimated depth of about 19-22 km of the magma source is lower than the assumed crustal thickness of about 25 km in the eastern Graham Land (Moyes and Hamer, 1983) and therefore indicative of an important westward reduction of the crustal thickness.

Finally, the westward increase in PH_2O/Ptotal conditions of the westward migrating plutons (Fig. 2c) can be attributed to the approach of the Aluk Ridge to the trench off the Anvers island that caused the dehydration of progressively younger oceanic crust at progressively shallower depths. Such a premature volatile release may explain the cessation of the magmatic activity, at least, 15 Ma prior to the arrival of the ridge at the trench of Anvers Island.

ACKNOWLEDGMENTS

The authors aknowledge the financial support provided by the grant e.17 from Instituto Antartico Chileno (INACH) during the field and laboratory researches. This work is a contribution to the IGCP project N°249 "Andean Magmatism and its Tectonic Setting".

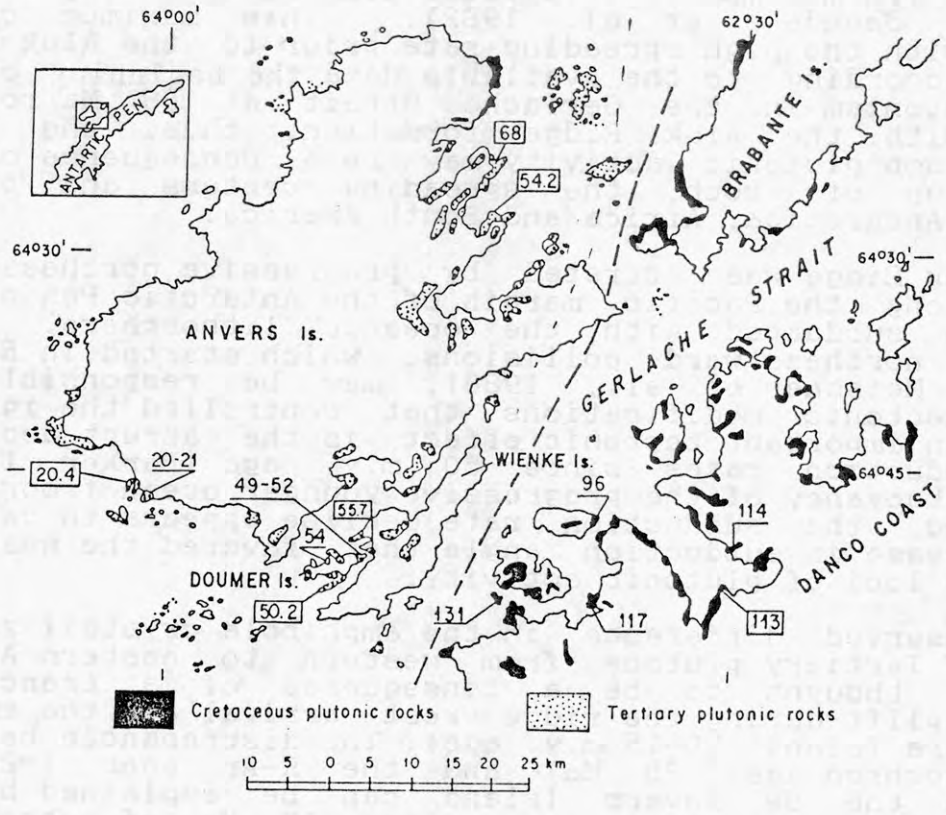

Fig. 1. Distribution of the plutonic rocks in the Gerlache Strait. Numbers indicate radiometric ages. Enclosed numbers are the ages obtained in this study. Dashed line separates Cretaceous and Tertiary plutonic domains.

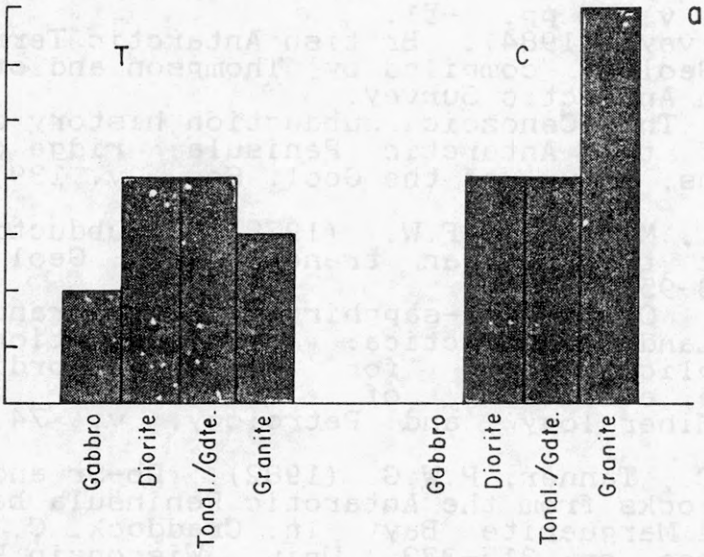

Fig. 2a. Hystogram of lithology. T: Tertiary plutonic rocks; C: Cretaceous plutonic rocks.

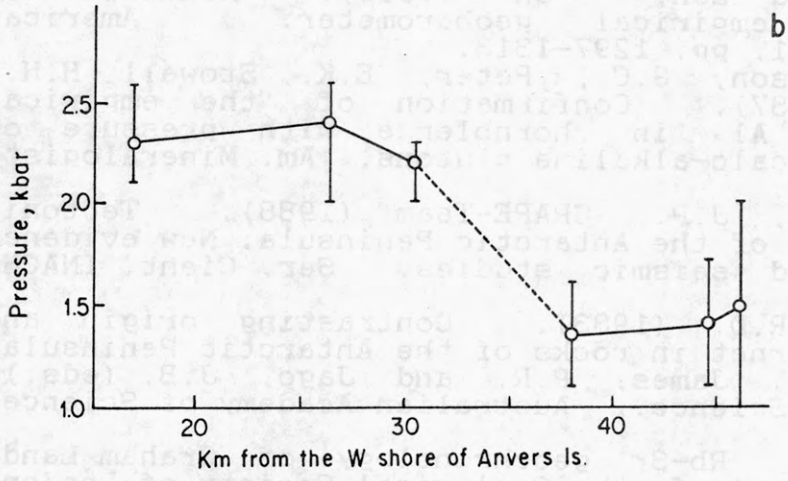

Fig. 2b. Spatial variation of pressure of amphibole crystallization in Tertiary granitoids.

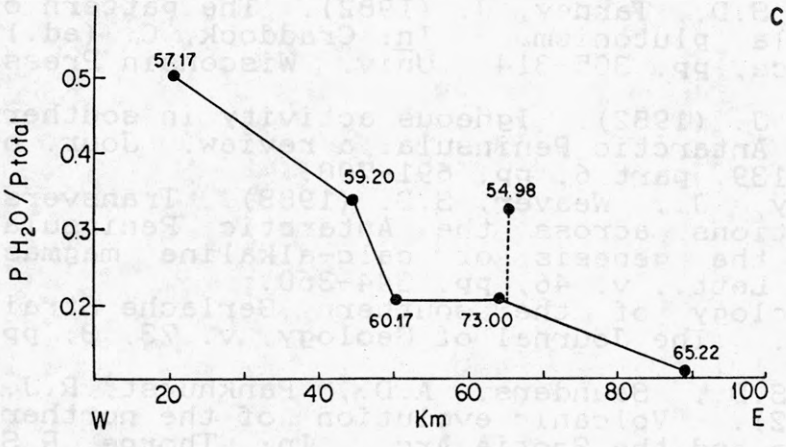

Fig. 2c. Gradient of PH02/PTOTAL in the Gerlache Strait Granitoids. Numbers indicate Si02 wt. %.

REFERENCES

Alarcón, B., Ambrus, J., Olcay, L. and Vieira, C. (1976). Geología del Estrecho de Gerlache entre los paralelos 64° y 65° Sur, Antártica Chilena. Serie Científica, Instituto Antártico Chileno, v. 1, pp. 7-51.

British Antarctic Survey (1984). British Antarctic Territory geological map. Geology compiled by Thompson and others. Cambridge, British Antarctic Survey.

Barker, P.F. (1982). The Cenozoic subduction history of the Pacific margin of the Antarctic Penisula: ridge crest-trench interactions. Jour. of the Geol. Soc., v. 139, part 6, pp. 787-802.

DeLong, S.E., Fox, S.E., McDowell, F.W. (1978). Subduction of the Kula ridge at the Aleutian trench. Bull. Geol. Soc. Am., v. 89, pp. 83-95.

Ellis, D.J. (1980). Osumillite-sapphirine-quartz granulites from Enderby Land, Antarctica: P-T conditions of metamorphism, implications for garnet-cordierite equilibria and the evolution of the depth crust. Contributions to Mineralogy and Petrology, v. 74, pp. 201-210.

Gledhill, A., Rex, D.C., Tanner, P.W.G. (1982). Rb-Sr and K-Ar geochronology of rocks from the Antarctic Peninsula between Anvers Island and Marguerite Bay. In: Craddock, C. (ed.) Antarctic Geoscience, pp. 315-323. Univ. Wisconsin Press, Madison.

Hammarstrom, J.M. and Zen, E-an. (1986). Aluminium in hornblende: an empirical geobarometer. American Mineralogist, v. 71, pp. 1297-1313.

Hollister, L.S., Grisson, G.C., Peter, E.K., Stowell, H.H., Sisson, V.B. (1987). Confirmation of the empirical correlation of Al in hornblende with pressure of solidification of calc-alkaline plutons. Am. Mineralogist, v. 72, pp. 231-239.

Meissner, R., Henriet, J.P., GRAPE-Team (1988). Tectonic features northwest of the Antarctic Peninsula: New evidence from magnetic and seismic studies. Ser. Cient. INACH, n°38, pp. 89-105.

Moyes, A.B., Hamer, R.D. (1983). Contrasting origin and implications of garnet in rocks of the Antarctic Peninsula. In: Oliver, R.L., James, P.R. and Jago, J.B. (eds.). Antarctic Earth Science. Australian Academy of Science, pp. 358-362.

Pankhurst, R.J. (1982). Rb-Sr geochronology of Graham Land, Antarctica. Journal of the Geological Society of London, v. 139, pp. 701-711.

Saunders, A.D., Weaver, S.D., Tarney, J. (1982). The pattern of Antarctic Peninsula plutonism. In: Craddock, C. (ed.), Antarctic Geoscience, pp. 305-314. Univ. Wisconsin Press, Madison.

Saunders, A.D., Tarney, J. (1982). Igneous activity in southern Andes and northern Antarctic Peninsula: a review. Jour. of the Geol. Soc. v. 139, part 6, pp. 691-700.

Saunders, A.D., Tarney, J., Weaver, S.D. (1988). Transverse geochemical variations across the Antarctic Peninsula: implications for the genesis of calc-alkaline magmas. Earth Planet. Sci. Lett., v. 46, pp. 344-360.

Scott, K. (1965). Geology of the southern Gerlache Strait Region, Antarctica. The Journal of Geology, v. 73, 3, pp. 518-527.

Tarney, J., Weaver, S.D., Saunders, A.D., Pankhurst, R.J., Barker, P.F. (1982). Volcanic evolution of the northern Antarctic Peninsula and the Scotia Arc. In: Thorpe, R.S. (ed.), Orogenic Andesites. Wiley, New York, pp. 371-400.

STRUCTURAL MAP OF THE AVIATOR - TUCKER GLACIERS AREA, NORTHERN VICTORIA LAND, ANTARCTICA

P.C. Pertusati *, Dipartimento Scienze della Terra, Università di Pisa - Italy
F. Tessensohn *, Bundesanstalt f. Geowissenschaften u. Rohstoffe, Hannover - Germany
C.A. Ricci *, Dipartimento Scienze della Terra, Università di Siena - Italy
G. Kleinschmidt *, Geologisch-Palaeontologisches Institut, Darmstadt - Germany

The area between the Aviator and Tucker Glaciers is of key importance in the geology of the Transantarctic Mountains because it allows the study of the relation of the three terranes which characterize this northern end of the Paleozoic Ross Orogén, i.e. the Wilson, Bowers and Robertson Bay Terranes.

After a first reconnaisance by GANOVEX III (1982/83) this suture area was studied more extensively in the austral summers 1988/89 and 1989/90 (GANOVEX V and ItaliAntartide IV and V), working from a joint camp. As a result of this research, a tectonic map of the zone has been prepared. The map will be published in a joint Italian-German publication which is in preparation. Because of the general interest in this key area a draft of the map is presented here in the form of a poster. All units in the area strike generally NW-SE.

Wilson/Bowers Suture:
The medium to high-grade Wilson and low-grade Bowers Terranes are characterized by different lithostratigraphic and metamorphic features and their junction forms the major suture of the area. On the Wilson side it is outlined by a thin belt of Dessent metamorphics (Dm on map) that can be followed from the Ross Sea up to the Mt. Supernal area. The Dessent metamorphics are made up of metabasites and metasediments that underwent

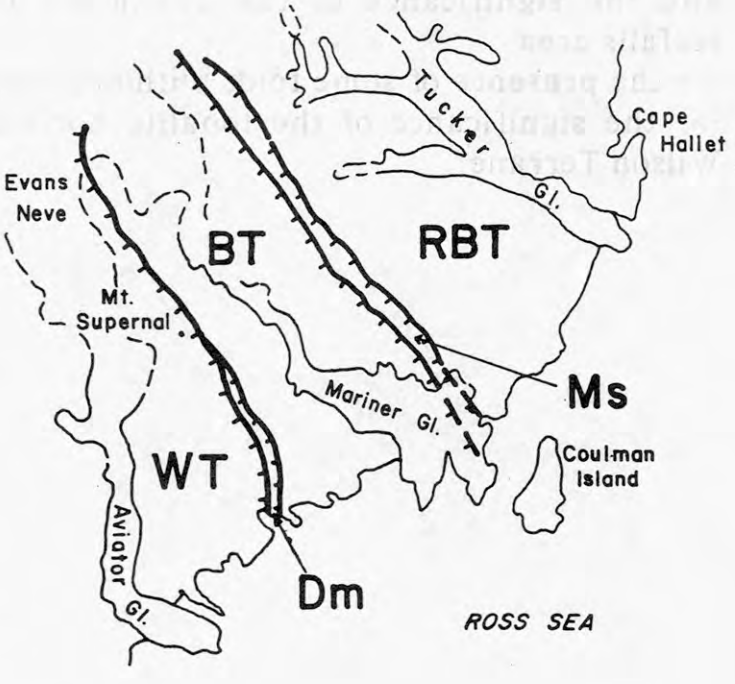

* on behalf of GANOVEX and ItaliAntartide teams

medium temperature and medium - high pressure amphibolite facies metamorphism. The Dessent rocks differ in their lithostratigraphic and metamorphic features from the rocks in both the Wilson and Bowers Terranes.

Upon more detailed observation, the field research allowed us to establish that the easternmost border of the Wilson Terrane is also outlined by a thin discontinous horizon of tectonically deformed tonalite rocks that can be followed from the Ross Sea up to the Niagara Icefalls area (north of Mt. Supernal).

Bowers and Robertson Bay Junction:
The Bowers and Robertson Bay Terranes show similar lithological, structural and metamorphic features and their junction is marked by a second order tectonic element: the Millen Schist belt. The Millen Schists are characterized by greenschist facies metamorphism and by a more complex structural deformation than the Bowers and Robertson Bay Terranes but, from a lithostratographic point of view,they show strong similarities with both adjacent Terranes.

All structural features (e.g. stretching and mineral lineations, facing of the folds and S-C mylonites) visible in the three Terranes, in the Dessent metamorphics and in the Millen Schist belt point to a northeast tectonic transport which brings higher grade units over lower grade ones.

Problems still open to discussion include:
--- the possible prolongation of the Dessent Unit north of Mt. Supernal and the significance of the ultramafic bodies found in the Niagara Icefalls area
--- the presence of some folds with opposite (SW) facing and
--- the significance of the tonalite horizon and its relationship to the Wilson Terrane.

SEDIMENTATION AROUND A POLAR MARINE GLACIER TONGUE, MACKAY GLACIER, SOUTH VICTORIA LAND

A.R. Pyne, P.J. Barrett, A.J. Macpherson, Antarctic Research Centre, Victoria University of Wellington, PO Box 600, Wellington, New Zealand.
R.B. Dunbar, Department of Geology & Geophysics, Rice University, PO Box 1892, Houston, Texas, USA.

The Mackay is an outlet glacier flowing through the Transantarctic Mountains into Granite Harbour (~ 77°S, mean annual temperature is -17°C) to form a floating ice tongue 3 km wide and 5 km long (Figure 1). The glacier is sufficiently thick (>430 m) in its central part for the basal ice to be at melting point, allowing the glacier to flow seaward into Granite Harbour with moderate speed (250 $m.a^{-1}$). The harbour itself is broad (19 km across) and opens into the Ross Sea, with which its waters freely circulate. Annual ice cover is 2.5 - 3 m thick, breaking out most years for about a month in late summer (February - March).

The Mackay Glacier-Granite Harbour system is interesting because it offers an opportunity for observing and measuring the processes that move sediment (and especially mud) from the Antarctic continent into the Ross Sea. The Ross Sea today has a number of basins floored with mud with a large terrigenous component of unknown origin, though the ultimate source must be the continent itself.

Our observations indicate that Mackay Glacier is transporting terrigenous sediment (~ 300,000 tonnes a^{-1}), almost entirely in a 6-m-thick basal debris layer, through the grounding line to melt out and sink to the harbour floor (Macpherson 1987). This is by far the dominant source of sediment as there is very little melt water runoff in the region. The only other significant sources are terrigenous mud brought in from the Ross Sea and biogenic material,largely opaline silica from diatoms. Our studies have been aimed at determining the rates and processes by which terrigenous mud is dispersed from its delivery point at the grounding line and mixed with biogenic sediment as it moves out into the harbour. The approach includes measuring texture and composition of sediment in the water column and on the sea floor, and measuring water temperature, salinity and velocity around the glacier tongue.

Sea floor cores and sediment trap samples show a progressive decrease in sand size debris and a corresponding increase in mud and biogenic sediment (mud size) away from the grounding line (Figure 1). We presume this occurs because sediment in the 6 m thick basal debris layer, which includes around 60 % gravel and sand, melts out and settles to the sea floor within a few hundred metres of the grounding line (based on a submarine glacial melt rate of 5-9 $m.a^{-1}$ (Macpherson 1987). The increasing proportion of mud seaward of the ice tongue is not solely from increasing biogenic sedimentation but implies delivery of terrigenous mud to the sea floor well beyond the tongue.

Measurement of conductivity and temperature profiles through the water column at the end and side of the glacier tongue reveal salinity values about 34.25 psu in the lower part of the water column, but decrease by 0.11 psu from 440m to the base of the floating glacier tongue at approximately 240m (Figure 2). These data indicate that the lower salinity layer is wedge shaped and thins towards the ice tongue grounding line. The water beneath the ice tongue might therefore be considered in general as a two layer system.

Bottom currents were been measured just seaward of the glacier tongue by an electromagnetic current meter 1 m above the sea floor in the deepest part of the harbour cross-section (702 m) over a fifty day period (Nov -Jan). Ten day mean speeds range between 6.9 and 4.3 cms^{-1} with intermittent speeds slightly in excess of 10 cms^{-1}. Mean flow was towards the glacier tongue (240^0 - 270^0T). The record shows periodic changes in current speed and direction that closely correspond to the main diurnal tidal components in the region, and hence we believe that the bottom currents at this site are tidally driven. The current meter was originally deployed to seek evidence of density currents flowing from beneath the glacier tongue. No short period flows were recorded that might indicate the passage of density currents.

Short term current velocity records including a 13 hour sea floor deployment at site h and profiles through the water column at sites h & i show that circulation beneath the ice tongue is complex. There is a four hour difference in current reversals between sites g & h (1 km apart) which indicates that a 1st mode internal tide develops within this restricted part of Granite Harbour. At times the lower layer flows in the opposite direction to the wedge-shaped layer above with a differential velocity up to 10 cms^{-1}. Within the wedge different current speeds and small salinity differences indicate vertical mixing by eddies with a diameter of as much as one half of the maximum thickness of the wedge. Because the density difference between the two layers is very small changes in the driving forces can cause a sloping isopycnal separating the two salinity layers.

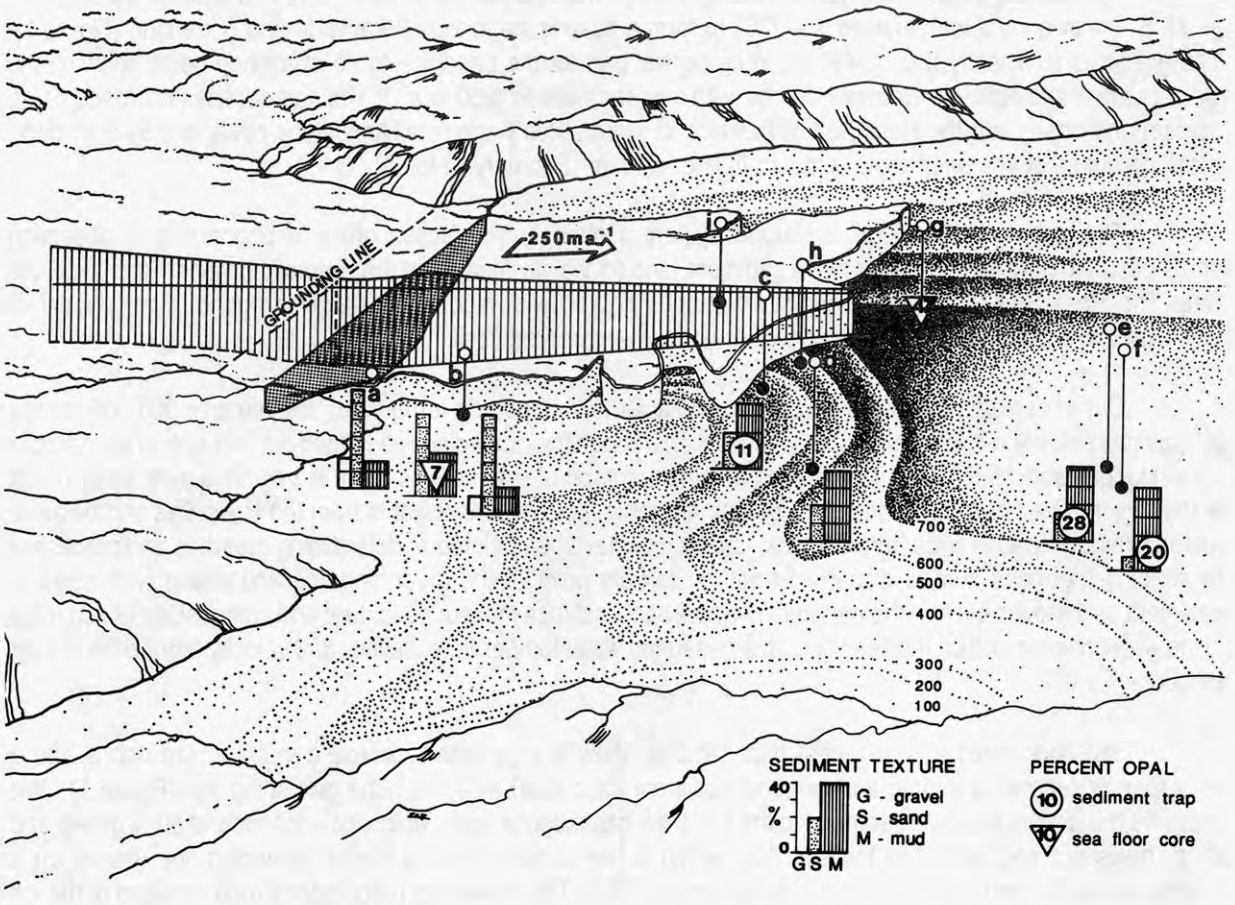

Figure 1. View northwards across Mackay Glacier Tongue which extends into Granite Harbour from the west. The glacier tongue is drawn as it was in 1988. Bar charts show increase in mud from beneath the glacier tongue to the basin floor seaward of the tongue, and an increase in opaline silica. Note that sediment trap material normally has substantially higher opaline values than sea floor material.

Site

a. Canyon position in 1983. Sample from berg with basal debris (field #83-64,83-65).
b. Canyon position in 1983(#83-31). Sediment trap sample 5m above sea floor and seafloor sample(260 m).
c. Terminus position in 1983 (#83-33). Sample from the sea floor (460 m).
d. Sea floor sample 550 m (#81-15).
e. Sea floor sample 704 m (#83-35).
f. Sea floor sample 700 m (#83-15).
g. S4 current meter site and sediment trap 1.5m above sea floor (702 m, MGT 88/89).
h. Terminus conductivity/temperature profile 598 m (Dunbar -site D).
i. Canyon conductivity/temperature profile, 475 m (Dunbar -site E).

The reduced salinity layer is probably formed largely by basal melting of the glacier tongue, although there could be a small contribution from subglacial outflow at the grounding line. Mud may become suspended by a tidal pumping mechanism but this may not be very effective because the tidal range here is only 1.1 m.

Our studies show that sedimentation in Granite Harbour is dominated by meltout of basal debris near the grounding line. Gravel and sand fall to the sea floor close by whereas very fine sand and mud are transported further afield in suspension by tidal currents to settle, along with biogenic debris, onto the basin floor. Both bottom current measurements and sea floor cores indicate that velocities are too low to be effective in sorting sandy sediment, and that density currents are rare or absent. We conclude that even though the glacier may be wet based it does not generate sufficient sub-glacial melt water at the grounding line to influence the deposition of sediments there.

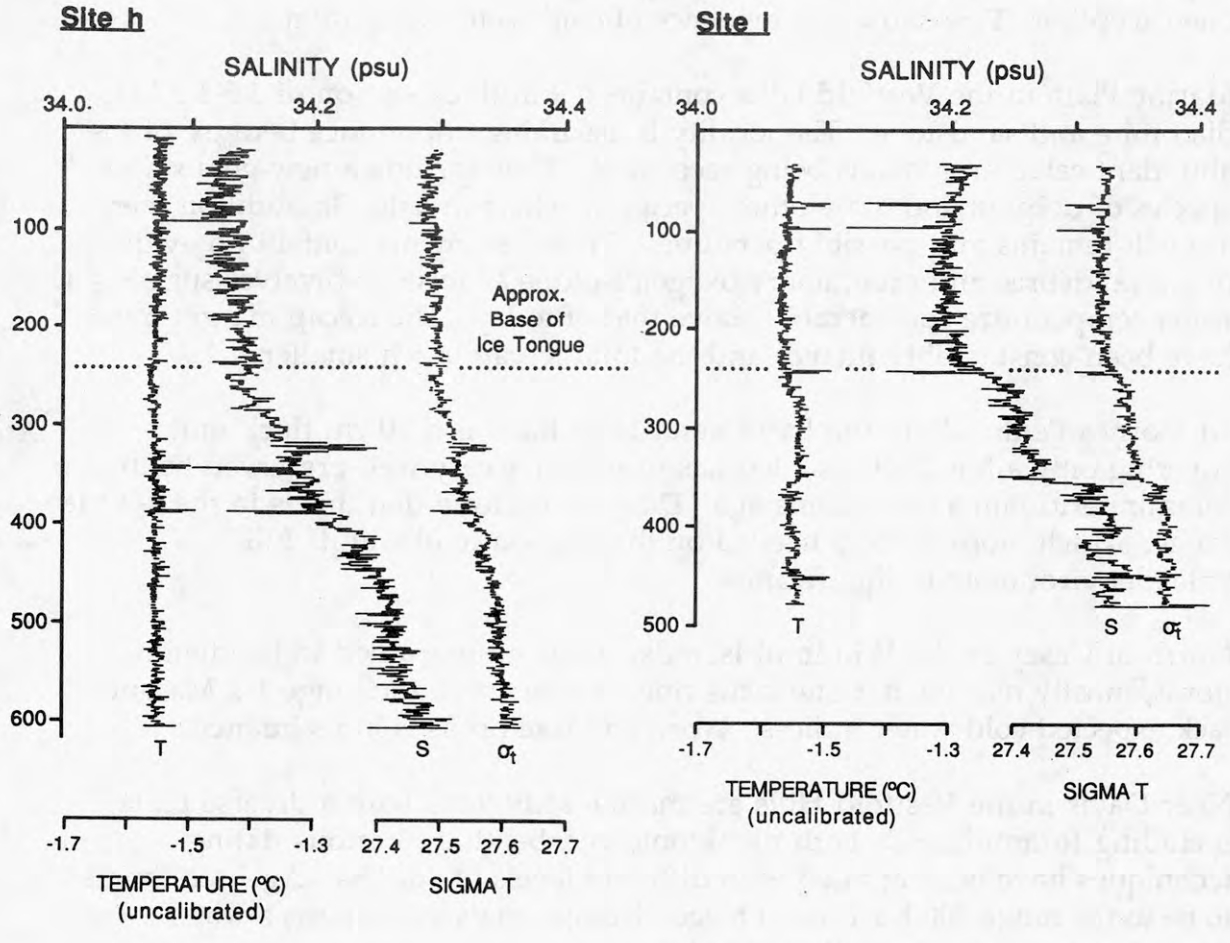

Figure 2. Profiles of temperature,salinity and density (sigma t) at site h. at the terminus of glacier tongue and site i. in the north side canyon.

REFERENCES

Macpherson, A.J. 1987. The Mackay Glacier/ Granite Harbour system (Ross Dependency, Antarctica) -a study in nearshore glacial marine sedimentation. Unpublished Ph D thesis, Victoria University of Wellington library.

Pyne, A.R. 1989. Antarctic Bottom Currents(K042). NZ Antarctic Record, v9-3 p28.

Dunbar, R.B. and Pyne,A.R.1989. Current velocities and sedimentation patterns in Granite Harbor fjord,southern Victoria Land,Antarctica.Antarctic Journal of the United States,v24-5,p136.

SOURCES OF INFORMATION ON THE LATE NEOGENE OF COASTAL EAST ANTARCTICA

Patrick G. Quilty
Australian Antarctic Division
Channel Highway, Kingston
Tasmania, Australia, 7050

Several localities in coastal East Antarctica have yielded thin sediment sequences of several Pliocene and younger ages. Most are marine but there is one exception. Few show any evidence of cold water deposition.

Marine Plain in the Vestfold Hills contains a 9 m thick section of 3.5-4.2 Ma diatomite and sandstone. The locality is assuming importance because of the abundant cetacean remains being recovered. They include a new genus and species of dolphin and three other species of whale to date. In addition there are fish remains and possibly penguins. These sediments contain no evidence of glacial debris, and preliminary oxygen isotope analysis of bivalves suggests a water temperature considerably above that of today. The icecap margin must have been considerably inland, and the total icecap much smaller.

At Stornes Peninsula in the Larsemann Hills there is a 40 cm thick unit, covering only a few hectares, that has provided a very well preserved benthic foraminiferid fauna of Pliocene age. Diatoms indicate that this is in the 2-3 Ma range. Much more work is needed on this section to obtain its full palaeoenvironmental significance.

North of Casey in the Windmill Islands, sediment entrained in ice diatom floras, mostly marine, but one lacustrine. These are in the range 1-2 Ma but lack expected cold water indices. Work on these floras is in its infancy.

Near Davis in the Vestfold Hills are marine sediments with a diverse biota, including foraminiferids both planktonic and benthic. Various dating techniques have been applied with different levels of success. Age is estimated to be in the range 300 Ka-1 Ma. Oxygen isotope analysis suggests a water temperature a little above that of today.

These sequences probably are biassed towards intervals of warm water and thus high sea level. They do, however, provide a source of data for hypotheses that are apparently in conflict with some of the ideas generated from deep sea sections. Much work, including deep sea drilling, is needed to make all stories compatible.

NEW EVIDENCE CONFIRMS THE EXISTENCE OF THE BELLINGSHAUSEN PLATE, OFFSHORE MARIE BYRD LAND

C. A. Raymond, Jet Propulsion Laboratory, California Institute of Technology, Pasadena, California 91109 USA
R.E. Bell, Lamont Doherty Geological Observatory of Columbia University, Palisades, New York 10964 USA

Marie Byrd Land (MBL) is one of many separate tectonic blocks that comprise West Antarctica. Along the Pacific margin of West Antarctica, the MBL margin extends from the Ross Sea to Thurston Island; it is a region of very sparse geophysical observations. The lack of seafloor spreading data in this region requires that models of Pacific-Antarctic (PAC-ANT) relative motion during the late Cretaceous-Early Tertiary rely solely on data from the well-mapped Chatham Rise on the New Zealand margin. Attempts to reconstruct the margins on opposite sides of the Pacific plate produce a misfit which first appears at anomaly 18 (Eocene) and increase in magnitude into the Cretaceous. The cause of the misfit is a kink in the azimuth of the seafloor spreading lineations on the Pacific plate at the approximate location of Fracture Zone 8.5. The misfit results in a wedge of crust on the MBL margin that cannot be accounted for with existing models of PAC-ANT spreading. Stock and Molnar (1987, *Nature, v.325*) proposed the existence of a short-lived plate,the Bellinghausen Plate, to fill this gap.

Recent geophysical observations from a *Polar Duke* cruise that transited the MBL margin provide several key fiducial magnetic anomaly points and seafloor structural information on the MBL margin to aid in evaluating the existence of the Bellinshausen Plate. We have used the new anomaly picks on the MBL margin to test rotation parameters derived by Stock and Molnar for PAC-ANT spreading, using only data south of FZ 8.5, derived under the assumption that a separate Bellingshausen Plate existed. We obtain a good fit of rotated Pacific anomaly picks with the Antarctic picks using the PAC-ANT stage pole of Stock and Molnar for the period A28-31 (~65-70 Ma). The total rotation angle we derive is smaller by ~10%, indicating Antarctic spreading was ~30% slower than Pacific during that stage of spreading. The fit of rotated and observed anomalies obtained using the Stock and Molnar pole confirms the existence of a separate Bellingshausen plate north of FZ 8.5.

Our data provides tighter constraints on the physical boundaries of the Bellingshausen plate. We have mapped a change in basement character from flat, undisturbed seafloor to rough seafloor with well-defined ridge flank structure. The morphologic change also coincides with a change in the character of the magnetic anomalies from long to short wavelength. A ridge-like structure is observed at the estimated location of the Bellingshausen-Antarctica spreading center, near 127°W, 69°S. This ridge structure coincides with a region of high amplitude, short wavelength gravity anomalies detected in Geosat data and shipboard gravity data. We interpret this structure to be the failed Bellingshausen-Antarctica spreading center, that ceased spreading around 42 Ma.

REVISED HISTORY OF EARLY CRETACEOUS SEAFLOOR SPREADING BETWEEN SOUTH AMERICA AND ANTARCTICA INFERRED FROM SATELLITE GEOPOTENTIAL DATA

C. A. Raymond, Jet Propulsion Laboratory, California Institute of Technology, Pasadena, California 91109 USA
W. F. Haxby, Lamont-Doherty Geological Observatory of Columbia University, Palisades, New York 10964 USA

Analysis of Magsat and shipboard magnetic data offshore Dronning Maud Land in the eastern Weddell Sea suggests that the Cretaceous Quiet Zone is more extensive than previously deduced from sparse shipboard observations. The Magsat satellite magnetic anomaly field reveals a large positive anomaly similar in characteristics to the anomalies observed over the Cretaceous Quiet Zones of the North Atlantic. The available shipboard magnetic data provides weaker evidence to support this hypothesis. Acceptance of the new age distribution for the crust implies relative motion between East and West Antarctica during the Early Cretaceous. We find supporting evidence in the Geosat gravity data that such relative motion took place.

We derive a revised plate kinematic model, based on these new observations, describing the motion of South America, Africa, East and West Antarctica during the Early to Late Cretaceous.

GRAVITY TRANSECT ACROSS THE TRANSANTARCTIC MOUNTAINS (TAM) SOUTH OF THE DRYGALSKI ICE TONGUE, NORTH VICTORIA LAND

T. F. Redfield
Dept. Geology, Arizona State University, Tempe, Arizona, 85287, USA.
J. Behrendt
United States Geological Survey, Denver Federal Center, MS 964, Box 25046, Denver, Colorado, 80225, USA.
D. Damaske, G. DeLisle, D. Moeller, G. Reitmayr, Joachim Sievers.
Bundesanstalt fuer Geowissenschaften und Rohstoffe, Hannover, FRG.

During GANOVEX VI new gravity data were collected in an east-west profile south of the Drygalski Ice Tongue. The profile extends 140 km across the TAM. The survey has been connected to northern gravity data (GANOVEX V) by a coastal transect. All data can be terrain corrected, and are constrained by satellite elevation (GPS) and ice-thickness measurements.

A pronounced regional Bouguer gravity gradient decreasing to the west by approximately 3 mgal/km is superimposed over a coastal belt of granitoid basement rocks (Figure 1). We interpret the gradient to be representative of the crust/mantle boundary within the study area. West of this belt (161° 30'East) Ferrar sills are exposed at the surface. We interpret the break-in-slope and the apparent flattening of the regional gradient to be an effect of the dense Ferrar sills and associated deep crustal fractionate replacing less dense basement. We attribute the "busy" local field below the Ferrar to be the product of still unreduced GPS elevation data and incomplete ice/terrain corrections. We estimate that the effect of complete corrections will prove less than 50 mgals, implying that some portions of the local anomalies are real.

The regional gravity gradient of the profile is steeper than that observed to the north (Mt. Melbourne quadrangle) and shallower than that reported to the south (McMurdo Sound). The absolute gravity values at the coastal points of origin differ by 60 to 100 mgal. In addition, topographic relief within the area is subdued relative to the TAM to the north and south. We speculate that the root structure of the TAM undergoes a change somewhere between the Mt. Melbourne quadrangle and the region south of the Drygalski.

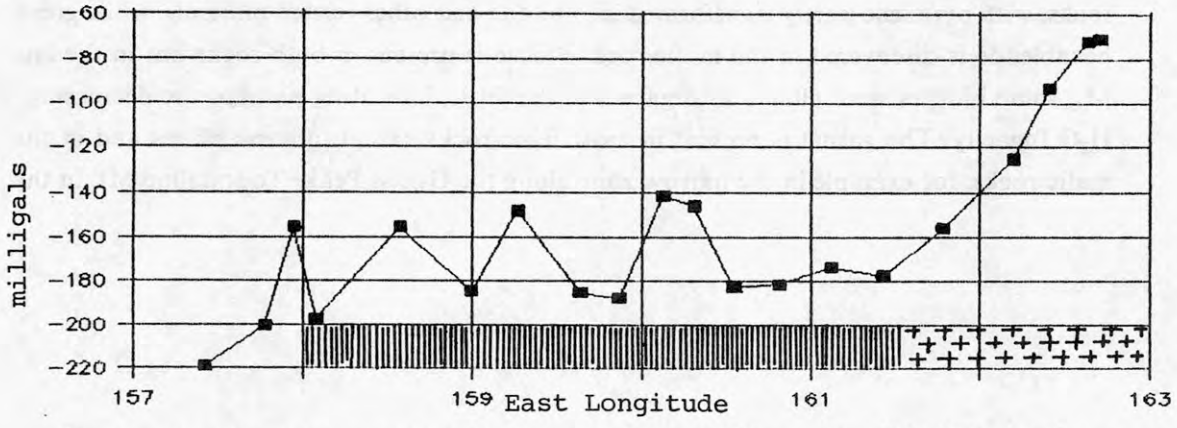

Figure 1: Bouguer gravity values dropping from sea (right) to land

EVOLUTION OF METAMORPHIC GEOLOGY OF ZHONGSHAN STATION REGION (LARSEMANN HILLS), EAST ANTARCTICA

Ren Liudong[1], Zhao Yue[1], Liu Xiaohan[2]
and Chen Tingyu[1]

1. Institute of Geology, Chinese Academy of Geological Sciences, Baiwanzhuang RD., Beijing, 100037, P.R. China.
2. Institute of Geology, Academia Sinica, Dewai Qijiahuozi, Beijing, 100029, P.R.China.

On the basis of detailed geological mapping (1:2000) in northern Mirror Peninsula and mapping (1:10000) in Stornes and Mirror Peninsulas and domestic research, some knowledge has been obtained in the petrology and metamorphic geology. The region is dominated by paragneiss, such as migmatic gneiss (metatexite), migmatic granite(diatexite), stromatic biotite–garnet gneiss, biotite gneiss, minor corderite–sillimanite gneiss, biotite–sillimanite gneiss and biotite–pyroxene gneiss, felsic pegmatite, most of them contain garnet, except that along the zone of Gneiss Peak–Tourmaline Mt. in the Stornes Peninsula and part of the zone from Seal Cove to the Nella Fjord in the Mirror Peninsula. At least four stages of deformation have been discerned by the relationships between foliation, fold and fracture, with the early deformation D_1 and D_2, foliations S_1 and S_2 especially the latter can be discriminated. S_1 usually occurs as residue between foliation S_2, and the needle–like sillimanite lineations of S_1 indicates the extensional setting when it was formed. S_2 is most strongly developed and controlled the regional structrue pattern. D_3 is shown by mesoscopic open–tight fold and the D_4 brittle fractures.

The region has undergone three stages of metamorphism. M_1, corresponding to D_1, is manifested by some residual sillimanite and biotite, M_2, contemporaneous with or in the late D_2, formed the granulite facies assemblages, e. g. Opx–Cpx–Pl± Hb ± Qtz in mafic rocks and Crd–Sil–Grt–Or–Qtz ± Pl ± Bt in felsic rocks. Some corderite coronae have been found in the late M_2. M_3, probably related with D_3, is most distinguished by the partial melting, but euhedral megacrysts of garnet and orthopyroxene concentrated in the leucosome had been formed at the initial time of the metamorphism M_3, suggesting near granulite facies condition had been reached.

The partial melting resulted in large amount of metatexite and diatexite in the felsic rocks, with pyroxene partly transformed into biotite and other related minerals. while green hornblende is discovered in the mafic rock. Biotite is present in both rocks but in the late M_3, some biotites were altered into garnet in the felsic, indicating perhaps the decreasing H_2O fugacity. The garnet is present in most felsic rocks except in some places and in the mafic rocks, for example in the narrow zone along the Gneiss Peak–Tourmaline Mt. in the

Stornes Peninsula and the zone from Seal Cove to Nella Fjord in Mirror P. especially the former. Mineral zones can be discovered in the field, with the order from inner to outer: garnet–corderite–tourmaline–potassium feldspar and biotite zones. Corderite is present in all zones except the garnet area. The corderite and tourmaline zones are narrow, 60–70m, while the last zone hundreds of meters wide.

The partial melting may result in the partly uplifting of the region by diapirism, We can take the quartz–rich diatexite in northern Mirror Peninsula as an example, where the body is surrounded by layered gneiss in which the small folds of D_3 are distinguished.

As to the geochronology, detrital zircons from diatexite in the northern Mirror P. give a range from 1200 ± 6Ma to 789 ± 20Ma ($^{207}Pb/^{206}Pb$ age of single zircon), which lay constraints on the formation age of the original rocks. Zircon from garnet–bearing granite(diatexite) yield 563–529Ma ages, and the pegmatite in Seal Cove gives the range 535–521Ma. By using $^{40}Ar/^{39}Ar$ biotite measurement, we have the results of plateau and isochron ages of metatexite 504.4 ± 1.4Ma, 506.6 ± 4.5Ma; diatexite 494.4 ± 1.3Ma, 495.9 ± 4.6Ma and pegmatite 485.8 ± 0.6Ma, 485.6 ± 7.8Ma, respectively. All the dates concentrate at the Pan–African event period (500Ma). As implied above, the M_2 is probably lower in H_2O fugacity, and the M_3 higher. Corresponding with the Pan–African event, the M_3 thermal event is presumbly independent of the M_2 and the last event could be coupled with the lower crust and / or upper mantle different from that of M_2, This last stage of metamorphism might be related to the eventual formation of the Gondwana supercontinent.

METAMORPHIC FACIES OF THE ROSS OROGENY IN THE WILSON TERRANE OF NORTHERN VICTORIA LAND, ANTARCTICA

C.A.Ricci, M.Meccheri, R.Palmeri, N.Rastelli, F.Talarico
Dipart. Scienze Terra, Università di Siena, Italy
B.Lombardo, Centro Studi Orogeno Alpi Occidentali C.N.R.Torino, Italy
P.C.Pertusati, Dipart. Scienze Terra Università di Pisa, Italy
M.Franceschelli, F.Pannuti ,Ist. Giacimenti Minerari,Università di Cagliari, Italy
G.Oggiano, Ist. Geo-mineralogico, Università di Sassari, Italy
G.Capponi, Dipart. Scienze Terra Università di Genova, Italy
D.Castelli, Dipart. Scienze Terra Università di Torino, Italy
A.Montrasio, Centro Studi Stratigrafia e Petrografia C.N.R. Milano, Italy
P.G.Rossetti, Dipart. Georisorse e Territorio, Politecnico di Torino, Italy

Northern Victoria Land lies at the Pacific end of the Transantarctic Mountains and comprises three major litho-tectonic units or terranes: Wilson, Bowers and Robertson Bay Terrane.

The Wilson Terrane formed during the Ross Orogeny (Cambro-Ordovician) which affected a "cover" of partly Cambrian age and a basement (containing granulite facies relics) possibly dating back to the Proterozoic. Both cover and basement were intruded by Cambro-Ordovician granitoid plutons.

In the cover sequence, the Ross metamorphism is of low-Pressure/high-Temperature and has a prograde character. It ranges from low greenschist to upper amphibolite facies and anatexis.

The older granulitic-migmatitic basement shows a strong Ross overprinting which has locally completely obliterated the pristine parageneses. The conditions of the retrogressive metamorphism are comparable to the highest grade recognized in the cover sequence.

On the basis of detailed petrological and structural studies, performed in three areas of the Deep Freeze and Eisenhower Ranges (Wishbone Ridge, Mt. Levick and Foolsmate Glacier), we were able 1) to recognize that both deformation and metamorphism of Ross age show a continuous development from low-grade to high-grade areas and 2) to distinguish five zones of increasing metamorphic grade in pelitic-quartzofeldspatic rocks and in calc-silicate rocks.

The metamorphic zones and their correlation are as follows (critical mineral associations are reported in brackets):

Metapelites	Calc-silicate rocks
Biotite *(Bt+Chl±Pyr?)*	Ankerite *(Ank+Cc+Chl)* Calcite+Biotite *(Cc+Bt+Chl)* Ca- amphibole *(Cam+Pl+Zo)*
Andalusite+Muscovite *(And+Ms±Crd)*	Diopside *(Di+Cam+Cc+Qtz±Grs)*
Sillimanite+Muscovite *(Sil+Ms +Crd)*	
Sillimanite+K-Feldspar *(Sil+Kfs+Crd)*	Wollastonite *(Wo+Di±Scp)*
Garnet+Cordierite *(Grt+Crd+Bt±melt)*	

Seven metamorphic zones can, therefore, potentially be distinguished and mapped: however, they have been mapped only for the three areas studied in detail (Wishbone Ridge, Mt. Levick and Foolsmate Glacier).

The mapping of the metamorphic zones on a larger scale is complicated by the discontinuity of the outcrops. However, a five-fold partition of the Ross metamorphism, corresponding to the five zones distinguished for pelitic rocks, could be made for the metamorphic rocks of the Eisenhower and Deep Freeze Range and extended, in a modified form, also to the Mountaineer Range metamorphics.

At the regional scale, it was impossible, on the basis of literature data, to make the distinction between the two zones of highest grade that were distinguished in pelitic rocks and, therefore, only a four-fold partition of the Ross metamorphism has been outlined for the whole Wilson Terrane of Northern Victoria Land.

STRUCTURE OF THE FOSDICK METAMORPHIC COMPLEX, MARIE BYRD LAND, WEST ANTARCTICA

S. M. Richard, Institute for Crustal Studies, University of California, Santa Barbara, CA, 93106-1100, USA

Setting and rock types

Most of the Ford Ranges, located in coastal Marie Byrd Land, are underlain by low-grade metasediments of the Late Proterozoic(?) Swanson Formation, intruded by Devonian Ford Granodiorite and Cretaceous Byrd Coast Granite [Wade et al., 1977, 1978]. We have been studying the Fosdick Mountains (145° W, 76° S), an east-west trending range formed of high-grade metamorphic rocks referred to as the Fosdick Metamorphic Complex. The complex consists of upper amphibolite- to lower granulite-facies metasedimentary rocks [Smith, this volume], intruded before, during, and after metamorphism by a variety of granitoids. This paper describes the structure of the metamorphic complex based on two seasons of field work (1989-1990, 1990-1991).

Two syn-metamorphic deformation events are recognized. The older event produced a steeply dipping gneissic foliation, largely transposed and obliterated by the younger event which produced the prominent, relatively planar gneissic layering in most of the complex. Lineations are scarce and not consistently oriented, suggesting that the finite strain ellipsoid is quite oblate. The geometry of late syn-metamorphic extensional shear fractures suggests a NNE component of extension within the shear zone. Retrograde extension fractures indicate a NNE extension direction during uplift. Late-stage, normal(?) faults trend north-south.

Gneissic foliation

Two generations of gneissic layering are recognized. Both are defined by mineralogic differentiation on a centimeter to decimeter scale and by gross lithologic layering on a 10-100 m scale, and apparently both formed under similar metamorphic conditions. The older, generally steeply dipping foliation (S_1) is preserved in large-scale, lozenge-like, low strain zones in the north-central part of the range. Tight to isoclinal folds with hinge surfaces parallel to this foliation (F_1) indicate that it represents a transposed older foliation, probably bedding. Where preserved, the S_1 foliation is typically strongly folded (F_2). Folds generally have long, gently dipping high strain limbs and short, steep limbs. These asymmetrical folds form a large-scale continuous crenulation fabric. High strain in the long limbs is indicated by attenuation of layering relative to that in the steep limbs. Cascades of recumbent, close to tight folds are also observed. F_2 folds trend ENE in the Ochs glacier area, but hinge lines trends swing to the SE at the eastern end of the low-strain domain.

Hinge surfaces of F_2 folds are sub parallel to their attenuated long limbs; these are interpreted to represent S_2. At the margins of the low strain zones the intrafolial lozenges preserving older fabric become thinner and straight gneissic foliation equivalent to the long limbs of the large-scale crenulation fabric becomes dominant. Intrafolial close to isoclinal folds are locally present but are not common in S_2.

In the western part of the range, large volumes of granitoid neosome invaded parts of the complex leading to formation of block gneisses, in which the blocks preserve the character and locally even the structure of the original gneiss. Gneissic foliation in the granitoid matrix of the block gneisses wraps around the blocks, commonly discordant to foliation within the blocks. The preservation of pre-existing structure in and between blocks in the block gneisses and the irregular gneissic foliation in the matrix between the blocks implies that invasion by the granitoid matrix and associated disaggregation to form the blocks post-dates the major deformation in the Fosdick gneiss complex.

Sparse mineral lineations defined by sillimanite in pelitic rocks or by hornblende (generally replaced by biotite) in dioritic rocks are present in the Fosdick metamorphic complex. Trends of both the sillimanite (N=26) and hornblende (N=15) mineral lineations scatter widely with weak concentrations plunging gently towards the E and SW.

Synmetamorphic faults

Syn-metamorphic minor faults cut the gneissic foliation at moderate to steep angles. These range from continuous faults (shear zones) to discrete discontinuities. Typically they contain unfoliated granitoid veins along the fault surface, ranging from 1-30 cm thick. A discrete surface of discontinuity characterizes the discontinuous faults. Gneissic foliation can be traced through the continuous fault zones, although it becomes highly attenuated in the central part, with geometry typical of a Ramsay-Graham shear zone. The two fault types are gradational with each other. Discontinuous faults commonly terminate along strike into continuous faults, and foliation commonly curves into the discontinuous faults with geometry identical to the continuous faults. Granitoid veins are thicker and more abundant along the discontinuous faults. Orientation of the synmetamorphic faults varies widely, but poles to the fault surfaces are weakly concentrated about a girdle oriented 020/70 NW.

Dikes

Mafic dikes were intruded continuously throughout the metamorphism and deformation of the Fosdick complex. The least deformed, youngest dikes are steeply dipping hornblende diorite, and cut gneissic foliation; older dikes are buckled and boudinaged, progressively rotated towards parallelism with gneissic foliation, and metamorphosed to fine-grained

biotite-plagioclase granofels. The dikes both cut and are cut by the synmetamorphic faults. Dike orientations scatter widely. This variation in orientation is interpreted to result from variable initial orientation and variable degrees of deformation. Steeply dipping, easterly trending dikes are the most common.

Structures associated w/ retrogression

Late-metamorphic pegmatites form irregular to planar veins. Planar veins are most abundant where the pegmatites cut mafic dikes. Drusy quartz and muscovite crystals line cavities within the pegmatite dikes, indicating decreasing metamorphic conditions and elevated fluid pressures. Thin muscovite-chlorite-quartz veinlets are younger than the pegmatites. These also contain cavities with drusy quartz and muscovite crystals. The planar pegmatites and muscovite-chlorite-quartz veinlets generally trend easterly and are vertical. They have very similar orientation distributions, with a modal orientation of 100/V. The similarity in orientation and mineralogy in cavities between the pegmatite dikes and younger veins suggests that they formed progressively in a relatively consistent stress field.

Brittle faults

The youngest structures recognized are north-trending minor high-angle faults. These typically have thin chloritic microbreccia zones along them, commonly with minor quartz veins and hematite staining. Faults in this set along the west side of the Ochs glacier have striations indicating that final movement was dip-slip. Parallelism of the Ochs glacier and other trunk glaciers draining the ice cap on top of the range with these structures suggests that they are controlled by north-trending faults.

Interpretation

The steep S_1 foliation may have originated as a steep foliation similar to that observed in the Dry Valleys area near Ross Island. Alternatively, S_1 and S_2 may have developed during a progressive deformation, with S_1 representing the steep limbs of large scale folds produced early in the deformation, and now largely obliterated by continued flow to produce a pervasive S_2. The change in F_2 fold orientation in the zone of crenulated S_1 is interpreted to reflect a pre-crenulation warp in S_1. The relatively planar regional character of S_2 reflects strain during metamorphism. The absence of a pervasive lineation indicates that this strain was largely a flattening deformation, consistent with the large scattering in the orientation of mafic dikes intruded during the metamorphic event. Orientations of syn-metamorphic faults are less scattered, and suggest a component of ENE extension late in the metamorphic history, consistent with a slight NE-trending preferred orientation of sillimanite mineral lineations in S_2 in the eastern part of the range. Retrograde pegmatites and muscovite-chlorite-quartz

fractures are more consistently oriented indicating that σ_3 was oriented approximately 00/010° during initial uplift of the gneisses. The north-trending faults are younger, and may be related to the final uplift of the Fosdick Mountains.

References

Wade, F. A., Cathey, C. A., and Oldham, J. B., 1977, Reconnaissance geologic map of the Boyd Glacier quadrangle, Marie Byrd Land, Antarctica: United States Antarctic Research Program, Antarctic Geologic Map A-6.

Wade, F. A., Cathey, C. A., and Oldham, J. B., 1978, Reconnaissance geologic map of the Gutenko Nunataks quadrangle, Marie Byrd Land, Antarctica: United States Antarctic Research Program, Antarctic Geologic Map A-11.

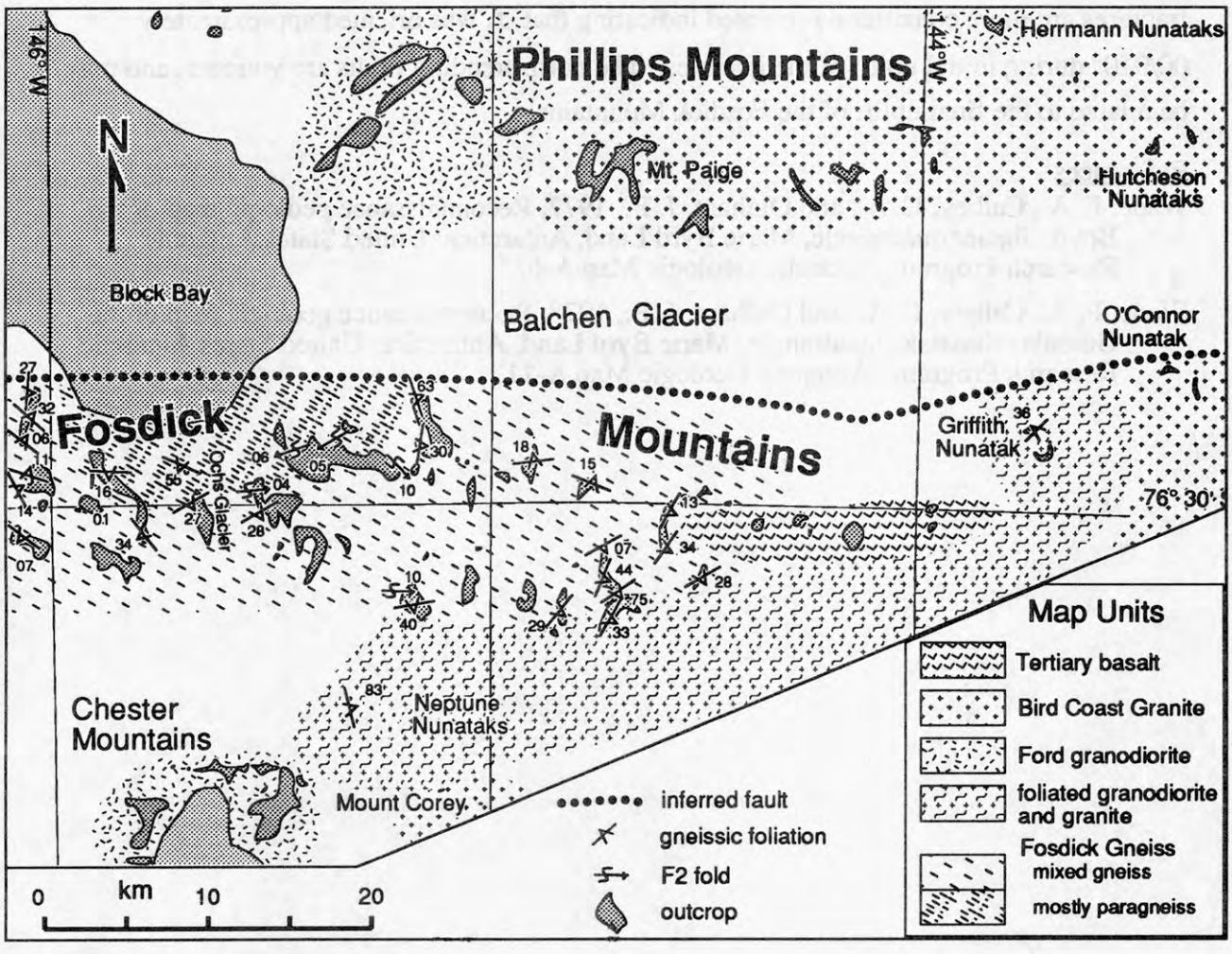
Phillips Mountains
Herrmann Nunataks
Mt. Paige
Hutcheson Nunataks
Block Bay
Balchen Glacier
O'Connor Nunatak
Fosdick
Mountains
Griffith Nunatak
Ochs Glacier
76° 30'
Chester Mountains
Neptune Nunataks
Mount Corey
144°W
146°W
N
0 km 10 20
inferred fault
gneissic foliation
F2 fold
outcrop
Map Units
Tertiary basalt
Bird Coast Granite
Ford granodiorite
foliated granodiorite and granite
Fosdick Gneiss
mixed gneiss
mostly paragneiss

GEOLOGICAL AND GEOPHYSICAL INVESTIGATIONS IN THE NORTHERN FORD RANGES, MARIE BYRD LAND, WEST ANTARCTICA: IMPLICATIONS FOR A ZONE OF LATE MESOZOIC, DEEP CRUSTAL MIGMATIZATION AND FLOW IN THE FOSDICK METAMORPHIC COMPLEX

Richard, S. M., Smith, C. H., Luyendyk, B. P., Institute for Crustal Studies, University of California, Santa Barbara, California, 93106-1100, USA;
Kimbrough, D. L., Department of Geological Sciences, San Diego State University, San Diego, California, 92182, USA

The Phillips, Fosdick, and Chester Mountains are found in the northern Ford Ranges of Marie Byrd Land (MBL). They trend east-west and are separated by about 15-20 km. Plutonic rocks crop out in the Phillips and Chester Mountains while the Fosdick Mountains comprise high grade metamorphic rocks. We conducted field studies during the 1989-90 and 1990-91 austral summers in these ranges, which included mapping, structural measurements, and sampling for isotopic, paleomagnetic, and petrological investigations. Our efforts focused mainly on the metamorphic rocks of the Fosdick Mountains.

The Fosdick and Chester Mountains form a south-dipping tilted block which shows a transition from high grade metamorphic rocks into plutonic rocks. The Fosdick Mountains provide an opportunity for direct observation of the deeper levels of continental crust in this segment of MBL. The Fosdick metamorphic complex consists primarily of a variety of migmatitic orthogneisses, with interlayered migmatitic metasedimentary rocks. Mixed orthogneiss and paragneiss predominate in the northern part of the complex, and grade southward, structurally upward into mostly granodioritic orthogneiss. Biotite, sillimanite, garnet, cordierite, quartz and K-feldspar are present in pelitic gneisses throughout the range. Petrologic observations indicate significant late-metamorphic decompression. Leucogranitic neosome bodies range from homotropic and crosscutting to gneissic and concordant, demonstrating that migmatization and the development of penetrative gneissic foliation were coeval. Preliminary U-Pb data indicate that migmatization occurred during Mesozoic time, overprinting older metamorphic events. We interpret that the protolith of the migmatite was a relatively homogeneous calcareous argillite, probably correlative with the Late Proterozoic Swanson Formation, intruded by granodiorite plutons (Devonian Ford Granodiorite?).

The Fosdick Mountains comprise a large-scale deformation zone. Older, steeply dipping gneissic foliation is preserved in low-strain, highly crenulated zones in the north-central part of the range. Straight gneisses in much of the rest of complex are interpreted to be transposed from this older foliation. This younger foliation dips predominantly S to SE. The lack of lineation in the gneisses indicates that deformation was largely by flattening; the orientation of syn-metamorphic minor faults suggests a small component of NNE extension during the deformation. Migmatization was accompanied by intrusion of mafic dikes. The orientation of the dikes is highly variable. Advanced partial melting led to the formation of block gneiss, in which lenses of paleosome and boudinaged dikes were engulfed in granitic neosome. Block gneiss formation was largely post-kinematic. Retrograde pegmatites and extensional veins trend ESE, consistent with NNE extension during initial cooling of the complex. $^{40}Ar/^{39}Ar$ isotopic data indicate rapid cooling of the Fosdick gneiss complex between 100 and 94 Ma.

Outcrops south of the Fosdick Mountains, in the Neptune Nunatuks and Chester Mountains, consist of granodiorite plutons (~353 Ma, U-Pb zircon) with pendants of greenschist to lower amphibolite-facies metasedimentary rocks. A similar tonalite to granodiorite plutonic complex crops out in the western Phillips Mountains north of the Fosdick Mountains; these are correlated with Ford Granodiorite [Wade et al., 1977, 1978]. The eastern Phillips and Fosdick Mountains and isolated nunataks east of the Chester Mountains are underlain by epizonal biotite granite

(~103 Ma, based on U-Pb zircon studies) correlated with the Byrd Coast granite [Wade et al., 1977, 1978].

Lithologic gradation from mixed migmatite and orthogneiss to foliated granodiorite to unfoliated granodiorite between the northern Fosdick and Chester Mountains suggests that the Fosdick complex originated in a sub-batholithic domain related to the Ford Granodiorite. U-Pb isotopic data indicating Mesozoic metamorphism suggests migmatization was coeval with the intrusion of Byrd Coast granites. These observations suggest that the two gneissic foliations may be significantly different in age. Chemical data from Byrd Coast granites [Weaver et al., 1991] make derivation of these plutons from migmatite complexes like the Fosdick Complex very unlikely. Heating associated with the plutonism may have resulted in minor mid-crustal melting without generating discrete magma bodies. The early deformation recorded in the Fosdick gneiss complex may be related to intrusion of the Ford Granodiorite, while the later Mesozoic deformation probably reflects some combination of flattening to accommodate intrusion of Byrd Coast granite and large-scale intracrustal flow related to the initial breakup of Gondwanaland.

The present physiography of the Phillips, Fosdick, and Chester Mountains may be related to basin-and-range style extension, possibly associated with extension in the Ross Embayment and uplift of the Transantarctic Mountains. The Phillips and Fosdick Mountains trend parallel to the Transantarctic Mountains (as viewed in polar grid projection), as do several other mountain ranges in the southern Ford Ranges. The geomorphology of the Fosdick Mountains suggests that it is a fault block with a steep northern side. A residual bouguer gravity anomaly of at least -50 Mgal [Beitzel, 1972] follows the Balchen Glacier which separates the Phillips and Fosdick Mountains, suggesting that the glacier is flowing through a graben between these mountains. Cenozoic basaltic volcanic centers crop out along an east-west trend in the eastern Fosdick Mountains, suggesting fault control of their distribution by unexposed, range-bounding, master normal faults. Importantly, the volcanic centers are the only outcrops of young basaltic rocks in the entire Ford Ranges, and they lie along the axis of the Fosdick metamorphic complex. The spatial association of young basalts with high grade metamorphic rocks may indicate a zone of thin, extended crust.

REFERENCE:

Beitzel, J. E., 1972, Geophysical investigations in Marie Byrd Land, Antarctica [Ph. D. dissertation]: Madison, Wisconsin, University of Wisconsin, 111 p.

Wade, F. A., Cathey, C. A., and Oldham, J. B., 1977, Reconnaissance geologic map of the Guest Peninsula quadrangle, Marie Byrd Land, Antarctica: U. S. Antarctic Research Program Antarctica Geological Map A-7: Reston, Virginia, U. S. Geological Survey, scale 1:250,000.

___, 1978, Reconnaissance geologic map of the Gutenko Nunataks quadrangle, Marie Byrd Land, Antarctica: U. S. Antarctic Research Program Antarctica Geological Map A-11: Reston, Virginia, U. S. Geological Survey, scale 1:250,000.

Weaver, S. D., Bradshaw, J. D., and Adams, C. J., 1991, Granitoids of the Ford Ranges, Marie Byrd Land, Antarctica, *in* Thomson, M. R. A., Crame, J. A., and Thomson, J. W., Editors, Geological Evolution of Antarctica: Cambridge, England, Cambridge University Press, p. 345-352.

DOUBLING THE KNOWN EXTENT OF THE ROSS SEA SEDIMENTARY BASINS

S.T. Rooney, Mobil Research and Development Corp., Dallas, Texas, U.S.A.

D.D. Blankenship, Byrd Polar Research Center, The Ohio State University, Columbus, Ohio, U.S.A.

R.B. Alley, Earth Systems Science Center, The Pennsylvania State University, University Park, Pennsylvania, U.S.A.

C.R. Bentley, Geophysical and Polar Research Center, University of Wisconsin-Madison, Madison, Wisconsin, U.S.A.

The Tertiary sedimentary basins of the Ross Sea extend almost 1000 km farther into the interior of West Antarctica than previously demonstrated, based on our recent geophysical studies. The Ross Sea is underlain by a series of ridges and troughs subparallel to the Transantarctic Mountains. The troughs occupy grabens formed by extension of the Ross Embayment, and contain ~1 km of sedimentary fill with low seismic velocities. Similar topography continues beneath the Ross Ice Shelf and the ice streams on the Siple Coast of the West Antarctic ice sheet, suggesting structural continuity. The experiments involved in this project spanned three Antarctic field seasons at two sites on ice stream B in West Antarctica: one site near the grounding line at the Ross Ice Shelf (DnB) and a site approximately 200 km upstream of the grounding line (UpB). In 1983-84 and 1984-85 a 50-km seismic-refraction profile was completed near UpB on ice stream B. In 1984-85, also near UpB but about 4 km to the side from the refraction profile, a 4.5 km multichannel seismic-reflection profile was collected for interval velocity analysis and for structural interpretation. In 1987-88 another seismic reflection profile, this one 9.4 km long, was collected near DnB. Our results show that the subglacial trough of ice stream B occupies a fault-bounded basin containing ~1 km of low-velocity sediments fully consistent with an inland extension of the Ross Sea basins.

THE DEEP STRUCTURE BENEATH ANTARCTICA INFERRED FROM RAYLEIGH AND LOVE WAVES

D.Rouland , Ecole et Observatoire de Physique du Globe
5,rue René Descartes,67084 Strasbourg cedex,France
G.Roult and J.P Montagner , Institut de Physique Du Globe
4,place Jussieu , 75130 Paris cedex 05, France

The deep structure beneath the antarctic continent is not well known due to the scarcity of geophysical studies performed up to now. In seismology the main reason is that few observatories operating in low frequency domain were operational in the high southern latitudes during the seventies and early eighties. Since 1982 high priority was given by french authorities to global seismic research programs, and particularly to seismological stations development such as in Territoires desTerres Australes et Antarctiques Francaises which have been either updated or created with use of recent and sophisticated technologies. In the present study we attempt to recover the upper mantle structure of Antarctica and the surrounding areas by analysing group and phase velocities of surface waves from digital 3-components broad band records. For this purpose we have selected a set of more than 150 direct paths connecting epicentres to GEOSCOPE stations located in southern hemisphere (Port aux Francais(PAF), Crozet(CRZF),La Reunion(RER), Dumont D'Urville(DRV), Noumea(NOC), Canberra(CAN) and Tahiti(PPT). To fill gaps in the azimuthal data distribution, some records from South Pole and southern SRO/GDSN seismological stations have been added to the initial set. The tomographic structure of shear wave velocities and their related anisotropies are retrieved from both the rayleigh and love wave dispersion data. The three-dimensional velocity variations and associated anisotropies are interpreted in terms of thermal and dynamic processes beneath the antarctic lithosphere.

EARTHQUAKE LOCATIONS AT MOUNT EREBUS VOLCANO, ROSS ISLAND, ANTARCTICA, AND DEVELOPMENT OF A WORKING VELOCITY MODEL - DETERMINATIONS USING MAN-MADE FLANK EXPLOSIONS AND SUMMIT ERUPTIONS

C.A. Rowe and J. Kienle, Geophysical Institute,
University of Alaska, Fairbanks, Alaska 99775-0800, U.S.A.

In this study, artificial explosions detonated on and near Mount Erebus volcano are used as test events to adjust the velocity model applied when locating natural earthquakes which occur in the vicinity of the volcano. Additionally, natural explosions within the summit lava lake are used as test events for the summit region.

The resulting velocity model for use with the earthquake location routine, HYPOELLIPSE, consists of a linearly increasing velocity gradient ranging from 3.55 km/sec at the volcano's summit to 4.6 km/sec at a depth of 7 km below the summit, over a homogeneous halfspace of velocity 6.1 km/sec. Analysis of the shot data reveals heterogeneities in the volcano's velocity structure, as do independent studies of the shallow regions and crater area, but these discrepancies cannot be addressed in the necessarily simple velocity model required by HYPOELLIPSE. Further, geometric raypath errors introduced by the simplified HYPOELLIPSE model can be addressed only by means of static station corrections. Errors introduced into earthquake locations as a result of these inadequacies are very small; the most significant effect is a systematic error in origin time for lava lake explosions. The apparent "pipe" distribution of earthquake hypocenters sometimes extending as deep as 5 km beneath the summit lava lake is likely to be an artifact of station distribution, and is corrected with the addition of summit station readings - it seems to be much more sensitive to presence or absence of summit station control than to the velocity model used in earthquake location.

Most earthquakes recorded with the network on Ross Island appear to occur within the summit lava lake, though a few locate deeper. Some earthquakes of tectonic appearance show a north-south trend cross-cutting Ross Island, and dike injection may have been observed in one unusual two-day swarm of over 600 volcanotectonic microearthquakes.

HEAT FLOW MEASUREMENTS AROUND ANTARCTICA
- A SUMMARY OF JAPANESE HEAT FLOW STUDIES OF LAST DECADE -

Takao Saki, Technology Research Center, Japan National Oil Corporation, 2-2-2, Uchisaiwai-cho, Chiyoda-ku, Tokyo 100, Japan.
Toshiyasu Nagao, Faculty of Science, Kanazawa University, 1-1, Marunouchi, Kanazawa 920, Japan.

Since 1980, the Japanese research vessel Hakurei has been conducting geophysical and geological surveys in offshore areas around Antarctica every Antarctic summer season. During the cruises, R/V Hakurei made seismic, gravimetric and magnetic surveys and, routinely coring operation to get sediment samples together with heat flow measurement. As a result, we obtained about 50 new heat flow data in the Antarctic Sea during the last decade.

In this presentation, we would like to review newly obtained heat flow data around the Antarctica and to present newly compiled heat flow contour map.

Temperature gradient measurements were made using mainly three types of devices (two Bullard types and a violin bow type). The maximum probe length was 7 m, however, in most cases, the probe length was 5 m. Thermal conductivities were measured with the use of commercial thermal conductivity meter named QTM (Quick Thermal Conductivity Meter). QTM uses the continuous heating method and assumes a semi-infinite medium.

One of the most notable feature of heat flow distribution around Antarctica is relatively high heat flow in comparison with that based on the age of the seafloor and estimated for a cooling plate model. The surface of the Antarctic plate is relatively cold in comparison with other plates. Even a mantle heat flow is the same, this cold Antarctic plate surface causes large temperature gradient. Therefore, we now consider that these relatively high heat flows are not real high heat flows but are apparent ones. They may be due to relatively cold Antarctic plate.

As an examples of regional features, in the Weddell Sea region, the eastern part shows relatively low heat flow in comparison with the western part, with the boundary between them at about 15^{o}W longitude.

A NEW SATELLITE IMAGE OF THE ANTARCTIC PLATE

D.T. Sandwell, Scripps Institution of Oceanography, University of California at San Diego, Geological Research Division A-020, La Jolla, CA 92093, USA.
I.W.D. Dalziel, L.A. Lawver, M. Wiederspahn, Institute for Geophysics, University of Texas at Austin, 8701 Mopac Boulevard, Austin, Texas 78759-8345, USA.

The AVHRR (Advanced Very High Resolution Radiometer) image of the Antarctic landmass and the recently declassified Geosat image of the oceanic lithosphere between 60°S and 72°S have been digitally combined in a new synoptic image that covers most of the Antarctic plate. North of 60°S, the 17 day ERM (Exact Repeat Mission) Geosat data, which has only 10% of the resolution of the total Geosat coverage, has been used. An overlay of the image identifies the main tectonic features of the continent, continental margin and the ocean floor. The ocean-continent boundary for most of the circumference of the Antarctic continent can be clearly identified although it is still obscured by ice coverage in a few areas. Prominent lineations in the seafloor gravity data indicate where most of the Gondwana fragments rifted away from the Antarctic continent. The AVHRR image is dominated by the Transantarctic Mountains that separate the East Antarctic craton from the discrete blocks of West Antarctica. The combination of the two images gives a better understanding of the actual extent of the Antarctic Peninsula and the craton. In several instances, seafloor features seen in the Geosat data seem to correlate with tectonic boundaries apparent on the AVHRR image. The very prominent fracture zones that constrain the reconstruction of Tasmania with the East Antarctic craton are parallel to such features as the Rennick Graben of North Victoria Land. The extension of the Udintsev Fracture Zone appears to continue into the Pine Island Bay region of West Antarctica which is the tectonic boundary between the Marie Byrd Land and Thurston Island blocks. An additional feature of the poster is reconstructions that show the relation of Antarctica to the other southern continents and Laurentia throughout the Phanerozoic based on marine geophysical, paleomagnetic, and geologic data.

ROLE OF FLUIDS IN CHARNOCKITE FORMATION IN THE LÜTZOW-HOLM BAY REGION, EAST ANTARCTICA: IMPLICATIONS FOR CO_2 INFILTRATION IN THE DEEP CRUST

M. Santosh, Centre for Earth Science Studies, P.B. 7250, Akkulam, Thuruvikkal Post, Trivandrum 695 031, India.
M. Yoshida, Department of Geosciences, Faculty of Science, Osaka City University, Osaka 558, Japan.

The Proterozoic deep crustal domain of Lützow-Holm Bay (LHB) in East Antarctica comprises an unbroken progression of amphibolite to granulite grade metamorphic rocks (Shiraishi *et al.*, 1987, *Geoph. Monogr.*, **40**, 309-318). Gneiss-charnockite sequences are widely represented in Ongul, which is adjacent to the amphibolite-granulite transition zone, as well as in Skallen and Botnneset, which are within the high grade segment towards south. The LHB region, in many respects, thus comprises an analogous sequence to those in southern India and Sri Lanka (Santosh, 1986, *Lithos*, **19**, 1-10; Hansen *et al.*, 1987, *Contrib. Mineral. Petrol.*, **96**, 225-244). Field, microstructural, mineral phase equilibria and fluid inclusion characteristics have yielded compelling evidence for fluid-controlled transformation of amphibolite facies gneisses to charnockites in southern India and Sri Lanka (*cf.* Santosh *et al.*, 1990, *J. Geol.*, **98**, 915-926). The LHB terrain in East Antarctica constitutes their Gondwanian counterpart, and hence investigations related to the role of fluids in charnockite formation in this terrain are fundamental to the modelling of fluid processes in East Gondwanian lower crust. This paper presents the results of a systematic petrologic and fluid inclusion study on amphibolite facies gneiss-charnockite associations in Ongul, Skallen and Botnneset. The temperatures attained during the granulite metamorphism show a broad overlap in the range of 650-800°C, with only marginal increase southward. The mineral phase equilibria barometry, computed from the chemistry of equilibrium mineral assemblages based on experimental calibrations, however, indicates an increase in pressure, from 5-7 kbar in Ongul through 6-8 kbar in Skallen up to 7-9 kbar in Botnneset. Optical fluid inclusion studies in the charnockite minerals (quartz, feldspars, garnet) show the common occurrence of trapped carbon dioxide, its composition determined by microthermometry and laser Raman spectrometry. The maximum CO_2 densities show a dramatic increase southward from Ongul (0.98 g/cm^3) through Skallen (1.05 g/cm^3) to Botnneset (1.10 g/cm^3) as shown in Fig. 1. The CO_2 isochores for individual terrains penetrate the P-T windows defined from mineral phase equilibria thermobarometry, suggesting that the carbonic inclusions were entrapped during peak metamorphic conditions and that they represent the ambient fluids which effected dehydration and charnockite formation. This is consistent with the stability of orthopyroxene in these samples, which, at the computed metamorphic P-T conditions, requires that water activities were low. In garnet-bearing samples we observed a decrease in the densities of CO_2 from garnet through feldspar to quartz, defining a fluid evolution path which is T-convex. The millimeter-scale density variations among adjacent minerals preclude a common post-metamorphic influx of CO_2, and suggest the distinct geodynamic environment of decompression-related metamorphic uplift (Fig. 2). This is analogous to the T-convex isothermal decompression paths proposed for the charnockites of southern India and Sri Lanka (*cf.* Santosh *et al.*, 1991, *J. Min. Pet. Econ. Geol.*, **86**, 27-44).

One of the major implications of our study pertains to the current debate on the role of fluids in granulite formation. Granulite facies rocks can be generated by a variety of processes such as, vapor-absent metamorphism, extraction of a partial melt leaving an anhydrous residue, and dilution of pore-fluids and resultant lowering of water activity by flushing with externally-derived CO_2-rich fluids (cf. Newton, 1989, *Ann. Rev. Earth Planet.*

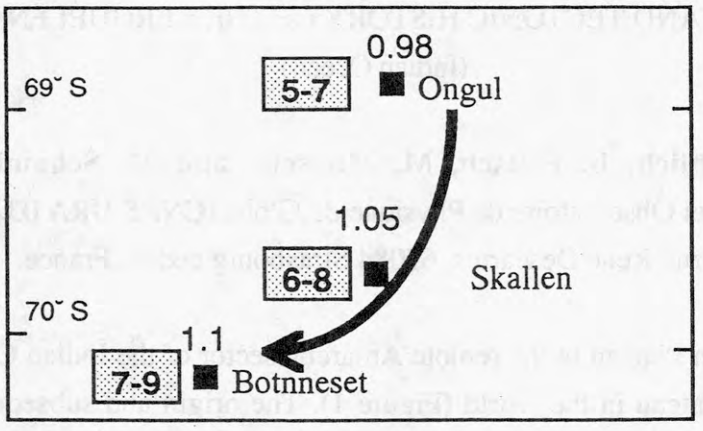

Fig. 1: Mineral phase equilibria pressures (within boxes) and carbonic inclusion densities for charnockitic rocks from Ongul, Skallen and Bottneset areas of the LHB. Note the progressive increase in both values southward.

Sci., **17**, 385-412; Santosh, 1991, *J. Geosci. Osaka City Univ.*, **34**, 1-53). The abundant occurrence of carbonic inclusions trapped within various minerals in the LHB charnockites, the systematic micro-scale density variations among early to late crystallized minerals, and the concommitant increase in density with increasing P-T conditions indicate that the LHB charnockites were derived through "carbonic metamorphism" in the lower crust (*cf.* Newton *et al.*, 1980, *Nature*, **288**, 45-50). A comparison of the present results with those from southern India and Sri Lanka suggests that CO_2 infiltration has been fundamental to the evolutionary history of the East Gondwanian deep crust. This study correlates charnockite formation with degassing of an attenuating continental lithosphere and transfer of CO_2-rich fluids to higher crustal levels through magmatic conduits. We suggest that CO_2 infiltration in the generally fluid-free deep crust might have been triggered by large-scale distensional tectonics in East Gondwana.

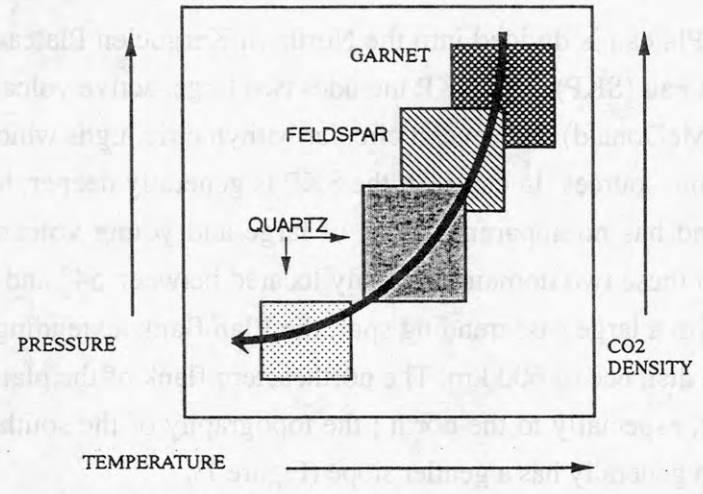

Fig. 2: Density variations in carbonic inclusions trapped within garnet, feldspars and quartz from the LHB area, shown schematically as a function of temperature and pressure. The data indicate a T-convex isothermal uplift history for the terrane.

STRUCTURE AND TECTONIC HISTORY OF THE KERGUELEN PLATEAU
(Indian Ocean)

R. Schlich, B. Fritsch, M. Munschy and M. Schaming
Ecole et Observatoire de Physique du Globe (CNRS URA 0323)
5, rue René Descartes, 67084 Strasbourg cedex, France.

The Kerguelen Plateau in the remote Antarctic sector of the Indian Ocean is one of the largest submerged plateau in the world (Figure 1). The origin and subsequent geologic and tectonic history of this imposing feature have long been a matter of debate and speculation. These outstanding problems were the primary topics addressed by several French and Australian multichannel seismic reflection surveys carried out on the plateau between 1981 and 1991 (cruises MD26, RS02, MD47 and MD67) and by deep sea drilling performed in 1988 by the Ocean Drilling Program (ODP, legs 119 and 120).

The Kerguelen Plateau extends over 2000 km from northwest to southeast between 46° and 64°S and is about 500 km wide over much of its length. The plateau is bounded to the south by the Princess Elizabeth Trough, and is otherwise surrounded by deep ocean basins : the African-Antarctic Basin lies to the west and the Labuan and Australian-Antarctic basins lie to the east (Figure 1). The plateau is situated in a part of the Indian Ocean where magnetic anomalies have not yet been identified and for which the Mesozoic evolution is not well known. Thus, the structure and tectonic history of the Kerguelen Plateau is likely to be important in understanding the evolution of the South Indian Ocean.

The Kerguelen Plateau is divided into the Northern Kerguelen Plateau (NKP) and the Southern Kerguelen Plateau (SKP). The NKP includes two large, active volcanic archipelagos (Kerguelen and Heard-McDonald) and several circular bathymetric highs which may represent additional young volcanic sources. In contrast, the SKP is generally deeper, has a much more subdued topography and has no apparent record of large and young volcanic sources. The transition zone between these two domains, roughly located between 54° and 57°S, exhibits a complex bathymetry with a large east-trending spur, the Elan Bank, extending westward from the main plateau over a distance of 600 km. The northeastern flank of the plateau is extremely steep and almost linear, especially to the north ; the topography of the southwestern flank is more complicated, but it generally has a gentler slope (Figure 1).

Two major sedimentary basins are known to exist on the Kerguelen Plateau ; one lies on the Northern Kerguelen Plateau, southwestward of Kerguelen between Kerguelen and Heard islands and the second, the Raggatt Basin, occupies a large surface on the Southern Kerguelen

Plateau. The average sediment thickness in these basins is about 2500 m with a maximum reaching 3500 m in the Raggatt Basin. All the sedimentary basins are resting upon smooth basement surface, suggesting subaerial erosion before subsequent subsidence and sedimentation. Internal basement reflections characterize most of the plateau. Basement reflections with other geological and geophysical information, indicate that the entire plateau is underlain by volcanic basement, suggesting that both the northern and southern domains have an oceanic origin. Basement areas with no internal reflections are associated mostly with basement ridges ; basement reflector wedges, indicative of volcanic flows, appear on the flank of these ridges (Figure 2). Dredging along the 77°E Graben (cruise MD48) and drilling at sites 738, 747, 749 and 750 (ODP legs 119 and 120) provided for the basement complex an Early Cretaceous age.

Correlation of multichannel seismic reflection profiles with drilling results provide new insight on the evolution and tectonic history of the Kerguelen Plateau. Interpretation of a composite profile, in the Raggatt Basin, between ODP Sites 748, 751 and 750, lead to the following results :

Before or during Albian time (110 Ma) , thick basalt flows formed the Kerguelen Plateau during successive volcanic episodes. As a result of the volcanic activity, basement synforms and basement ridges shaped the plateau. At this time much of the plateau was above sea level (Figure 3A).

Between 110 and 88 Ma, basement was strongly eroded and sediment filled the Raggatt Basin basement synform and covered the eastern basement ridge. Gradual and probably thermal subsidence affected the entire Raggatt Basin. Continental-type sedimentation (K1-K2) prevailed during this time span. At the beginning of the Turonian, the eastern Raggatt Basin was uplifted in association with faulting (Figure 3B). The uplift was followed by subsidence and can be interpreted as the result of extension along a northwest-southeast direction that will give rise to the eastern SKP margin.

After this tectonic event, the eastern part of the SKP subsided and pelagic sediment was deposited, whereas to the west the sedimentation regime remained at shallow water depths (K3). During the Campanian and the Maestrichtian carbonate mounds were developed in the western part of the Raggatt Basin suggesting a very slow subsidence. Later, the basin was uplifted (66 Ma) in association with the north-south tectonic event that formed the 77°E Graben. The western Raggatt Basin represent one of the rift flanks associated with the 77°E Graben (Figure 3C).

During the Paleocene, the western part of the Raggatt Basin subsided rapidly to 1000 m water depths. From the late Paleocene (58 Ma) to about 40 Ma, a slow thermal subsidence affected the entire SKP, which reached a depth of 1000-2000 m (P1). At 54-52 Ma, the sedimentation rate changed abruptly over most of the Raggatt Basin (P2) (Figure 3D).

At 38 Ma, an erosional event was observed on the entire plateau. This event is related to the separation by seafloor spreading of the Kerguelen Plateau-Labuan Basin and Broken Ridge-Diamantina Zone dated at 45-42 Ma. No sediment was deposited in the eastern part of the basin between middle Eocene and middle Pliocene times. In the central and western parts of the basin Oligocene and Miocene (PN1 and NQ1) sediments are present, and two erosional events were observed in the Miocene between 17 and 12 Ma and between 8 and 5 Ma (Figure 3E).

References

Schlich, R., Delteil, J., Moulin, J., Patriat, P., and Guillaume, R., 1971. Mise en évidence d'une sédimentation de marge continentale sur le plateau de Kerguelen-Heard. *C.R. Acad. Sci., Série 2, 272, 2060-2063.*

Houtz, R.E., Hayes, D.E., and Markl, R.G., 1977. Kerguelen Plateau bathymetry, sediment distribution and crustal structure. *Mar. Geol., 25, 95-130.*

Schlich, R., 1982. The Indian Ocean : aseismic ridges, spreading centers and oceanic basins. *In Nairn, A.E.M., and Stehli, F.G. (eds). The Ocean Basins and Margins (Vol. 6) : New York (Plenum), 51-147.*

Wicquart, E., and Fröhlich, F., 1986. La sédimentation sur le plateau de Kerguelen-Heard ; relations avec l'évolution de l'océan Indien au Cénozoïque. *Bull. Soc. Géol. Fr., 8, 569-574.*

Coffin, M.F., Davies, H.L., and Haxby, W.F., 1986. Structure of the Kerguelen Plateau province from SEASAT altimetry and seismic reflection data. *Nature, 324, 134-136.*
Munschy, M., and Schlich, R., 1987. Structure and evolution of the Kerguelen Plateau (Indian Ocean) deduced from seismic stratigraphic studies. *Mar. Geol., 76, 131-152.*

Schlich, R., Coffin, M.F., Munschy, M., Stagg, H.M.J., Li, Z.G., and Revill, K, 1987. Bathymetric chart of the Kerguelen Plateau. *Jointly edited by Bureau of Mineral Resources, Geology and Geophysics, Canberra, Australia, Institut de Physique du Globe, Strasbourg, France, and Territoire des Terres Australes et Antarctiques Françaises, Paris, France.*

Schlich, R., Wise, S.W., et al., 1989. *Proc. ODP, Init. Repts., 120, College Station, TX (Ocean Drilling Program).*

Coffin, M.F., Munschy, M., Colwell, J.B., Schlich, R., Davies, H.L., and Li, Z.G., 1990. Seismic stratigraphy of the Raggatt Basin, Southern Kerguelen Plateau : Tectonic and paleoceanographic implications. *Geol. Soc. Am. Bull., 102, 563-579.*

Schaming, M., and Rotstein, Y., 1990. Basement reflectors in the Kerguelen Plateau, South Indian Ocean : Indications for the structure and early history of the plateau. *Geol. Soc. Am. Bull., 102, 580-592.*

Rotstein, Y., Schaming, M., Schlich, R., and Colwell, J.B., 1990. Basin evolution in oceanic plateaus : Seismic reflection evidence from the Kerguelen Plateau, South Indian Ocean. *Mar. Pet. Geol., 7, 2-12.*

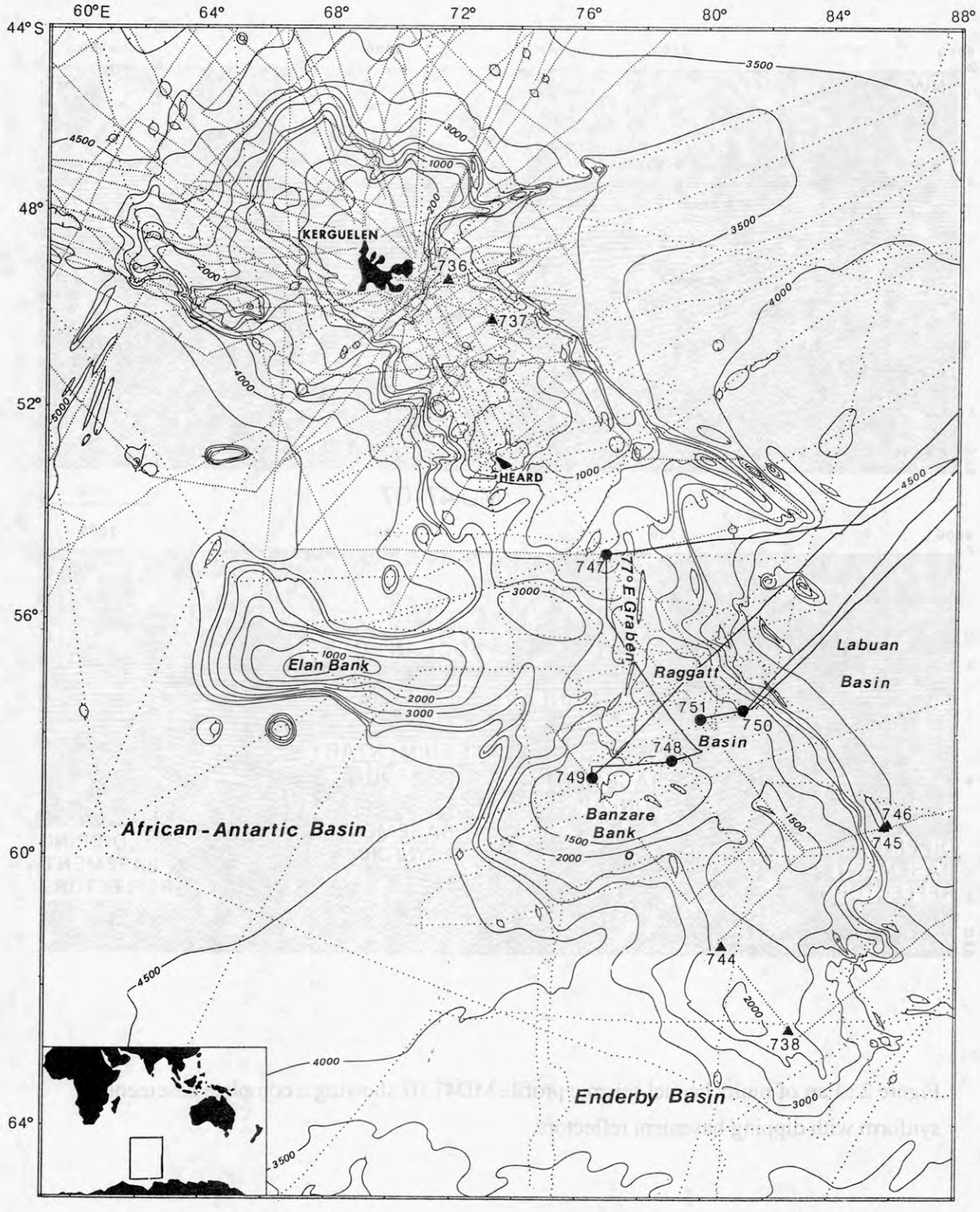

Figure 1 : Bathymetric chart of the Kerguelen Plateau after Schlich et al. (1987). The contour interval is 500 m. Location of Leg 119 (triangles) and Leg 120 (dots) ODP drill sites.

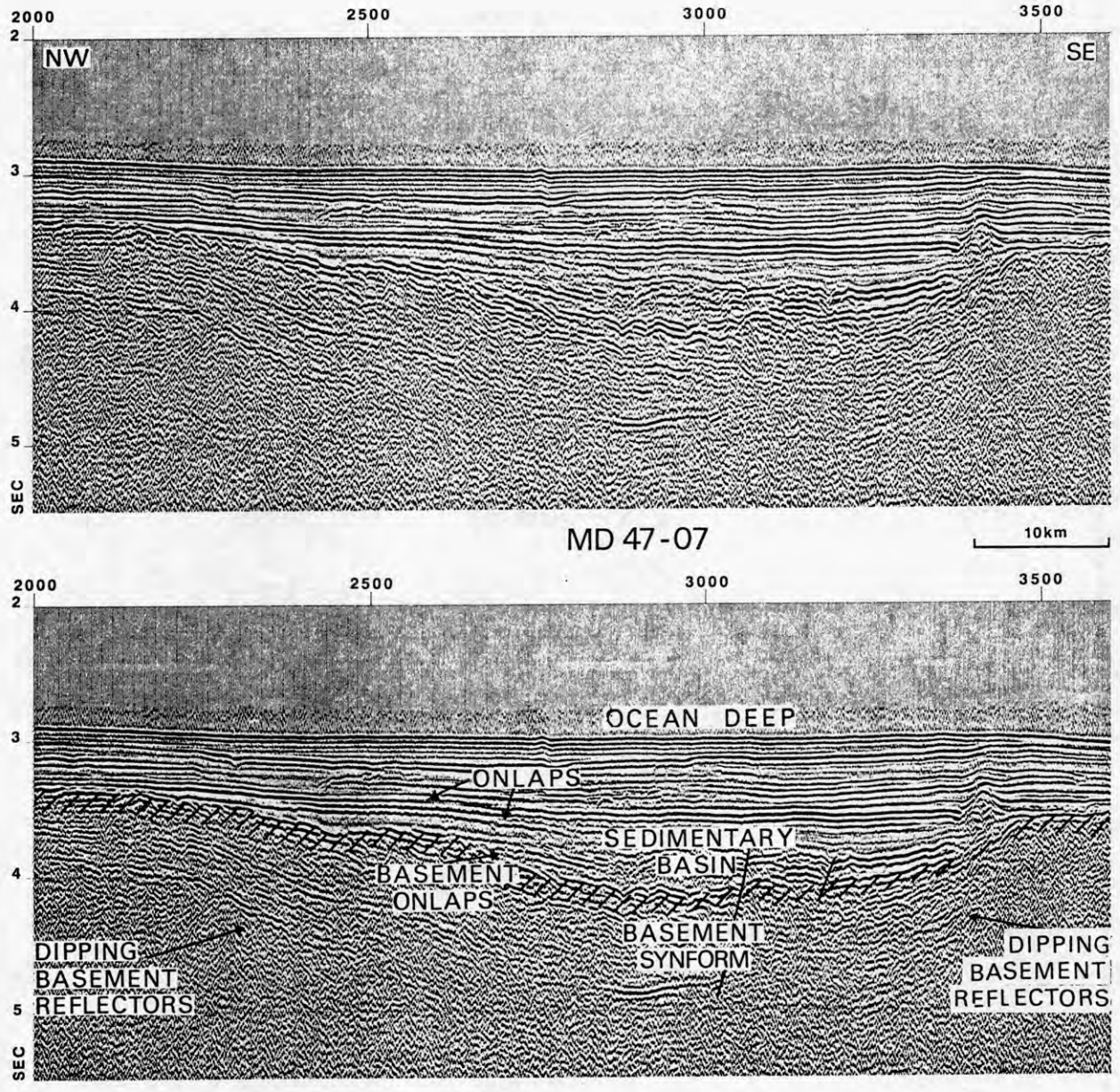

Figure 2 : Part of multichannel seismic profile MD47-07 showing a complete basement synform with dipping basement reflectors.

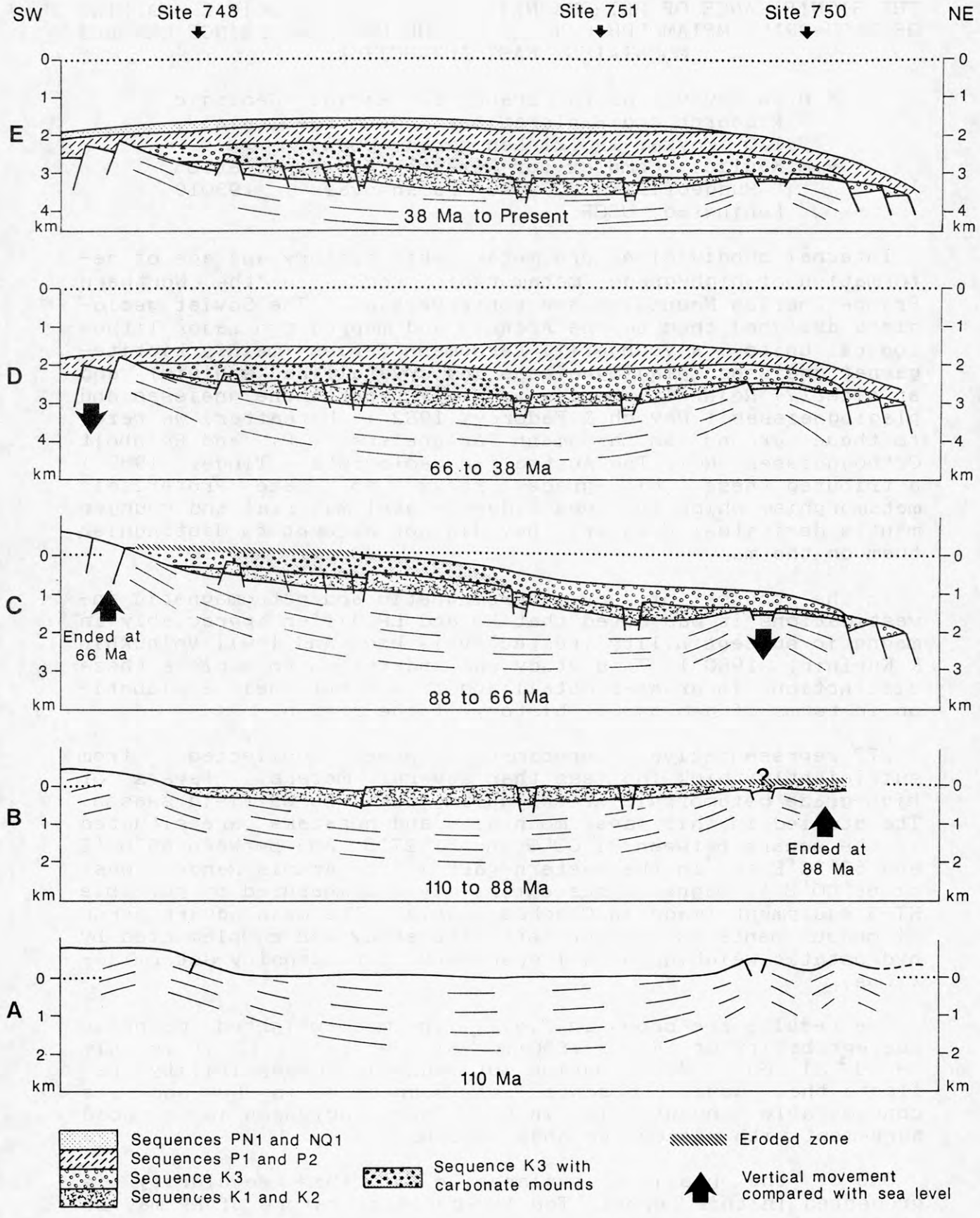

Figure 3 : Schematic representation of the evolution and tectonic history of the Raggatt Basin (Southern Kerguelen Plateau).

THE SIGNIFICANCE OF PETROMAGNETIC DATA FOR GEOLOGICAL MAPPING OF HIGH-GRADE METAMORPHIC ROCKS IN THE NORTHERN PRINCE CHARLES MOUNTAINS, EAST ANTARCTICA

M.B.Sergeyev, North Branch for Marine Geologic Research and Exploration " Sevmorgeologia ", 120 Moyka, 190121 Leningrad, USSR
V.M.Kaulio, Complex for Research and Exploration " Rudgeofizika " , 20 Faiansovaia , 193019 Leningrad, USSR

Internal subdivision, pre-metamorphic history and age of deformation of high-grade metamorphic rocks in the Northern Prince Charles Mountains are controversial. The Soviet geologists assigned them to the Archean and mapped two major lithological units : a younger(?) Larsemann Series (mainly biotite-garnet gneisses, plagiogneisses and crystalline schists) and an older(?) Reinbolt Series (mainly hypersthene gneisses and plagiogneisses)(Ravich & Fedorov, 1982). Hereafter, we refer to these groups as Larsemann Paragneisses (LP) and Reinbolt Orthogneisses (RO). The Australian geologists (Tingey, 1982) attributed these high-grade rocks to late Proterozoic metamorphism which involved older crustal material and younger mantle derivates; however, they did not attempt to distinguish them on the map.

In the course of early aeromagnetic and petromagnetic investigations it was noted that RO and LP differ appreciably in magnetic susceptibility (respectively high and low)(Volnukhin & Kurinin, 1980). This study was undertaken to explore these distinctions in greater detail and to attempt their explanation in terms of geological history of the region.

277 representative specimens were collected from sufficiently thick (no less than several meters) layers of high-grade metamorphic rocks during the 1988-89 field season. The studied in this paper mountains and nunataks are situated in the square between 71° 00′ S and 71° 27′ S and between 65° 00′ E and 67° 30′ E and in the western part of the Aramis Range (west of 66° 00′ E). Magnetic susceptibility was measured by portable KT-5 equipment (made in Czeckoslovakia). The mean square error of measurements is 6.3 per cent. The study was complemented by hydrostatic weighing of all specimens for density determinations.

The results are shown in Fig.1. The mean-weighted magnetic susceptibility of RO is $1850 \cdot 10^{-5}$ SI, while for LP it is only $69 \cdot 10^{-5}$ SI. Such distribution of magnetic susceptibility reflects the usual absence of magnetite in LP and its considerable concentration in RO. This conclusion is in good agreement with microscope observations.

One of the possible explanation of this regularity is presented in this report. The low-magnetic nature of LP may be explaned by their supracrustal origin. Magnetite is unstable in low-grade environment and with rare exceptions is not preserved at early stages of metamorphic alteration of supra-

crustal (sedimentary and volcanic) rocks. Increase in metamorphic grade, as a rule, is not accompanied by regeneration of magnetite, therefore high-grade supracrustal complexes generally must remain void of this mineral, although the later crystallization of magnetite in the high-grade supracrustal rocks is possible as a result of some ultrametamorphic and retrograde processes. Nevertheless, such crystallization of magnetite in LP took place only localy and therefore the LP generally are low-magnetic.

On the contrary, RO, as a rule, are high-magnetic and, on our opinion, it is in agreement with the supposition of their plutonic origin. It is necessary to note, that plutonic rocks may be primarely void of magnetite. In this case orthometamorphic rocks also generally must be void of magnetite. But if primary plutonic rocks content the considerable amount of this mineral, it must be preserved under high-grade conditions, because magnetite is stable in this environment. In this case, orthometamorphic rocks must be high-magnetic and, probably, it may be the explanation of high magnetic susceptibility of RO.

C o n c l u s i o n s :

- the existence in a high-grade metamorphic terrain of the Northern Prince Charles Mountains of lithologically distinct RO and LP is confirmed by differences in their magnetic susceptibility ;
-a high magnetic susceptibility of RO indicates their deep-seated plutonic origination ;
-a low magnetic susceptibility of LP is best explained in terms of their supracrustal derivation ;
-in our opinion, these data are more consistent with interpretation suggested by Australian geologists and imply that RO may represent mantle derivates, while LP represent relatively older reworked crustal rocks ;
-a strong distinction in magnetic susceptibility between RO and LP may be used for geological mapping of high-grade terrain in the Northern Prince Charles Mountains, including implementation of aeromagnetic survey.

REFERENCES

RAVICH M.G. & FEDOROV L.V. Geologic evolution of MacRobertson Land and Princess Elizabeth Land, East Antarctica.-in: Antarctic Geoscience., ed. by C.Craddock, The University of Wisconsin Press, Madison, 1982, pp. 499-504.

TINGEY R.J. The geologic evolution of the Prince Charles Mountains - an Antarctic Archean cratonic block.-in: Antarctic Geoscience., ed. by C.Craddock, The University of Wisconsin Press, Madison, 1982, pp. 455-464.

VOLNUKHIN V.S. & KURININ R.G. The physical properties of rocks of Lambert Glacier region. - in: Geophysical studies in Antarctica., NIIGA, Leningrad, 1980, pp. 52-58. (IN RUSSIAN : Fizicheskie svoistva gornih porod raiona lednika Lamberta.-in: Geofizicheskie issledovania v Antarktide).

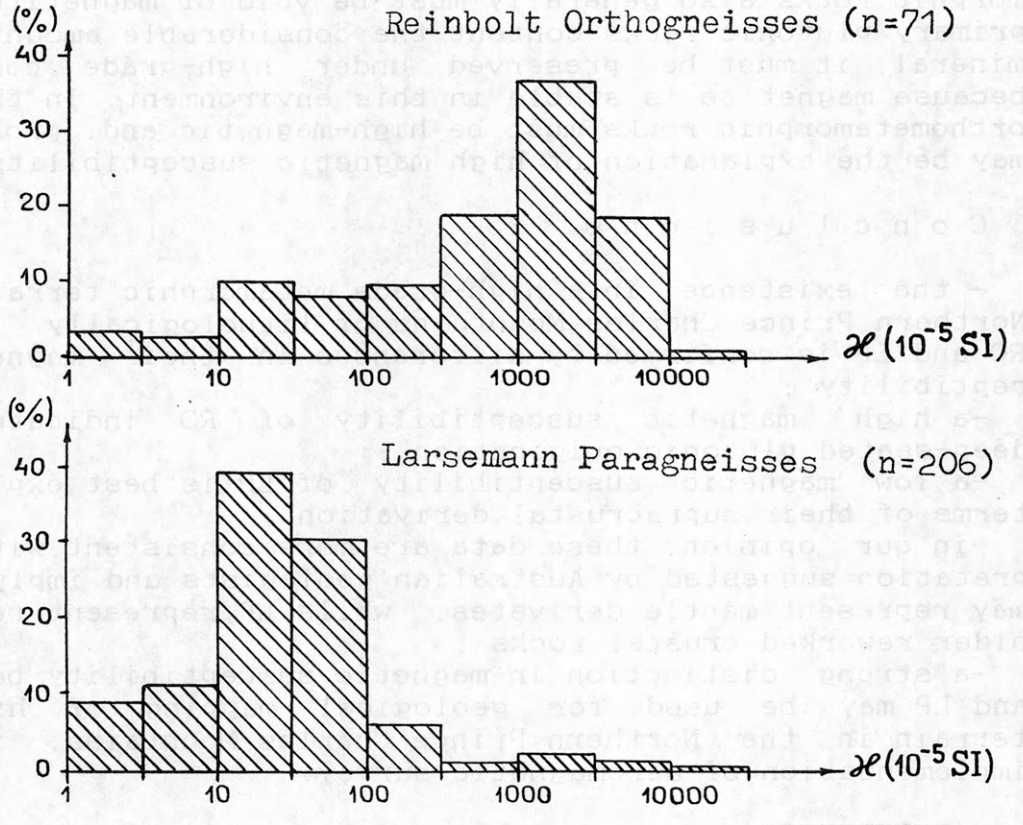

Fig. 1. Histograms of magnetic susceptibility of high-grade rocks collected during 1988-89 field season.

A Non-Marine Late Cretaceous Deposit -- Three Half Point Formation From King George Island, Antarctica

Shen Yanbin, Nanjing Institute of Geology and Paleontology, Academia Sinica, Nanjing, Chi-Ming-Ssu, 210008, China

A New lithostratigraphic unit -- Half Three Point Formation is defined on an inlet (62°13' 40" S, 58°59' 01" W) near Half Three Point of Fildes Peninsula of King George Island, South Shetland Islands. The sedimentary rocks cropped out consist of finely laminated dark-greyish tuffites, tuffaceous siltstones and mudstones containing pyrite and siderite. The formation is about 5.5 m and traceable laterally for approximately 30 m, being inundated by sea at both ends. It contacts with underlying Palaeocene agglomerates by fault and is unconformably overlain by Eocene andesitic lavas.

About 38 fungal spores, more than 40 forms of land-flora sporopollen and some megaflora were found from the formation. The palynomorph assemblage is of Late Cretaceous age (Campanian-Maastrichtian). The isochron age of tuffites by Rb-Sr whole-rock method is 70.4±1.93 Ma.

The calcite of sand-sized tuffites formed by calcitization during early diagenesis exhibits very light $\delta^{18}C$ values of -26.246%, PDB, and $\delta^{13}C$ values of -5.130 to 5.631%, PDB, which suggest that the calcitization is related to thermal freshwater originally. Tuffaceous mudstones contain lower B content of 48.4 ppm corresponding with that of lacustrine mudstones. Low $^{87}Sr/^{86}Sr$ ratio (0.703189-0.703320) indicates the tuffites being of continental origin.

Therefore, the formation might represent a lacustrine a deposit under low energy and reducing condition. The palynoflora indicated a humid and warm climate in this area.

Upper Cretaceous volcanic rocks so far determined on South Shetland Islands are only reported in Admiralty Bay, King George Island. These consist of basaltic lavas and andesitic lavas intercalated with few fossil leaves and woods, but no freshwater sediments. However, the finding of non-marine Late Cretaceous deposits is very significant to recognize the palaeogeography and palaeoclimatology on the west margin of magmatic arc in Antarctic Peninsula.

A REVIEW OF SATELLITE AND FIELD GEODETIC STUDIES IN THE JAPANESE ANTARCTIC RESEARCH AREA

K. Shibuya, National Institute of Polar Research,
Kaga 1-9-10, Itabashi-ku, Tokyo 173, Japan

Antarctic geodesy has become more important and more comprehensive for the research fields of oceanography, meteorology and glaciology. We have therefore conducted satellite and field geodetic studies with special application to Antarctic research in order to overcome some existing difficulty in the observation or in the data analysis. The following summarizes the results of each study.

1. Determination of geoid height at Breid Bay, East Antarctica

Any existing geopotential models suffer from the sparse coverage and small number of gravity and satellite geodesy ground data in and around Antarctica. We determined geoid height at the marginal ice zone of Breid Bay (70° 12'S, 23° 47'E) by the combined observation of TRANSIT positioning, GPS relative positioning and ocean tide observation. The plan of observation is schematically illustrated in Figure 1.

The estimated ground data of geoid height is 16.6 m above the WGS84 Earth Elliposoid. The TRANSIT positioning gave the ellipsoidal height at L0 point on the grounded ice sheet of Breid Bay to an accuracy of +- 4 m from the accepted 95 broadcast NNSS satellite passes. GPS relative positioning was made between L0 point and the deck of the Icebreaker "SHIRASE" (S point). The height difference between L0 point and S point is determined to an accuracy of +- 0.3 m from the analysis of 15 minutes' carrier phase data from 4 Space Vehicles by the doubly differenced phase method. The recording of sea level variation was made using the sea bottom pressure-transducer water level recorder for 4 days, together with monitoring of ship's attitude and meteorological data. The separation of S point from the local mean sea level is determined to an accuracy of +- 0.4 m. The standard deviation of the obtained geoid height can thus be considered as $\sqrt{4^2 + 0.3^2 + 0.4^2} \sim +-4$ m.

The obtained geoid height at S point is 3.4 m smaller than the WGS84 model geoid (18 order truncation), and 8 m smaller than the OSU-86D geoid of 250 order harmonics.

The method we applied here is operationally simple and appropriate for dense installation of geoid height control stations along the circum Antarctic coastal zone. More detailed discussion will be found in Shibuya et al. [1991].

2. Crustal Magnetic Anomalies by MAGSAT

Crustal magnetic anomalies in the Antarctic region are studied with the MAGSAT CHRONFIN data of 1790 passes [Takenaka et al., 1991].

GSFC(12/83) model was used to reduce the earth's core field to estimate the residual magnetic field. The obtained residual intensity data in the geomagnetic coordinates are averaged over 1 hour magnetic local time (MLT) and 1° invariant latitude, then grouped by taking the planetary magnetic activity index (K_p) as a parameter, to derive the Mean Polar Disturbance Fields (MPDFs).

The obtained MPDF for $K_p = 2_0$, for example, amounts to 50 nT at 85° S and decreases monotonically toward lower latitudes on the

dawnside. On the duskside, the MPDF takes a small value of 10 nT at 85° S, decreases to a negative peak of -30 nT at 78° S, recovers to a smaller positive peak of 20 nT at 62° S, and then decreases to zero at further lower latitudes. These characteristic features of the MPDF are attributable to the external fields produced by S_q^P currents with occasional eastward electrojet in the ionosphere and the magnetic field due to the westward ring current in the magnetosphere.

The MPDFs for K_p values from 0_0 to 2_0 were subtracted from the residual intensity data, and the resultant data were averaged for 3° by 3° in latitudes and longitudes to obtain crustal magnetic anomalies at a mean altitude of 450 km.

The obtained anomaly contours (Figure 2; 2 nT interval) in the oceanic area are negative for abyssal plains, while they are positive for ridges and plateaus. The tectonically active Scotia Sea microplate region is associated with negative anomalies. Land areas of Antarctica are characterized by three positive anomalies over Enderby Land, Gamburtsev Subglacial Mountains and Wilkes Land. Negative land anomalies are also definitely related to geologic provinces such as Queen Maud Land, Queen Mary Land, etc.

As compared with the crustal magnetic anomalies by the pass-by-pass correction method [Ritzwoller and Bentley, 1983], our MPDF correction results retain long-wavelength (~500 km) anomaly patterns with an enhanced correlation among the neighboring anomalies and show a clear correspondence to geologic provinces.

3. Tidal gravity observation at Asuka and Syowa Stations

Tidal gravity observations were made at Syowa and Asuka Stations in 1987. LaCoste & Romberg type G gravity meters with electrostatic feedback amplifiers were used. The feedback voltage outputs were recorded every 30 minutes for both stations. The selected data cover 2976 points from April 1 to June 1 for Syowa Station, and 8656 points from June 3 to November 30 for Asuka Station.

The obtained tidal gravity data were analyzed by using the 'BAYTAP-G' program [Ishiguro et al., 1983]. Oceanic tidal loading effects were corrected for by using the 'GOTIC' program [Sato and Hanada, 1984]. The δ factors corrected for oceanic tidal loading effects distribute from 1.130 (K_1) to 1.250 (M_2) for Syowa Station, and from 1.134 (P_1) to 1.330 (K_2) for Asuka Station.

The results for tidal components O_1, P_1, M_2 and S_2 are presented in Figure 3. For diurnal tides, there is no significant difference between the observed δ factors and the statistically deduced latitudinal dependence by Melchior and De Becker [1983]. For semi-diurnal tides, however, the observed factors at both stations are larger than the Wahr's theoretical predictions [1981] by 10-14%.

Since shorter period constituents (semi-diurnal tides), which reflect shallower crustal structures, deviated from the theoretical δ factors to more positive values as compared with longer period constituents (diurnal tides), the easily deformable ice sheet may have played an important role in the observed large δ factors of semi-diurnal tides in the Antarctic region. The larger admittance of gravity change for atomospheric pressure at Asuka Station (-0.27 μgal/mb) than that in mid-latitude observations (-0.35~-0.37 μgal/mb) may also be explained by easy loading deformation of the ice sheet by air mass for an extent of

30 km covering the site.
More detailed discussion is given in Ogawa et al. [1991].

References

Drewry, D. J. (ed.) (1983): The bedrock surface of Antarctica, in Antarctica; Glaciological and Geophysical Folio. Cambridge, Scott Polar Res. Inst., Sheet 3.

Grikurov, G. E. (1979): Geological World Atlas (1/10000000), Antarctica, ed. by Commission for the geological map of the world, International Geological Mapping Bureau, Paris, C. G. M. W.-Unesco, Sheet 17.

Ishiguro, M., Akaike, H., Ooe, M. and Nakai, S. (1983): A Bayesian approach to the analysis of earth tides, in Proc. 9-th Int. Symp. Earth Tides, ed. J. T. Kuo, 283-292, E. Schweizerbartische Verlagsbuchhandlung, Stuttgart.

Melchior, P. and De Becker, M. (1983): A discussion of world-wide measurements of tidal gravity with respect to oceanic interactions, lithosphere heterogeneities, Earth's flattening and inertial forces, Phys. Earth Planet. Inter., 31, 27-53.

Ogawa, F., Fukuda, Y., Akamatsu, J. and Shibuya, K. (1991): Analysis of tidal variation of gravity at Syowa and Asuka Stations, Antarctica, J. Geodet. Soc. Japan, 37, 13-30, (in Japanese).

Ritzwoller, M. H. and Bentley, C. R. (1983): Magnetic anomalies over Antarctica measured from Magsat, in Antarctic Earth Science by R. L. Oliver et al. (eds.), 504-507, Cambridge Univ. Press, Cambridge.

Sato, T. and Hanada, H. (1984): A program for the computation of oceanic tidal loading effects 'GOTIC', Pub. Int. Lat. Obs. Mizusawa, 18, 29-47.

Segawa, J., Matsumoto, T. and Kaminuma, K. (1984): Brief topography in Antarctic region for reference for gravity anomaly chart, Appendix for Antarctic Special Map Series, No. 3, Natl Inst. Polar Res., Tokyo.

Shibuya, K., Fukuda, Y. and Michida, Y. (1991): Determination of geoid height at Breid Bay, East Antarctica, Submitted to J. Geophys. Res.

Takenaka, J., Yanagisawa, M., Fujii, R. and Shibuya, K. (1991): Crustal magnetic anomalies in the Antarctic region detected by MAGSAT, J. Geomag. Geoelectri., 43, No. 6, accepted for publication.

Wahr, J. M. (1981): Body tides on elliptical, rotating, elastic and oceanless earth, Geophys. J. R. astr. Soc., 64, 677-703.

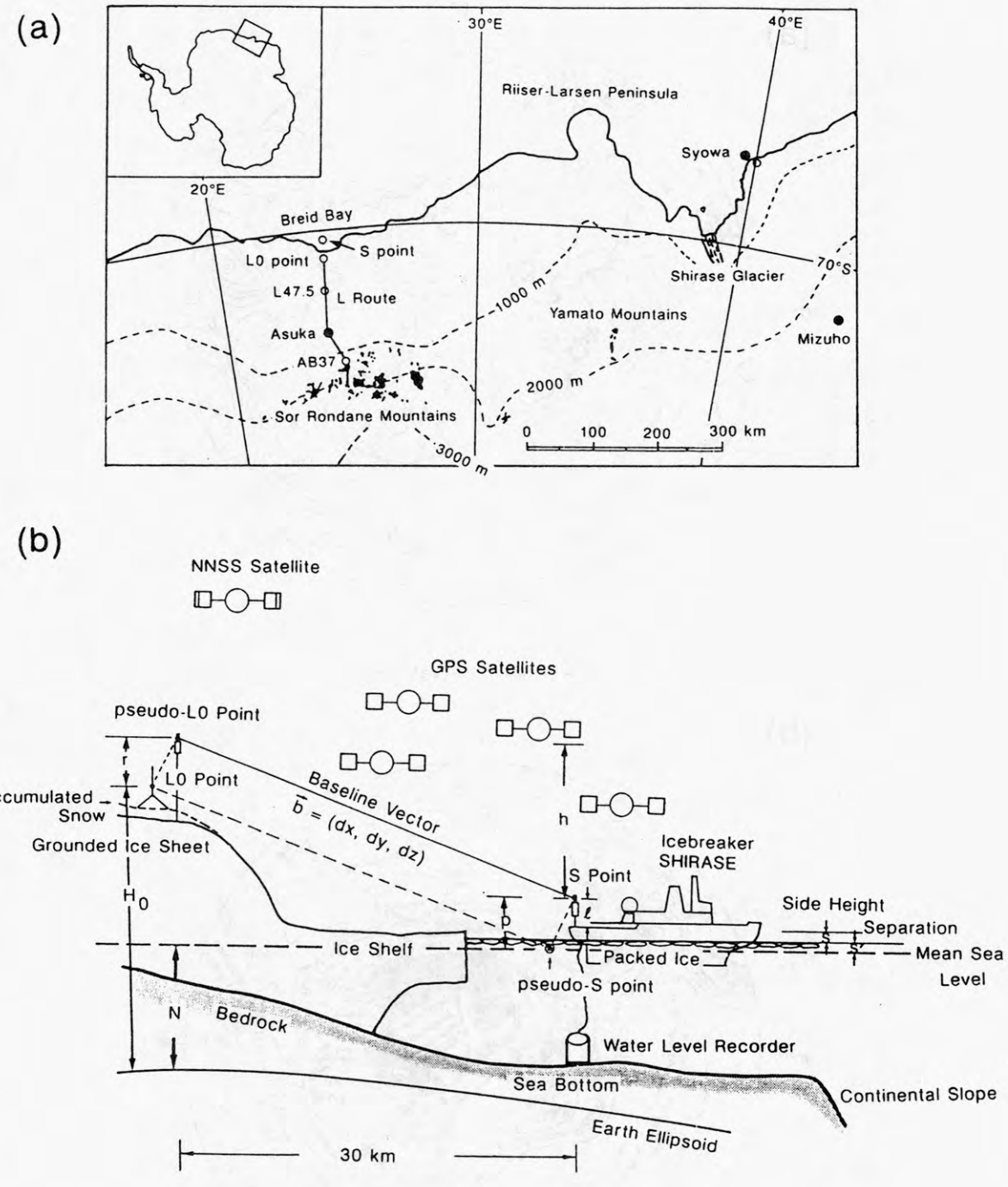

Figure 1

(a) Upper part shows research area by the Japanese Antarctic Research Expedition (JARE). The experiment was made in Breid Bay. (b) Lower part shows principle of geoid height determination. TRANSIT positioning was made at L0 point, which gave us ellipsoidal height H_0. GPS relative positioning between pseudo-L0 point and S point on the deck of "Shirase" gave us height difference h between the two points. Monitoring of sea level was made using the water level recorder, which gave us local mean sea level and consequently separation of S point p at a time of GPS relative positioning. Geoid height N_0 can be estimated using the above observed values.

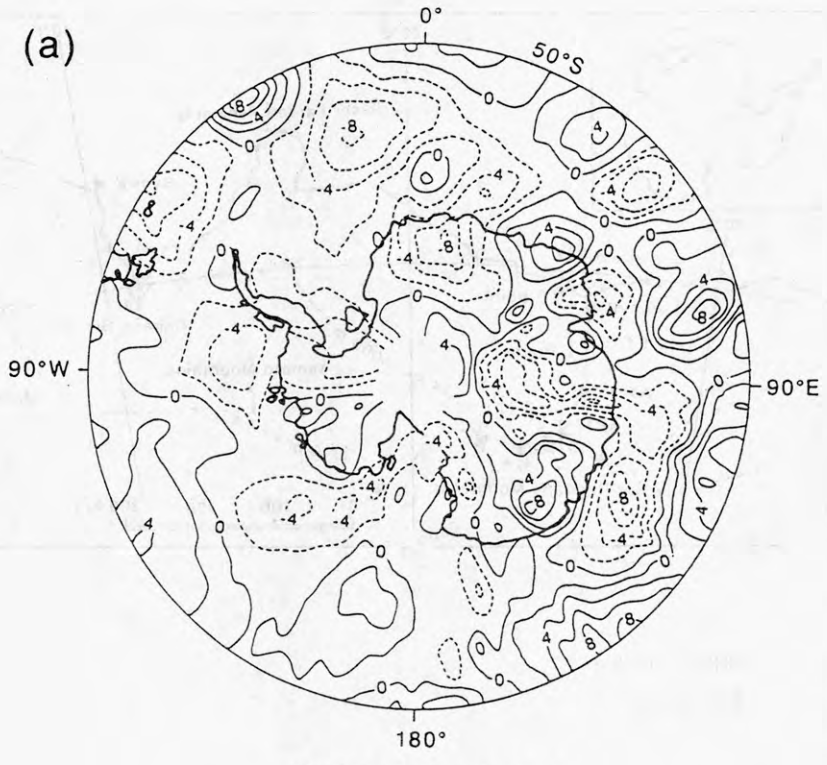

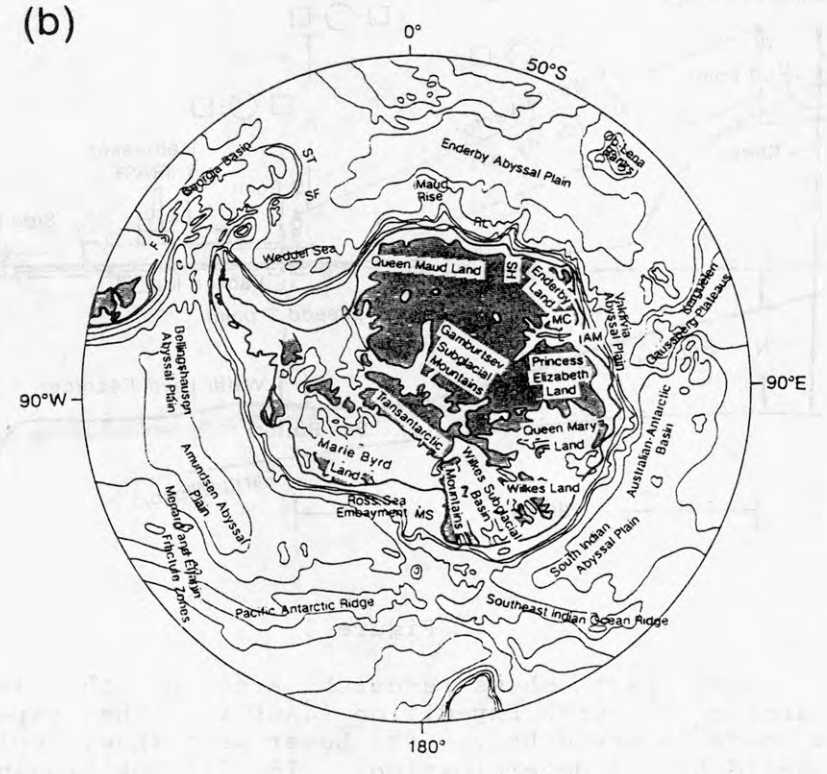

Figure 2.

(a) Crustal magnetic anomalies in the Antarctic region to the south of 50° S. Solid contours indicate positive, while broken contours indicate negative. (b) For comparison, simplified topography is illustrated by referring to Grikurov [1979], Segawa et al. [1984] and Drewry [1983]. Hatched area shows bedrock region with elevation above sea level. Bathymetric contours are drawn with 1000 m intervals.

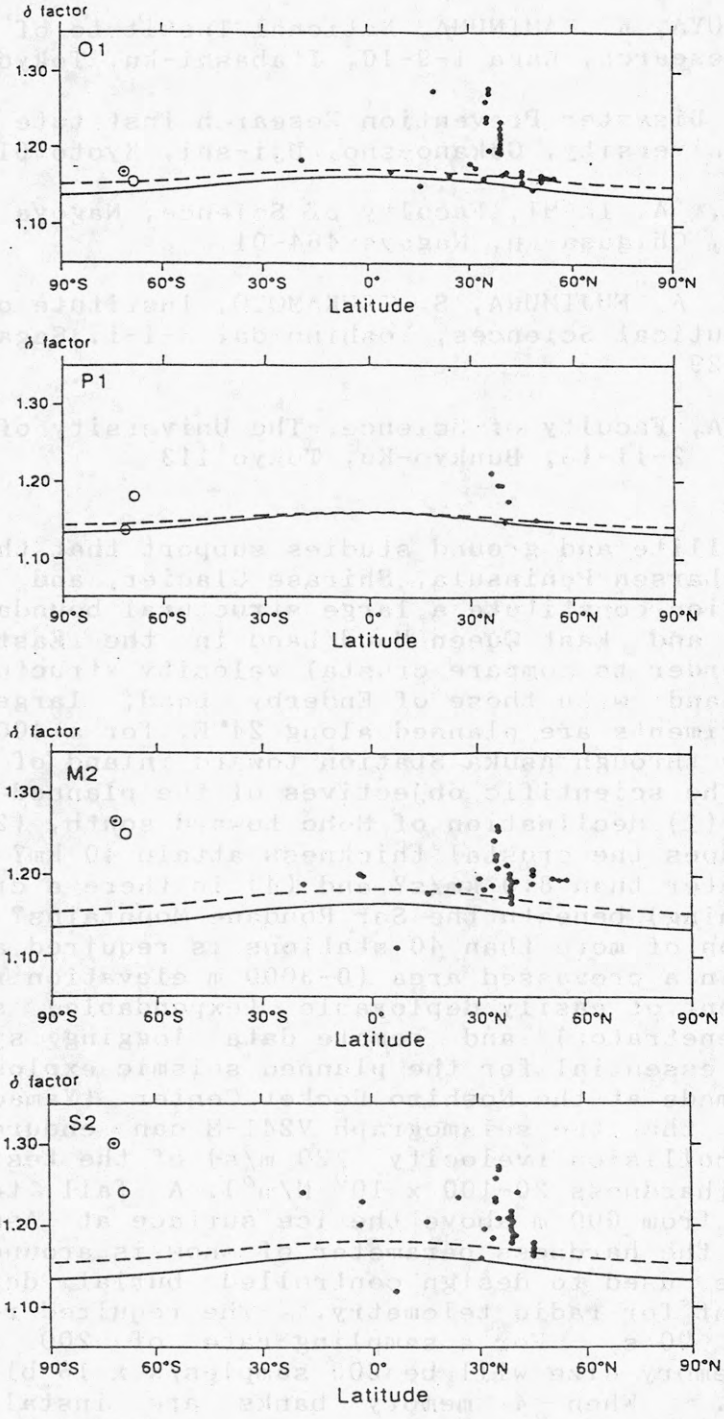

Figure 3.

The obtained δ factors for Asuka Station (dot circle) and Syowa Station (open circle). They are corrected for ocean load effects. Small solid circles indicate similar observed δ factors outside Antarctica. Solid and dashed curves, respectively, indicate theoretical latitudinal dependence by Wahr [1981] and statistically obtained latitudinal dependence by Melchior and De Becker [1983]. From top to bottom shows O_1, P_1, M_2 and S_2, respectively.

USE OF A PENETRATOR FOR PLANNED EXPLOSION SEISMIC EXPERIMENTS IN EAST QUEEN MAUD LAND

K. SHIBUYA, K. KAMINUMA, National Institute of Polar Research, Kaga 1-9-10, Itabashi-ku, Tokyo 173

K. ITO, Disaster Prevention Research Institute Kyoto University, Gokano-sho, Uji-shi, Kyoto 611

I. YAMADA, A. IKAMI, Faculty of Science, Nagoya University Furo-chyo, Chigusa-ku, Nagoya 464-01

H. MIZUTANI, A. FUJIMURA, S. TSUKAMOTO, Institute of Space and Astronautical Sciences, Yoshino-dai 3-1-1, Sagamihara-shi, Kanagawa 229

T. KANAZAWA, Faculty of Science, The University of Tokyo Yayoi-chyo 2-11-16, Bunkyo-Ku, Tokyo 113

Recent satellite and ground studies support that the Gunneras Bank, Riiser-Larsen Peninsula, Shirase Glacier, and the Yamato Mountains region constitute a large structural boundary between Enderby Land and East Queen Maud Land in the East Antarctic shield. In order to compare crustal velocity structures of East Queen Maud Land with those of Enderby Land, large explosion seismic experiments are planned along 24° E, for a 400 km profile from Breid Bay through Asuka Station toward inland of the Nansen Ice Field. The scientific objectives of the planned explosions are to detect (1) declination of Moho toward south, (2) where on the profile does the crustal thickness attain 40 km? (3) is Pn velocity greater than 8.0 km/s? and (4) is there a crustal root (local thickening) beneath the Sor Rondane Mountains?

Installation of more than 40 stations is required at intervals of 5-10 km in a crevassed area (0-3000 m elevation range), and the development of easily deployable (expendable) seismographs (Antarctic penetrator) and remote data logging system on a helicopter is essential for the planned seismic explosions. The shock test made at the Noshiro Rocket Center (Yamada et al., 1990) proved that the seismograph V241-M can endure +-5000 G shock by the collision (velocity ~220 m/s) of the test penetrator into sands (hardness 20-100 x 10^5 N/m^2). A fall test of the dummy loads from 600 m above the ice surface at Asuka Station showed that the hardness parameter of snow is around s = 8.3, which can be used to design controlled burial depth of the antenna element for radio telemetry. The required record length per shot is 90 s. For a sampling rate of 200 samples per second, the memory size will be 200 samples/s x 16 bits/s x 90 s = 288 Kbits. When 4 memory banks are installed in the penetrator, all the data for transmission is 288 Kbits x 4 = 1152 Kbits, which, by a transfer rate of 8 Kbits/s, can be transferred to the data acquisition system on the helicopter in 1152 Kbits ÷ 8 Kbits/s = 144 s ~ 2.5 min.

Detailed design of commands and data formats for radio-telemetory is now being made and some discussion is given in Shibuya et al. (1991).

References

Shibuya, K., Kaminuma, K., Mizutani, H., Fujimura, A., Tsukamoto, S., Yamada, I., Ito, K., Kanazawa, T., Takasaki, M. and Iga, A. (1991): Status report for the development of the Antarctic penetrator (No. 1, 1989-year program), Nankyoku Shiryo (Antarct. Rec.), 35, 92-117 (in Japanese).

Yamada, Y., Fujimura, A., Takagi, Y., Tsukamoto, S., Hirayama, S., Tanaka, S., Kusaba, M., Araki, H., Honda, R. and Mizutani, H. (1990): Penetrator onboard sensors in Fifth Report on Penetrator Shock Test ed. by ISAS SES Data Center, pp34-74, Inst. Space Astro. Sci., Sagamihara-shi.

Sm-Nd AND Rb-Sr AGES OF METAMORPHIC ROCKS FROM THE SØR RONDANE MOUNTAINS, EAST ANTARCTICA

K. Shiraishi, National Institute of Polar Research, Kaga, Itabashi-ku, Tokyo 173, Japan.
H. Kagami, Institute for Study of Earth's Interior, Okayama University, Misasa, Tohaku-gun, Tottori 682-02, Japan.

The Sør Rondane Mountains (71.5°-72.5°S, 22°-28°E) are underlain by medium- to high-grade metamorphic rocks, and plutonic rocks and minor dike rocks of diverse compositions (Shiraishi et al., 1991). Most of available geochronological data indicate an intense thermal event which are assigned to the plutonic activities in the early Paleozoic (eg. Picciotto, 1964). The oldest age, 2700 Ma was determined by U-Pb on detrital zircon from gneisses, but, the age of the main phase of the regional metamorphism remained uncertain (Pasteels and Michot, 1970). The aim of this study is to determine the ages of protoliths, of the main phase of the granulite facies metamorphism, and of succeeding tectonothermal events that affected the metamorphic rocks in the Sør Rondane Mountains. A preliminary report on these results was made by Shiraishi and Kagami (1989).

Description of the samples

The metamorphic rocks in the northern and eastern parts of the Sør Rondane are composed of pelitic to semipelitic gneisses and intermediate gneisses that may be derived from igneous rocks and mixtures of sedimentary and volcanic rocks. Thin layers and lenses of calcareous and basic rocks occur in many places. Tonalite associated with mylonitic schists of basic, semipelitic and calcareous compositions occupies in the southwestern part.

In the central and eastern parts of the mountains, orthopyroxene-bearing granulite facies mineral assemblages occur not only in the basic to intermediate gneisses, but also in acidic charnockitic gneisses. However, metamorphic zonation in the mountains has not been established. Sillimanite-bearing pelitic gneisses in the eastern Sør Rondane contain relict kyanite, suggesting the metamorphic facies series of medium-pressure type (Grew et al., 1989). Physical conditions of the peak granulite facies metamorphism of the analysed gneisses were estimated by Shiraishi and Kojima (1987) to be 800°C and 7-8.5kb based on geothermo-barometries. The metamorphic rocks show retrograde effects from plutonic intrusions and mylonitization for example retrograde kyanite in sillimanite-bearing pelitic gneiss (Asami and Shiraishi, 1987). Plutonic rocks are widespread throughout the Sør Rondane. Sakiyama et al. (1988) divided the plutonic activity into two stages based on the mutual intrusive relations and timing relative to the regional mylonitization. Previous geochronological work have established that the younger intrusives are early Paleozoic (Shiraishi et al., 1991).

Sampling For Nd and Sr isotopic studies, 10 whole-rock samples were selected from the northwestern part of Brattnipene in the central Sør Rondane Mountains. They were collected in a cliff 200 m high, which is predominantly composed of the enderbitic (tonalitic) gneisses with thin layers of mafic granulite. Conspicuous granite-pegmatite dykes intrusive into the enderbitic gneisses have retrograded them with no disturbance of foliation. The retrograde gneisses are bleached to light gray. The bleached zones are up to a few meters wide. Four enderbitic gneisses (1503B, 1503D, 1602D, 2502A) and two mafic granulites which are boudinaged interlayers 20 cm wide (1503C, 2502B), were collected from a single outcrop a few meters across. The analysed retrograde gneisses

include weakly foliated (1602A) and well-foliated gneisses (1602B, 1601C) and a mafic layer of 10 cm wide (1601A). Two of them (1602A, 1602B) crop out 50 m above the enderbitic gneisses sampling point. The other two retrograde gneisses (1601A, 1601C) were collected about 300 m distant in a direction subparallel to the strike, where a pegmatite dike of one meter wide occurs.

Petrography Mineral assemblages of the samples are given in Table 1. Mineral chemistry and geothrmo-barometry of the enderbitic gneisses were given by Shiraishi and Kojima (1987). The enderbitic gneisses are dark-colored medium- to coarse-grained rocks which partly show distinct foliation by elongated quartz grains and aggregates of mafic minerals. The gneisses commonly contain two pyroxenes and are up to 40 volume % quartz except for a mafic granulite. The dark-color is largely due to quartz and plagioclase. Brownish pargasitic hornblende is the dominant mafic mineral. Reddish brown biotite contains up to 4.4 wt. TiO_2 %. 1503D is the most quartzose gneiss and contains a trace amount of garnet (Mg/(Mg+Fe)=0.16). Mineral assemblages and chemistry retain granulite facies characteristics, but are overprinted by retrograde textures: yellowish brown biotite associated with quartz replaces a part of orthopyroxene, and greenish hornblende occurs along cracks in clinopyroxene.

The retrograde gneisses show intense retrograde textures. Hornblende usually shows strong color zoning; brownish green in the inner part and pale green to bluish green in the outer part. Some green hornblende with plagioclase form symplectitic pseudomorphs of orthopyroxene. Spherulitic aggregates of yellowish brown biotite occurs in addition to brown biotite forming the main foliation. Moreover, 1601C contains cummingtonite which is surrounded by pseudomorphic fine aggregates of bluish green tschermakitic hornblende and quartz. 1602B contains fine cummingtonite which is surrounded by bluish-green tschermakitic hornblende and fine epidote with quartz at the fringe of hornblende. These textures suggest the following hydration reactions (Mineral abbreviations after Kretz, 1983):

$Opx + Qtz + H_2O = Cum.$

$Cum + An + H_2O = Tsch + Qtz$

$Cam + An + H_2O = Ep + Qtz.$

Bulk chemical composition Chemical compositions of the eight samples including trace elements and REE have been analysed. There is no significant difference in major and trace elements composition for the non-retrograde and retrograde gneisses, thaving similar SiO_2 contents. It is noteworthy that Rb is low relative to K (K/Rb = 952-2991) and to Sr (Rb/Sr = 0.006-0.23). U and Th are also low. All chondrite-normalized REE patterns except for 1601A show relatively smooth and moderately fractionated patterns. However, spidergrams for incompatible element abundances in the retrograde gneisses are irregular relative to those for the non-retrograde enderbitic gneisses.

Isotopic data

Mass spectrometric analyses were made using a MAT261 mass spectrometer at Okayama University. $^{87}Sr/^{86}Sr$ ratios were normalized to $^{86}Sr/^{88}Sr=0.1194$ and $^{143}Nd/^{144}Nd$ ratios were normalized to $^{146}Nd/^{144}Nd=0.7219$.

Rb-Sr Data Rb-Sr isotopic data are given in Table 1 and plotted in Figs. 2 and 3. The $^{87}Rb/^{86}Sr$ ratios for all whole-rock samples are low and no meaningful isochron can be drawn due to the considerable scattering of the data. Four enderbitic gneisses and two mafic granulites, however, define an isochron of 978±52 Ma with initial ratio 0.70426 These rocks were collected within a few meters of each other. Among the four retrograde gneisses, two pairs occur adjacent to each other: 1601A occurs as a mafic layer in the gneiss (1601C) and 1602B is a well-foliated gneiss adjacent to the weakly foliated gneiss

(1602A). In Fig. 1, neither pair makes a meaningful isochron. Taking the mode of occurrence, petrographic and chemical characters into account, it is suggested that Rb-Sr isotopic compositions of the retrograde gneisses were disturbed by the retrogression. Deviation of six enderbitic gneisses plots from the isochron could also have resulted from later isotopic disturbance since these gneisses are also slightly altered to form retrograde minerals.

The internal mineral isochron for an enderbitic gneiss (1503D) yields 489±30 Ma with an initial ratio 0.70536 (Fig 2). However, biotite controls the age. The isochron age recalculated without biotite data is 556±26 Ma with an initial ratio 0.70510 and the age recalculated without hornblende data is 483±12 Ma with an initial ratio 0.70520.

Sm-Nd Data Sm-Nd isotopic data are given in Table 2 and plotted in Fig. 3. Sm and Nd contents of biotite and hornblende are very high realative to the commonly known values for these minerals possibly due to inclusion of accessory minerals such as apatite. The $^{143}Nd/^{144}Nd$ vs. $^{147}Sm/^{144}Nd$ ratios for all eight whole-rock samples define an isochron of 961±101 Ma with an initial ratio of 0.51163(εNd=+4.5). The calculated uncertainty is high due to the very small range in $^{147}Sm/^{144}Nd$ ratios. The internal mineral isochron for 1503D yields 624±18 Ma with an initial ratio 0.51193.

Discussion

Ages of the protoliths and granulite facies metamorphism The Sm-Nd and Rb-Sr whole-rock isochron ages are consistent within analytical uncertainities, viz. about 1000Ma. There are two possible explanations for the about 1000 Ma event: crust formation or metamorphism. Since REE mobility during metamorphism is still controversial (e.g. Grauch, 1989), we will examine the both cases. In fact, there is no distinct disturbance of REE patterns between the enderbitic gneisses and the retrograde gneisses. Model ages with respect to the depleted mantle (DM) for all samples range between 1220 and 1568 Ma(Table 2). The model ages are calculated based on εNd=+10.0 at present age. However, if we use εNd=+8.5 for the calculation, younger model ages between 1102 and 1291 Ma are indicated. These data are similar to the calculated isochron ages. Moreover, εNd=+4.5 at 1000 Ma suggests that the protoliths derived from the depleted mantle source. Hence, it is not unreasonable that the whole-rock Sm-Nd dating for the metamorphic rocks shows the crust formation age. The higher values of $^{147}Sm/^{144}Nd$ ratios of the analysed samples (mean 0.15) relative to those of the average continental crust (about 0.12: Moorbath and Taylor, 1986) support this assumption.

Alternatively, resetting of Sm-Nd whole-rock isochrons may have been possible under the estimated conditions of granulite facies metamorphism (800°C, 7-8.5kb) (McCulloch and Black, 1984). Re-equilibration of isotopic ratios during metamorphism depend on the scale of redistribution relative to sampling. Since the samples are obtained from a very localized region (within 300 meters), re-distributiuon of the Sm-Nd system is plausible, if dehydration reactions during the granulite facies metamorphism produce fluid incorporating not only large-ion-lithophile elementts but also LREE. In summary, we do not have any conclusive evidence to determine whether the Sm-Nd isochron age dates the protolith or the metamorphism at the moment. If Sm/Nd ratios of the enderbitic gneisses before 1000 Ma granulite facies metamorphism were lower than the present values, the model ages for depleted mantle give the maximum age of the protoliths.

On the other hand, the enderbitic gneisses are depleted in Rb as well as U and Th, and have very high K/Rb and low Rb/Sr ratios relative to the average continental crust. A large Rb-depletion that is assumed not to be a primary feature may be possible during

granulite facies metamorphism in combination with partial melt or fluid migration. Therefore, the Rb-Sr whole-rock isochron for the enderbitic gneisses yields the age of granulite facies metamorphism. Rb-depletion during granulite facies metamorphism has been reported from many Precambrian terrains (e.g. Moorbath and Taylor, 1986). If Sm-Nd data indicate the age of protolith, it means that the time of granulite facies metamorphism followed closely the emplacement of protoliths possibly by no more than 100 Ma which is the precision of our analyses. The close time relationship from crustal formation to granulite facies metamorphism have been reported from many granulite terrrains not only in Archean but also in Proterozoic (Jahn and Zhang, 1984; Moorbath and Taylor, 1986).

Successive thermal events Internal mineral isochron methods for Rb-Sr and Sm-Nd systems are useful to reveal the succesive thermal events which reset isotopic ratios in the mineral scale. Closure temperatures of Sm-Nd system in minerals is considered to be 620-660°C and those for biotite and hornblende in Rb-Sr system are considered to be about 320 and 530°C, respectively (Burton and O'Nions, 1990). Therfore, thermal event at 624±18 Ma might be significant. Retrograde textures are attributed to this event. U-Pb dating for zircon from granites near the present sample locality indicates two post-tectonic intrusive phases; 520±20 and 600±30 Ma (Pasteels and Michot, 1970). The older phase appears to be contemporaneous with the Sm-Nd mineral age of 624±18 Ma, whereas the younger one is consistent with the Rb-Sr mineral ages of 489±30 Ma.

Conclusion

In the central Sør Rondane Mountains, the geologic history which can be established with the available isotope data are as follows:

(1) Timing of the emplacement of the protoliths in the present region occurred about 1000 Ma and the granulite facies metamorphism followed shortly after the emplacement.

(2) A large depletion of Rb as well as U and Th was associated with the granulite facies metamorphism.

(3) The Sm-Nd system was reset in a mineral scale at 620 Ma possibly because of a granite intrusion.

(4) Successive granite intrusions reset the Rb-Sr mineral ages to be 560 and 480 Ma for closure temperatures of each mineral species.

References

Asami, M. and Shiraishi, K.(1987): NIPR Symp. Antarct. Geosci., 1, 150-168.

Burton, K.W. and O'Nions, R.K. (1990): Contrib. Mineral. Petrol., 106, 66-89.

Grew, E.S., Asami, M. and Makimoto, H.(1989): NIPR Symp. Antarct. Geosci., 3, 100-127.

Grauch, R.I.(1989): Reviews in Mineralogy 21, 147-167.

Jahn, B. and Zhang, Z.(1984): Contrib. Mineral. Petrol., 85, 224-243.

Kojima, S. and Shiraishi, K.(1986): Mem. Natl Inst. Polar Res., Spec. Issue, 43, 116-131.

Kretz, R.(1983): Am. Mineral, 68, 277.

McCulloch, and Black, L.P.(1984): Earth Planet. Sci. Lett., 71, 46.

Moorbath, S. and Taylor, P.N.(1986): Geological Society Special Publication, 24, 211-220.

Pasteels, P. and Michot, J.(1970): Eclogae geol. Helv., 63: 239-254.

Picciotto, E., Deutsch, S. and Pasteels, P.(1964): Antarctic Geology, North-Holland Publishing, 570-578.

Sakiyama, T., Takahashi, Y. and Osanai, Y.(1988): Proc. NIPR Symp. Antarct. Geosci., 2, 80-95.

Shiraishi, K. and Kojima, S.(1987): Proc. NIPR Symp. Antarct. Geosci., 1, 129-149.

Shiraishi, K. and Kagami, H.(1989): Proc. NIPR Symp. Antarct. Geosci., 3, 152.

Shiraishi, K., Asami, M., Ishizuka, H., Kojima, H., Kojima, S., Osanai, Y., Sakiyama, T., Takahashi, Y., Yamazaki, M. and Yoshikura, S.(1991): Geological Evolution of Antarctica. Cambridge Univ. Press, 77-82.

Table 1. Rb-Sr isotopic compositions of metamorphic rocks from the Sør Rondane Mountains.

Sample No.	Mineral Assemblages	Rb (ppm)	Sr (ppm)	$^{87}Rb/^{86}Sr$	$^{87}Sr/^{86}Sr$
Enderbitic gneisses					
85011503B	(Pl-Qtz-Hbl-Cpx-Bt-Opx)	2.47	291.8	0.0245	0.70436(4)#
1503C	(Pl-Hbl-Opx-Cpx-Bt)	3.59	238.2	0.0436	0.70484(6)
1503D	(Pl-Qtz-Opx-Hld-Bt-Cpx-Grt)	8.93	207.7	0.1244	0.70615(3)
Hbl		10.85	43.21	0.7269	0.71085(12)
Bt		162.8	16.30	29.47	0.90786(11)
Pl		4.44	186.0	0.0692	0.70559(4)
1602D	(Pl-Qtz-Hbl-Opx-Kfs-Cpx-Bt)	10.78	212.4	0.1468	0.70643(2)
9022502A	(Pl-Qtz-Opx-Bt)	38.30	165.3	0.6710	0.71356(1)
2502B	(Pl-Hbl-Opx-Bt-Cpx)	5.34	357.2	0.0433	0.70494(1)
Retrograde gneisses					
85011601A	(Hbl-Pl-Bt)	6.78	193.0	0.1016	0.70456(2)
1601C	(Qtz-Pl-Hbl-Bt-Kfs)	9.33	207.3	0.1302	0.70637(2)
1602A	(Pl-Qtz-Hbl-Cpx)	1.36	218.7	0.0180	0.70412(2)
1602B	(Pl-Qtz-Hbl-Bt-Cum-Ep)	2.98	327.9	0.0263	0.70358(2)

Numbers in parentheses for the $^{87}Sr/^{86}Sr$ ratios refer to the 2σ error in the last digit.

Table 2. Sm-Nd isotopic compositions and model ages of metamorphic rocks from the Sør Rondane Mountains.

Sample No.	Sm (ppm)	Nd (ppm)	$^{147}Sm/^{144}Nd$	$^{143}Nd/^{144}Nd$	T_{DM}^{Nd} ## (Ma)	ε_{Nd} (0Ma)	ε_{Nd} (1000Ma)
Enderbitic gneisses							
85011503B	4.93	20.03	0.1485	0.51256(2) #	1387	-1.60	+4.58
1503C	3.14	12.19	0.1554	0.51262(1)	1394	-0.43	+4.87
1503D W.R.	2.73	12.00	0.1376	0.51249(2)	1328	-2.58	+4.73
Hbl	94.78	288.0	0.1989	0.51275(2)			
Bt	9.20	28.60	0.1945	0.51273(1)			
Pl	0.83	5.07	0.0990	0.51234(2)			
1602D	3.44	13.94	0.1491	0.51254(2)	1446	-1.99	+4.12
9022502A	2.37	12.50	0.1145	0.51236(2)	1220	-5.48	+5.06
2502B	3.31	14.60	0.1137	0.51247(2)	1354	-3.28	+4.38
Retrograde gneisses							
85011601A	1.22	4.28	0.1716	0.51272(2)	1568	+1.52	+4.74
1601C	3.77	14.48	0.1574	0.51262(1)	1443	-0.47	+4.57
1602A	6.56	27.69	0.1432	0.51255(2)	1304	-1.83	+5.02
1602B	4.86	20.42	0.1439	0.51253(1)	1361	-2.20	+4.5

Numbers in parentheses for the $^{143}Nd/^{144}Nd$ ratios refer to the 2σ error in the last digit.

$T_{DM}^{Nd}=\frac{1}{\lambda}\ln\left[1+\frac{0.513153-(^{143}Nd/^{144}Nd)^{sample}}{0.2136-(^{147}Sm/^{143}Nd)^{sample}}\right]$, $\lambda=6.54\times10^{12}\,y^{-1}$

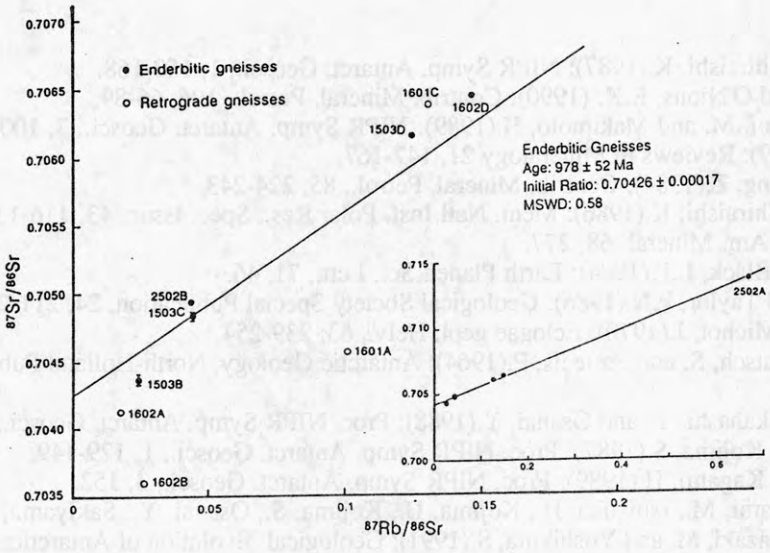

Fig. 1. Rb-Sr whole-rock isochron diagram of metamorphic rocks from the Sør Rondane Mountains.

Calculated error bars are shown with symbols, otherwise within the scale of symbols.

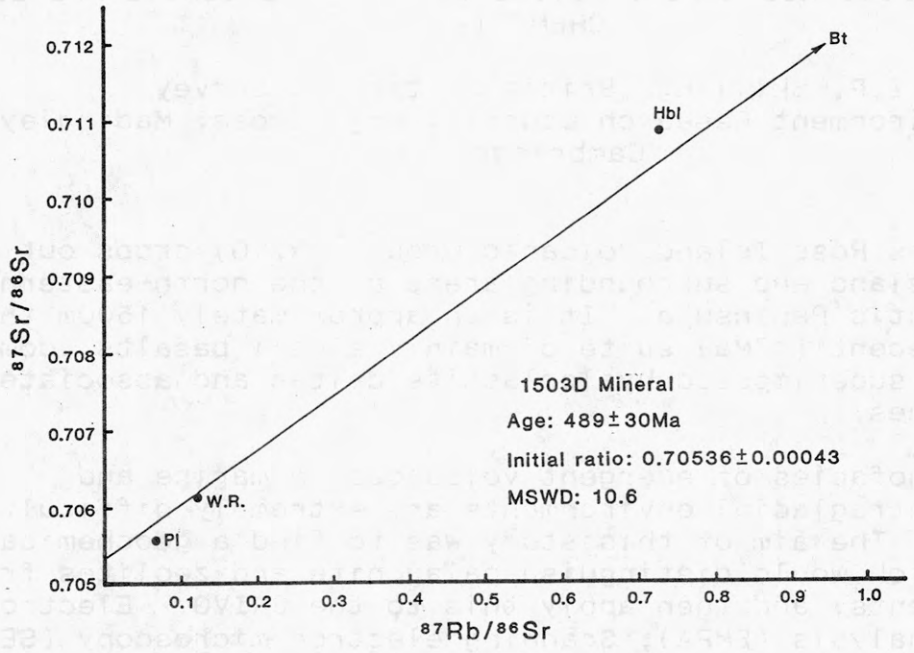

Fig. 2 Rb-Sr mineral isochron diagram of an enderbitic gneiss (1503D). W.R.: whole-rock, Hbl: hornblende, Bt: biotite, Pl: plagioclase.

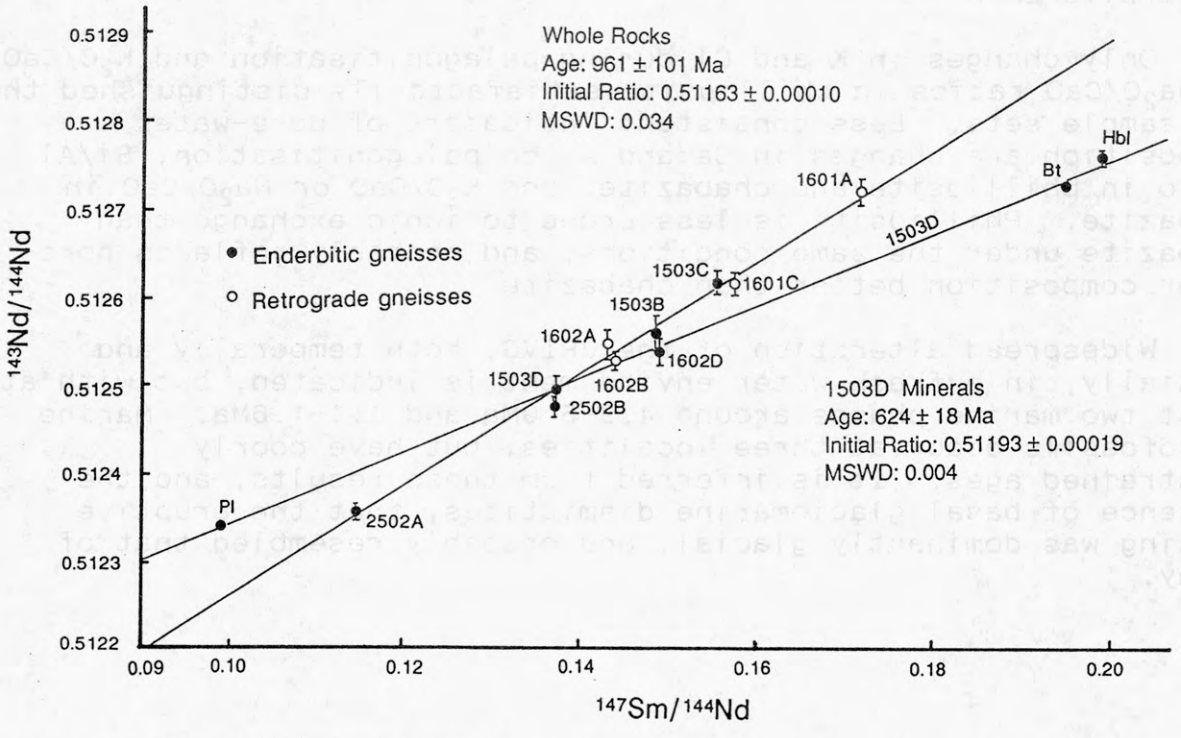

Fig. 3. Sm-Nd whole-rock and mineral isochron diagram of metamorphic rocks from the Sør Rondane Mountains.

Calculated error bars are shown with symbols, otherwise within the scale of symbols.

INTRAGLACIAL ERUPTIVE ENVIRONMENT OF THE MIOCENE-RECENT, JAMES ROSS ISLAND VOLCANIC GROUP: EVIDENCE FROM PALAGONITE AND ZEOLITE CHEMISTRY

I.P. Skilling, British Antarctic Survey,
Natural Environment Research Council, High Cross, Madingley Road
Cambridge, UK

The James Ross Island Volcanic Group (JRIVG) crops out on James Ross Island and surrounding areas at the north-eastern end of the Antarctic Peninsula. It is an approximately 1500m thick, Miocene to Recent (<7Ma) suite of mainly alkali basalts, dominated by multiple, superimposed hyaloclastite deltas and associated hyalotuff cones.

The lithofacies of emergent volcanoes in marine and freshwater/intraglacial environments are extremely difficult to distinguish. The aim of this study was to find a geochemical signature which would distinguish palagonite and zeolites from the two environments, and then apply this to the JRIVG. Electron microprobe analysis (EMPA), Scanning electron microscopy (SEM) and X-ray diffraction (XRD) analyses of JRIVG samples were compared with samples and published analyses from known eruptive environments. Si, Al, Ca, Mg, Fe, Ti were analysed by energy-dispersive EMPA and Na, K, Mn, P, Ba, Sr, Cl and F by wavelength-dispersive EMPA

Only changes in K and Cl during palagonitisation and K_2O/CaO or Na_2O/CaO ratios in phillipsite satisfactorily distinguished the two sample sets. Less consistent indicators of pore-water composition are changes in Ca and Al on palagonitisation, Si/Al ratio in phillipsite and chabazite, and K_2O/CaO or Na_2O/CaO in chabazite. Phillipsite is less prone to ionic exchange than chabazite under the same conditions, and probably reflects pore-water composition better than chabazite.

Widespread alteration of the JRIVG, both temporally and spatially, in a fresh water environment is indicated, but with at least two marine phases around 4.9-5.0Ma and 1.1-1.6Ma. Marine macrofossils occur at three localities, but have poorly constrained ages. It is inferred from these results, and the presence of basal glaciomarine diamictites, that the eruptive setting was dominantly glacial, and probably resembled that of today.

METASEDIMENTARY ROCKS OF WESTERN WILSON TERRANE (NORTH VICTORIA LAND - OATES LAND) AND GONDWANIDE CONNECTIONS TO AUSTRALIA

D.N.B. SKINNER, DSIR Geology & Geophysics, PO Box30-368
Lower Hutt, New Zealand.

Most reconstructions of Antarctica against Australia have had as their theme, the fit of SE Australia and Tasmania against Antarctica, and incidently, have shown a reasonable alignment of the eastern margins of the East Antarctic Craton of Wilkes Land and South Australia's Gawler Craton. However, they have not been able to spatially reconcile correlation of the Berg Group of Oates Land with either the Late Proterozoic Adelaide Supergroup or the Cambrian Kanmantoo Group of the South Australian Adelaide Geosyncline. Rock exposures in the Antarctic sector that should have been in contact with the Adelaide Geosyncline, consist only of early Palaeozoic granite (c. 146° to 147° E), Beacon Supergroup, and Ferrar Dolerite (c. 149° to 154° E), and outcrop along the north end of the Wilkes Subglacial Basin (WSB). Closure of the WSB to re-establish pre-Late Cambrian continuity would not only align Delamerian granites of South Australia with Ross granites of Oates Land to Terra Nova Bay, both with the same age range of 500-510 Ma, but would bring the discontinuous belt of metasedimentary rocks of the western Wilson Terrane (Berg Group, Morozumi Phyllites, Rennick Schist, and Priestley Formation) to a position corresponding to the eastern, more metamorphosed side of the Adelaide Geosyncline and its counterparts beneath the Murray Basin.

Although sparse age data on the Wilson Terrane metasedimentary rocks suggest that they are time equivalents of the Adelaidean to Kanmantoo rocks of South Australia, exact correlations are not yet possible. The Wilson Terrane metasedimentary rocks include comparable lithofacies sequences predominantly of flysch-like quartzose to quartzofeldspathic greywacke (with minor carbonates as cross-bedded nodules, lenses and layers), thinly layered carbonates (calc-silicates) associated with ferruginous and pyritic shales and quartzites, and more or less pelitic quartzites; minor volcanogenic rocks are known only from Priestley Formation, and significant more or less pure carbonates are known only from Berg Group and Priestley Formation. Although such lithofacies can be matched in the Adelaidean - Kanmantoo sequence, none of the three marker lithologies of the Adelaidean that would aid specific correlation - dolomites, glaciogene sediments, and stromatolites - are known in the Wilson Terrane. Neither do the exposures in Antarctica lend themselves to the facies sequence mapping that is the foundation for correlation within the Adelaide Geosyncline. Hence, although Berg Group and Priestley Formation may well be time equivalents of parts of the Cambrian Adelaidean-Kanmantoo, the evidence is insufficient to prove specific correlation.

GEOCHEMICAL EVOLUTION OF VOLCANOES IN THE EXECUTIVE COMMITTEE RANGE, CENTRAL MARIE BYRD LAND, WEST ANTARCTICA

J.L. Smellie, British Antarctic Survey, Natural Environment Research Council, High Cross, Madingley Road, Cambridge CB3 0ET, UK.
K.S. Panter, W.C. McIntosh and P.R. Kyle, Department of Geoscience, New Mexico Instute of Mining and Technology, Socorro, NM 87801, USA.

The Executive Committee Range is a linear chain of poorly known, late Miocene-Recent stratovolcanoes with large summit calderas. The volcanoes belong to the Marie Byrd Land volcanic province, which is hot-spot related and occurs within the West Antarctic rift system. In 1989-90, the West Antarctic Volcano Exploration (WAVE) project examined three of the volcanoes in detail. The erupted suite provides an excellent opportunity to examine the petrological evolution of sodic alkalic basalt magmas and their peralkaline differentiates. At Mount Cumming, trachyte lavas and welded pyroclastic fall deposits crop out around the caldera rim and the youngest activity consists of a basanite cone with mantle nodules. By contrast, the more extensive exposures at Mount Sidley and Mount Waesche contain a wide range of lithologies (lavas, pyroclastic fall and flow) with diverse compositions including alkali basalt, basanite, hawaiite, tephrophonolite, phonolite, trachyte and comenditic rhyolite. Crystal fractionation, involving the major phenocryst phases (mainly olivine, clinopyroxene, plagioclase and alkali feldspar), has exerted a dominant control on compatible element compositions. Rb, La, Ce, Y, Nb and Zr remained incompatible throughout the differentiation and each volcano can be distinguished uniquely by inter-element ratios involving these elements. A single magmatic series is present at Mount Waesche and each major eruptive phase displays evolutionary trends of evolved to less evolved compositions with time, suggesting sequential tapping down through a stratified magma chamber(s). The youngest activity at this volcano consists of recent eruptions of alkali basalt and phonotephrite tephra, which are preserved as layers in blue ice on the south side of the volcano. The evolution of Mount Sidley is more complicated and at least two magmatic series are well defined. The two series are distinguished by different incompatible LIL/HFS and HFS/HFS element ratios and they are separated by an angular unconformity, which must represent an important time gap as well as a petrological hiatus. The older series comprises phonotephrite, phonolite and trachyte compositions, whereas the younger series consists mainly of trachytes. Each of the magmatic series contains thick (>50 m), compound, trachyte lavas, which display considerable internal compositional variation suggesting significant evacuation of a stratified magma chamber(s) during their eruption. The most recent activity consists of several basanite cones, some of which contain abundant crustal and mantle nodules.

A LAYERED, AMPHIBOLITE TO GRANULITE FACIES, MIGMATITE SEQUENCE IN THE FOSDICK METAMORPHIC COMPLEX, WEST ANTARCTICA

Smith, C.H., Richard, S.M. Institute for Crustal Studies, University of California, Santa Barbara, California 93106-1100, USA

The Fosdick Mountains in western Marie Byrd Land consist of upper amphibolite to granulite facies rocks known as the Fosdick Metamorphic Complex. The complex exhibits planar metamorphic layering throughout; this is a transposition fabric bounding large-scale tectonic lozenges in which an older, steep-dipping fabric is preserved. In order of decreasing protolith age, the rocks consist of: (1) pelitic and psammitic gneisses; (2) granodiorite to monzogranite gneiss; (3) dioritic to granodioritic orthogneisses, locally garnet bearing, with minor granitoid intrusions; (4) syn-metamorphic granitoids; (5) mafic intrusions; and (6) biotite-muscovite granite. Units 1-4 form gently dipping, layered sequences of large, lenticular lithosomes, 10-30 m in thickness, which are laterally continuous for hundreds of meters. The order and spatial association of lithic units is variable. A coarse-grained, equant, granoblastic texture characterizes all of the migmatitic units.

The advanced degree of migmatization in the Fosdick complex generally obscures primary rock relations, and transposition imposes a gently dipping planar fabric throughout most of the range. However, pre-metamorphic, discordant, intrusive contacts are locally preserved, showing medium-grained biotite granodiorite (2, above) intruding paragneisses (1) which contain abundant calc-silicate nodules. The earliest intrusive rock is medium- to medium-coarse-grained granodiorite to K-feldspar monzogranite (2), with foliation defined by biotite selvages around feldspar porphyroblasts. The differentiated migmatitic fabric in this rock is distinct from the homogeneous foliation in younger, syn-metamorphic granitoids (4). The paragneisses (1) show mineralogic differentiation on a centimeter to decimeter scale, with sillimanite-garnet-biotite-cordierite melanosome interlayered with garnet- and cordierite-bearing quartz-plagioclase-K-feldspar leucosome. Paragneisses are localized along the northern front of the eastern Fosdick Mountains and in the central and western part of the range. In the east, they occur in laterally continuous layers, tens of meters thick, within sequences of layer-parallel granitoids of varying compositions (3). Elsewhere, crenulated paragneisses occur within large scale, low strain "lozenges" bounded by planar foliation zones. They are invaded by bodies of leucogranitic neosome.

Concordant granitoids (3) range from diorite and tonalite to biotite granodiorite. Diorite layers are typically fine grained and homogeneous, with large, equant, garnet porphyroblasts surrounded by light-colored, biotite-poor alteration rims. Granodiorite gneisses are medium to coarse-grained, containing variable amounts of biotite and garnet. Biotite extensively replaces primary hornblende in the diorite and granodiorite. Strongly segregated, thinly banded biotite-quartz-plagioclase-feldspar gneisses also occur within the layered sequences. The granodioritic rocks are intruded by anatectic leucogranites (4) which have a K-feldspar-biotite-quartz-plagioclase mineralogy adjacent to migmatitic granodiorite orthogneisses. Near migmatitic metapelites, the mineral assemblage of the leucogranites further includes abundant cordierite, garnet, and sillimanite. The anatectic intrusions commonly contain domains of heteroblastic, K-feldspar-and biotite-rich granitoid. Leucogranite forms the matrix for block gneisses which contain lenses and blocks of all of the above rock types. Mafic dikes (5) were intruded continuously throughout metamorphism. They are ensheathed and injected by locally derived leucogranitic material, are typically crosscutting to semi-concordant with surrounding layered gneisses, and are variably disaggregated. Massive, subvertical, fine-grained dioritic intrusions are either undisrupted or brittlely disaggregated by injected leucocratic melts. The youngest rock unit in the Fosdick Mountains is a homogeneous, equigranular, fine-medium-

grained, biotite-muscovite granite (6). The intrusive rock typically occurs in sub-vertical dikes, 1-10m thick, which sharply cut across the gneisses, orthogonal to layering. Distinctive mineral assemblages within the metapelitic paragneisses (1) of the lower strain "lozenges" contain evidence for four metamorphic episodes. Two upper amphibolite facies metamorphic events are recorded by overprinting mineral assemblages preserved within paragneisses. The first is associated with a steeply dipping gneissic foliation, and the second, with a shallowly dipping crenulation to transposition foliation. Pressure and temperature estimations based on field and thin section determination of stable mineral assemblages give amphibolite grade metamorphic conditions of 4-5 kb and 650-750°C. Almandine-cordierite associations within discrete crosscutting veins indicate that locally granulite-grade metamorphic conditions were reached. The third metamorphic event was a decompression phase, indicated by cordierite rims on garnet and discordant cordierite-bearing pegmatite veins, which was succeeded by a retrograde event marked by extensive chloritization.

Based on rock types and field relations, we interpret the protolith of the Fosdick complex as an argillaceous sedimentary sequence invaded by granodiorite intrusions. The protoliths for the metapelitic (1) and granodioritic (2) migmatites were probably correlative with the Late Proterozoic-early Paleozoic Swanson Formation and the Devonian Ford Granodiorite of the Ford Ranges. The depth of emplacement of the granodiorite into the pelitic metasediments is unclear, but the development of calc-silicate nodules in proximity to the contacts may indicate significant contact metamorphism. Further intrusion of a significant volume of granodiorite (3) may have provided necessary heat and transferred the metasedimentary material to sufficient crustal depths for the high grade metamorphism to occur. Association of the earliest amphibolite facies mineral assemblages with development of the steeply dipping S_1 foliation suggests that S_1 formed during metamorphism. In a like manner, the shallow S_2 transposition fabric is inferred to have formed during a second, overprinting, amphibolite to granulite facies metamorphism. The foliations may have resulted from two discrete deformational-metamorphic events, or from a single time-progressive episode. The concordant, sheet-like form of the dioritic to granodioritic gneisses (3) suggests that they were pre- to syn-kinematic with development of S_2; the intrusions may have provided a heat source for the concurrent high grade metamorphism. Leucogranite layers (4) are interpreted to be locally derived by anatexis during migmatization because their mineralogy is controlled by adjacent migmatized source rocks. Preliminary isotopic data indicate a Mesozoic age for peak metamorphism. Migmatization may have been coeval with intrusion of the Byrd Coast granites.

MINERAL INVENTORY OF ANTARCTICA

John F. Splettstoesser
Rockland, Maine 04841 U.S.A.

In the first major published inventory of Antarctic minerals, Stewart (1964) listed 222 known minerals from the entire continent. Although he did not visit Antarctica until 1960, he did considerable petrographic studies of rocks collected by others on earlier expeditions. The International Geophysical Year (IGY) of 1957-58 was the start of intense geological studies that continue to this day, even though geology was not an official IGY discipline. Nevertheless, geologic field work has now been done in all parts of Antarctica in a broad sense, and in detail in many areas. Many ice-free areas have yielded rocks and minerals previously unknown in Antarctica, and the earlier list of minerals by Stewart (1964) has grown considerably. It may be safe to say that Antactica contains a suite of minerals not unlike those on other continents, with only a few that are unique (e.g., antarcticite). Considering that only 1 to 2 percent of the continent is not covered by ice, many additional mineral types might occur beneath the ice, but might never be found and described.

A complete list of minerals found to date in Antarctica would have little practical value except for general reference purposes, but those that have economic potential in an appropriate geological setting and in sufficient quantity are of interest in helping to determine the present state of minerals potential for the continent. Further value of such a list is in the consolidation of not only common minerals but annotated entries for uncommon minerals, unusual geologic settings, comparisons with formerly contiguous Gondwana Land masses, location(s), and selected published references.

An exhaustive search of the literature has resulted in a list of all known minerals found in Antarctica to date, excluding those in meteorites, but including all land areas south of 60 degrees south and ferromanganese nodules on the seafloor.

Stewart, Duncan, 1964, Antarctic mineralogy. In R.J. Adie, ed., Antarctic Geology. North-Holland, Amsterdam, p. 395-401.

Numerical modelling of Transantarctic Mountain uplift and linked subsidence in the Ross Embayment

T. A. Stern[1] U. S. ten Brink[2] and M. H. P. Bott[3]

[1]*DSIR Geology and Geophysics, P.O.Box 1320 , Wellington, New Zealand*

[2] *Dept. of Geophysics, Stanford University, Stanford, CA 94305, USA.*

[3]*Dept. of Geological Sciences, University of Durham, Durham, DH1 3LE, UK.*

Introduction

Numerical modelling using both finite element and finite difference techniques provide important insights into geological processes. For example, stresses and associated strains can be estimated for mountain uplift and compared with geological and geophysical observations to ascertain the mechanical efficacy of any uplift model. The Transantarctic Mountains (fig.1) provide one of the best examples for such a modelling process as they are part of one of the largest and most continuous continental rift margins on earth. Adjacent to the uplifted mountains is the Victoria Land Basin which contains up to 7 km of Cenozoic sediments, as inferred from seismic reflection data (Cooper & Davey, 1985). The uplift and adjacent subsidence appear to be roughly coeval, suggesting the processes to be mechanically coupled.

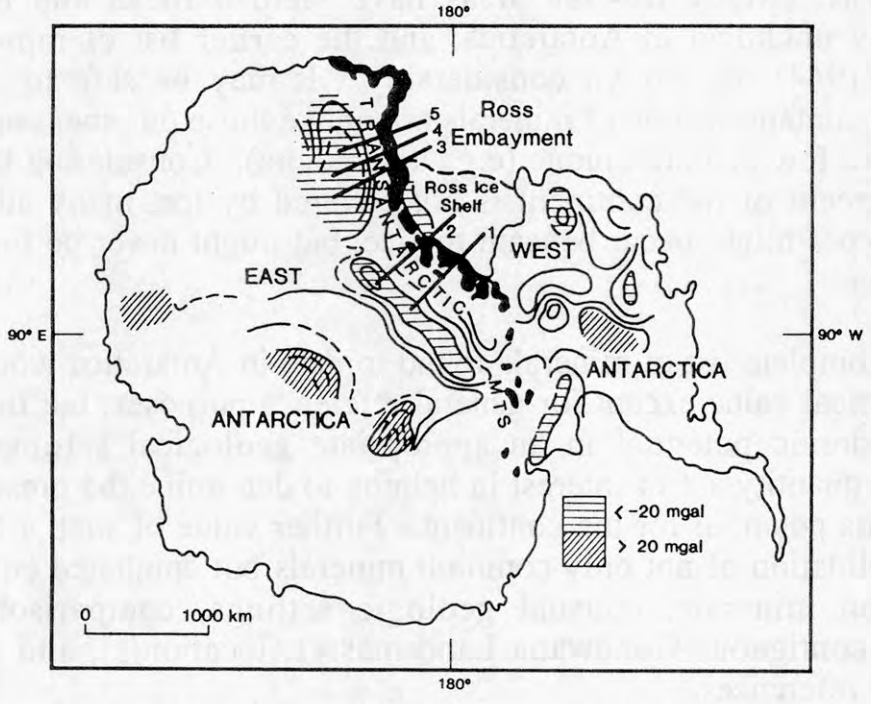

Fig. 1. Locality map and position of 5 topographic/subice profiles shown in fig.2. Free-air gravity anomalies after Bentley (1983).

Despite the extreme isolation of the Transantarctic Mountains, there are an unusually complete set of geological and geophysical observations that constrain the uplift and adjacent subsidence. Fission track studies suggest at least 5 km of Cenozoic uplift (Fitzgerald, et al., 1987). Within the mountains the Kukri Peneplain provides an excellent reference surface that has been up-warped at the mountain front to heights in excess of 3000 metres and slopes gently back beneath the ice cap. About six determinations of dip on the peneplain, at distances of roughly 40 km inland, suggest an average dip of about 2-3^{o} (see Stern & ten Brink,1989).

Evidence for flexure

Fig. 2 shows a stack of rock-surface profiles which passes through the Transantarctic Mountains and beneath the East Antarctic ice sheet. Locations of the profiles are shown in figure 1. Of apparent maximum uplift and the topographic low (the Wilkes Basin) beneath the ice cap. Such a

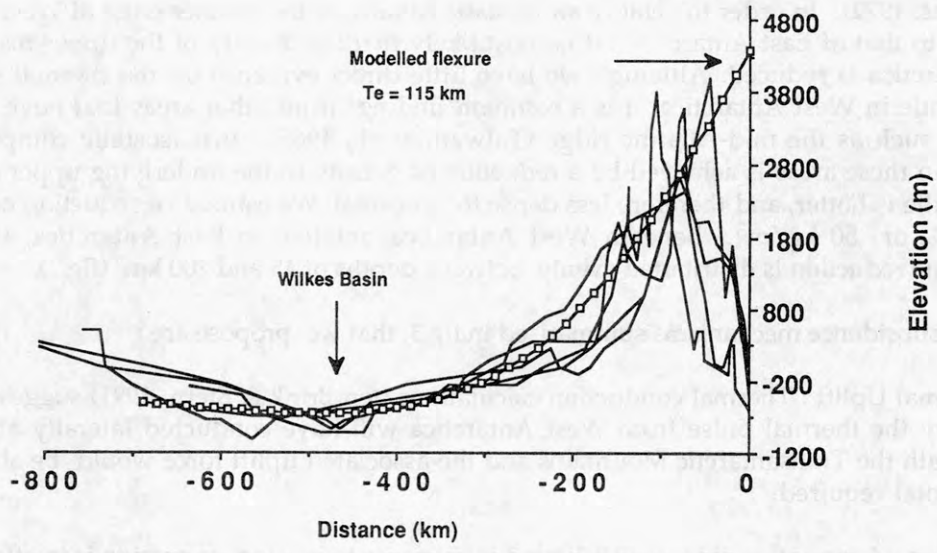

Fig.2. Five topographic-subice profiles through the Transantarctic Mountains and through to the Wilkes Basin . Results from Modelled flexure shown (after Stern & ten Brink, 1989).

distance, or half-wavelength, is typical of that for lithospheric flexure where the flexural rigidity (i.e."stiffness") of the lithosphere is high (an elastic thickness (T_e) of around 100 km). Corroborative evidence that the topographic pattern we see in fig.2 represents flexure of strong lithosphere comes from the pattern of free-air gravity anomalies shown in fig.1 where a broad free-air gravity low of about -50 mgal coincides with the axis of the Wilkes Basin. Such a long wavelength gravity pattern strongly favours a flexural origin for the Wilkes Basin rather than say a rift, or extensional origin.

Uplift Mechanisms

Figure 3 is a cartoon summarising our present knowledge of crustal structure at and adjacent to the each side of the front. The difference in crustal thickness of about 15 km between East and West

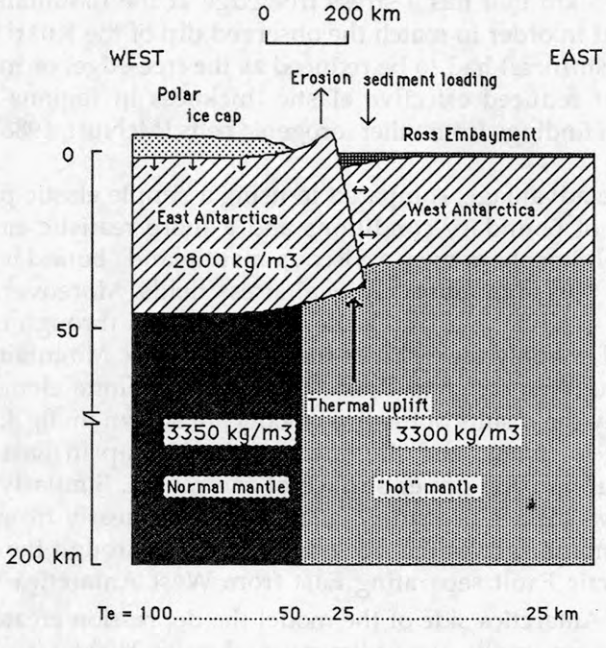

Fig.3. Conceptual model of uplift and subsidence at the Transantarctic Mountian Front.

Antarctica is within the range of that postulated by earthquake surface wave dispersion studies (e.g. Adams, 1972). In order to achieve an isostatic balance of the thinner crust of West Antarctica, compared to that of East Antarctica, it is most likely that the density of the upper mantle within West Antarctica is reduced. Although we have little direct evidence on the thermal state of the upper mantle in West Antarctica, it is a common finding from other areas that have undergone extension, such as the mid-Atlantic ridge (Talwani et al., 1965), that isostatic compensation of thin crust in these areas is achieved by a reduction of density in the underlying upper mantle; the upper mantle is hotter, and therefore less dense,than normal. We estimate a reduction of density of about 1.5%, or 50 kg/m^3, beneath West Antarctica, relative to East Antarctica, is sufficient provided the reduction is distributed evenly between depths of 45 and 200 km (fig.2).

The uplift-subsidence mechanisms summarised in fig.3, that we propose are :

a/ Thermal Uplift : Thermal conduction calculations (ten Brink & Stern, 1991) suggest that after 70 my the thermal pulse from West Antarctica will have conducted laterally about 60 km beneath the Transantarctic Mountains and the associated uplift force would be about 50% of the total required.

b/ Erosion : A mountain range will rebound in response to erosion, so erosion is in effect an uplift mechanism. Although fission track studies indicate at least 5000m of uplift, erosion has reduced the average elevation of the mountain front to heights of typically around 2500m. Thus erosion is an important factor in an uplift analysis of the Transantarctic Mountains.

c/ Isostatic forces : Isostatic forces are produced in the presence of a lithosphere that is cut by an inclined, normal fault as discussed first by Vening Meinesz (1950) and later by others. On the foot wall side of the fault uplift occurs while on the hanging wall side of the fault there is a net subsidence. It is this subsidence, assisted by sediment loading, that gives rise to the Victoria Land Basin.

Elastic Plate and Finite Element Models

The principal features of the flexural uplift profile(fig. 2) can be successfully modelled with a simple thin elastic plate model. Stern & ten Brink(1989) used a finite difference approximation to the elastic plate equation and showed that the total uplift of the Transantarctic Mountains, the dip on the Kukri Peneplain and the half-wavelength of 470 km can be explained by an elastic plate with an "effective" thickness of 115 km that has a stress free edge at the mountain front. i.e. a free-ended plate. We also found that in order to match the observed dip of the Kukri Peneplain the elastic thickness of the plate(or the stiffness) had to be reduced as the free-edge, or mountain front, is approached. This phenomena of reduced effective elastic thickness in regions of high plate curvature is entirely consistent with findings from other orogenic belts (McNutt, 1988).

The finite element approach has the advantage, compared to using a simple elastic plate model, of allowing a more complicated set of boundary conditions and a more realistic earth model. In particular, we allow for an elastic lithosphere over a viscous mantle and boundary forces to be applied at each end of the model, thus simulating regional stress fields. Moreover, with a finite element model we can study the behaviour of an elastic plate cut right through by an inclined fault. In other words we can model not only the uplift of the Transantarctic Mountains but also the apparent coeval development of the Victoria Land Basin. Details of the finite element model are given in Bott & Stern (1991) and only the results of the final model are shown in fig.4. In this model the right hand edge of the model is fixed and the effect of the ice cap in East Antarctica is introduced by a distributed pressure on the upper surface of the model. Similarly, the effect of erosion is incorporated as a negative surface pressure which increases linearly from a position 75 km east of the free-edge to a maximum right at the free-edge. Passing through the middle of the model is the proposed Transantarctic Fault separating East from West Antarctica which dips at 63^{o} and is stress-free. On the West Antarctica side of the model the depression created by isostatic forces is allowed to fill in, and therefore amplify, by sediments of density 2300 kg/m^3.

Shown in the three plots of fig.4 are the surface displacements the displacement vectors and the deviatoric stresses predicted. The surface displacements give a particularly good fit to the observed uplift in East Antarctica (fig.2) and the predicted 7 km of subsidence is in accord with the

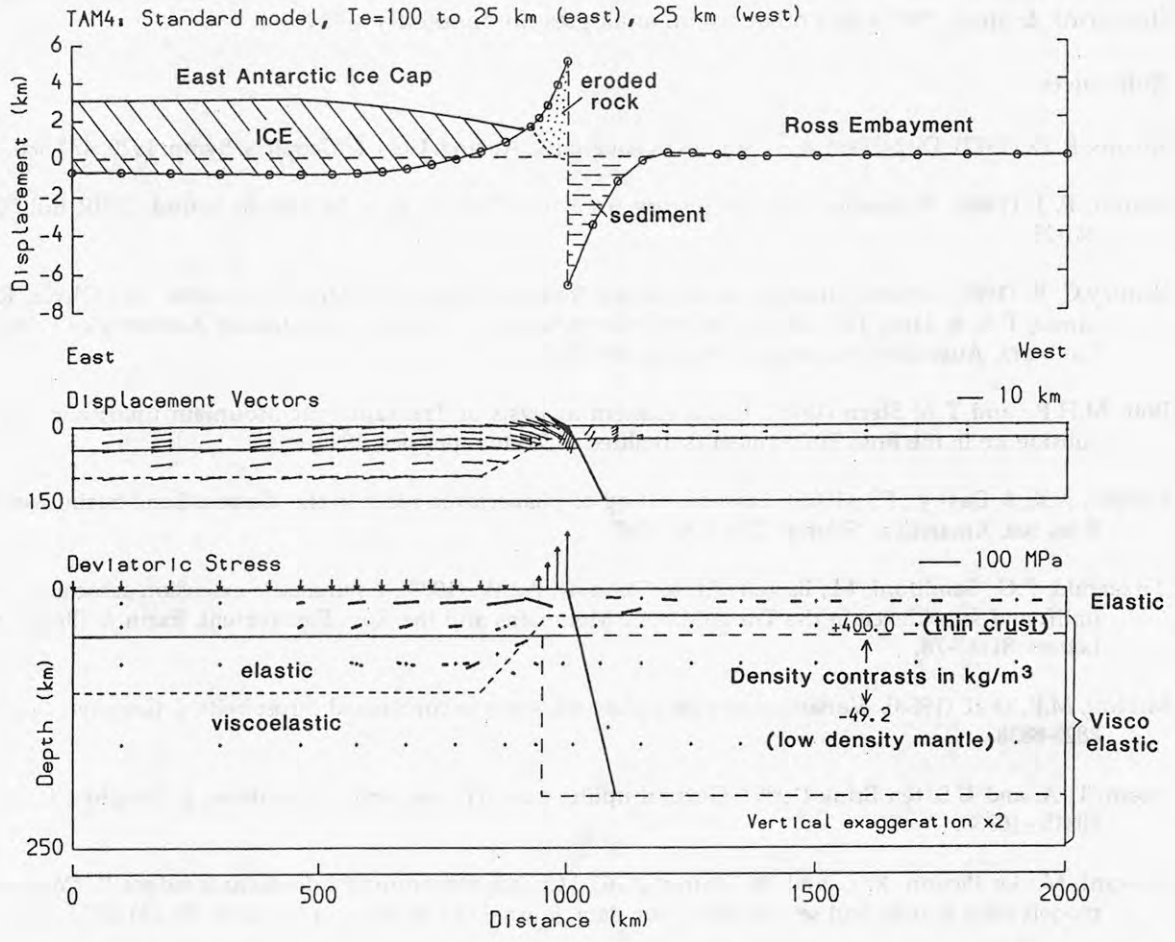

Fig.4. Results from the finite element model of Bott & Stern (1991). Top plot represents displacement of the upper surface of the earth, middle plot are displacement vectors where the right hand end of the model is kept fixed, and the bottom plot shows calculated deviatoric stresses superimposed on the physical model. Compressional stresses are shown by the solid bar, extension by the dash-dot-dash. Amplitude of stresses can be compared with the 100 Mpa scale shown.

proposed 5-7 km of Cenozoic sediments within the Victoria Land Basin (Cooper & Davey, 1985). About 8 km of total extension is all that is required for the uplift to take place (see displacement vectors in middle plot, fig.4).

Discussion

Our numerical models are designed to provide a first-order explanation for the Transantarctic Mountains uplift and adjacent subsidence in the Victoria Land Basin. The model is not definitive; it can and should be tested. For example, is the concept of a stress-free fault cutting through the whole lithosphere reasonable ? If there is a coupling across the fault it should be manifested in unconformities within the Ross Embayment, corresponding to the many glacial advances and retreats that are now (Barrett, 1989) being proposed for the East Antarctic ice cap on the basis of drill hole data .

What is the origin and character of the Wilkes Basin ? We argue strongly that the gravity anomalies and shape of the basin can be explained in terms of a flexural basin. However, that does not preclude the existence of a thick sedimentary sequence originating from an earlier period.

Exploration of the Wilkes Basin could be instigated with a multichannel seismic experiment located on the ice cap.

Finally, much can be learned by comparing the Transantarctic Mountains with other uplifted rift flanks around the world. A comparison has been done with Great Escarpment of southern Africa (ten Brink & Stern, 1991) but other useful analogies undoubtedly still exist.

References

Adams, R. D. (1972). Dispersion wave studies in Antarctica, Antarct. Geol. & Geophys. Symp. 1970, 473-480.

Barrett, P. J. (1989). Antarctic Cenozoic history from the CIROS-1 hole, McMurdo Sound. DSIR Bull. 245: 241-251.

Bentley,C. R. (1983). Crustal structure of Antarctica from geophysical evidence - a review , in : Oliver, R.L., James, P.R. & Jago, J.B. (eds.), Antarctic Earth Science : Canberra, Australian Academy of sciences: Canberra, Australian Academy of Science: 491-497.

Bott, M.H.P., and T.A. Stern (1991). Finite element analysis of Transantarctic Mountain uplift and coeval subsidence in the Ross Embayment (submitted to Tectonophysics, 1990).

Cooper, A.K. & Davey , F.J. (1985). Episodic rifting of phanerozoic rocks in the Victoria Land basin, western Ross Sea, Antarctica. Science, 229: 1085-1087.

Fitzgerald, P.G., Sandiford, M., Barrett, P.J. & Gleadow, A.J.W. (1987). Asymmetric extension associated with uplift and subsidence in the Transantarctic Mountains and the Ross Embayment. Earth & Planet. Sci. Letters. 81: 67-78.

McNutt, M.K. et al. (1988). Variations of elastic plate thickness at continental thrust belts, J. Geophys. Res., 93: 8825-8838.

Stern, T. A. and U.S. ten Brink (1989). Flexural uplift of the Transantarctic Mountains, J. Geophys. Res., 94: 10315 - 10330.

Talwani, M., Le Pichon, X. L. and M. Ewing, (1965). Crustal structure of mid-oceanic ridges 2. Computed models from gravity and seismic refraction data. Journal of Geophysical Research 70: 341-352.

ten Brink, U.S. & Stern, T.A. (1991) . Rift margin uplifts and hinterland basins: Comparison between the Transantarctic Mountains and the Great Escarpment of southern Africa, (submitted to JGR, 1990).

Vening Meinesz, F.A. (1950). Les Grabens africaines, resultat de compression ou de tension dans la croute terrestre? Bull. Inst. R. Colon. Belge, 21: 539-552.

TECTONIC CONTROLS ON JURASSIC MAGMATISM ALONG THE PROTO-PACIFIC MARGIN OF ANTARCTICA AND THEIR BEARING ON GONDWANA BREAK-UP MODELS

B.C. Storey, British Antarctic Survey, Natural Environment Research Council, High Cross, Madingley Road, Cambridge, CB3 0ET, U.K.
T. Alabaster, Sunderland Polytechnic, School of Environmental Technology, Benedict Building, St George's Way, Stockton Road, Sunderland, SR2 7BW, U.K.

According to active mantle hypotheses, continental rifting is initiated by doming above a mantle plume, whereas passive hypotheses consider that the presence of a plume only enhances break-up if the stress field is such that initial rifting is likely to occur. In the latter case, rifting may be the result of changes in plate boundary forces or caused by changes in absolute plate motions. However, the causal relationship between massive volumes of igneous activity along the proto-Pacific margin of Antarctica and the initial break-up of Gondwana during the Jurassic remains a matter of conjecture.

In the West Antarctic sector of Gondwana (Fig. 1), early stages of break-up are associated with the large Antarctic-Karoo-Tasman continental flood basalt province. Formation of this within-plate province was synchronous with active margin tectonics and development of both a proto-Pacific margin magmatic suite along the Antarctic Peninsula and the extensive *Tobifera* volcanic suite associated with formation of the Rocas Verdes marginal basin system of southern South America and South Georgia. Beneath part of the Antarctic-Karoo-Tasman province White and McKenzie [1989] have suggested the likely location of a plume, whereas Cox [1988] has preferred in this case to replace the notion of a *hot-spot* by a *hot-line*. In fact, Cox [1988] relates the main melting anomaly responsible for the flood basalt province to subduction and has drawn analogies between the province as a whole and back-arc spreading.

The West Antarctic sector of Gondwana is an excellent location in which to investigate possible relationships between tectonism, magmatism, and the onset of sea floor spreading in continental extension zones. In this presentation we consider the petrogenetic relationship between within-plate and Pacific margin magmatism and the tectonic controls on magma generation and lithospheric extension during the early stages of Gondwana break-up.

Geochemical and isotope data suggest the existence of a large, Middle Jurassic subduction-related magmatic province common to both the Antarctic Peninsula and southern South America. Moreover Pacific margin magmas were derived from an enriched lithospheric mantle source similar to that for the contemporaneous within-plate Ferrar-Tasman suite. Extension concurrent with subduction and oceanward migration of the magmatic focus resulted in a broad extensional province in a back-arc and inter-arc setting. High geothermal gradients and basalt underplating caused crustal melting on the east coast of the Antarctic Peninsula and formation of bimodal basalt-rhyolite suites. Enriched lithospheric initial rifting magmas were succeeded, at least in part of the Rocas Verdes basin, by transitional early drift magmas and then by entirely asthenospheric MORB magmas (Fig. 2) representing lithospheric rupture and sea-floor spreading (Alabaster and Storey, 1990a).

A plate interaction model (Fig. 3) is proposed for the initial stages of Gondwana

break-up relating the broad zone of lithospheric mantle melting to a reduction in plate boundary forces (Storey and Alabaster, in press). We suggest that the change from Gondwanide compression to lithospheric extension in the Jurassic may be linked to a change from shallow to steeply dipping subduction, and to a slowing of subduction rates caused by a decreasing age of the subducting plate. A possible reduction of compressive boundary stresses may have enabled unconfined, overthickened Permo-Triassic crust to extend because of gravitational instability, thus facilitating break-up. Ridge-trench interaction (Alabaster and Storey, 1990b) and formation of the Rocas Verdes basin, as a possible Gulf of California analogue, may have followed subduction of young hot oceanic lithosphere possibly causing a temporary cessation of subduction and a further reduction of plate boundary forces.

The presence of a mantle plume is not essential to our model. Decompression melting and passive upwelling of mantle diapirs beneath the rifting continental lithosphere may have formed the within-plate magmas. We do not, however, rule out the possibility of the chance unroofing of a plume during lithospheric extension which may be necessary to produce the large volumes and compositions of magma in the Karoo province.

Alabaster, T. and B.C. Storey. 1990a. Modified Gulf of California model for South Georgia, north Scotia Ridge, and implications for the Rocas Verdes back-arc basin, southern Andes. Geology, 18, 497-500.

Alabaster, T. and B.C. Storey, 1990b. Antarctic Peninsula continental magnesian andesites: indicators of ridge-trench interaction during Gondwana break-up. Journal of Geological Society, London. 147, 595-598.

Cox, K.G. 1988. The Karoo Province, in Continental Flood Basalts, edited by J.D. Macdougall, pp. 239-271, 1988.

Kyle, P.R., R.J. Pankhurst, and J.R. Bowman. Isotopic and chemical variations in Kirkpatrick Basalt Group rocks from southern Victoria Land, in *Antarctic Earth Science*, edited by R.L. Oliver, P.R. James, and J.B. Jago, pp. 234-237, Australian Academy of Science, Canberra and Cambridge University Press, Cambridge, 1983.

Pankhurst, R.J., I.L. Millar, F. McGibbon, M. Menzies, C.J. Hawksworth and P.R. Kyle. Evidence for the enriched source of the Jurassic Ferrar magmas of Antarctica, Terra Cognita, **6**, 204 (abstract only), 1986.

Storey, B.C. and T. Alabaster. In press. Tectono-magmatic controls on Gondwana break-up models: Evidence from the proto-Pacific margin of Antarctica. Tectonics.

White, R.S. and McKenzie, D. 1989. Magmatism at rift zones: the generation of volcanic continental margins and flood basalts. J. Geophys. Res., 94, 7685-7729.

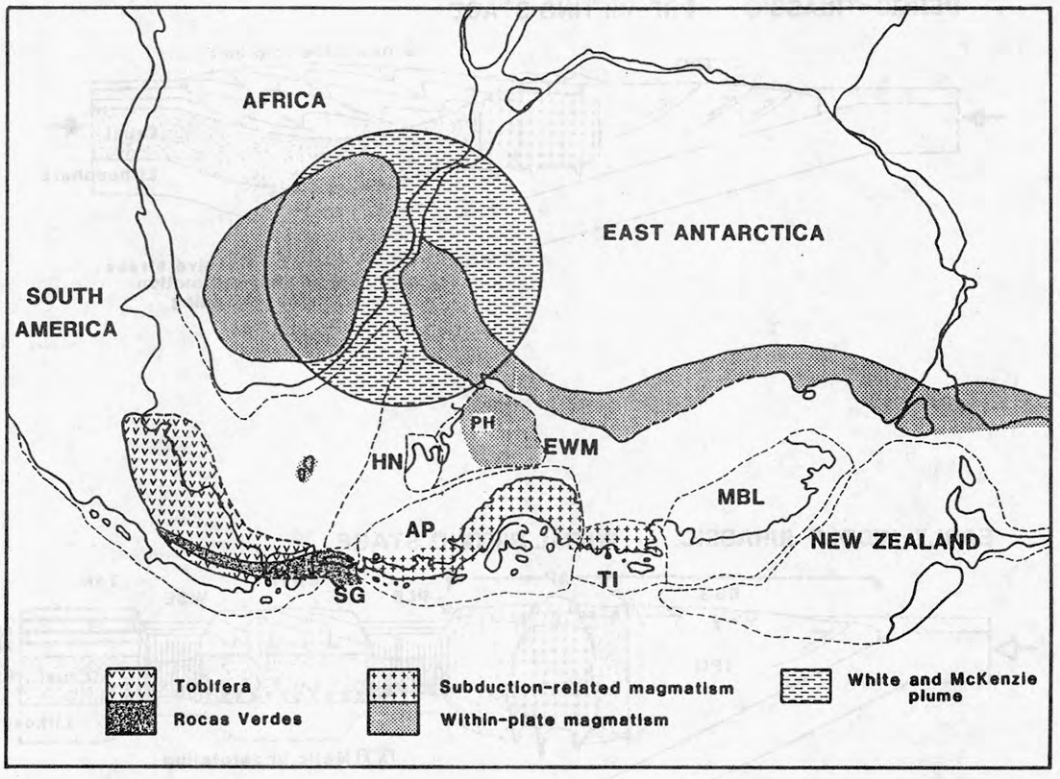

Figure 1. Distribution of Jurassic magmatism and the proposed location of the White and McKenzie (1989) plume on 180 Ma Gondwana reconstruction. AP, Antarctic Peninsula; HN, Haag Nunataks; EWM, Ellsworth-Whitmore Mountains; MBL, Marie Byrd Land; PH, Pirrit Hills; SG, South Georgia.

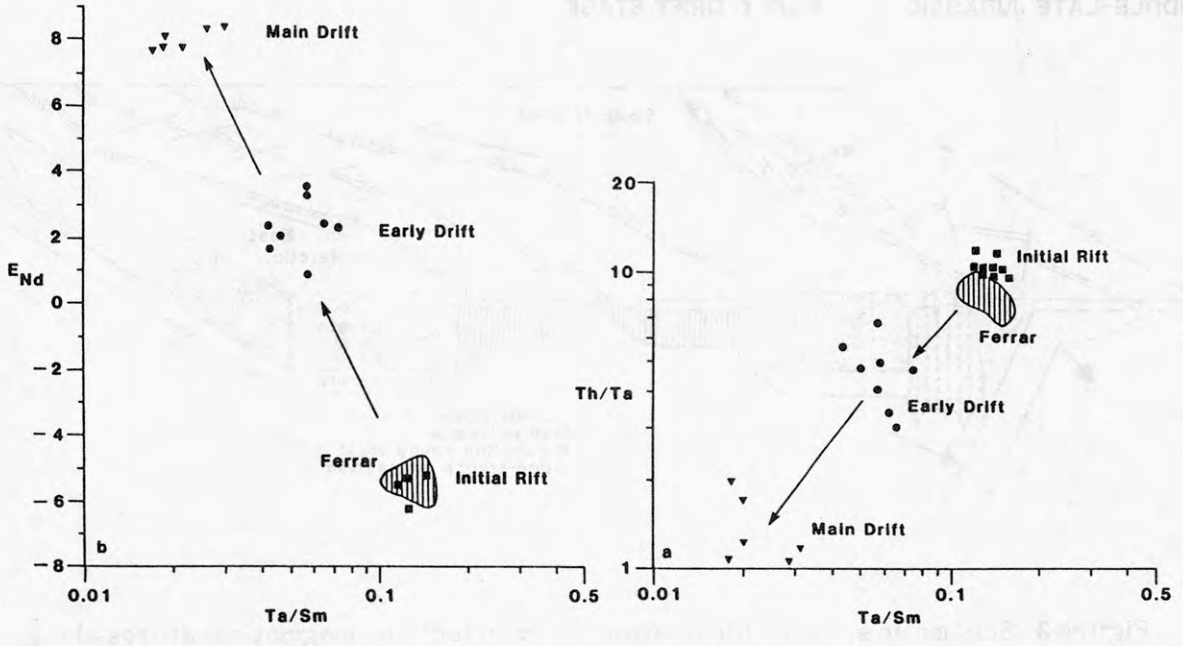

Figure 2. Plots of Th/Ta - Ta/Sm and E_{Nd} - Ta/Sm for stratigraphically controlled rocks with ≤60% SiO_2 from South Georgia and northern Antarctic Peninsula. Fields for Ferrar dolerites from Kyle et al. (1983) and Pankhurst et al. (1986).

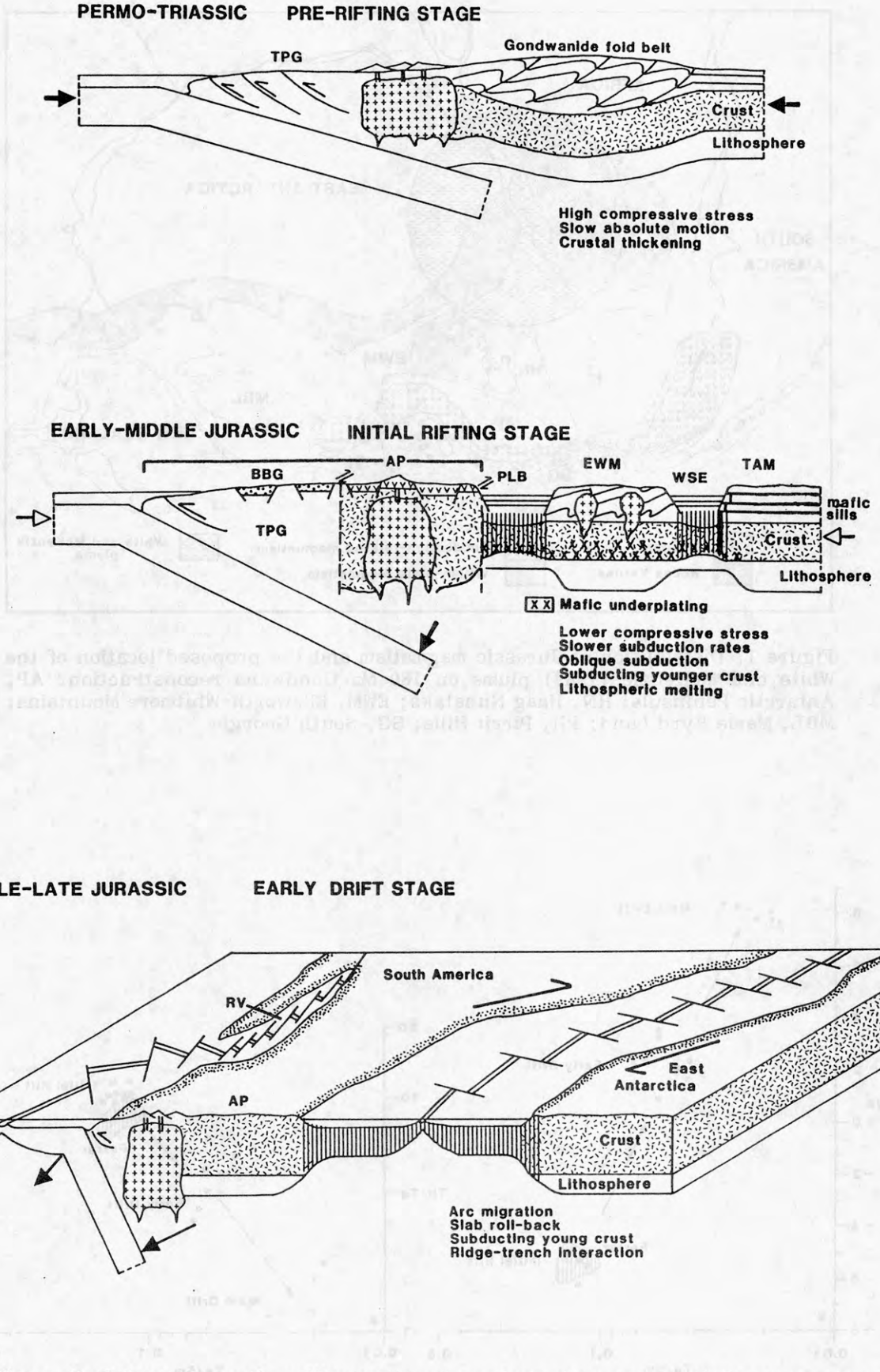

Figure 3. Schematic sections illustrating the main tectono-magmatic features along the proto-Pacific margin of Antarctica prior to and during the early stages of Gondwana break-up. BBG, Botany Bay Group fluviatile sedimentary rocks; TPG, Trinity Peninsula Group accretionary complex; AP, Antarctic Peninsula; EWM, Ellsworth-Whitmore mountains; TAM, Transantarctic Mountains; PLB, Palmer Land ensialic basin; WSE, Weddell Sea embayment; RV, Rocas Verdes.

UPPER PROTEROZOIC RIFT-RELATED BASIN AND BIMODAL VOLCANIC SEQUENCES IN THE PENSACOLA MOUNTAINS, ANTARCTICA: PRECURSOR TO CAMBRIAN SUPERCONTINENT BREAK-UP?

B.C. Storey, D.I.M. Macdonald, I.L. Millar, R.J. Pankhurst, British Antarctic Survey, Natural Environment Research Council, High Cross, Madingley Road, Cambridge, CB3 0ET, U.K.

T. Alabaster, Sunderland Polytechnic, School of Environmental Technology, Benedict Building, St George's Way, Stockton Road, Sunderland, SR2 7BW, U.K.

I.W.D. Dalziel, Institute for Geophysics, University of Texas at Austin, 8701 North Mopac Boulevard, Austin, Texas 78759, U.S.A.

Deformed Upper Proterozoic turbiditic sedimentary sequences are well known along the length of the Transantarctic Mountains although there is no consensus as to their tectonic significance. Both active and passive margin settings bordering the East Antarctic craton have been considered.

Data from the joint BAS/USAP West Antarctic Tectonic Project in the Pensacola Mountains suggest that Upper Precambrian clastic sedimentary rocks of the Patuxent Formation and associated bimodal volcanic rocks formed in an intra-continental rift setting. The greywacke-shale sequence was derived from a non-volcanic continental source and is typical of the mid-fan area of a continental slope or rise submarine fan deposit. Interbedded pillow basalts and intrusive basaltic sills have enriched trace and rare-earth element signatures similar to rift-related continental tholeiitic suites. The mafic rocks have ϵ_{Nd} values (+0.9 to +3.0 at t = 750 Ma) that are compatible with derivation from a subcontinental lithospheric mantle source. Associated felsic volcanic rocks have more crustal trace element and isotopic characteristics. These features are typical of the initial rifting stages in an intra-continental rift system and contrast with those of pillow basalts within the contemporaneous Goldie Formation in the central Transantarctic Mountains. The latter are oceanic basalts formed by sea-floor spreading in a wider ocean basin setting (Borg et al., 1990). Although the extent of these basins in Antarctica is unknown, they are part of a global array of Riphean basins ranging from broad intracratonic basins (e.g. in Australia) to complex branching aulacogen systems (e.g. Pan-African).

The opening of all these extensional basins may have been a prelude to the fragmentation of a supercontinent in the Early Cambrian with formation of the Cambrian passive margin shelf limestone sequences of the Transantarctic Mountains, eastern Australia, western South America, and both western and eastern Laurentia. If Laurentia rifted from the East Antarctic margin as recently proposed (Moores, 1991; Dalziel, 1991), parts of the conjugate margin of the Riphean rift system exposed in the Transantarctic Mountains may be recognizable along the western margin of the North American craton.

The Patuxent Formation of the Pensacola Mountains was strongly deformed during the Beardmore folding event prior to the Early Cambrian transgression. There are no known associated magmatic arc rocks. This important compressive tectonism does not however appear to have a counterpart in the Upper Proterozoic strata of southwestern North America.

Borg, S.C., DePaolo, D.J., and Smith, B.M. 1990. Isotopic structure and tectonics of the central Transantarctic Mountains. Journal of Geophysical Research, 95, 6647-6667.

Dalziel, I.W.D. 1991. Pacific margins of Laurentia and East Antarctica - Australia as a conjugate rift pair: Evidence and implications for an Eocambrian supercontinent. Geology.

Moores, E.M. 1991. The southwest U.S.-East Antarctic (SWEAT) connection: A hypothesis. Geology.

PRE-BEACON TECTONIC DEVELOPMENT OF THE TRANSANTARCTIC MOUNTAINS

Edmund Stump, Department of Geology, Arizona State University,
Tempe, Arizona 85287, U. S. A.

The recent hypothesis that western Laurentia was contiguous with Antarctica during the Proterozoic, with breakup and continental drift creating the Pacific margin of Gondwana at about the Precambrian/Cambrian boundary, offers a powerful framework for interpretation of events within the pre-Beacon record of the Transantarctic Mountains (TAM). Antecedent to this idea have been the suggestion of an outboard continental mass of Proterozoic age as indicated by isotopic data, and the suggestion of rifting during both the Late Proterozoic and the Early Cambrian as indicated by volcanism. When viewed as an intracontinental tectonic belt during the Late Proterozoic, the TAM find analogues in the Gariep-Ribeira-Damara belts of Africa and South America which remained embedded within Gondwana until breakup in the Mesozoic. During the early Paleozoic, however, the TAM became a continental margin tectonic belt, characterized by subduction and the movement of terranes. A continuing problem in the fine tuning of events during this interval is our uncertainty of the absolute ages of the boundaries of the Cambrian as defined the fossil record.

The earliest record of geological activity in the TAM comes from the Miller Range where the Miller Formation was deposited prior to deformation and intrusion by the Aurora orthogneiss at approximately 1.7 Ga. The Miller Formation has been thrust over younger rocks whose basement is not exposed; however, Sm-Nd model ages from granitic rocks from northern Victoria Land (NVL) and the central Transantarctic Mountains (CTM) suggest that the lower crust under most of the TAM is Early Proterozoic in age (2.0-1.7 Ga).

Widespread deposition occurred throughout much, if not all, of the TAM during the Late Proterozic. This includes the quartzose turbidites of the Patuxent Formation in the Pensacola Mountains (PM) and the La Gorce and Goldie Formations of the CTM, as well as the shallow-water clastics and carbonates of the Cobham and Argosy Formations in the CTM. It is my preference to correlate the Skelton and Koettlitz Groups of southern Victoria Land (SVL) with formations of this timeframe, although it is possible that they represent metamorphic equivalents of Cambrian-age rocks found elsewhere in the TAM. Metasediments of the Priestley Formation and Wilson Group in NVL may also have been deposited at this time, but it is perhaps better to consider them Early Cambrian in age, deposited post-breakup, and equivalents of the Kanmantoo Group of South Australia.

Depositional models of the Late Proterozoic sedimentary cycle have traditionally evoked continental margin settings, but with the paradigm of a contiguous Laurentia the basin receiving these sediments can now be viewed as two sided, intra or intercratonic, and formed by extension of cratonic blocks within the supercontinent. Such a basin is anagolous to early deposition in the Damara orogen, and provides the continental source to the east of the Goldie Formation implied by isotopic data. Extension is signaled by basalts of oceanic affinity in the Goldie and Patuxent Formations, as well as the bi-modally associated Gorecki Rhyolite in the Patuxent Formation. The dating of this volcanism is loosely constrained at approximately 800-750 Ma. Whereas the volcanism indicates extension, it does not necessarily imply the generation of a wide basin floored by oceanic crust. My preference is that of attenuated continental crust beneath the Goldie-La Gorce-Patuxent basin.

Sedimentation was followed by an period of convergence, the so-called Beardmore Orogeny, which folded the Late Proterozoic sedimentary rocks in a single episode under lower greenschist conditions from the PM to the CTM. This is demonstrated by angular unconformaties of Middle Cambrian Nelson Limestone on Patuxent Formation in the PM and Early Cambrian Shackleton Limestone on Goldie Formation at Cotton Plateau. To the west of Cotton Plateau in the Miller Range, thrusting at amphibolite conditions of the Miller Formation over Argosy Formation along the Endurance shear zone was another result of the Beardmore Orogeny. There

at least three episodes of deformation are associated with this event. At Cotton Plateau two episodes of folding are recognized in Goldie Formation, the earlier associated with the Beardmore Orogeny, the latter associated with the Ross Orogeny, which also folds Shackleton Limestone. Because only one episode of folding has been recognized in Goldie Formation east of Cotton Plateau, it is possible that convergence during the Beardmore Orogeny focused only along the western margin of the Late Proterozoic basin, in the vicinity of a major lower crustal boundary proposed from isotopic data. The lack of magmatic activity is a characteristic of the Beardmore Orogeny that argues against subduction to any great degree. Rather, convergence of continental blocks is more likely to have produced the deformational effects that are seen. Whether or not the deformation of the Beardmore Orogeny can be carried to the Wilson Terrane (WT) in NVL is uncertain, but by comparison, the Adelaide Supergroup of South Australia is not folded during the Late Proterozoic even though its sedimentation patterns can be interpreted as forming in a Late Proterozoic extensional environment akin to than in the CTM and PM.

The age of the Beardmore Orogeny remains an elusive quantity. Partly because of the lack of magmatism, partly because of an extensive thermal overprint suffered during the Ross Orogeny. Most of the dates which originally set the Beardmore Orogeny at approximately 680-620 Ma have been revised to numbers in the range of the Ross Orogeny or interpreted as due to excess argon. The older bound on the age is the 800-750 Ma dates on the interbedded basalts of the Goldie and Patuxent Formations. The younger bound on the age is pre-mid-Early Cambrian (Atdabanian), the oldest fossil age from the Shackleton Limestone, by which time the supposed split with Laurentia had occurred. Rb-Sr and K-Ar data from the Nimrod Glacier area (Miller, Argosy, and Goldie Formations) spread uniformly from typical Ross ages of 490 Ma back to about 570 Ma, with a scattering of ages on back to 1100 Ma that have been interpreted as due to excess argon. The dates in the high 500's Ma are intrepreted as caused by partial resetting of original Beardmore ages, but the exact timing is uncertain. Several pre-Ross-age granites may exist. The Lonely Ridge granodiorite from western Nilsen Plateau at 620 ± 13 Ma, the Carlyon granodiorite of the Darwin Glacier area at 568 ± 10 Ma, and the Surgeon Island granodiorite off the northern coast of NVL at 599 ± 21 Ma, all Rb-Sr, whole-rock isochron dates. The latter has been proposed to belong to a separate terrane in NVL, the Surgeon Island Terrane (SIT), with connections to Tasmania where Late Proterozoic orogeny is recorded, and possibly to the Lachlan province of southeast Australia.

The breakup of Laurentia and Gondwana comes somewhere close to the Precambrian-Cambrian boundary. If the Shackleton Limestone represents a shelf or platform deposit on the newly created, passive, continental margin, then the breakup is pre-Atdabanian. By the timescale of Harland et al. (1989) that is pre-560 Ma. The breakup unconformity in South Australia is set at the Precambrian-Cambrian boundary (570 Ma, Harland et al.). The age of the breakup from sedimentary subsidence curves globally is given within the range 626-555 Ma by Bond et al. (1984, EPSL, 70,325-345), but their best estimate for curves from western North America is 577.5 ± 22.5 Ma.

Aside from the Shackleton Limestone the only other known Early Cambrian limestones not associated with appreciable volcanics are in the Argentina Range. In both areas the rocks do not extend into the Middle Cambrian. The 1200 km distance between these two occurrences is covered by Beacon Supergroup and ice, so one could perhaps postulate continuity of an inboard carbonate shelf spanning this part of the TAM. A continuation of the Shackleton Limestone north of Byrd Glacier, however, would appear not to be justified. Some carbonates do exist in the Koettlitz and Skelton Groups, but they are not nearly as extensive as the Shackleton Limestone, and are more closely associated with clastic rocks, which argues for their correlation with Cobham and Argosy Formations. Lower crustal boundaries mapped from isotopic data indicate that approximately 125 km of dextral offset has occurred along Byrd Glacier, but this is not sufficient to project Shackleton Limestone into the Ross Sea east of the Dry Valleys. The offset in fact may be a result of displacement during the breakup, thus producing a northern boundary to the Shackleton basin. The suggestion that the

discontinuity down Byrd Glacier was produced by strike-slip faulting during formation of the Ross embayment is unlikely since there is no offset in the arcing of the Transantarctic Mountains Front at Byrd Glacier. Alternatively, the displacement along Byrd Glacier could have occurred at a number of other times prior to the uplift of the present day TAM, either pre- or post-Beacon.

Outboard of the carbonate platform sediments is an association of volcanics and carbonates, the Liv Group of the CTM and the Nelson Limestone-Gambacorta Formation-Wiens Formation of the PM. The age range of this association of rocks is perhaps Early to Middle Cambrian. Middle Cambrian trilobites are known from the Leverett Formation (Liv Group) and the Nelson Limestone. The Early Cambrian age, based on small tube fossils in the Taylor Formation (Liv Group), is less certain. The volcanic suite is bi-modal, at least in the Liv Group, indicating generation in an extensional environment. Whether the Early Cambrian age is accepted or not, this episode of volcanism indicates continued extension in the vicinity of the Antarctic continental margin, but outboard of carbonate platform deposits, as the ocean basin between Laurentia and Antarctica widened. It is unlikely that the outboard sequence is allochthonous to the Antarctic continental margin to any great extent for the correlative Goldie and Patuxent Formations are overlain by inboard Shackelton Limestone and outboard Nelson Limestone-Gambacorta Formation, respectively.

The extensional or passive margin regime in the TAM changed to one of subduction with resultant compresive deformation and magmatism at sometime during the Middle to Late Cambrian, the so-called Ross Orogeny. This event was probably diachronous throughout the length of the TAM, and it certainly is manifested differently at different places. The oldest isotopic dates are Rb-Sr whole-rock isochrons at about 550 Ma from the Lanterman Metamorphics of the eastern WT in NVL, and elsewhere in the WT early magmatism and metamophism are dated at about 535 Ma by the same technique. Deformation in the WT is syn-metamorphic. These dates are older than others associated with the Ross Orogeny elsewhere in the TAM, and may indicate that subduction began earlier in NVL while extension was occurring along the continental margin in the CTM and PM.

The main episode of compressive deformation probably occurred in the Late Cambrian, synchronous with and closely followed by extensive magmatism. Isotopic dates are seldom older than 510 Ma, and the large majority fall in the interval 500-470 Ma, with a spread several 10's of million years down from there, representing slower cooling at places. This approximately 500 Ma interval of compression and magma generation, which I have called the "Pannotios" event, occurred throughout Gondwana, signaling not only subduction along the Pacific margin, but the final consolidation of cratonic blocks within Gondwana , along the lines of late Proteorzoic orogenesis which in the Antarctic and Australian sector had become the line of breakup.

Ross deformation varies along the length of the TAM, and also as a function of distance from the mobile core of the orogen. On the cratonward side of the belt some rocks are actually unaffected by the deformation, e.g. the Shackleton Limestone at the head of Beardmore Glacier and the Mt. Walcott Formation of the Thiel Mountains, both of which are flat-lying. The Miller Range also was affected only by broad warps perhaps associated with intrusion of the Hope Granite. Intense compression, however, is indicated in the tightly folded Shackleton Limestone and Liv Group of the CTM.

Thrust faulting also occurred in the CTM. In the Duncan Mountains Duncan Formation is thrust over Fairweather Formation (Liv Group). The Duncan Formation has at times been correlated with the Goldie and La Gorce Formations, but no prior folding during the Beardmore Orogeny has been found. This may be explained by the argument implying that Beardmore deformation was focused along the western margin of the late Proterozoic basin and that the eastern occurrences of Goldie Formation escaped Beardmore folding. Alternatively the Duncan Formation could be a Cambrian slope sequence deposited outboard of the belt of carbonates and volcanics, and later thrust onto it. Another thrust fault is located in the La Gorce Mountains where La Gorce Formation is thrust over Wyatt Formation. The volcanic and hypabyssal Wyatt porphyries and associated marine, sedimentary Ackerman Formation are likely correlatives of the Thiel Mountains Prophyry and Mt. Walcott Formation that have been

Rb-Sr dated at about 495 Ma. These rocks are the youngest volcanics associated with the Ross interval, and likely represent surface manifestations of the extensive plutonic activity occurring at the time. Another faulted contact between La Gorce and Wyatt Formations occurs in the Cox Peaks roof pendent, where right-lateral, strike-slip motion is indicated. This locality is important for it demonstrates what has previously only been modelled, that some component of strike-slip motion was occurring during the Cambro-Ordovician in the TAM.

Deformation in the PM was less intense than in the CTM with an angular discordance beneath the Neptune Group of generally not more than 15 degrees, and no appreciable angular discordance with Devonian to Permain-age rocks above. The less intense Ross deformation in the PM may be due to its location in the cul-de-sac left by the departure of Laurentia, where subduction processes did not have as much freedom to work as they did farther along the more open Antarctic margin. This suggestion is supported by the relivitely minor amount of granitic plutonism in the PM when compared to the CTM, SVL, and NVL. The observation that Ross deformation occurred in the upper Scott Glacier area and the PM, which if a line were drawn between them would place the flat-lying Thiel Mountains in a more outboard position, may indicate that irregularities occurred in the continental margin at the time of breakup.

In SVL deformation of both the Koettlitz and Skelton Groups was mulitple, with three episodes occurring in many places. Due to the uncertainty of the age of these rocks, the timing of their deformation is also questionable. Both Beardmore and Ross structures are possible if the rocks are correlative with the Argosy and Cobham Formations, or the deformation could be primarily Beardmore. To be sure, extensive plutonism occurred in SVL around 500-470 Ma.

In the WT of NVL deformation also was multiple, but the episodes are thought to have occurred during one prograde metamorphic event. Cooling ages on metamorphic and plutonic rocks, as elsewhere in the TAM are around 500-470 Ma indicating a culmination of tectonism within the same timeframe as elsewhere. The interpretation is that deformation of the WT was Ross in age, albeit that this activity began earlier in the WT than the rest of the TAM.

Deformation and uplift of the Shackleton and Nelson Limestones produced karsted erosion surfaces. Locally derived clastic units of probable terrestrial origin overlie these surfaces, the Douglas Conglomerate and Starshot Formation in the CTM and the Neptune Group in the PM. Lacking fossils and cross-cutting plutonic rocks, the age of these deposits is loosely constrained by overlying Devonian strata and the age of the limestones beneath. If one considers that marine conditions persisted at least until the deposition of the Ackerman and Mt. Walcott Formations (circa. 495 Ma), then these terrestrial clastics may be younger, deposited after final retreat of the seas from the CTM and PM, perhaps in the Early or Middle Ordovician. The Neptune Group was not appreciably deformed before the late Paleozoic-Triassic Gondwanide Orogeny, consistant with the moderate tilting that occurred in the Nelson Limestone during Ross deformation. The Douglas and Starshot, however, were strongly folded during movements that postdate folding of the Shackleton Limestone, and may postdate the principal episode of Ross intrusion. Granitic cobbles are found in the polymict Douglas Conglomerate.

One other indication of post-500 Ma movement in the TAM is in NVL where it has been suggested that rocks east of the eastern boundary of the WT were removed after metamorphism and intrusion (Ross), but before docking of the Bowers terrane (BT). The argument centers on the truncated nature of trends in both the metamorphic and plutonic rocks compared to those of normal compressive continental margins. The removal of this considerable amount of material by thrusting at the converging boundary with BT seems unlikely. Rifting or strike-slip motion is preferred.

Intrusion of voluminous plutonic rocks at about 500 Ma is a unifying event throughout the TAM. Many authors have considered this magmatic arc to be the result of subduction beneath the continental margin from the Pacific. Recent isotopic data demonstrating a polarity in chemical trends reinforces this interpretation. The abrupt cessation of this magmatism may indicate a shutting off of subduction at this time.

Subsequently, the truncation of WT and deformation of Douglas Conglomerate may indicate reoriented but continuing plate motions at the continental margin.

In NVL two terranes, the Bowers (BT) and Robertson Bay (RBT), are generally thought to have been allochthonous to the Antarctic continental margin during the deposition of their sedimentary and volcanic rocks. Earliest activity in the BT is the formation of an intra-oceanic volcanic arc (Sledgers Group) fossil-dated as Middle Cambrian. Volcanism ceased and a regressive marine sequence (Mariner Group) of late Middle to Late Cambrian age followed conformably. A regional unconformity with little or no discordance was followed by deposition of coarse-grained clastic sediments probably of terrestrial origin (Leap Year Group). Some of the conglomerates are polymict indicating in part the proximity of a plutonic source (Carryer Conglomerate), others are primarily mature, quartzose clastics (Camp Ridge Quartzite). The Leap Year Group is unfossiliferous and may be either Late Cambrian or Early Ordovician in age.

To the east of the BT is the RBT, composed primarily of a quartzose turbidite sequence (Robertson Bay Group). Fossils in a limestone slump block in a unit near the top of the Robertson Bay Group (Handler Formation) exposed near the western boundary of the RBT indicate an age of uppermost Cambrian-lowermost Ordovician. Both the Bowers Supergroup and the Robertson Bay Group were deformed during a single, upright, folding episode at very low metamorphic conditions. K-Ar, whole-rock and mica dates from both terranes occur in the range 500-460 Ma indicating that the folding in both terranes was synchronous. Amalgamation of the terranes is likely to have occurred at the same time. Only in the boundary region between the BT and RBT is there formation of schists (Millen Schists), multiple deformation, and interleaving of Bowers Supergroup and Robertson Bay Group. A thrust fault, part of which is low-angle, is well exposed in one segment of the boundary, but the high-angle Leap Year Fault may record later vertical or strike-slip movement between the terranes.

The timing and mode of juxtaposition of the BT and RBT with the WT remains controversial. I prefer to move the terranes together after intrusion of the Late Devonian Admirality Intursives (370-360 Ma). I maintain that no Admiralty plutons have yet been demonstrated to intrude the WT. In addition, the chemical and isotopic polarity of the Admiralty Intursives indicates increased involvement of continental crust to the NNE, and implies subduction in that direction during their generation. The presence of the SIT at the northern margin of the RBT is consistent with this scenario. Neither the accretionary complex for this NNE subduction, nor for that matter the full width of the Glasgow arc (as suggested by others) remains. These could have been subducted during collision of the BT and RBT with the WT, but perhaps a better explanation is their removal by rifting or transform faulting in the same manner suggested for the eastern WT. Juxtaposition of the terranes would probably have occurred shortly after intrusion of the Admiralty Intrusives. Thrusting along the boundary (Lanterman Fault Zone) is indicated as the last motion between the BT and WT, but this zone is broad and highly splayed, and earlier strike-slip motions are possible. The spread of K-Ar ages down to less than 300 Ma in the BT but not the RBT, may be signaling argon loss during and following the juxtapositioning.

In summary, the tectonic development of the TAM can be viewed as commencing in the Late Proterozoic with extension and basin development along a linear zone within the supercontinent of Gondwana plus Laurentia. This two-sided basin received thick turbidite sediments in its axial region. Close to the end of the Proterozoic an episode of convergence (Beardmore Orogeny) caused folding and thrusting along the Antarctic side of this basin from SVL to the PM. At about the Precambrian-Cambrian boundary the continent of Laurentia broke off from Gondwana and began drifting away creating a passive continental margin adjacent to the widening Pacific Ocean. Carbonate platform deposits accumulated along the margin at least from the CTM to the PM during the Early Cambrian. Perhaps during the Early Cambrian and certainly during the Middle Cambrian extension in outer portions of the continental margin produced a suite of bi-modal volcanics associated with limestones. By Middle Cambrian subduction had begun along the continental margin in NVL, but it did not reach the CTM and PM until Late Cambrian. Tectonic activity, deformation and plutonism, culminated about 500 Ma throughout the TAM, and subduction ceased

shortly thereafter. Transverse motions along the continental margin continued in the Early to Middle Ordovician. Independently during the Middle and Late Cambrian, an early volcanic arc and ongoing sedimentation were creating the allochthonous BT, RBT, and SIT. These terranes were effected by an episode of subduction directed away from the TAM during the Late Devonian and shortly thereafter they were amalgamated with the Antarctic continental margin. Already by this time sediments of the Beacon Supergroup were accumulating above the eroded orogenic belt from SVL to the PM.

SELECTED REFERENCES

Adams, C.J.D., Gabites, J., and Grindley, G.W., 1982, Orogenic history of the Central Transantarctic Mountains: New K-Ar age data on the Precambrian-Early Paleozoic basement, in Craddock, C., ed., Antarctic Geoscience: University of Wisconsin Press, 817-826.

Borg, S. G., DePaolo, D. J., and Smith, B. M., 1990, Isotopic structure and tectonics of the central Transantarctic Mountains: Journal of Geophysical Research, v. 95, p. 6647-6667.

Borg, S.G., Stump., E., Chappell, B.W., McCulloch, M.T., Wyborn, D., Armstrong, R.L., and Holloway, J.R., 1987, Granitoids of northern Victoria Land, Antarctica: Implications of chemical and isotopic variations to regional crustal structure and tectonics: A.J.S., v. 287, p. 127-169.

Bradshaw, J.D., 1987, Terrane boundaries and terrane displacement in northern Victoria Land, Antarctica: Some problems and constraints, in Leitch, E.C., and Scheibner, E., eds., Terrane accretion and orogenic belts, AGU, Geodynamics Series, v. 19, p. 199-205.

Carmignani, L., Ghezzo, C., Gosso, G., Lombardo, B.,Meccheri, M.,Montrasio, A., Pertusati, P. C., and Salvini, F., 1989, Geology of the Wilson terrane in the area between David and Mariner Glaciers, Victoria Land (Antarctica): Memorie Societa Geologica Itaniana, v.33, p.77-97.

Findlay, R.H., Skinner, D.N.B., and Craw, D., 1984, Lithostratigraphy and structure of the Koettlitz Group, McMurdo Sound, Antarctica: New Zealand Journal of Geology and Geophysics, v. 27, p. 513-536.

GANOVEX Team, 1987, Geological map of north Victoria Land, Antarctica, 1:500 000, Explanatory notes: Geologisches Jahrbuch, v. B 66, p. 7-79.

Goodge, J. W., Borg, S. G., Smith, B. K., and Bennett, V. C., 1991, Tectonic significance of Proterozoic ductile shortening and translation along the Antarctic margin of Gondwana: Earth and Planetary Science Letters, v. 102, p. 58-70.

Laird, M.G., Mansergh, G.D., and Chappell, J.M.A., 1971, Geology of the central Nimrod Glacier area, Antarctica: New Zealand Journal of Geology and Geophysics, v. 14, p. 427-468.

Pankhurst, R.J., Storey, B.C., Millar, I.L., Macdonald, D.I.M., and Vennum, W.R., 1988, Cambro-Ordovician magmatism in the Thiel Mountains, Transantarctic Mountains, and implications for the Beardmore Orogeny: Geology, v. 16, p. 246-249.

Rowell, A. J., and Rees, M. N., 1989, Early Paleozoic history of the upper Beardmore Glacier area: implications for a major Antarctic structural boundary within the Transantarctic Mountains: Antractic Science, v. 1, p. 249-260.

Stump, E., 1987, Construction of the Pacific margin of Gondwana during the Pannotios cycle, in McKenzie, G.D., ed., Gondwana Six: Structure, Tectonics and Geophysics: AGU, Geophysical Monograph , v. 40, p. 77-87.

Tessensohn, F., 1984, Geological and tectonic history of the Bowers structural zone, North Victoria Land, Antarctica: Geologisches Jahrbuch, v. 60, p. 371-396.

Weaver, S.D., Bradshaw, J.D., and Laird, M.G., 1984, Geochemistry of Cambrian volcanics of the Bowers Supergroup and implications for the Early Paleozoic tectonic evolution of northern Victoria Land, Antarctica: Earth and Planetary Science Letters, v.68, p.128-140.

ALLUVIAL PLAIN SEDIMENTATION NEAR THE NORTHERN MARGIN OF THE DEVONIAN McMURDO BASIN, ROSS SEA REGION, ANTARCTICA: EVIDENCE FROM TAYLOR GROUP OF THE CONVOY RANGE, SOUTHERN VICTORIA LAND

R.Sykes, DSIR Geology & Geophysics,
PO Box 30 368, Lower Hutt, New Zealand

The 1200 m sequence of Devonian Taylor Group sediments (lower Beacon Supergroup) in the Dry Valleys of southern Victoria Land represents the depocentre of the regionally extensive McMurdo Basin. To the north, the sequence onlaps crystalline basement (Early Paleozoic and/or Precambrian) and thins considerably. The 300 m sequence in the Convoy Range is the northernmost occurrence of Taylor Group and excellent exposure permits detailed facies and paleocurrent analysis for this part of the basin.

Throughout the Convoy Range, Taylor Group consists almost entirely of a single, coarsening-upward sequence of quartzose sandstone. A consistent change in sedimentological character between the lower and upper parts of the sequence defines two distinct but partly interdigitating lithofacies: a floodplain facies and braided fluvial facies, respectively. Both facies are devoid of mudstone, carbonaceous matter and body fossils.

The floodplain facies is fine- to medium-grained and distinctly well-bedded. Parallel and ripple bedding predominate, with interbedded small-to medium-scale (<30 cm thick) trough and planar cross-bedding. These sediments are well bioturbated, with **Beaconites barretti, Beaconites antarcticus** and **Diplichnites gouldi** the principal ichnospecies present. Also prominent are large-scale (>30 cm) planar cross-beds, up to 2.5 m thick and up to 500 m or more in lateral extent. Their internal architecture of radiating, wedge-shaped sets, their lateral persistence, and predominant association with well-bedded strata rather than channels, strongly suggest a deltaic origin. These deltas prograded south to southeast into shallow lakes on the floodplain, away from the fluvial axis (see below). Small, isolated channels within the facies are interpreted as crevasse or distributary channels that supplied sediment to the delta fronts.

The braided fluvial facies coarsens upward from medium sandstone to slightly gravelly, coarse to very coarse sandstone. The facies is dominated by multistacked and multilateral sandstone channels, with only minor interspersed overbank deposits of laminated fine to very fine sandstone. The channels are typically shallow, less than 3 m, and about 20 m wide. Channel-fill sandstones are predominantly trough cross-bedded with most beds less than 50 cm thick but up to 1.5 m. Paleocurrent data indicates the fluvial system flowed east to northeast. Trace fossils are common but generally indistinct.

In summary, Taylor Group sediments in the Convoy Range represent part of an east to northeast-sloping alluvial plain, crossed by a major braided fluvial system and accomodating floodplain, lacustrine and lacustrine delta environments. The sediments described here are similar to and correlative with, the Arena Sandstone (floodplain facies) and Beacon Heights Orthoquartzite (braided fluvial facies) of Taylor Group in the Dry Valleys. A similar northeast-sloping alluvial plain environment has previously been interpreted for these formations and it appears likely that a single vast alluvial plain covered the whole Dry Valleys to Convoy Range area during this part of the Devonian.

PETROCHEMICAL CHARACTER OF THE GRANITES FROM THE SØR RONDANE MOUNTAINS, EAST ANTARCTICA

Yoshiaki Tainosho, Department of Geology, Faculty of Education, Kobe University, Nada-ku, Kobe 657.
Yuhei Takahashi, Geological Survey of Japan, 1-3, Higashi-1, Tsukuba 305.
Yasuhito Osanai, Department of Earth Sciences and Astronomy, Fukuoka University of Education, 729, Akama, Munakata 811-41.
Noriyoshi Tsuchiya, Department of Mining and Mineral Engineering, Faculty of Engineering, Tohoku University, Aobayama, Sendai 980.
Tohru Sakiyama, Natural history Museum and Institute project administration office, Cyuo-ku, Kobe 656.
Masaaki Owada, Department of Geology and Mineralogy, Faculty of Science, University of Yamaguchi, 1677-1, Yoshida, Yamaguchi 753.

1. Introduction

Granites directly reflect the composition of their source rocks. Many granites come from the deeper parts of the Earth's crust, their study can provide information about the nature of parts of that deep crust. Granites are widely distributed in the Sør Rondane Mountains, East Antarctica. These granites show patterns of regional variation in which discontinuities occur between provinces which internally are of a rather constant character. This paper represents the data as they relate to the recognition of petrological provinces.

2. Geological outline

The central part of the Sor Røndane Mountains consists mainly of granulite- and amphibolite-facies metamorphic rocks and granitic rocks (Kojima & Shiraishi, 1986; Ishizuka & Kojima, 1987). These metamorphic rocks can be devided into six lithologic units

numbered 1-6 from north to south that are bounded by north-dipping thrust faults(Osanai et al.,1991). The geochemical characters of the protoliths from each unit are clearly different. Granites occupying in the Sør Rondane Mountains, East Antarctica, are divided into the older(Late Proterozoic) and younger(Early Paleozoic) intrusive rocks. The Nils Larsen tonalite is the only Late Proterozoic intrusive. The younger intrusive rocks include various types of granites(Sakiyama et al.,1988;Takahashi et al.,1990,1991). Austkampane granites occur in the unit 1 area. Bergersen granites lie in the unit 2. Mefjell granites intrude unit 4. Vikinghogda, Tvitagen and Tanngarden granites are found in the unit 5. Dufek, Lunkeryggen and Rogerstopanne granites are situated at the unit 6.

3. Geochemistry of granitic rocks

3-1 Characteristics of the granites

Major and trace element analyses are presented in order to reveal petrochemical features of the granites. The Nils Larsen tonalite has a distinctively high MgO, CaO and low alkalis(Na_2O+K_2O) (Fig. 1). On the basis of its chemical and petrographic features, the Nils Larsen tonalite belongs to M-type granite which was presumably directly derived from the melting of subducted oceanic crust or the overlying mantle (White,1979). On the contrary, many of younger granites are chemically characterized by having high alkali, Zr and Nb contents and low

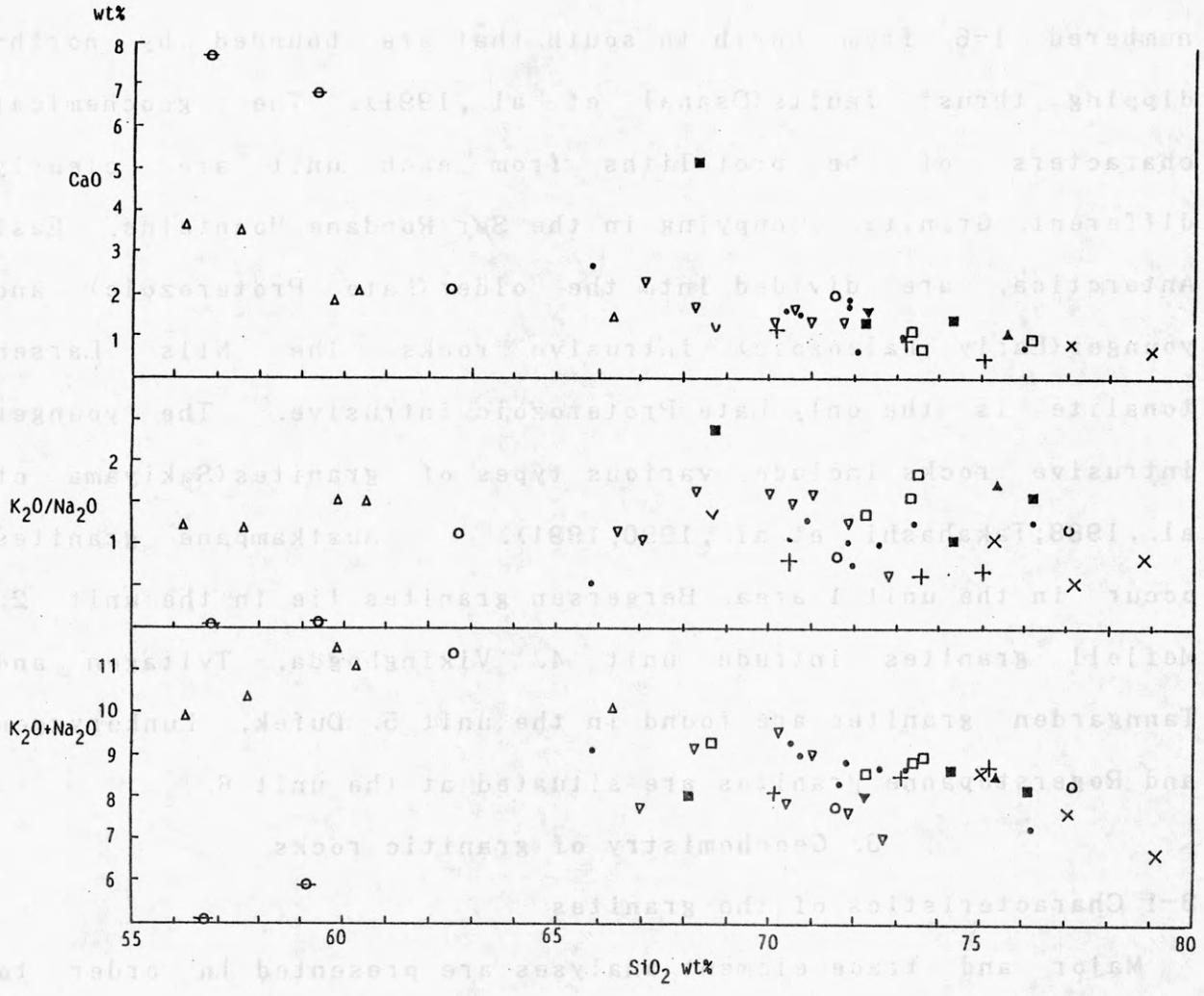

Fig. 1 Harker diagram for CaO, K_2O/Na_2O and K_2O+Na_2O in granites of the Sør Rondane Mountains. Same symbols as Fig. 2.

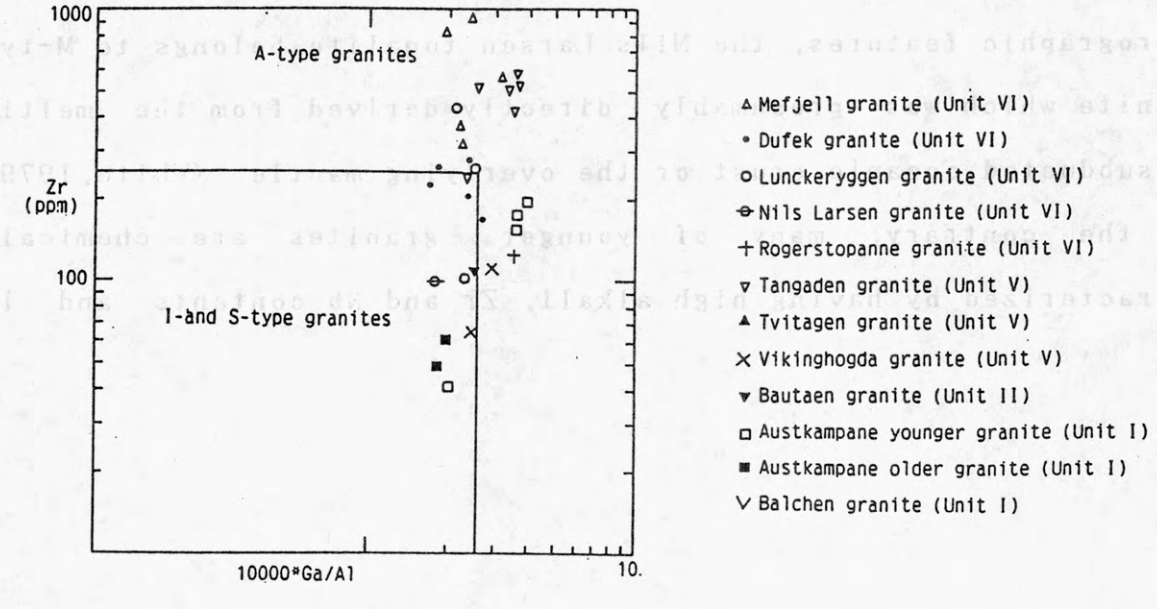

Fig. 2 10000*Ga/Al versus Zr A-type discriminant diagram of Whalen et al. (1987) for granites of the Sør Rondane Mountains.

CaO contents. In terms of trace elemets, the A-type granites are characterized by high Y, Nb, Zr and Ga content. On the 10000*Ga/Al-Zr diagram(Fig. 2), many of younger granites fall in the A-type granite field. Mefjell, Tangarden and Austkampane granites belong to A-type granites(Fig. 2). As defined by Loiselle and Wones(1979), the A-type granites occur along rift zones and within stable continental blocks. Other granites are plotted near the boundary of A-type and I-type granites(Fig. 2).

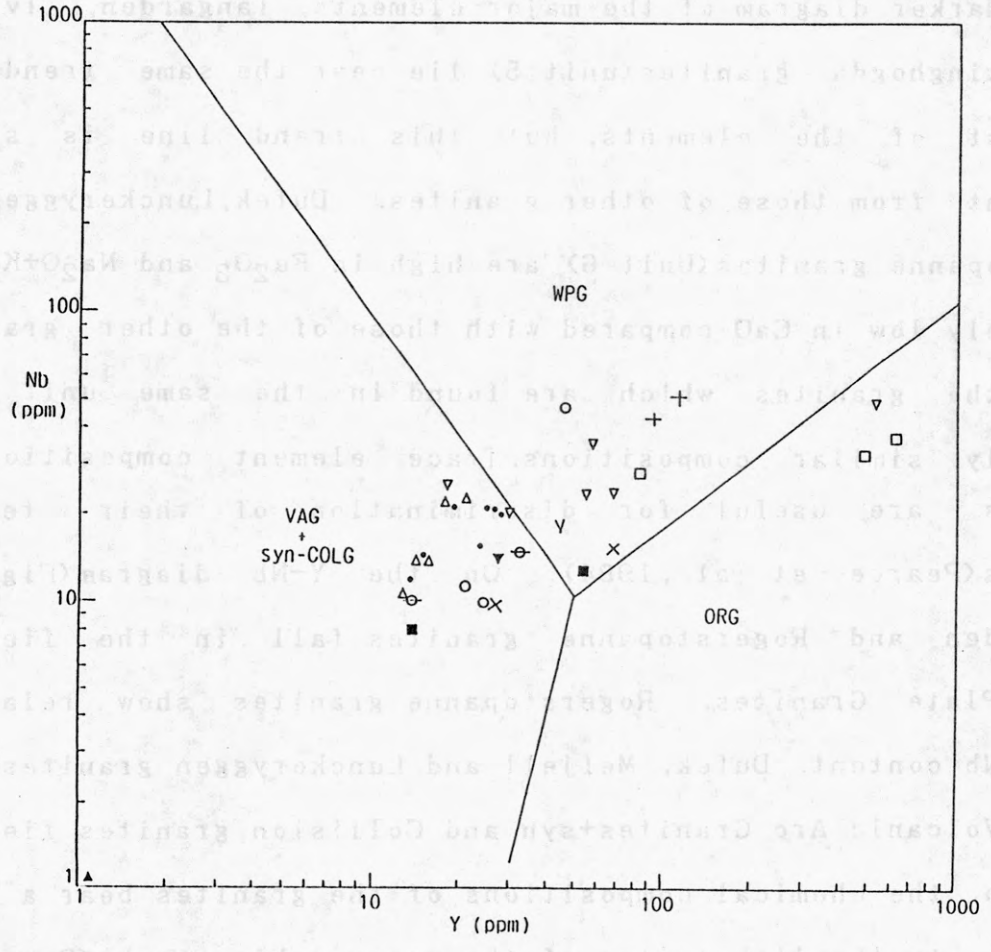

Fig. 3 Y-Nb tectonic discriminant diagram of Pearce et al. (1984). Same symbols as Fig. 2.

syn-COLG: syn-collision Granite
WPG: Within Plate Granites
ORG: Ocean Ridge Granites
VAG: Volcanic Arc Granites

3-2 Geochemical characteristics of each pluton

Chemical composition for major and trace elements of each pluton is shown in Fig. 1-3. Mefjell granites(unit 4) are rich in alkalis and BaO and somewhat enriched in Al_2O_3 and poor in MgO, CaO. Chemical composition of Mefjell granites is clearly different from those of the other granites. Austkampane granites(unit 1) have relatively higher alkalis and K_2O/Na_2O ratio and relatively lower MgO contents than the other granites. In the Harker diagram of the major elements, Tangarden, Tvitagen and Vikinghogda granites(unit 5) lie near the same trend line for most of the elements, but this trend line is slghtly different from those of other granites. Dufek, Lunckeryggen and Rogerstopanne granites(Unit 6) are high in Fe_2O_3 and Na_2O+K_2O and relatively low in CaO compared with those of the other granites. Thus, the granites which are found in the same unit have generally similar compositions. Trace element compositions of granites are useful for discrimination of their tectonic settings(Pearce et al., 1984). On the Y-Nb diagram(Fig. 3), Tanngarden and Rogerstopanne granites fall in the field of Within-Plate Granites. Rogerstopanne granites show relatively higher Nb content. Dufek, Mefjell and Lunckeryggen granites fall in the Volcanic Arc Granites+syn and Collision granites field. In addition, the chemical compositions of the granites bear a close relation to the lithologies of the metamorphic rocks(Osanai et

al. 1991). The NH_4^+ content of biotites in the granites is also related to the six lithologic units (Tainosho et al. 1991). The granites intrusive into a given unit have similar chemical characteristics in the same unit. These granites share distinct textural, modal and chemical features. Granites have chemical features that reflect their source compositions. In the Sør Rondane Mountains these features, and hence the source compositions, vary in a regional fashion. These chemical differences in those granite imply different tectonic histories of the different lithopheric blocks.

References

Ishizuka, H. and Kojima, H. (1987): Proc. NIPR Symp. Antarct. Geosci., 1, 113-128.

Kojima, S. and Shiraishi, K. (1986): Mem. Natl Inst. Polar Res., Spec. Issue, 43, 116-131.

Loiselle, M.C. and Wones, D.R. (1979): Geol. Soc. Am. Abstr. Programs, 11, 468.

Osanai, Y., Takahashi, Y., Shiraishi, K., Sakiyama, T., Tainosho, Y., Tsuchiya, Y. and Ishizuka, H. (1991): Proc. NIPR Symp. Antart. Geosci., 5, (in press).

Pearce, J.A., Harris, N.B.W. and Tindle, A.G. (1984): J. Petrol., 25, 956-983.

Sakiyama, T., Takahashi, Y. and Osanai, Y. (1988): Proc. NIPR Symp. Antart. Geosci., 2, 80-95.

Tainosho, Y., Takahashi, Y., Osanai, Y. and Tsuchiya, N. (1991): Proc. NIPR Symp. Antart. Geosci., 5, (in press).

Takahashi, Y., Arakawa, Y., Sekiyama, T. Osanai, Y. and Makimoto, H. (1990): Proc. NIPR symp. Antarct. Geosci., 4, 1-8.

Takahashi, Y., Tainosho, Y., Osanai, Y. and Tsuchiya, N. (1991): Program. Abstr. 11th Symp. Antarct. Geosci., 14-16.

Whalen, J.B. and Currie, K.L. and Chappell, B.W. (1987): Contrib. Mineral. Petrol., 95, 407-419.

White, A.J.R. (1979): Geol. Soc. Am. Abstr. Programs, 11, 539.

GEOLOGY AND GEOCHRONOLOGY OF THE GRANITOIDS IN THE SØR RONDANE MOUNTAINS, EAST ANTARCTICA

Yuhei Takahashi, Geological Survey of Japan, 1-3, Higashi-1, Tsukuba 305
Yoshiaki Tainosho, Department of Earth Sciences, Faculty of Education, Kobe University, Naka-ku, Kobe 657.
Yoji Arakawa, Institute of Geoscience, Universirty of Tsukuba, 1-1, Tennodai-1, Tsukuba 305.
Tohru Sakiyama, Natural History Museum Administration Office, 6-1-1, Nakayamate-dori, Chuo-ku, Kobe 650.
Masaaki Owada, Department of Geology and Mineralogy, Faculty of Science, University of Yamaguchi, 1677-1, Yoshida, Yamaguchi 753.

1. Introduction

Many intrusive rocks are emplaced into the metamorphic rocks of the Sør Rondane Mountains in East Antarctica(Fig. 1). They show various occurrences and petrography(Takahashi et al., 1990). Isotopic age data have been obtained by Belgian and Japanese scientists (Picciotto et al., 1964; Pasteels and Michot, 1970; Kojima and Shiraishi, 1986; Takigami et al., 1987, 1990; Takahashi et al., 1990).

We will first summarize the geology and geochronology of the granitoids in this mountains and then discuss the igneous activity in Early Paleozoic in the Antarctica based upon the isotopic initial ratios.

2. Geology

The intrusive rocks in the Sør Rondane Mountains include the Nils Larsen Tonalite, many granitic stocks, small dioritic to granitic bodies, and some small basic bodies. Our paper concerns the granitic stocks and small dioritic to granitic bodies, while the other

intrusive rocks (Nils Larsen Tonalite and basic rocks) will be discussed by other authors in this volume (Shiraishi et al.;Makimoto and Shiraishi).

Both concordant and discordant granitic bodies are exposed. The concordant granites include migmatitic granite (VIG, VEG and BG in Fig.1), foliated granite (AG and MG) and massive granite with migmatitic margin (PG and RmG). Discordant bodies consist of granite (LG and DG), syenite(SC) and diorite(D). In addition, small granitic sheet and dike have been found all over the area, but they are too small to be mapped out.

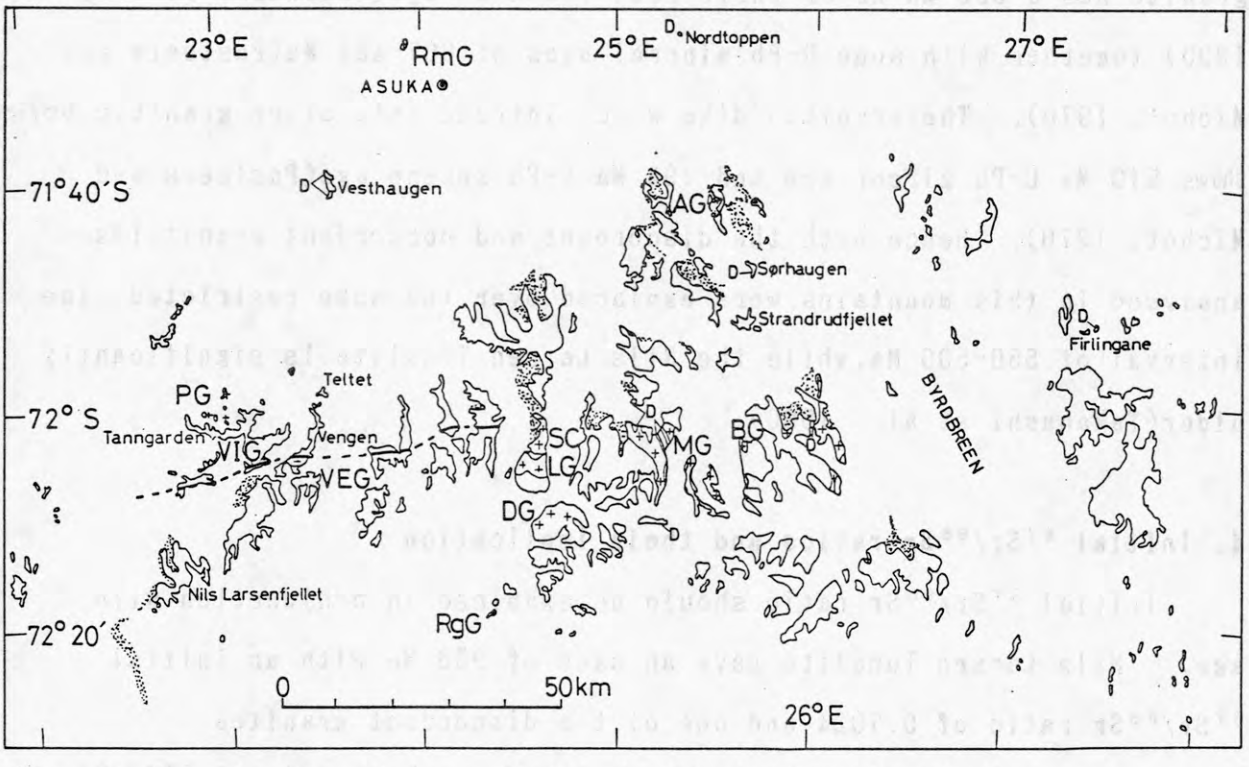

Fig. 1 Map showing the granitoids in Sør Rondane Mountains. Crossed symbols: granitic stocks(VIG:Vikinghogda Granite; VEG: Vengen Granite; BG:Bergersen Granite; AG: Austkampane Granite; MG:Mefjell Granite; PG:Pingvinane Granite;RmG:Romnoes Granite; RgG:Rogerstoppane Granite; SC:Syenite; LG:Lunckeryggen Granite; DG:Dufek Granite). D:diorite.

The modal compositions of the granitic stocks correspond to granite, quartz monzosyenite, and monzosyenite and syenite composition according to the IUGS classification.

3. Geochronology

The isotopic age data on the intrusive rocks are summarized into Fig.2. K-Ar and Rb-Sr mineral ages are generally younger than U-Pb mineral and Rb-Sr whole rock isochron ages. We infer that the U-Pb mineral ages and Rb-Sr whole rock isochron ages date the emplacement age of magma. One concordant granite has 521 and 552 Ma U-Pb zircon age(Pasteels and Michot, 1970), and a representative discordant granite has a 525 Ma Rb-Sr whole rock isochron age(Takahashi et al., 1990) together with some U-Pb mineral ages of 607-494 Ma(Pasteels and Michot, 1970). The granitic dike which intrude into other granitic bodies shows 510 Ma U-Pb zircon age and 498 Ma U-Pb sphene age(Pasteels and Michot, 1970). Hence both the discordant and concordant granitoids analysed in this mountains were emplaced over the some restricted time interval of 550-500 Ma,while the Nils Larsen Tonalite is significantly older(Takahashi et al., 1990).

4. Initial $^{87}Sr/^{86}Sr$ ratios and their implication

Initial $^{87}Sr/^{86}Sr$ ratio should be examined in conjunction with age. Nils Larsen Tonalite gave an ages of 956 Ma with an initial $^{87}Sr/^{86}Sr$ ratio of 0.7024 and one of the discordant granites (Lunckeryggen Granite) gave an age of 525 Ma with an initial $^{87}Sr/^{86}Sr$ ratio of 0.7050 (Takahashi et al., 1990). In addition to these, initial $^{87}Sr/^{86}Sr$ ratio for some granitic stocks are newly calculated from one sample each at assumed age, 500Ma ; 0.7041-0.7042 (Dufek Granite), 0.7053-0.7057(Mefjell Granite), 0.7056(Pingvinane Granite) and 0.7076 (Vikinghogda Granite)(Table 1).

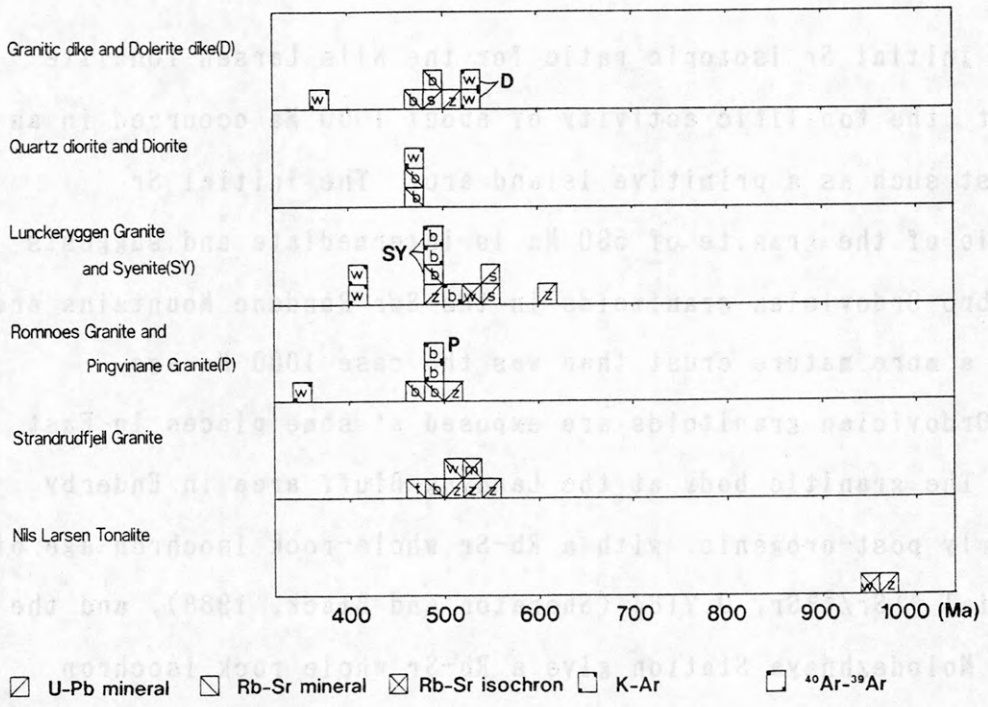

Fig. 2 Isotopic ages for the intrusive rocks in the Sør Rondane Mountains(Picciotto et al.,1963; Pasteels and Michot,1970; Kojima and Shiraishi,1986;Takahashi et al.,1990; Takigami and Funaki,1990). b:biotite, f:feldspar, s:sphene, z:zircon, m: mineral-whole rock, w: whole rock.

Table 1 $^{87}Sr/^{86}Sr$ isotopic initial ratio for the intrusive rocks in the Sør Rondane Mountains(Takahashi et al.,1990; Arakawa,unpublished data).

	n	isochron age	initial ratio(assumed age)
Lunckeryggen Granite	7	525±32	0.70504±0.00025
Dufek Granite		———	0.70413 (500 Ma)
			0.70419
Pingvinane Granite		———	0.70557 (500 Ma)
Mefjell Granite		———	0.70529 (500 Ma)
			0.70566
Vikinghogda Granite		———	0.70757 (500 Ma)
Nils Larsen Tonalite	5	956±39	0.70237±0.00019

The low initial Sr isotopic ratio for the Nils Larsen Tonalite suggests that the tonalitic activity of about 1000 Ma occurred in an immature crust such as a primitive island arc. The initial Sr isotopic ratio of the granite of 530 Ma is intermediate and suggests that the Cambro-Ordovician granitoids in the Sør Rondane Mountains are derived from a more mature crust than was the case 1000 Ma ago.

Cambro-Ordovician granitoids are exposed at some places in East Antarctica. The granitic body at the Landing Bluff area in Enderby Land is clearly post-orogenic, with a Rb-Sr whole-rock isochron age of 493 Ma, initial $^{87}Sr/^{86}Sr$, 0.7184 (Sheraton and Black, 1988), and the granite near Molodezhnaya Station give a Rb-Sr whole rock isochron age, 512 Ma, with an initial ratio, 0.7134 (Grew, 1978). The Granite Harbour Intrusives of Northern Victoia Land (Vetter et al.,1983) show the highly variable Sr and Nd initial(510Ma) isotopic ratios, 0.70649-0.71130 and 0.51151-0.51174 respectively (Armienti et al., 1990).

The Cambro-Ordovician granitoids in Sør Rondane Mountains have lower initial $^{87}Sr/^{86}Sr$ ratios than the granitoids of the other area of East Antarctica. It is concluded that they were producedin inner continent apart from the subduction zone and may be related with the internal fracturing of Gondwanaland(Osanai et al., in press).

References

Armienti, P., Ghezzo, C., Innocenti, F., Manetti, P., Rocchi, S. and Tonrini, S.(1990): Eur. J. Mineral., **2**, 103-123.

Grew, E. S. (1978): Geol. Soc. Am. Bull., **89**, 801-813.

Kojima, S. and Shiraishi, K.(1986): Mem. Natl Inst. Polar Res., Spec. Issue, **43**, 116-131.

Osanai, Y., Takahashi, Y., Shiraishi, K., Sakiyama, T., Tainosho, Y., Tsuchiya, Y., and Ishizuka, H.(1990): Proc. NIPR Symp. Antart.

Geosci., **5**, (in press).

Pasteels, P. and Michot, J.(1970): Eclogae Geol. Helv., **63**, 239-254.

Picciotto, E., Deutch, S. and Pasteels, P.(1963): Antarctic Geology (Adie, R. J. ed.), Amsterdam, North-Holland, 570-578.

Sheraton, J. W. and Black, L.P.(1988): Lithos, **21**, 37-52.

Takahashi, Y., Arakawa, Y., Sakiyama, T. Osanai, Y. and Makimoto, H. (1990): Proc. NIPR Symp. Antarct. Geosci., **4**, 1-8.

Takahashi, Y., Tainosho, Y., Osanai, Y. and Tsuchiya, N.(1990):Program ·Abstr. 11th Symp. Antarct. Geosci., 14-16.

Takigami, Y. and Funaki, M.(1990): Program·Abstr. 11th Symp. Antarct. Geosci., 48-50.

Takigami, Y., Kaneoka, I. and Funaki, M.(1987): Proc. NIPR Symp. Antarct. Geosci., 1, 169-177.

Vetter, U., Roland, N. W., Kreuzer, A., Lenz, H. and Besang, C.(1983): Antarctic Earth Science (Oliver R. L. et al. eds.), Australian Academy of Science and Cambridge, 140-143.

^{40}AR-^{39}AR AGES AND PALEOMAGNETIC STUDIES OF IGNEOUS AND METAMOROHIC ROCKS FROM SØR RONDANE MOUNTAINS, EAST ANTARCTICA

Y. Takigami, Kanto Gakuen University, Ohta-shi, Gunma 373, Japan
M. Funaki, National Institute of Polar Research, Kaga, Itabashi-ku, Tokyo 173, Japan
K. Tokieda, Shimane University, Matsue-shi, Shimane 690, Japan

In order to investigate the movement of East Antarctica during Precambrian and Pareozoic time, geochronological studies by the ^{40}Ar-^{39}Ar and K-Ar methods were performed together with paleomagnetic studies for igneous and metamorphic rocks collected from the Sør Rondane Mountains, East Antarctica (Fig. 1). Biotite samples separated from granite and syenite from Lunckeryggen and Pingvinane show ^{40}Ar-^{39}Ar plateau ages of about 500 Ma (Table 1 and Fig. 2), which are similar to a Rb-Sr whole rock age (526+16 Ma) for Lunckeryggen granite (Takahashi et al., 1990). K-Ar ages for biotite from Selungen and Otto Borchgrevink are 480-490 Ma, which are the same as the total-fusion ^{40}Ar-^{39}Ar ages of biotites from Lunckeryggen and Pingvinane. K-Ar and ^{40}Ar-^{39}Ar ages of 440-470 Ma were obtained for basaltic dykes and metamorphic rocks from Brattnipene, Selungen and other areas (Table 1, 2).

Compared with the reported age results for many regions of East Anarctica (e.g. Lützow-Holm Bay), the igneous activity of the Sør Rondane Mountains represented by the ^{40}Ar-^{39}Ar and K-Ar ages of 440-500 Ma was probably a part of the Late Ross Orogeny (Suzuki, 1986).

For the rocks dated by ^{40}Ar-^{39}Ar geochronology, paleomagnetic studies were performed (Funaki, 1990; Tokieda and Funaki, 1991). Virtual Geomagnetic Pole (VGP) positions are concentrated in the South Atlantic (Fig.3) and are consistent with the Zijderveld's (1968) studies of samples from the Sør Rondane Mountains. However, VGP positions of Cambrian - Ordovician samples from East Antarctica (Ongul Island, Mirny Station, etc) (Funaki, 1984) are distinctly different from that of the Sør Rondane Mountains (Fig.3). This result suggests that the Sør Rondane Mountains have been displaced relative to East Antarctica.

The ^{40}Ar-^{39}Ar age spectrum for K-feldsper samples from Lunckeryggen, which were separated from the same rock as biotite samples, show the stair-case type (Fig. 4). Slow cooling mechanism or weak thermal metamorphism may be the explanation of these age spectrum (Macdougall and Harrison, 1988). The minimum ages of 370-400 Ma are similar to the K-Ar ages obtained on some rocks from Lützow-Holm Bay, Yamato Mountains and Belgica Mountains (Hiroi and Shiraishi, 1986). However, the existence of a weak thermal event at about 370-400 Ma is not clear.

References

Funaki, M. (1984): Paleomagnetic investigation of McMurdo Sound region, southern Victoria Land, Antarctica. Mem. Natl Inst. Polar Res., Spec. C (Earth Sci.), 16, 300-308.

Funaki, M. and Tokieda, K. (1990): Natural remanent magnetizations of granite and syenite from Pingvinane and Lunckeryggen in the Sør Rondane Mountains, East Antarctica. Proc. NIPR Symp. Antarct. Geosci., 4, 67-79.

Hiroi, Y. and Shiraishi, K.(1986): Syōwa Kiti shūhen no chishitsu to ganseki (Geology and petrology around Syowa Station). Nankyoku no Kagaku, 5. Chigaku (Science in Antarctica, 5. Earth Sciences), ed. by Natl Inst. Polar Res. Tokyo, Kokon Shoin, 45-84.

MacDougall, I. and Harrison, T.M. (1988): Geochronology and thermochronology by the $^{40}Ar/^{39}Ar$ method. Oxford Monographs on Geology and Geophysics No.9. New York, Oxford University Press, 212p.

Suzuki, M. (1986): Nendai to chishitsu kubun (Geochronology and geological subdivision). Nankyoku no Kagaku, 5. Chigaku (Science in Antarctica, 5. Earth Sciences), ed. by Natl Inst. Polar Res. Tokyo, Kokon Shoin, 10-23.

Takahashi, Y., Arakawa, Y., Sakiyama, T., Osanai, Y. and Makimoto, H. (1990): Rb-Sr and K-Ar whole rock ages of the plutonic bodies from the Sør Rondane mountains, East Antarctica. Proc. NIPR Symp. Antarct. Geosci., 4, 1-8.

Takigami, Y., Kaneoka, I. and Funaki, M. (1987): Age and paleomagnetic studies for intrusive and metamorphic rocks from the Sør Rondane Mountains, Antarctica. Proc. NIPR Symp. Antarct. Geosci., 1, 169-177.

Tokieda, K. and Funaki, M.(1991): Tilting movement of Sør Rondane Mountains and possible apparent polar wander path for Precambrian to Cambrian-Ordovician. submitted in Proc. NIPR Symp. Antarct. Geosci., 5.

Zijdervelt, J. D. A. (1968): Natural remanent magnetizations of some intrusive rocks from the Sør Rondane Mountains, Queen Maud Land, Antarctica. J. Geophys. Res., 73, 3773- 3785.

Table 1. ^{40}Ar-^{39}Ar AGE

Sample site (rock type)	mineral	Plateau Age(Ma)	(Temperature; ^{39}Ar)	Total Age(Ma)
B414 Pingvinane (granite)	Biotite	498.5 ± 8.8	(800-1200 °C; 92.0%)	487.1 ± 8.8
B722 Lunckerggen (granite)	Biotite	501.1 ± 8.7	(800-1500 °C; 98.3%)	500.1 ± 8.7
	without Biotite		---------	453.2 ± 8.0
B740 Lunckerggen (syenite)	Biotite	499.7 ± 9.0	(900-1500 °C; 98.4%)	498.4 ± 9.0
	K-feldspar		---------	443.8 ± 8.1
B788 Lunckerggen (syenite)	Biotite	495.7 ± 8.9	(880-1500 °C; 92.8%)	491.8 ± 8.8
	K-feldspar		---------	413.6 ± 7.6
B858 Brattnipene (basalt dyke)	whole rock	exess Ar ---> isochron age 476.3 + 22.6 Ma		530.0 ± 9.2
1123 Nunatak 1550 (metadolerite)	whole rock	439 ± 13	(900-1500 °C; 99.3%)	438 ± 13
1120 Nunatak 1550 (gneiss)	whole rock		---------	412 ± 13

* samples 1120 and 1123 are after Takigami et al. (1987)

Table 2. K-AR AGE

sample	site	rock type	K (wt%)	rad ^{40}Ar (x10-5ccSTP/g)	air cont. (%)	Age (Ma)
B1	Selungen dyke	Bt (Qz monzonite)	5.76 ±0.04	11.3 ± 0.1	5.3	452 ± 6
B5	Selungen host	Bt (Qz syenite)	5.63 ±0.04	12.4 ± 0.1	1.2	492 ± 6
B140	Otto Borchgrevink	Bt (gneiss)	7.63 ±0.23	16.0 ± 0.1	3.2	479 ±15
B209	Nils Larsen	Bt (gneiss)	7.37 ±0.25	22.8 ± 0.2	1.3	662 ±23
B907	Vesthaugen	Whole rock (hornfels)	2.50 ±0.05	4.84 ± 0.04	0.5	439 ±10
B910	Vesthaugen (thermally metamorphosed trachybasalt?)	Whole rock	1.97 ±0.03	4.07 ± 0.03	0.1	467 ± 7
1098	Austkampane	Whole rock (gneiss)	1.07 ±0.04	2.17 ± 0.03	1.8	468 ±21
1117	Brattnipene	Whole rock (gneiss)	0.88 ±0.03	2.15 ± 0.22	5.4	551 ±56

* samples 1098 and 1117 are after TAKIGAMI et al. (1987)

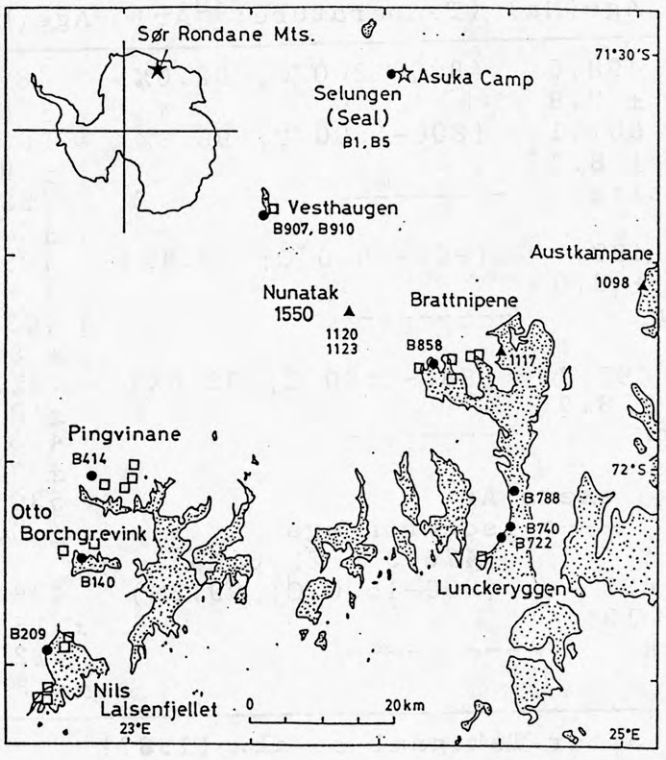

Fig.1.
Sampling sites in the Sør Rondane Mountains
●□ : Used for paleomagnetic studies
● : Used for geochronological studies

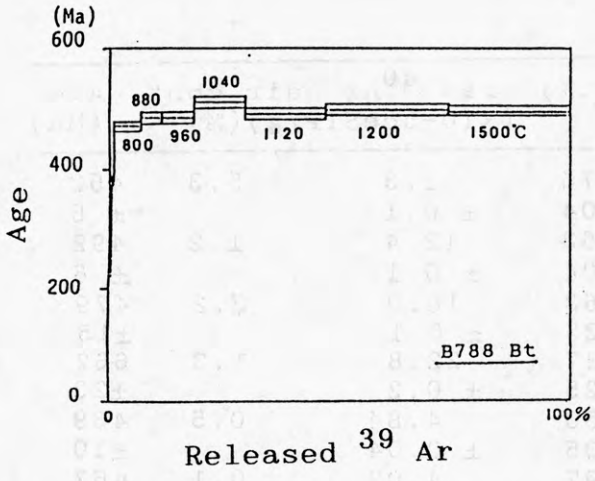

Fig.2. ^{40}Ar-^{39}Ar Age diagram of sample B788 Biotite
Virtical and horizontal axes indicate the age and the released fraction of ^{39}Ar in %. The bands in the age indicate errors of one standard deviation.

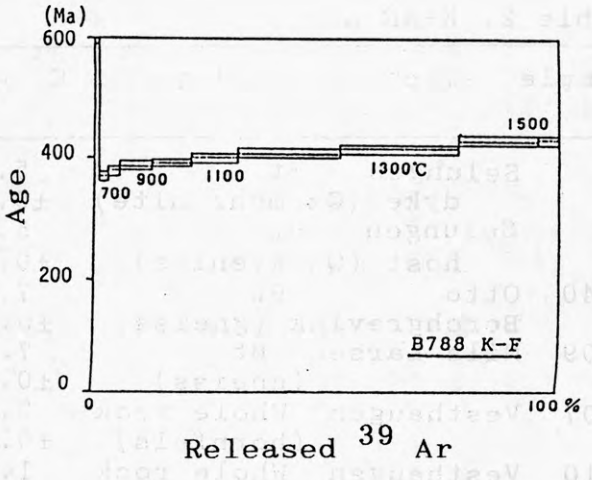

Fig.4. ^{40}Ar-^{39}Ar Age diagram of sample B788 K-Feldspar

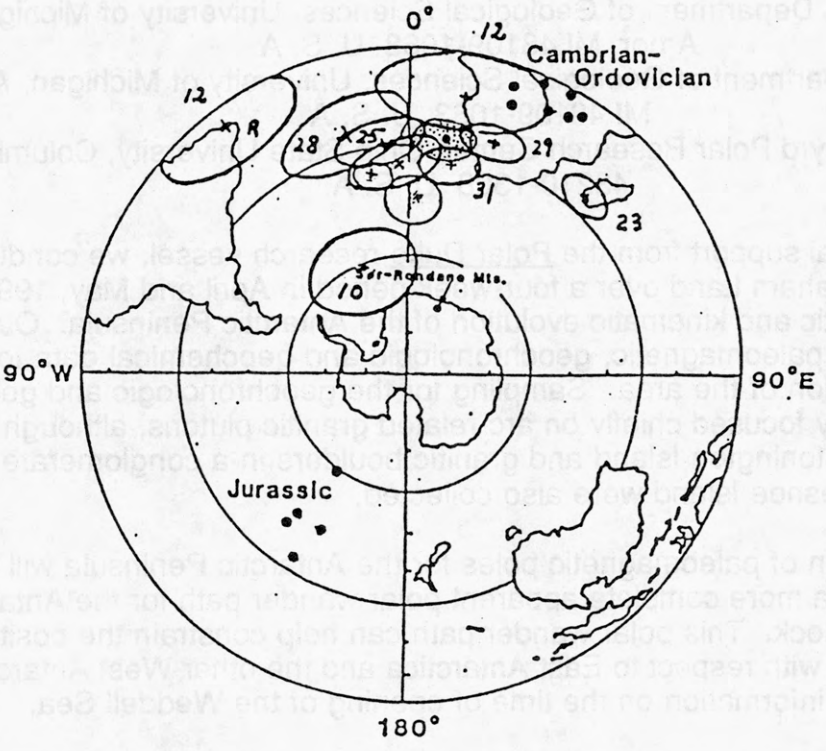

Fig.3. Virtual Geomagnetic Poles

⊕ : obtained from this study

• : obtained from previous studies for East Antarctica

⊙ : reported by Zijderveld (1968)

GEOCHRONOLOGIC AND GEOCHEMICAL CONSTRAINTS ON THE MAGMATIC AND KINEMATIC EVOLUTION OF THE WESTERN ANTARCTIC PENINSULA

J. A. Tangeman, Department of Geological Sciences, University of Michigan, Ann Arbor, MI 48109-1063 U. S. A.
S. B. Mukasa, Department of Geological Sciences, University of Michigan, Ann Arbor, MI 48109-1063 U. S. A.
A. M. Grunow, Byrd Polar Research Center, Ohio State University, Columbus, OH 43210-1308 U. S. A.

With logistical support from the Polar Duke research vessel, we conducted field work in western Graham Land over a four-week period in April and May, 1990, to assess the magmatic and kinematic evolution of the Antarctic Peninsula. Our approach is to use paleomagnetic, geochronologic and geochemical data to unravel the geologic evolution of the area. Sampling for the geochronologic and geochemical aspects of the study focused chiefly on arc-related granitic plutons, although some orthogneisses on Stonington Island and granitic boulders in a conglomerate close to a fault zone on Horseshoe Island were also collected.

Determination of paleomagnetic poles for the Antarctic Peninsula will result in the construction of a more complete apparent polar wander path for the Antarctic Peninsula crustal block. This polar wander path can help constrain the position of the Antarctic Peninsula with respect to East Antarctica and the other West Antarctic crustal blocks and provide information on the time of opening of the Weddell Sea.

Absolute crystallization ages will be determined by the zircon U-Pb dating method and metamorphic ages for the gneisses using a combination of the U-Pb and $^{40}Ar/^{39}Ar$ isotopic methods. Time constraints are vital to the precision of the apparent polar wander path constructed from the paleomagnetic data. These time constraints will also be used in conjunction with geochemical data to more clearly characterize the plutonic rocks along the western portion of Graham Land and to derive a model of calc-alkaline petrogenesis along the Antarctic Peninsula.

STABLE ISOTOPE COMPOSITION OF RECENT ANTARCTIC BIOGENIC CARBONATES AND ITS BEARING TO THE PROBLEM OF ANCIENT COLD WATER LIMESTONES

M. Taviani, Istituto Geologia Marina, CNR
via Zamboni 65, 40127 Bologna, Italy

Recognition of ancient carbonates formed at temperatures close to 0° C requires a better understanding of their modern polar counterparts. Among diagnostic characteristics, the geochemical signature can be considered a good tracer in those cases where no important diagenetic modifications occurred. Differently from temperate and tropical carbonates which also include cements, modern marine Arctic and Antarctic carbonates are almost exclusively skeletal. A growing field of research deals with the assessment of stable isotopic composition of modern and ancient polar carbonates. I plotted available published and unpublished $\delta\,^{18}O$ and $\delta\,^{13}C$ data of polar skeletal carbonates in Milliman's classic diagram. As can be seen in fig.1, Antarctic skeletal carbonates occupy a distinct field of existence which only partly overlaps the Arctic ones. Skeletal carbonates from Antarctica do not appear affected by glacier-dilution isotopic signals as is often the case in the Arctic thus representing a better model for cold-water limestones.

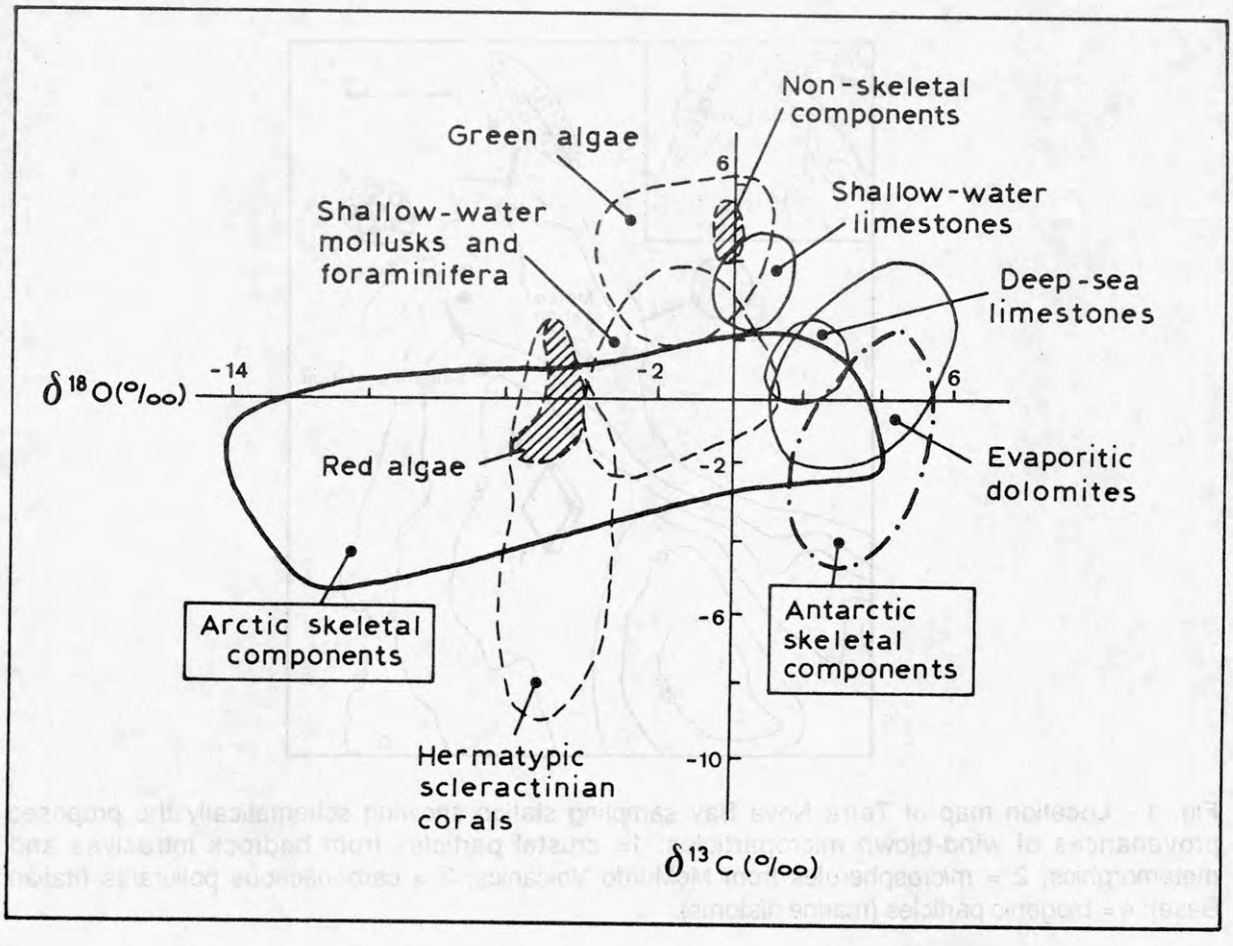

Fig. 1 - Stable isotopic composition of various marine Quaternary carbonates.

WIND-TRANSPORTED CRUSTAL MICROPARTICLES IN TERRA NOVA BAY (ANTARCTICA)

M. Taviani, S. Guerzoni, R. Lenaz, Istituto Geologia Marina, CNR, via Zamboni 65, 40127 Bologna, Italy

Interception of wind-blown dust in Terra Nova Bay by means of mesh-panels led to the recovery of a wide variety of µm-size insoluble particles subdividible into three major classes, i.e., crustal , biogenic and anthropogenic. Crustal microparticles represent the commonest category and were subjected to SEM-EDS inspection for identification. Most particles are silicatic crystal recognized as Quartz, Biotite, Illite, Hyperstene, Amphibole, Zircon. Carbonates (Calcite and Dolomite) are moderately abundant and Pyrite was also spotted. Microspherules of Al-Si-Fe composition have been considered as volcanic products. In consideration of the small particle size the transport of this crustal dust took place in suspension, while the problem remains concerning whether it represents remote material or whether abrasion and suspension took place directly on the Antarctic continent. As a working hypothesis, we suggest a local origin for most particles since there is a good correspondence between particle type and bedrock geology of this sector of Victoria Land. Further support derives from the observation that associated biogenic particles (i.e., the marine diatom *Nitzschia cylindrus*) can be tracked back to Antarctic sources.

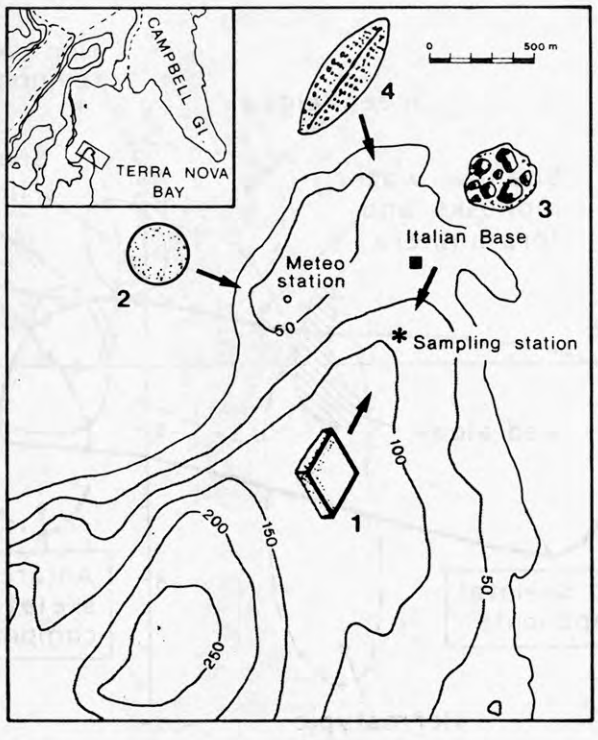

Fig. 1 - Location map of Terra Nova Bay sampling station showing schematically the proposed provenances of wind-blown microparticles: 1= crustal particles from bedrock intrusives and metamorphics; 2 = microspherules from McMurdo Volcanics; 3 = carbonaceous pollutants (Italian Base); 4 = biogenic particles (marine diatoms).

FOSSIL FORESTS FROM THE CENTRAL TRANSANTARCTIC MOUNTAINS

Edith L. Taylor, Ruben Cuneo and Thomas N. Taylor
Byrd Polar Research Center and Department of Plant Biology
Ohio State University, Columbus, OH 43210-1293 U.S.A.

During the 1990-1991 field season, two *in situ* fossil forests were studied and specimens were collected. One forest occurs in the upper Gordon Valley, near Mt. Falla (84° 11' 10" S, 164° 54' 28" E). This site is within the upper part of the Fremouw Formation and is believed to be Middle Triassic in age. The second forest occurs on Mt. Achernar, near the Law Glacier (84° 22' 23" S, 164° 37' 56" E). This site is within the Permian Buckley Formation. Both sites consist of upright stumps that have been permineralized in silica. The mean diameter of the stumps in Gordon Valley varies from 20-60 cm, while those on Mt. Achernar are smaller, averaging 9-18 cm. The mean distance between the trunks in Gordon Valley is 6.23 m; the Permian stumps average 1.95 m separation. The Gordon Valley site covers a large area (approximately 128 x 30.5 m) and includes 98 stumps in two stands. The Mt. Achernar site is about 20 x 12 m in size and includes 15 stumps. Using the point-quarter method, the density of trees at each site was determined. In Gordon Valley, mean density is 257.6 trees/hectare; on Mt. Achernar, mean density is much higher. These densities can be compared with that calculated for the Cretaceous fossil forest from Alexander Island (Antarctic peninsula) by Jefferson. An analysis of ring structure in the Mt. Achernar wood reveals that distinct growth rings are present. These are narrow (generally < 1.0 cm wide), although occasional, very large rings are present. The rings consist primarily of earlywood with a small proportion of latewood. The ring structure of the wood from these Permian and Triassic *in situ* forests can be compared with that previously examined from other sites in the Transantarctic Mountains, as well as with Jefferson's data from Alexander Island.

TRIASSIC SEED PLANTS FROM ANTARCTICA: A KEY TO UNDERSTANDING THE ORIGIN OF ANGIOSPERMS

Thomas N. Taylor, Department of Plant Biology, The Ohio State University, Columbus, Ohio 43210, U.S.A.
Edith L. Taylor, Byrd Polar Research Center, The Ohio State University, Columbus, Ohio 43210, U.S.A.

It is becoming increasingly clear that the transition from gymnospermous organization and reproduction to that encompassed by the flowering plants took place early in the Mesozoic. Dispersed pollen suggests that by at least Triassic time there were several pollen characters present that can be equated with angiospermy. There is far less information, however, from the megafossil record which can be used to document the structural and morphological changes that took place during the evolution of certain flowering plant features. One important source of such information are permineralized gymnospermous plant remains of early Middle Triassic age from the Fremouw Peak site in the Transantarctic Mountains. Recovered from this site are vascularized leaf-like cupules that measure up 2.5 cm in diameter. Anatomically the cupules are similar to leaves of Dicroidium. Cupules are multiovulate (2-5 seeds) with each of the seeds attached to the inner surface of the cupule by a delicate, elongate stalk. Seeds are triangular in transverse section and characterized by an unusual integument that is thickened only in the corners. Associated with the cupules are clusters of unilocular, elliptical pollen sacs, each approximately 2.0 mm long. Pollen grains are bisaccate and of the Alisporites or Pteruchipollenites type. Both organs represent the first permineralized reproductive structures of Triassic age that can be directly associated with the Mesozoic seed ferns, one group that has played a pivotal role in discussions regarding the origin of the angiosperms.

MODELING THE GEOMETRY OF ANTARCTIC CONTINENTAL MARGINS

Uri S. ten Brink, USGS, Branch of Atlantic Marine Geology, Woods Hole, MA 02543, USA
Alan K. Cooper, USGS, Branch of Pacific Marine Geology, Menlo Park, Ca 94025, USA

Continental margins around Antarctica are often characterized by a trough of up to 1 km deep near the coast and an unusually deep shelf (400-700 m deep at the shelf edge). In some places (e.g. Prydz Bay) the water depth increases monotonically from the shelf edge toward the coastal trough while in others (e.g., Weddell Sea, Haugland et al., 1985) a central high is located between the shelf edge and the trough.

Several factors may determine the geometry of the sea floor and the underlying stratigraphy in Antarctic margins. These are: 1. The load of the ice cap. 2. The isostatic response of the lithosphere. 3. The pattern of erosion. 4. The pattern of sedimentation. 5. Sea level changes. 6. Thermal and tectonic subsidence of the margin. 7. Possible compaction of the sedimentary section by an ice cap which has periodically covered the margin.

The effects of these factors (with the exception of compaction) were investigated using simple numerical models to simulate the sea floor bathymetry along a seismic line ODP-119 across Prydz Bay (Fig. 1; Cooper et al., in press). The seismic line is tied to five ODP boreholes which provide geological control. In these models we assume that prior to the existence of ice cap in East Antarctica the margin had a depth profile typical of low-latitudes margins, which gradually deepen from the coast to ~150 m at the shelf edge (Fig. 2a). The supply of water-suspended sediments to the margin has to a large extent terminated when the ice cap developed on land suggesting that further erosion and sedimentation on the shelf were caused by glacial advancement and retreat across the shelf (Hambrey et al., in press). In the absence of quantitative relationship between characteristic properties of the ice cap and erosion and sedimentation (e.g, Drewry, 1986, Brown et al., 1987), we measured the distribution of eroded and deposited material from the seismic section (Cooper et al., in press), but also explored hypothetical distributions of erosion and sedimentation. We further assumed that glacial advancement and retreat across the shelf occurred in cycles with periods ≥10,000 y implying that residual deformation of the asthenosphere from these movements is negligible (e.g., Cathles, 1975). Isostatic compensation to ice loading, erosion, sedimentation, and to sea-level change was therefore, assumed to be limited to the lithosphere and in our models was either local (Airy model) or regional (flexure) with variable rigidity across the margin. Following Hughes (1981, and pers. comm., 1990) the height (flow line) of the ice cap was calculated using an initial-value finite difference formulation with a basal shear stress of 0.3 bar. Regional isostatic response to ice loading was incorporated by iteratively calculating the ice flow and flexure until convergence was achieved. Lastly, we assumed that the margin has been undergoing residual thermal subsidence (e.g., Dunbar and Sawyer, 1989) because it was formed by rifting from Australia some 120 Ma (Lawver et al., in press). We assumed for simplicity linearly increasing subsidence from the coast (extension factor, β=1, no subsidence) to the shelf-edge (extension factor, β=6). A maximum of 460 m of thermal subsidence is expected to have occurred in the last 40 Ma, but only 90 m in the last 10 Ma.

Since we modeled only one chrono-stratigraphic horizon (i.e., the sea floor) and the effect of compaction was not investigated, the models consist of only one time step, which is the present situation. We can make the reasonable assumption that lithospheric rigidity has not changed significantly in Prydz Bay since the commencement of Antarctic glaciation and, therefore, the effects of erosion, sedimentation, and sea level can be considered cumulative. (This assumption may fail in more recently active margins, such as the Ross Sea).

At least two different models can fit the shape of the sea floor equally well (Fig. 2b): One which uses the observed distribution of sediments and erosion and allows for variations of the

other parameters. The other model assumes Airy local isostasy and lets all the other parameters including sedimentation and erosion vary. A model with Airy isostasy is simple because the shelf geometry is not affected by the loads of either the ice cap or the large prograding sequence of glacial sediments in the outer shelf. The areal extent and amplitude of erosion for the Airy model are, however, double the observed, while the extent and amplitude of the topset flat-lying sediments are less than half the observed (Fig. 2c).

The relative contribution of the different parameters to the unique shape of the Antarctic margins was investigated by the model which uses the observed distirbution of sedimentation and erosion. The model which best predicts the observed profile of the sea floor is one where the margin has a very high rigidity (elastic thickness, Te=100 km) and where thermal subsidence has been negligible (<100 m). Models with lower rigidity (including the extreme case of local isostasy) produce markedly different bathymetric profile with a central high in the middle of the shelf and an increasing depth both landward and seaward (Fig. 3a). By adding thermal subsidence the margin becomes much deeper and is tilted seaward over large part of the shelf (Fig. 3b).

While an elastic thickness on the order of 100 km was determined for East Antarctica (Stern and ten Brink, 1989), the rigidity (i.e., elastic thickness) of continental margins is, usually thought to be considerably smaller (e.g., ten Brink and Stern, in press). The thickness of post-rift pre-glacial sediments in the shelf in the vicinity of this profile is very small (0.5-2.5 km) (Cooper et al., in press) indicating little thermal subsidence and β, which is probably $<<6$. This suggests little thermal perturbation of the lithosphere along the transect. Since lithospheric rigidity is strongly dependent on temperature, no appreciable reduction in flexural rigidity is expected from land toward the margin. Models with lower rigidity across the margin may, on the other hand, fit better margins such as Weddell Sea (Haugland et al., 1985) with a local high at the center of the shelf.

The static contribution of the continental ice sheet to the shape of the margin is small (on the order of 100 m) regardless of the rigidity of the margin (Fig. 3c,d). This conclusion is also suggested by the bathymetry of Prydz Bay (Fig. 1) which shows that the deepest bathymetric contour is not parallel to the coast. The dynamic effect of the ice load may, however, be important as even a small initial depression may initiate and concentrate erosion close to shore.

The effect of sediment distribution on the shape of the margin is, on the other hand, significant. If instead of erosion close to shore and sedimentation toward the shelf's edge, we do not allow any erosion or sedimentation on the shelf, the shelf will deepen seaward (Fig. 3e). This geometry is observed in mature low-latitude margins where sediments by-pass the shelf and are deposited on the continental slope. If the volume of prograding slope sediments is excluded from the model, the entire margin will rise and a large part of it will be well above sea level (Fig. 3f). The exact geometry of such hypothetical margin will vary with the rigidity of the margin.

In conclusion: 1. The distribution of erosion in the inner shelf and sedimentation in the outer shelf is probably the single most important factor in determining the unique shape of Antarctic margins. 2. The static contribution of the ice cap to the shape of the margin is small. However, its dynamic contribution in initiating near-shore erosion may be important. In addition, the ice cap prevents the supply of water-suspended sediments to the margin making it "starved". 3. The flexural rigidity (i.e. isostatic response) determines the degree of interference between the various forces which shape the margin, and hence influences the geometry of the sea floor. 4. Thermal subsidence and sea level change do not seem to affect the gross shape of Prydz Bay.

References:

Brown, N.E., B. Hallet, and D.B. Booth, Rapid soft bed sliding of the Puget glacial lobe, J. Geophys. Res., 92, 8985-8997, 1987.

Cathles, L.M., The viscosity of the earth mantle, 386 pp., Princeton University Press, Princeton, N.J., 1975.

Cooper A.K., H. Stagg, and E. , Seismic stratigraphy and structure of Prydz Bay, Antarctica: Implications from ODP Leg 119 drilling: In Barron, J. and Larsen, B., eds., Scientific results of ODP Leg 119 drilling, Vol. B, College Station, Tx, Ocean Drilling Program, in press.

Drewry, D., Glacial geologic processes, 276 pp., Edward Arnold, London, U.K., 1986.

Dunbar, J.A., and D.S. Sawyer, Patterns of continental extension along the conjugate margins of the Central and North Atlantic oceans and Labrador Sea, Tectonics, 8, 1059-1077, 1989.

Hambrey, M.J., W.U. Ehrmann, and B. Larsen, The Cenozoic glacial record of the Prydz Bay continental shelf, East Antarctica: In Barron, J. and Larsen, B., eds., Scientific results of ODP Leg 119 drilling, Vol. B, College Station, Tx, Ocean Drilling Program, in press.

Haugland, K., Y. Kristoffersen, and A. Velde, Seismic investigations in the Weddell Sea Embayment, Tectonophysics, 114, 293-313, 1985.

Hughes, T.J., Numerical reconstruction of paleo-ice sheets, in: The last Great Ice Sheet, edited by G.H. Denton and T.J. Hughes, pp. 221-261, Wiley and Sons, New York, N.Y., 1981.

Lawver, L.A., J-Y Royer, D.T. Sandwell, and C.R. Scotese, Evolution of the Antarctic continental margins: In Thompson, M.A., ed., Proceedings of the 5th International Antarctic Symposium, Cambridge August 1987, Cambridge University Press, Cambridge, U.K., in press.

Stern, T.A. and U.S. ten Brink, flexural uplift of the Transantarctic Mountains, J. Geophys. Res., 94, 10315-10330, 1989.

ten Brink, U.S., and T.A. Stern, Rift-margin uplifts and hinterland basins: Comparison between the Transantarctic Mountains and the Great Escarpment of southern Africa, J. Geophys. Res., in press.

Fig.1

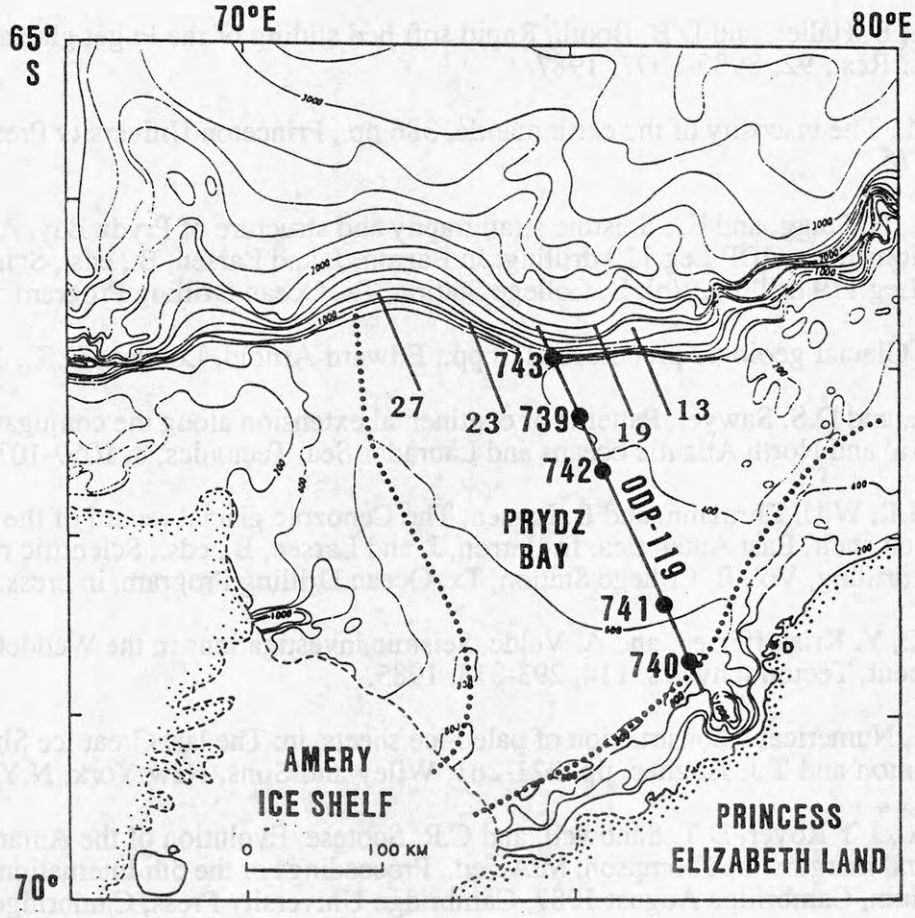

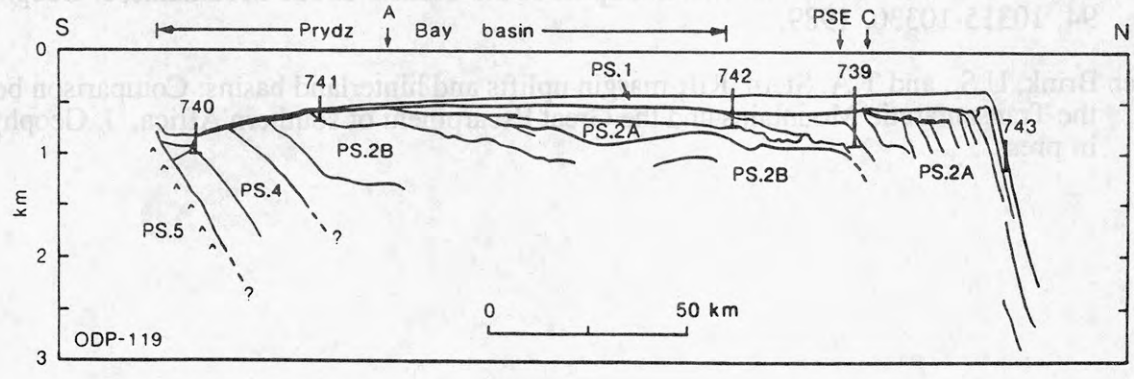

GLACIAL: PS.1 and PS.2A - late Eocene-early Oligocene through Holocene marine diamictite and diatomaceous sediment

NON-GLACIAL: PS.2B - Early Cretaceous nonmarine sandstone and siltstone
PS.4 - (?)Permian to Mesozoic red siltstone and sandstone
PS.5 - (?)Precambrian metamorphic rocks
PS.6 - (?)Mesozoic or Precambrian intrusive or metamorphic rocks

Fig.2

(a)

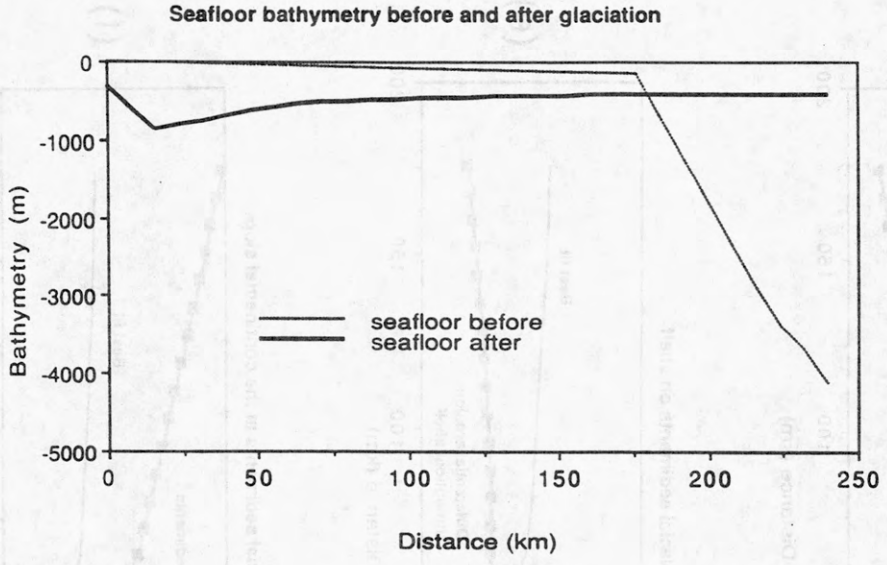
Seafloor bathymetry before and after glaciation
0
-1000
-2000
-3000
-4000
-5000
Bathymetry (m)
seafloor before
seafloor after
0
50
100
150
200
250
Distance (km)

(b)

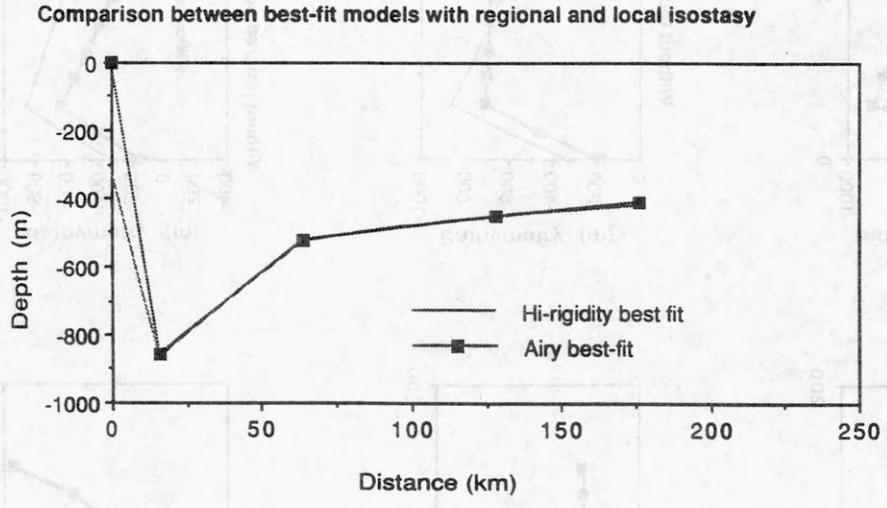
Comparison between best-fit models with regional and local isostasy
0
-200
-400
-600
-800
-1000
Depth (m)
Hi-rigidity best fit
Airy best-fit
0
50
100
150
200
250
Distance (km)

(c)

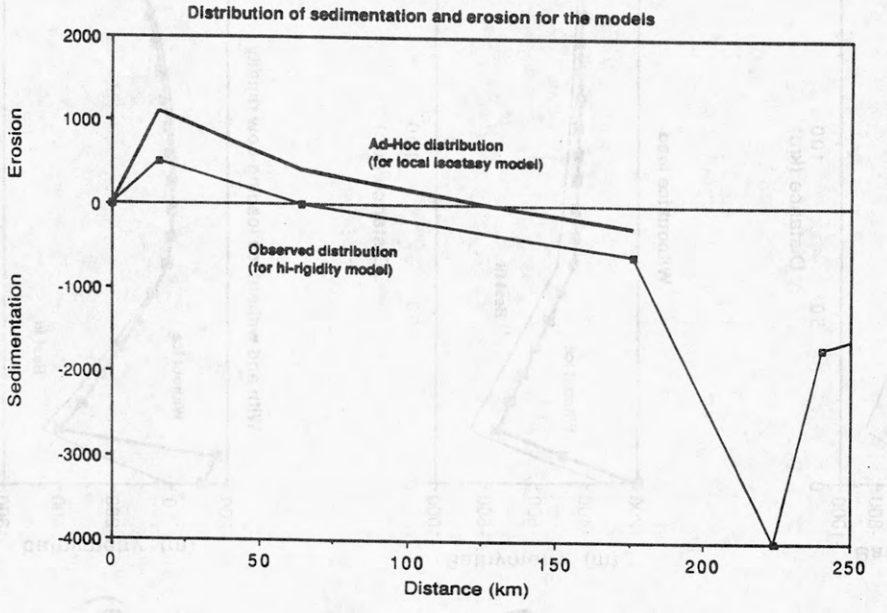
Distribution of sedimentation and erosion for the models
2000
1000
0
-1000
-2000
-3000
-4000
Erosion
Sedimentation
Ad-Hoc distribution
(for local isostasy model)
Observed distribution
(for hi-rigidity model)
0
50
100
150
200
250
Distance (km)

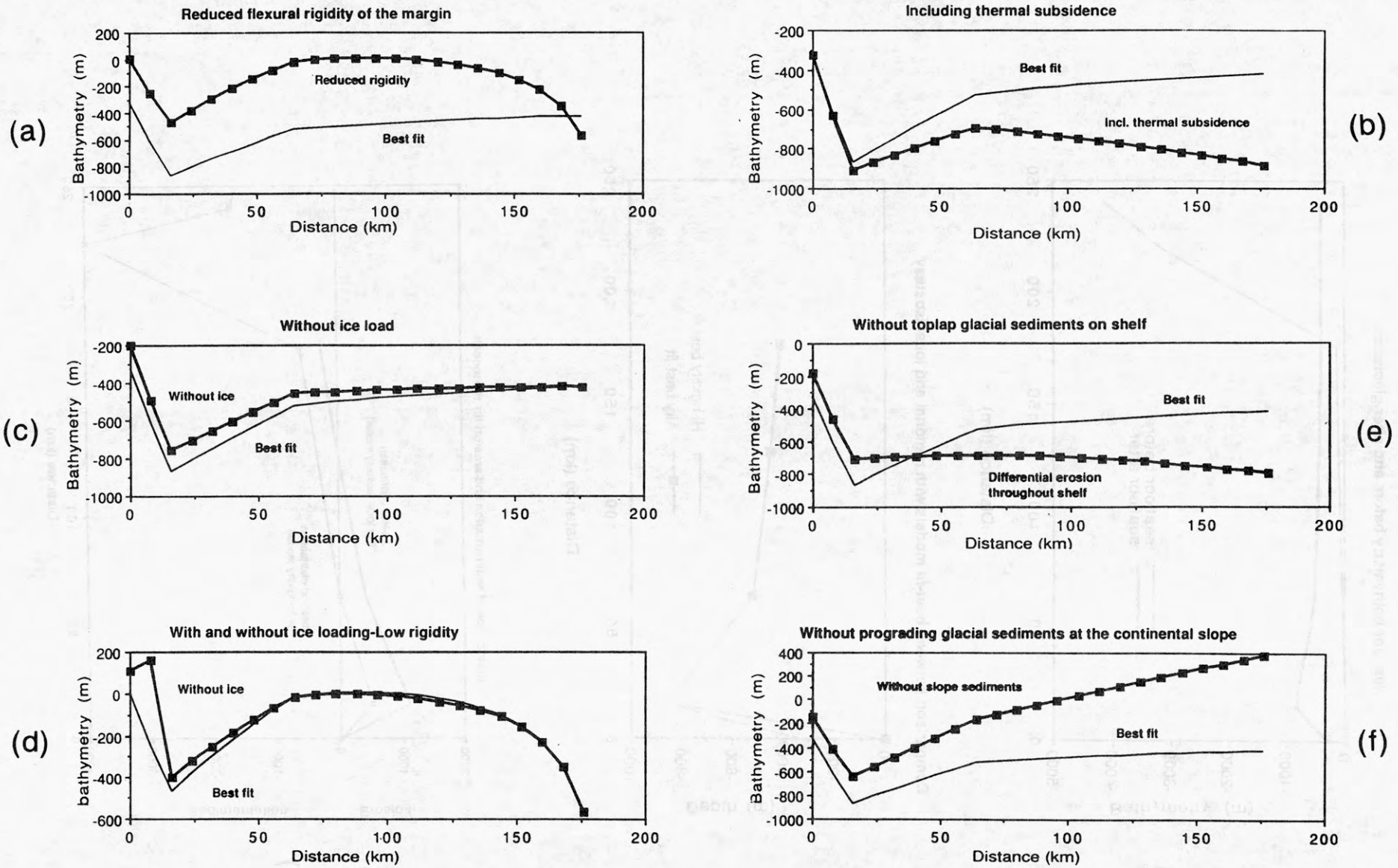
(a)
Reduced flexural rigidity of the margin
Reduced rigidity
Best fit
Bathymetry (m)
Distance (km)
(b)
Including thermal subsidence
Best fit
Incl. thermal subsidence
Bathymetry (m)
Distance (km)
(c)
Without ice load
Without ice
Best fit
Bathymetry (m)
Distance (km)
(e)
Without toplap glacial sediments on shelf
Best fit
Differential erosion throughout shelf
Bathymetry (m)
Distance (km)
(d)
With and without ice loading-Low rigidity
Without ice
Best fit
bathymetry (m)
Distance (km)
(f)
Without prograding glacial sediments at the continental slope
Without slope sediments
Best fit
Bathymetry (m)
Distance (km)

Fig.3

SEISMIC STUDY OF LITHOSPHERIC FLEXURE NEAR ROSS ARCHIPELAGO, ANTARCTICA

U.S. ten Brink, Branch of Atlantic Marine Geology, USGS, Woods Hole, MA 02543, USA
T.A. Stern, Geophysics Division, DSIR, P.O. Box 1320, Wellington, New Zealand
B C. Beaudoin, Department of Geophysics, Stanford University, Stanford, CA 94305, USA

Modeling indicates that a number of tectonic and stratigraphic features of intra-continental basins and passive continental margins may be determined by the rigidity of the lithosphere [1-3]. These features include the geometry of stratigraphic sequences and unconformities, the development of a coastal plain, an outer stratigraphic high and a hinge zone, the formation of break-up unconformities in rifts and the observed uplift of certain rift margins. Measuring the rigidity of the oceanic lithosphere is a comparatively straight forward task, but measuring the rigidity of the extended continental lithosphere is, on the other hand, difficult because there are few well-isolated and measurable loads [4]. In this regard, the situation of the young (~5 Ma, [5]) Ross Archipelago (which includes Mt. Erebus) (Fig. 1), is unusual. This volcanic group was emplaced on the thin continental lithosphere of the Victoria Land Basin in the Ross Embayment, which has undergone two episodes of extension in the past 60 Ma [6].

A multichannel seismic experiment on the Ross Ice Shelf in the vicinity of the Ross Archipelago was carried out jointly between Stanford University and the Geophysics Division of Department of Scientific and Industrial Research, New Zealand during the austral summer of 1988/89. The objective of the seismic experiment was to map the flexural deformation of the stretched continental crust. The 58-km-long profile, named RIS-2, was located so as to cross the apparent flexural deeps seen in the bathymetry and gravity maps around Ross Island ([7,8], Fig. 1) and as far as possible from the Transantarctic Mountains. The profile was collected using a 2.4 km-long 24-channel receiving array connected to a DFS-V recording system. The sound source consisted of 5 kg dynamite charges, spaced at 200 m intervals and placed at the bottom of 17 m-deep-holes (i.e., below the firn ice). The holes were drilled by a high pressure hot water drill with a drilling rate of 6 holes per hour. A 31.1-km-long unreversed wide-angle reflection profile was also shot along the reflection line using dynamite charges varying in sizes from 15 to 55 kg.

The Ross Ice Shelf in the study area is a thick ice layer (200-350 m) with velocity of 3.8 km/s overlying 700-800 m of water with a velocity of 1.44 km/s. A high velocity gradient (0.5 to 3.8 km/s) exists in the top 70 m of ice. The high-velocity and high-gradient ice lid introduces high energy and high-frequency, intra-water, and intra-ice multiples with stacking velocities ranging between 1.65 km/s and 2.6 km/s. This range of velocities overlaps the expected range of primary velocities from the sedimentary section. The multiples are of sufficient energy to mask primary reflections. Three approaches were combined to successfully remove the multiples: 1) Techniques based on the frequency content of the primary and multiple data. Intra-ice multiples were found to be mainly limited to frequencies > 35 Hz. Since these frequencies are naturally attenuated by scattering within the earth's crust, high-cut frequency filter was applied to remove inter-ice multiples in the crustal (> 3 s) portion of the section. 2) Techniques based on the shape of the wavelet (pre-stack and post-stack predictive deconvolution) were used to remove intra-ice multiples arriving at times equivalent to primary arrivals from the sedimentary layers. 3) Techniques based on velocity-discrimination. Long-period sea floor and intra-water multiples with low stacking velocities were removed using a technique of Inverse Velocity Stacking [9]. This technique models the data as a linear combination of parabolic events with weighting functions.

The processed reflection section (Fig. 2) shows a wedge of sedimentary layers which plunge northwestward toward Ross Island. The reflections appear to be truncated by a high-amplitude sea floor reflection. The sea floor reflection may correspond to the Ross Sea Unconformity, which is observed on many seismic profiles in the Ross Sea and is attributed to the advance of a grounded ice sheet [10]. Analysis of the reflection coefficient of the sea floor along profile RIS-2 does not

reveal a consistent change with distance as would be expected if erosion truncated successively deeper sediments along the line. It is, therefore, likely that the unconformity is overlain by a thin diamictite layer.

A discontinuous diffractive horizon which underlies the sedimentary wedge is interpreted as basement (B, Fig. 2). Two normal faults may displace the basement and the lowermost sedimentary horizon. A continuous reflection for 5 km below the basement appears at the SE end of the line at a two-way travel time of 7.2 s. It is overlain by a reflective section of almost 2 s thick. The band of highly reflective and laterally discontinuous reflections may be analogous to the reflective lower crust observed in seismic reflection profiles in other extensional provinces. In particular, a strong reflection at about 7.0-7.5 s has been observed on several reflection and refraction profiles in the Ross Sea where it was interpreted as the Moho [12,13]. Our observations, therefore, suggest that the shallow continental Moho continues from the Ross Sea south under the Ross Ice Shelf and that crustal thickness is ~21 km (for an average crustal velocity of 6.5 km/s).

The travel times of three continuous reflections within the sedimentary wedge (R1, R2, R3), as well as the sea floor (SF) and the basement (B), have been converted to depth using velocity information from stacking velocities for the first 1.5 s below sea floor and from the coincident refraction profile thereafter. The velocity increases from 1.8-2 km/s at the sea floor to 4.0-4.5 km/s at the bottom of the sedimentary wedge. In the Ross Sea, where ample multichannel seismic data exist, velocities of 1.7-2.3 km/s are interpreted to represent Mid-Miocene to recent sediments while the faster velocities represent Paleogene to Miocene marine and glacial sediments [11].

The deformation observed on seismic profile RIS-2 (e.g., the constant dip of the reflections and the possible faults cutting the basement) cannot be easily reconciled with flexural deformation. Comparison of predicted flexural profiles from three-dimensional elastic plate models with the observed depth section of profile RIS-2 indicates that the amplitude of the flexural deformation is too small to explain most of the northwestward tilt of the sedimentary section (Fig. 3a). The thickness of the sedimentary section increases from 0 to 3.6 km over a distance of 50 km while the largest flexural deflection reaches only 1/10 in magnitude (Fig. 3a). Furthermore, the dips on reflectors B, R3, and R2 are steeper than any dips along the calculated flexural profiles. The slope of the sea floor toward Ross Island can, however, be fit by a plate with high (Te=40 km) rigidity (the rigidity is expressed as the equivalent elastic thickness of the plate, Te), assuming that there has been little or no sediment deposition since the volcanoes formed. Alternatively, a model with a low rigidity (Te=5 km) fits reflector R1 and the sea floor (Fig. 3b) but only if variable erosion of several hundreds meters is postulated along the profile. Erosion contributes an upward force which alters the curvature of the deflection. The distributed erosion shown in Fig. 3b is an ad-hoc distribution which was chosen to fit reflector R1 and it does not have an observational basis. Other distributions of erosion will not fit the observed reflectors.

Two previously collected single-channel seismic profiles were also modeled. The bathymetry and sub-sea floor reflections in these profiles deepen toward Ross Island. An apparent flexural arch in these profiles is located at distances of 65-77 km from the peak of the volcanoes. These distances correspond to elastic thicknesses of 3-4 km. Modeling of the entire profiles with a three-dimensional elastic plate model shows that one of the profiles can be fit with a Te=5 km but the other profile cannot be fit with any reasonable parameters.

Gravity and bathymetry maps around the Ross Archipelago (Fig. 1) show a long (~200 km) trend of decreasing topography (by 100-300 m) and free-air gravity (by 40 mGal) from the east and SE toward Ross Island which were previously interpreted as evidence for a plate flexure with an elastic thickness of 20-25 km [14]. The results of profile RIS-2 and of the previously acquired seismic profiles suggest that a flexure model cannot be easily fit to the observed profiles. There are three possible reasons for the discrepancy: 1) The effect of loading does not extend far outside the

Ross Archipelago because the of the elastic thickness of the underlying plate is negligible (3-5 km). The inferred high temperatures in the uppermost mantle under Ross Archipelago [15] support this explanation and suggest a weak lithosphere with a maximum Te=6-11 km. 2) The flexural deformation is small in amplitude relative to displacement by faults regardless of the value of elastic thickness. The observed sedimentary wedge is, then, interpreted as a tilted and faulted block that is part of the southward continuation of Terror Rift. The trend in the gravity and bathymetry should therefore, also be interpreted as representing a deepening basement toward the Victoria Land Basin independent of flexure. 3) The least likely explanation is that evidence for flexure has been removed by glacial erosion of the uppermost section.

In addition to the results bearing on the rigidity of the stretched continental lithosphere, the observed sedimentary and crustal structure along profile RIS-2 also provides for the first time seismic evidence for the continuation of Terror Rift and a thin crust under the Ice Shelf. The experiment also demonstrates that multichannel seismic surveys can be effectively conducted on the Antarctic ice shelves.

References:

1. C. Beaumont, C.E. Keen and R. Boutilier, A comparison of foreland and rift margin sedimentary basins, Phil. Trans. Roy. Soc. London, A305, 295-317, 1982.
2. J.A Thorne and A.B. Watts, Seismic reflectors and unconformities at passive continental margins, Nature, 311, 365-368, 1984.
3. J. Braun and C. Beaumont, A physical explanation of the relation between flank uplifts and the breakup unconformity at rifted continental margins, Geology, 17, 760-764, 1989.
4. M.K. McNutt, Implications of regional gravity for the state of stress in the earth's crust and upper mantle, J. Geophys. Res., 85, 6377-6390, 1980.
5. R.L. Armstrong, K-Ar dating: late Cenozoic McMurdo Volcanic Group and Dry Valley history, Victorialand, Antarctica, N.Z. J. Geol. Geophys., 21, 685-698, 1978.
6. A.K. Cooper, F. J. Davey and K. Hinz, Crustal extension, sedimentary basins beneath the Ross Sea and the Ross Ice Shelf, Antarctica, in: Antarctic Geosciences - proceedings of the 5th Int. Antarctic Geosci. symposium, August, 1987 , Cambridge, U.K., M.R.A. Thompson, ed., Cambridge, in press.
7. F.J. Davey, K. Hinz and A.K. Cooper, Ross Sea gravity anomaly map, Miscellanous Series No. 2, Dept. Sci. Indust. Res., Wellington, New Zealand, 1987.
8. 36. Infomap 135, Antarctic Ross Sea Regions, 1:1,000,000, 3rd edition, Dept. of Survey and Land Information, Govt. Printer, Wellington, New Zealand, 1987.
9. D. Hampson, Inverse velocity stacking for multiple elimination, J. Can. Soc. Exploration Geophys., 22, 44-55, 1986.
10. H.A. Karl, E. Reimnitz and B.D. Edwards, Extent and Nature of Ross Sea Unconformity in the western Ross Sea, Antarctica, in: The Antarctic continental margin, geology and geophysics of the western Ross Sea, A. K. Cooper and F. J. Davey, eds., Earth Sci. Ser., 5B, Circum-Pacific Council for Energy and Mineral Resources, Houston, Texas, 1987.
11. A.K. Cooper, F. J. Davey and J. C. Behrendt, Seismic stratigraphy and structure of the Victorialand basin, western Ross Sea, Antarctica, in: The Antarctic continental margin, geology and geophysics of the western Ross Sea, see ref. 10.
12. L.D. McGinnis, R.H. Bowen, J.M. Erickson, B.J. Allred and J.L. Kreamer, East-West Antarctic boundary in McMurdo Sound, Tectonophys., 114, 341-356, 1985.
13. A. Trehu, T. Holt, J.C. Behrendt and J.C. Fritsch, crustal structure in the Ross Sea, Antarctica, preliminary results from GANOVEX V, Eos, 70, 1344, 1989.
14. T.A. Stern, F.J. Davey and G. Delisle, Lithospheric flexure induced by the loading of Ross Archipelago, and possible implications for the development of the Dry Valleys , southern Victorialand , Antarctica, in: Antarctic Geosciences , see ref. 6
15. J. Berg, R.J. Moscati, and D.L. Herz, A petrologic geotherm from a continental rift in Antarctica, Earth Planet. Sci. Lett., 93, 98-108, 1989.

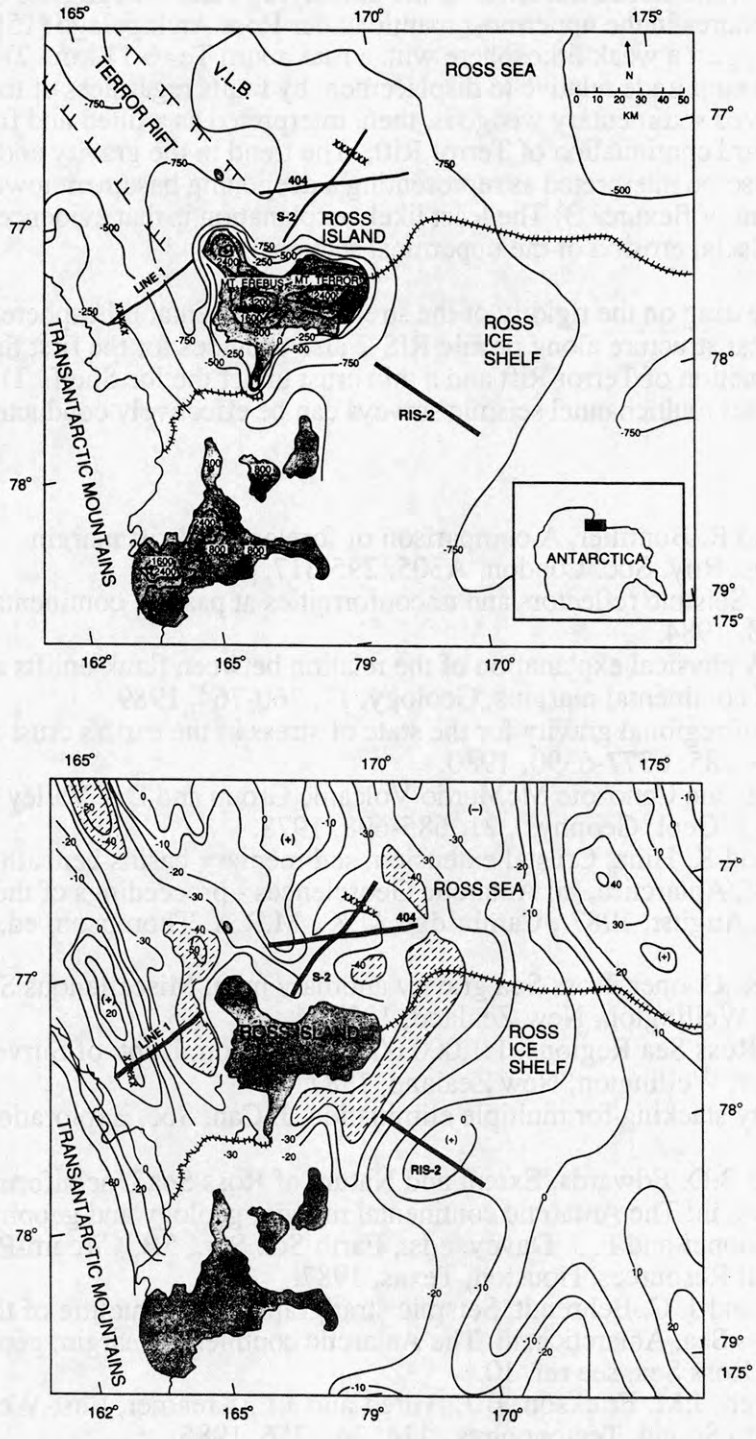

Fig. 1 a) Topographic and bathymetric map of the Ross Archipelago (shaded) and the surrounding Ross Embayment (after [7,8]). Heavy lines - the locations of seismic profile RIS-2 and other seismic profiles which were modeled. V.L.B. - Victoria Land Basin which includes the Terror Rift. Bold lines of crosses - the locations of the apparent flexural arch on these lines. The volcanic load of the Ross Archipelago includes the volcanic peninsula at the southern end of the region. b) Free-air gravity map of the Ross Archipelago and the surrounding Ross Embayment (after [7]). Contour interval 10 mGal. The map is based on sparse gravity data in the Ross Ice Shelf. Dotted areas - areas with gravity anomaly < -40 mGal. Other symbols as in a).

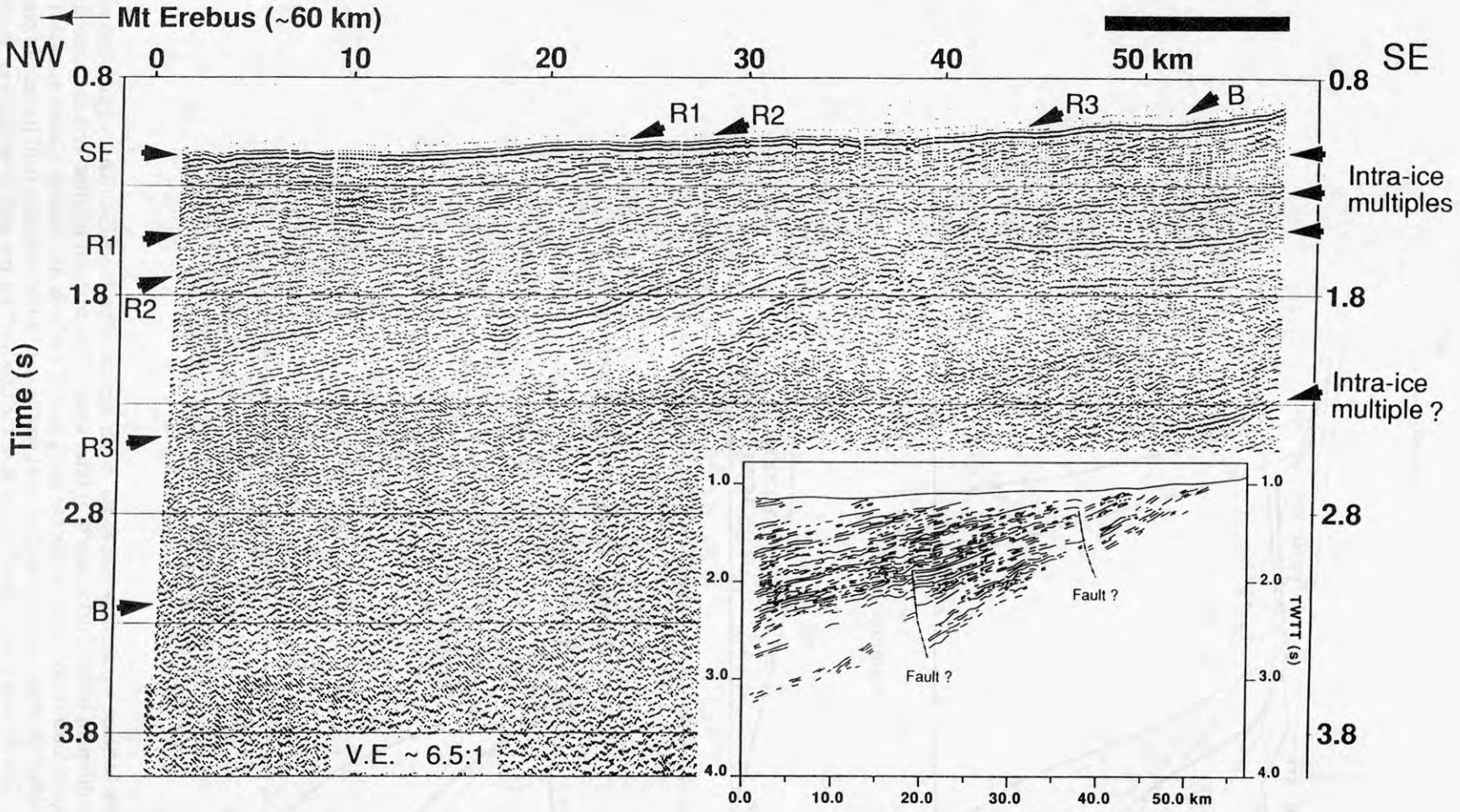

Fig. 2 Unmigrated stacked section of multichannel seismic profile RIS-2. B - basement, SF - sea floor, R1, R2, R3 - Internal sedimentary reflections. Inset shows line drawing of the profile.

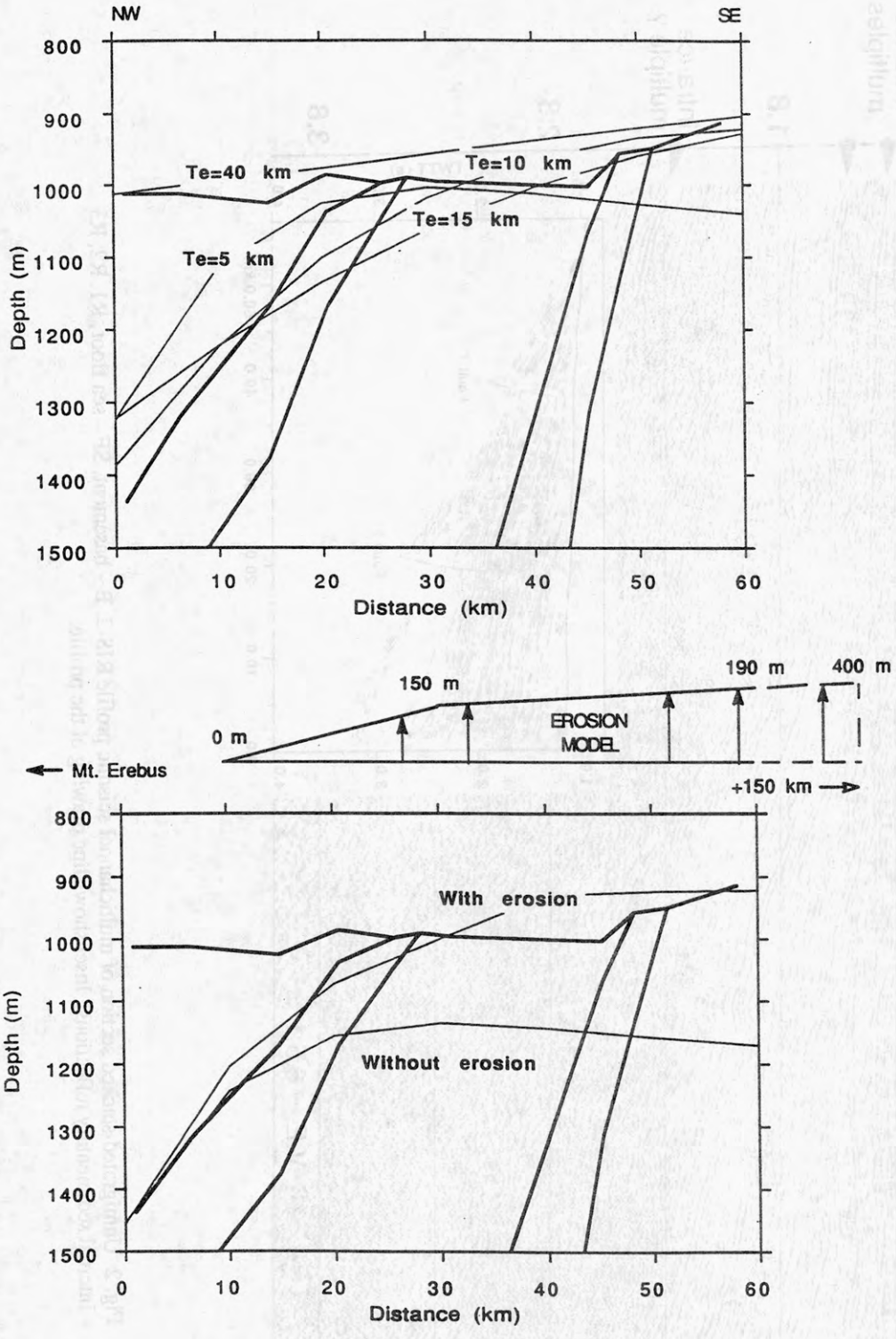

Fig. 3 a) Comparison between the shallow part of the depth section of profile RIS-2 (heavy lines) and modeled flexural profiles with different elastic thicknesses (Te) (thin lines). The modeled profiles were extracted from the deflection of three-dimensional elastic plate models due to the load of the Ross Archipelago (shown as shaded area in figure 1a). The individual reference depth of each flexural profile was shifted vertically until it could fit one of the observed reflectors. The vertical shift is justified because the depth of the pre-deformed sea floor in the Ross Embayment is not known b) Comparison between depth section and modeled flexural profile (Te=5 km) with and without differential erosion. The distribution of removed material is shown above the figure. Without erosion - unmodified. The reference depth for the models is arbitrary as discussed in a).

THE UPLIFT OF THE TRANSANTARCTIC MOUNTAINS IN VICTORIA LAND - SOME GEOLOGICAL CONSTRAINTS.

Franz Tessensohn, Bundesanstalt für Geowissenschaften und Rohstoffe, Stilleweg 2, 3000 Hannover 51, Germany.

The Transantarctic Mountains are considered to form the uplifted shoulder of the downfaulted Ross Sea rift system. The beginning of uplift is uncertain as is the age of subsidence in the rift. Slow and very fast uplift rates have been proposed. Fission track investigations in basement rocks have suggested a total amount of Cenozoic uplift in the order of 3-5 and 3-10 kms for different tectonic blocks of South and North Victoria Land, respectively.

Based on the results of recent mapping, especially in North Victoria Land, these proposed uplift rates are assessed here by reviewing the geological constraints for the maximum amount of uplift in each of these blocks. Terrestrial sediments and subaerial volcanics are used as constraining factors.

Terrestrial Beacon and Ferrar cover rocks are preserved all along the western slope of the Transantarctic Mountains in Victoria Land. The stratigraphically highest terrestrial rocks in this sequence include Kirkpatrick lavas and associated tuffs and sediments of Jurassic age. These rocks have all been deposited above sea level. Today they occur at elevations of 1500 to 3000 m. No younger sediments are known apart from Plio-Pleistocene glacial deposits.

More than 2-3 kms of postulated post-Jurassic uplift require a pre-uplift position of these subaerial lavas and sediments below sea level. If more than 10 kms are postulated, a subsidence of at least 7 kms below sea level is necessary prior to the uplift. Moreover, a post-Jurassic sedimentary load of some kms would be required to account for the critical isotherm (80-100°) of the apatite annealing zone in the basement. No post-Jurassic sediments are preserved in Victoria Land to account for such a marine phase. It would also be highly improbable in most rift models to have a downwarping of such a magnitude before final uplift of the rift shoulder.

In addition to the Beacon/Ferrar cover, Cenozoic subaerial volcanic rocks put further constraints on the young uplift history. As they cannot have been deposited below sealevel, their present elevations above sealevel give maximum values for the uplift since their time of extrusion. Different dated examples are discussed from the different tectonic blocks.

As a result, the simple evidence from terrestrial sediments and subaerial volcanics in the Victoria Land mountains contradicts an uplift of more than 2-3 kms in post-Jurassic times. The higher fission track values either require a (highly improbable) subsidence before the uplift or else there are some invalid assumptions in the application of the method.

FIRST HYPSILOPHODONTID DINOSAUR FROM ANTARCTICA

M.R.A. Thomson, British Antarctic Survey, Natural Environment Research Council, High Cross, Madingley Road, Cambridge CB3 0ET, U.K.

J.J. Hooker, Department of Palaeontology, Natural History Museum, Cromwell Road, London SW7 5BD, U.K.

The discovery of a new hypsilophodontid dinosaur in the Upper Cretaceous (Upper Campanian/Maastrichtian) sandstones of Vega Island, James Ross Island area, extends our knowledge of dinosaur distribution and is important in understanding high-latitude palaeoenvironments. This is only the second dinosaur to be reported from Antarctica, the first being an ankylosaur from the Campanian of north-west James Ross Island, itself (Olivero *et al.* 1991). Both dinosaurs occur in marine rocks and presumably represent drifted carcasses.

The hypsilophodontid was found on the western side of Cape Lamb and consists of parts of the skull, both upper and lower jaws, fore limbs, pelvis and vertebral column. It is estimated to have been about 5 m long and was thus rather large for a hypsilophodontid.

The stratigraphy of the Cretaceous rocks of Cape Lamb has been reviewed by Pirrie *et al.* (1991), who identified three main lithostratigraphical units in a 480 m-thick succession. Informally designated as members A (52 m), B (319 m) and C (111 m) they will be formally named in a second paper which addresses the stratigraphy of the whole of eastern James Ross Island (Crame *et al.*, in press). The scattered remains of the dinosaur were found loose on Member B between 171.5 and 186.5 m above the base of the section. They were closely associated with a rich marine fauna, including a variety of gastropods, bivalves, ammonites (especially *Gunnarites*) and decapod crustaceans. The isolated bones and partial skeletons of plesiosaurs are relatively common in Members B and C; a few mosasaur bones have also been found. Member B is interpreted as representing "a regressive-transgressive cycle within a shelf setting. Deposition was below storm wave base, with sedimentation in outer shelf and possibly mid to (?) inner shelf settings during regression" (Pirrie *et al.*, 1991).

Dinosaurs have been described from all other Gondwana continents and, since there is a considerable body of evidence to show that Antarctica supported forest vegetation during Jurassic and Cretaceous time (e.g. Francis, 1991), there was every reason to suppose that dinosaurs could have lived in Antarctica too. The palaeolatitude of the James Ross Island area in the Cretaceous was probably very close to that of today (64°S). Moreover, in the Northern Hemisphere dinosaurs are known from palaeolatitudes as high as 85°N (Parrish *et al.* 1987). By Late Cretaceous times Australasia had only just broken away from Antarctica, whereas the link between South America and the Antarctic Peninsula was maintained until the mid-Tertiary and faunal interchange should have been possible.

Hypsilophodontid dinosaurs are known from North America, Europe, China, Africa and Australasia. These are, however, nearly all Late Jurassic and Early Cretaceous occurrences and the Antarctic specimen represents one of the geologically youngest known members of the group. The only other Late Cretaceous one is *Thescelosaurus* from western North America. It is interesting that hypsilophodontids are usually rare elements in dinosaur faunas, yet this is the family to which only the second Antarctic dinosaur belongs. It provides tentative evidence of a time extension into the Late Cretaceous of hypsilophodontid diversity at southern high latitudes, already documented by Rich *et al.* (1988) for the Aptian/Albian of Australia.

References

Crame, J.A., Pirrie, D., Riding, J.B. & Thomson, M.R.A. In press. Late Cretaceous lithostratigraphy of the James Ross Island area, Antarctica. *Journal of the Geological Society of London*.

Francis, J.E. 1991. Palaeoclimatic significance of Cretaceous-early Tertiary fossil forests of the Antarctic Peninsula. *In* Thomson, M.R.A., Crame, J.A. & Thomson, J.W. *eds, Geological evolution of Antarctica*. Cambridge: Cambridge University Press, 623-27.

Olivero, E.B., Gasparini, Z., Rinaldi, C.A. & Scasso, R. 1991. First record of dinosaurs in Antartica (Upper Cretaceous, James Ross Island): palaeogeographical implications. *In* Thomson, M.R.A., Crame, J.A. & Thomson, J.W. *eds, Geological evolution of Antarctica*. Cambridge: Cambridge University Press, 617-22.

Parrish, J.M., Parrish, J.T., Hutchison, J.H. & Spicer, R.A. 1987. Late Cretaceous vertebrate fossils from the North Slope of Alaska and implications for dinosaur ecology. *Palaios*, 2, 377-89.

Pirrie, D., Crame, J.A. & Riding, J.B. 1991. Late Cretaceous stratigraphy and sedimentology of Cape Lamb, Vega Island, Antarctica. *Cretaceous Research*.

Rich, P.V., Rich, T.H., Wagstaff, B.E., McEwen Mason, J., Douthitt, C.B., Gregory, R.T. & Felton, E.A. 1988. Evidence for low temperatures and biologic diversity in Cretaceous high latitudes of Australia. *Science*, 242, 1403-6.

GEOLOGICAL RELATIONSHIPS IN GRANULITE FACIES GNEISSES OF THE PORTHOS RANGE, NORTHERN PRINCE CHARLES MOUNTAINS,ANTARCTICA.

D. E. Thost and B. J. Hensen, Department of Applied Geology,
University of New South Wales, Kensington 2033, Australia.

The Porthos Range in the Northern Prince Charles Mountains, Mac. Robertson Land, is composed of upper amphibolite to granulite facies metamorphic rocks. The most common rock type is felsic orthogneiss, which hosts lenses and layers of ultramafic and mafic granulite, pelitic gneiss and calc-silicate gneiss. These rocks are cross-cut by at least two generations of mafic dykes, and have undergone at least two partial-melting events resulting in the formation of leucogneiss bodies. Large intrusive bodies of charnockite are common, and pre-date the mafic dyke intrusion.

To varying degrees, these rock types have all been affected by a number of deformational events. D1 is expressed as a moderate to strong foliation, only preserved in the ultra-mafic and mafic gneiss pods and boudinaged layers. D2 is recognized as a series of low amplitude, disharmonic folds (F2), with wavelengths generally less than 50cm, again preserved only within ultra-mafic and mafic gneiss bodies. D3 has produced the dominant gneissic foliation in the area (S3) in both the felsic and pelitic gneisses. D1-D3 may represent a deformational progression during a single tectonic event. D4 folds S3, with steep easterly plunging fold hinges. F4 folds are tight to isoclinal, with wavelengths less than 5m. During D4, calc-silicates were mobilized, and cross-cut S3, generally axial planar to F4 folds. This was followed by charnockite and later mafic dyke intrusion. D5 is a heterogeneous deformation, co-axial with D4. In zones of high strain, it is manifest as a strong sub-vertical foliation (S5) and/or easterly plunging lineation (L5). These zones may be hundreds of metres wide. Separating these high strain zones are areas of large scale F5 folds, which refold S3, with wavelengths of 1-2km. The high strain zones anastomose between outcrops, resulting in the tightening of F5 hinge zones or transposition of limbs. D1-D5 occured under granulite facies conditions, as evidenced by the widespread occurrence of orthopyroxene in the felsic gneisses and mafic dykes.In D5 high strain zones orthopyroxene remains stable.

D6 produced small scale gently dipping shear zones and minor flexures. These shears are locally intruded by planar pegmatite dykes. A series of mylonites, which locally offset pegmatites, and pseudotachylites are assigned to D7. The interval D6-D7 reflects a decrease in grade, with late planar quartz and epidote-bearing veins being associated with a greenschist facies overprint. Rare, basaltic dykes cross-cut all the other rock types.

Geothermobarometry indicates maximum pressure-temperature conditions (D1-D5) of 700±50°C and 0.6±0.1GPa using garnet+orthopyroxene+quartz+plagioclase assemblages, and garnet+cordierite+sillimanite+plagioclase+quartz+biotite +K-feldspar assemblages in the metapelites. Somewhat higher peak temperatures are indicated by the stability of scapolite+quartz and scapolite+wollastonite+calcite in calc-silicates from the adjacent Aramis Range (Fitzsimons and Thost, in press). Coarse grained garnets in metapelites contain inclusions of cordierite, and less commonly sillimanite, suggesting a counter-clockwise prograde evolution for this terrane.

Fitzsimons I.C.W. & Thost D.E. 1991. Geological relationships in high-grade basement gneiss of the northern Prince Charles Mountains, east Antarctica. Australian Journal of Earth Sciences, in press.

THINNING RATE OF ICE SHEET ON MIZUHO PLATEAU, EAST ANTARCTICA, DETERMINED BY GPS DIFFERENTIAL POSITIONING

H. Toh, Ocean Research Institute, The University of Tokyo,
Minamidai, Nakano-ku, Tokyo 164, Japan
K. Shibuya, National Institute of Polar Research,
Kaga, Itabashi-ku, Tokyo 173, Japan

Two sets of GPS receivers were used in January 1988 during the 29th Japanese Antarctic Research Expedition (JARE29) in order to conduct differential positioning of stations on the Mizuho route relative to the astronomical point at Syowa Station. Noise sources common to both stations in satellite positioning are easily cancelled out, resulting in an elevation accuracy of ±0.1m. Simultaneous gravity measurements were also made using a LaCoste-Romberg gravimeter model G-515 at each differential positioning site.

The positions of 11 stations were determined through this method and compared with those observed in 1981 after appropriate conversion to the coordinate on WGS84 Ellipsoid. Three stations observed in 1981 (S16, H231 and Z33) were repeated in the 1988 measurements. Although a different positioning system (NNSS) had been used in 1981, which gave out more erroneous positions than those of GPS, the direct comparison of the heights yielded the thinning rates of ice sheet ($-\partial h/\partial t$) at the three stations as 0.57, 0.20 and 0.53 m/a, respectively. A comparison of these results with the simultaneous gravity measurements proved that they coincided with the changes of the gravity values caused by the height changes. For instance, the difference between the height change expected from the change of the gravity value and that determined by GPS positioning was less than 0.2m at station Z33.

The basal sliding velocity at station Z33 was also estimated using the thinning rate above and assuming the declination of the bedrock as of the order of 10^{-2}, which showed of the same order (10 m/a) as had been estimated by Mae (1979).

REFERENCE

Mae, S. 1979. The basal sliding of a thinning ice sheet, Mizuho Plateau, East Antarctica. *Journal of Glaciology*, Vol. 24, No. 90, p. 53-61.

Preferred Session : D-2

STRUCTURAL DEVELOPMNENT OF TRINITY PENINSULA GROUP IN BRANSFIELD STRAIT REGION, WEST ANTARCTICA

Antoni K. Tokarski Institute of Geological Sciences, Polish Academy of Sciences, ul. Senacka 1-3, 31-002, Kraków, Poland

Rocks of the Trinity Peninsula Group (Permo-Carboniferous - Triassic?) have been studied in the area of Cape Legoupil (Antarctic Peninsula) and on Hurd Peninsula (Livingston Island). These rocks, called respectively Legoupil Formation (Cape Legoupil) and Miers Bluff Formation (Livingston Island), show in both areas identical lithologies. These are: (1) black shale with minor intercalations of thin-bedded sandstone, (2) thin-bedded sandstone and shale with few intercalations of thick-bedded sandstone, and (3) massive non-bedded sandstone. Particular lithologies form complexes which pinch-out laterally and are repeated in vertical section. Particular complexes attain maximum thicknesses of: 140 m (1), 250 m (2), and 110 m (3).

In both areas, rocks of the Trinity Peninsula Group are folded into map-scale, east-verging folds. Numerous minor folds (amplitudes of few mm to few m) occur in black shales and thin-bedded sandstones and shales. The axes of minor folds are rougly parallel to those of the map-scale folds. No traces of shearing were found in reversed limbs nor in hinges of the map-scale folds. This may attest to gravitational origin of the folds. The orientations of fold axes are different in particular areas: N70E (Cape Legoupil) and N35E (Hurd Peninsula). This differentiation of orientations of the fold axes and eastward vergences of the folds are uncompatible with the eastward Mesozoic-Cenozoic subduction of the ancient Pacific ocean crust. The folding possibly pre-dated this subduction.

After folding, the rocks of the Trinity Peninsula Group in both areas were deformed only in brittle way. In Cape Legoupil area this deformation occurred in four stages: (1) jointing, (2) dyking, (3) faulting and, (4) jointing. None of these stages is compatible with Mesozoic-Cenozoic subduction.

On Hurd Peninsula, folded rocks of the Miers Bluff Formation were cut by: (1) strike-slip and normal faults belonging to several sets and, (2) magmatic dykes of two sets N45W (older) and N70E (younger) respectively. The orientations of the older set dykes are compatible with the Mesozoic-Cenozoic subduction, while those of the younger set with opening of Bransfield Strait.

GLORIA Survey of the Pacific Margin of the Antarctic Peninsula: tectonic fabric and sedimentary processes.

J Tomlinson, C J Pudsey, R A Livermore,
R D Larter and P F Barker,
British Antarctic Survey, Natural Environment Research Council,
Madingley Road, Cambridge CB3 0ET, UK.

The GLORIA survey occupied Leg 3 of RRS Charles Darwin Cruise 37, in March 1989. It covers 85000km^2 and involved 3100 line km of ship track, over 10 days. 3.5 KHz, single-channel digital seismic, magnetic and gravity profiles were also acquired. The main aims were to aid existing studies of shelf-slope-rise sediment transport (in the southwest) and of recent ridge crest subduction (in the northeast). The main objectives of the survey lie in sediment transport, in which the southwestern area may act as a model for the Antarctic continental margin in general, and in the tectonics of subduction, particularly imminent ridge crest-trench collision.

The digitally-acquired data swaths have been corrected for geometric and acoustic propagation effects, transformed onto a Lambert conical orthomorphic projection and digitally mosaicked.

Tectonic Background

During the Cenozoic, the Pacific margin of the Antarctic Peninsula has undergone a series of ridge crest collisions, which have migrated northeastward through time (Barker, 1982; Larter and Barker, 1991). The youngest occurred between the "C" and Hero fracture zones, between 5.5 and 3.1 Ma ago. In each collision zone, subduction stopped at the time of collision and, after an initial uplift phase lasting 1 to 4 Ma, the margin began to behave like a young passive margin, with relatively rapid thermal subsidence.

To the northeast of the Hero FZ, spreading stopped at about the time of the last collision (3-4 Ma ago), before the ridge crest had reached the trench: subduction continued, slowly, as a result of roll-back of the trench hinge, and has been accommodated by back-arc extension in Bransfield Strait.

The GLORIA survey picks out the typical, mainly rectilinear ridge/fracture zone fabric of ocean floor, in the northeast where sediment cover is thin, and the highly reflective accretionary prism at the South Shetland Trench. Also visible are linear chains of seamounts, apparently younging to the southeast, and an episode of pivoting subduction between the C and Hero FZ, preceding collision, which had already been seen in the magnetic anomalies (Larter and Barker, in prep).

The survey has raised many intriguing tectonic questions. In particular, the accretionary prism and trench extend farther to the southwest along the margin than the Hero Fracture Zone and the generally recognized southwestern end of Bransfield Strait. The extension in Bransfield Strait has not led to an offset of the fore-arc at this southwestern end, as might have been expected. We believe (Larter et al, in prep) this is explained by a southwestward extrapolation of the extensional zone of Bransfield Strait, via the graben-like deeps of Croker Passage and the northern Gerlache Strait.

The Continental Margin

Southwest of where the "C" FZ reaches the margin, the main influence on continental margin morphology is glacial/interglacial sedimentation, whereas northeast of the "C" FZ, the main influence is tectonic. That southwestern margin should have much in common with virtually all Antarctic margins.

The continental slope southwest of the "C" FZ is steep (up to 17^{o}) and yet depositional. Reflection profiles (Larter and Barker, 1989; 1991) show a prograded wedge of sediments beneath the outer shelf and slope. This is interpreted as consisting mainly of till and proximal glacimarine sediment, transported to the shelf edge in the base of grounded ice sheets during glacial maxima, probably across a broad front. Terrigenous sediment supply to the shelf edge during interglacials is minimal.

The GLORIA mosaic shows that the continental slope is uniformly smooth and steep, with no canyons or major collapse features such as slumps. Groups of small gullies are seen in the lower slope, where reflection profiles (see AMG845-08 on the adjacent poster) show some dissection. The shelf break follows a smooth sinuous line, not obviously influenced by topographic variation inshore, nor by ocean floor discontinuities.

Four major channels (I to IV) trend northwest across the continental rise. They include narrow meandering reaches with point bars and broad straight reaches with longitudinal bedforms. Channels I and III rise in a network of tributary gullies on the lower slope, Channel III flowing southwest along the foot of the slope for 30 km before turning northwest to cross the rise. A typical MCS profile along the rise (AMG845-04) shows a modern channel and the migration paths of one or more predecessors, within a sediment thickness of up to 1 km representing deposition over about 5 Ma. The channels thus migrate only slowly, compared with the glacial/interglacial cycle.

We suggest the channels are maintained by turbidity currents originating in small slumps and slides on the lower slope. The unsorted nature of glacial sediments on the upper slope, and their deposition from essentially a line source (rather than the point sources more typical of temperate shelves) may serve to limit the size of a turbidity flow originating on the slope (despite its steepness) and to distribute flows laterally along the slope. Each channel appears to drain a section of slope, and the rough topography along the base of the slope may result from erosion by both turbidity currents in lateral tributary channels and any indigenous bottom currents.

We plan next to sample the several provinces defined by the GLORIA sonograph, and establish the balance between slump, turbidite and nepheloid layer transport and redeposition of slope sediments, and the extent to which the cyclicity of sediment supply to the shelf break and upper slope is preserved in sediments of the continental rise.

References

Barker, P F. 1982. The Cenozoic subduction history of the Pacific margin of the Antarctic Peninsula: ridge crest-trench interactions. J Geol Soc Lond, 139, 787-801.

Larter, R.D. and Barker, P.F. 1989. Seismic Stratigraphy of the Antarctic Peninsula Pacific margin: a record of Pliocene-Pleistocene ice volume and paleoclimate. Geology, 17, 731-4.

Larter, R. D. and Barker, P. F. 1991. Neogene interaction of tectonic and glacial processes at the Pacific margin of the Antarctic Peninsula. In Macdonald, D.I.M., ed. Sedimentation, Tectonics and Eustasy Int. Assoc Sediment. Sp. Publ. Oxford, Blackwell.

Figure Captions

Figure 1. Location of GLORIA survey of Pacific margin of Antarctic Peninsula, RRS Charles Darwin cruise 37, 1989, showing major seabed features: fracture zones, seamount chains, channels.

Figure 2. Interpretative line drawing of part of MCS line AMG845-04, with seismic data from area corner-marked, crossing Channel I. Vertical exaggeration in water is 3.3:1

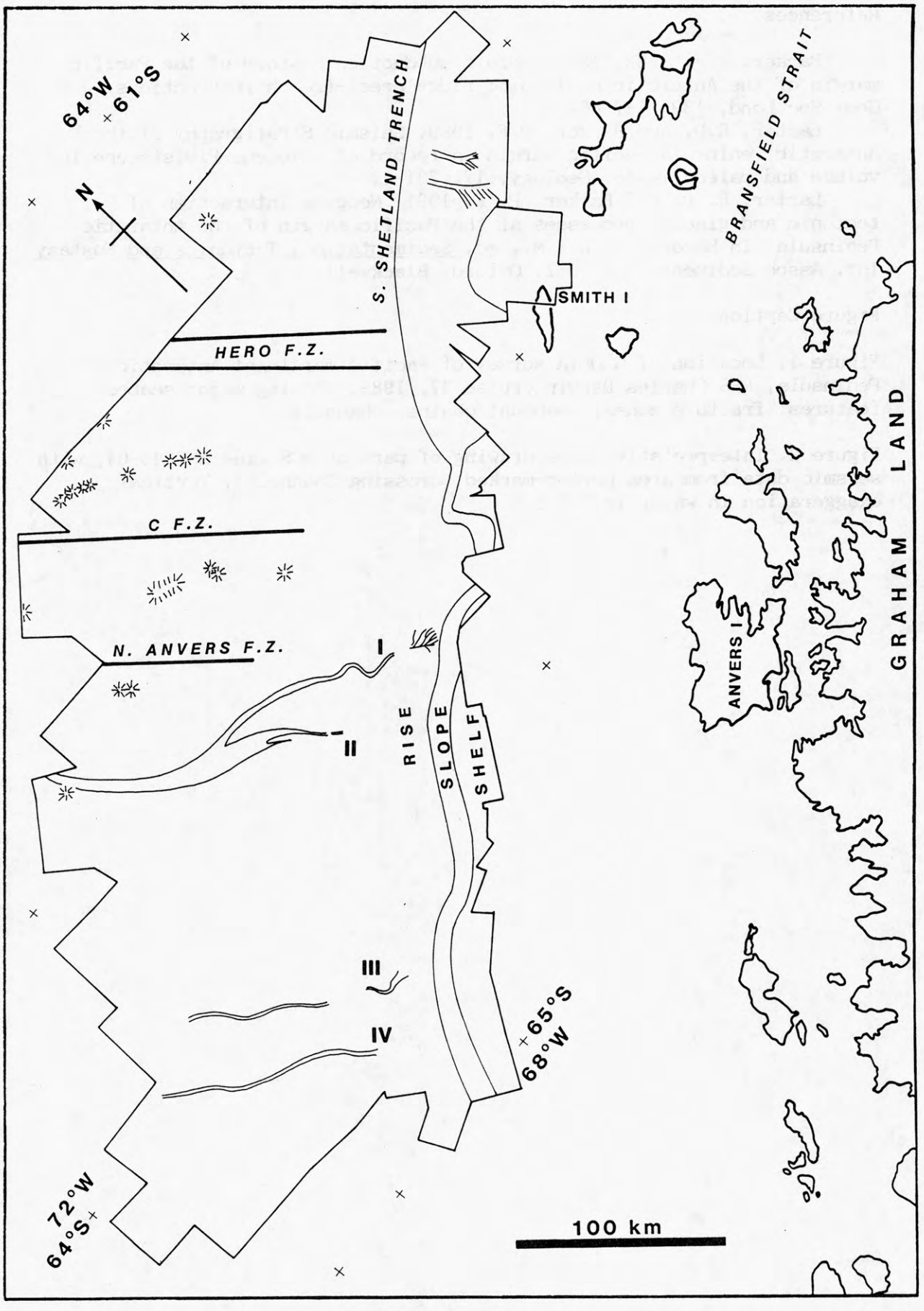
64°W
61°S
N
S. SHETLAND TRENCH
BRANSFIELD STRAIT
SMITH I
HERO F.Z.
C F.Z.
N. ANVERS F.Z.
I
II
III
IV
RISE
SLOPE
SHELF
ANVERS I
GRAHAM LAND
65°S
68°W
72°W
64°S
100 km

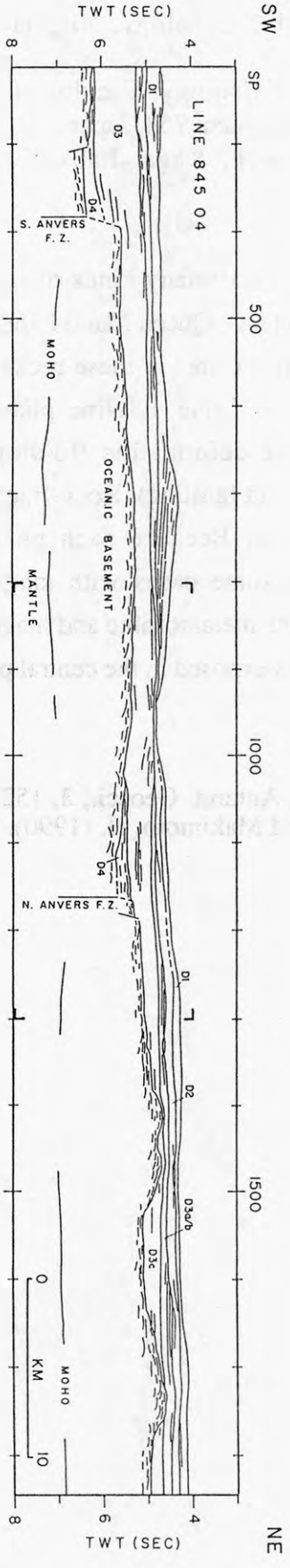
TWT (SEC)
SW
SP
LINE 845 04
S. ANVERS F. Z.
N. ANVERS F. Z.
MOHO
OCEANIC BASEMENT
MANTLE
D1
D2
D3
D4
D3a/b
D3c
0
KM
10
NE
500
1000
1500

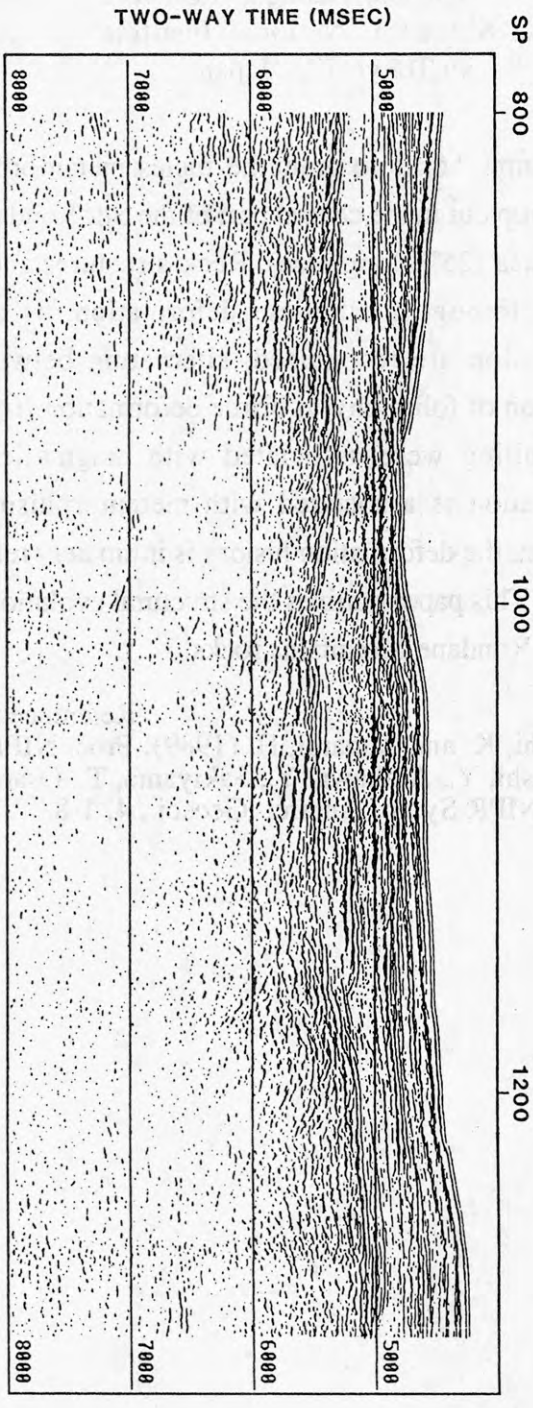
TWO-WAY TIME (MSEC)
SP
800
1000
1200
5000
6000
7000
8000

STRUCTURAL EVOLUTION OF METAMORPHIC AND INTRUSIVE ROCKS OF THE SØR RONDANE MOUNTAINS, EAST ANTARCTICA

T. Toyoshima, Graduate School of Science and Technology, Niigata University, Ikarashi, Niigata 950-21, Japan.
M. Owada, Department of Mineral Science and Geology, Faculty of Science, Yamaguchi University, Yoshida, Yamaguchi 753, Japan.
K. Shiraishi, National Institute of Polar Research, Kaga, Itabashi-ku,Tokyo 173, Japan.

Amphibolite to granulite facies metamorphic rocks and many kinds of igneous rocks crop out in the central part of the Sør Rondane Mountains, Queen Maud Land, East Antarctica (25°E longitude). Rock-structures and mineral textures in these rocks were formed through multiphase deformation, as outlined in Table 1. Nine phases of deformation are recognized, alternating between ductile deformation (folding and formation of foliation) to brittle deformation (fracturing and faulting). Rock-fracturing and faulting were associated with magmatic intrusions. Because each phase of deformation is associated with metamorphism and in some cases with magmatic intrusion, the deformation history is intimately related to the metamorphic and magmatic history. This paper outlines the structural evolution of rocks exposed in the central part of the Sør Rondane Mountains rocks.

References

Shiraishi, K. and Kagami, H. (1989): Proc. NIPR Symp. Antarct. Geosci., **3**, 152.
Takahashi, Y., Arakawa, Y., Sakiyama, T., Osanai, Y. and Makimoto, H. (1990): Proc. NIPR Symp. Antarct. Geosci., **4**, 1-8.

Table 1. Deformation history of the central part of the Sør Rondane Mts.

*: Shiraishi and Kagami (1989), **: Takahashi et al. (1990).

Deformation phase	Structure	Magmatism	Metamorphism	Movement picture	Age (Ma)
	bedding foliation (S1), tight to isoclinal fold		peak of prograde metamorphism ?		1000*
D1	(B1) and fracture with intrusion of charnockitic and basic rocks	charnockitic and basic	granulite to amphibolite facies ?		
D2	fracture with intrusion of gabbroic and tonalitic rocks	gabbroic and tonalitic			950**
D3a	mylonitic foliation (S3a) and tight fold (B3a)			southeastward to eastward displacement ?	
D3b	mylonitic foliation (S3b), tight fold (B3b) and fracture with intrusion of granitic rock	granitic and pegmatitic	amphibolite facies retrograde metamorphism		
D4	WNW-ESE trending tight to open fold (B4), minor shear zone and fracture with intrusion of granitic rock	granitic and pegmatitic		N-S trending compression and northward thrusting ?	
D5	N-S trending open to tight fold (B5)			E-W trending compression ?	
D6	fracture with intrusion of syenitic rock	syenitic	greenschist facies		
D7	NE-SW trending gentle fold (B7)				
D8	fracture with intrusion of granitic rocks	granitic and pegmatitic			500**

SEDIMENTARY FRAMEWORK OF THE ROSS SEA SHELF AND TECTONIC MOVEMENT BETWEEN EAST AND WEST ANTARCTICA

V. V. Traube, North Branch for Marine Geologic Research and Exploration "SEVMORGEOLOGIA", 120 Moyka, 190121 Leningrad, USSR

First observations on crustal structure of the open Ross Sea Shelf made near twenty years ago [Houtz and Davey, 1973] were recently complemented by more extensive geophysical studies. An important contribution was provided by the Soviet investigations aboard R\V "Geolog Dmitry Nalivkin" in 1987 and 1989. The survey included 8 000 km of MCS, HRS, magnetic and gravity observations concentrated predominantly in the eastern part of the shelf (Fig. 1).

A type section of the sedimentary cover of the Ross Sea Shelf includes three supersequences (Fig. 2). Internal subdivision of the lower supersequence (LS) is not possible with available resolution. The middle supersequence (MS) includes two sequences, while at least 5 sequences are recognized in the upper supersequence (US).

LS is largely controlled by deep basement depressions and sharply thins or completely wedges out on basement highs. Apparently it represents the fill of grabens related to extensional rifting during early Gondwana breakup. MS appears to constitute a thick regional cover which is less controlled by extensional events and decreases in thickness towards the outer shelf. US forms anomalously thick sedimentary body only in the eastern outer shelf but is thin elsewhere in the studied area.

The supersequences are divided by distinct regional unconformities V and VI. On the basis of DSDP data and general considerations these boundaries were assigned to Early Miocene and Middle(?) Eocene respectively [Traube, 1990].

One of the most important observations derived from our new time-isopach map for total sedimentary section (Fig. 3) is that the axial trends of individual basement depressions are controlled not only by longitudinal direction stressed in previous publications but also by a distinct NW orientation. The latter is delineated by a number of structural features parallel to the shelf break (e.g. subbasins in the Eastern Basin, boundary between subbasins B-1 and B-2 in the Central Basin, etc.).

According to earlier data [Robertson et al., 1982], the linear gravity anomalies on the Ross Ice Shelf are caused by deep structural control. Our work has shown that these regional gravity features may be continuously traced across the open shelf where they are represented by a system of NW-trending relative gravity lows associated with contrasting magnetic anomalies (Fig. 4, 5). We believe that the presence

of these anomaly zones supports the previous interpretation and may be explained in terms of crustal extension involving deep faulting, brecciation and local magmatic activity from deep sources. It is significant that the same extensional features delineate fracture zones in the Northern Victoria Land that control position of the major Glaciers, distribution of the Cenozoic volcanics and the Ferrar Group rocks and, possibly, even older structural trends (Fig. 6).

Therefore a prominent NW-trending crustal heterogeneity may be recognized across the Ross Sea area from at least the Siple Coast to the Northern Victoria Land for more than 2 000 km. It is evident not only from geological features on land, but also in distribution of deep gravity and magnetic sources and respective position of the extensional sedimentary basins.

We conclude that this en echelon S-shaped crustal suture reflects a major lithospheric shear probably responsible for right-lateral displacement of West Antarctica relative to East Antarctica along the Transantarctic failed rift[Schmidt, Rowley, 1986]. Initial indications of that shear are represented by LS in the Ross Sea extensional (pull-apart?) basins. Tectonic movement between East and West Antarctica continued throughout Cenozoic time and led to formation of the West Antarctic sub-ice rift system connecting the Ross and Weddell embayments.

REFERENCES:

Cooper A.K., Davey F.J., Behrendt J.C., 1987. Seismic stratigraphy and structure of the Victoria Land Basin, Western Ross Sea, Antarctica. In: Cooper A.K. and Davey F.J., eds. The Antarctic Continental Margin: Geology and Geophysics of the Western Ross Sea. CPCEMR Earth Sci. Ser., 5B, Houston, Texas, p. 27-76.

Houtz R., Davey F.J., 1973. Seismic profiler and sonobuoy measurements in Ross Sea, Antarctica. J. Geophys. Res., v. 78, no. 17, p. 3448-3468.

Robertson J.D., Bentley C.R., Clough J.W., Greischar L.L., 1982. Sea-bottom topography and crustal structure below the Ross Ice Shelf, Antarctica. In: Craddock C., ed. Antarct. Geosci. Madison (Univ. of Wisconsin Press), p. 1083-1090.

Schmidt D.L., Rowley P.D., 1986. Continental rifting and transform faulting along the Jurassic Transantarctic rift, Antarctica. Tectonics, v. 5, no. 2, p. 279-291.

Traube V.V., 1990. Ross Sea sedimentary basin. In: Ivanov V.L. and Kamenev E.N., eds. Geology and Mineral Resources of Antarctica (in Russian). Moscow, "Nedra", p. 193-211.

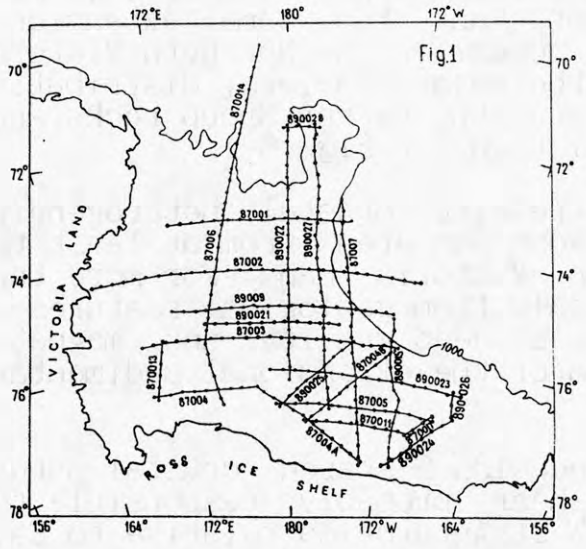

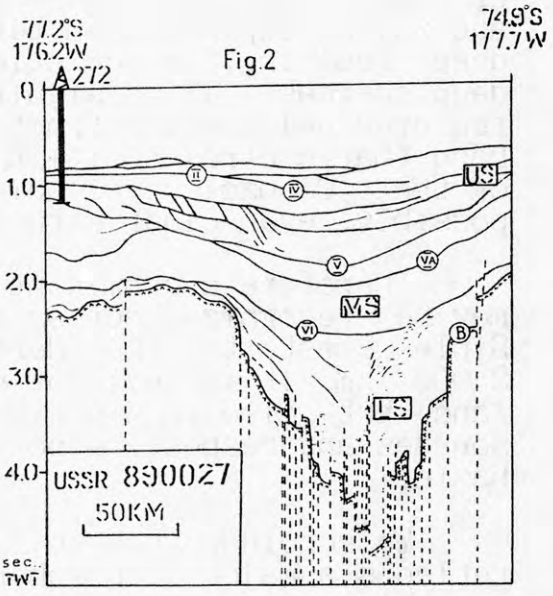

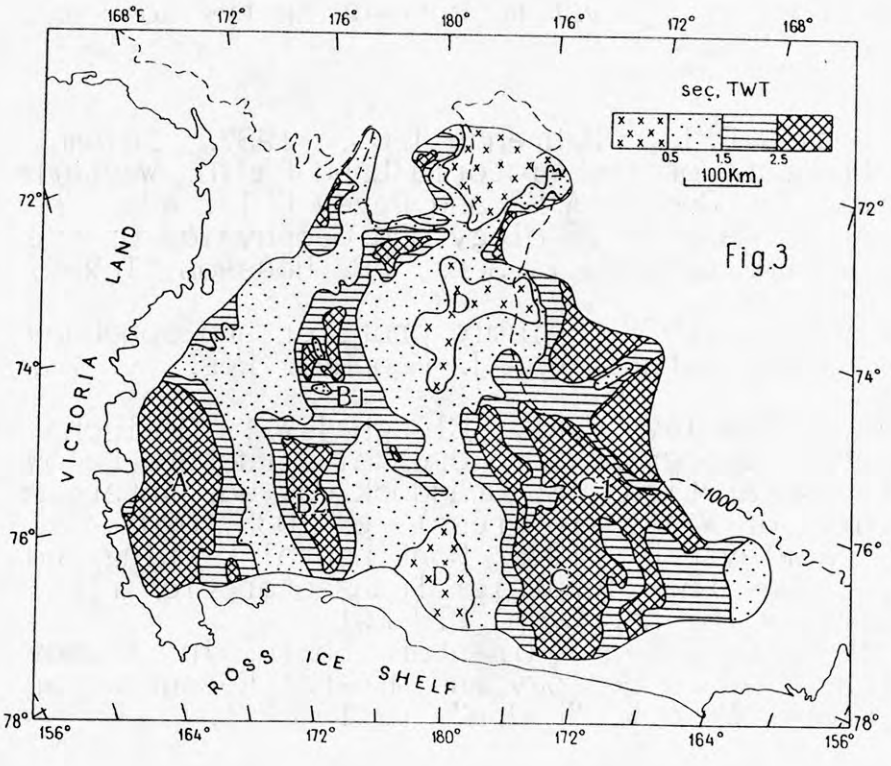

Fig.1. LOCATION OF R/V "GEOLOG DMITRY NALIVKIN" TRAKCLINES IN 1987 AND 1989.

Fig.2. TYPICAL EXAMPLE OF SEDIMENTARY COVER SUBDIVIDED INTO THREE SUPERSEQUENCES (LS-lower, MS - middle, US - upper). Numbers of unconformities in circles. B - surface of acoustic basement.

Fig.3.REFLECTION TIME INTERVAL BETWEEN SEA FLOOR AND ACOUSTIC BASEMENT. A - Victoria Land Basin, B-1 Northern Central Subbasin, B-2 Southern Central Subbasin, C -Eastern Basin, C-1 - marginal shelf subbasin, D-Central High. From Soviet and previously published data (Cooper et al., 1987).

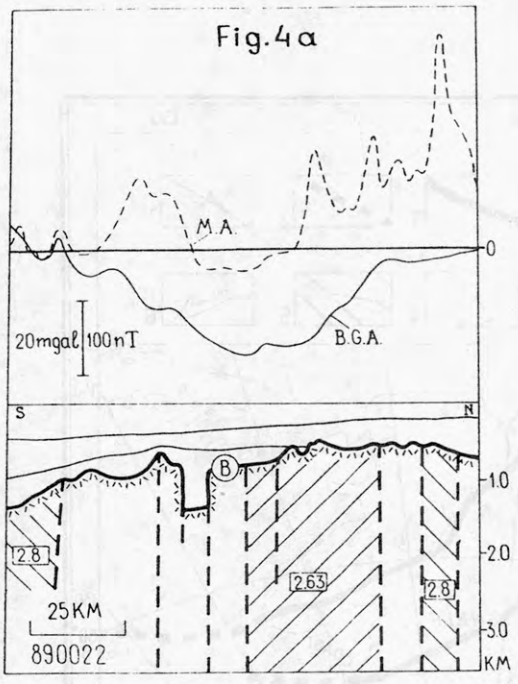

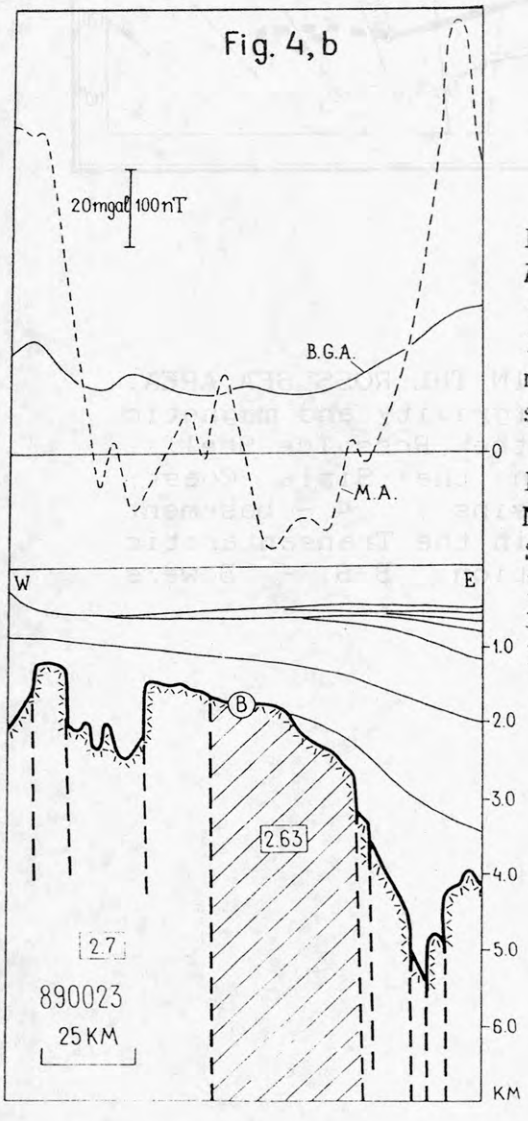

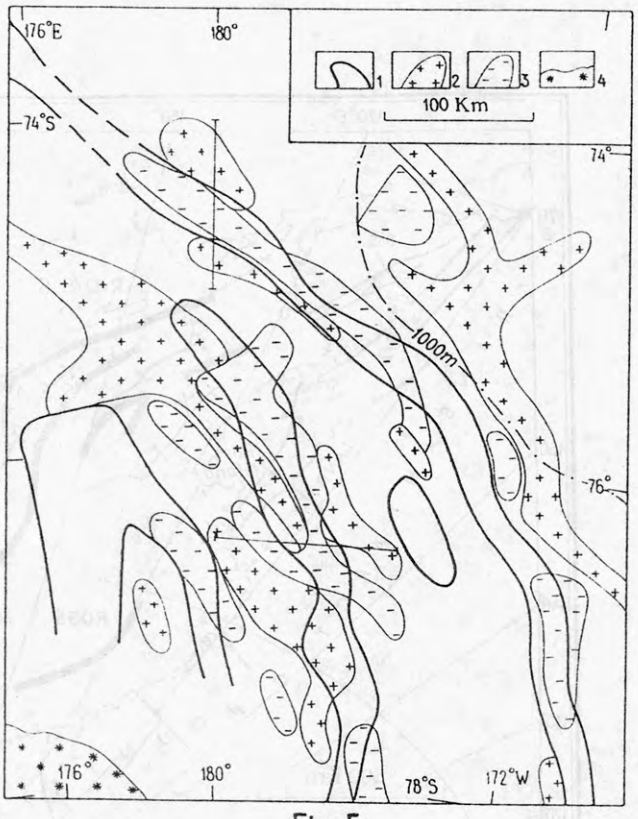

Fig.5

Fig.4. BOUGUER GRAVITY AND MAGNETIC ANOMALIES ALONG THE LONGITUDINAL (a) AND LATITUDINAL (b) SECTIONS OF INTERPRETED SEISMIC PROFILES. Basement densities in Mg/m^3. Location of sections is shown in Fig.5.

Fig.5. ZONES OF GRAVITY AND MAGNETIC ANOMALIES ON THE ROSS SEA SHELF. 1-regional Bouguer gravity lows, 2-regional magnetic highs, 3 - regional magnetic lows, 4-Ross Ice Shelf.

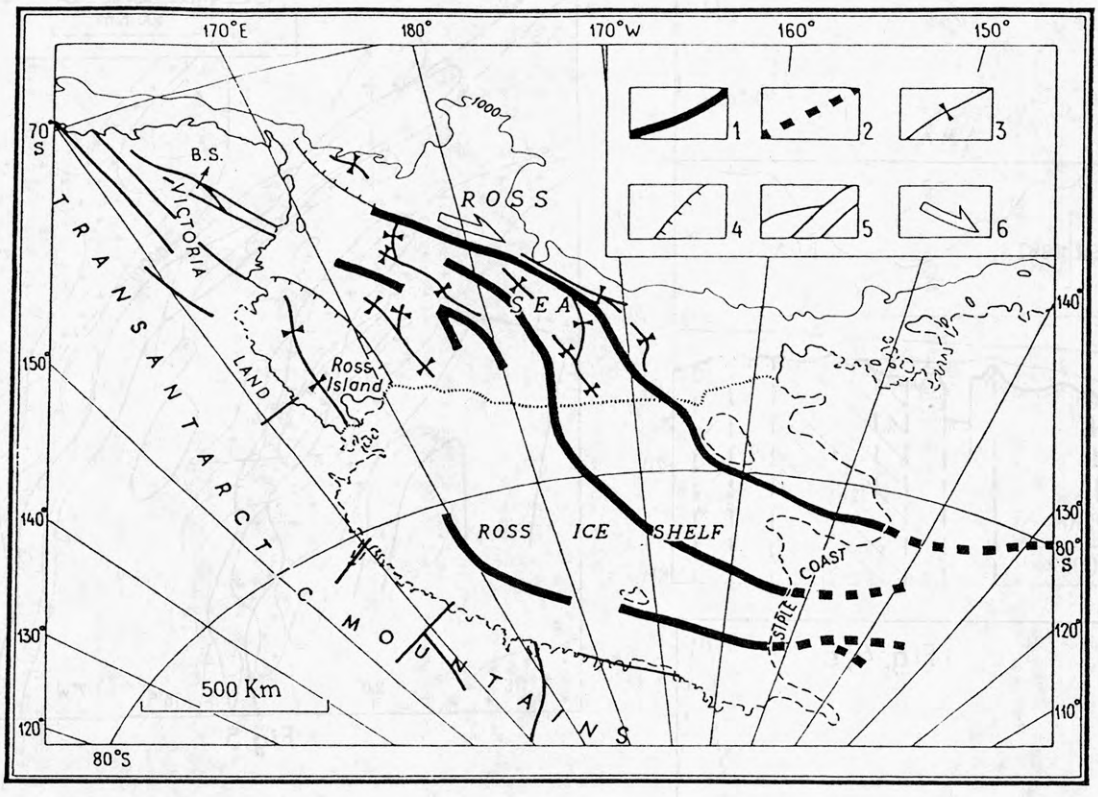

Fig.6. TECTONIC SEGMENTATION IN THE ROSS SEA AREA. 1-Zones of regional anomalies (gravity and magnetic in the open shelf, gravity on the Ross Ice Shelf); 2 - anomaly zones inferred on the Siple Coast; 3 - axes of sedimentary basins ; 4 - basement escarpments; 5 - major faults in the Transantarctic Mountains; 6 - shear direction. B.S. - Bowers Structure.

SEDIMENTOLOGY AND PALEOENVIRONMENTS OF THE BEACON STRATA AT BEAVER LAKE, PRINCE CHARLES MOUNTAINS
(poster presentation)

V.V. Traube, North Branch for Marine Geologic Research and Exploration "Sevmorgeologia", 120 Moyka, 190121 Leningrad, USSR

The Permian beds in the Beaver Lake area is the only known occurrence of Beacon sedimentation in central Antarctica. The first stratigraphic subdivision and general description of these rocks [Mond, 1972] was subsequently supplemented by more detailed studies [Ravich, 1974; Ravich et al.,1977] and some recent modifications [McKelvey, Stephenson, 1990]. Field observations were mostly concentrated on Flagstone Bench and along adjacent coast of Radok Lake and Pagodroma Gorge.

Apart from additional studies in the same locality, the author extended field research to the junction of Flagstone Bench and Jetty Peninsula (Fig.1). Two key sections each 160 m thick were documented in detail at sites 581 and 570 (Fig.2, I and II, respectively); they are 7 km apart and probably separated by a major fault.

The first sedimentary section is typical for the Flagstone Bench Formation. It consists of cross-bedded medium - to coarse-grained sandstones with some gravel admixture and clay galls; vaguely-bedded poorly-sorted sandstones rich in gravel; pale green and lilac siltstones and dark-brown or dark -red clays.

The sedimentary sequence at Jetty Peninsula includes a unique cycle (Jetty Formation) starting from deposition of olistolithes, boulderstones, breccias with large coal fragments, conglomerates with exceptionally coarse debris material (unit 2, Fig.2, II; Fig.3) indicating sharp activization of tectonic movements. The coarse unit grades in poorly sorted mixed rocks which in turn are succeeded by clays and limestones (unit 6, Fig.2,II). This unit is followed by a hiatus corresponding to stable tectonic period. Above disconformity there is a thick sandstone unit that represents a dramatic change in depositional environment.

The Jetty Formation and the overlying sandstone unit can be traced northward along Jetty Peninsula at least as far as site 585. However, this type section which is apparently rather persistent on the east coast of Beaver Lake, has no distinct equivalents elsewhere in the Radok-Beaver Lakes area and can not be correlated with any known section of the Amery Group.

Despite the lack of definite correlation, the Permian strata of both the Amery Group and the Jetty Formation belong

to continental paleoenvironments characterized by landsliding, fluviolacustrine, high-energy alluvial facies with predominant paleocurrent directions to NEN on Flagstone Bench and slightly more easterly trends on Jetty Peninsula (Fig.4).

Thick low-energy alluvial deposits of similar age are inferred in deep grabens underlying the Prydz Bay Shelf (Cooper et al., in press). Perhaps, in late Paleozoic - early Mesozoic time a single linear depression controlled transit of sediments across the present-day Beaver Lake area, Amery and Prydz Bay shelf into epicontinental depositional paleobasin subsequently rifted as the result of Gondwana breakup.

REFERENCES:

Cooper A.K., Stagg, H., Geist, E., in press. Seismic stratigraphy and structure of Prydz Bay, Antarctica: Implications from ODP Leg 119 drilling: In Barron J., Larsen,B., eds., Scientific Results of ODP Leg 119 drilling, Volume B: College Station, TX (Ocean Drilling Program), 57 pp.

McKelvey, B.C., Stephenson, N.C.N., 1990. A geological reconnaissance of the Radok Lake area, Amery Oasis, Prince Charles Mountains: Antarctic Science, v.2, N 1, p.53-66.

Mond, A., 1972. Permian sediments of the Beaver Lake area, Prince Charles Mountains. In Adie, R.J., ed. Antarctic geology and geophysics. Oslo, Universitetsforlaget, p.585-589.

Ravich, M.G.,1974. Section through the Permian coal-bearing sediments of the Beaver Lake area (Prince Charles Mountains, East Antarctica). In: "Antarctica", Repts. of the Comiss., 13, Moscow, "Nauka", p.19-35 (in Russian).

Ravich, M.G., Gor, Yu.G., Dibner, A.F., Lobanova, O.V., 1977. The stratigraphy of Upper Paleozoic Coal Measures (Beaver Lake Area, East Antarctica). In: "Antarctica", Repts. of the Comiss., 16, Moscow, "Nauka", p.62-75 (in Russian).

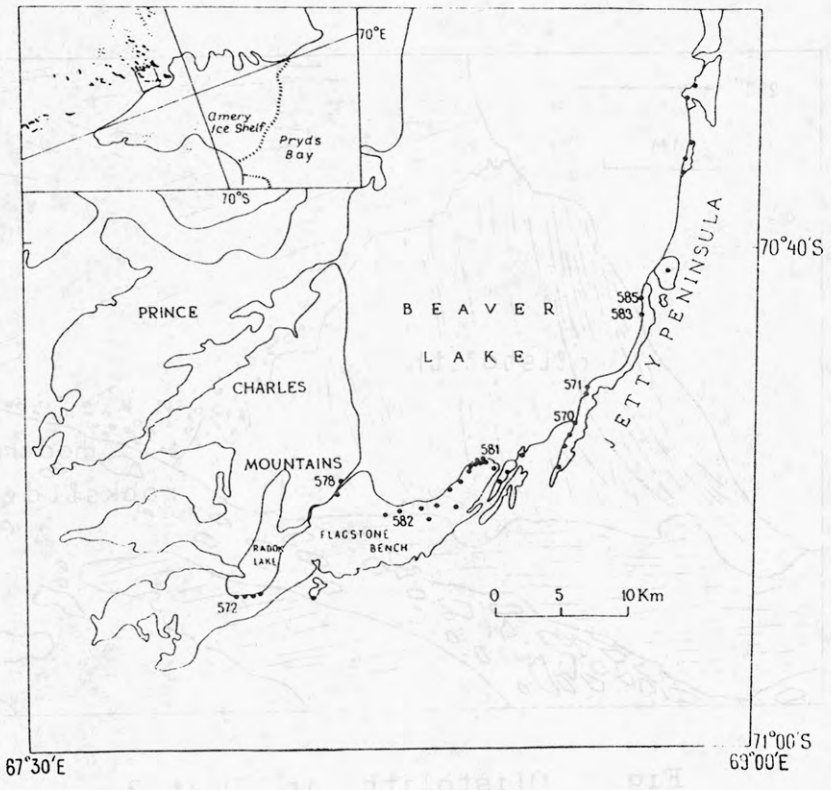

Fig.1. Sketch map of the Beaver Lake area. Black circles refer to the studied outcrops.

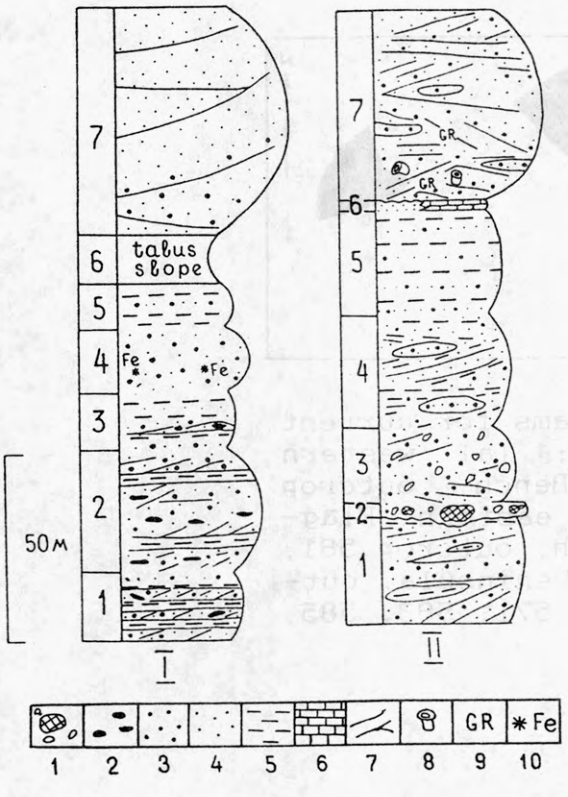

Fig.2. Sedimentary sections exposed in the eastern part of Flagstone Bench (I) and Jetty Peninsula (II): 1 - boulderstone, breccia, conglomerate; 2-clay galls; 3-gravel; 4 - sandstone; 5 -siltstone, clay; 6 - limestone; 7-cross bedding; 8 - silicified wood; 9 - detrital garnet; 10 -ferruginous concretions.

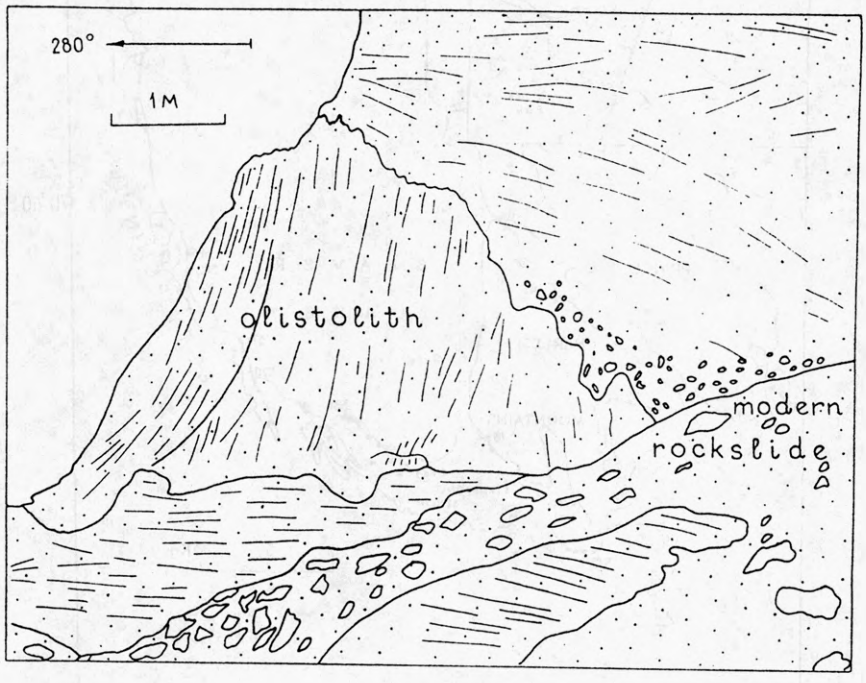

Fig.3. Olistolith in Unit 2 of the Jetty Peninsula sedimentary sequence.

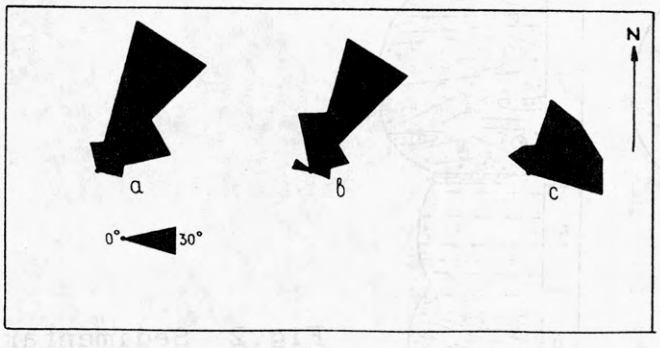

Fig.4. Rose diagrams for current directions: (a) western Flagstone Bench, outcrop 582, (b) eastern Flagstone Bench, outcrop 581, (c) Jetty Peninsula, outcrops 570, 571, 583, 585.

SOME NEW INSIGHTS INTO TECTONIC HISTORY OF NORTH-WEST WEDDELL SEA MARGIN (from Preliminary Results of the 1990 Marine Survey)

V.V. Traube, A.N. Rybnikov, North Branch for Marine Geologic Research and Exploration "SEVMORGEOLOGIA", 120 Moyka, 190121 Leningrad, USSR

A reconnaissance marine geophysical survey in the north-western Weddell Sea and the southern Scotia Sea was made on Leg 32 of R\V "Geolog Dmitry Nalivkin" in February - March 1990. The surveyed area considerably extended previous work by the UK and Japanese expeditions [King and Barker, 1988; Shinizu et al., 1989] (Figure 1).

Despite hostile weather conditions, 4900 km of survey profiles were obtained including continuous magnetic observations, depth sounding, gravity and HRS measurements and moreover 4 600 km of 48- to 24-fold MCS. Due to the unusually southward position of drifting ice edge, it was possible to extend some profiles beyond 65° S.

SIGNAL air-guns grouped by three to form 366 to 421 cu.in. sources and PRAKLA SEISMOS streamer 2400 m long with five RCL-2 depth regulators (10-25 m) were implemented for MCS survey; group length was 50 m, phones per group 64, shotpoint interval 25 m (9-12 s); maximum recording time was 6 s. Digital recording was provided by GRAD - AM equipment.

HRS survey was carried out using a 20 m streamer with 40 phones submerged to 2-4 m depth. Source signal ranged between 150 and 200 Hz. The depth of penetration was up to 800 m.

Gravity survey by GMN-K gravimeters was tied to ship anchoring sites near terrestrial gravity stations on Laurie and Elephant Islands. The accuracy of measurements was tested at 23 intersections. Magnetic gradiometer differential observations were recorded in both digital and analog mode.

Navigation was provided by NAVSTAR GPS.

By February 1991 only some preliminary results were available. They are given in a general review of sedimentary basins in the Weddell Province by Grikurov et al. (this volume).

More advanced interpretation of the collected data will be possible in the near future in terms of basins boundaries, structural features of seismic sequences, Cenozoic sedimentation, extentional tectonics and breakup events, crustal structure of the southern Scotia Arc and relation between different tectonic

provinces (including transition from the Jurassic Basin [LaBreque and Ghidella, in press] to the Weddell deep seabed).

REFERENCES:

Grikurov G.E., Ivanov V.L., Traube V.V., Leitchenkov G.L., Aleshkova N.D., Golynsky A.V., Kurinin R.G. (this volume). Structure and evolution of sedimentary basins in the Weddell Province.

King E.C., Barker P.F., 1988. The margins of South Orkney microcontinent. J. Geol. Soc., Lond., v. 145, p. 317-331.

LaBreque J.L., Ghidella M.E., 1991. Bathymetry, depth to magnetic basement and sediment thickness estimates from aerogeophysical data over the Western Weddell (in press).

Shimizu S., Morishima H., Tamura Y., 1989. Preliminary report of geophysical and geological survey off the South Orkney Islands, Scotia Arc region. Proc. NIPR Symp. Antarct. Geosci., 3, p. 52-64.

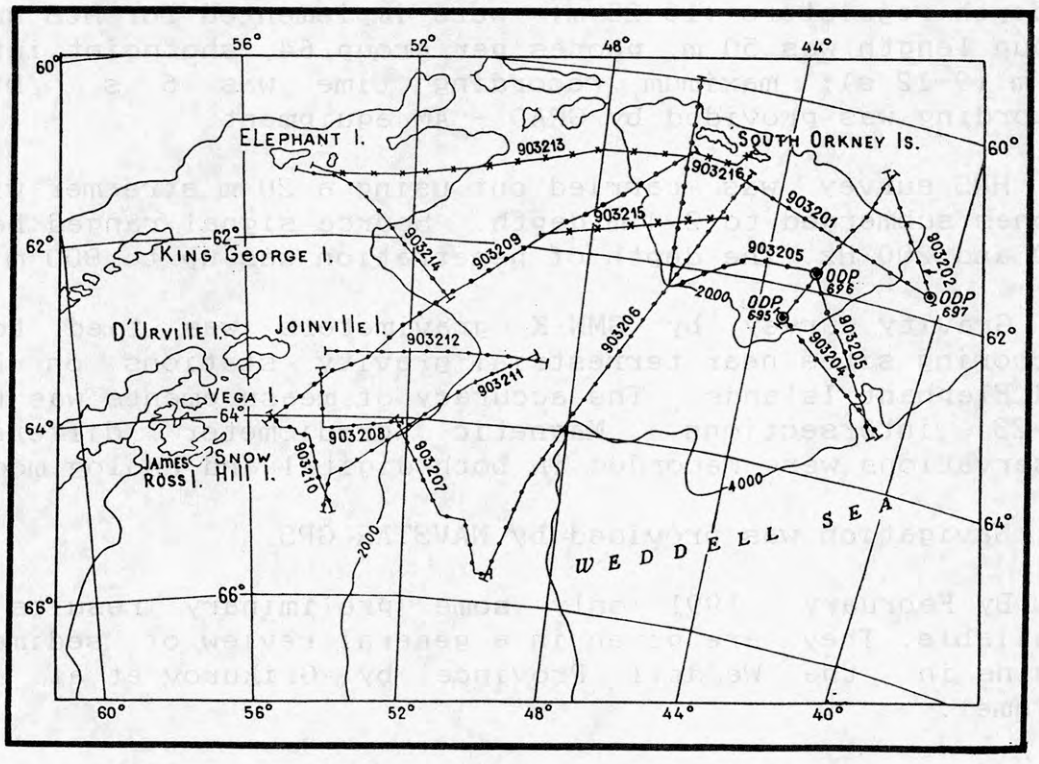

Figure1. LOCATION OF SHIP TRACKLINES RECORDED IN FEBRUARY - MARCH 1990. PROFILES 903213, 903215, 903216 WITHOUT MCS.

STRUCTURE AND ORIGIN OF PROGRADING SEQUENCES IN THE ROSS SEA BASIN

V. V. Traube, I. V. Zayatz, North Branch for Marine Geologic Research and Exploration "Sevmorgeologia", 120 Moyka, 190121 Leningrad, USSR

The Soviet MCS research in the Ross Sea in 1987 and 1989 aboard R/V "Geolog Dmitry Nalivkin" significantly contributed to studies of glacial sedimentation and related prograding sequences. A large progradational body established earlier in the Eastern Basin (Hinz and Block 1983), was intersected by several more seismic lines, and a previously unknown smaller sequence of similar character was discovered adjacent to the North Victoria Land; location of MCS lines where distinct prograding patterns were recorded is shown in Fig. 1.

Prograding supersequence (PSS) in the Eastern Basin is comparable in size to the Mississippi Delta (Frazier, 1967; Fig. 2); its thickness reaches 2.0 - 3.5 km with a depocenter extending beneath the present-day shelf break (Fig. 3). Internal structure of PSS is demonstrated in Fig. 4, lines 87003, 87004B, 890015.

The base of PSS is represented by unconformity V that can be traced immediately below the 17.5 Ma strata at the bottom of DSDP hole 272 (Steinhauff et al., 1987). The presence of aggradational sequences beneath unconformity V (Cooper et al., in press) indicates that this regional early Miocene boundary reflects the first grounding of the ice shelf at the paleoshelf edge in the eastern Ross Sea.

In the north-west Ross Sea shelf reflector V is observed above the base of a much smaller prograding sequence (Fig. 4, line 87006). Judging by a lower stratigraphic position here of the PSS base and the CIROS data (Barrett, 1989), the earliest grounding events along the Transantarctic Mountains front did occur in late Oligocene time.

To explain the huge volume of clastic material in the Ross Sea Basin involved in formation of the outer shelf topset beds, PSS and thick sedimentary apron farther downslope, one must assume repeated and deep glacial retreats allowing for rapid transportation of sediment from the Antarctic source area and vigorous accumulation on adjacent margin. Open marine paleoenvironments in late Tertiary time confirmed by micropaleontological data (Webb et al., 1984) must have interchanged with advances and groundings of ice sheet imprinted in at least a dozen of unconformities in the Upper Tertiary sequences.

Seaward migration of shelf break defined by paleoposition of successive unconformities is shown in Fig. 5 to demonstrate the summary progradational effect in the eastern Ross Sea. Evidently, shelf progradation was to a large degree controlled by a linear depositional agent, most likely an advancing ice front that must have been responsible for redistibution and seaward transportation of debris.

It is therefore evident that amount and regional extent of glacial fluctuations on the Ross Sea shelf could have been very considerable, and that sedimentation processes were affected by the retreats of ice sheet just as much as by glacial advances. The late Cenozoic history of West Antarctic ice sheet must have been more dynamic than previously suspected.

REFERENCES:

Barrett, P. J., 1989,ed. Antarctic Cenozoic History from CIROS-1 Drillhole. Dept. Sci. Industr. Res. Bull. 245, Wellington, 255p.

Cooper, A. K., Barrett, P. J., Hinz, K., Traube, V., Leitchenkov, G., Stagg, H. M. J. (in press). Cenozoic prograding sequences of the Antarctic continental margin: a record of glacio-eustatic and tectonic controls. Marine Geology.

Frazier, D. E., 1967. Recent deltaic deposits of the Mississippi delta: their development and chronology. Trans. Gulf -Cst Ass. Geol. Socs., 17, p. 287-315.

Hinz, K., Block, M., 1983. Results of geophysical investigations in the Weddell Sea and in the Ross Sea, Antarctica: Exploration in New Regions. Eleventh Petrol. Congr., Lond., PD 2(1), p. 1 - 13.

Steinhauff, D. M., Renz, M. E., Harwood, D. M., Webb, P-N., 1987. Miocene diatom biostratigraphy of DSDP hole 272: Stratigraphic relationship to the underlying Miocene of DSDP hole 270, Ross Sea. Antarct. Journ. US, v. XXII, No 5, p. 123-125.

Webb, P-N., Harwood, D. M., McKelvey, B. C., Mercer J. H., Stott, L. D., 1984. Cenozoic marine sedimentation and ice volume variation on the East Antarctic Craton. Geology, V. 12, P. 287-291.

Fig.1. Location of MCS Lines crossing the prograding sequences. Numbers refer to sections shown in Fig.4.

Fig.2. The Ross Sea prograding supersequence in comparison with the Mississippi Delta.

Fig.3. Map of reflection time (s, TWT) between seafloor and unconformity V.

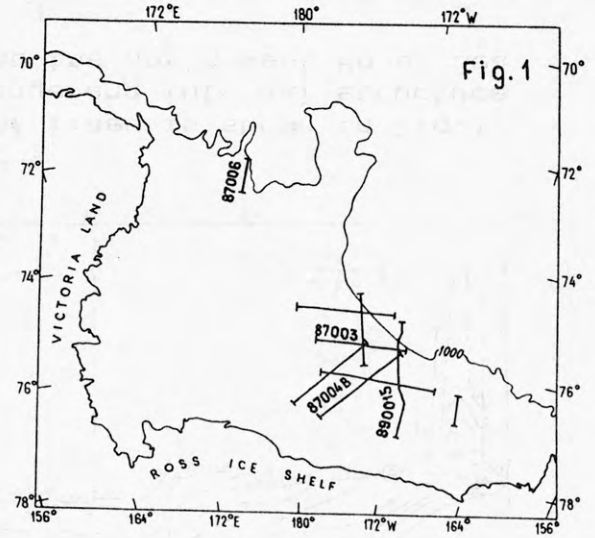

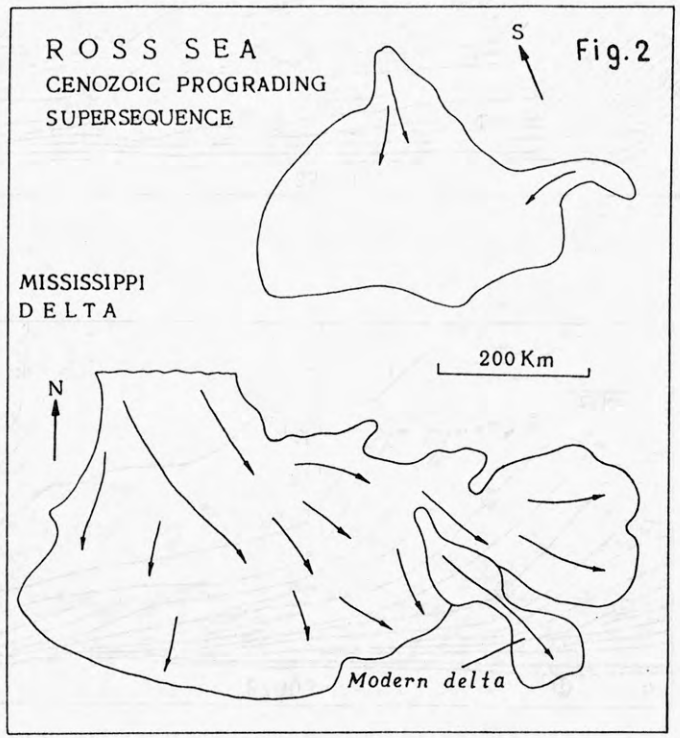

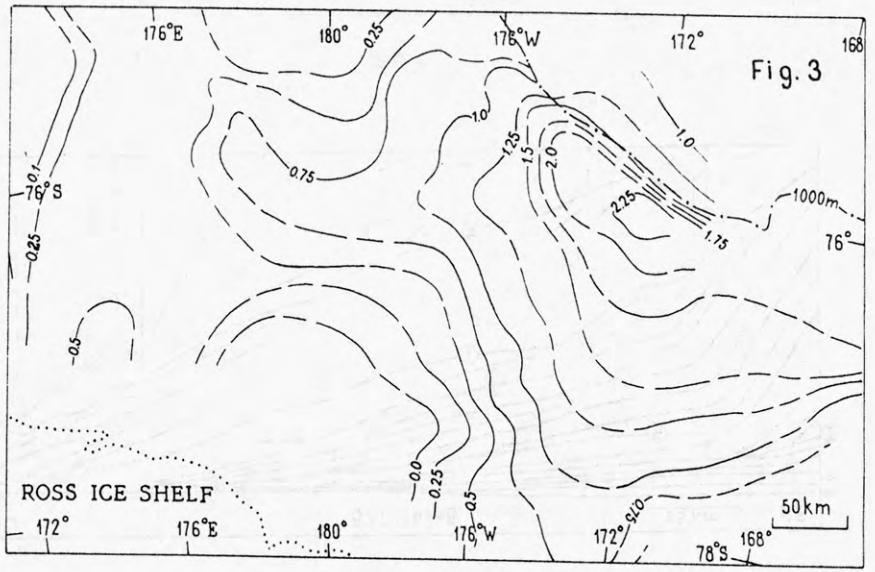

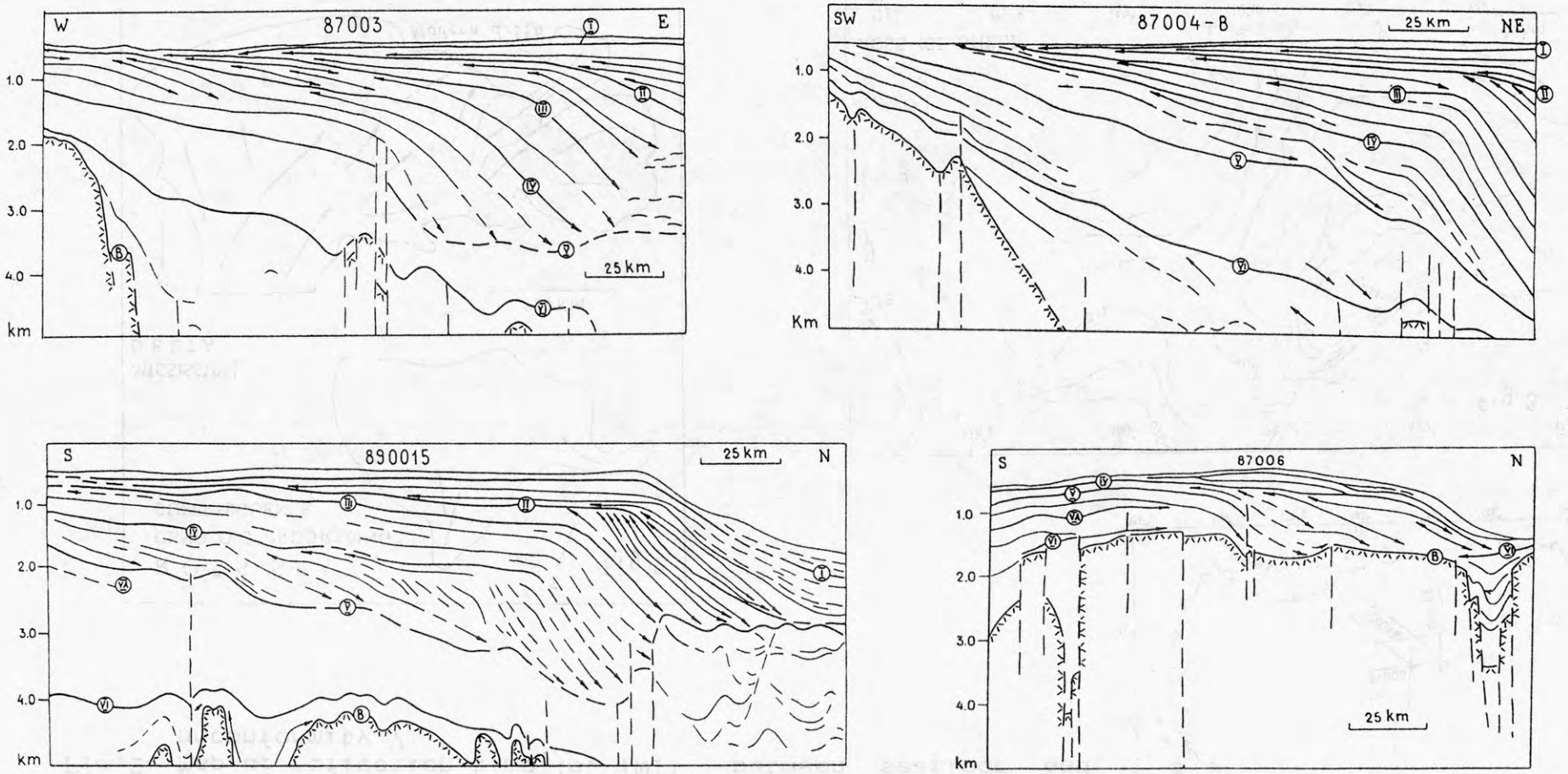

Fig.4. Interpreted sections of prograding sequences. Location of lines is shown in Fig.1. Note the difference in total volume, stratigraphic range and internal structure between prograding supersequences in the Eastern Basin and the north-west Ross Sea shelf.

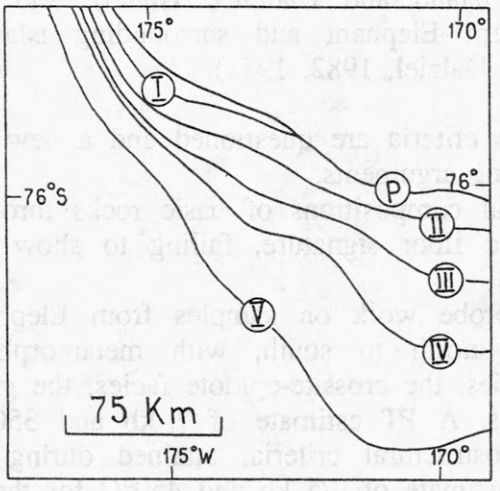

Fig.5. Advance of shelf break due to successive accretion of progradational sequences since the unconformity V time till the present time.

A NEW SUBDIVISION OF THE SCOTIA METAMORPHIC COMPLEX

Rudolph A.J. Trouw, Departamento de Geologia, Universidade Federal do Rio de Janeiro, Ilha do Fundão, CEP 21910, Rio de Janeiro, Brazil

The Scotia metamorphic complex of the South Shetland and South Orkney Islands, interpreted as an accretionary wedge, constitutes part of the active pacific margin of Gondwana. On the basis of contrasting metamorphic grade and possible age differences it has been subdivided into Terrane A of blueschist/greenschist facies (Smith Island, northern Elephant Island and Clarence Island), and Terrane B of epidote-amphibolite facies, (southern Elephant and surrounding islands and South Orkney Islands; Tanner et al. 1982; Dalziel, 1982, 1984).

In this paper these criteria are questioned and a new subdivision is proposed which considers the following arguments.

- The whole rock chemical compositions of basic rocks throughout the complex are predominantly of oceanic floor signature, failing to show any difference between Terrane A and Terrane B.
- Petrographic and microprobe work on samples from Elephant Island confirmed a gradual transition from north to south, with metamorphic assemblages of the pumpellyite-actinolite facies, the crossite-epidote facies, the greenschist facies and the epidote-amphibolite facies. A PT estimate of 7 kb and 350°C for the central part was, according to microstructural criteria, attained during the first deformational phase, whereas another estimate of 4/5 kb and 450°C for the southern part seems to reflect local conditions during the second of three deformation phases.
- Radiometric age dating failed to show a clear difference between north and south Elephant Island. However, differences in metamorphic age between the metamorphic rocks of the South Orkney Islands (~ 190 Ma), the Elephant Island group (70/120 Ma) and Smith Island (50/100 Ma), and the non-metamorphic sedimentary rocks from the Seal Islands just north of Elephant Island (< 25 Ma, based on fossils and K-Ar dating in a volcanic pebble) do appear to be real (Hervé et al., 1990, 1991; Trouw et al., 1990; Tanner et al., 1982).
- The South Orkney Islands metamorphic rocks, formerly grouped together with south Elephant Island because of their similar field appearance and metamorphic grade (Tanner et al., 1982; Dalziel, 1982, 1984), show a gradual transition from epidote-amphibolite facies to lower greenschist facies on Powell Island, similar to the transition on Elephant Island (but lacking blue amphibole). This illustrates that metamorphic grade is not a sound base for subdivision.

It is concluded that neither metamorphic grade nor lithology are reliable criteria for subdivision. Radiometric age data and chemical data seem to be more reliable. The following subdivision of subsequently accreted parts of oceanic affinity is proposed: a) South Orkney Islands metamorphic rocks (~ 190 Ma), b) Elephant Island group and Smith Island (50/120 Ma), c) Seal Islands Formation (< 25 Ma).

REFERENCES

Dalziel, I.W.D. (1982). The pre-Jurassic history of the Scotia arc: a review and progress report. In: Antarctic Geoscience, ed. C. Craddock, pp. 111-126. Madison; University of Wisconsin Press.

Dalziel, I.W.D. (1984). Tectonic evolution of a fore-arc terrane, southern Scotia ridge, Antarctica, Washington, DC; Geological Society of America Special Paper, 200, 32 pp.

Hervé, F., Miller, H., Loske, W., Milne, A. & Pankhurst, R.J. (1990). New Rb-Sr age data from the Scotia metamorphic complex of Clarence Island, West Antarctica. Zbl. Geol. Paläont. Teil I, H. 1/2, pp. 119-126.

Hervé, F., Loske, W., Miller, H. & Pankhurst, R.J. (1991). Chronology of provenance, deposition and metamorphism in the southern limb of the Scotia arc. In: Geologic evolution of Antarctica, eds. M.R.A. Thomson, J.A. Crame & J.W. Thomson, Cambridge, Cambridge Univ. Press.

Tanner, P.W.G., Pankhurst, R.J. & Hyden, G. (1982). Radiometric evidence for the age of the subduction complex in the South Orkney and South Shetland Islands, West Antarctica. J. Geol. Soc. Lond., 139, pp. 683-690.

Trouw, R.A.J., Pankhurst, R.J. & Kawashita, K. (1990). New radiometric age data from Elephant Island, South Shetland Islands. Zbl. Geol. Paläont. Teil I, H. 1/2, pp. 105-118.

GEOTRANSECT DRAKE PASSAGE - WEDDELL SEA, ANTARCTICA

Rudolph A.J. Trouw, Departamento de Geologia, Universidade Federal do Rio de Janeiro, Ilha do Fundão, CEP 21910, Rio de Janeiro, Brazil
Luiz A.P. Gambôa, Petrobrás S.A., Rio de Janeiro, Brazil

INTRODUCTION

The transect traverses the Antarctic Peninsula close to its northern extremity, where it is presently surrounded by oceanic crust. The opening of the Weddell and Scotia Seas and the ridge crest interactions along its western margin, transformed the peninsula into a tectonically unstable strip of continental crust, along which there has been rifting and wrench-fault related block movement. Because all the major tectonic boundaries are recognizable and most still active, it is a natural laboratory to study the interactions among lithospheric plates. This work is a condensed version of a panel and text submitted for publication in the Geotransect series of the IUGS. The major tectonic elements, in order of appearance from NW to SE, will be described in the next paragraphs.

DRAKE PASSAGE/ACCRETIONARY COMPLEX

The transect starts in the Drake Passage on oceanic crust varying from about 15 Ma at the northwestern end to about 25 Ma below the South Shetland Trench.

The morphologic and structural expressions of the South Shetland Islands accretionary complex appear clearly on the seismic sections. The subducted oceanic crust, the sediments and the prograding layers of the fore-arc basin can be observed on these profiles. No outer arc high exists adjacent to the South Shetland Islands and thus the lithologies of the fore-arc rocks can not be investigated directly. However, on both extremes of the South Shetland Islands, somewhat outboard of their main trend, relatively high P/T metamorphic rocks crop out, both on Smith Island and in the Elephant Island group. These have been interpreted as part of an accretionary complex, formed along the Pacific margin of Gondwana. The continuous trench and arc geometry suggests that these isolated outcrops are in fact uplifted fragments of a continuous accretionary complex, parallel to the trench. Since in the present transect corridor no such rocks crop out, an inset map of the Elephant Island group has been projected below the actual fore-arc basin in the interpretative cross-section.

The main lithologies in the Elephant Island group are grey, green and blue phyllites and schists, with local intercalations of calc-silicate rocks, marble, amphibolite and metachert (Dalziel, 1984). A dunite-serpentinite sheet on Gibbs Island has been described by de Wit et al. (1977).

Three metamorphic zones have been recognized on Elephant Island (Trouw et al., in press) with increasing metamorphic grade towards southwest: a low grade chlorite zone with pumpellyite, a garnet zone with blue amphibole and a biotite zone with garnet, hornblende and albite. The gradual changes between these zones suggest one prograde sequence of subduction related metamorphism of Sanbagawa type. The protoliths of these rocks, such as pelitic sediments, cherts, thin limestones and basaltic rocks, are interpreted as associated with a subduction zone environment.

The structure of the Elephant Island group has been described by Dalziel (1984) and Trouw (1988). Three deformational phases left their record: D1, D2 and D3. D1 seems to represent the subduction movements. Strain analysis resulted in a probable SW subduction direction with relation to the actual position of Elephant Island. This position however may result from rotation through 90° or more in a clockwise sense since mid-Cretaceous time, as proposed in several break up reconstructions of Gondwanaland. The second phase, D2, folded the earlier structures into open and tight south to SSE verging folds. This phase seems to represent late back-thrusting. Post-metamorphic structures with variable orientation are grouped together as D3 structures and may be related to heterogeneous uplift.

Most radiometric age determinations on rocks of the Elephant Island group by both K-Ar and Rb-Sr methods, have yielded ages in the range 80-120 Ma (Tanner et al., 1982; Dalziel, 1982; Hervé et al., in press; Trouw et al., 1990).

Few kilometers north of Elephant Island, at the Seal Islands, non-metamorphosed folded conglomerates and siltstones crop out, that are also part of the subduction complex. They contain microfossils of Miocene to Recent age (Trouw et al., in press).

SOUTH SHETLAND ISLANDS

The central part of the South Shetland Islands is mainly composed of volcanic and plutonic rocks of calc-alkaline affinity (Smellie et al., 1984) with few intercalated sedimentary rocks, constituting part of a magmatic arc of Cretaceous to mid-Tertiary age. This sequence, locally with sediments on top and at the bottom, overlies unconformably folded layers of Permian-Triassic turbidity current sequences, called Miers Bluff Formation. The youngest rocks in the Islands are Quaternary ensialic alkaline volcanics (Smellie, 1987) probably related to extension.

The Miers Bluff Formation crops out exclusively at Hurd Peninsula, Livingston Island (Smellie et al., 1984; Dalziel, 1972). A mainly steep standing sequence of at least three kilometers thick, without top or bottom exposed, is composed of sandstones, siltstones, shales and some rudites. The nature of bedding contacts, and internal sedimentary structures, point to a turbidity current origin. The composition of clastic material indicates a source area with metamorphic and sedimentary rocks, and also volcanic and plutonic rocks, probably representing an active magmatic arc on a continental margin. The age of the Miers Bluff Formation is poorly constrained. Most of the authors, referring to this formation consider it equivalent to the Trinity Peninsula Group, with probable Permian-Triassic sedimentation age (Pankhurst, 1983; Dalziel, 1984; Storey and Garrett, 1985).

A thick pile of magmatic arc volcanic and intrusive rocks locally exceeding several thousand meters of mainly calc-alkaline basaltic and andesitic lavas, covers most of the South Shetland Islands that appear on the strip map (Smellie et al., 1984; Birkenmajer, 1983). The age varies form Early Cretaceous in the west (Livingstone Island), to Tertiary in the east (King George Island). The detailed geology, chemistry and age determination for these islands have been described by Smellie et al. (1984) and, in particular King George Island, by Birkenmajer (1983 and references in Dalziel, 1989). At Cape Melville, King George Island, some 300 m of marine fossiliferous sediments of Early Miocene age occur on top of the volcanic pile (Birkenmajer, 1984) possibly indicating the end of the arc activity.

Smellie et al. (1988) described outcrops of ensialic alkaline basaltic volcanic rocks, related to Neogene and Quaternary extension on Livingston and Greenwich Islands, consisting mostly of dolerite plugs encased in stratified lapilli-tuffs. Lavas are extremely rare and the deposits were probably erupted from numerous small, overlapping volcanic centres. Birkenmajer (1983) described diabase dykes dated at 20-21 Ma, sealing normal faults related to extension at southern King George Island, possibly related to the initiation of the opening of the Bransfield Basin.

BRANSFIELD BASIN

The Bransfield Basin has been interpreted as formed by interarc spreading (Barker, 1982; Storey and Garrett, 1985; Parra et al., 1988; Gambôa et al., 1988). It separates the South Shetland Islands, the location of the latest volcanic arc activity, from the Antarctic Peninsula. The age of opening of the Bransfield Basin is unclear. The existent evidence indicates that the basin was formed less than 4 Ma ago. Based on the correlation of the basin with closed and folded basins south of the Hero Fracture Zone, Gambôa and Maldonado (in press) suggested that the opening of this basin could be older than previously proposed, probably as old as 20-21 Ma as the diabase dykes studied by Birkenmajer (1983).

The Bransfield Basin has an asymmetrical profile with a steeper slope along its northern margin and with a conspicuous spreading center closer to the South Shetland Islands. As shown by Gambôa and Maldonado (in press), the southern margin of the Bransfield Basin shows the structural and stratigraphic characteristics of an Atlantic type margin. Two main sedimentary sequences occur along this margin and are separated by a regional unconformity. The older sequence, interpreted as deposited during the rifting event that separated the South Shetland Islands from the Antarctic Peninsula is faulted and in many places tilted towards the continent. The younger sequence, above the unconformity, is not affected by faulting and dips gently towards the central parts of the basin forming the present southern margin of the Bransfield Basin and covers the interpreted basaltic crust near the spreading center.

ANTARCTIC PENINSULA AND BRANSFIELD PLATFORM

Since the Antarctic Peninsula and Bransfield Platform were united with the South Shetland Islands before the opening of the Bransfield Rift, the rock units are essentially the same as those described for the South Shetland Islands. The main difference is that Trinity Peninsula is apparently a higher uplifted, and therefore deeper eroded, part of the magmatic arc, resulting in the predominance of basement outcrops with abundant intrusives and few remainders of volcanic rocks. Another difference is that the age of the intrusives is considerably older (Middle Jurassic-Cretaceous), illustrating the north-westward migration of the magmatic arc in time, probably as a result of outward migration of the subduction zone accompanying the growth of the accretionary prism (Storey and Garrett, 1985).

The basement is composed of folded sandstones and shales, with few conglomerates, interpreted as turbidity current sequences and named Trinity Peninsula Group (TPG). The thickness is likely to exceed several thousand metres. Clastic fragments of metamorphic rocks, including garnets, suggest the presence of a metamorphic basement at depth, as shown on the interpretative cross-section. Deformation and regional metamorphism of the TPG increases towards the SW along Trinity Peninsula, from only tilted, faulted but little folded, unmetamorphosed strata at Hope Bay, to prehnite-pumpellyite facies, strongly folded and cleaved slates and phyllites further to the SW.

The age of the metamorphism and deformation is not precisely known, but must predate the overlying Upper Jurassic strata.

South of Hope Bay, in the Camp Hill area, and north of Botany Bay a group of continental sedimentary rocks rests with an angular unconformity on top of the TPG. These rocks, named Botany Bay Group contain well preserved plant remains and have been assigned ages ranging from Rhaetian to earliest Cretaceous (see Thomson and Pankhurst, 1983 and Farquharson, 1984, for discussion).

On top of these sedimentary rocks, again with a slight unconformity, rest volcanic rocks of the Antarctic Peninsula Volcanic Group (APVG). Very little of these volcanic rocks is now left in the area covered by the strip map. The period of this volcanism probably had its beginning in the Late Jurassic and continued until the Paleogene. Arc plutonism is represented by granites and granodiorites. The oldest pluton in the strip map area and also in the whole of northern Graham Land has yielded late Middle Jurassic K-Ar mineral ages of between 160-175 Ma. The huge granite body in the surroundings of Cape Roquemarel, visible on the strip map, and also in the transect, yielded Late Jurassic ages (142-146 Ma), but most other bodies produced Cretaceous ages in the range 90-110 Ma (Pankhurst, 1982). Magnetic anomalies below the Bransfield Platform led Garrett and Storey (1987) and Parra et al. (1988) to the hypothesis of the presence of a huge mafic igneous body in this site, possibly related to extension in the arc.

Ensialic extensional alkaline volcanics of Late Tertiary and Quaternary age cover the older sequences locally on the east side of the Peninsula.

LARSEN BASIN

This basin has been defined as the western margin of the Weddell Sea, adjacent to Graham Land (Macdonald et al., 1988). It is bounded to the east by the shelf-break towards the oceanic crust of the Weddell Sea and to the west, through steep faults, by the Antarctic Peninsula. It has been claimed that the opening of the Weddell Sea began in Middle-Late Jurassic times, but the main phase of opening was probably during the Early Cretaceous. It seems likely that the mechanism of formation of the basin was related to a major phase of Middle Jurassic - Early Cretaceous dextral transcurrent motion, causing the fragmentation of West Antarctica into crustal blocks separated by pull-apart basins. A recent review paper on the basin has been published by Macdonald et al. (1988). Geophysical data published by del Valle et al. (1988) and Keller et al. (1989) furnished some control on the thickness shown on the interpretative cross-section.

REFERENCES

Barker, P.F., 1982, The Cenozoic subduction history of the Pacific margin of the Antarctic Peninsula: ridge crest-trench interactions, Journal of Geological Society of London, v. 139, p. 787-801.

Birkenmajer, K., 1983, Late Cenozoic phases of block-faulting on King George Island (South Shetland Island, West Antarctica), Bull. Acad. Polon. Sci., Sciences de la Terre, 30, p. 21-32.

Birkenmajer, K., 1984, Geology of the Cape Melville area, King George Island (South Shetland Islands, Antarctica): pre-Pliocene glaciomarine deposits and their substratum, Stud. Geol. Polon., 79, p. 7-36.

Dalziel, I.W.D., 1972, Large-scale folding in the Scotia Arc, in: Antarctic Geology and Geophysics, edited by R.J. Adie, p. 47-55, Universitetsforlaget, Oslo.

Dalziel, I.W.D., 1982, Pre-Jurassic history of the Scotia Arc region, in: Antarctic Geoscience, edited by C. Craddock, p. 111-126, University of Wisconsin Press, Madison, Wisconsin.

Dalziel, I.W.D., 1984, Tectonic evolution of a forearc terrane, southern Scotia Ridge, Antarctica, Spec. Pap. Geol. Soc. Am. 200, 32 p.

Dalziel, I.W.D., 1989, Tectonics of the Scotia Arc, Antarctica, Field trip guidebook T 180, 28th Int. Geol. Cong., Amer. Geoph. Union, Washington, 206 p.

del Valle, R.A., Diaz, M.T., Febrer, J., Fourcade, M., Fournier, H.G., Gasco, J.C., Keller, M.A., Medina, F., Nuñez, H.J., and Pomposiello, M.C., 1988. Mid-Cretaceous boundary detected below the Seymour Island and its tracing offshore along the north-eastern coast of the Antarctic Peninsula by magnetotelluric measurements, Acta Geol. Geoph. Mont. Hung., vol. 23 (2-4), p. 265-286.

de Wit, M.J., Dutch, S., Kligfield, R., Allen, R. and Stern, C., 1977, Deformation serpentinization and emplacement of a dunite complex, Gibbs Island, South Shetland Islands: Possible fracture zone tectonics, J. Geol., 85, p. 745-762.

Garrett, S.W. and Storey, B.C., 1987, Lithospheric extension on the Antarctic Peninsula during Cenozoic subduction, Geol. Soc. Spec. Publ. no. 28, p. 419-431.

Gambôa, L.A.P. and Maldonado, P.R., in press, Geophysical investigations in the Bransfield Strait and in the Bellingshausen Sea-Antarctica, American Association of Petroleum Geologists Memoir.

Gambôa, L.A.P., Barrocas, S.L. and Maldonado, P.R., 1988, Investigações Geofísicas no Estreito de Bransfield e Mar de Bellingshausen-Antártica, Anais do XXXV Congresso Brasileiro de Geologia, Belém, V. 5, p. 2343-2357.

Hervé, F., Loske, W., Miller, H. and Pankhurst, R.J., in press, Chronology of provenance, deposition and metamorphism in the southern limb of the Scotia arc, in: Geologic Evolution of Antarctica, edited by M.R.A. Thomson, J.A. Crame and J.W. Thomson, Cambridge University Press, U.K.

Keller, M.A., del Valle, R.A., Diaz, M.T. and Rinaldi, C.A., 1989, Evolution of the Larsen Basin from a Seismic Section Analysis, 28th Int. Congr. Abstracts, vol. 2, p. 170-171, Washington.

Macdonald, D.T.M., Barker, P.F., Garrett, S.W., Ineson, J.R., Pirrie, D., Storey, B.C., Whitham, A.G., Kinghorn, R.R.F. and Marshall, J.E.A., 1988, A preliminary assessment of the hydrocarbon potential of the Larsen Basin, Antarctica, Mar. Pet. Geol., 5, 34-53.

Pankhurst, R.J., 1982, Rb-Sr geochronology of Graham Land, Antarctica, J. Geol. Soc. London, vol. 139, p. 701-711.

Pankhurst, R.J., 1983, Rb-Sr constraints on the ages of basement rocks of the Antarctic Peninsula, in: Antarctic Earth Science, edited by R.L. Oliver, P.R. James and J.B. Jago, p. 367-371, Australian Academy of Science, Canberra.

Parra, J.C., Yanez, G., and USAC Working Group, 1988, Aeromagnetic Survey of the Antarctic Peninsula and surrounding seas: Integration of the data obtained at different altitudes, Ser. Cient. INACH 38, p. 118-131.

Smellie, J.L., 1987, Geochemistry and tectonic setting of alkaline volcanic rocks in the Antarctic Peninsula: a review, J. Volc. Geotherm. Res., vol. 32, p. 269-285.

Smellie, J.L., Pankhurst, R.J., Hole, M.J. and Thomson, J.W., 1988, Age, distribution and eruptive conditions of late Cenozoic alkaline volcanism in the Antarctic Peninsula and eastern Ellisworth Land: review, Brit. Antar. Sur. Bull., v. 80, p. 21-49.

Smellie, J.L., Pankhurst, R.J., Thomson, M.R.A. and Davies, R.E.S., 1984, The geology of the South Shetland Islands: VI Stratigraphy geochemistry and evolution, Brit. Antar. Sur. Sci. Reps., no. 85, 85 p.

Storey, B.C. and Garrett, S.W., 1985, Crustal growth of the Antarctic Peninsula by accretion, magmatism and extension, Geological Magazine, v. 122, p. 5-14.

Tanner, P.W.G., Pankhurst, R.J. and Hyden, G.M., 1982, Radiometric evidence for the age of the subduction complex in the South Orkney and South Shetland Islands, West Antarctica, J. Geol. Soc. London, v. 139, p. 683-690.

Thomson, M.R.A. and Pankhurst, R.J., 1983. Age of post-Gondwanian calc-alkaline volcanism in the Antarctic Peninsula region, in: Antarctic Earth Science, edited by R.L. Oliver, P.R. James and J.B. Jago, p. 328-333, Australian Academy of Science, Canberra.

Trouw, R.A.J., 1988, Structural analysis of the Elephant Island Group, South Shetland Islands, Ser. Cient. INACH. 38, p. 141-162.

Trouw, R.A.J., Pankhurst, R.J. and Kawashita, K., 1990, New radiometric age data from Elephant Island, South Shetland Islands, Zentralbl. Geol. Paläont. Teil I, H 1/2, p. 105-118.

Trouw, R.A.J., Ribeiro, A. and Paciullo, F.V.P., in press, Structural and metamorphic evolution of the Elephant Island group and Smith Island, South Shetland Islands, in: Geologic Evolution of Antarctica, edited by M.R.A. Thomson, J.A. Crame and J.W. Thomson, Cambridge University Press, U.K.

Carbon and Oxygen Isotopic Compositions of Calc-silicate Rocks in the Sør Rondane Mountains, East Antarctica

N.Tsuchiya, Department of Resources Engineering,Faculty of Engineering,Tohoku University,Aoba-ku,Sendai,980.
Y.Osanai, Department of Earth Sciences and Astronormy,Fukuoka University of Education,729,Akama, Munakata, 811-41.
H.Wada, Institute of Geosciences,Faculty of Science, Shizuoka University,836,Oya,Shizuoka,422.

1.Introduction

The Sør Rondane Mountains extend 22° to 28° E and 71.5° to 72.5° S and is one of the largest inland mountain ranges in East Antarctica. These mountains mainly consist of high- and medium-grade metamorphic and plutonic rocks.

This paper presents stable isotopic compositions of carbon and oxygen of calcites in marbles and calc-silicate rocks from the central part of the Sør Rondane Mountains. Isotopic features provide an insight into how the metamorphic fluids interacted with carbonates during metamorphism(Rye et al.,1976).

The samples analyzed were collected during the 31st Japanese Antarctic Research Expedition(JARE-31)in 1989-1990.

2.Geological Setting

The metamorphic rocks in the Sør Rondane Mountains are divided into two groups(Van Autenboer,1969). One is the Teltet-Vengen group which is composed of high-grade gneisses and the other is the Nils-Larsen group which is composed of mylonitized tonalitic rocks(Shiraishi et al.,1991).

The metamorphic rocks of the Teltet-Vengen group are mainly composed of pelitic, psammitic gneisses and intermediate gneiss.Thin layers and lenses of calcareous rocks(e.g. marbles and calc-silicate rocks)are distributed in the northern and central parts of the mountains. The grade of metamorphism is of granulite facies(Kojima and Shiraishi,1986; Ishizuka and Kojima, 1987;Shiraishi et al.,1991).

Whole-rock Rb-Sr and Sm-Nd isochron dating shows c.1000Ma for granulite rocks from the northern part of the mountains (Shiraishiand Kagami,1988). Osanai et al.(1988) estimated the

metamorphic temperature and pressure of the granulite-facies rocks from pelitic system to be 750-850° C and 7-8 kbar, respectively. Many plutonic rocks which are mainly granite intruded into the metamorphic rocks as forming large masses at the time of 550-500 Ma(Takahashi et al.,1990,1991).

3.Samples and Analytical Methods

Analyzed calcite samples in marble and calc-silicate layers were collected from the Teltet-Vengen group in Menipa, central part of the Sør Rondane Mountains.

The calcite samples were collected in perpendicular to the strike of the layers at various distance from the contact with the nearest gneiss and/or mylonitized granite.

For carbon and oxygen isotope analyses of calcite, carbon dioxide gas was extracted by reacting calcite with H_3PO_4 as described by McCrea(1950). Resulting CO_2 was analyzed with a mass-spectrometer, Finnigan Mat 250, at the Institute of Geosciences, Shizuoka University. The experimental data are reported in terms of the quantity delta defined by $\delta(‰)=(R_{sample}/R_{standard}-1)X1000$, where $R_{standard}$ is PDB(Craig,1957).

4.Results

Figs.1 and 2 show carbon and oxygen isotopic compositions of marbles. Carbon isotope ratio ($\delta^{13}C$ value) ranges from -6.1 to 2.2‰ (Fig.1). Carbon isotope composition of the marble layer is heterogeneous and changes on the scale of 10 centimeters. In the middle part of the marble layer, $\delta^{13}C$ value is higher than 0‰. However, the $\delta^{13}C$ value decreases toward the boundary between the marble and gneiss on both sides. Oxygen isotope ratio($\delta^{18}O$ value) ranges from -17.1 to -15.8‰ and shows little change in the marble layer(Fig.1).

In No.N90012001 sample series, the $\delta^{13}C$ ranges from 0.5 to 3.3‰ and the $\delta^{18}O$ ranges from -11.7 to -7.3‰ (Fig.2). These values decrease toward the mylonite which is intercalated in the marble layers. The $\delta^{13}C$ value are nearly identical to that of N90011905 in the middle part of the marble layers. Near the boundary between the marble and mylonite, however, $\delta^{13}C$ values are higher than that at the boundary between the marble and gneiss of N90011905. $\delta^{18}O$ values are higher than that of N90011905.

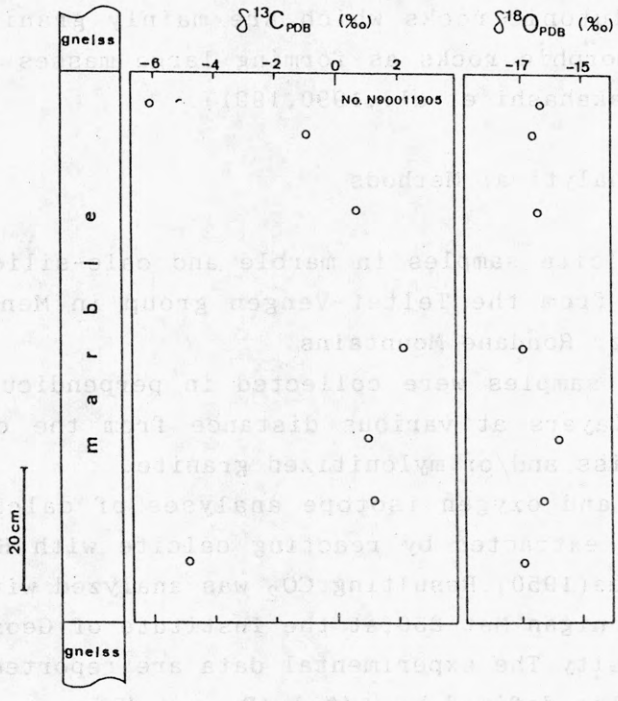

Fig.1 Carbon and oxygen isotopic compositions of marble (Sample No.N90011905).

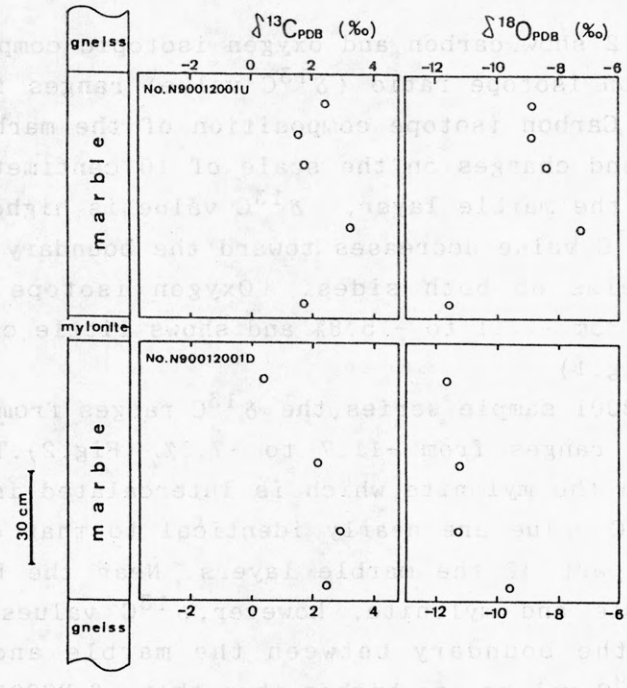

Fig.2 Carbon and oxgen isotopic compositions of marbles (sample No.N90012001U,D).

5.Mathematical Model of One-dimensional Metamorphic Fluid Flow

The isotope distribution patterns in the marble layers could be interpreted by a fluid flow model within the layers.One-dimensional fluid flow model is based on the following assumptions:

(1)Mass transport is controlled by conduction and advection in a porous medium.

(2)The diffusion constant and the porosity are constant(Bickle and McKenzie,1987).

(3)Metamorphic fluid is incompressible(Mckenzie,1984:Labotka et al.,1989).

The fundamental equation of mass transfer is

$$\frac{\partial C}{\partial T}=\frac{\partial^2 C}{\partial Z^2}-Pe\frac{\partial C}{\partial Z}, \qquad (1)$$

where T is dimensionless time,C the dimensionless concentration, Z the dimensionless distance and Pe the Peclet number that describes the tramsport characteristics in terms of a dimensionless constant. Pe is defined as vL/D, where v is the velocity of metamorphic fluid, L the characteristic length and D the diffusion constant.

The initial and boundary conditions are given as follows:

$C=1$, when $T=0$ (2)

$C=0$, at $Z=-1$ (3)

$C=0$, at $Z=0$. (4)

Analytical solution is obtained as follows:

$$C=2\pi\exp\left(\frac{Pe}{2}Z\right)\sum_{n=1}^{\infty}\frac{n\left\{\exp\left(\frac{Pe}{2}\right)(-1)^n-1\right\}sinn\pi Z}{n^2\pi+\frac{Pe^2}{4}}\exp\left\{-\left(n^2\pi^2+\frac{Pe^2}{4}\right)T\right\} \qquad (5)$$

Fig.3 shows that relationship between dimensionless distance Z and dimensionless concentration C from Eq.(5) at Pe=0. The calculated profiles are symmetrical against Z, which means mass transfer is controlled by conduction only. Fig.4 shows relationship between Z and C at Pe=20. Assuming that metamorphic fluid flows from left side to right side and that mass is transported

by conduction and advection, the calculated variation profiles of C for all dimensionless time(except T=0) are asymmetric against Z.

Variation of dimensionless carbon isotopic composition of No.N90011905 plotted against Z in Fig.3 is similar to the calculated variation profile at time T=0.02. Experimentally determined carbon isotopic composition of No.N90012001D is asymmetric against Z,and its variation profile is similar to the calculated profile at T=0.02(Fig.4). These results suggest that metamorphic fluid flowed from the mylonite to the gneiss through the marble layer. The dimensionless time T(0.02) suggests pressure depleted period with isothermal condition in retrograde path.

$\delta^{13}C$ value of the nearest position above the mylonite in N90012001U is slightly lower and $\delta^{18}O$ value of that decreases toward the mylonite, which means that metamorphic fluid flowed from the mylonite,however,quantitative analysis is not be possible by this mathematical model.

This model shows that discrepancy between the variation profiles of carbon and oxygen isotopic compositions in Figs.1-2 is due to difference between the temperature dependence of diffusion constants of carbon and oxygen.However,carbon and oxygen isotopic

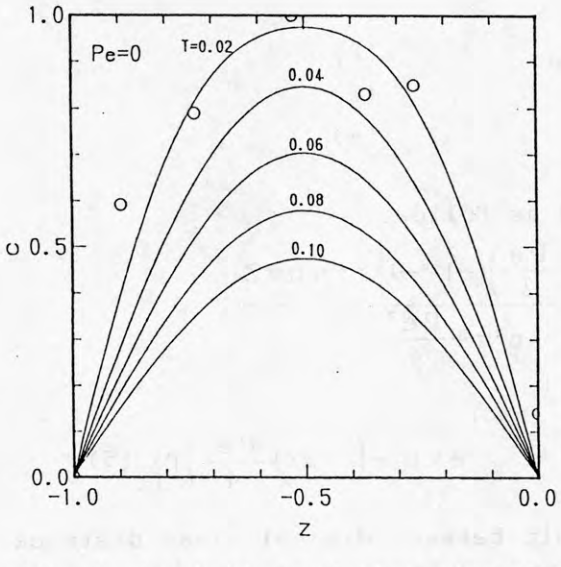

Fig.3 Variation of dimensionless concentration C plotted against dimensionless distance Z at Pe=0. Open circles represent dimensionless carbon isotopic composition of N90011905.

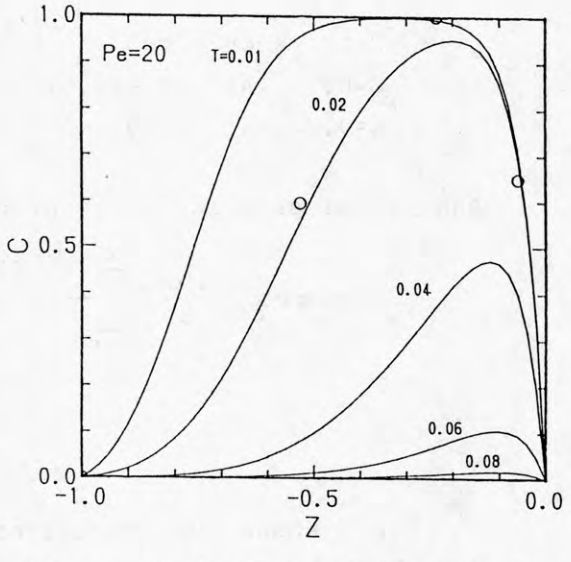

Fig.4 Variation of dimensionless concentration C plotted against dimensionless distance Z at Pe=20. Open circles represent dimensionless carbon isotopic composition of N90012001D.

compositions of marbles depend on fluid composition,isotopic compositions of fluid and fluid rock ratio. Therefore, the flat patterns of $\delta^{18}O$ values in Figs.1-2 suggest that the discrepancy mentioned above does not only depends on the temperature dependence of diffusion constants but only carbon-oxygen atomic ratio in fluid.

6.Conclusions

(1)Cabon and oxygen isotopic compositions of marbles and calc-silicate rocks are heterogeneous within thin layers.
(2)Variation profile of carbon and oxygen isotope compositions indicates that both advective and diffusive transport by metamorphic fluid are significant.

Acknowledgements

We are greatly indebted to Prof.Chida of Tohoku University for valuable discussion.

References

Bickle,M.J.and Mckenzie,D.(1987)Contrib.Mineral.Petrol.,95,384-392.
Craig,H.(1957)Geochim.Cosmochim.Acta,12,133-149.
Ishizuka,H.and Kojima,H.(1987)Proc.NIPR Symp.Antact.Geosci., 1,113-128.
Kojima,S.and Shiraishi,K.(1986)Mem.Natl Inst.Polar Res.,Spec. Issue,43,116-131.
Labotka,T.C. et al.(1988)Am.Mineral.73,1302-1324.
McCrea,J.M.(1950)J.Chem.Phys.,18,849-857.
Mckenzie,D.(1984)J.Petrol.,25,713-765.
Osanai,Y.et al.(1988)Proc.NIPR Symp.Antact.Geosci. (Abstract),2,170
Osanai,Y.et al.(1991)Proc.NIPR Symp.Antact.Geosci.,5.(in press)
Rye,R.O.et al.(1976)Geochim.Cosmochim.Acta,40,1031-1049.
Shiraishi,K. and Kagami,H.(1988)Program Abstr.9th Symp. Abstract.Tokyo,Natl Inst.Polar Res.,67-68.
Shiraishi,K. et al.(1991)Gelogical Evolution of Antarctica, Cambride Unive.Press,77-82.
Takahashi,Y. et al.(1990)Proc.NIPR Symp.Antact.Geosci.,4,1-8.
Takahashi,Y. et al.(1991)ibid.,5,(in press)
Van Autenboer,T.(1969)Antarct.Map Folio Ser.,Folio 12.

NEW ZEALAND'S GEOLOGICAL MAPPING PROGRAMME, SOUTHERN VICTORIA LAND, ANTARCTICA

I.M. Turnbull, DSIR Geology & Geophysics,
DSIR, Private Bag, Dunedin, New Zealand

Systematic 1:50 000 geological mapping of Southern Victoria Land began in 1980/81 when an Australian group studied and mapped Beacon Supergroup sediments in the Beacon Heights area. In 1982/83 and 1984/85 this group was joined by New Zealand Geological Survey staff and mapped the Shapeless Mountain and Mt Bastion areas. The programme was taken over by NZGS in 1987/88 in response to widespread demand for up-to-date geological maps. Three maps are published, with four more in preparation.

The mapping has produced much new data and significant re-interpretation of several aspects of Southern Victoria Land geology. Detailed mapping of basement Granite Harbour Intrusives, in conjunction with Otago University, has enabled recognition of 14 separate granitoid plutons between the Ferrar and MacKay glaciers, with several dike swarms, and rare gabbroic intrusives (Thundergut, St Johns maps). Newly established field relationships mean that previous radiometric ages can now be fitted into an intrusive sequence. Proterozoic granitoids have been deformed together with their host Koettlitz Group amphibolite to granulite metamorphic rocks, and have in turn been intruded by undeformed Ordovician plutons. New geochemical data shows the presence of several suites within the intrusive sequence.

Within the Devonian Taylor Group, Beacon Supergroup, the stratigraphy established at Beacon Heights (Beacon Heights map) has been extended over a large area, although revision is proposed in the north (Convoy Range map). A newly recognised unit, characterised by conglomerate with volcanic and lowgrade metasedimentary provenance, extends over much of the St Johns Range (St Johns map). A series of fining-upward cycles has been recognised in the south (Knobhead map), new trace fossil assemblages have been documented, and new paleoenvironmental interpretations can be made (Knobhead, Bastion, Shapeless, Convoy maps). Fault-fold offset of the Kukri Erosion Surface has been demonstrated, as has lateral transport of the Beacon sequence and erosion surface, above Ferrar Dolerite sills (St Johns map).

Mapping of surficial deposits and McMurdo Volcanic Group has confirmed previous observations. Up to five glacial episodes can now be recognised (Convoy Range, St Johns maps). No potentially economic mineral deposits have been found, apart from coal seams in the Mt Bastion area.

The eventual aim of the project is to produce a 1:250 000 scale regional map, with accompanying monograph, of the geology of Southern Victoria Land. The project will take another 10 years to complete, given current financial and staff constraints.

GLACIAL GEOLOGY AND MOUNTAIN UPLIFT IN NORTH VICTORIA LAND

Frederik (Dick) M. van der Wateren,
Geological Survey of the Netherlands, P.O.Box 157,
NL-2000 AD Haarlem, The Netherlands.
Anja L. L. M. Verbers,
Bundesanstalt für Geowissenschaften und Rohstoffe,
D-3000 Hannover, Germany.

Glacial geologic investigations have been carried out in North Victoria Land since the first German Antarctic North Victoria Land Expedition (GANOVEX) in 1979/80. Since GANOVEX IV (1984/85) exposure dating of deglaciated bedrock surfaces by means of ^{10}Be has aided the reconstruction of the glaciation and deglaciation history of the Pacific termination of the Transantarctic Mountains. Our field work during GANOVEX VI (1990/91) focused on the response by the North Victoria Land icesheet to the differential uplift of the area since about 50 Ma.

^{10}Be dating of the icefree summit plateaus between 1000 and 1500 m above the present day ice surface has yielded ages between 2.7 and 4.0 Ma. This sets a time limit to the termination of the inundation phase of the Transantarctic Mountains, which has been termed Queen Maud Glaciation elsewhere in the Transantarctic Mountains and has been correlated with the Sirius Formation. Successively younger exposure ages are found at lower levels, e.g. approximately 1 Ma at 300 m above present day ice surface.

The Late Cenozoic glacial history of North Victoria Land can be divided into two main phases. During the Pliocene a local icesheet in North Victoria Land covered a peneplain, the remnants of which are now found at altitudes between 2500 and 3200 m. The striation and erratic dispersal patterns on the highest surfaces indicate that the centre of the Pliocene ice mass lay in the mountain ranges southeast of the Rennick Graben. This area has undergone the highest amount of uplift during the last 50 Ma, and even today is part of the ice divide between the Pacific and Ross Sea drainage areas.

During the Early Pleistocene the ice began to cut valleys into this peneplain. Isolated terraces at altitudes between 1000 and 2500 m are the remaining traces of the early part of this erosion phase. Ice radar measurements show that the bottoms of the largest outlet glaciers are up to 900 m below their surfaces, suggesting that between 1500 and 2500 m of valley erosion has occurred during the last 1 to 1.5 Ma. Presently, the Rennick Glacier drains Talos Dome, a local ice centre of the East Antarctic icesheet, located more than 250 km to the west of the Pliocene ice centre.

The oldest ice flow directions we have found curve towards the Rennick Graben, confirming the existence of this depression during the Pliocene. The following radical change in ice drainage in our view has been caused by reactivation of the Mesozoic tension system and subsequent relative downward movement of the Rennick Graben. We conclude that differential uplift of the Transantarctic Mountains, in connection with the Cenozoic rifting in the Ross Sea, have forced the ice drainage to change from a more or less radial to a linear flow pattern.

A GLACIAL GEOLOGICAL RECONNAISSANCE OF THE SOUTHERN PRINCE ALBERT MOUNTAINS, VICTORIA LAND, ANTARCTICA.

A.L.L.M. Verbers, Bundesanstalt für Geowissenschaften und Rohstoffe, Postfach 511053, Hannover 51, D-3000 Federal Republic of Germany.
F.M. Van der Wateren, Geological Survey of The Netherlands, Postbus 157, NL-2000 AD Haarlem, The Netherlands.

A glacial geological reconnaissance of the area between the David and Mawson Glaciers took place during GANOVEX VI 1990/91 (German Antarctic North Victoria Land Expedition). The aim was twofold: to achieve a general idea of the glacial history of the area, and to find evidence of the relationship between the Cenozoic mountain uplift and this glacial history. Ice flow directions were determined, till samples were taken for grain size distribution, microfossil, chemical and thin section analysis. Soils were described and sampled for chemical analyses and algae were collected for ^{14}C dating. Quartz was sampled from glaciated surfaces for ^{10}Be exposure dating.

The area consists of a series of nunataks which rise stepwise in a southwestern direction from an altitude of 800m near the coast to 2300 m inland. Parallel to the coast a more or less continuous ridge of nunataks consists of Granite Harbour Intrusives. In general these granitic nunataks are glacially rounded and due to strong weathering, no striations or crescentic marks were found.

The inland area consists of the remnants of a tableland of Kirkpatrick Volcanics and Ferrar sills alternating with Beacon sandstone which is almost entirely buried by ice. The Beacon peneplain, underlying these rocks, dips a few degrees to the west. This results in subhorizontal plateaus and terraces, which are rounded on the edges by the ice.
The plateaus are covered with a thin, discontinuous layer of till. The surfaces show a desert pavement and polygons. Ventifacts are abundant, although much of the patina has crumbled away by weathering. No obvious erratics were found, the rounded clasts seem to be locally derived.

Most nunataks have glacial terraces on the north-northeastern side. They occur 100 m to 400 m below the the level of the glacial plateaus and again are covered with a thin till layer containing several erratics. The ventifacts show a great variety in their weathering degree. These glacial terraces are incised by cirques. Some of the nunataks are flanked by vast areas of ice-cored moraines.

We conclude from our field observations that the glacially eroded plateaus must have been icefree for a longer period than the lower glacial terraces, as they show a stronger degree of weathering. Erratics, striae and crescentic marks show an ice flow direction to the northeast. Erratics derived from the basement rocks only occur on the glacial terraces and not on the highest plateaus. This implies that the valleys have been cut at times when the summit plateaus already were ice-free, but the terraces were still covered with ice. This could be an indication of mountain uplift, although datings are not yet available.

REGIONAL GEOPHYSICAL IMAGING OF THE ANTARCTIC LITHOSPHERE

Ralph R. B. von Frese, Douglas E. Alsdorf, Timothy M. Stepp, Daniel R. H. O'Connell, and Heong-Hee Kim, all at Byrd Polar Research Center and Dept. of Geological Sciences, The Ohio State University, Columbus, Ohio 43210, U.S.A.

The geology of Antarctica and adjacent marine areas is perhaps the most poorly known of any region of the earth. This paper examines the characterization of the antarctic lithosphere by satellite magnetometry and altimetry-derived gravimetrics, ship-to-shore seismic refraction studies, passive seismic experiments, and airborne geophysical reconnaissance studies.

Satellite measured magnetic anomalies were recently compiled for studies of the antarctic lithosphere south of 40°S from nearly 2,500 orbits of NASA's Magsat mission. This effort necessitated the development of enhanced processing procedures for extracting the lithospheric component from the satellite magnetometer observations, including least-squares collocation for altitude normalization of the orbital data, and wavenumber correlation analysis to remove the extremely dynamic variations of the polar external geomagnetic field. Differentially adjusted for the properties of the earth's core magnetic field, the resultant radially polarized Magsat magnetic amomalies demonstrate associations with numereous crustal features. Lithopheric interpretations relate Wilkes Land, Enderby Land, and the Ellsworth-Whitmore microplate with regions of positive magnetization. Prominent negative magnetizations characterize the Transantarctic Mountains, Amery Basin, Gamburtsev Mountains, Queen Maud Land, and many of the oceanic basins. Oceanic rises are commonly associated with regions of positive magnetization, whereas active ridges are characterized by a complex pattern of predominantly positive magnetizations.

Gravity anomalies provide additional constraints for investigating features of the antarctic lithosphere and for limiting the interpretational ambiguities of the magnetic anomaly data. Much of the coverage of the study region is available as gravity anomalies derived from satellite altimetry surveys of the marine waters by the GEOS-3, Seasat and Geosat missions. Analysis of the 1990 release of Geosat altimetry data for the area between 60°S to 72°S indicates a high degree of consistency between altimetry-derived gravity anomalies and shipborne gravity data. For comparison with radially polarized Magsat magnetic anomalies, the vertical gradient of the altimetry-derived free-air gravity anomalies was computed at Magsat elevation (~375 km) using a high degree and order spherical harmonic expansion of the gravity data. The results suggest predominantly direct correlations between the regional geopotential field anomalies, where the oceanic ridges and rises tend to be characterized by positive contrasts of lithospheric density, and the basins by mostly negative density contrasts.

Insight on the geologic interpretation of the satellite elevation geopotential anomaly fields of Antarctica can be obtained from studying the comparable anomaly fields of various continental fragments of Gondwana (eg., South America, Africa, India, etc.) with ostensibly better resolved tectonic frameworks. These efforts suggest that satellite elevation geopotential anomaly fields can yield significant constraints on the geologic evolution of Gondwana. For example, lithospheric density and magnetic properties of the Bengal Gulf margin of India may be extrapolated via the global perspective of satellite geopotentential field anomalies as first order models of the Mesozoic margin of Enderby Land. Similarly, the Cenozoic margin of Wilkes

Land may be related to lithospheric models of the southeastern margin of Australia.

Because of the sparse distribution of land gravity observations over Antarctica, free-air gravity anomaly predictions derived from the OSU89A spherical harmonic expansion for the geopotential (up to n=360; Rapp & Pavlis, 1990) provide the only estimate of gravity variations for the continent outside of the Ross Sea and ice shelf. Regional free-air anomalies from this model are constrained by the satellite-derived GEM-T2 coefficients (up to n=36) where surface observations are absent. We are using the predictions to fill in between the widely distributed gravity observations and to assess the relative variations in those observations, specifically in the West Antarctic rift system. Once the regional free-air anomalies are rectified with the control provided by surface observations, terrain corrections for variations in bedrock topography and ice thickness are applied to give a residual that we are using to determine the most likely mechanism of isostatic compensation in the West Antarctic-Transantarctic Mountains (TAM) region. Any tectonic model proposed for the cause of rifting and uplift of the TAM is constrained by this mechanism. Terrain corrections are directly calculated by 3-D Gauss-Legendre quadrature from digital models (NISDC data provided by K. Jezek) for surface terrain, bedrock topography, and ice thickness that are sampled on a uniform 20 by 20 km grid. Likewise, the numerical models are being used to assess the terrain effects on airborne gravity and marine gravity, especially when obtained within 30 km of the rugged TAM. Because the free-air anomaly correlates with topography, the numerical models can be used to obtain a "best fit" prediction of subice topography in broad areas of East Antarctica where ice thickness data are entirely lacking. Finally, the long wavelength signature of the gravity field provides information on lateral variations in lithospheric thickness and the longest wavelength components in the geoid ($n<10$) can be used to model the termal state of the upper mantle beneath the continent.

Additional constraints on the lithospheric features of the continental margin of Antarctica may be obtained by ship-to-shore seismic refraction surveys. As part of the 1988-1989 German Antarctic North Victoria Land Expedition V (GANOVEX V) offshore-onshore seismic retraction experiment, an aseismic recording array was established in the TAM to record a tuned airgun array operated in the Ross Sea. The objective was to determine the crustal structure of the transition zone between the TAM and the Ross Sea by recording 3 onshore-offshore seismic refraction profiles across the TAM near Terra Nova Bay. Unfavorable ice conditions in Terra Nova Bay reduced two onshore-offshore profile lengths and necessitated reorientation of the third profile. Other GANOVEX V groups deployed onshore and offshore seismographs to provide constraints on the crustal structure of the Ross Sea and inland TAM portions of the profiles.

An 11 element digital seismograph array was established 65 km inland from the Terra Nova Bay on the Tourmaline Plateau icecap. The array consisted of a 1.2 km linear array of 8 vertical seismographs, deployed at 150 m intervals away from the array center, and an equilateral (160 m sides) triangular deployment of 3-component seismographs about the array midpoint. The array recorded digital seismic waveforms generated by a 43.5 liter airgun array fired shots at 250 m intervals in the Ross Sea. Data were recorded at offsets of 65-150 km along three onshore-offshore profiles. Data were also recorded during 3 marine seismic refraction experiments located > 230 km from the array. Virtually all the airgun shots comprising the 3 onshore-offshore refraction profiles were recorded by all or part of the array. Clear seismic signals from the three > 230 km marine seismic profiles were not detected on single components of ground motion or

on shot ensemble constant velocity stacks consisting of 55 traces.

The record sections contain lower crustal refracted first arrivals, wide angle PmP reflections, and Pn Moho refraction first arrivals which constrain the crustal thickness beneath the portion the TAM near the shoreline of Terra Nova Bay to approximately 22 km. Large amplitudes produced by the Moho triplication and the lower crust Pg-Pn crossover produced excellent signal-to-noise on single seismograms. Spectral calculations indicate signal-to-noise ratios exceeding 10 in the 2-20 Hz frequency range with ambient noise levels less than 0.1 millimicrons during most of the recording period.

The Ross Sea portion of the crustal model was derived from the results of McGinnis et al. (1985), Cooper et al. (1987(a)), and Cooper et al. (1987(b)), and Makris (personal communication). Ray tracing modeling of line 1 travel-time data indicate slow crustal thickening (1 km thickening per 10 km offset) beneath the TAM between the coastline and 20 km inland.

The travel-time and waveform data require a gradual crustal thickening transition zone between the TAM and the Ross Sea. Crustal thickness beneath the western portion of the TAM near Terra Nova Bay is significantly less than the 40 km assumed by Smithson (1972) and Davey and Cooper (1987) adjacent to McMurdo Sound. One explanation is that the TAM crust is thinner than assumed in the gravity modeling of Smithson (1972) and Davey and Cooper (1987). Smithson (1972) assumed a Ross Sea crustal thickness of 28 km. However, recent estimates of depth to Moho in the Ross Sea (McGinnis et al., 1985; Cooper et al., 1987b; Davey and Cooper, 1987; and ten Brink et al., 1989) suggest a crustal thickness of about 20 km. Thus the gravity data of Smithson (1972) could be explained by a gradual crustal thickening to only 30 km beneath the western portion of the TAM.

Crustal thinning related to the southeast extension of the Rennick Graben provides an alternative explanation of thinner crust found beneath the TAM in the study area. Line 1 is positioned along the southeast extension of the Rennick Graben. Our crustal model supports the hypothesis of Cooper et al. (1987a) and Fitzgerald and Gleadow (1988) that the granitic basement between the Rennick Graben and the Victoria Land Basin was thinned and uplifted. Whereas Davey and Cooper's (1987) gravity models postulate a rapid crustal thickening transition from 20 km to 40 km beneath the TAM coastline in the southern Victoria Land Basin, their gravity model near Terra Nova Bay is consistent with the slowly thickening crustal transition model. Thus, crustal attributes of the TAM observed here may be atypical of the TAM south of Terra Nova Bay.

Another valuable source of lithospheric information is available from the capture of seismograms generated by earthquakes. Although indigenous antarctic seismicity is virtually absent, Antarctica is located near the most seismically active plate boundaries in the southwestern Pacific and several other seimically active plate boundaries. These seismogenic regions provide teleseismic body waveforms suitable to probe the lithospheric structure of Antarctica. Analysis of the historical seismicity suggests, for example, that a passive seismic experiment located at the head of the Beardmore Glacier could expect at the 95% confidence level during a typical 2 month field season to record over 30 earthquakes with body wave magnitudes $\geq$5.5 over epicentral distances ranging from 30° to 95°. Comparable numbers of earthquake events may also

be observed by passive seismic experiments at the South Pole and the Byrd Catchment B-C sites. Accordingly, an integrated analysis of the seismograms collected at these sites would provide key constraints on crustal models along and across the Transantarctic Mountains, as well as the Ross Embayment and the West Antarctic Rift. Along 120° E from the South Pole, a comparable number of earthquake events can be anticipated which would help constrain crustal models of Wilkes Land and the Gamburtsev Mountains.

A quantum jump in our geological understanding of the continental interior of Antarctica will result from the combined application of airborne EM-radar, gravity, and magnetic surveys. Using fixed-wing aircraft like the DeHavilland Twin Otter, terrestrial regions of the order of 300 km by 200 km may be mapped at a 4-5 km grid spacing during a typical 2 month field season. Airborne EM-radars are capable of sounding ice up to 5 km in thickness, so that these surveys can provide valuable information on the subglacial topography. These data also will be required to obtain lithospheric anomalies from aerogravity surveys. Reduced for the ice thickness variations mapped by the EM-radar, a terrestrial aerogravity survey can provide a 4-5 km grid of gravity anomaly values to an accuracy of about 2 mgals or less. Accordingly, aerogravity surveys can yield unparalleled information concerning subice variations of geologic masses within the continental interior of Antarctica.

Experience in state-of-the-art aerogravity surveying suggests that the technical requirements for executing such surveys makes it unlikely that both EM-radar and terrestrial gravity anomalies can be simultaneous mapped from the same aircraft. However, even though EM-ice sounding surveys supplemented by dedicated aerogravity missions may be required, the total line-kilometer cost of the combined surveys will still be very small compared to the line-kilometer cost of any surface-based geophysical or geological investigation of the antarctic lithosphere.

The use of two aircraft will also facilitate the efficient collection of good quality aeromagnetic data. Airborne magnetometer systems can be inexpensively installed and operated on both aircraft as they are engaged in their respective primary functions of collecting aerogravity and EM-radar data. The flight-lines of the aerogravity survey can be flown in-between the lines of the EM-radar survey so that the two magnetic data sets can be ultimately merged to produce a higher resolution anomaly map at about a 2-2.5 km grid interval. Geologic applications of each of these data sets individually can be problematic due to the corrupting influences of the strong auroral current systems. However, both data sets are redundant in terms of the magnetic signals from the subice geology. Hence, procedures such as we have developed to separate lithospheric and external field effects in the Magsat data can be used to correlate both aeromagnetic data sets for their common geologic components. In this way, relatively high resolution and quality aeromagnetic anomaly maps might be readily generated in conjunction with airborne EM-radar and gravity survey operations.

The availability of mutually constraining gravity and magnetic anomaly fields offers significant advantages in geological applications. When analyzed in combination, these data sets greatly limit interpretational ambiguities for modeling the three-dimensional distribution of tectonic features between the uppermost mantle and the top of the crust. This is particularly critical for subsurface studies of the interior of Antarctica where direct observation of the geology

is possible for the most part only through very limited sampling by exorbitantly expensive drilling programs.

In general, combined airborne EM-radar, magnetic, and gravity surveys represent the most scientifically appropriate and cost-effective approach for initiating geological exploration of the continental interior of Antarctica. They will be required for effectively designing and executing higher resolution oversnow gravity and magnetic traverses, seismic experiments, scientific drilling, and other surface-based geophysical and geological programs. This approach will also be required to exploit fully lithospheric analyses of regional geopotential field anomalies mapped by satellite surveys.

State of the art aerogeophysical mapping of sub-icesheet geology is likely to involve the use of multiple aircraft because of special demands required for terrestrial aerogravity surveys. Accordingly, there would seem to be considerable incentive to coordinate the planning of aerogeophysical activities between agencies and groups which possess or plan to develop capabilities in antarctic aerogeophysics.

The results presented in this paper were obtained by research efforts supported in part by NSF through grants DPP-8313071 and DPP-8722536, NASA Headquarters through grant NAGW-736, the NASA Center for Real-Time Satellite Mapping through grant NAGW-973, and the Ohio Supercomputer Center.

References

Cooper, A. K., F. J. Davey, and J. C. Behrendt. 1987(a). Seismic stratigraphy and structure of the Victoria Land Basin, western Ross Sea, Antarctica. In: A. K. Cooper and F. J. Davey (Editors), The Antarctic Continental Margin: Geology and Geophysics of the Western Ross Sea. American Association of Petroleum Geologists, Houston, Texas, Earth Science Series, 5B: 27-76.

Cooper, A. K., F. J. Davey, and G. R. Cochrane. 1987(b). Structure of extensionally rifted crust beneath the western Ross Sea and Iselin Bank, Antarctica, from sonobuoy data. In: A. K. Cooper and F. J. Davey (Editors), The Antarctic Continental Margin: Geology and Geophysics of the Western Ross Sea. American Association of Petroleum Geologists, Houston, Texas, Earth Science Series, 5B: 93-118.

Davey, F. J., and A. K. Cooper. 1987. Gravity studies of the Victoria Land Basin and Iselin Bank. In: A. K. Cooper and F. J. Davey (Editors), The Antarctic Continental Margin: Geology and Geophysics of the Western Ross Sea. American Association of Petroleum Geologists, Houston, Texas, Earth Science Series, 5B: 119-137.

Fitzgerald, P. G., and A. J. W. Gleadow. 1988. Fission-track geochronology, tectonics and structure of the Transantarctic Mountains in Northern Victoria Land, Antarctica. Chemical Geology (Isotope Geoscience Section), 73: 169-198.

McGinnis, L. D., R. H. Bowen, J. M. Erickson, B. J. Allred, and J. L. Kreamer. 1985. East-west Antarctic boundary in McMurdo Sound. Tectonophysics, 114: 341-356.

Rapp, R.H., and N.K. Pavlis. 1990. The development and analysis of geopotential coefficients

to spherical harmonic degree 360. Journal of Geophysical Research, 95 (B13): 21,885-21,911

Smithson, S. B.. 1972. Gravity interpretation in the Trans-Antarctic Mountains near McMurdo Sound, Antarctica. Geological Society of America Bulletin. 83: 3437-3442.

ten Brink, U., T. Stern, I. Paintin, B. Beaudoin, T. Hefford, and J. McGinnis. 1989. Seismic investigation of lithospheric flexure within the Ross Embayment, Antarctica. EOS, 70(15): 468.

WESTERN DRONNING MAUD LAND IN THE FRAME OF GONDWANA

K. WEBER & J. JACOBS (Göttingen,FRG)

An orogenic event at ~1100 Ma is widespread in Gondwana. It corresponds to the Nimrod Event in the Transantarctic Mts and to the Kibara Event in Africa. Orogenic belts of Kibaran age (1200 Ma and 1000 Ma) surround the Archean Kaapvaal Craton (ZKC).

In western Dronning Maud Land west of Jutulstraumen-Pencksökket Rift Zone Archean rocks are exposed at Annandagstoppane at the western rim of Ahlmannryggen. It forms the ~3000 Ma old basement of the Middle to Upper Proterozoic Ritscherflya Supergroup (RS), which represents a intracontinental rift sequence. Magmatic biotites from mafic dikes and sills gave K/Ar-ages of 1109±33 and 1183±33 Ma which possibly date the minimum age of the RS. The RS can be correlated with similar platform sequences of the Umkondo Group of the ZKC. Their palaeopole plots closely to that of the Ahlmannryggen volcanics after its rotation back to a position in which the Ahlmannryggen forms the eastern rim of the ZKC. The Middle Proterozoic Soutpansberg and Waterberg Groups might be additional equivalents of units within the RS dated with 1800 - 1700 Ma. Thus, the cratonic basement of the Ahlmannryggen can be interpreted as a former part of the ZKC of Africa. New isotopical, geochemical and structural data show Middle Proterozoic rifting occured NW of the ZKC, where the ~1200 to ~1000 Ma old Sinclair Sequence repesents a failed rift of Kibaran age.

Heimefrontfjella and Mannefallknausane SW of the Ahlmannryggen form part of a 1200 to 1000 Ma old NW-SE trending and NE-facing mobile belt. Its amphibolite facies part consists of mafic to felsic metavolcanics and psammitic to pelitic and subordinate carbonatic metasediments, intruded by numerous granitoid plutons; the granulite facies part has similar lithologies intruded by charnockites. The amphibolite and granulite facies terrains are separated by a major shear zone. U-Pb zircon ages demonstrate that magmatic activity was confined to the time interval between 1130 and 1045 Ma and that metamorphism in the amphibolite facies rocks took place at around 1060 Ma. Older zircons were found only in psammitic metasediments which yielded discordant zircon fractions with ages between 1250 and 1450 Ma, and in a granulite facies metaquartzite, which contained concordant zircons with the following ages: 1104±5 Ma, 1215±15 Ma, ~1400 Ma, ~1700 Ma, ~2000 Ma. The youngest age is interpreted as age of granulite metamorphism, the older ages as those of detrital zircons.

The ZKC is rimmed to the south by the Kibaran Namaqua-Natal mobile belt which is dominated by metaigneous rocks and characterised by granulites and charnockites. Two-pyroxen granulites gave a metamorphic age of 1160 Ma. Rounded and zonend zircons from cordierite-orthopyroxen rocks gave a number of upper intercepts between 1300 Ma and 1700 Ma. These zircons have been interpreted as detrital; the upper intercepts are seen as inherited ages of the source material. This is similar to the Heimefrontfjella metasediments. The highest upper intercept age of 2000 Ma from the granulite facies metaquarzite documents a source material of Eburnian age, which is widespread in Namaqualand.

The Natal belt forms the Kibaran complex originaly nearest Heimefrontfjella. Its general strike and vergence can be traced into the D1 direction of Heimefrontfjella. The Mfongozi and Tugela Groups of the Natal area represent a metavolcanic-sedimentary sequence which seems to be comparable with the rocks of Heimefrontfjella. The Mapumulo Group in the southern part of the Natal metamorphic province is composed of banded gneisses, metapelites and intercalated mafic intrusions which are metamorphosed to almandine-amphibolite facies and further to the south to migmatites and granulites. The granulites are associated with charnockitic gneisses. Particularly the Leisure Bay granulites are intruded by various members of a charnockite suite. We correlate the rocks of the Mapumulo Group with the charnockitic sequence of Mannefallknausane and the southern Heimefrontfjella. Further northeast, the basement rocks of Kirwanveggen and Sverdrupfjella suffered magmatism, deformation and medium to high grade metamorphism in the same time span as the Heimefrontfjella.

We conclude, that Heimfrontfjella forms part of a Kibaran mobile belt along the southern and eastern rim of the ZKC. This belt can be traced from the Namaqua-Natal Belt via Heimefrontfjella, Kirwanveggen and Sverdrupfjella into the Kibaran metamorphics of the Mosambique Belt. The Archean basement of the Ahlmannryggen represents a fragment of the ZKC which is covered by the Middle Proterozoic platform sequenz of the Ritscherflya Supergroup.

MAGMATIC EVOLUTION OF A JURASSIC BACK-ARC BASIN SYSTEM IN NORTHEAST PALMER LAND, ANTARCTIC PENINSULA

H.E. Wever and B.C. Storey, British Antarctic Survey, Natural Environment Research Council, High Cross, Madingley Road, Cambridge, CB3 0ET, U.K.
A.B. Ford, U.S. Geological Survey, 345 Middlefield Road, Menlo Park, CA94025, U.S.A.
P.D. Rowley, U.S. Geological Survey, Box 25046, Denver, Colorado 80225 U.S.A.

Regional investigation within northeastern Palmer Land by a joint BAS - USGS field party suggests an extensional basin formed behind an active continental arc system during a period of crustal reworking and bimodal magmatism that commenced in the Early Jurassic. The basin was filled by thick sequences of arc-derived sedimentary rocks correlated with the Middle and Upper Jurassic Latady Formation of southeastern Palmer Land, and deformed during an Early Cretaceous compressional event.

The oldest plutonic rocks exposed in northeastern Palmer Land consist of a heterogeneous association of Lower Jurassic granitic gneisses formerly believed to represent pre-Andean basement. Field observations, and geochemical and isotopic data indicate two distinct types of deformed granitoids. One of predominantly metaluminous composition, has trace element concentrations similar to subduction-related I-type granitoids, an initial $^{87}Sr/^{86}Sr$ ratio of Ca. 0.706 and moderately negative ε_{Nd} (Ca. -3). The other, of peraluminous composition, has trace element contents indicating crustal derivation (S-type), a relatively high initial $^{87}Sr/^{86}Sr$ ratio (0.712 to 0.720), and low ε_{Nd} (Ca. -8). Although all known orthogneisses are younger than Palaeozoic, the ε_{Nd} determined for the S-type granitoids are among the lowest recorded from the Antarctic Peninsula and provide strong evidence for involvement of relatively old [Palaeozoic (?); $T_{dm} \approx$ 1.46GY] basement in the magma genesis of northeastern Palmer Land.

Mafic greenstones of the undated Hjort Formation form separate mappable units and occur as deformed doleritic sills within the sedimentary basin-fill sequence and as amphibolitic dykes within the Lower Jurassic granitoids. Based on trace element abundances three subgroups, with IAT (group I), E-type MORB (II) and CAB (III) characteristics, can be recognized. The greenstones of Group III show strong LILE/HFSE-enrichment (Th/Ta $\geq$ 5) and ε_{Nd} values (-2.3 to -5), typical for subduction-related basalts from active continental margins, whereas those of Group I and II show much less of a subduction-zone component (Th/Ta $\approx$ 2) and have higher ε_{Nd} values (+3.7 to -1.2). These features are explained by an origin within an extensional, ensialic, back-arc setting.

Felsic metavolcanic rocks of the undated Brennecke Formation also form separate mappable units and are interbedded with the Hjort Formation. They have geochemical and isotopic characteristics resembling those of the peraluminous plutons and are thus interpreted to be derived from a similar source region. It seems therefore likely that the rocks of the Brennecke Formation represent extrusive equivalents of the Lower Jurassic crustal-derived granitoids.

In conclusion, crustal attenuation along Palmer Land's eastern margin apparently commenced in the Early Jurassic and was contemporaneous with subduction-related magmatism. An associated thermal event caused large-

scale remobilisation of (?) Palaeozoic basement producing the voluminous crustal-derived granitoids and the silicic volcanic rocks of the Brennecke Formation. Crustal melting accompanying emplacement of doleritic sills of the Hjort Formation probably resulted from diapiric uprise of "hot" mafic mantle-derived material into basal crustal levels. Extension of the ensialic back-arc basin and the bimodal magmatism were coeval with and probably related to initial stages of Gondwana break-up. This activity predates the development of the Rocas Verdes basin in southern South America and thus cannot be regarded as its southwards continuation as has been postulated. Northeastern Palmer Land's onland record is obviously important in understanding basin evolution within this part of the proto-Weddell Sea. It suggests that there was continental extension in this area long before the main phase of Cretaceous sea-floor spreading in the Weddell Sea.

SEDIMENTOLOGY AND GLACIOLACUSTRINE HISTORY OF THE MIERS VALLEY, SOUTHERN VICTORIA LAND, ANTARCTICA; A STUDY IN POLAR LACUSTRINE PROCESSES.

G.S.Wilson*, Antarctic Research Centre, Victoria University of Wellington, P.O. Box 600, Wellington, NEW ZEALAND.
W.Dickinson, Research School of Earth Sciences, Victoria University of Wellington, P.O.Box 600, Wellington, NEW ZEALAND.
G.L.Lyon, Nuclear Sciences Group, Physical Sciences, DSIR, P.O.Box 31312, Lower Hutt, NEW ZEALAND.

The Miers Valley like many dry valleys in the McMurdo region has a complex stratigraphy of unconsolidated sediment mantling the valley floor. The sediment varies in lithology and thickness. Each sediment type has characteristic properties that identify it. These include; bedding features, grain size distribution, mineralogy, grain morphology, and, in the case of the most recent deposits, surface topography. The different sediment types are a direct result of their depositional environments and processes, and associated complex interactions.

Facies analysis and grain size distribution are used to divide the sediments into four main process related types: glacial, fluvial, aeolian, and lacustrine. The present Lake Miers is used to present a model for lake sedimentation in the valley.

Older sedimentation in the valley was dominated by glacial and lacustrine processes, with ice bodies extending both down valley (from the present valley glaciers) and up valley (from grounded ice in the Ross Sea). Moraine and ice damming has caused several lacustrine episodes in the valley during the period from 23,000 yBP to the present, with various evaporite phases recording the extent and nature of lacustrine deposition.

A new interpretation of the development and origin of the drift cones on the ice covered surface of Lake Miers is proposed. Sedimentologic evidence shows the drift mantling the cones to be glacial in origin and mineralogy and stable isotope data suggest a source from the present glaciers, at a time when both glaciers terminated within the present lake. The present form of the debris has resulted from the ablation of the lake ice cover. This ice rafting model is more consistent with ancient lacustrine deposits in the valley than previous models, as ancient lake sediments do not show any effects from ice overriding or diapirism. The lacustrine sediments result solely from settling and precipitation.

* Present address; Geology Department, 330 Bessey Hall, University of Nebraska, Lincoln, NE 68588-0340, U.S.A.

DATING OF PLIOCENE ANTARCTIC MARGIN SEDIMENTS; A NEW DEVELOPMENT OF THE ^{10}Be DATING PROCEDURE

G.S.Wilson*, Antarctic Research Centre, Victoria University of Wellington,
P.O. Box 600, Wellington, NEW ZEALAND.
R.J.Sparks, Nuclear Sciences Group, Physical Sciences, DSIR,
P.O.Box 31312, Lower Hutt, NEW ZEALAND.

Facies analysis of marine sedimentary strata from the Antarctic continental margin records the advance and retreat of glaciers and ice sheets. However, because of poorly constrained magnetostratigraphy and biostratigraphy, chronology of the sediment record is difficult to establish. Both of these methods are limited because of the large number of hiatuses in the records and their varying nature and length. Here we explore the possibility of dating the sediments directly by using the cosmogenic isotope ^{10}Be, with a half life of 1.5 Ma (Raisbeck and Yiou, 1984). Because of the nature of glaciomarine sedimentation at the Antarctic margin, assumptions commonly necessary to use ^{10}Be decay for dating sediments are not necessary when using absolute concentrations of ^{10}Be in conjunction with facies analysis (Wilson, 1990). This is possible because identification of depositional environments similar to the present day, along with present day ^{10}Be concentrations, provide reference values for constructing a local ^{10}Be logorithmic decay curve for each part of the margin.

Antarctic margin sediments have been cored in Ferrar Fjord by the CIROS-2 (Pyne et al.,1985) and DVDP-11 (McKelvey, 1975) drill-holes. Comparison of ^{10}Be abundances in the mudstone facies of the cores with that of modern sea floor mud allows the plotting of a decay curve with depth and an age to be estimated for each sample. A comparison of ages inferred in this way from CIROS-2 and DVDP-11 cores, which are 20 km apart but in separate valleys, provides a check on the consistency of the results.

The adsorbed cations are extracted from the sediment by leaching, and separation of the Beryllium from other cations is achieved by EDTA titration and ion exchange. A target sample of BeO is prepared for measurement in an Accelerator Mass Spectrometer (AMS). An existing ^{14}C AMS system has been modified to increase the yield of Beryllium and separate ^{10}Be from the isobar ^{10}B.

At present 20 samples from mudstone and siltstone horizons in the CIROS-2 and DVDP-11 cores have been measured. A preliminary interpretation shows a Plio-Pleistocene chronology for the sediments from these cores.

REFERENCES

Pyne,A.R., Robinson,P.H. & Barrett,P.J. (1985). Core log, description and photographs, CIROS-2, Ferrar Fjord, Antarctica. Antarctic Research Centre, Victoria University of Wellington: 80p.

McKelvey,B.C. (1975); Preliminary site report, DVDP 10 and 11, Taylor Valley; In Mudrey and McGinnis (Ed.) Dry Valley Drilling Project, Bulletin No. 5; Northern Illinois University; 16-60.

Raisbeck,G.M. & Yiou,F. (1984); Production of Long-Lived Cosmogenic Nuclei and their applications; Nuclear Instruments and Methods in Physics Research, B5, 91-99.

Wilson,G.S. (1990); Beryllium-10; A method for tracing and dating Antarctic ice sheet fluctuation in the Pliocene era (Abstract); Geological Society of Australia, No. 27, ICOG 7, Canberra, 112.

* Present address; Department of Geology, 330 Bessey Hall, University of Nebraska, Lincoln, NE 68588-0340, U.S.A.

MESOZOIC AND CENOZOIC KINEMATIC EVOLUTION OF THE TRANSANTARCTIC MOUNTAINS

Terry J. Wilson, Byrd Polar Research Center and Dept. of Geological Sciences,
Ohio State University, Columbus, Ohio, 43210, U.S.A.

The Transantarctic Mountains (TAM) appear to be a rift-margin uplift related to extensional tectonism within the Antarctic Plate during the Mesozoic and Cenozoic. The occurrence of Jurassic igneous rocks in a belt along the length of the present TAM has long been taken as evidence that extension and rift development within Antarctica began during the initial stage of fragmentation of the Gondwana supercontinent. Offshore seismic studies in the Ross Sea document a second rifting event, inferred to have commenced in the Eocene associated with the initiation of TAM uplift as dated by apatite fission-track ages. This study focused on structural analysis of brittle fault arrays and dolerite dike swarms of Jurassic and Cenozoic age in the TAM in southern Victoria Land and in the Beardmore Glacier region. Displacement directions during the Jurassic and Cenozoic rifting events have been reconstructed from the regional orientation patterns of these structures.

In both the southern Victoria Land and Beardmore areas, the Jurassic Ferrar dikes occur in *en echelon* arrays that form two prominent systems with NNW-NNE and ENE-EW trends. Mutual crosscutting and abutting relations indicate that emplacement of these subperpendicular dike systems overlapped in time. Mesoscopic normal faults cutting Beacon Supergroup strata occur together with the Ferrar dikes. Mutual crosscutting relations between these faults and dolerite dikes and sills, volcanic breccias and clastic dikes demonstrate that the faults are Jurassic in age. The normal faults occur in two sets striking NW and NE. The orientation patterns of the Jurassic faults and dikes are interpreted to reflect a triaxial strain field in which extension occurred in both NE-SW and NW-SE horizontal directions, and shortening occurred in the vertical direction. The similarity of the Jurassic orientation patterns in the southern Victoria Land and Beardmore areas documents a regionally consistent strain regime over a strike length of ca. 1000 km in the TAM. Previous workers documented a remarkably similar structural pattern in Queen Maud Land adjacent to the Weddell Sea margin, another 2000 km along the TAM. This strain regime is not compatible with translational motion between East and West Antarctica during initial Gondwana fragmentation, as proposed from geologic, paleomagnetic and marine geophysical data, requiring that any such translations postdated Ferrar magmatism and associated crustal extension.

Mesoscopic fault arrays cutting crystalline basement rocks were examined in coastal exposures in southern Victoria Land and near the mouth of the Beardmore Glacier. Because all of these faults occur in areas where Fitzgerald (1987, 1989) has documented offsets of fission-track age vs. elevation profiles, these faults are inferred to be of Cenozoic age. Faults along the TAM Front in southern Victoria Land do not have a N to NW strike parallel to the regional trend of the TAM and adjacent Victoria Land Basin. Instead, the fault orientations are rotated clockwise with respect to regional rift trends into a NNE to NE direction. The faults have dominantly normal dip-slip to oblique slip displacement with a component of right-lateral shear, with some faults subsequently reactivated in right-lateral strike-slip motion. Fault arrays along the major transverse physiographic breaks in the TAM marked by Granite Harbor/Mackay Glacier and Beardmore Glacier consist of NE-SW to E-W striking fault sets with normal or normal-oblique displacements. This indicates range-parallel extension across the morphologic troughs, consistent with the cross-strike graben structures suggested by many early workers. These graben may represent pull-apart features associated with transtensional deformation along the TAM. The fault patterns indicate that there is a significant component of right-lateral shear displacement along the TAM, and that the direction of displacement between East and West Antarctica during the Cenozoic was oriented obliquely, rather than perpendicular, to the regional trend of the TAM. The Cenozoic patterns can be explained by a right-oblique translation of Marie Byrd Land relative to East Antarctica since the mid-Cretaceous, consistent with existing paleomagnetic data.

AN EARLY TO MIDDLE JURASSIC GLACIATION - EVIDENCE FROM ALLAN HILLS, TRANSANTARCTIC MOUNTAINS

K. J. Woolfe, Research School of Earth Sciences, Victoria University of Wellington, P. O. Box 600, Wellington, NZ.

J. E. Francis, Department of Earth Sciences, University of Leeds, Leeds, LS2 9JT, UK.

Field work conducted during the 1990-91 Antarctic field season has uncovered evidence of Jurassic glaciation in the Mawson Formation at Allan Hills, southern Victoria Land, Antarctica. This unit was originally considered to be a glacial deposit by Gunn and Warren (1963), but was later reinterpreted by Ballance and Watters (1971) as a volcaniclastic lahar. Detailed mapping has revealed that the upper part of the formation is composed of volcaniclastic flows, but a previously undescribed lower diamictite is present which has no volcaniclastic component. This diamictite (Woolfe et al., in prep.) is composed of sandstone, siltstone, shale and coal clasts derived from the underlying Permian and Triassic strata (Weller Coal Measures, Feather Conglomerate and Lashly Formation) in a poorly sorted matrix, and is interpreted here as being of glacial origin.

This interpretation is supported by:

a) An extensive erosion surface (Mawson Erosion Surface (Woolfe et al in prep)) separates Beacon and Ferrar rocks at Allan Hills. This surface has over 400 m of sharp relief and indicates a period of erosion prior to the main magmatic phase of the Ferrar event (179 Ma).

b) A zone of intensely folded Beacon Supergroup sediments directly beneath Mawson A. The intensity of folding decreases downwards from the erosion surface over a few tens of metres. Within the zone of most intense folding, metre and decametre scale isoclinal folds have formed during complex brittle failure of interbedded sandstone and shale, cataclastic flow has occurred in some coal seams. Strain is partitioned into a zone subparallel with the Mawson Erosion Surface. The style and distribution of deformation is closely analogous to that observed locally beneath the Sirius Group, a known Cenozoic glacial deposit. This suggests that both the sub-Mawson and sub-Sirius strain resulted from similar processes, possibly ice contact drag folding at the

base of a dry-based glacier.

c) Striated clasts. Several clasts with striations were found within Mawson A. It is unlikely that these could have survived prolonged transportation as the clasts are composed of soft Beacon Supergroup sediments which do not hold striations well. These clasts represent direct evidence that diamictite and the sub-erosion surface deformation were glacially produced.

The age of the proposed glaciation is constrained by a Late Triassic microflora in the underlying Lashly Formation and a Middle Jurassic (179 Ma) radiometric age for the overlying Ferrar Group. At this stage it has not been determined whether this erosion, deformation and diamictite represents evidence of widespread glaciation in the Early to Middle Jurassic or whether it simply records the presence of a Jurassic alpine glacier at or near Allan Hills.

EARLY PALEOZOIC LAMPROPHYRE DIKES OF SOUTHERN VICTORIA LAND: GEOLOGY, PETROLOGY, AND GEOCHEMISTRY

B. Wu and J.H. Berg, Department of Geology, Northern Illinois University, DeKalb, IL 60115, USA

At the end of the Ross Orogeny (ca. 450-500 Ma.), lamprophyre dikes were extensively emplaced throughout the region of the present-day Transantarctic Mountains in southern Victoria Land. These dikes are locally dense and cut through the Precambrian metamorphic basement and granitic plutons (Granite Harbour Intrusives) parallel to the trend of the Transantarctic Mountains. The lamprophyres are the only basic rocks intruded in this region during the Ross Orogeny. In the Royal Society Range, lamprophyre dikes consist of a variety of ultramafic, alkaline, and calc-alkaline rock types including aillikite, camptonite, spessartite, and vogesite; whereas in the Dry Valleys and the Granite Harbour area, the lamprophyres are all calc-alkaline, mainly spessartites.

Most of the lamprophyre dikes are very fresh; some with minor alteration. All these rocks have typical panidiomorphic texture, but mineralogy varies with different rock types. The ultramafic lamprophyres contain phenocrysts of phlogopite and salite; the alkaline lamprophyres have diopside/salite and Ti-hornblende. In calc-alkaline lamprophyres, hornblende is the most common phenocryst; diopside/salite, biotite, and olivine also occur as phenocrysts in some rock types. Carbonate, apatite, and Fe-Ti oxides occur in all rock types, and are very common in ultramafic and alkaline lamprophyres. Some dikes contain an abundance of crustal xenoliths, including garnet granulites from the deep crust, and macrocrysts of diopside, garnet, hornblende, and phlogopite.

Both the ultramafic and alkaline lamprophyres have high abundance of compatible elements, with *Mg#*≤70%, Ni≤190 ppm, Co≤63 ppm, Cr≤550 ppm, and Sc≤31 ppm. They are also extremely enriched in LILE, HFSE, and LREE, with Ba≤4200 ppm, Sr≤1800 ppm, Nb≤65 ppm, and Ce≤195 ppm. These chemical features imply that these rocks may represent primary melts derived from low-degree partial melting of enriched mantle sources, likely metasomatized peridotites, and have undergone little or no differentiation from crystal fractionation. The calc-alkaline lamprophyres have a large range of chemical composition with SiO_2 = 46-65 wt% and *Mg#* = 35-72%, which, shown by their chemistry and petrology, are produced by crystal fractionation of diopside and hornblende. Their most primitive compositions, with *Mg#*≤72%, Ni≤210 ppm, Co≤75 ppm, Cr≤670 ppm ,and Sc≤34 ppm, are likely primary magmas derived from mantle sources. These rocks are also highly enriched in LILE and LREE, with Rb≤180 ppm, Ba≤1500 ppm, and Ce≤130 ppm, but display relatively strong depletion of HFSE, which is the characteristic of magmas generated above a subduction zone. The chemistry of these lamprophyres strongly suggests the existence of a subduction process and metasomatized mantle below southern Victoria Land during the Ross Orogeny.

XENOLITHS FROM THE VOLCANIC PROVINCE OF WEST ANTARCTICA AND IMPLICATIONS FOR LITHOSPHERIC STRUCTURE AND PROCESSES

R.J. Wysoczanski, Antarctic Research Centre and Research School of Earth Sciences, Victoria University, PO Box 600, Wellington, New Zealand.
J.A. Gamble, Antarctic Research Centre and Research School of Earth Sciences, Victoria University, PO Box 600, Wellington, New Zealand.

Xenoliths ranging in composition from peridotite and pyroxenite to mafic granulite and sintered granitoids have been collected from widely dispersed localities of alkaline volcanoes in West Antarctica including the Executive Committee Range (ECR), the USAS Escarpment, Mount Murphy and the Fosdick Mountains. The lithologies are thought to span a depth range from lithospheric mantle to lower and supra crustal rocks and as such can be used to construct stratigraphic sections through the lithosphere in vast areas where the summits of volcanoes are the only accessible rocks. The xenoliths range in shape form angular and blocky to well rounded probably reflecting the brittle nature of the deep lithosphere and the abrasive effects of transportation to the surface.

The mantle samples include spinel facies lherzolites and wehrlites which vary from protogranular to porphyroclastic in texture. Rare cross-cutting phlogopite veins provide evidence for multistage (infiltration and/or metasomatism) processes and the association of kaersutite with the wehrlites implies the interaction of silicate melts. Many xenoliths are oxidised, either as a result of entrainment in host magmas or due to the passage of oxidising fluids at source regions. The granulites (layered rocks equilibrated to temperatures and pressures of the granulite facies) are dominated by plagioclase (+ clinopyroxene ± olivine), are generally mafic (< 55% SiO_2), commonly layered on a scale of hand specimen and are rarely interlayered with ultramafic rocks. In contrast to xenolith populations from the Ross Sea Embayment, no garnet-bearing or two-pyroxene bearing granulite assemblages have been recorded from the ECR suites. Supra-crustal rocks are generally thoroughly sintered and melted.

Major element compositions of the mafic granulites indicate strong mineralogical controls on whole rock chemistry. Trace element abundances show generally low LIL and HFS concentrations (Rb = <3 ppm; Ba = 30 - 600 ppm; Zr = 30 - 357) with Zr/Nb = 1 - 11. Elements such as Ni (10 - 960 ppm) and Cr (< 5 - 1725 ppm) correlate with modal proportions of olivine and clinopyroxene. Sr, Nd and Pb isotopic studies and REE determinations will be undertaken.

The West Antarctic xenolith suites will be compared to suites from the Ross Sea Embayment sector of Antarctica, New Zealand and eastern Australia. The data tend to confirm that in these regions of lithospheric attenuation, the transition from lower crust to upper mantle is a diffuse zone of interlayered mafic and ultramafic rocks.

THE DISTRIBUTION AND DISPERSAL PATTERN OF CLAY MINERALS IN THE SURFACE SEDIMENTS OF THE BRANSFIELD STRAIT, ANTARCTICA

Ho Il Yoon, Myung Woo Han, Byong-Kwon Park and Sang-Joon Han

Polar Research Center, Korea Ocean Research and Development Institute, Ansan, P.O. Box 29, Seoul 425-600 (Korea)

Abstract

Provenance and dispersal pattern of clay minerals of the surface sediments in the Bransfield Strait are studied in their relation to the oceanographic data and climate in this area.

On the average, the clay minerals of the strait are composed of 45.56% illite, 40.65% chlorite, 4.43% kaolinite, and 9.36% smectite. The distribution pattern of the clay minerals demonstrates, away from the South Shetland Islands toward the Antarctic Peninsula, an increase in illite, and a decrease in kaolinite and chlorite. The proportion of smectite is the highest near Penguine and Bridgeman Islands, and decreases south- and southwestward.

Kaolinite in the northern half of the Bransfield Strait originates largely from the South Shetland Islands where humid and warm climate induces the chemical weathering of bed rocks. Chlorite-rich sediments in the northwestern strait seem to be derived partly from Smith Island where the metamorphic rocks rich in mica and chlorite predominate. The distribution of kaolinite and chlorite appears to have been influenced by the geostrophic current flowing northeastward from the Bellingshausen Sea. Illite is dominant on the shelf off the Antarctic Peninsula where the climate is colder and drier, and might have been derived from the Antarctic Peninsula in a detrital form. Smectite enrichment near Penguine and Bridgeman Islands seems to originate from the volcanic eruptions. However, the volcanogenic smectite is slightly dispersed southwestward by the intrusion of the saline and cold Weddell Sea water.

RE-EXAMINATION OF TECTONOTHERMAL HISTORY OF LUTZOW-HOLM BAY AREA, EAST ANTARCTICA

M. YOSHIDA, Department of Geosciences, Faculty of Science,
Osaka City University, 3-3-138 Sugimoto, Sumiyoshi-ku,
Osaka 558, Japan

Since the compilation of the tectonothermal history of Lützow-Holm Bay area in around 1980 (e.g. Yoshida et al., 1983, in Antarctic Earth Science, Austral. Acad. Sci.), much work has been done which is mostly concentrated on the petrological and geochronological topics. Incorporating these recent studies, a plate tectonic interpretation of this area during Late Proterozoic has been presented (Shiraishi et al., 1987, in Gondwana Six, Am. Geophys. Union). A correct understanding of tectonics of the Lützow-Holm Bay area, however, needs the incorporation of the tectonothermal history ranging back to Archaean. Petrological, structural and geochronolgical studies so far conducted in the area around Lützow-Holm Bay are reviewed and a revised model of tectonothermal history of the area is presented below.

The oldest rocks in the Lützow-Holm Bay area have recently been reported by Nakajima et al.(1988, Proc. NIPR Symp. Antarctic Geosci., 2). They are granulite facies metamorphic rocks cropping out in a southern outcrop of the bay, giving a ca 3000 Ma Rb-Sr whole rock isochron age. Distribution of Archaean rocks is unclear: they may be either inliers or a margin of relatively large Archaean terrain extending further south.

Some time before ca 2000 Ma, original rocks of some portions of rocks of the Lützow-Holm Bay area were formed. The first possible metamorphic event in this area is recorded as ca 1900 Ma from Pb-Pb and Rb-Sr whole rock isochron ages of charnockitic rocks and of gneisses occurring in the central portion of the Lützow-Holm Bay coast. The distribution of rocks suffered these early Proterozoic events are indistinct and could be similar to that suggested for the Archaean rocks.

Shortly before ca 1100 Ma, original rocks of considerable portions of Lützow-Holm Bay area which occur mostly in the Prince Olav Coast were formed. These rocks then sufferred intense intrafolial rootless folding and tight-isoclinal-recumbent meso- to mega-folding. This folding event was followed by the second metamorphic event which is recorded at ca 1100 Ma by Rb-Sr whole rock isochron ages of charnockitic rocks occurring in the same area where early Proterozoic

ages have been detected. The progressive amphibolite facies to granulite facies metamorphism in the most part of Lützow-Holm Bay area is attributed to this event.

The third metamorphic event is the high amphibolite facies metamorphism and migmatization associated with the upright folding and the local development of axial plane foliation. Rb-Sr whole rock isochron ages of ca 700 Ma obtained from various rocks throughout the area may reflect this metamorphism.

The forth metamorphic event is the widespread thermal event under low pressure low amphibolite facies metamorphism associated locally with gentle folding and ductile faulting. This event is considered to be at ca 500 Ma, reflected by K-Ar and Rb-Sr mineral and whole rock ages and Rb-Sr mineral isochron ages obtained from Prince Olav Coast to Lützow-Holm Bay. Intrusion of granite-pegmatite veins with U-Pb age of 470Ma took place relatively later phase during this event.

The area was gradually up-lifted and cooled to temperatures equivalent to the greenschist facies or slightly lower conditions, and at about 350 Ma, it reached the temperature at which argon loss stops as reflected by younger K-A ages. The area around Lützow-Holm Bay remained stable until the sudden shear-fracturing by extensional tectonics, which reflects the beginning of the total disruption of East Gondwana during Jurassic times.

TECTONICS OF PRECAMBRIAN EAST GONDWANA SURROUNDING ANTARCTICA

M. YOSHIDA, Department of Geosciences, Faculty of Science,
Osaka City University 3-3-138 Sugimoto, Sumiyoshi-ku,
Osaka 558, Japan
M. FUNAKI, National Institute of Polar Research, 1-9-10 Kaga,
Itabashi-ku, Tokyo 173, Japan

Paleomagnetic studies in recent years have considerably aided in fixing the positions of wandering continents in the Phanerozoic era. In contrast, models for the Precambrian show extreme divergence which is due to the previously poor quality of data. The acculate assembly of Precambrian continents on the strength of new geologic data base is yet to be attempted.

Jurassic and Cambro-Ordovician paleomagnetic data of good quality from Antarctica and Sri Lanka support a reconstruction model of East Gondwana (India -Sri Lanka-Antarctica) similar to that given by Lawver and Scotese (1987, in Gondwana Six, Am. Geophys. Union). Various geologic characteristics including lithologies, structures, metamorphic conditions and metamorphic P-T-t paths, from the latest Archaean to Jurassic, are also traceable and/or comparable in the same juxtaposition model as above.

Thus, it is suggested that there was no considerable breakup in this part of East Gondwana during the period from the latest Archaean to Jurassic. Neverthless, there is evidence of several episodes of tectonothermal events in the period under discussion, which indicate repeated episodes of intense differential movement among the crustal fragments. This study discusses a model for Precambrian global tectonics based on the structure, metamorphism, igneous activity, sedimentation, and palaeomagnetic record available from this part of East Gondwana.

LARGE-SCALE TOPOGRAPHY OF THE PRINCE OLAV COAST — LÜTZOW-HOLM BAY REGION AND ITS TECTONIC IMPLICATIONS

Y. Yoshida, National Institute of Polar Research, Kaga, Itabashi-ku, Tokyo 173, Japan

Antarctica is a unique continent, being subjected to a vast ice burden for most of the Late-Cenozoic. The ice sheet seems to preserve tectonic topographic features and even enlarges their relief, by glacial erosion combined with isostatic crustal adjustment. Therefore, bedrock topography gives tectonic information on local, regional and continental scales.

In the region from the Prince Olav Coast through Lützow-Holm Bay to Yamato Mountains, three major topographic features can be recognized: 1) a NE-SW trending straight coastline associated with the outer edge of the continental shelf, 2) the NW-SE trending Shirase Submarine Valley in Lützow-Holm Bay enbayment and Riiser-Larsen Peninsular — Gunnerus Ridge, and 3) the N-S trending Yamato Mountains. These large-scale topographic features originated with the breakup of Gondwana Land which involved pre-breakup uplift and subsequent faulting. However, later crustal movements seem to have influenced the region greatly. NW-SE or NNW-SSE trending crustal movements affected the NE-SW coastline, forming the fault valley and fault scarp system indicated by the Shirase Submarine Valley, Riiser-Larsen Peninsular — Gunnerus Ridge horst, and the Yamato Mountains, which may be essentially the continuation of the horst. Recent radio-echo sounding suggests that the Yamato Mountains are a fault block with a width of 50 km, occupying the marginal part of a uplifted peneplain at about 500 m above sea level. Traces of ice sheet glaciation on the summits of the mountains suggest relatively recent uplift of the area. The Sör Rondane Mountains, 200 km west of the Yamato Mountains, show E-W trending topographic features and the major fault structure extends in the same direction. Features of ice sheet glaciation suggest a more stable crustal setting compared with that of the Yamato Mountains. The seismic epicenters recently determined in the vicinity of Syowa Station seem to be located along the estimated faultline. This may indicate crustal movement is still active, though the amount of displacement may be slight. On the other hand, NW(NNW)-SE(SSE) topographic features would also be compatible with structures formed by a Proterozoic plate collision. The trend or zoning of the regional gravity anomaly coincides with these structures. These facts raise the question of the influence of ancient geological structures on relatively recent crustal movement.

LATE QUTERNARY ENVIRONMENT CHANGES IN ANTARCTICA AND THEIR CORRELATIONS WITH GLOBAL CHANGE

ZHANG Qingsong, Institute of Geography, Chinese Academy of Sciences, Beijing 100101, CHINA

Records from Antarctic ice free areas and ice cores testify that environmental and climatic changes in the Antarctic region are coordinated with global changes since the late Pleistocene. For instance, two ingressions occurred in the last glacial interstadial(50,000-25,000a.B.P.) and Holocene optimum(7,500-5,000a.B.P) periods on the Antarctic coast. The Antarctic Ice Sheet greatly expanded at the last glacial maximum (18,000a.B.P.) when Antarctic sea level was 100-150m lower than that at present. Three intervals of glacial advance and retreat have occurred on the front of the Antarctic Ice Sheet since 3,000a.B.P.. All these climatic events corresponded to those in the north hemisphere.

The Antarctic Ice Sheet which contains of 24.5 million cubic kilometres of ice, provides a massive cooling source affecting world climate. Either expansion or retreat of the Ice Sheet will significantly affect changes of sea level.

Some climatologists predict that sea level will rise several metres due to a rapid increase of temperature which will cause the Antarctic Ice Sheet to melt significantly in the next 50 years. Records from the Antarctica do not support this point of view. Although the temperature in Antarctic inland (Dome C) has increased by 0.3 C in the past 80 years, there is little evidence infer that the green house effect has disturbed the world wide cooling tendency which started 3,000a.B.P.. However, the course of such a limited temperature increase was very slow, and in the next 50 years, the temperature will not be able to reach as high as it was in the Holocene climatic optimum period. Even in that time the Antarctic Ice Sheet including ice shelves was still stable.

According to available tidal monitoring data recorded in past decades, the rise in sea level caused by melt water from the Antarctic ice may be less than 0.2m in the coming 50 years.

GEOCHRONOLOGICAL STUDY OF METAMORPHIC AND IGNEOUS ROCKS OF THE LARSEMANN HILLS, EAST ANTARCTICA

Zhao Yue[1], Song Biao[1], Wang Yangbin[1], Ren Liudong[1],
Li Jiliang[2], and Chen Tingyu[1]

1. Institute of Geology, Chinese Academy of Geological Sciences, Baiwanzhuang RD., Beijing, 100037, P.R. China.
2. Institute of Geology, Academia Sinica, Dewai Qijiahuozi, Beijing, 100029, P.R.China.

Metamorphic and igneous rocks in the Larsemann Hills are dominantly composed of low pressure granulite facies paragneisses and granitoids which are genetically associated closely with migmatization. Because extensive isotopic resetting occurred in the Precambrian basement of East Antarctica, the single grain zircon evaporation technique is adopted here to determine the crystallisation age of zircons, lest those should have lost most of their radiogenic lead.

Direct determination of the $^{207}Pb/^{206}Pb$ age of single zircon grains by use of the thermal emission mass spectrometer was performed in the Laboratory of Isotope Geochronology, Institute of Geology, Chinese Academy of Geological Sciences. A multicollecter MAT–261 mass spectrometer was used for this study and a Secondary Electron Multiplier was used as the ion beam detector. The linearity of the SEM detector system was monitored by daily analyses of the NBS 982 Standard .

Zircons were extracted from a garnet–bearing migmatitic gneiss ('yellow gneiss'), a biotite–bearing syenogranite ('late granite'),a leucocratic garnet–bearing migmatitic granite ('painted rock'), a garnet+biotite–bearing striped migmatitic gneiss (a part of 'blue gneiss') and granite–pegmatite . In order to determine zircon types, scanning electron microscope photographs and photomicrographs of the zircons from those samples were taken. Zircons from the garnet–bearing migmatitic gneiss, which is less foliated, are mostly clastic. Those from the biotite–bearing syenogranite are hypidiomorphic and elongated.

Preliminary measurement of the detrital zircons from the garnet–bearing migmatitic gneiss gives a range in age from 1200 ± 6Ma to 789 ± 20Ma. Zircons from the biotite–bearing syenogranite yield 563 ± 27Ma and 529+15 / −16Ma ages, similar to an age (560 ± 70Ma) of an approximate Rb–Sr total – rock isochron for the metapelites in Prydz Bay (Sheraton, J.W. & Black,L. P., 1984). Zircons from the granite–pegmatite dyke, which intruded the biotite–bearing syenogranite, yield age results of 535 ± 18Ma and 521 ± 11Ma.

The preliminary age results of biotite–bearing syenogranite may be considered as migmatization age of the Larsemann Hills. This conclusion is based on the observation that although the undeformed biotite syenogranite dyke cuts across the gneisses in Broknes Peninsula and Sigdoy Island, in northern Mirror Peninsula the syenogranite, with gneissic foliations along its borders which are concordant with surrounding rocks, is transitional to the unfoliated, and then less foliated migmatitic gneiss. Mineralogical and geochemical data indicate that the syenogranite has S–type characteristics and may therefore have been derived from partial melting of paragneisses (metapelites) in the Larsemann Hills (Stuwe K., Braun H.M., & Peer H., 1989). For this reason, the effect of the 'Pan African event' may be regionally important, at least in the Larsemann Hills.

More detail and further measurements of $^{207}Pb / ^{206}Pb$ age of the zircons, and systematic age results (Sm–Nd and Ar–Ar) of the gneisses and granitoids will be obtained and discussed.

THE CHARACTERISTICS OF THE ROCK-FORMING MINERALS AND APPROACH TO THE GENERATION AND EVOLUTION OF THE VOLCANIC ROCKS FROM THE FILDES PENINSULA, KING GEORGE ISLAND, WEST ANTARCTICA

*Zheng Xiangshen Li Jiaju

*Laboratory of Lithosphere Tectonic Evolution
Institute of Geology, Academia Sinica
P.O.Box 634, Beijing 100029, P.R.CHINA

Abstract

The Fildes Peninsula, where the Chinese Great Wall Station is located, is predominantly Early Tertiary volcanic rocks. The volcanic strata in the area studied have a uniform dip to the NNE or NE of 25 or less. Based on stratigraphy and rock associations, the present study has subdivided the volcanic rocks into two lithostratigraphic formations, each with two members (Zheng & Liu,1989a). The members consist of basaltic, andesitic and dacitic lavas with some basaltic volcanic breccias and agglomerate. The volcanic-clastic sedimentary rocks, which belongs to Fossil Hill Member and overlies disconformatbly on different positions of other members, contain few fossiliferous intercalations, within which some ripple-marks, mud cracks as well as bird tracks are found. The isotope chronological data (Davies,1982; Li, et al., 1990; Pankhurst, et al.,1980; Smellie, et al., 1984; Watts,1982; Zhu, et al., in publishing) show that the volcanism is Early Paleocene to Mid-Miocene. Subvolcanic bodies are wide-spread on the peninsula and include stocks and veins which are distributed along or near the fracture-fissure zones, and dykes concentrated around the volcanic centres. Petrographic and petrochemic data suggest that the lavas including basalt, basaltic andesite, andesite and dacite form a calc-alkaline association with low-K and high-Al characters (Zheng, et al., 1988; Zheng & Liu, 1989b). Although there are different components and structures in the rocks from distinctive volcanic phases, the major rock-forming mineral assemblages are similar and the contents and compositions of the major minerals vary with the chemical compositions of the rocks. Petrochemic evidences suggest a crystallization process of magma in the area studied.

I. Characteristics of major rock-forming minerals

The most important mineral phases in the volcanic rocks are plagioclase and clinopyroxene. The results of microprobe and X-ray diffraction (XRD) show that the plagioclase phenocrysts of basalt and basaltic andesite lavas are basic with the An content ranging from 93% to 57%. Normal and oscillatory zoning is well

developed, with the An contents in the central part of plagioclase phenocrysts over 80% and decrease towards the margin (An=74% - 49%). Phenocrysts in andesite and dacite are mainly labrador to andesine. Microprobe determination shows that the clinopyroxenes are mainly augite, only a few diopside and Mg-diopside. The compositions of the orthopyroxene in the rocks vary from bronzite in basalt and basaltic andesite to augite bronzite in subvolcanic rocks. The olivines are almost iddingsited, which have a ratio of Mg/Mg+Fe ranging between 78% and 87%, and are classified to Mg-rich chrysolite.

II. Relationship between Mineral Assemblage and Magma Evolution

Sakuyama(1981,1983) discussed the mineral assemblage and different petrochimic character of the calc-alkaline volcanic rocks generated from magma mixing and divided the rocks into N-type and R-type. Compared with Sakuyama's division, the main rock-forming minerals of the basaltic lavas from the Fildes Peninsula are of the features of N-type. The features are as follows.

1. The plagioclase phenocrysts havenormal and oscillatory zoning and with a regularly varying compositional range, e.g. from basic (bytownite or amphodelite) in the central part to labradorite and andesine in the outer part of crystals;
2. Clinopyroxene is the main mafic mineral in rocks and shows no zoning;
3. Amphible and quartz are absent in rocks and their CIPW norms;
4. Orthopyroxenes is mainly bronzite.

Above characteristics of the mineral assemblage suggest that the generation and evolution of the rocks from the Fildes Peninsula are the result of an equilibrium fractional crystallization in a magma chamber.

III. Trace Element Concentrations of Minerals

Main oxides of the minerals including feldspar, pyroxene, olivine and other accessory minerals have been analyzed and used in discussing fractional crystallization in magma evolution. We find that the fractionation of plagioclase and pyroxene, and minor olivine from a primary basaltic melt results in andesitic magma, then the separation of plagioclase and pyroxene controlled the generation of dacitic melt. Studies on the melt inclusions of augite crystals in basalt also supports our evidences for understanding the evolution of magmas under the control of mineral fractionation.

Contents of trace and rare earth element of some plagioclase and augite phenocrysts combining with that of related whole rocks and groundmass determined with INAA are published (table 1).

Plagioclase is rich in LREE and with sharply positive Eu anomaly. The total content of REE in plagioclases trends to decreasing from basaltic to andesitic rocks with increasing Eu anomaly and decreasing the LREE/HREE ratio.

Table 1 REE concentration of minerals and rocks (ppm)

	XN17				ZF37			ZF38		
	Rock	Pl	Cpx	Matrix	Rock	Pl	Cpx	Rock	Pl	Cpx
LA	9.15	2.16	1.29	12.1	5.40	0.674	1.47	13.1	1.08	1.41
CE	20.0	3.17	-	28.5	12.6	-	5.22	26.0	2.02	5.86
ND	10.8	1.52	4.98	14.6	8.33	0.888	4.09	18.9	-	5.53
SM	2.69	0.272	1.76	3.51	2.08	0.113	1.68	4.37	0.157	2.82
EU	1.13	0.227	0.634	0.965	0.74	0.228	0.576	1.40	0.319	0.874
TB	0.542	0.0511	0.408	0.494	0.349	0.0362	0.375	0.698	-	0.437
YB	1.42	0.120	1.05	1.70	0.96	0.109	1.07	2.05	0.169	1.58
LU	0.236	0.0216	0.119	0.175	0.141	0.0221	0.157	0.300	0.0331	0.236

The LREE/HREE ratio of clinopyroxene is less than 1. We can see that the fractionation of the above phenocrysts from magma would result in increasing the REE concentration of residual melts except Eu. So the Eu anomaly of evolved magmas became lower and lower, and which in dacite is going to be negative (Fig.1). Based on the contents of TE and REE in minerals, matrix and whole rocks, the magmatic evolution process controlled by fractional crystallization of plagioclase and pyroxene has been calculated with Reyleigh function (Gast,1968). In calculation the proportions of separated mineral are from the calculated results with major compositions and the partition coefficients is after Luhr and Carmicheal (1985). Calculated results confirm magmatic generation being under the control of plagioclase and pyroxene separated from melts.

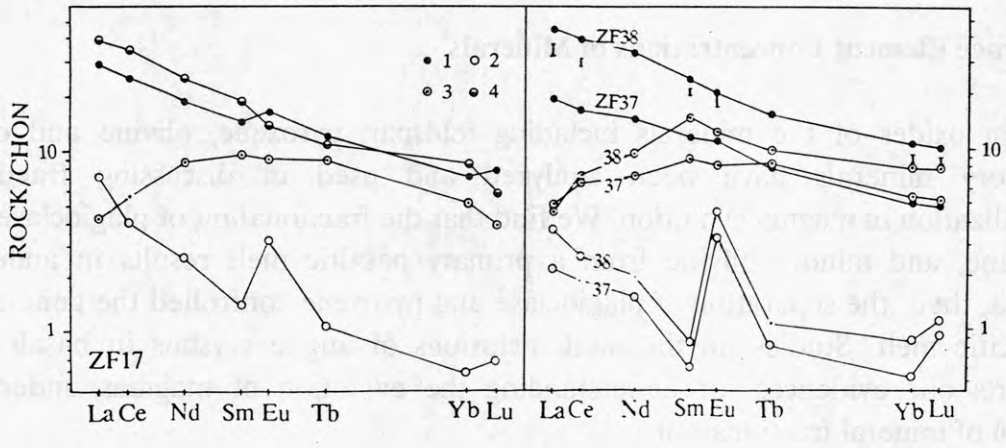

Fig.1 Rare Earth Element chondrite-normalized diagram showing the relationship within whole rock, Matrix glass, plagioclase and clinopyroxene

1. rock; 2. Pl; 3. Augite; 4. matrix of rocks

Conclusion

1. The main rock-forming minerals of the volcanic rocks from the Fildes

Peninsula are plagioclase and pyroxene which are very important separated phases in the process of magmatic generation and evolution;

2. Mineralogical assemblage and characteristics indicate that the rocks from studied area were formed in a equilibrium condition in magmatic chamber by plagioclase and pyroxene fractionation;

3. Trace and REE contents of rock-forming minerals, combining with major composition of rocks, should be used to discuss magmatic evolution and could have efficient effect.

Reference

Davies,R.E.S., 1982, The geology of the Marian Cove area, King George Island, and a Tertiary age for its supported Jurassic volcanic rocks, Brit. Ant. Surv. Bull., 51, 151-165.

Li Zhaonai, Liu Xiaohan, Zheng Xiangshen, Jin Qingmin, Li Guo. 1989. Tertiary volcanism and formation of volcanic rocks in the Fildes Peninsula, King George Island, Antarctica. In: Guo Kun ed. Proceeding of the International Symposium on Antarctic Research, Beijing: China Ocean Press, 114-118.

Luhr,J.F. and Carmichael,I.S.E., 1985, Jorullo Volcano, Michoacan,Mexico(1759-1774): the earliest stage of fractionation in calc-alkaline magmas, Contrib. Mineral. Petrol., 90, 142-161.

Pankhurst,R.J.Smellie,J.L.,1983, K-Ar geochronology of the South Shetland Islands, Lesser Antarctica, Apparent lateral migration of Jurassic to Quaternary island arc volcanism, Earth Planet. Sci. Lett., 66, 214- 222.

Sakuyama M. 1981. Petrological study of the Myoko and Kurohime Volcanoes, Japan: Evidence for magma mixing. J. Petrol., 22,553-583.

Sakuyama M. 1983. Petrology of arc volcanic rocks and their origin by mantle diapirs. J. V. Geotherm. Res., 18: 297-320. Smellie,J.L., Pankhurst,R.J.,Thomson, R.A. and Davies, R.E.S., 1984, The geology of the South Shetland Islands: VI. Stratigraphy, geochemistry and evolution, Bull. Brit. Antarct. Surv., 53, 39-84.

Watts, D.R., 1982, Potassium-Argon ages and paleomagnetic results from King George Island, South Shetland Islands, in: Antarctic Geoscience, ed. by Craddock, C., University of Wisconsin Press, Madison, 255-261.

Zheng,Xiangshen and Liu,Xiaohan, 1989a, Tertiary volcanic stratigraphy and volcanism in Fildes Peninsula, King George Island,West Antarctica, in: Advances on Geology, ed. by Wang, Sijing et al., China Ocean Press, Beijing, 163-176.

Zheng,Xiangshen and Liu,Xiaohan, 1989b, The petrological characteristics and evolution of tertiary volcanic rocks stratigraphy in the Fildes Peninsula, King George Island, Antarctica, In: Guo Kun ed Proceedings of the international symposium on antarctic research, Beijing: China Ocean Press, 142-150.

Zheng Xiangshen, Liu Xiaohan and Yang Reiying, 1988, The petrological characteristics of Tertiary volcanic rocks near the Chinese Great Wall Station area, West Antarctica, Acta Petrologica Sinica, 1, 33-47, (in Chinese with English abstract).

Zhu Ming, E Molan, Liu Xiaohan and Zheng Xiangshen, 1991, The isotope age of the volcanic rocks from the Feildes Peninsula and its corelation to stratigraphy, Antarctica. Antarctic Research (in Chinese with English abstract, in press).

CONTRASTING FLUVIAL STYLES IN THE WELLER COAL MEASURES AT ALLAN HILLS

K. J. Woolfe, M. J. Arnot, P. J. Barrett, Antarctic Research Centre, Victoria University, P. O. Box 600, Wellington, New Zealand.

J. E. Francis, Department of Geology and Geophysics, The University of Adelaide, GPO Box 498, Adelaide, Australia.

Reconnaissance field work in 1988-89 revealed an enigmatic fluvial sequence, in the Weller Coal Measures (Early Permian), at Allan Hills, southern Victoria Land. Continuous exposure of Member C over 10 km^2 shows well developed Well developed epsilon crossbedding, fining-upwards cycles and diverse paleocurrent directions suggest deposition by meandering rivers. However, epsilon crossbedding is developed in fine sandy mudstone, a lithology more characteristic of over-bank sedimentation, and sandstone bodies have sheet-like geometries. Both of these features are not readily explained by the traditional meandering river model (Allen 1965, 1970, Walker and Cant 1984). The strata were the subject of a more intensive study when Allan Hills was revisited during the 1990-91 austral summer.

Member C (of the Weller Coal Measures) at Allan Hills can be divided into fourteen, widely traceable, lithostratigraphic units. These units consist mainly of sheet-like sandstone bodies, containing subordinate shale, and laterally continuous coal seams up to 4 m thick. Two types of sandstone-sheet can be recognised on the basis of their sedimentary structures and paleocurrent signature.

Type 1 Sandstone-sheets

Type 1 sandstone-sheets consist mainly of decimetre-scale trough crossbedded medium to coarse sandstone or granule conglomerate. Pebbles, up to 30 cm in largest diameter, occur widely at the base of these sheets but the contact with underlying coal shows no relief. Internally type 1 sandstone-sheets are simple, consisting of stacked trough crossbeds and large isolated bar forms. Trough crossbedded sandstone grades vertically, and locally laterally, through ripple laminated fine sandstone into planar bedded or unbedded mudstone, commonly containing well preserved Glossopteris or Vertebraria Unit thickness ranges from 1 m to 4 m and in most cases the sheet appears to have been deposited by a single large scale event.

Six sandstone-sheets of this type are recognised in Member C at Allan Hills. Within each sheet paleocurrent directions, obtained from trough crossbed axes exposed on bedding plains, are very consistent indicating deposition by a unimodal flow (figure 1). Paleocurrent directions are also consistent between sheets (figure 2), showing that all the sheets were sourced from the east.

Type 2 Sandstone-sheets

The second type of sandstone-sheet is characterised by medium to fine sandstone with complex and commonly truncated sedimentary structures. Decimetre- and metre-scale trough crossbedding, ripple drift lamination (including climbing ripples), hummocks (HCS), swales and metre-scale epsilon crossbedding are all common. Shale lenses containing well preserved Glossopteris and Vertebraria are common, along with mudflake breccia lenses, silicified logs and stumps.

Paleocurrent directions from trough crossbeds, ripples and logs are highly variable and are mostly bimodal and polymodal (figure 3).

Interpretation:

Type 1 sandstone-sheets are interpreted as being deposited by a braided system. A crevasse splay origin is not favoured because all the sandstone-sheets of these type are sourced from the same direction. Instead it is inferred that the sheets were deposited at the distal end of an alluvial fan complex which periodically advanced across the flood plain from a basement high to the east of Allan Hills. Coarse angular feldspars suggest rapid unroofing of granitic basement and short transport duration. A single large striated boulder in the lowermost sheet suggests that periodic unroofing events may be related to glaciation in the highlands (Barrett et al. this symposium).

It is concluded on the basis of paleocurrent evidence and sedimentary structures that the internally complex sandstone sheets (type 2) were deposited by a meandering system. Well exposed cross-cutting relationships between internally complex (meandering) sandstone-sheets and split coal seams (figure 4) show that the meandering system and the coal swamp co-existed, and were adjacent to each other on the flood plain. The absence of shale and sandstone within coal seams juxtaposed to the sandstone-sheets suggests that crevasse splays and avulsions did not play a major role in flood plain sedimentation.

Conclusion

It is concluded that, for the most part, Member C at Allan Hills was deposited on a very low gradient, tectonically stable flood plain by co-existing blind meandering rivers (type 2 sandstone sheets) and coal swamps. Periodically braided sand-sheets (type 1) invaded the flood plain from the east. Coarse angular feldspar grains suggest limited transportation and it is inferred that the braided sand-sheets were sourced by alluvial fans draining off a granitic basement high to the east.

References

Allen, J. R. L. 1965: A review of the origin and characteristics of Recent alluvial sediments. **Sedimentology 5** : 89-191.

Allen, J. R. L. 1970: Studies in fluviatile sedimentology: a comparison of fining-upwards cyclothems, with spectial reference to coarse-member composition and interpretation. **Journal of Sedimentary Petrology 40**: 298-323.

Walker, R. G.; Cant, D. J. 1984: Sandy Fluvial Systems. **In**: Walker, R. G. (ed) Facies Models. **Geoscience Canada Reprint Series 1**: 71-89.

Figure captions

Figure 1 Composite rose diagram for lowermost type 1 sandstone-sheet in Member C at Allan Hills, trough crossbeds, n=250, directions are magnetic.

Figure 2 Composite rose diagram showing 210 trough crossbed axes from 6 type 1 sandstone-sheets indentified in Member A, directions are magnetic.

Figure 3 Composite diagram for a type 2 sandstone-sheet, ripples, n=242, all directions are magnetic.

Figure 4 Cross-cutting relationships between coal seams and internally complex sandstone-sheets (type 2), eastern wall of Pond Valley, Allan Hills.

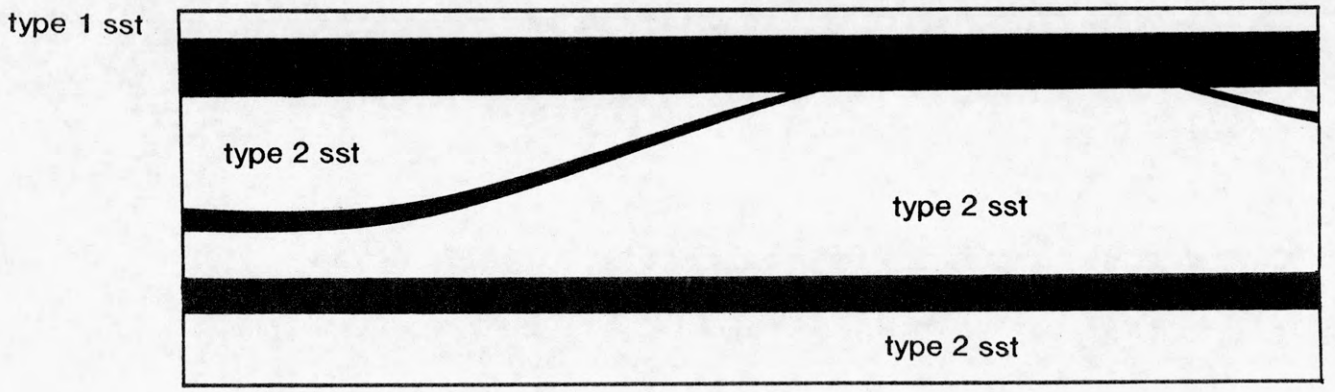

Fig.4

10 m

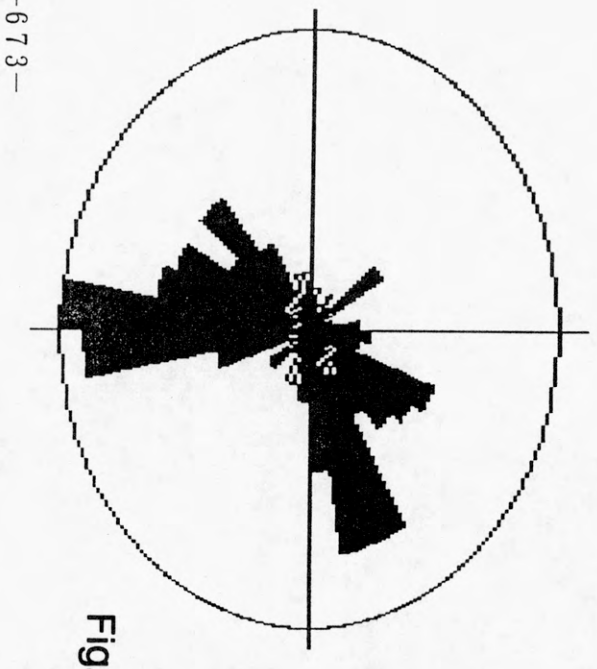

Fig.3

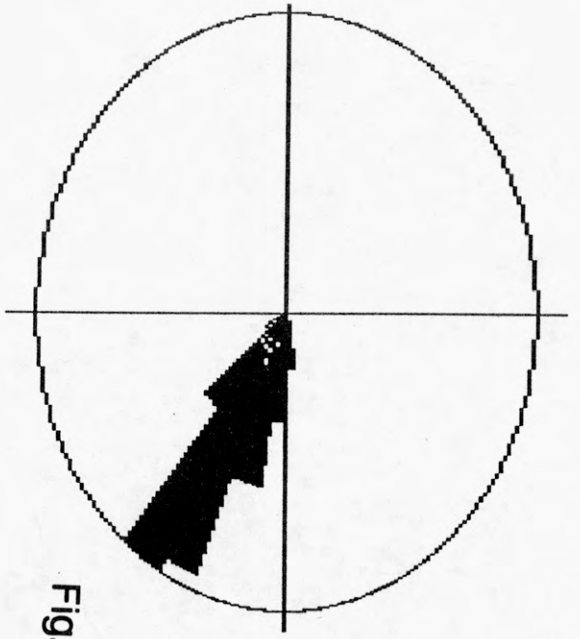

Fig.2

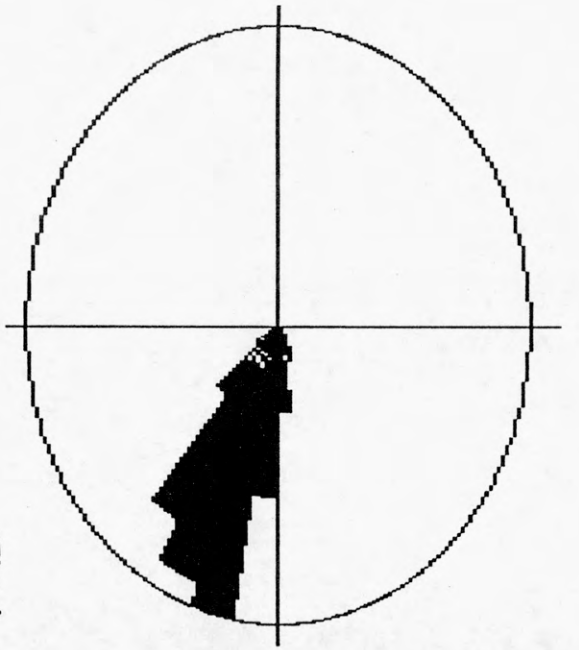

Fig.1